Proceedings of the first *fib* Congress 2002

fib 2002
Osaka Congress

fib
CEB-FIP

Concrete Structures in the 21st Century

Volume 2

Condensed Papers (2)

Organized by
Japan Prestressed Concrete Engineering Association
Japan Concrete Institute

Proceedings of the first *fib* Congress 2002

fib 2002 Osaka Congress

Concrete Structures in the 21st Century
Volume 2

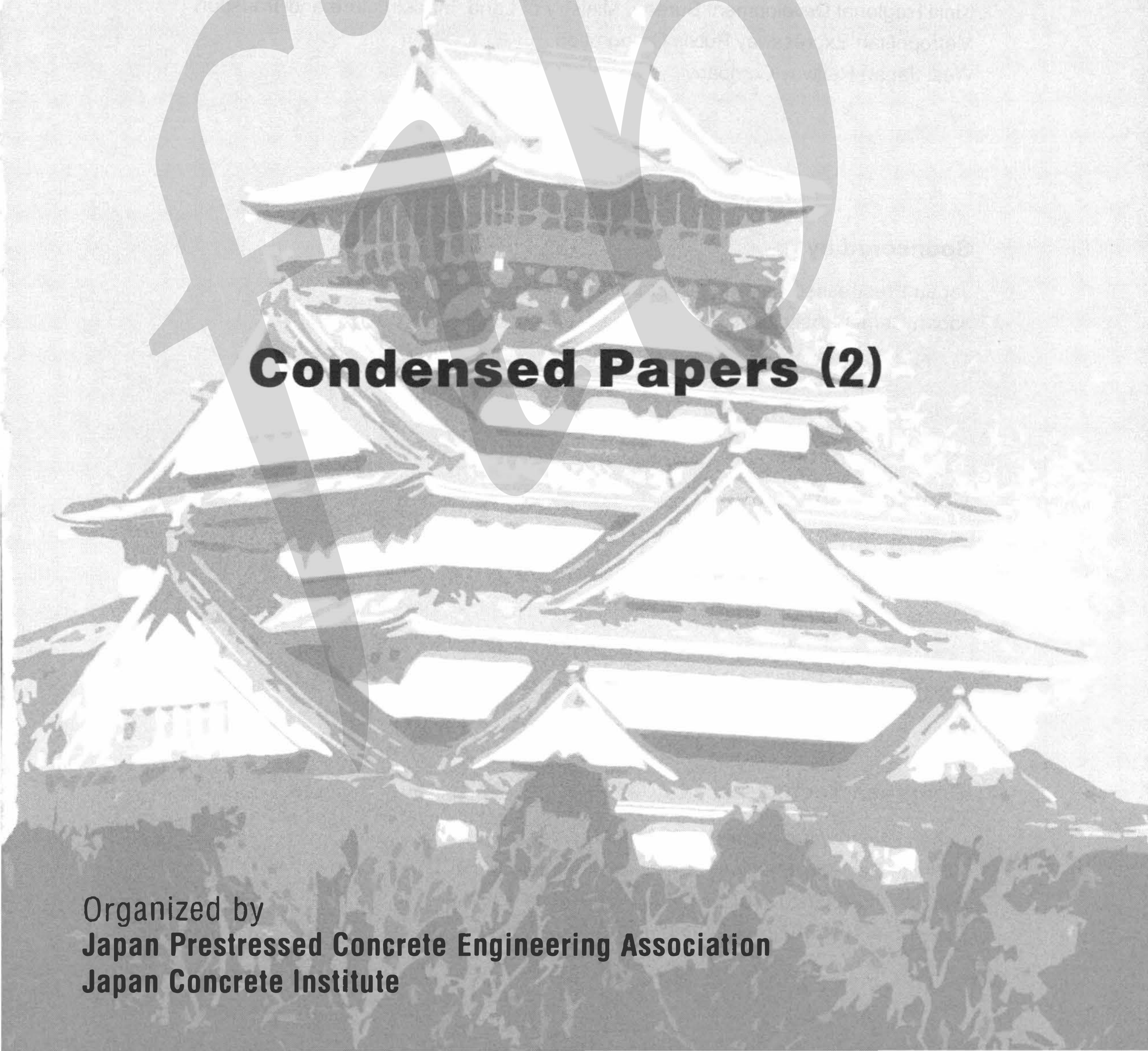

Condensed Papers (2)

Organized by
Japan Prestressed Concrete Engineering Association
Japan Concrete Institute

Officially Supported by

Ministry of land, Infrastructure and Transport, Japan
Osaka Prefectural Government
Osaka City

Supported by

Hanshin Expressway Public Corporation
Honshu-Shikoku Bridge Authority
Japan Highway Public Corporation
The Kansai Electric Power Co., Inc
Kinki Regional Development Bureau, Ministry of Land, Infrastructure and Transport
Metropolitan Expressway Public Corporation
West Japan Railway Company

Sponsored by

Japan Prestressed Concrete Contractors Association
Japan Cement Association

Contributed by

The Maeda Engineering Foundation
March 8 Symposium
Osaka Convention Bureau

Congress Secretariat

Japan Prestressed Concrete Engineering Association
On-site Secretariat Office : Rooms 805(8th floor of OICC)
Phone : 06-4803-5590(dial in, Intl : +81-6-4803-5590)
Fax : 06-4803-5592((dial in, Intl : +81-6-4803-5592)

Scientific Committee
Chairman
Joost Walraven

Co-chairman
Jun Yamazaki

Gordon Clark
Jim G. Forbes
Catherine E. French
Hans Rudolf Ganz
Steinar Helland
Shoji Ikeda
Tsutomu Kadotani
Hans-Ulrich Litzner
Giuseppe Mancini
Života Perišic
Tippur N. Subba Rao
Jiri Strasky
Tada-aki Tanabe
Ruediger Tewes
Taketo Uomoto
Michel Virlogeux
Fumio Watanabe

Secretary
Akio Kasuga
Takuya Mori
Tamio Yoshioka

Organizing Committee
Chairman
Shoji Ikeda

Yasuo Egashira
Tsutomu Fukute
Satoshi Kashima
Kenji Kitahashi
Kazuo Kobayashi
Hiroshi Komori
Kiyoshi Kono
Atsuhiko Machida
Hiromichi Matsushita
Shiro Morita
Masanobu Murata
Shojiro Nan-ya
Yasuyuki Odagiri
Tsunesuke Ogasawara
Toshio Ohkoshi
Yoshiteru Ohno
Michio Okahara
Tetsutaro Orito
Nobuhiko Sato
Katsuyuki Suzuki
Yoshiharu Takamatsu
Tada-aki Tanabe
Giichi Tanaka
Yasuo Tanigawa
Fuminori Tomozawa
Michio Uchida
Fumio Watanabe
Shigeyuki Watanabe
Hiroyuki Yamanouchi
Jun Yamazaki
Tsuneji Yasui

Executive Committee
Chairman
Jun Yamazaki

Masaru Hamada
Shizuo Hayashi
Katsushi Ikejiri
Tsutomu Kadotani
Akio Kasuga
Hiroto Kato
Hirotaka Kawano
Hiroshi Kikkawa
Hitoshi Kitayama
Kazuo Kobayashi
Tsutomu Kurotani
Makoto Kuwayama
Koichi Maekawa
Masao Maruyama
Hirozo Mihashi
Toyoaki Miyagawa
Takuya Mori
Hidenori Morikawa
Hiroshi Mutsuyoshi
Hiroyuki Nakajima
Hiroshi Nemoto
Minehiro Nishiyama
Junichiro Niwa
Hiroshi Noguchi
Yoshiteru Ohno
Kazuya Oshima
Keitetsu Rokugo
Masamichi Sano
Shunsuke Sugano
Masataka Sumi
Tsutomu Takazawa
Katsuki Takiguchi
Yukikazu Tsuji
Taketo Uomoto
Akira Wada
Fumio Watanabe
Hiroshi Yamashita
Tamio Yoshioka

Table of Contents

Session 7 | Development of new materials

RECENT DEVELOPMENTS IN THE PROTECTION OF PRESTRESSING STEELS

Hans Rudolf Ganz
Chief Technical Officer, VSL International Ltd,
Berne, Switzerland

Keywords: prestressing steel, corrosion protection, coatings, grouting

1 INTRODUCTION

Today's prestressing steels, i.e. cold drawn prestressing strand, cold drawn wire, and hot rolled prestressing bar, produced in accordance with well recognised standards such as ASTM A416, BS 5896, Draft EN10138, and JIS G3536 and 3109, or similar standards, are of an excellent quality, in general. These prestressing steels have outstanding properties in terms of strength, ductility, toughness, fatigue, stress corrosion, etc. and can be anchored safely with well proven and practical anchorage systems. However, to achieve durable prestressing tendons, the prestressing steels need to be adequately protected from corrosion. The objective of the corrosion protection must be to achieve a design life of the tendons which is comparable to that of the structure in which they are placed. The design of the corrosion protection systems should take into account that most parts of the tendons are not accessible during the design life, in general, and that individual components or the entire tendons, are not replaceable, in general. Even if special details are provided to allow replaceability of the tendons during the design life, it is the author's opinion that replacement should be considered an exceptional case which is only carried out in "emergency" situations, i.e. the corrosion protection system(s) shall be designed for the entire design life. Corrosion protection of prestressing steels includes temporary protection, and starts at the manufacturing place. It has also been recognised that a design for durability relying on a single layer of protection cannot guarantee reliable overall protection of the reinforcing and prestressing steels. Therefore, the concept of multi-layer protection has been created. In this concept the first and perhaps most important layer of protection is the overall concept and design of the structure. A key element in this design is to keep water off the structure and the reinforcement, and / or to assure that it drains quickly from the structure. A second layer of protection can be provided with water-proofing membranes in particular on critical surfaces exposed to water and other aggressive media such as de-icing salts. A third layer of protection in concrete structures is provided with dense concrete designed specifically for low permeability. The final layers of protection applied directly onto the prestressing steels are only called into action after the above mentioned layers have been breached. It is these final layers of protection applied directly onto the prestressing steel which are addressed in this paper.

These final layers of protection can be grouped into two main categories. The first category includes layers of protection which are applied to the prestressing steel during fabrication in the factory. The most common protection systems include: Grease and sheathing, zinc (or zinc-aluminium) coating, epoxy coating, and some more recent systems such as the "after bond" protection developed in Japan. Above systems can be used individually or in combination, e.g. zinc coating with grease and sheathing. These protection systems have in common that they can provide both temporary and permanent protection.

The second category includes layers of protection which are applied to the prestressing steel on site. The most common protection system in this category is the cementitious grout injected into the ducts of post-tensioning systems, and the concrete poured around the tendons in pretensioned applications. Also grease and wax have been used for injection of mainly external tendons. More recently, specific leak tight plastic ducts have been introduced to form a supplementary layer of protection for post-tensioning tendons, or even to form electrically isolated tendons. These systems have in common that a temporary protection of the prestressing steel may be needed if the time from installation and stressing to application of the permanent protection exceeds certain limits, in the order of one to several weeks, for very aggressive to benign climats.

Some of the above protection systems are quite old, others are quite recent. This paper will review the most commonly used systems for post-tensioning, i.e. grease and sheathing, zinc and epoxy coating of prestressing steel, and protection by cementitious grout, plastic ducts, and electrical isolation. Both temporary and permanent protection will be reviewed. The paper presents existing experience and new trends.

2 CONCLUSIONS

Factory applied corrosion protection systems can provide improved protection to the prestressing steel. They can provide both temporary and permanent protection at the same time. However, encapsulation of the anchorage zones is important to provide an equivalent protection as in the current tendon length.

In practice the only system used in significant quantity is the greased and sheathed monostrand mostly applied in building construction. This system has proven to provide reliable protection, if the anchorage zones are encapsulated, while still allowing for easy and reliable anchorage of the tendon by wedges.

The zinc coated strand, protected with wax and tightly extruded PE sheathing, has obtained a certain importance for stay cable applications. However, some progress is still needed to better control the fabrication process of zinc coating to assure consistent high quality of the finished product. The main query with epoxy coated prestressing steel used for post-tensioning is the assurance of a sufficiently constant coating thickness for reliable anchorage by wedges. Other factory applied protection systems do exist. However, their usage for post-tensioning is marginal.

The most common protection system applied on site is cementitious grout. As a consequence of recent problems the grout mix and testing procedures have been completely reviewed. Grout mixes which have been designed and tested with these new procedures, published by fib and others, assure an excellent quality of protection and durability of the tendons.

Special plastic duct systems have been developed for post-tensioning tendons. These plastic duct systems complement high quality grout mixes in an optimum way to provide fully encapsulated tendons. This provides redundant layers of corrosion protection which can guarantee the long term durability of tendons.

Electrically isolated tendons can further improve the level of protection, and permit to verify the actual protection at any time during the design life of the structure. This may provide important feed back to the client for his management system of the structure, and particularly the tendons.

With any protection system, factory applied or in situ applied, the tendons are eventually installed by people. High quality installation assuring long term durability can only be obtained if these activities are performed by experienced, qualified and well trained specialists. In particular this last aspect will still need to be introduced in most national and project specifications.

Prestressing steels are excellent materials for which we have long and good experience for their suitability for post-tensioning. However, the prestressing steels have to be adequately protected in accordance with the today's knowledge. It has been proposed to replace prestressing steels with non-corrosive fibre reinforced plastic materials. It is the author's opinion that these materials still have to go through a long development until they can provide performance and reliability for post-tensioning applications comparable with well protected prestressing steel.

ENHANCING THE DURABILITY OF POST-TENSIONED STRUCTURES BY IMPROVING THE QUALITY OF GROUTING

Dr. Hans Rudolf Ganz, Chief Technical Officer
Ms. Stephanie Vildaer, Materials Engineer
VSL International Ltd., Berne, Switzerland

Keywords: durability, grout, bleed, optimisation

1 INTRODUCTION

The durability of a post-tensioned concrete structure is a function of the number and quality of the layers of protection provided on the structure. These layers may include the design and concept of keeping water off the surface of the structure or draining it as quickly as possible, protection membranes on critical exposed surfaces, dense and low permeability concrete, leak tight and non-corrosive ducts like plastic ducts, and the cementitious grout. Depending on the environment at a particular site, a sufficient number of suitable layers should be specified to guaranty the durability of the structure. The grout in a post-tensioned structure is only the last line of defence, but an important one. VSL has launched an extensive R&D program in 1998 on the quality of grout and grout injection. The aim of this paper is to summarise selected results of this program.

2 GROUT MIX DESIGN

The main components of a cementitious grout are cement, water, and admixtures. For a selected cement and admixture the compatibility of the couple needs to be verified first. Then the optimum content of admixtures and water can be determined to assure the specified performance. The grout obtained from such a procedure is called an optimised grout in this paper.

A grout for post-tensioning should have good flow characteristics to provide good workability and to allow complete filling of the tendon duct. It needs to be stable to avoid bleed and sedimentation which would lead to the creation of voids after the injection. Other essential characteristics of the grout are to provide bond between prestressing steel and duct/structure for bonded post-tensioning, and to protect the prestressing steel from corrosion by providing an alkaline and low permeability environment.

2.1 Flowability

To achieve a viscosity of grout which can easily be pumped without use of plasticizing admixtures, water/cement ratios in the order of 0.4 - 0.45 are required. This is significantly more water than required for hydration of the cement. With suitable plasticizing admixtures the water/cement ratio can be reduced down to the order of 0.3 for the same viscosity. Grout mixes with low water/cement ratio are inherently more stable and less likely to show excess bleed, sedimentation and segregation.

The flow time of a particular grout mix should remain stable over a sufficiently long period of time, at a given temperature range, to avoid problems during injection due to stiffening of the grout. With suitable design and eventual use of specific admixtures, the flow time of grout mixes can be maintained stable over an extended duration of time, sometimes hours, even at high temperatures.

2.2 Stability of grout

Grout is a suspension of cement in water and admixtures. The stability of the grout suspension against sedimentation is mainly a function of the quantity of water. Recent investigations and experience on sites have shown that the bleed is also a function of the type of test specimen. The bleed was measured in different specimens for two grout mixes with comparable flow time. The grout called "Common Grout" used a plasticizing and expansive admixture with a water/cement ratio of 0.38. The grout called "Optimised Grout" used another plasticizing, and a stabilising admixture but without expansion with a water/cement ratio of 0.32. All four types of specimens were filled with the same batch of each grout mix. Table 1 and Fig. 1 summarise the results obtained for the different tests presented in [1,2].

Table 1 Comparison of results of different bleeding tests

	100 mm high container	1 m high tube without strand	1 m high tube with strand	Inclined Tube
Common grout	1 %	0% / expansion	2.5% / no expansion	15 %
Optimised grout	0 %	0%	0%	0.1 %

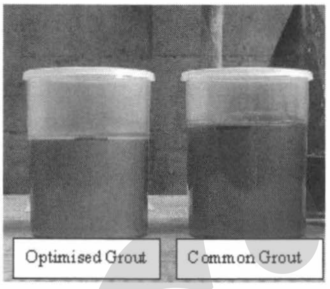

a) Standard bleed test in 100 mm containers

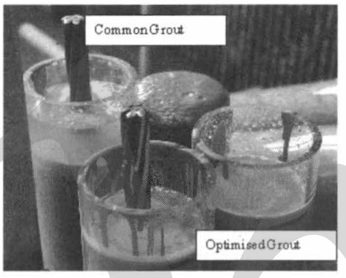

b) 1 m high tubes with and without strand

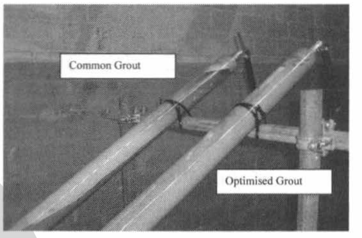

c) 5 m Inclined Tube with 12 strands

Fig. 1 Bleed and volume change behaviour in different test specimens

The Inclined Tube test is the only available type of test which is representative for the real conditions inside a tendon duct. The presence of the prestressing strands is particularly severe for bleed. This test therefore, should be used for the approval of a particular grout mix. In a situation of excess water, the cement particles tend to flocculate (form lumps), and settle (sedimentation), with the lighter water moving upwards, and collecting at the top of the grout (bleed). This sedimentation leads to an apparent reduction of grout volume in the order of a few percent of the initial volume, in the first few hours after injection. This movement of water may wash out certain components of the cement and admixtures, and thus may cause segregation of the grout.

Shrinkage of grout, on the other hand, is a completely different phenomenon which depends primarily on the type of the cement and to some degree on the amount of water. At 28 days maximum shrinkage values of optimised grout mixes were below 2000 μm/m, and hence, about one order of magnitude lower than the effect of sedimentation.

3 CONCLUSION

The required flowability of grout can be achieved with low water/cement ratio if a suitable plasticizer with confirmed compatibility with the cement is used. Such optimised grout mixes provide low bleed, low sedimentation and low volume change and do not leave voids in the tendons.

Standards tests for bleed should be reviewed. Wick-induced test and inclined tube test are representative of the real conditions inside a tendon duct and therefore, should be used instead of the small containers typically specified in today's standards.

On site, suitable procedures and well trained and qualified personnel are required to produce a high quality grout necessary for long term protection of the post-tensioning steel.

REFERENCES

[1] "Grouting of post-tensioning tendons", VSL Technical Report Series No 5, VSL International Ltd., Berne, 2002.
[2] "Grouting of tendons in prestressed concrete", Guide to Good Practice, fédération internationale du béton (fib), Lausanne, Draft January 2002.

Application of High Strength Fibre Reinforced Self Compacting Concrete In Prefabricated Prestressed Concrete Sheet Piles

Dr. W. Jansze
Spanbeton bv
Netherlands

Mr. M. Peters
Spanbeton bv
Netherlands

Dr. C. van der Veen
Delft University of Technology
Netherlands

Keywords: sheet piles, new materials, geometry, design, costs, production

1 INTRODUCTION

Since 1999 a joint research project (Spanbeton and Delft University of Technology) has been conducted to investigate the use of new concrete materials in prefabricated prestressed concrete sheet piles. Spanbeton produces 120 mm thick sheet piles with a normal concrete quality (C60). In a comparison study the use of a High Strength Concrete, a High Strength Fibre Reinforced Concrete, a High Strength Fibre Reinforced Self-Compacting Concrete and a Very High Strength Fibre Reinforced Self-Compacting Concrete were studied. It was concluded that the High Strength Fibre Reinforced Self-Compacting Concrete (HSFRSCC) was most competitive in sheet piles with a 50 mm thickness . The feasibility was proved by the production and installation of real size prototype sheet piles.

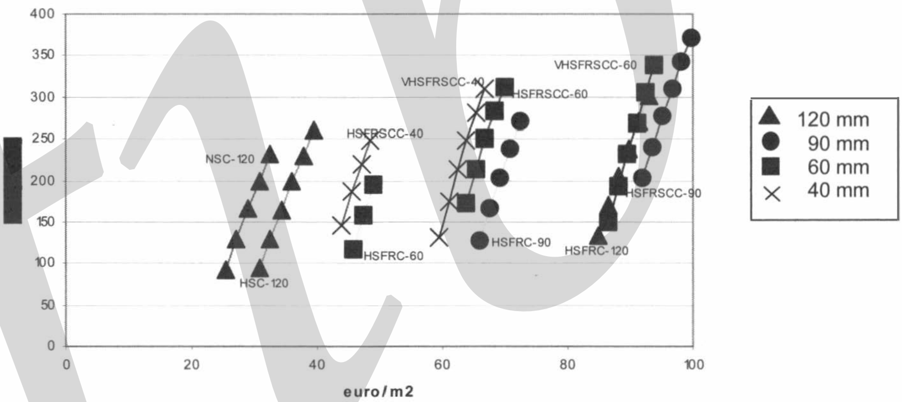

Fig. 1 M_e as a function of costs in [euro/m^2] and as a function of various mix designs and geometry

2 DESIGN AND COST COMPARISON STUDY ON CONCRETE MIXES

2.1 Goal of the study

The goal of the design and cost comparison study by Van der Kolk [2] was to investigate the possibilities to optimise the current Spanwand as a result of the use of new concrete mixes. The optimisation includes on the one hand a comparison of concrete mixes, and on the other hand the optimisation of the sheet pile geometry.

2.2 Concrete mixes

To explore the possibilities of new concrete mix designs, a comparison study was carried out in which five mixes were studied, 1. Normal Strength Concrete (NSC), 2. High Strength Concrete (HSC), 3. High Strength Fibre Reinforced Concrete (HSFRC), 4. High Strength Fibre Reinforced Self-Compacting Concrete (HSFRSCC) and 5. Very High Strength Fibre Reinforced Self-Compacting Concrete (VHSFRSCC). The amount of cement and silica fume significantly increases. High quantities of superplasticisers are used to obtain in good flow ability, fibres are added to improve ductility.

2.3 Comparison results

Figure 1 depicts the result of the design and cost comparison study. Due to the minimum cover on stirrups, it is not possible to reduce the thickness of both the NSC and HSC. Then, despite the higher compression strength of the HSC, the 120 mm sheet pile hardly improves because the tensile strength of HSC hardly increases. A 40 mm or 60 mm thick HSFRC sheet pile will give problems for the load cases concerning installation, but also concerning transport. The 90 mm and 120 mm thickness are relatively expensive compared to Spanwand. Also, the tensile strength of the HSFRC is too low. The 40 mm HSFRSCC and VHSFRSCC sheet pile will not give problems for any load case. It is clearly seen that the VHSFRSCC sheet pile will still have much higher costs (70%) than the HSFRSCC sheet pile (40%) compared to Spanwand. However, it must strongly be remarked that these 70% and 40% is much less than the 15, respectively 11 times higher mix costs. It is concluded that the HSFRSCC is the most suitable for application in sheet piles.

3 SHEET PILE OF HSFRSCC CONCRETE (C105)

3.1 Goal of the study

The goal of the study by Tol [5] was to translate the laboratory test of HSFRSCC into real sheet pile production at the Spanbeton factory, and carry out the first real installation test (by vibration) of three newly developed sheet piles. Also, experiments had to be carried out to validate the analytical calculation models and newly developed provisions.

3.2 Production of HSFRSCC sheet pile

The following results of the mix was reached at Spanbeton. A slump flow of 700-800 mm, a funnel flow time of 10 to 5 sec and a U-box value of 28 mm (322 mm of 350 mm height).

Fig. 2 Mould with strands for pile production

Fig. 3 Sheet piles on stock

3.3 Installation of HSFRSCC sheet pile

Three sheet piles were successfully installed into the ground by vibration. This test was the ultimate goal, because only then real loads act on the sheet pile. At the test site at about 12 m depth a sand layer was present, above, soft ground was present. During the vibration of the sheet piles a frequency of 1800 per minute was used. Total vibration time ranged between 15 and 7 minutes.

4 CONCLUSION

The main conclusion to be drawn from the various studies is that Spanbeton succesfully developed a new sheet pile geometry with HSFRSCC. This new concrete material stood at the basis of this new development. Accordingly, new concrete materials initiate product development. But also, product development speeds up the use of new materials at daily practise.

ACKNOWLEDGEMENT

This paper is mainly based on the master thesis works of Meindert van der Kolk [2000] and Robert Tol [2002] carried out at Spanbeton, for which the authors are indebted. The HSFRSCC mix design work carried out by Steffen Grünewald and Tony Bolo is greatly acknowledged.

FLEXURAL FATIGUE PROPERTIES OF FIBER REINFORCED CONCRETE

Mutsumi Mizukoshi
Sumitomo Osaka Cement Co,. Ltd.
JAPAN

Shigeyuki Matsui
Osaka University, Graduate School of Engineering
JAPAN

Hiroshi Higashiyama
Kinki University
JAPAN

Mitsuharu Teduka
Mitsubishi Chemical Functional Product, Inc.
JAPAN

Keywords: fiber reinforced concrete, steel fiber, carbon fiber, fatigue, crack development

1 INTRODUCTION

In this study flexural fatigue tests were performed. Specimens were small unreinforced beams made of carbon fiber reinforced concrete (CFRC), steel fiber reinforced concrete (SFRC), and plain concrete (PL) containing no fiber as comparison base. Crack development until ultimate failure caused by fatigue was observed. From the analyses of fatigue data about the crack propagation, reasonable S-N curves and serviceability limit of crack depth were proposed. Finally a design procedure applying the serviceability limit was discussed.

2 OUTLINE OF EXPERIMENT

2.1 Kinds of specimens

Table 1 shows the seven kinds of specimens used for the fatigue test.

Table 1 Kinds of specimens and mix proportion

Kinds of specimen	W/(C+EX) (%)	Gmax (mm)	Fiber length (Lf) (mm)	Gmax/Lf	s/a (%)	Vf (%)	Unit weight (kg/m^3)						C×(%) SP
							W	C	EX	S	G	Fiber	
CF-0.5	45	20	40	0.50	58	0.5	172	342	40	984	743	9.5	1.0
CF-1.0		20	40	0.50	66	1.0	185	371	40	1073	576	19	1.0
SF-A-0.6		13	30	0.43	51	0.6	159	316	40	868	888	47	1.4
SF-A-1.0		13	30	0.43	52	1.0	170	340	40	860	83.4	80	1.3
SF-A-1.5		13	30	0.43	56	1.5	181	365	40	891	737	118	1.3
SF-B-1.27		13	30	0.43	58	1.27	172	342	40	972	734	100	1.0
PL		13	-	-	43	0	153	302	40	737	1071	—	1.0

2.2 Experimental method

Fig. 1 shows the condition of the fatigue test. All specimens were subjected to a central concentrated load with the span length of 320 mm. The fatigue load was the pulsating load of a sine curve 5Hz using a servo type jack. The maximum load was changed from 60% to 95% of the static strength, and the minimum load was the constant value by which the bending tensile stress on the bottom surface became $0.29 N/mm^2$. As shown in **Fig. 1**, two crack propagation gauges were attached on the both side of specimen for sensing crack development by every 5 mm.

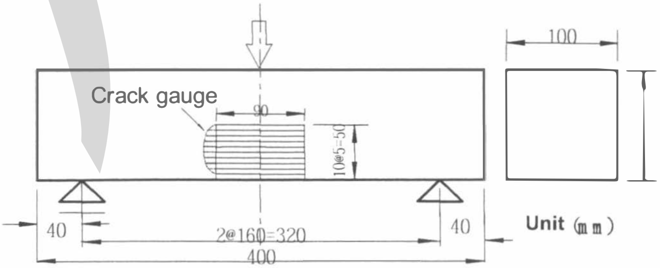

Fig. 1 Details of the the condition of the fatigue test

3 RELATIONS BETWEEN CRACK INITIATION LIFE AND CRACK PROPAGATION LIFE

A crack development diagram when maximum actual stress σ=6.0 N/mm^2 for all types of FRC except SF-A-1.5 was obtained as in **Fig. 2**. This clearly shows differences in the crack development speeds of each kind of concrete. This shows that after the crack depth has reached 15 mm, the crack development speed rises, and as soon as the depth exceeds 30 mm, failure occurs in a short time. Based on this, it is reasonable to conclude that the serviceability limit of CFRC and SFRC is the time when the crack depth is 15 mm.

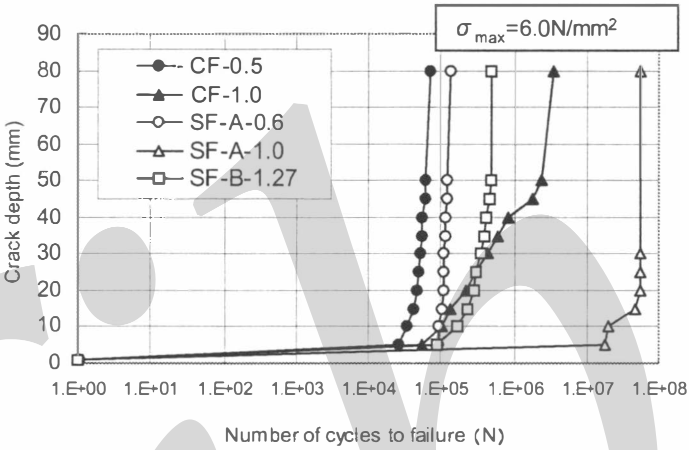

Fig. 2 The crack development diagram for all types of FRC (σ_{max}=6.0N/mm^2)

4 STUDY OF THE DESIGN FATIGUE CURVE

Until now, S-N diagrams were arranged with the mean fatigue lives. For actual design, more safety side definition should be taken into. Until now, it is general to use the fatigue curve presented with probability of survival p(N) 95%. In **Fig. 3**, the data of the serviceability crack depth of 15mm were rearranged with the data of non-failure. From such a diagram, a design fatigue curve could be determined by the 95% survival probability. The curve seems to be a favorable one instead of the 95% survival probability curve using the data of 15mm crack depth.

Considering the fact that even after 2 million fatigue loading cycles within the range of S from 60% to 70% any specimens did not fail, the fatigue limit may be set around the stress ratio.

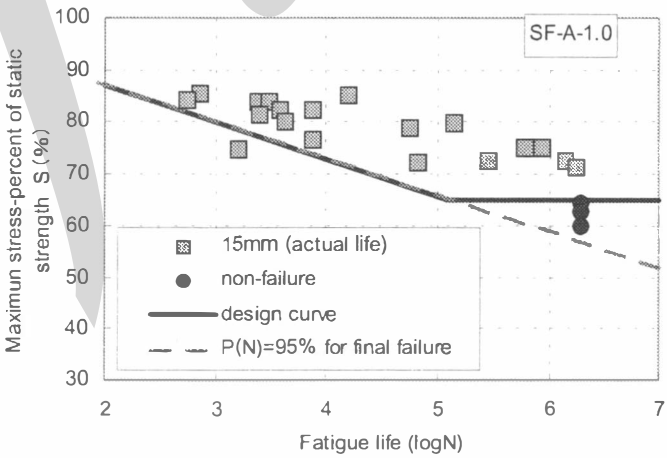

Fig. 3 The design use S-N diagram for FRC, for example, SF-A-1.0

CEMENT GROUT FOR POST-TENSIONING TENDONS PROTECTION - AN OVERVIEW OF RECOMMENDED PROPERTIES, MIXTURE PROPORTIONING, AND QUALITY CONTROL PROCEDURES

Ammar Yahia **Tamio Yoshioka**
Research Laboratory, Oriental Construction, Japan

Kamal H. Khayat
Dept. of Civil Engineering, Université de Sherbrooke
Canada

Keywords: Cement grout, bleeding, fluidity, corrosion, durability, steel tendon, post-tensioned.

1 INTRODUCTION

Although the importance of effective protection of post-tensioning steel tendons against corrosion is well recognized, the problems associated with the grouting operation have not been fully appreciated. Effectiveness of grouting has often been ignored or assumed to be satisfactory. However, since the few cases of tendon corrosion that have been reported in the late of 1980s and early 1990s, where a number of post-tensioned bridges were found to exhibit corrosion and failure of the tendons. The extent of this damage was such that it was deemed necessary to replace the bridge decks, and generated great concern about the durability of post-tensioned bridges. A working party has been set-up and immediately engaged to study the problem and prepare recommendations. Extensive development program involving some research activities, testing, and trials have been undertaken worldwide to review former practices and eventually develop new satisfactory materials, standards, and test procedures to secure durable structures. Considerable progress in developing a new generation of grouting materials and test procedures has been achieved. The objective of this paper is to review current technologies for specifying grouting materials and admixtures, test procedures, and mixture proportioning of grouts used to protect steel tendon in post-tensioned concrete structures. Various methods are presented to test flow properties, stability, and filling ability of cement-based grout. The review is limited to neat cement grout and does include mortar and resin-based grouts.

2 DURABILITY OF POST-TENSIONED CONCRETE STRUCTURES AND STRATEGIES FOR IMPROVEMENTS

The strategy adopted by the working party in 1996 included a range of improvements of past practice, including design detailing, construction workmanship and material properties. It introduced the use of a plastic sheath to offer an additional protective layer, improvement of grout properties to ensure complete filling of the duct, requirement for full scale trials for each project.

In North America the strategy adopted towards improving the durability of post-tensioned concrete structures have focused on improving grout materials, grout testing, and grouting practices. In France, two aspects are emphasized and considered as the key points to improving durability of post-tensioning tendons: emphasize the role of qualified companies in carrying the grouting operations and highlight the importance of approval acceptance procedures and quality control methods. The strategy adopted in Japan is highly emphasized on maintenance. Japan highway authority is encouraging prestressing methods that offer reliable anti-corrosive treatment and external cables to facilitate inspection. Another strategy consists of the application of pre-grouted prestressed tendons. In general, it can be stated that the primary efforts towards improving durability of post-tensioned concrete structures have focused on improving grout materials and practices and developing good quality grouts.

3 MAJOR ADVANCES IN CEMENT GROUT FOR POST-TENSIONING TENDONS PROTECTION

In the past 50 years, Portland cement meeting the requirement of ASTM C150 has been widely used in the grout. In general, Type II cement is selected whenever slower rise of temperature is required. In Japan, the use of Type I Portland cement is common. In North America, either Type I or Type II Portland cements have been used. On the other hand, blended cements conforming to ASTM C595 (Standard Specification for Blended Hydraulic Cements) can also be used if compatible with other grout ingredients. The partial replacement of cement by supplementary cementitious materials and mineral admixtures, to modify the properties of grout is a common practice worldwide. Actually a blended silica fume cement conforming to ASTM C595 (Standard Specifications for Blended Hydraulic Cements) is produced in Canada and widely used to proportion grouts for post-tensioning tendons protection [22]. Grouting technology is expected to shift to the use of binary or ternary blended cements in the future, both for technical and environmental reasons.

Various chemical admixtures, such as high-range water-reducer (HRWR), anti-bleeding admixtures, expansive agents, corrosion inhibitor admixtures, and air-entraining agents have been developed. The use of such admixtures to achieve specific properties is actually well accepted in grouting technology so long as they do not contain substances harmful to prestressing steel. Adequate compatibility with cement and mineral admixtures should be established by trial batches prior their uses on the site.

4 RECOMMENDED PROPERTIES OF GROUT

Some of the recommended properties of grouts considered suitable to secure adequate filling of ducts in post-tensioned concrete structures are summarized in Table 2.

Table 2 Recommended properties of grout

Authority	Fluidity	Bleeding	Volume change	Strength
Hope and Ip	12 to 15 s flow time (ASTM C 939 flow cone)	None (ASTM C 940)	Expansion of 6% to 7% (ASTM C 940)	7d: 45 MPa 28d: 60 MPa
Concrete Society TR No 47, 1994, UK	< 25 s after mixing < 25 s after 90 min (flow cone of 10 mm opening)	No bleeding Density variation < 10%	From 0 to 5%	> 27 MPA after 7 days
Canadian Standard, 1994, Canada	< 11 s flow time (standard flow cone with 13 mm opening)	Maximum bleeding of 1%	Maximum expansion of 5%	> 35 MPa after 28 days (4% to 8% of air)
Bastian et al., 1997	22%-23% flow time (Marsh cone with 10-mm opening)	None	Maximum of 2160 x 10^{-6}	
Khayat et al., 1999, Canada	< 61 s flow time (modified Marsh cone with 4.57-mm opening) < 70 s after 60 min	Zero static bleeding Bleeding under pressure < 10%	Maximum expansion of 5%	> 28 MPa after 7 days

5 SUMMARY AND OPINIONS

Considerable attention has been given to improve performance of grout used to protect tendons in ties of the grout, and investigating and developing better test methods for quality control. The perceived issue is that the duct should be completely filled to prevent the ingress and transport of contaminant along the tendon. This may be due to the field experience with post-tensioning systems in which inspection revealed partially grouted or ungrouted zones. It is therefore recognized that the corrosion of tendon in post-tensioned concrete structures can be a results of inadequate filling rather than poor performance of grout. In general, standards and specifications call for the use of well-proven admixtures to impart suitable fresh and hardened properties of grout given the type of application and exposure conditions

Although there is some difference of opinions regarding the suitable properties and the relative importance of these properties, grouts with improved placement characteristics as well as better engineering properties could be designed using admixtures and modifiers that are widely available. The difference of opinions is mainly due to differences in evaluation methods influenced to some extent by local practices. On the other hand, the suitability of these properties relies on the type of application, grouting equipment, and environmental conditions. Hence recommended properties should be regarded as guidance values, and actual properties required should be determined in accordance with the specific application and conditions at hand.

RC BEAM TEST USING T-HEADED BARS UNDER SHEAR, FLEXURE AND COMPRESSION

Toshiyuki Shioya, Yoshihiro Higuchi, and Hideyo Shiokawa
Shimizu Corporation
JAPAN

Masaaki Takagishi
Dai-ichi High Frequency Co., Ltd.
JAPAN

Key words: T-headed bar, shear strength, flexural behavior, compression, cyclic loading

1. INTRODUCTION

Since the Hyogo-ken Nanbu earthquake, earthquake-resistant design regulations have become more strict. In the case of civil structures, the amount of shear reinforcement or inner tie reinforcement of bridges have increased. In the case of high-rise buildings, by using high-strength concrete, column sections have become smaller, while the rebar arrangements of beam-column connections have become overcrowded. To improve the overcrowded rebar arrangement, the T-headed bar construction method, which directly shortens the building work period and reduces the cost, was developed [1]. The header of T-headed bars is processed firstly by heating the end of rebar up to 1300℃ using the high frequency induction method and then processed by pushing the end of the rebar into a holder. For rational construction methods, T-headed bars will become more popular. T-headed bars are effective for complicated rebar arrangements such as wall paneling structures or beam-column joints. In this study, assuming a wall paneling structure, shear tests, flexure tests and compressive tests were conducted using T-headed bars.

2. EXPERIMENTAL PROGRAM

Testing parameters were 180° hook, T-headed bar, no-anchorage, lap joint and axial force, based on actual construction conditions. In the case of shear tests, the tensile reinforcement ratio was 1.1%, and SD490 rebers were used (f_{sy}=490N/mm²). When reinforcing for shear, the shear reinforcement ratio was 0.13% and SD345 rebars were used. When lap joints were used, lap length was 20 ϕ (ϕ : diameter of main tensile reinforcement). In the case of flexure tests, the tensile reinforcement ratio was 0.4%, and SD345 rebars were used. When lap joints were used, lap length was 30 ϕ . When an axial force was applied, axial stress was set at 3.0N/mm² for all tests, and was reduced to 2.4N/mm².

The test models and the results are shown in Table 1. The dimensions and basic configurations are shown in Fig. 1.

The shear and flexure tests were carried out using simply supported models with four-point concentrated loadings.The compressive tests were conducted under uni-axial compression.

Table 1 Varieties of test models and the results

Specimen	Test parameters					Concrete		Test results		
	Failure mode assumed	Configuration of anchorage of rebar	Lap joint	Axial force	Others	Compressive strength f'_c (N/mm²)	Tensile strength f_t (N/mm²)	Maximum load + P_u+ (kN)	Maximum load - P_u- (kN)	Failure mode
No.1	shear	180° hook	×	×		34.7	3.13	971	893	shear
No.2	shear	T-headed	×	×		36.6	2.51	899	909	shear
No.3	shear	none	×	×		34.4	2.80	770	893	shear
No.4	shear	180° hook	○	×		37.2	2.10	851	657	bond spliting
No.5	shear	T-headed	○	×		36.4	2.84	781	661	bond spliting
No.6	shear	T-headed	×	×	position of T-headed bars	36.2	2.77	897	945	shear
No.7	flexure	180° hook	×	×		35.9	2.18	483	448	flexure
No.8	flexure	T-headed	×	×		31.2	1.94	425	499	flexure
No.9	flexure	180° hook	○	×		31.2	1.94	399	385	bond spliting
No.10	flexure	T-headed	○	×		31.0	2.43	422	392	bond spliting
No.11	flexure	180° hook	○	○		29.9	2.35	786	829	bond spliting
No.12	flexure	T-headed	○	○		29.6	2.35	811	866	bond spliting
No.13	flexure	T-headed	○	×	position of T-headed bars	29.6	2.35	399	395	bond spliting
No.14	shear		×	×	without shear reinforcement	30.7	2.30	608	575	shear
No.15	shear	T-headed	×	×	shear reinforcement provided afterward	30.7	2.30	851	661	shear
No.16	compression	180° hook	×			32.2	2.35	2902	*	compression
No.17	compression	T-headed	×			32.2	2.35	2974	*	compression

Main rebar for shear test: D32 , f_{sy}=529N/mm², f_{su}=706N/mm²,main rebar for flexure test: D19, f_{sy}=398N/mm², f_{su}=595N/mm²
Main rebar for compression test: D10, f_{sy}=403N/mm², f_{su}=550N/mm², tie bar: D10, f_{sy}=403N/mm², f_{su}=550N/mm²

3. TEST RESULTS

3.1 Table of test results

The test results are shown in Table 1. The results do not include self-weight.

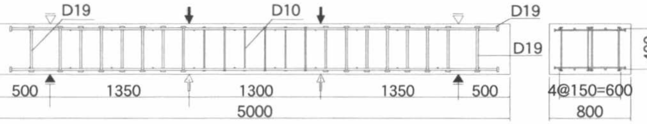

Fig. 1 Dimensions of specimen (No.8 specimen)

3.2 Shear capacity

Figure 2 shows the comparison between the values calculated using the Niwa-Okamura equation[2] and experimental values. The experimental values are almost the same as the calculated values.Therefore, it was concluded that the 180° hook and T-headed bar have the same function for shear reinforcement.

In the case of the specimen with shear reinforcement and lap joints (No.4, No.5), the shear strength is higher than the specimen without shear reinforcement, but is lower than the specimen without lap joints (No.1, No.2, No.6). It has been found that shear strength without shear reinforcement decreases as the number of lap joints increases [3]. The effects of bar cutoff on the shear strength of reinforced concrete beams is considerd to be 10-15%. If this effect is taken into account, the results can be explained. However, there are few cutoff test results, so these effects should be investigated.

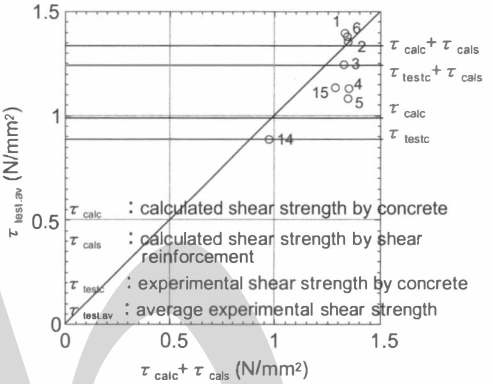

Fig. 2 Comparisons of Niwa-Okamura eq. and experimental values

3.3 Flexural behavior

The load-deflection relationship is very similar between No.7 and No.8 (Fig.3). Consequently, it is concluded that 180° hook and T-headed bar work well as ties of main reinforcement.

3.3 Compressive behavior

In the case of the specimens which failed in compression, the T-headed bar specimen was superior in compressive strength and ductility compared with the 180° hook specimen.

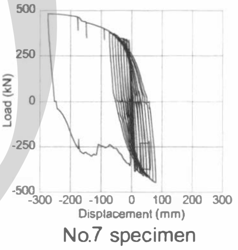

No.7 specimen

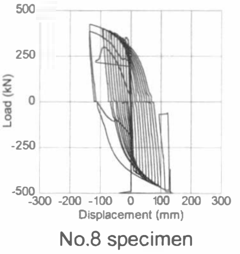

No.8 specimen

Fig. 3 Load-displacement at midspan

4. CONCLUSION

1) From the experimental results of shear tests, the shear capacity of the beam using T-headed stirrup bars was almost the same as that using 180° hook stirrup rebars.
2) From the experimental results of flexure tests, the binding capacity of T-headed tie bars was almost the same as that using 180° hook tie rebars.
3) From the experimental results of compressive tests, the binding capacity of T-headed tie bars was almost the same as that using 180° hook tie rebars.

In conclusion, T-headed bars are useful in a variety of ways.

REFERENCES

[1] Shioya, T., Nakazawa, H., Nagasawa, Y. and Takagishi, M.: Development of T-Headed bars, Proc. of JCI, Vol.22, No.3, pp.1291-1296, 2000.6 (in Japanese)

[2] Niwa, J., Yamada, K., Yokozawa, K. and Okamura, H.: Revaluation of the Equation for Shear Strength of Reinforced Concrete Beams without Web Reinforcement, Proc. of JSCE, No.372/V-5, pp.167-176, 1986.8 (in Japanese)

[3] Ozaka, Y., Suzuki, M., Terasawa, M. and Kobayashi, S.: Effect of Bar Cutoff on Shear Strength of Reinforced Concrete Beams, Proc. of JSCE, No.366/V-4, pp.133-142, 1986.2 (in Japanese)

DEVELOPMENT OF THE ENVIRONMENT-FRIENDLY HYBRID PERMEABLE CONCRETE PAVEMENT

Tetsuo KOBAYASHI
SUMITOMO OSAKA CEMENT CO.,LTD
JAPAN

Mamoru KAGATA Takayoshi KODAMA
KAJIMA ROAD CO.,LTD
JAPAN

Masaaki ITO
OZAWA CONCRETE INDUSTRY CO.,LTD
JAPAN

Keywords: Permeable pavement, Porous concrete, Noise reduction, Industrial by-product

1. INTRODUCTION

The hybrid permeable concrete pavement that is the topic of this report is constructed by integrating types of concrete with differing bending strengths and coefficients of water permeability by the Wet-On-Wet technique.

In other words, it is a highly durable compound concrete slab made by combining a surface course of permeable concrete that provides superior permeability with a binder course of permeable concrete with designated bending strength. The sub-base course is a rain permeable high strength mixture stabilized by cement. On account of its stiffness, it bears the concrete slab at the same time as it restricts the heat island phenomenon by working rain to permeate into the subgrade level and causing the evaporation of moisture.

The study included a trial use of fly ash and blast furnace slag fine aggregate as materials for the surface course and binder course concrete.

It also studied the effect of their replacement rates on various physical properties including the bending strength, permeability, and the aggregate scattering resistance on the surface of the pavement.

After the optimum mix proportion was determined, a trial execution was performed to evaluate its workability, physical properties, serviceability, protection of the roadside environment, and other items.

2. PAVEMENT STRUCTURE

Figure 1 shows the cross section of the pavement made by the trial execution.

The surface course was porous concrete with a coefficient of water permeability equal to that of drainage asphalt pavement.

The binder course was porous concrete with bending strength identical to that of ordinary paving use concrete.

These were laid one on top of the other by the Wet-On-Wet technique, and integrated as hybrid permeable concrete.

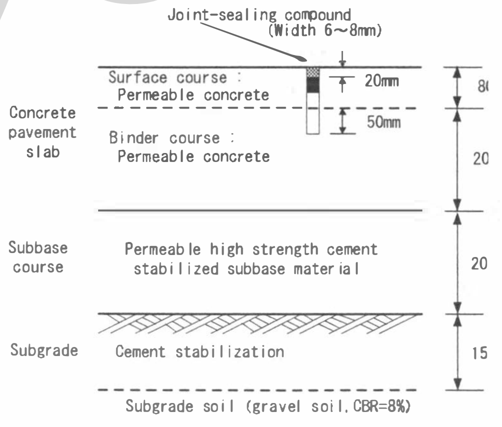

Fig. 1 Section of pavement

3. MIX PROPORTION DESIGN OF THE SURFACE COURSE CONCRETE

3.1 Target physical values

The target weight loss ratio based on the Cantabro test that is an index of aggregate scattering resistance was set at 15% or less by laboratory testing. The design bond strength (target of 4.0 N/mm^2 or more) was controlled by 7 days in order to use on traffic lanes early. The target consistency of the fresh concrete was set to achieve a compaction rate at 5 seconds of vibration during modified VC testing of 100±10%, on the premise that the concrete would be placed by a high compaction type finisher.

.3.2 Materials and mix proportion

Table 1 Mix proportion of surface course permeable concrete

Design Void (%)	FA/B (vol%)	W/B (%)	Unit weight(kg/m^3)					SP (B×%)
			B		W	S	G	
			HC	FA				
15	20	25	303	62	91	147	1531	1.0

HC:High early portland cement, FA:Fly ash,S:Blast furnace slag fine aggregate.

G:Crushed stone Gmax13mm, SP:Superplasticizer

4. TRIAL EXECUTION

4.1 Physical properties evaluation

Table 2 shows the results of bending strength and permeability testing of specimens taken at the trial execution site.

Table 2 The results of testing of specimens taken at the trial execution site.

	Item	Target value	Result
Binder course	Bending strength	5.2N/mm^{2}or more	6.13
	Coefficient of permeability	1.0×10^{-3}cm/sec or more	5.8×10^{-3}
Surface course	Cantabro test value	20% or less	18
	Bending strength	4.0N/mm^{2}or more	4.96
	Coefficient of permeability	1.0×10^{-2}cm/sec or more	2.8×10^{-2}
Monolithic specimen	Bond strength	1.0N/mm^{2}or more	2.62
	Bending strength	4.5N/mm^{2}or more	5.92

4.2 Conservation of the surrounding environment

(1) Restricting the heat island phenomenon

Figure 2 shows the results of measurements of the temperature on a single specified day. Compared with dense grade asphalt, the maximum temperature of the permeable concrete paving is lower and it warms and cools less easily.

(2) Noise reduction effects

A tire dropping test method developed by Kajima Road Co., Ltd. was performed to measure its noise reduction effects. The results of the frequency analysis shown in Figure 3 confirmed that the frequency 1 to 2 kHz sound pressure level that people are said to find unpleasant of the permeable concrete paving is lower than that of dense grade asphalt, confirming the noise reduction effects of this material

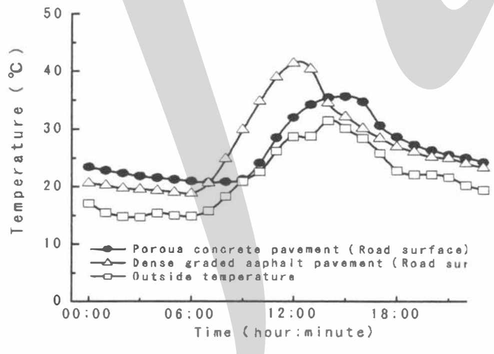

Fig.2 Result of road temperature

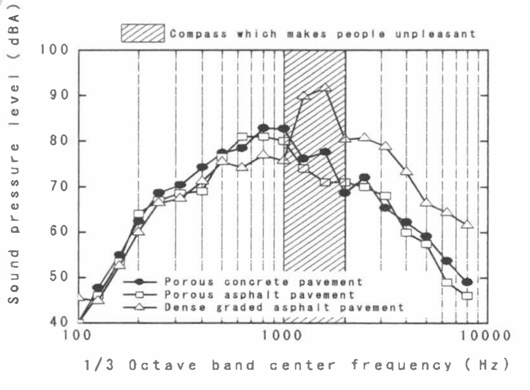

Fig.3 Result of frequency analysis

5. CONCLUSION

The results of the trial execution of hybrid permeable concrete pavement show that this pavement satisfied initial target values concerning its basic physical properties, driving safety, and conservation of the surrounding environment. A follow-up survey is now in progress. Plans call for its use to be expanded to include parking lots and toll gates on highways.

VERIFICATION OF SHRINKAGE AND CREEP IN CONCRETE CONTAINING GROUND GRANULATED BLAST-FURNACE SLAG BY EFFECTIVE PRESTRESS ON PC GIRDER

Hiroaki Tsuruta Hiromichi Matsushita
Kyushu University, JAPAN

Mamoru Esaki
Abe Kogyosho Co.,Ltd.
JAPAN

Yoshitaka Maeda
Nippon Steel Blast-Furnace Slag
Cement Co.,Ltd., JAPAN

Keywords: ground granulated blast- furnace slag, PC girder, effective prestress, shrinkage, creep

1 INTRODUCTION

The effectiveness of the use of ground granulated blast-furnace slag in order to ensure high durability of prestressed concrete structures has been ascertained on a laboratory test level[1]. However, there are few examples of investigation of the drying shrinkage and creep properties in actual-scale pretension-type PC structures that used ground granulated blast-furnace slag and required steam curing. Therefore, with the test specimens of the same pretension-type PC girders as those used in actual bridges, drying shrinkage and creep were measured for about a year in a case that the conventional high-early-strength portland cement only is used and in a case that ground granulated blast-furnace slag is used. After that, in order to confirm the ultimate strength and transformation behavior of girder, a static bending fracture test was carried out.

In this study, on the basis of results of a static bending fracture test conducted using these test specimens, an amount of effective prestress was verified and a relationship between load and displacement was compared and examined.

2 OUTLINE OF EXPERIMENT

2.1 Materials and mixture proportions

The materials used in this experiment are high-early-strength portland cement (density: 3.14 g/cm^3), ground granulated blast-furnace slag (density: 2.91 g/cm^3, specific surface area: 6100 cm^2/g) as an admixture, river sand from Saga prefecture (density: 2.55 g/cm^3, fineness modulus: 2.87) as a fine aggregate, crushed stone from Kumamoto prefecture (maximum size20mm, density: 3.00 g/cm^3, fineness modulus: 2.87) as a coarse aggregate, and polycarboxylic acid type superplasticizer (SP) as a chemical admixture.

Table 1 shows the mixture proportions of concrete. In the table, BFS in 'Name" indicates the case that ground granulated blast-furnace slag is used and HPC indicates the conventional case that an admixture is not used. The reason why the water/binder ratio is different is that the mixture proportions for BFS was determined so that the compressive strength of con crete, 34.3 N/mm^2, which is necessary for the introduction of a prestress of PC girders, is satisfied, and the slag replacement ratio was determined in consideration of resistance for damage by salt attack and material cost.

Table 1 Mixture proportions of concrete

Name	slag ratio (%)	W/B (%)	s/a (%)	Unit weight (kg/m^3)						Target Air(%)	Target slump(cm)
				W	C	GBFS	S	G	SP		
BFS	50	35	43	160	229	228	732	1143	2.29	2±1	10±2.5
HPC	0	40	43	160	400	-	768	1173	3.2	2±1	10±2.5

2.3 Test specimens and static bending fracture test

Test specimens were actual-scale pretension-type PC girders, which length was about 15m. Embedded strain gauges (gauge length;100mm) in sections having styrene foam at the center were embedded and axial strain were measured. Furthermore, the concrete temperature in the same places was measured using thermocouples. Girder specimens, prisms specimens and cylindrical specimens were all steam cured. Demolding was carried out in 19 hours after placing, and the specimens after demolding were stored in such a manner that they were exposed to rain.

The bending test was conducted by two-point loading with a support to support distance of 14,316 mm and an equal-moment span of 1,500 mm.

3 EXPERIMENT RESULTS AND CONSIDERATIONS

Fig.1 shows load-displacement in central part curve in bending test. In both cases of BFS and HPC, relationships between load and displacement in central part are very similar.

Then, we shall focus on the amount of effective prestress. In this paper, it was calculated by the following two methods.

a) Calculation using design values of drying shrinkage, etc.
b) Calculation using experimental values of drying shrinkage, etc.

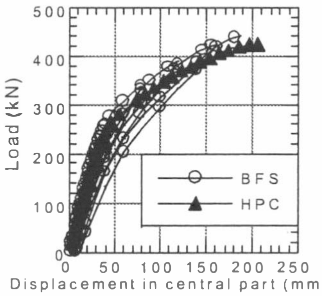

Fig.1 Load-displacement curve

The effective tensile stress(σ_{pe}) of prestressing steel for the bending test was calculated using the following equation given in the Specifications for Highway Bridges, by which a decreased amount by the relaxation($\Delta \sigma_{p\gamma}$) of prestressing steel and a decreased amount($\Delta \sigma_{p\phi}$) by creep and drying shrinkage were deducted from a tensile stress(σ_{pt}) of a prestressing steel immediately after introduction of prestress:

$$\sigma_{pe} = \sigma_{pt} - \Delta \sigma_{p\gamma} - \Delta \sigma_{p\phi}$$

Next, the amount of effective prestress is found from results of the static bending fracture test by the following two methods and compared with the amount of effective prestress found by calculation.

c) Calculation from the load under which crack was formed
d) Calculation from the load under which crack occurred again in repeated loading

When a crack was formed by loading, the concrete stress of a girder became bending stress (assumed to be 1.8 times the tensile strength) at the lower edge. Because the stress distribution by applied loads and the stress distribution by deadweight are known, the lower-edge stress of effective prestress can be calculated from these. Furthermore, the lower-edge stress is 0 when crack occurs again, the amount of effective prestress is found similarly.

As a result, the tensile stress of prestressing steel was calcurated as shown in Table 2. A decreased amount of tensile stress of prestressing steel by the elastic deformation of concrete was found by using the apparent Young's modulus in the lower part of a girder. Furthermore, the creep coefficient of the lower part of a girder and drying shrinkage strain of the middle part of a girder were used.

From Table 2 it is apparent that the effective tensile stress of prestressing steel in case of HPC during the static bending fracture test is equivalent to a value (878N/mm^2) calculated by the present design method, and that of BFS is larger than it. Furthermore, when a comparison was made between a girder in the case of BFS and a conventional girder in the case of HPC, it was found that the effective tensile stress in the case of BFS during the static bending fracture test is larger than that of HPC. This is because the strain by drying shrinkage and creep in case of BFS are smaller than that of HPC.

Table 2 Effective tens ile stress of prestressing steel

Time	Calculation methods	Effective tensile stress(N/mm^2)	
		BFS	HPC
Just after prestressing	a	1168	
	b	1162	1145
In bending test	a	878	
	b	1035	991
	c	1003	802
	d	1007	873

4. CONCLUSIONS

Judging from the above, it is said that there are no bad influences due to mix ground granulated blast-furnace slag to concrete on the ultimate strength, the transformation behavior of girder, effective prestress of prestressing steel. Therefore, from the point of dynamical view, it is said that pretension-type PC girder used ground granulated blast-furnace slag has similar performance to conventional PC girder used high-early-strength portland cement.

REFERENCES

[1] Development Examination Committee of Highly Durable PC Structures: Development of Highly Durable Prestressed Concrete Structures Using Ground Granulated Blast-Furnace Slag, The Society of Materials Science, Japan, 1998.3.

PROPERTIES OF SHRINKAGE AND CREEP IN CONCRETE CONTAINING GROUND GRANULATED BLAST-FURNACE SLAG, USED FOR A PRETENSION PC GIRDER

Yoshitaka Maeda
Nippon Steel Blast-furnace Slag Cement co.,ltd, JAPAN

Hiromichi Matsushita Hiroaki Tsuruta
Kyushu University
JAPAN

Yasukazu YOSHITOMI
Abe Kogyosho co.,ltd,
JAPAN

Keywords: Ground granulated blast-furnace slag, PC girder, drying shrinkage, creep

1. INTRODUCTION

It has been confirmed, in laboratory-scale tests, that ground granulated blast-furnace slag (GGBFS) is an effective admixture in order to improve durability of prestressed concrete (PC) structures [1]. However, there have been very few cases in which drying shrinkage and creep properties have been investigated of on an actual structure PC structures using BFS.

In this study, pretensioning type PC girders of the same size as those used for actual bridges were manufactured at a shop, and their drying shrinkage and creep in two different cases were measured for about one year. In one case, conventional high-early-strength portland cement (HPC) was used, and in the other case, BFS(density 2.91, specific surface area 6,100 cm^2/g) was used as the admixture. The drying shrinkage and creep of rectangular prism specimens, manufactured using the same materials as the above, were also measured, and compared to that of girders.

2. EXPERIMENTAL METHOD

Table 1 shows the Mixture Proportion. In the table, No.1 is a concrete using GGBFS (hereinafter referred to as GGBFS) and No.2 is the conventional mixture not using GGBFS (hereinafter referred to as HPC). In this experiment, river sand (density 2.55 g/cm^3,) for the fine aggregate, crushed stone (2005, density 3.00 g/cm^3,) for the coarse aggregate and superplasticizer (SP) for the chemical agent were used.

Fig.1 shows the types and sizes of the girders. To measure the strain of each girder, a strain gauge was embedded. Also the temperature at the same position was measured with a thermocouple. The size of the prism specimens was set at 10 x 10 x 40 cm.

The concrete for test girders and those for specimens were cast

Table 1 Mixture Proportion

Mix No.	GGBFS/B (%)	W/B (%)	s/a (%)	Unit weight (kg/m^3) W	HPC	GGBFS	SP	air (%)	slump (cm)
1	50	35	43	160	229	228	2.29	1.9	8.6
2	0	40	43	160	400	—	3.20	2.2	8.3

B:Binder (H+BFS)

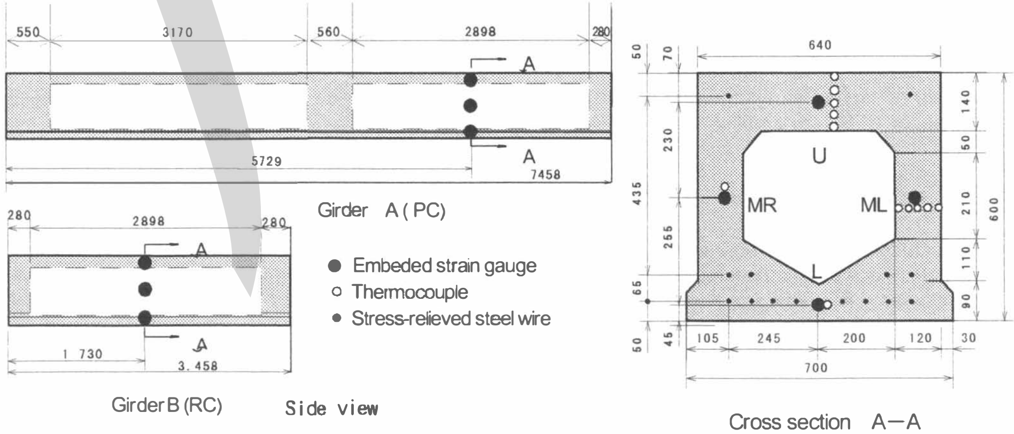

Fig.1 Test Girder

into molds and simultaneously steam-cured. 18 hours after the casting, they were demolded. After that, the test girders were left outdoors, and the prism specimens were tested both outdoors and indoors (20°C--RH 60%).

3. EXPERIMENTAL RESULTS AND CONSIDERATIONS

3.1 Drying shrinkage

Fig.2 shows drying shrinkage of Girder B, and Fig.3 shows drying shrinkage of prism specimens.

In the case of the test girders, the difference of strain between the GGBFS and HPC was small, and the strain of the GGBFS girder showed a tendency to become somewhat smaller in the long term.

The shrinkage of the specimens was larger for the GGBFS admixed specimens than for the HPC in the early stage of drying when tested under 20℃--60RH%, but it was smaller for the GGBFS when tested outdoors.

The specimens tested under the atmospheric condition of 20℃ --RH 60% showed strain values of over 600 $\times 10^{-6}$, but the shrinkage strain of the test girders and specimens exposed outdoors was found to be smaller than the design value 200 x 10^{-6} of dry shrinkage strain used for designing PC girders regardless of the presence of slag.

3.2 Creep

Fig. 4 shows creep strain of the lower part of girders A. Fig. 5 shows creep strain of the specimens.

The use of slag decreased the creep of the test girders. While creep of the GGBFS specimens was bigger than HPC under 20℃ --60RH%, the inequality was reversed with respect to outdoors.

The compressive stress working on the lower part of the test girders was nearly equal to that working on the specimens, but the creep was smaller for the test girders.

Table 2 shows the values of creep coefficient calculated using the strain of test girder A.. Although the values were different at different parts of the girder, all the values were found to be smaller than the design value 3.0 used for designing PC girders.

Table 2 Creep Coefficient of the test girders

Mixture	upper	middle	lower
GGBFS	1.42	0.90	0.70
HPC	1.66	1.19	1.07

4. CONCLUSION

Regarding the influence of ground granulated blast-furnace slag on the drying shrinkage and creep of prestressed concrete, the use of ground granulated blast-furnace slag increased the drying shrinkage of the specimens in the room at 20℃-RH 60%, did not change the drying shrinkage of the girders of the same size as PC girder used in actual bridges and decreased the creep of the test girders, and the values of dry shrinkage and the creep coefficient of PC girders were found to be smaller than the design values.

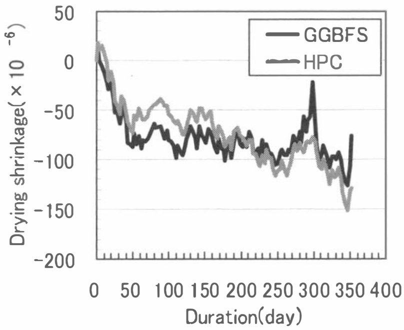

Fig.2 Drying shrinkage of Girders

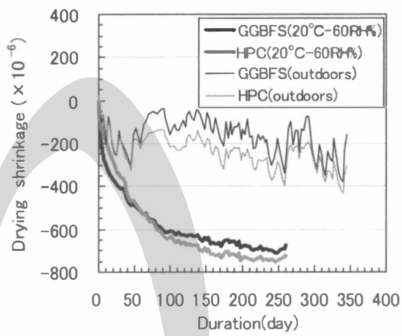

Fig.3 Drying shrinkage of prisms

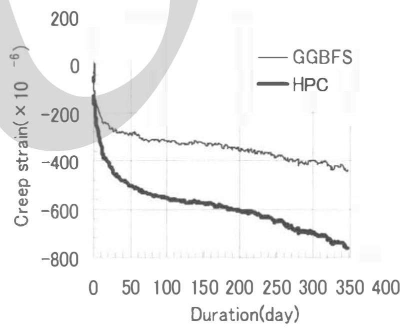

Fig.4 Creep strain of the test girders

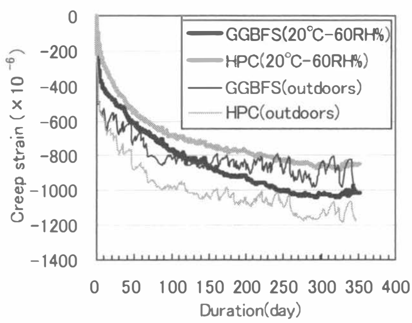

Fig.5 Creep strain of prisms

EVALUATION OF STRUCTURAL PERFORMANCE OF ULTRA HIGH PERFORMANCE CONCRETE

Tetsushi Uzawa, Weijian Zhao, Toshihiko Tsuka, Koichi Kano, Yoshihiro Tanaka, Taisei Corp., JAPAN
Shinpei Maehori, Taiheiyo Cement Corp., JAPAN

keywords: reactive powder concrete, fiber reinforced concrete, high-strength, ductiliy

1 INTRODUCTION

In recent years, many new high-rise reinforced concrete buildings have employed high-strength concrete with compressive strength as high as 100 N/mm². Increasing expectation of high-performance concrete as well as high-strength, a new generation concrete: reactive powder concrete (RPC) has been developed. Moreover an improved RPC (Ductal®) which has succeeded in balancing ultra high-strength and ductility by supplementing fibers was proposed by Orange et al [1] . The mechanical properties of Ductal, such as compressive strength, bending strength and fracture energy, are out of range compared with the ordinary reinforced concrete. Applying Ductal to long span bridges or high-rise buildings; it is possible to develop the new design approach that cannot be considered before.

This paper focuses on the evaluation of the structural performances of Ductal beams that may be a fundamental design and construction technology. The structural performances such as flexural strength, share strength, ductility and crack pattern have been investigated from the behavior of dozens of Ductal beams subjected to flexion and shear loading.

2 OUTLINE OF EXPERIMENTS

B series specimens have been tested to evaluate flexural performance of Ductal beams without longitudinal reinforcement. The beams of the B series change shear-spans in the same cross section. The cross section is 200 mm in height and 150 mm in width. R series tests have been conducted to study the shear performance of Ductal beams with longitudinal reinforcements. The specimens are I shaped beams with a narrow web of 40 mm in width. The outer dimensions of the cross section are 400 mm in height and 150 mm in width. The specimens of R1 and R2 are the same dimensions of the beams, however R2 has been produced without the supplementing steel fibers unlike R1 in order to evaluate the contribution of the steel fibers to the shear performance of Ductal beam.

Ductal is made of two components: the premixed cementitious matrix and steel fibers. The premixed cementitious matrix is composed of a cement mixed with ground siliceous material and quartz sand. Thanks to the use of superplasticizers, water to binder ratio of 0.08 is employed. The steel fibers, which are 0.2 mm in diameter and 15 mm in length, are added at the end of mixing process in a concrete mixer. The fiber content is kept at 2 % by volume. Tow specimens, B1 and B2, have been poured from both sides of formwork and the matrix flowed together at the center of the specimens. Other specimens have been poured from one side of the formwork continuously. Heat treatment of which temperature is 90 degrees has been carried out during 48 hours following normal temperature treatment of 48 hours.

The beams have been stressed by bending at 4 points. The specimens have been loaded to failure.

3 EXPERIMENT RESULTS

Figure 1 shows the relationship between the flexural stress at the bottom of the cross section and the vertical displacement at the mid-span. These deflection behaviors can be distinguishable in two types. The results of the B3 and B4 have shown significant flexural strength and structural ductility. The linear elastic behavior of these specimens has been observed until first cracks have appeared at a flexural stress of about 20 N/mm². After the linear elastic stage, nonlinear behavior has been observed and ultimate flexural stress has reached between 28 and 35 N/mm² with significant ductility. On the other hand, in the case of B1 and B2, the ultimate state has been observed at a flexural stress of about 16 N/mm² right after first cracks have appeared without sufficiently ductile behavior. The ultimate flexural stress of these specimens has been only half of the expected value of the flexural strength.

The difference of above two behaviors can be explained by crack patterns on the specimens. Figure 2 shows the crack pattern observed on the B2 and B4 as representative examples of the two behaviors, respectively. In the case of B1 and B2, a few cracks have appeared and spread nearby mid-span of the beam, whereas, in other cases, many fine cracks have appeared along the beam up to the ultimate state and one of the cracks has spread with degreasing the flexural stress. It is quite likely that the placing method of B1 and B2 has created defects in the beams where the matrix flowed together.

Figure 3 shows load-deflection curves of the R1 and R2 beams. In the case of R1 specimen, first flexural cracks have appeared on the lower flange at a load of 65 KN and diagonal cracks also have began to spread on the web at a load of 210 KN. Many fine cracks have appeared on the lower flange and web up to the ultimate carrying capacity of 525 KN. Propagation of two major diagonal cracks has led to decline of the carrying load with ductile behavior. Eventually, the upper flange of shear span has collapsed due to buckling as shown in Fig 4. On the other hand, in the case of R2 specimen, the stiffness after appearance of flexural cracks has been clearly low and the number of cracks has been very few compared with those of R1. The specimen has been broken into some pieces (see. Fig. 4) with brittle behavior as soon as diagonal cracks have been observed at a load of 324 KN. The calculated shear strength of the R1 and R2 are 25 N/mm² and 15 N/mm² respectively. These results clearly show that the steel fibers significantly improve the shear performance of Ductal beam instead of stirrups.

4 CONCLUSION

The paper addresses the structural performance of the ultra high performance concrete (Ductal) beams subjected to flexion and shear loading. The experimental work on the different structural beams has led to a number of results as follows.

1) Ductal beam without longitudinal reinforcements shows the nonlinear behavior with significant ductility, multiple cracks and increase of flexural strength. The first cracking strength is approximately 20 N/mm², and the ultimate flexural strength reaches approximately between 30 and 35 N/mm².
2) In the case of Ductal beam with longitudinal reinforcements, despite the absence of stirrups, no brittle behavior has been observed after many diagonal cracks have spread. The shear strength of the tested beam of which shear span to height ratio (a/h) is 2.0 has been estimated at 25 N/mm².
3) The placing technique is very important issue to keep the high performance of Ductal structures. In order not to create fiber orientation defects, it is necessary to take the continuity of flow and the uniformity of fibers into account.

REFERENCE

[1] Orange, G., Acker. P., and Vernet, C. : A new generation of UHP concrete : DUCTAL damage registance and micromechanical analysis, 3rd International Workshop on High Performance Fiber Reinforced Cement Composite, RILEM, pp. 102-112, 1999.

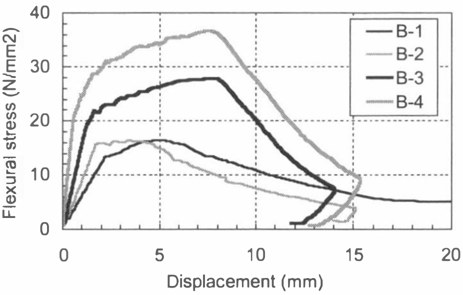

Fig. 1 Stress-displacement curves of B series

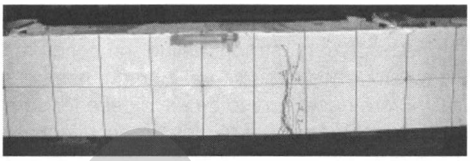

(a) B2

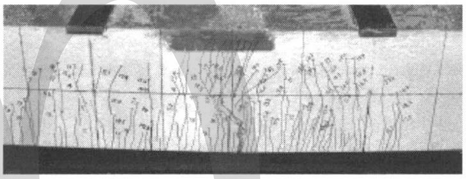

(b) B4

Fig. 2 Crack petterns between load points

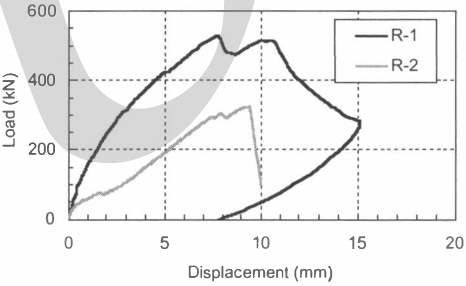

Fig. 3 Load-displacement curves of R1 and R2

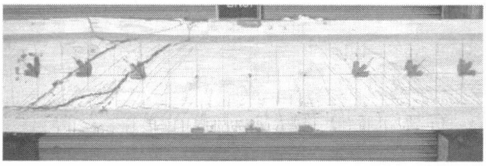

(a) R1

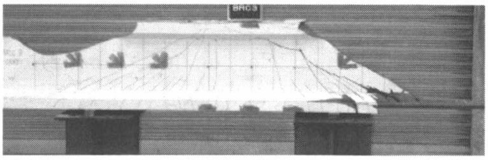

(b) R2

Fig. 4 Crack petterns of R1 and R2 specimen

STRENGTHENING PRESTRESSED-CONCRETE GIRDERS WITH EXTERNALLY PRESTRESSED PBO FIBER SHEETS

K.Hayashi※1, Z.S. Wu※2, K.Iwashita※2, T.Higuchi※3, S.Murakami※4
※1:ABE KOGYO SYO Co.,Ltd.,Japan
※2:Department of Urban & Civil Engineering, Ibaraki University,Japan
※3:TOHO EARTHTECH, Inc.,Japan
※4:Nippon Steel Composite Co.,Ltd.,Japan

Keywords External Prestressing, PBO fiber sheets (PFS), PC girder, Composite behavior, Crack-resistance

1 INTRODUCTION

In recent years, strengthening the concrete structures with externally epoxy-bonded FRP sheets to the tension face of structural element has been accepted for practical uses, and more functional uses of FRP are necessary to be developed for seismic reinforcing or upgrading of the structural capacity in further improvement of reinforcement effects and assurance of structural ductility.

During past several decades, prestressing technique has been advanced successively and applied widely for reinforcing large-scale civil and building structures. Based on the concept of prestressing technique,the authors have proposed a prestressing system for PBO(short for Polypara-phenylene-Benzo-bis-Oxazole) fiber sheets (PFS) which is first designed to be suitable for strengthening existing concrete structures, and investigated the reinforcement effects of prestressed PFS on PC beams.

This paper is mainly focused on investigating the effectiveness and efficiency of the developed prestressing method for PC beams with externally prestressed PFS. An experimental program is carried out to confirm the reinforcement effects on load-carrying capacity, stiffness characteristics, ductility, and resistance of crack opening of PC beams with the design variables including prestress level, reinforcement ratio, and impregnation of PFS before bonding to PC beams.

2 EXPERIMENTAL PROGRAM AND EXPERIMENTAL RESULTS

2.1 Test variables

In order to investigate the strengthening effects and composite behavior for large scale of PC structures with prestressed PFS, girder specimens with 10m span and 1m high as shown in **Figure 1** are designed. The material properties are listed in **Table 1**. In this study, the following test variables are considered to investigate the reinforcement effects:

1) Prestress levels 33% and 45% of f_{ts}※ (※ f_{ts} =3500N/mm^2, assumed effective strength of PFS)
2) PFS layers (3 and 4 layers)
3) Impregnation of PFS with epoxy after or before bonding to specimen surface

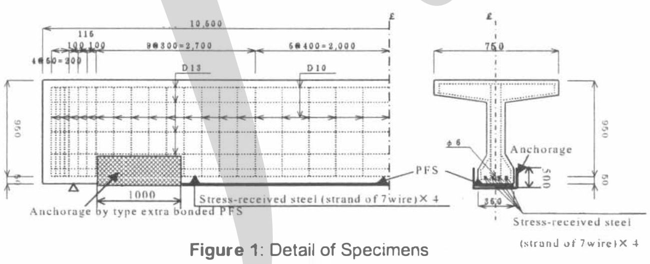

Figure 1: Detail of Specimens

Table 1: Summary of material properties

Concrete	Modulus of elasticity (GPa)	33.9
	Compressive strength (MPa	58.0
	Poisson's ratio	1.5
Stress-relieved steel SD295A	Modulus of elasticity (GPa)	200
	Tensile strength (GPa)	1.86
	Yielding strength (GPa)	1.57
	Introduced prestress (GPa)	1.10
PFS	Modulus of elasticity (GPa)	240
	Tensile strength (GPa)	4.0
	Limit of tensile strain (μ)	16700
	Thickness (mm)	0.128
	Unit weight (g/m^2)	200
Epoxy	Modulus of elasticity (GPa)	3.43
	Poisson's ratio	0.35

2.2 Strengthening effect on flexural behavior

The load versus displacement at mid-span of specimen with bonded PFS of three layers is shown in **Figure 2**, in which the result of normal PC beam (control specimen) is also shown in order to make a comparison. The control PC specimen without PFS strengthening fails due to the yielding of steel cables and concrete crushing. As for PFS-strengthened PC beam without PFS prestressing, the debonding initiates from the ends of a flexural crack almost at the mid-span and rapidly propagates to the end of PFS. For the prestressed PFS(33% prestress of assumed effective strength of

PFS)-strengthened PC beam, the initiation of debonding starts, also, from the end of flexural crack. Both strengthened beams occurs slightly load degradation due to the debonding propagation from the mid-span to the end of specimens and then maintains a constant loading level due to the effect of anchorage by U type extra bonded PFS until the final failure of the anchorage. The another prestressed PFS(45% prestress of assumed effective strength of PFS)-strengthened PC beam shows a PFS rupture failure mode. There are also great increases in cracking load of prestressed PFS-strengthened beams due to prestressing while the cracking load of the PFS-strengthened beam is same as the one of control beam without PFS strengthening.

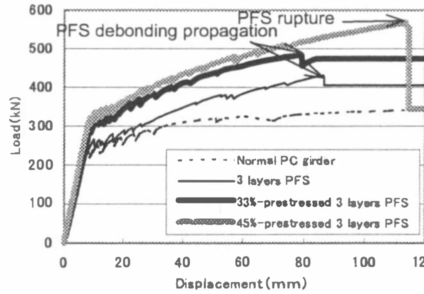

Figure2: Result of Load Versus Displacement Relationship

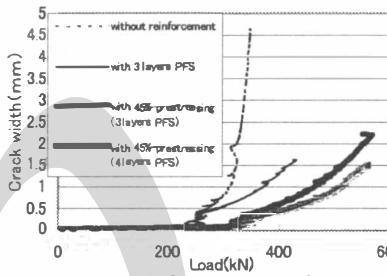

Figure3: Crack width in Different Specimens

2.3 Strengthening effect on cracking behavior

The crack width varying with the loading stage for four beams is shown in **Figure 3**. It is found that the crack dispersion can be improved by the prestressing of PFS. A great effect on crack resistance is observed in the case of the prestressed PFS-strengthened beams and it increases with the increase of the introduced prestressing force.

2.4 Bonding behavior due to impregnation process of prestressed PFS

Figure 4 shows the experimental results of load versus displacement relationship for two 33% prestressed PFS-strengthened beams with resin impregnation procedure before and after the prestressing procedure of PFS. The initiation of PFS debonding is delayed for the case of resin impregnation after the prestressing procedure of PFS comparing the case of resin impregnation before the prestressing procedure of PFS.

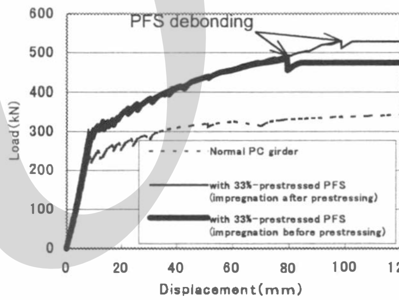

Figure 4: Bonding Capacity due to Impregnation Process of PFS

2.5 Strengthening effects due to the record of pre-loading before the bonding of prestressed PFS

Figure 5 shows the experimental results of load versus displacement relationship for two 45% prestressed PFS-strengthened girders with and without the record of pre-loading the bonding of prestressed PFS. The strengthening effects for the two girders are nearly same on load-carrying capacity, stiffness characteristics, and ductility. This result implies that the record of existing cracks for a PC girders have no influence on their structural performances and strengthening effects.

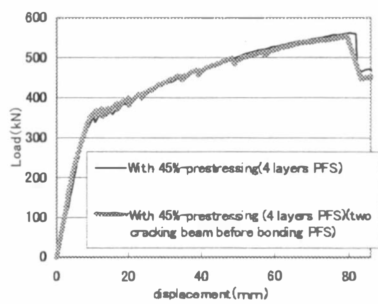

Figure 5: Comparison on Load versus Displacement Relationship of Specimens with and without pre-loading record before bonding prestressed PFS

3 CONCLUSIONS

1) Through pretension of PFS, significant improvements can be achieved in flexural strength, stiffness and crack resistance of the structure. The load levels of crack occurrence, compressive crushing of concrete and debonding from the ends of flexural concrete crack have a great increase.
2) Some considerations are suggested on determination of appropriate prestress level of PFS and structural optimization of reinforcement.
3) It is found that bonding capacity without impregnation process is higher than that with the process.
4) Strengthening effects for a PC girder with the record of cracks duets pre-loading before the bonding of prestressed PFS are nearly same as same type of intact structure.

EXPERIMENTAL BEHAVIOUR OF DEFICIENT RECTANGULAR COLUMNS WITH EXTERNALLY BONDED FRPs

Stathis Bousias Thanasis Triantafillou Michael Fardis Loukas Spathis Bill Oregan
Structures Laboratory, Dept. of Civil Engineering, University of Patras, GREECE

Keywords: concrete columns, deformation capacity, fibre reinforced polymers, retrofit, seismic upgrading

Non-seismically designed and detailed RC structures have been proven repetitively around the world as particularly vulnerable to strong earthquakes. Due to the significant cost of rehabilitation of such structures, retrofitting measures are taken striving to enhance their structural performance (ductility, strength, stiffness, or a combination of them). In improving one of member deficiencies, that of lack of ductility, conventional and more modern techniques (employing composite materials) have been applied, both basing their effectiveness in improving concrete deformability through confinement. The latter class of retrofitting techniques is less studied than the former, but its application is rapidly spreading worldwide. The experimental validation of the contribution of FRP fabric wraps in enhancing the ductility of RC members, has mainly focused on those with circular or at most square cross-section. For the far more common class of elements with rectangular cross-section, experimental results are lacking, especially when the obvious importance of section aspect ratio is considered.

In this paper the effectiveness of jacketing ductility-deficient columns with FRP fabric wraps as a means of enhancing their deformation capacity is experimentally investigated. The tests presented concern non-seismically detailed reinforced concrete columns subjected to cyclic uniaxial flexure and constant axial load. The level of the latter was relatively high to investigate its effect and the vertical-loading capacity of the column after the serious damage due to cycling of lateral loads.

Ten cantilever-type specimens emulating old construction, as far as materials used and lack of earthquake resistant detailing, were tested. The column net height was 1.6m and its rectangular cross-section was 250×500mm (Figure 1). Longitudinal reinforcement comprised four 18-mm bars with 559.5 MPa yield stress, 682 MPa tensile strength and uniform elongation at failure of 13%; transverse reinforcement was provided by 8-mm diameter smooth bars at 200-mm centres with 135°-hook at one end and a 90° hook at the other (286 MPa yield stress, 350 MPa tensile strength and 13% uniform elongation at failure). Low concrete strength f_c was chosen. Table 1 summarises the material characteristics. The basic parameters of the retrofitting scheme studied were: (a) the number of layers of the wrap material and the fibre material (carbon vs. glass), (c) the effect of previous, unrepaired damage, (d) the level of FRP-induced confinement in columns with cross-sectional aspect ratio other than 1.0, and (e) the effect of FRP wrapping in columns dominated by flexure or shear.

Table 1 Specimens and summary of test results

Specimen	Concrete strength f_c (MPa)	FRP for retrofitting		Normalised axial load ?=N/$A_c f_c$	Peak force (kN)	Drift at failure (%)
		Material	Layers			
S_0	18.3	-	-	0.38	190	2.5
S_C2*in*	16.7	Carbon	2	0.40	219	3.8
S_C2	18.1	Carbon	2	0.37	228	5.6
S_C5	17.9	Carbon	5	0.39	237	6.9(*)
S_G5	18.7	Glass	5	0.37	207	6.2
W_0	17.9	-	-	0.38	72	4.1
W_C2*in*	18.1	Carbon	2	0.37	67	6.6
W_C2	18.1	Carbon	2	0.37	73	7.8
W_C5	17.9	Carbon	5	0.39	75	7.5
W_G5	18.7	Glass	5	0.37	75	9.0

(*) test stopped without failure
(*) Specimen nomenclature: S (strong), W (weak), C (carbon), G (glass), *in* (initial damage)

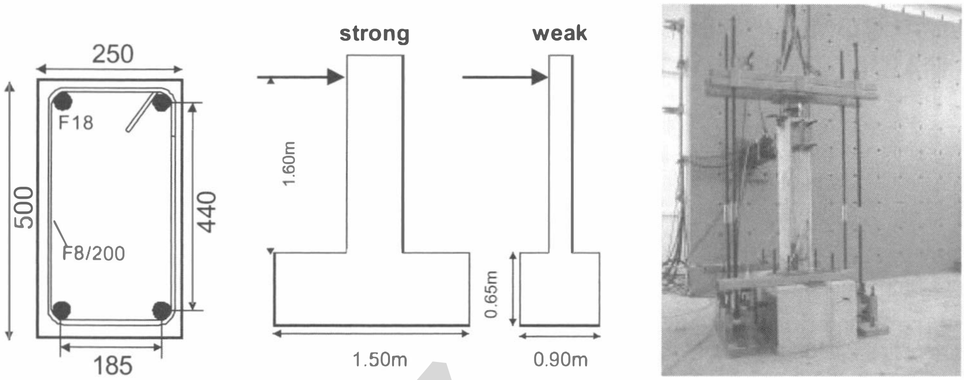

Figure 1: Specimen geometry and test set-up

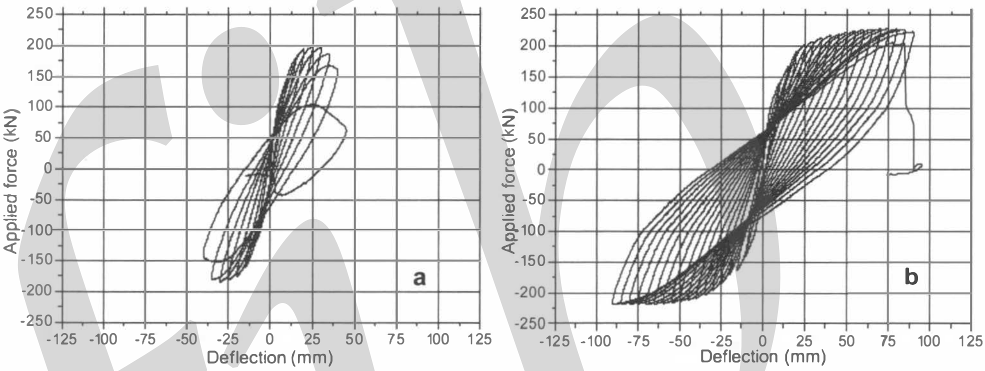

Figure 2: Force-deflection loops for specimens (a) S_0 and (b) S_C2

The following conclusions for columns in buildings constructed before application of modern seismic design are deduced from the experimental results:

(a) Deformation capacity and hysteretic response improve dramatically (Fig 2) when non-ductile regions are encased in continuous (carbon or glass) FRP jackets. Apart from being an easy to apply technique, it also proved extremely efficient in upgrading member deformability by at least a factor of 2.0, owing to the increased strain capacity of confined concrete in compression. The technique increases member strength marginally without modifying member stiffness.

(b) Compared to an undamaged and retrofitted specimen, those in which retrofitting measures were applied after initial damage may behave in a less favourable way, with more rapid strength loss due to FRP rupture. Since previously inflicted damage was not restored before retrofitting, confined concrete reaches earlier its crushing strain with less benefit from the FRP wraps.

(c) Increasing CFRP layers from two to five increases marginally member deformability and strength.

(d) Changing the type of material (glass instead of carbon fibres) but maintaining FRP jacket stiffness the same leads to an increase in number of FRP layers by 250%, with the GFRP retrofitted elements responding slightly better than the 2-layer –CFRP specimens.

(e) Due to the reduced confinement by the FRP over the rectangular cross-section, the improvement in strength and deformation capacity in the weak direction is much less than in the strong.

(f) Unretrofitted specimens exhibit a gradual loss of lateral and axial load resistance during the cycle that le to failure, whereas retrofitted ones maintained constant axial load (and practically lateral) force capacity, but lost it abruptly at failure.

REFERENCES

[1] Federation International du Beton, Externally bonded FRP reinforcement for RC structures, *fib* Bulletin 14, Lausanne, 2001.

COMPOSITE AND HYBRID STRUCTURE SYSTEMS MAKING THE MOST OF HIGH PERFORMANCE MATERIALS

Prof. Dr.-Ing. Dr.-Ing. e.h. Gert König
Institut für Massivbau und Baustofftechnologie
Universität Leipzig, Germany

Dr.-Ing. Reinhard Maurer
König und Heunisch Planungsgesellschaft mbH,
Leipzig, Germany

The most important steps in the further development are characterized by the following bridges.

1. The Bridge crossing the river Zwickauer Mulde, with an overall length of 171 m is the largest application of high-performance concrete C 70/85 in Germany by now. Almost 2,600 m3 concrete were processed for the slab bridge over 5 spans. With a structural height of 1.05 m and a maximum span of 39 m, the bridge has a slenderness of 37 (figure 1). The tramway bridge Jahnallee in Leipzig (figure 2) has a similar slenderness. Also the Havel river bridge in Brandenburg demonstrates the new design opportunities for concrete bridges by using high-performance concrete (figure 3).

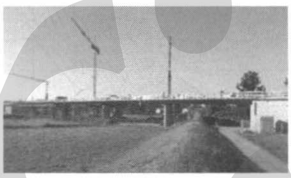

Fig. 1
Mulde Bridge near Glauchau

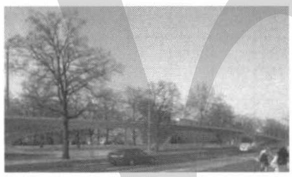

Fig. 2
Project: Jahnallee in Leipzig

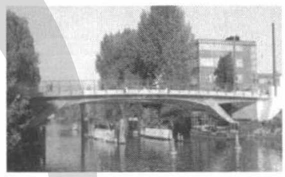

Fig. 3
Luckenberger Bridge, Brandenburg

2. Just before the end of the year 2001, the first bridge made of self-compacting concrete SCC 65 (web) and lightweight concrete SCLC 45 (deckslab) over the river Pleisse near Leipzig could be completed (figure 4).

Fig. 4 footbridge over the Pleiße made of SCC

3. The experience gained at these 4 bridges shows that the high-performance concrete can be aimedly applied if an according quality assurance and previous trial concreting are provided. However , the capabilities of this material are not exhausted at all yet because the construction methods were still adapted from traditional construction with common concrete.
4. The application of high-performance concrete together with steel also provides for a new dimension in the construction methods because the construction work can be carried out almost without any scaffolding or formwork.

This is evidenced by the following bridges:

The Prager bridge in Leipzig is a integral frame bridge without joints, whose steel frames in the corner region are filled with high-performance concrete C 55/67. This results in a braced delicate looking structure of extraordinary slenderness (figure 5).

Fig. 5 Prager Bridge, Leipzig

The bridge Karl-Heine-Bogen demonstrates another opportunity. Pipe structures are filled with high-performance concrete (LC 70/77) supporting semi-precast components made of lightweight concrete. The precast elements are combined to a continuous slab with cast in place concrete and internal tendons without bond (figure 6).

Fig. 6 Karl-Heine-Bogen, Leipzig

This can be generally further developed for bridge construction. First regarding drafts have been presented, sometimes by using UHPC. This results in sufficiently rigid bridge types with a most appealing design.

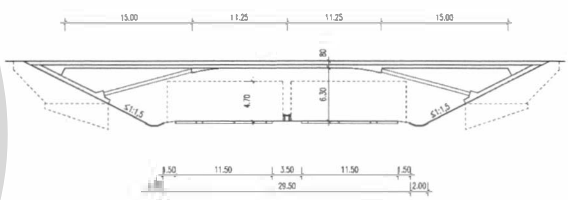

Fig. 7 Project: Motorway Overcrossing. Inclined-leg frame bridge of high performance materials (C 70/85, composite pipes)

APPLICATION OF HIGH PERFORMANCE LIGHTWEIGHT AGGREGATE CONCRETE FOR CONSTRUCTION OF PRE-STRESSED CONCRETE BOX GIRDER BRIDGE

Shuji Yanai
Research Engineer
Kajima Technical Research Institute
Tokyo, Japan

Shunichi Taniguchi
Civil Engineer
East Japan Railway Company
Sendai, Japan

Kazuhito Koizumi
Civil Engineer
East Japan Railway Company
Sendai, Japan

Hideki Ohkubo
Civil Engineer
Kajima Corporation
Tokyo, Japan

Keyword: high performance lightweight aggregate concrete, pre-stressed concrete bridge

1. INTRODUCTION

The NUMAKUNAI Bridge (shown in Photo 1) in Tohoku Shinkansen Line between Morioka to Hachinohe was constructed by concrete using high performance artificial lightweight aggregate [1] that had both higher strength and lower water absorption than the ordinary (shown in Photo 2). The bridge is the pre-stressed concrete box girder bridge having 11-spans. The specified concrete strength was $40N/mm^2$ and the unit weight of concrete was $1{,}800kg/m^3$. The concrete reinforced by polypropylene fiber was also applied to the part of over roadway and over railway to prevent accidents due to falls of concrete pieces.

Though it was the first application of this type of concrete to the large-scale structure, the properties of concrete were examined carefully. Mix proportion was selected by the laboratory tests carried out on workability, strength, durability and resistance to stripping-off. Field tests were also carried out in order to verify the workability of concrete at site.

In this report, the results of tests on High Performance Lightweight Aggregate Concrete, and the construction work were discussed.

Photo 1 Whole View of NUMAKUNAI Bridge

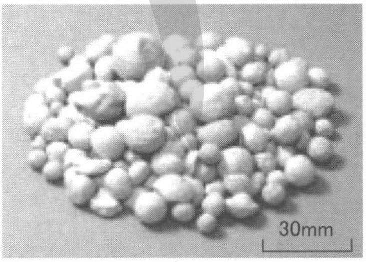

Photo 2 High Performance Lightweight Coarse Aggregate

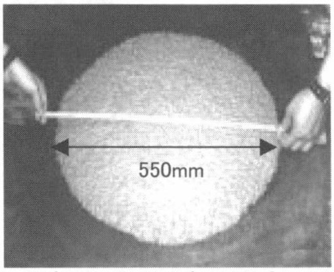

Photo 3 Property of Fresh Concrete

2. APPROACH

Mix proportion of High Performance Lightweight Aggregate Concrete was selected by laboratory test (shown in table 1) and it verified that the properties of fresh and hardened concrete were satisfied the characteristics value used in design (shown in Photo 3 and Table 2).

Field application tests, casting concrete to the large scale specimens (shown in Photo 4), were also carried out in order to verify the workability, pumpability, placeability, finishability, and so on.

Through these tests High Performance Lightweight Aggregate Concrete could be applied to actual construction work.

Table 1 Mix Proportions of Concrete

Air (%)	W/C (%)	s/a (%)	Unit Quantity (kg/m^3) W	C	S	G	SP (C×%)	VIS (W×%)
6.0	38.0	49.7	165	435	828	381	1.00 (4.35kg)	0.05 (82.5g)

W : Water C : High Early Strength Portland Cement
S : Pit Sand
G : High Performance Lightweight Corse Aggregate
SP : High Range Water Reducing Agent
VIS : Viscosity Agent (Welan Gum) [2]

Table 2 Test Results of Hardened Concrete

	Compressive Strength (N/mm^2)		Splitting Tensile Strength (N/mm^2)	Flexural Strength (N/mm^2)	Young's Modulus (kN/mm^2)	Durability Factor
Age	7days	28days	28days	28days	28days	—
Test Value	42.7	54.8	4.23	7.20	21.9	87.2
Design Value	—	40.0	1.89	3.43	19.0	(70.0)

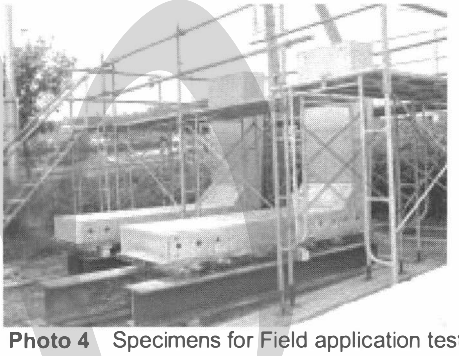

Photo 4 Specimens for Field application test

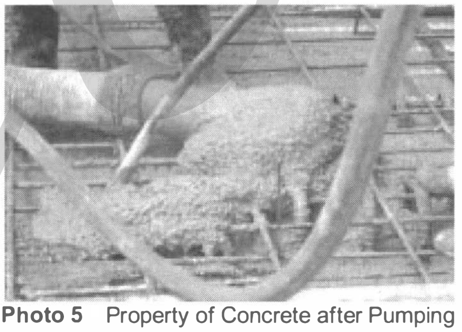

Photo 5 Property of Concrete after Pumping

3. CONSTRUCTION WORK

Concrete was transferred by pumping and consolidated by vibrators excessively. As shown in Photo 5, the workability of concrete after pumping was very satisfactory, and there was no clogging of the pipe and the pumping work could be performed without any problems. The quality of structure was also satisfactory.

The main girder was erected rapidly by the incremental launching method over the entire length of 380 m (shown in Photo 6). The length of a block was to be 35 m, and the execution cycle time of 1span was to be about 20 days.

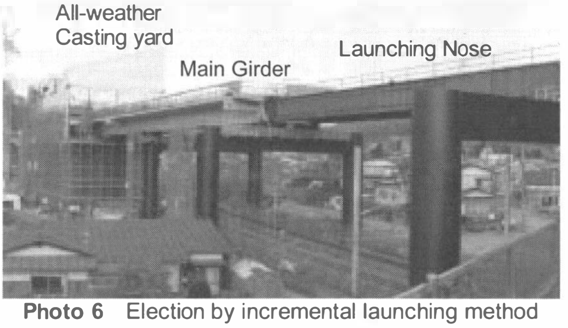

Photo 6 Election by incremental launching method

4. CONCLUSION

The construction work proceeded smoothly and the work could be completed successfully because the investigations and work controls were reasonably adequate. Since the costs could be reduced by about 10 %, the present technique may be anticipated to become one of the new cost-reduction technologies likely to be used in similar construction projects.

REFERENCES

[1] Okamoto,T., Hayano,H., Shibata,T., : Super Lightweight Concrete, CONCRETE JOURNAL, Vol.36, No.1, pp.48-52, January, 1998 (in Japanese)

[2] Yanai,S., Sakata,N., Nobuta,Y., Ishikawa Y., : Pumpability of High-performance Lightweight Concrete under the Influences of Mixture Proportion, Proceedings of JCI, Vol.22, No.2, pp.1405-1410, June, 2000 (in Japanese)

EXAMINATION FOR THE APPLICABILITY OF THE FIBER REINFORCED CONCRETE TO THE SUPERSTRUCTURE OF THE BRIDGE

Yasuo Fukunaga, Japan Highway, JAPAN
Hiroo Minami, Kajima corporation, JAPAN
Takenori Hiraishi, Kajima corporation, JAPAN
Noboru Sakata, Kajima corporation, JAPAN

Keywords: fiber reinforced concrete, preventing spalling

1 INTRODUCTION

Due to the concrete spalling related accident of the tunnel lining and peeling of the covering concrete of a viaduct of the Shinkansen Line which occurred in 1999, securing the safety of concrete structures, especially securing the safety to third parties, is strongly desired.

Spalling of concrete occurs due to extended cracks generated by initial defects, such as cold joints during the construction and corrosion of reinforcement bar due to salt damage and neutralization. As a manufacturing method for preventing concrete spalling incidents, studies [1][2] on methods of repair, such as continuous fiber sheets and steel plate adhesion, have been actively performed for established structures. It is thought that such methods of repair will be applied to many established structures in the future as well. However, spall prevention methods for established structures will require much labor and cost.

The present study has the objective of providing a structure with spall prevention capabilities at the time of construction, wherein fiber reinforced concrete using organic short fiber is targeted, laboratory tests were performed paying attention to the kind of fiber suitable for the prevention of spalling, and the basic physical properties and fiber dispersibility of fiber-mixed concrete, fiber concrete of blending determined from the laboratory test results were provided in a specimen which modeled a part of an actual bridge, wherein, at that time manufacturing, the pump sending ability, tamping properties, surface finish, etc. were investigated using an actual raw concrete plant, and after hardening the sample was taken out of the specimen and fiber dispersibility was checked.

2 LABORATORY TESTS

In this report, among the following five items performed in the laboratory test, the results are described for four items, which

Table 1 Performance comparison of fiber

Types of fiber	Organic fiber		Steel fiber
	Polypropylene	Polyvinyl alcohol	
Gravity (g/cm^3)	0.91	1.3	7.85
Diameter (mm)	1.0	0.66	0.6,0.8
Length (mm)	30	30	30
Form	Waveform	Straight	hook at both end
Tensile strength (N/mm^2)	450	900	1,000
Young modulus (*10^{4}N/mm^2)	1.0~1.5	2.9	2.1
Corrosive proof	Good		Rust by oxidization
Workability	Handling is good (Light weight)		Failure
	Dispersibility is good		Failure
Strengthening effect	Small		Large
Evaluation (about preventing spalling)	good	good	Failure

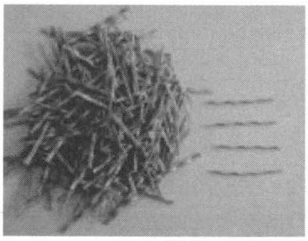

Photo 1 Polypropylene fiber

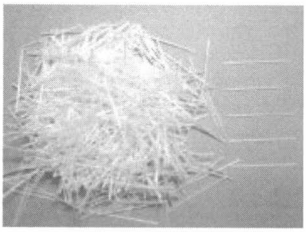

Photo 2 Polyvinyl alcohol fiber

excluded durability testing.

* Basic physical property evaluation test
* Dispersibility test
* Spall simulation test
* Fire-resistance test
* Durability test (Freeze-thawing test and salinity permeation promotion test)

The performance of the fiber used in the test is listed in **Table 1**, and the two kinds of fibers are shown in **Photos** 1 and **2**. As an example, results of spalling-off simulation test are shown in **Photos 3** and **4**.

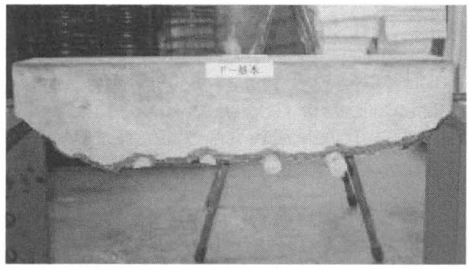

Photo 3 Result of spalling-off simulation test (Plain concrete, Progress in 48 hour)

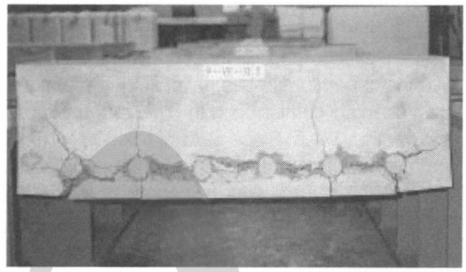

Photo 4 Result of spalling-off simulation test (P-VF-0.2, Progress in 48 hour)

3 WORKABILITY CHECK TEST

In the workability test, with the objective of applying the fiber concrete whose performance was confirmed in the laboratory test to the construction of the superstructure of the bridge, in order to grasp the influence on the scatter and workability of fiber during construction, installation of the fiber reinforced concrete was experimentally performed to a specimen of a box girder cross section. The results are reported here.

The shape of the specimen used for the experiment is shown in **Fig. 1**. The specimen is a simulation of the cross section of a prestressed concrete rigid frame bridge with a length of 90 m and a box girder cross section, where the cross section and the amount of reinforcement bar were determined assuming the design standard strength of concrete as 36 N/mm^2, and reinforcement bar was placed in the sample. The concrete was manufactured in a concrete plant in the city, and five agitator cars loaded with 4.5 m^3 concrete were used for the experiment. As to the fiber mixing ratios, it is confirmed in the laboratory test that a spall prevention effect can be provided by mixing Polyvinyl fiber of length 30 mm by 0.2 vol % or more to the concrete. However, in this experiment, considering the scattering of fiber during construction, the fiber mixing ratio up to the third car used for installation of the sample was set to 0.35 vol %. Also, in order to investigate the influence of mixed fiber on workability, concrete with no mixed fiber was applied as the fourth car in the hatched area in **Fig. 1**. The fifth car was not used for installation of the sample, and an experiment was performed on the dispersibility of fiber when the fiber mixing ratio was set to 0.2 vol %. Injection of the fiber was performed on site as the agitator car was rotated at high speed, where 5 kg of fiber was injected per minute. Here, in the middle and at the end of fiber injection, a high-speed rotation time was maintained when no fiber was injected for 30 seconds and 60 seconds, respectively.

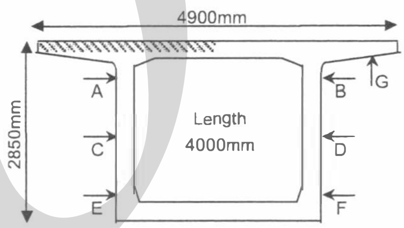

Fig.1 Shape of the specimen

In the experiment, about seven liters of concrete was sampled from the exhausted concrete from the first, third, and fifth agitator cars at the start, middle, and end of unloading, and the respective fiber mixing ratios were measured. Also, core borings shown in **Fig. 1** were sampled from the hardened samples, and their fiber mixing ratios were measured. Furthermore, in order to evaluate the pump pressure sending performance, the main oil pressure of the used concrete pumping car was measured.

4 CONCLUSION

The fruits of this research have been already applied, through workability check tests, to a bridge over a roadway (Polyvinyl fiber was applied) over the Second Tomei Highway and a bridge over the roadway of the Tohoku Shinkansen (Polypropylene fiber was applied).

FRESH MORTAR PROPERTIES AND STRENGTH OF REACTIVE POWDER COMPOSITE MATERIAL (Ductal®)

Masami Uzawa Tsuguya Masuda Kazuyoshi Shirai Yoshihide Shimoyama Yoshihiro Tanaka
Taiheiyo Cement Corporation, JAPAN Taisei Corporation, JAPAN

Keywords: ultra high strength, self-compactable, Reactive Powder Composite Material,

1 INTRODUCTION

As more skyscrapers are being built the demand for high strength concrete with compressive strength over 100 N/mm^2 [1] has been increasing year by year. Demands for materials with much higher strength will be far larger in the future.

In the history of the compressive strength of cement-based materials, the record of 600 N/mm^2 established by Roy, et al. in 1972 [2] had not been broken until 1992 when Lu and Young [3] marked 800 N/mm^2 based on the densest compaction theory. In 1994 Richard et al. [4] invented an 800 N/mm^2-class cement-based material with increased toughness, by mixing in metal fiber. This new material bom from an innovative concept of ultra high strength combined with high toughness was named RPC (reactive powder concrete) for the reactive powder they used. Since RPC of the 800 N/mm^2 class (RPC800) requires heating and pressing curing which is unpractical for commercial production, some propose RPC of the 200 N/mm^2 class (RPC200) which can be obtained by steam-curing. Strength of the RPC is almost one digit higher than that of normal high strength concrete, but there have been few reports on such materials in Japan.

Based on this RPC technique, the Taiheiyo Cement research group examined domestically available materials and their proportions. Consequently, a powdery premix of cement, ground siliceous material and some other powdered materials was developed, together with special water reducer and steel fiber to be used with this premix. Its commercial production started in Japan under the brand name Ductal® [5]. What makes this new material distinct from the above mentioned RPC is its wide applications ranging from structural members for bridges and buildings to replacement of iron and granite. Being completely different from concrete, this promising material is called Reactive Powder Composite Material (RPCM).

This report describes the constitution of the RPCM, the temperature dependency of its fresh mortar properties and the changes in its strength dependent on curing temperature and other conditions.

2 RPCM CONSTITUTION

The RPCM is steel fiber reinforced ultra high strength mortar consisting of premix containing cement, ground siliceous material and quartz sand, plus special water reducer and special steel fiber. Precuring and then steam-curing the fresh mortar prepared by mixing with water produces hardened RPCM with a compressive strength of 230 N/mm^2. Flow value (no hits) of the RPCM fresh mortar is about 270 mm; i.e., it is highly fluid and thus self-compactable. This excellent fluidity of fresh mortar results from a synergy of the premix and the special water reducer. The synergy further allows a reduction in the water ratio to the premix, remarkably, leading to the ultra high strength of hardened pieces. There are two factors that make such an extremely low water ratio (mass) of only 8% possible:

(1) the unprecedented proportioning of the premix which was established on the basis of the densest compaction theory : and
(2) the molecular design of the special water reducer which was determined by giving consideration to particle behavior at the extremely low water ratio so that both the cement and the ground siliceous material of different chemical properties may be dispersed effectively.

The combined use of the premix and the special water reducer achieves the extremely low water ratio.

The special steel fiber is deformed for better compatibility with hardened matrix, which achieves a maximum bending strength of 45 N/mm^2 (40 x 40 x 160 mm specimen). The steel fiber reinforces the hardened matrix under stress against cracking. After cracking, it gradually pulls off the hardened matrix with the increase in stress. Although the crack width increases as the steel fiber pulls off, the RPCM does not reach ultimate failure even with a displacement of 2 to 3 mm, demonstrating its high toughness.

3 RPCM FRESH MORTAR PROPERTIES

Table 1 shows the fluidity of the RPCM fresh mortar after mixing. The quantity of the solid water reducer that achieved a self-compactable mortar flow value of about 270 mm was 7.0 kg/m^3 at 20°C. The lower the ambient temperature, the smaller the quantity of the water reducer; the higher the temperature, the larger the quantity. The quantity of the water reducer was 6.4 kg/m^3 at an ambient temperature of 5°C, and was 7.6 kg/m^3 at 30°C. The temperature of the RPCM fresh mortar immediately after mixing was 6°C to 7°C higher than the ambient temperature. The flow value was about 270 mm where the fresh mortar was self-compactable.

Table 1 RPCM fresh mortar properties at different temperatures

Ambient temperature (°C)	Content (kg/m³)				Temperature immediately after mixing (°C)	Flow (mm)
	Water*	Premix	Water reducer (solid)	Steel fiber		
5	180	2297	6.4	157 (2% vol.)	11	270
20			7.0		27	278
30			7.6		36	265

* The figure of 180 kg includes the solid water reducer which was 6.4 kg, 7.0 kg and 7.6 kg, respectively.

4 COMPRESSIVE STRENGTH AND BENDING STRENGTH

Table 2 shows compressive strength, bending strength and modulus of elasticity obtained.

Table 2 RPCM strength properties

	Compressive strength (N/mm²)	Bending strength (N/mm²)		Modulus of elasticity (GPa)
		Initial crack strength	Maximum bending strength	
Mean value	238	24.9	46.1	52.2
Standard deviation	8.46	2.36	4.34	0.93
Number of specimens	50	50	50	10

The mean value for compressive strength was 238 N/mm^2, and a standard deviation of 8.46. This demonstrates the very high strength of the RPCM with small deviation. Design standard strength F_c can be defined as expressed by equation (1), in reference to the design standard strength calculation in the Architectural Institute of Japan Standard: $F_c = F_a - 1.73\sigma$ (1) With F_a as the mean value of compressive strength and σ as the standard deviation, F_c = 223 N/mm^2.

Figure 1 shows the stress-crosshead displacement curve during the bending strength measurement. The initial crack strength was determined from a small bump found at a stress of 25 N/mm^2 until which a very smooth curve was drawn. Although minor cracks develop in the RPCM matrix at the initial cracking, they are invisible to the naked eye since the matrix is heavily reinforced by the steel fiber contained in it.

The curve was serrated after that point as the steel fiber pulled off with the increase in the stress. Stress continued to increase until reaching a maximum bending strength of 45 N/mm^2; after which, that increase stopped while crosshead displacement increased. Stress decreased, without breaking. When the crosshead displacement reached 2.5 mm, the specimen still expressed a stress of 12 N/mm^2 while deforming. As demonstrated here, the RPCM is a highly tough material which does not break but deforms as the steel fiber pulls off.

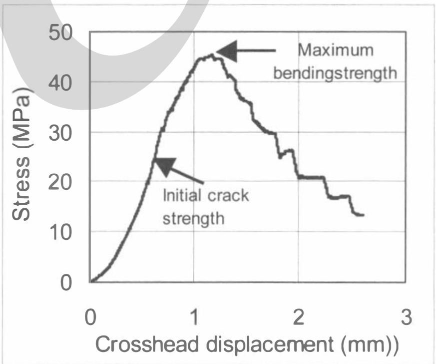

Fig. 1 Stress-crosshead displacement curve for RPCM during bending

REFERENCES

[1] Kuroha, K.: An application of concrete using AE superplasticizer. High Strength Concrete, Concrete Engineering, Vol. 37, No. 6, pp. 31-35, 1999 (in Japanese)

[2] Roy, D. M., Gouda, G. R. and Bobrowsky, A.: Very high strength cement pastes prepared by hot pressing and other high pressure techniques. Cement and Concrete Research, Vol. 2, No. 3, pp. 349-366, 1972

[3] Lu, P. and Young, J. F.: Hot pressed DSP cement paste. Material Research Society Symposium Proceedings, No. 245, pp. 321-328, 1992

[4] Richard, P. and Cheyrezy, M. H.: Reactive powder concretes with high ductility and 200-800 N/mm^2 compressive strength. Metha, P.K(ed.), Concrete Technology: Past, Present and Future, SP144-24, pp. 507-517, 1994

[5] http://www.taiheiyo-cement.co.jp/ductal/index.html

PHYSICAL PROPERTIES AND DURABILITY OF REACTIVE POWDER COMPOSITE MATERIAL (DUCTAL®)

Makoto Katagiri Shinpei Maehori Tsuyoshi Ono Yoshihide Shimoyama Yoshihiro Tanaka
Taiheiyo Cement Corporation, JAPAN Taisei Corporation, JAPAN

Keywords: durability, physical properties, reactive powder composite

1. INTRODUCTION

Researching records on the compressive strength of cement-based materials shows that the highest record had not been renewed for a long time since Roy et al.[1] recorded 600MPa in 1972. Richard et al.[2] developed a cement-based material with 800MPa-class compressive strength by further mixing in metal fiber to allow ductility, which gave rise to a new concept of super high-strength + high-ductility. This was named RPC (Reactive Powder Concrete) by Richard et al. from the point in which reactive powder was used. Also, since the 800MPa-class RPC (RPC800) lacks practicality in terms of production method because it requires high temperature and pressure for curing, RPC with approximately 200MPa (RPC200) is proposed, which can be manufactured by steam curing. Thus, RPC manifests strength nearly one figure higher than regular high-strength concrete; however, this material and its properties are scarcely reported on in Japan.

Based on this RPC technology, we studied prescriptions for materials, which can be procured in Japan. As a result, we developed premixed powder consisting of several types of powder, such as cement, silica particles, special water reducing agents, and special steel fibers, which were produced commercially under the trade name Ductal®[3]. This material is based on RPC, and has high added functions, such as high fluidity, the application field of which is not limited to replacing conventional concrete for bridges, etc., but extends to altematives for steel and natural stone. From these, this new material is called RPCM (Reactive Powder Composite Material), which is different from concrete.

In this text, we will report on the characteristics of RPCM physical properties and durability, such as shrinkage, frost resistance, neutralization, water permeability and abrasion resistance, obtained from experiments.

2. COMPONENTS OF RPCM AND SPECIMENS FOR EVALUATING PHYSICAL PROPERTIES AND DURABILITY

RPCM is a super high strength cement-based material reinforced with steel fiber. It consists of premixed powder in a carefully selected combination of cement, silica particles, siliceous sand, special water reducing agents, and special steel fibers. These are mixed with water and cast into a form to produce a hardened body with compressive strength as high as 230MPa and bending strength as high as 45MPa after 90℃-48hours steam curing.

Specimens for evaluating physical properties and durability were prepared by using the RPCM premix. Materials used and the typical mix proportions are shown in Table 1. Here, premix refers to a mix primarily of cement, silica particles, and siliceous sand. Also, the water-cement ratio is 0.22 and the amount of water reducing agent refers to a solid portion. And, 0.2mm diameter and 15mm long carbon steel wire was used for the steel fiber.

Table 1 Materials used, mix proportion, and fresh mix conditions

Unit amount (kg/m^3)				Mixture temperature (℃)	Flow (mm)
Water	Premix	Water reducing agent	Steel fiber		
173	2297	7	157 (2%/Vol)	27	278

3. PHYSICAL PROPERTIES AND DURABILITY OF RPCM

Evaluation tests on shinkage, frost resistance, neutralization, water permeability and abrasion resistance were carried out. The general terms of those evaluation methods are as follows:

- Shinkage: measured by embedded straingages after setting up to approximately 200 days with and without

steam curing.
- Frost resistance: according to JIS 6204 attached document 2, "Concrete freezing/thawing test method,"
- Neutralization: accelerated test under steady temperature and humidity controlled (20℃, 60%RH) at 5% CO_2 gas concentration.
- Water permeability: based on an inflow permeation method under water pressure of 150-350MPa.
- Abrasion resistence: according to ASTM C779 procedure A

The inflow permeation test was carried out by using a pressure tank as shown in Fig. 1. The specimen was placed in a rubber bag containing water and applier pressure of 150-350MPa from around the rubber bag. After maintaining the specified pressure for a designated period of time, a specimen was split to measure the depth of water permeation. The water diffusion coefficient was computed based on Murata's references[4].

As the results of experiments listed in Table 2, RPCM will be more durable than the ordinary concrete.

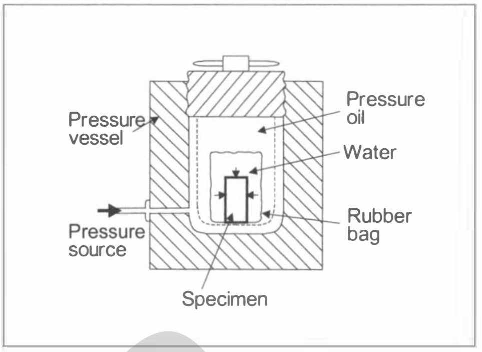

Fig. 1 Equipment for inflow permeation test

Table 2 Summy of experimental results

Property	Experimental method	Result
Shrinkage	Embedded strain gage	Total shrinkage: 550 μ , During Steam curing: 500 μ
Frost resistance	JIS A6204	Durability Factor :100% at 300 cycle
Neutralization	Accelerated under 5% CO_2 gas	Depth of neutralization: less than 0.1mm
Water permeability	Inflow permeation test under 150-350MPa	Diffusion coefficient: approximately $1x10^{-7}$ (cm^2/s)
Abrasion resistance	ASTM C779 procedure A	2.3 times of concrete and 1.8 times of gabbro

4. CONCLUSION

Several tests to evaluate physical properties and durability of RPCM were carried out. As the results of these tests, characteristics of RPCM physical properties and durability are summarized as follows:

1) Shrinkage measured approximately 500 μ by steam curing; however, subsequent shrinkage was small. Total shrinkage was approximately 550 μ .
2) The freezing/thawing test did not indicate any changes in the durability factor up to at least 300 cycles, and it was difficult to measure within the range of neutralization even from the results of the accelerated carbonation test. These indicated the superiority of RPCM for frost resistance and neutralization.
3) Water diffusion coefficients were evaluated by applying relatively high pressure in the inflow permeation method. As a result, the water diffusion coefficient of RPCM was estimated to be approximately $1x10^{-7}$ (cm^2/s).
4) In the abrasion resistance test, the depth of abrasion in RPCM was less than that of concrete and gabbro (black granite), which indicated its superiority for abrasion resistance.

REFERENCE

[1] Roy, D. M., Gouda, G. R. and Bobrowsky, A.: Very high strength cement pastes prepared by hot pressing and other high pressure techniques. Cement and Concrete Research, Vol. 2, No. 3, pp. 349-366, 1972
[2] Richard, P. and Cheyrezy, M. H.: Reactive powder concretes with high ductility and 200-800 N/mm^2 compressive strength. Metha, P. K. (ed.), Concrete Technology: Past, Present and Future, SP144-24, pp. 507-517, 1994
[3] http://www.taiheiyo-cement.co.jp/ductal/index.html
[4] Murata, J. Koshikawa, S. and Ito, Y.: Study on pressurized flow in concrete, Concrete Research and Technology, Vol. 11, No. 1, Jan, pp. 61-74, 2000 (in Japanese)

NEW SYSTEM FOR CONNECTING PRECAST CONCRETE BEAMS WITH HIGH PERFORMANCE CEMENTITIOUS COMPOSITES

Kenji Yoshitake Toshiyuki Shioya Morio Kurita Hirokazu Tanaka
Institute of Technology, Shimizu Corporation
JAPAN

Keywords: butt joint, lap splice joint, compact reinforced composite (CRC), precast concrete

1 INTRODUCTION

We propose two types of new connecting system between precast reinforced concrete members to facilitate the execution: the butt joint and the lap splice joint in which the lap length is extremely short. The re-bars, which extend from one face of the precast members, are anchored in the connection region by Compact Reinforced Composites (CRC) [1] [2]. CRC is a special type of fiber reinforced mortar with high compressive strength (130MPa), high bond strength and ductility. Adjacent re-bars from other precast beams are not tied to each other and the joints have no transverse re-bar. Flexural tests and flexural shear tests were carried out. This paper presents the effects of the steel fiber content, anchorage length, additional re-bars and lap length on the beam behavior.

2 EXPERIMENTAL PROGRAM

The specimens consist of two precast reinforced concrete beams and a connection region as shown in Fig. 1. Re-bars, which extend from one face of the precast members which are made of normal concrete, are anchored in the connection region by CRC without transverse re-bar, and adjacent re-bars from other precast beams are not tied to each other. CRC has extremely high bond strength, compressive strength and high flowability. Figure 1a shows the butt joint in which the anchorage length is 10*d* (where *d* indicates bar diameter) with additional re-bar and the main steel ratio is 0.5%. Figure 1b shows the lap splice joint in which the lap length is 10*d*. Figure 1c shows the specimen with the lap splice joint for flexural shear tests and the main steel ratio is about 1.2%. The influence of anchorage length, volume fraction of fiber content and additional re-bar for the butt joint, and volume fraction and lap length for the lap splice joint are investigated as shown in Table 1. Fresh and hardened properties of four mix proportions are given in Table 2. NC indicates the normal concrete which is used for the precast members. CRC-3 indicates that the material is CRC and volume fraction is 3%.

Table 1 Parameters and results of the tests

Specimen	Type of test	Lap splice length	Anchorage length	Joint material	Additional re-bar	Max. load (kN)	Failure Mode*
No. 1	flexure	No joint	No joint	No joint	—	129.1	BEND(Y)**
No. 2	flexure	0*d*	5*d*	CRC-0	—	44.9	SPLIT
No. 3	flexure	0*d*	5*d*	CRC-3	—	108.4	SPLIT(Y)
No. 4	flexure	0*d*	5*d*	CRC-6	—	91.6	BOND
No. 5	flexure	0*d*	5*d*	CRC-0	○	48.1	SPLIT
No. 6	flexure	0*d*	5*d*	CRC-3	○	122.6	BOND
No. 7	flexure	0*d*	10*d*	CRC-0	—	73.8	SPLIT
No. 8	flexure	0*d*	10*d*	CRC-3	—	139.6	SPLIT(Y)
No. 9	flexure	0*d*	10*d*	CRC-6	—	141.6	BEND(Y)
No.10	flexure	0*d*	10*d*	CRC-0	○	80.1	SPLIT
No.11	flexure	0*d*	10*d*	CRC-3	○	143.6	BEND(Y)
No.12	flexure	5*d*	—	CRC-0	—	65.0	BOND
No.13	flexure	5*d*	—	CRC-3	—	117.4	BOND(Y)
No.14	flexure	5*d*	—	CRC-6	—	129.0	BOND(Y)
No.15	flexure	10*d*	—	CRC-0	—	104.4	BOND(Y)
No.16	flexure	10*d*	—	CRC-3	—	130.3	BEND(Y)
No.17	flexure	10*d*	—	CRC-6	—	130.5	BEND(Y)
No.18	flexural shear	No joint	No joint	No joint	—	255.6	SHEAR(Y)
No.19	flexural shear	5*d*	—	CRC-3	—	210.2	BOND(Y)
No.20	flexural shear	10*d*	—	CRC-3	—	240.5	SHEAR(Y)

* BEND ; bending failure, SPLIT ; splitting of the CRC, BOND ; splitting bond failure, SHEAR ; share failure
** (Y) ; Max. load was attained after yielding of re-bar

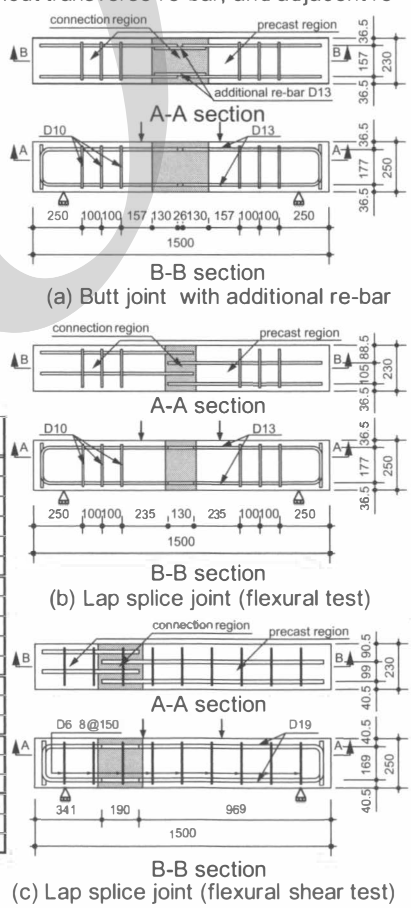

Fig. 1 Arrangement of reinforcement

Table 2 Material properties

Type of concrete	f'c (N/mm²)	ft (N/mm²)	Ec (kN/mm²)	Slump (mm)	Slump flow (mm)
NC	29.5	4.6	32.4	134	-
CRC-0	131.2	8.9	42.6	-	595
CRC-3	128.0	13.7	45.9	-	530
CRC-6	131.2	16.0	44.9	-	410

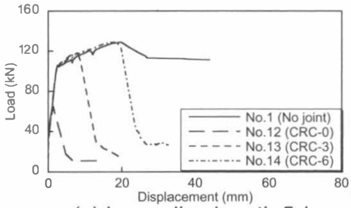

(c) Lap splice length 5*d*

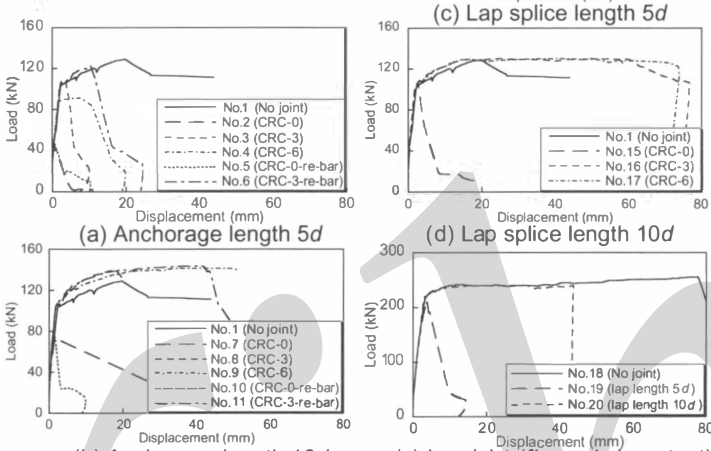

(a) Anchorage length 5*d* (d) Lap splice length 10*d*

(b) Anchorage length 10*d* (e) Lap joint (flexural shear test)

Fig. 2 Load displacement relationship

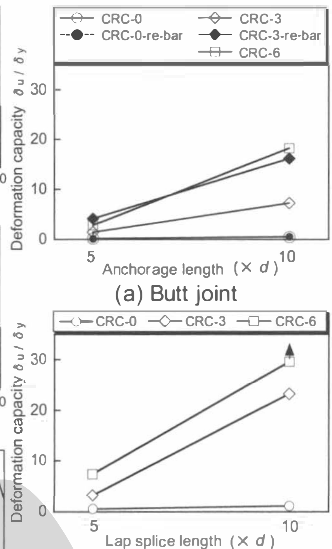

(a) Butt joint

(b) Lap splice joint

Fig. 4 Deformation capacity for flexural tests

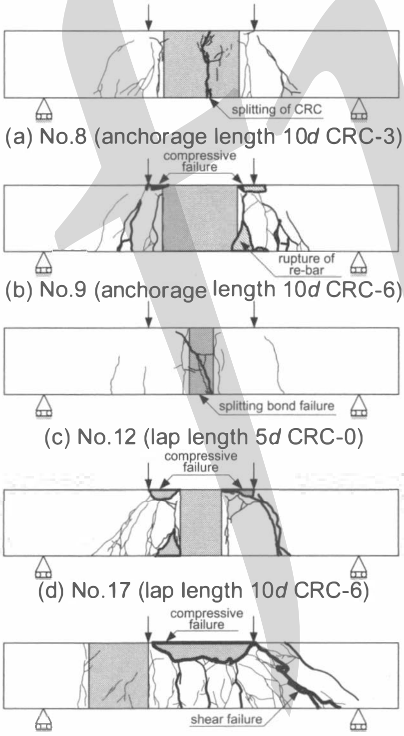

(a) No.8 (anchorage length 10*d* CRC-3)

(b) No.9 (anchorage length 10*d* CRC-6)

(c) No.12 (lap length 5*d* CRC-0)

(d) No.17 (lap length 10*d* CRC-6)

(e) No.20 (lap length 10*d* CRC-3)

Fig. 3 Crack patterns

3 EXPERIMENTAL RESULTS

The relationship between load and displacement at the center of the specimen, and the representative crack patterns are shown in Fig. 2 and Fig. 3, respectively. Three failure modes for the butt joint were observed: splitting of the CRC from the end of the re-bar, pull-out of the re-bar, and rupture of the re-bar. The proposed butt joint could transfer the full bending moment for an anchorage length of 10*d* and 6% steel fiber content. Likewise, the full moment could be transferred using the same anchorage length, 3% steel fiber content and an additional re-bar. For the lap splice joint, three failure modes were observed: splitting bond failure, pull-out of the re-bar, and rupture of the re-bar. Sufficient performance of the connection region was obtained for a 10*d* lap length with 3 and 6% steel fiber contents, and for flexural shear test, 10*d* lap length with 3% steel fiber content.

The relationships between deformation capacity and anchorage length of the butt joint and lap length are shown in Fig. 4. δ_u indicates the longitudinal displacement when the load decreased suddenly. δ_y is set to 2.5 mm which was the longitudinal displacement when the main re-bar of specimen No.1 yielded. The deformation capacity increased with increase of the volume fraction of the steel fiber. The additional re-bars was more effective as the steel fiber content increased.

4 CONCLUSIONS

We proposed a new butt joint and lap splice joint using CRC to facilitate the execution of the joint between precast members and investigated the performance of the joints. It was apparent from the test results that the proposed joint system could be very effective means to facilitate the execution of the joint.

REFERENCES

[1] Bache, H.H. : Concrete and Concrete Technology in a broad Perspective, CANMET/ACI
[2] Yoshitake, K., Tanaka, H., Kurita, M. and Shioya, T. : Flexural behavior of precast concrete beams connected by fiber reinforced cementitious composites, Proc. of JCI, Vol.23, No.3, pp.859 -864, 2001 (in Japanese)

PROPERTIES OF STEEL FIBER-REINFORCED CEMENTITIOUS COMPOSITES WITH 70 TO 180N/mm² OF COMPRESSIVE STRENGTH

Morio Kurita Toshiyuki Shioya Kenji Yoshitake Hirokazu Tanaka
Institute of Technology, Shimizu Corporation
JAPAN

Bendt Aarup
CRC Technology
Denmark

Keywords: short steel fiber, mortar, concrete, compressive strength, flexural strength, bond strength

1 INTRODUCTION

Recently research and development activities have been underway aiming at better performance of steel fiber-reinforced cementitious materials. It includes one to focus on fluidity to achieve a highly-flowable concrete in order to improve its filling capacity. Another is to dramatically improve a hardened concrete in performance by designing it with low water-binder ratio and high volume fraction of steel fibers to achieve a high compressive strength, high bond strength and ductility. This paper presents fresh and hardened properties of high-performance steel fiber-reinforced cementitious materials with 70 to 180N/mm² of compressive strength, and mainly delineates the result of a bond strength test (Pull-Out test) in terms of the compressive strength, diameter of reinforced bars, presence of steel fibers, the volume fraction of the steel fiber for highly-flowable SFRC[1] and CRC(Compact Reinforced Composite) [2].

2 EXPERIMENTS

Table 1 and **Table 2** respectively show the factors and levels of the experiment and the combinations of the tests. Three kinds of cementitious materials were used in these experiments. **Table 3** and **Table 4** show mix proportions applied to the test.
- NC: ordinary concrete with compressive strength of approximately 40N/mm².
- SFRC: highly-flowable steel fiber-reinforced concrete with compressive strength of approximately 70N/mm².
- CRC: super high strength steel fiber-reinforced mortar with compressive strength of approximately 130N/mm² and 180N/mm².

3 EXPERIMENTAL RESULTS

Figure 1 illustrates the relationship between the volume fraction of steel fiber (V_f) and the slump flow. The slump flow decreased as V_f got increased on an almost constant basis, which revealed that the

Table 1 Factors and levels

Factors	levels		
	NC	SFRC	CRC
Target strength(N/mm²)	40	70	130, 180
Re-bar	D19, D32, D51		
Vf (vol%)	0	0, 0.5, 1	0, 1, 2, 3, 6

Table 2 Combination of Experiments

Type of concrete \ Re-bar	D19	D32	D51
NC	0	0	0
SFRC	1	0, 0.5, 1	1
CRC-130	0,3	0,1,2,3,6	0,3
CRC-180	3	0,3	3

Table 3 Mix proportions of NC and SFRC

	NC	SFRC-0	SFRC-0.5	SFRC-1.0
Target slump, Target slumpflow (mm)	120	650	650	650
Target air content (%)	4.5	1.5	1.5	1.5
W/B	0.55	0.38	0.38	0.38
s/a (%)	42.7	65.0	65.0	65.0
Vf (%)	0	0	0.5	1

Table 4 Mix proportions of CRC

Mix.	CRC130-0	CRC130-1	CRC130-2	CRC130-3	CRC130-6	CRC180-0	CRC180-3
W/B	0.17	0.17	0.17	0.17	0.17	0.187	0.187
S/B	1.44	1.41	1.38	1.35	1.26	1.80	1.68
Vf (vol%)	0	1	2	3	6	0	3
note	land sand	land sand	land sand	land sand	land sand	bauxite	bauxite

flowability was significantly affected by V_f. **Figure 2** and **3** show the relationship between V_f and the compressive strength and flexural strength. For CRC130, the compressive strength achieved was about 130N/mm² at 28 days age. For CRC180, the compressive strength achieved was about 200N/mm² while SFRC was at 70-80 N/mm² and NC was at approximately 40N/mm². The relationship between V_f and the compressive strength showed no significant difference in the compressive strength regardless of the increase of V_f. The flexural tensile strength increased as V_f increased for both CRC and SFRC, which shows that containing steel fibers has contributed to improve the flexural tensile strength. **Figure 4** illustrates the relationship between the compressive strength and the bond strength per diameter of reinforcing bars regardless of the presence of steel fibers. It proved that the higher the compressive strength, the higher the bond strength. As long as the compressive strength was the same, it was found more bond strength could have been achieved with less diameter of reinforcing bar so that its size effect was confirmed. This tendency was not obvious until the compressive strength reached about 80N/mm² but it was in the region with more strength. **Figure 5** shows the relationship between the reinforcing bar diameter and the bond strength for CRC130 and CRC180. The bond strengths in both cases were almost in proportion to (-1/2) - (-1/4) power of the reinforcing bar diameter.

4 CONCLUSIONS

The flowability declined as the volume fraction of steel fiber increased. The bond strength increased on an almost constant basis as the compressive strength increased. As long as the compressive strength was the same, the bond strength tended to decrease when the diameter of the re-bars got larger. This tendency was confirmed in the region where the compressive strength exceeded 80N/mm².

REFERENCES

[1] Kurita, M. and Nomura, T.:Highly-flowable steel fiber-concrete containing fly ash, Proceedings of Sixth CANMET/ACI International Conference, Bangkok, SP178, 1998.

[2] Bache, H.H.:Concrete and Concrete Technology in a broad perspective, CANMET/ACI International symposium on advanced in concrete technology, Las Vegas, 1995

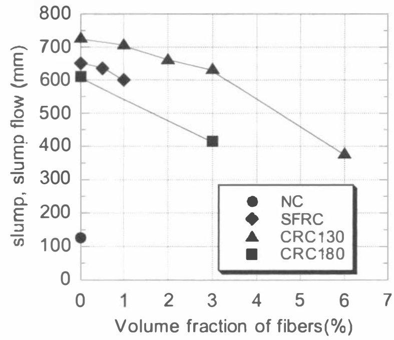

Fig. 1 Volume fraction vs. slump, slump flow

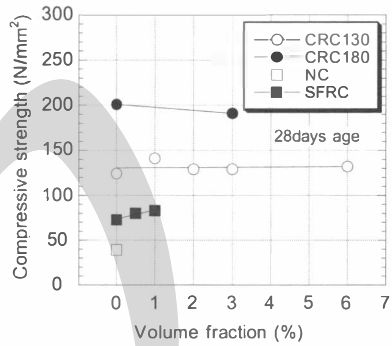

Fig. 2 Volume fraction vs. compressive strength

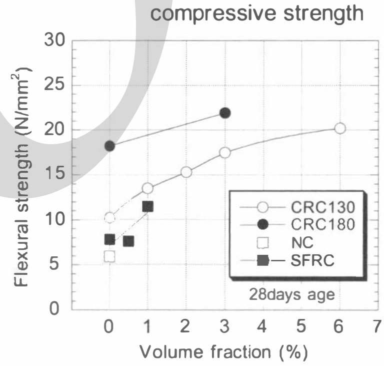

Fig. 3 Volume fraction vs. flexural strength

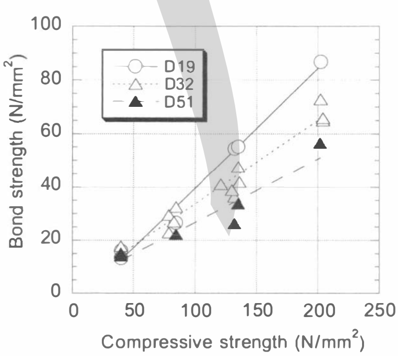

Fig. 4 Compressisve strength vs. bond strength

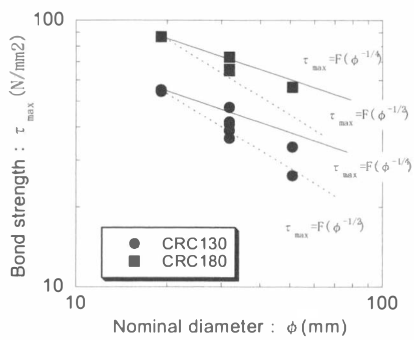

Fig. 5 Re-bar diameter vs. bond strength

THE DEVELOPMENT OF A NEW LAP SPLICE WITH HEADED ANCHOR BY GAS PRESSURE WELDING FOR PRECAST BEAMS

Masao Yamada Akira Sumi Hideki Kimura Yasumasa Miyautchi
Takenaka Corporation,JAPAN

Keywords;pre-cast,splice,lap splice,headed anchor by gas pressure welding

1 INTRODUCTION

The purpose of this reserch is rationalizing the reinforcing bar joint of precast beams in a high RC building, for the further promotion of precast concrete.

This research develops a new lap splice with headed anchor by gas pressure welding for joints of the reinforcing bar at the center of a pre-cast beam. A rational junction is possible at the central part of a beam, because the bending stress of beams is small in case of earthquake.

The headed anchor by gas pressure welding was originally developed as an anchoring method for the construction of a reinforcing bar.It forms a headed anchor (diameter of 2d, d:the diameter of main bar) at the end of a reinforcing bar. The new lap splice with headed anchor makes the joint length short by virtue of the compression effect of the headed anchor. Simple good lap splices are possible. Various experiments have been conducted in order to identity the fundamental performance of the joint.

2 EXPERIMENT PLAN AND RESULT

(1) Experiment plan

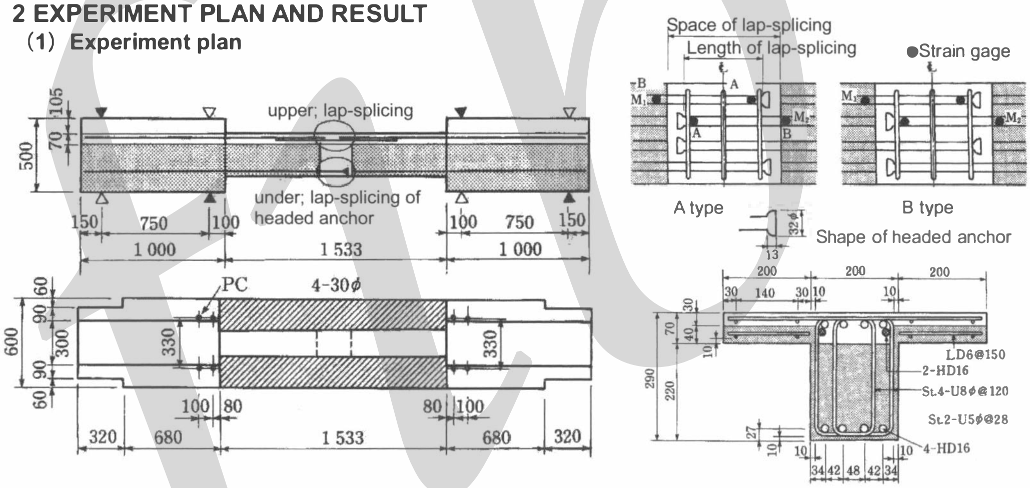

Fig.1 Details of test specimen(mm)

(2) Experimental result

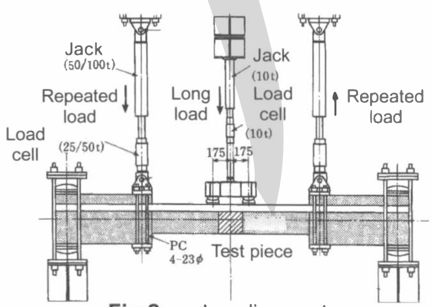

Fig.2 Loading system

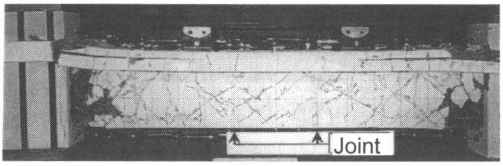

Photo 1 Final state(No.31)

3 PROPOSAL OF A DESIGNING METHOD

① The reinforcing bar of a joint part is subjected to tension as well over long periods of time as over short periods, and the stress should not exceed the permissible stress;

$$N=N_b+N_q \leqq f_a \cdot A_s \quad (1)$$

N_b;tensil force by bending moments
N_q;tensil force by shearing forces
f_a ;allowable unit stress in steel

② A bonding cleavage crack of a jointes part is not permitted over a long period of time as well as over a short period. That mean, the average bonding stress should not exceed the bonding cleavage strength τ_{co}.

$$\tau_{co}= (1.5+0.3b_i+15d_b/l_s) \cdot Ft/4 \quad (2)$$

③ Don't carry out bonding destruction to the degree of existence stress at the time of power-proof. That meam, the degree of joint part average bonding stress should not exceed the end bonding cleavage on-the-strength τ_{bu}.

$$\tau_{bu}=(1+50pw)\,\tau_{co} \quad (3)$$

pw;a ratio of stirrup

4 CONCLUSION

When satisfying the following conditions, it turns out that this new joint has a good performance

① Length of lap joint is more than 15db.
② It is made, as for a joint part, for a reinforcing bar on either side to become by turns.(B-type)
③ Concrete strength of lap joint is more than $Fc=30N/mm^2$.
④ Ratio of stirrup which a lap joint part is 0.7% or more.
⑤ The reinforcing bar may be less than D35.
⑥ The degree of long-term stress of bottom reinforcing bar is made below into $5.5kN/cm^2$ at the time of both-ends bending yeild.

By preparing a headed anchor in the reinforcing bar end of a joint part, about 1/2 joint length showed the possible thing compared with the common joint.

This new lap joint is used for Pre-cast Hight RC building. The execution of work is show in **Photo 2**.

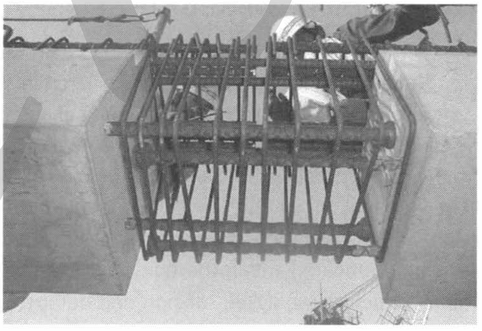

Photo 2 Execution of works

REFERENCES

[1]Sumi,A.,Yamada,M.,et al..,Study on structural behavior of PCa beams with lap-jointed main reinforcement with headed anchor by gas pressure welding., Annual paper ,JCI,Vol.20,No.3,pp.223-228,1998
[2]Sumi,A.,Kimura,H.,Yamada,M.,Miyauti,Y.,The development of the new lap splice with headed anchor by gas pressure welding for Pre-cast beam. Concrete Journal,JCI,No.425,pp.36-42,Feb.2001
[3]Yamada,M.,Sumi,A.,et al..Experimenntal studies on lap-splicing of Longitudinal deformed bars with headed anchor by gas pressure welding in RC beams(Part;3,4).outline of meeting,AIJ,pp.767-770,Sep.,1998
[4]Yamada,M.,Sumi,A.,et al..Experimenntal studies on lap-splicing of Longitudinal deformed bars with headed anchor by gas pressure welding in RC beams(Part;5). outline of meeting,AIJ,pp.615-616,Sep.,1999

STRENGTHENING OF WEST GATE BRIDGE APPROACH SPAN USING FRP COMPOSITE REINFORCEMENT

Amar Rahman, Pietro Brenni, Rob Irwin - BBR Systems Ltd., SWITZERLAND
Peter Onken - bow ingenieure, GERMANY

Keywords: FRP composite reinforcement, reinforced concrete bridge, structural strengthening

1. INTRODUCTION

The use of fibre reinforced polymers (FRP) as reinforcement for civil engineering structures is rapidly gaining in appeal. This is due to the many advantages which these types of materials afford over conventional steel reinforcement for certain types of applications. While no national design codes exist to date, several national guidelines, [1] offer the state-of-the-art in the selection of FRP systems and the design of civil engineering structures incorporating FRP reinforcement.

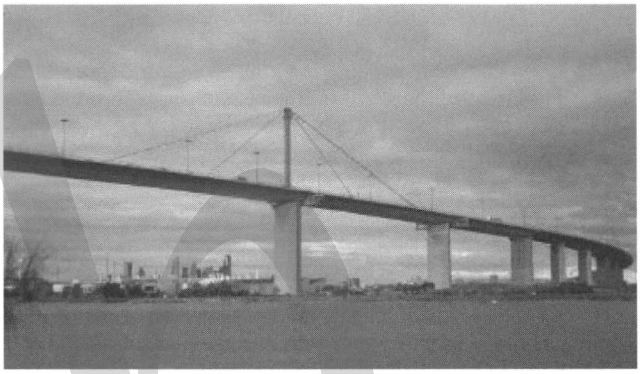

Figure 1: Overview of West Gate Bridge.

This paper outlines what is considered to be the world's largest application of FRP reinforcement in the strength enhancement of a prestressed concrete bridge, West Gate Bridge in Melbourne, Australia (Figure 1).

2. DESCRIPTION OF WEST GATE BRIDGE AND STRENGTHENING REQUIREMENTS

Due to a more than seven-fold increase in daily vehicle usage since its opening in 1978, the owner, state road authority VicRoads, decided to increase the number of lanes over a 670 m length of one of the concrete approach viaducts. This is achieved by utilizing a service lane without additional construction works on the superstructure. Also, an increase in design loads and changes in design philosophy in the most recent relevant Australian guidelines [2] compared to the 1960's code [3] were additional motivation for the strength enhancement of West Gate Bridge. A Design and Construct approach was chosen and the successful bid team provided a solution which incorporates external post-tensioning located within the box cells, together with carbon fibre reinforced polymer sheets and laminates. Structural analyses, design and detailing of the strength enhancement system was carried out by URS Australia Pty Ltd who engaged bow ingenieure of Braunschweig, Germany as specialist designers in the FRP field, while construction was carried out by Abigroup, with the assistance of Savcor Pty, Ltd. In addition to supply of the FRP reinforcement, BBR Systems Ltd, Zurich provided technical support [4].

3. STRENGTHENING SCHEME

Pre-tender analysis of the structure by VicRoads' consultants concluded that the structure had insufficient capacity in the following areas:

- Global hog of the box girder
- Combined shear and torsion near the piers
- Local sag movements in the deck slab
- Local bending capacity in the cantilever frame

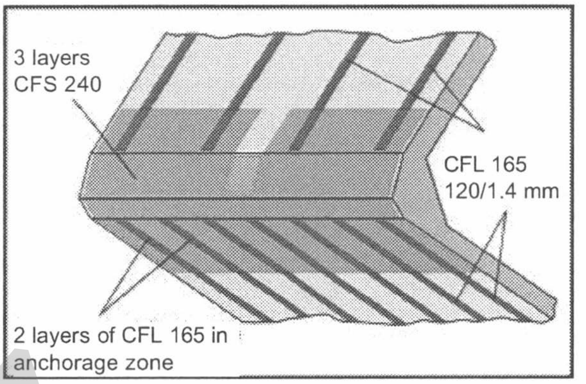

Figure 2: Detail of box girder torsional reinforcement with FRP.

The concept developed and offered by the tender team proposed enhancement of the box girder flexural capacity by means of conventional externally located, post-tensioned tendons located within the box girder cells. The other areas of concern were addressed by means of externally bonded carbon fibre reinforced polymer (CFRP) in the form of unidirectional sheets and laminates. Torsional forces were resisted by circumferential reinforcement of the box girder spine (external webs and soffit slab). Continuous shear flow reinforcement was achieved by slotting the laminates into the underside of the box girder deck slab. At the lower corner of the box girder, the web and soffit slab laminates were spliced by means of CFRP sheets wrapped around the bottom corner of the box girder (Figure 2). This area required special detailing to ensure that continuity of the reinforcement was achieved from laminate through sheet through laminate. Flexural capacity enhancement of the precast deck slab elements spanning between cantilever frames was provided by CFRP laminates, for both negative moment regions (laminates in slots cut in the deck slab) and positive moment regions (laminates bonded to the deck slab underside). Flexural enhancement of the cantilever frames combined the use of laminates and steel plates (for compression struts). VicRoads chose the solution using FRP reinforcement instead of bonded steel plates for reasons of economy. Additional material costs of FRP over steel were negated by practical aspects, as no heavy lifting, cutting or welding equipment were required as is the case with steel, and labour hours were significantly less. In addition, no disruption to traffic was necessary throughout the strengthening operations.

3. CONCLUSIONS

The Design and Construct contract was competitively won with an innovative solution to conventional steel plate technology proving to be more economical and quicker to execute. The pooled skills of the contractor, designer and technical advisors during the concept and tender stage provided the winning concept, which illustrates the advantages of D & C projects of this type.

Whilst design methods for FRP are still in their formative years, the contractor Abigroup and its designers, URS Australia assisted by bow ingenieure, Germany, aided by technical assistance in FRP technology from BBR Systems, have pioneered the large scale use of FRP for major bridge rehabilitation. The knowledge derived during the design and construct exercise will enable future major projects to proceed with confidence.

REFERENCES

[1] British UK Concrete Society Technical Report: TR-55, Design Guidance for Strengthening Concrete Structure Using Fibre Composite Materials, 2000.

[2] Austroads Bridge Assessment Group Guidelines for Bridge Load Capacity Assessment, BAG Guidelines, 1997.

[3] National Association of Australian State Road Authorities: Highway Bridge Design Specifications (NAASRA) 1965.

[4] BBR Systems, Ltd: A Guide to the Design and Application of BBR FRP Strengthening Systems, 2001.

DEVELOPMENT OF SMART CONCRETE

Hirozo Mihashi Tomoya Nishiwaki Yoshio Kaneko
Tohoku University, Sendai, Japan

Naohiro Nishiyama
Nishimatsu Construction Co., Yamato, Japan

Keywords: cracking, self-healing, thermal stress, microcapsule, self-control

1. INTRODUCTION

In recent years, smart materials have been thoroughly developed in various research fields in which a new type of material design has been incubated by the concept of installing smart functions such as sensing, processing and executing ones in the material itself. Shahinpoor [1] reported that smart materials are currently defined as materials capable of automatically and inherently sensing or detecting changes in their environment and responding to those changes with some kinds of actuation or action.

Based on such a new concept, several types of smart concrete have been developed [2-4]. In this paper, some ideas developed by the authors are presented. They are self-healing system for cracked concrete and self-controlling system for hydration heat which causes significant thermal stress. The new materials were verified by a series of experimental studies and those results are discussed.

2. DESIGN CONCEPTS OF SMART CONCRETE SYSTEM

A fundamental design concept for smart concrete of self-healing system was formulated. For achieving the sensing function, brittle pipes are embedded in concrete. Fracture of brittle pipes is induced by cracking in the concrete, and repair agent contained in the pipes penetrates into the space of cracks in the concrete.

A smart material to control the hydration heat of concrete was also developed by the authors. The new material consists of a microcapsule made with paraffin containing a hydration retarder agent. Whenever the temperature of concrete rises up to a certain degree, the microcapsule is melted releasing gradually the hydration retarder agent. As a result of the gradual release of the hydration retarder agent, the temperature of concrete is kept under the designed degree and thermal stress in the concrete structures can be controlled under a negligible level.

3. EXPERIMENTAL RESULTS AND DISCUSSION

Three point bending tests were carried out on single-notched beam specimens to verify the self-healing system for concrete. Fig. 1 shows the relation between the damage level (residual CMOD) and the strength recovery ratio for all series. It is clearly shown that the repaired specimens in the zone indicated by "*1" achieve the extremely good strength recovery. On the other hands, in case of the repaired specimens with larger residual CMOD than this zone, the repair agents used in this

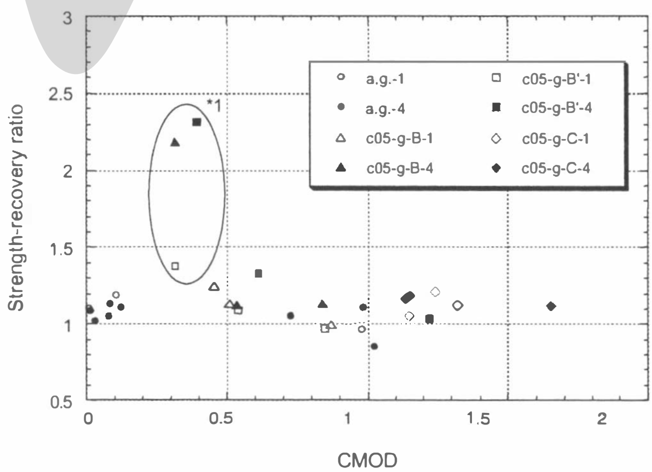

Fig. 1 Residual CMOD vs. strength recovery ratio

study didn't work well to recover the strength. Thus, it is obvious that selection of suitable repair agents and restraint of crack propagation could be very effective and important for the repair. Similar results were obtained for self-healing for water leakage, too.

Fig. 2 shows a typical relation between the time after placing concrete and the temperature of the cylindrical specimen. The increasing and decreasing rates of temperature and the peak temperature in concrete containing the microcapsules is much lower than that of plain concrete. This should lead to the mitigation of the thermal gradient in the concrete and thus the thermal stress.

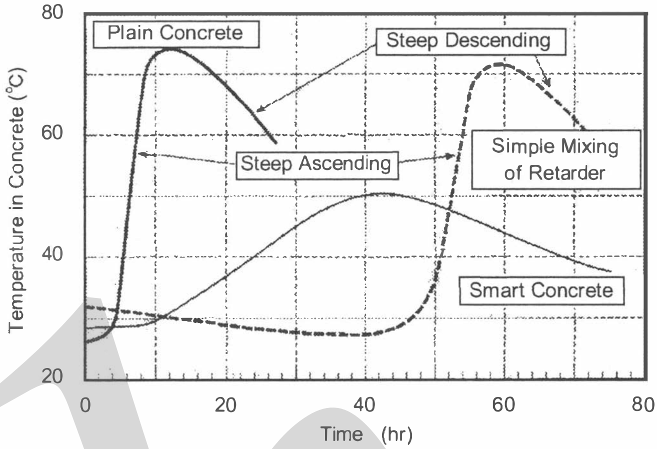

Fig. 2 Concrete temperature vs. age

4. CONCLUSIONS

The following conclusive remarks were obtained.

1) Once brittle pipes of the sensing function available for practical uses are developed, the system will work effectively to achieve the self-healing capability for both strength and prevention of water leakage. The restraint of crack propagation is an effective and important issue to achieve the self-healing capability.

2) The smart concrete containing microcapsules proved to be efficient in controlling the temperature under a certain level suitable for the steady hydration and in mitigating the thermal stress due to the heat of hydration in concrete. .

3) Results obtained in the experiments using large specimens proved that the controlling technology by means of the smart material can be applicable to practical uses in concrete technology.

REFERENCES

[1] Shahinpoor, M.: Intelligent civil engineering materials, structures and systems revisited, in Intelligent civil engineering materials and structures, Ansari, F., Maji, A. and Leung, C. (eds.), New York, ASCE, pp.44-61, 1997

[2] Dry, C.M.: Matrix cracking repair and filling using active and passivemodes for smart timed release of chemicals from fibers into matrixes, J. Smart Materials and Structures, Vol. 3, No.2, pp.118-123, 1994

[3] Mihashi, H., Nisiyama, N., Kobayashi, T. and Hanada, M.: Development of a smart material to mitigate thermal stress in early age concrete, Proc. International Workshop on Control of Cracking in Early Age Concrete, H. Mihashi and F.H. Wittmann (eds.), Sendai, Tohoku University, pp.343-350, 2000

[4] Mihashi, H., Kaneko, Y., Nishiwaki, T. and Otsuka, K.: Fundamental study on development of intelligent concrete characterized by self-healing capability for strength, Trans. of Japan Concrete Institute, pp.441-450, 2000

DEVELOPMENT OF HYBRID FIBER REINFORCED CEMENTITIOUS COMPOSITES

Hirozo Mihashi Atsushi Kawamata Yoshio Kaneko Hiroshi Fukuyama
Tohoku University Building Research Institute
JAPAN JAPAN

Keywords: fiber, hybrid, composite, ductility, cracking

1 INTRODUCTION

Concrete is one of the principal materials for structures and widely used all over the world. While advanced technologies of concrete have been recently focused especially on developping high performance concrete which possesses high compressive strength and durability, such concrete shows extremely brittle failure under shear and tension. To improve such a poor property, fiber reinforced cementitious composites (FRCC) have been developed [1]. Fibers are added not to improve the tensile strength itself but mainly to control the cracking, and to change the behavior of the cracked material by bridging of fibers across the cracks. Li [2] developed Engineered Cementitious Composites (ECC) based on a micromechanics approach, in which the volume content of synthetic fiber is less than 2%. Even with the small amount of fiber content, it has a property of pseudo-strain hardening and the ductility is much larger than that of ordinary FRCC. In the Li's work, it was clarified that bridging and snubbing of fibers on cracked surfaces under a certain condition are the key to acieve the multiple cracking which increases the ductility. However, the post peak behavior under compression is rather brittle, though ECC is extremely ductile under tension. Moreover the elastic modulus is much lower than that of ordinary concrete.

In this paper, the possibility of the hybrid fiber reinforced cementitious composites is studied to achieve a multiple phase controlling system of cracking to overcome those problem above mentioned, and the ductility is quantitatively evaluated. Three series of experimental study on FRCC are carried out, in which a specially-processed steel fiber (steel cord) is used to make FRCC more ductile. Three-point bending tests are carried out to measure the ductility. Since FRCC reinforced only with the steel cord shows brittle failure because of the high flexural-rigidity of the fiber, synthetic fibers are introduced to produce a hybrid fiber reinforcement with the steel cord. Since the matrix containing the synthetic fibers becomes more ductile, cracking resistance of the FRCC is much improved. As a result, hybrid FRCC (HYFRCC) produces a new type of cementitious composite which achieves ductile failure and high strength.

2 EXPERIMENTAL PROGRAM

Experimental studies were carried out in three test series as shown in Table 1. In the Series I, single type of fiber was mixed with cement paste, that is, steel cord and polyethylene. In Series II, the steel cord and synthetic fibers were mixed together to produce the hybrid cementitious composites. Series III was caried out to study the resisting mechanisms that are bond and snubbing of steel cord.

Used materials as the matrix in this study are Early strength Portland Cement, Silica fume, Superplasticizer and Viscous agent. Water-binder ratio (W/B) was 0.3. Various types of fibers such as steel cord, polyethylene, PVA and aramid were used and the fiber volume content was mostly 1.5 vol.%.

Table 1 Test series and experimental items.

Series	Experimental Items
I (FRCC)	single type of fiber
II (HYFRCC)	hybrid reinforced composites
III (Pull-out)	bond and snubbing

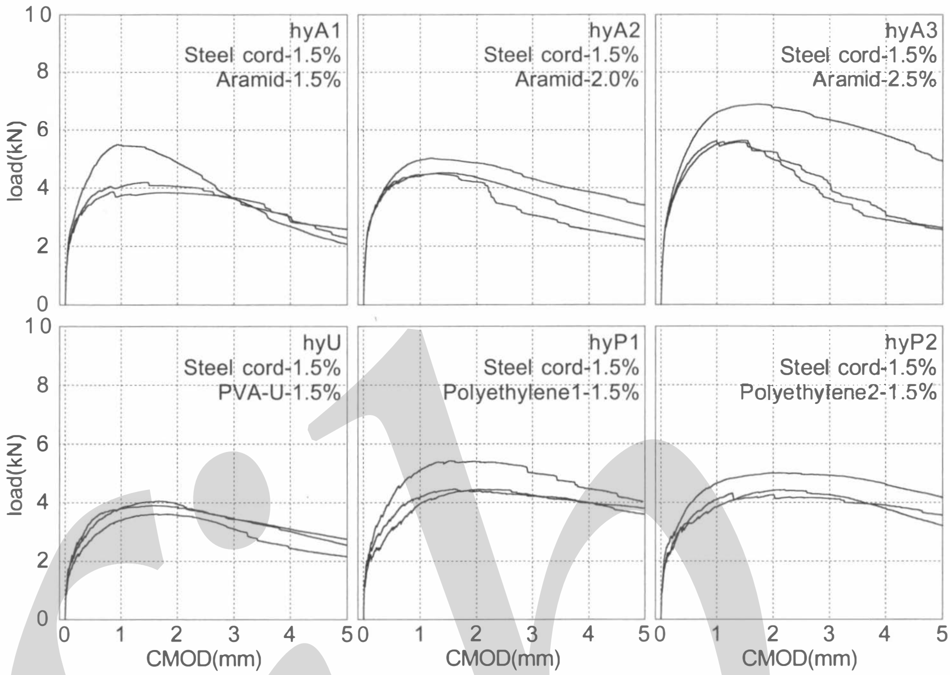

Fig. 1 Load-CMOD curves of HYFRCC in Series II.

3 EXPERIMENTAL RESULTS AND DISCUSSION

In Series I, it was shown that a single type of fiber can perform only for a limited range to resist cracking. In Series II, however, it was generally confirmed that the strength and the ductility were improved by the hybrid fiber reinforcement. Especially the strength and the post-peak ductility were improved by the hybrid fiber reinforcement in the case of PVA fiber and the polyethylene fiber.

4 CONCLUSIONS

This paper presented some results of a fundamental study on hybrid fiber reinforced cementitious composites (HYFRCC). Although even only steel cord reinforcement can work to improve the ductility of cementitious composites with a certain level, brittle macrocracking was observed near the notch of the specimens. On the other hand, multiple microcracking was observed near the notch of the specimens of HYFRCC, especially reinforced with the polyethylene fiber. The change of cracking behavior can provide HYFRCC with high-strength and high-ductility and also with the reduction of the crack width.

REFERENCES

[1] Rossi, P.: Ultra-High Performance Fiber Reinforced Concretes (UHPFRC) : An overview. Fiber-Reinforced Concrete (FRC) BEFIB' 2000, RILEM, pp.87-100, 2000.
[2] Li, V. C. and Leung, C. K. Y.: Steady-state and Multiple Cracking of Short Random Fiber Composites. Journal of Engineering Mechanics, ASCE, Vol.118, No.11, pp.2246-2264, 1992.

INNOVATIVE FOOTBRIDGE IN SEOUL
SEONYU FOOTBRIDGE

Mouloud BEHLOUL KC.LEE

Keywords: Ultra high performance concrete, Footbridge, Precasting, Tuned Mass Damper

1. INTRODUCTION

The city of Seoul is currently in the midst of a long-term project known as “New Seoul, Our Han River,” which consists in setting up easily accessible parks near the river, re-establishing the river's ecosystem, and organising a variety of cultural events. As part of this project, the city decided to create a park on this island and link it to the city by a footbridge to encourage visits by the public. Within the framework of co-operation and friendship between France and Korea and to celebrate the new millennium, a French architect, Rudy Ricciotti, was selected to design this footbridge.
The footbridge connecting Sunyudo Island to the river bank and city is 430 m long. It is composed of a 120-m arch spanning the Han River, with a steel footbridge at each end.
Rudy Ricciotti, working with the design department of Bouygues Travaux Publics, designed the arch using Ductal®. This choice allowed the bridge to have a very slender and thin structure, and it fulfilled the architect's desire to have an aesthetic and elegant arch.
Ductal® is a new generation of ultra high strength concretes that constitutes a breakthrough in concrete mix design. This family of concretes is characterised by a very dense microstructure and very high compressive strength reaching 200 MPa or more.
The arch was constructed by VSL Korea and Bouygues Travaux Publics.

2. DESCRIPTION OF THE ARCH

The 120-m arch (Fig 1.), which is composed of six prefabricated segments, is attached at each end to two massive reinforced concrete foundations. The arch has got a π-shaped cross-section (Fig 2.), consisting of a transversally ribbed upper slab and two girders. The width of this arch is 4.3 m and its depth 1.3 m. The structure is composed of a thin, 3-cm slab, which is supported by transversal ribs, each measuring 1.225 m, and two longitudinal ribs at the extremities of the transversal section. This ribbed slab is supported by two 16-cm-thick webs. The transversal ribs are prestressed by one or two 0.5” sheathed and greased monostrands. Specially adapted, small anchors were used to transfer the prestressing forces from the strands to the arch.

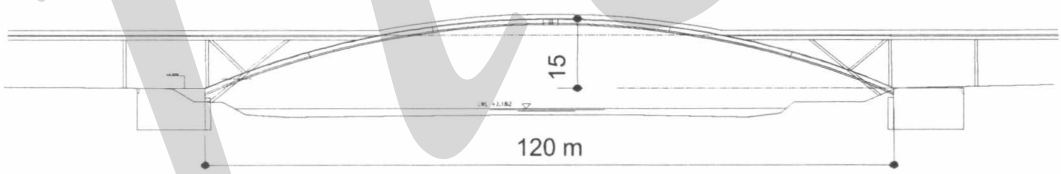

Fig 1. Elevation

In the longitudinal direction, the structure is prestressed by three tendons per web. There are nine strands in each of the lower pipes and 12 strands in the upper pipes. After completion of the stressing phase, all the pipes were grouted. The arch does not have any passive reinforcement.

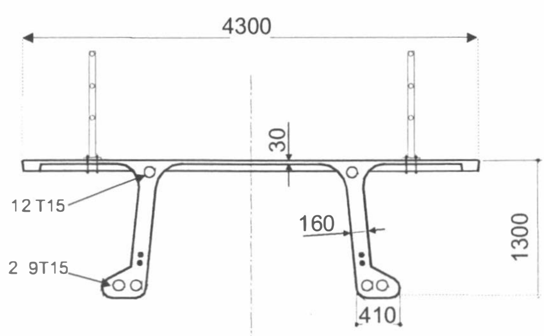

Fig 2. Transversal section

3. PRECASTING AND ERECTION

A 50-tonne steel mould was used to precast the segments. There is a cover on the top of the mould, and burlap is placed under the cover to help air escape. Polystyrene blocks are used as the mould form for the upper part of the slab. Also a 1-cm-thick polystyrene layer is added on the entire width of the formwork in order to relieve any vertical blockage.
Transversal and longitudinal keys are added in the mould to facilitate demoulding and to avert any blockage.

A special mixer provided by Bouygues is used to mix the Ductal®. This mixer makes batches of 1.5 m^3 and obtains the targeted properties: characteristic compressive strength of 180 Mpa, with a fluidity allowing for easy casting.
After demoulding, the segments are placed in a heat treatment chamber, and steam is injected. They are kept at 90°C for 48 hours.

The erection of the segments was accomplished with five temporary supports in the river. The photos opposite show the erection sequence. First, three segments, corresponding to half the arch, are positioned using a crane supported by a barge. The stitches between the segments were cast in place. After the upper part of the foundations is cast, the longitudinal cables are prestressed and the steel pipes are grouted. The same work is done on the second half of the arch.
Using two jacks, a horizontal force of 230 tons is applied between the two parts of the arch. After the central stitches are cast, the jacks are downloaded. At the end, eight continuity prestressing bars are installed and stressed

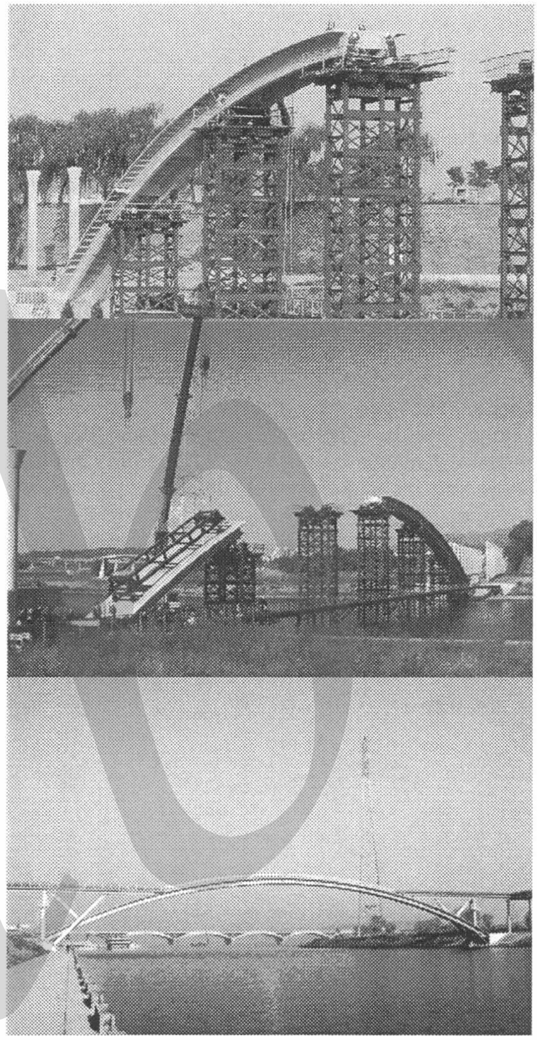

Photos 1. Arch erection sequence

4. TUNED MASS DAMPER

A special vibration study was done at an early stage of the project. The calculated natural frequencies of the arch are within the range of values that could make people crossing it uncomfortable.
Tuned mass dampers were designed to damp the vibrations of the modes next to the natural frequency cause by a pedestrian, with a limitation criteria of 0.2 m/s² for horizontal acceleration and 0.5 m/s² for vertical acceleration.
Preliminary dynamic tests were first made to determine the exact frequencies of the arch and their associated critical damping ratio. The maximal accelerations induced by a group of 30 people were also measured.
Four TMDs were designed and installed next to the central section of the arch. Control tests were then made to check the level of vertical and horizontal acceleration and verify that the comfort criteria are fulfilled.

DEVELOPMENT OF INITIAL DEFECT-FREE HIGH PERFORMANCE CONCRETE

Akihiro Hori, Tetsuya Ando,
Denki Kagaku Kogyo Co. Ltd, JAPAN

Yuichi Otabe, Yasunori Suzuki
Sumitomo-Osaka Cement Co. Ltd, JAPAN

Since high-flow concrete the utilization of which is increasing recently can produce large slump flow without generating separation so does not need compaction and so on in execution, it is exhibiting large effects in simplification of execution and in reducing noise with compaction. In addition, high compressive strength is frequently required for multistory structure and slim structure, and the demand for concrete with both high strength and high flow is increasing.

High-strength and high-flow concrete is required to use a method to decrease the water/binder ratio, to increase the unit binder quantity, or to add a thickener in order to satisfy required performance. As a result, the concrete is recognized to have tendencies to increase hydration heat and autogenous shrinkage and to be liable to thermal cracking.

As main methods to solve this problem from the material viewpoint, the use of low heat cement, expansive additive, shrinkage reducing agent, mixing materials (blast-furnace slag fine powder, limestone fine powder, etc.) may be adopted, but examples the effects of which have been quantitatively evaluated are few. Therefore, this test intends to solve the problem by proposing high-strength high-flow concrete jointly using low heat cement, expansive additive and shrinkage reducing agent, as well as to grasp the properties of the relevant concrete and to evaluate resistance to cracks caused by hydration heat and autogenous shrinkage. Furthermore, the test is to confirm the production feasibility in a real machine as well as to confirm the properties of the relevant concrete produced with the real machine by carrying out a model test using a concrete sample mixed in a ready-mixed concrete plant.

Table 1 Mix proportion of concrete

Mix No.	water-binder ratio (%)	s/a (%)	kind of cement	unit content(kg/m³) water	cement	EX1 *1	EX2 *2	S1	S2	G1	SR *3	AD (kg/m³)	AE (kg/m³)
1	34.6	53.6	low heat	184	506	25	—	580	248	747	16.0	4.8	0.02
2	34.8			184	504	—	25				16.0	4.8	0.02
3	34.6			184	502	30	—				—	4.8	0.03
4	34.8			184	499	—	30				—	4.8	0.03
5	34.3			184	535	—	—				—	4.8	0.03
6	36.0		ordinary	185	515	—	—				—	6.7	0.04

*1,*2: expansive additive
*3: shrinkage reducing agent

Mix No. 1 and No. 2 are the concrete proposed in this paper, and are jointly using expansive additive and shrinkage reducing agent in low heat cement. No. 3 and No. 4 are not added with shrinkage reducing agent, and No. 5 is not added neither expansive additive nor shrinkage reducing agent. No. 6 is a composition using ordinary Portland cement as cement, and is a blank for No. 1 - No. 5. All the concrete specimens are of mix having 60 N/mm^2 or higher as compressive strength at material age of 56 days, 65±10 cm as target slump flow, and 4.5±1.5% as target air quantity.

Evaluation of crack resistance of concrete above was carried out with a thermal stress testing apparatus shown in Fig. 1 and Photo 1.

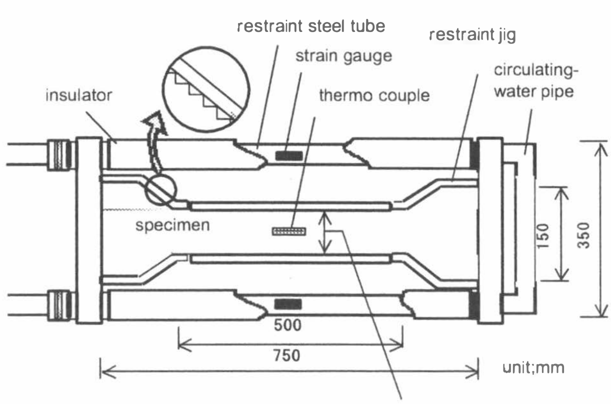

Fig. 1 Thermal stress testing apparatus

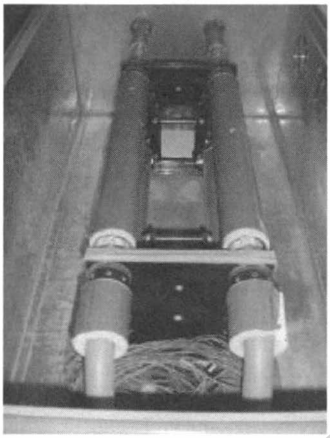

Photo 1 Testing apparatus

The measured stress to evaluate crack resistance of concrete is shown in Fig. 2. In comparison of tensile stress, the tensile stress generated at material age of 10 days was smallest in Mix No. 1 and No. 2 then increased in the order of Mix No. 3 and No. 4, No. 5, No. 6. Namely, in high-strength high-flow concrete using ordinary cement the stress generated accompanying with hydration heat and autogenous shrinkage is relaxed by changing cement to low heat cement, and the effect was promoted by using expansive additive. It was also confirmed that joint use of expansive additive and shrinkage reducing agent synergetically increases the effect.

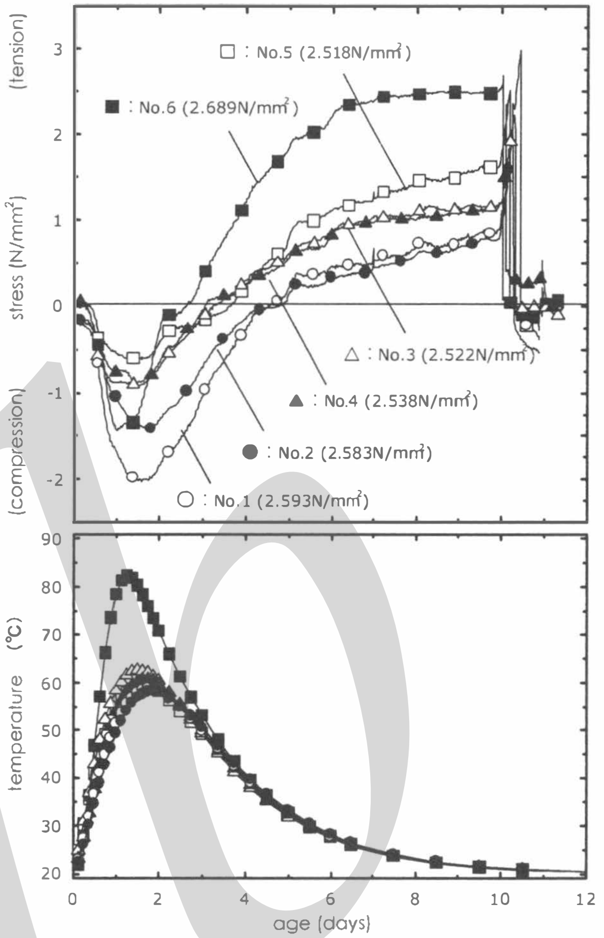

Fig. 9 Temperature stress measurement results

This study intends to propose a concrete composition which has resistance to crack generation from hydration heat and self shrinkage while satisfying high flow and high strength, and to grasp basic properties of the relevant concrete and evaluate the crack resistance with concrete values. The conclusions obtained within the range of this experiment are summarized as follows:

(1) It was confirmed that concrete with small self shrinkage and drying shrinkage as well as resistance to carbonation and crack formation can be obtained by using a high-strength high flow concrete composition proposed in this paper, namely, using low heat cement as cement and jointly using expansive additive and shrinkage reducing agent.

(2) It was confirmed that the effect of expansive additive, namely, introduction of expansion strain and compressive stress crack reduction effect is increased by joint use of expansive additive and shrinkage reducing agent compared with the composition using expansive additive only.

(3) It was confirmed that the concrete proposed in this paper is fully possible to produce with a real machine in a ready-mixed concrete plant, and the produced concrete has equivalent properties to concrete prepared in a laboratory test.

INCOMPATIBILITY BETWEEN CEMENT AND SUPERPLASTICIZER AND THE PREVENTION METHOD

Kazuo YAMADA and Shunsuke HANEHARA
Central Research & Development Center
Taiheiyo Cement Corporation, JAPAN

Keywords: incompatibility, polycarboxylate, superplasticizer, adsorption, sulfate ion

1 INTRODUCTION

Superplasticizer (SP) is one of the key materials for high performance concrete. Because of its superior dispersing effect of cement particles, it is possible to increase the fluidity even at low water cement ratio. Another important role of SP is fluidity retention. There are various requirements in the practical concrete works, therefore, many kinds of SP have been developed.

However, the fresh properties of concrete containing SP can be affected by various factors of ingredients and environments and the fresh properties are varied occasionally. These unexpected behaviors of fresh concrete have been called as incompatibility problems. In order to overcome these problems and to control the fresh properties of concrete, the working mechanisms of many kinds of SP such as poly-beta-naphthalene sulfonate (BNS) and polycarboxylate with polyether graft chain (PC) were studied. As a result, the working mechanisms have been elucidated in some degree for the fluidity just after mixing and the fluidity change with time[1)]. Moreover, some prevention methods of the incompatibility have been proposed based on cement characteristics and solution chemistry[2)]. The characteristics of cement and the solution chemistry however, can be affected by various factors such as the types of raw materials of cement, the processing conditions of cement and concrete and it is not easy to control constant. Therefore, it is convenient that the incompatibility can be prevented by modifying of the chemical structure of SPs.

Based on the information, one example preventing the incompatibility caused by the fluctuation of cement characteristics is demonstrated in this study by optimizing the composition of PC.

2 PREVENTION METHOD THE INCOMPATIBILITY

Because of the characteristics of PC, the fluidity just after mixing and the fluidity retention should be improved simultaneously. As for the fluidity just after mixing, the incompatibility can be minimized by enhancing the adsorbing ability of PC[3)]. This type of PC can be adsorbed onto cement hydrates in a similar manner regardless of the sulfate ion concentration. However, the fluidity retention is very poor because this type PC does not remain in the aqueous phase much. Therefore, some components that show fluidity retention effects are blended in the high-adsorbing-type PC.

3 BLENDING EFFECT OF PC (MORTAR)

At first, the blending effect of PC is examined. Characteristics of cement used (C1-1 & C3-1) are summarized in **Table 1**. Although C1-1 needs more dosage of PC than C3-1 to achieve same fluidity, the fluidity retention of C1-1 is better than C3-1. Five commercial PCs are used in this study as shown in **Table 2**. PC1 is a standard PC for high strength concrete for ready mixed concrete plants. PC2 and PC3 show higher adsorbing ability. PC3 and PC4 shows higher fluidity retention effect. PC1 is selected as the standard, PC2 or PC3 is mixed as high adsorbing ability type and PC4 and/or PC5 is mixed as fluidity retention type as shown in **Table 2**.

The flow of mortar was measured as the index. The water cement ratio (W/C) is 0.35 and the sand cement ratio was 2.0. ISO standard sand was used. Flow was measured by using a flow cone specified by JIS R5201.

The relationship between PC dosage and flow is shown in **Fig. 1** and the change with time is shown in **Fig. 2**.

Table 2 Mix proportion of PC (mass%)

	Std.	High ads.		Fl. retention	
	PC1	PC2	PC3	PC4	PC5
PC6	30	40	-	30	-
PC7	24	32	-	24	20
PC8	40	-	20	-	40

Table 1 Characteristic of cements (Normal Portland cement)

	Blaine	ig.loss	insol.	SiO_2	Al_2O_3	Fe_2O_3	CaO	MgO	SO_3	Na_2O	K_2O	f.CaO	s. R_2O	Hm	C_3A	C_4AF
C1-1	3310	1.27	0.08	21.54	5.65	2.85	64.16	1.30	2.08	0.24	0.40	0.5	0.64	49	10.2	8.7
C3-1	3100	1.99	0.07	21.06	5.06	2.90	64.74	1.09	1.97	0.15	0.30	0.8	0.23	20	8.5	8.8
C2-2	3820	0.99	0.07	21.88	5.95	2.99	62.07	2.46	2.16	0.30	0.42	0.9	0.51	87	10.7	9.1
C3-2	3130	1.74	0.47	20.23	5.41	2.91	64.85	1.36	1.99	0.16	0.32	0.7	0.38	37	9.4	8.8

Hm: Mass ratio of $CaSO_4.1/2H_2O$ in the total of $CaSO_4.1/2H_2O$ and $CaSO_4.2H_2O$. s.R_2O: Soluble alkaline.

When various PC dosage is compared with the different kinds of cement at the flow of 220mm, PC6 and PC7 show less difference than PC1. The change with time are negligible in the case of C1-1 for every PC. In the case of PC3-1, only PC7 shows less fluidity loss by half compared to others.

These results indicate that the incompatibility between cement and PC can be minimized when PC7 is used. It is difficult to minimize the incompatibility by simply blending a PC that shows good performance just after mixing and a PC that shows good fluidity retention effect. It is necessary to optimize the combination for this aim.

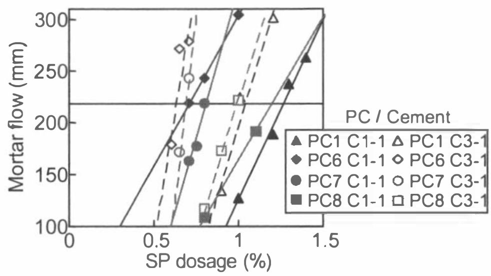

Fig. 1 Dosage of blended PC and mortar flow

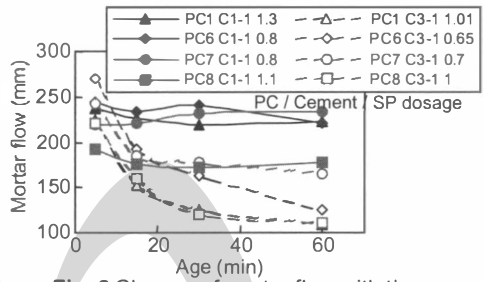

Fig. 2 Change of mortar flow with time

4 DEMONSTRATION OF THE OPTIMIZED PC IN A FORM OF HIGH-FLUIDITY CONCRETE

The effect of blending of PC is demonstrated by the high-fluidity concrete. Cements used in this concrete test (C2-2 & C3-2) are shown in **Table 1**. C2-2 needs more dosage of PC than C3-2 to achieve the same fluidity. The flow retention of C2-2 is better than C3-2. PCs used are several commercial PCs: PC1, PC9, and PC10 for high strength concrete and the specially synthesized PC: PC11. The mix proportion of high-fluidity concrete was as follows: G_{max}=20mm, W/C=0.37, cement content=400 kg/m^3.

The relationship between PC dosage and slump flow for each combination of PC and cement is shown in **Fig. 3** and the change with time is shown in **Fig. 4**. When the various dosages for the slump flow of 650mm are compared, the order of dosage is PC1 < PC10 < PC11 << PC9. The difference of the dosage between two cements is in the order; PC1=PC11=PC10<PC9. The change with time from the slump flow of 650 mm is in the order; PC9=PC11<PC1=PC10. The difference of the change with time between two cements is in the order; PC9=PC11< PC1=PC10.

From these results, it is concluded that PC11 can minimize the differences of the PC dosage for a constant fluidity and the change of fluidity with time when the cements being used are different.

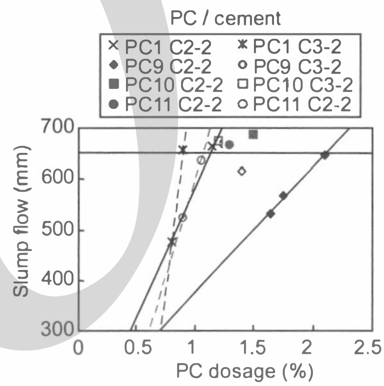

Fig. 3 PC dosage and slump flow

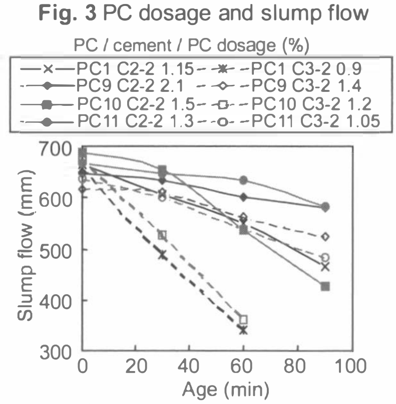

Fig. 4 Change of slump flow with time

5 CONCLUSIONS

In order to prevent the incompatibility problems between cement and SP, based on the understanding of the working mechanisms, a prevention method is indicated. It is demonstrated that the incompatibility between cement and PC can be minimized by adjusting the composition of PC.

REFERENCES

[1] Yamada, K. and Hanehara, S.: Interaction mechanism of cement and superplasticizers -The roles of polymer adsorption and ionic conditions of aqueous phase. Concrete Science and Engineering, Vol. 3, No. 9, pp. 135-145, 2001

[2] Yamada, K., Ogawa, S. and Hanehara, S.: Controlling the adsorption and dispersing force of polycarboxylate-type superplasticizer by sulfate ion concentration in aqueous phase. Cement and Concrete Research, Vol. 31, No. 3, pp. 375-383, 2001

[3] Yamada, K., Ogawa, S. and Takahashi, T.: Improvement of the compatibility between cement and superplasticizer by optimizing the chemical structure of the polycarboxylate-type superplasticizer. Proc. of the 2nd Int. Symp. on SCC, pp. 159-168, 2001

CHARACTERISTICS OF FIBER COMPOSITE CONCRETE AT HIGH TEMPERATURES

Mahmoud Abo El-Wafa Ph.D. Candidate
Masuo Yabuki Ph.D. Candidate
Toshiki Ayano Associate Professor
Kenji Sakata Professor
Department of Environmental and Civil Engineering
Okayama University, JAPAN

Keywords: fibrous concrete, high temperatures, surface cracking, mechanical properties

1 INTRODUCTION

At present, fiber reinforced concrete is steadily developing. Among the various types, polypropylene fiber composite materials with low fiber contents appear to be the most attractive due to ease of processing. The use of polypropylene fibers at low fiber volume fractions improves many aspects of the production and application of fiber reinforced concrete, including shrinkage and crack control [1]. The paper describes tests on (ϕ100 x 200 mm) concrete cylindrical specimens containing either polypropylene or steel fibers with a constant volume ratio (0.5 %). They are heated to temperatures in the range of 125 – 1000 °C to determine the effect of some variables such as; maximum temperature levels, rate of heating to maximum temperature level, holding time at maximum temperature level on the mechanical properties of fibrous concrete.

2 EXPERIMENTAL PROGRAM

The proportioning of the concrete mixtures for testing is summarized in Table 1. Fig. 1 shows a typical curve of temperature profile during the heating process.

Table 1 Mix proportion of concrete

Max. Size (mm)	Air (%)	Slump (mm)	W/C (%)	S/a (%)	Weight per unit volume(kg/m^3)				
					W	C	S	G	SP
20	2.0	150	46	45	159	350	800	1,040	1.75

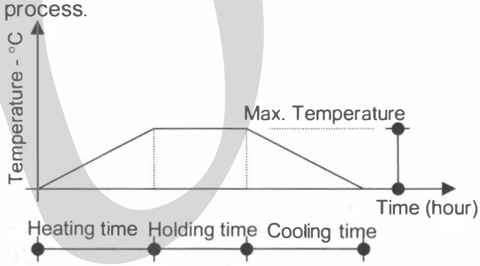

Fig. 1 Temperature profile during the heating process

3 EXPERIMENTAL RESULTS AND DISCUSSION

3.1 Maximum temperature levels

The exposure of concrete to high temperatures alters the microstructure in different ways. Initially, the temperature elevation results in the elimination of the water contained in the pore system and the consequent contraction of the paste with crack formation. Photos 1 and 2 show a group of specimens which are exposed to different temperature degrees (250, 500, 750 and 1000 °C). It is observed that the specimens, which have been exposed to high temperatures, show significant surface cracking, which is more evident in the plain concrete than in the fibrous concrete. Figs. 2 and 3 show the losses of concrete strength and Young's modulus appear to increase with increasing temperature degree of the fibrous concrete.

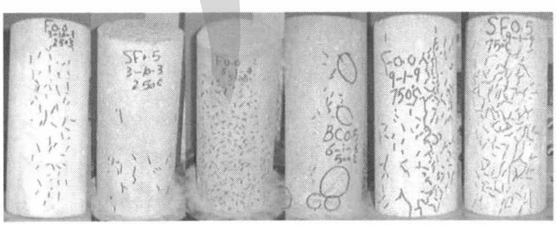

Photo 1 Effect of different temperatures on surface cracking

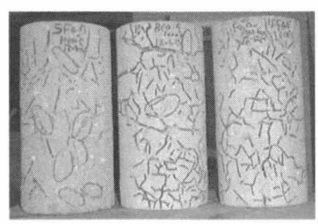

Photo 2 Surface cracking at 1000 °C

3.2 Rate of heating to maximum temperature level

Fig. 4 illustrates the group of specimens exposed to different rates of heating to a maximum temperature level. It is noticed that there are descending and ascending paths for the loss of concrete strength and this depends on the rate of heating to the maximum temperature level and the type of fibrous concrete. Also, it is clearly seen that the specimens reinforced with polypropylene fibers have the ability for carrying a higher rate of heating than the specimens reinforced with steel fibers and without fibers.

3.3 Holding time at maximum temperature level

As can be seen from Fig. 5, there is also a considerable variation in the loss of Young's modulus values, indicating that the different holding times at maximum temperature level have an effect on the loss of Young's modulus of fibrous concrete.

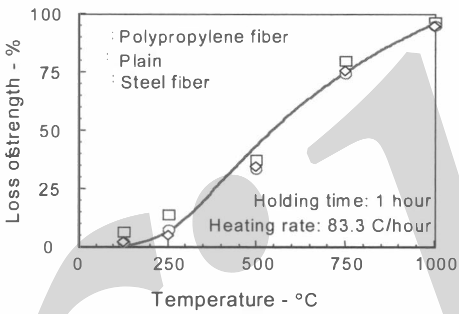

Fig. 2 Effect of temperature on loss of strength

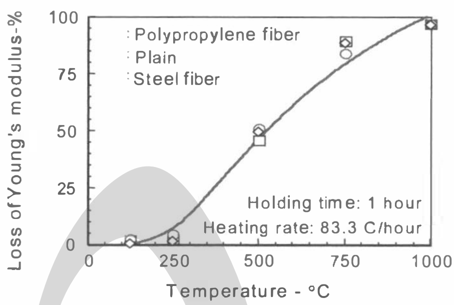

Fig. 3 Effect of temperature on loss of Young's modulus

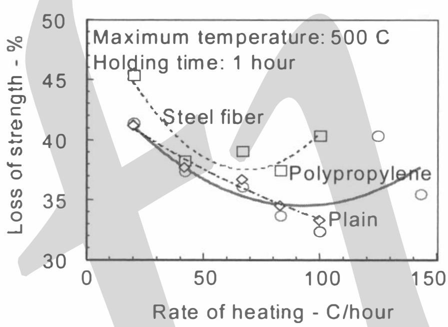

Fig. 4 Effect of different rates of heating on loss of concrete strength

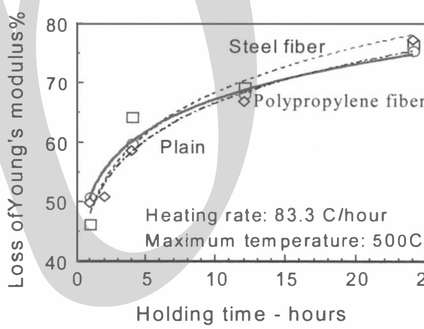

Fig. 5 Effect of different holding times on loss of Young's modulus

4 CONCLUSIONS

The experimental program was performed to investigate the mechanical properties of fiber composite concrete exposure to high temperatures in the range of 125–1000 °C. The results clarify that the changes in the mechanical properties of fibrous concrete on heating are due to a series of complex physical and chemical phenomena, which take place within the concrete. From these results, it is possible to appreciate the way the alteration of the fibrous concrete is reflected on the modification of its mechanical behavior at high temperatures. It is evident that the defects generated by the high temperatures enhance surface cracking propagation, reducing the stiffness, and affecting the fracture energy of the fibrous concrete. The risk of explosion increases with increasing the rate of heating to the maximum temperature level. The presence of steel fibers does not reduce the risk of explosion. On the contrary, within the same series, specimens with polypropylene fibers are most likely not to fail. The specimens reinforced with polypropylene fibers have the ability for carrying a higher rate of heating than the specimens reinforced with steel fibers and without fibers.

5 REFERENCES

[1] Ayano, T., Abo El-Wafa, M., Yabuki, M., and Sakata, K.: Resistance to cracking due to drying shrinkage by polypropylene fiber, Proceeding of the 2001 Second International Conference on Engineering Materials, San Jos, CA, U.S.A., pp. 705-712, 2001.

PRE-GROUTED PC MATERIAL WITH MOISTURE REACTIVE EPOXY RESIN

Keiichi Aoki
Japan Highway Public Corporation.
Japan

Kunihiro Mukai
Sumitomo Construction Corporation.,Ltd.,
Japan

Ryuuichi Takagi
P.S Corporation.,Ltd.,
Japan

Yoshihiko Touda
Sumitomo Electric Industries.,Ltd.,
Japan

Keywords: Grout, Prestressing Strand

1 INTRODUCTION

The Pre-Grouted Prestressing Strand is composed of prestressing steel coated with special epoxy resin and covered with a corrugated plastic sheath, as shown in Fig. 1. With controllable hardening time, initially it behaves as an 'unbonded' prestressing strand and finally behaves as a grouted (bonded) prestressing strand. [(1)]

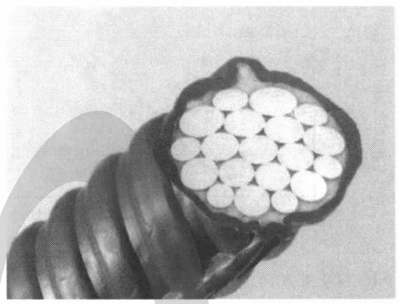

Fig.1 Pre-Grouted Prestressing Strand

The Pre-Grouted Prestressing Strand provides (A) anti-corrosion properties, due to the epoxy resin and the seamless polyethylene plastic wrapped around the bare material, (B) effective site work by elimination of the grouting process, which sometimes creates serious problems in quality, through improper grouting. After several evaluation programs, the Pre-Grouted Prestressing Strand has been applied to various concrete structures and is now regularly applied to transversal tendons for prestressing bridge decks. In this context, it was considered desirable to apply the Pre-Grouted Prestressing Strand to the main cable (longitudinal tendon) of the bridges girders as an alternative to the conventional grouting process. Normally the main cable should contain several temperature zones - in the massive concrete section, for example, the concrete generates excessive heat due to a hydration reaction during the concrete cure. To apply the Pre-Grouted Prestressing Strand to the main cable safely, new technology had to be developed to reduce the temperature sensitivity of the product.

This report discusses the latest technology applied to the Pre-Grouted Prestressing Strand; specifically, the 'Moisture Reactive Resin Technology' and its evaluation test results.

2 DEVELOPMENT OF THE NEW PRE-GROUTED PRESTRESSING STRAND

2.1 Application to Main Cables

During the curing process, prestressing materials placed in the massive concrete area may be heated up to 90°C, which exceeds the temperature range required to control the hardening time of the conventional Pre-Grouted Prestressing Strand (Fig. 2). To apply the Pre-Grouted Prestressing Strand to the main cable (which normally contains a massive concrete zone), the resin used in the Pre-Grouted Prestressing Materials has to exhibit low temperature dependence.

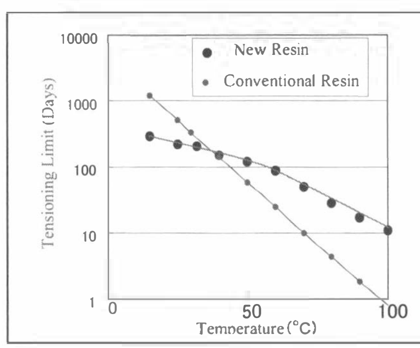

h tensioning limit of the new resin and conventional resin. (Samples exposed to constant temperature.)

2.2 Moisture Reactive Resin Technology

To reduce temperature dependence, 'Moisture Reactive Resin Technology' was introduced in the new Pre-Grouted Prestressing Strand. Generally, when an epoxy resin hardens, molecules of epoxy form a 3-dimensional structure with a support of a hardener that works as their 'connector'.

As shown in Fig. 3, the developed resin contains a hardener that is originally sealed by a 'capsule'. As Step-1, each capsule is gradually removed by a small quantity of moisture contained in the epoxy resin. This process is not influenced by temperature. The desiccant material contained in the resin absorbs extra moisture, which may come from the strand end or penetrate through the polyethylene, possibly accelerating epoxy curing. As Step-2, the epoxy molecule starts bridging (hardening) by the hardener. The conventional resin relied only on this process.

With 'Moisture Reactive Resin Technology', even prestressing strands are exposed to an environment of 100°C, the tensioning work can be done for up to 10 days as shown in Fig. 2.

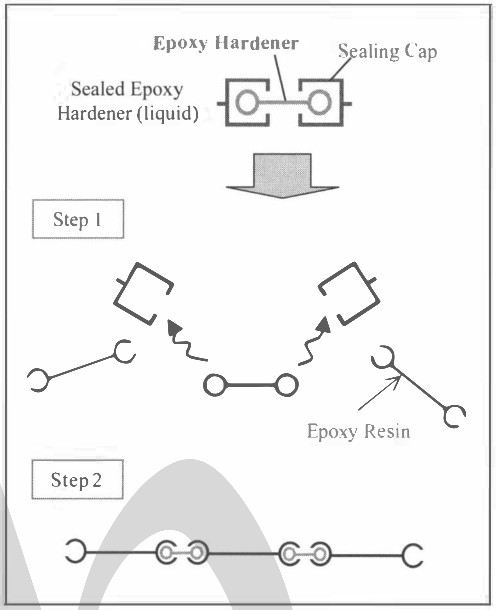

Fig.3 Hardening mechanism of the new resin

2.3 Estimated Tensioning Limit and Complete Hardening time in Actual Situations

Fig. 2 shows the tensioning limit when the Pre-Grouted Prestressing Strand is exposed to constant temperature. During actual bridge construction, after the temperature reaches its highest point, it then decreases to the outside temperature. Table 1 shows the estimated tensioning period limit and the complete hardening time as applied to the typical range of temperature in actual bridge constructions.

Table 1 Estimation of Hardening Time at Actual Use

	Maximum Concrete Temp	Average Outside Temp	Tensioning Period Limit	Hardening Period
Massive Concrete at hot region	95°C	28°C	1 Month	1-1.5 Years
Slab Concrete at Clod region	75°C	8°C	3 Months	2 Years

3 APPLICATION TO ACTUAL CONSTRUCTIONS

From August 2001, the Pre-Grouted Prestressing Strand has been applied to the main cables in the actual structures at Ichinomiya Kouka Bridge, Murahigashi Daini Kouka Bridge, Zaikeduka Kouka Bridge, Okoba River Bridge, Nobeno Kouka Bridge, Iburodani Bridge, and Nobeno Kouka Bridge. Fig 4 shows views of these construction sites.

To avoid damages to the polyethylene sheath, special attention is paid to using tools such as turn table for pay-off, guide rolls for installation pass line, and the like.

Fig.4 Site View of construction

REFERENCE

(1)Development of 'After-Bond' Prestressing Steel, Kazuo Suzuki, Osaka University, Takeshi Kobayashi, Sinko Wire Company Ltd., Toyokazu Minami, Shinko Wire Company Ltd., FIP – XIth International Congress on Prestressed Concrete, June 1990.

FUNDAMENTAL PROPERTIES AND FREEZING AND THAWING RESISTANCE OF EAF SLAG AGGREGATE CONCRETE

Han-Young Moon, Jung-Hoon Yoo, Woo-Yul Baek Seong-Soo Kim
Hanyang University in Korea Daejin University in Korea

Keywords: aging; electric arc furnace slag aggregate; expansion; freezing and thawing;

1 INTRODUCTION

Blast furnace slag is a high-valuable material that could be utilized as cementitious material and aggregate for concrete. On the other hand, electric arc furnace slag is unvalued material that can be utilized only in the road construction because of volume instability.

Generally natural aggregate is relatively stable and does not enter into complex chemical reactions with water. Unfortunately, however, electric arc furnace slag aggregate contains a small amount of free lime. The hydration of lime makes electric arc furnace slag aggregate unstable and liable to expand.

Hotwater and steam aging methods are common to stabilize electic arc furnace slag aggregate. Those also reduce the expansion for application in road construction. In case of aggregate for concrete, however, not only expansion of slag aggregate, but also durability of concrete is taken into consideration.

2 PROPERTIES OF EAF SLAG AGGREGATE

Non aging electric arc furnace slag aggregate shows maximum volume expansion in Fig. 1. Any aging method decreases the expansion of electric arc furnace slag aggregate. The reason is that the unstable free CaO in electric arc furnace slag aggregate is hydrated by hotwater or steam.

The capacity of $Ca(OH)_2$ must be known from electric arc furnace slag aggregate. We know $Ca(OH)_2$ dehydrates to CaO and H_2O at maximum, 550• . The weight of $Ca(OH)_2$ is

Table 1. $Ca(OH)_2$ of EAF Slag Aggregate (%)

Non aging	Air 1 mon.	Hotwater 1 d.	Hotwater 3 d.	Steam 3 d.	Steam 5 d.
0.1010	0.3525	0.6050	0.8620	0.8000	0.9420

$Ca(OH)_2$ from electric arc furnace slag aggregate is arranged in aging methods in table 1. This is that free CaO in it is changed into $Ca(OH)_2$ after reacting with H_2O. In this table, the more $Ca(OH)_2$ is, the more stabilization is in electric arc furnace slag aggregate.

The more exposed time to hotwater or steam is, the more $Ca(OH)_2$ is generated from electric arc furnace slag aggregate except air aging. In same exposed time, more $Ca(OH)_2$ is generated in hotwater than steam from electric arc furnace slag aggregate. Hotwater aging method has the most effect of stabilization on electric arc furnace slag aggregate than steam aging from Fig. 1 and table 1.

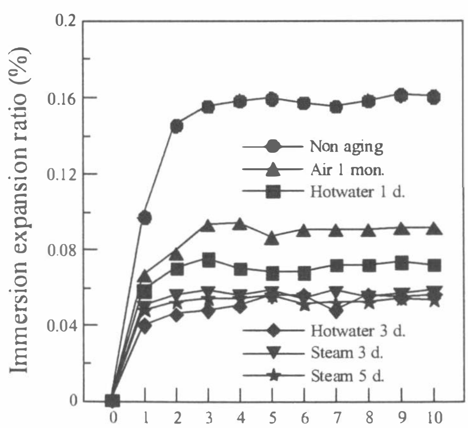

Fig. 1. Immersion Expansion Ratio of EAF Slag Aggregate

3 STRENGTH OF EAF SLAG CONCRETE

Fig. 2 is the relationship between the compressive strength of concrete and maximum immersion expansion of electric arc furnace slag aggregate.

There are harmful aggregate reactions in concrete that take place without the presence of alkalies. For instance, CaO, which can occur in slag, reacts with water. Such particles expand individually, producing uneven stress, and those that are close to an exposed surface produce popouts. In contradistinction with the aggregate reactions discussed above, there are reactions between aggregate and cement paste that are favorable for the concrete. The characteristic of these is that the reaction is not accompanied by excessive volume changes. For instance, a limited chemical reaction is believed to be beneficial with respect to the bond between the aggregate and paste. In Fig. 2, the more expansion of aggregate is the more compressive strength at early age, 7 days is. This expansion, especially in air aging electric arc furnace slag aggregate, makes bonds between the slag aggregate and paste dense. But in the long term, it is thought this expansion makes uneven stress gradually. At 91 days, strength of air aging electric arc furnace slag aggregate concrete therefore doesn't increase.

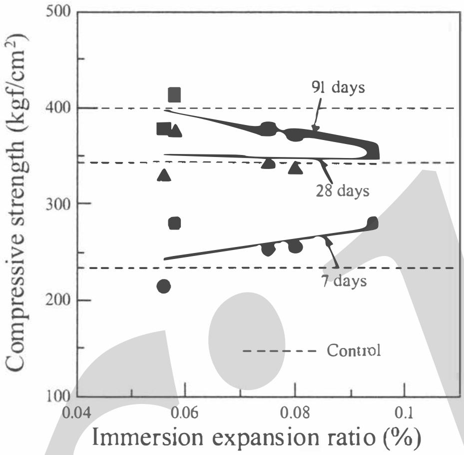

Fig. 2. Relationship between Immersion Expansion and Compressive Strength

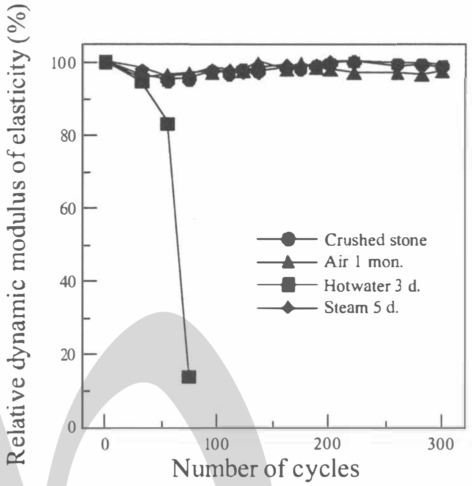

Fig. 3. Relative Dynamic Modulus of Elasticity of Concrete

4 FREEZING AND THAWING RESISTANCE OF EAF SLAG CONCRETE

Electric arc furnace slag aggregate concretes treated with air and steam aging are not different with the control concrete in relative dynamic modulus of elasticity in Fig 3. But hotwater aging electric arc furnace slag aggregate concrete has shown the failure before 75 cycles.

The frost resistance of properly air-entrained concretes made with different aggregate is determined by the internal structure, especially the pore structure of the aggregate, by its composition, and by the particle size. For instance aggregate having absorption of about 0.5% by weight or less are usually frost resistant under any practical circumstances. On the other hand, critically saturated aggregate of higher absorption can cause freezing failure because of high internal hydraulic pressure developed in the aggregate. In electric arc furnace slag aggregate, the absorption is about 1.6~2.0.

In hotwater aging, it is thought that unstable materials in electric arc furnace slag aggregate flow out into water, but in steam aging it doesn' t. This increases the small pores of hotwater aging electric arc furnace slag aggregate somewhat. This pore-size difference causes failure of concrete in frost action.

5 CONCLUSION

(1) The expansion of electric arc furnace slag aggregate processed by hotwater or steam aging is much lower than that of non aging. The reason is that the unstable free CaO inside non aging electric arc furnace slag aggregate reacts with H_2O.

(2) Compressive strength of steam and hotwater aging electric arc furnace slag aggregate concrete are good quality. But that of air aging concrete doesn't increase after 28 days. From the viewpoint of durability of concrete, hotwater aging electric arc furnace slag aggregate concrete has some problem.

(3) Considering properties of electric arc furnace slag aggregate, strength and durability of concrete using electric arc furnace slag aggregate collectively, sufficiently stabilized electric arc furnace slag aggregate by steam aging might have potentialities for concrete aggregate in the scope of this study.

TECHNOLOGICAL PROBLEMS OF MULTI-PERFORMANCE POROUS CONCRETE

Abderrazak Zouaghi
Technical Research Center, Kyowa Concrete Industry Co. Ltd. Japan

Takao Nakazawa
Miyazaki University, Japan

Fumio Taguchi
Civil Engineering Research Institute of Hokkaido, Japan

Keywords: required functions, required properties, optimum water-cement ratio, mixing methods, compaction methods and degrees

1 INTRODUCTION

Multi-performance porous concrete is a special type of lightweight concrete in which the fine aggregate has been partially or completely omitted. The porous concrete is designed to obtain higher percentage of continuous voids. The continuity and the higher percentage of pores make the material well suitable to store rainwater and control stormwater run-off; to improve water quality; to provide a drainage system and construction platform for concrete pavements; to be used as permeable concrete pavement; as greening concrete; as organism adaptable concrete; as an absorbing cover for noise, and so on. Consequently, this multi-performance porous concrete represents in someway a new avenue for the environment conservation and protection. However, as represented in **Fig.1** for any application the required functions and proprieties that porous concrete should fulfill depend on the percentage of voids. Up to date, all mixture proportioning are based mainly on the "desired percentage of voids ". Generally, these attempts do not consider one or more factors concerning the design and construction of porous concrete such as the search for optimum water-cement ratio, effect of mixing methods and effect of compaction methods and degrees etc. Therefore, the present research intends to clarify the effects of the above factors and concludes with a proposal for a method of proportioning porous concrete.

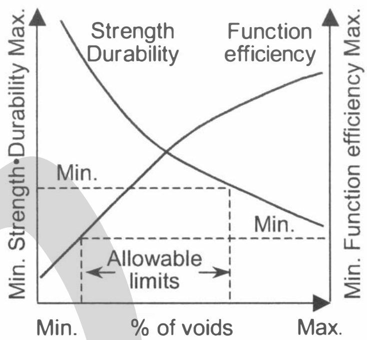

Fig.1 Conditions for porous concrete usage

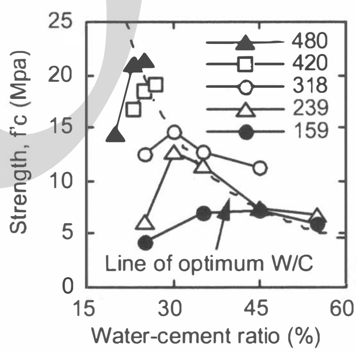

Fig.2 Compressive strength versus W/C water-cement ratio

2 OPTIMUMWATER-CEMENTRATIO

To investigate the effect of water-cement ratio, series of varying batches were mixed with water-cement ratios varying from 20 up to 55% and cement factors varying from 159 up to 480 kg/m^3. A 5-20 mm coarse aggregate was used. The volume of aggregates per cubic meter was kept equal to one cubic meter when calculated as a function of the bulk density determined in accordance with JIS A 1104. Consistency of porous concrete, which represents a unique set of challenges, was visually checked just after discharge from the mixer.

The cement paste matrix alone showed the expected increase in strength with decrease in water-cement ratio. However, as shown in **Fig.2**, the strength of porous concrete was not found to be a direct function of water-cement ratio and hence did not correlate with the properties of the cement paste matrix alone as reported in the literature. Consequently, unlike conventional concrete in which the strength is primarily controlled by the water-cement ratio, the strength of porous concrete is governed simultaneously by the water-cement ratio and cement factor. The findings agree with the test results obtained by other researchers. For a given percentage of voids, there is a cement factor and a corresponding optimum water-cement ratio that facilitates the migration of the paste toward the points of contact and thus leads to maximum strength. The relationship between optimum water-cement ratio and cement factor might be expressed as:

$$W/C = A \bullet C^{-B} \qquad (1)$$

where, W/C = water-cement ratio, C = cement factor, A and B = experimental parameters that depend on every factor that influences the strength of porous concrete.

3 EFFECT OF COMPACTION METHOD AND DEGREE

An important property of the porous concrete for the practical application is the behavior at compaction. Therefore, to understand the effect of compaction on porous concrete texture, percentage of voids, compressive strength and permeability, several porous concrete batches were mixed at 3 different cement factors and corresponding optimum water-cement ratios. Cylindrical specimens were then made using 4 different compaction methods with varied levels of compaction efforts for each.

Table 1 Effects of compaction methods on Vc, f'c and secant E of porous concrete made with cement factor 320 kg/m^3.

Compaction Method	Vc (%)	f'c (MPa)	E (GPa)
Self packing	38.60	6.13	9.70
Ramming 25 blows	26.76	11.92	13.53
Tamping 25 blows	27.22	12.62	15.03
I. Vibrating 5 sec	26.76	13.93	17.00
S. Compacting 5 sec	21.29	16.31	20.40

The densification of porous concrete specimens was largely responsible for the increase in compressive strength. The percentage rise in compressive strength between self packed porous concrete and that manually compacted for 25 blows were about 200%. However, the percentage rise in compressive strength between self compacted porous concrete and that mechanically compacted for 5 sec was nearly 300%. In addition, as **Table 1** shows, compacting the porous concrete by a surface vibrating tamper for 5 sec led up to percentages of voids (Vc) close to those expected from the mixture proportioning without causing migration of cement paste to the bottom of the specimen and reducing cohesion in the upper potion as well as closing the voids in the bottom portion i.e. rendering the material impermeable. Moreover, the secant modulus of elasticity of porous concrete compacted by the surface vibrating tamper for 5sec was higher than that for porous concrete compacted by other methods.

4 PERMEABILITY AND LONG-TERM DURABILITY

- Besides the mixture proportion, the permeability was proved to be dependent on the measurement devices and procedures.
- As per durability factor of 60, most porous concretes used in this investigation failed the freezing thawing durability test. However, no damage to the test specimens of porous concretes with a cement factor of 320 kg/m^3 was visually noted and the weight loss was less than 2% for all aggregate gradation used in this investigation.

5 CONCLUSIONS

Porous concrete is a multi-benefit strategy for environment protection and conservation. The potential for its usage is expected to increase as the problems outlined in this paper are seriously considered:

1. Mixture proportion of porous concrete should be performed as following:
   a) According to your application, choose the aggregate gradation and determine the required data on it (mainly: bulk density (T), solid content (G), specific gravity in saturated surface-dry condition (Ds) and percentage of water absorption (Q))
   b) Assume that the volume of aggregates per cubic meter is equal to one cubic meter when calculated as a function of bulk density.
   c) Select a minimum percentage of voids (Vc) that fulfill the required function of your product.
   d) Determine the cement factor that gives you maximum strength from the following equation:

   $$P = C/\rho_c + A \cdot C/\rho_w \cdot C^{-B} \quad (2)$$

   where: P = paste volume (P = 1 – (G + Vc)), ρ_c = specific gravity of cement, ρ_w = specific gravity of water, A and B are the same as defined in equation (1).
   e) Mix trial batch and determine: percentage of voids; unit weight; strength; etc. for compaction level desired.
   f) Adjust your mixture proportion using compaction degree as correction factor.
2. Need for quantitative and qualitative method to evaluate the consistency of porous concrete.
3. Need for permeameter setup.
4. Need for a regime that considers environmental conditions of the application site for evaluation of long-term durability.

INTRODUCTION OF A HIGH PERFORMANCE CABLE SYSTEM COMPOSED OF EPOXY RESIN COATED PC STRAND

Kei HIRAI* Tukasa KASHIWAZAKI* Naoyasu HIRAYAMA*
Takatugu FUJIKAWA** Keizou TANABE*

* KUROSAWA CORPORATION ENGINEERING & CONSTRUCTION, JAPAN
** KTB CORPORATION, JAPAN

Keywords: thin coated PC strand, rust prevention, fretting, fatigue strength

1. INTRODUCTION

Recently, a lot of results become available with regard to the development of coating PC strand to process rust prevention by epoxy resin in Japan. While the design to the external force of the structure was general up to now, Coated PC strand is more and more used in design for durability. Especially, effectiveness is admitted for the reduction of the life cycle cost, and the design which values durability has come to be actual practice. The method of coating epoxy resin in a thin film was investigated and developed, and each of the wires which composed the PC strand without burying a spiral ditch of the PC strand was confirmed to be able to use quite the same anchorage device as a normal PC strand, with enough achievement of the effect of rust prevention.[1] This paper introduces examples of application with various performances of rust prevention of epoxy resin coated PC strand, which coats each wire in the thin film. Further more mechanical properties, and cable systems are presented.

2. OUTLINE OF EPOXY RESIN COATED PC STRAND

The difference between the shape of the outer coated PC strand and the thin coaed PC strand is shown in Fig-1. The left figure shows the outer coated PC strand and the right shows the thin film coated PC strand. It can be confirmed that a spiral ditch of the outer coated PC strand has disappeared because it is thicker than the coat thickness. The spiral sulcus of the PC strand remains because each of the wires is coated in the thin film as for the thin film coated PC strand. The coat thickness for the outer coating needs to be more than 400 μ m. The coat thickness for the thin film coated PC strand is about 150 μ m.

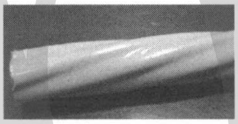

a. Outer coating PC strand

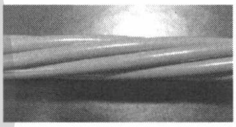

b. Thin film coating PC strand

Fig.1 Difference between outer coating PC strand and thin film coating PC strand

The difference between that two originates in the difference of the method of the coating. The thin film coating PC strand returns the strand ahead of the surface treatment more, processes the abrasive blasting to all of the seven wires, and does an electrostatic powder coating to all of the wires while the normal PC strand is coated on the outer coating PC strand in the untouched shape in this process.

3. VARIOUS PERFORMANCES OF THIN FILM COATING PC STRAND

Various performances of the thin film coated PC strand manufactured by a method of the coating which is quite different from the past method of the epoxy resin coating are shown.

3.1 Relation between coat thickness and pin-sized hole

The coating thickness was changed to 60 μ m-220 μ m compared with the board specimen and the strand specimen, and then, the number of generated pin-sized holes and the salt spray test were executed and the rusting rate was confirmed. The transition of the number of pin-sized hole generation is shown in Fig-2. According to the result by the confirmation of the number of pin-sized holes to the board specimen, it was confirmed that no pin-sized hole were found for a coating thickness of more than 90 μ m. Therefore, it was confirmed that the pin-sized holes were not generated, and enough rust prevention performance was demonstrated in the board specimen if it was more than 90 μ m.

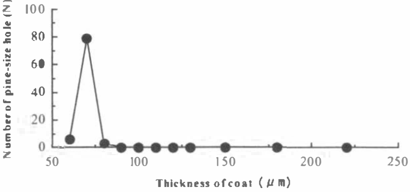

Fig-2 Transition of pin-sized hole generation

According to the result of the rusting after the salt spray test in the strand specimen, the rusting was not observes for the specimens with a coat thickness more than 100 μm after 1,000hr, and an enough rust prevention performance was confirmed.

3.2 Fatigue resistance capability

The fatigue resistance capability of a PC strand is lower than that of a round bar because of shape which is a spiral. The situation of the wire, which decreases the section by fretting corrosion, is shown in phot-2. It can be confirmed that the mark of the next wire, which has come into contact by fretting, has been clearly left according to the photo. According to the result of fatigue test shown in Fig-3, the normal PC strand exceeds 2,000,000 times when the stress range is 130N/mm^2. On the other hand, the thin film coating PC strand has ended at 4,000,000 times with the stress range of 245N/mm^2. It can be considered from this that the fatigue strength of thin film coated PC strand is 4,000,000 times or more in a stress range of 245N/mm^2. Moreover, according to the tension test result after fatigue testing, the breaking load satisfied the standard value in all specimens.

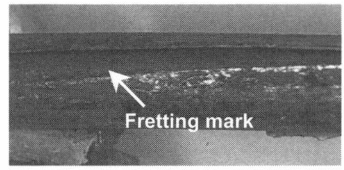

photo-2 Reduction-of-area by fretting

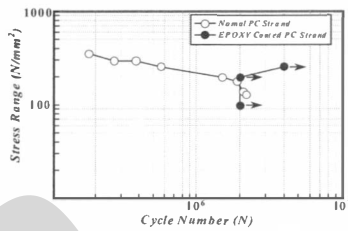

Fig-3 Compare Fatigue Strength

4. CABLE SYSTEM WHICH USED THIN FILM COATING PC STRAND

The outline of the cable system of 19S15.2 type shown in Table-3 is shown in Figure-5. This cable system adopts the one with different methods for both ends of the strand anchorage, using the compression fixed grip to the fixed side, and using the wedge to the movable side anchor tension member. Breaking by the anchorage zone is most probable when the fatigue testing of the cable is done, and it often breaks especially in the compression fixed grip part. The fretting of the strand increases by the concentration of stress at the grip and the effect of the cutting lack at the edge of the inner part of the grip when anchoring in the grip, and being tightened in addition. However, it was confirmed that the method of thin film coating was effective to the fretting prevention of the anchorage zone by the fatigue testing result of 19S15.2.

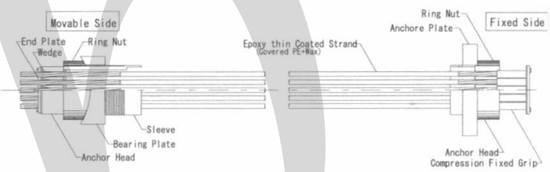

Fig-5 Cable Specimen for fatigue test (19S15.2)

5. SUMMARY

When the thin film coating PC strand was applied to the cable system, the effect of reducing the fretting phenomenon of the cable anchorage zone, which was a past weak point, was confirmed.

① The strand was confirmed to obtaining an excellent rust prevention performance by coating the thin film epoxy resin respectively.

② The coating can prevent pin-sized holes from being generated if it's thickness is larger 100 μm.

③ Fretting of the wires can be prevented by coating the thin film epoxy resin, and a fatigue strength of 4,000,000 times or more is possible in a stress range of 245N/mm^2.

④ The fatigue performance in the anchorage zone improves by applying a thin film coated PC strand to the cable system.

6. POSTSCRIPT

A lot of cables which use this epoxy resin coating PC strand are used for a Japanese and overseas construction and civil engineering structure.

PROPERTIES OF PRE-GROUTED PRESTRESSING TENDONS AND FLEXURAL BEHAVIOR OF CONCRETE BEAMS USING THE TENDON

Seiichiro Hirata, Mutsuhiko Ohnishi, Shoji Shirahama and Takeshi Kobayashi
Shinko Wire Co., Ltd., Japan

Keywords: Pre-grout,Flexural Behavior,Bond Strength

1 INTRODUCTION

The unbonded post-tensioning system is widely used for the construction of floors and roof slabs in buildings. However, the bonded post-tensioning system in which the tendons are bonded to the concrete by cement grouting is generally used for buildings and bridges required to be seismic-resistant. However, the work of grouting is very troublesome and the process is time-consuming. And incomplete grouting was often found in some PC girders bridges. The pre-grouted prestressing tendon has been newly developed for post-tensioning of concrete. Without grouting, this tendon has the same structural properties as the grouted tendon. The pre-grouted prestressing tendon is composed of a prestressing steel coated with a cold setting epoxy resin in a corrugated polyethylene sheath. The hardening time of the resin can be controlled by such amount of curing catalyst that hardens after stressing and then the bond with the concrete occurs through the sheath. It is expected that the pre-grouted prestressing tendon will be widely used instead of the tendon grouted with cement because the use of the pre-grouted tendon will lead to savings in labor and greater durability as well as improved seismic-resistance.

This paper presents the abstract and the properties of pre-grouted prestressing tendons and the flexural behaviors of the concrete beams using these tendons.

2 THE PROPERTIES OF PRE-GROUTED PRESTRESSING TENDONS

2.1 Properties of bond with concrete

The test was carried out when the compressive strength of the concrete had reached 30MPa. And a specimen with a tendon grouted with cement in a corrugated sheath was also used for comparison. The results of the pull-out test are shown in Table 1. It appeared that the bond of pre-grouted prestressing tendon with concrete was equivalent to that of the tendon with cement grout.

Table 1: Results of pull-out test

Specimen	Average bond strength, MPa
Pre-grouted prestressing tendon(PGP)	3.9
Prestressing steel with cement grout(CGM)	3.8

2.2 Fire-resistant property of the pre-grouted prestressing tendon

The test was carried out in accordance with JIS A1304 "Method of fire resistance test for structural buildings". A pull-out test was carried out using the specimens after the fire test. The test was carried out using pre-grouted prestressing tendons in addition to tendons grouted with cement with corrugate metal sheath for comparison.

The average bond strength of the pre-grouted prestressing tendon was about 4MPa in the pull-out test, so the cover for the average bond strength starts to decrease is estimated at about 55mm for 30minutes heating, about 65mm for 1hour heating and about 75mm for 2hours heating(Fig.1).

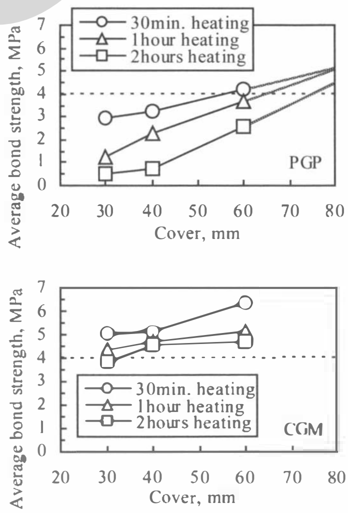

Fig.1: Average bond strength of test tendons after fire resistance test

2.3 Flexural behavior of prestressed concrete beam

The flexural specimens and the list of tendons used for the test beams are shown in Table 2. The test set up was with symmetrical two-point loading. The loading was increased linearly until the first crack occurred, and then the test was continued until the specimen fractured by incremental cyclic loading. The envelope curve relations between bending moment and mid-span deflection of the test beams are shown in Fig.2 and the relation between the bending moment and the maximum crack width is shown Fig.3. The crack patterns of each specimen are shown in Fig.4. It appeared that specimen PG had the same structural properties as CG.

Table 2: List of tendons used for test beams

Symbol	Tendon	State of bond
PG	Pre-grouted prestressing tendon	Bonded
CG	Prestressing steel with cement grout	Bonded
UB	Unbonded prestressing steel	Unbonded

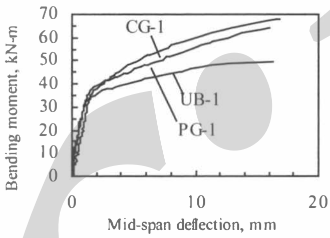

Fig.2: The relation between bending moment and mid-span deflection

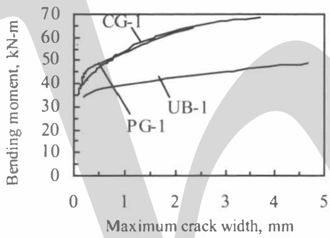

Fig.3: The relation between bending moment and maximum crack width

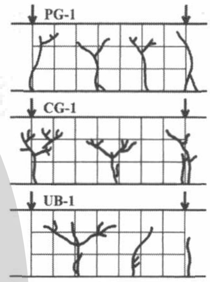

Fig. 4: Crack patterns

3 CONCLUSIONS

The epoxy resin has adequate mechanical properties for a grouting material for the prestressing tendon.

1. The bond strength of pre-grouted prestressing tendons are equal or superior to that of the prestressing steels with cement grout.

2. The concrete cover of a pre-grouted prestressing tendon needs about 55mm, 65mm and 75mm for 30minutes, 1 hour and 2 hours of fire-resistance respectively.

3. The concrete beams using pre-grouted tendons show a flexural behavior similar to the concrete beams using prestressing steel grouted with cement. A prestressed concrete member using pre-grouted prestressing tendons had about the same structural properties as that using tendons grouted with cement. Therefore, it was proved that a pre-grouted prestressing tendon has advantages for bonded tendon grouted with cement.

EXTERNAL CABLE USING EPOXY COATED STRANDS

Yasuhiro Hoshino Masato Yamada Motonobu Nishino
Sumitomo Electric Industry Ltd. Japan

Keywords: epoxy-coated strand, external cable, deviator

1 INTRODUCTION

Prestressing steel with factory applied corrosion protection gets much attention in various application fields, such as post-tensioning, stay cable and ground anchor. Although factory applied corrosion protection has not so much long history, it is usually highly reliable under well-quality-controlled production process and also effective for labor saving, rapid working process at job sites and tentative corrosion protection as well. Epoxy coated strand, prestressing steel with one of the major factory-applied-corrosion-protection, is very durable because of its thick and tough coating film, and there is no need to peel off the coating at anchorage zone, and has no anxiety to lose the protection material from the steel surface even under direct sun light like grease or wax. It is also very advantageous to be easily inspected from outside by naked eyes when it is deteriorated.

These advantages are highly evaluated and epoxy-coated strands are widely used as external cable in box girder bridges, as post-tensioning cable with grouting in hazard environment and also as tension member of ground anchor.

This paper reports the details about external cables using epoxy-coated strand. The main contents as follows,

- ·Composite Cycle Corrosion Test for Epoxy Film.
- ·3 Million Cycles of Full Scale Fatigue Test on 19 ϕ 15.2 Cable at deviated zone under complete non-grout environment.
- ·Evaluation of epoxy coating film under lateral pressure during tensioning using full-scale cable of 19 ϕ 15.2.
- ·Creep test of epoxy film under compression load.
- ·Actual Use of Epoxy Coated Strand Cable at Construction site.

2 COMPOSITE CYCLE CORROSION TEST FOR EPOXY FILM (JHS403－1992)

An examination was done based on the way of examining composite cycle test (JHS403-1992) prescribed by a Japan Highway Public Corporation(JH). Five type of test piece was tested. First 96 hours, the test pieces were irradiated in the sunshine-carbon-ark-light test machine. After that, they were carried out by the corrosion cycle examination shown as following prescribed as the seawater and general environment (A-law).

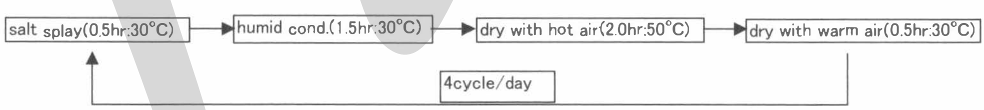

Fig.1 corrosion cycle

There was no abnormality was found on these samples. The judgment was based on the way of evaluating it in the composite cycle test of JH(Not found corrosion, softly, cracking and peeling off at coating : JHS403－1992).

3 THREE MILLION CYCLES OF FULL SCALE FATIGUE TEST ON 19 ϕ 15.2 CABLE AT DEVIATED ZONE UNDER COMPLETE NON-GROUT ENVIRONMENT

19 x ϕ 15.2 epoxy coated strands were twisted at two deviated zones was tested.

- ● Deviate angle: 14° ●Radius of deviation zone: r=3,000mm
- ● Grouting: Nothing ●Lower limit load: 2957.4kN(60% tension of nominal breaking load)
- ● Amplitude of load range: 129.2kN ●Frequency: 0.7Hz ●Number of cycles: 3 million cycles
- ● After the fatigue test, each epoxy strand at deviated zone was performed a breaking test.

There was no abnormality observed at epoxy-coated strand at fatigue test.

Epoxy film was well maintained on the surface of PC strand, which enable to keep performance of corrosion protection, after fatigue test. This test result shows that performance of the epoxy-coated strand applied to deviated zone well maintains its anti-corrosion property.

4 EVALUATION OF EPOXY COATING FILM UNDER LATERAL PRESSURE DURING TENSIONING USING FULL-SCALE CABLE OF 19 ϕ 15.2

Two types of 19 x ϕ 15.2 epoxy coated strand cable were tested, parallel cable and twisted cable.

- ●Radius of deviation zone : r=3,000mm
- ●A deviation part made of a polyethylene pipe installed in bended steel pipe.
- ●Tensile load: 3,789.9kN (90% load of yield point) Setting cable for deviation block and tension was given. A cable is moved 200mm with keeping the load. Then observe epoxy coating film at high pressure points by dismantling the sample.

After the test, enough thickness of the epoxy film was remained on the surface of the strand to keep performance of corrosion protection, as shown in fig-15, 16.

5 CREEP TEST OF EPOXY FILM UNDER COMPRESSION LOAD

The load test outline is shown fig-2. Test pieces were pressured by test machine with constant load (3.4t/100mm: Max pressure at deviation zone when 19 x ϕ 15.2 cable was strained.).

And measured displacement of a film thickness with the dial gauge.

After the test, enough thickness of the epoxy film was remained on the surface of pc strand to keep performance of corrosion protection. And then it expects that the film thickness will be maintained after 100 years because the creep of resin is settled.

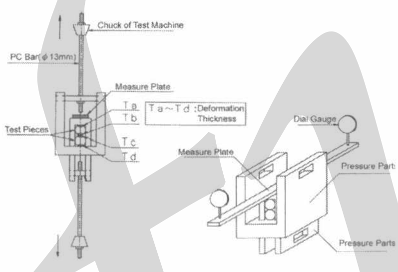

Fig.2 Test Exterior

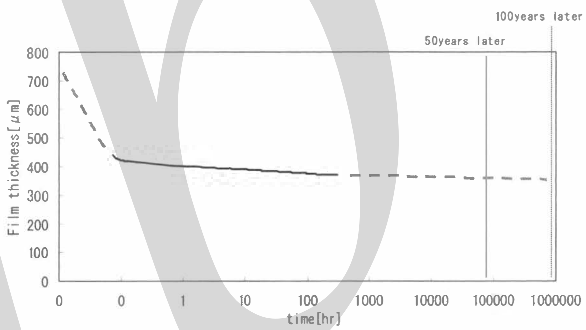

Fig.3 The amount of a film thickness change.

6 ACTUAL USE OF EPOXY COATED CABLE AT CONSTRUCTION SITE

An example of cable packaging is shown fig-4.application accessories to protect from damages of the epoxy coat were also made and supplied to the construction site.

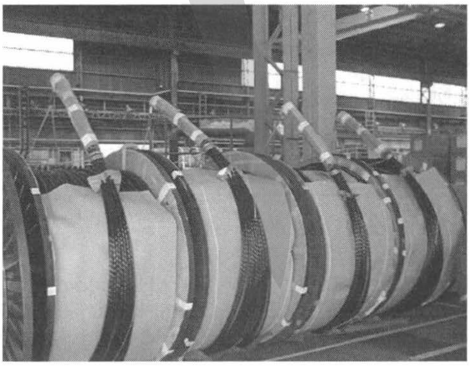

Fig.4 Packaging

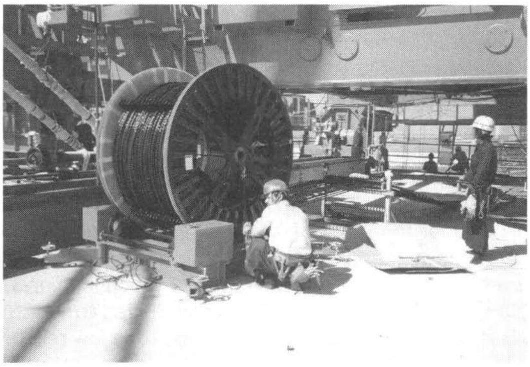

Fig.5 Installing cable

DEVELOPMENT OF ULTRA FAT PC STRAND

Shinichi Yoshida Takashi Ichiki Yoshihiko Touda
Sumitomo Electric Industry Ltd. JAPAN

Keyword: steel strand, high breaking strength

1 INTRODUCTION

The Steel Strand for Prestressed Concrete (PC strand) has recently become preferable to the PC bar in the use of prestressing materials in concrete bridges and buildings, because of its advantageous characteristics such as flexibility and longer cable length that enable easier construction. On the other hand, the breaking strength in single piece of a PC strand is lower than that of a PC bar. When PC strands are applied to large bridges or buildings, usual in these days , with multiple cables, PC strand is considered as a less efficient material than a PC bar which can be applied in only single piece.

According to these circumstances, a 19-wires PC strand of 28.6mm diameter, which is the biggest PC strand in the world, was developed to be applied to large structures in one single piece, enabling efficient construction. The advantageous characteristics are as follows:

(1) The nominal breaking strength is 949 kN, which is about 1.7 times higher than of a 19-wires PC strand of 21.8mm diameter and is equivalent to a PC bar of 32mm diameter.
(2) The major flexibility is not sacrificed by such a large diameter by adopting the Warrington type component of strand
(3) The anti-fatigue property, relaxation property, anchorage performance and bond performance with concrete are equivalent to those of a 19-wires PC strand of 21.8mm diameter.

Corresponding equipment such as the tensioning jack and the anchorage system for 28.6mm PC strand were also developed as well as the Ultra Fat PC strand (UFPS). UFPS began to be applied to actual structures since 1996. The quantity of it has reached over 5000MT in 2001.

2 PROPERTIES OF THE UFPS

2.1 Geometrical and mechanical properties

The outlook of UFPS is shown in Photo.1. The mechanical properties of UFPS and conventional materials (32mm PC bar and 21.8mm PC strand) are shown in Table1. The diameter of UFPS is 28.6mm and the breaking strength is 959kN, which is higher than the 949kN of the 32mm PC bar. The breaking strength is also over 1.7 times higher than that of the 21.8mm PC strand. The yield strength at 0.2% extention of UFPS is 837 kN, which is also higher than that of a 32mm PC bar and 1.7 times higher than that of a 21.8mm PC strand. The total elongation is 7.7%, which is over 3.5% of the lower limit in the ASTM standard. The relaxation losses, when it is initially loaded to 70% of 949kN and tested after 1000 h, is 1.3% of the initial load, which is less than the 2.5% of a low relaxation grade in the ASTM standard.

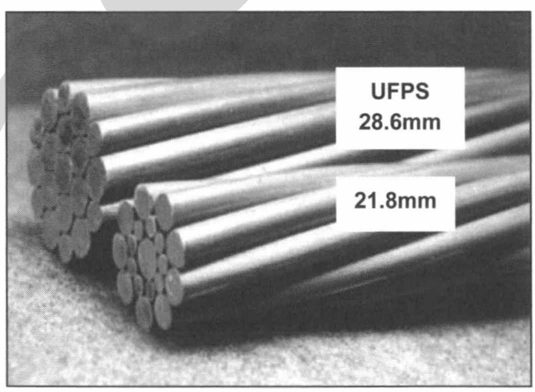

Photo.1 Outlook of UFPS

Table.1 Mechanical properties of UFPS

Material	Breaking strength (kN)	Yield strength at 0.2% extention (kN)	Total elongation (%)	Relaxation after 1000h (%)
UFPS	959	837	7.7	1.32
32mmPC bar	958	830	9.0	0.80
21.8mmPC strand	595	535	6.8	1.20

2.2 Flexibility

The cross section of a Seal type and a Warrington type component of a 19-wire strand are shown in Fig.1. The Warrington type is more flexible than the Seal type because of the outer wire of smaller diameter.

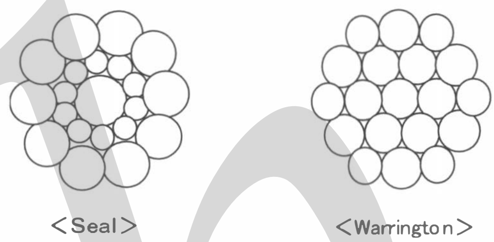

Fig.1 Seal and Warrington type of component of 19-wires

The flexibility of the PC strand is evaluated by actual bending the strand and installing it to the pipe in a concrete block, which aspect is shown in Photo.2. In this test, the number of workers are estimated and the radius of the bent strand are measured. Three type of strands, UFPS of Warrington, UFPS of Seal and 21.8mm PC strand, were tested. When the Seal type is adapt to the UFPS, 3 workers are required for its installation. On the other hand, only 2 workers are required when the Warrington type is adapted, because of the better flexibility.

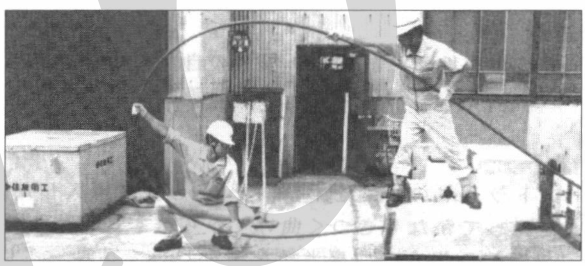

Photo.2 Aspect of flexibility test

3 APPLICATIONS

UFPS began to be applied to transversal tendons in actual construction in 1996. UFPS with Pre-Grout sheath shown in Photo.3. was applied mainly for transversal tendons and the quantity shown in Fig.2 has reached over 5000MT in 2001. This material also began to be applied as longitudinal tendons since 2001 because of the improvement of the Pre-Grout sheath.

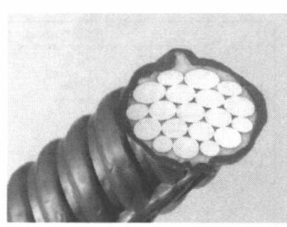

Photo.3 Pre-Grouted PC materials

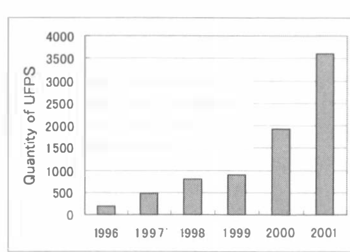

Fig.2 Quantity of UFPS

APPLICATION OF ACTIVATED FLY ASH IN MORTAR AND CONCRETE

Sanhai Zeng
Hubei Polytech University
CHINA

Rudolf Hela
Brno University of Technology
CZECH REPUBLIC

Keywords: Raw fly ash, Activated fly ash, Pozzolanic, Blended cement.

1 INTRODUCTION

Pulverized fly ash (PFA) is clearly abundant artificial pozzolan so far in the world. Though it has been successfully used in cement, mortar and concrete for its reduction of water, pozzolanic reaction with Ca(OH)2, increasing workability and durability of concrete, only approximately one third of it used in construction. It has changeable physical and chemical composition, also its limitation of lower early strength development in cement and concrete [1].

Intense research has been focused on the improvement of the early strength of cement, mortar and concrete containing fly ash, especially in high volume content. Increasing the fineness of fly ash apparently increasing the pozzolanic reactivity of fly ash. Elevating the curing temperature is also beneficial to the early strength development of fly ash concrete [2]. Some studies indicated that the addition of chemical activators could effectively activate or improve the pozzolanic of natural pozzolans . Alkali activated fly ash also has been reported to increase the pozzolanic activity of fly ash [3].

In this research, the raw PFA (RFA) was activated into two types of activated fly ash AFA-1 and AFA-2 with a specific method; aim at increasing the early strength of cement, mortar and concrete. The properties of AFA were tested. Mortar and concrete tests were carried out to assess the activity of AFA.

2 EXPERIMENTAL DETAILS

2.1 Material properties

All materials used in the tests came from Czech Republic market. The chemical and physical compositions of powder materials are listed in Table 1. The cement used in mortar and concrete is CEM I 42.5 R. The RFA is Chvaletice, a local power plant. The slag, $(CaO+MgO)/SiO_2>1$, $(CaO+MgO)/(SiO_2+AL2O_3)>1$,was used for comparative and blended tests. Three different fractions of sands for mortar tests are local river sands. Another river sand (0--4mm) and gravel (6-16mm) used for concrete tests according to Czech experience. The AFA-1 and AFA-2 were made from RFA with different activation treatments.

Chemical copmosition(%)						physical composition		
	CEM I 42 5 R	RFA	SLAG	AFA-1	AFA-2		Density (g/m^3)	surface (cm^3/g)
SiO_2	21 88	56.82	39.60	39.62	42.62	CEM I 42 4 R	3 14	3840
AL_2O_3	5 22	28.93	6.40	20.70	21.70			
Fe_2O_3	3 55	6.18	0.80	4.53	4.64	RFA	2 036	2426
CaO	61.5	1.79	38.00	18.24	22.34	RFA-1	2 42	2380
MgO	1.06	1.31	12.70	0.96	0.98	RFA-2	2 58	2401
Na_2O	0 21	0.32	-	0.21	0.24			
K_2O	0.97	1.79	-	1.30	1.34			
SO_3	3.83	0.5	-	5.38	6.38			

Table 1 Chemical and physical composition of powder materials

2.2 Mortar and concrete tests

The mortar mix proportion for all mortar tests containing the following amount of materials in mass: Cement: sand (three fractions): water=1:3:0.5.Cementicious for assessment of AFA activity: RFA, AFA-1 and AFA-2 represented cement at 15%, 25%, 35%, 45% content respectively, designed numbers are C-01, C-02, C-03, C-04 (for RFA); C-11, C-12, C-13, C-14 (for AFA-1); C-21, C-22, C-23, C-24 (for AFA-2). For comparative and blended tests, the pozzolans (RFA, AFA-1, AFA-2 and Slag) represented cement at 35% content, also blended RAF with AFA-1, AFA-2 and Slag tests were carried out, designed number were B-01, B-02, B-03, B-04 for RFA, AFA-1, AFA-2 And Slag respectively; B-05 (17%RFA+18%AFA-1); B-06 (17%RAF+18%AFA-2); B-07 (17%AFA-1+18%AFA-2); B-08 (17%S+18%RFA); B-09 (17%S+18%AFA-1); B10 (17%S+18%AFA-2) .All the sample were tested according to EN-197.The concrete tests were prepared according to Czech experience.

3 EXPERIMENTAL RESULTS

In this section, the average values of the test results are presented. Each value was obtained from three measurements.

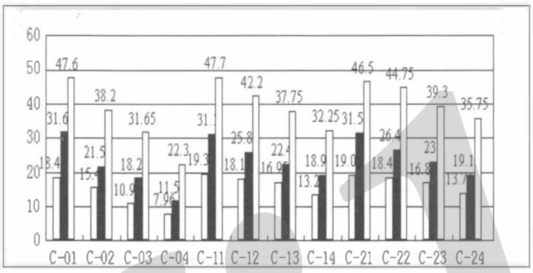

Fig.1 Mortar tests for assessment Activity of AFA

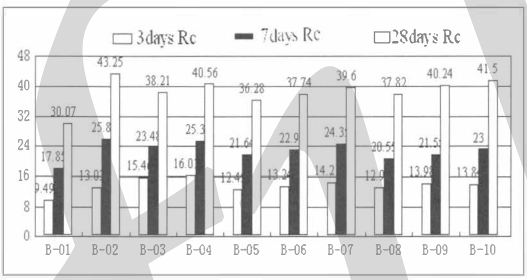

Fig.2 Comparative and blended mortar tests

flyash	strength (MPa)	cement /fly ash ratio(%)				
		100/0	70/30	60/40	50/50	40/60
RFA	3 days	23.85	10.18	7.18	5.49	4.30
	7 days		15.86	11.25	9.50	7.28
	28 days		24.87	21.17	19.45	17.34
AFA-1	3 days	28.49	15.36	12.07	9.49	9.00
	7 days		21.40	17.25	14.35	11.58
	28 days		31.23	27.28	24.87	22.46
AFA-2	3 days	36.14 (control)	17.70	13.24	10.31	8.40
	7 days		22.59	18.16	15.24	12.13
	28 days		31.55	28.36	25.80	21.50

Table 2 concrete tests

4 CONCLUSIONS

An attempt has been made to activate the activity of raw fly ash, especially to increase the early strength of cement, mortar and concrete containing fly ash. The experimental results showed that:

☐ Uniformed the chemical and physical composition after activating fly ash. This made the fly ash easily used and was more compatible with cement, mortar and concrete.

☐ Compared with raw fly ash, the activated fly ash not only increased the early strength of cement, mortar and concrete, but also the long-term strength. It has the same or much higher early strength development as slag.

☐ Changed the color of raw fly ash, which makes it more aesthetic.

☐ This activation method also can be used to other pozzolanic materials.

5 REFERENCES

[1] R.K.DHIR,F.H.HUBBARD,J.G.L.MONDY AND M.R.JONES. Proceeding of 2nd International Conference on Fly Ash, Silica Fume, Slag and Natural Pozzolans in Concrete. SP-91,PP693-721,1986.

[2] C.SHI AND R.L.DAY, Proceeding of 10th International British Block &Masonry Conference.Vol.3, PP.1153-1162, Calgary, July, 5-7, 1994.

[3] NGEL PALOMO AND SANTIAGO ALONSO. "Alkali activated fly ashes-New cemetitious for concrete".

A NEW CABLE TECHNOLOGY: THE "COHESTRAND"

Ivica Zivanovic Benoit Lecinq Jean-Philippe Fuzier
Freyssinet International
FRANCE

Keywords : suspension bridges, cables, strand, rehabilitation

1 INTRODUCTION

Over the past decade there has been considerable interest in the durability and maintenance of bridges. Bridge owners are becoming more and more conscious of the need for thorough inspection and scheduled maintenance, thereby increasing knowledge of the behaviour and vulnerability of cable structures, as cable failures are recorded on suspension bridges around the world. The cables of many structures are corroded and require replacement. The cable technology used is one hundred years old and needs to be completely renovated incorporating an improved corrosion protection and the concept of maintenance, monitoring and surveillance without traffic disruption in order to achieve more durable and economical structures.

2 DESCRIPTION OF THE COHESTRAND™

This paper presents the replacement of the suspension cable for the Chartrouse Bridge in France and the use of a new technique: the COHESTRAND™. This strand is based on the existing stay cable technology which has proven very successful. Over the past fifteen years, the rapid development of stay structures, in particular cable-stayed bridges have led to a remarkable improvement in the cables used.

This improvement has been firmly based on a solid program of research and development. The application of cables made up from multiple small strands and the advantages that this configuration brings to large cable construction :

- Individually protected small strands eliminate the danger of the spread of corrosion to the complete cable section. A strand is a small proportion of the cable capacity so that the loss of one or a few strands in a large cable through damage to their protection does not compromise the whole cable or reduce its capacity significantly.
- Individual 7-wire strands have a high fatigue resistance.
- Grouped individual strand anchorages allow cables of any capacity to be constructed.
- The stay strand anchorages have an elevated fatigue performance and are extremely compact.
- The provision of an external cable duct protects the strand sheaths from UV attack and ensures the extreme durability of the cable structure.
- Easy construction using light equipment.

As a result of these developments, stay cable technology is now far in advance of conventional parabolic cable technology with regard to corrosion protection, fatigue performance and durability.

This technology provides a cable system with an expected durability in excess of 100 years.

It is interesting to note that conventional parabolic cable technology has barely changed during the last 50 years.

The suspension cable systems proposed bring these hard won advantages to parabolic suspensions together with further advantages arising from the very compact anchorage and the concept of individually protected strand.

However, there are specific needs when this technology is applied to parabolic suspension cables: a tangential force has to be transferred at each collar connecting the hangers to the suspension cable, and so a secure bond must be created between the polyethylene sheath and the steel strand.

COHESTRAND™ used for the main suspension cable of the Chartrouse Bridge complies with these requirements. It is galvanised or galfanised (galfan is an alloy of steel and aluminium providing three times better corrosion protection than galvanising) and covered with a black High Density Polyethylene (HDPE) sheath which is fully bonded to the strand. The strand coating process can be applied to any 7-wire prestressing type strand.

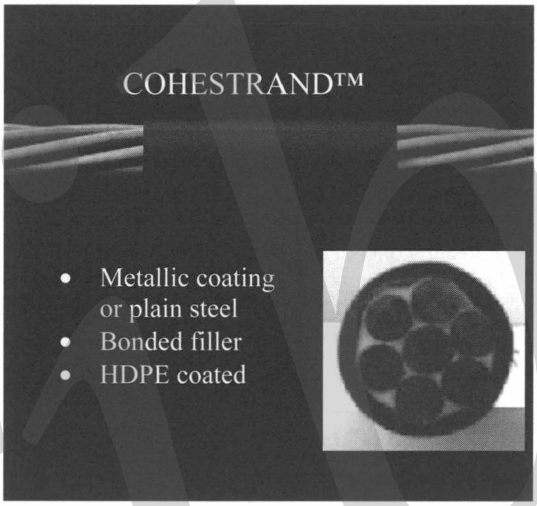

Fig. 1 COHESTRAND™

In addition special collar clamping systems have been developed to provide uniform stresses and fail safe transfer to the cable. The programme of the tests carried out on this new suspension device, and in particular the dynamic test carried out on a collar, shows that the collar behaves in a perfect way and that there is no damage on the various parts of the device nor on the strands in particular.

3 CONCLUSION

Moreover the performances of the COHESTRAND™ protection against corrosion, its adherence to steel and HDPE, instantaneous as well as in the long term or in fatigue, ensures its future in the prestressing and derived techniques area as well as that of cabled structures (suspended bridges, cable-stayed bridges with deviation saddles in pylons, etc.). The next application will be on Sungai Muar (in Malaysia) cable-stayed bridge with specific deviation saddles.

REFERENCES

[1] F.L.. Stahl and C.P. Gagnon : Cables corrosion in bridges and other structures - 1996
[2] LCPC / SETRA : Les ponts suspendus en France - 1989.
[3] N.J. Gimsing : Cables . IABSE Congress – Copenhagen / May 1996.
[4] J.A. Calgaro and R. Lacroix : Maintenance et réparations des ponts. Presse des Ponts et Chaussées – 1997.

DEVELOPMENT OF HEM ANCHORAGE SYSTEM FOR CABLE STAYED BRIDGE USING MULTIPLE CFRP STRANDS

Tetsuo Harada Naomi Sakaue
Nagasaki University, Nagasaki , JAPAN

Hiroshi Kimura Tsuyoshi Enomoto
Tokyo Rope Mfg Co. Ltd., Tokyo, JAPAN

Myo Khin
Dai-ichi Institute of Technology, Kagoshima, JAPAN

Masashi Soeda
Fukuoka University, Fukuoka, JAPAN

Keywords: CFRP strand, anchorage, cable stayed bridge

1 INTRODUCTION

The authors have studied an anchorage using Highly Expansive Materials (HEM) for Fiber Reinforced Polymers (FRP). Recently, the needs of CFRP tendon grips having larger prestressing capacity have been increased, because higher durability for a long term is required for large scale structures such as "Cable Stayed Bridge". In the near future, the HEM tendon grips having a capacity of 5,000kN will be necessary. At the first stage of the development of HEM tendon grips with large prestressing capacity, the HEM tendon grips having the capacity of 2,500kN have been developed. This HEM tendon grip consists of twelve CFRP strands with 15.2 mm diameter.

In order to design and fabricate the HEM multi-cables type tendon grip, further fundamental studies should be carried out. To be used as an anchorage for a cable stayed bridge, it is important to clarify the long-term behavior of prestressing force and fatigue characteristics of CFRP strands using HEM anchorage. In this paper, the design concept of HEM multi-cables type tendon grip is described firstly and followed by the evaluation of experimental results for long term behavior and fatigue characteristics of HEM multi-cables type tendon grip having the capacity of 2,500kN. Also, analytical studies were carried out on the mechanism of HEM anchorage and reported.

2 HEM TENDON GRIP WITH A CAPACITY OF 2,500kN

Here, the required tensile strength of tendon grip is aimed at 2500kN by using twelve CFRP strands having 15.2 mm diameter. The arrangement of twelve CFRP strands in the steel sleeve is shown in Fig.1. After setting CFRP strands in the steel sleeve, the slurry of HEM is poured into the small spaces between steel sleeve and CFRP strands. When the expansive pressure reaches over 50MPa, the tendon grip which is connected to the tension rod, can be tensioned by a center-hole jack up to the required prestressing level, and then, HEM tendon grip is fixed with a locking nut.

The expansive pressure was transmitted in a manner similar to that of a fluid in multi-cables type HEM anchorage. The expansive pressure is steady for long-term without decreasing. The length of steel sleeve is determined as 500 mm, considering the results of pull-out analysis and the transmission length of expansive pressure at both ends with wide diameter of steel sleeve.

3 LONG-TERM BEHAVIOR OF HEM ANCHORAGE WITH TWELVE CFRP STRANDS

One of the most important matter is to predict the loss of prestressing force for long-term characteristics of HEM anchor. It has been confirmed that the loss of prestressing force is caused by the pull-out displacement at loaded end for HEM anchor with a single strand. Here, the relationship between the loss of prestressing force and the pull-out displacement at loaded end was also examined.

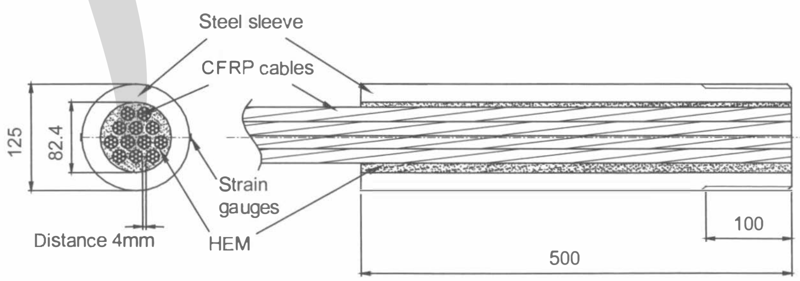

Fig.1 HEM tendon grip with twelve CFRP strands having capacity of 2,500

The simulation curve, which only considers the pull-out displacement, is estimated to be smaller than the experimental curve comparing with experimental one.

Then, the influence of relaxation of CFRP was considered. The relaxation function of CFRP strand can be changed to be expressed as a creep function. The simulation curve considering both the pull-out displacement and the relaxation of CFRP strand fits well to the experimental curve within 1000 hours. When the length of the CFRP strands is 10 m and considering only the pull-out displacement, the loss of prestressing force becomes within 1.5 % range. Therefore, the loss of prestressing force of CFRP strand for long-term should be considered mainly on the relaxation of CFRP strand in practice.

4 FATIGUE CHARACTERISTICS OF CFRP STRAND WITH HEM ANCHORAGE

To examine the fatigue characteristics of CFRP strand including HEM anchorage is vitally important, since the variation of prestressing force of cables in cable stayed bridge is caused by wind vibration, live load etc.

HEM anchorage and epoxy resin anchorage were used in the fatigue test. In the static tensile tests, the test results of tensile strength of CFRP strand were not affected by the kind of tendon grip naturally. However, it was found that the fatigue characteristics of CFRP strand(ϕ 15.2) using HEM anchorage are advantageous than the one using epoxy resin anchorage.

In the fatigue design of ordinal cable stayed bridge using steel cable, the required fatigue strength of cable can be considered sufficient as the amount of stress range from 200N/mm^2 to 400N/mm^2 by taking into account on safety factor. Based on the fatigue test results, the authors consider that the minimal required stress range of CFRP strand(ϕ 15.2) is 800N/mm^2 for HEM anchorage, and 600N/mm^2 for epoxy resin anchorage respectively. The fatigue strength of CFRP strand is around twice that of steel cable.

5 CONCLUSIONS

The results obtained in this study are summarized below.

(1) The mechanism of HEM anchorage can be explained well for both a single and multi-cable by using developed FEM model, in which the HEM layer is assumed as a shear spring. And twelve cables were treated as a single cable and performed uniformly.

(2) The loss of prestressing force is caused by the pull-out displacement at loaded end and the relaxation of CFRP strands. When the length of the CFRP strands is 10 m and considering only the pull-out displacement, the loss of prestressing force becomes within 1.5 % range. Therefore, the loss of prestressing force of CFRP strand for long-term should be considered mainly on the relaxation of CFRP strand in practice.

(3) From the fatigue test results of CFRP single strand with 15.2mm diameter, the allowable stress range of CFRP strand for fatigue load can be adopted to be in wide range. The required stress range of CFRP strand(ϕ 15.2) is 800N/mm^2 for HEM anchorage.

REFERENCE

[1] T. Harada et al.: “New FRP Tendon Anchorage System Using Highly Expansive Material for Anchoring”, FIP Symposium ’93, Kyoto, Proceedings Vol. II, pp.711-718, 1993.

[2] T. Harada et al.: “Development of Non-Metallic Anchoring Devices for FRP Tendons”, Non-Metallic(FRP) Reinforcement for Concrete Structures, Proceedings of the Second International RILEM Symposium (FRPRCS-2), E&FN SPON, pp.41-48, 1995.

[3] T. Harada et al.: “Behavior of Anchorage for FRP Tendons Using Highly Expansive Material Under Cyclic Loading”, Non-Metallic(FRP) Reinforcement for Concrete Structures, Proceedings of the Third International Symposium (FRPRCS-3), Vol.2, pp. 719-726, Japan Concrete Institute, 1997.

[4] T. Harada et al.: “Long-Term Behavior of Anchorage for Carbon Fiber Reinforced Polymer Strands Using Highly Expansive Material”, Fourth International Symposium, Fiber Reinforced Polymer Reinforcement for Reinforced Concrete Structures, (FRPRCS-4), ACI, SP-188, pp.843-853, 1999.

[5] T. Harada et al.: “Development of HEM Anchorage Having Large Capacity of 2500kN with CFRP Strands, (FRPRCS-5) fibre-reinforced plastics for reinforced concrete structures, Tomas Telford, Vol.2, pp.639-648, 2001.

DEVELOPMENT OF CARBON FIBER CABLE

Yoshihisa Minami Takashi Ishikawa Masakuni Uku Ippei Sakaki
Shinko Wire Company, Ltd.
JAPAN

Keywords: carbon fiber, CFRP, cable, anchorage, FEM analysis

1 INTRODUCTION

The so-called "new materials" are gradually used as a construction material and studies are being made if such materials can be practically applied to the main cables of future long span bridges for straight crossing(1). When considering the application of the new materials to the main tension elements, carbon fiber is particularly highlighted because it has many good features such as high tensile strength, high fatigue resistance, light unit weight, freedom from corrosion, freedom from magnetism and low relaxation loss(2)(3). What is more, the modulus of elasticity of carbon fiber reinforced plastics (CFRP) is similar to that of steel. If these favorable features can fully be utilized, we may be able to break through the area that the conventional technology is considered difficult to overcome. The weakness of the CFRP is that it is not as strong as steel against shear stress, which affects the anchorage efficiency.

This paper describes the development of CFRP cables and proposes a design method for the anchorage. The cable, which is now called "semi-parallel carbon fiber composite cable" (SPCC), was subjected to static and dynamic loading tests for the confirmation of the reliability of the cable system.

2 OUTLINE OF CARBON FIBER SEMI-PARALLEL WIRE CABLE (SPCC)

Table 1 gives the nominal specifications for the CFRP 5mm diameter wire used in this development. For a comparison, also given are the characteristics of 5 mm diameter galvanized wires for use in bridge cable.

Table 1 Nominal specifications for CFRP and galvanized wires

Item	Unit	CFRP Wire	Galvanized Steel Wire
Diameter	mm	5.0	5.0
Mass	g/cm^3	1.56	7.85
Unit Weight	g/m	30	154
Fiber Content	%	68	na
Breaking Load	kN	48	30.8 34.8
Tensile Strength	N/mm^2	2,450	1,570 1,770
Modulus of Elasticity	N/mm^2	165,000	196,000
Thermal Expansion	m/m/°C	0.2 10^{-6}	12 10^{-6}

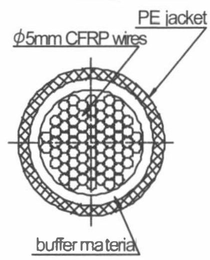

Fig. 1 A Cross-section of SPCC

A typical cross-section of an SPCC is shown in Fig. 1. Fig. 2 shows the detailed configuration of the anchorage system for the SPCC proposed herein. The anchorage was designed by incorporating the design concept of HiAm anchorage and the evaluation by finite element method (FEM). The shear stress that occurs along the interface between the wire surface and the load transfer media (LTM) was assessed by FEM analysis using a quarter 3-D elastic model of an anchorage. High anchorage efficiency was expected in case where the peak of the shear force was lowered by gradually reducing the rigidity of the LTM from the back end toward the front end of the conical cone.

3 CHARACTERISTICS OF CABLES

To investigate the fundamental properties of the SPCC, two Type SPCC19 specimens and two Type SPCC73 specimens were fabricated: One of the SPCC19 specimens consisted of a parallel wire bundle and the other consisted of a long lay wire bundle. The anchorages for the two SPCC19 cables were of the precedent EMPA type in both anchor sleeve and LTM formation, while the anchorages for the SPCC73 were designed in a manner described above. All anchorages were confirmed to have the shear stress, $_{rz}$ that satisfies the limiting value, $_{a}$, by FEM analysis. The design method by FEM analysis and the effects of long lay were evaluated by subjecting three specimens to static tensile test and one to a dynamic tensile test. During these tests, the displacements of the LTM cones and the strain of wires were measured.

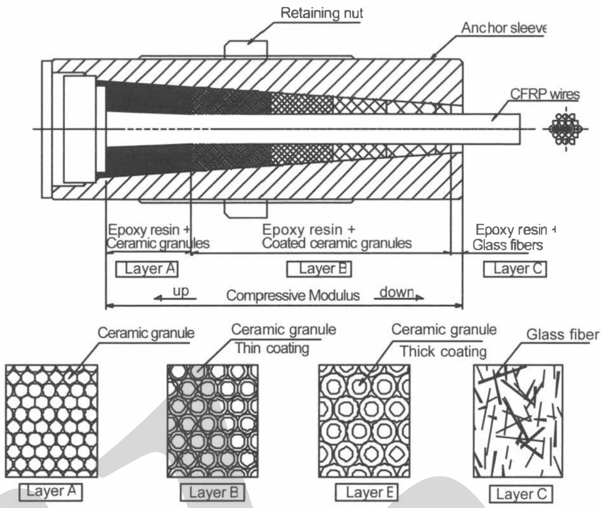

Fig. 2 Configuration of the anchor system

Table 2 Static tensile test results

Type Designation	Nominal Tensile Strength σ_u (N/mm^2)	Actual Tensile Strength σ_{max} (N/mm^2)	Tensile Efficiency σ_{max}/σ_u (%)	Point of Rupture	Displacement of LTM Cone ΔEP ※1 (mm)
SPCC19P	2,450	2,654	108	Free length	2.8
SPCC19SP	2,450	2,627	107	Free length	2.2
SPCC73SP	2,450	2,516	103	Free length	3.2

※1 Measured at 0.45 σ_u

The static tensile test results are summarized in Table 2. Both parallel wire cable and semi-parallel (long lay) cable specimens failed in their free lengths and developed more than 100% static tensile strength. Two million cycle fatigue test was carried out under the conditions shown in Table 3. There was no failure of wires and the anchorages under such severe conditions as no steel wire cables may survive.

Table 3 Loading conditions for dynamic tensile test

Definition	Force (kN)		Stress (N/mm^2)	
Upper	P_{max}	1,752	σ_{max}	1,222.6
Lower	P_{min}	1,250	σ_{min}	872.6
Amplitude	ΔP	502	Δσ	350

4 CONCLUSIONS

(1) Excellent performance of the SPCC system was confirmed in static and a dynamic tensile test. The design method of the anchorage proposed in this paper was justified.

(2) We have established a CFRP cable system that has reliability equal or superior to the current steel wire cable systems and is applicable to stay cables and external tendons on an industrial basis. Authors believe that the design method can be applicable to cable bands of very long suspension bridges with CFRP main cables.

REFERENCES

(1) S. Konno, M. Seiryuu, T. Takahashi and T. Takeda: Studies on ultra long span suspension bridges, Honshu-Hokkaido Bridge Symposium, June 1996 (In Japanese)

(2) S. Konno, S. Yamazaki, T. Noro and H. Maikuma: Material properties of carbon fiber cables for cable supported bridges, Bridge and Foundation Engineering, August 1997 (In Japanese)

(3) U. Meier: Carbon fiber-reinforced polymer modem materials in bridge engineering, Structrural Engineering International, 1/92, pp7-12

LOW LIFE CYCLE COST BUT HIGH PERFORMANCE REINFORCEMENT OF NEW CARBON FIBER CABLE FOR CONCRETE STRUCTURES

Toshiaki OHTA, Professor
Kohei YAMAGUCHI, Assistant
Aya OHTA, Research Worker
Kyushu University, Fukuoka, Japan

Keywords: Unresin Carbon Fibers, UCAS Method, Automatic Arrangement Reinforcement Robot

1. INTRODUCTION

UCAS is an abbreviation of Unresin Carbon fibers Assembly Systems. UCAS is a new construction system suited IT for applying of unresin carbon fibers cables (CF cable) or partially resin ones as reinforcement in concrete structures. These cables can be produced cheaply by using an automatic arranging reinforcement robot whereas preimpregnated and thermosetting processes are eliminated. And the cost of a usual preimpregnated one is very expensive in comparison with that of steel bars. These defects are improved by using UCAS.

This paper introduces a study on the application of an unresin CF cables reinforcement system produced by UCAS for concrete structures. The mechanical properties of CF cables and a bending test one full-scale precast concrete slab are presented. This slab test is aimed to clarify the slab performance at the design load level, the safety factor including the maximum capacity.

2. TENSILE PROPERTIES OF UNRESIN CF CABLE

CF is a strand of 12000 to 70000 continuous filaments, each of which has a diameter of approximately seven microns. The strand has a tensile strength from 10 to 20% of the nominal tensile strength that generally ranges from 3.5×10^4 to 4.8×10^4 N/mm^2, due to initial loosening. CF strand is, therefore, usually preimpregnated (unhardened resin is soaked), and is subjected to thermosetting at a temperature of 120 to 150 degree to obtain a strength slightly over 70% of the nominal strength. The process makes hardened CF more than about 5 times costlier than unhardened CF, and prevents general use of the hardened type for construction. Even if a decrease of tensile strength is considered, the unhardened CF is superior to the hardened type in cost. Table 1 shows the material properties of CF filaments stated by manufacture. Specimen details are presented in Fig. 1.

Table 2 shows the value of the material properties of all data for each type. It shows a high-level tensile strength, and the experimental elastic modulus is close to the one stated by manufacture. Based on safety

Table 1 Material properties of the carbon fibers stated by maker

Maker	Designation	Tensile strength [N/mm^2]	Elastic modulus [N/mm^2]	Ultimate strain [%]	Weight density [g/cm^3]	Cross section area [mm^2/strand]*
Toray	TORAYCA T700S (12K)	4800	2.3×10^5	2.1	1.76	0.46

* 1strand = 12K = 12000 filamens

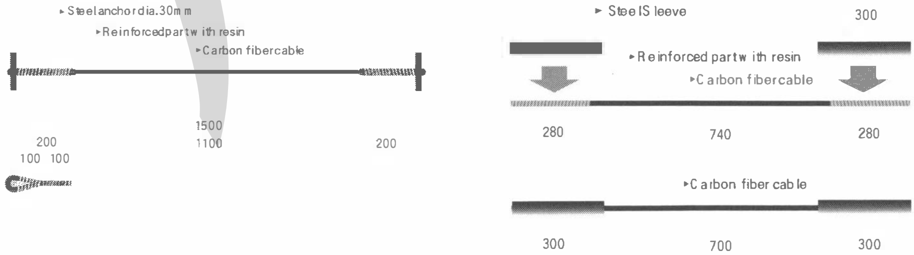

(a) Type A (b) Type B, C

Fig. 1 Specimen details

Table 2 Average of results

Type	Maximum load [kN]	Maximum tensile strength [N/mm^2]	Garantee tensile strength [N/mm^2]	Elastic modulus [N/mm^2]
A	30.9	1676 (34.9%)	1295 (27.0%)	2.03×10^5 (88.3%)
B	58.3	1583 (32.9%)	1381 (28.8%)	2.16×10^5 (93.9%)
C	81.9	1480 (30.9%)	1261 (26.3%)	2.08×10^5 (90.4%)
D	73.0	1323 (27.6%)	---	2.06×10^5 (89.5%)

considerations, the guaranteed strength was taken asthe average value minus 3 times the standard deviation.

3. BENDING TEST ON FULL-SCALE PRECAST CONCRETE SLAB

To investigate the bending performance of a full-scale concrete slab before application to a building in the Kyushu University, the slab with a length of 3.3m, a width of 1.0m and thickness of 14cm as presented in Fig. 2 was constructed. Both main and transversal reinforcement were made of unresin CF cables.

Fig. 3 shows the load - deformation relationship at the design load level of the slab. It can be observed that the design load is lower than the crack load (about 22kN). This means that the slab carries the service load under uncrackes conditions. The behavior in the uncrackes region is linear. In testing, the reloading process was done 5 times at this level. Photo 1 shows the specimen under testing.

4. CONCLUSION

The results of this experimental study are summarized as follows.

(1) The tensile strength of a CF cable is much lower than the tensile strength of a CF strand provided by the manufacturer : it ranges from 30% for a cable made of 120 strands to 35% for a cable made of 40 stands.

(2) The slab has enough capacity to carry the service load where the service load level was much lower than the crack load. The design load level of the slab is about one-forth of the crack load. Compared to the ultimate load, the service load level is about one-tenth. In this study, it was considered that the big grid pitch caused the unstable post crack response. The distance between the grid should be made smaller to prevent this problem.

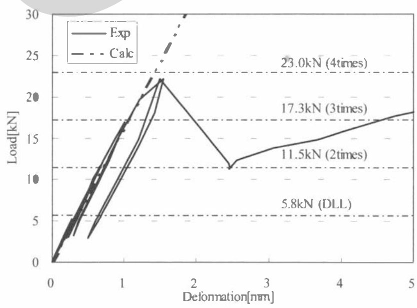

Fig. 3 Load - deformation relation-

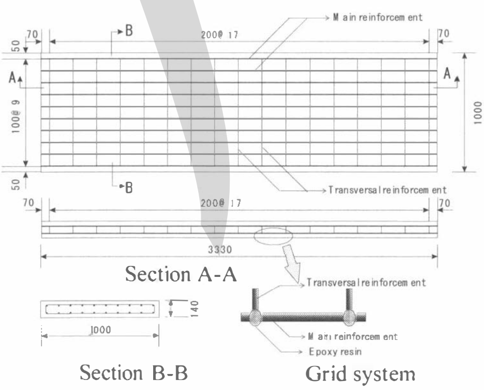

Fig. 2 Specimen detail

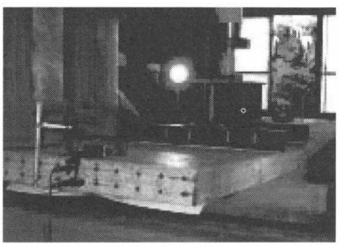

Photo 1 Slab under testing

INNOVATIVE ANCHORAGE SYSTEM FOR CFRP-TENDONS

Bernhard GAUBINGER Gerhard BAHR Günther HAMPEL Johann KOLLEGGER

Institute for Structural Concrete
University of Technology
Vienna, AUSTRIA

Keywords: anchorage system - carbon fiber reinforced plastics (CFRP) - new materials - prestressed concrete - stay cables

1. INTRODUCTION

Durability and load carrying capacity of high strength steel tendons may be affected by steel corrosion or weak performance under fatigue loading. Therefore, the interest in advanced composite materials (AC) - also known as fiber reinforced plastics (FRP) - which have so far shown their efficiency in domains of aircraft construction, mechanical engineering or sports industry has been noticeably increased in the last decade. Several types of these non-metallic advanced composites meanwhile have become available for practical application.

In civil engineering FRP offer great advantages due to their outstanding strength properties in fiber direction, low weight, resistance against corrosion and excellent fatigue behaviour as well as their chemical and magnetical inertness and low thermal expansion. In this connection glass- (GFRP), aramid- (AFRP) and carbon fiber reinforced plastics (CFRP) have mainly come into use. Research indicates that out of these advanced composite materials CFRP-elements seem to have the highest future potential and the best conditions as an adequate alternative to conventional prestressing steel tendons with respect to their mechanical and physical properties.

The outstanding properties of CFRP-elements are only valid in axial direction. However, the mechanical strength properties are very poor in lateral direction. So the key problem concerning their application is to find a suitable anchorage system which regulates the lateral stress distribution acting on the tensile element inside the anchor body, and simultaneously provides an as high system degree of efficiency as possible. Moreover, a direct replacement for conventional steel tendons is prevented at the time by the high material and manufacturing costs.

This paper presents a new type of anchorage as a further contribution to an efficient and reliable application of CFRP-prestressed elements in concrete structures is presented.

2. LATEST DEVELOPMENTS

An appropriate conical potting system was developed at the EMPA-Dübendorf (Switzerland). In this anchor model a gradient material with a low Young's modulus in the front section close to the load and a high Young's modulus at the end of the anchor socket was used as a casting matrix between the CFRP-element and the metal sleeve in order to distribute the high lateral pressure over the whole length of the anchor construction [1]. The way of manufacturing of such an anchorage is complicated since the casting process of the gradient matrix material can only be performed in vertical position.

As part of a research project by Dywidag Systems International, Munich, in cooperation with the Institute for Structural Concrete, Technical University of Munich, another kind of casting anchorage system was designed. In this model a homogeneous casting material has been used, so that the casting procedure could also be carried out in horizontal position. Thus the way of manufacturing could be simplified [2]. However, in order to get a regular distribution of the lateral forces the measurements of the anchoring socket had to be considerably increased which may lead to problems in the construction process (weight of socket, limited time of injection of the casting material).

3. DEVELOPMENT OF A NEW CASTING ANCHORAGE SYSTEM

The Institute for Structural Concrete at Vienna University of Technology is currently engaged in the development of a new anchorage system which takes the anisotropic material- and strength properties of CFRP-elements into account in order to reach a high degree of efficiency. Compared to the anchor models mentioned above a uniform stress distribution of the lateral pressure along the anchoring socket is obtained by its new geometric shape.

The central idea of the new model was to invert the geometric shape of the conical anchor body instead of using a gradient material so that the matrix material is widened in the part of the anchorage close to the load and gets smaller towards its end. Therefore, the conventional geometric shape of a conventional conical anchor body is mentally separated into segments and subsequently reassembled in inversed order as shown in figure 1a. The choice of the height h_i and the inclination α_i of the segment as well as the inner inclination of the metal sleeve β are the main parameters for the regulation of the stress distribution in the anchor body (figure 1b).

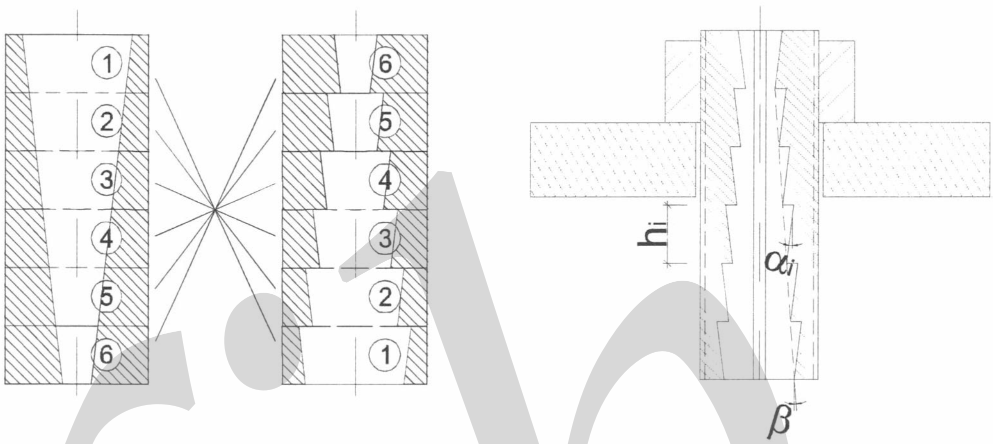

Fig. 1 Inversion of geometric shape (1a) and model of new casting segmented anchorage (1b)

Evaluations have shown that the concentrated peak of the lateral stresses emerges in the conventional system in the front part of the anchoring system whereas in the new model a nearly uniform stress distribution over the whole length of the socket can be reached (figure 2).

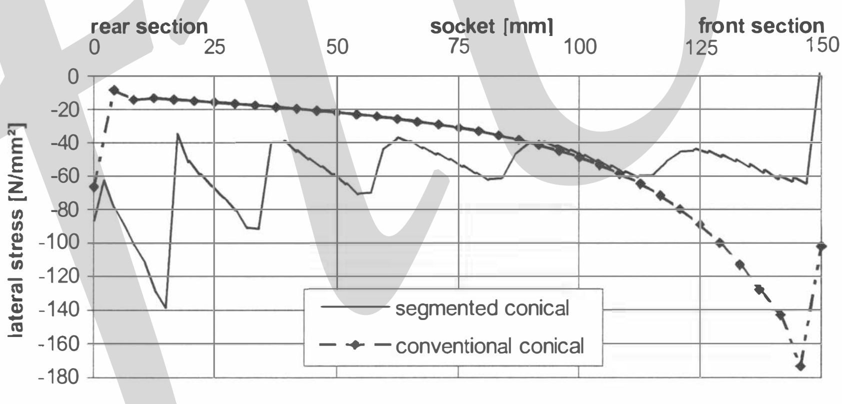

Fig. 2 Lateral stress distribution of the conventional and the segmented conical anchorage

CFRP-elements represent a viable alternative to conventionally prestressed steel tendons with respect to their outstanding material properties. The new anchorage system which is presented in this paper should be seen as a further development in the practical use of CFRP-prestressed systems with respect to economy, efficiency and cost-performance-ratio.

REFERENCES

[1] Meier, U.: Zwei CFK-Kabel für die Storchenbrücke. Schweizer Ingenieur und Architekt, No. 44, pp. 980-985, 1996.

[2] Windisch, A.: Zug- / Spannglieder aus Kohlenstofffaser-Kunststoff-Verbunden für das Bauwesen. Neue Werkstoffe in Bayern, München, 2000.

SMALL AND ECONOMIC ANCHORAGE FOR CARBON FIBER REINFORCED POLYMER RODS

Pascal Klein, Klein Engineering – BBR Systems, Zurich Switzerland
Dr. Amar Rahman, BBR Systems, Schwerzenbach Switzerland
Nik Winkler, Nik Engineering – BBR Systems, Horgen Switzerland

1 INTRODUCTION

Carbon fiber reinforced polymers have very promising characteristics: They provide impressive tensile strength combined with a very low specific gravity. Moreover they are not susceptible to corrosion and possess exceptional tension-tension fatigue resistance. Despite this appeal, two factors have unfortunately hindered more widespread application of this product, namely;

- Raw materials as well as manufacturing costs for the tendons are considerably higher than for conventional prestressing steel,
- State of the art technology for CFRP anchorage – patented by EMPA/BBR 1995 – is very sophisticated and therefore costly.

To date, the use of CFRP tendons has been limited to cases where conventional steel cannot fulfill the technical requirements (weight, fatigue, maintenance-free durability, electrical conductivity).

BBR Systems has developed a low-cost/low-tech small anchor for tendons with capacities of up to 1500 kN. The targets were defined as follows:

- Anchor sizes for single- and multi-rod tendons of up to 37 rods (Ø5 mm) taking into account aesthetic considerations.
- - Simple anchor installation (shop manufactured or on-site assembly).
- - Use of standard commercial parts in order to reduce costs.
- - Achieving an acceptable performance level through the application of readily-available low-cost manufacturing techniques.

This development is not considered to be in competition with products such as those manufactured by Shinko Wire Company, Ltd. The reduced anchor dimensions of the Shinko product totally preserves the efficiency of the anchor (i.e. failure occurs in the free length) whereas the low budget concept presented herein allows for failure in the anchor zone. This is considered to be acceptable for small size tendons since the full tensile strength of the carbon material will not be utilized in any case. In addition, the cost of the carbon material in such anchor sizes is in the same order of magnitude as that of the anchor.

2 DESCRIPTION OF SYSTEM

This system is a spin-off of the well known EMPA/BBR anchorage system for pultruded CFRP rods. The main design criteria are that the system be small and practical, in contrast to the original system which strives for highest possible anchorage efficiency.

2.1 System characteristics

Standard rod diameters are either 5 or 6 mm. These rods are split at the ends and fixed with an inside ring by a simple tool. This tool splits the rod into a central segment with a triangular cross-section and three equal exterior segments with a half-circular profile. The resulting flower shape is resembles the geometry required to achieve an optimum flow of the shear and compressive stresses in an anchor medium (Fig. 1).

2.2 Single rod anchorage:

The anchor sleeve is made of an M24 threaded bar with concentric boring. The flower end of the CFRP rod is pulled into the sleeve and cast-in with an epoxy resin filled with ceramic granules.

The threaded sleeve is 75 mm long and has a Ø5.5mm cavity for the Ø5mm rod and a Ø15mm external diameter to accommodate the cast-in flower end.

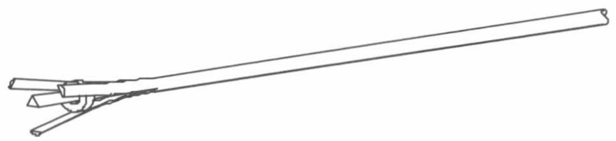

Fig. 1: Carbon rod with flower-shaped split end.

Splitting of the wire provides the following advantages compared with the straight round wire: The bonding surface is considerably increased – the cone produced by the external profiled segments follows a smooth curve and prevents shear peaks at the anchor sleeve exit – the conical shape occurs spontaneously under loading levels approaching fracture – simple straight drilling in the M24 threaded bar is less costly and the preparation of the rod (i.e. splitting) can be achieved with a simple tool.

2.3 Multi-rod anchorage:

The promising results obtained with single-rod anchors encouraged the extension of the system application to multi-rod systems.

Figure (put number here) shows an anchor for 37Ø5mm rods. The CFRP flowers are arranged in a hexagonal pattern for optimum use of the space.

The anchor body, made of steel and threaded on the outside surface, has 37 individual Ø5.5mm-drillings to receive the Ø5mm-rods. The free space between the flowers is cast-in with the epoxy compound filled with ceramic granules.

3 APPLICATIONS

Based on the results of the testing regime, this system is considered ready for implementation in particular fields, some of which are outlined below:

Architectural ties: The use of exposed tensile elements as interior architectural elements is gaining in popularity. These elements are currently manufactured mostly from stainless steel bars and ropes equipped with fancy fittings (terminations). CFRP components are highly recommended candidates for this niche market. The material would be suitable for in- and outdoor use for the suspension of canopy roofs, spiral staircases and transparent safety fences. The CFRP might be combined with aesthetic fittings made of stainless steel or titanium (e.g. open sockets, screw joints).

Guy cables: The low electric conductivity of CFRP is an advantage that makes expensive extra insulators superfluous. Steel guy cables moreover reduce the output efficiency of antennas (e.g. for mobile telecommunication). Small CFRP tendons are practical in such a context. CFRP cables are also in evaluation for use in suspension cables for long-span power transmission lines.

Earthquake engineering: Seismic performance of smaller precast structural and/or nonstructural elements can be combined with easy erection conditions by using connections in the form of unbonded carbon tendons.

Ground anchors: CFRP would be advantageous for two reasons: high corrosion resistance and ease of cutting to the required length in the case of temporary anchors. For ground anchors the size of the termination is crucial since it defines the size of hole to be drilled before installation. The drilling is a major cost contribution which must be kept as low as possible. The simplified anchorage meets this criterion.

For rock anchors no steel sleeve is required at all. The bundled flower ends would be pushed into the anchor hole and the anchorage body would be achieved by injection directly into the surrounding soil. Savings on terminations are combined with savings on corrosion protection measures.

Overhead support cables: Fiber reinforced plastics are in use for the suspension of overhead support cables for tram, bus and train lines. The required properties are: Lightweight, insulation and low maintenance cost.

CONTROLLING VIBRATION OF STAY CABLE

Yves Bournand
Head of New Developments
VSL International
St Quentin en Yvelines – France

Keywords : stay cable, vibration, damping systems

1. SUMMARY

Several solutions have been developed for the controlling of the stay cable vibrations on cable-stayed bridges. Some bridges are equipped with hydraulic and viscous dampers. Friction dampers have been developed and installed on some structures like chimneys and buildings. This paper presents a new development of a friction damper for cable-stayed bridges.

2. INTRODUCTION

The main advantages of the presented friction damper are the following:

- The damper is not activated for small and non-critical vibration amplitudes. Thus, we have reduced wearing and low maintenance costs.
  For UDDEVALLA Bridge, the friction force is adjusted to have an action of the damper only when the amplitude of vibration of the longest cable is exceeding 70 mm.
- The friction damper is designed to be easily installed on existing bridges where cables are subjected to unexpected vibrations.
- All components of the damper are accessible and can be easily inspected and replaced, if necessary, during the maintenance operations.
- The characteristics of the damper can be easily adjusted during the maintenance operations.
- The friction forces are practically constant and independent of the speed of the point to be dampened.
- The damping characteristics are insensitive to the frequency of the vibrations and to the temperature.
- The friction damper is designed so that the damping of the stay cable is not affected by longitudinal movement of the stay due to load variations.
- For better aesthetic, the damper can be placed at a reduced distance from the anchorage.

3. DESCRIPTION OF THE FRICTION DAMPER

The damper consists of two parts, see Fig. 1.

ASSEMBLY 1 is rigidly fixed to the cable by means of a steel collar (A) and moves together with the cable. The major element of Assembly 1 is the two wings (B) projecting transversely to the cable plane, with hard friction partners (C) being attached to the top side and the bottom side of the wings.

ASSEMBLY 2 is rigidly fixed to the bridge structure. It consists of two spring blade half-ring pairs (D), both of them together surrounding the cable and Assembly 1. The two superposed half rings are clamped against each other at the ends and fixed by bolts (E) to the substructure. Soft friction partners (F), which are pressed from the top and from the bottom against the hard friction partners (C) of Assembly 1, are held by the spring blade rings through an inwardly projecting plate (G).

The damper is activated during transverse vibration of the cable. This results in a periodic relative motion between Assembly 1 and Assembly 2. Thereby, friction force and damping reactions, acting against the movement, are produced between the soft and the hard friction partners.

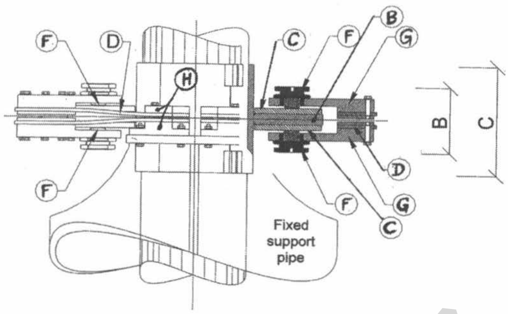

Fig. 1 – Friction damper description.

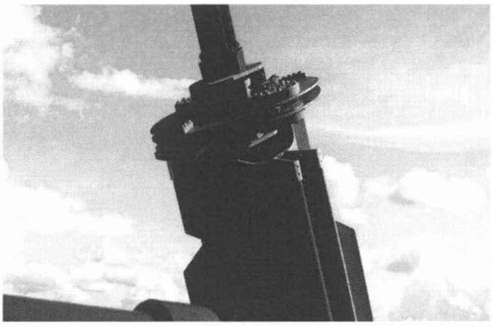

Fig. 2 – Friction damper, without the protection sleeve

4. DESIGN SPECIFICATIONS

The possibility of rain-wind induced vibrations is considered as the most onerous scenario. It is assumed that if an adequate solution to this type of vibration is found, it would also reduce the response due to other types of vibrations, e.g. vortex shedding and parametric resonance.
The analysis of the friction damper is based on the classical galloping theory.

The Figure 3 represents the cable stability diagram (damping VS amplitude), after the installation of the friction damper.

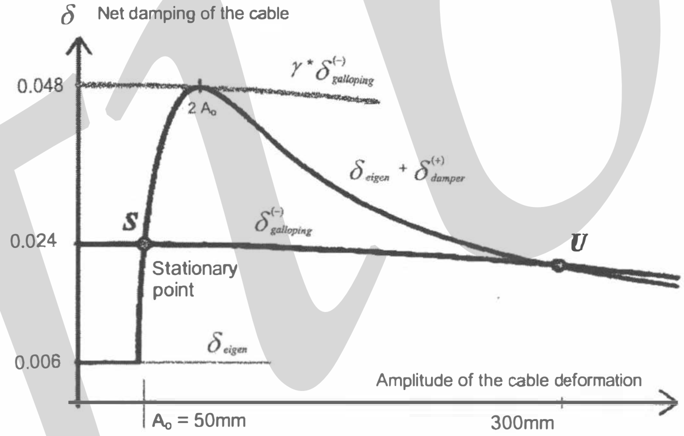

Fig. 3 – Cable stability diagram

5. REFERENCES

Friction vibration absorbers are installed since some years in different types of structures, as for examples:

- Elevated types of structures (chimneys)
- Equipped with multiple-plate friction absorbers developed in 1973
- Pedestrian bridges

Recent references in cable-stayed bridges:

- Uddevalla Bridge (Sweden)
- Gdansk Bridge (Poland)
- Badajoz Bridge (Spain)

APPLICATION OF HIGH STRENGTH PRESTRESSING STEEL TO PRESTRESSED CONCRETE MEMBERS

Masaru Kodama Shoji Shirahama, Dr. Eng.
R & D Department, Shinko Wire Company, Ltd.
Amagasaki, Japan

Keywords: prestressed concrete, prestressing steel, high strength, flexural moment, cracking pattern

1 INTRODUCTION

There are demands for strengthening concrete members to save labor and materials, and also to improve the durability of structures [1]. Therefore, high strength concrete and high strength reinforcing steels have been researched and put into practical structures in the field of reinforced concrete [2]. However, in the field of prestressed concrete, there have been little reports on high strength prestressing steel and its application. This paper presents some physical properties of a newly developed high strength prestressing strand that has a breaking strength higher than the conventional 270K-grade-strand. Flexural test results for the concrete beams post-tensioned with the high strength prestressing strand is also reported.

2 PROPERTIES OF HIGH STRENGTH PRESTRESSING STRAND

The physical properties of the newly developed high strength prestressing strand (hereinafter called "HT") and the conventional prestressing strand (the so called 270K grade in ASTM A416) (hereinafter called "NT") that is commonly used were investigated for tensile strength, stress relaxation, stress corrosion cracking and fatigue resistance.

The tensile properties of the 12.7mm diameter 7-wire prestressing strands are shown in Table 1. Yield load is defined as a proof load at 0.2% offset. Compared with NT strand, the HT strand had a tensile load higher by 23% and a yield load higher by 27%. As a result, the tensile strength of the newly developed strand was rated at 330K-grade, which is the highest strength for the 12.7 mm diameter prestressing strand ever achieved.

Table 1 Tensile properties of 12.7mm dia. 7-wire prestressing strand

Steel Type	Desig-nation	Tensile Load kN	Tensile Strength MPa	Yield Load kN	Yield Strength MPa	Yield Ratio %	Elongation %	Young's Modulus GPa
High strength	HT	235	2,380	224	2,260	95.0	7.8	191
Conventional	NT	191	1,930	176	1,780	92.2	7.6	191

Stress relaxation was tested under an initial stress of 70% of the ultimate tensile strength for 1,000 hours at a temperature of 20℃. The relaxation loss was 0.7% and 1.1 for HT and NT, respectively. Stress corrosion cracking test in a 20wt% NH_4SCN aqueous solution at 50°C satisfied the index proposed by the CEB-FIP Model Code 1990. The fatigue strength of the HT strand is equal to or higher than those of the NT strand when tested under the minimum stress of 50% UTS.

3 BENDING PROPERTIES OF CONCRETE BEAMS WITH HIGH STRENGTH STRAND

To investigate the fundamental properties, flexural tests were carried out for the concrete members post-tensioned with the above-mentioned HT and NT prestressing strands. The target compressive strengths of the concrete mixes were 30MPa, 65MPa and 100MPa. An ordinary Portland cement was used for all mixes with some admixtures. The grout mix was made from ordinary cement and a non-bleed and non-expansion type admixture was added with a water-cement ratio (W/C) of 45% for all concrete beams.

The dimensions of the concrete beams were 1,700 mm long and had a cross section of 150 mm in width and 240 mm in beam height. Loads were applied at two points symmetrically, with a shear span and a bending span of 500 mm each. The test program was planned combining two types of prestressing strands and three types of concrete. Measurements were made on the displacement at the center of specimen, the displacements at the loading points and the fulcrum, the concrete strain on upper and bottom at center of specimen, and cracking patterns of concrete.

Fig. 1 shows the cracking moment. In case of identical concrete strength, the cracking moment of concrete beams with the HT strands are larger than that of concrete beams with the NT strands. On the other hand, in case of identical strand strengths, the cracking moment of high strength concrete beams are larger than that of low strength concrete beams.

With the increase in the strength of prestressing strand and concrete, the flexural capacity increases.

There was no significant difference in the crack width of the concrete beams regardless of the difference in the strength of prestressing steels and concrete types used.

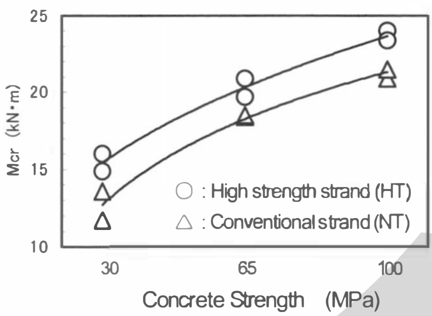

Fig.1 Cracking moment

4 CONCLUSION

The following conclusions can be drawn:

① Compared with the conventional prestressing strand, the newly developed high strength prestressing strand has a tensile strength higher by 23%, which is equivalent to 330K-grade, and a yield strength higher by 27% without sacrificing its ductility. Other properties such as stress relaxation, stress corrosion cracking and fatigue resistance were similar or superior to those of the conventional prestressing strand.

② Flexural tests were carried out on beams made of 30MPa, 65MPa and 100MPa grade concrete and post-tensioned with the high strength prestressing strands. It was confirmed that favorable characteristics of high strength concrete can be utilized by using the high strength prestressing strand that matches with the concrete strength because the cracking moment and the ultimate flexural capacity increase.

③ There is no significant difference in the cracking width regardless of the difference in the strength of prestressing strand and concrete.

REFERENCES

〔1〕 Kodama, M., Zaiki, T., Yamaoka, Y., Ibaraki, N., : Development of 2300MPa grade high strength uncoated stress-relieved steel strands, Proceedings of the 5th symposium on development in prestressed concrete, vol.5, pp.561-564, 1995.

〔2〕 Namiki, T., Sawai, N., Kuroha, K., Hara, T., : Application of high strength concrete with 1000kgf/cm2 to high rise building, Concrete Journal, vol.37, No.3, pp.35-38, 1999.3.
80, 1995.10.

SPRAYED FIBER REINFORCED PLASTICS (SFRPS) FOR REPAIR AND STRENGTHENING

T.Tsutsumi
Engineering Dep.
Fuji p.s. Corporation

J.Niwa
Professor Dr. Eng.
Department of Civil Engineering
Tokyo Institute of Technology

N.Banthia
Professor Dr. Eng.
Department of Civil Engineering
The University of British Columbia

N.Ozawa
Engineering Dep.
Vantec Corporation

Keywords: retrofit, strengthening, FRP, sprayed fiber

1 INTRODUCTION

To address some of the concerns such as the anisotropic characteristics and the poor damage tolerance of continuous fiber composites used for repair and strengthening of existing structures as mentioned above, recently a new method of applying fiber-reinforced polymers, called Sprayed Fiber Reinforced Plastics (SFRPs) for repair and strengthening of existing concrete structures, has been developed as an innovative technique to improve the performance of the FRP wraps. A research activity to make the basic performance clear was successfully done by the UBC (University of British Columbia) in Canada.

Here, a brief summary of the testing, is presented as a part of an ongoing program carried out to confirm the effectiveness of applying this technique to a domestic structure. The program is a collaborative research activity together with UBC for the purpose of proposing a design method.

2 THE CHARACTERISTICS OF SFRPS

In this method, the polymeric matrix and the fiber are simultaneously sprayed at a high speed on the surface of the concrete structure to be repaired. The sprayed composite is compacted pneumatically on the application surface, and is then finished with a roller. The length of the fiber can be adjusted in the process along with the type of polymer and the sprayed thickness. As it has a 2-D random orientation of the fibers, its properties are isotropic in the plane of application and the member, on which the spray is applied shows a non-linear behavior. In addition, the sprayed composites is somewhat tougher and more damage tolerant than a continuous fiber composite, which is brittle and fails in an uncontrolled manner.

SFRPs is mostly used for the manufacturing of bath-tabs and boats, which have an irregular shape and/or circular surface. Spray work is usually done like shown in Fig.1.

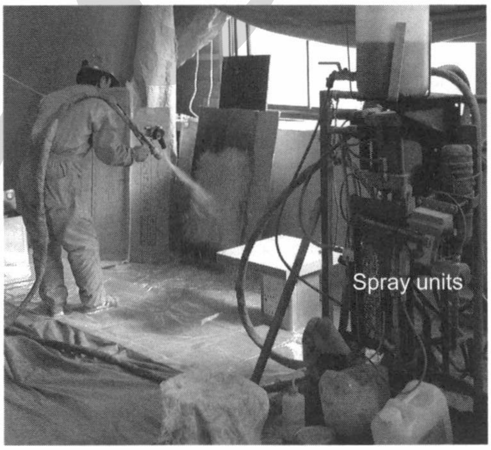

Fig.1 View of spray work together with spray unit

3 EXPERIMENTAL PROGRAMS

For the solution of the problem considering the use in Japan and the establishment of the system of the method, the investigation and the testing program have been planed and executed to make these unclear points clear.

The programs of the development of this method are composed of the purpose as follows.

1) Confirmation of workability and effectiveness of the spray direction
2) Establishment of the design method for members strengthened by SFRPs
3) Confirmation of the effectiveness and performance of the member designed and strengthened by SFRPs based on the 2)

4 APPLICATION AND PROPERTIES OF SPRAYED FIBER

The following conclusions were obtained from testing the uni-axial strength, bond strength, bending strength and compression strength on a cylinder.

1) An increase in the length of the fiber increased not only the tensile strength of the composite, but also its ductility, though the scatter of the curves needs to be investigated.(Fig.2)
   This result means that the combination of various lengths of fibers could be chosen considering the needs of strengthening and the ease of spray work.
2) The bond strength between concrete and composite is larger than the tensile strength of the composite. On the other hand, debonding between concrete and composite by the shear deformation might occur.
3) Bending and compression behavior of the members that are strengthened with SFRPs shows a higher energy absorption. In addition, the effectiveness of strengthening and the mode of failure could be estimated to some extent.(Fig.3 and 4)
4) As SFRPs composite possibly fail at the thin portion. Therefore maintaining a constant thickness is highly needed. This is expected to reduce with the experience and a more skilled workmanship of a nozzleman.

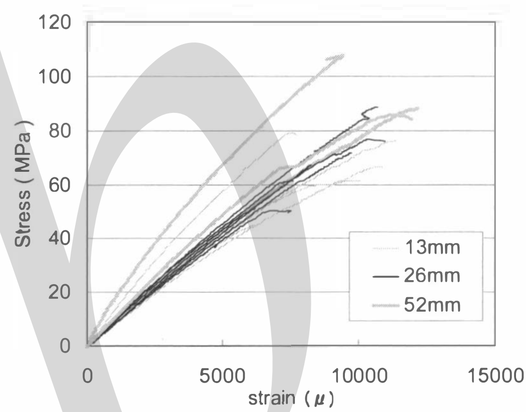

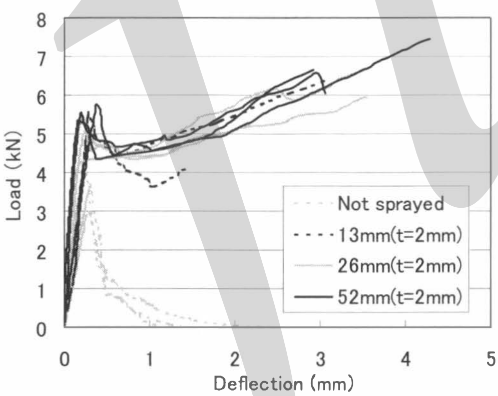

Fig.3 Load-Deflection Curve

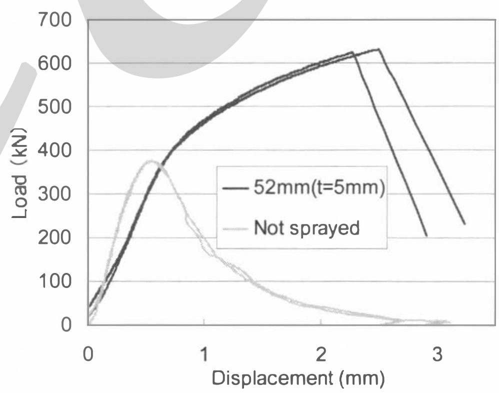

Fig.4 Load-Displacement Curve

REFERENCE

[1] Banthia, N. and Boyd, A.J., Sprayed Fiber Reinforced Plastics for Repairs, Canadian J. of Civil Engineering, 2000

[2] Banthia, N. Boyd, A.J.Jhonson, M.M.Ross, S.L and Sexsmith, R.J., Sprayed Fiber Reinforced Polymers for Infrastructure Restoration, Proc,2nd Inter. Conf. on Engineering Materials, 2001. Volume2. pp213-221

[3] JSCE, Guidelines of repair and strengthen for concrete structure using continuous fiber sheets, Concrete Library 101, 2000.7

RHEOLOGICAL AND SETTING BEHAVIOUR OF MORTAR AND CONCRETE

Prof. Dr.-Ing. G. Thielen, Dipl.-Ing. S. Kordts, Dr. rer. nat. G. Spanka
German Cement Works Association
(Research Institute of the Cement Industry)
GERMANY

Keywords: Flow and Setting behaviour of concrete, cement/plasticizer interaction

High strength, high performance concretes, reactive powder concrete and also self compacting concrete are distinguished from traditional concretes through a low water to cement or water to fines ratio. Adequate workability is important for production, transportation, placing and compacting of concrete.

1 WORKABILITY OF CONCRETE

The flow of concrete depends mainly on the volume percentage (V-%) of the paste in the mix composition, on the rheological properties of the paste and on the grinding curve of the coarse aggregate. The paste includes all solid particles ≤125 µm (called fines), the mixing water and eventually the admixtures. Fig. 1 shows for given concrete compositions the measured flow 45 minutes after mixing (a_{45}) in relation to the cement paste volume for different water cement ratios. Adequate workability of concrete can only be achieved, if the paste volume of concrete is higher than a minimum level of about 250 l/m^3. Paste volumes beyond this limit only improve the flow values, if the paste shows adequate rheological properties. Changing the rheological properties of the paste in the direction of lower viscosity – either, by increasing the water cement ratio (see fig. 1) or by adding plasticizers (see fig. 2), will improve the flow of concrete with given paste volumes.

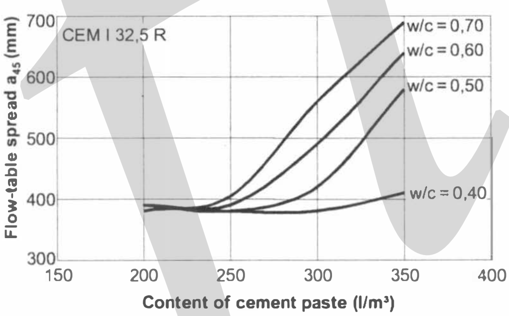

Fig. 1: Workability of concrete (flow-table spread after 45 min) depending on the content of paste volume and of the w/c-ratio [1]

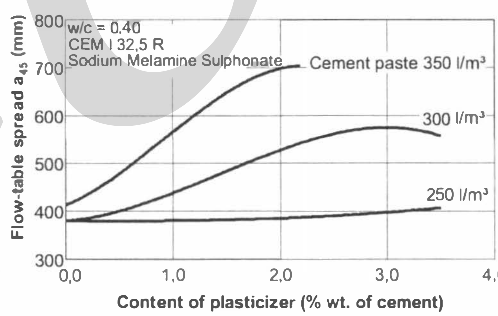

Fig. 2: Workability of concrete (flow-table spread after 45 min) depending on the quantity of plasticizer [1]

2 MINIMUM WATER DEMAND OF PASTES

The most important novel developments in concrete technology - high performance concretes - are based on low water to fines ratios. The magnitude to which the water to fines ratio can be reduced depends on the workability and in particular on the flow behaviour of the paste, mortar or concrete. Considering the rheology of the paste, a minimum water to fines ratio is necessary to assure adequate flow behaviour. This limit is defined by the minimum water content (w_{min}) which is necessary to cover the particle surfaces and more important to fill the pore voids between the particles and by that to reduce the capillary forces acting in the pores. In high performance concretes the total pore volume of the paste is significantly reduced by adding an optimal quantity of a finer filler to the cement.

Cement pastes can only develop adequate flow performance if the water content is sufficient to fill the total pore volume of the mix, which for normal cements amounts to 40 – 50 V.-% and which corresponds to a minimum water-cement ratio of about 22 – 28 M.-%. Beyond this limit the flow behaviour of pastes can be controlled by additional water and/or the use of plasticizers.

3 SHEAR RESISTENCE OF THE PASTE

Adequate workability of low water mixes requires pastes with a low yield limit -necessary for adequate flow behaviour- and an with sufficiently high dynamic viscosity -necessary for adequate resistance against bleeding and segregation. Low yield of pastes requires deflocculation of the solid particles. Polycondensate based plasticisers (eg, naphthalene sulphonate) deflocculate by pure electro-static repulsion whereas copolymer based plasticisers (eg. polycarboxylatethers) cause in addition steric repulsive forces and allow better to control the cement /plasticiser interactions in view of strength development and setting behaviour. The dosage of plasticisers must be controlled to values smaller than saturation in order to avoid segregation of the particles.

4 SETTING BEHAVIOUR

Although controlled by the design of the concrete mix and verified by initial tests, practical problems may arise when the initial flow decreases with time in a way which is incompatible with project dependent transportation and placing requirements. Stiffening and early setting of the fresh mortar and concrete are often caused by evapuration or adsorption losses of mixing water but may also be caused by uncontrolled interactions between plasticizer and cement during the early hydration reactions. To quantify possible negative interactions between cement and plasticizer and their influence on the stiffening and setting behaviour of fresh mortar and concrete a series of tests has been carried out with mortars of similar initial rheological characteristics. The mortars were composed with a water content corresponding to the water demand of the cement for standard consistency [2]. The dosage of each plasticizer added was equal to the corresponding cement paste saturation dosage. For all mixes the stiffening was monitored by measuring the time depending mortar spread according to [3]. Fig. 3 shows the loss of flow of 3 mortars composed of the same cement and 3 plasticizers. This figure demonstrates the different level of initial flow of the mortars having similar initial rheological properties. Since the loss of flow with time is not very different for the three plasticizers, the time of adequate workability is mainly influenced by the level of initial flow.

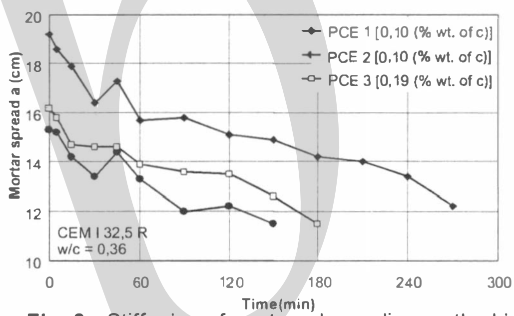

Fig. 3: Stiffening of mortars depending on the kind of plasticizer (Dosage of active agent at the saturation point of corresponding cement pastes)

Table 1 shows the time during which the flow of the mortar is higher than the minimum level required for adequate workability (a_{45} > 12 cm). As can be seen from this table, the duration of adequate workability depends very much on the combination of cement and plasticizer although all the mixes had been designed to show similar initial rheological properties.

Tab. 1: Cement-plasticizer combinations: Time to reach zero-work-ability (12 cm mortar spread flow after 15 shocks)

Cement	SNS	SMS	PCE 1	PCE 2	PCE 3
	Workability time [min]				
CEM I 32.5 R 1	120	120	210	90	120
CEM I 32.5 R 2	270	210	270	150	180
CEM I 32.5 R 3	180	150	360	360	300
SNS, SMS, PCE see tab. 1					

REFERENCES

[1] Thielen, G; Spanka, G.; Grube, H.: Adjusting the consistency of concrete using Superplasticizers; Concrete technology reports 1995 – 1997; ISBN 3-7640-0376-6; pp. 61-68

[2] DIN-EN 196-3: Methods of testing cement – Part 3; Determination of setting time and soundness; German version EN 196-3: 1995-05

[3] EN 459-2: Building lime – Part 2: Test methods; 5.5.2.1.2 Flow table; German version EN 459-2: 1995-03

DESIGN AND SAFETY OF STEEL FIBRE REINFORCED CONCRETE STRUCTURAL MEMBERS

Horst Falkner
Prof. Dr.-Ing.
Technical University at Braunschweig
Braunschweig, GERMANY

Ulrich Gossla
Dr.-Ing.
Köhler+Seitz Consulting Engineers
Nürnberg, GERMANY

Keywords: steel fibre concrete, safety, crack width, underwater concrete, slab on piles

1 INTRODUCTION

Recently there is an increasing number of projects with structural elements made of steel fibre reinforced concrete. Steel fibres are used instead of ordinary steel reinforcement or in addition to reinforcing bars. Both, under service and ultimate loading conditions, the fibre reinforcement is subjected to carry tensile loads.

The addition of steel fibres to plain concrete changes its mechanical properties. Depending on the type and amount of fibres an increase in ductility and better cracking behaviour can be achieved. Especially by the use of steel wire fibres remarkable stresses can be transferred across cracks. The fibre itself can be seen as a kind of reinforcement. A verification concept for SFRC structural members can be derived from this principle.

2 TESTS AND INVESTIGATIONS

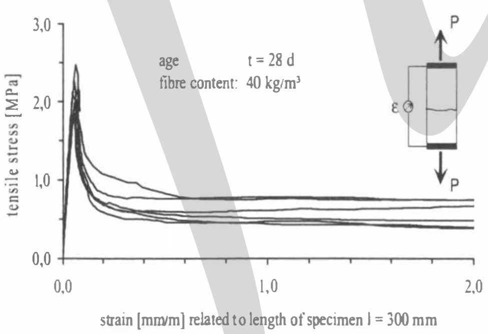

Fig. 1: Direct tension tests on SFRC

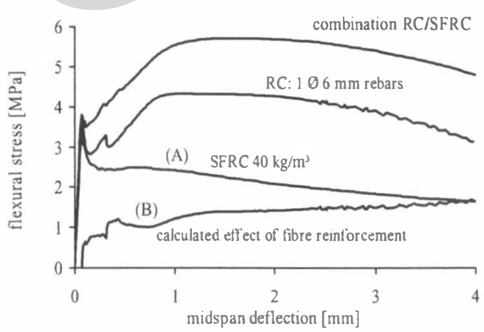

Fig. 2: Bending tests with combined reinforcement

Fig. 1 shows a direct tension tests of a steel fibre reinforced concrete cylinder. With the use of high strength wire fibres, remarkable stress transfer across the crack can be achieved. There is an almost ideal plastic behaviour after cracking. Taking this into account fibres can be seen as equivalent reinforcement. Also the effects of combination of fibre and ordinary bar reinforcement as shown in Fig. 2 proves that in certain cases steel fibres may replace or reinforce ordinary steel bars.

3 CRACK WIDTH IN COMBINED BAR AND STEEL FIBRE REINFORCE MEMBERS

Crack control with fibre and bar reinforcement has been studied at the Braunschweig University. Large scale tests and site experiments on a test track of German Rail have proven that steel fibre concrete increases the durability of non ballast track for high speed railway lines (Fig. 3).

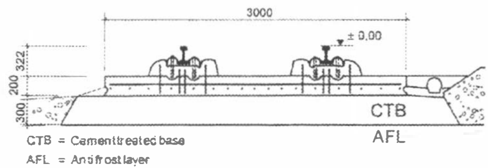

Fig. 3: Non ballast track system

The test specimen with an additional steel fibre reinforcement of 40 kg/m³ showed an entirely different behaviour (Fig. 4). For this case the initial crack width of approximately 0.05 mm increased to only 0.18 mm after 3 million loading cycles. This indicates clearly that the fibres are able to reduce the surface crack width considerably, thus resulting in an improved serviceability behaviour.

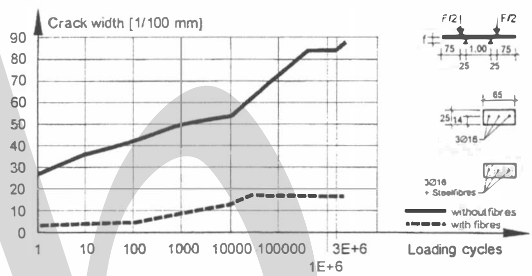

Fig. 4: Fatigue test set-up for crack width of RC and combined RC/SFRC beams

4 SAFETY ANALYSIS AND APPLICATION IN STRUCTURAL MEMBERS

With the results from material tests statistical analysis was carried out to find characteristic values and deviations. By performing a reliability analysis, safety factors for SFRC have been defined. With this knowledge further large scale tests on flat slab type specimens as well as on underwater concrete specimens have been carried out.

In the results of these large scale tests and numerical analysis, huge projects have been carried out in Europe, recently.

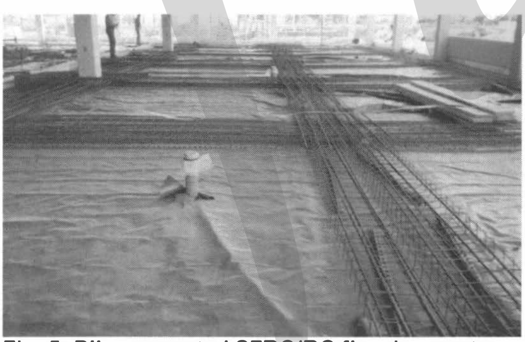

Fig. 5: Pile supported SFRC/RC flooring system

Fig. 6: SFRC underwater concrete in Berlin

This paper presents outstanding applications of SFRC such as for underwater concrete slabs in the huge excavation pits in the centre of Berlin at Potsdamer Platz, industrial floors on piles with combined bar and steel fibre reinforcement, ductile high performance concrete columns for high rise buildings in Frankfurt and elsewhere.

DRAINAGE OF UNDERGROUND STRUCTURES AVOIDANCE OF DEPOSITS

Jan Dirk Chabot, M. Sc. Civil Engineering
Amberg Engineering Ltd.
CH-8105 Regensdorf/Zurich, Switzerland

Keywords: Drainage, preventing lime deposits, reduction maintenance costs

1. INTRODUCTION

The groundwater drainage of existing and new underground structures must allow a permanent pressureless drain of entering water. It must enable correct function also with reduced maintenance due to the costs or prevention of traffic-interruptions. If, however, the drainage system collapses as a result of poor design or neglected maintenance, severe consequences for the security and the durability of the underground infrastructure will arise [1].

The use of hardness-stabilizer is a way to cut the expenses for maintenance of the tunnel drainage and to ensure its function. Even the design of a tunnel-drainage can be simplified with this system.

2. LIME DEPOSITS AND PREVENTION

2.1. Problem

Drainage systems of underground structures are often blockaded by lime deposits (sintering) after shorter or longer periods. In drained underground structures the pressureless drainage must be at all time ensured, to prevent a waterpressure build-up, possible deformations to the structure and visible leakages [2]. Removing these deposits from drainage systems not only requires a sufficient access to the drainage system, but also involves costly frequent maintenance work, causing nuisance to tunnel traffic.

The method described hereafter provides a reliable means of preventing the formation of lime deposits in drainage systems. [3].

2.2. Lime deposits

Lime deposits, i.e. formations occur to the precipitation of calcium carbonate out of the ground- or seepage water. This process is likely to appear in almost standing water as well as in flowing water or in zones of leaking water or damp points (drainage slots, cracks and joints in tunnels as well as in hydropower dams).

The calcium proportion in lime deposits is generally above 95%

Calcium saturated groundwater usually loses approx. 5 - 10 % of its total lime content in the drainage system. The rate of sintering is more or less constant. After an intensive contact to cementeous construction materials like injections or sprayed concrete this rate can be much higher.

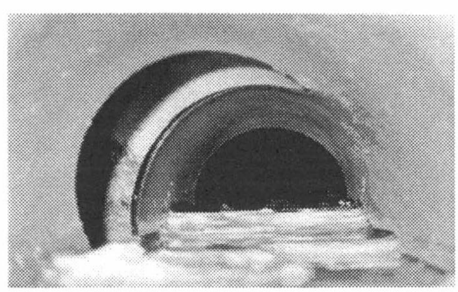

Fig. 1 Hard, white deposits with high rate of sintering in drainage pipes.

2.3. Lime-carbonic acid equilibrium of groundwater

The precipitation process can be described roughly by the lime-carbonic acid equilibrium. This equilibrium will be shifted by external influences when groundwater enters an underground structure. Dissolved calcium can dissipate. This process can be drastically accelerated, if the groundwater comes into longer contact with cement-containing building materials. This raising of the pH-value from e.g. original 6-8 to over 10-11 leads to the complete precipitation of the dissolved calcium from the entering groundwater. So also in zones with low mineralised groundwater heavy deposits can occur.

2.4. Lime deposits prevention methods

Common methods to deal with sintering in drainage systems are regular cleaning or siphoning in order to avoid CO_2-emissions.

Both the first methods do not influence the process of sintering, whereas the **hardness stabilization** controls the sintering process, since the conditioning of the drainage water with chemicals inhibits the precipitation of lime.

Steric and electrostatic effects lead to a better disperse: On the one hand the growth of the lime deposits is inhibited and, on the other hand, crystals are kept in suspension in the water. Both effects rely on physical and not on chemical processes.

In the presence of the agent, the dissolved calcium cannot precipitate anymore; the calcium hardness of the water is being „stabilized%(hence the name), and the water remains hard till the tunnel head.

The hardness stabilizer can be dispensed in either liquid or solid form. Dispensing liquid hardness stabilizer into drainage water is achieved by means of a fixed-place dosing station. The required dosage rate of the stabilizer to the water inside the drainage pipes is based on the average water flow at the end of the drainage section being treated.

Pellets containing solid hardness stabilizing agent are alternatively used for low flow rates or are foreseen in dry packages to keep the inlets of drainage pipes free of deposits.

2.5. Economic aspects of hardness stabilization:

The experiences of hardness stabilization with liquid dosing stations to date have shown excellent cost efficiency.

The economics of a number of installations has been investigated. Conventional cleaning costs of Tunnel drainage systems have been compared with the maintenance and cleaning costs after the installation of hardness dosing units. The investigated 7 cases showed cost reductions of 40 to over 70% for maintenance in hardness- stabilized drainage systems.

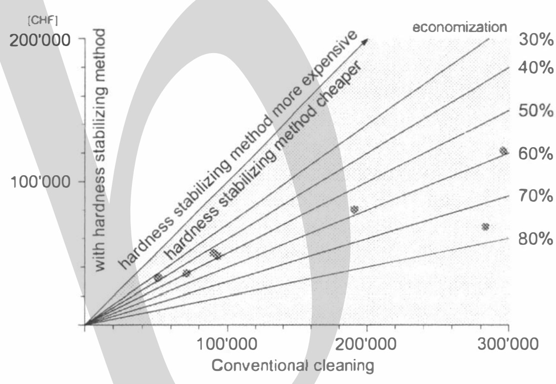

Fig. 2 Cost-comparison scheme of conventional cleaning and hardness stabilization method in 7 Swiss railway and road tunnels. (1 CHF = approx. 80 æ)

2.6. Environmental aspects

The stabilizer consist of polyamide, biologically degradable; water pollution class 0 in Switzerland.

2.7. Conclusions preventing methods

Hardness stabilization provides a lasting method to prevent the occurrence of sintering in drainage systems of deep foundations, railway, and road tunnels. The water conditioning is based on physical processes preventing the precipitation of lime in the drainage pipes, even using lower additives concentration of 1 to 2 ppm. The method is environmental friendly. Also the 57 km long Gotthard Base Railway Tunnel through the Swiss Alps presently under construction as well liquid as solid hardness stabilizer are foreseen in itś drainage system.

REFERENCES

[1] Chabot J.D., Wegmueller M.C.: Effects of groundwater on the durability of underground construction works. Institute for Construction and Planning Management, ETH Zurich, Sept. 1997 (in German)

[2] Chabot J.D.: Drainage of tunnels new aspects. Tunnel, No. 2/2002, Bertelsmann Fachzeitschriften, Germany, 2002

[3] Galli M.: Hardness stabilization of the drainage water, Schweizerischer Ingenieur und Architekt, No. 12, pp. 9-13. March 2000 (in German)

PUNCHING SHEAR STRENGTHENING OF EXISTING SLABS

Maria Anna Polak
Department of Civil Engineering
University of Waterloo
CANADA

Ehab El-Salakawy
Department of Civil Engineering
University of Sherbrooke
CANADA

Keywords: punching shear, strengthening, flat plates

1 INTRODUCTION

Flat reinforced concrete plates supported on columns are simple and economical. They are widely used for example in high-rise buildings and parking garages. The most economical design for the connection between a slab and a column is when the slab is placed on top of the column, without a capital or a drop panel. However, this type of reinforced concrete slab-column connection causes high shear stresses in the slab. In reinforced concrete structures, the dominant mode of failure should not be shear because it is very brittle and nonductile. In order to ensure a ductile (flexural) failure mode of a reinforced concrete slab, proper reinforcement for shear should be provided in the slab around the column. However, if the shear reinforcement, for whatever reason, has not been provided during the construction phase, strengthening of the connection for shear becomes a difficult issue.

The paper presents a new technique for strengthening of reinforced concrete slabs around the column area. The technique is simple to apply to existing slabs, does not chance the appearance of a slab and provides adequate means for increasing punching shear strength. It allows changing a failure mode form punching shear to flexural thus providing needed ductility to the slab -column system. The technique consists of new steel reinforcement properly placed around the column area. The initial laboratory tests designed to check the effectiveness of the new method involved strengthening six slab-column edge connections. The paper presents the reinforcement, the method for applying it to the slab and the results of the initial tests. Previously tested slabs without shear reinforcement (similar to the strengthened slabs) failed in a brittle punching shear mode. The strengthened slabs, in all tested cases, showed increased strength and flexural, ductile modes of failure.

2 NEW TYPE OF REINFORCEMENT

The new shear strengthening reinforcement, shear bolts, are the type of reinforcement which can be used for strengthening and rehabilitation of reinforced concrete flat slabs to prevent shear failures. Shear bolts can be applied to a hardened reinforced concrete slab at any time. They consist of the reinforcing bar anchored at both end at slab surfaces (Fig 1). The installation requires drilling of a small hole (approximately the diameter of the bar) through the slab and anchoring the bolt at both ends. The bolts are not bonded to the slab and no prestressing is required. The anchorage can be, but does not have to, embedded in the slab. If the anchorage is embedded in the slab, the resulting strengthened slab looks almost exactly like the original slab (Fig 2). The shear bolts must be placed in a certain designed configuration around the column.

3 TESTS ON SLABS WITH SHEAR BOLTS

The developed reinforcement was tested for strengthening of slab column edge connections. The tests with shear bolts were part of a larger test programme (phase I) on punching shear behaviour of slab-column edge connections (El-Salakawy et al. 1999, 2000, and 2002). The lack of simple and efficient strengthening technique for punching in slabs prompted the new phase (phase II) of the research. In this new phase, twelve specimens were tested; six of them were strengthened with shear bolts. The six tested specimen contained different arrangements of shear bolts, openings and two had additional strengthening with GFRP laminates.

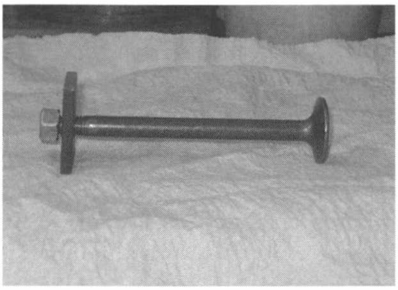

Fig. 1 Shear Bolt

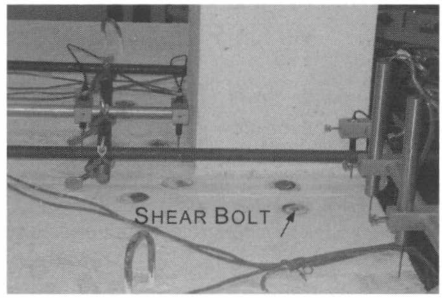

Fig. 2 Slab strengthened with shear bolts

4 TEST RESULTS

All strengthened specimens, except for one, failed in a ductile manner. The specimen SX-1SB (one row of steel bolts) failed in a mixed flexural-punching mode. For the two specimens SX-GF-SB and SH-GF-SB, strengthened with GFRP and shear studs, failure was accompanied by debonding of GFRP laminates (no rapture of GFRP was observed).

Figures 3 shows the maximum measured deflections at the column stub for the specimens without openings. The specimens behaved essentially the same as the specimen with shear studs (in XXX-R shear studs were placed inside the slab during construction).

Fig. 3 Load-deflection of strengthened specimens

REFERENCES

[1] El-Salakawy, E., Polak, M.A., Soudki, K., (2002).“New Shear Strengthening Technique For Concrete”, ACI Structural Journal, accepted.

[2] El-Salakawy, E.F., Polak, M.A. and Soliman, M.H., (1999). “*Reinforced Concrete Slab-Column Edge Connections With Openings*”, ACI Structural Journal, Vol. 96, No. 1, Jan.-Feb., pp. 79-87.

[3] El-Salakawy, E.F., Polak, M.A., Soliman, M.H., (2000). *"Reinforced Concrete Slab-Column Edge Connections With Shear Studs,"* Canadian Journal of Civil Engineering, Vol. 27, No. 2, pp. 338-348.

POLYMER MODIFIED LIGHTWEIGHT CONCRETE REINFORCED WITH POLYPROPYLENE FIBERS

Ksenija Jankovic, Ph.D.
Research Associate
Ljiljana Loncar, B.Sc.Civ.Eng.
IMS Institute, Bulevar vojvode Misica 43, 11000 Belgrade, YUGOSLAVIA

Keywords: polymer, lightweight concrete, expanded polystyrene grains, polypropylene fibers.

1 INTRODUCTION

Polymer modified concrete (PMC) is a composite consisting of two matrices: organic, which is a product of polymerization and inorganic, which is a product of cement hydration.

PMC has improved properties when compared with non-modified concrete. This concrete has high tensile and flexural strength, good adhesion to various bases, high resistance to frost and chemical agents, better waterproofness [1].

The PMC properties depend, not only on composition but also on the way of preparation, compacting and curing of such concrete [3]. PMC curing differs from ordinary concrete because the humid condition of curing is suitable for hydration process and dry condition to polymer matrix forming. Optimum regime of curing and concrete technology fabrication is defined in the first phase of experimental work.

Lightweight concrete reinforced with polypropylene fibers has better ductility, tensile and bending strength than lightweight concrete without fibers [2].

By using expanded polystyrene grains, concrete with different bulk density can be obtained.

On the basis of characteristics of PMC, fiber concrete and concrete with expanded polystyrene grains, it has been assumed that polymer modified concrete with expanded polystyrene grains reinforced with polypropylene fibers shall be material which will preserve good properties of all types of concrete, i.e. by using polymer lightweight fiber concrete, with satisfying compressive and tensile strength, decreased water absorption and with increased ductility and tensile strength can be obtained.

In the second phase of experimental work, which is shown in this paper, the concrete with various compositions were designed by varying cement, water and polystyrene grains quantity. The influence of concrete composition on its bulk density, compressive and splitting tensile strength and water absorption are observed.

2 EXPERIMENTAL WORK

Experimental work included six kinds of concrete with 2.5 % (mixtures A and B) or 1.9 % (other) admixture of polymer (dry material, concerning cement content).

Curing of polymer modified concrete is different compared to normal concrete, because hydration needs wet conditions, but formation of organic (polymer) matrix needs dry conditions. Accordingly, it is necessary to determinate combination of wet and dry conditions that produces the best polymer modified concrete's properties. Concrete was cured 1 day in wet conditions, 6 days in water and after that in dry conditions.

Concrete mixtures were made with following materials:

- Normal portland cement (mixtuers A and B), with 15 % additive of pozzolane (C, D) or with 30 % additive of slag (E, F) which, according to Yugoslav standards, are marked PC 45 (compressive strength is approximately 45 N/mm^2 in the age of 28 days).
- Fine river aggregate was separated into fractions 0/4, 4/8 mm.
- Expanded polystyrene grains 2/5 mm with bulk density 15 kg/m^3 .
- Polymer latex BSR (butadiene styrole rubber) with 33.00 % (mixtures A and B) or 47.37 % (other) of dry material in dispersion.
- Silica fume with 17240 cm^2/g specific surface.

Concrete mixtures are shown in Table 1.

Table 1 Quantities of component materials of concrete

Type of concrete		A	B	C	D	E	F
Cement (kg/m^3)		550	550	550	550	585	550
Aggregate (kg/m^3)	0/4	400	500	560	560	595	560
	4/8	400	500	560	560	595	560
Water (kg/m^3)		220	220	190	205	225	214
Polystyrene grains (kg/m^3)		3.73	3.73	2.5	2.5	2.5	3.0
Polypropylene fiber (kg/m^3)		3.40	5.10	4.0	4.0	4.0	4.0
Silica fume (kg/m^3)		25	25	25	25	25	25
Plastisizer (kg/m^3)		-	-	4.4	4.4	4.4	4.4
Polymer (kg/m^3)		41.2	41.2	22.0	22.0	23.4	22.0

3 THE RESULTS OF INVESTIGATIONS

Compressive strength was tested on the cube specimens of 10 cm edges. Tensile strength was tested on cube specimens of 10 cm edges by splitting. Water absorption was tested on specimens 28 days old. The results were shown in Table 2.

Table 2 Properties of concrete

Type of concrete	A	B	C	D	E	F
Bulk density (kg/m^3)	1650	1890	1950	1880	2050	1985
Compressive strength (N/mm^2)	16.0	26.7	32.9	25.4	30.0	27.0
Tensile strength (N/mm^2)	2.0	2.7	3.2	2.6	3.1	3.0
Water absorption (%)	8.0	6.5	3.7	4.2	3.8	4.1

4 CONCLUSIONS

Comparing kinds of concrete A and B it can be concluded that concrete with lower bulk density has better ratio between compressive and splitting strength. The values of splitting tensile strength are 1/8 (for concrete A) and 1/10 (for concrete B) of compressive strength value.

Comparing kinds of concrete with different value of polystyrene grains (E and F) it can be concluded that concrete with lower quantity of polystyrene grains has greater bulk density and compressive strength and lower water absorption. Increase of 0.5 kg/m^3 grains gives 70 kg/m^3 lower bulk density, 10 % lower compressive strength and 10 % greater water absorption.

Finally it can be concluded that:

- Increase of polystyrene grains quantity give lower bulk density
- With lower bulk density compressive strength is lower
- With lower bulk density water absorption is greater
- With lower bulk density tensile / compressive strength is greater
- Using admixture plastisizer w/c is lower
- Using admixture plastisizer water absorption is lower
- Using admixture plastisizer bulk density is greater.

REFERENCES

[1] ACI Committee 548: Guide For The Use Of Polymers In Concrete, ACI Journal / September - October '86, USA, 1986.

[2] Chen, P.W. and Chung, D.D.L.: A Comparative Study of Concretes Reinforced with Carbon, Polyethylene, and Steel Fibers and Their Improvement By Latex Addition, ACI Materials Journal, Vol. 93, No. 2, March-April 1996, pp. 129-133

[3] Jankovic, K. : Polymer Modified Concrete Based On Recycled Bricks - Choice Of Curing, VII INDIS and CIB W-63, FTN-IIG, University of Novi Sad, Novi Sad, Yugoslavia, 1997, Vol. II, pp. 115 - 123

DEVELOPMENTS OF CONCRETE IN RUSSIA.

Andrei Zvezdov, DSc, Yuri Volkov
Scientific Research, Design and Technological
Institute on Concrete and Reinforced Concrete,
Russia

Keywords: stressed concrete, polystyrene concrete, low water demand binder, non-shrinkage concrete, HPC, hazard action.

An application of complex chemical admixtures in concrete technology during last years were essentially increased. One of such admixtures of MB group is produced by mixing silica fume, superplastisizer and cement hardening regulator. Because the microsilica component is rather expensive the research the research works were carried out for the purpose to replace partially the fumesilica with fly ash. The study revealed that in this admixture up to 50% silica fume can be replaced with fly ashes. The results and other data is given in the table 1.

Table 1 Data on concrete strength with MB modifier, microsilica (MS) and fly ash (FA)

Percentage, % in admixture		Strength, MPa at 28 days	Water tightness, bar	Frost resistance, cycles
MS	FA			
100	-	72,6	16	1000
70	30	76,2	16	1000
50	50	72,0	16	800
10	90	52,4	14	300

One of serious problems of modern concrete construction in Russia is the increased requirements to thermal resistance of building envelope structures. For conditions of Moscow the thermal resistance of outside walls of apartment buildings was increased by three times. The researches have shown, that one of most effective, and main durable thermal isolating material is the concrete making of the aerated cement paste and light weight aggregate.

Modified polysterenconcretes (PC) were developed with especially low thermal conductivity which heatconductivity is lower 30%, than for ordinary polysterenconcrete

Table 2 Data on thermal conductivity of polysterenconcrete (PC)

Density, kg/m^3	Coefficient of thermal conductivity, W/m°C	
	Ordinary, PC	Modified, PC
200	0,070	0,055
300	0,092	0,064
400	0,113	0,080
500	0,132	0,103

It gives the opportunity for application of such material not only in outside walls of buildings, but also even for a heat insulation of industrial refrigerators.

Researches on technology of multi component cement, were carried out and as a result a creation of a new class of binder is achieved cement of a low water demand (ZNV). ZNV is made by a joint grinding of portland cement and dry plastisizer. The addition of other components is possible as fly ash and slag.

The application of ZNV allows to reduce one duration of a heat curing concrete or even abandon it.

Table 3 Data on concrete strength made with low water demand binder — ZNV

Cement ZNV Content, kg/m^3	W / ZNV	Concrete strength, MPa		Frost resistanc, cycles
		1 day	28 day	
350	0,27	100	152	800
450	0,23	131	171	900
550	0,2	142	183	1100

The interesting results were obtained in developing at the expansive admixture for concrete for compensating shrinkage. This class of binders can be received directly during production of a concrete mix by admixing of the expansive admixtures with ordinary portland cement.

Table 4 Data on concrete strength made with expansive admixture

Selfstressing, MPa	Compressive strength, MPa	Water tightness,bar	Frost resistance, cycles
0,71-0,84	46-52	12	350

In conditions of Siberia, where the frosts reach 50 degrees below zero the special concrete designed for such severe conditions of operation are developed.

Besides concrete for common construction application a number of special concrete, including sulfuric concrete, polymer concrete, refractory etc., were developed. Refractory concrete the fire-resistant aggregates prepared with nigh aluminia cement ($A\ell_2 0_3$>50 %) can sustain temperature up to 1800^{0}C. New material is the heat refractory cellular-concrete with average density 400 kg / m^3 and above for temperatures of application up to 1600^{0}C.

The "know-how" production of light weight coarse aggregates directly from slag melts was developed, i.e. manufacturing of aggregates for concrete becomes a part of technological cycle of production of iron.

With introduction of a pore-forming additives into a slag melt using the special technologies the light weight aerated aggregate as it is called the granulated slag – glass aggregate can be produced, which basic characteristics are given in the table.

Table 5 Data on characteristics of granulated slag-glass aggregate

Bulk density, kg / m^3	300-400	450-600	650-800
Coefficient of thermal conductivity, W/m°C	0,095-0,1	0,11-0,12	0,13-0,15
Water-saturation for 1 hour, %	24-21	18-13	12-8

Energy consumption for manufacturing granulated slag-glass aggregate is lower up to 10 times (!), in comparison with keramzite production.

REFERENCES

[1] Reinforced concrete in XXI century, NIIZHB, Moscow, 2001,683 pages (in Russian).
[2] 1-st All-Russia conference on problems of concrete and reinforced concrete, Proceedings, 3 volumes, 1820 pages. Moscow, September 9-14, 2001(in English and Russian)

THE CHARACTERISTICS OF HIGH DAMPING RUBBER BEARING AND EARTHQUAKE RESPONSE OF THE BRIDGE USED RUBBER BEARING

Masahiro Koshitouge Jun Shimada
The Yokohama Rubber Co., Ltd
Japan

Keywords: high damping rubber bearing, isolation bearing, earthquake response

1 INTRODUCTION

The damping performance of high damping rubber bearing (hereinafter called "HDR") is about 0.14 in terms of the equivalent damping constant, a higher damping performance is now needed. We have developed a rubber material which improve the damping performance in comparison with that for conventional HDR. The material properties are cleared by experiments. And HDR developed was assembled to undergo static and dynamic tests, which cleared fundamental properties, deformation performance, and durability that were necessary for isolation bearings. Further, static designs for the HDR developed and the conventional HDR were carried out to confirm that the seismic isolation efficiency of the former is higher than the latter.

2 FUNDAMENTAL PROPERTIES

To express a damping performance, we have a constant named the equivalent damping constant, which is determined by a formula as below and the hysteresis loop for shear stress vs. shear strain as shown in Fig.1. Where the shear stress is the lateral force divided by the steel plate area of the isolation bearing, and the shear strain is the lateral displacement divided by the total rubber thickness of the isolation bearing.

$$heq = \frac{1}{2\pi}\frac{\Delta W}{W} \qquad (1)$$

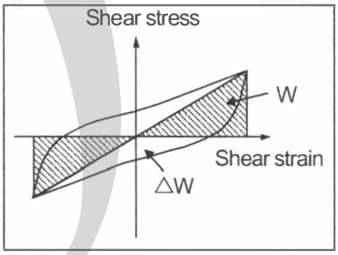

Fig.1 Equivalent damping constant

where, heq is the equivalent damping constant, W is the elastic energy of isolation bearing, and ΔW is the total absorbed energy of the isolation bearing. Using the new rubber material developed, the properties of the isolation bearing are evaluated by dynamic tests on a scaled down model. The test model is shown in Fig.2. The size of that is 135mm×135mm×74.4mm. it is made by laminating rubber sheets with 130mm×130mm square and 3mm thick and 3.2mm thick steel plates alternately to form 4 rubber layers. Table 1 indicates the test conditions. Fig.3 shows the equivalent damping constant, which are determined by each hysteresis loops, taking the shear strain on the axis of abscissa. The equivalent damping constant of the HDR developed is larger by approximately 20% than that of the conventional HDR.

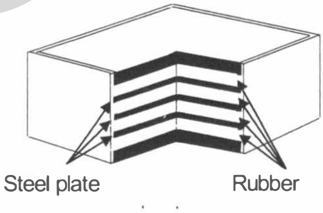

Fig.2 Test model

Table 1 Test conditions

Compression stress (N/mm^2)	6.0
Frequency (Hz)	0.5
Shear strain (±)	1series : 0.25,0.5,0.75,1.0,1.5,1.75,2.0
	2series : 0.25,0.5,0.75,1.0,1.5,1.75,2.0,2.5,3.0

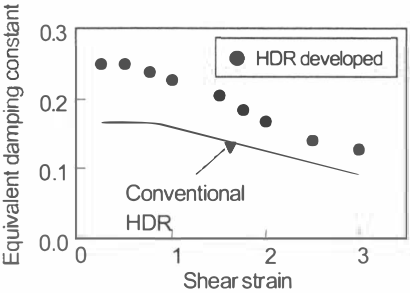

Fig.3 Effect of shear strain on the equivalent damping constant

3 LATERAL DEFORMATION PERFORMANCE

To evaluate the performance of the HDR developed in its ultimate lateral deformation, a test model is assembled to undergo a destructive test. The test model is 620mm × 620mm × 179.5mm in size. The thickness of rubber is 13.5mm multiplied by 5 rubber layers. Fig.4 shows the curve of shear stress vs. shear strain obtained by the test. Fig.7 gives about 4.3 of shear strain at the break, which exceeds 3.5, the target value, then confirms a sufficient performance in the lateral deformation.

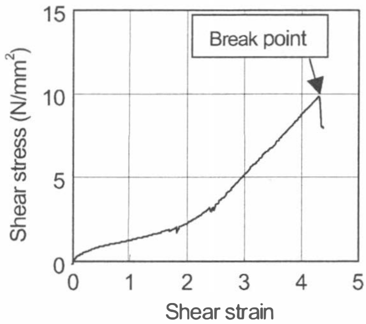

Fig.4 shear stress vs. shear strain

4 DURABILITY

To evaluate the change of the properties in the HDR developed in case of repeated compression force, compression force is repeated on the bearing under 0.7 shear strain. The test model is 420mm × 420mm × 134mm in size. The thickness of rubber 9.0mm multiplied by 6 rubber layers. The test model is taken out from the fatigue tester, before the fatigue test and every 500,000 cycles, to conduct the lateral test and compression test to evaluate the change of the fundamental properties. Fig. 5 shows the changes of the lateral stiffness and the equivalent damping constant caused from the compression force repeated. Where the axis of abscissa indicate the number of cycles of compression force, and the axis of coordinate indicate the ratio of the lateral stiffness, that is standardized at the value before the fatigue test. A change in the number of compression cycles seems to barely affect the properties. Consequently, the HDR developed barely changes the fundamental properties against the compression force repeated, then has an excellent durability.

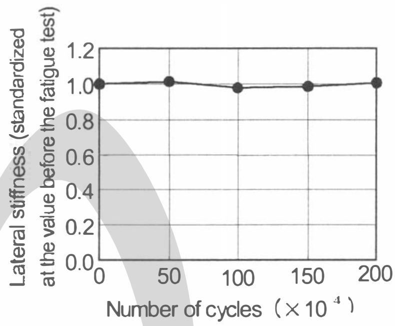

Fig.5 Changes of the lateral stiffness

Table 2 Conditions of the parallel designs

	P1,P4	P2,P3
Maximum reaction force (kN)	2,600	6,200
Reaction force due to dead weight (kN)	1,600	4,500
Lateral stiffness of the substructure (kN/m)	50,000	90,000

5 COMPARISON STUDY

Static designs for the HDR developed and the conventional HDR were carried out respectively, according to the current code in Japan[1]. 3-span continuous reinforced concrete bridges supported by P1,P2,P3, and P4 piers are used in this study. The condition of the parallel designs is shown in Table 2. And table 3 shows the resulted design items. The damping performance of a whole bridge using the HDR developed is, here, 0.177, and it is about 25% better than 0.142 of using the conventional HDR. Eventually, the inertia force of the bridge at an earthquake is decreased, and the lateral displacement of the superstructure is also decreased from 340mm to 310mm. Further, as the volume of the bearings is decreased, a decrease in cost is observed.

Table 3 Result of the parallel designs

HDR	developed		conventional	
Pier	P1,P4	P2,P3	P1,P4	P2,P3
Size(mm)	600× 140	850× 120	600× 140	900× 116
Total volume(cm²)	137,100		144,360	
Disp. of the superstructure	310		340	
Damping of a whole bridge	0.177		0.142	

6 CONCLUSION

A HDR with a better damping performance than conventional HDR has been developed. The properties of the HDR developed were confirmed by dynamic loading tests, destructive test and fatigue test. Further, comparison studies of designs using the HDR developed and the conventional HDR, were made, and confirm that the seismic isolation efficiency of the HDR developed is higher than that of the conventional HDR.

REFERENCES

[1] Specification for highway bridges, and the instruction thereof, Part V: Design, Dec. 1996; Japan Road Association

DESIGN OF AN EARTHQUAKE-RESISTANT EXPANSION JOINT WITH UNSEATING PREVENTION SYSTEM

Kazuhiko Kawashima
Tokyo Institute of Technology
JAPAN

Gaku Shoji
Tsukuba University
JAPAN

Masahiro Koshitouge   Satoshi Shimanoe
The Yokohama Rubber Co., Ltd.
JAPAN

Keywords: expansion joint, seismic design, bridge, shock absorber, unseating prevention device

1 INTRODUCTION

It is obvious from the recent earthquakes such as the 1994 Northridge, USA, 1995 Kobe, Japan, 1999 Chi Chi, Taiwan and the 1999 Duzce, Turkey earthquakes that near-field ground motions with long pulses are destructive for bridges [1]. It is recognized from such an experience that enhancing ductility of structural system is essential for preventing collapse in an extreme earthquake. It is well known that under an extreme excitation, the unseating prevention devices are effective to maintain the integrity of a total bridge system. It prevents an excessive relative displacement between decks or between a deck and an abutment, and even prevent drop of a deck that dislodges from its support. Variety of unseating prevention devices such as cable restrainers, a connection of adjacent decks and a connection of a deck to a substructure have been used worldwide.

Relative displacement developed at an expansion joint is quite large under a strong near-field ground motion. It sometimes reaches over 0.5 m in a 10 m tall standard viaduct with a span length of 30-50 m [2]. Consequently it is required to provide an expansion joint that accommodates a large relative displacement. Since it is not easy to provide such a large gap between two adjacent decks, it is most likely that poundings occur between adjacent decks. Poundings results in a transfer of large lateral force from a deck to the other, no matter how the damage of a deck as a direct result of pounding is localized and limited. This results in damage in piers and bearings in the other deck. Consequently it is effective to provide a shock absorber between adjacent decks for the mitigation of pounding effect.

Since the 1995 Kobe Earthquake, the design requirements for relative displacement, shock absorbing mechanism, unseating prevention devices and measures for preventing settlement of a deck have been extended. It makes required to provide many devices to encounter such a requirement, and this makes the space on a pier at the end of deck busy. This is a problem for maintenance, too. This is not restricted only in Japan, but is a common problem in the design of bridges in the seismic prone regions worldwide.

We developed a new expansion joint that accommodates a large relative displacement with a function of unseating prevention device at the same time. This was developed from a desire that a whole-in-package device that accommodates every function required at the end of deck should be developed. As a first trial, we developed a package that has function of an expansion joint and an unseating prevention device. It is called “big joint.” It simplifies the structure of an expansion joint and an unseating prevention device, and it contributes to save the space.

2 BIG JOINT

Fig. 1 shows the big joint. It has a function of expansion joint and unseating prevention device. An expansion joint consists of rubber cells, and longitudinal and lateral beams. The lateral beams penetrate the openings in the longitudinal beams. The rubber cells and the lateral beams are connected each other by curing adhesion. The wheel weight of vehicles is first supported by the lateral beams, and it is then supported by reinforced concrete slabs through the longitudinal beams.

The longitudinal beams have to be strong enough to support the wheel weight [3]. Consequently, the longitudinal beams can be used as an unseating prevention device for both compression and tension between adjacent decks [4]. Two lateral beams at the ends (end lateral beams) are anchored to the reinforced concrete slabs by anchor bolts so that sufficient strength is assured to transfer the lateral force from a big joint to decks.

Relative displacement accommodated by a big joint can be extended by increasing number of the rubber cells. As long as 500 mm displacement can be accommodated by a standard type big joint

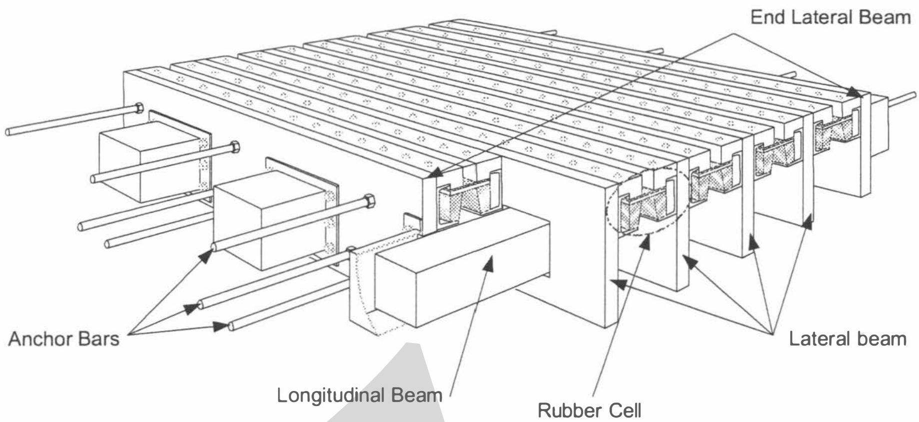

Fig. 1 Basic Structure of the Seismic Expansion

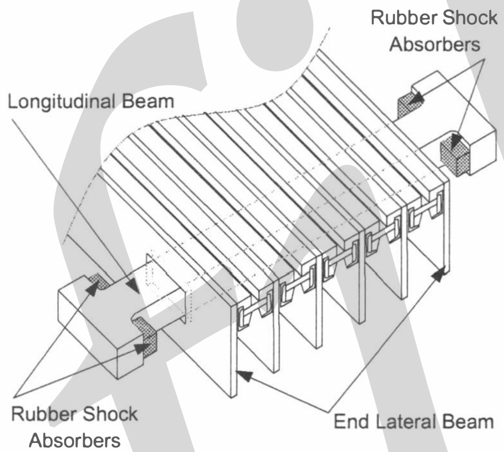

Fig. 2 Longitudinal Beam on the Edge Structure

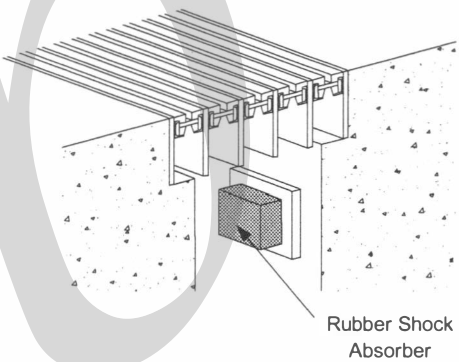

Fig. 3 Installation on the Girder Edge

although further extension is feasible. It should be noted that the big joint accommodates a relative displacement in not only longitudinal direction but transverse direction.

Figs. 2 and **3** show rubber shock absorbers that resist tension and compression. For tension, four rubber shock absorbers per longitudinal beam are provided at protuberances. For compression, shock absorbers are accommodated at one of the decks.

For developing the big joint, various experiments were conducted for rubber shock absorbers. The seismic performance of the big joint was also tested using a 0.6 m wide proto-type model.

REFERNCES

1) Kawashima, K., Seismic Design and Retrofit of Bridges," Key Note Presentation, Proc. 12th World Conference on Earthquake Engineering, Paper No. 1818 (CD-ROM), Auckland, New Zealand.
2) Kawashima K., and Shoji G., 1999, "Effectiveness of Restrainers to Mitigate Pounding between Adjacent Decks subjected to a R Strong Ground Motion", Proc. 12th World Conference on Earthquake Engineering, Paper No. 1435 (CD-ROM), Auckland, New Zealand.
3) Japan Highway Joint Association, 1999, "Manual for Expansion Joint (Draft)", Tokyo, Japan.
4) Japan Road Association, 1996, "Design Specifications of Highway Bridges, Part V Seismic Design", Tokyo:Maruzen.

REPLACEMENT OF THE ISOLATION BEARING OF YAMAAGE BRIDGE

K. Okada S. Suzuki
Tochigi Prefecture
JAPAN

K. Osawa
Kawada Construction Co.,Ltd.
JAPAN

C. Sudoh
Bridgestone Corporation
JAPAN

T. Nishi
The University of Tokyo
JAPAN

T. Suda
Oriental Construction Co., Ltd.
JAPAN

F. Yazaki
The Yokohama Rubber Co., Ltd.
JAPAN

Keywords: Seismic isolated bridge, High damping laminated rubber bearing, Shear deformation-release, Rubber bearing's replacement

1 INTRODUCTION

Yamaage bridge (Fig.1) is a seismic isolated bridge of 6 span continuous prestressed concrete (PC) box girder, with the length of 246.3 m, which was constructed in 1992 in Karasuyama-town, Nasu-county, Tochigi-prefecture as then one of the largest seismic isolated bridges, in Japan, using the high damping laminated rubber bearing. [1]

The feature of a seismic isolated bridge consists in the active reduction of inertia force caused from earthquakes by using isolation bearings, which means both a seismic isolating ability to realize longer periods and a damping ability to restrain excessive displacements.

Such features of the present bridge were confirmed in term of vibration properties, at the time of completion, through vibration tests using a rapid release hydraulic jack or a vibrator.[2]

Further, a shear deformation-release of the high damping laminated rubber seismic isolator was carried out after two years from the completion(1994), when the creep and shrinkage of concrete had been thought to have completed. This work confirmed the propriety of designed deformation as intended initially. And it was a unique one which used synchronized hydraulic jacks on the bridge pier to jack up the bridge girder and needed some reinforcing of the pier.

The replacement of isolation bearings scheduled for this year (2002) is to take them out to evaluate the durability of nine years after commission of the bridge. For this purpose, tests for checking compression properties, horizontal deformation properties, and internal physical properties of the seismic isolator will be carried out nine years after the installation for use.

This report presents the detail of the shear deformation-release practiced at Yamaage bridge, and a proposed plan of the replacement of seismic isolators, which may be informative for construction / maintenance of seismic isolated bridges in the future.

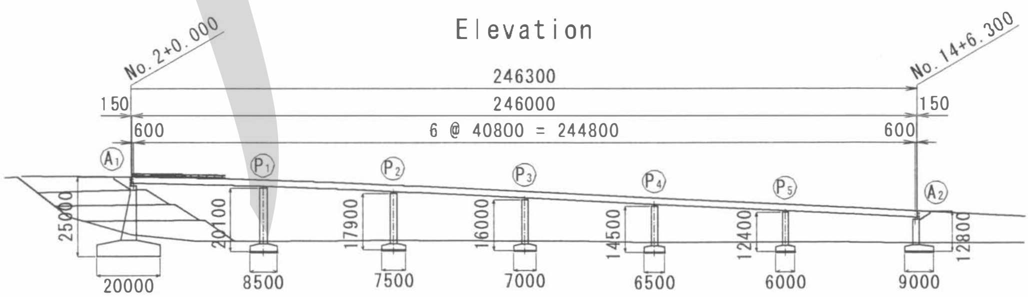

Fig.1 Elevation of Yamaage bridge

2 REPLACEMENT OF THE ISOLATION BEARING

2.1 Outline of the replacing work

This work is made to implement confirming tests for compression properties, and horizontal deformation properties of the isolation bearing to evaluate its endurance about nine years after the commission of the bridge, which includes collecting two existing bearings, and substituting them to new ones. The work, including a total suspension of traffics at night, is scheduled for the end of February, 2002. This report presents the detail of a preliminary investigation, confirmation tests for work, the stresses study, and the plan of supporting work.

2.2 Plan of the supporting work

Different from the above mentioned work for shear deformation release, this work needs to secure working space to substitute bearings. Therefore, as shown in Fig.2, we are planning to assemble temporary towers in front of the pier and to do jacking.

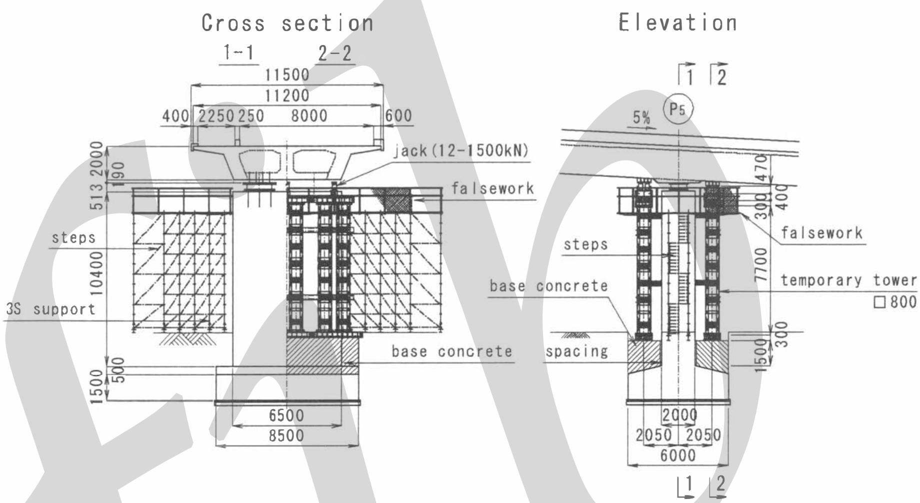

Fig.2 Plan of the supporting work for substituting isolations

3 ACKNOWLEDGEMENT

The present report describes the detail of the work for releasing shear deformation of isolation bearings, and a plan of the work for replacing them for their endurance evaluation, in a seismic isolated bridge that applied a high damping laminated rubber bearing for the first time in Japan. Let's present, in the future, a detail of the work for substituting the isolation bearing and the consideration resulted from the data of physical property tests for collected bearigs. We should add that the work for substituting isolation bearings is promoted as a part of the project named "Research/Development of Seismic Laminated Rubber Bearings for Bridges and Buildings" which is subsidized from the Standard Creation Research and Development Fund of the New Energy Development Organization (for Industrial Technology)(NEDO).

Finally, we hope the work will be informative for maintenance and repair works, and substituting works of bridge isolation bearings (the demand of which is considered to increase in future), further for the development of verifying methods for soundness and seismic properties of a whole bridge, accompanying these works.

REFERENCES

[1] Ikeda,T.,Kumakura,K.,Ohzeki,K.,and Abe,N.; Design of Karasuyama No.1 bridge (Seismic isolated bridge),*Bridge and Foundation*, Jun.1991, pp.5~10

[2] Kawakami,K.,Kumakura,K.,Tani,H.; Design and vibration test for Yamaage bridge – Seismic isolated bridge using high damping laminated rubber bearing, *Civil engineering*, Vol.48,No.8, pp.53~61

EVALUATION OF COMPRESSION FORCE STABILITY OF LAMINATED RUBBER BEARING FOR SEISMIC ISOLATION OF BUILDING

Tohru Sakaguchi , Fumihiko Yazaki — The Yokohama Rubber Co., Ltd., Japan
Toshikazu Yoshizawa — Bridgestone Corporation, Japan
Toshio Nishi — The University of Tokyo, Japan

1. PREFACE

Laminated rubber isolators are widely used as a general and key component of seismic isolated buildings. The compression limit is a very important property. A compression loading test to grasp this critical performance was conducted to destruction of the sample, and the result is now presented, by which their high critical performance is demonstrated and a safety design for the product is confirmed. Formulas of the buckling limit of the laminated rubber bearing and the stress of the inside steel plate have been proposed in the ISO(Draft). Using curves of the load/displacement in the compressive direction obtained by the test this time, a comparison study on the stresses at the buckling and the break in the curve, and the stress determined by the formula is carried out to evaluate the propriety of the formula.

2. OUTLINE OF THE TEST

The rubber is a natural rubber with the shear modulus of elasticity of 0.4N/mm^2. The shape factors are of S_1: 24 – 30 and S_2: 5 – 5.6. The effective sizes of the inside steel plate are ϕ150 and ϕ250, respectively. The inner diameter of the inside steel plate is 5% of the effective size. Test object A is to respond to the designed compression force, 10N/mm^2, and Test object B, 15N/mm^2. The seismic natural period of both objects is 3 –4s.

Table1 Specification of the test object

Test object	A	B
Rubber	Natural rubber	
Shear modulus of elasticity G (N/mm^2)	0.4	
Outer diameter of inside steel plate(mm)	ϕ150	ϕ250
Inner diameter of inside steel plate(mm)	ϕ7.5	ϕ12.5
Thickness of inside steel plate(mm)	1.0	2.0
Material of inside steel plate	SPCC	
Rubber thickness/layer(mm)	1.5	1.8
Number of rubber layers	20	25
Total thickness of rubber(mm)	30	45
S_1	24	33
S_2	5.0	5.6

Formulas for the buckling limit and the stress of the inside steel plate ,regarding to the ISO[1] proposes ,are as follows,

- Formula for the buchkling limit $\sigma_{cr} = \pi/4 \cdot \eta \cdot G \cdot S_1 \cdot S_2$ ……①
- Formula for the stress of the inside steel plate $\sigma_s = 1.5 \cdot \sigma \cdot t_r/t_s \ \gamma_m$ ……②

3.TEST RESULTS

(1) Growth of the destruction and the section by the break

Photo 1 is the section after the compressive destruction, Fig. 1 are compression force/strain curves of the test objects, A and B, respectively, in the vertical direction. Referring to Fig. 1 and Photo 1, the inside steel plate in the central laminated rubbers begins to swell out laterally, which corresponds that the compression force/strain curve begins yielding at the time when the compression force is about 100N/mm^2 . Subsequently, with increasing the swelling out accompanied by increasing the compressive load, a deformation as in a secondary mode proceeds. Regarding the destruction, the inside steel plate for each layer starts abrupt break immediately after that for the lowest layer breaks.Referring to Photo 1, it is observed that the break generated along a oblique surface, which means the compressive destruction occurred by a tensile break of the steel plate.

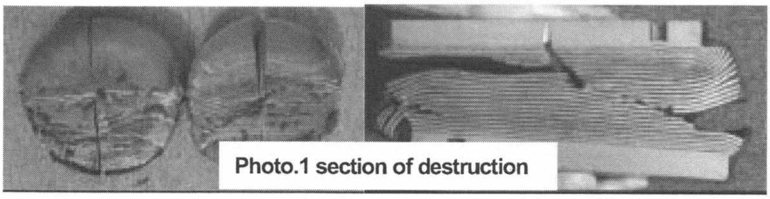
Photo.1 section of destruction

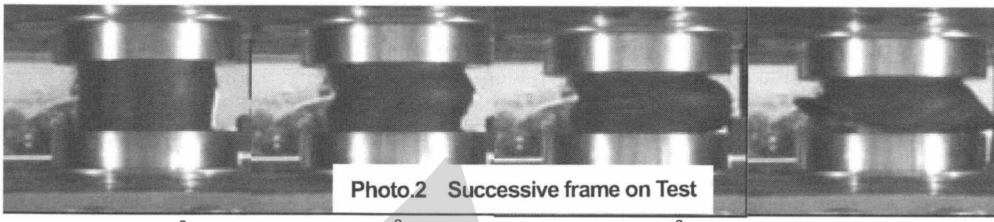
Photo.2 Successive frame on Test

100 N/mm² 140 N/mm² 200 N/mm² Destruction

(2) Curves for the compression force/strain

Table 1 Test results

Test object	A-1	A-2	Design formula	B-1	B-2	Design formula
Compression force at yielding(N/mm^2)	92	113	52 (by ①) 62 (by ②)	100	107	70 (by ①) 104 (by ②)
Max. compression force: σ_{max} (N/mm^2)	-	141	80 (by②)	-	200	133 (by ②)

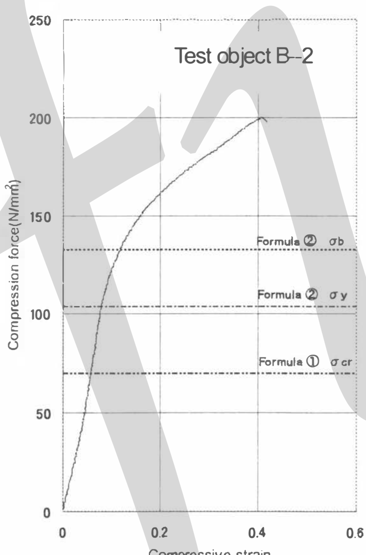

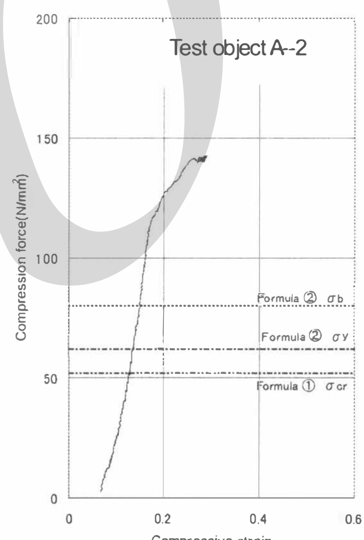

Fig.1 Result of Test

4.CONCLUSION

The compression limit of laminated rubber bearings proved, comparing with the design compression force, to be high enough. Further, the design formula based on the ISO standard[1] stands on the safety side of designing, the propriety of which is proved.

The test object used this time have typical shapes and use typical rubbers, which are widely used for seismic isolation buildings. The test object this time is a standard test object as defined in the ISO standard. Each dependency and critical performances thereof must be cleared in future.

References:

1) ISO/CD 22762 Date: 2002-01-23

FIRE RESISTANCE OF DUCTAL® ULTRA HIGH PERFORMANCE CONCRETE

M. Behloul, VSL, France
G. Chanvillard, Lafarge Central Research Laboratory, France
P. Casanova, Lafarge SA, France
G. Orange, Rhodia CRA, France

Keywords: fire resistance, ultra high performance concrete, material, structure, simulation

1 INTRODUCTION

After a joint research programme lasting more than five years, Bouygues, Lafarge and Rhodia have for the first time launched a range of ultra high performance fibre-reinforced concretes: Ductal®. These products are suitable for use across the whole construction industry and are now being used in civil engineering applications (e.g. bridges and footbridges, anchor plates and sewage works), building works (e.g. wall cladding, acoustic panels and sun screens), industrial structures (e.g. beams and large-span roofing sections) and other technical applications. Fire resistance is one of the main issues for development in the building industry. Fire resistance is determined both by the choice of materials used and by the structure's design. To address this issue, Bouygues, Lafarge and Rhodia have developed the Ductal® AF range, which possesses excellent fire resistance properties, and have validated this behaviour on various configurations of load-bearing elements.

Like all concretes, UHPCs are M0 classified and slow the spread of fire. However, the very low porosity of UHPCs leads to greater internal stresses. In these materials, the porosity is totally enclosed, which prevents water vapour (steam) from escaping. This increases the pressure within the material and causes the spalling phenomenon. Part of the solution for eliminating spalling has been to use organic fibres. This approach is now becoming outdated in the field of HPC fire behaviour. In fact, various northern European countries and Japan recommend the use of polypropylene fibres in their national legislation. Above 150°C, polypropylene fibres begin to soften and melt, thereby providing escape routes for trapped steam.

Using organic fibres does however lead to a loss of rheology and strength that must be countered by fine-tuning the formulation. The Ductal® AF range was developed with this end in mind. It offers outstanding fire behaviour while still offering high slump flow and strength (200 MPa in compression). This article describes the extensive campaign of tests that were conducted at both material and structural level in order to validate the behaviour of these products. The formulas were tested in ISO fire conditions by independent laboratories (CSTB, SFC and VTT). Some elements had received heat treatment as standard with the Ductal® range.

2 MECHANICAL CHARACTERISATION OF THE MATERIAL ACCORDING TO TEMPERATURE

The purpose of this part is to define the behaviour of Ductal® AF when exposed to the high temperatures that typically occur during a fire. The stated results were obtained during two different test campaigns:

- A campaign conducted on cured Ductal® AF as part of the European project HITECO [1]. For the purposes of this document, we shall refer to these tests as the HITECO campaign.
- A second campaign, conducted at the Société Française de Céramique's laboratory, using both cured and uncured Ductal® AF [3]. It should be noted that the tests on the uncured specimens were performed after maturing them under water for four months. For the purposes of this document, we shall refer to these tests as the SFC campaign.
-

3 TESTS ON STRUCTURAL ELEMENTS

Columns and beams, loaded or unloaded, with or without thermal treatment, were submitted to an ISO 834 fire. The tests were performed at CSTB laboratory [5] for unloaded specimens and at VTT laboratory [6] for loaded specimens. Figure 9 below shows the ISO 834 fire curve used for the tests, i.e. $\Delta T = 345\log(8t+1)$.

3.1 Tests on columns

The sizes of the columns are 200*200*900 mm. The columns do not include any reinforcement. 4 tests were made in VTT's laboratory using an ISO fire curve.

Reference	Fire duration	External temperature reached
BY-Ductal#1 : Heat treated column	89 min	984 °C
BY-Ductal#2 : Heat treated column	82 min	972 °C
BY-Ductal#17 : non-heat treated column	95 min	994°C
BY-Ductal#18 : non-heat treated column	85 min	977°C

3.2 Beam tests

3 prestressed beams were fabricated. One beam is tested unloaded under ISO fire, the second beam is tested loaded under ISO fire and the third one is tested at room temperature to determine the ultimate capacity. The length of the beam is 6.15 m. The transversal section has an I-shaped form. The height of the transversal section is 24 cm, the width of the flanges is 15 cm. The beams are prestressed by 2 0.6-inch tendons positioned at the lower part.

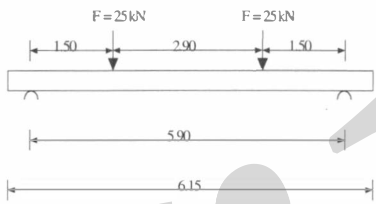

Figure 1. Loading conditions

The beam was loaded for the fire test. Two jacks located 1.5 m from the bearing points each applied a 25 kN downward force. The maximum bending moment was 42 kN.m. This value includes the applied load (37.5 kN.m) and the moment generated by the beam's own weight. The breaking strain measured at room temperature is 88.83 kN.m: the loading rate applied during the fire test was therefore

The test lasted 36 minutes. The photo below shows the state of the beam after the test, during which a bending failure occurred. No spalling was observed. The photo shows that failure was caused by the pre-stressing cables: the crack was straight and the upper part of the beam was undamaged.

4 CONCLUSIONS

This work enabled the fire behaviour of Ductal® AF to be clearly identified. This range of product is perfectly suitable for use in fire-resistant applications. This formula is not susceptible to spalling. The metal fibres ensure high strength even at high temperature. Because there is no spalling, a calculation-based approach can be adopted to determine the fire resistance of Ductal-AF parts. This calculation should be performed using the variations in the compression and direct tensile strengths measured for the material.

- The temperature field can be calculated using the assumptions given in the Fire French DTU [2] (boundary conditions and flow formulae).
- Compressive strength, Young's modulus and free strain data for different temperatures are given in 3.4, 3.5, 3.6 and 3.7 of this document.
- The load-induced thermal strain can be approximated using a bilinear law:

Temperature	LITS in 0/00/q
20	0
350	0
1000	-80

REFERENCES

[1] European project BRITE EURAM III - BRPR-CT95-0065 HITECO
[2] "Méthode de prévision par le calcul du comportement au feu des structures en béton" (*Predicting the fire behaviour of concrete structures – a calculation-based method*), French code of practice DTU P 92-701, 2000
[3] Tests report year 2001, Société Française de Céramique, Paris, France
[5] Tests report year 2000, Centre Scientifique et Technique du Bâtiment, Marne la Vallée, France
[6] Tests report year 2001, VTT BUILDING TECHNOLOGY, Finland

Session 8 | Durability of concrete structures

DURABILITY AND SERVICE LIFE OF CONCRETE STRUCTURES

Odd E. Gjørv
Professor, Dr.techn.
Norwegian University of Science and Technology, NTNU
Department of Building Materials
Tondheim, NORWAY

Keywords: steel corrosion, freezing and thawing, alkali-aggregate reaction, durability design, construction quality, life cycle management

1 INTRODUCTION

In most countries, concrete structures make up a very large and important part of the national infrastructure, and both the condition and performance of all these stuctures are very important for the productivity of the society. Since there is a growing amount of deteriorating concrete structures, however, not only the productivity of the society is affected, but it also has a great impact on resources, environment and human safety. In the present paper, a brief outline and review of current knowledge and experience on durability and service life of concrete structures is given.

2 DETERIORATION

Although carbonation-induced corrosion still represents a durability problem for many concrete structures, it is primarily an uncontrolled penetration of chlorides which represents the most technically difficult and serious problem to the durability and safety of concrete structures. Already in 1917, Wig and Furguson [1] pointed out the problem with steel corrosion in concrete structures in marine environment after a comprehensive survey of concrete structures in U.S. waters. Still, an uncontrolled penetration of chlorides into concrete structures either from marine environment or from deicing salt represents a big challenge to the professional society (Fig. 1).

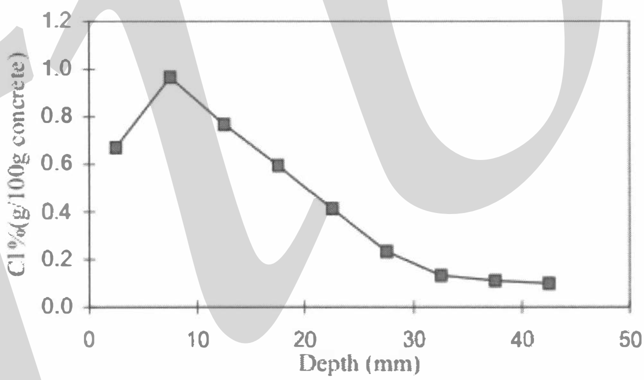

Fig. 1 Penetration of chlorides into a concrete harbor structure (1993) after 8 years of exposure.

The freeze-thaw resistance of concrete has been the subject for extensive research throughout a major part of the last century, but also this type of deterioration still represents a durability problem in many countries. This is primarily due to the widespread use of deicing salt on concrete pavements and highway bridges.

Although the first durability problems caused by alkali-aggregate reaction (AAR) were observed on several Californian concrete structures already in 1940, it has taken a long time to recognize AAR being a general durability problem. In many countries, maintenance costs due to AAR make up a large proportion of the total maintenance costs of concrete structures.

3 CODES AND PRACTICE

Most concrete codes for concrete structures have been upgraded a number of times during the last 30 years, but current code specifications to concrete durability are still almost exclusively based on the traditional requirements to concrete composition, construction procedures and curing conditions, and where requirement to compressive strength is the only performance criteria. For several reasons, this descriptive approach has shown to yield insufficient and unsatisfactory results. In recent years, therefore, much research work has been carried out in order to develop new procedures and recommendations both for durability design, improved construction quality and life cycle management. However, almost nothing from that has been incorporated in current concrete codes. Thus, for concrete structures in marine environment, the new European concrete code only recommends a concrete quality of a lower level than what was recommended for offshore concrete platforms approximately 30 years ago.

4 DURABILITY DESIGN

Although the deteriorating processes such as AAR and freezing and thawing also represent severe durability problems, most of the recent research on durability design has so far been related to concrete structures in chloride containing environments.

Since the parameters both for concrete durability and environmental exposure typically show a high scatter, the introduction of a probabilistic-based service life design has proved to be very valuable. Although there is still a lack of relevant data, this methodology has already been successfully applied to several new concrete structures, where strict requirements to durability and long-term performance have been specified. Basically, the chloride penetration is most commonly modelled by Fick´s 2nd Law in combination with a time dependent diffusion coefficient. In order to include the uncertainty of the various parameters involved, a similar approach as that used for structural design is applied, and where the analysis is principally based on:

- A limit state, e.g. onset of steel corrosion
- A reliability index expressing the probability of failure

5 CONSTRUCTION QUALITY

Traditionally, most engineers look for numerical solutions to solve their problems, and this is also the case for approching the durability problems for concrete structures. Although numerical solutions must play an important role in the design for concrete durability, the issue of construction quality and variability must also be firmly grasped, before any rational approach to durability design can be achieved. Since current programs for quality assurance and quality control are normally based on prescriptive requirements which are not easy to verify and control, new concrete structures are normally completed and handed over to the owner without any documentation on the in situ quality produced. Through a numerical approach to the service life design, however, a set of specific durability parameters must be defined and introduced, and since such parameters can more easily be measured and controlled, this can also provide a basis for performance-based quality control and hence, a documentation of the achieved concrete quality can be obtained.

6 CONCLUDING REMARKS

The growing amount of deteriorating concrete structures in many countries does not only represent technical and economical problems. This is poor utilization of natural resources and hence also the background for the Lofoten Declaration of 1998 [2], which appeals to the professional society to take more appropriate steps and measures to direct the concrete technology towards a more sustainable development.

In the traditional design of concrete structures, problems related to durability and execution of work have through many years been underestimated. Main emphasis has been given to mechanical properties and structural capacity, while durability design, construction quality and life cycle management have been neglected. Also the owners of the concrete structures have very seldom been coming up with special requirements for durability and long-term performance of their structures.

In recent years, an extensive amount of research work has been carried in order to better understand and control several of the most important deteriorating mechanisms, and never before has so much basic information and knowledge about concrete durability been available. The great challenge to the professional society is, therefore, to utilize and transform more of this existing knowledge into good and appropriate engineering practice.

REFERENCES

[1] Wig, R.J. and Ferguson, L.R.: What is the trouble with concrete in seawater? Engineering News Record, Vol. 79, pp. 532, 641, 689, 737 and 794, 1917.

[2] Concrete technology for a sustainable development in the 21st century, Proceedings from an international workshop in Lofoten, Norway, June 1998, ed. by O.E. Gjørv and K. Sakai, E & FN Spon, London and New York, 386 p., 2000.

CORROSION INDUCED FAILURES OF PRESTRESSED CONCRETE STRUCTURES

Ulf Nuernberger
University of Stuttgart
GERMANY

Keywords: prestressed concrete, corrosion, failures

1 INTRODUCTION

Rarely occurring fractures of prestressing steel and failures of prestressed concrete structure can, as a rule, be attributed to corrosion induced cracking. The mechanism of these failures often is not well understood. In this connection it is difficult to establish the necessary recommendation not only for design and execution but also for building materials and prestressing systems in order to avoid future problems.This paper gives a survey about corrosion induced failure mechanisms of prestressing steels with a particular emphasis on post-tensioning tendons.

2 FRACTURE MECHANISMS OF PRESTRESSING STEEL

Depending on the prevailing corrosion situation and the load conditions as well as the prestressing steel properties the following possibilities of fracturing must be distinguished [1]:

- **Brittle fracture** due to exceeding the residual load capacity. Brittle fracture is particularly promoted by local corrosion attack (pitting and wide pitting corrosion) and hydrogen embrittlement.
- Fracture as a result of **hydrogen induced stress-corrosion cracking.**
- Fracture as a result of fatigue and corrosion influences, distinguishing between **corrosion fatigue cracking** and **fretting corrosion/fretting fatigue.**

2.1 Brittle fracture

Influence of corrosion

If the prestressing steel incurs a local corrosion attack in the form of pitting corrosion, the load bearing capacity may get lost at an early stages due to brittle fracture.The performance characteristics of corroded prestressing steels can be determined in tensile, fatigue and stress corrosion tests.

High strength prestressing steels show a far more sensitive reaction to corrosion attack than reinforcing steels, and this increasingly in the sequence tensile test - fatigue test – stress corrosion test In case of uneven local corrosion a corrosion depth of 0.6 mm may suffice for breaking a cold deformed wire under tension of 70 % of the specified tendon strength of about 1800 N/mm^2. At pitting depth of above 0.2 mm cold drawn wires may show fatigue limits (fatigue limits for stress cycles of N = 2 · 10^6) of 100 N/mm^2 and less. Like-new smooth surfaced steels normally show a fatigue limit of more than 400 N/mm^2. In all the performance characteristics of prestressing steels local corrosion attack has the most detrimental effect on the behaviour to hydrogen induced corrosion cracking. In a test developed by FIP the prestressing steel is immersed under tension into an ammonium thiocyanate solution. A minimum and average time of exposure before failure is specified. For cold drawn wire and strand these values are in the order of 1.5, respectively 5 hours. In an example these life times are underrun at corrosion depths of > 0.2 mm.

Effect of hydrogen (hydrogen embrittlement)

In a specific corrosion situation prestressing steel corrosion may release hydrogen which is then absorbed by the prestressing steel. also if the prestressing steel is free of any tensile stresses (not prestressed). The steel will not crack, but depending on the quantity of hydrogen absorbed and the specific hydrogen sensitivity the prestressing steel may become brittle. This may have an adverse effect on the mechanical characteristics, more so on the deformation properties than on the tensile strength.

2.2 Fractures because of stress-corrosion cracking

Stress-corrosion cracking is understood to mean crack formation and crack propagation in a material under the effect of mechanical tensile stresses and of an aqueous corrosion medium. The risk of fractures due to hydrogen induced stress corrosion cracking results from the joint action of very prestressing steel properties and environmental parameters. What is needed is the presence of hydrogen which comes into being under certain corrosion conditions through the cathodic partial reaction of the corrosion. During the corrosion process hydrogen atoms have be set free and get absorbed by the steel. In sensitive steels the hydrogen under the effect of mechanical stresses can create pre-cracks in critical structural areas such as grain boundaries. These cracks may grow and result in material fracture. From the practical point of view one can say that hydrogen assisted damages are only possible

- in acid media or if the steel surface is polarized to low potentials (e. g. if the prestressing steel has contact with zinc or galvanized steel),
- in the presence of promotors such as sulphides, thiocyanate or compounds of arsenic or selenium,
- and under crevice conditions, because the electrolyte in the crevice is poor in oxygen.

In concrete structures the attacking medium is mostly alkaline and acid media are limited to exceptions. Nevertheless, in natural environments the pitting induced H-SCC can take place. Pitting induced H-SCC means crack initiation within a corrosion pit. In the corrosion pits the pH-value falls down because of hydrolysis of the Fe^{2+}-ions. Especially effective is the attack of condensation water or salt enriched aqueous solution (bleed water), when erecting the constructions. In prestressed construction chloride contaminati-on supports a local corrosion attack. Therefore all types of uneven local corrosion should be prevented to exclude failures because of hydrogen assisted cracking. Plastic flow in steel favours an absorption of atomic hydrogen. If a dynamic load of low amplitude is superimposed, the lifetime will more and more decrease with rising amplitude.

2.3 Fractures because of fatigue and corrosion

Prestressing steels can only be subject to a noticeable steel stress in dynamically strained reinforced concrete structures if there is concrete in a cracked state. The stress amplitudes of prestressing steel due to acting high dynamic loads (e. g. a high traffic load of a bridge) may then amount to > 200 N/mm^2 in the crack region. In the uncracked state the steels will show ranges of stress of clearly less than 100 N/mm^2. Cracks in concrete may occur in partially prestressed structures. Since such cracks tend to open and to close in a superimposed fatigue stress the following facts must be considered:

Corrosion fatigue cracking

If corrosion promoting aqueous media penetrate through the concrete crack to the dynamically stressed tendon, corrosion fatigue cracking is possible although this type of corrosion has not been observed in prestressing steel construction so far. Corrosion fatigue cracking manifests itself in that a metallic material under dynamic stress in a reactive corrosion medium (water, salt solution) will show a much more unfouverable fatigue behaviour than under fatigue loading in air. A decrease of the fatigue limit by corrosion is the more distinct the higher the strength of the steel and the more aggressive an attacking medium are. Hence the high strength prestressing steels, when e. g. simultaneously attacked by an aqueous chloride-containing medium, may show a very unfavourable fatigue behaviour.

Fretting corrosion / fretting fatigue

In the vicinity of concrete cracks due to fatigue loading displacements between the tendon and the injection mortar or the steel duct respectively will occur in a cracked component. In bended tendons a high radial pressure acts at the same time on the fretting prestressing steel surface. If air advance to the fretting location through the concrete crack a fretting corrosion is favoured. Fretting corrosion is described as damaging a metal surface similar to wear as a result of oscillating friction under radial pressure with a partner. In the presence of oxygen oxidation of the reactive surface will take place. In concrete embedded tendons, subjected to a relative movement and a radial pressure in the concrete crack between prepressing steel and duct or injection mortar respectively, tolerable fatigue limits of about 150 N/mm^2 for cycles to fracture of $2 \cdot 10^6$ were found.

Also the anchorages of the tendons, due to fretting corrosion influences, show a fatigue limit which is reduced compared with the free length. Under dynamic stress of the anchored tendon the fatigue limit, depending on the type of anchorage, is reduced to values between 80 and 150 N/mm^2.

REFERENCES

[1] Nürnberger,U.: Corrosion and corrosin protection in civil engineering. Bauverlag,Wiesbaden 1995

SOME COUNTERMOVES TO HIGH-DURABILITY OF THE PRESTRESSED CONCRETE BRIDGE IN MARIN ENVIRONMENTS

Yosikuni Kamimura
Okinawa Prefecture
Japan

Satoshi Takano Masaki Yanagita
Kouri-Bridge Project office
Japan

Koichiro Onzuka
P.S.Corporation
Japan

Keywords : precast segmental block, high-durability, chloride damage

1. INTRODUCTION

The Kouri-bridge is a prestressed concrete road bridge, length of 1,960m which connects Kouri-Island and Yagachi-Island both located north of Okinawa prefecture. This bridge is constructing with the precast segmental block, segment block is made of the short-line match cast system method, and its erection method applied is a balanced cantilever construction method using a large scale truss girder. Total number of the segments is 550 pieces, and the weight of a segment is from 80 to 110 ton. This bridge is one of the longest among the bridges of this type in Japan.

Since it is constructed in such a severe marine environment, deterioration effect due to the chloride damage is expected to be significant. Therefore, by implementing preventive countermeasure for concrete deterioration due to chloride damage, prior to the construction, it is intended to achieve "A Minimum Maintenance Bridge".

In this paper, actual measures for enhancing the durability will be reported.

2. ATTMPT FOR ACHIEVING HIGH DURABIRITY

When considering how to achieve high durability of Kouri-bridge, causes for deterioration of existing concrete bridges are, in many case, corrosion of the embedded steel (reinforcing bar, prestressing steel wire) in concrete. Factors inducing this corrosion are considered to be cracks in the concrete generated by various causes such as neutralization of the concrete or alkali-aggregate reaction.

Therefore, the following three points were taken care of, during the construction of the bridge.

2.1 Concrete

Although the design compressive strength of this bridge is designed to be 50 N/mm², early strength development to not less than 14 N/mm² at ages 15-18 hours is necessary to remove the form on the next day of the placement day, in order for shortening the cycle of segment manufacturing. As autoclaving is generally implemented for development of the early strength, "High-early strength expansive agent" was used for fulfilling this requirement in this case. In addition, a high range air entraining water-reducing agent was applied to reduce as much water content as possible in order to produce dense and impermeable concrete against the salt.

The mix proportion of concrete used for manufacturing segments is as shown in Table-1.

Table-1 Mix proportion of concrete

W/C	S/a	Water	Unit amount (kg/m³)					
			Ordinary	Fine agg-	Fine agg-	Coarse ag-	Chemical	Mineral
%	%	Kg	cement	regate①	regate②	regate	admixture	Admixture
33.5	42.9	156	436	307	447	1004	4.66	30

Remarks Chemical admixture : High-range air entraining agent
Mineral admixture : High-early strength expansive agent

2.2 Steel (Reinforcing bar, Prestressing steel wire)

All type of reinforcing bar used are epoxy resin coated, except a part of joint rebar in the curb at manufacturing of the segment, where stainless deformed rebar was used. This because it takes 2 to 3 years from the production of the segment by the completion of the bridge surface, and potential UV deterioration of the epoxy coated reinforcing bar (changing color into yellow, or chalking) during this long construction period is considered.

For prestressing steel wire and fittings, epoxy resin coated products are specified to be standard, and the sheath is all made of polyethylene. Conditions of prestressing steel wire and fittings are as shown in Photo-1 to Photo-2.

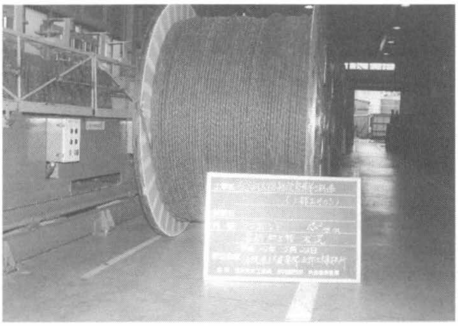

Photo-1 Epoxy coated prestressing wire

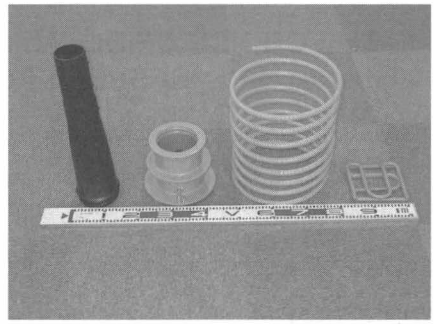

Photo-2 Fitting for bondage

2.3 Treatment of joints between segments

It has been pointed out that the sheath is not continuous at the joint part for the precast segment bridge and that prevention measure against the migration of the chlorides is not sufficient at these joints. Therefore , a polyethylene sheath coupler has been proposed in order to ensure the continuity of the sheath, and its effect of shutting the salt migration was confirmed by experiment. However it had not been applied for any bridge in service, a specimen of the polyethylene sheath coupler (called as PE coupler here) was manufactured and tested for confirmation of its applicability in construction, prior to the erection of the bridge segment.

Configuration of the PE coupler used are as shown in Figure-1 and Figure-2.

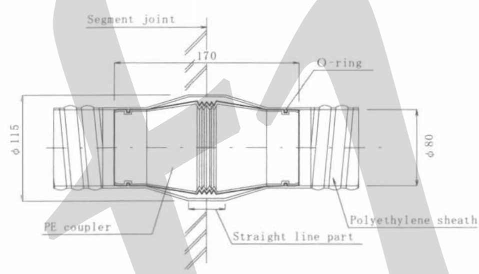

Figure-1 Configuration of PE coupler

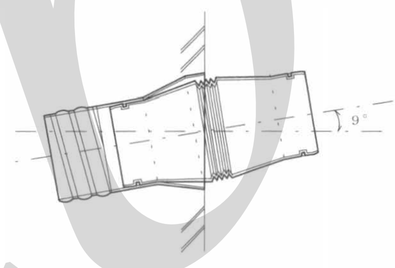

Figure-2 Adjustment for angle change

An O-ring (made of rubber) is attached in order for preventing grout from leaking out and chlorides from migrating inward, and the center part of the PE coupler is devised to be expandable. For changes in angle of the cable at the segment joint, a straight line part is designed to be kept outside of the PE sheath, at which it is cut easily at any required angle.

3. CONCLUSIVE REMARKS

As most of the new structure are now designed and constructed with consideration of minimizing their life cycle cost, low maintenance cost and long life are required for PC road bridges. As mentioned before, from the viewpoint that deterioration due to salts becomes critical defects in achieving high durability for the PC road bridges, corrosion prevention of the steel was mainly implemented for this bridge. However, no matter how high quality material is specified for protection from salt attack, if its properties were not properly understood, or its construction were not properly done, the structure finally made would not have high durability.

REFERENCE

1) Yoshiki Tanaka, "Development of corrosion prevention technology at the joint part of the PC bridge constructed by precast segmental method" Prestressed Concrete, Vol.41, No.5, Sep.1999

THE CHOICE OF DETAILS IN BRIDGE DESIGN WITH RESPECT TO DURABILITY

Damir Tkalcic, BSc.CE, Petar Sesar, MSc.CE, Ana Krecak, BSc.CE
Civil Engineering Institute of Croatia,
Janka Rakuše 1, HR-10000 Zagreb, Croatia
tel. +385-1-6144-725, fax: +385-1-6146-200, e-mail: dtkalcic@zg.igh.hr

Keywords: durability, design, construction detail, furnishing, structure life

1 INTRODUCTION

Durability of bridges is defined by their capability of posessing demanded level of security and usability in certain period of time. Security of bridge is its capability to bear outside influences, and its usability is its capability to fulfill demands of its users. The life of a bridge is influenced by factors which emerge during its design, construction and later in bridge exploitation.
Some of this factors are: design, construction, influence of the enviroment, consequences of bridge exploitation and loads that are implemented on it, maintenance etc.
The influence of detail choice from the design point of view on several types of different bridge constructions and static system which were designed or construction proces supervised will be made in this report.
The durability of bridges is considered to be around 100 years. However the bridge parts have shorter durability. The right choice of details and their implementation can prolong their durability and lower the cost of maintenance. The emphasis will be given to the choice of bearing details, drainage details and details of expansion joints.

2 FURNISHING DETAILS

Since construction of several highway sections is under way in Croatia, different types of bridge structures and statical system are being implemented in design. Bridges consist of structural parts that are used for loadings transfer and parts, so called furnishings, which are used to ensure safe and smooth traffic over the bridge. The emphasys will be given only on three furnishing details which eather represent cost in maintenance or their failure can lead to loss of structures stability and safety. That are bearings (elastomer or teflon), drainage details and expansion joints.

2.1 Bearings

Bearings are structural elements that have purpose of transferring loadings from superstructure to piers or abutments. During that process, bearings have to enable or prevent displacements and rotation of structural elements. In this report problem of concrete hinges will not be analised. Bearings can be elastomeric or teflon. Those elastomeric are put on piers which bear less structures movement. Teflon bearings are put on those piers which bear bigger structures movement. On continuous structure systems the movement at the ends of the structure is bigger than at structures made of freely supported beams. Therefore teflon bearings which can bear bigger movement are to be placed at piers which are most distant to the displacement centre. Closer to the displacement centre, where displacement are smaller, elastomeric bearings can be placed.

The main difference between continuous structures and simple supported structures are in the number of bearings needed and in their sizes. On structures with continuous static system girders are supported by means of cross girder which lies on two or three bearings and therefore less bearings are needed but they are bigger (Fig. 1).

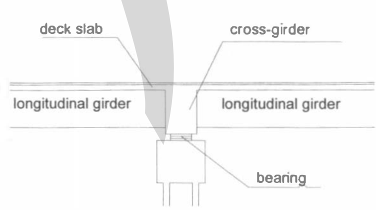

Fig. 1: Bearing detail on continuous structural system

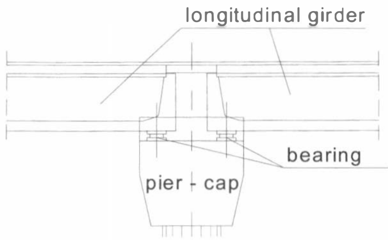

On simple supported structural systems there are a lot more bearings needed because each beam end is supported by bearing. Since the bearing size is smaller they do not permit big displacement therefore shorter expansion sequences are recommended (Fig. 2).

Fig. 2: Bearing detail on simple supported structural system

2.2. Drainage

Drainage of the bridges is one of the most important bridge parts with respect to structures durability. It is a known fact that water has a big destructive energy. Therefore directing waters path off the bridge has to have big designers attention. The pipe system has to be as simple as possible, parts have to be exposed for inspection, cleaning, repair and replacement (Fig. 3). During drainage design, sufficient slopes and terms of water flow has to be ensured. The choice of material, quality of design and economical optimisation have to be at its best value.

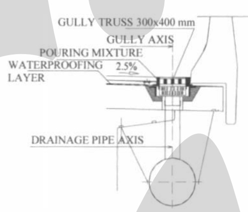

The best material is definitely the one that can last longest like steel or some synthetic materials. The main items designer has to bear in mind while drainage design are: gully distance, transversal slopes and pipes, pipes diameter, gully – pipe joints, pipehanger details, revision shafts arrangement etc.

Fig. 3: Properly designed drainage detail

2.3 Expansion Joints

Expansion joints help overpass the gap between superstructure and abutment and while doing so they have to enable mutual horizontal and vertical displacements, displacements of structures parts as well as safety and comfort during passing over it. Expansion joint has to be easily checked, repaired and replaced when needed. The factors that influence durability of expansion joints are: technical solution (structural shaping), material quality, execution quality, placing precision, maintenance.

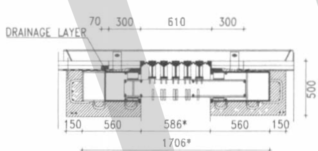

With respect to durability and precise placing of expansion joint there are two important issues: achieving good and longlasting connection between expansion joint and superstructure and geometrical precision of expansion joint placing. Asphalt around expansion joint has to be placed with special care and it is recommended that asphalt around expansion joint is poured (Fig. 4).

Fig. 4: Expansion joint detail

3 FURNISHING DESIGN REVIEW

During bridge design there are some uncertainties what is a sufficient level of furnishing detail design. In time shortage often detailed representation of furnishing is missed out. Later during construction problems like placing, fitting in, connecting with other parts etc emerge. Designer, revisor, employer and contractor are equaly responsible for that situation. Therefore while commissioning, designing, controlling and constructing, all the participants should pay more attention to furnishing drawings, calculations and ensuring that controle and quality ensuring program is implemented properly.

DURABILITY INVESTIGATION OF PRESTRESSED CONCRETE BRIDGE AFTER A PERFORMANCE PERIOD OF 50 YEARS - TAIHEI BRIDGE -

Ryoichi Komonmae Takashi Ohura Yoshinori Okuda
P.S. Corporation
JAPAN

Kazuyuki Torii
Kanazawa University
JAPAN

Keywords: Durability, Self potential, Neutralization, Chloride content, Loading test

1 INTRODUCTION

Taihei bridge which is the first prestressed concrete bridge with pretension T shaped girder, was built in Japan, in 1952. This bridge was located very closed to the Japan Sea, and was dismantled after service period of 50 years because of the river improvement. The authors examined about the durability and ultimate strength of girders removed from Taihei Bridge constructed in the early stage of prestressed concrete technology in this country.

2 INVESTIGATION ABSTRACT

Fig.1 shows the reinforcement arrangement drawing of Taihei bridge. This investigation is to carry out material tests of concrete which were mechanical properties and estimated mix proportion, chloride content, depth of neutralization and prestressing steel wire of Taihei bridge. Furthermore, the authors are to carry out bending test (span:10m) and shear test (span:6m,a/d=2.3) using main girder of Taihei bridge.

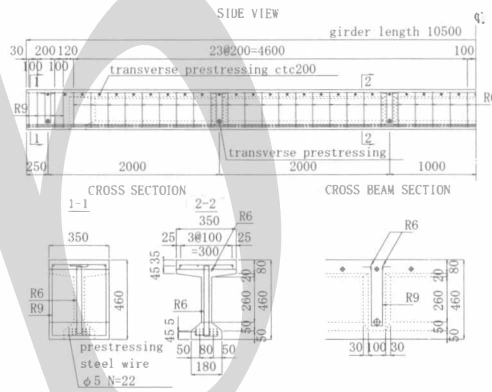

Fig.1 Reinforcement arrangement drawing of main girder

3 MATERIAL TESTS

3.1 Mechanical properties of concrete

Fig.2 shows the relationship between compressive strength and static elastic modulus using a core sampled from main girder. The average compressive strength of concrete was 64.3 N/mm^2. Furthermore the value of static elastic modulus corresponding to compressive strength was considerably greater than the value in the actual guideline. However, the static elastic modulus corresponding to a compressive strength of concrete of 60 N/mm^2 given in the "Guidelines for the Design and Construction of Prestressed Concrete, the Japan Society of Civil Engineers, 1961" is 45.0 N/mm^2. Thus, the test results for Taihei bridge compared to the guidelines at that time, are appropriate.

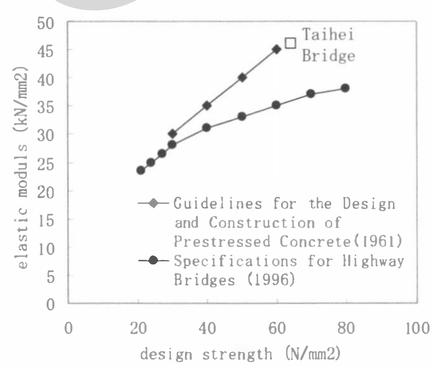

Fig. 2 Relationship between compressive strength and static elastic modulus

3.2 Estimated mix proportion

Table 1 shows the results of estimation of mix proportion of concrete. The obtained water to cement ratio of 33% of the concrete may be considered to be more appropriate than that obtained by the results of compressive strength tests given earlier. Another noteworthy feature is that the weight per unit volume of concrete is very high.

Table 1 Estimation of mix proportion of concrete

Weight per unit volume (kg/m^3)	water-cement resio (%)	Weight per unit volume of concrete (kg/m^3)		
		cement	water	aggregate
2460	33	438	144	1878

3.3 Depth of neutralization and Chloride content

Practically no neutralization zone existed over the entire cross section of the girder as indicated by spraying the phenolphthalein solution on the cross section of the outside girder positioned on the offshore side. Fig. 3 shows the distribution of chloride content of the through core sampled from the web of the outside girder positioned on the offshore side. The chloride content on the surface on the offshore side was extremely high. However, the chloride content beyond 2 cm below the surface was practically negligible.

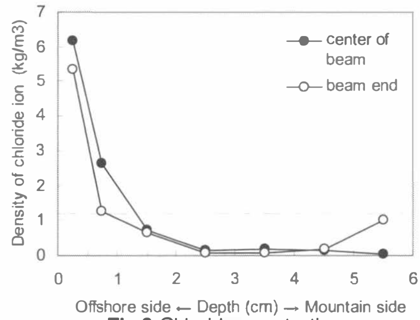

Fig.3 Chloride penetration

3.4 Mechanical properties of prestressing steel wire

Table 2 shows the mechanical properties of prestressing steel obtained from tensile tests. The yield load and Young's modules are rather small compared to the current standard value. Although the steel wires of the Taihei bridge had been used for a long period, the actual relaxation value was greater than the standard value. It is thought from these result that the prestressing steel using Taihei bridge was not subjected to blueing.

Table 2 Mechanical properties of prestressing steel

Item	Test result	Standard value
Diamater	5.02mm	5.00±0.05mm
Tensile Load	33.17kN	Grater than 31.9kN
Yield Load	26.42kN	Grater than 27.9kN
Young's modulus	194.67kN/mm^2	(Nomally 200kN/mm^2)
Elongation	4.17%	Grater than 4.0%
Reraxation	3.33%	Grater than 3.0%*

* The relaxation rate after 10 hours given here indicates the standar value prescribed in JIS-3536 of 1988

4 LODING TESTS OF PC GIRDER

4.1 Bending test

Fig. 4 shows and load-displacement curve according to the results of the bending tests and non-linear two-dimensional FEM analysis. The results of non-linear FEM analysis in which case using effective tensioning force estimated from the load at which crack propagation re-starts (σ_{pe}=660N/mm^2) agreed well with the results of bending tests. The failure load exceeded the flexural strength by beam theory. The final failure occurred by breakage of the prestressing steel. The strain measured in the concrete at the upper edge at failure was about 2600 x 10^{-6}.

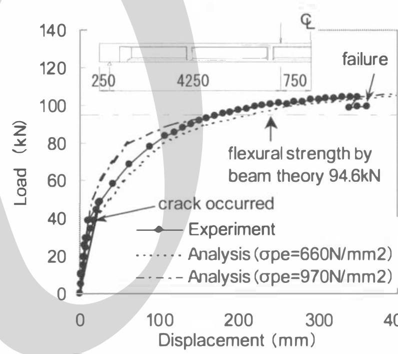

Fig. 4 Load-displacement curve Bending test

4.2 Shear test

Fig. 5 shows the load-displacement (at the center of span) curve based on the results of the shear tests. After a diagonal crack occurred from the loading point toward the supporting point, a flexural crack occurred in the isoflexural zone, and ultimately, the girder failed at the position of the diagonal crack. Failure of the stirrup was confirmed on the failure surface. The failure load was approximately 2.5 times the value of the shear strength given in the Standard Specifications for Design and Construction of Concrete Structures (Design Part).

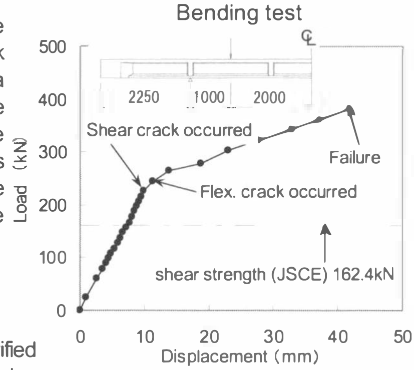

Fig. 5 Load-displacement curve Shear test

5 CONCLUSION

Taihei bridge was studied and the results of the investigation verified that the bridge is a sound PC bridge with very high durability, having maintained its mechanical properties even after 48 years of use.

REFERENCE

[1] Douniwa: Glimpses of PC works in the initial stages, Civil Engineering Works, Nov. 1964 Supplement, pp. 231-235, 1964/11.

[2] Technical Sub-committee on Concrete, the Cement Association of Japan: Estimation of mix proportion of hardened concrete, Cement Concrete, No. 251, pp. 2-3, 1968.

COUNTERMEASURES FOR CHLORIDE-INDUCED CORROSION OF STEEL BARS IN COASTAL CONCRETE BRIDGE IN A SEVERE SALINE ENVIRONMENT

Minobu Aoyama and Masahiro Nomura
Civil Engineering Research and Planning Department, Quest Engineer Co., Ltd., JAPAN

Kaoru Sakamoto
Hokuriku Branch, Japan Highway Public Corporation, JAPAN

Kazuyuki Torii
Department of Civil Engineering, Kanazawa University, JAPAN

Keywords: chloride-induced corrosion, chloride ion, durability design, PC bridge, LCC

1. Introduction

The Oyashirazu coastal bridge is a PC bridge with high piers, which was constructed along the coast of the Sea of Japan in the period of 1985 to1987, and hence exposed to a severe saline environment. Based on the survey concerning the wind-laden chloride ions around the construction site and its influence on the deterioration of concrete structures, in the planning, designing and construction of this bridge, we employed some countermeasures against the chloride-induced corrosion of steel bars as far as possible; improving the shape of pier and slab, increasing the cover depth of steel bars, and in special cases, coating the surface of the concrete and so on.

About 15 years have already passed since the Oyashirazu bridge was constructed. A recent survey showed that chloride ions have penetrated to a considerable extent into the bridge piers that are directly struck by the waves. For this reason, in the period of 1998 to 2000, a surface coating was applied to prevent further penetration of chloride ions into the affected RC piers. This type of countermeasure was also applied to other parts of the superstructure of the bridge to prevent the chloride-induced corrosion of the steel bars.

This paper describes (1) countermeasures for chloride-induced corrosion of the coastal bridge at the time of construction, (2) surveys conducted prior to the maintenance of the bridge, (3) repair methods for the deteriorated parts, and (4) evaluation of various countermeasures. In addition, the most suitable countermeasure to improve the durability of concrete bridges in coastal areas is discussed from the viewpoint of Life Cycle Cost (LCC).

2. Outline of coastal bridge

The Oyashirazu coastal bridge is a prestressed concrete road bridge, 3,373m in length and of height 16~36m above sea level. One third of them are above seawater.

High waves arise on the Oyashirazu Coast; the rate of occurrence of 1m or higher waves is 47% and that of 2m or higher waves is 8.9% over a one-year period.

3. Countermeasures at the time of construction

The amount of chloride that had accumulated and penetrated into the concrete is shown by the Fick`s second diffusion law (Formula 1), and the required cover depth was calculated to be 7cm for the superstructure and 10cm for the substructure.

$$C = C_o\left(1 - \mathrm{erf}\left(X/(2\sqrt{DcT})\right)\right) \qquad \text{Formula 1}$$

C: chloride content at the position (g/cm3)
Co: Surface chloride content (g/cm3),
X : Depth from the surface (cm)
Dc: Diffusion coefficient (cm^2/sec)
T: Time passed after construction (sec)

Hollow slabs or box-beams were used for the superstructure because they have less surface area.

Some parts of the superstructure were painted, and corrosion-proof panels were attached for isolation of chloride ions.

4. Maintenance

The changes in chloride ion penetration into concrete with were investigated. The amount of chloride penetration was shown with characteristic values, Co and Dc. Co shows the saline environment and Dc shows the process of chloride penetration. With these values, we predicted chloride penetration and studied protective countermeasures.

Our monitoring revealed that many cracks extended over the bridge piers in sea water, and a great quantity of chloride ions had accumulated on them. Based on these results, we coated the surface of the piers to prevent chloride ions from penetrating into the steel members and to prevent rust. For the areas with a higher density of chloride penetration, we chipped the surface, and for the damaged areas, we chipped to the depth of the back of the reinforcing bars. The chipped areas were repaired and the surface of the concrete was painted.

5. Countermeasures to assure durability

The recommendations for the countermeasures to secure the durability of concrete bridges in a severe saline environment were carried out.

The main results obtained in this study are as follows;

1. The chloride ion penetration in future could be predicted from both values of Co and Dc, which show the degree of environmental factor in saline environment, and the materials characteristics respectively.
2. In the maintenance work, it was required to monitor the chloride ion penetration, and to conduct the surface coating if necessary.
3. Blast-furnace slag cement concrete effectively controlled the chloride ion penetration into concrete.
4. The surface coating was also effective in protecting the structure from chloride ions, its durability being expected for 20 years or longer.
5. The corrosion-proof panel attachment in the form was the most effective method and excellent for improving the durability of concrete.
6. The shape of concrete structure was determined so as to have the minimal surface area.
7. From the viewpoint of LCC, in a severe saline environment, the surface treatment such as the corrosion-proof panels should be applied in the sea and shoreline areas from the beginning construction.
8. From the viewpoint of LCC, in a mild saline environment, increasing the cover depth or surface coating was more advantageous, but in this case, the monitoring was inevitable for the maintenance work.

REFERENCES

[1] Minobu Aoyama, “Countermeasures for Chloride-induced Steel Corrosion in Concrete Road Bridges”, Journal of Japan Concrete Institute, pp.74-79, 1987.9 (in Japanese)

[2] Japan Highway Association, “Investigation on Chloride-Induced Steel Corrosion of Oyashirazu Coastal Bridge”, 1997.3 (in Japanese)

[3] Japan Society for Civil Engineers, “A New Standard Specification for Maintenance of Concrete Structure”, pp.11-14, pp.61-62, 2001.1 (in Japanese)

DETAILED ASSESSMENT OF CONCRETE STRUCTURES AFFECTED BY REINFORCEMENT CORROSION

J. Rodríguez
Dr. Civil Engineer

L. Ortega
Civil Engineer

GEOCISA
MADRID (SPAIN)

D. Izquierdo
Civil Engineer

C. Andrade
Dr. Chemist

Institute Eduardo Torroja of Construction Sciences
MADRID (SPAIN)

Key words: Concrete structures, reinforcement corrosion, structural assessment.

1 INTRODUCTION

The aging of structures is produced by a continuous interaction with the ambient which leads into a deterioration of the material. Thus, it is essential to know of the deterioration mechanisms, and how this deterioration influences the safety of the whole structure. Although several deterioration process may affect concrete structures, the reinforcement corrosion has been recognised the most important one for its economical consequences. The main effects of reinforcement corrosion can be classified into three main groups:

- Those, which affect the reinforcement section, reducing the effective area and steel ductility.
- Those, which are related to concrete integrity (cracking and spalling).
- Those, which affect the interaction concrete – reinforcement due to the bond reduction.

2 DETAILED ASSESSMENT OF CONCRETE STRUCTURES AFFECTED BY REBAR CORROSION

The main objective of a structural assessment is the residual safety level determination, in order to establish an adequate intervention program with the higher degree of available information. On the other hand, a structural assessment can also be used for calibration of more simplified methodologies [1], [2]. Three are the main aspects to be analysed in a structural assessment.

- Action, or better action effect, evaluated on the structure.
- Deterioration process evaluation.
- Safety and serviceability limit states verification.

The last two aspects will be commented below for structures affected by reinforcement corrosion:

2.1 Deterioration process evaluation

The attack by corrosion will be appraised by using a *penetration attack,* **Px** ,which is the loss of reinforcement radius. **Px** is the main parameter that will allow a correlation with the general effects previously mentioned on the composite section concrete – steel [4]. This parameter can be measured visually from the residual diameter or estimated by means the corrosion rate $\mathbf{I_{corr}}$.

Reinforcement corrosion provokes on concrete – steel section the effects previously mentioned. These effects are related to the $\mathbf{P_x}$ value according to following principles:

Effective steel section reduction. Depending on the type of aggressive and type of corrosion, their influence on the effective steel is quite different (homogeneous or pitting corrosion).

Cover cracking. The oxides generated in the corrosion process provoke a tensional state in the concrete cover that will produce cover cracks, reducing consequently the cross section of the concrete element and therefore their load bearing capacity.

Loss of bond. The concrete – steel bond is the responsible of the bar anchorage in the element ends and the composite behaviour of both materials. However, corrosion provokes a reduction in bond due to the cover cracking and stirrups corrosion. Finally a limit state of bond can be achieved.

Rebar ductility. Several tests of corroded rebars have shown an important reduction in the rebar ductility not only in the final strain of the rebar but also in the strain – stress curve of the corroded rebar. The tests show that the yield point is diffuse and the final strain is considerably reduced. However in all cases the final value of the ultimate strain is above 1% which is the value to be used in Ultimate Limit State.

2.2 Structural analysis

The structural analysis can be carried out following the main principles of structures with linear – elastic analysis, it is important to identify whether the section has or not cracks produced by corrosion or not in order to reduce their stiffness in the structural model.

3. LIMIT STATE VERIFICATION

3.1. Ultimate limit states For slab and beams, a conservative value of the ultimate bending moment can be calculated by using the classical models adding correction in order to take into account the reduced steel section and the concrete section spalled. A possible reduction due to bond deterioration due to corrosion should be considered, specially if the corrosion attack is on the tensile zone of the elements without stirrups. In order to check the ultimate axial effort of a column element, the reduction should be applied on the concrete section in the case of spalling and if there are no stirrups in a zone due to the failure produced by corrosion, a reduction in the longitudinal bars subjected to compression due to risk of buckling.

3.1.2. Serviceability Limit States For the deflection and crack checking due to loading the same expressions provided by Eurocode 2 can be used, reducing the steel section, the spalled concrete and the cracking if it exists. However is the owner of the structure who has to establish their acceptable degree for their structures.

4 FINAL REMARKS

An adequate tool for a convenient management of structures, has been developed to be a first order requirement. After a preliminary inspection, that tries to identify the damage level of the structure and the environmental characteristics that surrounds it, a structural assessment on the element in order to evaluate the intervention urgency is carried out. Detailed assessment allows a complete verification of the element safety in a similar manner as that proposed by the Limit State theory.

REFERENCES

[1].- **J. Rodriguez, J. Aragoncillo, C. Andrade, D. Izquierdo** *"Manual de evaluación de estructuras afectadas por corrosión de la armadura"* CONTECVET IN30902I (2000)

[2].- **BE 4062** *Manual for assessment of residual service life of reinforced concrete structures*.DG XII. C.E.C. internal document (1995)

LESSONS LEARNED FROM THE VERTICAL TENDON CORROSION INVESTIGATION OF THE SUNSHINE SKYWAY BRIDGE HIGH LEVEL APPROACH PIERS

Teddy Theryo, P.E.
Assistant Vice President
Parsons Brinckerhoff
Tampa, Florida, U.S.A.

Pepe Garcia, P.E.
District Structures & Facilities Eng.
Florida Dep. of Transportation
Tampa, Florida, U.S.A.

William Nickas, P.E.
State Structures Design Eng.
Florida Dep. of Transportation
Tallahassee, Florida, U.S.A.

Keywords: corrosion, tendon, post-tension, pour-back

DISCLAIMER

This paper is the summary of an extensive PT system investigation, inspection, and testing related to the high level approach piers of the Sunshine Skyway Bridge. The information, ideas, and recommendations expressed in this paper are solely those of the authors, and not necessarily represent the opinion of the Florida Department of Transportation and Parsons Brinckerhoff Quade and Douglas, Inc.

1 INTRODUCTION

The Sunshine Skyway Bridge over lower Tampa Bay on the west coast of Florida, U.S.A. has a total length of 6,6 kilometers. The bridge is part of Interstate 275, and links the major metropolitan areas of Tampa/St.Petersburg and Brandon/Sarasota in the West Coast of Florida. The bridge was open to traffic in April 1987. The bridge consists of a 1219,50 m main cable stayed bridge, 1481,70 m high-level approach spans, and 3969,50 m low-level approach spans. The focus of this paper concentrates only on the high-level approach piers. The high level of north and south approaches consists of twin trapezoidal precast post-tensioned (PT) box girder superstructures supported on precast post-tensioned hollow elliptical column segments centered at 41 m. During a special bridge inspection of the high-level approach columns in August 2000, severe tendon corrosion was discovered in column 133 NB (northbound structure). Eleven of seventeen 12,7 mm strands tendon of one of the four tendon legs, specifically SE (southeast) had severely corroded in the external region, immediately below the column cap. The NE (northeast) tendon exhibited significant pitting corrosion, but no strand failure was identified. Because of the above findings, the Florida Department of Transportation (FDOT) to contract the services of Parsons Brinckerhoff Quade and Douglas, Inc. (PBQD) to perform comprehensive tendon corrosion and structural analysis investigations.

2 INVESTIGATION APPROACH

A comprehensive corrosion investigation of the PT System in the bridge high-level approach piers column was initiated in September 2000. The original focus of the investigation was to assess the condition of the PT System below the transition point in the 28 columns that were partially filled with water for an unknown period of time. Water in many of these columns had a high concentration of chloride. The investigation was divided into three phases of investigations. The Phase 1 was to conduct extensive destructive and non-destructive testing of Column 133 NB, while Phase 2 to develop a testing strategy to the rest of the columns. The Phase 3 was the actual testing implementation in accordance to the Phase 2 testing protocol. Investigation methods and techniques used in this phase included visual inspection, vibration, half cell potential, and electrical continuity check, bore scope, water ponding, and concrete coring examination. Grout, water, and duct samples were also collected for testing.

3 THE FINDINGS OF THE INVESTIGATION

The investigation of the PT System in the column as represented by three distinct regions of the column, above and below transition point as follows: The column cap region, the external tendon region and the thick wall region.

The findings in the Column Cap Region included the deficiencies, cracking of pour-back (non-shrink grout or epoxy material anchorage protection) area and severe tendon corrosion and strands failure were discovered. In addition, voids due to bleed water were also identified in the PT trumpet areas. In the external region, strand failure was only found in SE tendon of Column 133 NB. Besides strand corrosion, a significant number external tendon ducts crack and hollow sound was found. No strand corrosion was found in the hollow sound areas, where the exposed strands were well protected by the polyethylene duct. In the thick wall region severe tendon corrosion in the bottom recess of the column was discovered, where 50% of the tendon cross sectional area was considered failed. The observation of excavation in the bottom recesses areas indicated a significant number of primary damaged ducts.

4 STRUCTURAL EVALUATION

In addition to the corrosion investigation, a comprehensive structural calculation was performed for the restoration of column 133NB to its original design requirement and for evaluation of other high-level approach columns in case of PT tendons deficiency found during the investigation.

5 IMPORTANT LESSONS LEARNED AND RECOMMENDATIONS

The following important lessons learned and recommendations were drawn from the above findings in the investigation. It is expected that these recommendations would enhance the durability of similar structure in the future.

1) Designers shall recognize the environmental impact to structural corrosion vulnerability in aggressive environments.

2) Construction methods and testing must be subjected to comprehensive corrosion prevention and constructibility reviews.

3) Corrosion detection methods should be included during the construction and service life of the structure.

4) Historical data must be accurately and completely documented to facilitate the analysis and repair of deficiencies.

5) PT redundancy system or practical replacement capabilities should be incorporated.

6) No pre-cast concrete hollow column section should be specified below the waterline.

7) No PT tendons should be located in columns below the highest water splash zone elevation.

8) Grouting operation for vertical tendons should be carefully planned, tested, and monitored. Stage and vacuum grouting should be specified in the upper section of tendons in combination with a pressurized sealed PT system and zero bleed grout.

9) Provide multiple levels protections at anchorages, including permanent grout cap, epoxy material pour-back and polymer coating over the pour-back.

10) Criteria and construction methods designed to accelerate construction or reduce costs must not compromise the required structural durability.

REFERENCES

1) "Sunshine Skyway Bridge Post-tensioned Tendons Investigation, Part 1: General Introduction" Final Draft Report, Parsons Brinckerhoff Quade and Douglas, Inc, in association with Concorr Florida, Inc. and Kissinger Campo & Associates Corp., February 6, 2002

2) "Sunshine Skyway Bridge Post-tensioned Tendons Investigation, Part 2: Investigation of the High Level Approach Span Piers" Final Report, Parsons Brinckerhoff Quade and Douglas, Inc, in association with Concorr Florida, Inc. and Kissinger Campo & Associates Corp., February 13, 2002

RELATIONSHIP BETWEEN CRACK WIDTH AND HYPOTHETICAL TENSILE STRESS OF PARTIALLY PRESTRESSED CONCRETE MEMBERS

Wenying Li
Black & Veatch
U.S.A.

Yoshiteru Ohno
Osaka University, Professor
Japan

Ziduan Shang
Osaka University

Keyword: hypothetical tensile stress, crack width, PPC member, RC member

• SIGNIFICANCE OF WORK

The computation of crack width is one of the most important considerations in designing partially prestressed concrete (PPC) members. However, crack width evaluation, which includes calculations of crack interval, steel stress in cracked section, etc., is very tedious using current procedures. As a simplified evaluation procedure, CP110 (English code, 1970) applied hypothetical tensile stress concept. Hypothetical tensile stress is defined on the assumption that the entire section is still effective even after cracking has occurred. Factors such as concrete strength, section depth, tensile reinforcement ratio had been included in CP110 in evaluating crack width. But several other factors that closely related to crack width like clear cover, average prestress level were not considered yet.

In this paper, relationship between crack width and hypothetical tensile stress was derived in order to simplify procedure of evaluating crack width in reinforced concrete and PPC members. The instantaneous and long-term crack widths are calculated according to PRC Recommendation of Architectural Institute of Japan (AIJ). Factors that were taken into account in developing the simplified procedure include concrete strength, reinforcement ratio, beam depth, concrete clear cover, average prestress, shrinkage and creep.

• BASICAL DIFINITION

Hypothetical tensile stress σ_f is defined by the following equation,

$$\sigma_f = \frac{M}{Z} - \left(\frac{P}{A} + \frac{P \cdot e}{Z}\right) \tag{1}$$

Where, M is flexural moment, P is effective prestress, A is section area, e is eccentricity, Z is section modulus

• MODEL SECTION AND PARAMETERS

To pursue the quantitative relationships of σ_f – W_{av}, a model section was selected as Fig. 1. Based on the chosen model section, the following parameters are considered to develop the relationship of σ_f – W_{av}.

1) Concrete compressive strength f_c: 200, 300, 400, 500, 600 kgf/cm^2
2) Tensile reinforcement ratio p_t, diameter of steel bar ϕ, and number of steel bar used n
3) Beam depth D: 30 ~ 120 cm
4) Concrete clear cover c: 3, 4, 5, 6, 7, 8, 9, 10 cm.
5) Average prestress σ_g: 0, 10, 20, 30, 40 kgf/cm^2.
6) Dry shrinkage strain ε_{sh}: 0, 1, 2, 3, 4 ($\times 10^{-4}$).
7) Bond decreasing coefficient C_r: 1 ~ 0

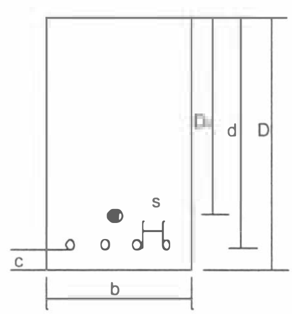

$b = 40cm$
$D = 80cm$
$A_s = 20.28cm^2$
$f_c = 300kgf/cm^2$
$c = 5cm$
$s = 9.17cm$
$n = 4$
$A_p = 0$
$\sigma_g = 0$

Fig.1 Model section

Generally, σ_f – W_{av} relationship of the model section can be written as following equation.

$$\sigma_f = k w_{av} + \sigma_{f0} \tag{5}$$

To investigate effects of above factors, equation (5) can be rewritten as

$$\sigma_f = k \sigma_{f0s} \frac{1}{w_{av0}} w_{av} + \sigma_{f0} \tag{6}$$

Where

$k = k_1 k_2 k_3 \cdots \qquad \sigma_{f0s} = 3.49 MPa \qquad w_{av0} = 0.1mm \qquad \sigma_{f0} = \sigma_{f0i} m_1 m_2 m_3 \cdots \sigma_{f0i} = 10.1 kgf/cm^2$

k_1, k_2, k_3… and m_1, m_2, m_3… are coefficients reflecting every factor's effect to the slope and intercept of equation (5), respectively. σ_{f0s} and σ_{f0i} are the values of slope and intercept of model section when $w_{av0} = 0.1mm$. Thus the procedure to determine relationship of σ_f - w_{av} shall be the investigations of how the slope k and intercept σ_{f0} vary with each factor.

• PRINCIPAL RESULTS

Following results are summarized on the basis of the all formulation procedures in this paper:

$$\sigma_f = k\sigma_{f0s} \frac{1}{w_{av0}} w_{av} + \sigma_{f0}$$

$$\sigma_{f0s} = 34.9 \quad kgf/cm^2$$

$$w_{av0} = 0.1mm$$

$$k = k_s k_c k_D$$

$$k_s = 2.15 p_t - 0.07\phi' + 0.22$$

$$k_D = 0.69 D' + 0.31$$

$$k_c = -0.76c' + 1.76$$

$$\sigma_{f0} = \sigma_{f0i} m_{(Ft)} m_s m_c m_{Cr} + \Delta m_p + \Delta\sigma_{f0sh}$$

$$\sigma_{f0i} = 10.1 kgf/cm^2$$

$$m_{(F_t)} = 1.03 F_t' - 0.03$$

$$m_c = 1.2c' - 0.2 \qquad m_s = -0.12n + 1.5$$

$$m_{cr} = C_r \qquad \Delta m_p = 1.3\sigma_g$$

$$\Delta\sigma_{f0sh} = -6.3 \times 10^4 \times \varepsilon_{sh} \times N_1 \times N_2 \times N_3$$

$$N_1 = 1.43 p_t$$

$$N_2 = D'/(0.7D' + 0.3)$$

$$N_3 = -0.25c' + 1.25$$

• CONCLUSIONS

The relationship of hypothetical tensile stress and crack width developed here has the following features:

- Factors, which should be taken into account here for instantaneous crack width estimation, are concrete strength, tensile reinforcement ratio, diameter of steel bar, number of steel bar, section width, concrete clear cover and average prestress.
- Proposed method can also be applied to long-term crack width estimation by considering those effects due to concrete shrinkage and creep.
- Hypothetical tensile stress calculated from proposed method is well agreed with that from CEB78, but relatively small than that from CP110.

ACKNOWLEDGEMENT

The authors would like to thank Dr. Li, Zheng-Bao in Daisue Construction Company Ltd. and Mr. Iwada in NTT Series, who assisted abundantly on this research.

REFERENCES

[1] Recommendations for Design and Construction of Partially Prestressed Concrete (Class III of Prestressed Concrete) Structures, Japan Architectural Institute, 1986.
[2] CEB-FIP: CEB-FIP Model Code for Concrete Structures, Jan. 1978.
[3] Recommendations for Design and Construction of Prestressed Concrete Structures, Japan Architectural Institute, Nov. 1998.
[4] British Standards Institution, Code of Practice for The Structural Use of Concrete, CP110 Part 1, p.68, 1972

FLEXURAL BEHAVIOR OF REINFORCED CONCRETE COMPOSITE BEAMS WITH PRECAST ELEMENTS CRACKED DUE TO CONSTRUCTION LOAD (SHORT-TERM FLEXURAL BEHAVIORS)

Ziduan Shang, Osaka University
Yoshiteru Ohno, Osaka Univ., Professor, Japan
Zhenbao Li, Beijing Polytechnic University, China
Wenying Li, Black & Veatch, U.S.A.

Keywords: precast composite beam, construction load, stiffness, crack, deflection

1 SIGNIFICANCE OF WORK

Precast concrete, for their high quality and low cost of construction, were often designed and widely used in reinforced concrete and prestressed concrete structures in recent years. However, to ensure crack will not occur during the construction stage, either full prestress was induced on precast flexural elements or specific shore systems were designed to support them because the designer cannot precisely evaluate the crack width and deflection in the service stage if precast elements had been cracked during the construction stage. This prevailing situation, on design and construction, cannot make precast concrete members demonstrate their comprehensive function in pursuing the very purposes of high quality and low cost.

In order to change the present concept of the design of the precast structure and make the precast concrete members more widely and conveniently used during construction, this study was focused on reinforced (RC) and partially prestressed (PPC) concrete composite flexural members, whose precast elements supposedly un-shored and cracked due to the construction load at construction stage. Two series counted eight concrete composite beams were prepared and loaded considered three critical factors: the level of construction load, the depth of precast element, and the existence of prestress on precast element. This paper was devoted to the study of this kind of composite beams on the following three purposes: 1) to investigate the short-term flexural behaviors; 2) to give a precise section stress analysis method; and 3) to recommended a new and accurate method for the evaluation of short-term deflection. Sustained loading will continue for several years to investigate the development trend of long-term stress, crack width and deflection. Fig.1 shows the details of specimens and loading method of this experiment.

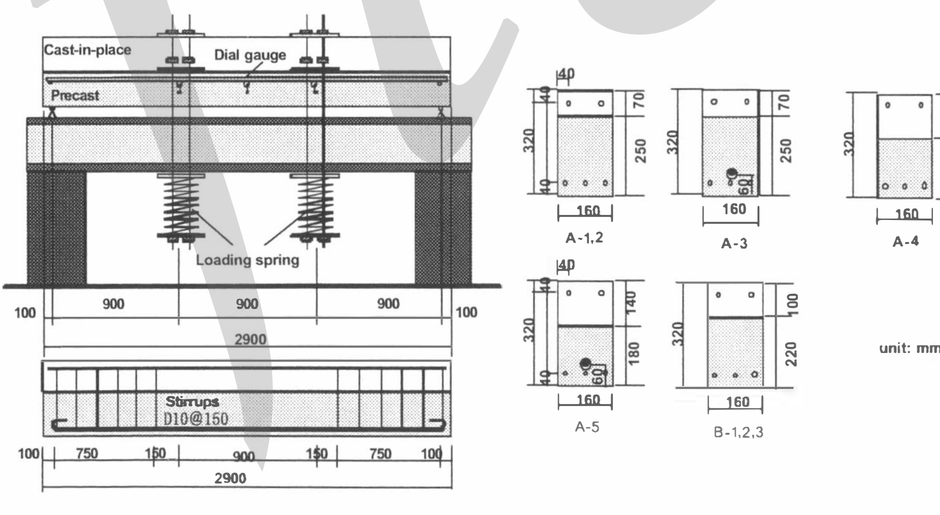

Fig.1 The way of loading and reinforcement details of specimens

2 CONCLUSIONS

- The loading of construction load on precast element will lead to an existence of compressive stresses at the top of precast section, this stress condition usually cannot be offset by the service load loaded subsequently. As a result, this kind of composite member has greater effective concrete area on its section, and therefore exhibited a greater initial anti-flexural stiffness than that of full cast-in-place member toward service load. Corresponded to the loading of P_2, composite beam exhibited a smaller increment on tensile reinforcement strain than that of full cast-in place beam (Fig. 2, Fig. 3)

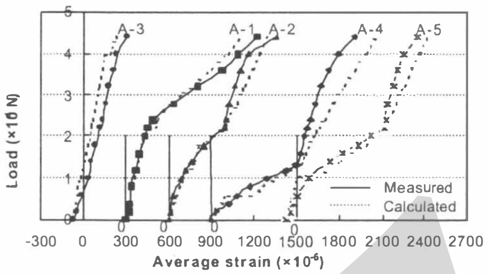

Fig. 2 Relation of load and average tensile reinforcement strain

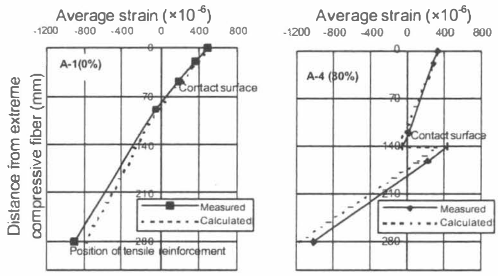

Fig. 3 Initial strains distribution of critical section in mid-span

- Un-shored construction process may lead to a cracked precast element at construction stage, but this does not mean a greater initial crack width will result at service stage. On the contrary, according to theoretical analysis and experimental results reported in this paper, it is possible to control initial crack width within a permissible range (Fig. 4).
- Precast composite members constructed by the means of un-shored method may produce large initial deflection because of relatively larger δ_1 (deflection in construction stage). But, if good combination of construction load and precast element can be made on design or inducing moderate prestress on precast element, δ_1 can be controlled to a acceptable amount, which would has little negative effect on total initial deflections. Furthermore, because greater effective concrete area makes initial anti-flexural stiffness becomes greater, it is possible to anticipate a good long-term flexural behaviors at precast composite members (Fig. 5).
- Recommended approaches for section analysis and deflection calculation can well evaluate the initial behaviors of this kind of members, calculated values are agreed well with those from experimental measurements.

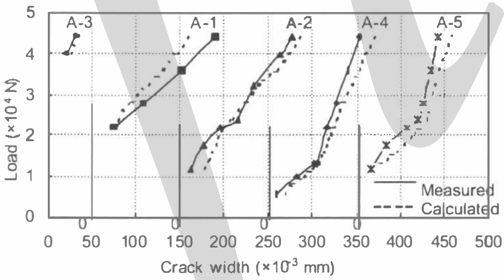

Fig. 4 Relation of load and initial average crack width

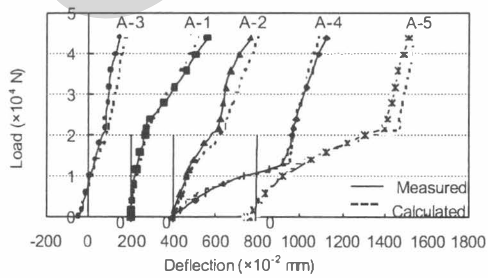

Fig. 5 Relation of load and initial deflections

REFFERENCES

[1] Architectural Institute of Japan: Design and construction code for prestressed concrete (PC) composite members and commentary, 1994

[2] Architectural Institute of Japan: Recommendations for Design and Construction of Partially Prestressed Concrete (class III of Prestressed Concrete) Structures

[3] Zhenbao Li, Yoshiteru Ohno and Kazuo Suzuki: Calculation of Stress in Partially Prestressed Concrete Composite Section, The 4th Symposium on Developments in Prestressed Concrete, Japan Prestressed Concrete Engineering Association, Oct.1994

COMPARISON OF WATERPROOFING SYSTEMS FOR CONCRETE BRIDGES: JAPAN, GERMANY GREAT BRITAIN

Koichiro Shito, Japan Highway Public Corporation
Yasushi Kamihigashi, Japan Highway Public Corporation
Yoshiharu Mizugami, Japan Highway Public Corporation
Ken'ichi Hida, Chiyoda Engineering Consultants Co.,Ltd., Tokyo Japan
Rob Stroeks, Chiyoda Engineering Consultants Co.,Ltd., Tokyo Japan
Prof. Dr.-Ing. Alfred Haack, STUVA, Cologne Germany
Richard Jordan, TRL, Crowthorne Great Britain

1 INTRODUCTION

The use of drain asphalt for roads and road bridges has increased in recent years. The significance of this to concrete bridge structures in particular has called for more stringent performance requirements and improved evaluation standards for waterproofing systems in Japan. For this reason, comparative investigations between (1) Japan and Germany, and (2) Japan and Great Britain have been carried out. As part of these investigations, the performance of several waterproofing systems has been tested in each other's country, in accordance with the test methods in use in that country. This paper describes the differences in requirements and standards, and presents the applied methods and obtained results of the performance tests.

2 PRESENT STANDARDS

Present standards in the three countries are divided in requirements to the material that is used and requirements to the total system of waterproofing material, bond layers, protective layers etc. Table 1 shows a summary comparison.

Table 1 Comparison of standards

	Standard	Requirements for material	Requirements for system
Japan	Japan Highway Public Corporation Notification (1994): sheet type (a waterproof sheet is applied to the concrete slab by pasting or welding) and paint type (a liquid paint is applied to the concrete slab by heating or solvent).	Resistance to heat, resistance to chemical and low temperature flexibility.	Resistance to water penetration (before and after local loading), shear and tensile bond strength (before and after 7 days immersion) and crack behavior.
Germany	TP-BEL-B Part 1 (1999): single layer welded bituminous membranes and Part 3 (1995) for liquid polyurethane coating in conjunction with two layers of poured asphalt (protective layer and covering layer).	Weight and thickness of sheet, tensile force, water impermeability, heat resistance, low temperature flexibility etc.	Tear off resistance, crack bridging (dynamic, static), shear strength etc.
Great Britain	BD 47/99 (1999), the latest version of Departmental Standard BD 47 that was introduced in 1994: Certification tests are specified for sheet systems and liquid applied systems. Normally, systems must be overlaid with a protective layer of red sand asphalt.	Resistance to water penetration, handling tests on sheet membranes (as rolls and as strips), resistance to pin/blow holing of liquid applied membranes, etc.	Resistance to chloride ion penetration, tensile adhesion (waterproofing to concrete), resistance to freeze-thaw, resistance to heat ageing, thermal shock and heat ageing and crack cycling (dynamic and static), surfacing to waterproofing system shear test, surfacing to waterproofing system tensile bond test, etc.

3 COMPARATIVE INVESTIGATION

In order to compare standards in use in Japan, Germany and Great Britain, three representative Japanese types of waterproofing (pasted sheet type, welded sheet type, liquid type) were sent to Germany and Great Britain for performance tests. At the same time, two German types (sheet type, liquid type) and one British type (liquid type) waterproofing was sent to Japan. All tests for performance verification were carried out in accordance with guidelines in use in the country of testing. Table 2 compares results of tests concerning resistance to water penetration, shear bond strength, tensile bond strength and crack behavior ([1], [2], [3]).

Table 2 Results of tests on material requirements of waterproofing

Test country	Material		Resistance to water penetr.	Shear bond strength		Tensile bond strength		Crack behavior	
	Country	Type							
Germany	Japanese	P	No leakage		0.29^{**} N/mm^2	8℃	$1.71/1.88^{*}$ N/mm^2	-20℃	No cracks visible
						23℃	$1.37/1.33^{*}$ N/mm^2	70℃	No cracks visible
		W	No leakage		0.41^{**} N/mm^2	8℃	$1.08/0.89^{*}$ N/mm^2	-20℃	No cracks visible
						23℃	$1.01/1.47^{*}$ N/mm^2	70℃	No cracks visible
		L	Leakage after 30 min.		0.70^{**} N/mm^2	8℃	$2.52/2.01^{*}$ N/mm^2	Crack through the bitumen coating	
						23℃	$1.68/1.90^{*}$ N/mm^2		
Great Britain	Japanese	P	No leakage	-10℃	1.37 N/mm^2	-10℃	(0.80 N/mm^2)***	-10℃	No cracks visible
				23℃	0.36 N/mm^2	23℃	(1.02 N/mm^2) 1.33 N/mm^2	23℃	No cracks visible
				40℃	0.09 N/mm^2	40℃	(0.40 N/mm^2)	40℃	No cracks visible
		W	No leakage	-10℃	>1.73 N/mm^2	-10℃	(0.50 N/mm^2)	-10℃	No cracks visible
				23℃	0.56 N/mm^2	23℃	(0.77 N/mm^2) 1.44 N/mm^2	23℃	No cracks visible
				40℃	0.17 N/mm^2	40℃	(0.44 N/mm^2)	40℃	No cracks visible
		L	No leakage	-10℃	>1.73 N/mm^2	-10℃	(0.55 N/mm^2)	23℃	All specimens were fully cracked after initial crack opening
				23℃	0.64 N/mm^2	23℃	(0.82 N/mm^2) 1.61 N/mm^2		
				40℃	0.20 N/mm^2	40℃	(0.36 N/mm^2)		
Japan	German	W	0.0ml	-10℃	F=1.3 N/mm^2 S=3.4%	-10℃	F>1.0N/mm^2	Up to 2.3mm crack	
				20℃	F=0.4 N/mm^2 S=3.5%	20℃	F=0.6N/mm^2 7 day 160%		
		L	0.0ml	-10℃	F=1.3N/mm^2 S=2.3%	-10℃	F>1.2N/mm^2	Up to 5.8mm crack	
				20℃	F=0.6N/mm^2 S=2.2%	20℃	F=1.1N/mm^2 7 day 113%		
	British	L	0.0ml	-10℃	F=0.07N/mm^2 S=0.5%	-10℃	F=0.2N/mm^2	Up to 15.4mm crack	
				20℃	F=0.13N/mm^2 S=0.8%	20℃	F=0.2N/mm^2 7 day 28%		

P: Pasted type sheet, W: Welded type sheet, L: Liquid type

* The first value is bond between sheet and concrete, second value is bond between sheet and asphalt

** Value after exposure to heat and alternating temperatures

*** Values in parenthesis are for tensile adhesion of membrane to concrete

4. CONCLUSION

Due to differences in weather conditions such as temperature and humidity, as well as type and construction of waterproofing system etc., it is not possible to make clear and simple comparison, but the following points have been stated:

- Tests on the German system in Japan: all tests were passed according to JH standards. At low temperature flexibility tests, 1 in 5 test specimen (sheet) were broken. Although this is in line with the JH standards, it is believed that the damage occurred due to the thickness of sheet (4.5mm).
- Tests on the British system in Japan: in the shear and tensile bond test, the waterproofing system remained firmly bonded to the concrete and the failures occurred at the bond between the red sand asphalt and the waterproofing system. The shear and tensile bond strengths measured in Japan were lower than those measured on the same system in Britain.
- Tests on the Japanese system: the Japanese systems did not pass all tests in Germany and Great Britain. Especially the items resistance to chloride ion, resistance to aggregate indentation and crack cycling are significant. These items are not included in the present JH standards and it was decided to consider them in the preparation of new standards.

Based on the above findings and other investigations, a new Japanese standard is proposed.

REFERENCES

[1] STUVA-tec, Investigations of Japanese and German waterproofing systems for deck slabs of bridges, 2001

[2] R.W. Jordan, Investigation of characteristics of waterproofing systems for concrete bridge decks, TRL Limited, 2001

[3] Japan Highway Public Corporation, Investigation concerning improvement of waterproofing for concrete bridge slabs, 2000

RAPID MEASUREMENT METHOD OF CHLORIDE CONTENT IN HARDENED CONCRETE

Tatsumi Ohta Yasuhiro Kuroda
Shimizu Corporation, Institute of Technology
Tokyo, JAPAN

Keywords : chloride content, rapid measurement method, hardened concrete, concrete powder from drilled holes

1 INTRODUCTION

In Japan, chloride contents are often measured according to the method prescribed by the Japan Concrete Institute (JCI) [1]. In general, it takes several days to obtain the results because the JCI method includes various processes. However, there are some rapid measurement methods that can present chloride content in hardened concrete at investigation sites immediately [ex. 2]. These rapid methods use a rotary hammer drill to pulverize hardened concrete into powder before testing with a salinometer. Acid without water or hot water is used to extract the chloride. Despite its simplicity, it may be difficult to prepare these materials at investigation sites. This study proposes a new rapid method that enables chloride content measurement at normal daily temperatures, using concrete powder removed directly from structural members with a rotary hammer drill, demineralized water, and a handheld salinometer.

Chloride content is obtained as follows: First, more than 10.0 g of concrete powder is produced using a rotary hammer drill. Next, 10.0 g of the gathered concrete powder is sorted and mixed with 10.0 g of demineralized water at a temperature of 5 to 35^{o}C. Then, to extract the chloride content, the concrete powder with demineralized water is kept still for 0.5 to 2.0 hr. When the prescribed time has passed, the samples are remixed for about 1 min, then, using a handheld salinometer, the soluble chloride content is measured and converted to total chloride content, taking account of the temperature and time of extraction.

This rapid method was validated by the following experiments.

2 EXPERIMENTS

A two-part experiment was conducted, Series I and Series II.

Series I compared the results of the proposed rapid method and the JCI method. Several concrete samples removed from 2 investigation sites (sample A and B) and exposed specimens at the seaside (sample C) were used. Rapid measurements were conducted at 5, 20 and 35^{o}C and 0.5, 1.0, 1.5 and 2.0 hr. In general, since only soluble chloride content can be measured by the handheld salinometer and the chloride content solidificated in concrete such as Friedel's salt depends on the type and unit content of cement, the proposed method cannot be applied to all hardened concrete. However, at investigation sites, approximate total chloride can be obtained immediately by this rapid method.

Series II determined the effect of the sampling method, that is, 'the drilling method' and the JCI method on the rapid measurements. Concrete powder from drilled holes (drilled powder) and concrete ground according to the JCI method (JCI sample) were used. The drilled powder was gathered by drilling concrete with a rotary hammer drill, and the JCI sample was obtained by grinding concrete to pass through a 149 μm sieve. The particle size distribution of these powders was measured by a laser diffraction instrument. The effect of 10 and 18 mm drill size on the rapid measurements was also studied. In Series II, the temperature of extraction was set at 20^{o}C.

3 RESULTS

3.1 Series I

The relationship between the extraction temperature and the measured results by the rapid method is shown in Fig.1. The chloride content closely corresponded to the temperature of extraction. On the other hand, the time of extraction was not thought to contribute to the rapid measurements. The results of the rapid measurement (soluble chloride) are shown in Fig.2, compared with the results by the JCI method (total chloride). In Fig.2, the results at an extraction time of 1.0 hr and a regression line ($y=\alpha\cdot x$) are indicated. The regression line showed a good proportional relationship between the results by the rapid method and the JCI method. Coefficient α, decreased with the temperature and time of extraction, as shown in Fig.3.

The soluble chloride content measured by the rapid method was affected by the temperature and time of extraction. Thus, multiple regression analysis was conducted regarding the relationship between coefficient α, temperature and time. As a result of the analysis, coefficient α, had a good correlation with the inverse of the extraction temperature and time. Consequently, total chloride contents can be evaluated by multiplying coefficient α, obtained by the multiple regression equation (α = 1.235 + 8.437 / temp [^{o}C] + 0.383 / time [hr]) by the results measured by the rapid method.

3.2 Series II

The measured results of the drilled powder and the JCI samples by the rapid method are shown in Fig.4. Chloride contents of the drilled powder and the JCI samples were almost the same at any distance from the surface of the exposed specimen. A laser diffraction instrument was used to reveal the particle size distribution of the samples. The drilled samples had almost the same particle volume as the JCI samples. Also, the chloride contents of concrete powder produced by a rotary hammer drill with a drill size of 10 and 18 mm were almost the same. Consequently, the drilling method is adequate to obtain samples for chloride content measurement.

4. CONCLUSION

Several experiments were conducted to establish a new rapid measurement method of the chloride content in hardened concrete at investigation sites using concrete powders and a handheld salinometer. From the measurements, the following conclusions were derived: 1) There is a good correlation between the inverse of the extraction temperature and time and coefficient α, which is the ratio of the measured results by the rapid method and the JCI method. 2) Total chloride content can be approximately evaluated, using the coefficient determined by the extraction temperature and time and the measured results by the proposed rapid method, though this method cannot be applied to all hardened concrete. 3) When soluble chloride content in hardened concrete is measured by the rapid method, the sample can be obtained by the drilling method using a rotary hammer drill with a drill size of 10 to 18mm in diameter.

REFERENCES

[1] Japan Concrete Institute: Proposed JCI Standard - Test methods of corrosion and corrosion protection of concrete structure (JCI-SC), 1991 (in Japanese)
[2] Tomosawa, F., et al.: Simple method of test for chloride ions in hardened concrete, Proceedings of the Annual Meeting, AIJ, pp.353-354, 1985 (in Japanese)

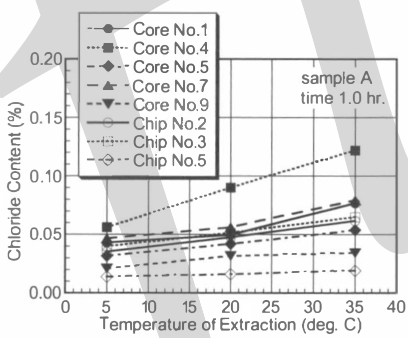

Fig.1 Relationship between extraction temperature and chloride content

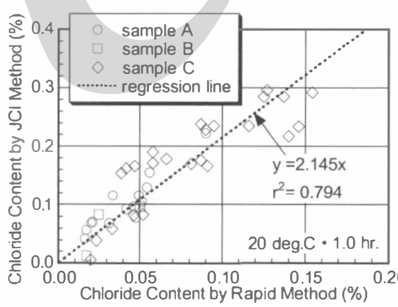

Fig.2 Results measured by rapid method and JCI method

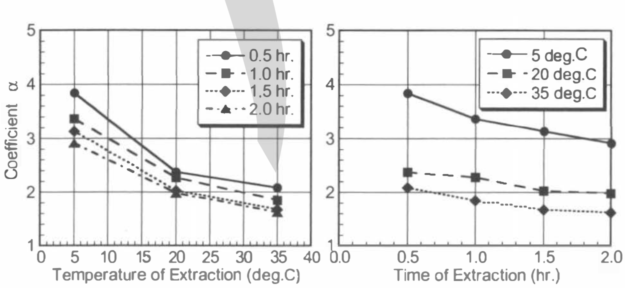

Fig.3 Relationship between extraction temperature and time and coefficient, α

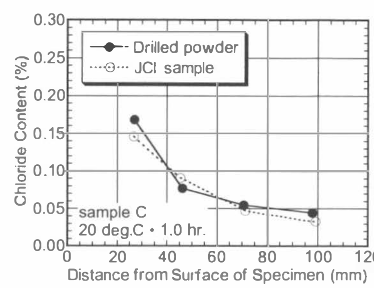

Fig.4 Effect of sampling method on rapid measurement

DURABILITY OF CONCRETE SUBJECTED TO COMBINED DETERRIORATING ACTIONS OF CHLORIDE ION PENETRATION AND FREEZING AND THAWING

Nobufumi TAKEDA Shigeyuki SOGO
Technical Research Institute of
Obayashi Corporation, JAPAN.

Keywords: durability, combined deterioration, chloride ion penetration, freezing and thawing action

1 INTRODUCTION

When designing concrete structures focusing on durability, durability checking should be conducted based on long-term deterioration prediction. Though many structures are subjected to composite deterioration, the progress of such deterioration is yet to be elucidated. The 1999 edition of the Japan Society of Civil Engineers' (JSCE) Standard Specification for Design and Construction of Concrete Structures [Construction] provides a method of deterioration prediction for each deterioration mechanism, but does not provide methods for composite deterioration. Combined deterioration by freezing and thawing action and chloride attack have been discussed in the literature[1],[2],[3],[4], but the accumulated data are scarcely sufficient for allowing deterioration prediction.

This paper reports on a study on concrete structures in a marine environment in a cold climate conducted with the aim of quantitatively grasping the combined effects of chloride ion supply and freezing and thawing action on the durability of concrete. The results of investigation into the progress of deterioration under freezing and thawing in seawater, as well as chloride ion penetration in concrete subjected to freezing and thawing are described.

2 OUTLINE OF EXPERIMENTS

The following two series of tests were conducted:

Series I : In accordance with the freezing and thawing test method specified in JSCE Standard using tap water and seawater as freezing water in the specimen container .

Series II :Cyclic seawater spraying and drying (salt spray testing) after freezing and thawing testing (sequence as shown in **Fig.1**). After freezing and thawing testing was completed, salt spray tests were conducted. One cycle of salt spray testing comprised spraying of seawater at a rate of 200 ml/m^2/hr for 12 hours at 30°C using artificial seawater and drying at a temperature of 40°C and relative humidity of 60% for 12 hours each day.

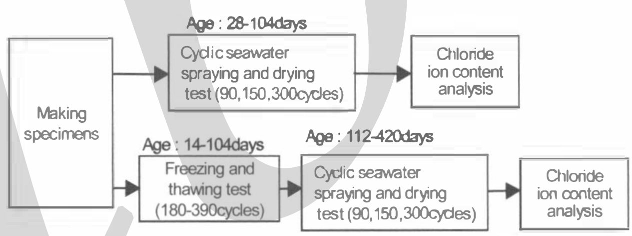

Fig.1 Sequence of Experiment (series II)

Beam specimens 100 by 100 by 400 mm were used. The water-cement ratios were 0.4, 0.5, and 0.6. The air content varied between 1.3% and 7.4%. In Series I , specimens were fabricated by adding chloride ions at concentrations of 0, 2.5, 5.0, and 10.0 kg/m^3 during mixing. The dynamic modulus, mass change, and depth of scaling were measured using a laser non-contact displacement meter. And the diffusion coefficient (Dc) was calculated by measuring the chloride ion content distribution.

3 RESULTS

3.1 Deterioration due to cyclic freezing and thawing in seawater

Fig.2 shows the changes in the relative dynamic modulus (REd) during freezing and thawing tests. When compared at 300 cycles of freezing and thawing, the REd in seawater is lower than in tap water by 5 to 10 percentage points and 10 percentage points or more with a W/C of 0.4 and 0.5, respectively. With a W/C of 0.6, the REd reduction is also faster in seawater. **Fig.3** shows the changes in the mass during the freezing and thawing tests. In the case of seawater, the mass losses are greater at between 5% and 10% at 300 cycles with a W/C of 0.4 and more than 10% at 150 cycles or less with a W/C of 0.5 or more, exhibiting faster progress of scaling than in tap water. When concrete is subjected to freezing and thawing in a chloride-supplying environment, the deterioration of concrete is evidently recognized as surface scaling.

3.2 Deterioration of concrete with inherent chlorides under freezing and thawing

Fig.4 show the changes in the REd of concrete containing initially added chloride ions during the freezing and thawing tests. The reduction in the REd was accelerated as the chloride ion content in concrete increased. When concrete containing chlorides added during mixing is subjected to freezing and thawing, the deterioration is recognized as reductions in the dynamic modulus due to fine cracking within concrete.

3.3 Chloride ion penetration in concrete deteriorated by freezing and thawing

Fig.5 shows the relationship between REd and the ratio of the diffusion coefficient with freezing and thawing action (D_2) to the diffusion coefficient without freezing and thawing action (D_1). The diffusion coefficient of chloride ions in concrete subjected to freezing and thawing is similar to that in concrete without such action when the relative dynamic modulus is over 80%. However, when the REd decreases to 50% and 20%, the diffusion coefficients increase to 2 times and 6 times or more, respectively, the values of concrete without freezing and thawing action.

4 CONCLUSIONS

When concrete is subjected to freezing and thawing in a chloride-supplying environment, the diffusion coefficient of chloride ions increases. It is therefore necessary to use a diffusion coefficient taking account of the freezing and thawing action when checking durability of structures in a combined deterioration environment involving chloride ion supply and cyclic freezing and thawing.

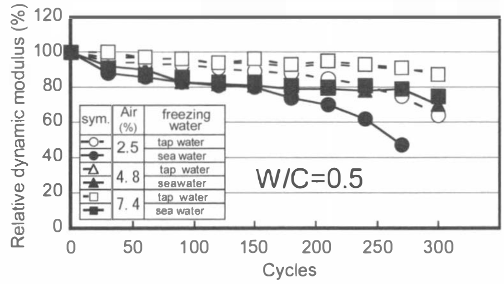

Fig.2 Change in dynamic modulus

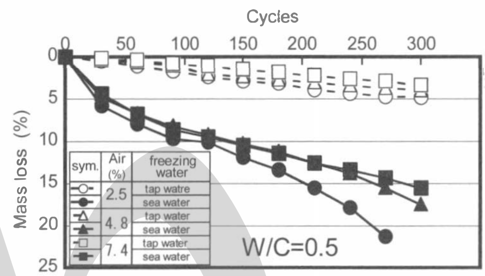

Fig.3 Change in mass loss

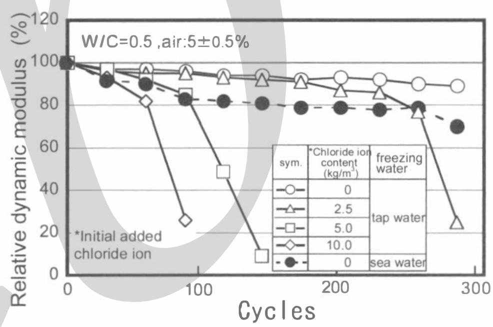

Fig.4 Change in relative dynamic modulus

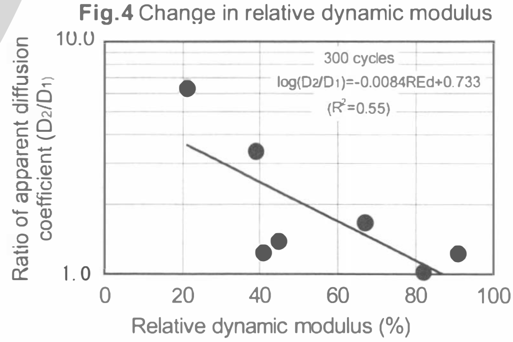

Fig.5 Relationship between REd and the

REFERENCES

[1] Fujii,T.,Fujita,Y.:Influence of chlorides on scaling deterioration of hardened cement paste, Journal of Materials, Concrete Structures and Pavements, Proceedings of Japan Society of Civil Engineers, No.360, pp.129-138, Aug.,1985

[2] Saeki,N., Fujita,Y.: Performance of concrete coastal and cold environment, Concrete Journal, Vol.25, No.4, pp.4-12, Apr.,1980.

[3] Tukinaga,Y.,Shoya,M.,Hara,T., : Study on the frost damage concrete due to application of chloride, JCA Proceedings of Cement & Concrete,No.47,pp.468-473,May, 1993

[4] Itabashi,H.,Miura,T., : Experimental study on effects of de-icing salts on the deterioration of concrete, JCA Proceedings of Cement & Concrete,No.47,pp.456-461,May, 1993

THERMODYNAMICS LAW APPLIED FOR THE DIFFUSION OF CHLORIDE IONS IN CONCRETE

Worapatt RITTHICHAUY Takafumi SUGIYAMA Yukikazu TSUJI Tsutomu SUDA
Department of Civil Engineering Gunma University, JAPAN
Oriental Construction Co.Ltd. JAPAN

Keywords: ion migration, multicomponent solution, generalized Fick's first law, Onsager phenomenological coefficient, thermodynamics law

1 INTRODUCTION

Recently, the durability of reinforced concrete structure is significantly concerned, especially in some environmental conditions such as saline environment or nuclear waste-disposal containment barriers. An important process concerning to the deterioration of the concrete structure is the ion transport through a cement-based material. The penetration of some aggressive ions and the leaching of some metallic ions from concrete pore structure that caused by diffusion are the main factors that directly affect to the durability of concrete structures. Therefore, it is necessary to develop a reliable calculation model for the diffusion transport, which can be used for accurate prediction of such phenomenon. For the diffusion of ions in concrete, the multicomponent system of the ions in pore solution of a cement-based material should be mainly considered for reality. The concentrations of the co-existing ions have the significant influence on the mobility of each ion [1]. The researches of ion transport in a cement-based material considering to the co-existing ions in the multicomponent solution have been carried out by Otsuki N. et al. [2], in which, the flux of an ion is calculated by the Nernst-Plank Equation, electro-neutrality constraint and Debye-Hückel theory.

The purpose of this research is to apply the theories of the ion transport in a multicomponent solution for calculating the matrix of mutual diffusion coefficients of every ion existing in the pore solution in a cement-based material. This diffusion coefficient is designated as D_{ij}, the mutual diffusion coefficient of i_{th} species influenced by the interaction from j_{th} species. The calculation of this model is based on a generalized form of Fick's first law that was suggested by Onsager. This generalized form is composed of the Onsager phenomenological coefficient [3] and the thermodynamic force between ions occurred by the gradient of electrochemical potential. Consequently, from this D_{ij}, the flux and/or the concentration profile of each ion can be calculated from the generalized Fick's second law.

The validation of this calculation model for D_{ij} was verified by the comparison with the experimental results. It is shown that by using the presented method of calculation and comparing to the experimental results, the calculated amount of the total chloride ions that penetrated into mortar specimen exhibited fairly close to that from the experimental results.

2 ELECTROLYTE DIFFUSION ACCORDING TO THE THERMODYNAMICS LAW

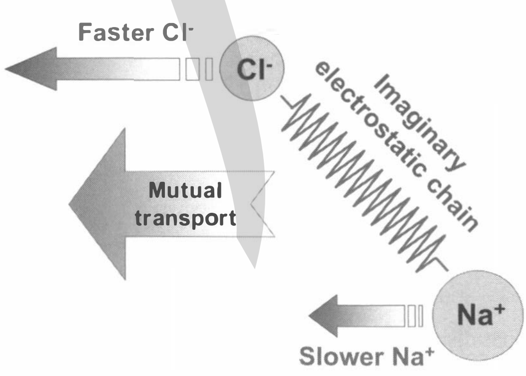

Fig.1 Electrolyte diffusion for system of Na^+ and Cl^-

In an electrolyte diffusion process, the movement of an aqueous species will occur by the driving forces that created from the concentration gradient of that species itself and by those of the other species [1,3]. Moreover, another driving force is the gradient of electrical potential created by the difference between mobility of cation and anion. It can be illustrated schematically in **Fig.1**. Assuming that in a binary electrolyte solution composed of NaCl, the faster Cl^- and the slower Na^+ are constrained by the electrostatic force, to move at the same rate. In addition to this, because of the electro-neutrality constraint, these two ions must maintain the same diffusive flux through out the transport in the solution.

The flux of NaCl can be characterized by a single diffusion coefficient, i.e. mutual diffusion coefficient, which is an average of the diffusion coefficients of Na^+ and Cl^-. This mutual diffusion coefficient can be imaginatively considered as a chain tying Na^+ and Cl^- together. The faster Cl^- will be going to accelerate the slower Na^+, while at the same time, the slower Na^+ will decelerate the Cl^-. All of these accelerating and decelerating effects produce a mutual diffusion coefficient, which is considered to be the similar manner for a multicomponent solution system that composed of various ionic species.

3 THE CALCULATION MODEL OF MUTUAL DIFFUSION COEFFICIENT

The generalized form of the Fick's first law suggested by Onsager [3], which can relate the flux of i_{th} species (J_i) to the concentration gradient of j_{th} species ($\partial C_j/\partial x$) by the mutual diffusion coefficient (D_{ij}), is shown in the following expression.

$$J_i = -\sum_{j=1}^{n_s} D_{ij} \frac{\partial C_j}{\partial x} \tag{1}$$

By the definition of the Onsager phenomenological coefficient [3] and the thermodynamic force between ions occurred by the gradient of electrochemical potential [1], D_{ij} can be calculated from the following equation.

$$D_{ij} = \delta_{ij} D_i^0 \left(1 + \frac{\partial \ln \gamma_i}{\partial \ln C_i}\right) - \left\{ \frac{z_i D_i^0 C_i}{\sum_{k=1}^{n_s} z_k^2 D_k^0 C_k} z_j D_j^0 \left(1 + \frac{\partial \ln \gamma_j}{\partial \ln C_j}\right) \right\} \tag{2}$$

By using above equations and the finite difference analysis, the transport of ions concerning to the interaction from all coexisting ions in pore solution of a cement-based material can be determined.

4 CONCLUSIONS

The validation of presented calculation model for mutual diffusion coefficients for ions transport in a cement-based material is shown in **Fig.2**. The calculated results are compared with the experimental results of a mortar specimen exposed to 0.5 M NaCl solution for one year. Because of the uncertainty of the material's tortuosity (τ), which is very complicated to determine, the simulation of ions penetration into the mortar specimen was made by assuming τ = 3, 5 and 7. The results from this figure show that with a particular amount of tortuosity, the amount of total chloride is slightly changed and the best approximation is according with τ = 7.

It can show that by using this model for the transport of the ions in a multicomponent solution coupling to the chemical equilibrium model, i.e. a chloride binding isotherm, we can predict the amount of penetration of chloride ions into a cement-based material.

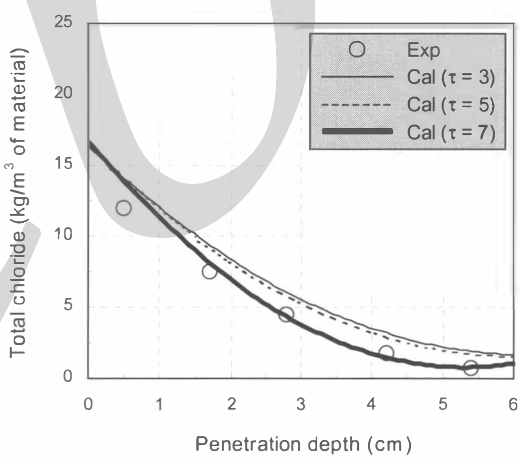

Fig.2 Calculated and experimental results of mortar specimen exposed to NaCl solution for one year

REFERENCES

[1] Andrew, R. Felmy and John, H. Weare, "Calculation of Multicomponent Ionic Diffusion from Zero to High Concentration: I. The System Na-K-Ca-Mg-Cl-SO4-H2O at 25," Geochimica et Cosmochimica Acta, Vol.55, pp.113-131, 1991

[2] N. OTSUKI, S. MIYAZATO, H. MINAGAWA and S. HIRAYAMA, "Theoretical Simulation of Ion Migration in Concrete," Concrete Research and Technology, Vol.10, No.2, pp.43-49, May, 1999

[3] P. C. Lichtner, C. I. Steefel and E. H. Oelkers, "Reactive Transport in Porous Media: Review in Mineralogy, Vol.34," The Mineralogical Society of America, pp.147-157, 1996

INFLUENCE OF REBAR CORROSION ON STRUCTURAL PERFORMANCE OF REINFORCED CONCRETE JOINTS

Mitsuyasu Iwanami
Port and Airport Research Institute
Yokosuka, JAPAN

Fuminori Sato
Maeda Corporation
Tokyo, JAPAN

Hiroshi Yokota
Port and Airport Research Institute
Yokosuka, JAPAN

Keywords: joint of reinforced concrete members, structural performance, corrosion, bond, localization of deformation

1 INTRODUCTION

Marine concrete structures are exposed to extremely severe condition. Chloride ions in sea water easily penetrate into concrete, and the atmosphere in marine areas is rather humid. Consequently, corrosion of reinforcing bars in concrete occurs, resulting in decrease in the structural performance [1].

In this study, influence of rebar corrosion at the joint of reinforced concrete members was investigated, where the stress condition is considerably severe in ordinary concrete structures. At the joint of T-shaped reinforced concrete specimen, corrosion of rebars was locally induced by electrolytic action. From the result of loading tests, influence of degree of corrosion was investigated on structural performance such as load bearing capacity and deformability. Moreover, finite element analysis was conducted considering bond deterioration between rebars and concrete due to corrosion. On the basis of the analytical results, an evaluation method of structural performance was examined for existing concrete structures damaged by rebar corrosion.

2 EXPERIMENTAL RESULTS

The specimens used for the experiment were T-shaped reinforced concrete beam-to-column connected members modeling a joint of reinforced concrete structures. Figure 1 shows the geometry and dimensions of the specimen. Longitudinal rebars in the joint suffered from artificially accelerated corrosion by means of electrolytic technique. The degree of corrosion was controlled by changing the duration of electrolytic test, and four cases of deterioration in the specimens were prepared including the sound one, according to the reference [2]. Loading test was conducted on these specimens. The specimen was fixed to the load-bearing-floor through the beam by PC bars. Repeated horizontal force was applied by a hydraulic jack attached to the load-bearing-wall. A cross-sectional loss of rebars was used to evaluate corrosion state of rebars in concrete. In the measurement, longitudinal rebars were taken out from the column of the specimen after the loading tests, and corrosion product attached to the rebar surface was perfectly removed by sand-blasting and chemical reaction of citric acid.

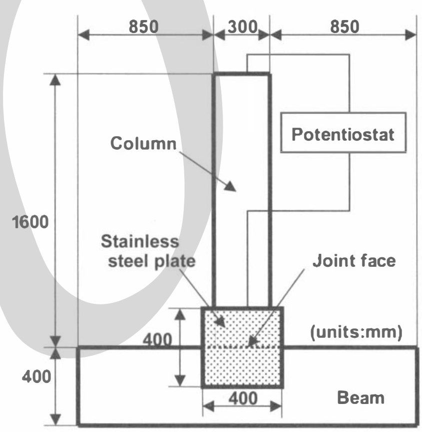

Fig.1 Dimensions of specimen and setup of electrolytic test

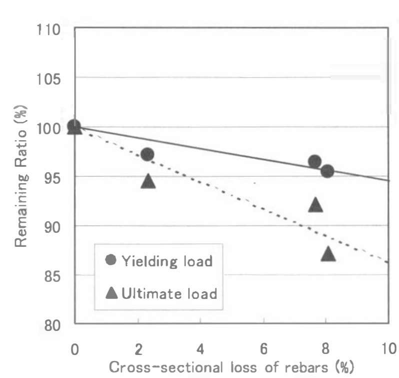

Fig. 2 Influence of rebar corrosion on load bearing capacity

Figure 2 shows the relationship between cross-sectional loss of rebars and the load bearing capacity. From this figure, it was found that yielding and ultimate loads gradually decreased with increase in cross-sectional loss of rebars. Furthermore, the rate of decrease in ultimate load was larger than that in yielding load. The reason for this was the deterioration of bond between rebars and concrete due to corrosion. That is, degradation of the bond took away a tension-stiffening effect of concrete, and performance of crack distribution was lost. Only one crack among several bending cracks opened extremely. Consequently, localization of deformation brought about, resulting in less increase in load after yielding of rebar.

As to the measurement of crack pattern, the crack widths of the sound specimen (Level 0) decreased monotonically from the joint face to the loading point, with demonstrating the same shape as the gradient of actual moment acting in the column. On the other hand, when the longitudinal cracks due to rebar corrosion have occurred in the column, only one crack near the joint face opened extremely wider than the other cracks. Furthermore, the number of cracks in the column became less as rebar corrosion progressed.

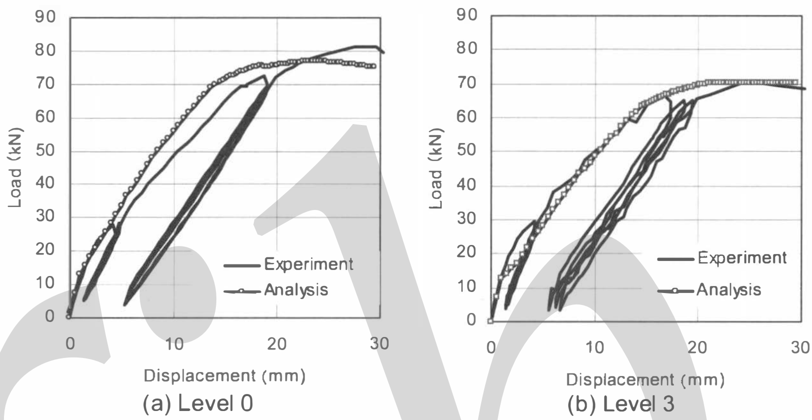

Fig. 3 Comparison of relationship between load and displacement at loading point

3 FEM ANALYSIS

To analytically evaluate the influence of rebar corrosion at the joint on its structural performance, finite element analysis was conducted taking deterioration of bond between rebars and concrete into account. The analytical results were compared with the results of loading tests. For considering decrease in bond properties between rebars and concrete due to corrosion, a bond element was introduced, which had the two specific parameters; shear strength and shear modulus. In this analysis, shear modulus was modifying appropriately in accordance with the state of rebar corrosion. As a result, as to the relationship between load and displacement at the loading point, the analytical result coincided well with the experimental one, as shown in Fig.3. Furthermore, it was made clear that the FEM analysis conducted in this study enabled to well simulate the phenomena of pullout and slippage of rebars, which caused decrease in performance of crack distribution and localization of deformation.

4 CONCLUSION

1) As deterioration of the specimen progressed due to rebar corrosion, cross-sectional loss of rebars in concrete increased. Load bearing capacity, such as yielding load and ultimate load, became worse in accordance with the degree of rebar corrosion.
2) The bond properties between rebars and concrete degraded due to rebar corrosion, resulting in loss of tension-stiffening effect and decrease in performance of crack distribution. Therefore, deformation of the column concentrated in the joint, in which corrosion of rebars occurred.
3) FEM analysis was executed considering both loss of cross-section of rebars and decrease in bond properties between rebars and concrete. By appropriately modifying characteristics of the elements in consideration with the state of rebar corrosion, decrease in performance of crack distribution and localization of deformation at the joint face were simulated well, corresponding with the experimental results.

REFERENCES

[1] Yokota, H., Fukute, T. Hamada, H. and Akiyama, T : Structural Assessment of Deteriorated RC and PC Beams Exposed to Marine Environment for More Than 20 years. Proceedings of the 2nd International RILEM/CSIRO/ACRA Conference, Melbourne, Australia, pp.209-219, 1998
[2] Port and Harbour Research Institute Ed. : Manual for Maintenance and Repair of Port Structures. Coastal Development Institute of Technology, 1999 (in Japanese)

DURABILITY OF A PRESTRESSED CONCRETE TRUSS IN AGRESSIVE ENVIRONMENT

Péter Lenkei
Pécs University, Hungary

Károly Kovács
Quality Control and Innovation in Building Plc., Hungary

Keywords: durability, Dt and NDT investigations

1 INTRODUCTION

The first precast and prestressed concrete truss in Hungary was designed in 1960 and executed in the city of Pécs, Hungary in mid 1961. The 24 m span industrial hall with a bridge crane was designated for the mechanical and chemical processing of uranium ore.

The frame of the one span hall frame consisted of in-situ precast large concrete elements: two Vierendeel columns and the post tensioned truss.

The prestressed concrete version to cover a span of 24 m was chosen for higher resistance to and better durability in moderate aggressive environment. The truss was shaped (polygonal fully compressed top chords, straight and fully prestressed bottom chord and only some of the diagonal chords slightly tensioned) to have predominantly compressive concrete stresses.

The one single piece trusses were casted and cured in horizontal position under their final place. The post tensioning of the three cables (20Ø5 mm high strength wires each) were carried out in the horizontal position too, when the concrete strength had reached 80% of its design strength. The effective mean strength at the age of 28 days was 30.6 MPa.

The injection of the cables was carried out under high pressure, neither plasticizer nor accelerator were used in the cement paste.

Two of the trusses were subjected to a loading test. The maximal deflection under 85% of the design load (excluding self weight) was 15 mm, which is equal to 1/1600.

The technological process in the hall had been continuously carried out for 35 years, with limited but permanent sulphuric acid, carbon dioxide and other emissions.

2 THE INVESTIGATIONS IN 1991

In summer 1991 after 30 years of service an investigation was carried out, including several non-destructive measurements and surface carbonization tests [1].

The *strength of concrete* was measured by Schmidt hammer. The overall mean concrete strength, corrected with the concrete technology factors was equal to 37.6 MPa. This higher value compared with the initial 30,6 MPa was partly due to the strength increase in time and due to the inaccuracy of this NDT test.

The *carbonization process* was checked by the thermo-analytical measurements on a derivatograph of small surface pieces taken from different trusses. The measurements showed well defined quantity of residual carbon hydroxide. The relative mass reductions were definitely higher in the region of acid emission.

The *crack measurements* were taken in the chords and joints of the trusses by hand microscope (magnifying by 25 times) and no visible cracking was observed.

The *deflection measurements* were taken on the bottom of the trusses by geodesic method. The results proved, that practically no truss deflections occurred during the 30 years service over the measured in the initial loading tests.

The *overall survey* of the structure showed no corrosion of the non-prestressed reinforcement, except the places of extensive moisture penetrations (leaks).

Summing up the 1991 investigations it was stated, that after 30 year use in moderate aggressive environment the post tensioned trusses were in good condition. This was due to the good quality of workmanship, to the effective cover of the reinforcement and to the fact, that no chemical additives were used.

3 THE RESULTS OF THE 2000/2001 INVESTIGATIONS

Due to the termination of the uranium ore mining near this chemical factory it was decided to decommission in 2000 and demolish in 2001 the chemical hall with the above described post tensioned trusses. This gave an unique opportunity to make detailed in-situ and laboratory investigations of the structures. It was aimed to make as much as possible *parallel DT and NDT investigations* [2].

In December 2000 the simultaneous evaluation of the *Schmidt hammer and the ultrasonic tests* on the concrete strength of the trusses resulted in 35.34 MPa mean concrete strength. This is a little less than 10 years ago.

The *phenolphthalein test* showed god surface basicity.

The *corrosion meter* showed practically no corrosion on the non-prestressed reinforcement.

No *surface cracks* were observed. For this the protective paint (which was applied for easier decontamination of the structures) had to be removed from all the places observed.

As a conclusion it was stated, that the concrete structure is in a good condition.

In June 2001 after the demolition of the structure two pieces from the prestressed bottom chord and two pieces from the non-prestressed diagonal chords were used to drill out *concrete core samples*. The concrete of the bottom chords had high level compressive pre-loading (from the post-tensioning) from early ages, but the diagonal chords stress level was very low. Altogether 14 concrete core samples of Ø73 mm were used for strength measurements and additionally 4 core samples were used for thermoanalytical investigations.

Some parts of the concrete truss were affected by the demolition process. This resulted in microcracking of several concrete core samples taken from the bottom chord. The microcracking was checked by high resolution microscope.

The non-microcracked core samples (4 from the diagonal chords and 3 from the bottom chord) gave a mean concrete compressive cylinder strength of 32.24 MPa, which is ~10% less than the mean strength observed by the NDT investigations one year earlier. This was due to the overestimated strength values of the NDT investigations.

The microcracked core samples were of two kinds. One was taken from the direction of the prestressing force and the mean strength was 23.06 MPa, the other was taken from the right angle to that direction and the mean strength was only of 20.11 MPa.

The strength differences were supported by the analogous differences of the concrete specific weights, due to the compaction by the pre-loading.

The *thermoanalytical measurements* showed only slight surface carbonization of the concrete, like in 1991.

4 CONCLUSIONS

The investigations reported showed the following tendencies:

- the NDT test by Schmidt hammer, even in conjunction with ultrasonic test or taking into account the concrete technology factors gave 5-15% higher results than the DT core sample tests, in the higher concrete strength area (C 20 and higher),
- early compressive pre-loading e.g. early age post-tensioning can considerably, 5-10% increase the concrete strength (due to higher compaction) but only in the direction of pre-loading,
- the good quality concrete technology using protective coatings, even in moderate aggressive environment will prevent concrete carbonization.

REFERENCES

[1] Lenkei, P. and Pálmai, I.: Thirty years experience with a prestressed concrete truss in a moderate agressive environment, FIP Symposium, Budapest '92, Proceedings, pp.247-257, 1992

[2] Lenkei, P. and Kovács K.: Program for comparison of NDT and DT methods of structural concrete evaluation, RILEM-IMEKO-Expertcentrum Conference „Non destructive testing and experimental stress analysis of concrete structures" Kosice, Proceedings, pp. 34-36, 1998

REQUIRED PERFORMANCE AND METHOD OF TESTS FOR WATERPROOFING SYSTEMS

Koichiro Shito, Japan Highway Public Corporation
Yasushi Kamihigashi, Japan Highway Public Corporation
Yoshiharu Mizugami, Japan Highway Public Corporation
Izumi Tanikura, Japan Construction Method and Machinery Research Institute
Ken'ichi Hida, Chiyoda Engineering Consultants Co.,Ltd., Japan
Yuichi Ishikawa, Chiyoda Engineering Consultants Co.,Ltd., Japan

1 INTRODUCTION

At present, the Japan Highway Public Corporation (JH) applies waterproofing to all bridge structures, as measure to improve the lifespan. The performance of waterproofing materials presently used fulfills the existing JH standards of 1994 ([1]) at the time of application, but tend to decrease soon after that. Symptoms that imply this decrease include water leakage at the bottom side of the concrete slab (indicating increased content of water and salt in concrete, Photo 1) and damage to pavement (indicating blistering and separation of waterproofing, Photo 2).

In order to find solutions for this problem and to keep in line with international developments such as ISO standards, it was necessary to clarify required performance and lifespan of waterproofing, and to lay down specifications for performance verification. This paper reports about the new proposed standards for waterproofing of concrete bridge slabs.

Photo 1 Water leakage (bottom of slab)

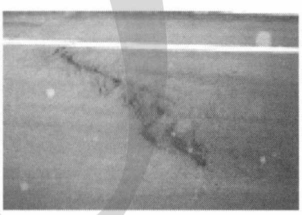

Photo 2 Damage to pavement

It is necessary to apply not only a suitable waterproofing layer but at the same time an effective drainage system that removes rainwater and other liquids rapidly (Figure 1).

Waterproofing systems

Improve the lifespan of concrete slab	Improve the lifespan of pavement
Apply waterproof layer	**Effective drainage system**

Figure 1 Concept of waterproofing systems

2 PROPOSED STANDARD

Investigations have shown that foremost importance should be placed to avoid items that decrease the quality of concrete or have a negative effect to the durability of pavement. Requirements to avoid the former type of items include resistance to water and resistance to salt. These requirements must be maintained under difficult conditions such as moving traffic loads and cracks in concrete that open and close. Requirements to avoid the latter type of items include that the tensile and shear bond strength between concrete slab and pavement must not be affected, neither during construction neither during operation.

Based on the maintenance planning for pavement, the design lifespan of waterproofing is set at 30 years. During this lifetime the requirements as shown in Table 1 must be fulfilled.

Table 1 Standardized requirements to waterproofing

No.	Requirement	Stage
1	Resistance to water	During construction and operation
2	Resistance to salt	
3	Good tensile bond	
4	Good shear bond	

The four requirements described above (resistance to water and salt, tensile and shear bond strength) are to be maintained at all location, under all conditions (during construction and during operation) and at all times. In order to verify this, it is necessary to verify these items after applying all types of loads and conditions that are to be expected during construction period and operation period of waterproofing systems. These conditions and loads are specified in the proposed standard, based on comparative investigation about Japanese, German and British standards ([2]).

For the verification, test specimens are prepared consisting of concrete slab, waterproofing layer and pavement layer. As shown in Figure 2, loads and conditions expected during construction period are applied and tests are carried out. After that, loads and conditions expected during operation period are applied and additional tests are carried out.

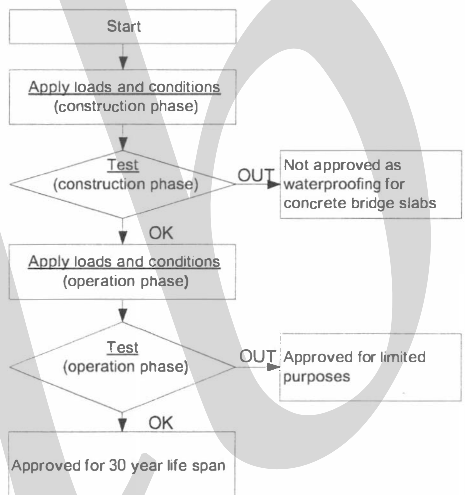

Figure 2 Verification flow

3. CONCLUSION

Test methods for waterproofing systems of concrete bridge slabs was discussed. The findings can be summarized as follows:

- A manual was proposed in order to clarify required performance and lifespan of waterproofing, and to lay down specifications for performance verification.
- The proposed manual is planned to be made official in due time.
- The data obtained from the performance tests according to this manual will be saved in a database for future reference.
- It is objected to further improve the knowledge about the lifespan of waterproofing for concrete bridge slabs, and to develop materials that enable cheap and fast realization of waterproofing.

REFERENCES

[1] Japan Highway Public Corporation, Guideline for Design and Construction of Waterproofing Systems for Concrete Bridge Slabs, Notification, 1994

[2] K. Shito, Y. Kamihigashi, Y. Mizugami, K. Hida, R. Stroeks, A. Haack and R. Jordan, Comparison of Waterproofing Systems for Concrete Bridges: Japan, Germany and Great Britain, The First FIB Congress 2002

CHLORIDE PERMEABILITY OF HIGH-STRENGTH CONCRETE

Yoshiki Tanaka, Public Works Research Institute, JAPAN
Manabu Fujita, Japan Prestressed Concrete Contractors Association, JAPAN
Haimoon Cheong, Korea Highway Corporation, KOREA
Hiroshi Watanabe, Hirotaka Kawano, Public Works Research Institute, JAPAN

Keywords: chloride attack, diffusion coefficient, electric conductivity and wet/dry condition

1 INTRODUCTION

High-strength concrete (HSC), with a design strength of 70 to 80 MPa, is expected to reduce the life cycle cost of bridges and other concrete structures. HSC has the advantage of a high degree of durability as well as other advantages such as being lightweight and good constructability due to the reduced size of cross-section. Since HSC is a very dense, chlorides are less likely to permeate into HSC than into conventional concretes. Nevertheless, HSC's permeability has not been quantitatively clarified yet. This paper shows the results obtained from the 1-year ponding, 3-year exposure and electric conductivity tests using concrete with differing water / cement ratio (W/C).

Table 1 Mix proportions

No.	W/C	s/a	W (kg/m³)	C (kg/m³)	S (kg/m³)	G (kg/m³)	SP (%)	AE (%)	Proportion of paste (L/m³)
1	0.30	0.40	150	500	669	1031	1.8	0.006	310
2	0.40	0.40	173	433	667	1028	1.2	0.006	310
3	0.55	0.40	196	356	669	1030	0.5	0.006	310
4	0.30	0.40	130	433	711	1096	2.5	0.006	268
5	0.30	0.40	173	577	620	956	1.5	0.006	357
6	0.25	0.40	173	692	583	898	2.3	0.006	393

Cement: High early-strength Portland cement
Super plasticizer: Polycarbonate type AE: Air entraining agent

2 TEST PROCEDURES

Specimens for the salt-water ponding test were cylindrical in shape, 100 mm diameter x 200 mm height. Mix proportions of specimens are shown in Table 1. After three days of wet curing, specimens were kept indoors, without wet curing, for a few months. Following curing, the specimens were ponded in salt-water with 5% NaCl. Acid-soluble chloride ions were measured at ponding periods of 4, 13 and 52 weeks (1 year).

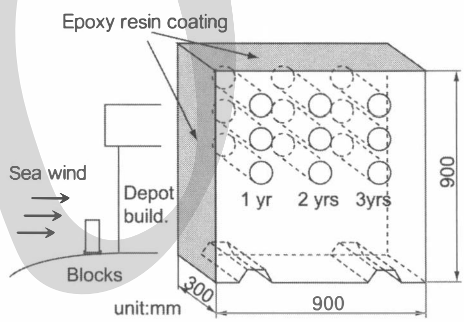

Fig. 1 Exposure test setup

The specimen used in the exposure test is shown in Fig. 1. Profiles of chloride ions of cores taken from the blocks were determined at exposure periods of 1, 2 and 3 years. Concrete for the blocks were taken from the same batch as those used in the ponding test. After curing similar to the ponding test, the blocks were exposed at a site, approximately 20 m from the coastline, near the Sekiya Mouth of the Shinano River. Annual averages of airborne chloride ion levels in the site were 2.1 to 3.0 mg/dm^2/day. The diffusion coefficient of the chloride ingress was calculated by means of a curve fitting based on the Fick's second law.

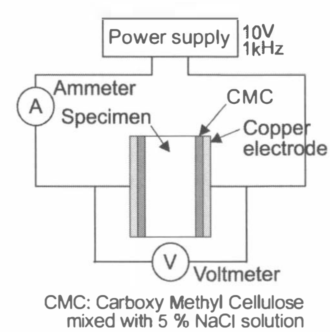

Fig. 2 The method of measuring electric conductivity

The conductivities of both test specimens were measured at about 16 months of age, using the remaining parts of the cores, by means of the setup shown in Fig. 2. The electric conductivity of concrete can be used as an index to express the wet and dry conditions as well as the denseness of hardened concrete.

3 RESULTS AND DISCUSSION

Figures 3 and 4 show the relationship between the diffusion coefficient and W/C, obtained from the ponding and the exposure tests over several periods. The dataset could not be fitted appropriately when the depth of chloride ingress had reached less than the slice pitch of 10 mm. According to the results from the both tests, smaller W/C could realize the lower diffusion coefficient of chloride ions.

Figure 5 shows the relationship between the diffusion coefficient and the electric conductivity. In the case of the ponding test, a correlation between the logarithm of the conductivity measured under the saturation and the logarithm of the diffusion coefficient was clearly observed. On the other hand, in the case of the exposure test, there was no correlation between the conductivity of natural dry concrete and the diffusion coefficient. These results suggest that the diffusion coefficient was influenced by dry conditions in the concrete as well as the deneseness of the pore structures. In the case of W/C of 0.25 and 0.30, conductivities up to 50 mm deep might differ from those up to 20 mm, of which the range was effective in determining the diffusion coefficient.

The diffusion coefficient of the 1-year immersed specimens (Fig. 3) was much greater than that of the exposed blocks (Fig. 4). This may have been caused by the dry condition of the exposed surface. Consequently, it has been suggested that the diffusion coefficient of the typical ponding test may be excessive for a durability design of structures located in the air, or in the same conditions as the exposure test.

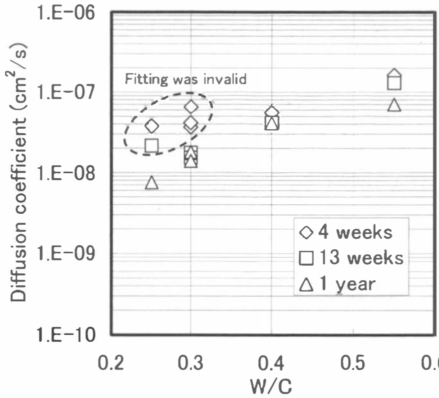

Fig. 3 Relationship between diffusion coefficient and W/C from the ponding test

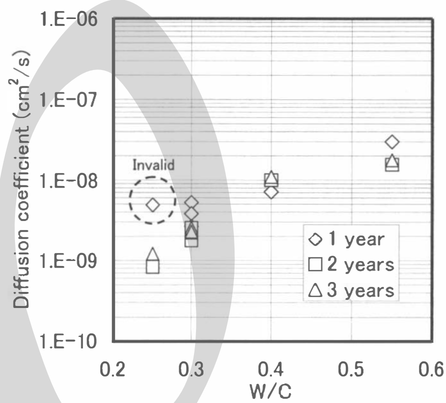

Fig. 4 Relationship between diffusion coefficient and W/C from the exposure test

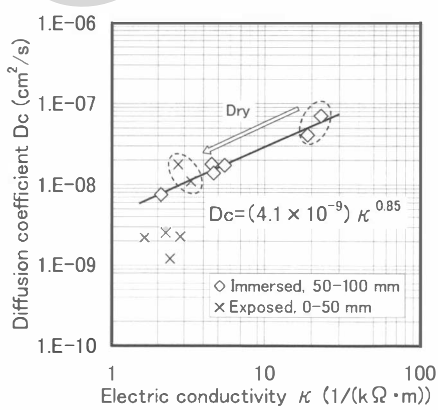

Fig. 5 Relationship between diffusion coefficient and electric conductivity

4 CONCLUSIONS

1) Whichever test was applied, either the salt-water ponding test or the exposure test, the smaller the W/C, the smaller the diffusion coefficient as an index of the chloride permeability, in the range of W/C from 0.25 to 0.55.
2) The diffusion coefficient of the 1-year ponding test was much greater than that of the exposure test despite the same batch of concrete being used. This seemed to be influenced by the dry condition of the exposed blocks. Consequently, it is suggested that the diffusion coefficient obtained from the ordinary ponding test may be excessive for applying to the practical durability design of the structures located in the air.

ACKNOWLEDGEMENTS: The authors thank the Sekiya Branch and the Shinanogawa-karyu Construction Office, the Ministry of Land, Infrastructure and Transport, Japan for co-operating with the exposure test.

CORROSION RESISTANCE OF STAINLESS STEEL REBAR IN CONCRETE WITH HIGH CHLORIDE CONTENT

Sungho Tae

S.H.Tae, T.Noguchi, M.Kanematsu
Tokyo University, Japan

T.Ujiro
Kawasaki steel Corporation, Japan

Keywords：Stainless steel rebar, Corrosion resistance, Limit of chloride content

1 INTRODUCTION

The corrosion of RC structures demonstrates very complicated forms of deterioration intermingled together but all pointing to a decrease in the durability of RC structures by the corrosion of the reinforcing bars. For this reason, many studies have been performed to discover the best method of preventing corrosion in reinforcing bars. However, most of them have been disproportionately concentrated on the improvement of concrete quality such as the increase in concrete cover thickness, optimization of water-to-cement ratio or the addition of corrosion resistant materials. In America and Europe, standardized high corrosion resistance stainless steel has already been employed in those areas damaged by salt as a method of enhancing the corrosion resistance of the reinforcing bar through its characteristic improvements [1]. Whereas, in Japan, there have not been many studies on the corrosion resistant reinforcing bars. However, considering the ever increasing maintenance cost for RC structures, it is desirous to conduct the study on the corrosion resistant reinforcing bars that does not require a life cycle cost. Accordingly, when a low stainless steel rebar containing fewer Cr and Ni elements is made available, the excessive concrete cover thickness can be reduced and the regulation on the water-to-cement ratio will become less strict, at which time the lifetime of RC structures can be extended by using the highly cost effective anticorrosion steel rebars that remain unaffected by corrosion under corrosive environments.

2 OUTLINE OF THE EXPERIMENTS

2.1 Materials

The experiment has been conducted on concrete with only one water-to-cement ratio being 0.6 to 1. Five levels of chloride ion contents, being 0.3, 0.6, 1.2, 2.4 and 24 kg/m^3 of concrete were applied, which were adjusted using NaCl (first class reagent). The NaCl was used dissolved in mixing water. A total of 8 types of rebar specimens including SD345 of JISG3112 (bar type concrete reinforcing steel), 6 types of stainless steel rebar with different Cr contents and SUS304 stainless steel rebar were used in this experiment. Table 1and Table 2 indicate the basic components of the reinforcing bars and the mix proportion of concrete. In the specimen, two types of rebars were arranged at the left and right sides in two layers, with one type of rebar in each layer as shown in Fig.1.

Table 1 Reinforcing bar composition, wt.%

Steel bars	C	Si	Mn	P	S	Cr	Ni	Mo
SD345	0.2280	0.31	1.34	0.029	0.020	0.084	0.04	0.016
0Cr	0.0120	0.32	0.50	0.031	0.006	0.005	0.01	0.001
5Cr	0.0150	0.28	0.53	0.027	0.006	5.020	0.01	0.001
9Cr	0.0107	0.28	0.53	0.028	0.006	9.140	0.01	0.001
11Cr	0.0117	0.28	0.53	0.028	0.004	11.00	0.01	0.001
13Cr	0.0117	0.28	0.53	0.028	0.004	13.05	0.01	0.002
16Cr	0.0113	0.29	0.53	0.027	0.004	15.98	0.01	0.002
SUS304	0.0630	0.31	1.01	0.026	0.006	18.36	0.04	0.053

Table 2 Mix proportion of concrete

W/C (%)	Water (kg/m^3)	Cement (kg/m^3)	Sand (kg/m^3)	Coarse Aggregate (kg/m^3)	s/a (%)	Slump (cm)	Air (%)	Air entraining agent (g/m^3)
60	185	308	810	970	46	18	4.5	20

2.2 Experiment method

The acceleration of corrosion for each specimen was achieved by repeated high and low temperature curing as well as wet and dry curing. Each curing cycle consisted of one-day high temperature/humidity (temp. 60,humidity 95) curing and one-day low temperature/humidity (temp. 30, humidity 50) curing. Measurement of half-cell potential was conducted once 5 cycles of corrosion accelerated curing had been completed.
Additionally, the corrosion area and the weight loss were measured after pulling out the rebars at such time when 50 cycles and 65 cycles of the corrosion accelerated test had been completed.

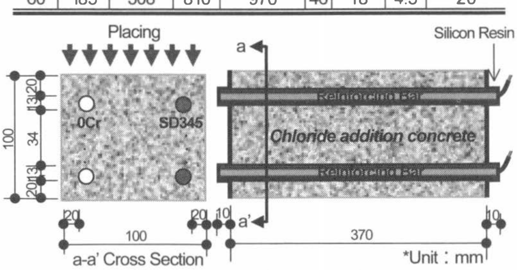

Fig.1 Details of test specimen

3 RESULTS OF EXPERIMENTS AND DISCUSSION

Furthermore, for the concrete containing a chloride ion content of 0.3 and 0.6kg/m^3, the half potential of the SD345 and 0Cr rebar were already observed at the 5cycles, to be near –0.35V, which is the criteria for corrosion in ASTM. For the concrete containing 1.2 kg/m^3 of chloride ion, the rebar having a Cr content above 5% showed half-cell potential greater than –0.35V, even at the 65cycles. In the case of 2.4kg/m^3 chloride ion content, for the stainless steel rebar with Cr content above 9%, the measured half potential value was higher than –0.35V. In the case of the chloride ion content of the concrete exceeding 24kg/m^3, the measured half-cell potential of all the rebars except SUS304 was below –0.35V.

The higher the Cr content, the lesser the corrosion area regardless of the chloride ion content. For the same types of rebars, the corrosion area became higher as the chloride ion contents increased. Such a trend was conspicuous in SD345 and 0Cr rebars. However, in the case of the 5Cr rebar containing 5% Cr content, a rapid increase in the corrosion area was not observed even when the chloride ion content had increased from 2.4kg/m^3 to 24kg/m^3. This was due to the fact that the rebar were protected by the passive coating formed by the reaction between chromium and oxygen despite the increase of chloride ion content. As for the 9Cr stainless steel rebar, the corrosion area was measured to be 20% at 24kg/m^3 of chloride ion content at the 65cycles of the corrosion accelerated testing.

Fig.2 shows the relationship between the chloride ion content and the weight loss by corrosion for different types of rebars for 50 and 65 cycles of corrosion accelerated testing. According to Fig.2, the weight loss by corrosion increased along with the increase of chloride ion content irrelevant to the types of rebars. Also, for 50 cycles of corrosion accelerated testing, corrosion occurred to the SD345 and 0Cr rebar in the concrete containing a chloride ion content of 0.3kg/m^3. As well, the weight loss by corrosion did not increase remarkably while the chloride ion content showed an increase up to 1.2kg/m^3. However, the weight loss by corrosion increased with the increase of chloride ion content, and the measured weight loss by corrosion for the SD 345 rebar, which contains much carbon, was about 3 times as high as that of 0Cr rebar when the chloride ion content was 24kg/m^3. Furthermore, corrosion occurred to the 5Cr rebar when the chloride ion content of the concrete was 2.4kg/m^3. However, any rapid increase in the weight loss by corrosion was not observed even when the chloride ion content had increased to 24kg/m^3. This was the same trend as that of the increase in the corrosion area. For the rebar with Cr content exceeding 9%, a weight loss by corrosion less than 0.5% was observed in the concrete with chloride ion content of 24kg/m^3. The 65 cycles of corrosion accelerated testing indicated the same trend as the 50 cycles.

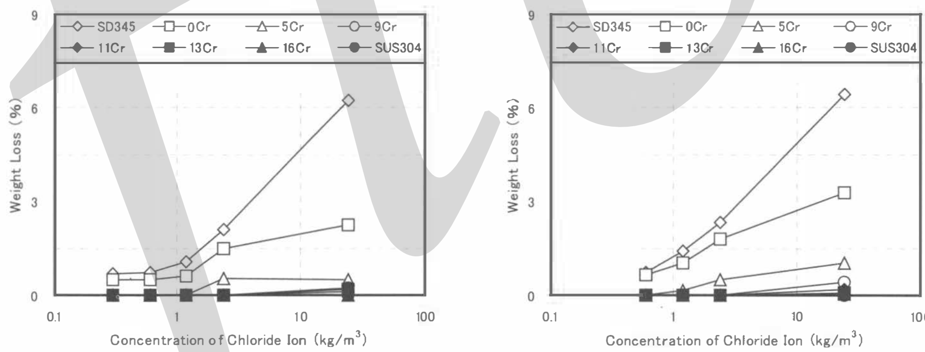

(a) 50Cycle (b) 65Cycle

Fig.2 Weight loss

4 CONCLUSION

1. Irrelevant of the chloride content, the corrosion area and the weight loss by corrosion were low when the Cr content was high.
2. Cr content required for corrosion resistance was above 5% and 9% when the chloride ion contents were 1.2kg/m^3 and 2.4kg/m^3, respectively.
3. For concrete containing a chloride content of 24kg/m^3, it is expected, although not yet confirmed, that the stainless steel rebar with a Cr content greater than 11% has corrosion resistance.

Literature

[1] Yamaji, T., Aoyama,T., Yamagawa, M. and Simizu, T. : Corrosion property of a Stainless steel rebar in the concrete inside, repair and reinforcement of a concrete construction, up grade symposium article report, pp.69-74, Vol. 1, 2001

CHLORIDE PENETRATION AND CORROSION ANALYSIS IN REINFORCED CONCRETE STRUCTURES

Byung Hwan Oh
Professor, Department of Civil Eng
Seoul National University, Korea

Bong Seok Jang
Senior Researcher, Korea Institute
of Construction Materials, Korea

Keywords : chloride diffusion, corrosion, reinforced concrete

1 INTRODUCTION

The reinforced concrete structures exposed to sea environments suffer from corrosion of steel bars due to chloride ingress. The purpose of the present study is to explore the effects of steel bars on the chloride penetration and to determine realistically time to corrosion considering the existence of steel bars. Many design variables including rebar diameter, cover thickness of rebar, and water-cement ratio have been considered in the analysis to see the effects of those variables on the chloride penetration.

2 CHLORIDE DIFFUSION MODEL

2.1 Diffusion equation

The diffusion of chloride ions is generally assumed to follow the Fick's second law. The general diffusion equation can be written as follows,

$$\frac{dC_f}{dt} = \frac{dC_f}{dC_t} div\left[D_{cl} grad\left(C_f\right)\right] \tag{1}$$

where, C_t = total chloride ions (per concrete weight, g/g) , C_f = free chloride ions(per concrete weight, g/g), t = time, D_{cl} = diffusion coefficient , and dC_f / dC_t = binding capacity.

2.2 Binding isotherm

Some parts of chloride ions penetrated into concrete are bound and do not affect directly the corrosion of steel bars. The following nonlinear binding isotherm was used in this study,

$$C_b' = \left(C_f'\right)^A 10^B \tag{2}$$

where C_b' = bound chloride ions (per gel weight, mg_{cl} / g_{gel}), and C_f' = free chloride ions (per one liquid liter, mol / l).

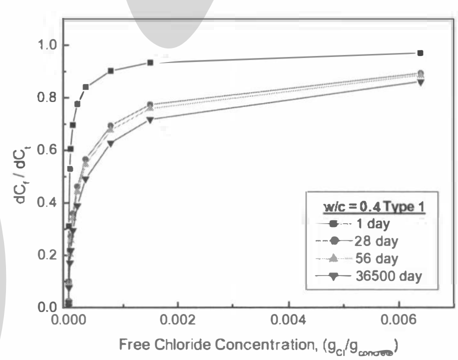

Fig. 1 Variation of dC_f / dC_t according to age

The binding capacity, dC_f / dC_t, has been also determined using the previously defined material properties. Fig.1 describes the variation of dC_f / dC_t according to free chloride concentration for various ages. It can be seen that the values of dC_f / dC_t are much larger at very young ages compared with those of mature concrete at older ages. This is because the free chlorides are reduced with increasing age.

3 CHLORIDE DIFFUSION ANALYSIS CONSIDERING REINFORCEMENTS.

The major variables used in the diffusion analysis include bar diameters, cover thickness of rebar, and water-cement ratios. The chloride penetration into concrete wall or column members exposed to seawater can be analyzed by modeling the cross-section of the member in two dimension.

The chloride diffusion analysis were implemented for various cases and some results are depicted in Fig.2. Fig.2 shows the chloride profiles penetrated into concrete for the member with rebar diameter d =10 mm and cover thickness c=20 mm. Fig.2 indicates that the penetrated chlorides increase with time. However, the most important finding here is that the chlorides accumulate in front of the reinforcing bar and that it shows much higher chlorides values at the location of rebar, compared with those without considering reinforcement. This is due to the fact that the chloride penetration cannot take place through the rebar and the rebar plays a role to curb further penetration of chlorides locally.

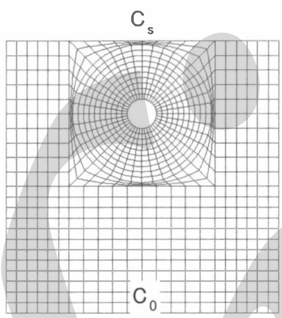

Fig.2 Finite element meshes

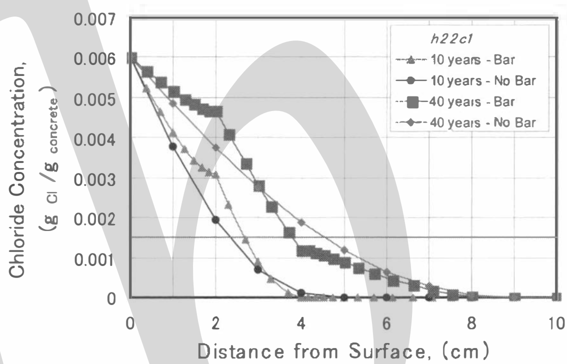

Fig.3 Effects of reinforcement bar on chloride diffusion

4 CONCLUSION

The conventional diffusion analysis has neglected the existence of steel bars in concrete. However, the existence of steel bar may influence greatly the diffusion process in reinforced concrete members. The purpose of the present paper is, therefore, to study primarily the effects of reinforcements in chloride diffusion of concrete structures.

The present study indicates that the chlorides are accumulated in front of a reinforcing bar and the accumulation of chlorides is much more pronounced for the case of larger-size bar. The major reason of chloride accumulation in front of a bar is due to the fact that the chloride diffusion does not occur through the reinforcing bars. The higher accumulation of chlorides at the bar location causes faster corrosion for reinforcing bars. The present study indicates that the effects of reinforcements must be properly considered in the chloride diffusion analysis for more accurate and realistic prediction of service life of concrete structures.

ACKNOWLEDGEMENT

The support from National Research Laboratory Program of Korea is grestly appreciated

REFERENCES

[1] Broomfield, J.P., "Corrosion of Steel in Concrete : Understanding, Investigation and Repair," Rilem, E & FN Spon, 1997.

[2] Tang, L, Nilsson, L.O.(1993), "Chloride Binding Capacity and Binding Isotherms of OPC Pastes and Mortars," Cement and Concrete Research, V.23, No.2, pp.347-353.

ELECTRICAL ISOLATION AS ENHANCED PROTECTION FOR POST-TENSIONING TENDONS IN CONCRETE STRUCTURES

J. Ayats, Special developments in PT engineering
A. Gnägi, PT Systems development
B. Elsener, ETH Zürich, Institute for Building Materials

Keywords: Electricaly Isolated Tendons, monitoring, durability

1. INTRODUCTION

Prestressing created new possibilities for the structural use of concrete. Today technology allows producing steels with very high strength, but these materials are more susceptible to brittle fracture caused by corrosion and hydrogen embrittlement [1].

Research and investigations on a great number of structures have shown that corrosion of the prestressing steel occurs at points where water and chloride ions can penetrate. The metallic ducts can not be considered as a barrier against corrosion. All these facts have lead to demands for improved performance of the PT systems in corrosion protection and the possibility to monitor the tendons.

2. HISTORY AND STANDARDS

2.1 Milestones to Electrically Isolated Tendons (EIT)

In the 1960s, corrugat ` plastic PT tendon sheathing was introduced as more cost efficient solution. The petrol crisis (1970) was responsible that plastics ducts disappeared again. When investigating fretting fatigue and fretting corrosion of tendons with metallic ducts, polymeric materials were introduced again for tendon ducts. This was the starting point of a fully isolated tendon. The increasing concern about corrosion and stray currents of the high strength steel lead to the requirement for electrical isolation of all 945 permanent ground anchors at the railway station Stadelhofen, Zürich, in 1985; this was the break through for EIT.

2.2 Reference to Standards

Several reports recommendations and guidelines are giving guidance for EIT. The most complete document regarding EIT, is the Guideline for "Measures to ensure the durability of post-tensioning tendons in RC concrete structures" [2], published by the Swiss Federal Highway Agency and the Swiss Railways in 2001. The guideline [2] proposed three categories for Post-Tensioning tendons in terms of corrosion protection. Tendons of category c) require complete electrical isolated to avoid stray currents and to allow to monitor the integrity of the tendon encapsulation. The Guideline [2] indicates criterias for the choice of the categories and gives information for the measuring procedure and the interpretation of the results.

3. MONITORING OF ELECTRICALLY ISOLATED TENDONS

The use of electrically isolated tendons allows to control the electrical isolation and the integrity of the duct after construction and to monitor the corrosion protection of the steel strands during service life with simple AC impedance measurements (usually called ‚electrical resistance measurements').

3.1 Electrical connections and measuring procedure

The measurements require a sound electrical connection to each individual tendon and another connection to the rebars. Monitoring of the electrically isolated tendons is performed with AC impedance measurements at frequency of 1 kHz (LCR meter ESCORT 131). From laboratory studies the limiting values for a sound encapsulation was found to be 500 kΩ*m (59 mm PT Plus duct).

3.2 Field Results – control the integrity of the duct after construction

The flyover "P.S. du Milieu" near Avenches is about 100 m long and consists of six sections with five columns. The anchorage zone is constructed with robust plastic ducts and plastic sleeve and electrically isolated anchorages. Six electrically isolated tendons (length 100 m, PT PLUS duct diameter

59 mm) were measured in order to control the integrity of the duct after construction. Five of the six tendons showed ohmic resistance between 7 kΩ and 28 kΩ, thus fulfilling the criteria of 500 kΩ*m. Tendon nr. 6 had a short circuit. The capaitance values measured (234 ± 4 nF) of the 100 m long tendons were in agreement with the laboratory data (2.33 nF/m) and allow thus to check the diameter and wall thickness of the duct.

3.3 Field Results – long term monitoring

On another flyover, "Prés du Mariage" (length 49.3 m, PT PLUS duct, diameter 76 mm), the ohmic resistance was monitored from the time of grouting up to three years. The six individual tendons showed a certain scatter, but the overall trend is an increase of the resistance with time; in the log R vs log t plot a straight line with a slope of about 0.5 can be observed. This indicates that the increase of the resistance is very rapid at the beginning but slows down after some months becoming asymptotic after several years. This continuous increase of the electrical resistance can be explained by the hydration of the grout and the surrounding concrete and the subsequent drying out; this trend is expected to continue in the future service life of the structure. This allows to detect the ingress of water in a very early stage: if (chloride containing) water reaches a defect in the duct, the concrete and the grout get wet and the electrical resistance of this tendon will not increase any more but decrease steadily. Thus the measurement of the electrical impedance at the normal inspection intevals represents a simple but very effective early warning system to detect a corrosion risk situation.

4. THE VSL ELECTRICALLY ISOLATED POST-TENSIONING TENDON

The combination of two existing post-tensioning system components like the anchorage of the VSL Composite System 2000 (CS 2000) and the VSL PT-PLUS duct [3] integrates a complete and practical solution for an electrically isolated post-tensioning tendons (EIT).

The anchorage is made of a combination of steel, high performance mortar and plastic taking advantage of progress in material technology, manufacturing and design. The CS 2000 anchorage series is made to accommodate up to 37 prestressing strands diameter 0.6", grade 1860 MPa.

The PT-PLUS plastic duct fully encapsulates and isolates the strand bundle by nature and continuity along tendon. Detailing is most important at anchorage level in order to guarantee full encapsulation and electrical isolation. The elements that complete the encapsulation at the anchorage are a standard PT-PLUS coupler with inlet, the plastic trumpet, the insulation plate and the protection cap made of plastic.

These corrugated ducts for internal bonded PT tendons offer attractive features and several advantages for use with curved tendons for internal post-tensioning:

Full encapsulation of tendon	⇒	durability
Electrical isolation of tendon	⇒	monitoring, early warning system
Enhanced fatigue strength	⇒	durability
Low friction of PT-PLUS duct	⇒	efficiency of prestressing
Reduced weight of components	⇒	handling (transport, installation)

5. APPLICATIONS

As already mentioned, long and proven experience with electrically isolated ground anchors and tendons has been accumulated since 1985 (railway station Stadelhofen, Zürich). The first application in bridges was in 1992 the flyover "PS du Milieu" near Avenches (Vaud). At present EITs comprising 19 and 22 strands of 15 mm are being installed in the Rhone Bridge at Raron (Valais). The Italian Railway Authorities will use EIT for the new high speed train lines.

REFERENCES

[1] FIP Recommendations, "Corrosion protection of prestressing steels" 1996.

[2] Guideline "Measures to ensure the durability of post-tensioning tendons in RC concrete structures" Swiss Federal Highway Agency and Swiss Railways, EDMZ (2001)

[3] H. R. Ganz: "Plastic ducts for enhanced performance of post-tensioning tendons", FIP Notes 1997/2, The Institution of Structural Engineers, London, pp 15-18 (1997)

MECHANICAL PERFORMANCE OF PRE-TENSIONED PRESTRESSED CONCRETE BEAMS WITH 10 YEARS CATHODIC PROTECTION UNDER MARINE ENVIRONMENT EXPOSURE

Toshiyuki Aoyama
P.S Corporation
Japan

Hiroshi Seki
Waseda University
Japan

Masami Abe
Port and Airport Reserch Institute
Japan

Kazuhiro Ikawa
Nakabohtec Corrosion Protecting CO.,LTD
Japan

Keywords: Cathodic Protection, Prestressed Concrete, Corrosion, Long-term exposure test, Marine environment

1 INTRODUCTION

The reinforcing steel in RC and PC members can be protected from corrosion by cathodic protection. This form of protection, however, suffers from certain drawbacks: 1) the build-up of alkaline ions around reinforcing steel causes softening of the concrete after long periods with a potential difference applied between anode and cathode [1]; 2) concrete softening leads to reduced bond strength between concrete and reinforcing steel [1][2]; 3) the reinforcing steel suffers damage due to hydrogen embrittlement after long periods of protection [1][2].

This paper discusses the effectiveness of cathodic protection for prestressed concrete structures under marine environment through a study of actual structures. All specimens had an initial chloride ion concentration of 9 kg/m^3, and were exposed to marine environment for ten years. The experimental work consisted of electro-chemical tests on the embedded PC strands, loading tests on the beams, corroded condition of PC strands and mechanical property of corroded strand.

2 EXPERIMENTAL PROCEDURES

2.1 Outline Of Test Beams

Figure 1 gives details of the pretensioned PC test beams and their dimensions. The beams were 325 mm deep and 4 m long. The PC strands consisted of 7 twisted strands measuring 9.3 mm in diameter, with 5 of these tendons in the lower flange and 2 in the upper flange.

2.2 Cathodic Protection Systems

The arrangement of anode materials was as shown in Fig. 2. The anode material in the impressed current system was titanium; this was either in the form of mesh attached to the beam surface or wires 1.5 mm in diameter buried 5 mm below the concrete surface. In the case of the titanium wire anode, the individual wires were arranged as marked ① to ⑨ in the figure. The sacrificial anode system comprised a protective sheet, a back-fill material, and a zinc sheet anode.

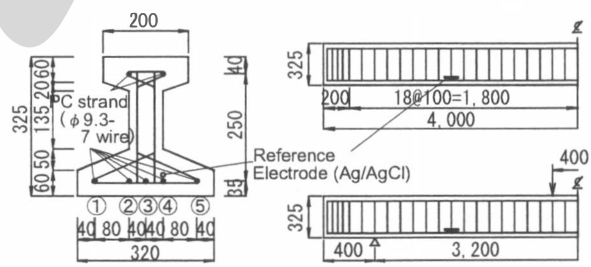

Fig.1 Dimensions of PC Beams

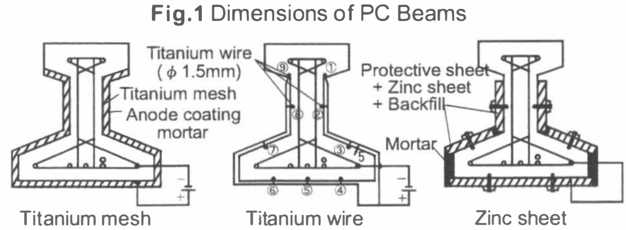

Fig.2 Cathodic Protection Systems

3 TEST RESULTS

3.1 Load Application Test

Loading tests were carried out on the beams by setting up a span of 3,200 mm, while the pure flexural-moment tests were with a span of 400 mm. A "dummy beam" was used for load application tests immediately after beam fabrication.

Table 1 shows the cracking and ultimate loads. The cracking loads of beams with titanium mesh, titanium

Table 1 Test Result

	Cracking load (kN)	Ratio	Ultimate load (kN)	Ratio	Type of failure
Dummy	78.5	1.00	205.0	1.00	Flexure (Compression zone is failure)
No -cathodic protection	58.8	0.75	132.4	0.65	Flexure (Compression zone is failure and strand ③ failure)
Titanium mesh	98.1	1.25	210.8	1.03	Flexure (Compression zone is failure)
Titanium wire	98.1	1.25	135.3	0.66	Flexure (Strand ①,⑤ failure and compression zone failure)
Zinc sheet	93.2	1.19	205.9	1.00	Flexure (Compression zone failure)

wire, and zinc sheet protection exceed the dummy beam load value (the value measured at zero years). Where there was no-cathodic protection, however, the cracking load decreased to approximately 75% that of the dummy beam. The ultimate loads of beams with titanium mesh and zinc sheet protection exceeded the dummy beam load value. However, with no-cathodic protection or in the case of titanium wire protection, the ultimate load decreased to approximately 65% that of the dummy beam. It is therefore concluded that the flexural characteristics of beams protected by the titanium mesh and zinc sheet methods do not degrade even after ten years of cathodic protection.

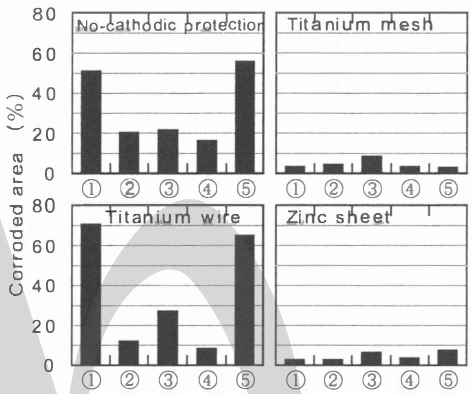

Fig.3 Corroded Area of PC Strands

3.2 Corroded Area of PC Strands

Figure 3 shows the corroded area of the PC strands. In this figure, numbers ①~⑤ correspond to positions ①~⑤ on the PC strands in Fig. 1. These results indicate that beams protected by the titanium mesh and zinc sheet methods suffered little corrosion of the PC strands, and this coincides with the electro-chemical tests on the embedded PC strands findings. For beams with no-cathodic protection and with titanium wire protection, PC strands embedded near the outer edge of the flange suffered serious corrosion. The reason for corrosion affecting PC strands in the case of beams with protected by the titanium wire method is that current stopped flowing. This ineffectual corrosion protection came about because insufficient current flowed, a result of concrete degradation around the titanium wire. The concrete degradation around the wire can be attributed to the small area of the anode material; as a result, the electric current density was very high over a limited area.

4 CONCLUSION

Ten-year tests were carried out on I-section pretensioned PC beams exposed to severe environmental conditions. The results of these tests are summarized below.

(1) Beams with protected by the titanium mesh and zinc sheet methods had the same flexural properties at ten years as beams tested in the initial stage (at zero years). In contrast, beams with no-cathodic protection exhibited considerably reduced flexural capacity at the age of ten years.

(2) PC strands embedded in the concrete showed no sign of corrosion in the case of beams with titanium mesh and zinc sheet methods of cathodic protection. On the other hand, the reason for corrosion affecting PC strands in the case of beams with protected by the titanium wire method is that current stopped flowing. This was a consequence of the small size of the titanium wire anode, which had a diameter of 1.5 mm, leading to degradation of the concrete around the wire.

REFERENCES

[1] Koji, Ishii,: Application of Cathodic Protection to Pretensioned Prestressed Concrete Members, Doctoral Thesis, 1996.10

[2] Takao, Ueda: Application of Desalination Method for Concrete Members Deteriorated with Salt Attack, Doctoral Thesis, 1999.6

SIMULATION ANALYSIS FOR THE PROGRESS OF CARBONATION REACTION BASED ON CHEMICAL REACTION IN CONCRETE

Naoto Mashiko, Hiroshi Ueki
Metropolitan Expressway Public Corporation
JAPAN

Masaaki Murakami
Japan Information Processing Service Co., Ltd.

Takaharu Goto
Taiheiyo Consultant Co., Ltd.

Keywords: neutralization, carbonation, analytic model, actual structures

1. INTRODUCTION

The neutralization of concrete is one of the major causes of exfoliation of concrete. Exfoliation of concrete occurs because steel reinforcements, which do not rust in alkaline concrete, begin to rust in neutralized concrete, swell in size and push out the cover concrete. In 1996, Metropolitan Expressway Public Corporation took note of the neutralization of concrete as a measure of the life of concrete structures, and structured an analytic model by which to forecast the progress of concrete's carbonation due to the infiltration of carbon dioxide (CO_2).

Concrete's carbonation is a phenomenon in which CO_2 in the air invades concrete, diffuses through fine pores in it and dissolves in the water solution in the pores, and the dissolved CO_2 reacts with calcium hydroxide ($Ca(OH)_2$) and carbonates the concrete.

Analytic model faithfully embodies three stages of the mechanism of carbonation: (1) the stage in which CO_2 diffuses through fine pores, (2) the stage in which CO_2 dissolves in the water solution in the pores and reacts with $Ca(OH)_2$ and (3) the stage in which substances in the solution in the pores other than CO_2 and $Ca(OH)_2$ maintain a chemical equilibrium.

In fiscal 2000, we conducted an accelerated carbonation test, using a specimen prepared in a laboratory, and compared the chemical reaction of concrete in the analytic model with that of concrete in actual structures for verification. We confirmed that the analytic model could simulate the progress of carbonation with sufficient accuracy as proposed in [1]:.

In fiscal 2001, we took core specimens from actual concrete structures of the 1965-74 decade (the water-cement ratio, 41%) and ones constructed in the 1975-84 decade (the water-cement ratio, 50%), analyzed them and by using various data obtained through the analysis, and studied the applicability of analytic model to actual structures. We confirmed that the analytic model enables us to accurately forecast the progress of carbonation in actual structures. In addition, we compared the analytic model with the neutralization checking formula shown in the Standard Specifications for Design and Construction of Concrete Structures, Execution, of the Japan Society of Civil Engineers (JSCE), revised in 1999 and confirmed the usefulness of the model.

2. ANALYTICAL METHOD

This model enables one to calculate the concentration of each chemical species at each point of time and forecast the progress of carbonation by repeatedly calculating in the time direction.

START	
Step 1	Initial equilibrium
Step 2	Calculation of diffusion
Step 3	Boundary condition
Step 4	Calculation of equilibrium
FIN	

In Step 1, the equilibrium before the start of carbonation is calculated. In Step 2, the diffusion of CO_2 is calculated. In Step 3, the concentration of CO_2 in the surface of concrete is given as a boundary condition. In the dissolution of CO_2 and each chemical species, reaction occurs in an instant and the equilibrium is attained. Therefore, in Step 4, the above equilibria are calculated, and the concentration and pH degree of each substance are calculated. Calculations for the process from Step 2 to Step 4 are repeated as a time loop.

3. RESULTS OF ANALYSIS

The depth of concrete neutralization according to the JSCE formula is expressed as follows:

$$Y=\beta * (-3.57+9.0*W/C)\sqrt{t}$$

Y is the depth of concrete neutralization (mm);
t stands for the material's age (number of years);
W/C stands for the water-cement ratio;
β is the coefficient that expresses the environmental effect (dry environment; 1.6).

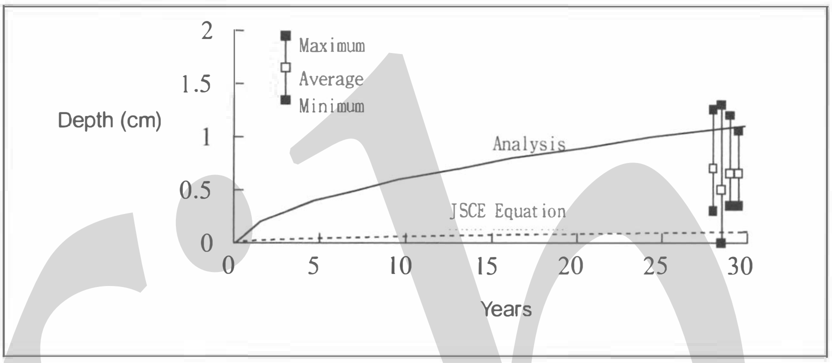

Fig. 3.1 Change in the depth of concrete neutralization in a balustrade of 41% W/C ratio

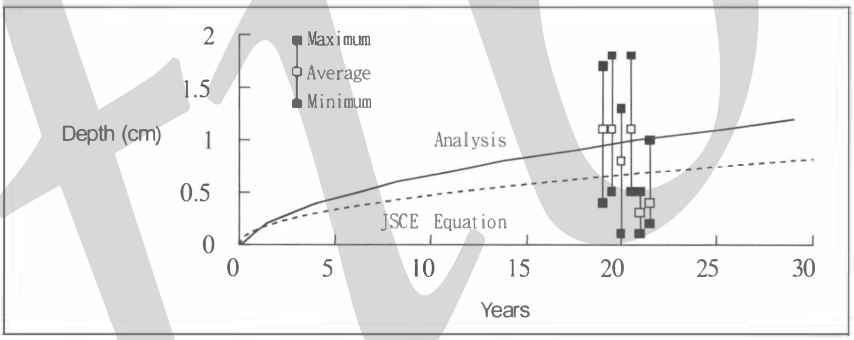

Fig. 3.2 Change in the depth of concrete neutralization in a balustrade of 50% W/C ratio

For the purpose of this report, we conducted analysis of carbonation using a diffusion coefficient and mixture obtained by analyzing cores sampled out from actual concrete structures, and examined whether it is possible to apply our model to actual structures. The results can be summarized as follows:

- The model makes it possible to express the depth of neutralization within the maximum and minimum of actually measured values.
- According to the JSCE formula, the forecast value proves lower than the actually measured value if the water/cement ratio is 40%.

We think that further investigations into actual structures are necessary, but it is possible to make the obtained results reflected in setting a proper covering depth to provide against concrete neutralization in the construction of new structures. In the case of existing structures, it is possible to forecast their residual life from the viewpoint of neutralization and use the results to prevent neutralization and contributing to their safety.

REFERENCE

[1] Konishi, Y: Research of a Simulation Model on a Carbonation Concrete. REAAA 10th Conference

ATMOSPHERIC CONCRETE DETERIORATION

ROSTISLAV DROCHYTKA
drochytka.r@fce.vutbr.cz
VÍT PETRÁNEK
petranek.v@fce.vutbr.cz
Brno University of Technology, Faculty of Civil Engineering,
Institute of Technology of Building Materials and Components.
Veveri 95, 662 37 Brno, Czech Republic

Keywords: concrete deterioration, atmospheric gases, carbonation, suplhatization

1 INTRODUCTION

The consequence of present industrial production volume is the increased air pollution. This means a negative effect not only on the environment, but even a harmful influence on building structures. The increased aggressiveness of surroundings causes failures of structures, which can significantly decrease the utility value of building structure and its durability. In the next reading the attention is paid particularly to a brief summary of present knowledge concerning the area of atmospheric concrete corrosion.

2 TYPES OF AGGRESSIVE GASES AND VAPOURS IN THE ATMOSPHERE

The next chapters discuss the chemical effects of gaseous materials, to which realistically concrete structures can be exposed. These are particularly carbon dioxide CO_2, sulphur dioxide SO_2 and sulphur trioxide SO_3 respectively, H_2S, N_xO_y.

The concentration of carbon dioxide in the atmosphere is mostly stable and it is about 60 mg CO_2 in 1 m^3 of air. In larger cities the concentration of SO_2 significantly increases, especially in winter months, because of the bad quality of brown coal combustion in local heating. The hydrogen monosulphide in gaseous form is a gas present particularly in agricultural objects and similar places. Nitrogen oxides are mostly products of road transport but we can find these compositions even in air pollution products of the chemical industry.

Water vapor similarly as carbon dioxide and other gases from the atmosphere penetrate the capillary porous materials by diffusion. The diffusion forms in materials conditions for the corrosion process. Therefore the diffusion is normally the deciding and the controlling factor of corrosion.

3 CARBONIZATION OF CONCRETE

Carbon dioxide causes in contact with cement binder formed by basic hydration products of binders a neutralization reaction normally called carbonization, because the products of this reaction are different carbonates. Decisive for the given degradation is certain moisture content. If the pores are practically full of water the concrete carbonization is significantly slower or it stops. The presence of certain moisture in concrete is the condition for the carbonization to take place, because it is an ionic reaction. The completely dry concrete doesn't react with CO_2 and other gases at all. It exists then a certain optimum or range of concrete moisture in which the carbonization of concrete will progress with highest velocity. (fig.No.1)

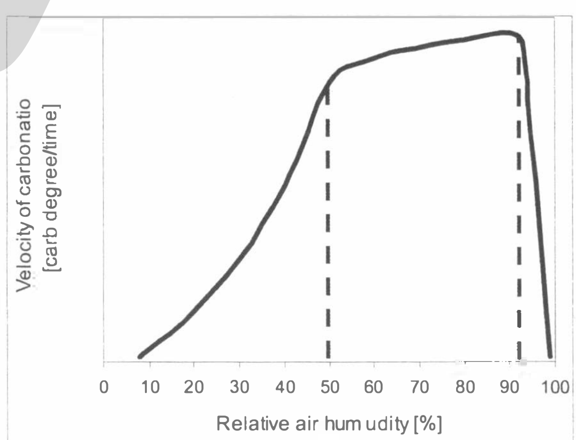

Fig. 1 Dependence of carbonization velocity of concrete upon the relative air humidity according to Prof. Matoušek, Brno UT.

Four stages of carbonization

The carbonization process was divided following our long term experience and measurements into four stages. These stages of concrete carbonization are substantial for the correct proposal of concrete structure rehabilitation.

I. Portlandite $Ca(OH)_2$ transforms in insoluble $CaCO_3$ which fills partially the pores. The main physico - mechanical parameters of concrete properties improve in this stage.

II. Carbon dioxide CO_2 attacks the other hydration products of concrete. The product of these reactions is $CaCO_3$ together with the amorphous gel of silicic acid. These components remain in a pseudo-morphous state after the hydration products of binders or as very fine-grained crystalline new formations of $CaCO_3$. The properties of concrete, do not change too much, the mechanical properties fluctuate around the original values.

III. The recrystallization of earlier formed new $CaCO_3$ formations. Numerous and relatively coarse more than ten times greater crystals of calcite and aragonite are formed. The physico-mechanical properties of concrete deteriorate. A significant decrease of pH value.

IV. The degree of carbonization oK is near 100%, coarse crystals of aragonite and mainly of calcite pervade the whole structure of cement body. In extreme case a concrete strength loss takes place. The pH value is so low that a significant corrosion of reinforcement takes place.

Table 1 Classification of concrete into stages of carbonization

Stage	Carbonization degree °C [%]	Modification change degree °MC [-]	pH [-]
I.	Less than 55	More than 0,5	12,6 –10,8
II.	55 - 73	0,5 – 0,4	10,8 – 9,6
III.	73 – 85	0,4 – 0,8	9,6 – 8,0
IV	More than 85	More than 0,8	< 8,0

4 SULPHATIZATION OF CONCRETE

The sulphatization process of SO_2 and also the synergic effect of CO_2 and SO_2 were examined experimentally. It was proved, that the moisture together with SO_2 concentration determine the quantitative and even the qualitative presence of intermediate products formed in the corroded material in different surroundings.

The samples were exposed to gaseous atmosphere containing 5, 20, 30 % of SO_2 with a relative air humidity of 45, 75, 95 % for the period of 180 days. During the corrosion the samples were tested by physico-mechanical and -physico-chemical methods (XRD, DTA, TG, SEM etc.).

The content of $Ca(OH)_2$ decreases with increasing humidity, concentration of SO_2 and time. A new phase is formed – $CaSO_3.½H_2O$, which successively is transformed in gypsum. This takes place especially with samples stored in medium with higher moisture content. A similar genesis was observed even during the formation of the second intermediate product of corrosion – $CaSO_4.½H_2O$.

The calcium carbonate in the form of calcite, vaterite or aragonite formed by primary carbonization decomposes by the influence of higher relative moisture faster than by the influence of increasing SO_2 concentration. On the contrary the content of reaction products i.e. $CaSO_3½H_2O$ or $CaSO_4.½H_2O$ but even of $CaSO_4.2H_2O$ increases the influence of progressing corrosion. In the case of higher humidity dominates gypsum, in the case of lower - calcium sulfite hemihydrate. The higher SO_2 concentration on the contrary conditions the formation of calcium sulphates (SO_4^{2-}) where the value of medium is decisive for the formation of dihydrate or hemihydrate. Interesting are the strong decreases of pH. Generally we can state that with lower concentration of SO_2, the influence of the medium is dominating but with higher concentration of SO_2 the relative humidity is no more of such importance.

More significant decrease of compression strength values take place after a longer treatment (at least 180 days) in all samples with higher relative moisture of surrounding. Here the SO_2 concentration value determines more the decrease of strength.

From realized long-term research on the Institute of Building Materials and Components the following scheme of concrete corrosion by SO_2 and CO_2 gases respectively was derived. In the sense of four stages of carbonization it is possible to formulate from the resulting information also four or five stages characterizing the concrete sulphatization.

REFERENCES

[1] Matoušek, M., Drochytka, R.: Atmosférická koroze betonů, IKAS, Praha Czech Republic, 1998

A STUDY ON THE ION DIFFUSIVITY AND DEGRADATION OF CEMENT MORTAR DUE TO CHEMICAL ATTACK

Makoto HISADA
Public Works Research Institute, Construction Technology Research Department, JAPAN
Tatsuhiko SAEKI
Dept. of Civil Engineering and Architecture, Niigata University, JAPAN
and
Shigeyoshi NAGATAKI
Research Institute for Industrial Technology, Aichi Institute of Technology, JAPAN

Keywords: ion diffusivity, chemical attack, cement hydrates, pore volume

1 INTRODUCTION

The authors tried to clarify the diffusivity of harmful ions for concrete durability, and the change of physical/chemical properties of hardened cement mortar exposed into chemically damaging conditions. In this study, $NaCl$, $CaCl_2$, HNO_3, $NaNO_3$, Na_2SO_4 and H_2SO_4 were selected as the electrolyte for making harmful solutions.

As the first discussion about the mechanisms of chemical attack, ion diffusivity of each solution in mortar specimen was discussed. Ion diffusion cells were used in these investigations.

In the second stage, for the investigation of the chemical change of mortar specimens, the cement hydrates, $Ca(OH)_2$, CSH, and AFm were quantitatively measured. Furthermore, micro pore volume and Vickers hardness were measured as the change of physical properties of mortar. Through these measurements, the relation between ion diffusivity and the change of mortar properties were discussed.

2 TEST PROCEDURES

In this study, ordinary Portland cement (density: 3.16 g/cm^3, specific surface area by Blaine: 3320 cm^2/g) was used. As fine aggregate, 3 kinds of Japanese quality-controlled silica sands (particle size: under 0.3 mm, 0.42-1.68 and 0.15-0.59 mm), were prepared for making mortar. The average density of these fine aggregates was 2.62 g/cm^3. Mixture proportion of each mortar, 0.55 of W/C and 50% of sand (by volume) was prepared in this study.

In this investigation, ion diffusion cell, which followed the migration cell system recommended in AASHTO-T227, were prepared. For the ion diffusion cell, 10mm disk specimens were used. In one side of cell, 950ml of electrolyte solution, and the other side, 950ml of de-ionized water were approximately prepared. As the electrolyte solution, $NaCl$, $CaCl_2$, HNO_3, $NaNO_3$, Na_2SO_4 and H_2SO_4 were selected. There should be noted that except the concentration of H_2SO_4 solution (prepared as 0.1 mol/L), all electrolyte solution was prepared as 1.0 mol/L since H_2SO_4 solution is quite aggressive to the deterioration of cement mortar.

As the degradation cell, 20mm disk specimens were used. The properties of concentration, volume of each electrolyte solution and exposure time were as same as ion diffusion cell.

3 MEASUREMENT

Concentration of diffused ion, the amount of calcium hydroxide ($Ca(OH)_2$, CH), calcium silicate hydrate (CSH) and mono-sulfate hydrate (AFm) were measured by using degradation cell specimens.

As the parameter for the change of physical property of hardened mortar due to the chemical attack, Vickers hardness and total pore volume of hardened mortar was measured.

4 DISCUSSION ON THE DIFFUSIVITY AND DEGRADATION OF CEMENT MORTAR

4.1 Diffusivity of ion through cement mortar

Generally, the ion diffusion through cement matrix, especially in case of 1-dimention such as diffusion cell in this study, can be explain by Fick's 1st low. However, the difference can be easily recognized in each cases from the test results.

4.2 Change of the amount of cement hydrates

The amount of $Ca(OH)_2$, CSH and AFm in mortar exposed in each electrolyte solution were discussed. In SO_4^{2-} group, the degradation of cement matrix due to both of solution can be seen in every cement hydrates. Addition, in Cl^- group, the degradation of cement matrix in every cement hydrates can be seen specially in case of $CaCl_2$ solution. Comparing to each ion group, the damage level of degradation was the smallest in Cl^-. However, it should be noted that $Ca(OH)_2$ can be degraded by exposed into NaCl solution, i.e., into sea water. Also, there should be noted that when people use $CaCl_2$ as the de-icing salt, the concrete structure will be chemically damaged.

4.3 Change of pore volume and Vickers hardness

According to the change of total pore volume and Vickers hardness of cement mortar exposed in each solution, it can be said that the physical damage of cement mortar clearly occurs in case of HNO_3 and H_2SO_4 solutions. However, in case of $NaNO_3$, Na_2SO_4,and $CaCl_2$, the change of total pore volume and Vickers hardness can not be seen so remarkably as the chemical change.

From these results, it can be concluded that the relation between the level of chemical and physical degradation of cement matrix due to harmful electrolyte solution cannot be classified from the viewpoint of ion group. More discussion must be done including the consideration of another influencing factors, such as pH or electric properties of solution.

5 DISCUSSION OF THE MECHANISMS OF DEGRADATION OF CEMENT MORTAR DUE TO CHEMICAL ATTACK

Discussing about the relation between the amount of $Ca(OH)_2$ and CSH, AFm, it can be recognized following important tendency.

1) Even when AFm is disappeared from cement matrix, $Ca(OH)_2$ still remains.
2) Even when $Ca(OH)_2$ is disappeared from cement matrix, CSH still remains.

From these tendencies, the deterioration mechanism of cement matrix due to chemical attack should be explained that AFm firstly damaged and disappeared from cement matrix, and secondary, $Ca(OH)_2$, and CSH can be remained until at final level.

6 CONCLUDING REMARKS

Through this investigation, following conclusions were mainly explained.

(1) Ion diffusivity in cement matrix is difficult to evaluate by using only diffusion phenomena, which is explained by the Fick's first low. Addition, the another factors, such as the electric condition of cement matrix, the properties of electrolyte, relation between the solution and cement hydrate, and so on, must be considered in close discussion about ion diffusivity.

(2) Diffusion co-efficient of ion must be evaluated with the consideration of source electrolyte when inspecting and designing the durability of concrete structure against the chemical attack.

(3) It should be noted that $Ca(OH)_2$ can be degraded by exposed into NaCl solution, i.e., into sea water. Also, there should be noted that when people use $CaCl_2$ as the de-icing salt, the concrete structure will be chemically damaged.

(4) As the deterioration mechanism of cement matrix due to chemical attack, it can be proposed that AFm firstly damaged and disappeared from cement matrix, and secondary, $Ca(OH)_2$, and CSH can be remained until at final level.

ROLE OF CHLORIDE IONS IN MORTARS SUBJECT TO SULFATE ATTACK

Han Young, Moon Seung Tae, Lee
Dept. of Civil Engineering,
Hanyang University, Korea

Keywords: chloride ions, sulfate resistance, expansion

1. INTRODUCTION

The co-existent presence of sulfate and chloride ions, especially, in groundwater and marine environments causes the deterioration of concrete structures due to steel corrosion and sulfate attack. Generally it was recognized that, in hardened cement matrix, the relevant phase that binds chloride ions to form Friedel' s salt, thereby causing its removal from its deleterious role of corrosion promotion, is tricalcium aluminate. However, many researchers have reported that the chloride ions in sulfate solution play a significant role in mitigating the sulfate attack.

In the present study, the effect of chloride ions on deterioration of ordinary portland cement mortar was evaluated.

2. EXPERIMENTAL PROCEDURE

2.1 Materials and test solutions

Ordinary portland cement (OPC) mortar specimens with water to cement ratio (w/c) of 0.35, 0.45 and 0.55 were prepared. Test solutions used for this experiment were 5% sodium sulfate solution and 3.5% sodium chloride solution + 5% sodium sulfate solution.

2.2 Test Techniques

According to ASTM C 39, 50 mm cube specimens for compressive strength were measured as using a compression testing machine. The SDF, which is expressed as compressive strength loss of cubic mortar specimens, was determined using the following equation.

$$SDF\ (\%) = (Sw - Ss) / Sw \times 100$$

P_W : the compressive strength of mortar cured in pure water
P_S : the compressive strength of mortar immersed in chloride-sulfate or sulfate solution

Expansion measurements of prism mortar specimens, 25×25×285 mm size, were performed according to ASTM C 1012 and measured on three mortar specimens withdrawn from test solutions. The average value was adopted.

3. RESULTS AND DISCUSSION

3.1 Sulfate deterioration factor and expansion due to sulfate attack

Fig. 1 remarkably indicates the beneficial effect of chloride ions in mortar specimens exposed sulfate solution. In other words, in case of mortar specimens with 0.45 w/c in chloride-sulfate solution at 270 days, the SDF value was approximately 1.4% compared to 26.2% of value in sulfate solution. The expansion of mortar specimens with w/c of 0.45 was 0.51% and the specimens were destroyed due to excessive expansion after 210 days of immersion period, compared with an expansion of 0.05% displayed by mortar specimens in sulfate-chloride solution as shown in Fig. 2. As a related study, the work carried out by Ogawa was reported that the formation of expansive sulfoaluminate hydrate is reduced in the presence of chloride ions. Chloride ions enter the structure of monosulfo- aluminate hydrate replacing sulfate ions, and also modifying the morphology of the ettringite, relatively non-expansive crystals instead of the usual elongated ones. In other words, Chloride ions responsible for steel corrosion in concrete have a positive effect to lessen the expansion as well as the strength loss with respect to sulfate deterioration.

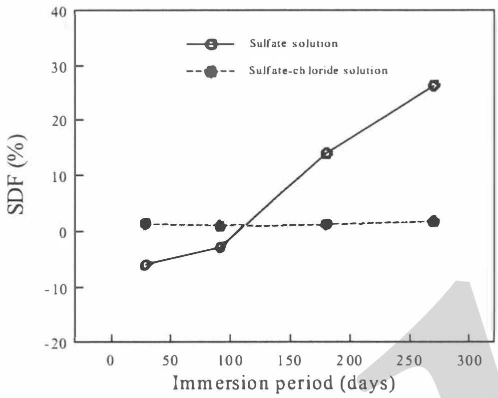

Fig. 1 SDF vs. immersion period (w/c=0.45)

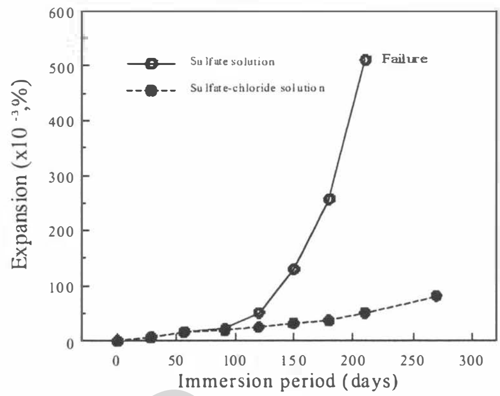

Fig. 2 The expansion of mortar (w/c=0.45)

3.2 XRD analysis

The x-ray diffractograms for the powder of OPC paste samples (w/c = 0.45) drawn from sodium sulfate solutions and chloride-sulfate solution are presented in Fig. 3 and 4, respectively. The importance of the observation from these diffractograms was the somewhat large intensity peaks for portlandite of paste sample immersed in a sodium sulfate solution, compared with those in a sulfate-chloride. As expected, due to reaction of chloride ions, the peaks for calcium chloro-aluminate hydrate (Friedel's salt) in paste immersed in sulfate-chloride solution were investigated.

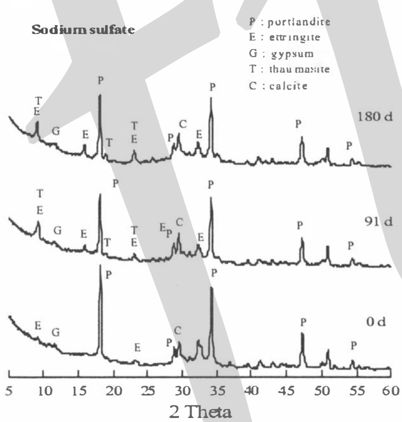

Fig. 3 XRD analysis of paste immersed in sulfate solution

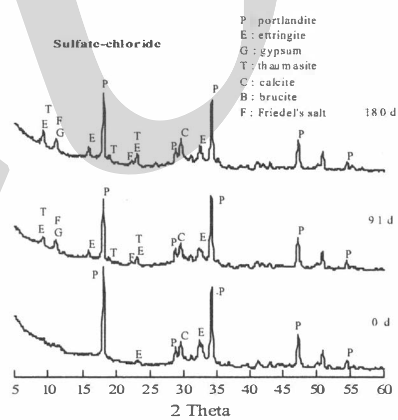

Fig. 4 XRD analysis of paste immersed in sulfate-chloride solution

REFERENCES

[1] Ogawa K. and Roy D.M., : C_4A_3S Hydration, Ettringite Formation, and its Expansion Mechanism; III. Effect of CaO, NaOH and NaCl; Conclusions, Cement and Concrete Research, Vol.12, No.2, pp.280-287, 1982.

[2] Al-Amoudi O.S.B., Rasheeduzzafar, M. Maslehuddin and Abduljauwad S.N., : Influence of Chloride Ions on Sulfate Deterioration in Plain and Blended Cements, Magazine of Concrete Research, Vol.46, No.167, pp.113-123, 1994.

A STUDY ON THE HIGH STRENGTH CONCRETE WITH GROUND GRANULATED BLAST-FURNACE SLAG AGAINST ICE-MELTING ADDITIVES

Yasuhiro Dan
Nippon Steel Blast-fumace Slag Cement co.,ltd, JAPAN

Yasukazu Yoshitomi
Abe Kogyosho co.,ltd, JAPAN

Kazuo Kobayashi
Osaka Institute of Technology, JAPAN

Yujiro Wasa
Abe Kogyosho co.,ltd, JAPAN

Keywords: ice-melting additives, ground granulated blast-fumace slag, high strength concrete, surface deterioration, freeze-thaw resistance

1. INTRODUCTION

In this study, chemical erosion and freeze-thaw resistance were examined especially in the case of factory-made high-strength concrete using three main ice-melting additives: sodium chloride, calcium chloride and calcium magnesium acetate.

2. OUTLINE OF EXPERIMENT

Because the experiment is conducted on high-strength concrete, high-early-strength portland cement (H) was used as cement and ground granulated blast-fumace slag (BFS) with a specific surface area in the range of 6000 cm^2/ g was used The replacement ratios of ground granulated blast-fumace slag was chosen as 50% (BFS50) and 70% (BFS70). The design compressive strength of concrete was 50 N/ mm^2.at 28 days .

For the curing of concrete, steam curing of factory-made products was conducted as a standard, and the experiment was carried out partly also for standard curing. (Steam curing condition :precured at 20 ℃ for 3 h, raised to 55 ℃ in 3 h and held for 6 h)

Three types of ice-melting additive of sodium chloride (NaCl), calcium chloride ($CaCl_2$) and calcium magnesium acetate (CaMg $(CH_3COO)_4$) were used, and as the concentrations of the solution for immersion test of concrete specimens, 10%, 20% and 30% were used at which surface deterioration is considered to occur early.

3. EXPERIMENT RESULTS AND DISCUSSION

3.1 Appearance Observation

In test specimens immersed in a $CaCl_2$ solution, in the case of use of H alone, surface mortar spalled off and a coarse aggregate was exposed. However, in the case of mixing of BFS, deterioration was scarcely observed. In a CaMg (CH_3COO)$_4$ solution, scaling and white precipitates(magnesium hydroxide) were observed in the case of use of H alone, while in the case of mixing of BFS scaling did not occur and white precipitates were scattered about.

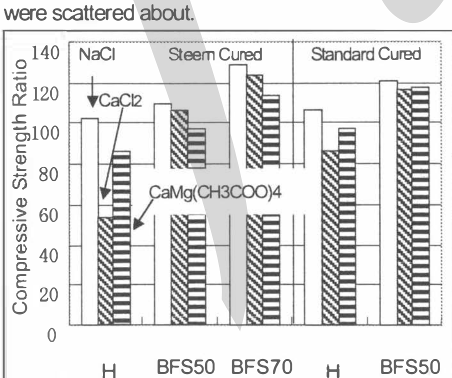

Fig.1 Compressive Strength ratio to value before immersion

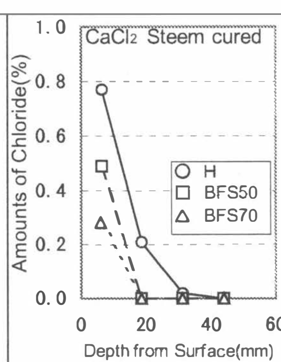

Fig.2 Amount of infiltrated chloride

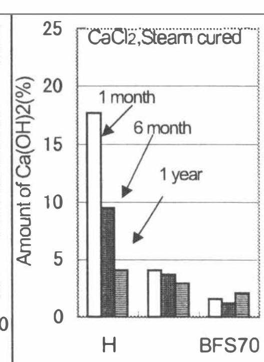

Fig.3 Amount of Ca(OH)2

3.2 Compressive Strength

Fig.1 shows the ratio of the compressive strength after 1 year immersion to the compressive strength before immersion. (The compressive strength before immersion in the case of steam curing was 66.4 N/ mm^2 for H, 61.5 N/ mm^2 for BFS50 and 58.6 N/ mm^2 for BFS70, in the case of standard curing was 64.2 N/ mm^2 for H and 61.8 N/ mm^2 for BFS50.) In the case with BFS, after both steam curing and standard curing, compressive strength tends to be equal to values before immersion or a little larger than them. Thus it was also ascertained that deterioration is not apt to occur.

3.3 Infiltration of Cloride

Fig.2 shows the amounts of infiltrated chloride concrete after 1 year immersion in a $CaCl_2$ solution in the case of steam curing.As is already known, in the case with BFS, chloride concentrate on the surfaces of test specimens and do not infiltrate into the interior, whereas in the case with H alone chloride infiltrate into the interior of the test specimens.

3.4 Stucture of Hardened Cement and Hydrate

In the case with BFS, the average pore size is small and this seems to be a factor responsible for the suppression of deterioration due to ice-melting additives. Fig. 3 shows the result of a differential thermal analysis of $Ca(OH)_2$ in a $CaCl_2$ solution.In the case with H alone in a $CaCl_2$ solution and a CaMg $(CH_3COO)_4$ solution where the deterioration of the surfaces of the test specimens proceeds greatly, the amount of $Ca(OH)_2$ decreases greatly with increasing immersion period and this seems to be a great factor responsible for surface deterioration.

In the case with BFS, the amount of $Ca(OH)_2$ before immersion is small and changes with an increase in immersion period are also small.

3.5 Freeze-Thaw

Test specimens were immersed in ice-melting additives solutions and water until the 28th day age after form removal and a freeze-thaw repetition test was conducted on these test specimens. The result of measurement of the relative dynamic elastic modulus is shown in Fig. 4.

In products whose entrained air content is adjusted in the case with BFS, the durability index is 100 or so even after immersion in either solution and freeze-thaw resistance was sufficient. It seems that the improvement in freeze-thaw resistance is closely related to the denseness of the structure of hardened concrete.

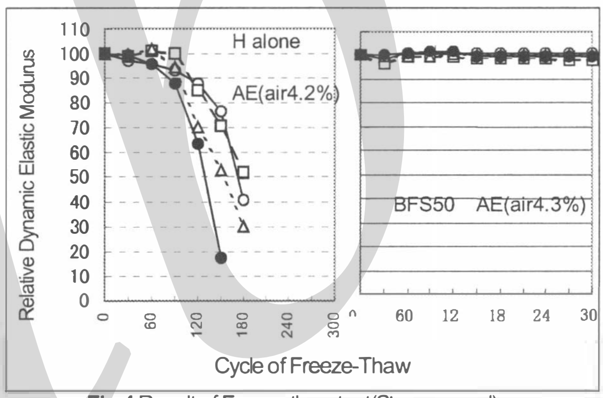

Fig.4 Result of Freeze-thaw test(Steam cured)

4. SUMMARY

As a result of this experiment, the following were ascertained:

(1) When ground granulated blast-furnace slag is mixed, surface deterioration was not observed after 1 year immersion in any ice-melting additive solution.

(2) The deterioration by ice-melting additives is due to the denseness of the structure of hardened concrete and the decomposition of calcium hydroxide by ice-melting additives.

(3) A freeze-thaw test was conducted after immersion of specimens in a ice-melting additive solution. Test specimens immersed in a ice-melting additive solution tend to be a little inferior in freezing-thaw resistance.

(4) Freeze-thaw resistance is higher in the case mixing ground granulated blast-furnace slag than in the case using high-early-strength portland cement alone.

(5) Satisfactory freeze-thaw resistance can be attained by introducing about 4% of entrained air in the case with ground granulated blast-furnace slag.

SOLIDIFIED CEMENTITIOUS MATERIAL-STRUCTURE MODEL WITH COUPLED HEAT AND MOISTURE TRANSPORT UNDER ARBITRARY AMBIENT CONDITIONS

Tetsuya ISHIDA Koichi MAEKAWA
Department of Civil Engineering, University of Tokyo, JAPAN

Keywords: moisture transport, thermodynamics, creep, shrinkage

1 INTRODUCTION

Moisture transport processes in cementitious materials and related mechanical behaviors, such as creep and shrinkage, are strongly dependent on temperature inside pores. In order to evaluate material and structural behaviors under arbitrary temperature conditions, it is essential to establish a model that can deal with thermodynamic aspects based on a microphysical approach.

2 NUMERICAL MODELING BASED ON STRONG COUPLING OF MOISTURE AND HEAT TRANSPORT

The mass balance equation for vapor and liquid water in a porous medium can be expressed as

$$\frac{\partial S(P_l)}{\partial t} + div\left(\mathbf{J}(P_l, \nabla P_l, \nabla T)\right) + Q = 0 \tag{1}$$

where, P_l: liquid pore pressure, T: temperature, S: potential term, J: flux term, and Q: sink term involving water consumption due to hydration reaction and bulk porosity change effects [1]. The equilibrium state of moisture is described by applying principal thermodynamic theories, such as, Gibbs energy balance and the Clausius-Clapeyron equation, to the moisture existing in pore structures. Regarding moisture transport, both vapor and liquid are taken into account, and temperature, vapor density, and pore pressure differences are specified as their driving forces.

3 NUMERICAL SIMULATIONS

The formulations proposed in this study were implemented into the finite-element computational program DuCOM [1]. The constituent material models are based on microphysical phenomena such as hydration, moisture transport, and the formation of pore-structure, and they take into account the inter-relationships between these in a natural way. Moisture behaviors under the gradient of temperature as well as moisture gradient were simulated. In the analysis, 60%RH and temperature of 20 °C were given as boundary conditions, whereas the deepest nodes (5cm from the exposure surface) in the mesh were specified as restrained in terms of temperature. A constant temperature of 80 °C was given to these nodes. Figure 1 shows the moisture distribution inside concrete after 2 days and 16 days drying. After 16 days drying, the amount of water at the middle of the specimen (portion at 1.5 ~ 2.5cm from the surface) shows a peak value. The analytical result means that the vapor coming from the center at 80 degrees Celsius becomes liquid phase again at the middle section where temperature is low enough to condense vapor into liquid water.

It is well known that creep, shrinkage, and their coupling behaviors show strong dependency on moisture condition, temperature, pore structure, and hydration process of concrete. The authors have been developing an integrated computational system for thermo-physics and structural mechanics, which can deal with time-dependent behavior of young aged concrete as well as mechanical behavior of hardened concrete, such as deformation, ductility, fracture, and cracking [2][3]. A sensitivity simulation was carried out to demonstrate the influence of temperature on the mechanical behavior of concrete. The specimens analyzed here are cylindrical specimens of radius 10cm and height 20cm. After 1 days of sealed curing, the specimens were subjected to both loading and drying (80%RH). The loading stress was 10 MPa, and a number of unloading-loading cycles was applied. The results of time-dependent mechanical behaviors under different temperature are shown in Fig.2. It can be seen that the behaviors of the specimens are strongly affected by ambient temperature. In this analysis, no intentional parameters to represent temperature effect are used. The specimen exposed to the temperature of 65°C shows larger deformation with time, reflecting temperature-dependent moisture profile, hydration,

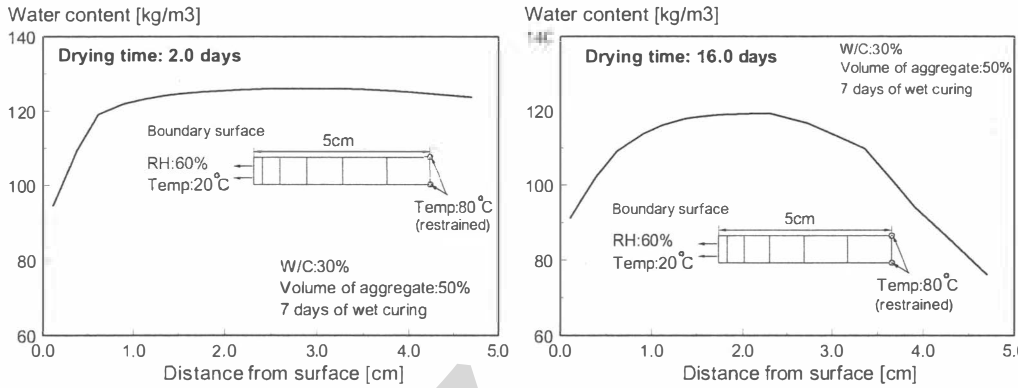

Fig.1 Moisture distribution under temperature gradient

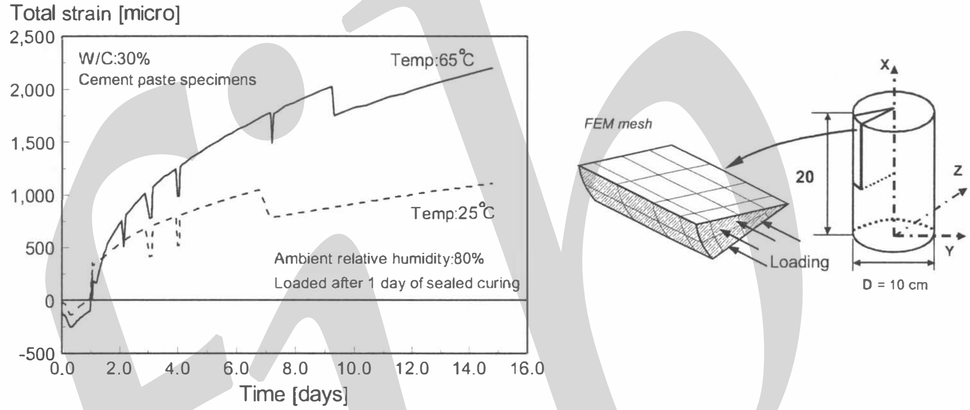

Fig.2 Time-dependent mechanical behaviors of specimens subjected to both drying and loading under different ambient temperatures

and micro-structure formation. In the model, visco-elastic and visco-plastic deformations are described by the viscosity of liquid water, moisture distribution, and microstructure profiles. Moreover, capillary stress generated by drying and self-desiccation is taken into account as the driving force for the deformation of cement paste as well as applied external forces. Analytical results implicitly involve these influential factors on mechanical behaviors of concrete, once initial and boundary conditions are given to the system.

4 CONCLUSIONS

In this study, a strong coupling system of moisture equilibrium/transport and heat energy is proposed. The mass balance equation, moisture capacity, and permeability, which highly depend on temperature, were formulated based on thermodynamic theory. By these modeling, it becomes possible to predict the moisture transport driven by temperature gradient as well as the pore pressure in a natural way. Furthermore, by combining the proposed thermodynamic model with solidification model of hardening concrete, it was shown that the system can reasonably simulate temperature-dependent mechanical behaviors.

REFERENCES

[1] Maekawa, K., Kishi, T., and Chaube, R.P.: Modelling of concrete performance, E&FN SPON, 1999.
[2] Ishida, T. and Maekawa, K.: An integrated computational system for mass/energy generation, transport, and mechanics of materials and structures, Concrete Library of JSCE, No.36, pp.129-144.
[3] Mabrouk, R.T., Ishida, T., and Maekawa, K.: A unified solidification model of hardening concrete composite, Proceedings of International Workshop on Control of Cracking in Early Age Concrete, Sendai, 2000.

ESTIMATION OF CA-LEACHING DETERIORATION OF CONCRETE WITH DIFFERENT WATER-CEMENT RATIO USING NUMERICAL ANALYSIS METHOD

Nobuaki Otsuki[1)], Hiroshi Minagawa[1)], Shinichi Miyazato[2)], Bouavieng Champaphanh[1)]
1): Tokyo Institute of Technology, Japan, 2): Kanazawa Institute of Technology, Japan

Keywords: Ca-leaching, Nernst-Plank equation, solid-liquid equilibrium, water-cement ratio

1. INTRODUCTION

As the calcium hydrate contained in concrete dissolves into water around the concrete structure, the concrete becomes porous. This type of deterioration is known as "Ca (Calcium) leaching deterioration". In the design of the special concrete structures that remain in contact with water for over 100 years, this type of deterioration must be estimated. The purposes of this study are (1) to establish a prediction method for Ca-leaching deterioration using numerical analysis method, (2) to verify the validity of the prediction method, and (3) to estimate the relationship between Ca-leaching deterioration and different water-cement ratio.

2. THE SUMMARY OF THE PREDICTION METHOD

2.1 Fundamental theory

The prediction method consists of an ion migration equation and a model of Ca-leaching from cement paste to pore solution. Equation (1) considering Nernst-Plank equation, Debye-Hückel equation, and Electro-neutrality condition is used for the ion migration equation.

$$J_{ion} = -k \cdot T \cdot B_{ion} \cdot \left(1 + \ln 10 \times C_{ion} \times \frac{-0.51 \cdot Z_{ion}^2}{2 \cdot \sqrt{I} \cdot \left(1+\sqrt{I}\right)^2}\right) \cdot \frac{\partial C_{ion}}{\partial x} - k \cdot T \cdot Z_{ion} \cdot B_{ion} \cdot C_{ion} \cdot \frac{\sum_i \left(Z_i \cdot \left(1 + \frac{\partial \ln \gamma_i}{\partial \ln C_i}\right) \cdot B_i \cdot \frac{\partial C_i}{\partial x}\right)}{\sum_i \left(Z_i^2 \cdot B_i \cdot C_i\right)} \quad (1)$$

where, i is ionic species, J is flux (mol/cm^2/sec), k is Boltzman number (=1.38$\times 10^{-23}$J/K), T is temperature (K), B is absolute mobility (cm/sec/dyne), C is concentration of ion (mol/cm^3), I is ionic strength (mol/l), x is distance from exposure surface (cm), e is elementary electric charge (=1.60$\times 10^{-19}$C), Z is ionic charge number.

Incidentally, it is not appropriate to adopt the absolute mobility in the dilute solution as an ion migration index of concrete when equation (1) is applied to concrete. Therefore, the apparent absolute mobility B_i shown in equation (2) is used as an ion migration index of concrete.

$$B_i = \frac{\varepsilon}{\tau^2} \cdot B_{0,i} \quad (2)$$

where, ε is pore ratio (cm^3/cm^3), τ is trotuosity factor(=$\sqrt{2}$), B_0 is absolute mobility in dilute solution (cm^2/sec/dyne).

The pore ratio increases with Ca-leaching. In this study, it is assumed that the porosity created by leaching a given quantity of calcium hydroxide is equal to the volume of the same quantity of $Ca(OH)_2$ crystal (C-H). Thus, the dependence of pore ratio on Ca-leaching is evaluated by equation (3):

$$\varepsilon = \varepsilon_0 + \frac{M_{CH}}{d_{CH}} \cdot \left(C_{c0} - C_c\right) \quad (3)$$

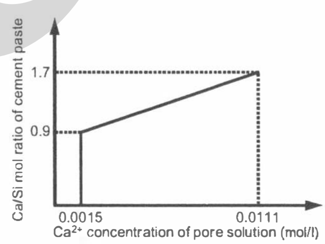

Fig. 1 Liquid-solid equilibrium model

where, ε_0 is initial pore ratio (cm^3/cm^3), M_{CH} is molecular weight of C-H (=74 g/mol), d_{CH} is density of C-H (=2.23 g/cm^3), C_{C0} is initial concentration of Ca of solid phase in unit concrete volume (mol/cm3), C_C is concentration of Ca of solid phase in unit concrete volume (mol/cm3).

In order to predict Ca-leaching deterioration, it is necessary to model Ca-leaching from cement paste to pore solution. In this study, it is assumed that (i) the calcium hydrates in cement paste are C-H and C-S-H only, (ii) Ca-leaching from C-S-H occurs after C-H dissolves perfectly, (iii) Ca-leaching from C-H depends on chemical equilibrium given by equation (4), (5) and (6).

$$C_{H^+} \cdot C_{OH^-} = K_w \quad (4), \qquad C_{Ca^{2+}} \cdot C_{OH^-}^2 = K_{sp} \quad (5), \qquad \sum_i Z_i \cdot C_i = 0 \quad (6)$$

where, K_w is the ion product of water (mol^2/l^2), K_{sp} is the solubility constant of C-H (mol^3/l^3). Moreover, Ca-leaching from C-S-H is modeled as shown in **Fig. 1** that follows an previous study [2].

2.2 Method of analysis

The one-dimensional finite difference method was adopted in this study. The boundary condition, which is the ion concentrations of the outside water, is assumed to be equal to C_{ion}=0. The initial values of concrete are (i) pore ratio, (ii) ion concentration in pore solution, and (iii) concentration of C-H, C-S-H, and Si in solid phase per unit concrete volume. The initial values of (i) and (ii) are determined by the experimental results. Also, the initial value of (iii) is determined using a model of the hydration reaction [3].

3. CONFIRMATION OF THE VALIDITY

In order to confirm the validity of the prediction method, the prediction results after 100 years are compared with the results of a survey of the existing member that had been in contact with water for about 100 years [4]. **Fig. 2** and **Fig. 3** show the relationships between the prediction and the survey. From this figure, it is obvious that the prediction correspond with the survey.

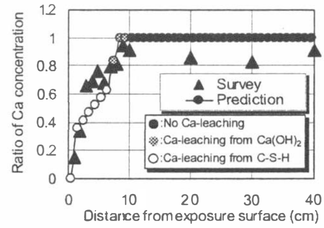

Fig. 2 Relationship between the prediction and the survey about ratio of Ca concentration ($=C_c/C_{c0}$)

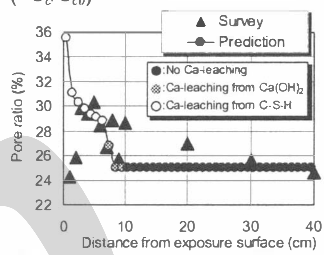

Fig. 3 Relationship between the prediction and the survey about pore ratio

4. Estimation of Ca-leaching Deterioration with Different Water-Cement Ratio

The relationship between Ca-leaching deterioration and different water-cement ratio is estimated using the prediction method. The mix proportion is W/C=40, 50, 65% and unit aggregate content is equal to 1400 kg/m^3 in each water cement ratio.

Fig. 4 shows the estimated result on the pore ratio. **Fig. 4** shows that Ca-leaching progress is fast as water-cement ratio increases. This is because the Ca^{2+} flux increases as water-cement ratio increases. The concrete of high water-cement ratio is so porous that it is easy for Ca^{2+} to migrate. In addition, it is shown that the pore ratio after Ca-leaching in the deep region depends on the initial pore ratio. However, there is not a difference between the pore ratios of each water cement ratio near the exposure surface too much in comparison with the deep region. Amount of increase of pore volume in the region where Ca perfectly dissolves from cement paste is high in case of low water-cement ratio. This is because the pore ratio after Ca perfectly dissolves depends on the volume of the cement paste in unit concrete volume. Since the volume of cement paste in unit concrete volume increases as water-cement ratio is lower, this result is obtained.

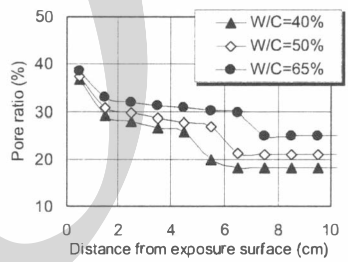

Fig. 4 Relationship between water-cement ratio and estimation about pore ratio

7. CONCLUSIONS

(1) A prediction method for estimating the Ca-leaching deterioration was constructed. Also, the validity of the prediction method was confirmed comparing the prediction and the survey of the existing member.

(2) From a predicted result, it is shown that Ca-leaching progress is fast as water-cement ratio increases. Also, the pore ratio after Ca-leaching in the deep region depends on the initial pore ratio. However, there is not a large difference between the pore ratios of each water cement ratio near the exposure surface where Ca perfectly dissolves.

REFERENCES

[1] Berner, U.: A Thermodynamic Description of the Evolution of Pore Water Chemistry and Uranium Speciation during the Degradation of Cement, PSI-Bericht Nr.62, 1990

[2] A. S. Soejono, H. Seki : The Evaluation of the hydration organization and the porosity in concrete using the hydration reaction model, Proceedings of Japan Concrete Institute, Vol. 21, No. 2, pp. 19-24, 1999. (in Japanese)

[3] Y. Yokozeki, Y, Furusawa, K. Watanabe, K. Koseki, M. Daimon, N. Otsuki, M. Hisada : Numerical Modeling for Predicting the Degradation of Cement-based Materials due to Calcium Leaching, RILEM/CIB/ISO International Symposium on Integrated Life-Cycle Design of Materials and Structures ILCDES 2000, 2000

STUDY ON WATER-PROOF-LAYER FOR REINFORCED CONCRETE SLABS IN ROAD BRIDGES

Kenji NOMURA
The University of Tokyo, JAPAN

Taketo UOMOTO
Industrial Institute of Science
The University of Tokyo, JAPAN

Keywords: water-proof-layer, asphalt concrete, rutting, density, freezing and thawing

1 INTRODUCTION

Several factors such as drainage pavement, excessive use of de-icing salts, adoption of revised prestressed concrete design methods that allow cracking in concrete, increased heavier vehicles, have possibly contributed to premature deterioration of RC slabs in road bridges in Japan. Though using a water-proof-layer between the concrete slab and the asphalt pavement is considered one of the ways of protecting the underlying concrete from water ingress (and hence, reinforcement corrosion, etc.), there is very little experimental evidence to establish the efficiency of such a treatment. To better understand the function of the waterproofing layer, experiments were carried out in the laboratory using specimens with and without waterproof layer. In this paper, the results obtained from the aggregate movement during compaction of the asphalt layer, density measurements and rutting of the asphalt layer, and the performance after cyclic exposure to freezing and thawing are reported.

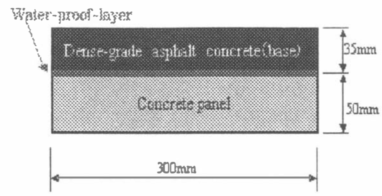

Fig,1 Specimen

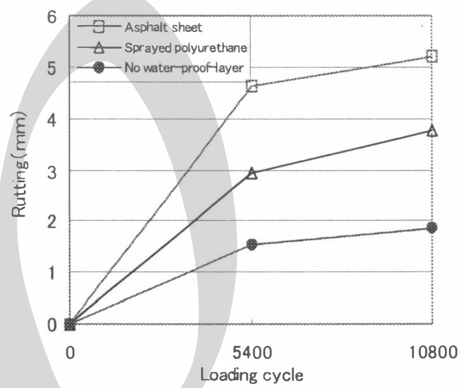

Fig.2 Rutting of asphalt concrete

2 RUTTING OF ASPHALT CONCRETE

Cyclic loading tests were carried out for cyclic loading arrangement using a wheel tracking-testing machine. The tests were carried out in a chamber whose temperature was maintained at 60°C. The tire used was 50mm wide and had a weight of 686N, to ensure a pressure (to the asphalt surface) at 0.6272N/mm^2, which may be classified as 'heavy traffic'. The tests were run for 10800 cycles over a 6-hour period. Observations for the depth of rutting in the asphalt concrete surface were made at the end of 5400 and 10800 cycles.

As the result, it was found out that the rutting of asphalt concrete with water-proof-layer was larger than the one without water-proof-layer as shown in **Fig.2**.

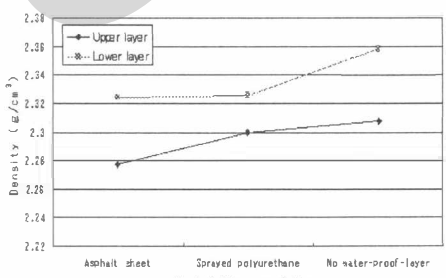

Fig.3 Density of asphalt concrete

3 DENSITY TEST OF ASPHALT CONCRETE

The asphalt concrete of each specimen was divided into 4 parts in the plane view, and into 2 parts in the elevation, namely upper layer and lower layer. **Table1** shows mix proportion of asphalt concrete.

Table1 Mix proportion of asphalt concrete (weight%)

Modified Asphalt Type II	Single-sized crushed stones S-13(grade 6)	Single-sized crushed stones S-5(grade 7)	Coarse sand	Fine sand	Filler
5.8% (1.030)	35.8% (2.705)	20.1% (2.641)	23.4% (2.627)	9.8% (2.613)	5.1% (2.700)

( ) :Specific gravity

As the result of applied loading, it can be seen that (a) density of the upper layer is lower than that of the lower layer, and, (b) the density of the asphalt concrete in both layers is highest in the case when no water-proof-layer is used as shown in **Fig.3**.

4 OBSERVATION OF MOTION OF AGGREGATE PARTICLES IN ASPHALT CONCRETE

In order to compare the differences of behaviors of asphalt concrete in the case with and without water-proof-layer under compaction-work, the photographs of aggregate particles in asphalt concrete were taken against the situations of asphalt concrete under compaction-work by roller compacter. They were taken before compaction, after 13th and 26th cycle of compaction. Particle Tracking Velocimetry[1] was used in this photo-analysis. The movement of particles at the intersection points in the mesh considered was expressed as vectors.

Fig.4 to **Fig.5** shows the result of displacement vectors of aggregate particles in asphalt concrete between 13th and 26th cycle. **Fig.4** shows the case with sprayed polyurethane under the asphalt concrete. In this case, the amount of movement at Y-direction was relatively large despite the second half of the compaction. **Fig.5** shows in the case without water-proof-layer under the asphalt concrete. In this case, the amount of movement at Y-direction was small. It seemed that the aggregate-particles were dispersed at X-direction symmetrically. It was considered that the compaction force was transferred uniformly from roller compactor to the asphalt concrete.

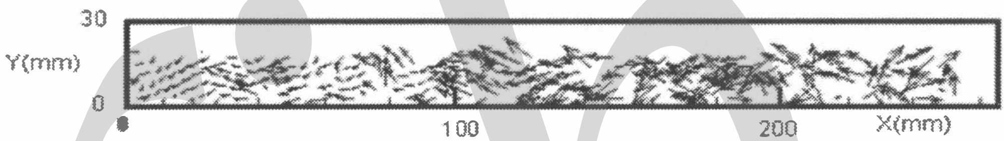

Fig.4 The case with sprayed polyurethane

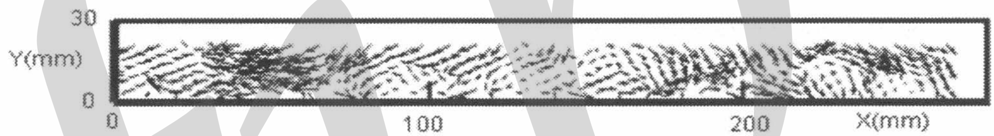

Fig.5 The case without water-proof-layer

5 FREEZING AND THAWING TEST

Freezing and thawing test on the asphalt concrete surface was done because there were a lot of instances where de-icing agents were used in road bridges.

The result of freezing and thawing test shows cracks occurring on the surface of asphalt concrete when water-proof-layer is used as shown in **Fig.6**.

6 CONCLUSIONS

The conclusions in this study were as follows.

1) The rutting of asphalt concrete due to tire loading in the case of water-proof-layer was larger than the case without water-proof-layer.
2) The density of asphalt concrete in the case of water-proof-layer becomes smaller than the case without water-proof-layer.
3) There are differences of aggregates' behavior in the cases with and without water-proof-layer under the compaction work.
4) The resistance of freezing and thawing of asphalt concrete in the case with water–proof -layer was smaller than the case without water-proof-layer.

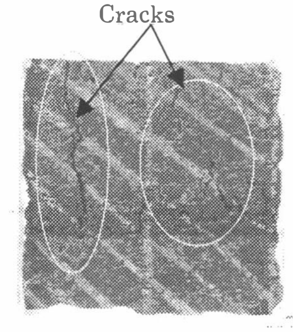

Fig.6 Surface condition in the case of water-proof-layer

REFERENCES

1.Tetsuo Saga et al:Development and evaluation on the correlation based PTV method, Saitama Univ. March 2000, JSME, pp171-172

A STUDY OF HIGH PERFORMANCE GROUT FOR POST-TENSIONED STRUCTURES

Chengning WU, Akira Okuma
Oriental Construction Co., Ltd., Japan

Masaki ISHIMORI, Hiroshi HAYASHI
Taiheiyo Cement Co., Ltd., Japan

Keywords: high performance grout, high fluidity, non-bleed, low permeability, high strength

1. INTRODUCTION

Cementitious grout is injected into ducts of post-tensioned structures to prevent the corrosion of tendon and also bond the tendon to the concrete. So, the grout is very important to the post-tensioned structures because it determines the durability and the mechanical properties of the structures.

The effect of the grout on the structure depends on the properties of the grout, such as fluidity, pumpability, bleeding, volume change, permeability and strength. In order to ensure the durability and mechanical properties of the structures, some new type cementitious grouts, those that have the properties of non-bleeding and normal fluidity or low fluidity have been developed in the United States of America and Japan [1][2]. However, grout with high fluidity is required to be injected into the ducts in the space between the sheath and the tendon, however this is too narrow to be injected with normal or low fluidity grout. The grout has to have not only a high fluidity, but also pumpability, non-bleeding, low volume change, low permeability and high strength. This grout is named high performance grout (HPG).

In order to develop HPG, it is necessary to investigate the effects of the materials on the properties of the grout. In this study, the effects of cements, superplasticizers and mineral admixtures on the properties of grout are researched. As the results, a pre-mixed HPG is developed. This paper reports the mix proportion and properties of HPG.

2. RESULTS AND DISCUSSION

2.1 Selection of materials for HPG

It is considered that types of materials used in grout can affect the properties of the grout greatly. Therefore, the selection of materials is very important to develop HPG. In this study, the selection is of the three main materials used in grout, which are cement, superplasticizer and mineral admixture are carried out.

A corroding to the results of the test, it is clear that grout made with low-heat portland cement has a higher fluidity than that of grout made with normal portland cement. And the fluidity loss of the grout in the low-heat portland cement with time is less than that of the NPC grout.

Polycarboxylic type superplasticizer gives grout a higher fluidity and the fluidity of the grout can be maintained for more than 90 minutes. It is evident that the polycarboxylic type superplasticizer is better than the naphthalene sulfonate type superplasticizer for producing HPG.

Because silica fume has a very huge specific surface area, it can be used instead of polymer anti-bleeding admixture to reduce bleeding of grout. The grout admixed with silica fume has higher resistance to bleeding under pressure than normal non-bleeding grout. The fluidity of the grout doesn't change with temperatures.

2.2 Composition of high performance grout

A according to above the studies, low-heat portland cement, polycarboxylic type super-plasticizer, silica fume and some other materials can be used to produce HPG. The composition of HPG is shown in Table 1. All the materials are pre-mixed and pre-packaged in the factory to insure the quality of the grout. On site, only mixing water is weighed and the water to powder (W/P) of the grout can be adjusted from 24% to 31% to get required fluidity. These W/P ratios are much lower than 45% that is used in normal grout (NG).

Table 1 Composition of high performance grout

Material	Content (wt%)
Low-heat portland cement	79%-94%
Polycarboxylic type superplasticizer	0.05%-0.30%
Silica fume	5%-15%
Lime type expansion-causing admixture	1%-6%

2.3 Properties of HPG

(1) Fluidity and pumpability

In this study, fluidity of HPG is measured with JP flow cone. The results of the test are shown in Fig. 1. The efflux time of HPG with W/P of 31% is approximate 3 seconds, which is shorter than that of NG (usually more than 4 seconds). It means that the fluidity of the HPG is much higher than that of NG.

The change in fluidity of the HPG with temperatures and time is so slight that it can be ignored, which means that it has excellent pumpability.

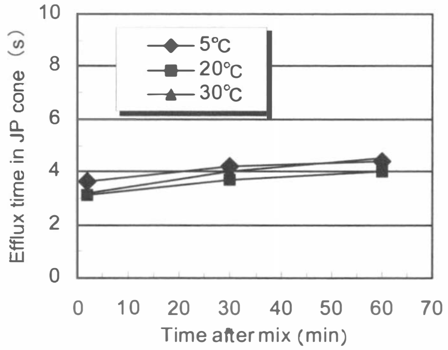

Fig. 1 Fluidity of high performance grout

(2) Setting time

The initial setting time of the HPG is 6.5 hours and its final setting time is 7.7 hours, which are approximate 4.5 hours shorter than those of the NG. There are not any standards to the setting time of grout in Japan now. But it is believed that the shorter setting time of HPG will not become a problem for injecting work because the fluidity can be maintained for more than one hour.

(3) Resistance to bleeding

In Japan, the bleeding test is a non-pressure test. However, sometimes the grout in the duct is under pressure, especially in vertical ducts. In these cases, the non-bleeding type grout measured under non-pressure tests may bleed. In order to investigate the bleeding behaviors of HPG under pressure, a pressure-bleeding test was carried out in this study. The pressure used was 0.5MPa and was equivalent to the pressure that occurs in a duct that has 25m vertical rise. The result of the test is shown in Fig. 2. According to the figure, it can be shown that the pressured bleed of HPG is much less than that of NG.

(4) Compressive strength

The compressive strength of HPG at age of 28 days is higher than 90 N/mm^2. So, HPG suits not only common prestressed concrete structures but also the prestressed concrete structures where high strength concrete is used.

(5) Volume Change

In this study, a lime type expansion-causing admixture is used instead of the gas-forming agent to improve the volume stability of grout. The expansion rates of HPG are from 0.07% to -0.07%. And these expansion rates satisfy both the specifications of JPCCA and JSCE.

(6) Permeability

Permeability of grout is measured by the rapid chloride permeability test (ASTM C1202). The ability of HPG to resist the penetration of chloride ions is much higher than that in NG because the values of charge passed in HPG is only one fourteenth that of NG. It is believed that the use of silica fume and low W/P contribute to make HPG have high resistant to penetration of chloride ions.

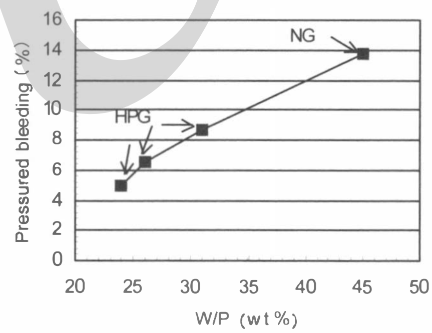

Fig. 2 Pressured bleed of HPG and NG

3. SUMMARY AND CONCLUSION

HPG produced with low-heat portland cement, polycarboxylic type superplasticizer, silica fume and lime type expansion-causing admixture has high fluidity, high pumpability, non-bleeding, low pressure bleeding, low volume change, low permeability and high strength. HPG is expected to improve grouting injection and consequently durability of post-tensioned prestressed concrete structures.

REFERENCES

[1] Japan prestressed concrete contractors association, Execution manual for grouts and pre-grouted tendon used in post-tensioned structures, 1999

SIMULATING THE GROUT FLOW IN POST-TENSIONED CONCRETE STRUCTURE DUCTS TO PREDICT THE FILLING PERFORMANCE

Ammar Yahia, Tamio Yoshioka, Shinzo Eguchi
Research Laboratory, Oriental Construction Inc., Japan

Takahiro Shinozaki
Research Center of Computational Mechanics, Inc., Japan

Keywords: grout, simulation, durability, post-tensioned, rheology

1 INTRODUCTION

Grouting operation is carried out to adequately encapsulate the steel tendon with an alkaline environment to prevent corrosion and to serve as a barrier to the ingress of external contaminants. This is by far the most important operation essential for the safety and durability of post-tensioned concrete structures. The objective of this study is to evaluate the applicability of computational fluid dynamics in simulating the flow of cement grout in post-tensioned concrete structure duct.

The flow of cement grout in typical two-parabolic segments duct is successfully simulated and visualized. The effects of viscosity of the injected grout and the eccentricity of the tendon in the duct are analyzed. At this step, the numerical simulation is carried out from the viewpoint of visualizing the flow pattern of grout in the duct and evaluating the effect of grout properties and eccentricity of the tendon in the duct on the filling process of the duct.

2 THE PROFILE OF SIMULATED DUCT AND FINITE ELEMENT (FE) MESH

The flow domain consists in the annular space between the duct and tendon. The profile of the duct and the finite element (FE) mesh of the cross sectional area considered in this simulation are shown in Fig.1.

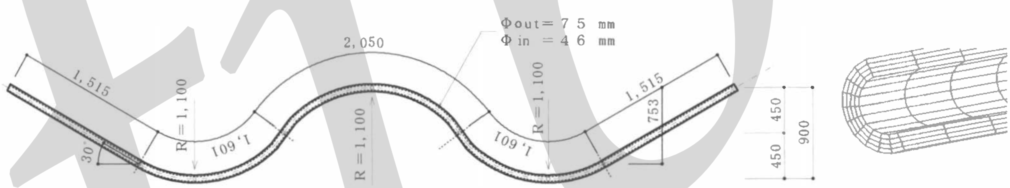

Fig. 1 Profile of the simulated duct and the cross section of the FE mesh

Since the problem is symmetric about the center plane of the duct in the flow direction; only half of the duct is simulated. The flow domain is divided into 11500 elements and 9150 nodal points.

3 PROBLEM FORMULATION

3.1 Governing Equations

$$\begin{cases} \nabla . u = 0 & \text{(Conservation of mass)} \quad (1) \\ \rho\left(\dfrac{\partial u}{\partial t} + u . \nabla u - g\right) - \nabla . \tau = 0 & \text{(Conservation of linear momentum)} \quad (2) \end{cases}$$

The symbols ρ, u, g, and τ are the density, velocity field, gravitational acceleration, and stress tensor, respectively.

The fluid volume is represented by a characteristic marker concentration F. The value of F is unity within the tracked fluid and zero outside. The advection of the marker concentration is governed by:

$$\frac{\partial F}{\partial t} + u . \nabla F = 0 \qquad (3)$$

3.2 Boundary Conditions

The velocity boundary conditions consist in assuming a no-slip formulation, which mean that the velocity vanishes on the duct and tendon walls. The symmetry boundary condition is on the other hand applied at the duct centerline. This consists in constraining the radial velocity to be zero while the axial component is left free. The grout is assumed to enter the duct at a constant flow rate (constant velocity). In order to create a uniform flow at the entrance of the duct, a small portion (100 mm in length) is considered to be initially filled. On the other hand, the filling fraction at the entrance is kept constant by mean of a filling boundary condition.

4 ANALYSIS AND DISCUSSIONS

4.1 Filling Pattern of the Duct

The 3-D simulated flow of grout (viscosity = 0.6 Pa.s, yield stress = 3.8 Pa) in a typical duct in which an eccentric tendon is placed confirms the flow pattern generally observed in the field (Figs. 2).

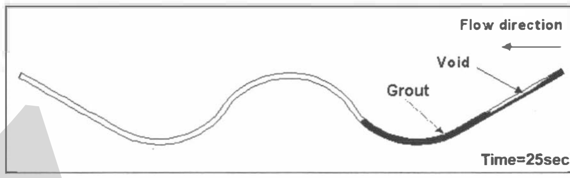

Fig. 2 The filling pattern of the duct

4.2 Effect of the Eccentricity of the Tendon

Larger void at the high side of the duct is obtained in case of eccentric position of the tendon. Indeed, at the concave segment the tendon is located at top of duct, hence resulted in easily flow of grout at bottom portion, but a difficult movement at top.

Furthermore, it is observed that contrarily to a central position of the tendon in the duct, where the grout has been subjected to uniform shear- rate during its flow, the presence of eccentricity inside the duct may however results in non-uniform shear-rate flow.

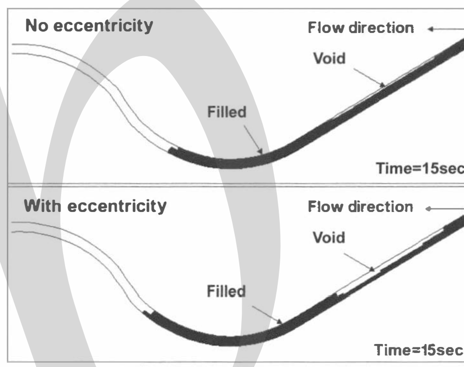

Fig. 3 Effect of eccentricity of the tendon on filling

4.3 Effect of Viscosity of Grout

These values of viscosity may represent low, moderate, and high viscosity grout, respectively. The flow rate of grout is fixed at 28 L/min. Figure 4 shows the effect of viscosity of grout on its flow behavior in the duct. When using high viscosity grout is the eventual increase of pressure inside the duct to achieve a constant flow rate during grouting operation.

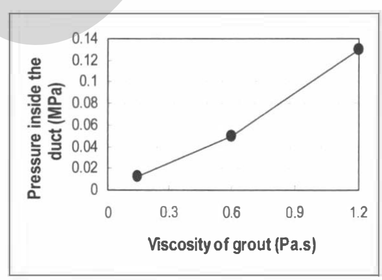

Fig. 4 Effect of viscosity on pressure in duct

5 SUMMARY AND PERSPECTIVES

Through this research authors aim to introduce a useful tool that can be used to optimize proper grouting parameters and evaluate the ability of grout to fill the duct and provide adequate coating of the steel tendon. Preliminary results presented in this paper regarding the 3-D flow of grout in two-parabolic segments duct confirm the capability of CFD to successfully simulate the grouting operation. At this step of the ongoing research, the basic aspect of the numerical model is verified by visualizing and comparing the simulated flow pattern in the duct to that observed in experiments. Next step will focus on the validation of the numerical simulation and this will involve experimental measurements on identical model, thus allow a quantitative comparison between numerical results and experimental data. Once the validation of the numerical model with the experimental results is achieved, the use of the proposed CFD model to simulate the grouting process will be confirmed. This should results in a useful and saving-energy tool that can be used to rationalize the grouting operation of post-tensioned ducts.

QUANTITATIVE ASSESSMENTS ON FILLING PERFORMANCE OF PC GROUT

Jun-ichi Izumo
Kanto Gakuin University, Japan

Shin-suke Mizukami
P.S. Corporation

Keywords: grout, filling performance, plastic viscosity, yield stress, flowability

1 INTRODUCTION

The defects due to inadequate grouting have been reported in Japan. It is required that the materials and the grouting practice are newly developed to assure that grout can be done perfectly and improve durability of post-tensioned structures.

The objective of this study is to formulate the angel at the tip part of grout in flow and propose the method that can evaluate the filling performance by taking into grout viscosity and the grouting conditions.

2 TEST PROGRAM

The authors have developed the new experimental test device that can visibly evaluate the filling performance of PC grout[1]. The outline of the test setup is shown in Fig. 1. The inclination at the tip part of grout in flow and the velocity are analyzed with the digital video pictures. The 6 types of grout with different viscosity; 29 grouts were prepared for the test to evaluate the effect of the grout viscosity on the filling performance.

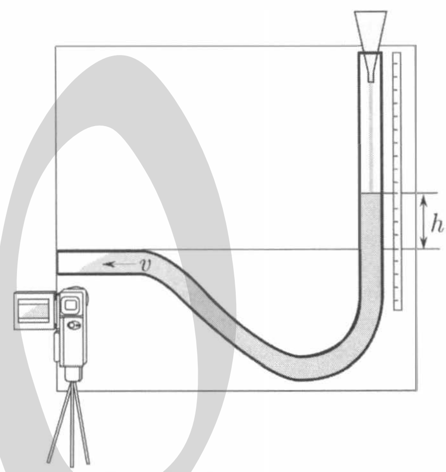

Fig. 1 Outline of test method

3 TEST RESULTS AND DISCUSSION

The observed tip part of grout in the horizontal part of the duct are shown in Fig. 2. When the angle is almost greater than 20 degrees, the complete filling is confirmed through the tests.

In reference to the free body including the tip part of grout as shown in Fig. 3, the angle ƒÆat the tip part of grout can be formulated as follows

$$\tan\theta = \frac{4(\tau_f + \mu \frac{v_m}{D}) - \rho g D \sin\alpha}{\rho g D(c_1 + 2c_2)} \qquad (1)$$

where
D = diameter of duct
τ_f = yield stress
μ = coefficient of plastic viscosity
μ_0 = coefficient of viscosity of water
α = inclination of duct
ρ = density of grout
v_m = average velocity of grout
g = gravitational accelration

$c_1 = \dfrac{1}{1+0.35\ln(\mu/\mu_0)}$: coefficient

$c_2 = 4\times10^{-3}\tau_f$: coefficient

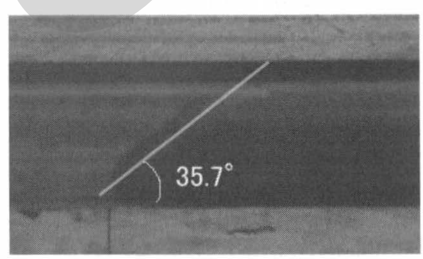

(a) In the case of complete filling

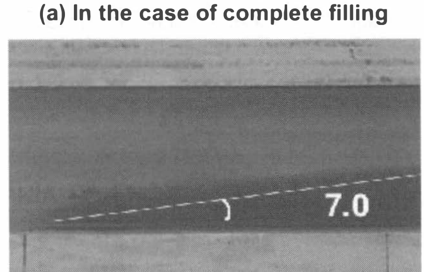

(b) In the case of incomplete filling

Fig. 2 Angle at a tip part of grout

The introduced analytical model has been verified through the tests done by the authors and the other researchers [2][3]. The 189 test results including the authors' test were used for the verification of the proposed model. The yield stresses of grout were in the range from 2.0 Pa to 181.7 Pa. The 3 types of the diameter were 32 mm, 50 mm and 70mm in the tests. The inclination α of the duct were in the range from zero to 20 degrees. Fig. 5 indicates the analytical results and the test results. The correlation coefficient is 0.97 for the total tests. It is considered that the analytical results are in good correspondence with the test results.

The parametric study on the filling performance is also done by using the Eq.(1). When the diameter is changed as 32mm, 50mm and 70mm respectively, the relationship between the velocity and the yield stress in the case of α= 0 degree and ρ= 2000kg/m^3 is obtained as shown in Fig. 5. From the simulations, It is recognized that the effect of the diameter on the filling is larger compared with the effects of the inclination and the density if the yield stress is constant.

4 CONCLUSIONS

(1) The good filling condition has been confirmed through the test when the angle at the tip part of grout is almost greater than 20 degrees.
(2) It has been confirmed that the calculated angles at the tip part of grout are in good correspondence with the observed ones
(3) Through the parametric study, the velocity and the yield stress of grout needed for the good filling is affected especially by the diameter and the inclination of the duct.
(4) The complete filling is possible if the appropriate viscosity and the velocity of grout are determined according to the diameter and the placement of the duct at the grouting program

REFFERENCES

[1] Izumo, J. : Study on Testing Method for Evaluating the PC Grout Performance, Journal of Prestressed Concrete, Vol.42, No.5, 2000.9 (in Japanese)
[2] Nishimura, M., Ito. K. and Uomoto, T.: Effect of Rheological Property and Injection Condition of Grout Material on Post-tensionning PC grout, Proceedings of the Japan Concrete Institute, Vol.22, No.2, pp-1399-1404, 2000 (in Japanese)
[3] Ito, K., Adachi, I. and Uomoto, T.: Fluidity Effect on Filling of Grout for Prestressed Concrete, Proceedings of the 55 Annual Coferrence of the Japan Society of Civil Engineers, V-409, 2000.9 (in Japanese)

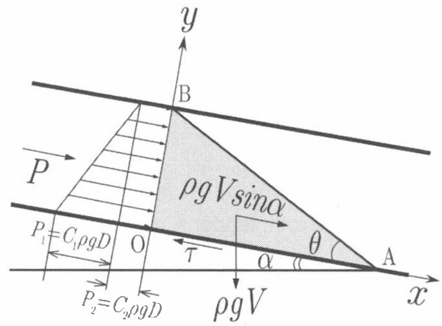

Fig. 3 Equilibrium of grout

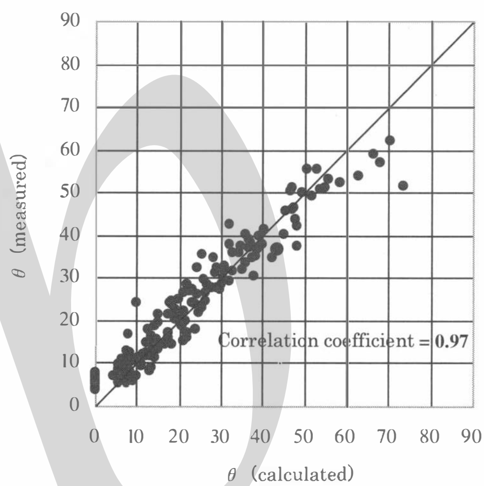

Fig. 4 Analytical results compared with the total tests

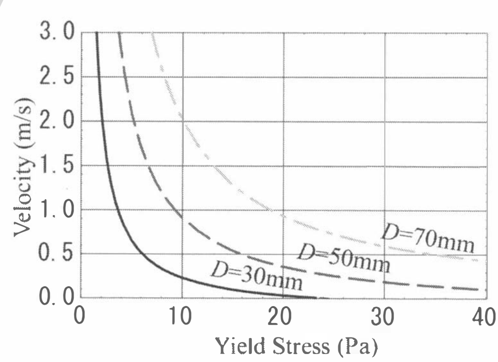

Fig. 5 Relationship between velocity and yield stress (Diameter changed)

GROUTING Of SEGMENTAL POST-TENSIONED BRIDGES IN AMERICA

Brett H Pielstick P.E.
Vice President
PTG Construction Services Company, USA

Keywords: Grout, tendons, durability, inlets, outlets

1 INTRODUCTION

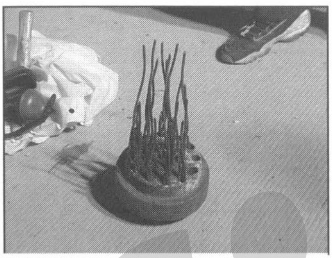

Picture 1.1 – Corroded

Over the past several years the post-tensioned concrete bridge industry in America has experienced several tendon failures due to corrosion. These isolated failures instituted additional investigations conducted in Florida as well as several other states, which have determined that several structures have shown some types of grouting deficiencies. Some of the grouting deficiencies had voids with no corrosion present, but others showed corroded ducts and/or post-tensioning strands. As a result, the owners and the industry have evaluated the process of grouting and have developed a course of action to improve the grouting and thus the long-term durability of these structures.

2 IMPROVEMENTS PLANS FOR GROUTING

As a result of the grouting deficiencies the industry has established several guidelines for better grouting methods. The PTI Specification for Grouting of Post-Tensioned Structures (1), The Concrete Society Technical Report 47 (2), as well as the ASBI "Interim Statement on Grouting Practices" (3) address several areas to improve the grouting process. First, several design details have been changed to improve recharge characteristics and performance of the post-tension systems. Second, several changes to the grout material have been recommended. The use of anti-bleed or no bleed grout is recommended and in Florida is required. Third, improvement of the grout equipment will provide a consistent mix and density for the grout. Fourth, training and certification for grouting technicians and inspectors is required. The ASBI and the Florida Department of Transportation have created training and certification programs for inspectors and grouting technicians.

2.1 Design Details

In an effort to improve corrosion related durability problems several changes in design details have been recommended through the American Segmental Bridge Institute " Interim Statement on Grouting Practices", The Florida Department of Transportation Design Guidelines, The Concrete Society Technical Report 47 and PTI Specification for Grouting of Post-Tensioned Structures. New anchorage zone protection details provide protection from air and water recharge (figure 1). Multi-layer protection is recommended to provide redundancy in the system. The position of the inlets and outlets are related to the direction in which the grout flows, the inclination (vertical rise and fall) of the ducts and the couplers, and the allowable grout pressure (figures 2). The details for their location may be addressed in the plans but nevertheless the inlets and outlets should be placed as follows:

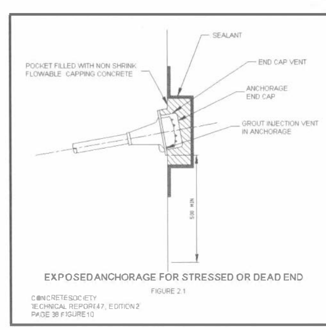

Figure 2.1- Anchor Detail

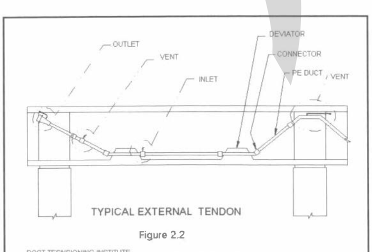

Figure 2.2- Outlet Location

1) At all Anchorages.
2) The high points of the duct, when the vertical distance between the highest and lowest point is more than 20 inches
3) An inlet shall be placed at or near the lowest point of the tendon.
4) Outlets should be placed at all high points
5) At major changes in the cross-section of the duct, such as couplers and anchorages.
6) At other locations recommended by the Design Engineer or the Construction Engineer.

2.2 Improved Grout Material

In an effort to provide a more consistent grout material, the Florida Department of Transportation is requiring a pre-bagged bleed resistant grout. The ASBI and PTI have recommended anti-bleed or low bleed grouts meeting a series of performance requirements. These grouts have reduced the size and number of voids due to bleed water. Although these grouts reduce the void potential the anchorages should still be probed or visually inspected when the grout has set.

2.3 Improved Grouting Equipment

All of the grouts need to be mixed with the proper water-cement ratio using the right equipment. The type of mixer and the time the grout is mixed is a determining factor in the quality of the grout. The manufacturers instructions should be followed using a colloidal or shear type mixer to obtain a homogeneous mixture. Over mixing of grout will result in variable density grout while under mixing of grout will produce an inconsistent poor grout.

2.4 Training of Grout technicians and Inspectors

From the problems discovered in Florida, the training of grout personnel was identified as one of the key components to getting a good grouting job. The grout foremen, inspectors and supervisors must be competent and knowledgeable in correct grouting procedures to prevent repeating the problems found.

Florida has developed several programs and requirements to assure the technicians performing grouting operations have the proper training. These programs include a one-day training seminar with classroom and field demonstration. In addition Florida is developing a grout training video for the laborers on the grout crew. This video is being developed to introduce the laborers to correct grouting procedures and to explain the importance of their work to the overall durability of the structures. ASBI also has developed a three-day training program for the Certification of grouting technicians. This program has been developed to train the Formen and Inspectors in theory and field procedures to achieve a properly grouted structure and will be required in the future by FDOT.

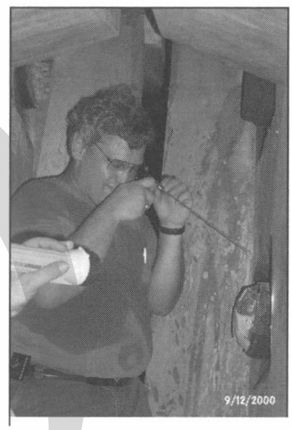

Picture 2.4.1 - Bore Scope

3 CONCLUSIONS

Although no structural deficiencies have been noted to date on segmental post-tensioned bridges in America, the industry has mobilized to address the grout problems to further enhance the durability of these structures. In an effort to improve the grout protection system changes to the design details, grout material and training of the grout technician have been implemented to improve the grout and increase the long term durability of the post-tensioned structures.

REFERENCES

[1] **"PTI Guide Specification – Specification For Grouting Of Post-Tensioned Structures"** Post-Tensioning Institute, Phoenix, AZ. First Edition, February, 2001

[2]**"The Concrete Society – Concrete Society Technical Report 47"** The Concrete Society, Telford Ave., Crowthorne, Berkshire Revision 2

[3] **"American Segmental Bridge Institute – Grouting Committee – Interim Statement on Grouting Practices"** American Segmental Bridge Institute, Phoenix, Arizona, December 4, 2000

[4] Shokker A.J., Koester, B.D., Breen, J.E., and Kreger, M.E., **"Development of High Performance Grouts for Bonded Post-Tensioned Structures".** Research Report 1405-2 Center for Transportation Research, October 1999

PROPERTIES OF PRESTRESSED CONCRETE STRUCTURES 30 YEARS AFTER COMPLETION AND THE IMPROVEMENT OF THE QUALITY OF GROUT THAT IS A FACTOR INFLUENCING DURABILITY

Misao Sugawara, Dr. Eng.
Kyokuto Kogen Concrete Shinko Co., Ltd.
Japan

Keywords: Neutralization of concrete, grouting detection, high viscosity grout

1. INTRODUCTION

In this paper, the author will confirm the durability of concrete that has been carefully installed using appropriate materials through measurement of creep in concrete over a period of 30 years with respect to an actually constructed PC bridge and through investigation of the changes in quality of concrete of the bridge that has been in use over a long period.

Moreover, with respect to prestressed concrete, the author also explains the importance and method of grouting of the PC cable that is an issue specific to such construction.

As part of the investigation, the author explains a method of monitoring the status of the injection of grout through non-destructive tests.

2. THE PROPERTIES OF PC BEAMS AFTER THE LAPSE OF A LONG PERIOD FROM CONSTRUCTION

2.1 Long-term Measurement of the First Daidogawa Bridge

The First Daidogawa Bridge has a span of 30 meters and is a PC railway bridge employing the Freyssinet method that was completed in 1954.

A measurement point for measuring stress using a removable strain meter (Giken type) was embedded in the PC beam and the creep of the concrete was measured over 30 years after applying tension to the PC steel material.

As the measured value became saturated about 4 years after completion, this fact was reported to the Japan Society of Civil Engineers.

This measurement was performed on a time to time basis over 30 years but the measured value of the creep has changed very little after the 4th year (Fig. 1).

Moreover, the rigidity of the beams as measured through deflection upon passage of trains is as originally calculated.

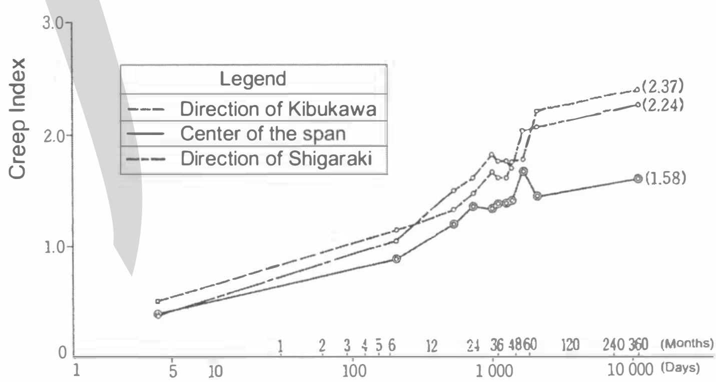

Fig. 1 Changes over Time of the Creep Index

2.2 Properties of the Kogen Bridge after Use over a Long Period of Time

This bridge is the first post tension type PC railway bridge constructed in Japan and was completed in 1953.

The railway route became unnecessary after the bridge had been in use for about 30 years and the bridge itself was therefore removed and tests were conducted on resistance to bending, the quality of the concrete and other factors.

The results of these tests indicate that the quality of the concrete is equivalent to the quality upon first construction (Table 1).

Moreover, prior to destructive testing, X-ray was used to investigate the status of grouting and the occurrence of rust in the PC steel was monitored through measurement of natural potential.

Table 1 Properties of the Concrete used for the Kogen Bridge Approximately 30 Years after Completion

Assumed composition	Cement (kg/m^3)	530
	Water (kg/m^3)	150
	Aggregate (kg/m^3)	1,780
	W/C (%)	28
Compressive strength	Fc-1 (N/mm^2)	44.2
	Fc-2 (N/mm^2)	43.2
	Fc-3 (N/mm^2)	46.1
	Average (N/mm^2)	44.5
Neutralization	Core No. 1	Less than 1mm
	Core No. 2	Less than 1mm

3. IMPROVEMENT OF THE QUALITY OF GROUT

In Japan, there are numerous cases of inadequate grouting in important PC bridges causing erosion of the PC steel materials.

In 1994, the PC Construction Industry Association of Japan conducted a large scale grouting test using legacy type admixture and 3 types of non-bleeding admixtures and 15 types of sheaths measuring between 5 meters and 15 meters. As a result of this test, the association agreed that from April 1997, non-bleeding grout should be used, flow meter should be used and a skilled engineer should be in attendance. This was in line with the TR-47 report announced by the British Concrete Society.

Several large scale experiments have been undertaken on admixtures for grout and method of injection after this. The author and colleagues have confirmed in injection tests involving Conbex 208 Neo, which can make high viscosity and non-bleeding grout that careful grouting allows completely filling of the sheath with grout.

4. CONCLUSION

The author believes that concrete with adequate durability may be achieved if the constructor is adequately cognizant of the properties of concrete and works carefully in conformance with standard specifications. It is clear that achieving complete grouting is an important issue specific to prestressed concrete. This is all the more reason for the importance of establishing methods of inspection to confirm whether or not adequate filling with grout has been achieved.

REFERENCES

(1) Sugawara, M.: Improvement of PC Grouting Work and Grout Quality in Japan, Cement & Concrete No.603, p.p. 8～15, May 1997 (in Japanese)

(2) Shimomura, Hisamatsu, Hayashishita: On the Investigation of a PC Railway Bridge (Kogen Bridge) Constructed in the Early Stages. Symposium of the PC Engineering Association, Oct. 1990

(3) Fuzier, J.: On the TR No.47, Durable Bonded Post-Tensioned Concrete bridges, Asia Pacific Technical Seminar at Singapore, Dec. 1996

DESIGN CRITERIA FOR LONG TERM PERFORMANCE OF CONCRETE STRUCTURES SUBJECTED TO INITIAL MODIFICATIONS OF STATIC SCHEME

M. A. Chiorino G. Lacidogna
Politecnico di Torino, ITALY

Antonio Segreto
S.I.C. Consulting Engineers, ITALY

Keywords: creep, change in static system, delayed restraints, stress redistribution, cracking, durability

1 INTRODUCTION

In modern reinforced or prestressed concrete structures the final construction is frequently the result of a sometime complex sequence of phases, which may include one or multiple modifications of the initial structural system. In practice, after the preliminary assemblage of prefabricated elements, or the independent casting in situ of different portions of the construction, higher degrees of mutual connection between the different parts and/or higher levels of external restraining are introduced in one or, most frequently, successive steps. The aim is to reduce the long-term creep deformations, achieve a more favorable stress distribution for the live loads, and increase the ultimate strength and robustness of the structure.

However, as a consequence of the creep behavior of concrete and of the introduction of these additional mutual or external restraints, that prevent the free creep displacements due to the pre-existing permanent actions (e.g. self-weight and initial prestressing), the corresponding stress distribution in the original structural system is progressively altered. More specifically, redundant reactions arise at these restraints. Their values, and consequently also the distribution of the internal stresses in the new structural system, varying continuously with time, tend to approach the values and the distribution that would be obtained applying the same permanent static actions to the structure in its final static configuration. As a general indication the higher is the residual creep deformation capacity of the structure after the application of the delayed restraints, the higher is this tendency.

If proper design and construction criteria are not adopted to counteract these effects, or to reduce their importance through convenient strategies (like e.g. a high level of load balancing in prestressed structures), the long-term serviceability and durability of the structure may be adversely affected, due to the possible appearance of undesirable cracking in regions where the stress redistribution introduces tension stresses or increases their original values. In conclusion, in the case of concrete structures that are built sequentially, care must be taken in order to avoid that the advantages on their global performance deriving from the progressive introduction of additional restraints shall be jeopardized by the consequences of neglecting the inevitable stress redistributions taking place due to creep.

Reliable methods for the estimation of these creep induced effects are therefore needed in order to appropriately define the convenient countermeasures in terms e.g. of additional reinforcing and/or prestressing in the new developing tension regions. Besides the discrete approaches in space and time, compact methods for a global evaluation of the creep induced structural effects are strongly needed, especially in the preliminary design stages, as well as in the control of the output of the final detailed numerical investigations and safety checks. The paper focuses on the development of such compact procedures and shows examples of application to practical design situations characterized by different sensitivities to these creep-induced effects.

2 COMPACT ANALYTICAL METHODS

The paper shows that these estimations may be performed in a very compact form, without the need for any simplifying approximation (normally yielding unacceptably large errors in these type of problems), on the basis of the theory of linear viscoelasticity for aging materials, through an extensive use of the redistribution function $\xi(t,t_0,t_i)$. This function, which depends on the creep properties of the concrete under consideration and on the ages t_0 of the application of the permanent static actions and t_i of the successive modifications of the static system, models the progressive variation of internal stresses and external reactions taking place due to creep after the introduction of the delayed restraints. The theoretical fundaments are the 3^{rd} and 4^{th} *theorems of linear viscoelasticty* demonstrated by the first author for the general case of materials characterized by a compliance function J, representing the creep properties of the material, of a completely general form (showing e. g. - as it is the case for concrete - both an aging and a delayed elastic behavior). The problem is governed by the following general relationship which applies to concrete structures that are, or may be considered as, homogeneous from the point of view of the creep properties, and to rigid restraints [1]:

$$S^{j+1}(t) = S^{el,1} + \sum_{i=1}^{j} \xi(t,t_0,t_i)\, \Delta S^{el,i} \qquad (1)$$

where, $\Delta S^{el,i}$ is the correction to be applied in the associated elastic problem to the elastic solution $S^{el,i}$ in order to respect the geometrical conditions imposed by the Δn_i additional restraints of static scheme $i+1$, imagined as applied before the permanent static actions. Eq. (1) allows a very concise description of the phenomena under consideration evidencing that the long-term values of the creep-induced stress redistribution determined by every successive modification of the static scheme at times t_i - which may be separately evaluated and then superimposed - depend both on the corresponding long-term values of ξ and on the differences between the reference elastic stress configurations for the permanent static actions evaluated *after* and *prior* to each modification of the scheme.

Similar compact formulations, still employing the redistribution function ξ introduced for homogeneous structures with rigid restraints, may be derived for an approximate solution of continuos beam structures built sequentially in span-length sections showing different creep properties, due e.g to differences in age of concrete and/or size and geometry of cross section [2].

3 CASE STUDIES

With reference to the results of the previous analysis, the paper shows an application to two case studies of cantilever built bridges (Figs. 1 and 2) characterized by a different sensitivity to the creep-induced stress redistributions, precisely as a consequence of the different magnitude of the variation in the reference elastic stress distributions, when passing from the original static scheme to the final one (change of static system by connection at mid-span). A major factor in defining the importance of this nominal elastic variation is represented, in these type of structures, by the level of "load balancing" due to the prestressing applied *prior* to the introduction of the continuity restraint, which is normally the result of a choice combining design requirements, construction constraints, technical and economical evaluations. The estimated final redistribution is influenced by the creep prediction model (Fig. 3).

Figs. 1 and 2 1st and 2nd case studies: Vallone Marzo Bridge (left) and Gesso River Bridge (right)

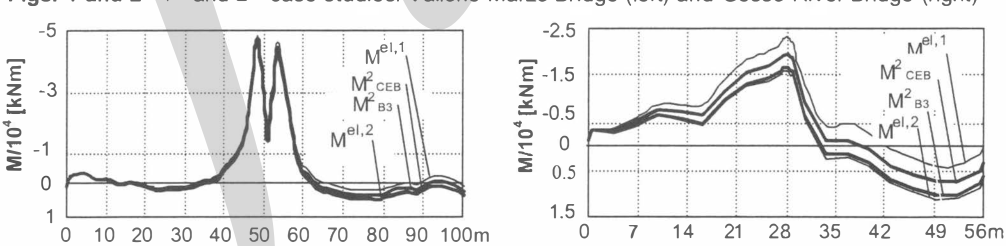

Fig. 3 Moment redistribution due to creep: estimated long-term bending moments M^2 in the final structures (CEB and B3 creep prediction models). Comparisons with elastic moments $M^{el,1}$ (static system 1) and $M^{el,2}$ (static system 2) (left: 1st case study, right: 2nd case study)

REFERENCES

[1] Chiorino M.A. and Lacidogna G. : General unified approach for creep analysis of concrete structures. Revue française de génie civil, Vol.3, No.3- 4, pp. 173-217, 1999

[2] Chiorino M.A., Dezi L.,Tarantino A.M. : Creep analysis of structures with variable statical scheme: a unified approach. Creep and Shrinkage – Struct. Design Effects ACI SP-194, pp. 187-213, 2000

REHABILITATION OF A CONCRETE CHIMNEY BY PRESTRESSING RINGS

Augustin Popaescu
Consultant INCERC Bucharest
ROMANIA

Ion Dumitrache
STIZO DSP Bucharest
ROMANIA

Ioan Mateescu
ROMEXIM Bucharest
ROMANIA

Keywords: prestressing, strength, durability, repair, strengthening

1 INTRODUCTION

Concrete chimneys built 25 – 35 years ago for electrical power plants present different durability deteriorations, but several of them present also vertical cracks due to thermal actions and low horizontal hoop reinforcement.

For rehabilitation of these chimneys there are different kind of strengthening and repair methods, but difficulties of application on this type of structure bring some limitations of use of the methods.

The paper describied the conception and methods for strengthening / rehabilitation of an existing concrete chimney of about 80 m and 30 years old. The chimney site is located in the environment of an electrical power plant and in the vicinity of chemical industry.

2 MAIN DETERIORATION AND CAUSES

In the following are describied the deteriorations observed on outside part of chimney (inside deteriorations not included in the paper) :

- horizontal cracks due to casting deficiencies at repeated forming lifts
- vertical cracks along the sustaining rods of lifting forming,especially on the lower chimney part, due to thermal actions plus wind effects;crack width of 1–2 mm on exterior side but not pierced
- corrosion and expansion corrosion of several horizontal reinforcement bars due to low concrete cover

3 STRENGTHENING AND REPAIR METHODS APPLIED

3.1 Strengthening by circumferential prestressing

An original method for strengthening by post-tensioned monostrand rings with permanent protection, proposed for strengthening of Govora Chimney by Prof. Dr.Augustin Popaescu (Ref. [1]), consists in:

- Strands (seven wire) with low relaxation, 15.3 mm(0.6”) dia., in sheat of PE tube of 2mm thickness and internal grease. Cross section=140 mm^2, $F_{p\,0.01}$=189 KN, $F_{p\,0.2}$=220 KN, F_{pr}=248 KN . Low relaxation : 2.5% for 1000 hrs
- Anchorage X shape, double protected (grease, shrink tube)

Both supplied by STIZO-DSP Bucharest from Dywidag (Germany)

- Polypropylene PPAS tube, 32 mm dia. (2mm thickness), antiultra-violet additivated, as supplementary protection for freeze and sun ray. Supplied by Romexim Bucharest (Romania).

3.2 Deteriorations repair with high bond materials, reliable surface protection.

The main aim of repair works was the reestablishing the concrete continuity in the cracks, repair of deteriorations using high bond materials and ensured a surface protection against humidity, sun rays, freeze and corrosive chemical penetration.

For reestablishing the concrete continuity we stated that the causes of cracking are mainly the thermal effects and also concrete shrinkage(already finished). So, for the reestablishing the concrete continuity in the cracks Prof. Popaescu recommended both the high bond injection resin with low viscozity to penetrate the cracks from fine width and permanent compressive stress induced by circumferential prestress (specified in **3.1**).

Main repair materials were choosed from SYMONS products (DAYTON Corporation USA), supplied by ROMEXIM Bucharest representing SYMONS in Romania, like as follows:

Injection resin : ResCon 302 HM-LV – high strength bond, low viscosity epoxy injection resin (including adhesive system) capable of penetrating concrete cracks from 0.12 to 6 mm in thickness.

Repair mortars: - Epoxi mortar based on ResCon 302 HM-LV resin;

-Cement mortar with improved bond strength, freeze/thaw and abrasion resistance and greater compression strength by admixture with Strong Bond, an acrilic latex bonding agent.

Surface protection : Spray-Rite^{TM} – polymer modified cement product for concrete texture, water resistant and ResCon 117 – epoxi penetrating sealer to provide an effective subsurface barrier to inhibit moisture migration and corrosive chemical penetration.

Both the strengthening and repair methods proposed were accepted and introduced in the project for strengthening and repair of 80 m chimney at Govora Electrical Power Plant, elaborated by Electrical Power Design Institute in Bucharest (ISPE).

4. SOME ASPECTS OF EXECUTION

All execution works on exterior side of the chimney were performed by STIZO DSP Company Bucharest using self climbing platforms for both inferior half and superior half of the chimney.

First, the repair of concrete surface was done : vertical and horizontal cracks injection using ResCon 302 resin and local repair concrete deteriorations with repair mortars.

Application of surface protection with Spray-Rite for concrete texture and ResCon 117 – epoxi penetrating sealer . Figure 1 presents the chimney during repair operations.

Strengthening by circumferential prestressing was performed in the following stages for each monostrand :

- preparation of the strands with double tubs
- erection at position of a strand, anchorage montaje, post-tensioning
- local protection of anchorage and the ends of tube

Figure 2 shows anchorage X shape and prestressing jack and figure 3 the chimney after accomplishment of works.

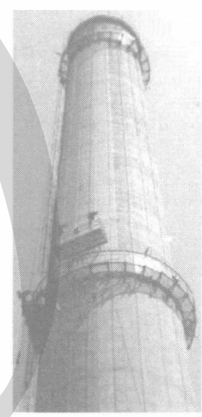

Fig.1 Chimney during repair operations

5. CONCLUDING REMARKS

Methods for strengthening/ rehabilitation of an existing concrete chimney of about 80 m and 30 years old, including increasing of horizontal reinforcement capacity by circumferential prestressing and repair of the surface deteriorations with high bond materials reestablishing the concrete continuity in the cracks and surface protection, permitted a reliable rehabilitation, with acceptable costs and a short period of execution works.

6. ACKNOWLEDGEMENTS

Authors acknowledge the contribution of the Electrical Power Design Institute in Bucharest (ISPE), main designer Eng. Luiza Serban and Technical Expert Prof. Radu Agent in providing the first strengthening of a chimney by prestressing using monostrands with permanent protection and repairs with modern materials.

REFERENCES

[1] Popaescu, A., Dumitrache I., Mateescu I. - OSIM Patent (Romania) 115902 / 28.07.2000 <Method of prestressing or strengthening of chimneys, with pretensioned rings of monostrands with permanent protection>.

[2] SYMONS Chemical Products Handbook, 1993, Symons Corporation, Des Plaines, IL 60018, USA

Fig.2 Anchorage X shape and prestressing jack

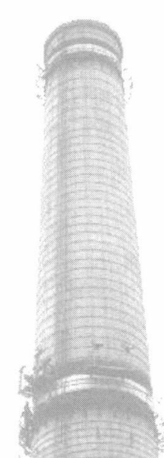

Fig.3 Circumferential prestress

PERFORMANCE OF REINFORCED CONCRETE BEAMS STRENGTHENED BY EXTERNAL PRESTRESSING TENDONS IN COMPARISON TO OTHER STRENGTHENING METHODS

Joao Bento de Hanai
Professor of Civil Engineering *
e-mail: jbhanai@sc.usp.br

Tatiana Gesteira Martins de Almeida
M.Sc. in Structural Engineering *
e-mail: tatiana@cpunet.com.br

Department of Structural Engineering
University of Sao Paulo at Sao Carlos, Sao Carlos - BRAZIL

Keywords: strengthening, beam, reinforced concrete, prestressed concrete, external tendons.

1 INTRODUCTION

This paper mainly focuses the experimental study conducted by ALMEIDA (2001) [1] in the analysis of strengthening methods with external prestressing tendons. A comparison of its results is made with those obtained by REIS (1998) [2] who analyzed strengthened reinforced concrete beams with addition of steel bars or plates and concrete on the tensioned face.

2 EXPERIMENTAL PROGRAM

The experimental program consisted of the strengthening and analysis of three reinforced concrete beams with a T-shape transversal section and 3 m span, as shown in Fig. 1.

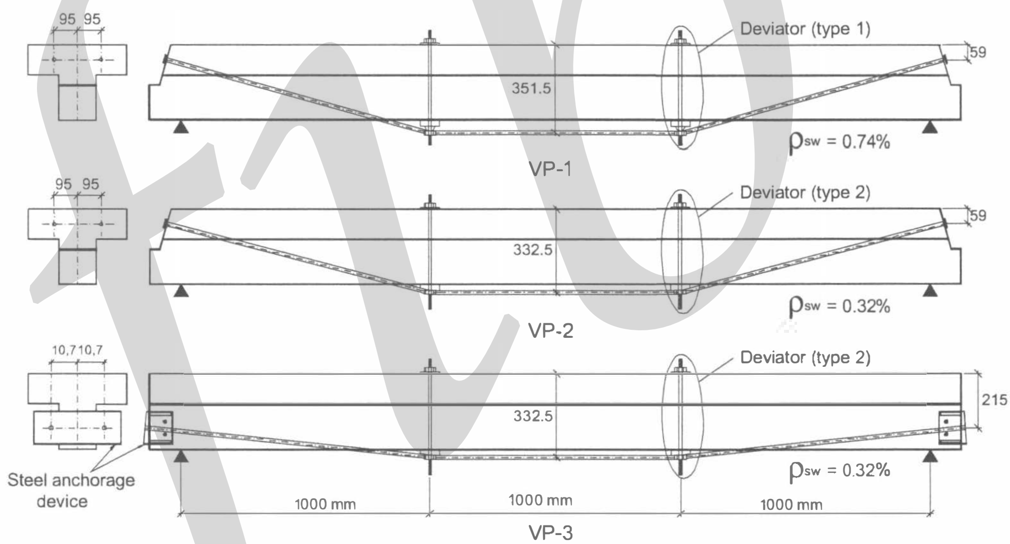

Fig. 1 Tendon profiles and shear reinforcement ratios

The parameters that changed during the tests were the shear reinforcement ratio and the profile of the external tendons.

3 TEST PROCEDURE

The tests consisted of three stages: pre-loading, prestressing of tendons and final loading up to collapse. In the first stage, an increasing loading was applied to the beam until a 40 kN force was achieved. In the second stage, the external force applied remained constant while the prestressing tendons were positioned and tensioned. The third stage began after the anchorage of the tendons, with increase of the applied force until the collapse of the beam. The flexural cracks appeared when the force was approximately 70 kN. Shear cracks appeared when the force was 130 kN for VP-1 and VP-2 and 115 kN for VP-3. The longitudinal reinforcement started yielding when the force reached 160 kN for the three tested beams.

During the tests, the average value of the forces applied by the two hydraulic jacks was registered, and all the present results refer to this value. To allow the analysis and comparison of the behavior of the three tested beams, graphics were elaborated with the average values of the measurements: beam deflection at the mid span, longitudinal reinforcement strain, compression concrete strain, and stirrup strain.

4 COMPARISON TO BEAMS TESTED BY REIS (1998)

REIS (1998) [2] tested reinforced concrete beams with original section (before strengthening) and longitudinal and transversal reinforcements similar to the VP-1 beam. The VA series beams were strengthened by addition of regular steel bars to the tension zone. The additional bars were enveloped by a high-performance mortar that bonds the new reinforcement to the original beam. The VC series beams were strengthened by the attachment of a steel plate to their inferior face. The attachment of the plates was done by steel connectors and high-performance grout.

Diagrams in Fig. 2 illustrate the comparison among the beams tested by REIS [2] and by the present authors.

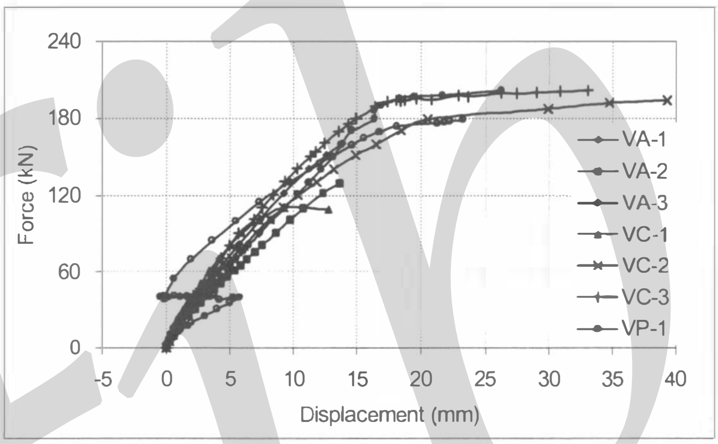

Fig. 2 Force *versus* deflection at mid span – comparison to REIS (1998) [2]

5 CONCLUSIONS

From the analysis of the results it is possible to conclude that external prestress highly contributes for the increase of the flexural and shear resistances, improving the service behavior through significant reduction of deflection and cracking. The tests showed that prestressing of external tendons when applied to beams under loading may lead to a total deflection recovering. Existent flexural cracks may be closed with prestressing of tendons.

It was observed that the tendon profile had no significant effect over the stiffness of the beams. The depth of the tendon in the mid span is the most effective characteristic for deflection control. Otherwise the shape of the external tendon has a great influence in the shear resistance. The shear cracking is significantly affected by the changes in the tendon geometry. For the tested beams, a larger deviation angle of the tendon leaded to a higher shear cracking resistance.

From the comparison between the strengthening methods it was possible to notice that despite its smaller stiffness, the beam strengthened with external tendons (VP-1) presented smaller deflections in service conditions. The favorable effect of prestress over the shear resistance was clearly observed. The strains in the stirrups in VP-1 were quite inferior than those found in the other beams until the collapse.

REFERENCES

[1] ALMEIDA, T.G.M. (2001) Strengthening of reinforced concrete beams by means of prestressing external tendons. São Carlos. 142p. Master Degree Thesis. In Portuguese.

[2] REIS, A.P.A. (1998). Strengthening of reinforced concrete beams by addition of steel bars or steel plates and high performance cement mortar. São Carlos. 179p. Master Degree Thesis. In Portuguese.

REPAIR AND REINFORCEMENT OF THE OYAKAWA BRIDGE AND TWO OTHER BRIDGES

Kiyohisa Kondo, Former Director-General, Akita Construction Office, Tohoku Regional Construction Bureau, Ministry of Land, Infrastructure and Transport,Japan
Susumu Ishikawa, Civil Engineering Division, Tohoku Branch, P.S. Corporation,Japan
Masami Yamashida Business Development Division, Tohoku Branch, P.S. Corporation,Japan
Keiichi Murakami, Technology of Civil Engineering Division, Tohoku Branch, P.S. Corporation,Japan

Keywords: chloride attack, external cable, cathodic protection

1 INTRODUCTION

Prestressed concrete bridges, which were once believed to be highly resistant, are now doubted for their durability. Prestressed concrete bridges are possibly damaged by chrloride attack, frost damage, carbonization, and alkali silica reaction. Measures against chloride attack are especially important in designing and constructing resistant bridges in Japan, which is surrounded by the sea. This paper describes surveys, repair, and reinforcement of bridges that were affected by chloride attack in coastal regions of Akita, which is located in the northwestern part of Japan, facing the Japan Sea.

The Oyakawa, Koyakawa, and Araiso Bridges are simply supported post-tensioned T-girder bridges on National Highway No. 7, which extends from Niigata Prefecture in the northwest area of Japan to Aomori Prefecture. These bridges and other structures in these regions suffer severe chloride attack due to cold weathers and strong west winds from the sea, which contain large quantities of salt.

2 SURVEY RESULTS, REPAIR AND REINFORCEMENT

The rest of this section describes the results of the surveys and repair and reinforcement of the Oyakawa, Koyakawa, and Araiso Bridges.

2.1 Oyakawa Bridge and Koyakawa Bridge

The Oyakawa and Koyakawa Bridges, which were constructed in 1964, were treated in 1982 with partial repair of the structural members, external cable reinforcement, steel plate lining, and fiberglass reinforced plastic sheeting to repair the parts damaged by chloride attack. Damage by chloride attack still progressed thereafter, and a survey in 1996 revealed new cracks and breakage of prestressing steels (Figure 1). The damage was serious, and the salt contents in the concrete near the steels exceeded the limit value, suggesting that the deterioration would further advance. We judged that the bridges were seriously deteriorated and new bridges needed to be constructed. To secure traffic until the completion of the new bridges, we repaired the structural members of the old bridges and reinforced them with external cables and carbon fiber sheets.

Fi g.1 Breakage of a prestressing wire (Oyakawa Bridge)

2.2 Araiso Bridge

The Araiso Bridge, which was constructed in 1965, showed less cracks and breakage of prestressing steels than the other bridges. To prolong the use of the bridge, external cable reinforcement and cathodic protection were applied after the repair of the structural members. Cathodic protection maintains steels within an electrochemically stable range and prevents the reinforcement and prestressing steels within the main girder from corroding by continuously sending a weak electric current from the surface of the concrete to the steels. In this bridge, an electric current was sent only to the lower flange to protect the steel that is most important in terms of strength.

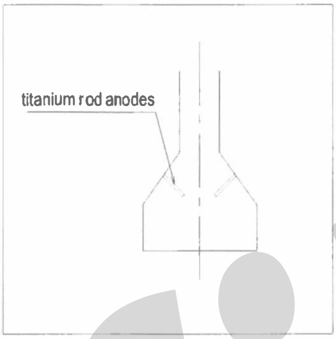

Fig.2 Outline of cathodic protection

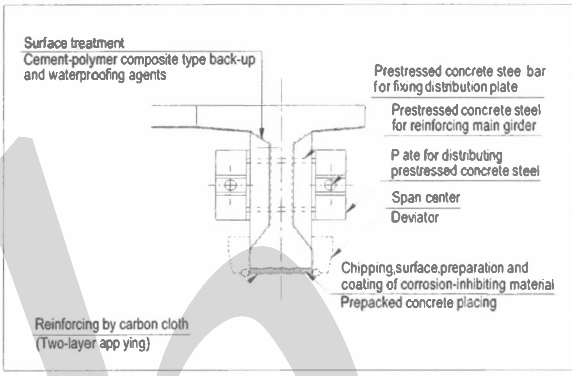

Fig.3 Outline of repair and reinforcement

3 CONCLUSION

National Highway No. 7, where the Oyakawa, Koyakawa, and Araiso Bridges are built, is crowded with heavy and other vehicles and must be securely maintained since there are no alternative routes.

The Oyakawa and Koyakawa Bridges, which were deteriorated and concerned for insufficient safety, were repaired and reinforced in 1998 to ensure the safety until their replacement. The strengthening of main structures was effective and ensured their safety for a period of three years or until the completion of new bridges in 2001.

The Araiso Bridge, which was less deteriorated and further from the service limit than the other two bridges, were repaired and strengthened using cathodic protection and other measures to enable the bridge to be used for a long time. The bridge has so far not shown any problems and is in service.

This survey and repair and reinforcement works showed the following conclusions:

1) Structures along the coast of the Japan Sea are prone to chloride attack and suffer serious damage, such as breakage of prestressing steels.

2) Repair of the structural members is effective to prevent chlorides from entering, and external cable and carbon fiber sheet reinforcements are effective to improve the strength.

3) Cathodic protection prevents prestressing steels from corroding and breaking by salts in concrete, and is an effective measure for elongating the life of bridges.

4) Repair of the structural members and application of external cable reinforcement and carbon fiber sheets are effective for ensuring short term safety of bridges. The use of these measures together with cathodic protection was found to be effective for securing long term service. It is therefore necessary to select repair and strengthening methods that are appropriate for the purpose.

REFERENCES

(1) Kon, Kazuo, Ishikawa, Susumu and Keiichi Murakami: Repair and Reinforcement of the Oyakawa Bridge and two other bridges (in Japanese), Proceedings of the 23rd Japan Road Congress (B), No. 6034, p.314, October 1999.

REPAIR STRATEGY BASED ON FRACTURE CONTROL DESIGN CONCEPTS IN CRACK INJECTION REPAIR

Minoru Kunieda, Kosuke Wakatsuki, Toshiro Kamada and Keitetsu Rokugo
Department of Civil Engineering, Gifu University
JAPAN

Keywords: crack injection repair, fracture control design, concrete structures, un-injected cracks

1 INTRODUCTION

Crack injection repair is one of the common techniques for the cracks. New injection materials and methods have been developed for durable repairs. Most cracks move due to loads, temperature, moisture and other factors, and it is important to understand the potential for crack movement prior to designing the crack repairs [1]. Effective, reliable repair strategies are necessary for durable repair on a lifecycle cost basis.

In this study, the fundamental performance of the reinforced concrete beams repaired by crack injection techniques was investigated. This paper also presents the material selection based on the fracture control design concepts focusing on the controlled behavior of the repaired concrete members might be important for durable repair.

2 OUTLINE OF EXPERIMENTS

Two kinds of the reinforced concrete beams were tested, each having the size of 100×100×600mm(smaller specimens) and 100 × 300 × 1800mm(larger specimens). The geometries of larger specimens are shown in Fig. 1. The four point bending tests were carried out to induce the cracks (first cracks) in original specimens, as shown in Fig. 1. The epoxy and polymer cement slurry (SBR) were used as the injections. The obtained first cracks were classified into two main groups; (a) injected cracks each having the crack width of 0.2-0.8mm were repaired by the crack injection techniques, (b) un-injected cracks each having the crack width under 0.04mm were not repaired. After the injection repair, the bending tests used for the original specimens were also carried out at 7days for epoxy injection, and at 28days for polymer cement slurry injection.

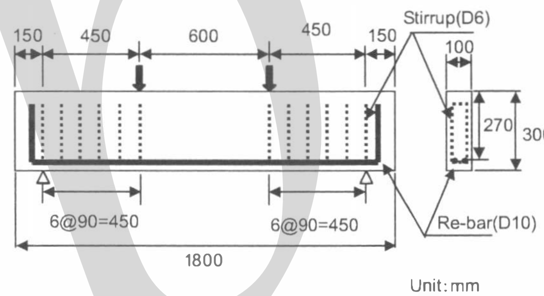

Fig. 1 Test setup (Larger specimen)

3 CRACK INJECTION REPAIR BASED ON FRACTURE CONTROL DESIGN CONCEPTS

3.1 Fracture control design concepts in crack injection repair

Figure 2 shows the crack patterns depend on the type injection. It can be observed that new cracks propagate through either the injection materials due to cracking of the injection itself, or the bulk concrete. The concept that new cracks form through the injections, however, helps to detect the new cracks in repaired concrete structures. After repairing the cracks, only the repaired cracks should be inspected.

3.2 Performance of repaired specimens depends on un-injected cracks

The relationships between moment and curvature in larger specimen are shown in Figs. 3(a) and 4(a), and the crack opening displacement of each crack in repaired specimens is shown in Figs. 3(b), (c) and 4(b), (c). For the un-injected cracks, the opening displacement became larger with increasing applied load. The un-injected cracks having larger crack width in each loading level would affect not only the mechanical behavior of repaired members but also the durability related to permeability of substance. For a durable repair in severe conditions, the un-injected cracks in concrete structures

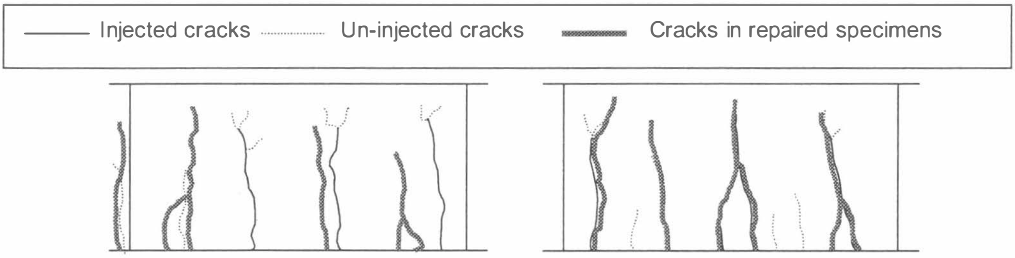

(a) Epoxy injection(Specimen No. 1) (b) Polymer cement slurry injection(Specimen No. 4)

Fig. 2 Examples of crack patterns in moment span of larger specimens

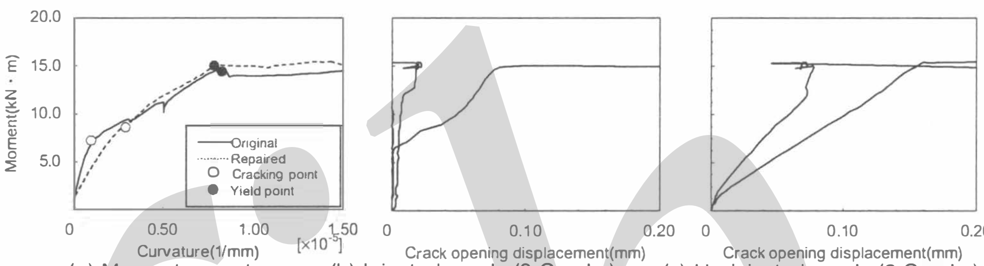

(a) Moment-curvature (b) Injected cracks(3 Cracks) (c) Un-injected cracks(2 Cracks)

Fig. 3 Results of larger specimens with epoxy injection(Specimen No. 1)

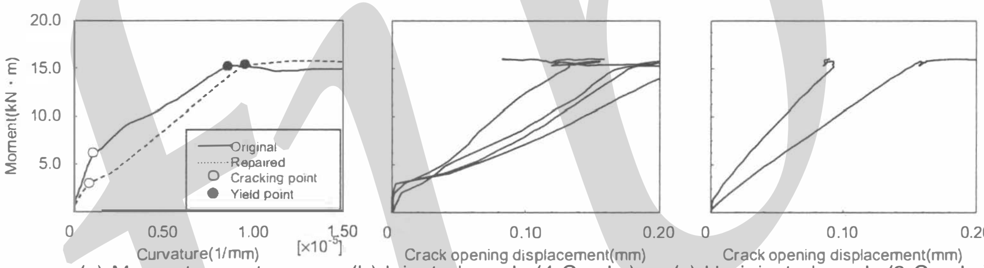

(a) Moment-curvature (b) Injected cracks(4 Cracks) (c) Un-injected cracks(2 Cracks)

Fig. 4 Results of larger specimens with polymer cement slurry injection(Specimen No. 4)

should be detected, or injecting and coating techniques should be used together.

4 CONCLUSIONS

The fracture control design concepts in the crack injection repair were discussed. The following conclusions were obtained:

(1) Two typical cracking behaviors due to the difference of injections could be observed; either new cracks form through the injections due to cracking of the injection material, or new cracks propagate through the bulk concrete. This cracking behavior could be also observed through the moment-curvature relations.

(2) The crack injection repair based on the fracture control design, in which the new cracks propagate through the injections, helps to monitor the repaired structures in a maintenance framework.

(3) Locally, the opening displacement of the un-injected cracks was larger than that of the injected cracks at lower loading levels. Repair strategies that focus on the un-injected cracks in crack injection repair are also important for a durable repair.

REFERENCES

[1] P. H. Emmons : Concrete Repair and Maintenance Illustrated, R. S. Means, 1993

IMPROVEMENT IN PERFORMANCE OF CONCRETE STRUCTURES BY USING SANDY FIBER MESH

Hiroshi Nakai
Sumitomo Construction Co., Ltd.
JAPAN

Norio Terada Atsushi Honma Koichi Nishikawa
Japan Highway Public Corporation
JAPAN

Keywords: spalling off, durability, aramid fiber mesh sheet

1. INTRODUCTION

In the search for durability, the Japan Highway Public Corporation is studying the application of fiber-reinforced concrete. In part, this has involved the trial application of a construction method of wrapping bridges with fiber sheet. This was performed on newly constructed bridges over highways and main line bridges over principal trunk roads. This construction method improves durability by suppressing initial cracks, and lessens the risk of damage to third parties by preventing spalling off when concrete deteriorates in the future.

As shown in Fig. 1, the SAM method involves lining the form with fiber sheet before concreting, thus placing the fiber sheet, coated with silica sand, near the concrete surface. The function of the fiber sheet is to control the crack width and to enhance durability by preventing spalling off in the future. Fiber sheet (SAM sheet) is a combination of aramid fiber bundles placed in three directions, coated with silica sand on one side (see Fig.2). Aramid fiber bundles having strength per piece of 740N provide capacity of 30kN per meter of SAM sheet.

2. SPALLING OFF PREVENTION PERFORMANCE

We conducted experiments to simply evaluate spalling off prevention under severe conditions. RC specimens were a height of 400mm and a width of 200mm. Pressure was applied to the covering thickness of 45mm, using chemical splitting agent, by assuming expansion of reinforcement.

Extreme spalling off occurred on the reference specimen without SAM sheet, no spalling off occurred and the crack width was controlled in the specimen with fiber sheet placed on three sides. It is apparent that spalling off prevention is substantially improved by incorporating SAM sheet (Fig.3).

3. AXIAL TENSILE TEST

We conducted axial tensile test, and used the diameter of reinforcement and the presence or absence of SAM sheet as parameters. Axial tensile tests were conducted using a specimen having a deformed bar at the center, a cross-section of 100 x 100 and a length of 1000mm, as shown in Fig.4. The loading pattern adopted is as follows: after a new crack was detected, the load is removed once and, after installing a pi-gauge, the load is gradually increased. This pattern was repeated until the fifth crack was detected. After detection of the fifth crack, the load was increased continuously until the average strain reached a value three times as large as the yield strain of reinforcement.

Fig.5 shows the relationship between the load and the average crack width for each specimen. This figure shows that the crack width is less, for a given load, when a larger diameter of reinforcement is used and also, when SAM sheet is used, the crack width tends to be less as the number of sheets used increases. It is qualitatively considered that the SAM method does functionally reduce the crack width.

4. APPLICATIONS

The Japan Highway Public Corporation started trials of the spalling off prevention method using sandy tri-axial aramid mesh sheet in April 2000, and used 18,000m² of SAM sheet in 15 bridges at 11 sites in fiscal 2000. Additionally, the use of 30,000m² of this sheet is expected in fiscal 2001. Use of this sheet has also begun in other public construction work, and we expect that the performance requirements for newly installed structures with critical crossing conditions will include spalling off prevention performance as well as improved durability.

5. CONCLUSIONS

The principal objectives of the SAM method are the prevention of spalling off and the improvement of durability, and then the results of axial tensile tests and axial compression tests indicate an improvement in the dynamic performance of concrete structures. It is our intention to clarify other performance aspects of this method, such as the control of cracks in concrete structures.

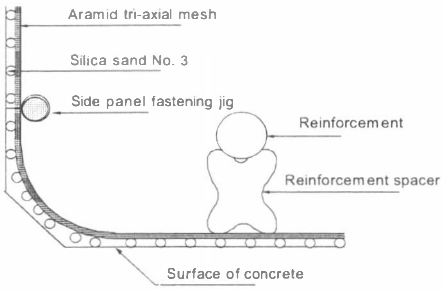

Fig. 1 Outline of the Placement of Fiber Sheet

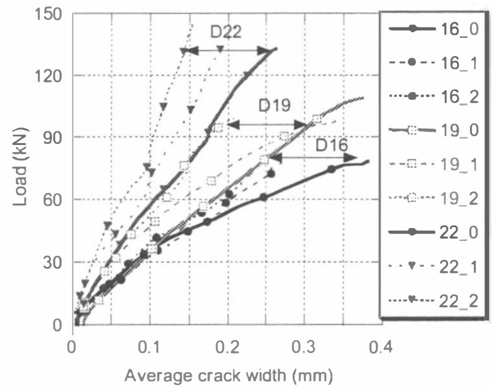

Fig.5 Relationship Between Load and Average Crack Width
(Ex: 16_1 16=Rebar D16 / 1=SAM sheet 1layer)

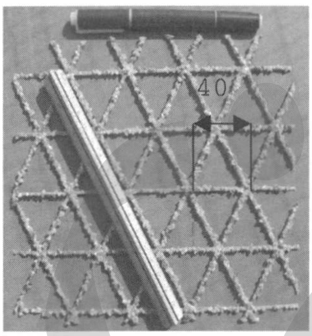

Fig. 2 SAM Sheet (Sandy Face)

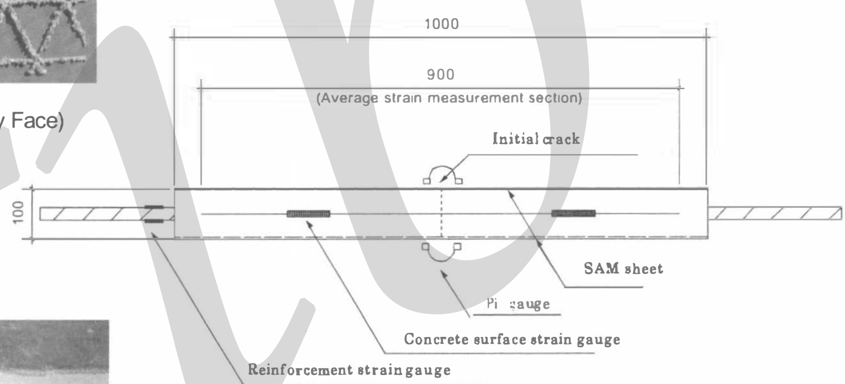

Fig.4 Outline of the Axial Tensile Test Specimen

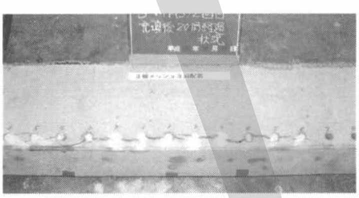

(a) Specimen with SAM sheet

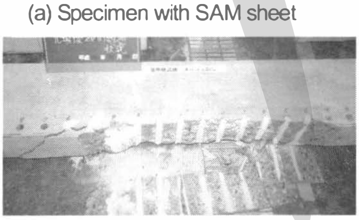

(b) Reference specimen

Fig. 3 Result of force spalling off tests

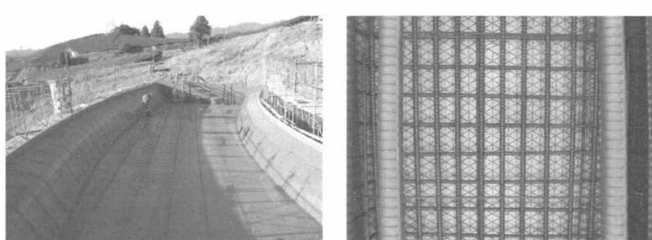

Installation of sheet on an over bridge At the main girder

Fig.6 Application of the SAM Method

COUNTERMEASURES AGAINST THE EXFOLIATION OF COVER CONCRETE USING FIBER REINFORCED CONCRETE

Keiichi Aoki
Japan Highway Public Corporation
Engineering Department, JAPAN

Shuichi Okamoto Kazunao Yokota Yoshihiro Tanaka
TAISEI Corporation
Technology Center, JAPAN

Keywords: polypropylene fiber, exfoliation, cover concrete

1 INTRODUCTION

At the bridge over major trunk lines such as roadways, highways, and railways, there is high possibility of leading some accident due to exfoliation of covering concrete. It is considerably difficult to inspect and execute due to problem of traffic regulation such as close traffic when future maintenance or repair are concerned.

Accordingly, under the guidance of The Bridge and Structural Engineering Division of Japan Highway Public Corporation, a study for fiber reinforced concrete for precautionary measures (arrangement of net fiber and mixture of cut fibers) is now being carried out.

This paper presents the results of the studies that the precautionary prevention measures for exfoliation of cover concrete using polypropylene fiber reinforced concrete on the laboratory or the site, and the concreting of the actual bridge.

2 OUTLINE OF FIBER

Polypropylene cut-fiber used for this time, is called "BARCHIP" that was developed by Taisei Corporation in cooperation with Hagiwara Kogyo. The fiber, as shown on Photo.1, is the organic fiber with the length of 30mm and the specific gravity of 0.91. This has a tensile strength of 440 N/mm^2 and a modulus of elasticity of 9800 N/mm^2. The characteristic of this fiber is that the surface of the fiber is processed to make uneven, is executed a special process to get not repel water, and is carried out to improve its bond with cement matrix and its dispersion of mixer performance.

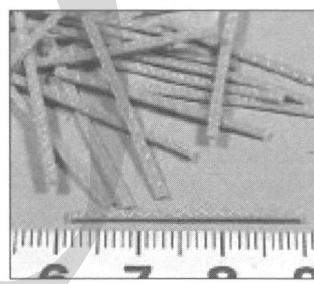

Photo.1 Polypropylene fiber

3 CHECK TEST FOR EXFOLIATION RESISTANCE AGAINST AGAINST FATIGUE LOAD

Fig.1 shows an outline of the bending fatigue test. The simulated exfoliation part that is supported by only fiber that was located under edge of the beam center for check the exfoliation resistance due to mixture of fibers. There are 3 cases as 0.25, 0.5, and 1.0 vol.% for the fiber contents. The condition of load was set up to be occurred the allowable stress (184N/mm^2) and 90% of the yield stress (347N/mm^2) of reinforcement. The load carrying speed was 1 Hz. At this fatigue test, there was no falling of the simulated exfoliation section for all cases. In the case of specimen with 0.5 vol.% fiber contents, there was also no falling even though 2 million times by the allowable stress. Moreover, as shown on Photo.2, the simulated exfoliation section was also no falling when gentle load was given until compressive edge was destroyed.

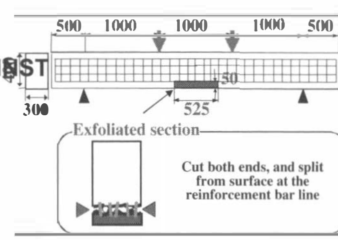

Fig.1 The test beam

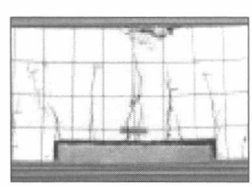

Photo.2 Exfoliation section after

4 EXECUTION TEST AND APPLICATION OF POLYPROPYLENE FIBER TO THE ACTUAL BRIDGE

4.1 Pumping test

The total length of pipes is about 50m or about 76.5m as exchanged horizontal conveying distance. The pumping were carried out with 3 different speed such as 10, 20, 40m^3/h. As items to be tested, a quality of the fresh concrete at before and after pumping, the compressive strength, and the pressure loss in pipe were measured. Generally, the slump and air content were no major changes after pumping. Also there was no trouble such as blockade of pipe occurred when pumping was suspended for maximum 54 minutes and then restarted. The pressure loss in pipe is conceivable that fiber reinforcement concrete has similar quality to the high-strength concrete used superplasticizer. Therefore, there is no problem to pumping the fiber concrete with fiber contents of 0.5%, fundamentally, in case of possibility of pumping by base concrete.

4.2 Application of fiber concrete to the actual bridge construction

The bridge that was applied polypropylene fiber concrete was “2nd Meishin expressway Yamamura-1 bridge” of the Japan Highway Public Corporation / Chubu Regional Bureau / Yokkaichi Construction Branch. The details of the bridge are as follows: the length is 52 meters, the effective width is 19.94 meters, and the structure is PRC with two-span continuous three main girders. The quantity of concrete for casting concrete was approximately 620 m^3 and it was concreted by 95m^3/h of speed using 3 pumping cars. Photo.3 shows the reinforcement arrangement of a web, and Photo.4 shows concreting. The result of measurements of slump and air content were within the limits of control. There were no troubles occurred during concreting. The workability of polypropylene fiber concrete was the same as common concrete. From the result of measurement of the fiber contents in fresh concrete by the water screening test, It was confirmed that only agitating fibers during transportation of concrete can be fully fixed and dispatched; the average of fiber contents was 0.51% and the standard deviation was 0.019 against 24 times of measurements.

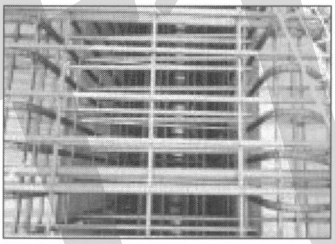

Photo.3 Reinforcement arrangement at a web

Photo.4 Concreting polypropylene fiber concrete

5 CONCLUDING REMARKS

The possibility of exfoliation of covering concrete would be extremely low if normal design and execution management have been carried out. But it is difficult that to keep away from some cracks due to unexpected load, drying shrinkage or cracks of corrosion expansion due to the influence of carbonation. In the worst case, covering concrete might be exfoliated.

The execution method that is introduced for this time, is studying from a standpoint as “Do not make to exfoliate concrete piece if covering concrete will be exfoliate” by the effect of restriction of chips. Furthermore it can be expected for fiber reinforcement concrete to control initial cracks due to drying shrinkage. Therefore in the future, we would like to study this method as an overall.

REFERENCES

[1] JSCE : Execution guide of concrete pumping, Concrete Library, No.100,2000

BASIC PROPERTIES OF SHOTCRETE TO CONTROL WEATHERING OF ROCK-BED

Hisatoshi SHIMADA, Fumio TAGUCHI, Susumu YOSHIDA, Isao YAMAZAKI
CIVIL ENGINEERING RESEARCH INSTITUTE OF HOKKAIDO, JAPAN

KEYWORDS: shotcrete, yield value, plastic viscosity, rebound, discharge rate of concrete

1. INTRODUCTION

To prevent small and large rock falls on rock slopes, measures to control rock bed weathering and crack development must be taken. In this prevention, mortar concrete spraying has been conducted conventionally. Shotcrete has been used for protection and reinforcement of rock slopes, as well as for primary lining of tunnels in the NATM method and various other applications. It has also been used for repair and reinforcement of concrete structures in recent years. However, because the quality of shotcrete depends greatly on working conditions and worker skill, especially of the nozzle man, and quality varies more greatly than normal concrete due to the specifics of the construction method, there is doubt in its reliability as a concrete structure.

While research on the clarification of the mechanism of shotcrete has been active in recent years, mainly concerning the NATM method, research has seldom been conducted on pumping capacity and workability of shotcrete for protection of rock bed. Because the composition of and construction methods for shotcrete are different for NATM and protection of rock bed, types of concrete and construction machinery suitable for the respective conditions of use are employed. It is therefore impossible to apply the research results obtained from shotcrete for NATM directly to shotcrete for protection of rock bed.

Under such circumstances, the authors have conducted compressive strength, bending, bond strength and freezing-thawing tests for shotcrete used for controlling weathering of rock bed and small rock falls, and have studied basic properties required for shotcrete[1][2]. As a result, it was revealed that these properties were influenced greatly by internal defects caused by discharge properties or force-feed conditions rather than by the properties of the concrete itself.

In this study, the effects of the fresh properties of concrete on pumping capacity and workability using non-AE, AE and fiber reinforced concrete with different cement contents and water-cement ratios were investigated, with the purpose of stabilizing the quality of shotcrete used for prevention of weathering of rock bed.

2. TEST RESULTS AND DISCUSSION

Table 1 shows the apparent yield value and apparent plastic viscosity. The apparent plastic viscosity tended to increase when steel fiber was mixed, while it did not vary greatly by the difference in the cement content and unit water volume. It indicates that the separating resistance of fresh concrete increased by mixing steel fiber.

Figure 1 shows the relationship between the discharge rate and slump. The discharge rate of concrete tended to increase with an increase in slump. The discharge rate decreased when steel fiber was mixed.

Figure 2 shows the relationship between the pressure in the pipe and slump. The initial pressure of the spray machine tended to increase with an increase in slump. The pressure in the pipe also tended to increase with an increase in plastic viscosity.

One reason for such tendencies of the discharge rate and slump was the use of a rotor-type spray machine. The discharge rate was considered to have increased because the volume of concrete filling each cylinder would

Table 1 Apparent yield value and apparent viscosity

Symbol	Apparent Yield Value (N·cm)	Apparent Viscosity (N·cm·min)	Slump (cm)
Plain	13.51	0.052	2.4
C390	6.90	0.048	7.4
C420	3.69	0.034	21.0
W180	10.17	0.047	5.6
W189	5.85	0.049	7.4
AE	10.14	0.070	5.8
AEST	10.68	0.125	8.2
ST	—	—	2.4

increase with an increase in slump in the case of a rotor-type spray machine.

A possible reason for the increase in pressure of the spray machine with an increase in slump is as follows: If there is an object inhibiting air flow in the pipe, the air pressure increases to force the object out. This pressure is believed to be determined by the proportion of the inhibitor to the cross section of the pipe. In this study, as mentioned above, the concrete volume per discharge into the pipe increased with an increase in slump and the proportion of concrete to the cross section of the pipe increased, causing an increase in pressure of the spray machine.

The pressure at each measuring point of the pipe was thought to have increased because the frictional force generated between concrete and the pipe wall increased with an increase in plastic viscosity.

The reason for a decrease in discharge pressure by mixing in steel fiber is regarded as follows: A decrease in discharge rate means the consumption of more time for spraying the same amount of concrete. As mentioned above, material adhered to the pipe wall for a longer period of time when concrete with a high plastic viscosity was force fed, due to the larger friction force generated between concrete and the pipe wall. It was therefore expected that the discharge rate would decrease in cases where steel fiber was mixed.

Figure 3 shows the relationship between the rebound ratio and discharge rate. It includes the data of tests conducted in the past, and the rebound ratio tended to decrease with an increase in discharge rate and began to increase again at a certain point.

The cause for the re-increase of the rebound ratio was thought to be that the volume of sprayed concrete that runs down without adhering increases with an increase in flowability even if the discharge rate also increases with an increase in flowability as shown in Fig. 1 above.

An increase in discharge rate can therefore be effective in reducing rebound loss. Close attention is however required in spraying concrete with high flowability because it may run down without adhering.

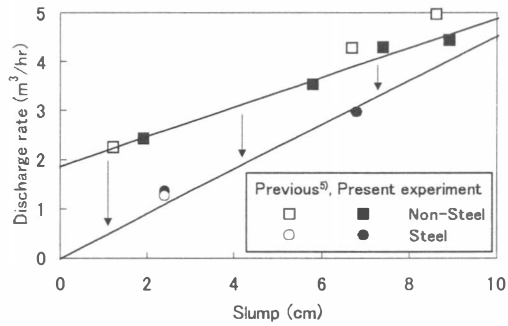

Fig. 1 Relationship between discharge rate of concrete and slump

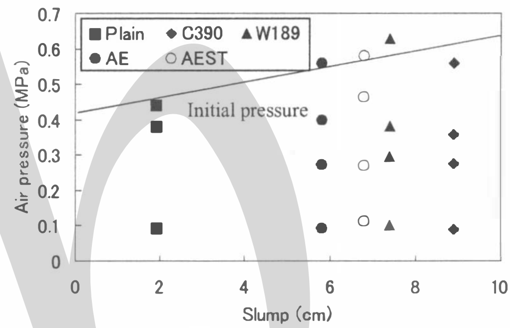

Fig. 2 Relationship between air pressure and slump

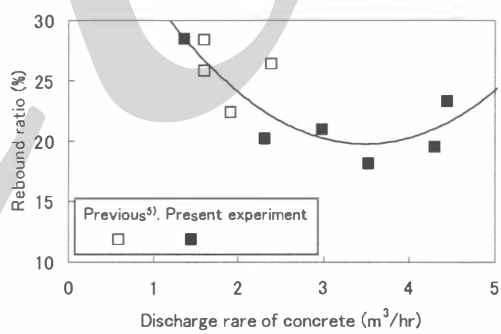

Fig. 3 Relationship between rebound ratio and discharge rate of concrete

REFERENCES

[1] YOSHIDA Susumu et al.: Freezing-Thawing Resistance of Shotcrete for Controlling Weathering of Rock Bed, 55th Annual Meeting of the Japan Society of Civil Engineers, V-228(2000) (in Japanese)

[2] YAMAZAKI Isao et al.: Fresh Properties of Shotcrete for Controlling Weathering of Rock Bed. Hokkaido Branch of the Japan Society of Civil Engineers, No. 56, Section V, pp.476-479 (2000) (in Japanese)

DEVELOPMENT AND APPLICATION OF POLYMER IMPREGNATED CONCRETE

Tsuyoshi Tanaka Dr. Ken Tsuruta Dr. Takafumi Naitou
Ozawa Concrete Industry CO.,LTD,JAPAN

Keywords : PIC, permanent form, durability, efficiency of construction

1 INTRODUCTION

The research and development of Polymer Impregnated Concrete (PIC , hereafter) has been conducted since 1960's and in 1970s[1], the method impregnating polymer partially into the surface concrete of structures such as road bridges slab and hydraulic dam came into practical use in the U.S In Japan, several type of PIC products have been developed[2], but most of those products have not applied to practical use because of technical and economical problems.

Permanent concrete formwork panel made of PIC (PIC form, hereafter) has been developed in 1985, and it is now widely known as practical application of PIC. At present, more than 100,000m^2 of PIC form have been used in concrete structures in Japan. This paper describes the outline of development and application of PIC form.

2 SUMMARY OF PIC FORM

The PIC form is a precast concrete panel fully impregnated with polymer and has a thickness ranging from 15～100 mm. The surfaces of the PIC form which come into contact with placed concrete are treated in a special manner to assure a high bond capability of the PIC form with placed concrete.

The typical mixture of base concrete consists of normal portland cement ,river sand and river gravel, as shown in Table 1,and the compressive strength of the base concrete is usually 40 N/mm^2.

Table 1 Mixture of base concrete

Gmax (mm)	W/C (%)	S/a (%)	Unit Volume (kgw/m^3)					
			W	C	S	G	Fiber	Admixture
10	35	58	175	500	958	715	95	3.5

The manufacturing process of PIC form is as shown in Fig.1. The impregnating liquid is methylmetacrylate (MMA).

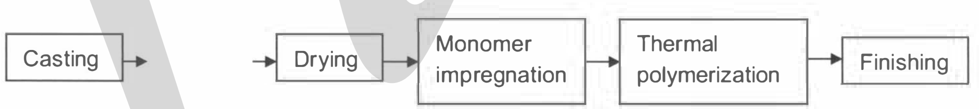

Fig. 1 Manufacturing process of PIC

The PIC form has a roughened back surface as shown in Fig.3,so it showed excellent bond strength with placed concrete.

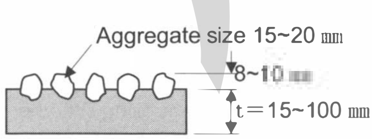

Fig. 2 Section of PIC form

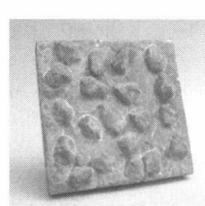

Photo 1 Back surface of PIC form

Photo 2 PIC form for round section

Table 2 Results of the physical property test of PIC form

Test Contents		Test Result
Compression strength	ϕ 10×20 cm	120～150 N/mm^2
Modulus rupture	10×10×40 cm	24.0 N/mm^2
Splitting strength	ϕ 15×15 cm	8.0 N/mm^2
Young's modulus	ϕ 10×20 cm	4.0×10^4 N/mm^2
Poisson's ratio	ϕ 10×20 cm	0.2
Specific gravity		2.4
Coefficient of linear expansion	−40℃～+50℃	1.1×10^{-5}/℃

3 APPLICATION OF PIC FORM

PIC form has been used in various types of concrete structures. The rates of its application on new structures and old structures for repair are both 50%. And 70% of PIC form have been used to improve the durability of structures, and 30% have been used focusing on the efficiency of construction.

In harbor structure and water tunnel, the main purpose of the use of PIC form is mostly improving the durability of structures, and in concrete bridges and steel framed reinforced concrete structure, the main purpose is mostly improving the efficiency of construction. However, the both purposes can be expected in a high durability of construction by the use of PIC form.

Table 3 States of application of PIC form

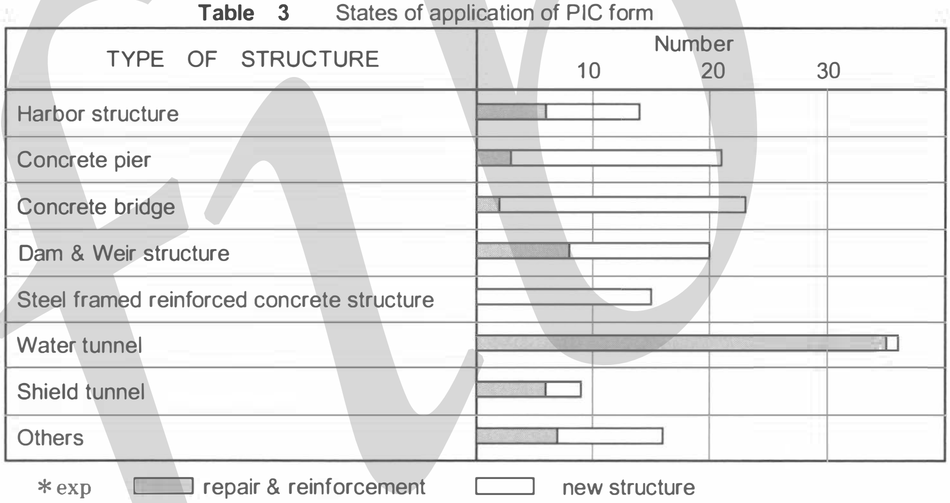

4 EXPECTATION IN THE FUTURE

In Japan, the durability of structures is regarded as of major importance, since the introduction of performance evaluating design method. And repair of old structures is increasing in recent years.

PIC form, which utilizes superior property of PIC and is ideal method to cope with those situations, will be used more widely in the future.

REFERENCES

[1] W.Glen Smoak : Surface Impregnation of New Concrete Bridge Decks ; Public Roads Vol.40 No.1, 1976

[2] T.Tazawa : Fundamental Study of PIC Products ; Concrete Journal Vol.9 No.1, 19

[3] Public Works Research Center : The Recommended Practice [PIC form] of The Ministry of Construction in Japan [PIC form],1994

PERFORMANCE TESTS OF PRECAST PRESTRESSED CONCRETE SLABS PRODUCED USING GROUND GRANULATED BLAST-FURNACE SLAG (6,000 cm^2/g)

Hiroshi Yokoyama*, Shigeharu Takano*
*Abc Kogyosho Co., ltd.
3-13-3 Rokujyo Omizo, Gifu, Gifu 500-8638, JAPAN

Hideaki Sakai**,
** Japan Highway Pubulic Corporation
4-16 Tukasa, Toyota, Aichi 471-0831, JAPAN

Keywords: ground granulated blast-furnace slag, prestressed concrete, precast slab

1 INTRODUCTION

The economical plate girder system is adopted for the entire The New Tomei and Meishin Expressways, which have prestressed concrete (PC) slabs and girder spacing of approximately 6 m (Figure 1). The structure is developed to rationalize the construction and reduce the construction costs and labor by increasing the cross sectional areas of the main girders using the recently developed techniques for manufacturing and welding thick steel plates, which enable to reduce the number of main girders. To further rationalize construction and reduce construction period and costs, Precast PC slabs manufactured in factories are used on the expressways (Figure 1).

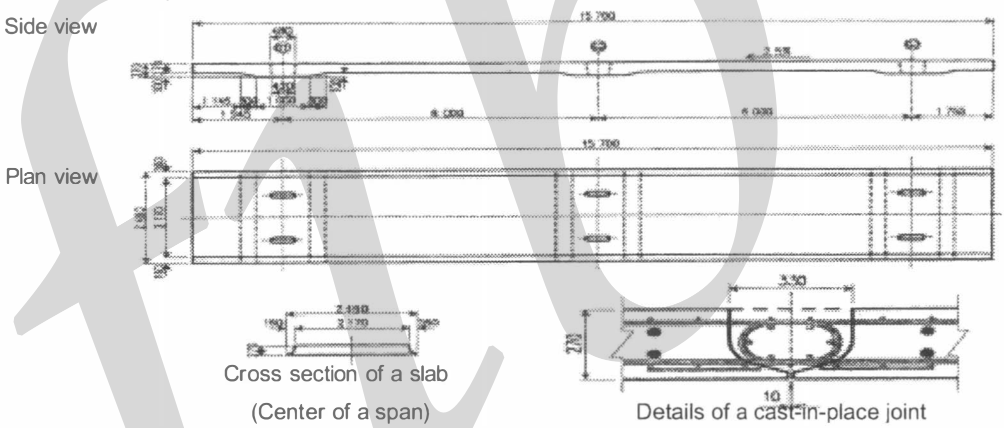

Figure. 1 Precast prestressed concrete slab

This paper describes the performance tests of precast PC slabs that were manufactured by substituting part of rapid hardening Portland cement by ground granulated blast-furnace slag.

2 APPLICATION TESTS OF THE GROUND GRANULATED BLAST-FURNACE SLAG FOR PRECAST PC SLABS

Before the production of the precast PC slabs that are shown in Figure 1 using the ground granulated blast-furnace slag, the following performances were tested since blast furnace slag had not been used to produce such large slabs:

The performance tests compared concrete specimens that were made of only high-early-strength Portland cement and those that were produced by substituting 50% of the Portland cement by ground granulated blast-furnace slag of 6,000 cm^2/g to examine the applicability,especially considering with the shrinkage.

2.1 Drying shrinkage of the concrete specimens

The concrete was tested for drying shrinkage in a laboratory to examine the shrinkage of the concrete. The shrinkage was tested by also considering the standard steam curing at the prestressed concrete factory.

The measurements according to the JIS A 1129 are shown in Figure 2. The tests showed that the shrinkage was larger in the blast furnace concrete than the rapid hardening concrete initially, but was similar in both concretes in long terms.

So, concrete produced using ground granulated blast-furnace slag are possibly treated as the conventional concrete in long terms.

2.2 Shrinkage of full-scale slabs

Figure 3 shows the strain histories of the full-scale concrete slabs, including the shrinkage at the points of monitoring (autogenous and drying shrinkage), prestress, creep of prestress, and all other effects by temperature change.

It is conclude that the strain of the full-scale concrete slabs are strongly affected by the temperature change of the steam used for curing up to the material age of 3 days. The histories of shrinking strain were derived for the 3-day full-scale concrete slabs. A comparison of shrinking strain after derived between the blast-furnace and rapid hardening slabs is shown in Figure 4 with the design strain.

The strain monitoring of the full-scale specimens showed that the shrinkage of the concrete slab produced using the ground granulated blast-furnace slag is equivalent to that of high-early-strength concrete slabs in long terms and satisfies the design shrinkage.

3. CONCLUSION

Analyses were conducted to compare the concrete made of high-early-strength Portland cement and the concrete made using ground granulated blast-furnace slag at a substitution ratio of 50%, such as mixing tests, material tests, and test preparation of full-scale precast prestressed concrete slab specimens. The applicability of the slag to produce precast prestressed concrete slabs was tested and confirmed.

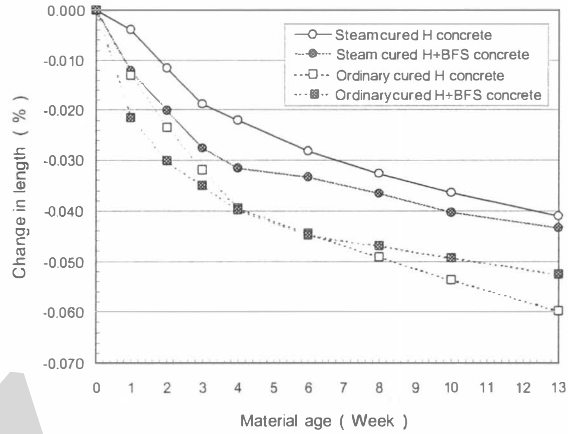

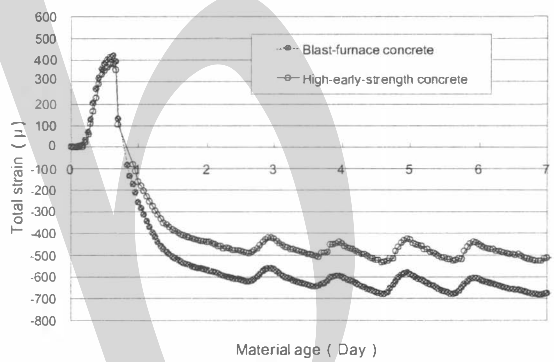

Figure. 3 Total actual strain behavior of full scale concrete slab

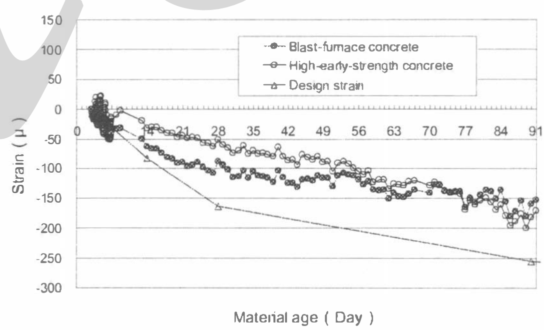

Figure. 4 Shrinkage and design strains of full scale concrete slabs three or more days after placing (values of three days after placing were put as zero)

PRESTRESSED CONCRETE PAVEMENT AND LIFT-UP METHODS FOR CONSTRUCTION OF TOKYO INTERNATIONAL AIRPORT

Kiyoshi Usuda
P.S. Corporation
JAPAN

Hisaaki Kato
Director of Tokyo International Airport Construction Office
Ministry of Land Infrastructure and Transport , JAPAN

Keywords: airport, prestressed concrete pavement, lift-up method, grout

1 INTRODUCTION

In Japan, most principal cities are located near the coast since its central areas are mountainous. It is difficult to acquire large sites in inland districts to construct airports, and many airports are therefore built on reclaimed land sections from the sea, such as the Tokyo International Airport, which is the first international airport in Japan. To construct airports on a reclaimed land section, various technological problems must be solved, such as uneven settlement of the ground.

The conventional methods for repairing the concrete pavement of aprons needed to suspend the use of the airport for a certain period of time to replace, overlay, and cure concrete.

An epoch-making method, which is called the lift-up method and uses prestressed concrete pavement (hereinafter referred to as the "PC pavement"), was developed and implemented to repair the inclination of the aprons by working in the nighttime and using the airport in the daytime.

In the Offshore Extension Project of Tokyo International Airport, the pavement structures were determined by predicting the amount of settlement. The PC pavement is used for 1) aprons that were predicted to have large residual settlements and are heavily used, 2) and aprons on which a cargo terminal was built, which was predicted to have a smaller settlement than the peripheral area since there was an underground structure.

2 LIFT-UP METHOD

2.1 Outline of the lift-up method

The lift-up method restores a subsided concrete pavement section by installing exclusive motor driven hydraulic jacks on the section at predetermined intervals (approximately 5m), controlling the jacks with a computer to simultaneously apply pressure to a PC pavement slab and reaction slabs on the base course of the pavement, lifting the PC pavement slab to a predetermined height, and filling the gap between the slab and the base course with grout.

2.2 Determination of the lift-up process

To control cracks on PC pavement slabs to not exceed the allowable crack values determined by the design while lifting up, the stress of the PC pavement slabs were determined by finite element analysis. The finite element analysis to derive the dead weight from a given design lift-up height was performed by assuming a flat plate on the elastic ground, following the assumption of Winkler for the reaction of the ground, and assuming that the ground reaction becomes zero when the PC pavement plates are lifted up from the ground.

The reaction of jacks and the amount of grout were also determined. The height of lifting was determined to not exceed the predetermined maximum value.

3 DEVELOPMENT OF GROUT MATERIALS

Grout materials are gravitationally filled in the space between a lifted up PC pavement slab and the base course. Therefore, the grout materials must be flowable and have small bleeding percentages to not leave voids beneath the slabs after hardening.

To execute lift-up works in the nighttime and to use the entire airport from the early morning, there were only two hours to cure the grout. Materials were selected from those that show the required strength in two hours.

3.1 Determining the strength of grouts

The strength of grouts was decided based on the following computational analyses:

(1) Computational conditions

The design load was four wheels of a leg of Boeing 747-400. The depth of the grout layer was assumed to be 10 cm based on the maximum height that can be lifted at once. Deformation moduli of 0.98, 2.9, 4.9, 9.8, 49, 98, and 196 N/m2 were used. The depth of a PC pavement slab was assumed to be 18 cm.

(2) Computational methods

1) Analysis by multi-layer elasticity theory (BISAR)

The BISAR analysis analyzed five layers from the surface to the subgrade.

2) Finite element analysis (three dimensional finite element method)

Finite element analysis was conducted by substituting the part lower than the PC pavement slab and the grout layer by a spring. The spring constant was K75 = 0.07 KN/mm3, which is the coefficient of bearing capacity of the base course that the Design Manual for Airport Concrete Pavement prescribes for PC pavement slabs.

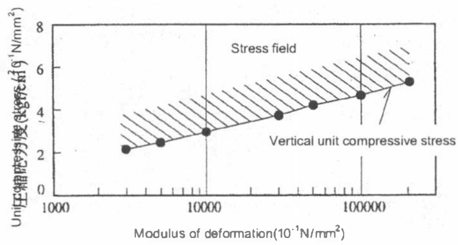

Fig.1 Unit compressive stress of grout layer (just after placement)

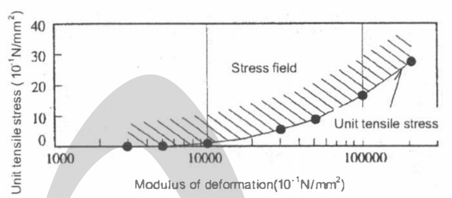

Fig.2 Unit tensile stress of grout layer (7 days after placement)

(3) Computational results

The relationships between deformation modulus and compressive stress that were derived by the two analytical methods are shown in Fig.1. Excessively large values were excluded. Based on the design concept described above, the 7-day compressive strength of at least 2 N/mm^2 was used, which corresponds to the hatched area in the figure. The relationship between deformation modulus and tensile strength are shown in Fig.2. Since the tensile strength was possibly not accurate for materials with small deformation moduli, the materials of 7-day strengths in the hatched area were used.

4 ACTUAL LIFT-UP WORK

The Tokyo International Airport has been repaired five times using the lift-up method to correct the inclination of the aprons. The analytical results of a lift-up process are shown in Table 1.

Grouting was conducted every day from 23:00 to 6:00. Approximately 750 m3 of grout was applied to correct the inclination of 21,000 m2 in 6 months.

No abnormality of the PC slabs was observed during nor after the work. The lift-up method was shown to be a technical solution against uneven settlement of the ground.

Table1 Computational results of lift-up process

Stage	Step	Lift-up length (mm)	Volume (m^3)	Displacement measuring point	Lift-up point	20t-25t point	Maximum value (t)	Vuffer slab (m^3)	Total (m^3)	Day
1	1	20	9.04	50	47	1	24.90	0.00	9.04	1
2	2	18	13.33	53	48	2	21.27	0.00	13.33	2
2	3	18	12.83	49	49	0	19.88	0.00	12.83	3
3	4	18	12.45	59	51	1	23.72			
3	5	18	8.86	48	48	1	20.90	0.00	21.31	4
3	6	18	8.43	46	46	1	20.37			
3	7	18	7.41	44	44	0	19.15	0.00	15.84	5
↓	↓	↓	↓	↓	↓	↓	↓	↓	↓	↓
6	36	12	7.28	56	52	0	17.32			
6	37	12	7.08	56	52	0	18.71	0.29	14.65	38
6	38	12	6.97	56	52	0	19.96			
6	39	12	5.56	55	39	1	21.77	1.52	14.05	39
		Total	728.72		4472			16.32	745.04	39

THE EFFECTIVE APPLICATION OF QUALITY ASSURANCE PRINCIPLES FOR PRODUCING DURABLE CONCRETE STRUCTURES THE PROBLEMS AND THE SOLUTIONS

Stuart Curtis
(Retired) Manager, Bridge Construction Services
Roads and Traffic Authority, New South Wales, Australia
Keywords: concreting processes, preventive planning, pre-contract communications

1 QUALITY ASSURANCE ------ IS IT WORTH THE EFFORT?

The experience of many engineers and concerned construction personnel around the world is that quality assurance (QA) has not given them **assurance** about the **quality** of their concrete structures. The increasing implementation of QA contracts over the last 15 years has coincided with an increasing recognition that the durability of many of our recently built concrete structures is significantly lower than for most of those built several decades ago. To design and construct for a predictable service life of 100 years is now a major challenge, requiring effective pre-contract communication and on-going partnering, involving all parties, including sub-contractors and suppliers. The potential construction and contractual problems need to be identified by the client and/or designer/specifier, and addressed by the tender documents in such a way that all tenderers are required to plan for, describe, and provide clearly in their tender price for appropriate preventive actions .[1]

Early in the planning for the massive Storebaelt Project in Denmark, involving two great bridges and a tunnel, the construction authority, A/S Storebaeltsforbindelsen, (ASS), made a brave decision ***"to specify that all work should adhere to QA standard ISO 9001, which requires that the contractor throughout the contract period in due time demonstrates that work methods, execution, and inspections are being planned and documented efficiently."***[2]

ASS has recently published a fine book on the Storebaelt Project which includes some honest appraisals of the successes and failures in the execution of the various contracts. Unfortunately, because of the initial decision to prescribe a very complex concrete mix which imposed very narrow tolerances; the resulting contractual disputes, and subsequent massive payouts, have clouded the industry's recognition of the major advances which were made.

2 ADAPTING ISO 9001 FOR CONCRETE CONSTRUCTION

Construction by QA contract is becoming increasingly common, at least in Europe, and in 1997, one of fib's predecessors, CEB, published a Bulletin providing guidelines ***"to assist in the creation and implementation of a user friendly and flexible quality system based on the ISO 9001 series"*** [3] However, additional guidelines and examples are needed in view of the major changes in ISO 9001:2000. Such guidance is necessary because ISO 9001 was developed for factory-based manufacturing industries, and focuses on the inspection and testing of product samples. Consequently ISO 9001 assumes that all processes can be controlled, whereas most concreting processes can't be fully controlled, because they are subject to the vagaries of weather and other site and human factors which are partly uncontrollable. Therefore to meet the needs of the construction industry, there needs to be a major refocusing on the quality system elements of **validation** and **monitoring**, (previously process control),**purchasing**, (subcontracting),and **preventive/corrective action**.

To illustrate this need, reference is made to the following quote from the ASS Book, "***Supervising an ISO 9001 contract faced the staff with tasks that for most were quite unfamiliar****: evaluation of quality planning, and of suppliers and sub-contractors, supervision of (QA system) corrections, the use of audit results, and evaluation of education and training, are not traditional supervision activities.* ***These required training in audit techniques rather than technical skills."*** To that last sentence the author would like to shout **"No, no, no!"** The experienced design and construction engineers working for the client or the prospective contractor must not let their project be hijacked by the "QA experts".

Auditing needs to be process-oriented, with the greatest focus on those processes with greatest risk. Audits and auditing requirements must be planned around identified problems, and effective auditing can only´be carried out by people with the relevant technical experience to visualize the processes and the potential problems associated with them. Furthermore, the critical construction and monitoring procedures need to be prepared and implemented by people with appropriate experience and authority as well as a belief that QA does work and a commitment to make it work. [1]

It must be realised that ISO 9001 is not a sacred document. Its principles can be applied effectively under a variety of contractual arrangements. For example, while it is usual in Europe for the contractor to be contractually responsible for monitoring the processes, recording non-conformities, and developing corrective and preventive actions, these responsibilities could be assigned to the client or his agent. Most importantly **ISO 9001 should not be regarded as a stand-alone document**. In a contract specification **it should be intimately linked with an interpretive document**, which makes the relevant ISO 9001 requirements specifically applicable to the critical construction processes. For example, in relation to validation of processes (clause 7.5.5 of ISO 9001: 2000), the client will need to state in the construction specification, which processes will require validation, and, if desired, any details of how the validation should be carried out, (including qualifications of inspectors etc)

3 REQUIREMENTS FOR DURABILITY

It is universally agreed that durability of reinforced concrete structures depends on the quality of the cover concrete. **The basic potential problem areas are** (a) **failure to achieve specified cover** (b) **failure to achieve specified quality of concrete** when compacted in the forms (for marine concrete the key requirement is resistance to chloride penetration) (c) **failure to apply specified curing**.

As a result of recent recognition of the widespread phenomenon of early age cracking in bridge decks and road pavements, [4] attention must also be paid to (d) **development of cracks, due to drying and autogenous shrinkage.**

Unfortunately, with the possible exception of cover distance, we don't have much confidence any more that currently specified, (often conflicting) prescriptive and/or performance requirements will ensure that the design minimum service life will really be achieved. Despite the tremendous amount of research that has been done around the world over the last five decades, the industry is still a long way from being able to specify durability requirements such that the performance of the completed structure can be effectively tested and verified. As has been stated in a recent paper [5] by one researcher who is trying to bridge the gap between concrete technology and structural design, **we must develop a methodology for specifying durability** which can build upon whatever levels of knowledge and experience are available, from prescriptive, deemed-to-comply requirements to methods involving testing for electrical resistivity or penetration of chlorides, and even diffusion coefficients.

One of the greatest disappointments for engineers and concrete researchers alike, is that it is virtually impossible to transfer the information gained on one project so that the it can be applied on another. This problem will not be solved until the industry can reduce the variability of concrete as it is supplied, and the inhomogeneity which is so often produced by nonconformities in the placing/compacting process, as well as irregularities in curing. Even on the same project, it is often difficult to compare the test results for the fresh and hardened concrete sampled during construction, with the preliminary mix design data. However, computer-simulation techniques developed in the last decade [6] appear to be opening the way for a systematic qualitative understanding of the many factors involved in the concrete hardening process. Provided concrete can be produced more consistently on site, it would appear that these computer simulation techniques could be harnessed to short cut the processes of property evaluation and service life prediction with a good degree of accuracy.

Effective QA is the missing factor without which the best efforts of concrete researchers and design engineers will not produce predictably durable concrete structures. The author advocates that these efforts be integrated through a co-operative international construction-site–based research project.

REFERENCES

[1].Curtis, S.: Design for durability by bridging the gap between designer's intent and construction contract practice. Proc. Fifth International Conference on Durability of Concrete, Barcelona, Spain. Supplementary Papers pp.823-837, 2000

[2].Gimsing, N.: Concrete Technology, publ. by The Storebaelt Publications, 271pp.,1999

[3].CEB Bulletin 234, Quality Management,(Guidelines for the implementation of the ISO Standards of the 9000 Series in the construction industry),1997

[4].Mehta, P.K., and Burrows, R.W.,: Building durable structures in the 21st century, Concrete International,Vol.23,No.3,March,pp 57-63,2001

[5].Andrade, C., Alonso C., Arteaga, A., and Tanner, P.,: Methodology based on the electrical resistivity for the calculation of reinforcement life, Proc. Fifth International Conference on Durability of Concrete, Barcelona, Spain. Supplementary Papers pp 899-915, 2000

[6].Bentz, D.,: Modelling cement microstructure; pixels, particles, and property prediction, Materials and Structures,Vol.32,No.217,April,pp 187-195,1999

CONTROLLED PERMEABILITY FORMWORK - FOR DURABLE CONCRETE

Morten Gantriis Sørensen
Technical consultant
Fibertex A/S, DENMARK

Keywords: Durability, Aggressive environment, Lifetime enhancement

1 INTRODUCTION

Concrete structures that are located in aggressive environment and not suitably protected against aggressive elements deteriorate very fast. Normally it is the diffusion of chlorides into the concrete that is the dominating factor in these structures deterioration. When the chlorides reach the re-bars the steel corrodes causing a volume increase and the concrete shatters. There are several ways of protecting the structure, but they all deal with the symptoms of the problem – bad concrete quality. It is generally acknowledged that the durability of a concrete structure is highly dependent of the w/c-ratio of the concrete mix design. While wanting a low w/c-ratio for better durability and denser concrete, in practice the concrete needs a certain workability to be properly placed. Generally coatings are applied to compensate the fact that a relatively high w/c-ratio is needed to properly place the concrete, but another solution is to drain the concrete after it has been placed.

Controlled permeability Formwork (CPF) liner is a fabric that is installed on the formwork before the concrete is cast. It consists of a filter and a drainage layer. It is a non-woven fabric made from fine polypropylene fibres needled together in a non-structured order. The fabric is thermally bonded on one side creating a filter, while the non-thermally bonded side functions as a drainage layer. The filter is designed to retain cement particles (mean pore size of approx. 30 microns), while letting water pass. Once the liner is installed the formwork is fixed into place in the exact same way as without a liner, and the concrete is cast. When the concrete is vibrated it becomes plastic and able to give away water from a depth of 15-20mm. The water is drained through the drainage layer, led under the formwork and out of the system.

2 ANALYSIS METHODS

2.1 Determining the water cement ratio in hardened concrete

In order to investigate the effect of using CPF there are several approaches. The obvious one is to determine the durability of the concrete when CPF is used as apposed to when it is not used. These improvements of the durability, however, have come because of a denser surface concrete with a lower w/c-ratio. This directs the attention to the question: "at what level is the w/c-ratio in the surface". To investigate this matter two methods are used. One method is to extract a cylinder from a test wall, cut the cylinder into slices and heat them up to determine the water content. At 105°C the free water (pore water) leaves the specimen, and at 1100°C the chemically bonded water evaporates. Then by weighing the cement in the totally dry specimen, you can determine the w/c-ratio for a specific slice. Another method is a denseness measurement through the depth of the concrete. This can be done by using X-ray equipment, where x-rays are sent through the specimen into a detector. The detector counts how much is left of the stream after it has penetrated the specimen. Thereby you get measurement of the denseness (and thereby the w/c-ratio), as a porous concrete with a high w/c-ratio will let more rays pass, than a dense concrete with a low w/c-ratio. The results of the two tests are shown in Fig. 2.

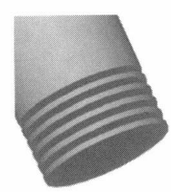

Fig. 1. The extracted cylinder cut into slices.[1]

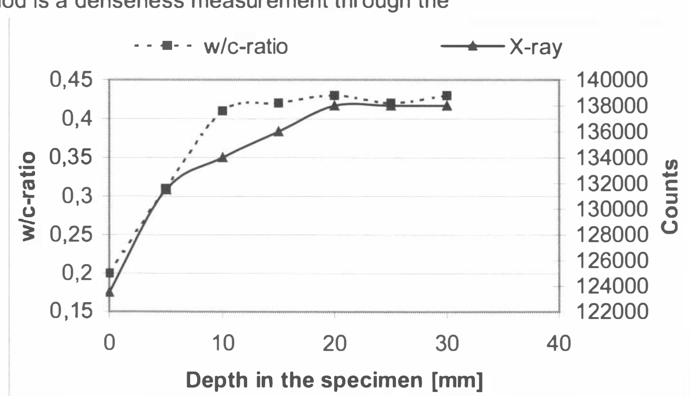

Fig. 2. Result of w/c-ratio experiments by sintering and x-ray.[1]

2.2 Durability enhancements

As mentioned in 2.1 the durability enhancements of the concrete is another way of showing the effect of using CPF. Several reports have been written on this subject, and this section will be based on a report made by Taywood Engineering Ltd. for Fibertex A/S in 1998. The concrete used in this test is for aggressive environment, and has a compressive strength of 45 Mpa after 28 days. The recipe is shown in Table 1

Table 1. Concrete recipe used in the durability tests

Material	Amount [kg/m^3]
Cement	340
Stone 20mm	793
Stone 10mm	397
Sand	645
Water	180
W/c-ratio [%]	0.53
Compressive strength (28 days) [Mpa]	45.5

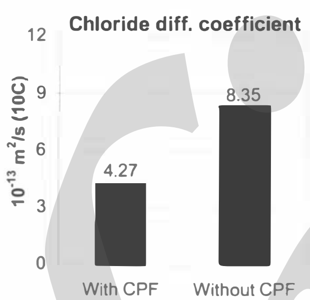

Fig. 3. Chloride diffusion coefficient according to TEL proforma Ref: 1303/MW001/JM issue 1.

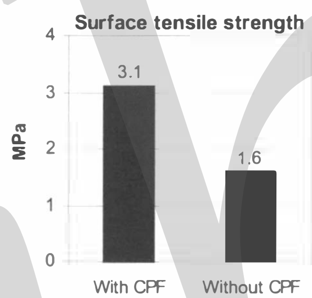

Fig. 4. Surface Tensile strength according to BS 1881 p. 207

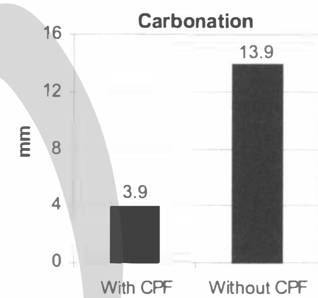

Fig. 5. Carbonation depth by accelerated test according to EN 104-839

3 LIFETIME CALCULATION

Provided that ingress of chlorides is the deterioration reason, and that the main transport mechanism is diffusion it is possible to calculate when the concentration of chlorides is critical at the rebars. The calculation is performed with Fick's 2. law of diffusion, under the following conditions:

$C_s = 0.2\%$ (= 2 vol%)	*The concentration of clorides at the concrete surface [% of concrete mass]*
$C_0 = 0\%$	*The initial concentration of clorides in the concrete [% of concrete mass]*
$C_{cr} = 0.05\%$	*The critical concentration of clorides at the rebars [% of concrete mass]*
$x = 0.035$	*Distance from the surface to the rebars [m]*
$D_{10,CPF} = 4.27 \cdot 10^{-13}$	*Diffusion coefficient in seawater at 10°C when using CPF* $[m^2 \; s]$
$D_{10,Non\ CPF} = 8.35 \cdot 10^{-13}$	*Diffusion coefficient in seawater at 10°C when not using CPF* $[m^2 \; s]$
$t = ?$	*Time until* C_{cr} *is present [sec.]*

The lifetime can now be calculated by Fick's 2. law of diffusion:

$$\frac{C_s - C_{cr}}{C_s - C_0} = erf\left(\frac{x}{2\sqrt{D \cdot t}}\right) \quad \Rightarrow \quad t_{Non\ CPF} = 23.1 years \quad t_{CPF} = 45.2 years$$ [2]

[1] Morten Gantriis Sørensen, Effect of using CPF when casting concrete, 2001 (In Danish)
[2] Birgit Sørensen, Chloride transport in concrete, 1990 (In Danish)

RESULTS OF EXTREME LONG DURATION OF A RELAXATION TEST (42 YEARS) ON PRESTRESSING STEEL

H.R. Mueller, dipl.Ing. ETH
Consulting Engineer, Herrliberg-Zurich, Switzerland

Sten Zetterholm, dipl. Ing. ETH
EMPA , Dübendorf-Zurich, Switzerland

Keywords: Bridge over river Thur near Zurich, Isothermal relaxation of cold drawn prestressing steel, long-term measuring (42 years) , formula CEB-FIP Model Code 90 as a plausible rule for relaxation.

1 INTRODUCTION

The road bridge over river Thur at Andelfingen (CH) was opened to traffic in May 1958. It was the longest post-tensioned concrete bridge (293 m) in Switzerland at that time and is still in good condition. The prestressing contractor recommended for checking of the long-term behaviour of the bridge permanent measuring of the prestressing forces by means of a built-in mechanical Dynamometer in a selected tendon. For more than 20 years readings of this calibrated force-measuring instrument were organised by the PWD.

Results of these readings were discussed and published in [1]. It was noted that after this long duration the tension in the measured tendon, initially registered as 690 MPa (70.4 kp/ mm^2) , decreased to the value of 644 MPa (65.7 kp/mm^2), i.e. 6.7 %. This reduction contains all the losses due to creep and shrinking of concrete as well as due to relaxation of prestressing steel. The relaxation may be estimated to max. 40 % of all the losses, say 2.7 %, according to calculations made for a similar bridge. The tendon (BBRV) has 42 cold drawn wires dia. 6 mm, quality 1370/1570 MPa, type: as drawn.

2 RESULTS OF RELAXATION TEST

To gain more insight in the behaviour of cold drawn steel under constant elongation, the BBR-Group designed a device enabling the long-term measuring of loss of prestressing force in a tendon. A small tendon, 2,5 m long, with 8 wires dia. 6 mm is placed into a stiff steel box and anchored with button heads. The tendon force is permanently measured with a Dynamometer. The test was ordered 1959 as a relaxation test at the Swiss Federal Laboratories for Materials Testing and Research (EMPA).

Table 1 Measured values and calculated values of relaxation losses, time in hours (log t) and in years, calculation with formula MC 90, CEB-FIP [3], f_0 = 1080 MPa.

Time in hours (log t)	0	1	2	3	3.3	3.5	3.9	4	4.2	4.4	4.5	4.6	4.9	5	5.1	5.2	5.5	5.6
Losses in % (readings)	0.4	1	1.7	2.5	2.9	2.9	3.6	3.7	4.1	4.8	4.5	5.6	5.8	6	6.3	6.4	7.3	7.6
Losses in % (formula)		1.1	1.6	2.5	2.8	3.1	3.7	3.8	4.2	4.5	4.8	5	5.7	5.8	6.1	6.3	7	7.4
Time: years							1				4		10			19	32	**42**
Phase	A				B							C					D	

The relaxation device as well as the readings of force during the first 3½ years are reported in the Proceedings of the third F.I.P-Congress Rome – Naples 1962 [2], see phases A and B in Table 1 above. Phase C is reported in [1]. Since no further long term results of relaxation were known, readings continued up to now (phase D) and are compared with the formula in CEB-FIP Model-Code 90 [3]. The authors do not know of any other long-term relaxation tests of this duration.

$$\rho_t = \rho_{1000}\left(\frac{t}{1000}\right)^k \quad (1) \qquad\qquad k = \log \frac{\rho_{1000}}{\rho_{100}} \quad (2)$$

Value for (2) in Table 1 is 0,183

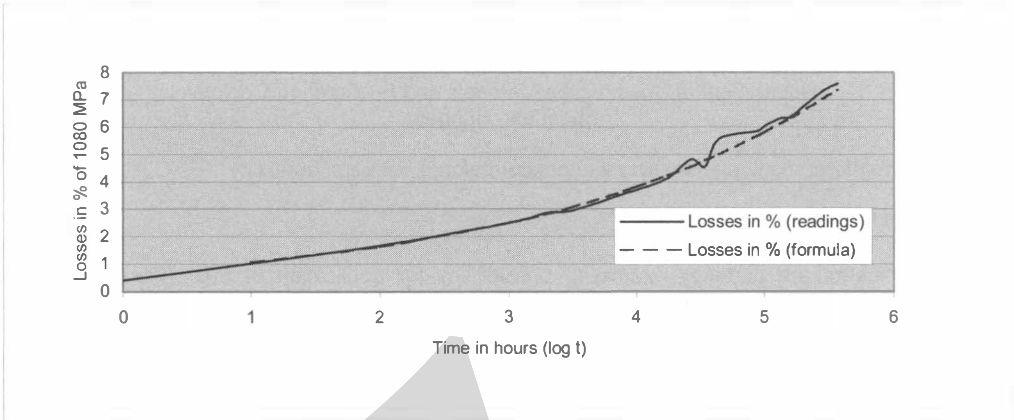

Fig.1 Relaxation losses in log scale, f_0 = 1080 MPa

The intention was, to follow up the decrease of tendon force as long as possible. The results are summarised in Table 1 and plotted in log scale in Fig. 1 above.

3 DATA OF TESTED MATERIAL AND PRETREATMENT BEFORE RELAXATION

Cold drawn wires dia. 5.93 mm, indented, as drawn, no heat treatment after drawing; f_u 1570 MPa, $f_{p\,0.2}$ 1177 MPa, λ_{10} 6.7 %, φ 47 %, Length of sample 2540mm, F 221 mm^2, Temperature 20^o ± 1 C. (not secured!), Accuracy of force ±0.8 % at 300 kN load. Program of the test: Stress to 1128 MPa (0.72 f_u),block 10 Minutes (constant elongation), lower stress to 1080 MPa (0.69 f_u)and start reading.

4 DEVELOPMENT OF RELAXATION TEST METHODS

Earlier, only creep of steel was known, i.e. increase of elongation of a steel sample , loaded with a constant weight. But this method did not describe the behaviour of a stressed tendon in prestressed concrete, where elongation is - after a first period of creep and shrinkage of concrete - blocked, and therefore better simulated with the relaxation test. In the early sixties, a broad discussion regarding relaxation started within FIP and was one of the topics of the Symposium in Madrid 1968. But up to 1979, no standard of a relaxation test was available, until RILEM/FIP/CEB gave with RPC-15 a first Recommendation. Today we have the prEN ISO 15630-3: 1999 (ISO/FDIS 15630-3): “Steels for the reinforcement and prestressing of concrete -Test methods - Part 3: Prestressing steels”. The tests are very sensitive to temperature variations!

5 CONCLUSION

Nowadays relaxation of cold drawn steel for prestressing is a good documented materials property. Isothermal tests up to 1000 hours are sufficient, but must be secured for new materials with long-term tests (min.1 year). CEB-FIP formula of MC 90 is well verified. The rule of thumb, that the value of final relaxation may be estimated as three times the value of loss after 1000 hours and is on the safe side.

REFERENCES

[1] Birkenmaier M. et al. : “Long-term measurements on prestressed concrete bridges”, Schweizerische Bauzeitung, Heft 14, 1978, pp 280 – 288 (in German).
[2] Ros M.R.et al.: ”Research and long-term measurements on prestressed constructions in Switzerland”, Fourth Congress of the F.I.P, Rome-Naples 1962, Volume 1, Theme I, Paper 27, pp 210 – 239, C and CA, London 1963.
[3] CEB-FIP MODEL-CODE 1990, CEB, Bulletin d’Information No. 213/214, May 1993 : Chapter 2.3.4.5 “Relaxation” , p 80, fib-Secretariat, Case Postale 88, CH-1015 Lausanne.

NON-METALLIC REINFORCEMENTS TO IMPROVE DURABILITY

Prof. György L. Balázs – Adorján Borosnyói
Budapest University of Technology and Economics
Department of Construction Materials and Engineering Geology
Budapest, Hungary

Keywords: reinforcement, prestressing tendon, corrosion, FRP bars, durability

1. INTRODUCTION

Civil engineers are currently examining possibilities for application of FRP (Fibre Reinforced Polymer) reinforcing and prestressing materials to overcome serious deterioration of concrete structures due to corrosion of steel reinforcement.

Corrosion resistant, non-metallic reinforcements are made of high strength fibres of glass, aramid or carbon embedded into a resin. FRP bars have tensile strengths of 700 to 3500 N/mm^2, Young's moduli of 38000 to 300000 N/mm^2, failure strains of 0.8 to 4.0 %. Their further advantages are superior resistance to corrosion, as well as to acidic or to alkaline solutions, high tensile strength, low self-weight, electromagnetic neutrality, high fatigue strength, low relaxation and good long-term characteristics.

Environmental effects can considerably influence long-term characteristics of FRPs. Liquids (water, alkali and salt solutions) can diffuse into resins of FRPs that can cause decrease in mechanical characteristics. Carbon Fibre Reinforced Polymers (CFRP) show superior resistance to environmental attacks and have very high tensile strength (2000 to 3500 N/mm^2), high strength-to-weight ratio, magnetic neutrality, excellent fatigue strength, low relaxation and good long term characteristics. CFRP tendons show linear elastic behaviour and brittle failure with considerable release of elastic energy.

Due to various surface treatments of non-metallic reinforcing bars bond strength can be even more than that of deformed steel rebars.

2. STUDIES

An experimental study has been carried out on prestressed concrete beams pretensioned either with CFRP or steel tendons at the Faculty of Civil Engineering, Budapest University of Technology and Economics. Test beams had an I cross-section with relatively thin web and did not contain any other longitudinal reinforcement but prestressed pretensioned tendons (Fig. 1). CFRP prestressing tendons were ∅5 mm Carbon-Stress® wires with sand coated surface produced by NEDRI Spanstaal BV, Venlo, the Netherlands (f_{fu} = 2700 N/mm^2; E_f = 158800 N/mm^2; ε_{fu} = 1,7%). Concrete used in specimens had characteristic compressive strength of concrete cubes was f_{ck} = 57,4 N/mm^2 at the age of 28 days. Steel wires used for control specimens were ∅5,34 mm indented cold-drawn steel wires (1770.5,34 ST) produced by D&D, Hungary (f_{pu} = 1770 N/mm^2; $f_{p0\,1}$ = 1450 N/mm^2; E_p = 195000 N/mm^2; ε_{pu} = 3,5%). Each prestressing tendon was pretensioned to 26.3 kN load that means 1340 N/mm^2 initial prestress in the CFRP tendons and 1174 N/mm^2 in the steel wires.

Load vs. deflection responses of both steel and CFRP prestressed members were linear before reaching the cracking load with almost equivalent stiffness. Exceeding the cracking load, load vs. deflection diagrams of CFRP prestressed members remained linear with lower stiffness on the contrary to steel prestressed members, which showed slight non-linearity. Bilinear behaviour was due to the linear elastic behaviour of CFRP prestressing tendons. Typical load vs. deflection responses are indicated for beams prestressed with two tendons in Fig. 1.

In the case of FRP reinforced or prestressed members usually bilinear load-deflection response was observed in other tests. Our tests also confirm this behaviour.

Strength of FRPs in transverse direction can be considerably minor to that of longitudinal direction. Therefore shear actions are of great interest in FRP reinforced concrete members. In most of the cases FRPs can resist less than 50 percent of their tensile strength if loading is perpendicular to the fibre axis. In our experiments CFRP tendons broke during shear failure on the contrary to steel wires, which kept the failed element in one piece. So the dowel action of CFRP tendons was found to be negligible.

Cracks generally occur in reinforced concrete structures where the principal tensile stress from loads or restraint forces exceeds the tensile strength of concrete. Cracks occur at random positions according to locally weak sections in the concrete matrix. The compatibility of strains between concrete and reinforcement is no more maintained at a crack as concrete stress dropped to zero. With increasing the distance from the crack the tensile stress in the concrete increases as force is transferred by bond stresses. At some distance the compatibility of strains between concrete and reinforcement is again maintained. The better the bond properties of the reinforcing bar, the shorter the length for re-establishing strain compatibility. Fig. 2 represents change of crack spacings and number of flexural cracks, respectively.

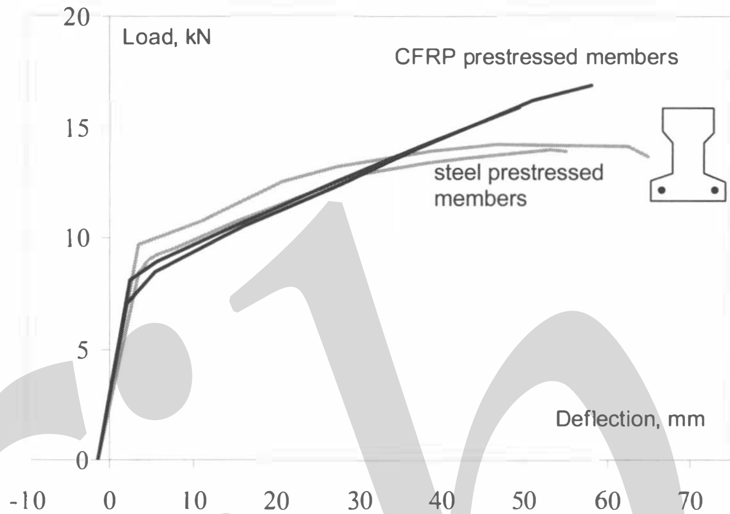

Fig. 1 Load vs. deflection responses of beams prestressed with two steel or CFRP wires

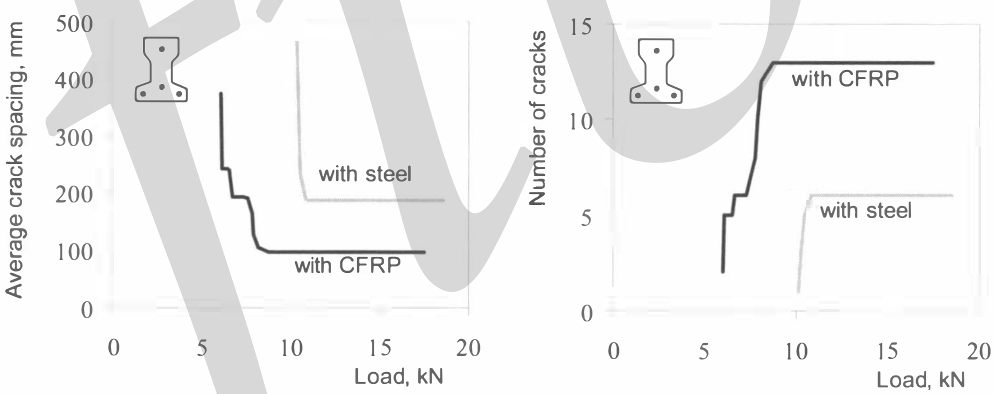

Fig. 2 Average crack spacing and number of flexural cracks for test members prestressed with four tendons

3. CONCLUSIONS

Based on an extensive experimental study the following conclusions can be drawn:

- Load vs. deflection response of CFRP prestressed members was practically bilinear, while that of steel prestressed members showed slight non-linearity. Bilinear behaviour of CFRP prestressed beams was mainly caused by the linear elastic prestressing material.
- Dowel action of CFRP tendons seemed to be negligible.
- Sand coated surfaces of CFRP prestressing tendons gives a preferable cracking behaviour of close cracks with small widths.

A STUDY ON THERMAL CRACK CONTROL OF THICK CONCRETE WALLS

Takeshi Suzuki Hiroshi Ishizaki Manabu Ito
Hanshin Expressway Public Corporation
Japan

Masamiti Eto
Shimizu Corporation
Japan

Keywords: thick wall, thermal crack, low-heat portland cement

1. INTRODUCTION

It is becoming a common way to construct underground structure for highways in metropolitan region because of the demand of an environmental concern and effective land use. When a cut and cover tunnel method is adopted, thermal crack in a thick concrete wall should be considered. Low-heat portland cement （L cement） is coming into use recently to control a thermal crack in a thick concrete wall.

The experiment in laboratory, the field experiment and the numerical analysis were conducted to investigate the effectiveness of L cement. As a result of experiment in the laboratory, the early compressive strength of the concrete using L cement became high when it was cured in high temperature. The compressive strength increased smoothly even after the curing period. This property is effective to control the thermal crack of thick concrete.

Next, the field experiments were conducted and very few crack was observed. Accordingly it was identified that L cement was effective for the thermal crack control. On the other hand, when thermal crack control measures is planned, precise thermal stress and the crack width should be estimated. It was shown that the estimation is improved when the suitable creep compensation coefficient depending on stress path is considered based on the results of the experiment and the numerical analysis.

Furthermore, parameter analysis was conducted by the finite element method (F.E.M) with a discrete crack model. As parameters, the construction season, type of cement, reinforcement content, structure dimensions were chosen.

As a result, the L cement was effective for the thermal crack control of thick concrete walls.

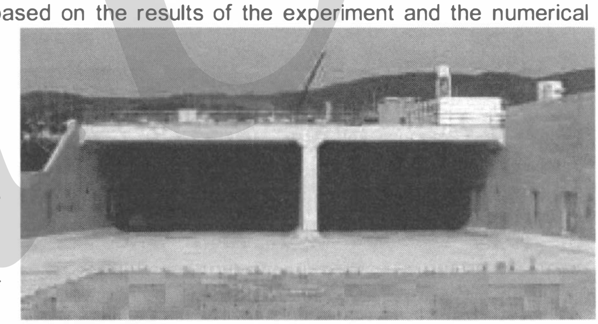

Photo-1 Entrance of cut and cover tunnel

2. PROPERTY OF L CEMENT

Fig.1 shows compressive strength property of L cement and Compressive strength under high temperature curing is stronger than that under standard curing. Adiabatic temperature rise test was also conducted and L cement's temperature rise was approximately 15 degree lower than that of slag cement.

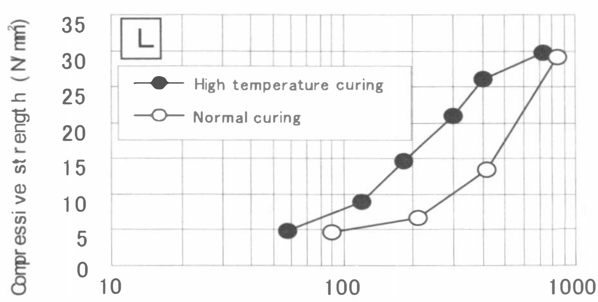

Fig.1 Compressive strength property of L cement

3. COMPARISON OF L CEMENT AND SLAG CEMENT ON THE REAL STRUCTURE

Experiment work on the real structure was conducted at Hanshin Expressway Kobe Yamate Line to examine the effectiveness of L cement. Fig-2 shows the section of the cut and cover tunnel which thermal crack measurements were conducted.

Comparison of L cement and slag cement were conducted on the diaphragm wall. Fig-3 show crack map of the fourth block diaphragm wall, for which slag cement was used and 0.3 mm width crack was observed on the diaphragm. On the other hand, Fig-4 shows crack map of third block diaphragm wall, for which L cement was used. Even though severe condition for thermal crack, as for all walls, for which L cement is used, harmful crack didn't appear.

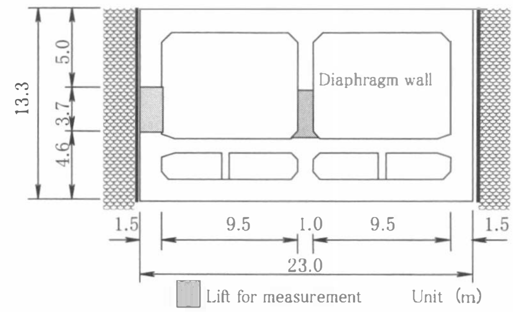

Fig.2 Cut and cover tunnel section

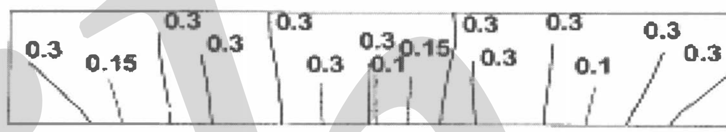

Values are crack width measurement (in mm)

Fig.3 State of crack (slag cement)

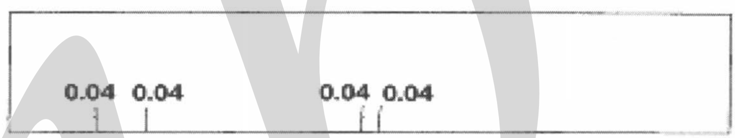

Values are crack width measurement (in mm)

Fig.4 State of crack (L cement)

4. CRACK WIDTH ANALYSIS

Crack width was calculated by F.E.M using discrete crack model and contents in analysis adopted the results of tests. Measurement results and numerical analysis were compared to verify the adequacy for numerical analysis.

Fig-5 shows crack width comparison of analysis and measurements results concerning diaphragm of fourth block diaphragm wall, for which slag cement was used. Analysis of fourth block was consistent with measurement results. Consequently, I think crack width on thick concrete wall can be estimated practically by FEM analysis using discrete crack model.

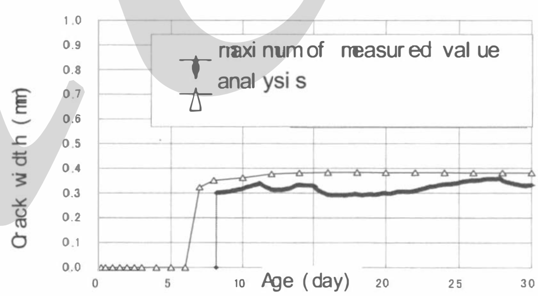

Fig.5 Results of crack width analysis(4block)

REFERENCES

1) Japan Society of Civil Engineers: STANDARD SPECIFICATIONS FOR CONCRETE STRUCTURES-1996, Materials and Construction

2) Iriya, K., : Study on creep of early aged concrete (doctor's dissertation), Nagoya Institute of Technology 1999

3) Eto, M., : Development of technique Reducing Thermal Stress for Mass Concrete (doctor's dissertation), Nagaoka University of Technology 1999

THE RESEARCH OF THE INFLUENCE OF THE DEGREE OF FILLING OF THE SPACE BETWEEN THE AGGREGATE GRAINS WITH THE CEMENT PASTE ON THE CONCRETE COMPACTNESS

Ph.D. Zoran Grdic Ph.D. Dusan Petkovic Mr.sci. Gordana Toplicic-Curcic
Faculty of Civil Engineering, Beogradska 14 st., Nis, Yugoslavia

Keywords: cement paste, space in the aggregate, consistency, concrete compressive strength

1 INTRODUCTION

Durability and resistance to the atmospheric influence are the characteristics that are almost regularly required in concrete and concrete structures. In that aspect, the compact, well-composed concrete, produced from the quality components has the advantage over other types of concrete. It is known that the characteristics of concrete depend on the realised structure of the mutual ratio of the aggregate and cement paste in concrete. Regarding this issue, the very voluminous researches of the influence of the degree of filling of the space between the aggregate grains with the cement paste on the certain characteristics fresh and hardened concrete have been done; in this paper, only a part relating to the change of consistency and compressive strength will be shown. A special attention has been paid to the realised concrete structure. Three different types of fresh concrete structure can be discerned, depending on the relation of the cement paste quantity and aggregate, figure 1.

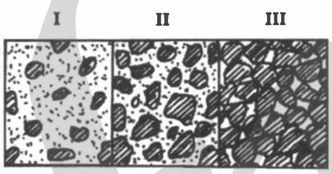

In the structure I, the cement paste is predominant. The aggregate grains are significantly divided with the paste so that it can be considered that there is no inter-reaction of the grains. The grains have influence only in the zone of contact with the paste and the magnitude of the influence is directly dependent on the specific surface of the grain. Such concrete mixtures most frequently have good fluidity and can easily be built in.

Fig. 1 Types of fresh concrete structures

Structure II, as a rule, enables production of the very compact concrete. At a concrete corresponding structure II, the amount of cement paste is smaller in respect of the structure I, but there is enough of it to fill in the space between the aggregate grains and to separate them slightly. Concrete with such structure are more difficult to build in, in respect of the concrete mixtures of the previous type. In the structure III, the aggregate is dominating. The cement paste enfolds the aggregate grains with a thin film, but there is no enough of it to fill in all the space between the grains. The friction effect is far more prominent than in the structure II and the fluidity of such mixtures is almost negligible.

2 EXPERIMENT

For making of the concrete the alite type Portland cement with 15% of slag. The aggregate was from a river is divided in four fractions. No additives were used in making concrete. Apart from the possible theoretical calculation of the space volume between the aggregate grains used for the making of concrete is measured experimentally. For that purpose, the equipment as in figure 2 was used.

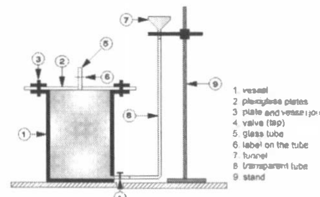

Fig. 2 Equipment for measuring of the space volume between the grains in the aggregate

For each of three different granulometric compositions the amount of concrete was varied from 250 to 500 kg for 1m^3 of concrete in 50 kg steps. Three water/cement ratios 0,46, 0,52 and 0,58 were varied for each possible previous combination. In such a way, 54 various compositions of concrete were made, and all three possible cases pertaining the mutual relationship of the cement paste volume and space volume between the aggregate grains were covered. In other words, it was possible to analyse the characteristics of each previously described concrete structure.

3 DISCUSSION OF THE RESULTS

Here the so-called structural concept of the understanding of concrete is important because its properties are connected to the realised structure of the fresh (i.e. hardened) concrete. Degree of filling of the space between the aggregate grains with the cement paste (k_e) is calculated for each concrete mixture as:

$$k_e = \frac{V_{cp}}{V_{s,exp}} \quad (1)$$

where V_{cp} is the cement paste volume, $V_{s,exp}$ is space volume in the aggregate, experimentally measured. The value of k_e parameter ranged between 0,977 and 2,256. The change of consistence (w) expressed in webe grades in function of the change of parameter k_e is given in the form:

$$w = f(k_e) = a \cdot e^{b \cdot k_e} \quad (2)$$

Graphical display is given in figure 3.

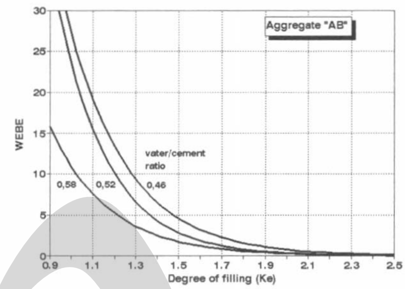

Fig. 3 Change of consistency in function of the change of parameter k_e for aggregate AB and for the values of ω_c = 0,46 – 0,58

Dependence of concrete compressive strength at 28 days of age ($f_{pb,28}$) on the parameter (k_e) is found in the form of the third degree polynomial function:

$$f_{pb,28} = f(k_e) = a + b \cdot k_e + c \cdot k_e^2 + d \cdot k_e^3 \quad (3)$$

Graphical display of compressive strength change in function of the parameter k_e change is given in figure 4.

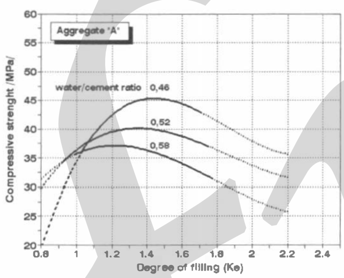

Fig. 4 The change of compressive strength in function of the parameter k_e change for aggregate A and for the values of ω_c = 0,46 – 0,58

4 CONCLUSION

The influence of the degree of filling of the space between the aggregate grains with the cement paste on the type of consistency should be observed in the light of the realised structure of concrete, taking into account as well the granulometric composition and water/cement ratio. Generally, with the increase of the degree of filling of the space between the aggregate grains with paste (k_e factor) from 0,9 to 2,5 the concrete consistency changes from very rigid to very liquid.

The maximum values of compressive strength are realised when the degree of filling of the space between the aggregate grains ("k_e" factor) is within relatively narrow range that can be considered optimal. This range depends on the water/cement ratio and granulometric composition. Concrete has structure II in the "k_e" factor optimum values zone.

REFERENCES

[1] Grdic, Z. : Contribution to the investigation of correlation dependence of physical-mechanical concrete characteristics on cement paste quantity and component characteristics, Doctoral dissertation, Faculty of Civil Engineering, Nis, 2001 (in Serbian)
[2] Grdic, Z. : The influence of admixture on cement paste texture changes, Facta Universitatis, Series Architecture and Civil Engineering, Vol.1, No.1, University of Nis, 1994
[3] Muravljov, M. : Technology of Concrete, Gradjevinska knjiga, Beograd, 2001 (in Serbian)

DURABILTY PROBLEMS IN HIGH STRENGTH CONCRETE BRIDGES

Satish Chandra
Chalmers University of Technology
412 96 Göteborg, Sweden

Keywords; Durability, Cracking, high early strength cement

1 INTRODUCTION

Concrete made in ancient period with lime pozzolana cements was long lasting which is evident with some of the structures existing today in good condition like Pantheon in Rome. While there is growing evidence of premature deterioration of the 20th century reinforced concrete structures that are constructed with modern portland cement. It causes worry and necessitates to find out the causes which adversely affect. The speed of construction increased at a high rate, which was met by the use of high early strength concrete (HESC). Portland cements have been developed through the years by increasing C_3S content from 30% for example in 1950s to 60% in 1990.s.The fineness increased for the same period from 1000 cm^2/g to 4000 cm^2/g, the factors giving high early strength. This paper reviews the influence of the change in cement composition and environmental conditions on the deterioration process.

HESC generally contains high amount of cement, therefore they shrink more and produce higher temperature during early hydration. This decreases the resistance of concrete to crack formation. At the same time HESC tends to increase the elastic modulus and reduce the creep coefficient, which increase the crack formation, Fig,1 shows how this would effect the principal factors influencing the cracking behavior of concrete.

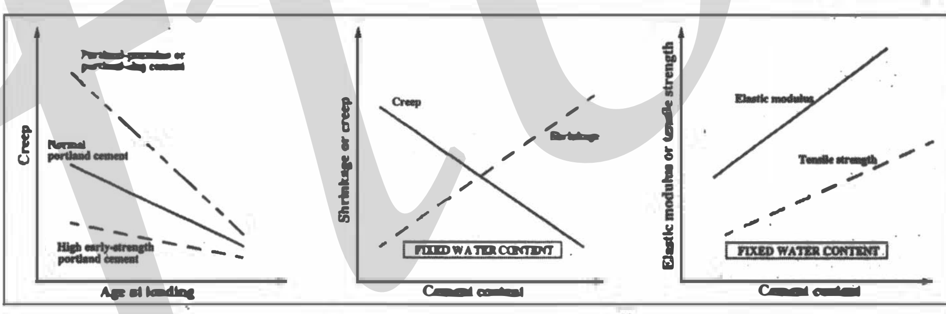

Fig.1. Relationship between concrete strength and other properties [1]

Strength being the cardinal property, concrete is designed basing upon its strength, under the belief that the high strength will increase the durability also. But this is not supported by the field experiences. The pier caps in 11 km elevated transit line in Teipei's have shown cracks [2]. The cause of damage is reported to be high cement content. Similarly investigations of Krauss & Rogalla [3] have shown that more than 100,000 bridge decks is USA showed transverse cracking even before the structures were less than one month old. A combination of thermal and drying shrinkage caused most of the cracks. Recently 2 bridges Alviks and Grandel in Stockholm have shown cracks. These are 3 years old bridges and costed about 20 million US$ to build. The cause of cracking is not yet known.

Deterioration of concrete is generally reported to be due to the miscalculations, misconceptions, wrong interpretations of the building codes and not the least due to the bad workmanship [4]. Apart from these factors which are common for the normal concrete, modern portland cement, which is used for making high strength concrete seems to play foremost role in the deterioration process . Thus cracking is directly related to the durability properties which in turn is closely connected with the use of early high strength cements.

2 ENVIRONMENT

Environment is another factor, which has been aggravated through the years and the concrete structures face more aggressive environmental abuse and has deleterious effect on the durability.

3 SYNERGISTIC EFFECT

Concrete does not deteriorate by one factor. There are many factors, which take part in the deterioration process simultaneously or successively. Their cumulative effect is more than the sum of individual damage. Therefore when considering the service life of actual structures, the results of laboratory tests on concrete durability should be used with caution because the cracking behavior of concrete is highly dependent upon the specimen size, curing history, and environmental conditions.

4 INTERNATIONAL SPECIFICATIONS & THEIR SYNERGISM

There are many international committees who deal with the specific problems and there is no synergy between them. Apart from this, in some countries international codes are used with out taking into consideration local environmental conditions, quality of the material and the working precision. It seems that it is necessary to build co-ordination committees, which can join the links between the committees and will create a closer working –relation between the architects, material specialists and the builders. This will reduce the possibilities of cracking at early age and will thus increase the durability.

For making high strength concrete with good durability avoiding cracking at early stage attention is to be given on concrete proportioning and selection of the material. It advisable to use mineral admixtures like fly ash and slag. These give dilution effect and reduce the heat of hydration. Consequently the thermal shrinkage is significantly decreased and thereby the early stage cracking is decreased.

REFERENCES

1. .Mehta, P.k.; Durability-critical issues for the future, Concrete International, July , pp 27-37. 1997.
2. Shapiro, D. Cracked pier caps delay rapid transit line, Engineering News Record, December 19, p 53, 1994.
3. K.rausS, P.D., and Rogalla, E.A., Transverse cracking in newly constructed bridge decks, NCHRP Report 380, Transport Research Board, Washington, D.C., 126 pp , 1996.
4. handra, S, Cederwall, K., and Nillson, Ingvar, Durabiity problems in Swedish Concrete bridges, P.K.Mehta Symposium on Durability of Concrete, May, Nice, pp 223-241, 1994..

THE INFLUENCE OF AGGREGATES ON CONCRETE DURABILITY A REVIEW

Claudio Sbrighi Neto
Brazilian Concrete Institute
FAAP Engineering School – São Paulo Brazil

Email : csbrighi@yahoo.com

Keywords : aggregates, durability, concrete

Most technical literature about durability points out six major factors that affect it : characteristics of materials comprising concrete, exposure conditions, loads imposed to structure, practice used during construction and structural design[1]. From the point of view of majority of buildings and structures, mainly those of more technical and economic relevance, the durability and the strength have equal importance. However, durability is complex and not easy to determine. If we try to find tests to determine durability we reach only freezing and thawing tests of concrete specimens, tests to evaluate some combination of Portland cement and aggregates and indirect electronic tests[2].

The complexity to determine concrete durability is great but, in general it is possible to classify four main categories of destruction agencies of concrete[3]:

- deficiencies or weakness of concrete itself from failure to follow a good practice construction, sometimes such weakness of concrete itself can be a way or an opening wedge for serious damage by actual attack;
- chemical or mechanical attack by outside agencies other than weather cycles;
- reaction between the constituents of concrete itself;
- cyclic forces of weather.

In this context the aggregates which occupy three quarters of solid volume of concrete have an important role to play mainly after lately changes in its sources. The scarcity of good quality aggregates near mostly of great cities, environmental codes and rising costs of disposal are promoting a renewed interest in using waste products. Many countries are facing the problem of a growing burden of waste materials accompanied by a shortage of primary materials and waste utilization as concrete or mortar aggregate is an “easy” and non expensive exit.

Waste materials originated by industrial or mining processes and treatment of solid urban waste commonly show a large variability of chemical and mineralogical composition, great microstructure diversity and sometimes biological contamination. In contrast, usual natural aggregates for concrete show a constant mineralogical and microstructural composition and regular shape and well defined superficial texture.

A secure use of alternative aggregates involves a well conducted research including :

- chemical aspects(in general with determination of organic compounds);
- physical tests with emphasis in porosity properties;
- petrographic examination where microstructural aspects must be considered.

When alternative sources of aggregates are considered to apply in concrete production the necessity to verify its influence on a long term behavior multiply, specially in industrial areas or places where environmental conditions can change fast. This happens because the addition of external causes and internal structural non stability can accelerate significantly concrete degeneration processes.

The resolution of problems based only in immediate economic/ecological aspects can lead to long term non stable materials with maintenance cost growing or, in extreme, risks for building structural stability. Beside technical aspects it is necessary to consider risks to human health when a contaminate raw material, specially by heavy metals or organic compounds, can be lixiviated or solubilizated during service life of concrete structure and reach the environment. Changes in environmental conditions like acid rain or groundwater pollution can modify the stability and mobility of certain chemical elements and organic chain incorporated by contaminants. Therefore, accurate research must be run to avoid risks the population health. Some kinds of phenolic resins are good example of mobility change when pH conditions vary. Its solubility can reach high levels in low pH and great stability in alkaline conditions.

One example of aggregate evaluation where durability aspects is adequately considered can be found in Sbrighi Neto et al[4].and Tango[5]. This paper describes step by step a procedure to evaluate used foundry sand and discuss the role of many contaminants in durability of concrete and human health if the concrete were lixiviated during service life of concrete.

REFERENCES

[1] Concrete Manual, International Conference of Building Officials ; third edition – second priting, 1991, California, USA

[2] Ferreira, R.M. and Jalali, S. "Evaluation of tests commonly used for measuring concrete durability" International Conference of Sustainable Construction into Next Millenium : Environmental Friendly and Innovative Cement Based Materials. Federal University of Paraíba, João Pessoa, Brazil, 2000

[3] Guide to durable concrete. ACI – American Concrete Institute, USA, 1982

[4] Sbrighi Neto, C., Tango, C.E.S., Lotti, F. and Quarcione, V.A , "Methodology to evaluate used dry sand as concrete aggregate", Proceedings of 14 th. CIB World Building Congress, Construction and Environment(KTH), Gavle, Sweden, 1998

[5] Tango, C.E.S., "Mixture proportioning fundaments for structural masonry concrete blocks" 5th. International Seminar on Structural Masonry for Developing Countries. Santa Catarina University/University of Edinburgh/ANTAC – Florianópolis, Brazil Aug.1994. Proceed. pp. 21-30. In Portuguese(Fundamentos da dosagem de concreto para blocos).

DURABILITY OF THE 85 YEARS OLD REINFORCED CONCRETE WATERPLANE HANGAR IN TALLINN

Sammal Olav and Marmor Heino
ETUI BetonTEST Ltd
Tallinn, Estonia

Keywords: reinforced concrete shell spherical, barrel, service life: 85 years, rehabilitable

1 INTRODUCTION

1911 in Russia of tsarist period was planned Tallinn-Porkala fortification zone and to build also a waterplane hangar (reinforced concrete “shed”) in Tallinn Mine Harbour.

The construction was designed and built (according to the results of the competition) by Danish firm Christian & Nielsen from 1915 to 1917. The first piles were driven in in 16.03.1916 and in 13.10.1917 was stopped the further financing of the building (it was spent 1 854 600 roubles). They could finish about 75% of the building (there were no gates).

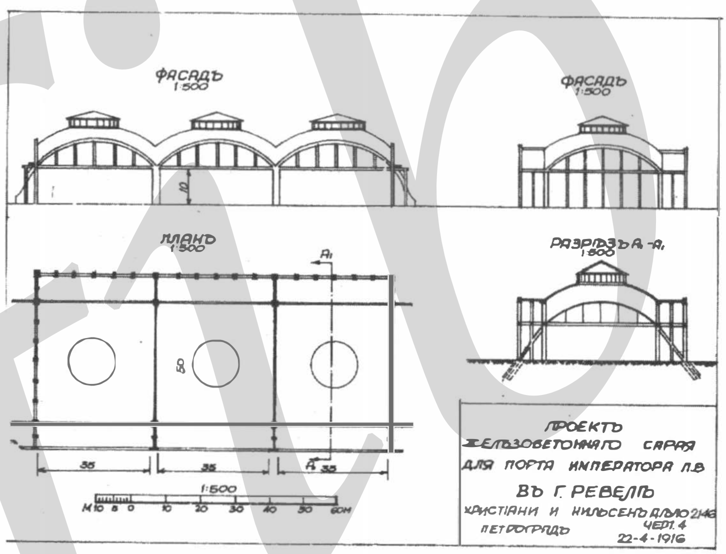

Fig 1 The design of the waterplane hangar. Christian & Nielsen. Petersburg branch office of the firm Christian&Nielsen (designers Sven Schultz, K.N. Höjgaard) 22.04.1916.

Hangar is made up of three spherical (four-square dimension) shells 36x36m, which are joined together side by side. The spherical parts of the building are surrounded from three sides with short barrel shell elements 36x6,1m. In borders shells rest on monolithic reinforced concrete ferms and through them on columns frame systems with sloping supports (spatial frames). Ferms-bordermembers are two hinged structures which form with the shell the monolithic joint. The dimensions of the building are: 120x48m, high max. 24m from the ground. The detailed-drawings of the constructions are not remained. The thickness of the concrete shells is 60-110-260mm.

The object is situated in Estonia, Tallinn Küti str.17. Considering of that time`s building custom it was a conspicuous construction and is one of the most important results of the world engineering point of development of reinforced concrete shells. It is still perceivable the clearness, laconics and reliability of the structural solution of the construction, although it is in the condition like before collapse. In the scale of the world this construction is particularly valuable because of its service life- more than 85 years in spite of conditions through two world wars and of certain period (1940--2000) where there was no continuing normal maintenance.

1999/2000y ETUI BetonTEST Ltd (Olav Sammal, PhD, Heino Marmor, PhD) realized more detailed examination of the hangar and composed the renovation suggestions.

It is very desirable to collaborate with international organizations fib (CEB-FIP), Danish government and the firm's "Christian & Nielsen" (COWI) experiences, UNESCO and others in restoration process of the waterplane hangar.

Figuratively this condition of waterplane hangar can be estimated as **"time-fused construction"** and quit little time is left before the building might be collapsed. That would be a worldwide loss.

In spite of this the hangar is rehabilitable and renovateable.

Fig 2 Waterplane hangar in Tallinn 2000 y (west facade)

CONSTRUCTION TECHNOLOGY FOR MONOLITHIC CONCRETE BRIDGES IN MOSCOW MEGACITY

Gadaev N
Elgad Int,
Russian Federation

Perevoznikov B
Souzdorproect, State Enterprise
Russian Federation

Seliverstov V
Giprotransmost J.S.Co,
Russian Federation

Keywords: monolithic concrete, system engineering, module, launching, technological system

1 INTRODUCTION

Current plans of the Russian capital on streets infrastructure improvement require building a large number of overbridges. Reinforced concrete bridges form a significant part of overall bridge infrastructure in the city.

Starting from the nineteen-sixties last century the Russian concrete bridge construction was mainly oriented on precast (prefabricated) concrete bridge superstructures. Therefore technology of concrete highway superstructure construction in Russia was predominantly based on employment of prefabricated shop units, thus speeding up the erection process. Later (early nineteen-nineties) various studies proved the cast-in-place or monolithic superstructures to be more beneficial and durable compared to that of precast concrete. The durability issue is one of the important aspects for the bridges and especially for the bridges in urban cities where traffic congestion and requirement of uninterrupted traffic flow do not allow easy access to build a new structure or repair/replace the deteriorated existing one. The mentioned constraints have called for development of efficient structural - technological system. The paper introduces the structural-technological system with particular emphasis on construction of superstructures with monolithic prestressed concrete in limited urban areas and presents construction issues based on the method of launching.

2 STRUCTURAL-TECHNOLOGICAL SYSTEM

2.1 General description of the system

General description is based on theoretical assumptions of construction process from the position of system engineering concepts. In this light function of the structural-technological system and its parameters are reviewed.

The main function of the system is determined as production of superstructures from monolithic reinforced concrete at construction site by transformation of material resources, energy (mainly by means of mechanisms and machines) and project (design) information. In more detailed aspect the system is presented as combination (totality) of modules, accomplishing some functional transformations and links between them (physical, technological, informational). Modules are considered as structural units of the system and each module represents a functionally independent structure or mechanism. Furthermore the module may be structural, technological, logical (coordinating, informational).

Main structure is an element forming the system, saying more precisely – a structural module of superstructure, repeated N times. Forming factors of the system are configuration of the main structure, its integrity, structural parameters, space position.

Specific (individual) system modules are falsework, forms, main structure, jacking-pushing device.

Technological modules are preparatory woks, formworks, reinforcement works, concreting works.

Internal creation of modules, their functioning and functional links between modules in subsystems “falsework-soil”, “forms-falsework”, “main structure-forms” are in the full paper in relevant subsections.

The following subsystems are outlined: “main structure-temporary structures” and “technology of work execution-mechanization”. These subsystems cover the aspects of preparatory works, formworks, reinforcement placement works, concreting works and also mechanisms and equipment for preparation and placement of non-prestressed reinforcement, installation of prestressed cables and prestressing operation.

High efficiency of the whole structural-technological system was mainly determined by a formation of the given subsystems using modern technologies and equipment.

The application of the new structural-technological system began in 1997. Efficiency of this system has been proved on a number of built bridges. For concrete overbridges, constructed within the frame of large-scale transportation project "Reconstruction of the Moscow Ring Road", launching of monolithic concrete superstructures was successfully implemented (e.g. for the overbridge constructed in 1997 at 11 km of the Moscow Ring Road see Fig. 5). Overview of this large-scale project was given in ref. [1]. However this report does not specifically cover details of monolithic concrete superstructure launching. Specific features of superstructure launching used for construction of monolithic concrete overbridges over the Ring Road around Moscow are discussed in detail in the full paper.

Length of superstructure concrete casting section is chosen so that superstructure joints in the final design configuration would be in zone of minimum moments. According to this point, the length of the first and the last launching superstructure sections are considered to be 0,65 of side spans length, and the length of intermediate launching superstructure sections to be 0,5 of the central span length. Naturally the other factors, which influenced the choice of superstructure launching length, are also taken into account: e.g. quantity of concrete casting was limited to 300 – 350 cubic meters.

3 DURABILITY ASPECTS

Modern bridge building is characterised by industrial production, persistent increase in concentration of material and technical resources at one particular building site. In these conditions requirements to quality of materials and reliability of structures are very high. Therefore establishment strict requirements to quality control and managing technological processes and also to quality control of final product is needed. Besides quality control is playing major role in assuming durability (which is in turn reliability category) of concrete bridges.

ISO International standards on quality systems 9000-series are used in Russia. Within the frame of this paper a technical aspect of quality control is one of the most important items. Therefore some points of quality control in respect to application to the structural-technological system are reviewed further.

In the Russian practice general requirements to quality control of construction works are stipulated in SNIP 3.01.01-85* (Building norms and regulations. Organisation of construction). The following modes of quality control are outlined (depending on location and time of carrying out checks in technological process): incoming inspection of supplied materials, parts, elements, structures e.t.c., and also technical documentation; operational inspection (in-process inspection) conducted during the process of work execution or immediately after their completion; completed product inspection conducted upon completion of overall construction or its stages, various types of work or other items of inspection.

To provide a high quality of construction works for the structural-technological system, a special quality control system has been developed and applied. This developed system combined commission inspection of all specific works (stressing of cables, installation of forms and reinforcement, content and strength of concrete, concrete casting) and acceptance of final product by means of testing. The adopted system of quality control proved its efficiency during construction.

4 CONCLUSION

Construction technologies adopted in the former USSR and Russian Federation for launching of reinforced concrete prestressed superstructures (precast or monolithic) was very labour consuming (4,5 man-hour/m^3 for precast concrete and 2,83 man-hour/m^3 for monolithic concrete), this resulted in enlargement of construction period. Based on the recent experience reflected in the paper, the average rate of construction is 2,76 linear m of superstructure per day. The developed structural-technological system is 5 times less labour consuming compared to the existing analogues in Russia.

The described in the paper structural-technological system for erection of monolithic concrete superstructures by method of launching has been employed on a number of bridges. This system allows execution of works on a tight (limited) space, satisfies requirements of environmental protection and proved its efficiency in specific urban conditions of Moscow megacity.

REFERENCES

[1] Perevoznikov B.F., Seliverstov V.A. Reconstruction of the Moscow Ring Road. Structural Engineering International, Vol. 9, No.2, IABSE, Zurich, 1999 (p.p. 137-142).

DURABILITY SPECIFICS FOR PRESTRESSING

Ivica Zivanovic Benoît Lecinq Jean-Philippe Fuzier
Freyssinet International
FRANCE

Keywords : prestressing, durability, corrosion protection, monitoring.

1 INTRODUCTION

The invention of prestressed concrete was welcomed as a considerable achievement. However, this new material has not always fulfilled its promises ; recent concerns were expressed during the past years in several countries regarding the durability of prestressing. In fact, corrosion of post-tensioned tendons in internally grouted ducts has occurred in a small number of post-tensioned concrete highway bridges.

These problems have been presented and discussed at Ghent University (15-16 November 2001) during the workshop sponsored by IABSE and ***fib*** : « Durability of post-tensioning tendons ». A summary of this workshop is presented hereafter, then the answers brought by Freyssinet acting as supplier and installer. These answers concern the prestressing technology itself (anchorage, ducts and vent), the procedures of threading, tensioning and grouting, the development of new grouts and other corrosion protective materials. Monitoring systems should also be considered.

This is the route towards « Intelligent Prestressing » and « High Performance Prestressing ».

2 THE GHENT WORKSHOP

2.1 Inventory and condition

The various investigations carried out in different countries lead to more or less the same findings. They are summarized hereafter :

a) design defects
b) construction defects.

2.2 Investigation and Repair

a) Corrosion of prestressing tendons
b) Monitoring
c) Repair with additional prestressing.

2.3 Strategies for improvement

Various countries have adopted strategies to improve the durability and quality of post-tensioning tendons. However, we could say that most of them follow the principles set up by the U.K. TR47 which recommends :

- improvements covering design detailing construction workmanship and material properties
- the used continuous corrosion resistant ducting, specifications for the grout and procedures to ensure filling of ducts and removal of air
- re-use of only properly qualified and trained personnel
- the introduction of requirements for full scale trials on every project.

3 TOWARDS HIGH PERFORMANCE PRESTRESSING

Improvements on the current processes for a better durability of post-tensioning cannot be achieved by any single action on its own but require parallel developments in the grouting materials, grouting techniques, grouting equipments and QA/QC systems.

It is recognized that proper installation and use of a system is as important as the performance of the system components for the successful application of prestressing.

It has therefore been the objective of the various actions to develop :

- better grouts which have improved properties : flowabilities, bleed, volume change, stability ;
- more realistic tests of grout performance ;
- improved grouted techniques, equipments and specifications ;
- QA systems which can be applied during and immediately after grouting ;
- inspection and long-term monitoring systems.

Presentation of new solutions and technologies developed by Freyssinet to improve the quality of prestressing is given hereafter :

- Plastic ducts (Plyduct®, Endovent®)
- Plastic couplers (Liaseal®)
- Individually protected strand (Cohestrand®, greased strand)
- Thixotropic grout (Smartgel®)
- Electrically insulated tendon.

In fact, **Durability**, **Ductility**, **Safety** and **Replaceability** will be key parameters of the **High Performance Prestressing**.

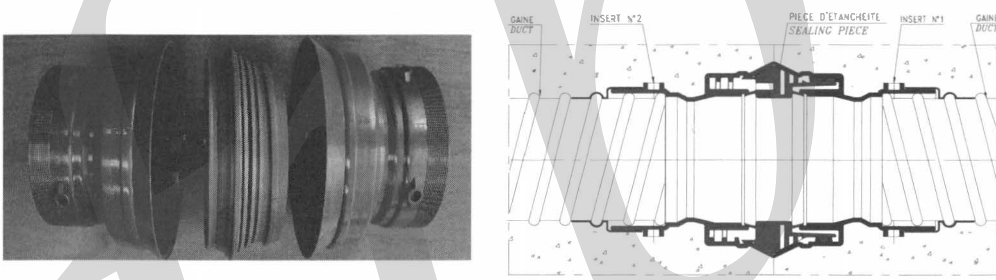

Fig. 1 Liaseal®

4 CONCLUSION

This paper has summarised in chapter 2 the remarkable work which has been done by owners, engineers and specialised contractors during the last five years to improve the durability of post-tensioned tendons. As previously said such a result cannot be obtained by any single action on its own but it requires parallel development in the design, the post-tensioning technologies, the grout and grouting and the overall construction. The technology developed by Freyssinet and presented in chapter 3 is an example of development following these above principles and it represents a large step towards High Performance Prestressing.

REFERENCES

[1] Durability of Post-Tensioning Tendons. Ghent Workshop (Belgium) / 15-16 Nov. 2001.
[2] R. Woodward : Durability of post-tensioned tendons on road bridges in the United Kingdom. Ghent Workshop (Belgium) / 15-16 Nov. 2001.
[3] Post-tensioned Concrete Bridges. Anglo-French liaison report 1999.
[4] P. Matt : Performance of Post-Tensioned Bridges in Switzerland and practical experience with a New Generation of Tendons. ASBI 2000 Convention – Brooklyn (USA).

Session 9 | High-performance concrete

A PERFORMANCE DESIGN METHOD OF RC STRUCTURES USING HIGH STRENGTH SELF-COMPACTING CONCRETE AND HIGH STRENGTH STEEL BARS

Tetsuya Mishima
Maeda Corporation, JAPAN

Keywords: Long Life Span, Super Quality Concrete, Self Compacting, High Strength, High Durability, Performance Evaluation, Design, Construction, Maintenance

1 INTRODUCTION

With increases in maintenance cost to prevent the deterioration of concrete structures, self-compacting, high-strength and highly durable concrete has recently been drawing attention as a technical solution to extend the life span of structures. Self-compacting, high-strength and highly durable concrete is also known as super quality concrete (S.Q.C) in Japan, and is defined as the "concrete with a water-binder ratio less than 40% that is expected to produce high strength exceeding a design strength of 60 N/mm^2, and ensures sufficient compaction to prevent any construction defects". Concrete structures using S.Q.C and high-strength steel, and reinforced with steel fibers as required are referred to as S.Q.C structures. The initial cost of S.Q.C structures is equivalent to that of conventional reinforced concrete structures but S.Q.C structures are more durable, so they require much less life cycle cost including maintenance cost.

2 CHARACTERISTICS OF S.Q.C STRUCTURES

2.1 S.Q.C mix proportions and materials

Highly flowable concrete generally contains powder, adhesive admixture or both. S.Q.C mainly contains powder. Mix proportions are listed in **Table 1**. The draft guideline for design and construction of S.Q.C structures specifies the following quality requirements for S.Q.C.

1) Concrete should be self-compacting.
2) Water-binder ratio of concrete should be less than 40%.
3) Concrete should have an autogenous shrinkage less than 200 x 10^{-6} at 28 days.
4) Design strength of concrete should be 60 to 100 N/mm^2 at 56 days.

Table 1 S.Q.C Mix Proportions

Mix Proportion	Required Strength	Target Slump Flow	Water-Binder Ratio	Target Air Content	Unit Content of Material (kg/m^3)									
					Water	Cement	Admixtures			Fine Aggre-gate	Coarse Aggre-gate	Chemical Admixtures		Steel Fiber
							Fly Ash	Iron-blast Furnace Slag Powder	Silica Fume			AE and High-range Water Reduce Agent	AE Agent	
	(N/mm^2)	(mm)	(%)	(%)	W	C	FA	BS	SF1	S	G			SF2
LC72	72	600	38.6	4.0	165	427				891	827	4.27	8.5	
FA72	72	600	34.9	4.0	165	378	95			809	827	5.91	35.5	
BS72	72	600	41.5	4.0	165	199		199		891	827	4.18	10.0	
BL96	96	650	32.6	3.5	165	506				852	811	6.83	10.1	
SF120	120	650	25.7	3.0	165	578			64	750	795	12.84	51.4	
BS120	120	650	22.0	3.0	165	675		75		681	795	13.13	9.0	
SFRC	72	600	28.9	5.5	165	571				1039	510	11.40	15.4	80

Maximum Size of Coarse Aggregate Particle = 20mm

2.2 Unit costs of materials and construction cost

The Development & Propagation Association of S.Q.C Structures has been designing S.Q.C structures and estimating costs under various conditions. The estimates show that S.Q.C structures require lower construction cost because smaller volumes of concrete are placed and smaller quantities of excavated material are produced if the cross section of the structure can be reduced. **Fig 1** shows a cost comparison for bridge piers.

3 SEISMIC RESISTANCE

Fig 2 shows bending moment-displacement curves for typical specimens as examples of experimental results[1),2)]. Specimen No. 1 had a longitudinal steel ratio equivalent to that of No. 0, and was made of high-strength material. The experimental result shows that the yield strength M_y of specimen No. 1 became larger than that of No. 0 in proportion to the increase in the yield strength of longitudinal steel but that ultimate displacement was almost the same for the two specimens. It was thus found that increasing the strength of S.Q.C column members was possible while maintaining their ductility, and that S.Q.C column members could absorb energy and resist seismic forces better than ordinary reinforced concrete members. Specimen No. 9, which was designed to have a reduced cross sectional area so as to be provided with flexural strength equivalent to that of No. 0, had ductility equivalent to or higher than that of No. 0. Thus, S.Q.C members could maintain their strength and ductility even after their cross sectional area was reduced to 60 to 70% of that of ordinary reinforced concrete members. It was therefore found possible to reduce the weight of the structure and increase seismic resistance at the same time.

4 FLOW OF DESIGN

This section outlines an example of design presented in the attachment to the guideline. A flow of reviewing a design example is shown in **Fig 3**. The review process is divided into two major phases: material design and performance evaluation of the structure. In material design, physical properties (characteristic values) are determined and performance for construction work is evaluated. Performance evaluation of the structure consists of the evaluation of performance requirements for safety, serviceability, durability and seismic resistance.

REFERENCES

[1] Kondoh, Mishima, Shimono and Sato: A study on ductility evaluation methods for reinforced concrete members using high-strength material, Proceedings of the Japan Concrete Institute, No. 3, pp 217-222, 1999 (in Japanese).

[2] Kondoh, Mishima, Tanimura and Sato: A study on ductility checking methods for reinforced concrete members using high-strength material, Proceedings of the 55th Annual Conference of Japan Society of Civil Engineers, Vol. 478, pp 958-959, September 2000 (in Japanese).

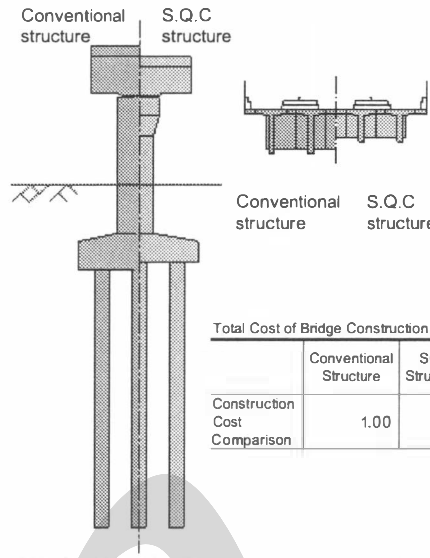

Total Cost of Bridge Construction

	Conventional Structure	SQC Structure
Construction Cost Comparison	1.00	0.97

Fig 1 Trial Design and Cost Comparison

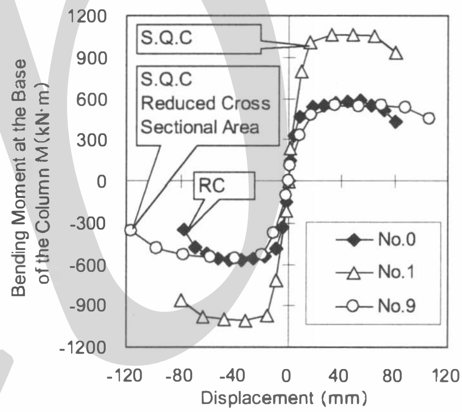

Fig 2 Bending Moment-Displacement Relationships

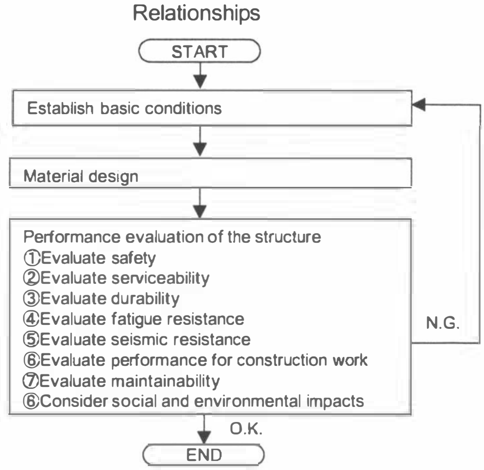

Fig 3 Flow of Overall Design

HIGH STRENGTH CONCRETE USING LOW HEAT PORTLAND CEMENT AND SILICA FUME

Yuichi Otabe   Takayoshi Kobayashi   Tetsuo Kobayashi   Yasunori Suzuki
Sumitomo Osaka Cement
JAPAN

Keywords: high strength concrete, low heat portland cement, silica fume, design of mix proportion, autogenous shrinkage

1 INTRODUCTION

Since demands for high strength concrete have increased recently, silica fume has been used due to its micro filler effect in concrete. Another effect such as reduction in viscousness of high strength concrete with a large quantity of binder is also expected. However, there are some problems to be solved, such as high temperature rise and large autogenous shrinkage during the hardening process. They not only cause an initial defect in concrete structure due to cracking formations, but also prevent strength development over long terms due to heat generation. Since low heat portland cement is effective in reducing such heat generation, its application to high strength concrete is increasing gradually.

In this study, properties of strength of high strength concrete using low heat portland cement and silica fume were confirmed in experiments on full-sized specimens, and the design of mix proportion was discussed in light of these results. Furthermore, time-dependent changes of fluidity and autogenous shrinkage in regard to the concrete were clarified, and countermeasures were also proposed.

2 OUTLINE OF EXPERIMENTS

2.1 Material and mix proportion

For high strength concrete, low heat portland cement and silica fume were used, while the replacing rate of silica fume was 10% of the weight of cement. Fine aggregates were hill sand and crushed sand. Coarse aggregate was crushed stone. Polycarboxylic acid was used as a superplasticizer.

The water-binder ratios of high strength concrete were 16%, 20%, 24% respectively, while the quantity of water was kept constantly at 140kg/m^3. The quantities of superplasticizer were determined by trial mixing to yield slump flow between 60 to 70cm.

2.2 Items of experiment

Various examinations were carried out on concrete manufactured at the ready-mixed-concrete factory. The points examined concerning fresh concrete properties are slump flow, L-type flow, and V-type funnel for flowability and air content. For hardened concrete, compressive strength of both standard cured specimens and drilled cores were measured. Furthermore, both time dependent change of fluidity and autogenous shrinkage were measured.

3 RESULTS

3.1 Strength and design of the mix proportion

The results of the compressive strength of standard cured specimens and cores are shown in Fig.1. In

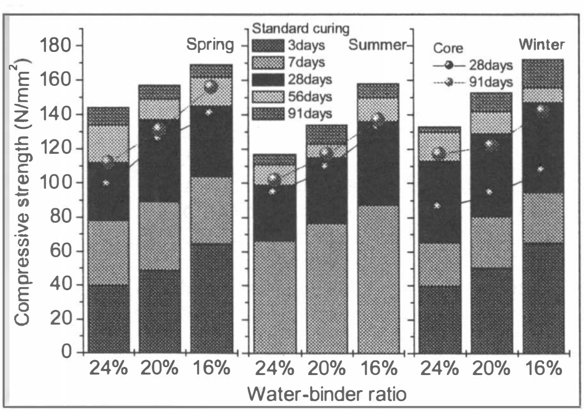

Fig.1 Compressive strength

mix-proportion design satisfying required structural concrete strength, it is necessary to calculate a required average strength by adding S value, which expresses the difference of the strength between standard cured specimens and cores, to specified design strength and standard deviation provided that S value could be quantified any water-binder ratio. Therefore, it is possible to determine a required average strength by Eq. (1).

$$mF \geqq Fq+mSn+2\sigma, mF \geqq 0.9(Fq+mSn)+3\sigma \quad (1)$$

Where, Fq is the specified design strength, mF is the average strength under standard curing at m days, mSn is the difference of strengths between standard cured specimens at m days and cores at n days, σ is the standard deviation ($\sigma=0.1Fq+0.1mSn$). The S value is calculated using a proposed equation as follows:

$$mSn = \frac{1.2(Am-An)}{1.2An-0.2Am} \cdot Fq + \frac{AnBm-AmBn}{1.2An-0.2Am} \quad (2)$$

where, A and B are the slope and the intercept in the linear equation of the relationship between binder-water ratio and strength.

The method of design mix proportion by using Eq. (1) and Eq. (2) is proposed here.

3.2 Fluid retentivity and autogenous shrinkage of high strength concrete

The results concerning fluid retentivity are shown in Fig.2. Although the slump flow decreased greatly when not adding retarder, time dependent changes decreased by adding a very small quantity of retarder. As a result, the fluid retentivity has been improved considerably without delaying setting time and the reduction in early age strength.

The result of autogenous shrinkage strain is shown in Fig.3. When either a retarder or a heat controlling agent was used, autogenous shrinkage could be reduced considerably compared with the case where both were not used. Furthermore, the reduction effect became larger when the both agents were used together. It was recognized that controlling hydration of the interstitial phase by retarder and heat controlling agent could contribute to the reduction in autogenous shrinkage.

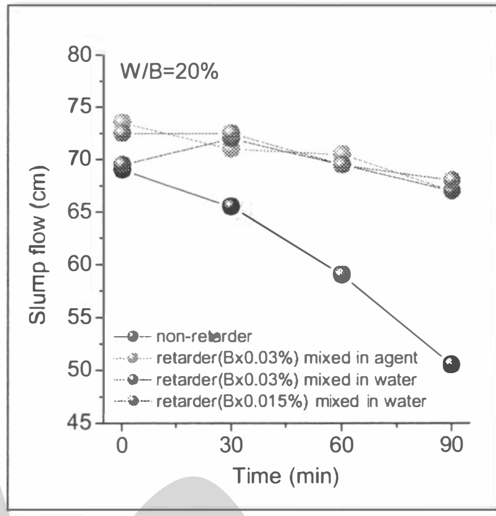

Fig.2 Change of slump flow

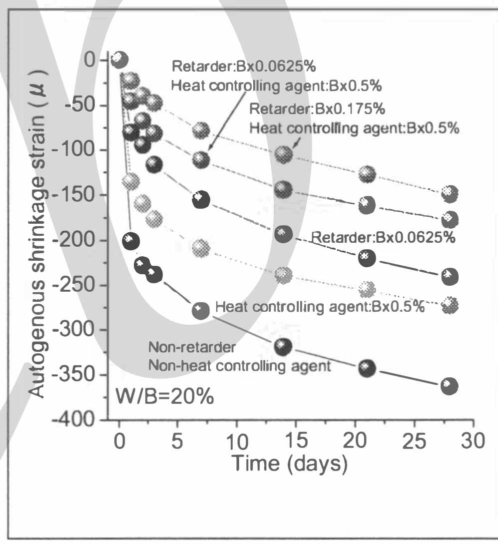

Fig.3 Autogenous shrinkage

4 CONCLUSION

[1] A method of design mix proportion was proposed because S value could be calculated at any water-binder ratio.

[2] The use of a retarder was effective not only the improvement of fluid retentivity but also reduction in autogenous shrinkage. Furthermore, autogenous shrinkage was lowered noticeably by using in combination with a retarder and a heat controlling agent.

SELF-COMPACTING LIGHTWEIGHT CONCRETE – A NEW HIGH-PERFORMANCE BUILDING MATERIAL

Viktor Mechtcherine Michael Haist Alexander Hewener Harald S. Müller
University of Karlsruhe, GERMANY

Keywords: self-compacting concrete, lightweight aggregates, rheometer tests, fibre reinforcement

1 INTRODUCTION

Self-compacting lightweight concrete (SCLC) is a new high-performance building material, which combines the well-known advantages of lightweight concrete with those of self-compacting concrete (SCC). Due to its favourable physical properties, its low unit weight and high strength in combination with an excellent workability and low noise emission during concreting SCLC might find a broad application in the practice of construction, especially in the production of precast elements and at the rehabilitation and reconstruction of buildings, respectively. This paper reports on the development and optimization of appropriate mixes for SCLC as well as on its rheological and mechanical properties.

The principal demands conceming the rheological properties of SCC, like high flowability, safe deairing and sufficient cohesion of the batch as well as a high resistance against segregation also apply to self-compacting lightweight concrete. However, with regard to the development of suitable mixes for SCLC, some specific phenomena have to be considered:

(1) flowing and self-compaction of the fresh concrete occurs at a reduced rate due to a lower unit-weight,
(2) lightweight aggregates adsorb a part of the mixing water, which can lead to a premature stiffening of SCLC as well as to the total loss of self-compactability,
(3) lightweight aggregates show a pronounced tendency to segregate (attributed to buoyancy).

The first phenomenon results from basic physical laws and cannot be overcome. Since for a proper execution of building work the concreting rate should not drop below a certain limit, the reduction of the unit weight of concrete is only reasonable up to some minimum value, which however cannot be defined so far.

In order to limit the adsorption of water by the porous lightweight aggregates they may be slightly pre-wetted by a defined amount of water.

The optimisation of the rheological properties of the binder paste and the mortar is the key to a successful production of SCLC (see Fig. 1). By optimising the viscosity and the shear resistance of the binder paste and the mortar the resistance of SCLC against segregation can be increased dramatically so that a sufficiently high cohesion is achieved while maintaining a high workability of the fresh concrete.

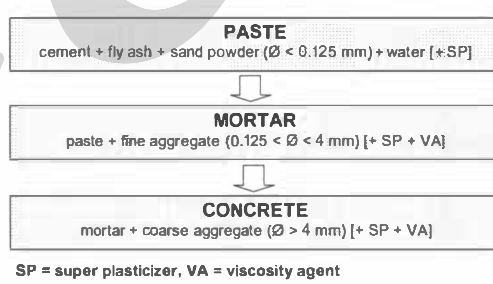

Fig. 1 Flow chart for the development of SCLC

2 INVESTIGATION ON PASTE AND MORTAR

Since the rheological properties of the powder paste are of significant importance to the self-compactability of SCC, in the first step, an extensive experimental program was carried out in order to determine the effect of the V_w/V_p ratio and the composition of the powder on its viscosity and shear resistance. On the basis of the obtained results optimum paste mixes could be produced.

Next, the experiments on mortar were performed. They showed a significant effect of the paste content on the rheological behavior of the mortar. Both the shear resistance τ_0 and the viscosity μ decrease with increasing paste content (Fig. 2).

Further, the V_w/V_p ratio was varied, revealing a strong dependency of the shear resistance and the viscosity from the water content. According to these results, the influence of both parameters, the paste and the water content, seem to be connected with each other.

An addition of 0.15 mass% (% by mass of cement) of viscosity agent indicated no effect on the rheological parameters of the mixture (here: with PC_M = 67 vol.%, VA = 1.5 mass% o.c. (o.c. = of cement) and V_w/V_p = 0.763) while a higher dosage of viscosity agent (0.3 mass%) led to a significant increase of the shear resistance τ_0 and the viscosity μ of the mortar.

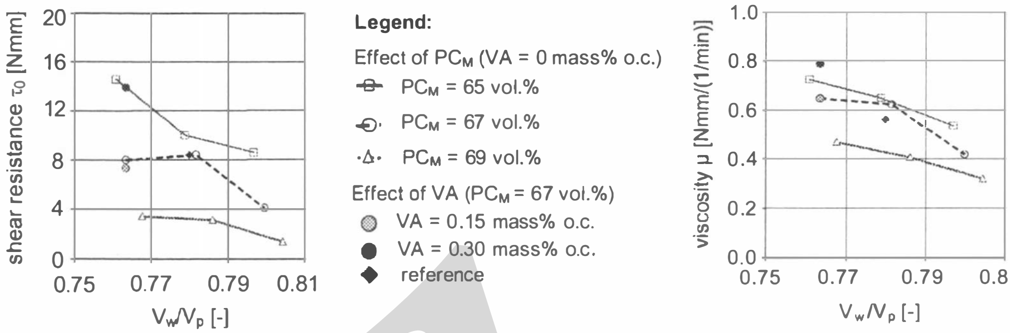

Fig. 2 Effect of the V_w/V_p ratio on the shear resistance τ_0 (left) and the viscosity μ (right) of mortar with expanded clay sand for different paste contents PC_M and viscosity agent contents VA (in % by mass of cement) in mortar

3 INVESTIGATION ON CONCRETE

Based on the results of the mortar tests, four different mortar mixes were developed for the investigations on concrete. Subsequently, these mixes were combined with different kinds and amounts of lightweight coarse aggregate.

The slump flow values of all developed mixes ranged between 63 and 72 cm and thus correspond to the usual values for SCC. However, the corresponding spreading time t_{50} and the v-funnel flow time were significantly higher than the average flow time for SCC. With decreasing unit weight of the investigated SCLC a pronounced increase of the flow time could be observed [1].

Table 1 Properties of hardened self-compacting lightweight aggregate concretes

concrete	compressive strength [MPa]		modulus of elasticity [MPa]	ρ_{dry} [kg/dm³]
	28 d	90 d	28 d	
SCLC 1	48	59	17 900	1.78
SCLC 2	39	43	12 900	1.43

The properties of hardened concrete for two representative SCLC mixtures are given in Table 1. Both concretes exhibit high compressive strengths at specific unit weights of 1.78 kg/dm³ and 1.43 kg/dm³, respectively. The modulus of elasticity corresponds well to the modulus of elasticity for normal lightweight aggregate concretes as estimated according to the German building code DIN 1045-1 on the basis of the measured compressive strength of SCLC.

4 SCLC WITH FIBRE REINFORCEMENT

Within this research project, the effect of the addition of different amounts of steel, polypropylene and glass fibres on the rheological properties of fresh SCLC as well as on the properties of hardened SCLC was investigated. The workability of SCLC remains sufficient only up to some defined percentage of fibres. This "limit content" depends strongly on the type of fibres. Considering the mechanical properties of SCLC, the addition of 0.5 vol.% of steel fibres increases the fracture energy by a factor of 100 compared to SCLC without reinforcement, whereas the compressive strength and the flexural tensile strength of this concrete remained almost unchanged. Details may be found in [2].

REFERENCES

[1] Müller, H. S., Mechtcherine, V.: Self-compacting lightweight concrete. In: State-of-the-Art Report „Self-compacting concrete ". DAfStb, No. 516, pp. 74-84, 2000 (in German).

[2] Hewener, A.: Self-compacting lightweight concrete with fibre reinforcement. Diploma thesis, Institute of Concr. Struct. and Build. Materials, University of Karlsruhe, Germany, 2001 (in German).

THE DEVELOPMENT OF SEMI-SELFCOMPACTING CONCRETE AS A FILLING MATERIAL FOR COMPOSITE STRUCTURES

Toru Yamaji
Port and Airport Research Institute, JAPAN

Sohsuke Kitazawa
National Instisute for Land Infrastructure Manegement Ministry of Land, Infrastructure and Transport, JAPAN

Toshio Azuma Nobufumi Yamagata
Kyusyu Regional Development Bureau, Ministry of Land, Infrastructure and Transport, JAPAN

Nobuaki Shiraishi
Coastal Development Institute of Technology, JAPAN JAPAN

Osamu Kiyomiya
Kiyomiya Laboratory, Waseda University

Takeshi Yamato
Dept.of Civil Eng., Fukuoka University, JAPAN

Keywords: semi-selfcompacting concrete, composite structure, immersed tunnel

ABSTRACT

In recent years, typical immersed tunnels have been built as steel-concrete composite structures made from self-compacting concrete with a slump flow of around 650 mm. However, production control, construction control and quality control of self-compacting concrete are complicated, as well as more costly than ordinary types of concrete. To solve the problems, the authors have developed a type of concrete with a slump flow of approximately 450 mm and are now performing experiments about it. We define the concrete as "Semi-selfcompacting Concrete as a Filling Material", and describe as semi-selfcompacting concrete below. This type of concrete can be provided the required compactability with few supplementary vibrations, and is less costly and gives easier production control, construction control and quality control than self-compacting concrete.

The objective of this study is to investigate the performance and compactability of the semi-selfcompacting concrete by performing various experiments.

The conclusions obtained by this study are as follows:

(1) For semi-selfcompacting concrete with slump flow of approximately 450 mm, the authors could confirm the effects of fluctuations in surface moisture and fineness modulus of fine aggregates on fresh concrete properties of self-compacting concrete, as shown in Fig.1. This degree of the effects seemed to be less than that of powder-type self-compacting concrete, and equal to that of combination-type self-compacting concrete. These results suggest the need to take appropriate control of fluctuations in surface moisture of fine aggregate especially, which heavily effects compactability.

(2) The semi-selfcompacting concrete that produced at a ready mixed concrete plant satisfied the required fresh concrete characteristics. The slump flow is decreased by less than 50 mm even after 90 minutes of mixing as shown in Fig.2. This indicated that this concrete also has good performance in actual construction.

(3) The change in fresh concrete properties of the semi-selfcompacting concrete before and after concrete pumping was very little. Pumping properties of this concrete is considered to be excellent.

(4) It was confirmed that the semi-selfcompacting concrete satisfied the required compactability, when the concrete was placed on the top floor plate or bottom floor plate of an immersed tunnel modeled in this study, with applying supplementary vibrations at four vibrating positions near the corners of the plate for five seconds at a frequency of about one minute (as shown in Fig.3).

(5) The semi-selfcompacting concrete was confirmed to have good quality after hardening.

(6) It was confirmed that semi-selfcompacting concrete provides excellent strength characteristics and chloride permeability, even on exposing in seawater. Thus, it should provide adequate durability in marine environments.

Based on the results described above, the authors concluded the suitability of semi-selfcompacting concrete for the production of immersed tunnels of composite structure. In future research, we plan to concentrate our efforts on determining the allowable range of slump flow, on investigating the stability of fresh concrete properties, and on verifying the suitability of concrete for wall members.

REFERENCES

[1] Japan Society of Civil Engineers : Construction Guidelines for Self-Compacting Concrete. Japan Society of Civil Engineers Concrete Library 93, pp. 157-159, Oct. 1998 (in Japanese)

[2] Oka, R., Iwaki, M. and Sakata, N. : Effect of Special Viscosity Agent on the Performance of Self-Compacting Concrete. The 48th Annual Science Lecture Meeting of Japan Society of Civil Engineers, V-56, pp.138-139, Sept. 1993 (in Japanese)

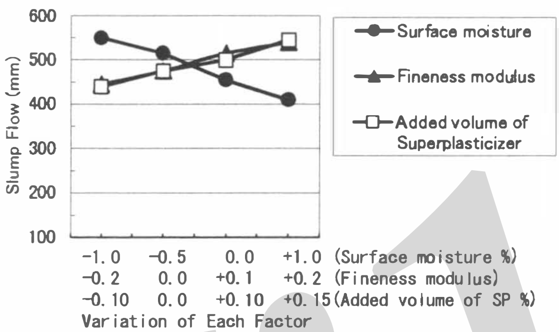

Fig.1 Changes in Slump Flow Caused by Variation of Different Factors

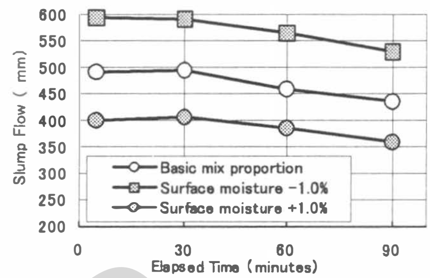

Fig.2 Change in Slump Flow Caused by Surface Moisture of Fine Aggregate

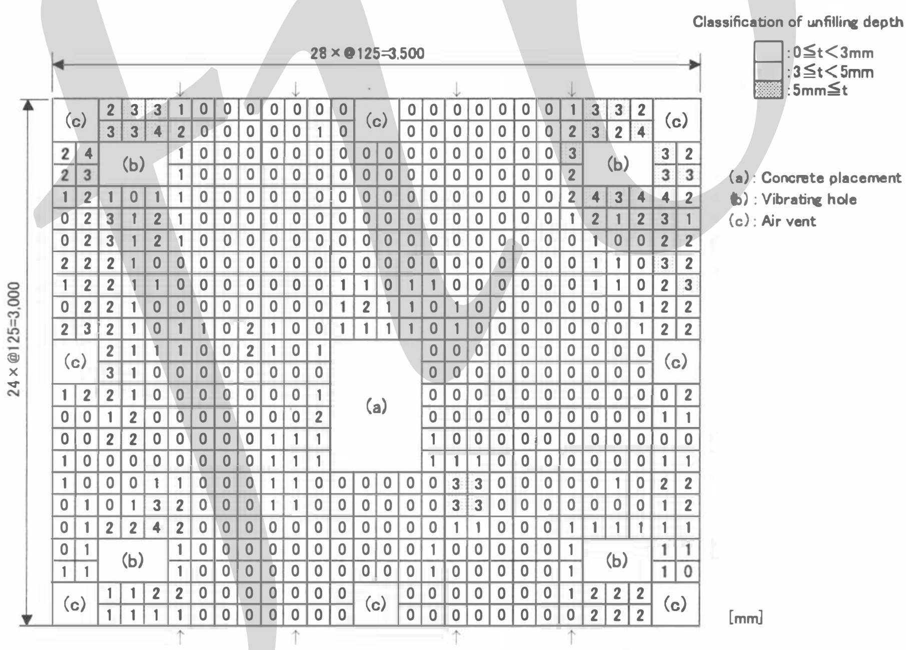

Fig.3 Unfilling Depth on Top Surface of Concrete (Slump flow=500 mm)

DEVELOPMENT OF NEW TYPE CONCRETE ADMIXTURE FOR PREVENTING LEAKAGE OF WATER THROUGH CRACKS

Masanori Tsuji Takehiro Sawamoto
Science University of Tokyo, JAPAN

Koichiro Shitama
Maebashi Institute of Technology, JAPAN

Keywords: Superabsorbent polymer, Admixture, Leakage, Curing, Shrinkage crack

1 INTRODUCTION

In recent years, many kinds of superabsorbent polymers have been synthesized. The superabsorbent polymers used in this study can hardly absorb water under alkaline condition in fresh and hardened concrete, but can absorb much water under neutral or acid condition and set to gel.

In this study, these superabsorbent polymers are proposed as a new type of concrete admixture in order to make hardened concrete waterproof even when small defects under constructions and cracks due to temporary loads, drying shrinkage, temperature change, etc. occur. These superabsorbent polymers absorb water under neutral or acid conditions leaking through the cracks and set to gel, so that the cracks are immediately filled up with the gel.

On the other hand, this admixture of superabsorbent polymers is also effective to save job curing concrete at the early age and to prevent the cracking of concrete caused by the initial drying shrinkage. The surface of concrete can be covered with gel only by wetting the surface of concrete after the removal of forms because the superabsorbent polymers around the concrete surface absorb immediately the water and set to gel. Therefore, the concrete surface is coated with the gel and protected from drying.

2 EXPERIMENTS

In this study, the white and ball forms superabsorbent polymers that were made from acrylic acid were examined. The properties of superabsorbent polymers and mix proportion of mortar are respectively shown in Table 1 and Table 2.

Experimental apparatus for leaking test are shown in Fig.1. The specimens were cured in the air at 20±2℃ until at the age of 7 days, and a crack was occurred to penetrate cross section at the center of the specimen by bending.

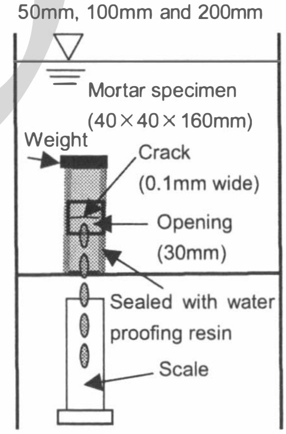

Fig.1 Apparatus for leaking test

Table 1 Properties of superabsorbent polymer

Polymer type	Water absorption in pure water (g/g)	Average grain diameter before absorption (μm)	Density before absorption (g/cm³)	Strength of gel
A	200～300	Under 280	0.9～1.0	High
B	600～800	Over 50	0.8～1.0	Medium

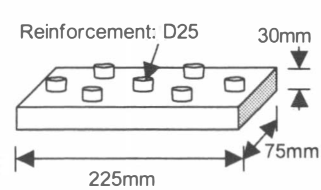

Fig.2 Specimen for drying shrinkage crack test

Table 2 Mix proportions of mortar

Mortar flow	W/C (%)	S/C	Percentage of polymer to mortar volume (%)
230±10	30,40,50	1.0	0, 0.2, 0.4, 1.0, 2.0, 3.0

On the compressive strength test, specimen sized 50 by 100mm was wetted by pouring water for 10 minutes after the removal of mold at the age of 24 hours. And then the specimens were cured in the air at 20±2℃ until loading test. For the purpose of comparison, the specimens were always kept in the water after the wetting.

The mortar specimen shown in Fig.2 was dried in electric dryer at 40℃ for 96 hours after casting mortar, and cracks caused by initial drying shrinkage were observed.

3 TEST RESULTS

Some examples of test results reported in this paper are shown in Fig.3～Fig.5

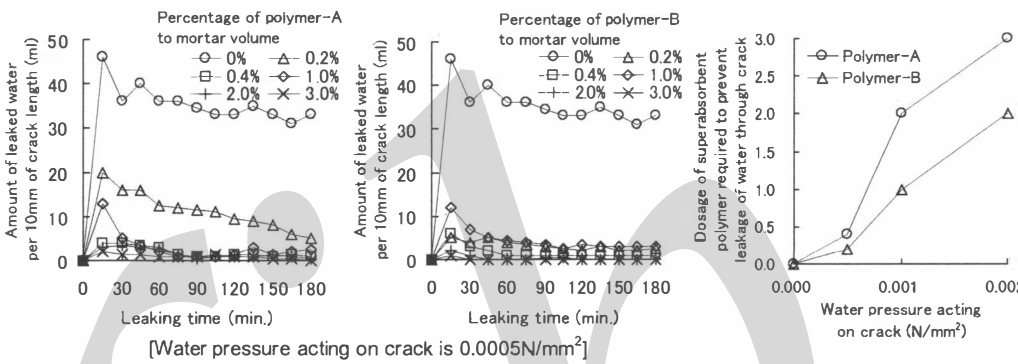

Fig.3 Test result of leakage of water through crack (W/C=50%)

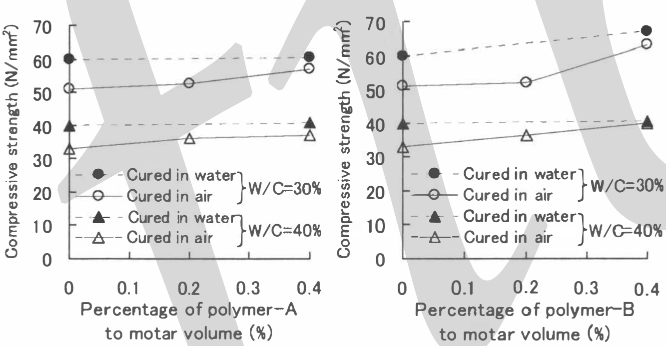

Fig.4 Test result of compressive strength at age of 7days

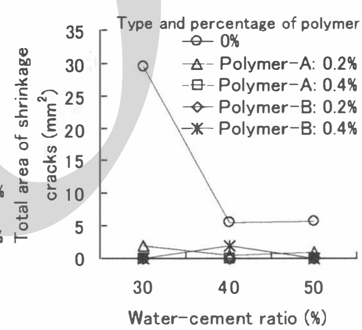

Fig.5 Test result of drying shrinkage crack

4 CONCLUSION

(1) The leakage of water through crack is showing a tendency to be great decrease when the superabsorbent polymers are added about 0.5% to the mortar volume contained in concrete.

(2) Even though concrete is cured in air, the compressive strength of concrete containing superabsorbent polymers is almost the same as that of the concrete always cured in water by wetting concrete surface for some minutes after removal of forms.

(3) Adding the superabsorbent polymer in concrete is great effective to prevent cracking of concrete caused by the initial drying shrinkage.

For actual application of the surperabsorbent polymer to admixture for concrete, it is important to be considered that the surperabsorbent polymer may store chloride from outside of concrete and condense the chloride, and then may accelerate corrosion of steel bar.

SHEAR DESIGN OF HIGH STRENGTH CONCRETE BRIDGE GIRDERS

Neil M. Hawkins Daniel A. Kuchma
Department of Civil and Environmental Engineering
University of Illinois at Urbana-Champaign, Urbana, IL 61801, USA

Keywords: shear, high strength concrete, bridges

1 INTRODUCTION

Enormous advances have been made in concrete technology over the last two decades. In North America it is now possible to obtain ready-mixed concrete with strengths as high as 15,000 psi (103 MPa) and plant produced concrete products with strengths of 20,000 psi (137 MPa). Further, in laboratory tests, strengths as high as 100,000 psi (690 MPa) have been achieved. High Performance Concrete (HPC) holds the promise of helping the concrete industry correct serious infrastructure deterioration problems and of spanning longer distances more effectively.

North American Codes for the design of buildings and bridges, such as ACI 318 Building Code and AASHTO Bridge Code, were developed primarily from test data with concrete strengths in the 3,000 to 5,000 psi (21 to 34 MPa) range. Understandably, designers frequently question the validity of the provisions of those codes for high strength concrete (HSC) structures. Both ACI and AASHTO are trying systematically to ensure that their documents are appropriate for HSC. However, laboratory testing of HSC structural components has not kept up with the advances in concrete technology. There are serious gaps in existing knowledge that need to be addressed if HSC structures are to perform satisfactorily. No gap is more serious than the inadequacy of information on the shear strength of HSC beams [1]

In 1993, the US Federal Highway Administration (FHWA) began a program to implement the greater use by the States of HPC bridge structures. The FHWA sponsored HPC bridge demonstration projects and held showcase workshops. The concrete used in those bridges had design strengths of up to 10,000 psi (69 MPa). However, because many of the resulting bridges had actual strengths well in excess of that level, their performance provides information for strengths up to 15,000 psi (103 MPa).

In 2001 the National Cooperative Highway Research Program (NCHRP) initiated a three-year study (Project 12-56) on “Application of the LRFD Bridge Design Specifications to High-Strength Structural Concrete: Shear Provisions” with the authors as the lead investigators. A review panel of State and FHWA bridge engineers guides the study, which has two phases. Phase I has been completed. It involved review of experience related to the use of HSC in bridges, identification of barriers to the expanded use of HSC, determination of HSC research needs, and the development of an experimental research program to generate data on the shear strength of HSC beams. Phase II began in May of 2002 and is the experimental research program as approved by the review panel. This paper describes the findings from the first phase of Project 12-56 and details of the experimental research program.

2 SHEAR DATA BANK

The AASHTO LRFD specifications for shear design utilize a sectional model based on the modified compression field theory [2]. The Phase I [3] Interim Report identified the most important HSC barriers as the requirements for crack control reinforcement, minimum transverse reinforcement, nominal shear resistance, and the determination of the factors relating the effect of the longitudinal strain and the inclination of the diagonal compressive stresses to the shear capacity of the concrete. Appropriate details for the proposed test program to address those barriers were identified using an interactive shear data bank developed by Dr. Kuchma (www.cee.uiuc.edu/kuchma/sheardatabank). That data bank contains the results from about 2000 beam tests. Most tests have been on small heavily reinforced beams subjected to concentrated loads and having shear span to depth ratios of about 3. Those are not likely to be the goveming shear conditions present in the HSC girders of the future.

The data bank was used to generate plots of shear stresses at failure versus different variables. Typical results are shown in Figs. 1 and 2 for reinforced concrete (RC) and prestressed concrete (PC) beams, respectively. For the 1287 RC members and the 587 PC members, there are very few test results for specimens containing either heavy shear reinforcement or HSC. For proportioning concrete based on field experience or trial mixes, or both, the ACI Code requires two groups of 30 test results for establishment of a one percent probability that the average of three consecutive tests will be below the specified strength and a one percent probability that an individual test will be less than 90% of the specified strength. If the same type of reasoning is applied to the data of Figure 2 for example, the maximum concrete strength for which statistically significant nominal shear strengths can be validated using existing data is about 8,000 psi (55MPa).

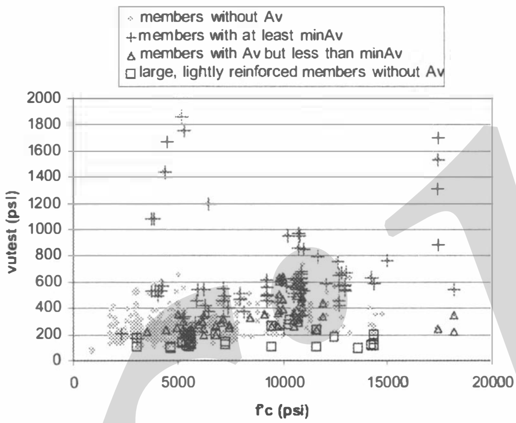

Fig. 1 Ultimate shear stress versus concrete strength for RC members

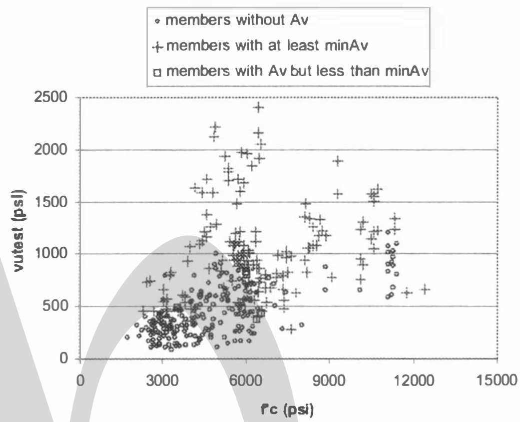

Fig. 2 Ultimate shear stress versus concrete strength for PC members

3. TEST PROGRAM

Based on the understanding developed from the Phase I work, the Phase II experimental program is focusing on testing large bulb-tee pretensioned bridge girders consisting of a 63 inch (1600 mm) deep precast concrete member composite with an 8 inch (203 mm) thick cast-in-place slab. Three test series will be made. The first series involves 16 uniform load tests on 8 simple span beams for which the primary variables are concrete strength, ranging between 10,000 and 18,000 psi (69 and 124 MPa); and the amount of shear reinforcement, ranging between the minimum currently specified by AASHTO and a maximum of 0.15 times the concrete strength. Secondary variables are the strand profile, straight or harped; and the type of shear reinforcement, deformed bar or welded wire fabric. Half of the tests will be on beams with 18,000 psi concrete. Several specimens for this test series have been cast and testing of those beams has commenced.

The second series will involve 8 tests on 18,000 psi simple beams made continuous over a central support and either embedded or not embedded in that support. These tests will allow examination of the issues associated with shear strength when negative moments are present. The third series will involve 8 tests on 18,000 psi simple beams for which the focus will be on the effects on shear strength of end detailing associated with strut and tie modeling, bond of the strand, and anchorage design. To follow the progress on this project, please visit www.cee.uiuc.edu/nchrp.

REFERENCES

[1] Collins, M.P., Mitchell, D. and MacGregor, J.G. : Structural design considerations for high strength concrete. Concrete International, ACI, May 1993, pp. 27-34.
[2] Vecchio, F.J. and Collins, M.P. : The modified compression field theory for reinforced concrete elements subject to shear. ACI Journal, V. 83, No. 2, Mar.-Apr. 1986, pp. 219-231.
[3] Hawkins, N.M. and Kuchma, D.A. : Application of the LRFD bridge design specifications to high strength structural concrete: shear provisions, phase I. Interim Report to NCHRP Panel 12-56, University of Illinois, Feb. 2000.

DEPENDENCE OF SHEAR CAPACITY OF REINFORCED CONCRETE BEAMS WITHOUT SHEAR REINFORCEMENT ON SIZE AND CONCRETE STRENGTH

Manabu FUJITA Kaori MATSUMOTO Takehiko OODATE Ryoichi SATO
Sumitomo Construction Co., LTD., Japan Hiroshima University, Japan

Keywords: shear capacity, high strength concrete, size effect, fracture mechanics

1. INTRODUCTION

Previously, the authors conducted shear tests on RC simple beams without shear reinforcement with the aim of determining the effect of concrete strength and the effect of member size on the shear fracture characteristics of RC beam members, using as parameters the compressive strength of the concrete f'_c (36-100N/mm^2), the effective depth d (250-1000mm), and the ratio of the shear span a and the effective depth d (hereafter "shear span ratio a/d"). The results of these tests confirmed that shear fracture of high strength concrete (HSC) was characterized by conspicuous localization of cracking as compared to ordinary strength concrete, and that the propagation of these cracks was rapid, resulting in more brittle fracture. Since the localization of cracking results from the tension softening of concrete, a study using fracture mechanics was conducted to determine the size effect on the nominal shear stress intensity τ_c (hereafter "shear capacity") when diagonal crack occurs.

2. COMPARISON OF THE DESIGN CODE FORMULAS ON TEST RESULTS

The fracture mode was diagonal tensile fracture in all cases. Fig.1 shows a comparison between the test results and the shear capacity derived using each of the design code formulas. The JSCE formula [1] and the CEB-FIP formula [2] provided an evaluation that were slightly in the danger zone in the d=1000mm case for HSC, but for the other cases the evaluation was in the safe zone. On the other hand, with the ACI formula [3] that did not consider the size effect, almost all of the evaluations for HSC were in the danger zone. From the above, it is clear that the shear capacity of HSC cannot be properly evaluated using the existing design code formulas.

3. STUDIES ON SHEAR CAPACITY FOR RC BEAMS USING FRACTURE MECHANICS

3.1 Characteristics and localization of crack

Crack localization was noted on the compression side from the center of the cross-section in each test specimen from test results. This trend was more noticeable for greater effective depths, and still more noticeable for greater compressive strengths. This difference in the localization of cracking is thought to be related to shear capacity and the size effect on shear capacity.

Crack localization results from the localization of the fracture process zone due to the tension softening of the concrete. The larger the member size is, and furthermore the greater the compressive strength is, the more conspicuous the localization of cracking will become. For this reason, it is thought that consideration for the application of fracture mechanics will be effective in making more rational evaluations of the size effect on the shear capacity of HSC.

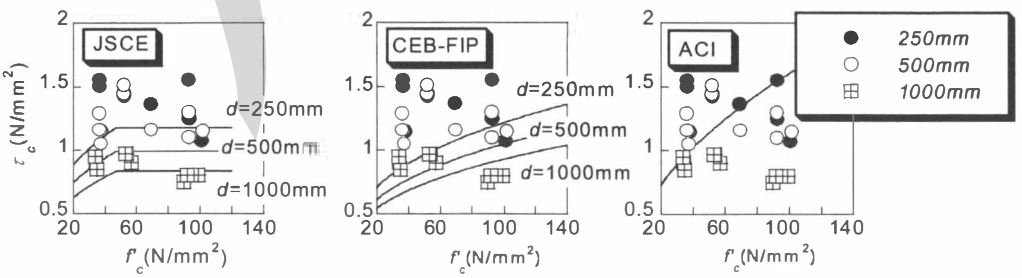

Fig.1 Comparison of formulas on design code to test results

3.2 Evaluation of characteristic length for concrete

In this study, each evaluation of the fracture energy G_f and the characteristics length l_{ch} by Hillerborg et al [4] was conducted. From this, it can be confirmed that, for $f'_c \leqq 85\text{N/mm}^2$, the value of G_f increases as compressive strength increases, but for $f'_c > 85\text{N/mm}^2$, the value tends to decrease. Fig.2 shows the relationship between f'_c and l_{ch}. From this figure, it can be seen that, as compressive strength increases, the value of l_{ch} decreases. The broken line in Fig.2 represents the results of regression analysis. The regression analysis and the test results showed an extremely high correlation, with a correlation coefficient of 0.9.

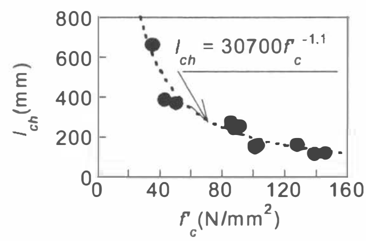

Fig.2 Dependence of compressive strength on characteristics length

3.3 Approach to size effect using fracture mechanics

In this study as well study of Hillerborg et al[8], a study of the size effect on τ_c was conducted using l_{ch}. To increase the accuracy of the study results, the results of a similar previous study were added to the results of this test. The l_{ch} was derived from the regression formula [see 3.2]. In this study, in order to consider the impact of concrete strength, the shear capacity was standardized by using the 1/3 power of the compressive strength in accordance with the design code formula of CEB-FIP. The results of the study are shown in Fig.3. Also, in order to check the impact of compressive strength on the size effect, levels were established with $f'_c \leqq 30\text{N/mm}^2$ as L'(low strength), $30 < f'_c \leqq 80\text{N/mm}^2$ as M' (medium strength) and $f'_c > 80\text{N/mm}^2$ as U' (high strength).

From Fig.3, it can be seen that, as d/l_{ch} increases, $\tau_c/f'_c{}^{1/3}$ tends to decrease. In addition, in Fig.3, the low strength L' values are near the solid line, while the high strength U' values are near the broken line, and the medium strength M' values are distributed between the solid and broken lines. When assuming the actual structure level (for example; beam and PC members on bridge superstructures), the range of d/l_{ch} can be thought of as being equal greater than 1. The results of regression analysis for L' and U' in the range of $d/l_{ch} \geqq 1$ were almost completely proportional to the –1/4 power and the –1/2 power of d/l_{ch}, respectively. Accordingly, each of the following theorems was determined by the method of least squares.

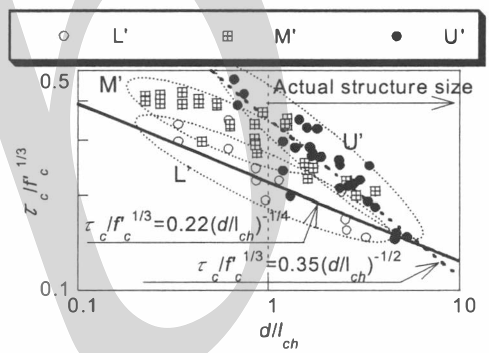

Fig.3 Study of size effect using l_{ch}

Low strength concrete : $\tau_c \big/ \sqrt[3]{f'_c} = 0.22(d/l_{ch})^{-1/4}$ HSC : $\tau_c \big/ \sqrt[3]{f'_c} = 0.35(d/l_{ch})^{-1/2}$

4. CONCLUSION

The conclusions derived from this study can be summarized as follows:

(1) The design code formulas by the JSCE, ACI and CEB-FIP overestimate the shear capacity of HSC of approximately $f'_c = 100\text{N/mm}^2$ and large size, resulting in evaluations in the danger zone.

(2) When characteristic length was used to study the size effect on shear capacity τ_c in accordance with fracture mechanics, the τ_c proportional to the effective depth at the actual structure level changed from to the –1/4 power to the -1/2 power of the effective depth as the compressive strength increased, and the τ_c of HSC was proportional to the effective depth to the –1/2 power.

REFERENCES

[1] JSCE : Standard Specification for Design and Construction of Concrete Structure, Design, 1996.

[2] ACI : ACI Manual of Concrete Practice Part 3, 1999.

[3] CEB-FIP : Model Code 1990, Bulletin D'Information No.213/214, Lausanne

[4] Per Johan Gustafsson et al : Sensitivity in Shear Strength of Longitudinally Reinforced Concrete Beams to Fracture Energy of Concrete, ACI Structural Joumal, May-June, pp.286-294, 1988.

EXPERIMENTAL STUDY ON SHEAR CAPACITY OF REINFORCED CONCRETE BEAMS USING SELF-COMPACTING HIGH-STRENGTH HIGH-DURABILITY CONCRETE

Natsuo HARA Tetsuya MISHIMA Takayoshi YAMADA Masao KONDOH
Maeda Corporation Japan

Keywords: shear capacity, self-compacting high-strength concrete, high-strength reinforced bar

1 INTRODUCTION

Using high-strength self-compacting concrete and high-strength reinforcement bars, the cross sections of members can be minimized. In these cases it is important to evaluate shear strength. In the method described in the Standard Specifications for Design and Construction of Concrete Structures issued by JSCE (Japan Society of Civil Engineers) [1], the shear strength of a slender member is calculated based on the modified truss theory, and an upper threshold value is defined for both the shear stress shared by concrete portion and the stress shared by shear reinforcement. A recent study by Shimono et al. [2] revealed that while the shear force shared by the concrete portion of structures composed of self-compacting concrete and high-strength shear reinforcement plateaus at a certain level, the shear forces working in the shear reinforcement increase up to its full strength. However, this results was obtained from loading tests on beam specimens using concrete with a target compressive strength of larger than 72 N/mm^2. The authors performed loading tests on beam specimens using concrete with two different target compressive strengths (30 N/mm^2, value for normal concrete structures, and 50 N/mm^2), in order to verify the relationship between concrete strength and the plateauing of the shear force shared by the concrete portion of a structure. Based on the results of the loading tests and previous studies, the authors proposed a method for evaluating the shear strength of reinforced concrete structures.

2 OUTLINE OF EXPERIMENTAL TEST PROGRAM

Table 1 shows the details of the five specimens used in the tests. Self-compacting concrete with a target compressive strength of 50 N/mm^2 was used for specimens No. 1 to No. 4, and normal concrete with a target compressive strength of 30 N/mm^2 was used for specimen No. 5. Except for specimen No. 1, high-strength shear reinforcement (specific yield strength: 685 N/mm^2) was provided in the shear spans of each specimen.

3 TEST RESULTS

3.1 Summary of test results

The summary of tests results is shown in **Table 2**. The calculative values in the table were derived based on the Standard Specification of JSCE. [1], [3]:

3.3 Deformation

Fig.3 shows the relationship between the working shear force and deflection at the mid-span. Loading tests (results: given in **Table 2**) showed that specimen No. 1, which was not provided with shear reinforcement, lost the load-bearing strength immediately after the occurrence of diagonal cracks. In contrast, shear force working in other specimens provided with shear reinforcement continued to increase after the occurrence of diagonal cracks. The crack growth continued until the shear failure, and the cracks eventually reached the compression edge. Test results for specimens No. 2 and No. 5,

Table 1 Specification of test beams

Specimen	Dimension: Width (mm)	Dimension: Effective Height (mm)	Dimension: Shear Span (mm)	Concrete: Design Strength (N/mm^2)	Longitudinal Reinforcement: Dia.-Nos.	Longitudinal Reinforcement: Design Yield Strength (N/mm^2)	Shear Reinforcement: Dia.-Pitch (mm)	Shear Reinforcement: Design Yield Strength (N/mm^2)	Shear Reinforcement: Ratio (%)
No.1	400	350	1050	50*	D29-4	685	–	–	–
No.2	400	350	1050	50*	D29-4	685	D6-100	685	0.16
No.3	400	350	1050	50*	D29-4	685	D10-200	685	0.18
No.4	400	350	1050	50*	D29-4	685	D6-75	685	0.21
No.5	400	350	1050	30	D29-4	685	D6-100	685	0.16

Table 2 Summary of test results

Specimen	Material strength			Calculation			Experiment		Comparison	
	Compressive strength of concrete	Yield strength		Shear capacity			Shear capacity		Exp./Cal.	
		Longitudinal bars	Shear reinforcement	Diagonal crack occur	Carried by shear reinforcement	Ultimate Shear Capacity	Diagonal crack occur	Ultimate Shear Capacity	Diagonal crack occur	Ultimate
	f'_c (N/mm^2)	f_{sy} (N/mm^2)	f_{wy} (N/mm^2)	$V_{c\ cal}$ (kN)	$V_{s\ cal}$ (kN)	$V_{y\ cal}$ (kN)	$V_{c\ exp}$ (kN)	V_{yexp} (kN)	$V_{c\ exp}/V_{c\ cal}$	$V_{y\ exp}/V_{y\ cal}$
No.1	51.0	698.2	—	201.1	—	201.1	194.7	194.7	0.97	0.97
No.2	49.4	698.2	746.6	198.9	143.9	342.8	178.9	381.0	0.90	1.11
No.3	51.0	698.2	803.0	201.1	174.3	375.4	169.1	376.8	0.84	1.00
No.4	55.2	698.2	746.6	206.5	191.9	398.4	186.2	437.4	0.90	1.10
No.5	27.8	698.2	746.6	164.3	143.9	308.2	144.6	274.5	0.88	0.89

which had the same shear reinforcement ratio and used concrete with different target compressive strengths, showed a significant difference in the ultimate shear strength. While the difference in the working shear force between the two specimens at the time for the visual inspection of diagonal cracks was about 34 kN, the difference in the ultimate shear strength between them was as large as 107 kN.

3.4 Strains in shear reinforcement

Fig.4 shows the distribution of strains in shear reinforcement for specimens No. 2 to No. 5 at four stages during loading tests. The strains of specimens No. 2 exceeded the yield strain, when the shear force was about 0.8 $V_{y,\ exp}$. On the other hand, the strains of the shear reinforcement of specimen No. 5 using normal concrete with a target compressive strength of 30 N/mm^2 did not reach the yield strain, even when the shear force was $V_{y,\ exp}$.

5 CONCLUSION

(1) The shear strength at the time of diagonal crack occurrence plateaus if the compressive strength of concrete exceeds 50 N/mm^2.

(2) If the compressive strength of self-compacting concrete is larger than 50 N/mm^2 and the specific yield strength of the shear reinforcement is equal to or smaller than 785 N/mm^2, the stresses in the shear reinforcement increase up to its full strength.

REFERENCES

[1] Japan Society of Civil Engineers: Standard specifications for design and construction of concrete structures,1996.

[2] Simono et al. : Experimental study on shear capacity of reinforced concrete beams using high-strength materials. Proc. of the Japan Concrete Institute Vol. 21, No.3, pp.175-180, 1999. (in Japanese)

[3] Niwa et al.: Revaluation of the equation for shear strength of reinforced concrete beams without web reinforcement, Concrete Library International of Japan Society of Civil Engineer, No.9, pp.65-85,1987.

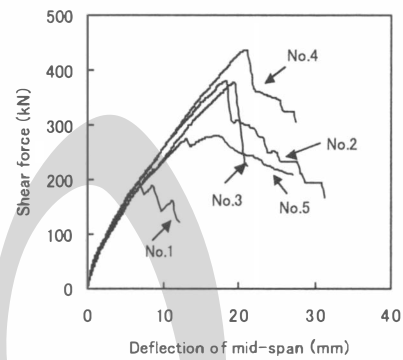

Fig.3 Shear force vs. mid-span deflection

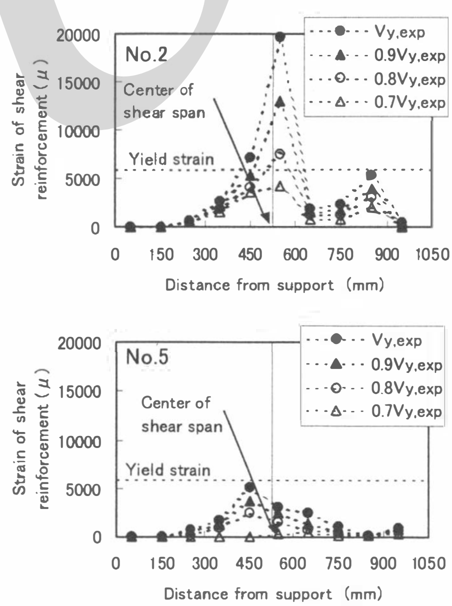

Fig.4 Distribution of strains in shear reinforcement

SHEAR BEHAVIOUR OF REINFORCED HIGH-PERFORMANCE CONCRETE BEAMS WITH HIGH-PERFORMANCE REINFORCEMENT

Sébastien Bemardi
Centre d'Etudes et de Recherches de l'Industrie du Béton, FRANCE

Bruno Mesureur, Philippe Rivillon
Centre Scientifique et Technique du Bâtiment, FRANCE

Michel Lorrain
Institut National des Sciences Appliquées de Toulouse, FRANCE

Keywords: reinforced high-performance concrete, shear, cracking

1 INTRODUCTION

Due to the evolution of materials and principally of concrete with the birth of high-performance concrete (HPC), it appeared necessary to undertake new experimental investigations in order to assess the possible consequences on the structural behaviour of reinforced concrete elements and their applications. However, a reinforced high-performance concrete means a better concrete (mechanical properties, durability) but also a better reinforcement with the improvement of its steel mechanical characteristics.

The study of HPC associated with high-performance reinforcement (HPR) has come to the attention of the BHP 2000 French National project involving the CSTB in collaboration with Toulouse University. The first part of this experimental research was devoted to the study of bonding laws and cracking behaviour of ties and rectangular beams (completed by a finite element model), especially at the serviceability limit state. In addition to the encouraging results that were obtained, the second part was dedicated to the study of shear behaviour, in particular at the ultimate limit state.

In this article, the shear behaviour of high-performance reinforced concrete beams (rectangular and T-shape cross section), under short-term imposed load, is investigated experimentally. A comparison was made between ordinary reinforced concrete (ORC) beams and high-performance reinforced concrete (HPRC) beams in order to highlight the increase of mechanical properties of materials on the shear strength and the diagonal cracking. All these test members are provided with high-performance steel for longitudinal reinforcement.

2 EXPERIMENTAL PROCESS

Test parameters are given in the table 1 and an example of a test device is shown in figure 1.

Table 1 Parameters for shear tests

	Rectangular beams					T-shape beams			
Test specimens	M100C HPR	M100C OR	M40 OR	M100C HPR	M100C OR	M30 OR	M30 HPR	M100C OR	M100C HPR
f_{cm} (MPa)	105	98	42	102	91	33		108	
$\rho_L = A_s/b_0d$ (%)	2.06					1.90			
f_y (MPa)	650	565	565	650	565	560	660	560	660
$\rho_t = A_{sy}/b_0s$ (%)	0.17 (1 stirrup)		0.34 (3 stirrups)			0.45		0.30	

HPR: High-Performance Reinforcement / OR: Ordinary Reinforcement

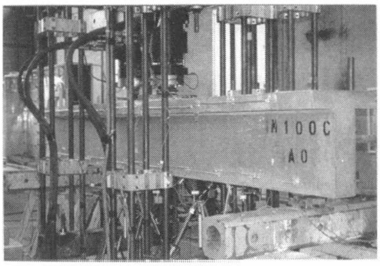

Fig. 1 Example of experimental device for T-shape beams tests

3 RESULTS

3.1 Shear strength at the ultimate limit state

In table 2, experimental shear resistance values are compared with some design codes and formulations (partial safety factors $\gamma_s = \gamma_c = 1.0$).

Table 2 Experimental/Design shear strength ratio

	Test specimens	EC2 [1]	BAEL [2]	ACI	Kordina [3]
R beams	M100C - 1 HPR stirrup	0.89	1.52	1.30	1.03
	M100C - 1 OR stirrup	0.85	1.47	1.25	0.98
	M40 - 3 OR stirrups	0.83	1.03	0.93	0.85
	M100C - 3 HPR stirrups	0.91	1.36	1.19	1.02
	M100C - 3 OR stirrups	0.73	1.10	0.96	0.81
T beams	M30 - OR stirrups	1.37	1.51	1.31	1.24
	M30 - HPR stirrups	1.38	1.50	1.32	1.27
	M100C - OR stirrups	1.08	1.44	1.25	1.03
	M100C - HPR stirrups	1.22	1.60	1.39	1.17

3.2 Diagonal cracking

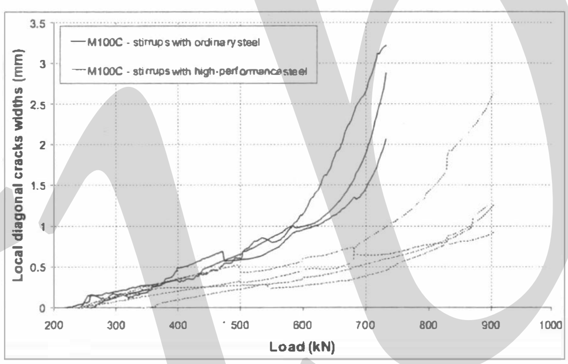

Fig. 2 Influence of the yield strength of the stirrups on the local diagonal crack widths

CONCLUSIONS

Further to the analysis of the experimental results, the following conclusions can be drawn:

- global shear behaviour is the same between HPRC and ORC beams ;
- shear cracking load increases with the use of HPC but not with HPR (Young's moduli are the same) ;
- shear strength increases with the use of HPR (in a proportion equal to the yield strength ratio) and HPC ;
- results don't allow to conclude that shear crack widths are reduced with the use of HPR / HPC.

REFERENCES

[1] Eurocode 2 : Calcul des structures en béton et Document d'Application Nationale. P18-711-0, ENV 1992-1-1, Afnor, Paris, Décembre 1992.

[2] Fascicule n° 62 - Titre I - Section I, Régles techniques de conception et de calcul des ouvrages et constructions en béton armé suivant la méthode des états limites. BAEL 91 révisé 99. Bulletin Officiel, fascicule spécial N° 99-8, Avril 1999.

[3] Kordina E. H. K., Blume F. : Empirische Zusammenhänge zur Ermittlung der Schubtragfähigkeit stabförmiger Stahlbetonelemente. Deutscher Ausschuss für Stahlbeton, Haft 364, Ed. Ernst & Sohn, Berlin, pp. 3-52, 1985.

BENDING AND SHEAR CAPACITIES OF REINFORCED SUPER LIGHTWEIGHT AGGREGATE CONCRETE BEAMS

Masashi Funahashi
Maeda Corporation
Japan

Hiroshi Yokota
Port and Airport Research
Institute, Japan

Natsuo Hara
Maeda Corporation
Japan

Junichiro Niwa
Tokyo Institute of
Technology, Japan

Keywords: super lightweight concrete, shear resistance, density, conversion term, reverse cyclic load

1 INTRODUCTION

The super lightweight aggregate (SLA), which was developed recently in Japan, has an absorption ratio of less than 5% and a specific gravity of between 0.8 and 1.2. These characteristics are superior to conventional lightweight aggregates. The freeze-thaw resistance, which is a drawback of conventional lightweight aggregate concrete, has been dramatically improved. Furthermore, SLA concrete has exceptionally low specific gravity of 1.2 to 1.8. The improved freeze-thaw resistance and exceptionally low specific gravity make it possible to apply SLA concrete to not only structures built on land but also those in marine.

Because SLA has high strength itself, SLA concrete is also applicable to structures where high strength is required such as prestressed concrete members. However, there are some problems in design, because the increases in tensile and shear strengths are smaller than those in compressive strength. Therefore, in the current JSCE standard specification for concrete structures, the shear capacity of a lightweight concrete beam is constantly reduced to be 70% as that of general normal-weight concrete [1]. This reduction factor for the shear capacity of lightweight aggregate concrete might restrict an economical design in dimension or reinforcement of members when structures are designed. The reduction is also considered in Europe; that is, tensile strength and shear strength of lightweight concrete would be reduced by applying a conversion term that is a function of the density of concrete [2]. Therefore, reinforced SLA concrete beams, which have various densities of concrete, were experimentally load-tested to investigate their basic mechanical properties of flexural and shear strengths.

Reinforced SLA concrete beams with controlled density of concrete were experimentally loading-tested to discuss their shear and flexural failure modes and capacities in this paper. Moreover, methods to evaluate the strength of SLA concrete are proposed here.

2 EXPERIMENTAL TESTS

2.1 Shear loading-test

Shear resisting behaviors of SLA concrete were investigated by a series of experimental loading tests using reinforced concrete simply supported beams. Test beams were manufactured with controlled density of concrete, 2300, 1800, 1500 and 1200 kg/m^3 to investigate the influence of the density of concrete. No shear reinforcement was provided in the shear spans of beams.

The calculated shear capacity was obtained by Eq. (1) proposed by Niwa et al. [3], which was used in the JSCE design standard for concrete structures as simplified equation without considering the effect of a/d.

$$V_c = 0.20(0.75+1.4d/a)f_c'^{1/3}(1000/d)^{1/4}p_w^{1/3}b_w d \qquad (1)$$

where, V_c is the shear capacity in concrete (N), a is the length of shear span (mm), d is the effective depth of a beam (mm), f_c' is the compressive strength of concrete (N/mm^2), p_w is the longitudinal reinforcement ratio (%), b_w is the width of a beam (mm).

Fig. 1 shows the shear carrying capacity at the diagonal tension cracking of SLA concrete beams. It was made clear from the experimental results that the shear resisting capacity of SLA beams is dependent on the density of concrete. The effect of the density of concrete to shear resisting capacity is not taken into account in the current design code in Japan as mentioned before. However, in the draft of revised version of Eurocode-2 [2], a density of concrete is considered as the conversion term that is a factor to calculate the shear capacity of lightweight concrete beams using that of general normal-weight concrete beams. The conversion term, η_s, is expressed as follows:

$$\eta_s = 0.4 + 0.6(\rho / \rho_0) \qquad (2)$$

where, ρ is a density of concrete in kg/m^3, ρ_0 is a density of normal-weight concrete.

The shear strength of concrete to govern the shear capacity of concrete beams has not well been quantified. However, the shear failure mechanism is considered to have close relation to the tensile splitting strength of lightweight concrete. Through try-and-error examination to find the most reasonable conversion term, η_s to predict the shear capacity of SLA beams has been proposed as follows:

$$\eta_s = (\rho / \rho_0)^{3/2} \qquad (3)$$

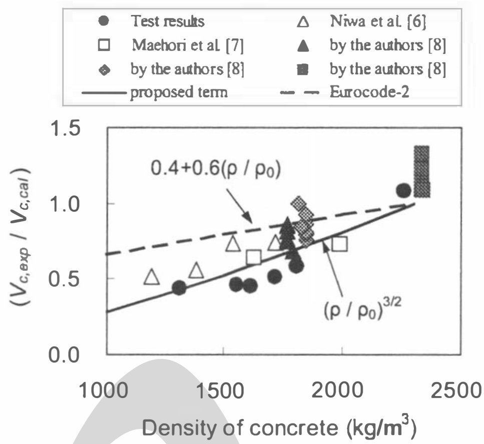

Fig.1 Shear capacity versus density of concrete

2.2 Flexural loading-test

Bending capacities of SLA concrete beam were investigated by monotonically increasing flexural loading-tests and reverse cyclic flexural loading-tests. Reinforcement is provided in the whole span of a beam to prevent the shear failure before longitudinal rebar yields.

Mix L is SLA concrete mixed with SLA0.85 as coarse aggregate. N is general normal-weight concrete, and B stands for blended aggregate concrete: a part of crushed stone was replaced by SLA.

The experimental bending capacities of all beams in any concrete mix, which were not only monotonically increasing loaded but also reverse cyclic loaded, were larger than those of calculated capacities. The ductility ratios of MN*i* beams were 8 to 11. On the other hand, the ductility ratios of both of ML*i* and MB*i* beams were 6 to 7, which were slightly reduced compared to those of normal-weight concrete. When $(V_c'+V_s)/V_m$ was calculated with considering the conversion term (η_s) for V_c, those of ML*i* and MB*i* beams were 1.8 to 1.9 and slightly smaller than those of MN*i* beams (2.2).

The ductility ratio increased as $(V_c'+V_s)/V_m$ increased. This means that it is possible for RC members using SLA concrete to maintain enough ductility, if the reduction of shear capacity of SLA concrete is compensated by extra shear reinforcement.

3 CONCLUSIONS

Major conclusions drawn from this study were as follows:

(1) The shear capacity of SLA concrete beams at diagonal tension failure decreased as the density of concrete became small. The conversion term was proposed to express this reduction with the density of concrete, ρ, as $(\rho / \rho_0)^{3/2}$.

(2) When SLA concrete is applied to the members subjected to cyclic loading, it is possible to maintain enough ductility ratio if the required value of $(V_c'+V_s)/V_m$ for the member is satisfied.

REFERENCES

[1] Japan Society of Civil Engineers : Standard Specification for Concrete, Design, 1996 (in Japanese)

[2] Walraven, J. : Design of Structures with Lightweight Concrete: Present Status of Revision of EC-2, Proc. of the Second International Symposium on Structural Lightweight Aggregate Concrete, Kristiansand, pp.57-70, 2000.6

[3] Niwa, J., et al. : Revaluation of the Equation for Shear Strength of Reinforced Concrete Beams without Web Reinforcement, Proceedings of JSCE, No.372, V-5, pp.167-176, 1986.8 (in Japanese)

STUDY ON THE FRESH AND HARDENED PROPERTIES OF CONCRETE CONTAINING SUPERPLASTICIZERS FOR ULTRA HIGH-STRENGTH CONCRETE

Takumi Sugamata Tomomi Sugiyama Satoshi Okazawa

NMB Co., Ltd. Central Research Labs., JAPAN

Key words: ultra high-strength concrete, superplasticizer, viscosity reducing effect, thixotropy, hysteresis loop

1. INTRODUCTION

The use of ultra high-strength concrete designed to have compressive strength of 100 N/mm^2 or grater is increasing in Japan. The authors developed a polycarboxylate-based superplasticizer (SPN) capable of imparting high deformability and lowering the viscosity to ultra high-strength concrete having a water-binder ratio of 20% or below. The authors compare the viscosity-reducing effect of this SPN with a conventional superplasticizer (SPC) in ultra high-strength concrete, defining the force required to initiate flowing motion from a stationary state as being due to a difference in thixotropy. The authors also clarified strength development and durability of hardened concrete having water-binder ratios of 22% down to 12%---an area in which there is very little published literature.

2. OUTLINE OF CONCRETE TESTS

2.1 Study of fresh properties of ultra high-strength concrete

The unit weight of water was 150 kg/m^3 in all concretes. Water-cement ratio (W/C) was varied from 14 to 25%. Silica fume cement (density: 3.08 g/cm^3, Blaine value: 5,600 cm^2/g), land sand (surface dry density: 2.57 g/cm^3, water adsorption: 2.15%, F. M: 2.76) and Crushed hard sandstone (surface dry density: 2.65 g/cm^3, F. M.: 6.74, M.S: 20 mm) were used. The testing temperature was 20°C. In mixing the concrete with a shovel prior to measurement of temporal changes in properties, it was found that the force required in the case of concretes containing SPN was lower than SPC. In this study, it is defined as a difference in thixotropy. The effects of the superplasticizers were quantitatively compared based on hysteresis loops obtained from measurements taken using a rotating viscometer. Measurements were taken under the following conditions. Firstly, specimens were mixed and then left in the outer tube of the rotating viscosity meter and further left to sit for 30 minutes. A second measurement was taken 60 minutes later. The area under the ascending and descending approximate curves derived from the relationship between shear force and shear rate for each superplasticizer were compared.

2.2 Study of properties of hardened ultra high-strength concrete

The binding material was low-heat Portland cement as specified in JIS R5201 (density: 3.22 g/cm^3; Blaine value: 3,280 cm^2/g) with 10% (by weight) replacement by fine silica fume powder (density: 2.20 g/cm^3; BET: 19.8 m^2/g). SPN was added to the binder. The unit weight of water was 150 kg/m^3 in all concretes. Only the water-binder ratio (W/B) was varied, at 12, 15, 18, and 22%. (These concrete specimens are referred to as LS12, LS15, LS18 and LS22 hereafter.) For purposes of comparison, concrete having an ordinary compressive strength (W/C 55%), made from ordinary Portland cement specified in JIS R 5201 (density: 3.16 g/cm^3, Blaine value: 3,350 cm^2/g) was prepared (OP55). The following hardening qualities were measured: compressive strength, freeze-thaw, change in length, amount of chloride ion permeation, and distribution of pore diameter.

3. RESULTS OF CONCRETE TESTING

3.1 Influence of superplasticizer on concrete deformability and viscosity

Table 1 shows the results of the fresh concrete properties. Compared with SPC, a lower dosage of SPN was needed to achieve the target slump flow. SPN exhibited high dispersibility. Concrete containing SPN exhibited dispersion stability, with little change in slump flow over time compared with concrete containing SPC. Regardless of the W/C, the T50 as an index of viscosity values of the SPN specimens are smaller than those of the SPC ones, demonstrating a lower viscosity. The difference in viscosity increased as W/C decreased. The extent of increase in T50 over time was lower in the SPN specimens. Compared with SPC, SPN exhibits high viscosity-reducing effect not only at the time of mixing, but during the period after mixing.

3.2 Influence of superplasticizer on thixotropy

Figure 1 shows the results of the thixotropy tests (hysteresis loop). Regardless of the superplasticizer, the calculated area increased over time compared with the value immediately after mixing, as the concrete was allowed to stand (the standing method). On the other hand, when the specimens having same time elapsed as the standing method were mixed immediately prior to measurement (the agitating method), the areas containing both superplasticizers are almost equivalent to those at mixing time. In a comparison of thixotropy made by subtracting the area obtained by the agitating method from the area obtained by the standing method, the thixotropy of the SPN concrete was found to be roughly one third that of the SPC concrete. A reduction in thixotropy results in a reduction in placement work, i.e., placement of concrete by buckets, re-pumping pressure to move concrete in the pipe, and trowel work. The authors consider that the ability of an SP to reduce the thixotropy of concrete will become a new function of superplasticizers.

3.3 Properties of hardened ultra high-strength concrete

The maximum compressive strength of 1-year-old standard-cured specimen of LS18 was 170 N/mm^2. On the other hand, the authors found that LS12 specimens obtained the greatest strength development under simple adiabatic curing: 163 N/mm^2 at the age of 56 days. Studies of resistance to freeze-thaw resistance, drying shrinkage and ability to obstruct chloride permeation revealed that ultra high-strength concrete had superior durability to OP55. Based on the measurements of the total pore volume (see **Fig. 2**), the excellent strength development and durability of ultra high-strength concrete are considered to be due to the compact organizational structure of these pores. It should be noted that the process of compaction of the pores in ultra high-strength concrete makes hardly any progress between 28 days and 6 months. Once the 6-month stage is passed, the total pore volume gradually decreases. The authors will in future study the changes in pore volume in older concrete, along with studies of hydration progress in cement composites with water-binder ratios of 20% and below, as well as the changes in their structure.

4. CONCLUSIONS

Studies of the fresh concretes showed that this new superplasticizer exhibits comparatively higher dispersibility than conventional superplasticizers, moreover, it reduces both viscosity and thixotropy. This superplasticizer will help improve the placeability of ultra high-strength concrete. The authors studied the strength development and durability of hardened concrete specimens with W/Cs down to 12% (a level for which there is hardly any published literature), and showed that the superior strength development and durability are due to the compaction of the pore structure.

Table 1 Properties of fresh ultra high-strength concrete

W/C (%)	SP Kind	SP Dosage (Cx%)	Slump flow (cm)/T50 (sec.) Time (min.) 0	30	60	90	L30/L50 (sec.) Time (min.) 0	60	Air content (%)
25	SPC	1.2	68.0	70.0	64.0	60.0	2.6	4.9	1.8
			5.3	5.6	9.4	15.7	8.0	13.3	
	SPN	1.1	70.0	68.0	64.0	62.0	2.1	3.4	1.6
			4.5	5.3	7.1	12.4	6.8	10.6	
22	SPC	1.4	67.0	70.0	65.5	60.5	3.2	6.2	1.7
			7.9	8.1	12.3	18.9	10.6	15.3	
	SPN	1.2	69.5	70.0	68.0	64.0	2.5	3.5	1.8
			6.8	7.5	8.8	12.2	8.1	10.8	
20	SPC	1.8	66.0	68.5	66.0	63.0	4.6	7.3	2.0
			9.5	10.8	13.7	16.8	17.0	24.1	
	SPN	1.3	68.0	67.5	68.5	67.0	2.9	3.6	1.8
			8.0	8.9	10.2	11.7	9.1	11.6	
18	SPC	2.2	64.0	68.5	67.5	65.0	6.4	10.1	1.9
			13.0	14.5	17.6	21.9	21.5	30.1	
	SPN	1.5	68.0	69.0	68.0	68.0	3.7	5.1	1.8
			9.5	10.5	12.7	14.2	12.0	17.0	
16	SPC	3.5	63.0	60.0	-	-	-	-	2.3
			29.8	33.5	-	-	-	-	
	SPN	2.2	69.0	69.5	-	-	-	-	1.9
			18.6	21.2	-	-	-	-	
14	SPC	4.5	52.0	45.0	-	-	-	-	2.2
			49.8	-	-	-	-	-	
	SPN	3.0	70.0	70.0	-	-	-	-	2.0
			25.1	26.2	-	-	-	-	

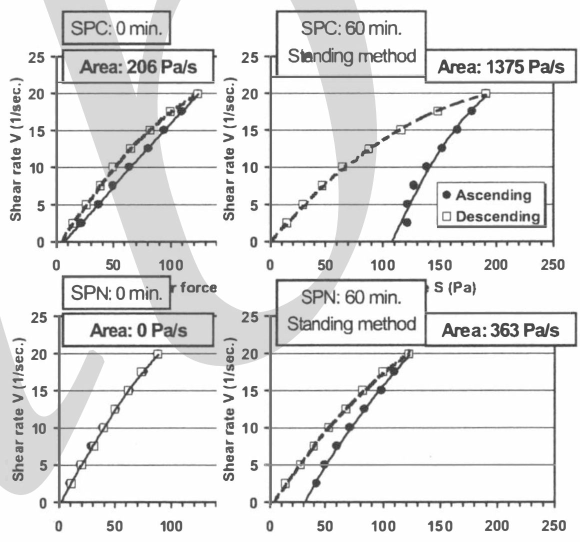

Fig. 1 Comparison of hysteresis loops

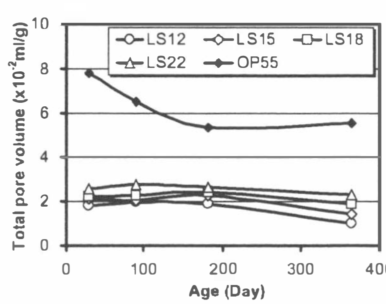

Fig. 2 Total pore volume

THE OPTIMIZATION OF THE SUPERPLASTICIZER FOR THE SELF-COMPACTING CONCRETE

Tatsuya Mizunuma, Daisuke Hamada, Takahiro Sato, Masaaki Shimoda
Kao Corporation, JAPAN

Keywords: Self-compacting concrete, polyethertype superplasticizer

1 INTRODUCTION

Self-compacting concrete (SCC) has been studied by many researchers because of its superior performances such as quality improvement and productivity improvement [1]. SCC requires both segregation resistance and high flowability to get enough self-compacting ability. Furthermore, high early strength is also desired for SCC in precast concrete factories to make production-cycle-time shorter. To meet these requirements, superplasticizers are required several performances, high dispersability, high segregation resistance (viscosity) and less setting retardation.

In this paper, the relationship between the chemical structure of polycarboxylate type superplasticizers in which poly-ethylene-oxides (PEO) chains were grafted and these required properties were studied. From the experimental results, the optimized structure of superplasticizer for SCC used in precast concrete is proposed.

2 SUPERPLASTICIZER

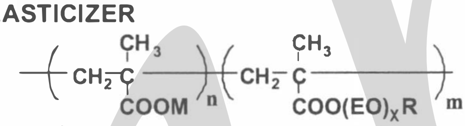

(1)

x=10,20,40,130,200,300 and n:m=8:2. Molecular weight=30000-80000 (PEG conversion)

3 RESULTS AND DISCUSSION

Polycarboxylate type superplasticizers were said to be dispersing cement particles mainly by steric repulsion which was caused by grafted chains which consist of poly-ethylene-oxides (PEO). Fig.1 shows the relationship between the length of PEO chains of polycarboxylate type superplasticizer shown in formula (1) and their dispersability. The cement paste flow of dispersability tended to be increased as PEO chain became longer and had the maximum peak around X=150moles.

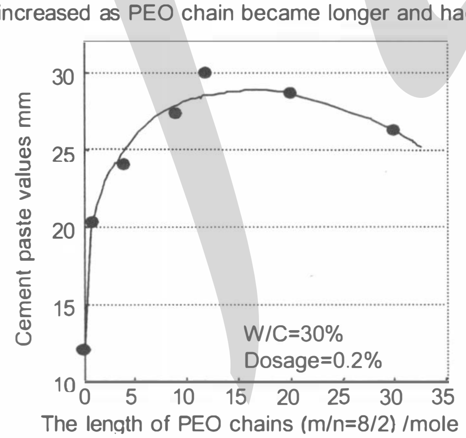

Fig.1 Influence of the length of PEO chains on dispersability of superplasticizer

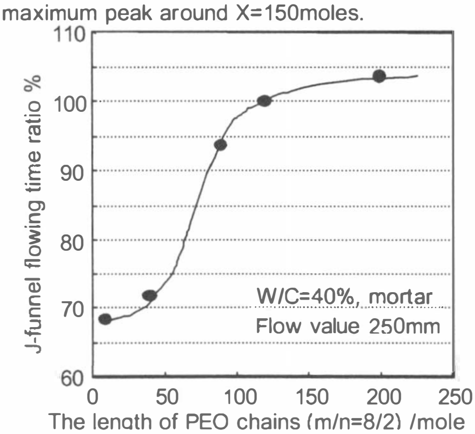

Fig.2 Influence of the length of PEO chains on viscosity of mortar

Fig.2 shows the relationship between the length of the above-mentioned PEO grafted chain and the J-funnel flowing time ratio of the mortar which is the indication of the mortar viscosity. The flowing time ratio tended to increase with the increase of PEO chain length in molecules and become constant at the length of more than 100 mole.

Fig.3 shows the relationship between the grafted PEO length of superplasticizer molecules and the second peak time of exothermic hydration. The peak time trended to be shortened with the increase of the length of PEO chain.

Fig.4 shows the adsorption amount of each superplasticizer with different length of grafted PEO chain. The longer the grafted PEO chain became, the less the adsorption amounts to the cement of each superplaticizer became, which seemed to be related to the hydration speed shown in Fig.3. It was suggested that the superplasticizer with the longer PEO chains could disperse cement particles effectively with small adsorption amount, forming thick adsorbing layer.

The conformation of the polycarboxylate type superplasticizer with grafted PEO chains, especially the conformation of PEO chains, was investigated by polarized FT-IR analysis. The FT-IR absorption peak at 1103cm-1 indicates standing PEO conformation, and that of 1147cm-1 indicates lying PEO conformation, respectively. In Fig.5 which is FT-IR chart of the superplasticizer adsorbed on silica plate, the broad peak of PEO chain was found at 1100cm-1 - 1150cm-1, which indicated that PEO chain might be swinging on cement particle. The superplasticizer with long PEO chain of 130 mole was supposed to exist on cement particle with the conformation of reverse conical shape shown as in Fig.5. In this case, the absorbed area on cement particle is so coarser and smaller that cement particles become much easier to hydrate, which resulted in much less setting retardation.

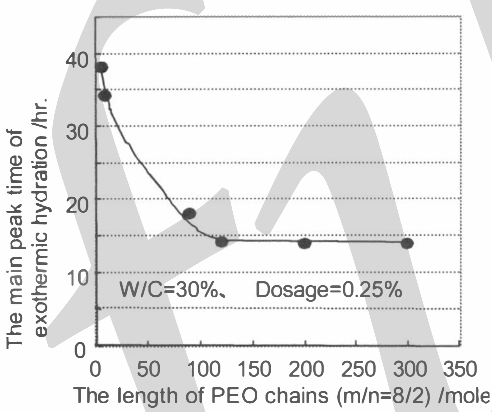

Fig.3 Influence of the length of PEO chains on the hydration ratio of cement

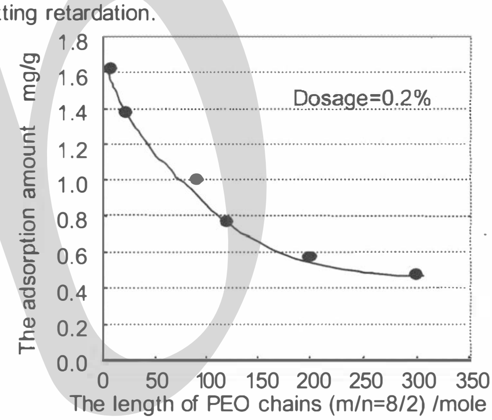

Fig.4 Influence of the length of PEO chains on the hydration ratio of cement

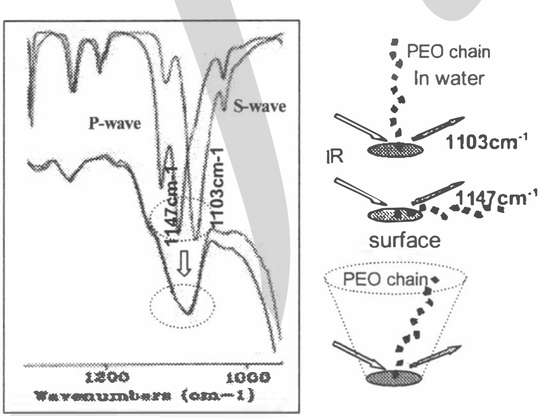

Fig.5 Polarized FT-IR analysis of the superplasticizer adsorbed on silica plate

REFERENCES

[1] Ozawa,K., Maekawa,K., Kunishima,M., Okamura,H.: Development of high performance concrete based on the durability design of structures. Proceedings of the second East-Asia and Pacific Conference on Structural Engineering and Construction (EASEC-2),Vol.1,January,PP445-450,1989

[2] Hamada, D., Sato, T., Yamato, F. and Mizunuma, T., "Development of New Superplasticizer and Its Application to Self-compacting Concrete", Superplasticizer and Other Chemical Admixtures in Concrete, Proceedings; Ed. Malhotra, V., M., 6th CANMET/ACI International Conference, Nice, France, 2000, pp.269-290.

EFFECT OF SURFACE MOISTURE OF SAND ON FLUIDITY OF FRESH MORTAR

Makoto Hibino and Kyuichi Maruyama
Nagaoka University of Technology, JAPAN

Keywords: surface moisture of sand, pre-mixing, mortar flow, funnel through time

1 ABSTRACT

In the current mixing process of mortar for self-compacting concrete, the surface moisture content of sand greatly influences the fluidity of fresh mortar and the change of fluidity with elapse of time. The aim of the present study is to examine the fluidity mechanism of fresh mortar. In order to reproduce variance in the surface moisture of sand the mixing water was divided into three parts and the fine aggregate was added in dry condition. Varying the surface moisture content of sand from 0.5 to 5.0%, the mortar fluidity was determined at intervals of 5, 20, 35 and 65 minutes after mixing. The test result showed that even if the specified mixture proportion was identical, the mortar with smaller content of surface moisture of sand increased the initial flow while it had a large reduction rate of the flow diameter with elapsed time.

2 EXPERIMENTAL DETAILS

Properties of materials used in mortar test are described in Table 1. Two types of superplasticizer (*SP*): polycarboxylate type (*PC*) and naphthalene sulfonate type (*NS*) were used. Both agents include a slump-controlling component, which inhibits reduction in slump flow with elapsed time.

The mixing procedure is shown in Fig. 1. The mortar volume of a batch was 1.5 litter and sand volume was fixed at 40% of mortar volume. Fine aggregate was added in dry condition and mixed for one minute with the mixing water (*Ws*) which performs the surface moisture of sand. After that, the cement was added and mixed with wet sand for 30 seconds. The authors represent this process as "pre-mixing".

In order to evaluate the fluidity of fresh mortar flow test and funnel test [1] were carried out at 5, 20, 35 and 65 minutes after mixing.

Table 1 Properties of materials

Cement (C)	Ordinary portland cement Density: 3.15 g/cm^3 Specific surface area: 3500 cm^2/g
Fine aggregate (S)	Silica sand Density: 2.59 g/cm^3 Fineness modulus: 2.84 Absorption: 0.74%
Superplasticizer (SP)	Polycarboxylate-type (PC)
	Naphthalene sulfonate-type (NS)

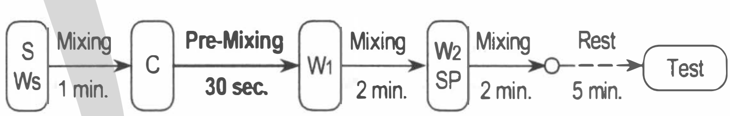

Fig. 1 Mixing procedure *Method A*

3 EFFECT OF SURFACE MOISTURE OF SAND

3.1 Change in initial fluidity

The effect of surface moisture of sand on the initial fluidity determined at 5 minutes after mixing was investigated. The mixture proportion of mortar: water-powder volume ratio (*w/p*) and *SP* dosage was decided to attain the fluidity adapted to the self-compacting concrete, which exhibits approximately 260mm in mortar flow and eight seconds in funnel through time. The relationship between the surface moisture and the initial fluidity is shown in Fig. 2. With rising surface moisture content, mortar flow reduced and funnel through time enlarged. Therefore, even if the specified mixture proportion is identical, it is considered that fresh concrete loses its self-compactability with increasing surface moisture of sand.

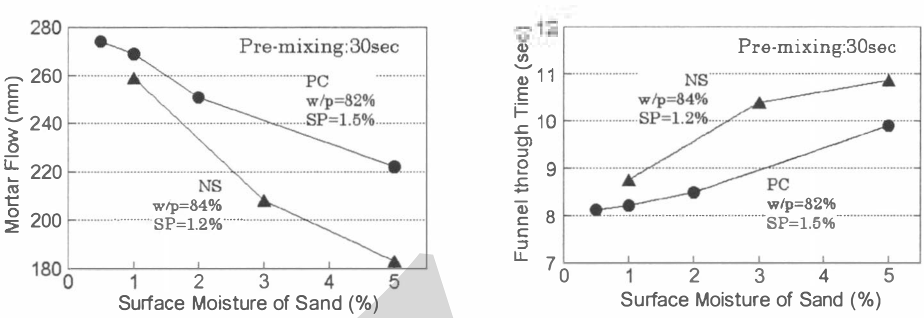

(a) Mortar flow (b) Funnel through Time

Fig. 2 Change in initial fluidity due to variance in surface moisture of sand

3.2 Change in fluidity with time

The effect of surface moisture on variance in fluidity with elapse of time was investigated. Mortar flow was measured at 5, 20,35 and 65 minutes after mixing. The test results are shown in Fig. 3. Significant drop in mortar flow with the elapse after mixing was noted irrespective of kinds of superplasticizer. It is, therefore, considered that the slump-controlling component did not perform sufficiently. In case of *PC* addition, it was observed that variance in mortar flow depended on the quantity of surface moisture of sand. The mortar with 5% surface moisture content showed smaller variation as compared with that having 1% surface moisture.

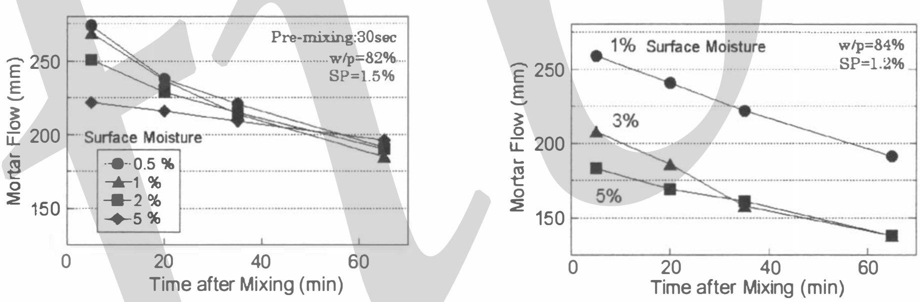

(a) Polycarboxylate-type (b) Naphthalene sulfonate-type

Fig. 3 Change in mortar flow with the elapse after mixing

4 CONCLUSION

(1) Even if the specified mixture proportion was identical, the mortar with smaller content of surface moisture of sand increased the initial flow while it had a large reduction rate of flow diameter with elapse of time.
(2) The above effect depended on the mixing procedure; it only rose in case when the pre-mixing was conducted in manufacturing.
(3) The initial hydration of cement induced in the pre-mixing period affected the activity of superplasticizer: particularly the slump-controlling component, thus changing the fluidity of fresh mortar.

REFERENCES

[1] M. OUCHI: "State of the Art Report on Self-Compactability Evaluation for Mix-Proportioning and Inspection", Proceedings of the International Workshop on Self-Compacting Concrete, JSCE Concrete Engineering Series No. 30, pp. 111-120, 1998

EXPERIMENTAL STUDY ON STABLE PRODUCTION OF SELF-COMPACTING HIGH PERFORMANCE CONCRETE

Hiroto Arima Masayoshi Sadakane Toshiki Ayano Kenji Sakata
Takadakiko Co.,Ltd. Okayama Univ.
JAPAN JAPAN

Keywords: self-compacting high performance concrete, fine aggregate, high filling performance

1. INTRODUCTION

Hybrid structure is already beginning to be adopted not alone including the superstructure of bridge but the substructure of it. Especially, a rigid connection with steel superstructure and concrete substructure is examined positively and is executed actually. In steel-concrete connection, it is difficult to compact using vibrator for filling of concrete structurally. Therefore, it is desired that self-compacting high performance concrete is applied for execution of hybrid structure with high safety and reliability. As a matter of course, the self-compacting high performance concrete must have the high filling performance.

On the contrary, extraction of natural aggregate is got tough in term of nature conservation. But the good natural aggregate wield a very large influence over quality of the concrete.

Under these circumstances, this study aims at development of self-compacting high performance concrete that has an independent on a kind of fine aggregate. Moreover, the mix-proportion which can hold the filling performance simultaneously for a long time is also revealed.

2. EXPERIMENTAL METHODS

2.1 Materials

Three kinds of the fine aggregates, river sand, sea sand and crushed sand are used. In addition, limestone powder and superplasticizer are also used as necessary.

In all materials about mix-proportion of the concrete, values of maximum size of aggregate (=Gmax), air content (=Air), water-cement ratio (=W/C), unit water content (=W) and unit cement content (=C) are kept constant.

2.2 Testing methods

The test is conduct to evaluate the capabilities of fresh concrete and we set evaluation criteria for the experiment (**Table 1**).

Table 1 Testing methods and Evaluation criteria

Methods	Items	Evaluation criteria
Air content test	Air content	
Slump cone test	Flow time (500mm in diameter)	5~20sec
	Slump-flow	650~750mm
U-type test	U-type filling height	300mm or more
	Time (until flow of fresh concrete stops)	
V-flow test	V-funnel time	10~25sec

3. EXPERIMENTAL RESULTS

3.1 EFFECTS OF DIFFERENCE OF FINE AGGRAGATES

The U-type filling height is 300mm or more, when river sand is used. Conversely, the U-type filling height isn't it for any sand ratio whatsoever, when sea sand and crushed sand. The relationship between sand ratio and U-type filling height for 1.5% of superplasticizer are shown in **Fig. 1**.

3.2 EFFECTS OF LIMESTONE POWDERS AS ADMIXTURES

When limestone powder is adjoined in mix-proportion using sea sand and crushed sand, the U-type filling height is 300mm or more. 80kg/m^3 of limestone powder particularly is good enough to accomplish over 300mm of the U-type filling height. The relationship between limestone powder content and U-type filling height are plotted in **Fig. 2**.

3.3 EFFECTS OF SEGREGATION-INHIBITING AGENT

The segregation-inhibiting agent is admixture with reducing variations of fresh concrete performance owing to fluctuations of the water content. On experiments, the fluctuations of water content are mixed without mix-proportion. All items satisfy requirements of the evaluation criteria in the –10kg/m^2 to +15kg/m^2 range of the fluctuations of water content regardless of a kind of sand. The relationship between fluctuations of water content and U-type filling height are shown here (**Fig. 3**);

3.4 TIME KEEPING THE PERFORMANCES

In execution, the time that elapses before fresh concrete is arrived from concrete plant to site is very important for performance of the fresh concrete. The performance deteriorates with time. We have an eye to retentivity of fresh concrete performance for 150 minutes, and carry out an experiment by adjusting of superplasticizer ratio. It is used river sand as fine aggregate. The performance of after 150 minutes satisfies the evaluation criteria, when superplasticizer ratio is 1.6% or more. However, there is a possibility segregation of concrete, when superplasticizer ratio is 2.0% or more. The relationship between elapsed time and U-type filling height are shown in **Fig. 4**.

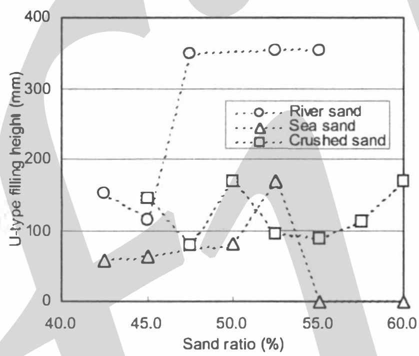

Fig. 1 The relationship between sand ratio and U-type filling height

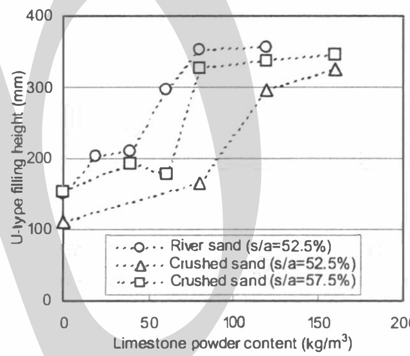

Fig. 2 The relationship between limestone powder content and U-type filling height

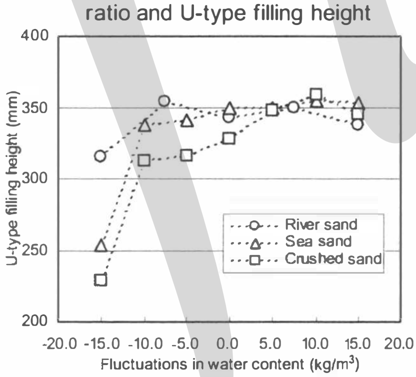

Fig. 3 The relationship between fluctuations of water content and U-type filling height

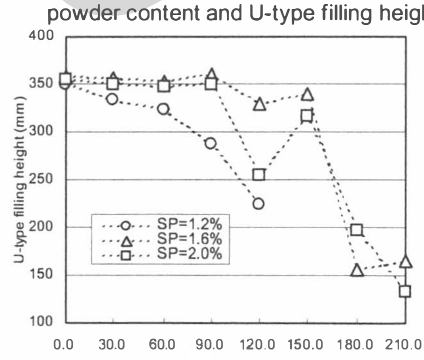

Fig. 4 The relationship between elapsed time and U-type filling height

REFERENCE

[1] Okamura H, et. al. Standard Specification for Design and Construction of Concrete Structures, JSCE, November 1999.

[2] Uomoto T, et. al. Guidelines for execution of self-compacting high performance concrete, Concrete Library of JSCE, No. 93, November 1999.

PUMPABILITY OF HIGH STRENGTH CONCRETE

Hideaki TANIGUCHI Manabu FUJITA
Sumitomo Construction Co., LTD., Japan

Sadaaki NAKAMURA
PC Bridge Co., LTD., Japan

Masaaki TANAKA
Fuji P.S Corporation, Japan

Hiroshi WATANABE
Public Works Research Institute, Japan

Keywords: high strength concrete, pumpability, fluidity, compressive strength, pressure loss

1 INTRODUCTION

On the Pumping of high strength concrete (HSC), the relationship between the pressure to the pumping speed and the effect on the properties of fresh/hardened HSC has not been clarified yet [1,2]. And also pump planning requires the pre-confirmation of the pumping pressure on the pump machine. This paper describes the results of pumping experiments to study these problems of HSC with design strength 60 MPa or greater. This experiment is one of the joint researches on the part of the Public Works Research Institute and the Japan Prestressed Concrete Contractors Association.

Table 1 Materials and mix proportion

W/C (%)	s/a (%)	Unit content(kg/m^3)				
		W	C	S	G	SP
25.0	45.0	160	640	699	868	10.2
W/C	Water cement ratio (weight)					
s/a	Sand aggregate ratio (volume)					
W	Water					
C	Ordinary portland cement(3.16)					
S	River sand and crushed sand(2.60)					
G	Crushed stone(2.64), Max size 20 mm					
SP	Superplasticizer(polycarboxylate)					

values in ( ):density(g/cm^3)

2 EXPERIMENTAL PROGRAM

Table 1 shows the materials and mix proportion for HSC. The water cement ratio was set to 25 %, which would ensure a compressive strength of 80 MPa or greater for the concrete at a material age of 28 days. Based on existing documentations [3,4], the slump flow before pumping was set to 55-60 cm. As shown in Figure 1, two types of piping condition (pipe diameter was 125 mm) were installed. The concrete piston-pump machine with the capacity of a maximum pumping rate of 100 m^3/h was used and the pumping rate was decided about 15-45 m^3/h.

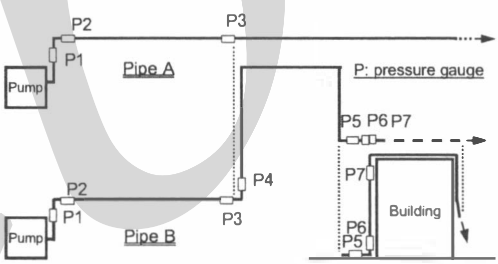

Figure 1 Layout of pipes

3 PROPERTIES OF CONCRETE

Table 2 shows the changes of the properties of concrete due to pumping. Almost no changes were observed in the slump flow after pumping with a pumping rate of 29 m^3/h for Pipe A and 25 m^3/h for Pipe B. However, when the pumping rate exceeded 30 m^3/h, a slump flow drop of about 7 cm was measured. The V-funnel flowing time was about 20 seconds before pumping, but after pumping it dramatically changed to about 10 seconds down. Judging from the fact that the V-funnel flowing time can be used to evaluate the viscosity of the concrete, this phenomenon is considered to result from a drop in the viscosity of the concrete [3]. The air content

Table 2 Changes of the properties of concrete due to pumping

Piping Codition	Pipe A		Pipe B		
actual pumping rate (m^3/h)	29	46	25	33	39
Slump flow (cm)	1	-7	-2	-8	-6
V-funnel flowing time (seconds)	-13	-12	-11	-11	-14
Air content (%)	1.5	1.5	0	0.5	1.5
Comprssive strength(28days)	0.94	0.87	0.97	0.93	0.78

The values of fresh concrete are the differences of values to after pumpimg and before pumping. The values of compressive concrete are after pumpimg devided by before pumping.

tended to increase with pumping.

The compressive strength after pumping tends to decrease as the pumping rate increases, and dropped suddenly at the pumping rates of 25 m^3/h or greater on Pipe B. For this reason, the pumping rate should be kept as low as possible in order to ensure compressive strength. The decrease of compressive strength was determined to be the result of an increase in the air content due to pumping as shown in Table 2.

4 PUMPING PRESSURE

As shown in Figure 2, the unit pressure loss of HSC in this experiment were larger than the values of the Recommendations. The conversion values calculated the pumping pressure of pump piston were greater than pressure loss of horizontal pipe that was actually measured by pressure gauges. Figure 3 shows the relationship between the conveying distance and the unit pressure loss. The unit pressure loss increased as the position came nearer to the cylinder of pump machine, and this trend became more noticeable as the pumping rate was increased. In the Recommendations, the type of pump is selected by using a value 1.25 times the pumping pressure measured at the position for calculating pressure losses. However, the values calculated in this experiment were 2.1-2.6. Moreover, the exchanged horizontal length per a upward bending pipe in the vertical direction exceeded 10 m when the pumping rate was high, and was longer than the 6 m value in the JSCE Recommendation.

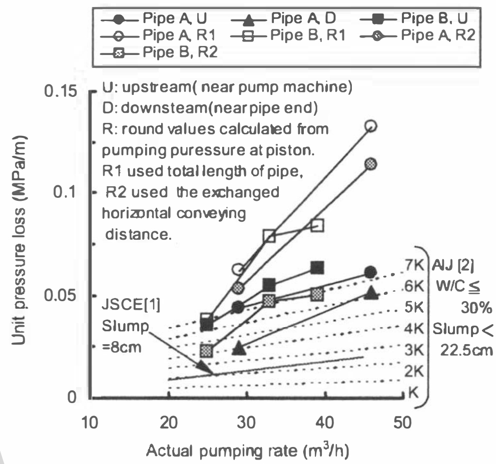

Figure 2 The relationship between actual pumping rate and unit pressure loss

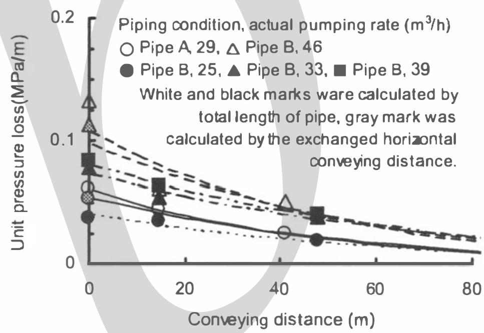

Figure 3 The relationship between the conveying distance and the unit pressure loss

5 CONCLUSIONS

Pumping in this experiment decreased the slump flow with pumping rates exceeding 30 m^3/h and reduced the flowing time of V-funnel by about 10 seconds in all cases. Since the air content tended to increase along with pumping, this had a major significant impact on the compressive strength of hardened concrete.

The unit pressure loss of a horizontal pipe containing HSC was greater than loss in one containing ordinary concrete, and the effect of the pumping rate was also significant. With HSC, the pressure near the cylinder of pump machine tended to be great. Moreover, The exchanged horizontal length per a upward bending pipe was larger than the value of JSCE Recommendation.

REFERENCES

[1] Japan Society of Civil Engineers: Recommendation for Pumping Concrete, 2000.
[2] Architectural Institute of Japan: Recommendation for Practice of Placing Concrete by Pumping Methods, 1994.
[3] Taniguchi, H. et al: Studies on the Quality Change of Super Workable Concrete due to Pumping, Concrete Research and Technology, Vol.9, No.1, pp.71-85, Jan., 1998.
[4] Taniguchi, H. et al: Studies on the Pressure Loss Attendant with Super Workable Concrete Pumping, Concrete Research and Technology, Vol.10, No.1, pp.25-39, Jan., 1999.

UTILIZATION OF SECONDARY RAW MATERIALS IN THE TECHNOLOGY OF SELF-COMPACTING CONCRETE (SCC) IN THE CZECH REPUBLIC

Rudolf Hela
hela.r@fce.vutbr.cz

Lenka Bodnarova
bodnarova.l@fce.vutbr.cz

Bmo University of Technology, Faculty of Civil Engineering,
Institute of Technology of Building Materials and Components
Veveri 95, 662 37 Bmo, Czech Republic

Keywords: self-compacting concrete, waste materials, stone filler, fly ash, foundry sand

1 INTRODUCTION

This contribution gives the results of work aimed at the development of SCC formulas with the addition of waste materials. The alternative to adding waste materials into the self-compacting concrete and thus using their specific properties is a big contribution in dealing with the issue of industrial waste processing. To be concrete, we verified the possibility of addition of fly ash from power stations, foundry sand and stone filler and their effect on the properties of both fresh and set self-compacting concrete.

2 EXPERIMENTAL WORK

The system of SCC formula development respected the local resources of raw materials and the possibility of selected industrial waste adding into SCC. The conducted tests pursued the following targets:

- Design of model formulas for the SCC technology for the maximum aggregate grain size of 8 mm and 16 mm from gravel and crushed natural aggregates with the use of industrial waste as a substitute of admixtures for the 0.25 mm fraction;
- Design and laboratory verification of complete methodology of fresh concrete rheologicall property testing, inclusive of testing equipment design and construction;
- Determination of major physical and mechanical properties of set SCC with an emphasis on study of volumetric changes;
- Study of set SCC structure and homogeneity;
- Verification of stone filler, power plant fly ash and foundry sand effect on highly liquefied concrete.

3 RESULTS

Suitable granulometric curve generally applicable to all types of natural aggregates was found. Following extensive research, self-compacting concrete formulas for aggregate with the maximum grain size of 8 mm and 16 mm were designed and fully tested.

Table 1 Proposed composition of 1m^3 of self-compacting concrete

	Maximum grain size 8 mm	Maximum grain size 16 mm
CEMENT 42,5R	400 kg/m^3	350 kg/m^3
Water	208 kg/m^3	200 kg/m^3
Admixture	As required by producer	As required by producer
Stone dust	190 kg/m^3	150 kg/m^3
Aggregate 0 – 4 mm	890 kg/m^3	827 kg/m^3
Aggregate 4 – 8 mm	573 kg/m^3	251 kg/m^3
Aggregate 8 – 16mm	-	501 kg/m^3

Fresh self-compacting concrete property testing: In the course of the fresh SCC mixture testing it tumed out that the most suitable method for evaluation of the basic characteristics is Orimet in combination with J-Ring.

SCC property testing and evaluating: To obtain a complete picture of the set self-compacting concrete properties, the following tests were carried out:

- Study of concrete compressive and tensile bending strengths after 3, 7 and 28 days
- Determination of volumetric changes of concrete after 3, 7, 14, 28, 48 and 72 days of maturing
- Determination of the relaxed and instantaneous modulus of elasticity
- Study of homogeneity.

The fact that the designed principles allow to design concrete with the maximum aggregate grain size of 8 to 16 mm is promising. The generally published fear of excessive concrete shrinkage was not proved. The progress of the concrete compressive strengths, on the contrary, is much more favourable than in common concrete; there is rather a problem to make a quality SCC with compressive strengths lower than 25 MPa after 28 days of normal maturing.

Evaluation of set SCC homogenity: The test procedure was developed to verify the set SCC properties, especially to evaluate concrete homogeneity when cast into structures higher than 1.0 m. The non-destructive ultrasonic method was used to evaluate the influence of the height of casting on the set concrete surface quality but also on the vertical homogeneity according to the ultrasonic wave propagation velocity in the tested sample.

SCC macrostructure examination: Another possibility of SCC quality evaluation is the macrostructure examination. The set concrete macrostructure was examined using the SONY optical microscope with the output to the digital imaging, magnification x 220. The evaluations were made in the form of a comparison between the overall view of the set concrete structure and a detailed picture of the gravel aggregate grain contained in the structure. In all evaluated samples, concrete broke over the aggregate grains, the reference concrete showed fractured grains of soft metamorphic rocks and minerals but the SCC fractured over quartz and feldspar grains, too.

4 EXAMPLES OF PRACTICAL EXECUTIONS

The results gained verified the possibility of full use of the local resources for SCC mixture production in the Czech Republic. This was as well verified through practical applications of SCC, for example at casting of the monolithic reinforced concrete walls of the Moravian Gallery archive in Bmo and at casting the supporting raker footings and cooling tower jacket in Ostrava – Trebovice heating plant.

5 FURTHER RESEARCH TRENDS

Further research will include the study of various superplastificizer influences on the rheology of cement grouts with fine industrial waste admixtures. Their properties will be tested on grouts using a technical viscosity meter. The output should include relationships between various property changes of the starting materials and the final viscosity of cement grouts when using the planned experiment methods. The character of the pore structure will be tested on the set grouts using the mercury porosimetry method and the character of macropores (spacing factor) using an optical microscope. Furthermore, properties of the SCC mixtures with the maximum grain size of 22 mm will be tested when using rough crushed aggregates preventing locking in reinforced structures and concrete component segregation. The tested formulas complying with the rheological conditions of fresh SCC will further be subject to tests of volumetric change in the early stage of maturation and at various temperatures, possible loading creep and SCC behaviour at long-lasting cyclic freezing.

REFERENCES

[1] Hosek, J., Kolar, K.: 2000. "Self-compacting-concrete". Beton a zdivo (2).
[2] Person, B.: Creep, shrinkage and elastic modulus of self-compacting concrete. In: Proceed of First Int. Symp. On Self-Compacting Concrete. Stockolm, 1999, 239 – 250.
[3] Masek, O.: Design of suitable formulas for the self-compacting concrete technology and verification of selected physical and mechanical properties. Degree work. TU Bmo, Bmo 2000.

This work was published with backing of GACR, within the research project No. 103/01/0814 „Microstructural features and related properties of cement based highly liquefied composites" and research project CEZ - MSM 26110008, name of the project is: "Research and Development of New Materials and Securing their Higher Durability in Building Structures"

HIGH STRENGTH SELF-COMPACTING COLORED CONCRETE FOR RITTO BRIDGE SUBSTRUCTURE (NEW MEISHIN EXPRESSWAY)

Yoshimitsu Nakajima, MAEDA Corporation, JAPAN
Akihiro Nakazono, Japan Highway Public Co., JAPAN
Seiji Mori, MAEDA Corporation, JAPAN

Keywords: self-compacting concrete, high strength concrete, integral colored concrete, air pipe cooling, thermal analysis

1 Introduction

Ritto Bridge, part of the New Meishin Expressway, is located in the Shiga Prefecture Nature Park, and ecological landscape design was considered due to its location. **Fig.-1** shows the landscape design of this bridge. Piers of these main towers have hexagonal hollow sections with four curved faces as shown in **Fig.-2**. Since this bridge had long spanned form, high strength concrete (design strength = 50 MPa) and also high strength reinforcing bars (yield strength = 685 MPa) were required to satisfy the earthquake resistance. Accordingly, high-strength self-compacting concrete was applied to the construction of this pier.

Beige was chosen as the color of the bridge to match the ground color of surrounding mountains. Integral colored concrete using inorganic pigment is applied to obtain a natural feeling of concrete surface.

2 Mix proportions and properties of high strength self-compacting concrete

In-house trial mixes, plant trial mixes and mock-up tests were carried out, and mix proportions of high strength self-compacting concrete were developed. All properties of concrete were confirmed to satisfy the specified requirements. Mix proportions and testing results are shown in **Table-1**.

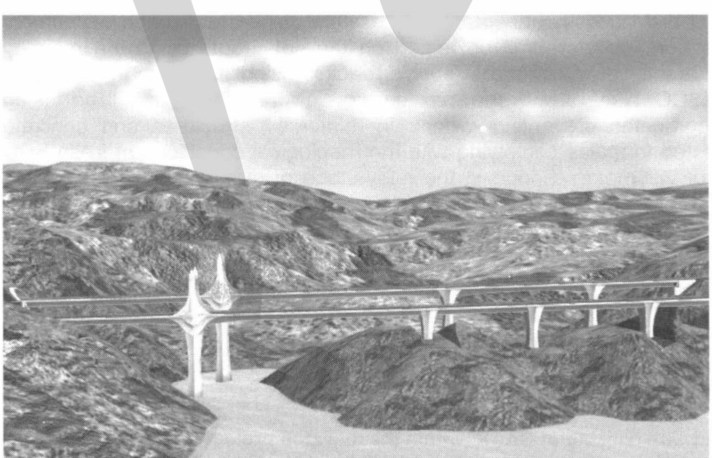

Fig.-1 Design of Ritto Bridge

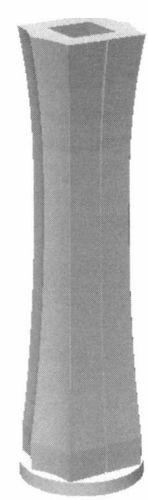

Fig.-2 Shape of A-P3 pier

Table-1 Mix proportion and test results

Mix proportion (In-house trial mix)												
design compressive strength (MPa)	water cement ratio (%)	maximum aggregate size (mm)	slump flow (cm)	air content (%)	Unit weight (kg/m^3)							
					Cement	Water	River sand	Crashed rock		Super-prasticizer	Pigment
								20mm	13mm		
50	33.0	20	60±5 65±5*	4.5±1.5	470	155	868	505	336	6.11	14.1

Test result										note
Testing time from mixing complete	Slump flow (cm)	flow time 50cm (sec.)	flow time stop (sec.)	U type filling (cm)	V type funnel (sec.)	Air content (%)	Concrete Temp. (°C)	Compressive strength (MPa)		*Target slump flow was revised when push up height of pump rose.
								7days	28days	
5	63.0	6.1	34.0	33.8	11.8	4.3	19.0	41.1	74.0	

3 Summary

Approximately 3,200m^3 of high strength self- compacting colored concrete was placed to A-P3 pier. The following was obtained through the trial mix, mock-up trial and actual construction.

High strength self compacting colored concrete was proportioned with low heat portland cement and inorganic pigment to satisfy all requirements specified in the JSCE's "Recommendations for Self-compacting High Strength High Durable Concrete Structure" [1] and the JH's "Guidance for Construction of High Performance Concrete".

Thermal properties of high strength self-compacting colored concrete were verified through the adiabatic temperature rise test, and thermal analysis with the air pipe cooling method (**Fig.-2**) was carried out to prevent thermal cracks. The efficiency of air pipe cooling was confirmed by a mock-up trial of air pipe cooling. This method was applied to the actual construction, and harmful cracking was avoided. As a result, the efficiency of the air pipe cooling was confirmed.

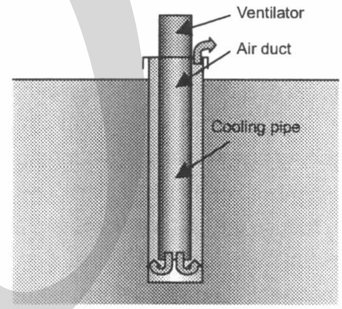

Fig.-2 Air pipe cooling method

Quality of concrete was checked more frequently than that of normal concrete at the ready mixed concrete plant and also on site to keep good quality. Whole concrete testing apparatus of self-compactability [2] was also applied for quality control.

Compressive strength of concrete at 28 days satisfied the specific strength. Strength at mold stripping was tested and the relationship between maturity and strength at mold stripping was verified.

Vented form was applied to avoid air holes. Furthermore, it was left on the concrete surface after formwork removal to protect the concrete surface from dirt. It proved to have a beneficial effect on the concrete surface, as evidenced by the few air holes that formed on the surface.

References

[1] Japan Society of Civil Engineers: Recommendations for Design and Construction of Self-compacting High Strength High Durable Concrete Structure, Concrete Engineering Series 105,2001.6

[2] M. Kubo, M. Nakano, S. Sugano, M. Ouchi: The Quality Control Method of Self-compacting Concrete Using Testing Apparatus for Self-Compactability Evaluation, Proceedings of The Second International Symposium on Self-Compacting Concrete, pp555-564, Oct., 2001

APPLICATION OF HIGH FLUIDITY CONCRETE WITH FLY-ASH TO COAL STORAGE SILOS

YOSHIHIRO YAMAGUCHI TAKEHITO KITANO
The Kansai Electric Power Co., Inc.
JAPAN

TORU KAWAGUCHI TAKESHI OHIKE
Technical Research Institute,
Obayashi Corporation JAPAN

Keywords; high fluidity concrete, fly-ash, mock-up test, mix proportion, execution plan

Outline

Kansai Electric Power Company Inc. is now constructing Japan's largest concrete coal-storage silos (each measuring 60 m in diameter, 78.45 m in height, with storage capacity of 100,000t. see Fig.1) at its Maizuru power plant. The bottom area of such silos around the coal removal outlet is where compaction with a vibrator is virtually impossible, so the new high-fluidity concrete method with its outstanding self-compactibility is used instead.

In connection with the construction, an investigation was conducted on the basic properties of high-fluidity concrete in which the proportion of fly-ash mixed in is varied when determining mix proportions. Then, using the selected concrete mix, a large-scale model test was conducted in which the quality of the structural concrete was verified in terms of compactibility, compressive strength and other factors.

We here report the results of the field testing with the large-scale model and mix selection test together with the quality control results. Japan's largest-ever volume of high-fluidity concrete (17,000 m^3) at one construction site was placed here.

The main factors in the mix selection test were the fly-ash mixing rate and the water binder ratio. The fly-ash was employed for the admixture. The concrete proportioning was tested by varying the fly-ash mixing rate at 20%, 30% and 45%, respectively. Mixing in a higher proportion of fly-ash was found to reduce the unit water content and increase fluidity. However, it became evident from mixing in fly-ash at over 30% that maintaining the segregation resistance by assuring compressive strength is important. Moreover, the more fly-ash mixed in, the faster the neutralization took place. The results of accelerated for 26 weeks showed that there was about three times the neutralization depth at a 45% mixing ratio than at 30%. In the end, a fly-ash mixing proportion of 30% was adopted.

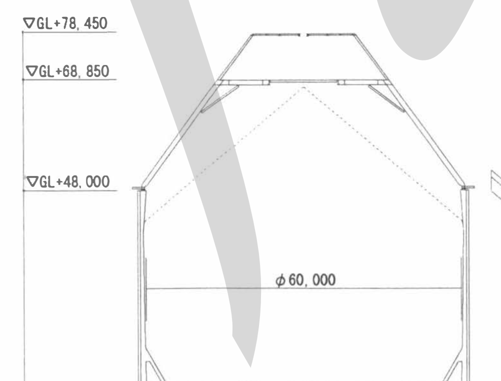

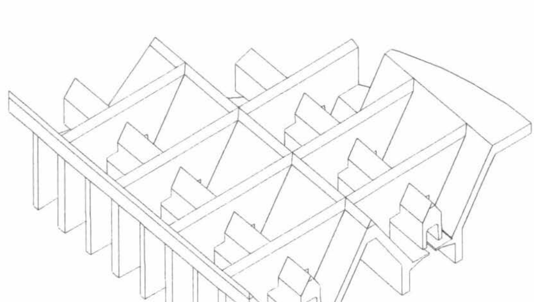

Fig.1 Coal-Silo Cross-Sectional Drawing and Hoppr Drawing

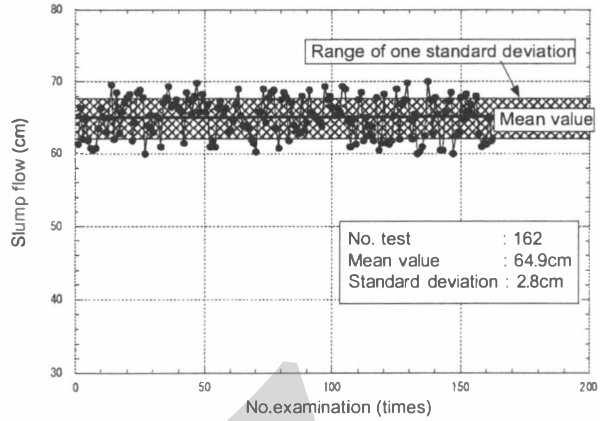

Fig.1 Slump Flow Control Results in Construction Work

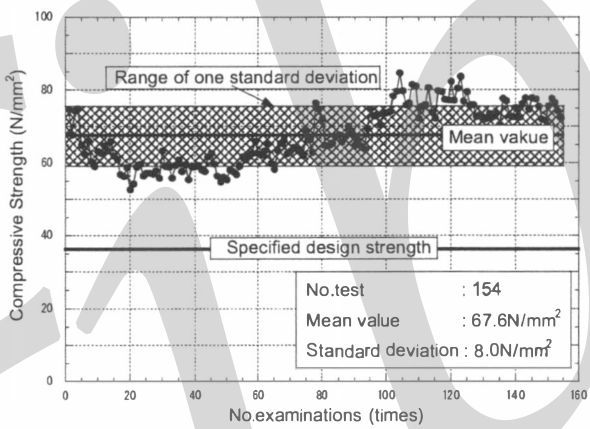

Fig.2 Results of Compressive Strength Control

The work on the large-scale model made it possible to verify the fresh concrete properties, the placing equipment procedure, flow conditions, the presence/absence of segregation, the quality of the structural concrete etc. It became clear that as long as the appropriate fluidity and material segregation resistance were maintained, even without any compacting the structure concrete quality requisites could be satisfied in the construction.

Figure 2 and Figure 3 present the slump flow test results and site sealed-cured cylinder test results for compressive strength control, respectively, both of which are representative of quality control results during the construction period. The Figures indicate the range of the mean values and one standard deviation.

In light of Figure 2, the slump flow, which is the key factor in good or bad high-fluidity concrete work with self-compaction, completely satisfies the control range of 65+5 cm and at the same time delivers excellent control with a standard deviation of only 2.8 cm. Then, in Figure 3, despite the seasonal weather factor that affects the compressive strength when placing concrete, the compression strength of the control cylinder in 13-weeks exhibited good control results with a mean 67.6 N/mm² and a standard deviation of 8.0 N/mm².

The actual construction project took about eight months, from the end of September 2000 to the end of May 2001. In the field construction the high-fluidity concrete work was done under strict quality control, resulting in a concrete structure of remarkably high quality.

APPLICATION OF SELF-COMPACTING CONCRETE TO PRECAST CONCRETE PRODUCTS

Tetsuya Oyamada, Takeo Nagai, Masahiro Suzuki
P.S.Corporation, JAPAN

Keywords: Self-compacting concrete, precast concrete products, fine limestone powder

1. INTRODUCTION

A serious problem at factories that manufacture concrete products is the generation of serious noise and vibration during vibrating compaction. This is coupled with a growing need in recent years for manufacturers to take advantage of the benefits of concrete, creating products with a greater variety of functions, and with a greater emphasis on the exterior beauty of concrete products and for more complex concrete-product shapes.

Self-compacting concrete (abbreviated as SCC below) can completely fill products with thin wall, permitting the work to be performed efficiently, even without vibrating compaction. The prices of the raw material are a little higher than for conventional concrete, but the use of SCC is counted on to lower the total cost by shortening the production process and increasing the efficiency of production. But at this stage, there are few examples of the regular use of SCC in factory production.

In light of these circumstances, for several years we have carried out trial mixing and plant mixing at our factories to apply SCC to the manufacture of factory products. The products treated are precast factory products with specified concrete strength of 50 MPa or higher. This report explains the SCC is developed and presents examples of how it has used this new material.

2. DEVELOPMENT OF SCC

2.1 Mix proportions design

This concrete consists of a powder-type SCC made using high-early-strength Portland cement and fine limestone powder. The fine limestone powder used had a Blaine value of about 3,500 cm^2/g. The fine aggregate is often crushed sand. The superplasticizer containing air-entraining agent used was of the polycarboxylic-acid-type.

The mix proportions of SCC must be established taking two opposed properties into account: flowability and segregation resistance. We control the flowability and segregation resistance of SCC by the values of its slump flow (abbreviated as S.F. below) and its 50-cm flow time (abbreviated as T_{50} below). However, the concrete is observed visually to assess the segregation of its materials. Table 1 shows the target values for fresh concrete testing. The factors considered most carefully are S.F. and T_{50}, and in accordance with accepted test results, the values of higher viscosity are set. A lower viscosity mix proportions is used to make SCC applied for sites where it will flow a long distance, primarily by the pump-feeding technique. But in order to use as much existing equipment as possible in production, as there is a high risk of segregation when fresh SCC is transported within the factory, consideration must be given to increasing the viscosity to prevent materials from such segregation.

We determine the mix proportions through the following study procedure. Among these items, the three items that are underlined are those to which particular attention is paid, based on the results of testing and research performed by our factories, in order to produce factory-use powder-type SCC products of stable quality.

Table 1 Items studied

Items studied	Target values
Slump-flow value	60±5cm, 65±5cm
50-cm flow time	8±3sec.
Air content	4.5±1.5%
Compressive strength	Appropriately controlled at each age

(1) Setting the unit volume of coarse aggregate
The unit absolute volume of coarse aggregate that presumably does not reduce flowability is approximately 300l/m^3.
(2) Setting the unit water content
The unit water content varies according to the materials used, but its suitable value is between 150 and 165 kg/m^3.
(3) Setting the water–cement ratio (unit cement content)
(4) Setting the total powder content
If the cement does not provide enough powder, fine limestone powder is used to set the total quantity of powder including both cement and fine limestone powder between 520 and 550 kg/m^3.
(5) Setting the air content
(6) Setting the unit content of fine aggregate

2.2 Points that must be carefully considered during execution and quality control

The following points must be carefully considered to ensure that the quality of SCC remains stable when fresh and after hardening.
(1) Controlling the unit water content → Administration by moisture gauges
(2) Improvement of the buckets used for transporting the concrete → Using buckets with concrete outlet made of rubber
(3) Decision of the pouring interval → The pouring interval of concrete is stipulated at or below 2 m
(4) Joint use of light vibration → In order to remove surface air bubbles certainly
(5) Use of surface finishing agents → A membrane curing agent, a neutral detergent, hardening accelerator, or the like are useful

3. APPLICATION CASES

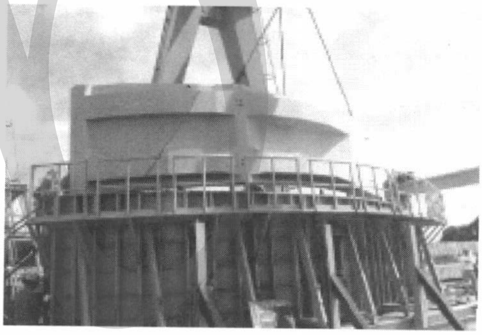

Photo. 1 PC snow barrier

The products made by SCC has been 11 applications, such as U-shaped PC girders, PC sleepers, PC snow barriers, PC snow shelters, SRC members for stadiums and etc. The were products were that risky to make with conventional concrete, because of their complex cross-sectional shape, small reinforcement intervals, and thin-wall members. But thanks to the use of SCC, we overcame these problems, shipping superior products that are free of pouring defects. The use of SCC has resulted in the development of new pouring methods, permitting more efficient and more economical product manufacturing[1],[2]. With steam curing, the compressive strength when the formwork is removed satisfies the required demould strength.

We proposed a vertical casting formwork and used SCC to make PC snow barriers and PC snow shelters. Photo. 1 shows this work in progress. The concrete is poured from buckets, it fills the formwork smoothly, and can be completed much more quickly.

4. POSTSCRIPT

At this stage, the number of specified articles is limited but, the number of applied articles is tending to increase, and demand is predicted to rise in the future. We are working eventually to acquire the capability of using self-compacting concrete to manufacture most factory products, at all of our factories.

REFERENCES

1) T. Nagai, T. Kojima, T. Miura : Application of high-strength/superworkable concrete to thin-wall prestressed concrete products, Magazine of Concrete Research, Vol.51, No.3, pp.153-162 (1999)
2) Tetsuya OYAMADA, Tadashi FUJIWARA, Dong JIANG, Kunishige KATABIRA : Adaptabirity of high fluidity concrete containing limestone powder for concrete products, The 4th Beijing International Symposium on Cement and Concrete, Vol.2,pp-524-529(1998)

CONSTRUCTION OF THE FIRST FRENCH ROAD BRIDGES IN ULTRA HIGH PERFORMANCE CONCRETE

Thierry Thibaux
Technical Manager
EIFFAGE TP FRANCE

Jacques Antoine Tanner
BSI Project Manager
EIFFAGE TP France

Keywords : Ultra high performance concrete BRIDGES

ABSTRACT

Under a research program led by the Ministry of Development, two innovative road bridges have been built at Bourg-Lès-Valence, France, using an ultra high performance fibre-reinforced concrete (UHPC). This article describes the construction of the decks of these two bridges using BSI special industrial concrete, a self-placing concrete having a compressive strength of 175MPa in which fibre reinforcements allow the elimination of passive reinforcements.

The document also takes stock of the research and the many tests performed as this project was implemented, the results of which were used in preparing the French recommendations for the design of UHPC structures, applicable to fibre-reinforced concretes beyond 150MPa.

1 - DESCRIPTION OF THE STRUCTURES

Each of the two bridges, OA4 and OA6, has two isostatic spans (22m for OA4, 20.5m for OA6) crossing the 2x2 lane expressway that bypasses the city of Valence, France. The decks of the two structures are identical in the transverse direction and comprise a set of 5 Π-shaped precast BSI beams (fig. 1 – fig.2).

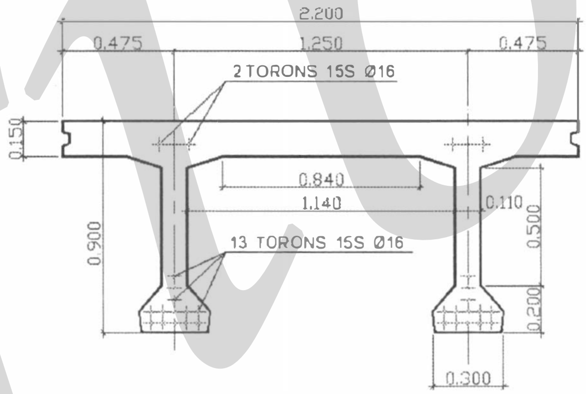

Fig. 1 : Cross-section of a precast beam

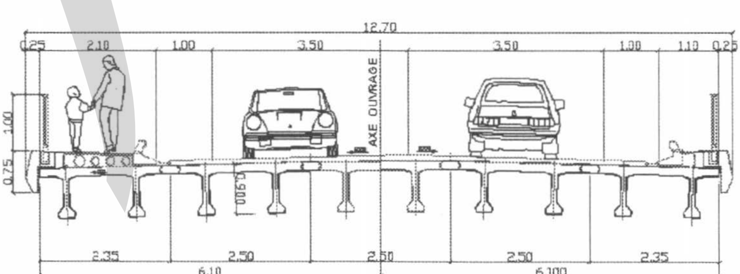

Fig. 2 : Cross-section of the deck

These beams have no reinforcements other than the connections between elements. In the longitudinal direction, the beams are prestressed by 15 mm strands

This results in an especially light deck having an equivalent thickness of 0.25m (against 0.75m for a conventional prestressed slab bridge and 0.37m for a ribbed deck made of high-performance B80 concrete). This weight saving could prove decisive in projects involving long spans.

2 - CHARACTERISTICS OF THE BSI

The BSI, a self-placing fibre-reinforced concrete, includes a high percentage of fibres to prevent brittleness and take out local forces and, in the case of this project, the transverse bending of the deck.

Table 2 : Technical Characteristics of the BSI

• Mean compressive strength at 28 days	190MPa
• Characteristic compressive strength at 28 days	175MPa
• Characteristic tensile strength of the matrix at 28 days	8MPa
• E-modulus	64GPa
• Density	2.8 T/m3
• Fibre content	0 to 3%
• Self-placing	

3 - DETERMINATION OF THE CONSTITUTIVE LAW

These new fibre-reinforced materials behave differently from conventional concretes. At the ultimate limit state (ULS), the ductile behaviour contributed by the fibres is modelled by a constitutive curve expressed by a tensile stress vs crack opening law (σ/w). Post-cracking tensile strength was until now measured by direct tension on a notched specimen.

The working group assigned to draft the new design rules for UHPC replaced this delicate test by a bending test on notched prisms. The intrinsic constitutive curve of the material is deduced from this bending test using the inverse method developed by G. CHANVILLARD. An extensive campaign of tests was carried during construction to validate the assumptions.

4 - PRODUCTION OF THE BEAMS

The beams were precast in 2 months (two days per beam) by the HURKS BETON company. Since the BSI is totally self-placing, even with a 3% fibre content, concreting is a simple and quiet operation. The precast beams were delivered by train and joined together by keys cast in situ of BSI prepared in an ordinary concrete plant.

5 - CONCLUSION

The innovative structures at Bourg-Lès-Valence, the first road bridges built in ultra-high-performance fiber-reinforced concrete, are already a reference allowing more general use of UHPC. The publication of the Provisional Design Recommendations [1] gives future Operating Authorities a reference to use in establishing their specifications and engineering design firms a starting point for their calculations.

However, while these conventional bridges with their small spans have served to validate the performance of the material, they have not yet revealed all the freedom and daring in design UHPC make possible. The toll --gate of the Millau Viaduct, which will have an elegant roof based on a thin BSI shell, is the next step in the development of this new material.

6 - REFERENCES

[1] SETRA-AFGC – « Bétons Fibrés à Ultra Hautes Performances – Recommandations Provisoires », AFGC-SETRA, 2002.

FEASIBILITY STUDY ON APPLICATION OF HIGH-STRENGTH CONCRETE TO PRESTRESSED CONCRETE FLEXURAL MEMBERS

Keita Furubayashi Katsuhiko Kangawa
P.S.Corporation,JAPAN

Tadashi Nakatsuka
Osaka-University
JAPAN

Hiroshi Muguruma
Kyoto-University
JAPAN

Keywords: high-strength concrete, jumping phenomenon, minimum ratio of prestressing steel

1 INTRODUCTION

High strength concrete with capacity ranging from 100 to 200MPa will be aimed to use practically in Japan, recently. High strength concrete has so high tensile strength that consideration must be paid to jumping phenomenon caused by transference of tensile resultant of concrete to reinforcement, namely, sudden large increase in curvature of cross sections and stress of reinforcing steels at initial cracking moment of concrete flexural members.

This paper describes the characteristics of jumping phenomenon by analyzing prestressed concrete beam sections with concrete strength ranging from 20 to 200MPa, reinforcing steel ratio of 0.2, 0.4 and 0.6%, and several prestressing levels.

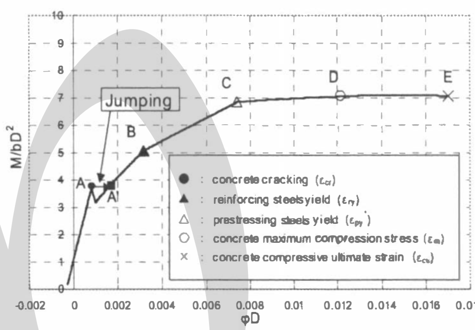

Fig.1 $M-\phi$ curve in prestressed concrete flexural members

2 ANALYTICAL RESULTS

Point A representing the cracking stage illustrated in $M-\phi$ curve shown in Fig.1 leaps promptly to point A'. This sudden large increase in curvature and stresses of prestressing and reinforcing steels is called *jumping phenomenon*. The jumping phenomenon, based from analytical results, is discussed in detail in the succeeding paragraphs.

2.1 Minimum ratios of prestressing steels ($_{min}P_p$)

To explain the characteristics of the jumping phenomenon, Fig.2 shows $M-\phi$ curves obtained from four different cases with concrete of 100 and 200MPa, and prestressing steel ratio of 0.0767 and 0.2343% . In the first case where $F_c = 100MPa$ and $P_p = 0.0767\%$, the cracking capacity is approximately equal to the yield capacity. This result means that the yielding of prestressing steels takes place just after crack occurs in tensile concrete. After prestressing steels yielding, the curvature visibly increases at a nearly constant moment until the concrete fails by reaching its ultimate strain ε_{cu} . Since the second case of $P_p = 0.0767\%$ and higher strength concrete of $F_c = 200MPa$, shows higher cracking capacity than the yield capacity, the section fails immediately after cracking due to rupture of prestressing steels. In the third case with larger P_p of 0.2343% under F_c of $200MPa$, because the yield capacity gets higher level similar to cracking capacity, the failure pattern is almost same as the first case, in which concrete crack and prestressing steels yield occur simultaneously. Conversely, in the last case of $P_p = 0.2343\%$, $F_c = 100MPa$, which the concrete strength is low, but the ratio of prestressing steels is large, as the cracking capacity becomes smaller, the resistance of moment increases ordinarily with increase in curvature until compression failure of concrete. From the above results, it has been discovered that the jumping phenomenon depends mainly on the amount of prestressing steels and concrete strength.

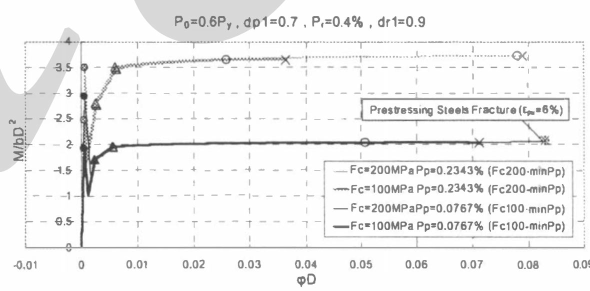

Fig.2 $M-\phi$ curve by minimum ratio of prestressing steels

2.2 Influence of concrete strength to $_{min}P_p$ and $_{max}P_p$

Analytical results describing the influence of concrete strength on $_{min}P_p$ and $_{max}P_p$ are shown in Fig.3. The horizontal axis denotes concrete strength, and the vertical axis denotes values of $_{min}P_p$ and $_{max}P_p$. As concrete strength becomes higher, $_{max}P_p$ increases significantly, but $_{min}P_p$ rises slowly. This result indicates that as the concrete strength gets higher, the range of allowable quantities of prestressing steels becomes wider, and that the use of high strength concrete to prestressed concrete members is feasible. However, it will be difficult to arrange large quantities of prestressing steels at the anchorage zones of prestressed concrete members. Thus, it is necessary to develop super high-strength prestressing steels and anchorages for high-strength concrete.

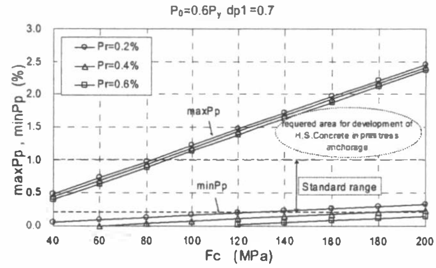

Fig.3 Relation of Fc , $_{min}P_p$ and $_{max}P_p$

2.3 Relations among stress of reinforcing steel, prestressing level and concrete strength

In this paragraph, the effect of prestressing level on the stress of reinforcing steel is examined using sections with reinforcing steel ratios of 0.2 , 0.4 and 0.6% , and concrete strengths of 100 and $200MPa$. In the calculation, prestressing steel ratio P_p is varied while keeping the initial prestressing force in constant at $0.6P_y$ (P_y ; yield force of prestressing steels)

Looking at Fig.4 showing the analytical results, the following tendencies were observed. Stresses of reinforcing steels after cracking decrease significantly in the shape of hyperbolic curves as the ratio of prestressing steels increases. This result demonstrates that prestressing level is key factor affecting σ_{st} and crack width. In addition, while holding P_p constant, the reinforcing steel ratio P_r behaves indirectly proportional to σ_{st} . On the other hand, with P_r being held constant, the $\sigma_{st} - P_p$ relations for concrete with various F_c appear to be parallel. This result shows that for concrete with $F_c = 200MPa$, to keep the value of σ_{st} equal to the case when, $F_c = 100MPa$, the quantity of prestressing steels should be doubled.

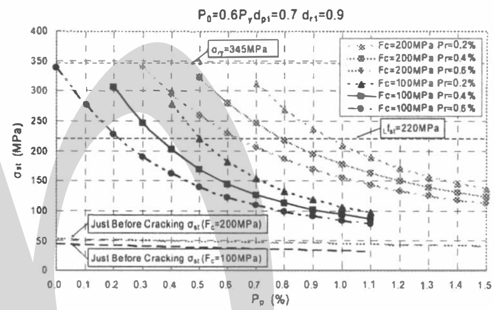

Fig.4 Relation of Fc , σ st and P_p

CONCLUSIONS

1) As concrete strength increases, the range of the allowable quantity of prestressing steels becomes wider suggesting that use of high-strength concrete for prestressed concrete members is feasible. However, it is necessary to develop super high-strength prestressing steels and anchorage for high-strength concrete.
2) With sections having the same amount of steel reinforcements, stresses of steel reinforcements after cracking decrease significantly in the shape of hyperbolic curves as the ratio of prestressing steels increases. This result observed in both cases of 100 and 200MPa concrete demonstrates that prestressing level is a key factor affecting the stress of reinforcing steels and crack width of flexural concrete members.

ACKNOWLEDGEMENT

This investigation was carried out by the working-group belonging to PC Committee in The Society of Materials Science, Japan. The authors would like to thank the group members for their useful suggestions relating to this study.

REFERENCES

1) Hiroshi Muguruma et al.: "Stress-Strain Curve Model for Concrete with a Wide-range of Compressive Strength", Proceedings of the 3rd International Symposium on Utilization of High Strength Concrete, pp21-32, Lillehammer, Norway, June 1993.
2) Hiroshi Muguruma, Fumio Watanabe and Minehiro Nishiyama : "Minimum Amount of Tensile Reinforced Concrete Flexural Members with High-Strength Concrete ", Proceedings of FIP Symposium on Concrete 95 Toward Better Concrete Structures, Vol. 1, pp.329-335, Brisbane, Australia, Sept., 1995
3) Tanigawa, Nakatsuka and Hatanaka : "Concept and Design of Reinforced Concrete", the second edition, Morishita, Japan, 1994 (In Japanese)

ON THE DESIGN AND CONSTRUCTION OF SHIRARIKA RIVER BRIDGE – A PC BRIDGE MADE OF HIGH PERFORMANCE LIGHTWEIGHT CONCRETE

Michihito Yamazaki, Shinichi Takemoto
Hokkaido Branch, DPS Bridge Works Co., Ltd., JAPAN

Yasuyuki Shibata, Hajime Nakamura
Hokkaido Regional Bureau, Japan Highway Public Corporation, JAPAN

Keywords: high-performance lightweight aggregate, lightweight concrete, 3D stress analysis, full-scale model test

1 INTRODUCTION

The Shirarika River Bridge is a prestressed concrete (PC) highway bridge designed and built with high-performance lightweight concrete (HL concrete) using recently developed high performance artificial lightweight aggregate. The use of lightweight concrete in Japan started with natural lightweight aggregate and became popular in 1960s when artificial lightweight aggregate of reliable quality was commercially available, recording about 50 cases of civil engineering application every year from 1967 to 1970. After that, however, lightweight concrete has not been used so often. With the introduction of pumping, blockage in pump tubes was reported frequently. Although it was found to be caused by the unique water absorption characteristics of the artificial lightweight aggregate, the problem was not dealt immediately. It was also revealed that fatigue durability and other deterioration mechanism of lightweight concrete had not been studied sufficiently.

The high performance artificial lightweight aggregate adopted for the current bridge has a reduced water absorption ratio by about 1/3 and nearly twice the strength compared with the conventional artificial lightweight aggregate. With the improvement of pumpability and durability, it was decided to use the new aggregate in a PC highway bridge on an experimental basis. In order to use the HL concrete, fundamental data about lightweight concrete was collected through various tests and experiments [1-2]. Since the water-cement ratio is lower and the cement content is higher in the HL concrete than in normal concrete commonly used in PC bridges, the heat of hydration in massive concrete members was expected to be high. For a comparison between the HL concrete and normal concrete, three-dimensional (3D) analysis was carried out for the thermal stress in a full-scale model of the pier-head section. Based on the results, the full-scale model, embedded with a pipe cooling system was prepared using the HL concrete to observe the temperatures and check for cracks. This paper discusses characteristics of the HL concrete and describes the 3D thermal stress analysis (using FEM analysis), the full-scale test and the construction of the Shirarika River Bridge.

2 OUTLINE OF THE BRIDGE

A side view and cross-sectional views of the Shirarika River Bridge are shown in Fig. 1. Summary of the project is described below.

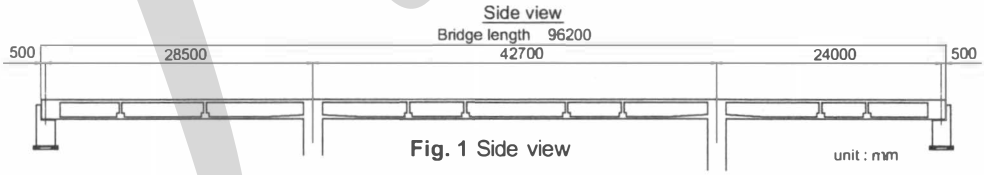

Fig. 1 Side view

- Project name: Hokkaido Highway Shirarika River Bridge (PC Superstructure) Project
- Construction period: from September 1999 to December 2001
- Construction site: Kuroiwa, Yakumo-cho, Hokkaido
- Road classification: Type 1, Class 2, B Standard
- Bridge length: 96.200 m
- Spans: 28.500 m + 42.700 m + 24.000 m
- Full width: 11.400 m
- Live load: B live load
- Concrete: Lightweight concrete (Type 1)
- Coarse aggregate: high performance artificial lightweight aggregate

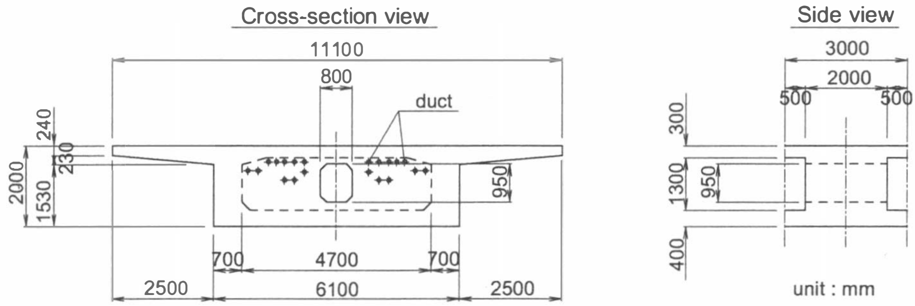

Fig. 2 Layout and dimensions of the full-scale model

3 THERMAL STRESS ANALYSIS AND THE FULL-SCALE MODEL TEST

The structural layout and dimensions of the full-scale pier-head model are shown in Fig. 2. A 3D thermal stress analysis was carried out for the full-scale model, considering only 1/4 of the model due to symmetry. From the results of the unsteady heat conduction and thermal stress analyses, thermal stress due to the heat of hydration was determined, and the thermal cracking index was computed. The temperature variation of normal concrete (Case 1) and HL concrete (Case 2) is shown in Fig. 3. From this result, it was decided to use high-heat resistant type for pre-grouted tendons for transverse prestressing of the slabs.

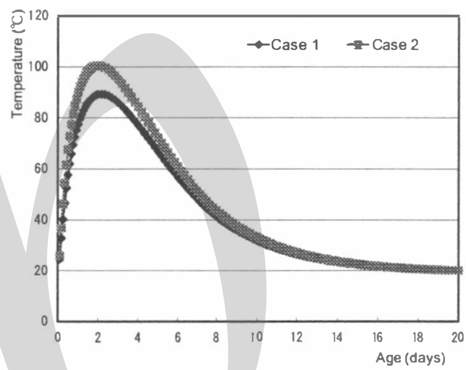

Fig. 3 Temperature variation from 3D thermal stress analysis

A full-scale model test of the pier head was carried, where the occurrence of initial cracks was visually checked. The observed temperature variation was compared against the analysis results, and confirmed the applicability of the high-heat resistant pre-grouted tendons. Pumpability was also checked during concrete placing to examine the workability of the mix. Since the preliminary temperature analysis suggested that the maximum concrete temperature might reach around 100°C, pipe cooling was provided by embedding pipes. In the construction of the pier-head section of the actual bridge, the concrete temperature at placing was kept low by pre-cooling, placing at night and by improving the pipe cooling system. Consequently, the concrete temperature at placing was successfully controlled to a range between 18°C and 20°C, leading to a maximum concrete temperature of the pier-head section as low as 86.0°C.

4 CONCLUSIONS

Following conclusions are made from the test results.

(1) The maximum temperature of a mass concrete member using the HL concrete varied depending on the concrete temperature at placing, and the rise in the temperature from placing was 80°C.
(2) No initial cracks developed in the full-scale model.
(3) Embedded pipe cooling in the HL concrete was effective only locally and showed no significant effects at a distance more than 10 cm from the pipes.
(4) The amount of the temperature rise estimated by the 3D thermal stress analysis was almost equal to that obtained by the full-scale model test and also to that observed during the actual construction.

REFERENCES

[1] Hamada, Y., et al.: Shear capacity of PC beam members using high performance lightweight concrete. Proc. of the 9th Symposium on Developments in Prestressed Concrete, pp. 739-744, Oct., 1999 (in Japanese)
[2] Tamura, S., et al.: Strength characteristics of PC anchorage zones using high performance lightweight concrete. Proc. of the JCI, Vol. 22, No. 3, pp. 871-876, 2000 (in Japanese)

SHRINKAGE PROPERTIES OF HIGH STRENGTH CONCRETE CONTAINING FLY ASH

Hoi-Keun Lee Joon-Young Im Kwang-Myong Lee Byung-Gi Kim
Department of Civil and Environmental Engineering Admixtures Team, R&D Center
Sungkyunkwan University, KOREA Kyunggi Chemicals Ltd., KOREA

Keywords: high strength concrete, autogenous shrinkage, drying shrinkage, fly ash

1 INTRODUCTION

Shrinkage characteristics of high strength concrete (HSC), autogenous and drying shrinkages, are quite different from those of normal strength concrete (NSC). Although autogenous shrinkage mechanism is basically the same as that of drying shrinkage, there exists a fundamental difference between two shrinkage phenomena. That is, the autogenous shrinkage develops progressively within the mass of a non water-cured concrete. On the other hand, the drying shrinkage is a localized phenomenon that starts to develop at the surface of concrete [1]. The objective of this study is to investigate shrinkage properties including autogenous and drying shrinkage of HSC with and without fly ash. The fresh and mechanical properties of concrete are also presented.

2 EXPERIMENTAL WORK

ASTM Type I Portland cement and low-calcium fly ash were used as the cementitious materials. Washed river sand and crushed granite were used as fine and coarse aggregate, respectively. Table 1 shows the mix proportions of the eight types of concrete used in this study. Mixes 1-4 do not contain fly and are designated as OPC concrete, whereas the others contains fly ash of 20% of cementitious materials (cm) by weight and are designated as FA concrete.

Table 1 Mix proportions of concrete per m^3

Mix no.	Water (kg)	Cement (kg)	Fly ash (kg)	Fine aggregate (kg)	Coarse aggregate (kg)	AE (cm×%)	SP (cm×%)	w/cm
1	185	370	-	754	969	0.5	-	0.50
2	158	450	-	672	1061	-	1.5	0.35
3	155	500	-	626	1074	-	2.0	0.31
4	148	550	-	617	1060	-	2.4	0.27
5	185	296	74	744	956	0.5	-	0.50
6	158	360	90	661	1043	-	1.5	0.35
7	155	400	100	614	1054	-	2.0	0.31
8	148	440	110	605	1038	-	2.4	0.27

Note: AE = air-entraining water reducing admixture, SP = superplasticizer

Concrete prisms with 100x100x400 mm were prepared to measure drying shrinkage and autogenous shrinkage. The first measurement of drying shrinkage strain of concrete was carried out at 7 days after casting using an embedded strain gauge under temperature at 20$^{\circ}C$ and relative humidity of 60%. Autogenous shrinkage of concrete had been measured according to the method proposed by Japan Concrete Institute (JCI) since the curing age of 6 hrs.

3 RESULTS AND DISCUSSION

3.1 Properties of fresh and hardened concrete

Iinitial slumps of NSC mixtures (Mix 1 and 5) were measured 190 mm, while those of HSC mixtures (Mixes 2-4 and 6-8) were 225±20 mm. At 28 days, compressive strengths of FA concrete slightly lower than that of OPC concrete.

3.2 Autogenous shrinkage

Figure 1 shows that autogenous shrinkage increased as w/cm decreased for both OPC and FA concretes. Moreover, a great part of autogenous shrinkage of the HSC was developed within a few days after casting, and this may cause early-age cracking. Besides, FA concrete showed lower autogenous shrinkage than the OPC concrete with the same w/cm due to the delayed hydration reaction and more free water [2]. However, in spite of the use of fly ash, the HSC with low w/cm still exhibits large autogenous shrinkage.

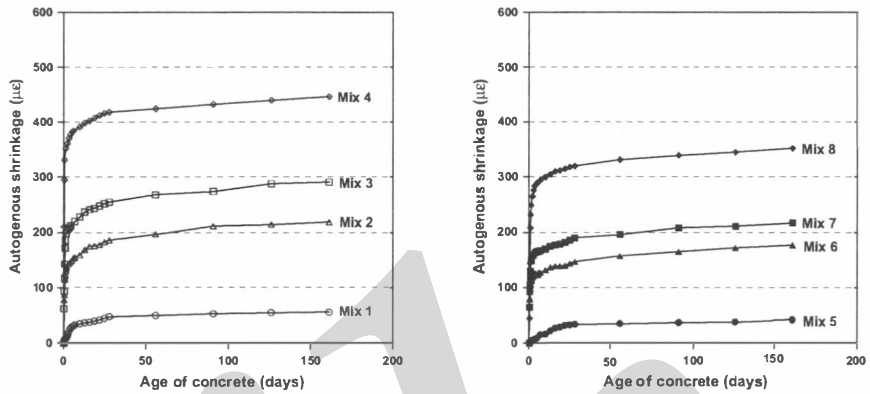

(a) OPC concrete (b) FA concrete

Fig.1 Autogenous shrinkage of concrete with various w/cm

3.3 Drying shrinkage

Figure 2 shows that the HSC exhibited lower drying shrinkage than that of NSC at any given ages because the HSC had small amount of porosity caused by its low w/cm. Moreover, the FA concrete had slightly higher drying shrinkage than OPC concrete. Since drying shrinkage of concrete are directly associated with the water held by gel pores in the range 3 to 20 nm, concrete containing fly ash that is capable of pore refinement usually shows higher drying shrinkage [3].

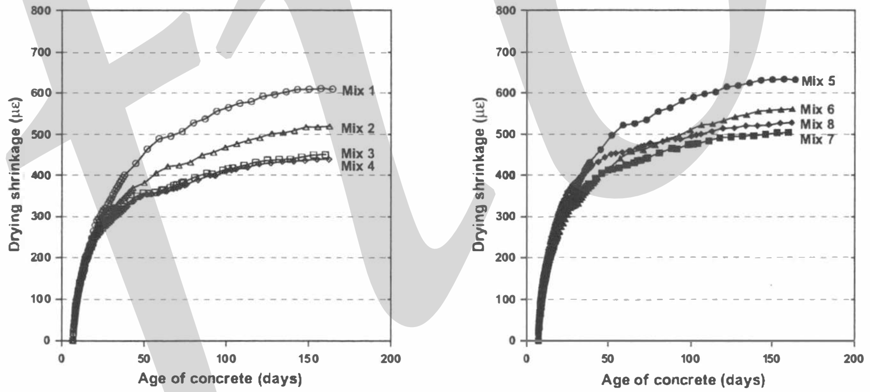

(a) OPC concrete (b) FA concrete

Fig.2 Drying shrinkage of concrete with various w/cm

4 CONCLUSIONS

(1) Autogenous shrinkage of concrete was more rapidly developed as the water to cementitiious materials ratio decreased. Fly ash would reduce the autogenous shrinkage of concrete.

(2) Drying shrinkage of high strength concrete was less than that of normal strength concrete because the HSC has small amount of porosity due to its low w/cm. Fly ash concrete exhibited greater drying shrinkage than ordinary concrete due to finer pores in fly ash concrete.

REFERENCES

[1] Aitcin, P. -C. : High performance concrete, E&FN Spon, 1998
[2] Tangtermsirikul, S. : Effect of chemical composition and particle size of fly ash on autogenous, 1999
[3] Mehta, P. K. and Monteiro, Paulo J. M. : Concrete, Prentice Hall, 1993.

EVALUATION AND COMPARISON OF SEALED AND NON-SEALED SHRINKAGE

Osamu Kuramoto — P.S. Corporation, JAPAN
Toshiki AYANO, Mahmoud Abo El-Wafa, Kenji SAKATA — Department of Environmental and Civil Engineering, Okayama University, JAPAN

Keywords: drying, shrinkage strain, autogeneous, moisture

1 INTRODUCTION

The purpose of this study is to propose the method to obtain autogenous shrinkage of non-sealed specimen under drying experimentally. The specimen was heated at 950C in order to obtain the bound water of cement paste. It will be shown that even if the start of drying of the specimen is different, the relationship between the development of drying shrinkage and moisture loss can be expressed by the same curve when the autogenous shrinkage under drying is obtained on the basis of bound water.

2 EXPERIMENTAL APPROACH

Mortar is used for test. The water to cement ratio is 20.0% by weight. The sand to cement ratio is 65.5% by weight. The superplasticizer is used 1.5% of total cement content. The dimension of specimens for measurement of moisture and shrinkage is 40x40x160mm. All surfaces, except the two parallel drying surfaces, of the specimens under drying were sealed by aluminum sheet. All surfaces of the specimen for measurement of autogenous shrinkage were sealed by aluminum sheet. The length change in the longitudinal direction was measured using a linear gauge with a minimum division of 1/1,000mm. The specimen was supported by two pins that consist of the pointed head of the linear gauge and the support. All specimens were put into the room with relative humidity of 60% and temperature of 20℃.

3 EXPERIMENTAL RESULTS AND DISCUSSION

Fig.1 shows the change of evaporable moisture content and bound water content. The sealed specimen does not lose any moisture. As it is clear from this figure, the bound water increases and evaporable moisture content decreases with the lapse of time. Fig. 2 shows the relationship between autogenous shrinkage and bound water content of sealed specimen. This relationship can be expressed simply by by-linear line. The tuming point of the by-linear line is at the bound water content of 50%. Fig.3 shows the bound water content of non-sealed specimen. As earlier the start of drying, the bigger the change of bound water content. Fig.4 shows the two types of autogenous shrinkage of mortar which starts to dry at 3days. The curve expressed by open circles is obtained on condition that the autogenous shrinkage is independent of drying [1]. The increase of autogenous shrinkage is calculated in time with the age of specimen under drying. The other curve expressed by filled circles is based on bound water of non-sealed specimens. That, the following hypothesis is used. The autogenous shrinkage is the same when the bound water content is the same irrespective of sealed or non-sealed. The value of vertical line in Fig.5 and Fig.6 is the development of drying shrinkage. That is obtained by dividing the drying shrinkage at each drying time by the regressed ultimate drying shrinkage. The moisture loss of mortar is on the horizontal line. The drying shrinkage shown in Fig.5 is obtained in the condition that autogenous shrinkage is independent of drying. The relationship between the development of drying shrinkage and moisture loss is different in the start of drying. But, when the drying shrinkage is determined by autogenous shrinkage based on the bound water, the relationship between the development of drying shrinkage and moisture loss can be expressed by the same curve as shown in Fig.6.

4 CONCLUSIONS

In this study, the bound water content is obtained from the difference between moisture loss of specimen heated at 950C and that dried at 105C. It is shown that the relationship between drying shrinkage and moisture loss can be expressed well when the autogenous shrinkage of dried specimen is determined on the basis of the bound water content.

REFERENCES

[1] Yang YANG, Ryoichi SATO and Kenji KAWAI, Evaluation of Autogenous Shrinkage and Drying Shrinkage Based on Bound Water Content of Cementitious Materials, Journal of Materials, Concrete Structures and Pavement, No.690/V-53, pp.109-120, November 2001 (in Japanese)

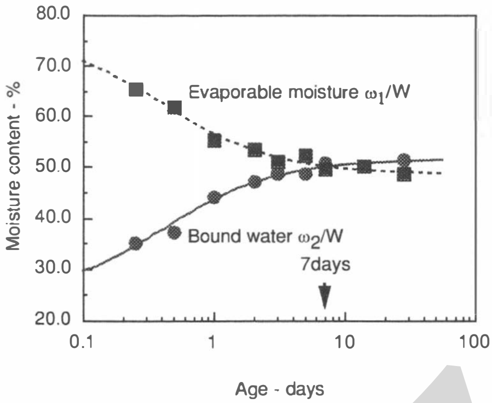

Fig.1 Relationship between evaporable moisture and combined water in sealed specimen

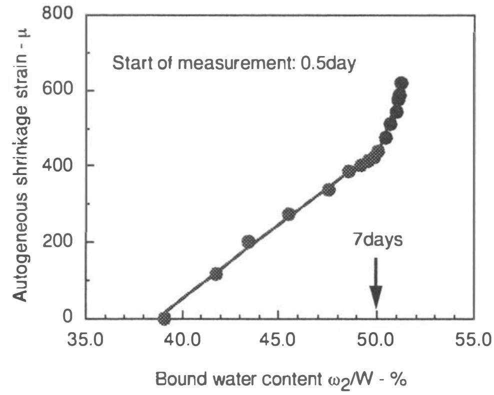

Fig.2 Relationship between autogenous shrinkage and bound water content

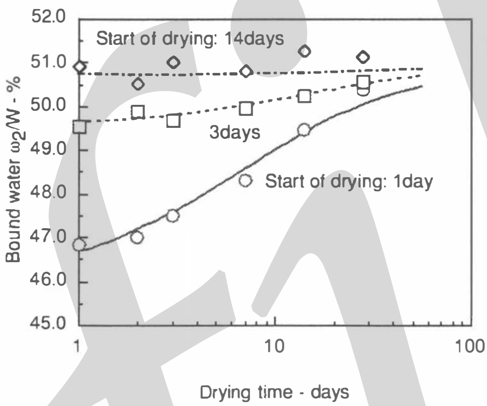

Fig.3 Change of bound water content of non-sealed specimen

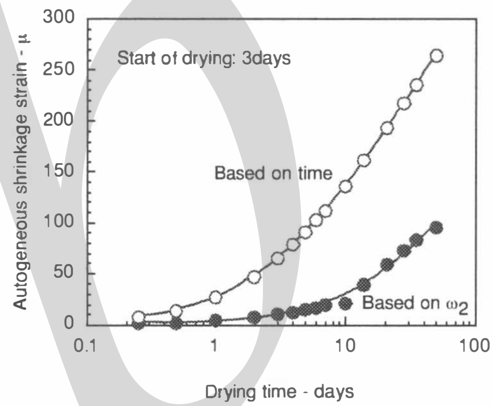

Fig.4 Autogenous shrinkage of specimen under drying

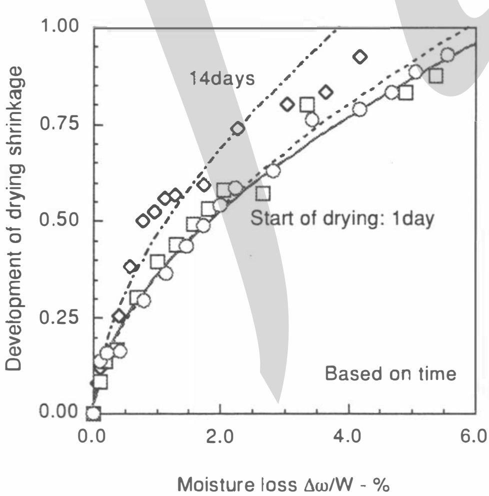

Fig.5 Autogenous shrinkage strain is considered to be independent of drying

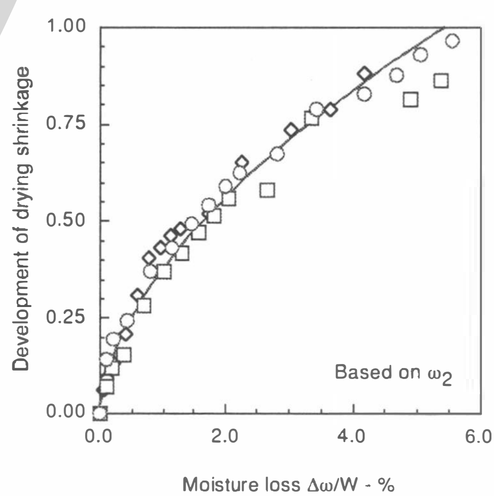

Fig.6 Autogenous shrinkage was obtained on the basis of the bound water content

LONG TERM BEHAVIOUR FOR CANTILEVER BRIDGES IN HPC

Dr. C. van der Veen
Delft University of Technology
the Netherlands

Mr. N. Kaptijn
Ministry of Public works and Water Management
the Netherlands

Keywords: High performance concrete, creep, shrinkage and deflections.

1 INTRODUCTION

The use of high performance concrete (HPC) has increased rapidly during the last few years. Starting from 1994 a few solid plate bridges were constructed in HPC. In 1997 the erection of the second 'Stichtse' bridge was completed in the Netherlands. It was the first application of HPC in a cantilever bridge. The span lengths are 80, 160 and 180 m. Near Rotterdam a second cantilever bridge made in HPC with a main span of 190 m was finished in 2001. Both bridges have been built with the in situ free cantilever construction method. They consist of a box-girder cross-section and a variable construction depth.

In order to predict reliable deflections of the bridges during lifetime, information about creep and shrinkage of the HPC is necessary. The experimental data of creep and shrinkage of HPC are still limited. For that reason experiments have been carried out to investigate the time dependent concrete properties. Besides specimens tested in the Stevin laboratory, some specimens were stored inside the box-girder bridge in order to measure e.g. shrinkage under the same weather conditions as the actual bridge. Furthermore, deflection of the bridge has been measured during constructions and during lifetime of the bridge.

2 EXPERIMENTS

Experimental research was performed on the HPC-mix. After 28 days the cubic compressive strength is about 100 N/mm^2.

During construction of the bridge concrete specimens were cast. The moulds adopted for the prismatic specimens had a size of 100 X 100 mm in cross-section and 400 mm in length. All the specimens were kept in the mould for 24 hours after casting. A part of the specimens were transported to the Stevin laboratory and put in a curing room at a temperature of 20°C and a relative humidity of about 50%. The other part of the specimens was stored in the bridge until the test. Tests have been carried out at a concrete age of 14, 28 and 365 days.

In each series of tests the following variables have been measured:

- shrinkage
- creep
- modulus of elasticity and cylindrical strength.

Shrinkage measurements have been started at a concrete age of 14 days in order to measure mainly the drying shrinkage. Autogeneous shrinkage is supposed to occur mainly in the first days after casting. Predictions were made by using the models according to the CEB-FIP model code 1990 (MC90), model code 1978 (MC78) and the Dutch code (DC). It was found that all the codes underestimate the shrinkage.

During construction of the bridge two concrete specimens were cast and placed inside the box-girder, Van der Veen [1]. These prismatic specimens were 1000 mm in length, 600 mm high and 320 mm thick. The thickness of the specimens was equal to the web thickness of the box girder.

Consequently, comparable shrinkage values could be expected as in the real structure, because the relative humidity and temperature are more or less equal. Shrinkage was measured along 4 lines. The results till a concrete age of about 1400 days are shown in Fig. 1. The measurements started about 24 hours after casting (directly after demoulding). A sharp increase in the shrinkage values was observed in the beginning, which was caused by the autogeneous shrinkage. After reaching a maximum shrinkage value at 550 days an unexpected descending branch was found for older concrete.

This phenomenon could not be explained and was not reported as a result elsewhere. More research in this field has been started to understand this feature.

Creep experiments have been performed on the prismatic specimens at a concrete age of 14 and 365 days at a stress level of 10 MPa and 20 MPa, respectively. all predictions of the codes overestimate the deformation very much. The MC90 overestimate the deformation by about 50%.

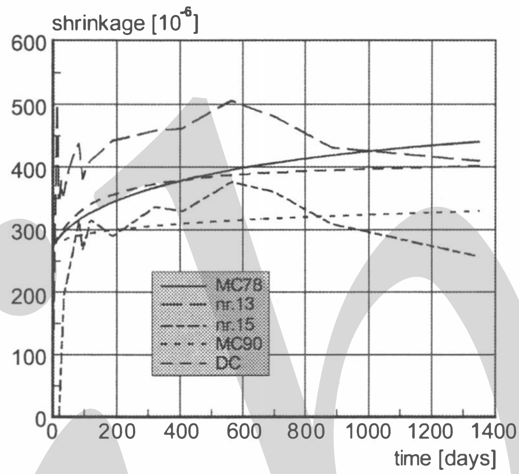

Fig. 1 Shrinkage of specimens in the bridge

3 LONG TERM BEHAVIOUR

After the cantilever bridge was made continuous and just before and after the asphalt layer was put on the bridge deck the midspan deformation was measured and predicted by a computer program. The results are close to each other.

After 1,2,5 an 10 years the midspan deflection will be measured. Based on the results during monitoring the deflection a fresh calculation has been made. The results were very much the same, only when the actual (mean)values for the material properties were used.

4 CONCLUSION

On the basis of the experimental results and field measurements mentioned above, the following main conclusions can be drawn:

- Field measurements on concrete specimens showed an unexpected feature. After about 550 days a concrete expansion instead of shrinkage was observed.
- Autogeneous shrinkage should be added to the predicted values calculated according to the CEB-FIP Model Code.
- Creep deformation of HPC is overestimated by at least 50% if the Model Code is applied.
- A calculation of the deflection of a cantilever bridge based on the Model Code overestimate the deflection very much.
- A reasonable prediction was found when the MC 90 was applied with the actual values of the material.

5 REFERENCES

[1] Veen, C. van der and Horeweg, E.M.; "Monitoring of cantilever bridges in HPC", (in Dutch) Stevin report 25.5-99-11, Delft, 190 pages.

AN ESTIMATION OF COUPLED DEFORMATION AND STRESS FROM AUTOGENOUS SHRINKAGE AND THERMAL EXPANSION OF HIGH-STRENGTH CONCRETE MEMBERS

H. Hashida N. Yamazaki
Institute of Technology, Shimizu Corporation, Tokyo, Japan

Keywords: autogenous shrinkage, thermal expansion, high-strength concrete, shrinkage stress

1 INTRODUCTION

Reinforced concrete members made of high-strength concrete are subjected to stress due to coupled strain resulting from autogenous shrinkage and thermal expansion/contraction, which may cause severe cracking at early age. In the paper, the coupled strain of concrete specimens under semi-adiabatic curing was measured and estimated both components, autogenous shrinkage and thermal expansion. Actual strain and shrinkage stress in full-scale model columns were then investigated by comparing the estimated values with the experimental measurements.

2 EXPERIMENT AND RESULT

Eight types of concrete were prepared for laboratory tests (Table 1). Four types of cement or binder were used: ordinary Portland cement (OPC), belite-rich Portland cement (BPC), BPC with 5% replaced by mass with silica fume (BSC) and blast fumace slag cement (OBC). The changes in the autogenous

Table 1 Mix proportions

Mix	W/B (%)	W	C	SF	S	G	f_{cs} (N/mm²)
		kg/m³					
BPC40	40	168	420	—	785	975	76.8
BPC27	27	165	611	—	697	940	101
BPC20	20	165	825	—	581	896	119
BSC20	20	165	784	41	606	856	123
OPC40	40	168	420	—	780	975	68.2
OPC27	27	165	611	—	692	940	97.4
OPC20	20	165	825	—	573	896	109
OBC27	27	165	611	—	751	859	109

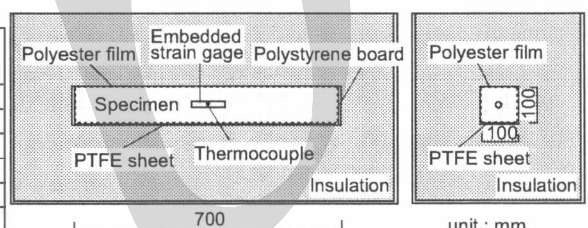

Fig. 1 Test specimen for semi-adiabatic curing

shrinkage strain at a constant temperature of 20°C and the total strain under semi-adiabatic curing i.e. the strain composed of autogenous shrinkage and thermal expansion, were measured (Fig. 1).

Two types of ready-mixed concrete, OPC-Rm and BPC-Rm with materials and mix proportions similar to OPC27 and BPC27, were used for an experiment on full-scale members (Fig. 2).

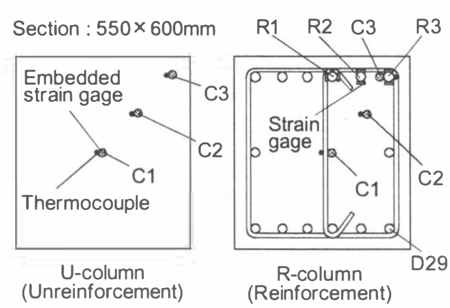

Fig. 2 Full-scale model columns

Fig. 3 shows separations of the actual strains of OPC27 under semi-adiabatic curing into thermal strains and autogenous shrinkage strains, with the coefficient of thermal expansion being assumed in one case to be constant and in another case to be increasing [1, 2]. A reasonable and nearly exponential curve of autogenous shrinkage strain was obtained when the increasing coefficient of thermal expansion was applied. From the relationship between the maximum temperature in the history and the ratio of the development of autogenous shrinkage in the history to that of 20°C-curing ($\varepsilon_{as} / \varepsilon_{as20}$), the autogenous shrinkage of OPC's and BPC's is highly dependent on the temperature conditions (Fig. 4). It should be noted, however, that OBC27 and BSC20 show higher developments.

These results indicates that by taking account of the increase of thermal expansion coefficient with

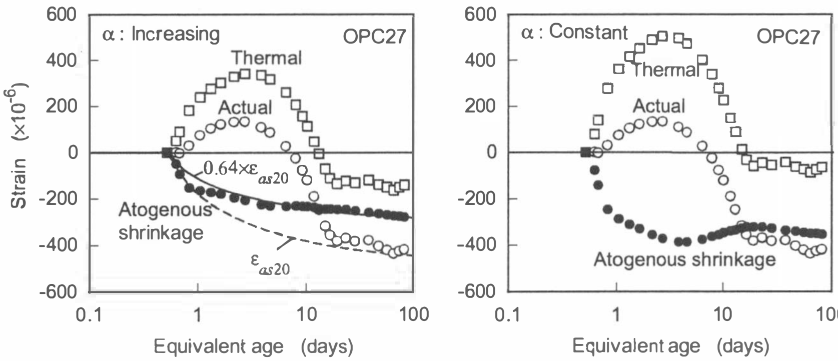

Fig. 3 Separations of actual strain of OPC27 under semi-adiabatic curing into thermal strain and autogenous shrinkage strain

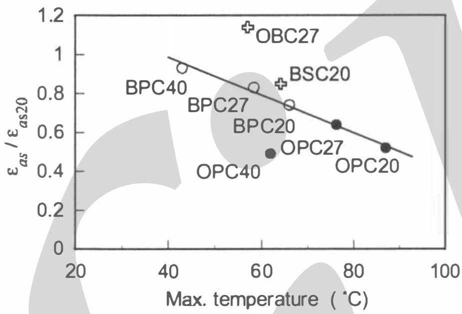

Fig. 4 Effect of maximum temperature on autogenous shrinkage

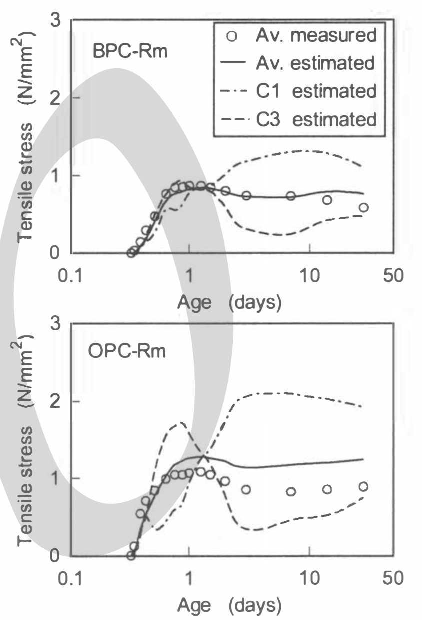

Fig. 5 Measured and estimated stresses in R-columns.

age, it was possible to estimate the coupled strain of high-strength concrete members subjected to a high temperature history. While autogenous shrinkage of concrete with usual Portland cement subjected to a high temperature history was considered to be smaller than that of 20°C-curing, autogenous shrinkage of concrete with admixtures was considered to be larger when the admixture content was high.

Fig. 5 shows the measured average stress, converted from the strain of reinforcing bar, and the estimated stress in R-columns, using the creep analysis described in [3]. While the average stress estimated of BPC-Rm agrees well with the measured one, that of OPC-Rm overestimates the measured one, corresponding with cracking. It was considered that the stress at the corner (C3) of OPC-Rm up to the age of 1 day was too high to protect against the crack.

3 CONCLUSION

These results make clear that the estimating approach including the concept of strain composed of autogenous shrinkage and thermal expansion are very useful for the analysis of actual strain and stress of high-strength concrete structural members.

REFERENCES

[1] Bjøntegaard, Ø. & Sellevold, E.J., Thermal Dilation-Autogenous shrinkage: How to separate? Proc, Intern. Workshop on Autogenous Shrinkage of Concrete, Hiroshima (Ed. by Tazawa, E.), pp.245-256, 1999
[2] Neville, A.M., Properties of Concrete, 3rd Edition. Longman Scientific & Technical, p.493, 1986
[3] Hashida, H. & Yamazaki, N., A calculation method of autogenous shrinkage stress in high-strength concrete structures subjected to elevated temperature at early age, J. Struct. Constr. Eng., AIJ, No.537, pp.7-12, 2000 (in Japanese)

CALCULATION OF SELF-INDUCED STRESS IN EARLY-AGE CONCRETE USING CREEP AND RELAXATION MODEL

I. Maruyama and T. Noguchi
Tokyo University, Japan

P. Lura and K. van Breugel
Delft University of Technology, The Netherlands

Keywords: self-induced stresses, early-age concrete, creep, modeling

1 INTRODUCTION

High-Performance concretes, characterized by low water-binder ratio, are particularly sensitive to self-desiccation of the cement paste during the hydration process, which is a principal cause of autogenous shrinkage. If an external restraint is present, autogenous shrinkage, added to temperature-induced deformations, may lead to high self-induced stresses, possibly causing surface and even through cracks. In order to estimate the cracking risk, it is of vital importance to accurately calculate the self-induced stresses. In this calculation the early-age creep behavior of the concrete plays a prominent role, since the self-induced stresses will be substantially reduced due to relaxation.

In this contribution, two recent models describing early-age creep and relaxation in concrete, namely Lokhorst's model (based on the degree of hydration concept) and Westmann's model (based on the early-age development of the mechanical properties), are discussed. The potential of the two models to predict the development of self-induced stresses in early-age concrete is evaluated by comparison with the experimental results obtained with a Thermal Stress Testing Machine (TSTM).

2 MODELS

Lokhorst's model is a constitutive model for hardening concrete, in which the evolution of the microstructure is explicitly accounted for [1]. In this model, concrete is composed of unhydrous cement, cement gel and aggregates. Each component possesses particular physical properties and they interact according to the geometry of the microstructure determined with the simulation program HYMOSTRUC [2]. New elements, representing the newly formed cement gel, are added to the microstructure with progress of the hydration process. This enables to simulate the microstructural development and its effect on the deformational behavior, which is highly influenced by the course of the hydration process, i.e. by the formation of new hydration products.

On the other hands, Westman's model [3], an easy-to-handle engineering model, is expressed as:

$$\varepsilon_{c\sigma}(\Delta t_{load}, t_0) = \sigma_c(t_0)\left[\frac{1}{E_c(t_0)} + \frac{\phi(\Delta t_{load}, t_0)}{E_{ck}}\right] \tag{1}$$

where:
$\varepsilon_{c\sigma}$ = creep strain at time $t_0+\Delta t_{load}$
Δt_{load} = time interval after loading at concrete age t_0
$\sigma_c(t_0)$ = applied stress at concrete age t_0
$E_c(t_0)$ = modulus of elasticity at time of loading
E_{ck} = modulus of elasticity of concrete at 28 days of age
$\phi(\Delta t_{load}, t_0)$ = creep coefficient

In this equation three factors appear that simulate the phenomena occurring during hardening of concrete. One deals with the modulus of elasticity and the others with the creep phenomenon.

3 EXPERIMENTS AND PARAMETERS OF THE MODELS

In order to determine the parameters in the models, several basic experiments were conducted with a concrete with w/c ratio 0.37. The model suggested by Westman needs the values of E_{ck} and of a parameter *s* to simulate the development of elastic modulus. By comparison with the experiments, the parameter *s*, determined by least-square method, was set as 0.119 and E_{ck} as 38.2 GPa. A creep test with constant load was carried out to determine the other parameters in Lokhorst's model and in Westman's model. The tested specimens had a prismatic shape (100x100x400 mm^3). The loading age was 1 day and the applied stress was 40% of the compressive strength at that age. In Fig. 1 the measured creep compliance of the specimen divided by the applied stress is shown with the simulated curves according to Lokhorst's and Westman's model. The following values were used for the constants in Lokhorst's model: a=2.4 x 10^{-5}, n = 0.3, $\lambda = 1-\mu = 0.815$. Moreover, a parameter for calculating the bridging volume (called bridge length factor in [4]) was set to 2.5. In Westman's model, ϕ_0 = 1.12 and t_ϕ = 1000 days were used. Finally, autogenous shrinkage of concrete was measured in a previous research [5]. The fitted autogenous shrinkage curve as a function of time, determined by least square method, is expressed as:

$$\varepsilon_{auto}(t) = -151.66 + \frac{1207.78}{0.01504 + t} \tag{2}$$

where t is the time after setting [hours]

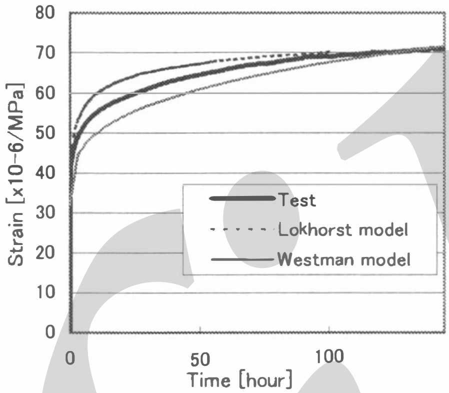

Fig. 1 Specific compliance curves of test result, Lokhorst's model and Westman's model. Loading age 1 day.

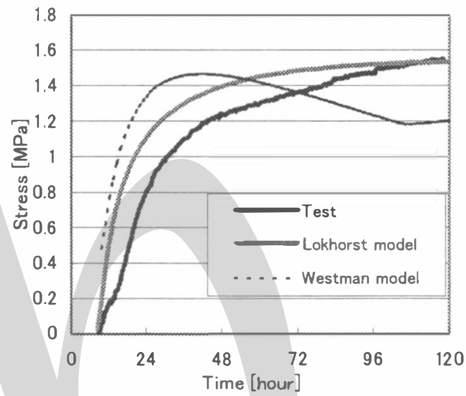

Fig. 2 Stress development under fully restrained condition and simulation results by Lokhorst's model and Westman's model.

4 EVALUATION AND CONCLUSION

Fig.2 shows the self-induced stresses developed in the first 5 days of hardening by a concrete specimen whose autogenous deformation was fully restrained. The specimen was cured at 20 ℃. The experiment was performed with a TSTM (Temperature Stress Testing Machine) [5]. By comparison of measured and calculated results, Westman's model, an easy-to-handle engineering model, is a good tool for a rough calculation of the self-induced stresses at early-age. On the contrary, Lokhorst's model shows a good agreement with the actual process of stress development. A disadvantage of this model is that a simulation of the hydration development performed with the program HYMOSTRUC is needed. Nevertheless, it is believed that Lokhorst's model has a great potential for both research and practical engineering purposes.

REFERENCES

[1] Lokhorst, S. J. and Breugel, K. van: Simulation of the effect of geometrical changes of the microstructure on the deformational behaviour of hardening concrete, Cement and Concrete Research, Vol.27, No.10, pp.1465 - 1479, 1997

[2] Breugel, K. van: Simulation of Hydration and Formation of Structure in Hardening Cement- based Materials, Ph.D thesis, Delft University of Technology, 1991

[3] Westman, G.: Concrete Creep and Thermal Stresses, Doctral thesis, Luleå University of Technology, Oct. 1999

[4] Lokhorst, S. J.: Deformational behaviour of concrete influenced by hydration related changes of the microstructure, Research report, Delft University of University, 1996

[5] Lura, P., Breugel, K. van and Maruyama, I.: Effect of curing temperature and type of cement on early-age shrinkage of high-performance concrete, Cement and Concrete Research, Volume 31, Issue 12, pp1867-1872, 2001

THE EFFECT OF REINFORCEMENT ON EARLY-AGE CRACKING IN HIGH STRENGTH CONCRETE AND NORMAL STRENGTH CONCRETE

Dipl.-Ing. M. Sule Prof.dr.ir. K. van Breugel
Delft University of Technology, THE NETHERLANDS

Keywords: early-age cracking, crack criterion, high strength concrete

1 INTRODUCTION

High strength concrete (HSC) has been developed for carrying higher loads than normal strength concrete (NSC). High strength concretes are realized by applying low water-cement ratios and admixtures. A low water-cement ratio leads to a denser microstructure, which makes HSC an ideal material for durable structures. However, HSC undergoes additional volume changes during hardening, so called autogenous shrinkage. Under restrained conditions this makes HSC even more prone to cracking in the early stage of hardening than NSC. With reinforcement this cracking can be controlled.

In order to enhance our understanding of the influence and effect of reinforcement on early-age cracking, an experimental research project was conducted [3]. Unreinforced and reinforced concrete specimens were tested in a Temperature Stress Testing Machine (TSTM). In this test device the concrete hardened under sealed condition and the deformations were 100% restrained. Consequently stresses were generated in the specimen, which could lead to cracking when the tensile strength (or strain capacity) of the concrete was exceeded.

In this contribution the results obtained with HSC (w/c ratio=0.33) are compared to the results of NSC (w/c ratio=0.5). Both concrete mixtures were subjected to semi-adiabatic hardening conditions. Test variables were the reinforcement percentages (0%, 1.34%, 3.02%) and configurations (1 and 4 reinforcing bars). In parallel with the TSTM test the free deformation of the plain and reinforced concrete was measured. From these measurements the effect of the reinforcement on the free deformation of reinforced specimens could be deduced.

Due to autogenous shrinkage HSC undergoes a larger deformation than NSC at early age. Therefore higher stresses are generated in HSC under full restraint. Nevertheless, the experimental results clearly show the effect of reinforcement on free deformation and stress development in both mixtures at early age. It was found that specimens reinforced with four reinforcing bars undergo substantial microcracking before the first through-crack occurs. This increases the strain capacity of the structural element prior to the occurrence of a dominant crack. Applying reinforcement can thus mitigate the proneness of HSC to early age cracking.

In addition to the presented experimental results, this paper quantifies the advantage achieved by applying a strain criterion instead of a stress [1] or a temperature [2] criterion for judging the cracking tendency of reinforced young concrete.

2 ANALYSE

Reinforcement bars are applied to carry loads and to control the crack width. In our experiments the effect of reinforcement on cracking NSC and HSC at early age was investigated. It was found that with the help of reinforcement, concrete elements can crack without sudden failure as observed in plain concrete. Microcracking proceeds large stress drops in reinforced specimens. This was especially found in specimens reinforced with four rebars.

An important property for cracking behaviour in reinforced concrete specimens is the bond between reinforcement and concrete. It enables the transmission of stresses in the cracking zone. In pull-out tests it was found that in NSC bond stress develops at about the same rate as cube compressive stress. In HSC it was found that cube compressive stress develops faster.

In NSC as well as in HSC it was found that especially specimens reinforced with four rebars can build up stress while generating smaller cracks. Large drops of the nominal stress in the specimen, indicating wider cracks, are postponed in this way. In order to verify whether indeed microcracking can be held responsible for the observed development of the nominal stresses prior to the moment of the formation of wide cracks, a number of cracks have been impregnated with fluorescent epoxy (Fig. 1). It can be seen that in the middle of a cross section (further away from rebars) the crack is wider and almost straight (Fig. 1, left). In the vicinity of the rebars (Fig. 1, right) the crack splits. It is assumed that these small cracks initiate the through-crack.

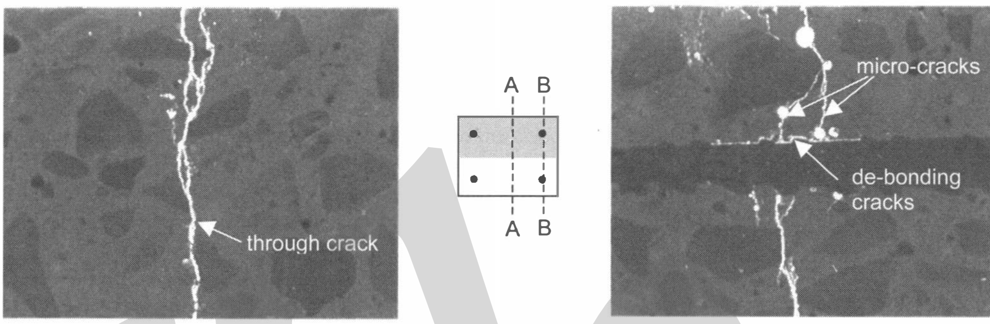

Fig. 1 Crack pattern in reinforced specimens in the middle of the specimen (left, section A-A) and in the vicinity of the rebars (right, section B-B)

Therefore reinforced specimens seem to crack later than plain specimens. In order to quantify the gain in tensile strain capacity prior to the moment of the occurrence of wide through-cracks achieved by applying reinforcement, the free deformations measured from the moment that the concrete stresses pass the zero until the moment of through-cracking were analysed (stress-inducing deformations) (Fig. 2).

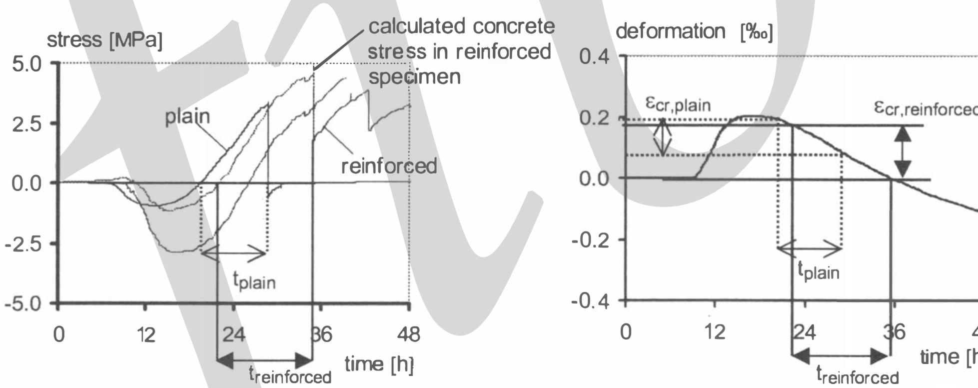

Fig. 2 Stress development and cracking in a reinforced (4∅12) and a plain HSC specimen cured semi-adiabatically. Tensile strain capacity $\varepsilon_{cr,reinforced} > \varepsilon_{cr,plain}$.

REFRERENCES

[1] Breugel, K. van, Lokhorst, S.J., 1999, "Stress-based crack criterion for concrete at early ages", Proc. IABSE symposium, Rio de Janeiro, CDROM, pp. 665-672.

[2] Eberhardt, M., Lokhorst, S.J., Breugel, K. van, 1994, "On the reliability of temperature differentials as a criterion for the risk of early-age thermal cracking, Proc. of the international RILEM symposium on thermal cracking in concrete at early age, pp. 353-360.

[3] Sule, M., Breugel, K. van, 2001, "Cracking behaviour of reinforced concrete subjected to early-age shrinkage", Materials and Structures, Vol. 34, June 2001, pp 284-292.

CRACKING BEHAVIOR OF REINFORCED HIGH-PERFORMANCE CONCRETE BEAMS WITH HIGH-PERFORMANCE REINFORCEMENT

Bruno Mesureur, Philippe Rivillon
Centre Scientifique et Technique du Bâtiment, FRANCE

Sébastien Bemardi
Centre d'Études et de Recherches de l'Industrie du Béton, FRANCE

Michel Lorrain
Institut National des Sciences Appliquées de Toulouse, FRANCE

Keywords: reinforced high-performance concrete, high performance steel, bending, cracking

1 INTRODUCTION

The study of high-performance concrete associated with high-performance reinforcement has come to the attention of the BHP 2000 French National project involving the CSTB in collaboration with Toulouse University. In this article, we deal with an experimental investigation on the mechanical behavior of high-performance reinforced concrete beams (rectangular cross section), under short-term imposed load.

The improvement of mechanical strengths of the two constitutes of reinforced concrete on the cracking behavior of tension ties and bending beams under short term imposed load was investigated experimentally. The mechanical strength of the concrete (the mean compressive strength varying from 30 to 100 N/mm²) and the longitudinal reinforcement ratio (ρ_l) were taken as tests parameters, and the yield steel strength was 830 N/mm².

We observed no significant change on the mean crack spacing due to the better mechanical strength of concrete. Under imposed load, the use of HSC (High Strength Concrete) allows 30 % reduction of the mean crack width during the stabilized cracking phase. This phenomenon is due to a reduction of the beam deflexion related to an increase of the bond between steel and concrete.

2 EXPERIMENTAL PROCESS

Table 1: parameters for bending tests and geometry of the test beam

Test lab	Beam reference	Concrete	Mean concrete strength [N/mm²]	Longitudinal reinforcement	Section h x b (cm²)	d (cm)	A_s (cm²)	B =2(h-d) (cm²)	$\rho = A_s/B$ (%)	Length (m)	Span (m)	Distance between loading points(m)
INSAT	M40 fy 620	M40C	42	2 HA 16 CS	28.3 x 15	25.7	4.02	78	5.15	3.60	2.80	1.20
	M75 fy 540	M75C	79	2 HA 16 CS								
	M75 fy 830	M75C	79	2 HA 16 HPS								
	M100 fy540	M100C	99	2 HA 16 CS								
	M100 fy 830	M100C	99	2 HA 16 HPS								
CSTB	M30/3HPS	M30C	31.6	3 HA 16 HPS	40 x 20	36	6.03	160	3.77	5.00	3.90	1.30
	M75/3HPS	M75C	93.2	3 HA 16 HPS								
	M100/3HPS	M100C	109.2	3 HA 16 HPS								
	M30/4HPS	M30C	31.6	4 HA 16 HPS			8.04	160	5.02			
	M75/4HPS	M75C	93.2	4 HA 16 HPS								
	M100/4HPS	M100C	109.2	4 HA 16 HPS								

Fig. 1: Example of experimental device for tie (respectively beam) tests

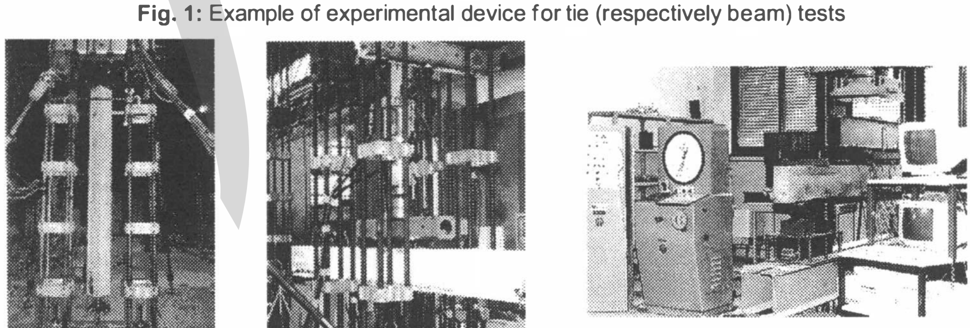

3 RESULTS

The present experimental study allows us to describe the crack behavior of rectangular HSC beams reinforced with high performance steel compared to normal RC beams. The tests were carried out under static short term loading.

Further to the analysis of the experimental results, the following conclusions can be drawn:

- The increase of the concrete strength has a significant influence upon:
  - The stiffness of the structure that increases
  - The deflection of the beam that decreases,
  - The load inducing the first bending crack and the rupture load that increase,
  - The crack widths that are about 30% lower compared to those cracks in standard RC beams,
  - The steel stresses at the conventional limit state of cracking ($w_k \leq 0.3$ mm) that is +20 % higher.

But it does not seem to have any influence on the crack.

- The increase of the steel yield strength has a significant and direct influence on the yield capacity of the structure

But it does not seem to have any influence on deflection of the beam, the crack spacing nor the cracking load

- The reinforcement ratio ($\rho = A_s/B$), does not seem to influence the structure's behavior.

The models that are proposed in the modern design codes (e.g. EC2 or CEB-FIP model code 90) show a good compliance with the experimental results within the range of the steel grades and the concrete strengths that were considered in the present study.

4. CONCLUSIONS

HSC are mainly used for civil engineering works, i.e. for structures with large spans for which the dead load partly governs the stress level in time. We do not have any sufficient experience about the long-term behavior of HSC. Therefore we are not able to draw yet conclusions regarding the effect of long lasting loads on the cracking of such HSC structures. However, existing results on the durability and the long-term strain of HSC seem to be very promising.

The use of HSC for structures reinforced with high performance steel would allow the designers to accept higher steel stresses and thus increase the bearing capacity of structures for a given span or increase the spans for a given load. However, it appears that the steel stress should be limited to about 700 N/mm².

5. REFERENCES

[4] BERNARDI S., *La fissuration des poutres en béton de hautes performances armées d'armatures à hautes performances sous sollicitations de flexion - Étude préliminaire - Dimensionnement des poutres* - Rapport du CSTB, Projet National BHP 2000, Opération Plan Génie Civil, Groupe BHP-AHP, Marne-la-Vallée, juin 1997, 28 pp.

[5] BRICE L.P., *Idées générales sur la fissuration du béton armé et du béton précontraint* - Annales ITBTP, n°198, juin 1964.

[16] MESUREUR B., RIVILLON Ph. *Comportement des ouvrages en béton de hautes performances armés d'aciers à haute limite élastique. Étude des lois d'adhérence en régime statique et endommagement en fatigue* - Rapport de recherche du CSTB, Projet National BHP 2000, Opération Plan Génie Civil, Groupe BHP-AHP, Marne-la-Vallée, septembre 1996, 105 pp.

[17] MESUREUR B., RIVILLON Ph. *Étude des bétons à hautes performances armés avec des armatures à hautes performances. Études des lois d'adhérence et du mode de fissuration en régime statique* - Cahier du CSTB n° 2979, Marne-la-Vallée, septembre 1997, 37 pp.

[19] MESUREUR B., RIVILLON Ph., BERNARDI S. *Étude de la fissuration par traction de tirants en bétons de hautes performances munis d'armatures de hautes performances* - Rapport d'essais du CSTB, Projet National BHP 2000, Opération du Plan Génie Civil, Groupe BHP-AHP, Marne-la-Vallée, février 1998, 28 pp.

REINFORCING STEEL – CONCRETE BOND

OF HIGH STRENGTH CONCRETE

Prof.Dr.Eng. Cornelia Magureanu
Technical University of Cluj Napoca
ROMANIA

Keywords: bond , high strength concrete

1 INTRODUCTION

The interest of applying of high strength and high performance (HSC/HPC) concrete for structural members increases. Unfortunately, beside some durability aspects also several design prospects are not cleared definitely , especially the bond behavior of reinforced concrete at various environmental conditions.

This paper outlines the experimental programme and its results on the bond behavior of the conventional deformed reinforcement OB37 , with a diameter of 10 mm. In this study , the hardened concrete properties and the bond behavior were experimentally investigated at 7 , 28 and 56 days.

It should not be forgotten , that HSC/HPC shows certain special features with respect to the bond properties . HSC/HPC has a higher tensile strength in comparison to normal concrete. Due to this fact it could be possible , that concrete members made of HSC/HPC and reinforced with smooth bars , tend to a good behavior in the bond.

2 DETERMINATION OF BOND BEHVIOUR OF SMOOTH BAR IN HSC/HPC

2.1 Experimental programme

The programme aimed at investigation the bond behavior in HSC/HPC of conventional deformed reinforcement , OB 37. In order to assess the development of the bond properties in different methods of curing after concreting can be described shortly as follows : curing under water 28 days , than in standards storage at 20^0 C ± 2^0 C and 60 % ± 5 % relative humidity (curing A) ; simulation of corrossive conditions : 28 days under water and then in chemical solutions : 1% (Na_2SO_4 + $MgSO_4$) – curing B ; 1% (NH_4)$_2SO_4$ – curing C ; 2% (NH_4)$_2SO_4$ –curing D.

Altogether 60 pull-out tests were performed. In order to assess the time development of the bond properties in relation to the strength development of the concrete, the tests were performed at an age of 7 , 28 and 56 days. The tests programme was set up to evaluate the bond characteristics of normal conditions and after 28 days in corossive conditions (when t_0 = 28 days).

Acompanying to the pull-out tests the typical hardened concrete properties like compressive strength (strength classe C70/85) , splitting tensile strength were measured.

3 PULL-OUT TESTS UNDER MONOTONING LOADING

The bond behavior under monotonic loading was tested on RILEM specimens. The free length was obtained by encasing the smooth bar (OB 37) with a plastic tube and sealing it with elastic silicon material.

The bond stress – slip – curves at 56 days in curing condition A , B , C and D are presented in Fig. 1. The bond – stress at slip 0.1 mm decreased to curing B with about 25 % ; for curing C with about 40 % ; for curing D , with 45 % , face to curing A

The adding the polypropilene fibers FIBRIN in concrete the bond between the fibres and matrix is strong that, the bond stress developed at concrete and reinforcing steel is greater with about 15% - 20 % than the bond stress developed at concrete without FIBRIN and reinforcing steel at 28 and 56 days (Fig. 2).

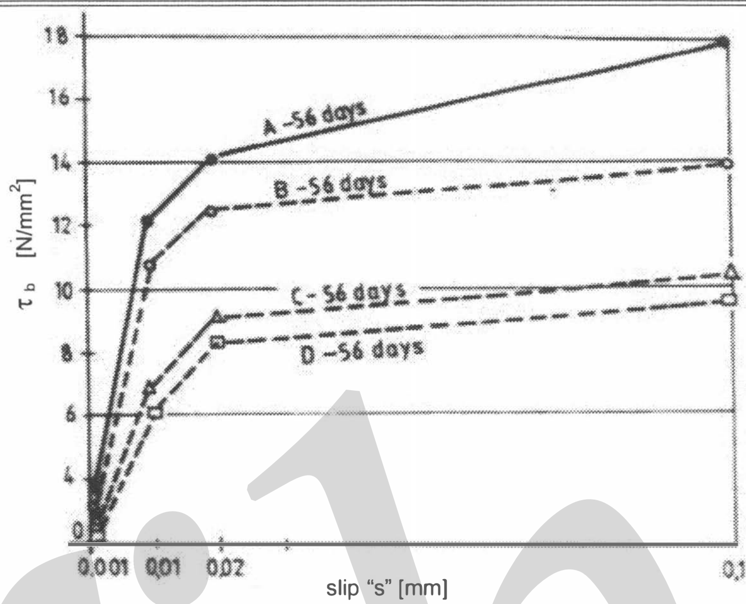

Fig.1 Bond stress – slip curve at 56 days

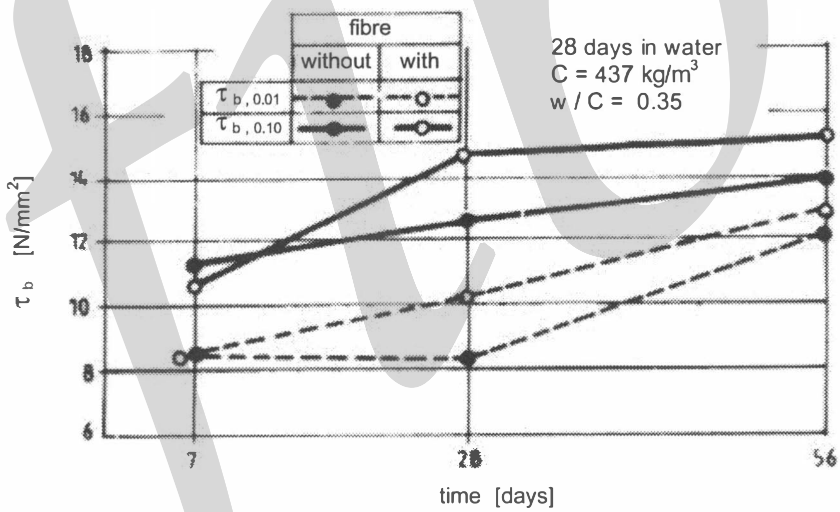

Fig. 2 Influence of polypropilene fibers FIBRIN on the bond stress (casting position II face to reinforcing bar)

REFERENCE

[1] Aitcin, P.C. : High – Performance Concrete . E & FN SPON London , 1998

[2] Magureanu, C. Onet, T. Pintea, D : Physical and mechanical characteristics of high performance concrete kept in different environmental conditions . International Conference on High Performance Materials in Bridges and Buildings. July 29 – Aug. 3, 2001 , Kona , Hawaii.

STRUCTURAL PROPERTIES OF HIGH PERFORMANCE LIGHTWEIGHT CONCRETE

Dante Galeota Matteo M. Giammatteo Michele Zulli
Department of Structural Engineering, University of L'Aquila, ITALY

Keywords: high-strength high-performance lightweight aggregate concrete, EC2 design rules, partial safety factor for concrete, structural properties.

1 INTRODUCTION

A research program has been conducted by the University of L'Aquila and Unicem – Italy, in order to study various aspects of high-strength/high-performance lightweight aggregate concrete. The purpose of this study was to analyse the results of several experimental research studies on the structural behaviour of lightweight aggregate concrete. On the basis of the test results, current EN 1992 – 2nd draft EC2 design rules were checked in order to examine the implication of the material properties on the design procedures. Due to the generally semi-empirical nature of many design procedures suggested in EC2, it appears important to compare these procedures against the results obtained in experimental research.

2 CONCRETE

Compressive strength. The concrete compressive strength (f_{cm}) depends primarily on the water/cement ratio, on the degree of hydration and, in the case of lightweight aggregate concrete, on the strength and stiffness of aggregates. From test results, it can be seen that f_{cm} tends to increase as the unit weight increases and the water/cement ratio decreases. The experimental development of f_{cm} versus age is compared with the predictions from EC2 and with a modified formulation given by Han and Walraven. The EC2 formulation underestimates the compressive strength at early ages.

Modulus of elasticity. Experimental values of E_{cm} and f_{cm} from the literature and from the writers are compared with the previsions of EC2 and two proposed relations. The EC2 formulation overestimates the modulus of elasticity.

Tensile strength. Using the EC2 expressions, the relationships between experimental results from the present study and other research of axial tensile strength (f_{ctm}) and f_{cm} are obtained. The best fit to the experimental data and the proposed relation for f_{ctm} is shown.

3 ULTIMATE LIMIT STATES

Stress-strain diagram for structural analysis. All the stress-strain curves from different authors, obtained from uniaxial compressive tests, have somewhat similar character: the ascending part is almost linear up to the peak stress; the descending part exhibits a very steep drop in load-carrying capacity. On the basis of the experimental results, the bilinear curve seems to be the more appropriate approximation for the design work.

Flexural capacity – Calibration of the partial safety factor γ_c for concrete. The flexural capacities of 37 singly and doubly reinforced high-strength lightweight aggregate concrete beams were calculated using two stress-strain models (parabola-rectangle and bilinear) for concrete and two models (elastic-plastic and elastic-hardening) for reinforcing steel. The calculations were made by using the actual material strength for concrete and for reinforcing steel, constant values were assumed for ε_{c1} and ε_{cu}. Each calculated moment M_{th} was normalized with the corresponding experimental failure moment M_{exp}. It was found that the ratio M_{th}/M_{exp} is normally distributed. In order to investigate the effect of different values of γ_c and γ_s in approximating a satisfactory reliability index β, the material design strength for concrete and reinforcing steel were calculated by varying γ_c from 1.5 to 1.7 and γ_s from 1.1 to 1.2. The flexural capacities were also calculated following the recommendations of *fib*-Bulletin 8 and EC2. For all assumed γ_c values, β was greater than 3.8 which is the value suggested in Eurocode 1. The β values calculated according to *fib*-Bulletin 8 and EC2 are quite similar to those obtained by using the bilinear model and γ_c=1.5, γ_s=1.15. The ultimate limit state design for reinforced high-strength lightweight aggregate concrete beams in flexure can be carried out by using the procedures used for normal weight concrete. There is no need to increase γ_c.

Shear capacity – Members without shear reinforcement. A number of shear data from tests performed by the writers and from literature were analysed. In order to compare directly the theoretical previsions (EN1992-1, 2nd draft EC2, section 10) of the ultimate shear stress (v_u) with the test results, the EC2 equation was calibrated by the available set of shear data. The design values for the shear capacity were obtained, according to the procedure suggested by Taerwe. The aforementioned procedure led, for the available set of data, to the following design equations:

$$v_u = \frac{0.13}{\gamma_c}\eta_1 k\left(100\rho_\ell f_{ck}\right)^{1/3}\left(2.5d/a\right) \quad , \quad a < 2.5d \qquad (1)$$

$$v_u = \frac{0.13}{\gamma_c}\eta_1 k\left(100\rho_\ell f_{ck}\right)^{1/3} \quad , \quad a \geq 2.5d \qquad (2)$$

Shear capacity – Members requiring design shear reinforcement. The experimental values of v_u were compared with the predictions based on the variable strut inclination method (EN1992-1, 2nd draft EC2, section 10). According to this method, the concrete strut inclination (θ) can be chosen between 21.8° and 45° and the reduction factor (ν) for the crushing capacity of the concrete is formulated as:

$$\nu = 0.45\left(1 - f_{ck}/250\right) \qquad (3)$$

The expression used in the prediction of the ultimate shear stress is:

$$\frac{v_u}{f_{c1}} = \sqrt{\psi(1-\psi)} \qquad (4)$$

where $f_{c1} = \nu f_{cm}$ and $\psi = \rho_{sw} f_{yw}/f_{c1}$, with ρ_{sw} = transverse shear reinforcement ratio and f_{yw} = yielding stress of the stirrups. The comparison with the experimental data under discussion shows that the above method tends to overestimate the shear capacity.

4 IN SERVICE BEHAVIOR – LONG-TERM DEFORMATION

Shrinkage. In order to observe the shrinkage strain (ε_{cs}) development versus age, three specimens of high-strength lightweight aggregate concrete (f_{cm}=70MPa, ρ_c=1920kg/m^3) were tested. The mean values obtained during the tests were compared with the theoretical predictions according to EC2 (Section 10, clause 10.3.1.3) and AFREM. The contribution of autogenous shrinkage was ignored in both formulations; in fact the measures of ε_{cs}, during testing, started 1 day after demoulding. The AFREM formulation was corrected by the coefficient η_3 suggested in EC2 (Section 10, clause 10.3.1.3). The AFREM model fits the experimental results quite well.

Creep. The creep coefficient (φ) of high-strength lightweight aggregate concrete (f_{cm}=70MPa, ρ_c=1920kg/m^3) was studied by means of long-term compressive tests. The experimental results were compared with the predictions obtained according to EC2 and AFREM. Once again the AFREM model, corrected by using the coefficient η_2 suggested in EC2 (Section 10, clause 10.3.1.3), yielded satisfactory predictions.

Long-term deflection. Long-term flexural test was also performed on a simply-supported hollow-core slab, made of lightweight aggregate concrete with similar structural characteristics (f_{cm}=65MPa, ρ_c=1920kg/m^3). The observed long-term deflection for the hollow-core slab was theoretically reproduced by using the moment-area method, with the shrinkage strain and the creep coefficient development calculated according to EC2 and AFREM. In spite of some differences between the experimental and the predicted curves, probably due to seasonal variations on the environmental conditions, the AFREM models gave the more satisfactory results.

REFERENCES

[1] 3rd Int. Symp. on Utilization of High-Strength/High- Performance Concrete, Lillehammer, Norway, 20-29.6.1993.
[2] 5th Int. Symp. on Utilization of High-Strength/High- Performance Concrete, Sandefjord, Norway, 20-24.6.1999.
[3] 2th Int. Symp. on Structural Lightweight Aggregate Concrete, Kristiansand, Norway, 18-22.6.2000.

RECENT APPLICATIONS OF HIGH PERFORMANCE CONCRETE IN GERMAN BRIDGE ENGINEERING

Gert König Martin Zink
König, Heunisch und Partner, Oskar-Sommer-Strasse 15-17
D-60596 Frankfurt am Main, GERMANY

Keywords: high strength concrete, bridge, prestressing, shear

1 INTRODUCTION

The introduction of high performance concrete (HPC) in German bridge engineering began about 10 years later than in other countries. Since 1998 about 7 pilot bridges have been built. In addition to the existing standard the design basis for prestressed HPC-structures was examined [1]. One of the most important advancements from the tests was a mechanically based formulation for the flexural shear capacity of rectangular sections. A principal influence of the compression zone height on the shear capacity of members without shear reinforcement was found [6]. The shear capacity V_0 of the compressive zone is in small beams accompanied by the tensile forces carried in the fracture process zone of the inclined cracks. Tension stiffening causes a higher tension chord rigidity than calculated with pure reinforcement and therefore a small influence of the shear slendemess a/d is observed. Dowel action of the reinforcing bars or crack friction are not of any major importance in flexural shear failure. Both effects are activated after the failure process has already started by crack propagation into the compression zone [6]. The empirically found expressions of the model code '90 cover the major influences quite well, even for high strength concrete.

In 2001 the first two German HPC bridges were successfully completed, where casting was done in several jobs. Both bridges, one near Glauchau and the other in the City of Brandenburg, may serve as pilot applications preparing the use in large superstructures of bridges in the autobahn network.

2 BRIDGE ACROSS THE RIVER ZWICKAUER MULDE NEAR GLAUCHAU

The first bridge presented has two separate superstructures with five spans of 31.0 m – 39.0 m – 37.0 m – 35.0 m – 29.0 m (fig. 1). Prestressing is designed for decompression of the extreme fibre under 50 % of the classified live load. Tendons of 7-wire strands (prestressing steel St 1570/1770) with small anchorages designed for the specified concrete class C 70/85 were used. Each superstructure is creted in five jobs within a 3 week cycle. The total bridge area of both superstructures is 3506 m².

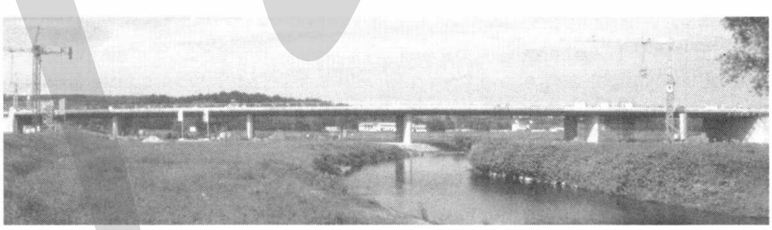

Fig. 1 Glauchau bridge with a main span of 39 m and a slenderness of 1:37

Glauchau is the first German HPC bridge where joints with couplers are necessary as in most larger bridges. The size of the jobs reaches up to nearly 300 m³ of concrete C 70/85. With a width of about 10 m and spans up to 39.0 m the superstructures are close to the size of common bridges in the autobahn network. The state authorities want to gather some more experience with this project. The feasibility of large bridges, principles for the bidding procedure, the construction and the quality management had to be examined. One further aim is to find a reliable basis for the economic evaluation of bridges designed in HPC. Higher material costs and improved quality control lead to some increase in prices that must be compared with a higher value due to improved durability, savings in material quantity, piers and foundations.

A key role for the success of the project is the development of a mix design meeting all the requirements, especially the long workability time of about 4 hours. The mix design had to be developed by the contractor. Requirements were specified conceming a high resistance against freeze-thaw action and a maximum temperature of 70 °C in the superstructure during hydration. The use of a portland cement free of C_3A phases and the choice of a PCE-type superplasticizer was favoured. The combination of silica fume with fly ash was proposed in the call for bids to reduce the cement content under 400 kg/m³. Each contractor invited for bidding had to prove it's ability and will to produce, cast and cure a high performance concrete with the specified properties. Detailed aspects of material tests, the reduction of hydration heat, the type of superplasticizer preferred and the required workability over a job were discussed during the pre-qualification. The cement content finally was the lowest used for a C 70/85 in all the German bridge projects. The silica dosage is extremely high and the added fly ash dosage is close to the permitted maximum. The mix design is shown in table 1.

Table 1 Mix design for the C 70/85

Materials		Content [kg/m³]
Cement CEM I 42,5 R-HS	*z*	360
Silica-slurry (w_{sf} = 0,5 *sf*)	*sf*	35 + 35
Fly ash	*fa*	120
Sand [mm] 0/2 a Coarse aggregate [mm] 2/8 Coarse aggregate [mm] 8/16		1831
Mixing water	w_0	100
Superplasticizer (*PCE*-Type)	*fm*	1.65 % *z*
Retarder, basic dosage	*vz*	0.20 % *z*
w/b		0.32

The workability achieved without significant loss of slump was about 4.5 hours. Penetration tests proved a friendly setting behaviour during the following 3 to 4 hours. The deformations of the scaffolding caused no problems during the creting process. A placing capacity of 40 m³/h was reached. The temperature of fresh concrete had to be limited to 25 °C with regard to the maximum temperature allowed. In total about 2620 m³ of C70/85 were needed for both superstructures. The compressive strength achieved on site was about f_{cm} = 92 MPa after 28 days. A small deviation was ensured by the quality management.

3 LUCKENBERGER BRIDGE AT THE CITY OF BRANDENBURG

In the city of Brandenburg the old bridge leading the Luckenberger street across the Havel had to be replaced. Due to the requirement to keep the Havel free from any river piers, a span of about 40 m was needed. However, due to the tramway, the geometry of the roadway had to be similar to the old bridge with spans of only 12 m. As a result, a very slender structure was required (fig. 2). In the pre-design of the bridge the deformations due to live loads from the tramway and individual traffic were critical. HPC was introduced first for its higher modulus of elasticity to reduce the deformations. The high slenderness of the strutted girder was finally decisive for the use of HPC. The concrete lab involved and the mix design used were the same as in the Glauchau project.

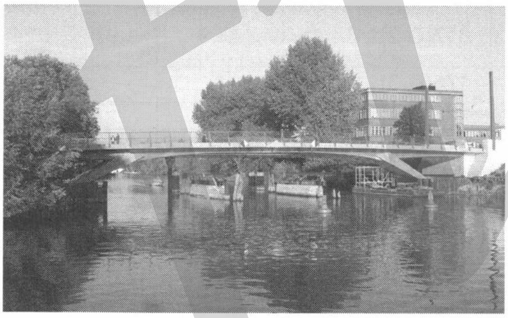

Fig. 2 Luckenberger Bridge, City of Brandenburg

4 CONCLUSION

The application of high strength concrete C70/85 with about f_{cm} = 90 MPa in two larger bridges was successful. The principles for the bidding procedure and the quality management system for HPC-bridges worked well in both projects. Both applications show the importance of an accurate mix design and a complete quality control system. Sufficient experience and know-how of the contractors invited for bidding should be checked during a pre-qualification.

REFERENCES [References 2-5 and 7 see full paper]

[1] *Bernhard, K., Brameshuber, W.* and *Zink, M.*: Prestressed High-Performance Concrete in German Bridge Engineering. LACER No. 3, p. 275-291. University of Leipzig 1998

[6] *Zink, M.*: Diagonal Shear Cracking in Slender Concrete Beams. LACER No. 5, p. 305-332. University of Leipzig 2000

SLABS WITH LIGHTWEIGHT AGGREAGATE CONCRETE OF HIGH STRENGTH

Sumio Hamada Mingjie Mao Isamu Yoshitake Hiroshi Tanaka
Dept. of Civil Eng. Yamaguchi University, JAPAN Kurimoto, Ltd., JAPAN

Keywords: lightweight aggregate, slab, punching shear, pre-stressed concrete

1 INTRODUCTION

The purpose of present study is to evaluate experimentally the punching shear strength of lightweight concrete slab, and to propose the punching shear strength equation for the slab with lightweight aggregate concrete. In the experiments, the comparative loading test between the RC slab and PC slab was carried out. The present study reports the applicability of the proposed equation to the both reinforced concrete and pre-stressed concrete slabs with lightweight aggregate concrete.

Table 1 Detail of materials

	Cement		Fine aggregate			Coarse aggregate				Admi-xture
Type	OPC	HPC	S-1	S-2	S-3	G-1	G-2	G-3	G-4	
Density g/cm^3	3.15	3.13	2.64	1.90	2.58	2.71	1.49	2.7	0.85	1.05
Absorption %	---	---	1.40	19.0	---	0.5	32.0	---	1.8	---

Table 2 Mix proportion

Mix No.	W/C	s/a	Unit Quantities, kg/m^3					Strength at 28days N/mm^2		
			W	C	S	G	Ad	Comp.	Tens.	Ratio
1	0.37	0.42	162	443(OPC)	387(S-1) 229(S-2)	617(G-2)	1.11	47.9	1.97	1/24
2	0.28	0.47	158	550(HPC)	771(S-3)	176(G-3) 222(G-4)	11.0	55.1	2.62	1/21
3	0.26	0.47	150	570(OPC)	609(S-3)	323(G-3)	11.0	45.6	3.45	1/13
4	0.36	0.42	156	430(HPC)	747(S-3)	1048(G-1)	4.3	40.3~61.2	----	1/10
5	0.30	0.41	146	500(OPC)	716(S-3)	1030(G-1)	4.0	45.9~52.0	----	1/10

2 EXPERIMENTAL PROGRAM

Table 1 gives the detail of materials in the present study. Mix proportions of the concrete tested are listed in **Table 2**. All specimens were square shaped slab; and the reinforcing bar with diameter of 10mm were set with a constant space in both directions. Specimens in **Fig.1** were nominated first 2 letters after structure system, and the letter or letters following the hyphen express coarse aggregate. The slab thickness, which affects the punching shear strength, varies in range of 100 to 160 mm.

3 EXPERIMENTAL RESULTS AND ESTIMATE EQUATION

The maximum loads of each specimen are indicated in **Fig.1**. The failure patterns of all specimens were punching shear failure in present study. The results shown in **Fig.1** indicate little difference between RC and PC slab strengths for lightweight aggregate concrete. The result implies that even pre-stressing to structure cannot effectively to reinforce the weakness of lightweight aggregate concrete such as tensile or shear strength.

The ratios of the analytical value based on above equations to the experimental value are illustrated on the upper side of each bar graph shown in **Fig.2**. The upper side of each bar graph in the lightweight concrete slab indicates that those equations tend to overestimate the punching shear strength. This tendency may be due to lower tensile and shearing strength of lightweight concrete than the strengths of normal concrete.

The lower side of each bar graph shown in **Fig.2** indicated the experiment-calculation ratios in case of the 50percents of tensile strength shown and 70percents of shearing strength. As shown in calculated results of **Fig.2**, the calculated values became closer to the experimental values, which implies that the punching strength of lightweight concrete slabs are affected by the tensile and shearing strength of the concrete. In addition, those equations employed in this study provide the ratio near to 1.0 with the high accuracy for the PC slabs of normal concrete, except for some data. The experiment calculation ratios indicate that strength of some slabs with normal concrete are less than 1.0, and these results seem to be caused by applicable strength range.

These tendencies obtained herein may imply that the tensile strength and shearing strength are affected significantly the design punching shear strength rather than the compressive strength. In order to ensure the appropriate design of bridge slab, test of the tensile strength must be required for the design of concrete slab at least. It is, otherwise, necessary to establish the proper estimation method of tensile strength toward to high-strength or lightweight concrete.

4 CONCLUSIONS

The conclusions are listed as follows:

(1) The punching strength of slabs is significantly affected by the tensile strength. Since the lightweight aggregate concrete is fairly weak in tension, the punching shear strength with lightweight aggregate concrete becomes lower.

(2) The equation proposed herein for the punching shear strength of the slab agrees well the experimental results.

(3) Tensile test must be required for design of concrete slab with new materials, when it is designed for concrete slabs.

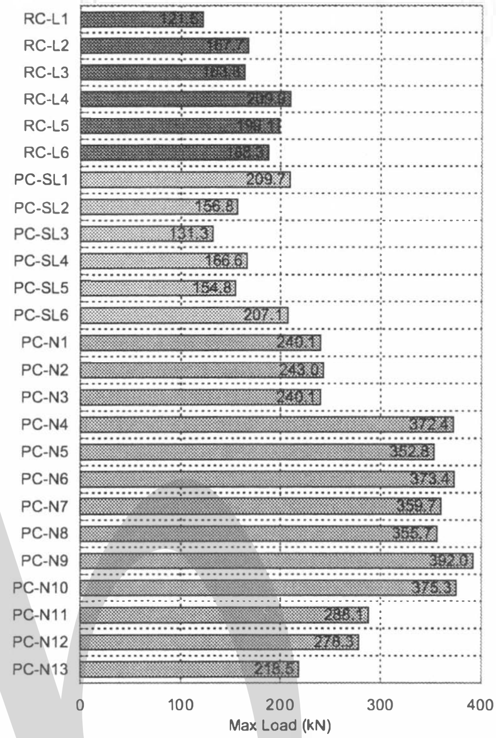

Fig.1 Punching shear test results

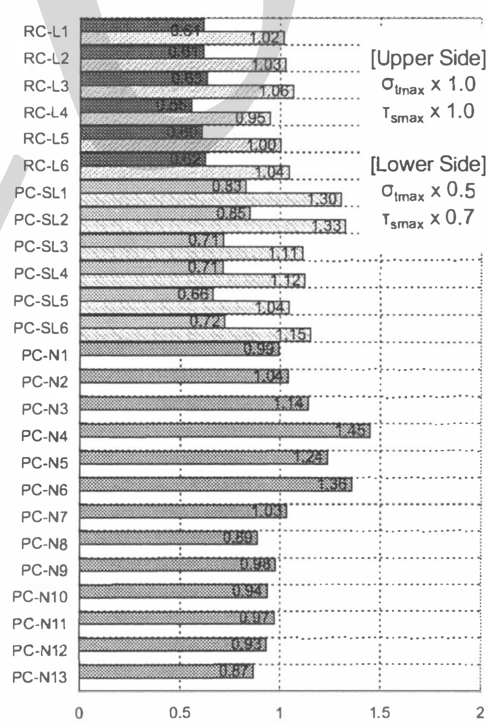

Fig.2 Experiment-calculation ratio

DEVELOPMENT OF HIGH STRENGTH AND LIGHTWEIGHT PRECAST PRESTRESSED CONCRETE SLAB

Sadaaki Nakamura Ryo Yamashita Kiyoroku Fukayama
PC Bridge Co., Ltd.
JAPAN

Ryoichi Onobe
Ishikawajima Construction
Materials Co., Ltd., JAPAN

Keywords: High-strength lightweight precast PC slab, Durability, wheel load traveling test

1 INTRODUCTION

In recent years, cases of damaged reinforced concrete slab in highway bridges have been reported, resulting from an increase in vehicle size and traffic density. A slab replacement method using precast slabs can be considered as a viable method for repairing and reinforcing the damaged slab. In the replacement method, reducing the structure weight by replacing the existing slab with a precast slab, effectively decreases the stress on the steel main girder and substructure stressed from vehicles larger than the design vehicle and traffic volumes larger than anticipated. Furthermore, the transportation and erection costs associated with a lightweight precast slab are economical compared to traditional methods. The high strength and lightweight precast PC slab is designed to take advantage of these benefits. Thus, authors have developed precast prestressed concrete slab (hereinafter referred to as "PC slab") using high strength and lightweight concrete so as to make the most of the above advantages.

The authors conducted the material performance tests on the high strength and lightweight concrete and the structural performance tests on the precast PC slab. This report mainly discusses the durability of the high strength and lightweight precast PC slab against fatigue. The fatigue durability was evaluated by the crank type wheel load traveling test (hereinafter referred to as "wheel load traveling test").

2 OVERVIEW OF THE HIGH STRENGTH AND LIGHTWEIGHT PRECAST PC SLAB

Fig. 1 shows the structural overview of the high strength and lightweight precast PC slab. The concrete slab has the following specified properties: a compressive strength of 50N/mm^2, unit weight of 19.0kN/m^3 or less, and static modulus of elasticity of 22.0kN/mm^2 or more.

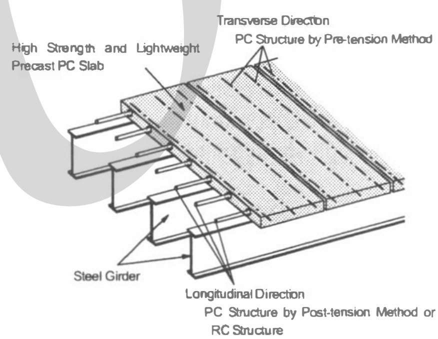

Fig.1 Overview of High Strength and Lightweight Precast PC Slab

3 PERFORMANCE TEST OF HIGH STRENGTH AND LIGHTWEIGHT PRECAST PC SLAB

3.1 Outline

In order to verify the performance required of the high strength and lightweight precast PC slab, material and structural performance verification tests using a full-scale test specimen have been carried out. In this paper, the flexural loading test and the wheel load traveling test are mainly reported.

3.2 Flexural Loading Test

Fig. 2 shows the load - displacement relationship resulting of the flexural loading test. The measured deflection at the time when a flexural crack occurred at the center of the span was 3.8 mm, and the measured deflection near the ultimate state was about 22 mm. This means that the deflection of the precast PC slab is not excessive at a service limit, and that it has excellent ductility under the strength limit state. Thus, it is understood that the high strength and lightweight precast PC slab has sufficient performance against bending moment.

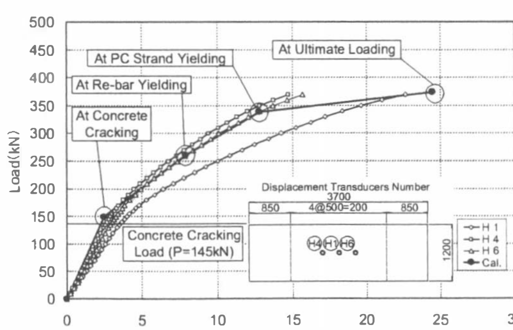

Fig. 2 Load – Displacement Relationship

3.3 Wheel load traveling test

(1) Test Method

In order to verify the durability against fatigue of the high strength and lightweight precast PC slab, the wheel load traveling test was conducted. Dimension of the test specimen was 2800 mm wide x 4500 mm long x 180mm thick. The slab was designed as fully prestressed concrete slab with a span of 3.0m. Fig. 3 illustrates the specimen installation condition and the crank type wheel load traveling test equipment. After the concrete had reached it's predetermined compressive strength and that strength was verified, increasing, incremental load was applied. The load pattern was the same manner adopted by the Public Works Research Institute of the Ministry of Land, Infrastructure and Transport [1].

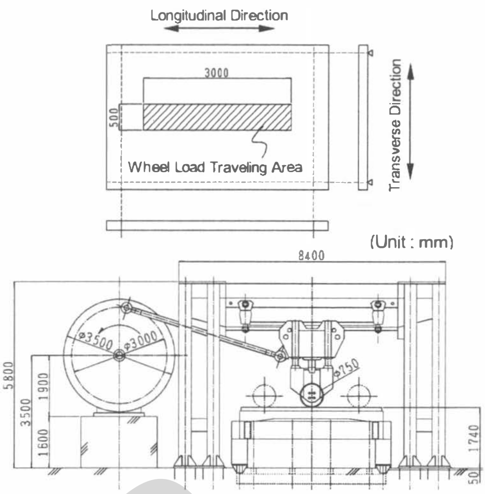

Fig.3 Crank Type Wheel Load Traveling Test Equipment

(2) Test results and discussions

1) Cracking load and ultimate load

Occurrence of concrete cracking was determined by visual inspection. The first crack was found in the longitudinal direction at a load of 373kN and 480,000 traveling operations. Subsequently, cracks developed with the increase of load and traveling frequency. An abrupt increase in displacement was observed at a load of 471kN and 593,000 traveling operations until failure of the specimen by punching shear force occurred.

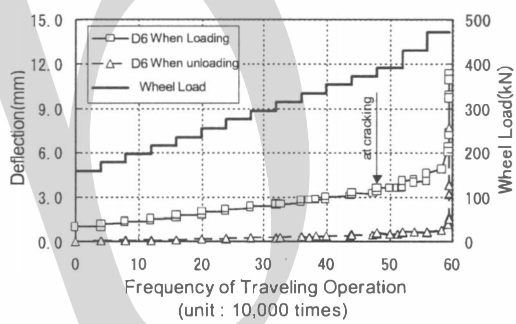

Fig.4 Relations between Deflection and Frequency of Traveling Operation

2) Deflection of the slab

Fig. 4 demonstrates the considerable change in deflection as measured by deflection gage D6, where the deflection has reached its maximum value. Hence, it is apparent that deflection significantly increases with an increase in load after a reduction in rigidity occurs, caused by the emergence of cracks.

3) Comparison with RC slab

Fig. 5 shows the comparison of the results of the wheel load traveling test on the RC slab (hereinafter referred to as "RC8") and the high strength and lightweight precast PC slab. As reported in the reference [1], the RC8 experienced punching shear failure at a load of 275kN in 260,000 traveling operations. For the RC8 test specimen, the slab was 250mm thick and the compressive strength of concrete was 27.6N/mm^2. Comparably, the high-strength lightweight precast PC floor slab with a thinner slab thickness of 180mm was able to endure a higher load and more traveling operations than the RC8 test specimen. Furthermore, deflection at the center of the specimen with respect to the same load is smaller, indicating that the rigidity is higher for the high strength and lightweight precast PC slab than that of the RC8.

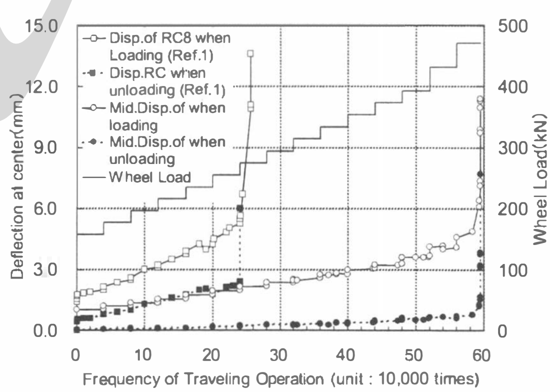

Fig.5 Comparison with RC8

REFERENCES

[1] Public Works Research Institute of the Ministry of Land, Infrastructure and Transport : Joint study report on the development of fatigue durability evaluation technique in the wheel load traveling test of highway bridge slab (Part 2), 1999. 11.

STRENGTH CHARACTERISTICS AT ANCHORAGE ZONE OF PC STRUCTURES USING HIGH-PERFORMANCE LIGHTWEIGHT CONCRETE WITH LOW WATER ABSORPTION

Satoshi Tamura Yuzuru Hamada
DPS Bridge Works Co., Ltd.
Japan

Thiru Aravinthan
University of Southern
Queensland, Australia

Junichiro Niwa
Tokyo Institute of
Technology, Japan

Shinpei Maehori
Taiheiyo Cement
Corporation, Japan

Keywords: high-performance lightweight aggregate, anchorage zone, anchor plate, bearing strength

1 INTRODUCTION

Research and development of lightweight aggregates have been increasingly progressing in the recent years. Recently, two types of high-performance lightweight aggregate (HLA) for concrete have been developed in Japan.

By applying such HLA concrete for prestressed concrete bridges, the self-weight of the girder can be reduced remarkably resulting in reduced loads in the sub-structure and foundation of the bridge. However, it has been known that the mechanical characteristics such as bearing strength and tensile strength of lightweight concrete are lower than that of the conventional normal concrete. Therefore, when applying such HLA concrete to PC structures, it is necessary to evaluate the load-bearing characteristics and failure mechanism of anchorage zone for the verification of the safety of structures, where high stress concentration is expected, especially when multi-anchorage system is used. In this research, it was proposed to use an additional anchor plate with larger area together with the standard anchor plate to reduce the high local stresses at the anchorage zone when HLA concrete is used. An experimental investigation was carried out on full-scale model specimens of an anchorage zone to clarify the load-bearing capacity, crack distribution and failure mode of such anchorage zone made of HLA concrete using the two types of anchor plates. Moreover, a three dimensional FEM analysis was carried out to verify the stresses in the anchorage zone in order to determine the shape and size of an anchor plate as well as the amount of reinforcement to be provided in the anchorage zone, which was later compared with the experimental results. The results of this investigation are discussed in this paper. These results were applied for the design of the anchorage system and reinforcement detailing of Shirarika-River bridge, a PC box girder bridge constructed using HLA concrete, for the first time in Japan [1].

2 TEST PROGRAM

The test variables are outlined in Table 1. The experiment consists of four specimens with test variables such as type of concrete, type of anchor plate, amount of reinforcement. The width, thickness and height of all the four specimens were set to 800 mm, 400 mm and 1600 mm, respectively. The thickness was decided based on the minimum thickness needed for the specific anchorage system.

To utilize the most commonly used external tendon, namely multi-strand tendon type 12S12.7 mm (SWPR7B), Freyssinet anchorage system 12T13M220 was used. It included a square anchor plate of 240 mm x 240 mm. For Case-3 and Case-4, an anchor plate that was developed for low-strength

Table 1 Type of specimen

Specimen	Concrete	Anchor plate	Standard section L(mm)	Reinforced section L'(mm)	Amount of reinforcement [rebar size(mm),spacing(mm)] A_{s1}	A_{s2}
CASE-1	NC*1	ST*3	L=L'=1600		$A_{s1}=A_{s2}$=D19@100	
CASE-2	HLA*2	ST*3	800	800	D19@100	D22@50
CASE-3	HLA*2	ST*3+LS*4	700	900	D19@100	D19@75
CASE-4	HLA*2	ST*3+LS*4	1200	400	D19@100	D19@50

*1: Normal concrete *2: HLA concrete *3: Standard type *4: Low strength type

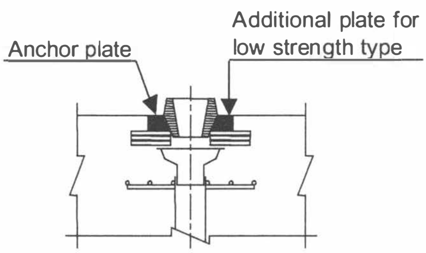

Fig.1 Outline of anchor plate

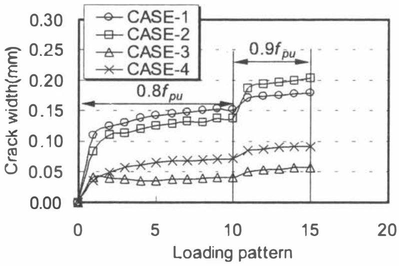

Fig.2 Variation of crack width with loading

concrete was used together with the standard anchor plate. The layout of this anchor plate is shown in Fig. 1. The idea of using an additional anchor plate was to enlarge the bearing area so that the local stress concentration caused in the anchorage zone could be reduced. It was found from FEM analysis that by using this additional plate, the stresses could be drastically reduced leading to an effective and economical anchorage system when HLA concrete is used for PC structures. The dimensions of the additional anchor plate were decided as 310 mm x 310 mm, which nearly increased the bearing area by about 70%.

3 TEST RESULTS AND DISCUSSION

The increase in the crack width with loading cycle is shown in Fig. 2. It can be seen that at 0.8f_{pu} loading, where f_{pu} is the tensile strength of prestressing steel, the crack width of Case-2 is nearly the same as that of Case-1, since the amount of reinforcement in Case-2 was nearly three times that of Case-1. Moreover, Case-3 and Case-4 showed relatively small crack widths compared to Case-1 and Case-2, due to the arrangement of an additional anchor plate together with the standard anchor plate. From the above results it is evident that by providing an additional anchor plate in the anchorage zone for PC structures with HLA concrete, it can drastically reduce the crack width as well as the number of cracks. Therefore, the necessity of providing large amount of reinforcement (as much as three times) can be eliminated, improving the workability at the construction site.

The values of strain obtained from experiments were compared with those of FEM analysis. The experimental and analytical results show good agreement, especially in the area of the post-peak region. Considering the ultimate failure, the maximum applied load for Case-1 with normal concrete was 3845 kN. In Case-2, some spalling of concrete was observed, but the specimen was able to withstand further loading till 4800 kN. In the other two cases, even though load was increased up to 4800 kN, there was no ultimate failure, indicating that they satisfy the necessary safety conditions at ultimate state.

4 CONCLUSIONS

An experimental investigation was carried out on the anchorage zone of prestressed concrete structures with HLA concrete. The following conclusions were obtained from the current study.

- By using an additional anchor plate with appropriate reinforcement detailing, it is possible to drastically improve the reduction of the crack width and number of cracks in the anchorage zone of PC structures with HLA concrete.
- In an anchorage zone where HLA concrete is used, an additional anchor plate can provide the sufficient ultimate capacity and the sufficient safety for failure, considering the ultimate strength of prestressing tendons.

The above experimental results were applied in the design of the anchorage system of Shirarika-River bridge, a PC box girder bridge, constructed using HLA concrete for the first time in Japan. As a result, it was possible to develop an economical anchorage system and prevent any cracking in the anchorage zone.

REFERENCES

[1] Yamazaki, M., et al. : On the design and construction of Shirarika-River bridge – A PC bridge made of high performance lightweight concrete, Proceedings of fib 2002 congress, Osaka, Oct. 2002. (submitted for publication)

EFFECTS OF PENETRATIVE CONDITIONS OF WATER FOR CURING ON STRENGTH OF CONCRETE

Komsan Maleesee
TOKAI UNIVERSITY
Graduate School of Engineering

Tetsurou KASAI
TOKAI UNIVERSITY
Faculty of Engineering

Keywords: penetrating water, self-desiccation, pressure curing, AE-admixture added water for curing

1 INTRODUCTION

The reaction between cement and mixing water causes difference of the hardened paste. In the case of high strength concrete, the mix proportion does not have enough water to complete the hydration. The penetrating water from outside is important to continue the hydration reaction. However, in the low water-cement ratio (w/c) and large specimen, the curing water cannot completely penetrate to fill pores formed during the hydration reaction thus causing different degree of hydration and degree of self-desiccation in the surface layer and in the bulk of the specimen. For this reason, influence of dynamic character of high strength concrete is considered in these experiments. Additionally, possibility of applying the same method of curing and testing on the normal strength concrete and on the high strength concrete will be discussed.

In this research, the effects of penetration of curing water on cementitious materials are experimentally investigated in five aspects: volume content of each compound in hardened cement paste, self-desiccation in hardened cement paste, effect of penetrating of water in hardened cement paste on degree of self-desiccation, effect of penetrating water in the mortar specimen for water pressure curing (10MPa-curing) on the strength and effect of AE-admixture added water for curing (AE-water curing) on strength of mortar specimen. For these purposes, the specimens with water-cement ratio 0.2, 0.25, 0.3, 0.4, and 0.6 were prepared and study of the effects of the penetration of water into the specimens was conducted. The larger range of self-desiccation was found for the low water-cement ratio specimen. Furthermore, an increase of strength of specimen was clearly found for the low water-cement ratio specimen threatened by water pressure curing or AE-water curing.

2 RESULTS AND DISCUSSION

2.1 Effect of penetrating water in the specimen for water pressure curing on the strength

It is known that large range of self-desiccation occurs in the cement paste with low water-cement ratio because water from outside cannot penetrate in the central part of the specimen. The self-desiccation affects strength of mortar by decreasing of hydration. It was found that the strength test with water-cement ratio of 0.25 for normal curing (Water-curing) the strength becomes lower with larger distance from the surface as shown in Fig.1. For the specimen that is treated by water pressure curing (10MPa-curing) it is found that the strength become higher than the normal curing or wrapping due to the penetration of water into the specimen. However, the specimen with w/c of 0.60 in case of

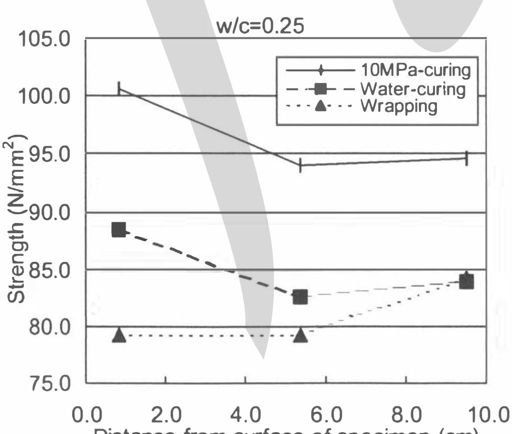

Fig.1 Relation between strength and penetrated water distance (w/c=0.25)

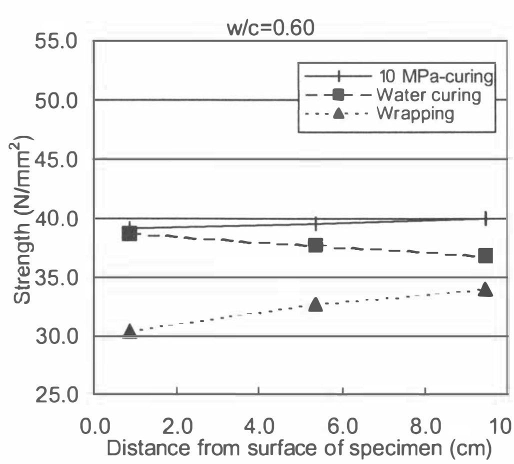

Fig.2 Relation between strength and penetrated water distance (w/c=0.60)

water pressure curing and normal curing the relation between strength and penetrated water distance from the surface does not seems largely affect the strength of specimen as shown in Fig.2 because the amount of water in the specimen is sufficient to complete the hydration reaction.

2.2 Effect of AE-water curing on the strength

As was already discussed, the specimen with water-cement ratio of 0.25 for water pressure curing comparing to the specimen curing by normal curing or wrapping shows the higher strength due to the water pressure penetrates deep into the specimen. For AE-water curing, Alkyl-ether based air-entraining agent mixing with water to reduce surface tension energy, the amount of water that penetrates into the specimen is larger than for the water-curing specimen so the larger strength is become as shown in Fig.3. From this experiment in case of AE-10MPa curing, AE-water curing maintaining pressure of 10MPa, the strength becomes largest.

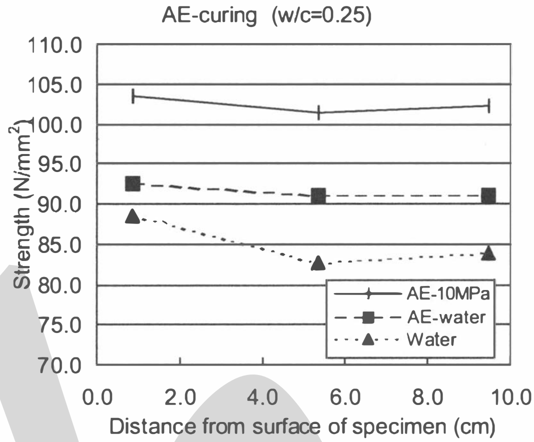

Fig.3 Relation between strength and penetrated water distance for AE-curing (w/c=0.25)

3 CONCLUSSIONS

The high-strength concrete with low water-cement ratio, threatened by standard curing of normal concrete, exhibit different degree of hydration and degree of self-desiccation for bulk and surface layer because of the non-uniformity of concrete structure. The degree of the penetrating of the water into the specimen and degree of self-desiccation are changed with curing water. Further investigations in order to find the appropriate curing condition, as standard for the high-strength are needed.

REFERENCES

[1] E.Tazawa: Autogenous Shrinkage of Concrete. Proceeding of the International Workshop organized by JCI, pp.3-67 (1998)
[2] H.F.W. Taylor: Cement chemistry 2^{nd} edition, pp. 227-255 (1997)
[3] E.Tazawa and S.Miyazawa: Influence of Constituents and Composition on Autogenous Shrinkage of Cementitious Materials, Magazine of Concrete Research, No. 178, pp. 15-22 (1997)

EFFCT OF STRESS RATE ON TENSILE STRENGTH OF HIGH-STRENGTH CONCRETE

Hiroshi Watanabe
Independent Administrative Institution
Public Works Research Institute
Construction Technology Research
Department,Japan

Tateo Nagai, Masahiro Suzuki, Shinichi Takemoto
Japan Prestressed Concrete Contractors
Assosiation,Japan

Key words: Direct tensile strength, slow loading test, high-strength concrete

1 INTRODUCTION

The tensile strength of concrete is an important property for evaluating the cracking resistance of structures. Normally, the tensile strength is determined in accordance with the method of test for splitting tensile strength of concretete shown in JIS A 1113(1993). However, the stress rate of tensile stress produced in actual structures by concrete drying shrinkage and thermal expansion or shrinkage is much lower than the tensile stress rate prescribed in the JIS tensile strength test method. If the tensile strength of concrete fluctuates depending on the stress rate, then the concrete tensile strength value obtained with the test specimens prescribed in JIS must be corrected, with consideration given to the effect of stress rate, and this value used to examine cracking.

CEB-FIP MC90[1] (hereafter "MC90") also includes a method of evaluating tensile strength that considers the impact of the stress rate. However, these studies have focused on the large stress rate domain, the so-called impact loading domain, and it is unclear whether or not these results apply to the cases with low stress rates postulated in this paper.

Partly due to the fact that the tests are difficult to conduct, there is only a limited amount of experimental data for the low stress rate domain. This paper describes a study of effct of stress rate on concrete tensile strength, targeting a stress rate lower than that prescribed by tensile strength method of JIS .

2 TEST METHOD AND TEST CONDITIONS

The test specimens were removed from the form at the age of one day. The method of curing was sealed curing (in which the test specimens were removed from the mold at the age of one day and then their entire surface was sealed with aluminum foil tape (0.05 mm) left to stand indoors at a temperature of 20°C until the loading age.

The test specimen was a square pillar measuring 100 x 100 x 400 mm. Figure 1 shows the shape of the notched test specimen. The direct tensile strength test was performed using A. Yoshimoto et al. report[2] as a reference. Four bolts measuring 8 mm in diameter and 120 mm in length and having screw threads (albeit with no screw threads on the pointed end) were fastened to each end of the mold at the positions shown in Figure 1. Therefore each test specimen had a total of eight bolts embedded in its two ends, so tensile force would be transmitted by the adherence between these bolts and the concrete. Loading was conducted with the use of a weighting control loading tester. In order to reduce the stress rate, a spring with a low spring constant was interposed. Table 1 shows the test conditions. The settings for stress rate used in this test were rates equivalent to the concrete tensile strength test method (splitting tensile test) in JIS A 1113: approximately 1/10 and 1/100 of the JIS rate.

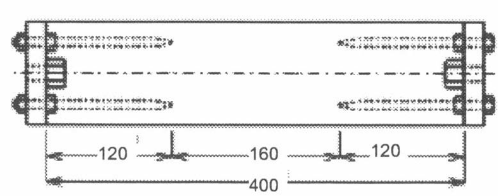

Fig.1 Shape and size of uniaxial tensional test specimen

3 TWS RESULTS AND DISCUSSION

Figure 2 shows the relationship between stress rate and direct tensile strength for a loading age of 28 days for mixes H-75 and H-25. The solid line in the figure represents the average value for the nine test specimens. In addition, figures in parentheses indicate ratios for which the direct tensile strength with a stress rate of 392 kPa/min is standardized (1.0). As shown in the figure, when W/C=25%, there was no constant trend in the relationship between stress rate and tensile strength. In contrast, with W/C=75%, a trend in which the tensile strength decreased as the stress rate decreased was confirmed.

Regarding the method used to evaluate the impact of stress rate on tensile strength, in MC90, concrete strength was included in the parameters. With regard to the tensile strength f_{t0} obtained for the stress rate σ 0 used as the standard ,the tensile strength f_t at a stress rate of σ 1 is expressed by the following equation. The effect of the compression strength f'c of the concrete is expressed as coefficient δ .

$$f_t = f_{t0}\left(\frac{\dot{\sigma} t}{\dot{\sigma}\, 0}\right)^{\delta} \qquad (1)$$

$$\delta = 1/[10 + 6\{f'c/f'co(=10MPa)\}] \qquad (2)$$

As shown in MC90, equation (1) was originally designed to express values with a stress rate of 0.1 MPa/sec or greater, which is different from the values targeted in this test. Figure 3 shows the relationship of coefficient δ and concrete compressive strength. The points plotted in the figure are the results obtained in this test. The dotted line in the figure represents the results of calculations when compressive strength was included in Equation (2). The effect of stress rate on concrete tensile strength was not as great as shown in MC90, but it can be seen that the impact of stress rate on compressive strength was quantitatively the same result.

Table 1 Test conditions

Mixture	Loading age (days)	Stress rate (kPa/min)	Number
H-75	28	392 29.4 2.45	9
H-25	28	392 29.4 2.45	9

H-75:Using high-early-strength portrandcement ,W/C=75%
H-25:Using high-early-strength portrandcement ,W/C=25%

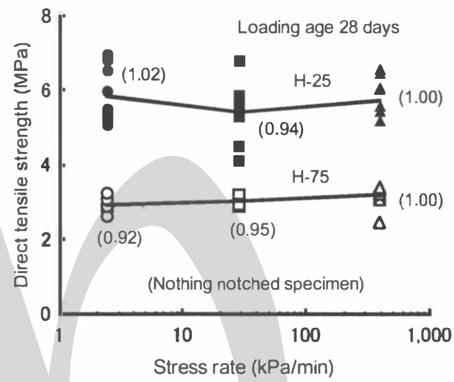

Fig.2 Relationship stress rate and direct tensile strength

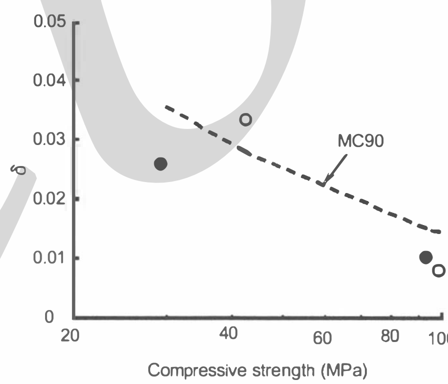

Fig.3 Relationship compressive strength and δ

4. CONCLUSION

(1) Tensile strength of concrete decreased as the stress rate decreased. But the effct of stress rate diminished as compressive strength of concrete increased.
(2) It is thought that the equations in CEB-FIP MC90 can approximately evaluate the effct of tensile stress rate on tensile strength of concrete even in slow loading.

REFERENCES

[1] CEB-FIP MODEL CODE, pp.2-22-24, 1990
[2]Akira Yoshimoto, Hiroshi Hasegawa, Keiji Kaneyuki, Hiroaki Shirakami: "Study of a concrete test specimen for pure tension testing" (Cement Technology Yearly 32, 1978, pp. 231 – 234.

DETERIORATION OF MORTARS WITH OR WITHOUT SILICA FUME IN VARIOUS SULFATE SOLUTIONS

Han Young, Moon Seung Tae, Lee Ho Seop, Jung Hong Sam, Kim
Hanyang University
Korea

Seong Soo, Kim
Daejin University
Korea

Keywords: pozzolanic reaction, sulfate attack, silica fume

1. INTRODUCTION

The superior resistance of concrete mixtures containing silica fume against sodium sulfate attack is attributed to, in addition to the filler action by the finer particle size of silica fume, the pore refinement process occurring due to the conversion portlandite into secondary C-S-H gel by strong pozzolanic reaction. It is reported that the secondary C-S-H gel, although less dense compared with primary C-S-H gel formed in normal cement, is nevertheless to be effective in filling up the large capillary pores in concrete. Additionally the reduction in the amount of portlandite due to the pozzolanic reaction is also beneficial in reducing the susceptibility to sodium sulfate attack. However a concrete containing silica fume exposed to magnesium sulfate environment suffers from softening types of sulfate deterioration compared with sodium sulfate environment. In other words, in concrete containing silica fume the reduction in the quantity of gypsum may mitigate sodium sulfate attack while increase of M·S-H gel due to the reaction of secondary C-S-H gel with Mg^{2+} ions enhances magnesium sulfate deterioration of concrete [1, 2]. In the present study, the expansion and strength loss behaviors of mortar with or without silica fume (w/cm = 0.45) exposed to sodium sulfate, magnesium sulfate and both mixed sulfate environment were evaluated.

2. MATERIALS AND EXPERIMENTAL PROCEDURE

2.1 Materials and specimens preparation

In the present study, OPC mortar specimens with water to cementitious material ratio (w/cm) of 0.45 were prepared. Silica fume was added as partial replacements of cement at 5%, 10% and 15% by weight of the total cementitious material.

2.2 Test methods

Length change measurements of prismatic mortar specimen, was performed according to ASTM C 1012 and measured on three mortar specimens withdrawn from test solutions. The average value of length change was adopted. The deterioration of cube mortar specimens was also investigated by measuring the strength deterioration factor (SDF), which was calculated as follows:

$$SDF\ (\%) = (Sw - Ss) / Sw \times 100$$

Sw = average compressive strength of mortar specimens cured in water (MPa)
Ss = average compressive strength of mortar specimens immersed in sulfate solution (MPa)

3. RESULTS AND DISCUSSION

3.1 Length change and silica fume replacement

In Fig. 1, after 120 days of immersion, the SF-0 mortar specimen experienced much larger length change than any of the mortar specimens with some silica fume replacements. At a period of immersion of 180 days, the control mortar (SF-0) had disintegrated due to excessive expansion, whereas the mortar specimens using silica fume with 5, 10, and 15% replacement for cement recorded the length change values of 0.024%, 0.015%, and 0.023% at 270 days of immersion, respectively. The data on length changes for mortar specimens immersed in magnesium sulfate solution (Fig. 2) indicate a qualitative trend similar to those observed in the mortar specimen without silica fume up to 180 days. However, length changes of the control mortar specimen after 210 days of immersion showed a lower magnesium sulfate resistance with respect to expansion. The deterioration of mortar specimens in magnesium sulfate solution was significantly related to SDFs in comparison to length change.

3.2 SDF and silica fume replacement

The extent of SDF increase was very similar up to 270 days, except for the mortar specimen without silica fume (SF-0), as shown in Fig. 3 This indicates that the beneficial effects of partial replacement of silica fume were clear after an immersion period of 91 days. The content of silica fume (5 to 15%) didn't significantly effect on the resistance of SDF increase by sodium sulfate attack. Fig. 4 shows the SDF with increasing age of mortar specimens exposed to magnesium sulfate attack during the test. This figure indicates that strength deterioration of mortar specimens with silica fume was more pronounced than that of mortar specimens without silica fume irrespective of immersion period.

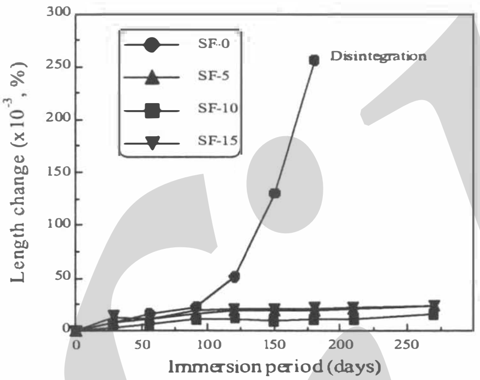

Fig. 1 The length change of mortars immersed in sodium sulfate solution

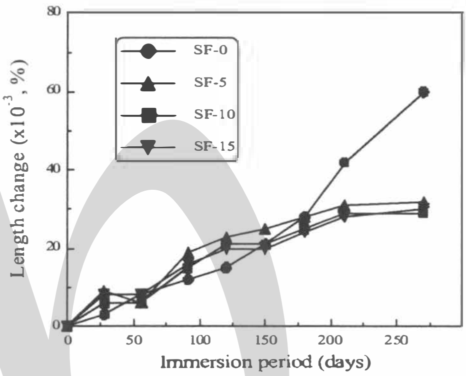

Fig. 2 The length change of mortars immersed in magnesium sulfate solution

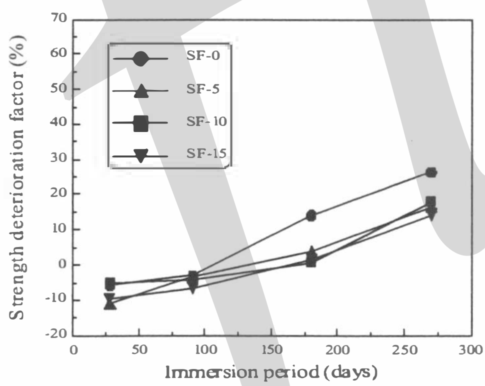

Fig. 3 The SDF of mortars immersed in sodium sulfate solution

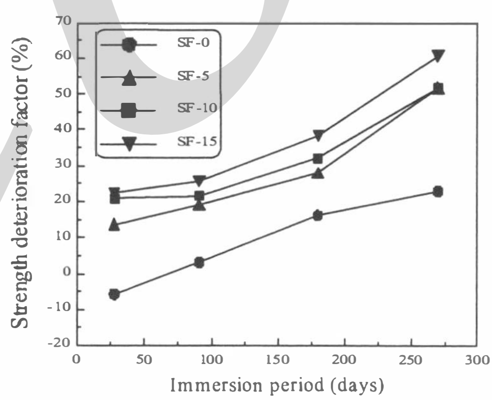

Fig. 4 The SDF of mortars immersed in magnesium sulfate solution

REFERENCES

[1] Bonen, D., and Cohen, M.D. : Magnesium sulfate attack on portland cement paste – II. Chemical and mineralogical analyses. Cement and Concrete Research, Vol. 22, pp. 707-718, 1992.

[2] Al-Amoudi, O.S.B., Maslehuddin, M., and Saadi, M.M. : Effect of magnesium sulfate and sodium sulfate on the durability performance of plain and blended cements. ACI Material Journal, No. 92, pp. 15-24, 1995.

SHRINKAGE AND CREEP OF HIGH STRENGTH CONCRETES CONTAINING SILICA FUME

A. A. Ramezanianpour
AmirKabir University, Iran

M. Mazloom
Shahid Rajaee University, Iran

Keywords: high-strength concrete, silica fume, elastic modulus, creep and shrinkage.

INTRODUCTION

Nowadays high-strength and high-performance concrete is widely used throughout the world and to produce them it is necessary to reduce the water/binder ratio and increase the binder content..

In high performance concrete, which contains high quality and expensive materials, cracking provides the greatest concerns for the designers; because harmful materials can penetrate from them to the concrete easily and start to destroy it and also corrode reinforcement. Some of these cracks are related to drying and autogenous shrinkage of concrete. Therefore, to improve the durability of high-strength concrete, its autogenous and drying shrinkage should be concerned and necessary work on its mix design should be implemented to minimize them. Creep is also an important time –dependent behaviour of concrete which needs more investigation.This paper compares strength, elasticity, shrinkage and creep of high-strength concretes containing different levels of silica fume.

TEST PROCEDURE

specimens were kept in a controlled environment of 20±2°C and 50±5% relative humidity throughout the test duration. Compressive strength specimens remained in 20±2°C water all the time.

The specimens of autogenous shrinkage and basic creep were sealed with aluminum waterproofing tape after moist curing for 7 days. This type of sealing is very effective since the specimens showed very minimal weight loss. The OPC control mix recorded a weight loss of 0.03% after 240 days.

RESULTS AND DISCUSSION

For concrete stored in water, the development of compressive strength with age is shown in Table 1. It can be seen that the compressive strength development of concrete mixtures containing silica fume was negligible after the age of 90 days; however, there is a 26% and 14% strength rise in control concrete after one year compared to its 28 and 90 days strength respectively.

Table 1. Development of compressive strength with age (MPa)

Concrete mixes	Age-days						
	7	14	28	42	90	365	400
OPC	46	52	58	62	64	73	74
SF6	50.5	58	65	69	71	73	73
SF8	52	62	68	71	73	72	73
SF10	52	61	67.5	71	74	74	73
SF15	53	63	70	73	76	75	76

Figure 1 shows the results of shrinkage test for cylindrical specimens of 150 by 300 mm. ACI 209R-92 [1] and also CEB-FIP 1990 [2] committees have executed a lot of investigations in this field and presented good prediction methods for shrinkage. However, as shown in these figures, the committees above could not predict the shrinkage of concrete containing silica fume properly.

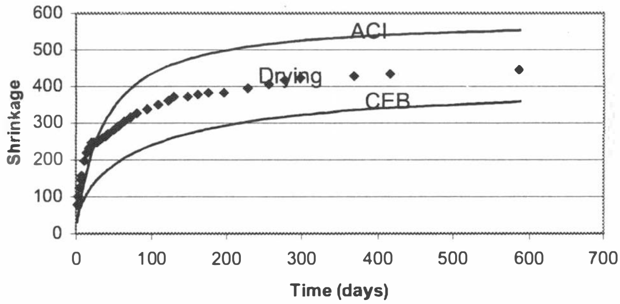

Figure 1-Shrinkage 0f 150 by 300 mm specimens containing 10% silica fume (microstrain)

Figure 2 shows the results of specific creep for cylindrical specimens of 80 by 270 mm loaded at the age of 28 days. As shown in this figure, the ACI andCEB-FIP committees could not properly predict the creep of high-strength concrete containing silica fume.

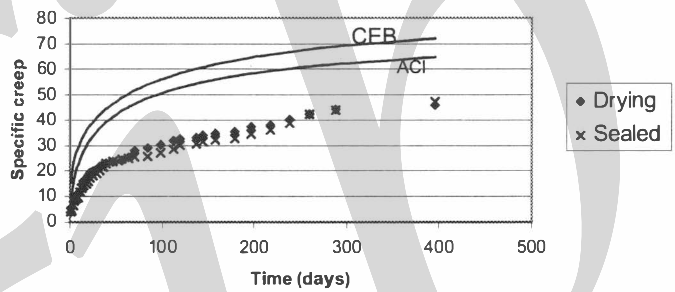

Figure 2- Specific creep 0f specimens containing 10% silica fume (microstrain/Mpa)

CONCLUSIONS

From the results presented in this paper, the conclusions are:

1. The prediction methods presented by the ACI [1] and CEB [2] could not properly estimate the creep and shrinkage of high-strength concrete specimens of this research.
2. Silica fume did not affect the total shrinkage; however, as the proportion of silica fume increased, the autogenous shrinkage of high strength concrete increased and its drying shrinkage decreased.
3. Drying creep was negligible in the high-strength concrete specimens investigated here; consequently, there was no interaction between creep and shrinkage, also specimen size and the relative humidity of the atmosphere had no effect on creep.

REFERENCES

[1] ACI Committee 209, Prediction of creep, shrinkage and temperature effects in concrete structures, ACI Manual of concrete practice, Part 1, 1997, 209R 1-92.
[2] CEB-FIP Model Code for Concrete Structures 1990, Evaluation of the time dependent behavior of concrete, Bulletin d'Information No. 199, Comite European du Beton/Federation Internationale de la Precontrainte, Lausanne, 1991.

STEAM CURING METHOD AND DURABILITY OF HIGH-EARLY-STRENGTH HIGH-FLOWING CONCRETE

Suguru TOKUMITSU Masaaki FUKUDA Masashi SOEDA Takeshi YAMATO
Fuji P.S Corporation, JAPAN Fukuoka University, JAPAN

Keywords: high-flowing concrete, steam curing, carbon dioxide emission, chloride ion penetration

1 INTRODUCTION

This paper presents the steam curing method and durability of high-flowing concrete for precast prestressed concrete products. The authors have developed High-early strength, High strength, and High-flowing concrete (hereinafter referred to as "HHH concrete"). Normally, the steam curing is controlled under 65°C in the air. In case of using a large quantity of cementing materials, however, this traditional steam-curing pattern probably causes problems to reduce the compressive strength and durability by overheat of hydration. This paper presents the temperature change in concrete through accelerated curing, the test result of compressive strength of the concrete up to the age of one year, and the difference between penetration resistance of chloride ion and carbonation resistance.

2 CONCRETE MIXTURES

The cementing materials used for the concrete mixtures are JIS R 5210 high-early portland cement and JIS A 6206 ground granulated blast-furnace slag (hereinafter referred to as "slag"). Crushed stones with a maximum diameter of 20 mm were used for course aggregates. Equal volumes of two different crushed sands were mixed for fine aggregates. The high performance water reducing agent used was a high performance AE superplasticiser in the sort of polycarboxylic acid in conformity with JIS A 6204. The mixture proportions are given in Table 1. The slump-flow of HHH concrete satisfied the requirement, 650±50 mm.

Table 1 Mixture proportions of concrete

Mixture no.	Fineness, cm^2/g		Weight per unit, kg/m^3					
	Cement*	Slag†	Cement*	Slag†	Water	Fine aggregate	Coarse aggregate	Super-plasticizer
1	4530	-	420	0	160	844	992	4.00
2	4530	4260	350	150	175	990	818	4.25
3	4530	6120	350	150	175	990	818	4.50
4	4530	4260	250	250	175	990	818	4.00
5	4530	6120	250	250	175	990	818	4.75
6	4530	-	500	0	175	998	818	5.00

* High-early strength portland cement † Ground granulated blast-furnace slag

3 EXPERIMENTS

The shape of actual size beam model is shown in Fig. 1. Four types of combination of curing method and the mixture combinations were tested. Three cylindrical specimens for testing of long term compressive strength were cast with actual size beam model at the same time. Some curing methods of cylinder were tested. Prism specimens were used for both chloride ion penetrating test and carbonating test. One cylinder was used as a specimen for the electric resistant test. Compression strength tests were conducted at the age of 1, 7, 28, 91, and 365 days. Spraying chloride solution to prism specimen and drying were repeated so that the chloride ion could penetrate into the specimen. Carbonation of prism specimen was accelerated in the carbonation accelerating chamber.

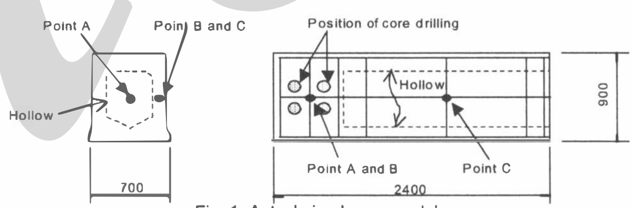

Fig. 1 Actual size beam model

4 RESULT AND DISCUSSIONS

4.1 COMPRESSIVE STRENGTH

Result of the tests, the heat of hydration of HHH concrete, therefore, becomes higher than usual concrete. The compressive strength of actual size beam model at the age of one day exceeded the required strength of 35 N/mm^2 at prestressing, in spite of no steam heating application to the concrete. The compressive strength of cylinders at the age of 28 days exceeded the design strength of 50 N/mm^2

Table 2 Rough estimate of carbon dioxide emission

		Ordinary concrete		HHH concrete		Decrease from ordinary concrete, %
		Weight per volume, kg/m^3	Carbon dioxide emission, kg-C/m^3	Weight per volume, kg/m^3	Carbon dioxide emission, kg-C/m^3	
Materials	High-early strength portland cement	420	95.76	350	79.80	
	Ground granulated blast-furnace slag	—	—	150	3.15	
	Coarce aggregate (crushed stone)	856	1.62	941	1.78	
	Fine aggregate (manufactured sand)	1080	2.04	845	1.60	
	Total	—	***99.42***	—	***86.33***	***13.2***
		Usual steam curing		Improved steam curing		Decrease from ordinary concrete, %
Curing		Use of fuel oil, l/m^3	Carbon dioxide emission, kg-C/m^3	Use of fuel oil, l/m^3	Carbon dioxide emission, kg-C/m^3	
	Heavy oil	20.3	15.022	2.5	1.87	87.6
Total	—	—	***114.44***	—	***88.19***	***22.9***

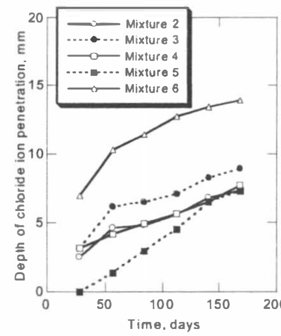

(b) Air-curing after steam curing

Fig. 2 Depth of chloride-ion penetration versus time

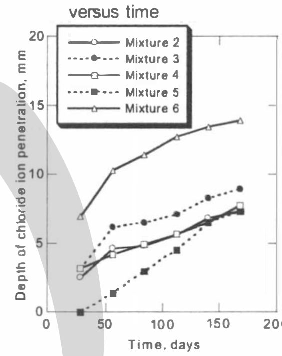

Air-curing after steam curing

Fig. 3 Carbonation depth versus time

The above indicates that it is a better way to suppress the curing temperature as low as possible within the range of satisfying the required performance for a long period of time.

4.2 CARBON DIOXIDE EMISSIONS

Based on those results of experiments, the curing method of products was improved. Changing the steam curing method reduces the carbon dioxide emission by about 88%, as compared with traditional steam curing. Approximately 23% reduction of carbon dioxide emission is expected per product. (Table 2)

4.3 RESISTANCE OF CHLORIDE-ION PENETRATION

The example of penetrated chloride ion penetration depths versus testing period is given in Fig. 2. The penetrated chloride ion depths of HHH concrete reduced to a half of usual concrete after 6-month accelerated penetration. The differences of chloride ion depths ranging from Mixture 2 to Mixture 5 were observed after 6-month accelerated penetration ranged from 2 to 3 mm, being little affected by the fineness of blast-furnace slag.

4.4 CARBONATION DEPTH

The example of the carbonation depths versus testing period is given in Fig. 3. Generally, it is said that the carbonation velocity in the slag-mixed concrete is faster, compared with the case of using only portland cement as cementing materials. The difference of carbonation depths of all mixtures were less than 5 mm. Curing pattern, fineness of slag, and slag content, however, had no effect to carbonation depth in general within this experiment.

5 CONCLUSIONS

1) The heat of hydration of HHH concrete is higher than the usual mixture for prestressed concrete products. 2) Accelerated curing temperature of HHH concrete should be controlled within the range of satisfying the required performance. 3) Approximately 23% reduction of carbon dioxide emission is expected per product due to the use of HHH concrete and change in steam curing method. 4) Chloride ion penetration resistance of HHH concrete was about two times better than usual mixture for prestressed concrete products. 5) Influence of the slag fineness to chloride ion penetrating resistance was small in HHH concrete. 6) Influence of the slag fineness and replacement rate to carbonation resistance was small in HHH concrete.

REFERENCES

[1] Japan Society of Civil Engineering (JSCE): Recommendation for construction with use of high-flowing concrete. Concrete Library 93. (in Japanese).
[2] M.SOEDA, T.YAMATO, Y.SATO and Y.EMOTO: Freezing and thawing durability of high flowing concrete using different cementitious materials, CANMET/ACI, pp.933, SP170-48, 1997.

STUDY ON THE EARLY AGE CRACKING OF HIGH-STRENGTH CONCRETE

Shigeto Sato, Masafumi Imai, Masahiro Suzuki, and Yoshinori Nakata
Japan Prestressed Concrete Constructors Association,
JAPAN

Hiroshi Watanabe
Public Works Research Institute,
JAPAN

Keywords: autogenous shrinkage, high strength concrete, restraining stress, thermal strain.

1 INTRODUCTION

Members built using high-strength concrete have a superior durability due to its low permeability. However, the unit cement content in the high-strength concrete is high which increases the thermal strain resulting from cement hydration and the autogenous shrinkage, therefore special considerations should be taken against initial cracking in order to insure a high durability. These considerations include a correct estimation of restraint stresses resulting from thermal and autogenous shrinkage stresses of concrete, and examination of the hazardous level of crack occurrence. However, the correct estimation of the restraint stresses is not easy in high-strength concrete due the large development of thermal and autogenous shrinkage strains simultaneously changing of physical properties of concrete.

In this study, the sequential changes of the strain occurring in concrete were measured for specimens subjected to the thermal history that a cast-in-situ high-strength concrete member would undergo. Tests simulating the real conditions were done to measure restraint stresses resulting from restraining this mentioned strain, and the effect of concrete temperature and creep on the restraint stresses were examined.

2 TESTING METHOD

2.1 Restraining tests

The tests were conducted in conformity with Japan Concrete Institute's "Testing Method of Concrete Autogenous Shrinkage". For consideration of hydration heat and thermal stress, the formwork was made of expanded-polystyrol and the concrete specimen was subjected to a high thermal history. The specimen dimensions are shown in Figure 1. Test cases are shown in Table 1 and details of the concrete mix proportion, which has target strength of 100 N/mm², are shown in Table 2.

The restraining steel bar used to constraint concrete deformation was D32 deformed bar, however, the length of the retraining steel bar would change because of the changes in concrete temperature when using deformed reinforcement bars. Consequently, when the temperature of the specimen reaches a peak, the restraint stresses that occur during the cooling time would not be possible to measure. In order to overcome this problem, tests using ϕ 30 invar bar with a low coefficient of linear expansion (1.0 x 10^{-6} / ℃) were performed as well. In addition, a control specimen without restraining steel bar was also prepared to measure the concrete strain under non-restrained condition.

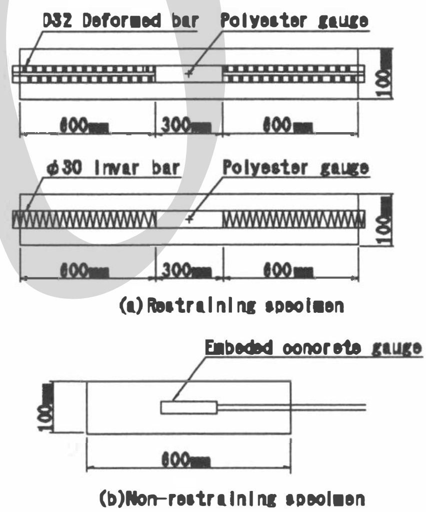

Fig. 1 Dimensions of specimens

Table 1 Test cases

Concreting Temperature (℃)	Restraining test		Non-restraining test
	D32 Deformed bar	ϕ30 Invar bar	
5	○	○	○
20	○	○	○
40	○	○	○

Table 2 Mixproportion

G_{max} (mm)	Target Value		Water cement ratio (%)	Sand-coarse aggregate ratio (%)	Unitweight (kg/m³)			
	Slump (cm)	Air content (%)			W	C	S	G
20	23±2.5	2.0	25	42.6	160	640	687	941

The specimens were subjected to different thermal history cases by setting the concreting temperature (concrete casting temperature) to three differentvalues:5, 20,and40 ℃.

2.2 Estimation of effective modulus of elasticity of concrete

Using the restraint stresses that were measured from restraining tests ($\Delta\sigma c$) and the difference between non-restrained concrete strain and restraining steel bar strain($\Delta\varepsilon sf - \Delta\varepsilon cf$), the effective modulus of elasticity of concrete was estimated by the following equation:

$$E_{ce} = \frac{\rho E_s \Delta\sigma_c}{\rho E_s\left(\Delta\varepsilon_{sf} - \Delta\varepsilon_{cf}\right) - \Delta\sigma_c} \quad (1)$$

Where: *Ece* the effective modulus of elasticity of the concrete, *Es* of the modulus of elasticity of the restraining steel bar, and ρ is the ratio of the section area of the restraining steel bar to the sectionareaoftheconcrete.

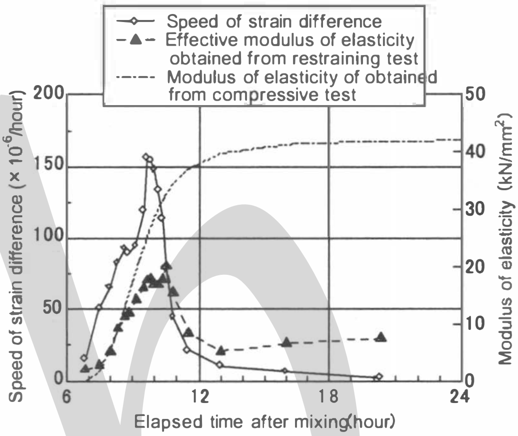

Fig. 2 Changeinthespeedofstraindifference andeffective modulus ofelasticity (D32 Deformed bar,20 ℃) ϕ

3 TEST RESULTS

In the case of using deformed bar as restraining steel,when($\Delta\varepsilon sf - \Delta\varepsilon cf$) starts to appear in a very early age after concreting and the concrete temperature rises, it was possible to measure the restraint stresses. As for the case of using invar bar, when the concrete temperature drops, the occurring thermal shrinkage and restraint stresses could also be measured. The restraint stresses thatdevelopinthe concrete are affected not only by ($\Delta\varepsilon sf - \Delta\varepsilon cf$), but also by the development of the modulus of elasticity of concrete. Figures 2 and 3 show the difference between non-restrained concrete strain and restraining steel bar strain at 20 ℃ as an example in the case of the specimens constrained with D32 deformed bars and invar bars, respectively. At very early ages, the effect of creep on the obtained approximate value of the effective modulus of elasticity of the concrete varies according to concreting temperature. This effect of creep depends as well on the speed of change of the difference between concrete strain and restraining steel bar strain. Particularly,whenthespeedofthestraindifferencedecreases,thecreepeffectbecomesremarkable and the effective E modulus tends to decrease. After concrete temperature drops, the value of restraining stresses approaches the value calculatedusing therealmodulusofelasticity.

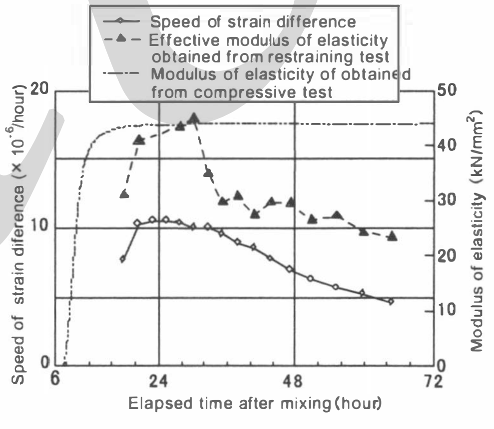

Fig. 3 Changeinthespeedofstraindifference andeffective modulus of elasticity (ϕ 30Invarbar,20 ℃)

ANALYSIS OF PRELOADED REINFORCED CONCRETE COLUMNS STRENGTHENED WITH HIGH-PERFORMANCE CONCRETE JACKETS

Adilson Roberto Takeuti
M.Sc. in Structural Engineering
e-mail: atakeuti@sc.usp.br

João Bento de Hanai
Professor of Civil Engineering
e-mail: jbhanai@sc.usp.br

Department of Structural Engineering
University of São Paulo at São Carlos, São Carlos - BRAZIL

Keywords: strengthening, reinforced concrete, column, high-strength concrete, jacket

1 INTRODUCTION

This paper presents some results of an ongoing research program on strengthening mechanisms in reinforced concrete columns, especially dedicated to observe preloading, time-dependant and confinement effects. Particularly, the results of two series of tests on preloaded and non-preloaded columns are presented and discussed. In these series also two kinds of transverse reinforcements in the high strength concrete jackets were tested.

The application of high-strength concrete in the jackets seems to be interesting especially to avoid excessive enlargement of the column dimensions. Takeuti and Hanai [1] observed a good composite performance of strengthened concrete columns subjected to axial loads.

2 TEST RESULTS

Fig.1 shows the stress-strain diagrams of the type S1 and S2 test specimen respectively. From both diagrams, evidences of a non-linear behavior of the preloaded columns can be easily seen to appear at a stress level of about 30 MPa. Possibly, this is due to the progressive damage of the inner concrete whose average compressive strength was 32.7 MPa. From this stress level onward, there is a progressive loss of rigidity, but the ultimate load capacity was nearly the same.

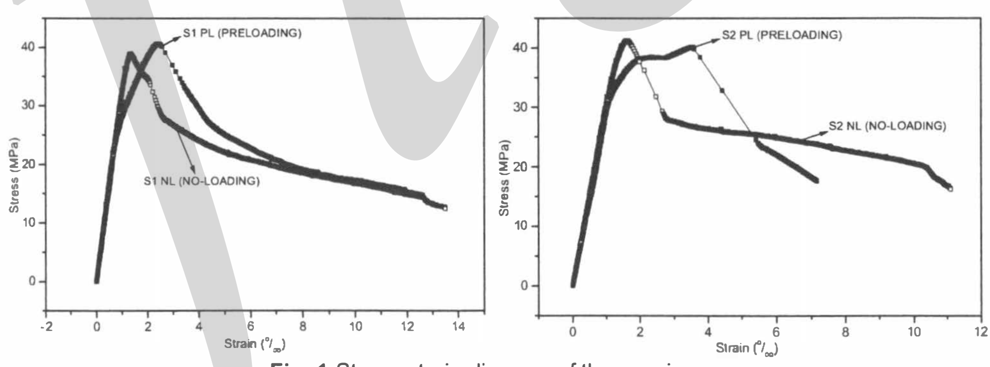

Fig. 1 Stress-strain diagram of the specimens

The ultimate load of the strengthened columns can be predicted from the equilibrium conditions of the longitudinal forces assuming perfect bonding between concrete and reinforcement. Five criteria were applied to evaluate the ultimate load of a composite section.

Table 1 shows the results of the theoretical predictions according to the five aforementioned criteria. It can be seen that the second criterion and those related to confinement models result in better-predicted results. This evidence leads to the conclusion that when there are good confinement conditions, the concrete section of the core contributes to the ultimate load capacity, whether or not the primary column is preloaded.

Table 1 Comparison between the theoretically and experimentally obtained ultimate loads

	Calculated / Test			
	S1 PL	S1 NL	S2 PL	S2 NL
Test	1627.7 (1)	1556.8 (1)	1607.4 (1)	1651 (1)
Reference [1] ($F_{u,int}$)	1.31	1.37	1.70	1.65
Reference [1] ($F_{u,inner}$)	0.83	0.87	0.98	0.96
Reference [2]	0.90	0.95	1.04	1.02
Reference [3]	0.84	0.88	0.99	0.96
Reference [4]	0.85	0.89	1.00	0.98

The most significant difference between the behavior of the preloaded and the non-preloaded columns is their deformability as shown in Fig. 1. The preloading of the primary column introduces a certain level of internal damage and creep in the concrete as well as pre-deformation of the steel bars.

Other tests are presently in progress on different preloading ratios, distinct column section shapes and other transverse reinforcement ratios.

3 CONCLUSIONS

In spite of the present test program not being completed, some preliminary conclusions can be drawn as a reference framework for further analyses:

- The concrete core section (primary column) contributes to the ultimate load capacity provided an efficient confinement is provided;
- The effect of preloading does not seem to significantly affect the ultimate load capacity. However, it modifies the strain capacity of the specimen depending on the level damage of the concrete and the reinforcement of the primary column and the confinement conditions;
- Accurate analyses of the behavior of preloaded columns with time must be carried out in order to understand and to give a realistic interpretation of the phenomena;
- The preloading system based on prestressed strands is efficient and cheaper than the servo-hydraulic system.

4 ACKNOWLEDGEMENTS

The authors express their gratitude to FAPESP (São Paulo State Research Foundation) for the financial support and to the companies Silmix/Camargo Corrêa Metais S.A., Holdercim Brasil S.A., MBT Brasil Indústria e Comércio Ltda., Weiler-C. Holzberger & Cia. Ltda., Gerdau S.A. and Jeruelplast Artefatos Plásticos Ltda. for providing the materials used in the test program.

REFERENCES

[1] TAKEUTI, A.R.; HANAI, J.B. (2000) Reinforced concrete columns strengthened with high performance concrete jackets. In: JOHAL, L.S. (Paul), ed. *The economical solution for durable bridges and transportation structures* (Proc. of the PCI/FHWA/FIB International Symposium on High Performance Concrete, Orlando, USA, Sept. 25-27, 2000). Chicago, PCI. p.439-448. (ISBN: 0-937040-65-7)

[2] CUSSON, D. ; PAULTRE, P. (1994). *Confinement model for high-strength concrete tied columns.* University of Sherbrooke, SMS-93/02, October, 54p.

[3] SAATCIOGLU, M.; RAZVI, S. R. (1992). Strength and ductility of confined concrete. *Joumal of Structural Engineering*, v. 118, n. 6, pp.1590-1607.

[4] FRANGOU, M.; PILAKOUTAS, K; DRITSOS, S.E. (1995). Structural repair/strengthening of R.C. columns. *Construction and Building Materials*. v. 9, n.5, pp.259-265.

INFLUENCE OF A MODIFIED SILICA FUME ON THE CHARACTERISTICS OF HIGH PERFORMANCE CONCRETE

Mahmoud Nili
Ass. Prof.
Bou Ali Sina Uni.
Iran

Ali Akbar Ramazanianpour
Prof.
Amir Kabir Uni.
Iran

Ali Taheri
Ass. Prof.
Delf. Uni.
Iran

Keywords: modified silica fume, high performance concrete, superplasticizer

1 INTRODUCTION

In recent years the use of high performance concrete ,(HPC), as an ideal construction material increased considerably. The mix proportions of HPC is normaly based on type I cement in combination with supplementary pozzolans ,such as silica fume and also superplactizer and the other additive or admixture depending on the environmental condition.

It is obvious realized that although silica fume enhance the key properties of concrete, but its performance such as transportation and application in concrete manufacturing process represent certain problem due to its ultra finness and dustability. Many efforts is doing to use silica fume in dry compacted state with bulk weight around 500 kg/m3 with of course, using simulatanously superplacticizer to enhance workability.

A complex material comprise silica fume, superplasticizer and a set regulator (MSF)at a powder form with bulk density of 750-800 kg/m3 was manufactured[1]. The influence of (MSF) on characteristics of fresh and hardened concrete is studied and the results are compared with those obtained with silica fume and also without any additive.

2 DESIGN OF EXPERIMENT

2.1 Properties of Materials

Ordinary portland cement was used. Satutated surface dry density of river sand and crushed stone with 20 mm maximum size were 2.54 and 2.7 respectively.

2.2 Mix proportions and test procedures

Mix proportions with slump value about 150 mm are given In Table 1.The following tests were done: setting time, slump loss,compressive strength, permeability and micro-photographs of mixtures

Table 1: Mix proportions of concrete

Series	Cement (kg)	Water (kg)	MSF (kg)	SF (kg)	Sand (Kg)	Coarse agg.(kg)
1	400	* 192	-	-	899	909
2	372	**192	-	28	899	909
3	372	192	28	-	899	909
4	340	192	60	-	899	909

*,** superplacticizer was used %1.8 and %2 of cement content

3 TESTING RESULTS

The results of **compressive strength** for all different mixtures is shown in Fig. 1. As it is shown %10 replacement cement by MSF at 3 , 7 and 28 days enhanced compressive strength %72, %47 and %37 respectively. However, In series 2, which cement replaced %7 by silica fume, the compressive strength at 7 and 28 days increased %2 and %10 respectively.

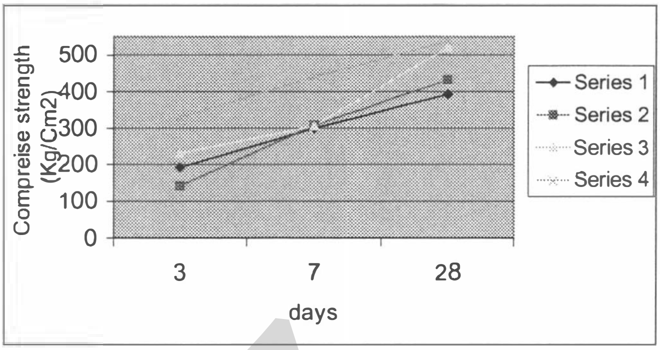

Fig.1 Compressive strength of different mixtures versus age

The water levels of specimens from surface in **permeability test** for all series was very low (below 2 cm), which may be attributed to low water cement ratio of concrete mixtures. The results of **slump loss test** declare that the slump of concrete mixtures (series 3 and 4) remain constant and decreased to about zero till 90 minutes and show a more plasticity than the mixtures 1 and 2 which slump loss were happened after about 15 minutes. Setting of the conrete mixtures was evaluated via **penetration test.** In mixture 2, which cement replaced by SF, the setting time decreased relative to the mixture 1 as a conventional series. However, in series 2 and 3, the both initial and final setting time increased considerably. Finally, the visual **Scanning electron** photomicrographs of the hydrated pastes at 3 days in series 2, 3, 4 show a high dense hydration solution than series 1. It may be attributed to ettringite (like crystals) which is appeared in the paste of series 1.

4 CONCLUSION

1. Using MSF powder on the basis of silica fume,superplacticizer and set regulator, high performance concrete mixture can be found,
2. High strength, dense formation ,more plasticity condition with time and simple application were found by using MSF compare to the the mixtures made with and without SF.

REFERENCES

[1] Kaprielov, S., Sheinfeld, A, Batrakov, V.: Properties of concrete s with complex modifier based on silica fume and superplacticizer. 5th CANMET/ACI International Conferrence on superplacticizers and other chemical admixtures in concrete (oct.1997 Italy)
[2] ASTMC403-88 Test for Time of Setting of Concrete Mixture by Penetration Resistance
[3] V.M.Malhotra, Developments in the use of superplasticizers, Amer. Concr. Ins. Sp. Publicn. No. .68 , pp .561(1981)

Session 10 | Recycling

THE STATE OF USING BY-PRODUCTS IN CONCRETE IN JAPAN AND OUTLINE OF JIS/TR ON "RECYCLED CONCRETE USING RECYCLE AGGREGATE"

Hirotaka KAWANO
Public Works Research Institute, JAPAN

Keywords: by-products, recycle, recycled aggregate, recycled concrete,

1. ABSTRACT

In the last few decades much research and development has been conducted on the reuse of many kinds of by-products in concrete and many papers have been published every year. However, although large quantities of several kinds of by-product materials are used in concrete today, the reuse of many kinds of by-products has not grown in spite of intensive research and development.

This paper outlines the state of reuse of by-products in concrete in Japan and outlines the problems related to reuse. It also summarizes the JIS Technical Report, TR A 0006 “Recycled Concrete Using Recycled Aggregate” published in 2000.

2. PURPOSE OF RECYCLING

The ultimate purpose of recycling materials is to minimize the impact of human activities on the environment and the planet. From this viewpoint, the first priority of concrete engineers is to maximize the lifespan of concrete structures, because buildings and infrastructures must be used for a very long time and, generally speaking, **reuse** of concrete and/or **recycling** of concrete materials is not easy technically or economically. We must also **reduce** the waste from concrete structures before considering how to reuse or recycle it. And when using by-products in concrete, we must also consider the influence on the quality of the structures, especially durability.

3. THE STATE OF REUSE

Table 1 outlines the state of reuse of many kinds of by-products related to concrete. In the full paper, the state of cement, mineral admixtures, aggregates and demolished concrete is shown.

4. BARRIERS AGAINST REUSE

There are several reasons why it is difficult to extend the sustainable use of concrete materials:

a. lack of suitable laws
b. lack of codes, specifications, standards and guidelines
c. cost
d. poor image
e. lack of experience
f. low quality
g. variations in quality
h. too many kinds and too large amounts of by-products
i. inefficient supply system
j. lack of proper information

The full paper contains brief discussions for each item.

5. OUTLINE OF JIS/TR ON "RECYCLED CONCRETE USING RECYCLE AGGREGATE"

Japan has a history of more than a quarter of a century of research on the reuse of demolished concrete for concrete again, and yet relatively little concrete has been recycled in this way. The JIS Civil Engineering Committee made a recommendation in 1998 to establish new JIS standards to encourage the use of recycled materials in the construction industry. In response, the Japan Concrete Institute formed a committee for establishing new JIS drafts for recycled materials for concrete in 1998 and 1999. One of the drafts was published as a JIS Technical Report, TR A 0006 "Recycled Concrete Using Recycled Aggregate" in 2000. A TR is the preliminary stage for the JIS draft.

Table 1 By-product materials used in concrete

Category 1: From non-construction industries to concrete

Usage	By-product materials
Cement	◎ sulfur, ◎ fly ash, ◎ blast furnace slag, ◎ converter slag, ◎ copper slag, ◎ mold sand for cast iron, ○ burned ash of garbage (for Eco-cement), ◎ tires, wooden panels of pinball machines, waste oil as fuel
Mineral admixtures	○ ground granulated blast furnace slag, ○ fly ash, ○ silica fume, □ ground granulated glass, △ burned ash of garbage, □ dust from ion casting, ○ lime powder, □ stone powder, △ burned ash of sewage sludge, □ rice husk ash
Chemical admixtures	◎ lignin, etc.
Aggregate	○ blast furnace slag, ○ copper slag, ○ ferro-nickel slag, □ electric furnace oxidized slag, □ crushed glass, ○ fly ash aggregate, □ bricks, roof tiles, pottery, △ melted slag from burned ash of garbage, △ melted slag from burned ash of sewage sludge, □ dust from ion casting, □ chopped plastics, □ paper, □ mud

◎: being used constantly, ○: standardized, △: being studied, □: required to be used

Category 2: From concrete to concrete

sludge from concrete plants → cement, ○ sludge water from concrete plants → concrete
○ reuse of attached mortar in agitator drum using retarder
△ reuse of refused concrete (concrete, cement, aggregate), ● recycled aggregate
△ stone powder from recycle treatment of aggregate

●: being studied intensively

Category 3: From concrete to other materials

△ sludge from concrete plants into cement → alkalizing material for soil or water, ground stabilizer
? cylinder specimen for compressive strength test,
◎ crushed concrete → subbase material for pavement,
△ crushed concrete → filler for asphalt concrete, ground stabilizer
? demolished concrete members → foot protection of levees, fish reefs

The full paper shows the background of establishing TR A 0006, then describes the following policies for making the TR:

- A new JIS is to be created for recycled concrete, not recycled aggregate.
- Recycled concrete must be standardized independently from JIS A 5308.
- Applicable sections in structures where recycled concrete can be used are limited.
- In order to facilitate quality control, the number of classes of recycled concrete should be minimized.
- Considering the variations of recycled concrete, an adequate margin of quality for designated uses must be allowed, which will also simplify quality control.
- When skilled engineers use recycled concrete, they can extend its scope of application.

The full paper also outlines the structure of the TR.

6. CONCLUSION

Concrete engineers and researchers must take a broad perspective when evaluating the relevant technologies for reusing and recycling concrete materials.

LIFE CYCLE DESIGN BASED ON COMPLETE RECYCLING OF CONCRETE

Masaki Tamura
Tokyo Metropolitan University
JAPAN

Takafumi Noguchi
The University of Tokyo
JAPAN

Fuminori Tomosawa
Hokkaido University
JAPAN

Keywords: lifecycle design, recycle design, resource conservability, complete recycling,

Summary

Concrete is a useful material for construction, concrete structures are generally expected to last for decades or more than a century. However, most of the concrete structures built in the past have been demolished and removed much earlier than their intended service lives. Why? Of course, this is mostly attributed to such reasons as outdated design, limitations in the space renewability, and technical problems including performance degradation of equipment and the structural bodies. However, the effects of social issues, such as the market mechanism that promotes consumption of new products while restricting recycling of used products and the absence of administrative guidance by policies towards recycling, cannot be disregarded. Technical development is necessary for the next generation in consideration of such social curtailment of service lives of structures.

This paper reviews concrete structures as products based on the concept of lifecycle design and presents a model of recycling design, the design factor of lifecycle design. The outline of completely recyclable concrete, with which closed-loop circulation of component materials is realized by recycling design, is presented as well.

Table1 shows the recycled products of concrete can be classified into 6 categories. Figure 1 shows the material flow of concrete structures provided by existing forward process systems. Figure 2 shows the hierarchy of the design concepts – a hierarchical system of material elements necessary for designing a material product, i.e., a building, together with design concepts necessary for formulating a sustainable life-cycle loop.

Table 1 Classification of regenerated concrete based on forward process production systems

Type of circulation	Method of replacement	Type of recycled concrete	Quality of recycled aggregate		Application of recycled aggregate / recycled concrete				
			Coarse	Fine	Main frame	Sub frame	Back filling	Special treatment	Examples
Open loop 1)	Down cycle 3)	(1) No use	Low	Low	×	×	○	---	Paving stone, Earthen floor stone
		(2) Low quality 1	Low	Low	×	○		---	Subslab concrete, Back filling concrete, Leveling concrete
		(3) Low quality 2	Low	(Virgin)	×	○		—	Foundation slabs, Earthen floor slabs
		(4) Low quality 3	High	Low	×	○		Cement paste must be strengthened	Concrete in contact with ground, Foundation, Cast-in-place concrete piles
	Level cycle 4)	(5) High quality 1	High	(Virgin)	○	○		Production system for high quality aggregate must be utilized	Ordinary reinforced concrete structure
Closed loop 2)		(6) High quality 2	High	High	○	○		Production system for high quality aggregate must be utilized	Ordinary reinforced concrete structure

Definitions:

1) **Open loop** : A form of circulation in which, when a product approaches its limit of service and the product or its components are to be renewed, disposal elements and/or newly introduced elements are involved, expanding the area of circulation.

2) **Closed loop** : A form of circulation in a closed area in which, when a product approaches its limit of service and the product or its components are to be renewed, no disposal elements or newly introduced elements are involved.

3) **Down-cycle(ing)** : A method of renewal in which, when a regenerated material is to be used as a component of a regenerated product, the quality/performance of the regenerated product is lowered and the resource conservability of the component is not ensured. In case of (ing), the form of renewal is to be carried out continuously.

4) **Level-cycle(ing)** : A method of renewal in which, when a regenerated material is to be used as a component of a regenerated product, the quality/performance of the regenerated product is retained, ensuring the resource conservability. In case of (ing), the form of renewal is to be carried out continuously.

5) **Resource conservability** : a property of materials to be able to continue circulation in different products during its service life and after demolition/separation, it can be used as materials for products having the same or higher qualities.

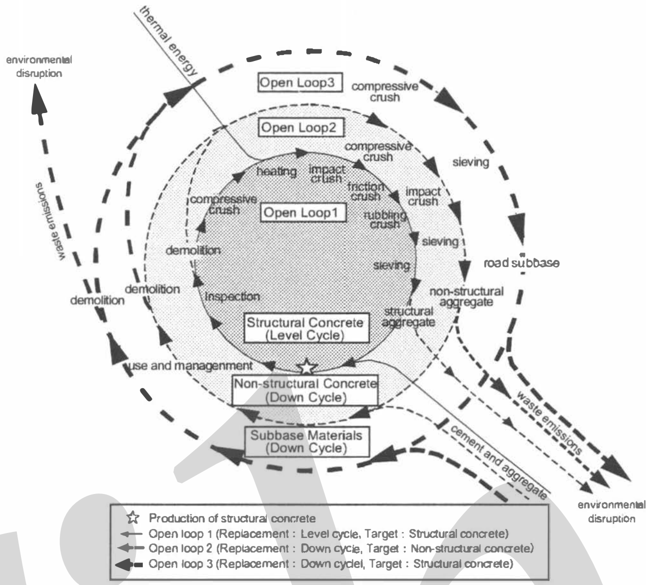

Fig. 1 Open-loop material flow of conventional concrete structures

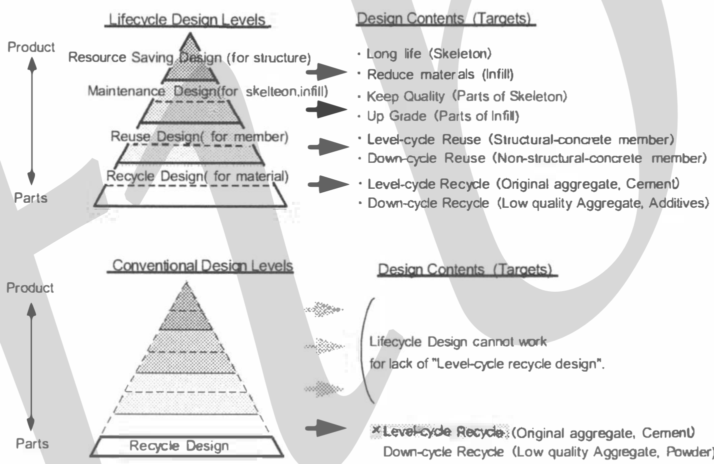

Fig. 2 Hierarchy of design concept incorporated in lifecycle

Research and development involving "recycling" as a keyword should clarify what recycling design ought to be and how it ought to be carried out and examine if it is essentially effective in establishing a sustainable global environment for the present and future. Otherwise, environmental technology intended to improve the issue of the global environment could be chained to another vicious circle.

Toward the future, in addition to technologies for treating existing stock, it is vital to establish production systems whereby new stock serves as resources by actively introducing lifecycle design involving recycling design, which incorporates inverse processes of production.

REFERENCES

Tomosawa F., Noguchi T. and Tamura M.: Towards Zero-Emissions in Concrete Industry: Advanced Technologies for Concrete Recycling, Three-Day CANMET/ACI International Symposium on Sustainable Development of the Cement and Concrete Industry, Ottawa, pp147～pp,160,1998

Tamura M., Noguchi T., Tomosawa F. and Kitsutaka Y.: Concrete Design toward Complete Recycling, Proceedings of fib-SYMPOSIUM -Concrete and Environment-, CD-ROM, Berlin, 2001

Noguchi T. and Tamura M.: Concrete Design toward Complete Recycling, Structural Concrete, Volume 2, Number 3, pp.155-167, 2001

DEVELOPMENT OF CONCRETE RECYCLING SYSTEM

Yasuhiro Kuroda Hiroshi Hashida Nobuyuki Yamazaki Kazuyuki Nakamura
Shimizu Corporation Tokyo Electric Power Company.
JAPAN JAPAN

Keywords: concrete rubble, recycled structural aggregate, concrete recycling system, fine-powder

1 INTRODUCTION

The 21st century has been called "the era of the environment," in which the construction industry has an important role of creating a recycling-based society for natural resources and materials. Concrete accounts for an especially large proportion of construction wastes, and its recycling should be promoted.

At present, most concrete wastes are reused in road subbases. However, the production of concrete wastes is predicted to exceed the demand for subbase materials in several years, and so other methods of reuse must be developed since the final disposal facilities are already almost full. On the other hand, construction activities require vast amounts of aggregates. Also in terms of external diseconomies, methods should be urgently developed to utilize concrete wastes to produce new concrete. The authors studied and developed a closed loop concrete system to solve these problems.

2 OUTLINE OF THE SYSTEM

An outline of the system is schematically shown in **Figure 1**. The system surveys the concrete building to be demolished in advance, examines the recyclability of the concrete, obtains concrete rubble by appropriately demolishing the building and separating the wastes, and then produces recycled structural aggregates from the concrete rubble by removing as much mortar and cement as possible using a heating and rubbing method [1]. The recycled aggregates have almost the same properties as the original aggregates and can be used for the same purposes such as constructing structures. The authors mixed concrete using the recycled structural aggregates (hereinafter referred to as "sustainable concrete", examined its strength and durability, and confirmed that the concrete can be used for ordinary building structures [2].

The fine-powdered materials produced while recovering aggregates mainly consist of cement, and could be used as cement materials. The use of the powder as cement filler and ground improvement material, and also as a material before calcination is being investigated.

This closed-loop concrete recycling system thus enables 100% of concrete to be recycled. However, the system had not been used to construct an actual building. This paper describes the results of the first application of the system.

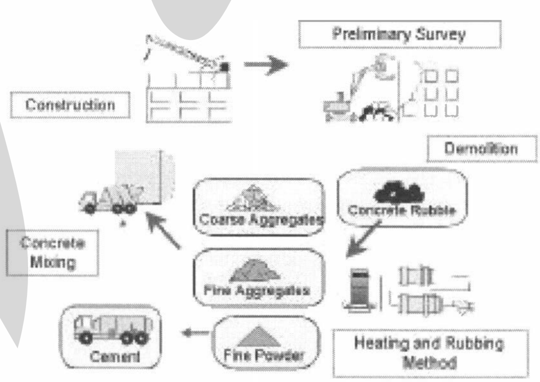

Figure 1 Closed-loop concrete recycling system

3 OUTLINE OF THE PROJECT

The system was demonstrated by constructing an actual laboratory building at the Institute of Technology, Shimizu Corporation. An outline of the project is:

- Name of the project: Renovative extension of the Acoustic Laboratory of the Institute of Technology, Shimizu Corporation
- Place: Etchu-jima 3-4-17, Koto-ku, Tokyo
- Structure: Reinforced concrete structure, partially steel structure, three levels above the ground
- Building area: 363.41 m^2 , Total floor area: 667.75 m^2

An exterior view of the laboratory after completion is shown in **Photograph 1**. The laboratory was built by recycled structural aggregates recovered in a pilot plant [3] using the heating and rubbing method (**Photograph 2**). The aggregates have equivalent quality designated by Japanese Industrial Standard.

Photograph 1 External view of the laboratory

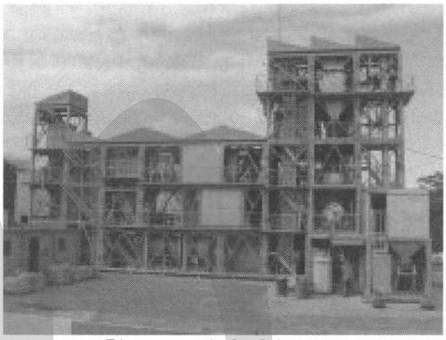

Photograph 2 Pilot plant

4 CONCLUSION

This paper briefly described the closed-looped concrete system, which reuses 100% of concrete wastes by separating and recovering fine and coarse aggregates and fine-powder from concrete wastes, and uses the aggregates for building structures and the fine-powder as cement materials and materials for improving the ground. It also described the first application of the system to construct a building.

The sustainable concrete which is produced using this system is mixed as ordinary concrete, and is equally workable as and has equivalent properties to ordinary concrete. This full-scale trial construction and other tests showed that, by surveying the concrete to be demolished in advance and examining whether the concrete is appropriate for reuse, the sustainable concrete and aggregates recovered by the heating and rubbing method can be used to construct buildings. Consequently, this system showed validity on the whole concrete recycling from demolition to construction

REFERENCES

[1] Koga, Y., Tateyashiki, H., et.al. : A process for separating aggregate from concrete waste during the dismantlement of Nuclear Power Plants, Radioactive Waste Research, Vol.3 No.2, pp.17-26, 1997 (in Japanese).
[2] Kuroda, Y., Hashida, H., et al. : Basic Properties of Concrete Using High Quality Recycled Aggregate, Proceedings of the JCI, Vol.21, No.2, pp.1105-1110, 2000 (in Japanese).
[3] Shima, H., Tateyashiki, H., et.al. : New technology for recovering high quality aggregate from demolished concrete, International Seminar on Recycled Concrete, Sponsored by Niigata University and Japan Concrete Institute, pp.33-44, September 2000.

STUDY ON THE APPLICATION OF ARTIFICIAL LIGHTWEIGHT AGGREGATES MADE FROM FLY ASH TO BE USED IN PC BREDGES

M. Sakurada, H. Watanabe, T. Ohura
P. S. Corporation
JAPAN

M. Suzuki
Tohoku University
JAPAN

Keywords: fly ash, lightweight aggregate, PC beam, load test, PC slab, wheel running fatigue test

1 INTRODUCTION

A new type of artificial lightweight aggregates made from fly ash, hereinafter called FAA, has been developed recently in Japan [1], [2]. The main raw material of FAA is fly ash which accounts for 85% of the coal ash. The FAA has some excellent characteristics, which are high strength and low water absorption as compared with the conventional lightweight aggregate. The application of FAA to prestressed concrete structure enables the following. Hereinafter, prestressed concrete and reinforced concrete are called PC and RC, respectively.

1) The industrial waste, fly ash, can be utilized effectively.
2) The concrete structure can be lightened by 10% to 20%.
3) The aseismicity of the concrete structure can be improved.
4) Resistance to freezing and thawing can be improved as compared to concrete with conventional lightweight aggregate.

However, since the tensile strength, bond strength, Young's modulus and fatigue strength of the lightweight concrete has been regarded lower, it is necessary to confirm the behavior of the PC member with FAA. Therefore, the authors carried out 1) bending tests, 2) shear tests, 3) stress measurement of prestressing strands and 4) a wheel running fatigue test, and the application of FAA to the PC bridge was studied.

2 PROPERTIES OF THE NEW TYPE OF LIGHTWEIGHT AGGREGATE, FAA

Table 1 shows the properties of FAA in this study. The two kinds of FAA have the lowest water absorption of all aggregates made from fly ash, therefore, concrete with these FAA has a high strength, high resistance to freeze and thawing, and high facility of pumping as compared to concrete with conventional lightweight aggregate which has high water absorption. Photo.1 and Photo.2 show the appearances of the two kinds of FAA.

Table 1 Properties of FAA

			FAA-M (UL)	FAA-H (TL)	Natural Stone (N)
Aggregate	Absolute dry density	g/cm^3	1.30	1.81	2.80
	Water absorption ratio	%	0.81	2.23	0.72
	Type of air space	—	Independent	Non air space	—
	Main raw material	—	Fly Ash	Fly Ash	Gravel
Concrete	Unit Weight	kg/l	1.85	2.05	2.35
	Compressive strength	MPa	70	100	100
	Tensile strength	MPa	2.8	3.1	3.1
	Young modulus	GPa	23	26	33
	Freeze and thawing	—	Durable	Durable	Durable

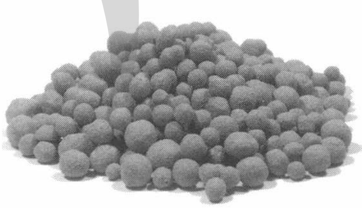

Photo 1 FAA-M (UL)

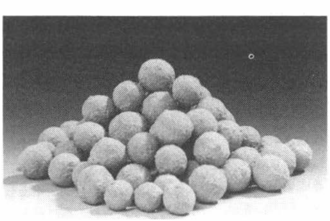

Photo 2 FAA-H (TL)

3 BEHAVIOR OF PC BEAM AND PC SLAB WITH FAA

1) Flexural Behavior of PC beam

Fig.1 shows the load-displacement curves in bending test. Each curve of FAA (TL and UL) is almost similar to natural aggregate (N) from the beginning through the end of loading. This means that the PC beam with FAA has almost the same performance as the ordinary PC beam with natural aggregate in respect of cracking strength, ultimate flexural strength and ductility.

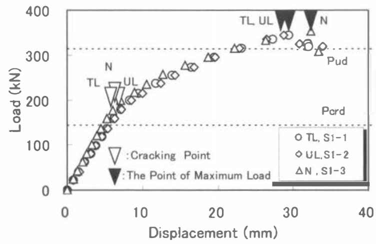

Fig. 1 Results of bending test

2) Shear capacity of PC beam

Fig.2 shows the load-displacement curves in shear test. As for the PC beams, each curve of TL and UL is almost similar to that of N from the beginning through the end of the loading. However, as for the RC specimens, the curve of UL is lower than that of TL. It can be said that the shear capacity of the PC beam with FAA is equal to that of the ordinary PC beam with natural aggregate, but the shear capacity of the RC beam with lighter FAA is lower than that of the RC beam with heavier FAA. This means that the prestressing increases the shear capacity of the concrete beam with FAA, and that effect is larger for the concrete beam with lighter FAA.

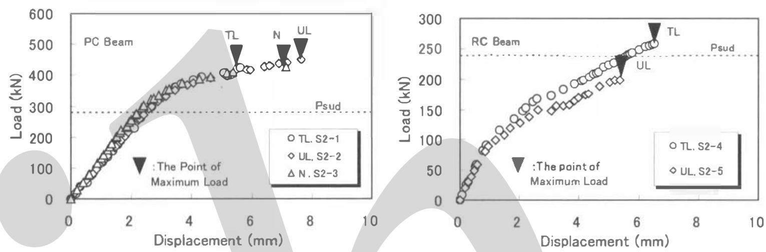

Fig. 2 Results of shear test

3) Transfer length of prestressing strand

Fig.3 shows the transfer length of prestressing strands. As the transfer length of UL and TL is 1m which is almost equal to that of N and the length is about 65 times the 15.2mm (the diameter of the prestressing strand), it can be said that the transfer length of the PC beam with FAA is almost equal to that of the ordinary PC beam with natural aggregate.

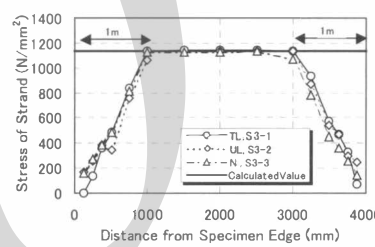

Fig. 3 Transfer length of strand

4) Effective stress of prestressing strand

Fig.4 shows the time dependent loss of stress of prestressing strand in respect of PC beam with UL. The calculated stress at after 3 months is obtained with the common design method regulated in Japanese specification. In the calculation, the creep and drying shrinkage of concrete and the relaxation of prestressing strand are considered. The measured stress of the prestressing strand is almost equal to or over the calculated stress both just after prestressing and at after 3 months. It can be said that the prescribed prestress can be introduced in the PC beam with FAA like the PC beam with natural aggregate.

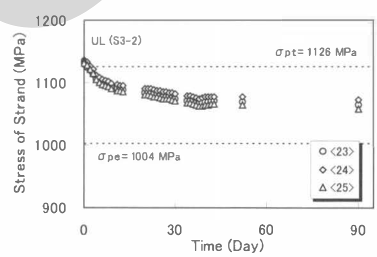

Fig. 4 Effective stress of strand

5) Fatigue endurance of PC slab

Fig.5 shows the relationship among loading cycles, load and displacement in wheel running fatigue test in respect to PC slab with UL.. The displacement is measured at the center of the specimen. It seems that damage from fatigue of this PC slab is small since the displacement gets linearly larger corresponding with the increase of the load. This result indicates that the PC slab with UL has enough fatigue endurance.

From all the above results, it is verified that the FAA can be applied to the PC bridge, and it can be said that the fly ash can be a promising resource for lightweight aggregate.

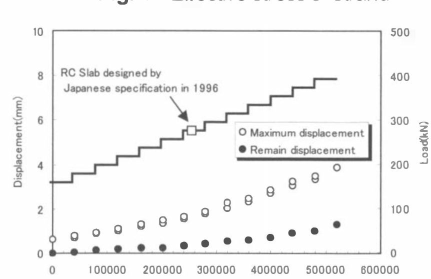

Fig. 5 Result of wheel running fatigue test

PERFORMANCE AND APPLICATION OF ECOCEMENT: A NEW TYPE PORTLAND CEMENT MADE WITH MUNICIPAL WASTE INCINERATOR ASH

Hiroshi HIRAO and Shigeru YOKOYAMA
Taiheiyo Cement Corporation, JAPAN

Keywords: Ecocement, waste, municipal waste incinerator ash, chlorine, recycle

1 INTRODUCTION

Municipal waste, the main waste products of domestic life, reached 50 million tons in 1997 in Japan. Most of it is usually reduced in volume to about 1/10 by incineration, and then disposed in landfill sites without being recycled. Moreover, the incinerator ash often contains toxic substances such as dioxins and heavy metals that call for very expensive care and treatment. Ecocement has been developed to provide a solution to these problems [1)2)]. The fundamental targets in the development of Ecocement are:(1) As much as 50% of the raw meal has to be replaced by incinerator ash or other waste materials such as sewage sludge, (2) The cement has to have general wide use, (3) Both the manufacturing process and the products have to be environment-friendly, (4) The entire process has to be a complete recycling system.

2 CHEMICAL DESIGN OF ECOCEMENT

A typical chemical composition of incinerator ash in Japan is shown in **Table 1**. Incinerator ash generally includes much more amounts of Cl, Na_2O, K_2O and P_2O_5 as well as Al_2O_3 than natural raw meals such as clay. Therefore, using incinerator ash close to 50% of raw meal leads to an increase these components in cement. Taking this into consideration, two types of Ecocement, (1) Normal type and (2) rapid-hardening type, are designed. Also, a typical chemical and mineral compositions of Ecocement is shown in **Table 2** in comparison with NPC.

Table 1 Chemical composition of incinerator ash

Major components (%)

ig. loss	SiO_2	Al_2O_3	Fe_2O_3	CaO	MgO	SO_3	Na_2O	K_2O	Cl
11.0	22.9	19.7	5.6	30.4	4.8	2.1	3.3	2.6	8.5

Minor components

TiO_2 (%)	P_2O_5	ZnO	CuO	Cr (ppm)	As	Cd	Hg	Pb	F	CN	PCB
0.9	1.8	0.6	0.6	438	55	11	3.5	311	120	ND	ND

Table 2 Chemical and mineral composition in Eco-cement

Type of cement	Chemical composition (%)									
	ig. loss	SiO_2	Al_2O_3	Fe_2O_3	CaO	MgO	SO_3	Na_2O	K_2O	Cl
Normal type	0.6	19.1	8.1	4.5	62.7	1.4	3.7	0.05	0.00	0.04
Rapid-hardening type	0.8	15.5	11.0	1.9	58.5	1.4	8.8	0.60	0.00	1.00
NPC	0.6	22.2	5.1	3.0	63.8	1.4	2.0	0.30	0.20	0.00

Type of cement	Mineral composition (%)					
	C_3S	C_2S	C_3A	$C_{11}A_7 \cdot CaCl_2$	C_4AF	$CaSO_4$
Normal type	49	12	14	–	13	7.7
Rapid-hardening type	44	11	–	17	8	15.0
NPC	56	19	9	–	9	3.4

2.1 Normal type

For the Normal type, the number of moles of Cl in the raw meal is designed to be equal to that of alkalis and metal components. Consequently, Cl is vaporized as compounds with alkalis and metal components in the sintering process and reduced down to below 0.1%.

2.2 Rapid-hardening type

Cl in the raw meal has to be in excess relative to alkalis in order to reserve Cl for the formation of $C_{11}A_7 \cdot CaCl_2$, eliminating C_3A. The $C_{11}A_7 \cdot CaCl_2$ phase contributes to rapid hardening. The Cl content in the final product is approximately 1%. Performance of this cement is similar to that of the rapid-hardening Jet cement which develops that performance because of $C_{11}A_7 \cdot CaF_2$.

3 MANUFACTURING PROCESS

The two types of Ecocement can be produced from the same production line. The whole process basically consists of the same unit processes used for NPC production: raw meal preparation, sintering and finishing processes. Since incinerator ash generally contains heavy metals such as Pb, Zn, Cu, Cr and As, a metal recovery process is designed and connected to the cement production line to recover these metals from the kiln dust.

4 PHYSICAL PROPERTIES

4.1 Normal type

This type of Ecocement develops nearly the same physical properties as NPC. The specific surface area of normal type Ecocement is higher than NPC, but the setting time of it is almost the same as NPC. The compressive strength of mortar with normal type Ecocement is a little lower than that of NPC because of the lower calcium silicate minerals.

4.2 Rapid-hardening type

The most distinguishing character of this type of Ecocement is the very short setting time and high early-strength development as observed in the test ages of 3 hours, 1 day and 3days, because calcium chloro-aluminate actively hydrates and rapidly forms ettringite. This is in the category of rapid hardening cement. The use of a retarder such as citric acid or other appropriate additives like blast furnace slag extends the setting time.

5 APPLICATION

Normal Ecocement can be used just as NPC; thus, it is suitable for very wide use. Properties of concrete with normal type Ecocement are described below. The rapid-hardening Ecocement contains a high chloride ion content of 1%; therefore, non-reinforced concrete products are a major area of application.

An example of mixing proportion and properties of fresh concrete with normal type Ecocement are shown in **Table 3**[3]. The unit amount of water and air entraining agent in concrete with normal type Ecocement are a little more than those with NPC. The changes of slump of concrete with normal type Ecocement with time are almost the same as those of NPC at ordinary temperature. The setting time of normal type Ecocement is 1 to 2 hours longer than NPC. The unit amount of chloride ion dissolved into free water in fresh concrete with normal type Ecocement is much lower than the 0.3 kg/m^3 (the upper limit specified in JIS A 5308). The relationships between cement-to-water ratio and compressive strength are shown in **Fig.1**[4]. The compressive strength of concrete with normal type Ecocement is a little lower than that with NPC as in the case of mortar. The cement-to-water ratio and compressive strength of concrete with normal type Ecocement has proportional relationship irrespective of curing condition as in the case with NPC. Therefore, concrete with normal type Ecocement can obtain the same compressive strength as that with NPC by decreasing the water-to-cement ratio.

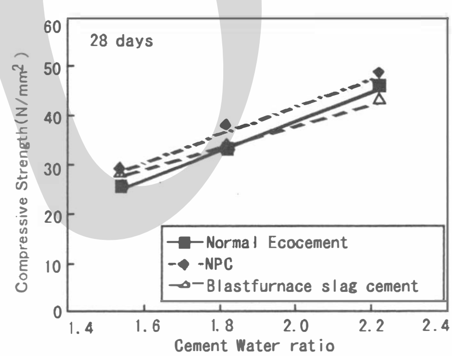

Fig. 1 Relationship between c/w and compressive strength of concrete under standard curing

Table 3 Mix proportion and properties of fresh concrete

	w/c (%)	s/a (%)	Unit weight (kg/m^3)				WRAE (C×%)	AE Agent (C×%)	Fresh Concrete		
			[illegible]	C	S	G			Slump (cm)	Air (%)	Cl$^-$ (kg/m^3)
Normal Ecocement	55.0	45	166	301	810	1040	0.25	0.0050	12.5	4.6	0.03
NPC		47	163	297	849	1006		0.0030	12.5	4.7	0.03
Blastfurnace slag cement		46	161	293	831	1024		0.0065	13.0	5.0	0.03

REFERENCES

1) OBANA,H., ANZAI,T. and FUKUNAGA,T., Proceedings of International Symposium on Environmental Issues of Ceramics, pp.63-67 (1994)
2) UCHIKAWA,H. and OBANA,H., World cement, pp.33-36 (1995)
3) TANAKA,S and YOSHIMOTO,M: Journal of research of the TAIHEIYO CEMENT CORPORATION, No.140, pp.92-100 (2001)
4) TERADA,M and MEIARASHI,S: Concrete Journal, Vol.37, No.8, pp.26-30 (1999)

PROPERTIES OF REPEATEDLY RECYCLED COARSE AGGREGATE CONCRETE

Takehiro Sawamoto Masanori Tsuji
Science University of Tokyo, JAPAN

Keywords: Recycled coarse aggregate, Strength, Durability, Colloidal silica, Non-freezing agent

1 INTRODUCTION

Recycled aggregate concrete should be widely used in the near future and it should also be repeatedly recycled. To sustain the properties of recycled aggregate, energy required in general processes manufacturing recycled aggregate must be more than that required to produce ordinary crushed stone aggregate, and also when the number of times recycling increases, final waste to be disposed must be more as byproduct. Therefore, it will be helpful to conserve or reduce energy in the recycling process that concrete waste can be recycled to be aggregate for concrete only by primary crushing and sieving. When the aggregate is recycled repeatedly, micro cracks remaining in the aggregate as well as mortar contained in it must increase. Thus the properties of repeatedly recycled coarse aggregate concrete must be low, and the recycled aggregate concrete can be applicable only to the low quality concrete.

In this study, some techniques to improve properties of repeatedly recycled coarse aggregate concrete, even when the aggregate is recycled only by primary crushing and sieving, are presented.

2 NEW TECHNIQUES TO IMPROVE PROPERTIES OF REPEATEDLY RECYCLED COARSE AGGREGATE CONCRETE

2.1 Absorption of colloidal silica solution into repeatedly recycled coarse aggregate (S)

The technique for repeatedly recycle coarse aggregate to absorb colloidal silica solution as a pozzolanic liquid was proposed to improve the compressive strength, the resistance against carbonation and chloride penetration, and the capability for shear transfer at interface along diagonal tension cracks. The absorbed colloidal silica is assumed to fill up micro cracks remaining in the recycled coarse aggregate and to set to gel by pozzolanic reaction.

2.2 Addition of cement clinker particle to repeatedly recycled coarse aggregate concrete (P)

The technique adding cement clinker particle in concrete was applied to make the resistance against carbonation and chloride penetration better. The grading of the cement clinker particle is similar to sand. The cement clinker can supply $Ca(OH)_2$ in much longer term compared with ordinary cement, therefore the repeatedly recycled coarse aggregate concrete can be kept in alkaline condition much longer.

2.3 Absorption of non-freezing agent into repeatedly recycled coarse aggregate (F)

To achieve higher resistance against repeated freezing and thawing action, the technique for repeatedly recycle coarse aggregate to absorb non-freezing agent solution was developed.

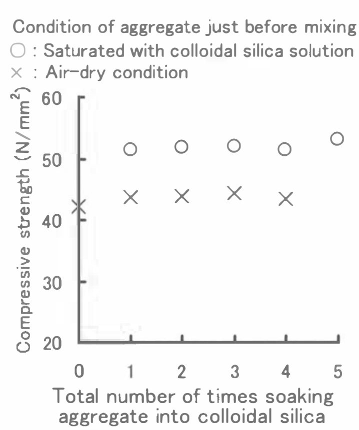

Fig.1 Compressive strength of concrete (RC5 : W/C=40%)

3 TEST RESULTS

Some examples of test results reported in this paper are shown in Fig.1～Fig.5

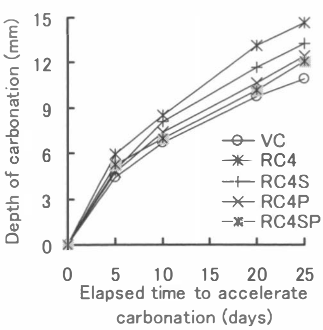

Fig.2 Carbonation depth of concrete (W/C=65%)

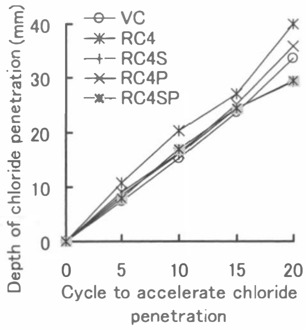

Fig.3 Depth of chloride penetration (W/C=65%)

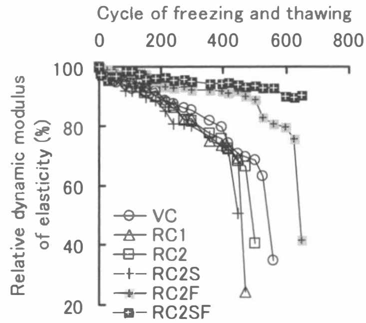

Fig.4 Freezing and thawing test result (W/C=55%)

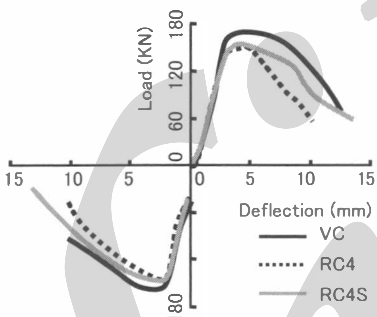

Fig.5 Load-deflection curve (W/C=45%)
[In case of shear failure on beams]

Note :
- **VC** means virgin aggregate concrete
- RC1 to RC5 means concrete consisting of coarse aggregate recycled 1 to 5 times, respectively
- S means the applied technique mentioned in 2.1 [Absorption of colloidal silica solution into repeatedly recycled coarse aggregate]
- P means the applied technique mentioned in 2.2 [Addition of cement clinker particle to repeatedly recycled coarse aggregate concrete]
- F means the applied technique mentioned in 2.3 [Absorption of non-freezing agent into repeatedly recycled coarse aggregate]

4 CONCLUSION

(1) When repeatedly recycled coarse aggregate is manufactured only by primary crushing and sieving, as the number of times recycling coarse aggregate increases, the power consumption required to crush decreases by more than 50% of that required to crush ordinal stone.
(2) When repeatedly recycled coarse aggregate is soaked in colloidal silica solution just before mixing, compressive strength of concrete becomes higher. This technique makes strength of repeatedly recycled coarse aggregate concrete enough to construct ordinary concrete structures.
(3) Elastic modulus of repeatedly recycled coarse aggregate concrete is significantly smaller compared with that of natural coarse aggregate concrete. The parallel model of natural coarse aggregate contained in recycled aggregate and total content of mortar in recycled aggregate and mortar matrix will be applicable to estimate the elastic modulus of repeatedly recycled aggregate concrete.
(4) As the number of times recycling coarse aggregate increases, carbonation and chloride penetration into repeatedly recycled coarse aggregate concrete becomes faster. However, the technique saturating recycled coarse aggregate with colloidal silica solution just before mixing concrete and the technique adding cement clinker particle to concrete can improve the durability of repeatedly recycled coarse aggregate concrete.
(5) Recycled aggregate concrete tends to be weaker against repeated freezing and thawing action. However, the technique for recycled aggregate to absorb colloidal silica solution and non-freezing agent can effectively improve the resistance against repeated freezing and thawing action.
(6) Maximum load and toughness of reinforced concrete that consists of repeatedly recycled coarse aggregate are lower when the reinforced concrete fails by shear. However, the technique for recycled aggregate to absorb the colloidal silica solution can significantly improve the unrespectable tendency.

STRENGTH AND DEFORMATION OF RECYCLED CONCRETE

Kinga Pankhardt Salem G. Nehme
Department of Construction Materials and Engineering Geology
Budapest University of Technology and Economics, Hungary

Keywords: recycled aggregate, concrete properties, Young's modulus, strength, neural networks

1. INTRODUCTION

Large volume of concrete waste generated during demolition makes it difficult for landfills to accommodate. Saving natural sources the recycling of building materials is one of the most important them in the waste management of EU. Our study shows, how mechanical properties of concrete are influenced when using recycled aggregate.
Are recycled materials competitive to natural aggregates?
The concrete from the demolition of a construction can be recycled as aggregate in new construction. It is generally combined with a natural aggregate when used in new concrete. Several developments have made recycling more economical.
Recycled materials are used both as aggregates to concrete (recycled concrete aggregate) and to layer of roads eg.

- **Recycling factor**: The amount of pre- and/or post-consumer material used to manufacture a recycled product (expressed as a percentage of the total content).
- **Recycled product:** Any product that is manufactured in part or in whole of recycled materials.

Recycled coarse aggregate is made of concrete with a crasher on the construction site.

2. EXPERIMENTAL STUDIES:

Analysis of recycled aggregate:
Picnometer method, aggregate in water saturated and surface dry condition.

- Water absorption after 10 Min (W_{10min}) or 24 h (W_{24h})
- Density

Analysis of fresh concrete

- Water-cement ratio

Analysis of hardened concrete

In order to determine the effect of recycled aggregate on the compressive strength, tensile strength and elastic modulus -using various proportion of natural and recycled aggregates- were tested in comparison to concrete containing 100% natural aggregate. [1,2]

3. THEORETICAL STUDIES:

At mesoscopic scale, concrete may be regarded as a three-phase composite consisting of coarse aggregate, mortar matrix and interfacial zones. (fig.1.)
The main influence factors of pore content of recycling concrete:

- type and pore content of used recycling aggregate,
- by producing of fresh concrete,
- by water/cement ratio,
- hydratation of cement,
- curing of concrete.

We calculated the pore content of recycling concrete with Neural Networks. [3]

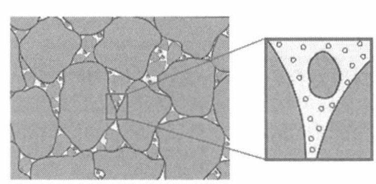

Fig.1. Porosity of concrete

4. RESULTS:

Mechanical properties of recycled aggregate depend on the art of demolition. Recycling concrete greatly saves energy compared to mining, processing and transporting natural aggregates.
The tensile and splitting strength of recycled concrete increase.
When calculating deformations, the V% of recycled and natural aggregate must be given.
By calculating the Young's modulus (W. Manns) reducing factors have to be applied.
Creep increases, because of the more cement content.

If frost and salt resistance is essential, concrete recycling-grains below 4 mm are not suitable for the production of concrete and must be replaced by sand.

The verification phase of the system demonstrates that the choice of Neural Network is able to learn the porosity depending on the factors: water/cement ratio, degree of hydration, cement content, air content of fresh concrete, d_{max} of aggregate, fineness modulus of aggregate.
Fig. 2. gives the graphical representation of the calculated and estimated porosity:

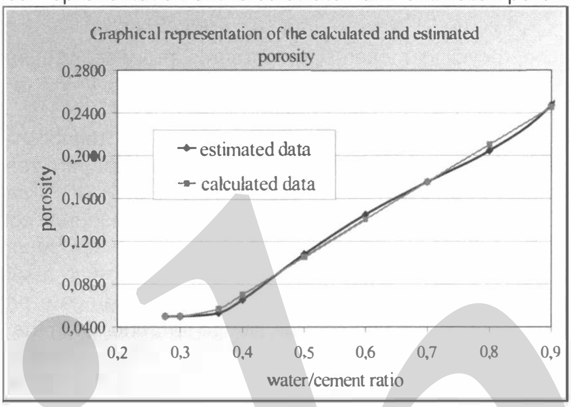

Fig. 2. Comparison of the calculation and the approximation of the porosity of concrete, cement content 350 kg/m^3, degree of hydration 1, initial porosity 0, d_{max} = 32 mm, fineness modulus 6.3.

Lot of the models consider that a fracture process zone exists at each crack tip and that a certain amount of fracture energy is needed for crack propagation. In our study we show, in many cases the crack tip starts at the pore.
The development of interface-surfaces is prevented by rough surface aggregate, because of the adhesion. (fig. 3.)

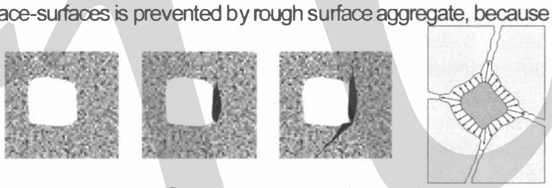

Fig. 3. Development of interface surfaces.
The 'softening'-zone of microcracks is ≈2,5 d_{max}. By increasing d_{max}, the zone of microcracks increases too. [4]

Following steps summarise the design considerations to minimise the pore content:
1. recycling concrete should be saturated,
2. by small water/cement ratio plastisizer should be applied,
3. detect the airspace-volume in recycling aggregate,
4. optimal duration of vibration.

To summarize the way to recycled concrete, we want to realise the recycling in the waste management, there are many factors to take into account. For successful realisation the same concept cannot be applied in every country, because of national traditions in building, and the use of different construction materials, different standards have to be developed.

5. REFERENCES:

[1] Pankhardt Kinga: Recycling of concrete , 2. International seminar on ECS, 24-25 May, 2001 Prague, pp 35-41.
[2] R. Haase, J. Dahms: Baustoffkreislauf am besonderen Beispiel von Beton… Beton 8/1996 S.480-486
[3] Charaf, H. and Vajk, I. (1995): Neural networks can be trained faster. *IFAC ACASP'95* Budapest.
[4] William Prager: Einführung in die Kontinuumsmechanik, Birkhäuser Verlag Basel uns Stuttgart, 1961

PROPOSED REQUIREMENTS OF MOLTEN SLAG AGGREGATES PRODUCED FROM MUNICIPAL SOLID WASTES AND SEWAGE SLUDGE

Yoshinobu Nobuta, Kajima Corp., JAPAN
Keishi Tobinai, Mitsubishi Material, JAPAN
Yasunori Suzuki, Sumitomo Osaka Cement, JAPAN
Kenji Nakura, Shimizu Corp., JAPAN
Yukikazu Tuji, Gunma Univ., JAPAN

Keywords: standardization, recycling, molten-slag aggregate, proposed requirement

1. INTRODUCTION

For promoting more usage of recycled materials such as demolished concrete, industrial by-products, municipal solid waste and so on for construction, standardization on their quality as material resources is indispensable. Japan Concrete Institute (JCI), in the view of future standardization as Japan Industrial Standard (JIS), organized a research committee for 5 different materials of recycled aggregate, Eco-cement, crushed-stone powder, municipal solid waste and incineration ashes of sewage sludge. After mainly reviewing the research results available at present, the committee proposed the draft requirements for molten slag aggregate produced from municipal solid waste (MSW) incineration slag/ash and sewage sludge for concrete in the form of a JCI standard, which is regarded as a pre-JIS, in consideration of the data insufficiency. Reported in this paper are the background and the overview of the JCI requirements for molten slag aggregate for concrete.

2. OUTLINES AND BACKGROUND OF ESTABLISHING JCI REQUIREMENTS – Draft

2.1 Applicable aggregate and concrete

The Ministry of Environment (MOE) holds the view that dioxins and PCB contained in slag decompose in the melting process at a temperature of 1,200°C or higher and that the items to be covered by the leaching standard are limited to the following six: cadmium, lead, hexavalent chromium, arsenic, total mercury, and selenium. This draft standard specifies the aggregate containing molten slag made from MSW or sewage sludge by being melted at 1,200°C or higher and granulated from the aspect of environmental safety. It also covers molten slag made innocuous in terms of dioxins.

The scope of concrete is defined in the stipulation as follows: "Concrete containing molten slag aggregate shall generally be applied to cast-in-place concrete in a relatively low design strength range of 21 N/mm^2 or less or replaceable precast concrete products. In order to ensure durability, the water-cement ratio (W/C) of concrete containing molten slag aggregate shall be not more than 55%."

The scope of application is defined in the stipulation as stated above in consideration of the limited field experience, insufficient data regarding long-term stability, and scarce trial application to reinforced concrete structures. The W/C is required to be not more than 55% to ensure durability. Since the strength of concrete containing molten slag aggregate is normally between 60 and 80% of that of normal aggregate concrete, W/C of around 50% provides a compressive strength between 20 and 40 N/mm^2. Also, W/C of 55% or less ensures durability to a certain extent. On the other hand, limiting the scope to an excessively low strength range may narrow the possible uses. These are the reasons for specifying W/C of not more than 55%. However, the use of molten slag aggregate for concrete with a higher strength level is not necessarily restricted provided the performance of the slag aggregate in the concrete, such as strength and durability, are confirmed.

2.2 Types and classes of aggregate

Molten slag is divided into water-granulated slag and air-cooled slag. Water-granulated slag is made by quenching molten slag by direct contact with water to obtain glassy granules or sand suitable for fine aggregate. Air-cooled slag is made by cooling it in the atmosphere to allow it to crystallize into lumps primarily used for coarse aggregate. Molten slag air-cooled to a high degree of crystallization by cooling at a low rate may be particularly referred to as slow-cooled slag, but it is included in the air-cooled slag here for the sake of convenience. Coarse and fine aggregates of molten slag for concrete are each divided into four grading classes in this standard: 25-5, 20-5, 15-5, and 10-5 mm for coarse aggregate and 5 or less, 2.5 or less, 1.2 or less, and 5-0.3 mm for fine aggregate. The fine grading class of 1.2 mm or less and coarse grading class of 5-0.3 mm are specified in consideration of the case of blending with normal fine aggregate. No alkali-silica reaction has reported in concrete using molten slag aggregate. However, this does not necessarily assure innocuousness of all molten slag aggregate. When using aggregate not judged innocuous by testing or untested, measures should be taken to suppress alkali-silica reaction.

2.3 Qualities of aggregate

Care should be exercised to prevent inclusion of deleterious amounts of dirt, mud, organic impurities, and the like. Also, the aggregate and the structure or work piece using the aggregate should be confirmed as not polluting the environment throughout the processes of storage, transportation, and production, as well as in use. It is also advisable to take measures during the production process to inhibit leaching of hazardous substances mentioned previously for leaching to be limited to the specified values. MOE Notification No. 13 was adopted as the material test standard for the relevant grading in Japan, though the leaching time differs from that of the prEN standard.

It is desirable to confirm that the contents of typical hazardous chemical components in molten slag aggregate are limited to the values given in the requirement. Metallic aluminum aggregate can react with calcium hydroxide and water in concrete, generating hydrogen gas. The standard requires confirmation by the mortar test because of the scarcity of data available on the relationship between the hydrogen gas generation and metallic aluminum content of molten slag aggregate. The metallic iron content is specified not to be more than 1.0% from the standpoint of preventing corrosion staining where aesthetic appearance of concrete surfaces is required.

Table 1 Quality of molten-slag aggregate (proposal)

Classification	Item	Coarse aggregate	Fine aggregate
Chemical components	Calcium oxide (as CaO) %	45.0 or less	
	All sulfur (as S) %	2.0 or less	
	Sulfur trioxide (as SO_3) %	0.5 or less	
	Metal aluminum %	Expansion ratio of the mortar by JSCE-F 522 must be 2.0% or less.	
	Metal iron (as Fe) %	1.0 or less	
	Amount of chlorides (as NaCl) %	0.04 or less	
Physical properties	Density under oven-dry g/cm^3	2.5 or more	2.5 or more
	Rate of water absorption %	3.0 or less	3.0 or less
	Soundness %	12 or less	10 or less
	Solid volume %	55 or more	53 or more
	Percentage of abrasion %	40 or less	-----
	Amount of material passing standard sieve 75 μ m in aggregates [1)]	1.0 or less	7.0 or less

Note 1):Amount of material passing sieve 75 μ m in aggregates when wearing the surface of concrete out is made into 1.0% or less with coarse aggregate, and is made into 5.0% or less by the fine aggregate.

The physical properties of molten slag aggregate are required to fulfill the specifications given in Table 1. Since molten slag aggregate may become porous depending on the treatment conditions, the absorption and soundness were specified to exclude porous aggregate. Also, crushing may cause particles having inadequate shapes to be generated. Since such particles can produce adverse effects on the workability of concrete, the solid volume percentage was specified. Unlike clay and silt passing a 75μm sieve included in normal aggregate, fine particles included in molten slag aggregate does not adversely affect the qualities of concrete, but is rather expected to contribute to reductions in the amount of bleeding water. It is therefore desirable to use such powder as much as practicable. Accordingly, molten slag powder is treated similarly to JIS for crushed stone and manufactured sand.

3. CONCLUDING REMARKS

The Recycling Standardization Committee established a JCI Requirement (draft) for the qualities of molten slag produced from MSW and sewage sludge from the users' standpoint based on a survey of past research accomplishments. The committee considers that it is preferable to formulate the technical report or JIS in cooperation with producers after supplementing insufficient data.

REFERENCES

[1] Public Works Research Institute, "Manual of assessment of test result on recycled materials for public works – draft" and "Development of utilization of waste for construction", Ministry of Construction, 1999.9 and 1986
[2] Yamaura T., "Applicability of molten slag produced from sewage sludge", Ready-Mixed Conc., No.9, 1992
[3] Kitatsuji M. et al, "Fundamental study on applicability of molten slag produced from municipal solid waste as fine aggregate for concrete", Proceeding of Agricultural and Civil Engineering, No.6, Vol.65, pp.1-8, 1997
[4] Naruse H. et al, "Study on applicability of molten slag produced from municipal solid waste as aggregate for concrete", Report of Ube Mitsubishi Research Institute, No.1, pp.47-56, 2000
[5] JTCCM, "Report on standardization of recycling system of construction materials", pp.182-230, 2000.3
[6] JSWME, "Committee report on leaching tests of heavy metals from eco-cement materials", pp.8-20, 2000.3.24

FRACTURE MECHANICS ON CONCRETE WITH RECYCLED AGGREGATE

K. Zilch M. Cyllok
TU München, Lehrstuhl für Massivbau, Munich, Germany

Keywords: recycling, laps, cracks, serviceability

1 INTRODUCTION

The building industry and building owners anticipate increasing crack widths due to the use of concrete with recycled aggregate (recycling concrete). Crack widths beyond the limitation of the German standard DIN 1045-1 [1] lead to recourse claims, hence it is necessary to analyse fracture mechanics on recycling concrete. Funded by the Bavarian State Ministry for Regional Development and Environmental Affairs, large slab specimens of up to 100% from building rubble recycled aggregate with laps were tested to investigate cracks at the serviceable limit state (SLS) as well as other SLS-criteria and the performance of the lap section at the ultimate limit state (ULS).

2 TEST WITH SLAB SPECIMENS

2.1 Test specimens

All specimens have the same geometry (Fig. 1), but different compositions, see Table 1. Five 420 mm overlapping bars (Ø16) serve as a longitudinal reinforcement.

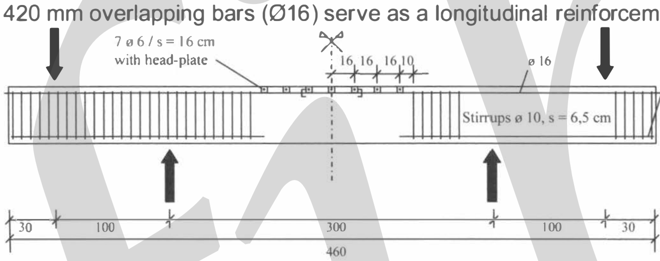

Fig. 1 Dimensions and bar arrangement of the specimens

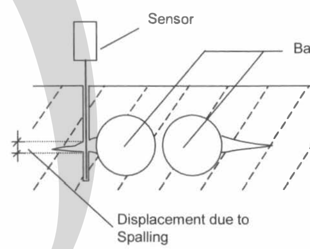

Fig. 2 Spalling displacement of cover measured with sensor

The recycled aggregate is regular crushed building rubble from an ordinary aggregate dealer. It was stored till production time in a dry room at approx. 20°C. A mix without additional water was put in the mixer and for D3 and D4 water was added till the consistency of the D1 and D2 was reached to provide the extra needed water.

Table 1 Properties and compositions of fresh concrete in slab-specimens

	CEM I 32,5 R [kg/m³]	Fly Ash [kg/m³]	All aggr. [kg/m³]	Nat. aggr.	Crshd concr.	Crshd brick	Crshd sand-lime-brick	Water		Super-plasticizer [g/kg$_{cem}$]	ρ_{cm} [kg/m³]	Flow table value [cm]
								Basic [kg/m³]	Add [kg/m³]			
D0	245*	-	1980	100%	-	-	-	210	-	-	2430	41
D1	382	-	1699	-	100%	-	-	210	-	3,7	2290	42
D2	338	-	1821	35%	65%	-	-	186	-	8,3	2340	47
D3	245	109	1596	-	50%	20%	30%	194	52	9,0	2160	53
D4	272	117	1631	-	34%	33%	33%	222	19	12,8	2150	43
*:	For composition 0 CEM I 42,5 was used.											

2.2 Test procedure and results

Loads were applied in stages in which crack widths, crack patterns and concrete strains were taken. Deflections in three points between the two supports at a pitch of 500 mm, stresses and slippage of the reinforcement (especially in the lap) as well as the actual displacement of the concrete cover due to spalling, see Fig. 2, were measured continuously. Finally loads were increased till failure.

Table 2 shows that at the same compressive strength (D1 and D2 have over strengths) modules of elasticity of the recycling concretes are 10% to 35% lower than the recommended value of DIN 1045-1 [1], which is normal. The splitting tensile strengths given in Table 2 are for all specimens in the same range. For all specimens bond failure without full spalling of the concrete cover over the lap occurred beyond the ULS-load-stage.

Table 2 Properties of the slab specimens

Type	E cm [N/mm²]	f cm,cube [N/mm²]	f ctm [N/mm²]	w cent 1) [mm]	w end 2) [mm]	w bent 3) [mm]	M Ru,meas / M Ru,calc
D0	28800	27,1	2,3	-	0,20	0,20	1,06
D1	22800	38,9	2,6	0,04	0,12	0,20	1,29
D2	26300	46,3	2,7	-	0,04	0,20	1,31
D3	19700	31,1	2,3	0,10	0,20	0,28	1,22
D4	19100	28,7	2,9	0,14	0,20	0,28	1,30

Note 1: Measured maximum crack width in the centre of the lap zone
Note 2: Measured maximum crack width at the end of the lap zone
Note 3: Measured maximum crack width outside the lap zone

Fig. 3 shows a typical bond failure situation of the lap-section of the specimens. This illustrated failure of D4 (similar to D3) shows extreme crack widths not encountered in the tests of the specimens D0 to D2. Furthermore for D3 and D4 spalling starts earlier and also the bars in the laps of these specimens start to slip earlier.

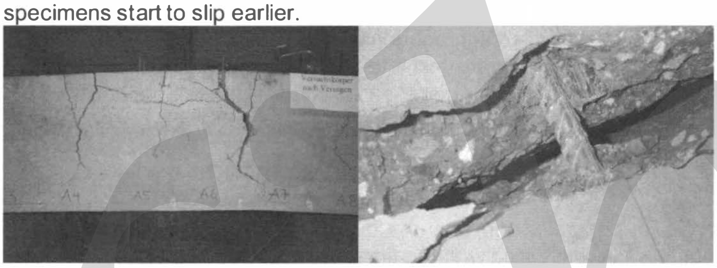

Fig. 3 Lateral and detailed view of the failing lap section of specimen D4

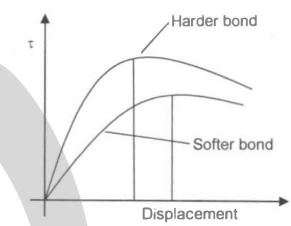

Fig. 4 τ-displacement relationships (qualitative)

Assuming a softer bond for these compositions this can be explained. This doesn't contradict the fact that the resistance of the lap is not reduced as a harder bond doesn't per se transmit a higher maximum force than a softer bond, see Fig. 4.

What about cracking? The cracks are initiated at different stages: For D1 and D2 ca. 3 cracks appeared at 0,33 M_{rk} (a third of the SLS-load-stage), while for D3 and D4 about 12 to 14 cracks could be found at the same level. At the SLS-load-stage of 1,0 M_{rk} when for all specimens the crack initiation was completed, the crack spacing for D0 to D2 was wider (15 cm to 20 cm) than for D3 and D4 (under 10 cm), as exemplarily displayed in Fig. 5 and Fig. 6. The greater crack widths for D3 and D4 (Table 2) result from the softer bond and the narrower crack spacing and the early initiation are caused by a great number of soft spots (e.g. sand-lime-stone aggregate).

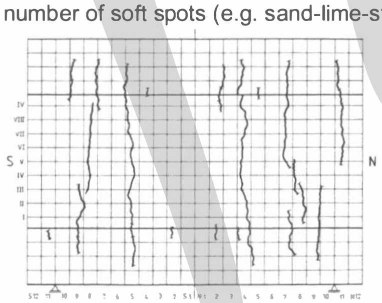

Fig. 5 Crack pattern for D2 at SLS-load-stage

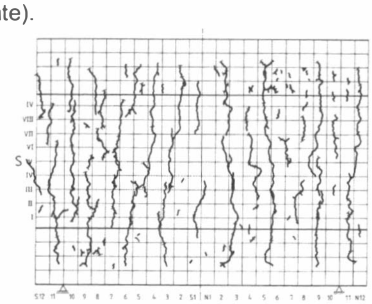

Fig. 6 Crack pattern for D4 at SLS-load-stage

3 CONCLUSION

Laps in concrete with recycled aggregate at the ULS and SLS were tested and proved that they comply with the requirements member resistance, crack widths, steel stresses and deflection.

4 REFERENCE

[1] DIN 1045-1, Concrete, reinforced and Prestressed concrete structures – Part 1: Design, Berlin: Beuth, Jul., 2001

STANDARDIZATION OF TECHNOLOGY TO UTILIZE RECYCLED MATERIALS FOR CONCRETE

Yukikazu Tsuji
Gunma University, JAPAN

Yasunori Suzuki
Sumitomo Osaka Cement, JAPAN

Keywords: standardization, recycled aggregate, Eco-cement, crushed-stone powder, molten-slag aggregate, Technical Report

1 INTRODUCTIN

Research on utilization of recycled materials has been advanced regarding recycled aggregate, Eco-cement and crushed-stone powder, municipal solid waste, incineration ashes of sewage sludge, and so on. For the widespread usage of these recycled materials, standardization is indispensable.

The paper reports the circumstances and the summary of each establishment regarding the Technical Report (TR)[1] on concrete using recycled aggregate and Eco-cement, the draft proposal of TR on crushed-stone powder and the Japan Concrete Institute (JCI) draft standard of molten-slag aggregate by which a draft proposal was stipulated in the research committee for standardization of technology to utilize recycled materials for concrete established in JCI.

2 DIFFICULTY AT TIME OF STIPULATING JIS OF RECYCLED MATERIALS

When using recycled materials for concrete, generally the quality of the concrete with recycling material is sub-standard. Although it was a big difficulty at the time of stipulating JIS, this difficulty has still not been solved at this time. Since existing concrete-related JIS does not assume the above-mentioned situations, when stipulating JIS of recycled materials or standardizing, it was made to recognize that the obstacle is serious. Then, it could only start with the argument about recycled materials changing the character of the standard of JIS. The committee members had to unify on how the concrete with recycled materials is used.

Therefore, in the recycling standardization committee, we stopped stipulating the JIS draft proposal and decided to stipulate the TR draft proposal classified into type II of the TR in the order of Eco-cement, recycled aggregate, and other recycled materials.

3 STANDARDIZATION OF RECYCLED MATERIALS

In order to incorporate recycled aggregate into the JIS system of conventional concrete, the TR draft proposal of the concrete using recycled aggregate was stipulated first (Table 1). In addition, the recycled aggregate produced by crushing hardened lumps of residues from ready mixed concrete is also included, but with some restrictions. And as for the use of the standard type of which the nominal strength is 12MPa, it is desirable to limit to the components of high strength or high durability, such as backfilling concrete, between stuffing concrete, leveling concrete, and sub-slab concrete are not required. In addition to the standard type, the salinity-control type (less than 0.3 kg/m^3) and the customized type (the maximum of nominal strength is 18MPa) are prepared.

Table 1 Quality of Recycled Aggregate (TR A 0006:2000)

Item	Recycled coarse aggregate	Recycled fine aggregate
Rate of water absorption %	7 or less	10 or less
Amount of material passing standard sieve 75 μm in aggregates %	2 or less	10 or less

Concerning crushed-stone powder, it is limited to what passes through a 75 μm sieve in which the by-product is separated by dry process at the time of manufacture of a crushed stone or a crushed sand, and the draft proposal of TR was proposed. Such crushed-stone powder may be used for the purpose of increasing the material's separation resistance of concrete. The cause of the limitation as mentioned above is that the direction of the fine powder which passes through a 75 μm sieve can lessen a unit weight of water from the examination result of mortar and concrete. Moreover, although it was thought possible to also use the crushed-stone powder from drying cake manufactured by wet process, experiment data was insufficient, so it was limited to dry type.

The issue of standardization of molten slag which utilizes the incineration ashes of a municipal solid waste and a sewage sludge to concrete was taken up. When using municipal-solid-waste incineration ashes, a sewage sludge and its incineration, the leach-out problem of toxic substances, such as heavy metals, was a big problem. Although based also on the manufacture method, it is becoming clear by melting and slag-izing municipal-solid-waste incineration ashes, a sewage sludge and its incineration ashes that the leach-out of toxic substance does not pose so big a problem. Therefore, the quality of molten-slag aggregates was specified by JCI.

Eco-cement is resources circulation type cement. In addition to the mineral composition of usual cement, the Eco-cement developed at the beginning contained $C_{11}A_7$ and $CaCl_2$ as a calcium aluminate system clinker mineral, and the amount of chloride ion was 5000 ppm or more, and it was a regulated set type. Then, progress of dechlorine technology was made and the normal type Eco-cement which also usually controlled the amount of chloride ion from portland cement to many grades was developed. In standardization, we decided to usually specify two kinds, a normal and a regulated set type (Table 2).

Table 2 Quality of Eco-cement (TR R 0002:2000)

Item		Normal-type Eco-cement	Regulated-set-type Eco-cement
Specific surface area	cm^2/g	2500 or more	3300 or more
Setting time	Initial setting min	60 or more	5 or more
	Final setting hour	10 or less	1 or less
Soundness	Putting method	Goodness	Goodness
	Le Chatelier's method	10 or less	10 or less
Compressive strength N/mm^2	1 day	-----	15.0 or more
	3 days	12.5 or more	22.5 or more
	7 days	22.5 or more	25.0 or more
	28 days	42.5 or more	32.5 or more
Magnesium oxide	%	5.0 or less	5.0 or less
Sulfur trioxide (as SO_3)	%	4.5 or less	10.0 or less
Ignition loss	%	3.0 or less	3.0 or less
Total alkali	%	0.75 or less	0.75 or less
Chloride ion	%	0.1 or less	0.5 or more and 1.5 or less

4 CONCLUSION

The results of the research committee's investigation into the standardization of the practical use of technology of recycled materials in concrete which was established in JCI in 1998 have been shown. TR R 0002 (Eco-cement) and TR A 0006 (Concrete using recycled aggregate) have already been released. TR draft proposal of crushed-stone powder was presented, and the specifications of the molten-slag aggregate of municipal solid waste and sewage sludge were also presented as a JCI standard (proposal). The paper focused on the areas which resulted in this standardization.

Unfortunately, it seems that concrete made using recycled materials would result in a reduction in quality. Even the quality of concrete would be varied. However, in appreciating the worries of our society regarding environmental problems, we would like to propose the standardization of recycled materials used in concrete. It would be tremendous if this proposal could be adopted by JIS from now on, and at the same time be accepted by the people of Japan, so a new industry can be born.

REFERENCES

[1] Standards Department in Agency of Industrial Science and Technology, "About foundation of the Technical Report (TR) system ," Standardization journal, Vol.27, 1996,p.7

OUTLINE OF TECHNICAL REPORT FOR ECOCEMENT (TR R 0002: 2000)

Shigeru YOKOYAMA
Taiheiyo Cement Corporation, JAPAN

Keywords: Ecocement, incinerator ash, recycle, heavy metal, chloride ion

1 INTRODUCTION

In Japan, municipal waste (e.g. garbage) reached 50 million tons in 1996. It has continued to increase with the rising level of living, the changing life-style and population concentration in urban areas. Rapid increase in municipal and industrial waste has been causing several serious environmental problems. For years, municipalities have chosen the use of garbage incinerators so that the life of the disposal sites can be extended by reducing the volume of dumping materials. The incinerator, however, does not give a final solution as it produces ash which has to be dumped, keeping the municipalities still looking for the next site. Moreover, the incinerator ash often contains toxic substances such as dioxins and heavy metals which call for very expensive care and treatment.

Ecocement is a new type of Portland cement being developed not only to solve the municipal and industrial waste problem caused by limited availability of landfill sites, but also to contribute to the protection of the environment.

Ecocement is heated to more than 1300°C in the sintering process. Toxic organic substances are completely decomposed and heavy metals such as lead are volatilized to separate from cement clinker.

Concerning prevention of environmental pollution, the Ecocement manufacturing plant has to meet strict standards for emission, eliminating NOx, SOx, HCl, dioxins and any other toxic substances. The product, Eco-cement, has to be safe when it is used, for instance, safe regarding leach-out of toxic substances from concrete. Any secondary pollution must not be caused.

The development of Eco-cement was a collaboration project between the New Energy Development Organization (NEDO; an extra-governmental organization of the Ministry of Economy, Trade and Industry (MOETI)) and three private companies.

Two big local governments have approved the construction of commercial plants; Ichihara Ecocement plant (in Chiba pref.) as the first commercial Ecocement plant in the world has been working since April, 2000 and produces 110,000 ton-cement/year (using 90,000 t/y of incinerator ash), and Tokyo Ecocement plant (at Tama district of Tokyo) that produces 200,000 ton-cement/year (using 130,000 t/y of incinerator ash) is now under construction.

Technical Report for Ecocement (TR R 0002: 2000) was published on May 22, 2000.

This paper describes the standardization of Ecocement and discussion in the committee of the Japan Concrete Institute (JCI).

2 BACKGROUND of TR FORMULATION

With the aim of realizing a resource-recycling society, the Ministry of Economy, Trade and Industry (MOETI) designated the Ecocement as a recommended technology in the “Eco-town” projects. The Ministry of Environment also approved the technology as a method of treating and utilizing incinerator ash. In these circumstances, standards for Ecocement have been strongly desired.

The MOETI assigned formulation of a technical report to the Japan Standards Association (JSA) to accelerate discussion for early publication and standardization of the technical information for Ecocement. JSA re-assigned the work to JCI, which in turn organized a committee, in which Working Group 5 took the leadership of formulating the draft for Technical Report (TR R 0002: 2000) as Type II.

3 SUMMARY of TR

3.1 Definition

Standardization of Ecocement aims to promote active popularization/use of recycled materials. Ecocement is defined as follows:

(1)Ecocement

It is well known that Portland cement is currently produced using industrial waste. Ecocement is regarded as cement made using much more waste as raw materials than normal Portland cement. Ecocement is designed to use primarily municipal waste incinerator ash, and sewage sludge or other waste materials more than 500kg of the raw materials to produce a ton cement.

The qualities of Ecocement depend on chloride ion contents. Ecocements produced from incinerator ash containing chloride ions are classified normal Ecocement and rapid-hardening Ecocement. The two classes of Eco-cement can be produced from the same production line by controlling the amount of Cl in cement clinker.

(2)Normal ecocement

Normal Ecocement is a class of cement in which chloride ions content is reduced to less than 0.1 mass % of cement by dechlorination of the cement raw materials during production, The properties of this class are similar to those of ordinary Portland cement specified in **JIS R 5210 (Portland cement)**[2)3)] and can be used for plain concrete and general reinforced concrete.

(3)Rapid-hardening ecocement

Rapid-hardening Ecocement is a class of cement having a chloride ion content of 0.5 to 1.5% by mass of cement. It shows rapid-hardening properties, with chloride ions in the materials being bound in cement minerals. It is can be used for plain concrete.

3.2 Quality of Ecocement

The quality specifications are given in Table1 in comparison with commercial cement values.

Table1 Quality of Ecocement

Quality		Class	Normal Ecocement			Rapid-hardening Ecocement		
			Standard	Commercial cement		Standard	Commercial cement	
				ave.	std. dev.		ave.	std. dev.
Density		g/cm^3	–	3.16	–	–	3.18	–
Specific surface area		cm^3/g	2,500min.	4,320	133	3,300min.	5,055	59
Setting	Initial setting	h-min	1-00min.	2-19.	13	–	0-11.	1
	Final setting	h-min	10-00max.	3-25.	13	1:00max.	0-21.	1
Stability	Pat method		Good	Good	–	Good	Good	–
	Le Chaterier method	mm	10max.	–	–	10max.	–	–
Compressive strength N/mm2	1d		–	–	–	15.0min.	24.5	1.6
	3d		12.5min.	29.7	1.5	22.5min.	35.2	1.7
	7d		22.5min.	41.1	1.7	25.0min.	39.2	1.7
	28d		42.5min.	53.2	1.7	32.5min.	48.9	2.5
Magnesium oxide		%	5.0max.	2.08	0.11	5.0max.	1.69	0.02
Sulfur trioxide		%	4.5max.	3.75	0.17	10.0max.	8.19	0.12
Ignition loss		%	3.0max.	1.25	0.08	3.0max.	1.26	0.01
Total alkali		%	0.75max.	0.43	0.06	0.75max.	0.39	0.03
Chloride ion		%	0.1max.	0.054	0.009	0.5-1.5	0.879	0.022

PHYSICAL - MECHANICAL PROPERTIES OF POLYMER MODIFIED CONCRETE WITH RECYCLED BRICK AS AGGREGATE

Prof. Mihailo Muravljov Prof. Aleksandar Pakvor
Faculty of Civil Engineering, University of Belgrade,
Bulevar kralja Aleksandra 73, 11000 Belgrade,
YUGOSLAVIA

Ksenija Jankovic, Ph. D.
Research Associate
IMS Institute, Bulevar vojvode Misica 43,
11000 Belgrade, YUGOSLAVIA

Keywords: polymer modified concrete, recycled aggregate concrete, brick, physical - mechanical properties.

1 INTRODUCTION

Deposit of large quantity of building materials resulting from demolition of structures or from natural or other catastrophes, represents a significant ecological problem. That is why the possibility of recycling waste building material seems often justified and sometimes even the most optimum solution.

On the basis of characteristics of polymer portland modified concrete (PMC) and concrete made on the base of crushed brick, it has been assumed that concrete, modified by polymer on the base of recycled brick, shall be material which will preserve good properties of both types of concrete.

Determination the influence of used polymer and cement quantity on the some modified concrete properties is shown in this paper.

Experimental work included few types of concrete made with different cement content (250 or 350 kg/m^3), and the same consistency (slump about 5 cm), and with 0, 4 or 8 % admixture of polymer (dry material) concerning cement content.

The PMC properties depend, not only on composition but also on the way of preparation, compacting and curing of such concrete. All types of concrete were curing as follows: one day in wet conditions, six days in water and the rest in air as proposed in [2].

The influence of polymer on concrete composition on its compressive and bending strength, module of elasticity, coefficient of heat conductivity, resistance to frost and waterproofness are observed.

2 EXPERIMENTAL WORK

2.1 Component materials and concrete mixtures

Experimental work included six kinds of concrete. Concrete mixtures were made using pure Portland cement, which, according to Yugoslav standards, is marked PC 45 (its compressive strength is approximately 45 N/mm^2 when it is 28 days old). Crushed bricks were separated into fractions 0/4, 4/8, 8/16 and 16/32 mm. Concrete mixtures B, C, E and F were made using polymer “Polibet” (produce by “Prvi Maj”, Cacak, Yugoslavia). It was latex BSR, with 47.4 % of dry materials in dispersion. One part of water providing the required consistency (slump about 5.0 cm) of the mixture (free water i.e. effective water). Quantity of absorbed water is equivalent average value of water absorbed by aggregate after 30' as proposed in [1]. Concrete composition is shown in Table 1.

Table 1 Quantities of component materials of concrete

Type of concrete		A	B	C	D	E	F
Cement (kg/m^3)		350	350	350	250	250	250
Aggregate (kg/m^3)	0/4 mm	469	458	458	504	487	487
	4/8 mm	161	157	157	173	167	167
	8/16 mm	214	210	210	230	222	222
	16/32 mm	496	485	485	533	514	514
Water (kg/m^3)	Absorption	224	219	219	240	232	232
	Free	79	51	36	40	38	28
Polymer (kg/m^3)		-	29.6	59.1	-	21.1	42.2

2.2 The results of investigations

By testing the specimens of cube having 15 cm long edges compressive strength of concrete was established. The obtained strengths of all kinds of concrete examined after 28 days are shown in Table 2.

Bending strength of concrete was tested on prismatic specimens of dimensions 15 x 15 x 60 cm. One concentrated force on half of specimen span (l = 50 cm) was taken as the loading. The obtained strength of all concrete examined after 28 days is shown in Table 2.

Modulus of elasticity has been examined for all kinds of concrete after 28 days on cylindrical specimens d/h = 15/30 cm. The results are shown in Table 2.

Waterproofness has been tested according to Yugoslav standard (on cylindrical specimens d/h = 15/15 cm; 8 hours at 1 bar, 8 hours at 2 bars, etc.). The specimens of concrete D satisfied at water's pressure at 8 bar. Other concrete satisfied at water's pressure at 12 bars.

According to Yugoslav standard frost resistance was tested on prismatic specimens of the dimension 12 x 12 x 36 cm by nondestructive method (after 25 freezing and thawing cycles decrease of dynamically modules if elasticity was tested; maximal decrease after testing is 25 %). Number of freezing and thawing cycles, which satisfied decrease of dynamically modulus of elasticity, is shown in Table 2.

Coefficient of thermal conductivity of concrete was tested for concrete A, C and E. Laboratory coefficient of thermal conductivity λ at the mean temperature t_M = 10 ^oC is shown in Table 2.

Table 2 Properties of concrete

Type of concrete		A	B	C	D	E	F
Compressive strength	N/mm^2	28.4	20.9	23.0	19.0	20.3	15.9
Bending strength	N/mm^2	1.9	2.2	2.0	2.3	2.2	2.1
Modulus of elasticity	GPa	14.5	11.1	11.6	13.6	11.7	11.5
Frost resistance	Number of cycles	125	125	150	50	150	75
Coefficient of thermal conductivity	W/ (mK)	0.556	-	0.544	-	0.505	-

3 CONCLUSIONS

Analyzing results of investigations it can be conclude that polymer modified concrete based on recycled bricks has approximately same value of compressive and bending strength, worse modulus of elasticity, better waterproofness and frost resistance, than concrete without polymer.

Polymer modified concrete has less absorption than unmodified concrete, so it is more waterproof. Polymer modified concrete has greater air content and less absorption than unmodified concrete. That is a reason why it has better frost resistance.

Measurement thermal conductivity values of lightweight concrete, with (or without) polymer, can be of opinion like as satisfied low. In addition to relative high bulk dry densities, here can be talking about concrete that have relatively small thermal conductivity, e.g. good thermal performances.

Concrete based on recycled brick can be used for production of various solid and hollow construction blocks. Beside their function as thermal insulators, such blocks, with regard to their mechanical characteristics, can have an important role in the bearing walls of buildings.

REFERENCES

[1] Hansen,T. : Recycling of demolished concrete and masonry, Report of Technical Committee 37-DRC Demolition and Reuse of Concrete, RILEM, E & FN SPON, London, UK, 1992.

[2] Jankovic, K. : Polymer modified concrete based on recycled bricks - choice of curing, VII INDIS and CIB W-63, FTN-IAG, Proceeding, Vol. II, Novi Sad, Yugoslavia, 1997, pp 115 - 123

[3] Jankovic, K. : Polymer modified concrete based on recycled brick, dissertation, Faculty of Civil Engineering, University of Belgrade, Yugoslavia, 1999, (on Serbian)

RECYCLING OF WIRE-ROPES FOR RC, PC AND FRC STRUCTURES

Géza Tassi
Budapest University of Technology
and Economics, Budapest, HUNGARY

Béla Magyari
Innomat Ltd.
Kecskemét, HUNGARY

József Szlivka
Archi+Med L
Budapest, HUNGARY

Keywords: recycling, wire-ropes, prestressing strands, fibre reinforcement

1 INTRODUCTION

Wire-ropes are widely used in various fittings all over the world. Because of the very strict regulations, these ropes must be replaced much before they loose their load capacity. Recycling of this material is advantageous from the environmental protection point of view and as well as economy. The object of the present investigation is to prove the applicability of worn out wire-ropes in concrete construction. [1], (Fig.1)

2 TECHNOLOGICAL PROCEDURE FOR PROCESSING THE USED WIRE-ROPES AND THE CHARACTERISTICS OF THE RECYCLED MATERI AL

The most suitable methods for processing this material are the following: a) cleaning and cutting followed by quality control, b) producing strands, cleaning and cutting followed by quality control, c) cutting the rope to gain fibre reinforcement. According to the quality control results and classification, the effective cross section can be utilised in 100, 82 and 67%, and the design stress 100, 70 and 60% of the original steel. It was proven experimentally that the bond properties of recycled strands correspond to the requirements.-

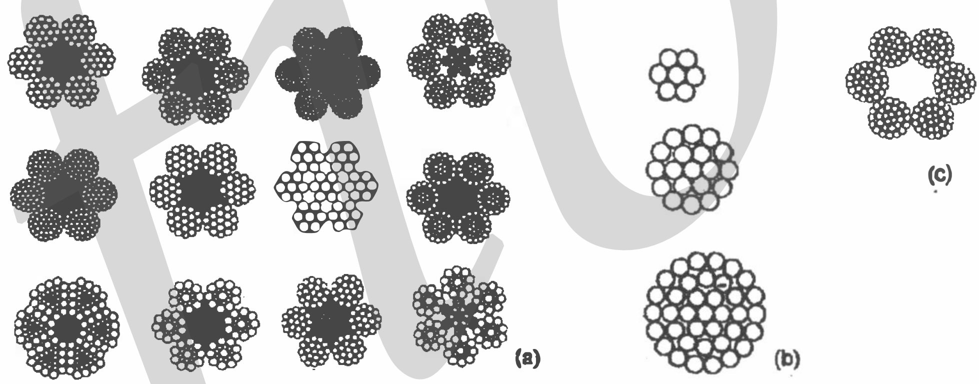

Fig.1 Cross sections of ropes suitable for recycling
(a) Arrangement of ropes (b) strands gained from ropes to be used as prestressing tendons (c) a rope which was used to produce fibre reinforcement

3 BEAM TESTS

Prestressed pre-tensioned beams were tested. The testing arrangement, the geometrical data, as well as the grade of the concrete were equal. Two beams were prestressed by original strands while four beams by recycled ones. The crack patterns, crack widths and load capacities did not show any significant variation between the beams with original and those with recycled strands. [7]

4 APPLICATION OF RECYCLED FIBRES

Fibre reinforcement was made with used ropes consisting of thin wires. A series of experiments were carried out with the same concrete mix (note: additional cement was added in the case of fibre reinforcement). Cubes were made for testing the characteristics of cube strengths, bearing resistance and beams for flexural behaviour. All the FRC specimens were made with commercial as well as recycled fibres. The flexural members were with two different reinforcing bars as well as without. It was found that cube strength was influenced slightly by fibre reinforcement. The effect of fibres is also low in bearing strength but more significant in toughness in case of a force transmitted on a section of the cube. The beam tests have shown a slightly increasing flexural tensile resistance and a more significant total deformation work with increasing amount of fibres. The essential finding is that there was no noteworthy difference in the use of commercial versus recycled fibres. [8], [9], [16], [18], (Fig.2).

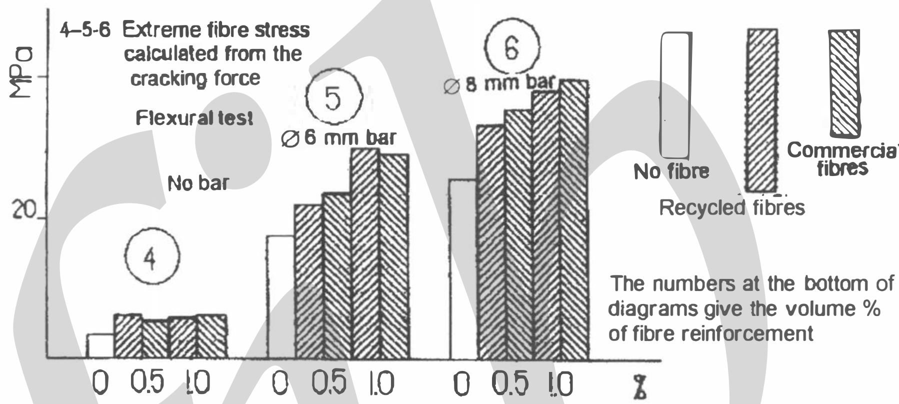

Fig.2 Comparison of test results

5 CONCLUSIONS

Experimental laboratory analyses and practical applications show the advantages of recycled wire ropes. Properly prepared worn out ropes can be utilised as prestressing strands and as fibre reinforcements. Of course, the recycled material is not destined to replace the factory made new steel at all kind of structures, but the recycling offers a reliable and economic solution in many cases. [23] It can be stated that the application is a benefit for the environmental protection.

REFERENCES

[1] Kuryllo, A., Mamontov, N.P. : Research on beams prestressed by strands gained from steel ropes. (In Russian), LPI, Lvov, 1955.

[7] Tassi, G., Szlivka, J., : Recycling of wire-ropes in reinforced concrete structures., (In Hungarian), Scientific Publications of the Department of structural Engineering, Budapest University of Technology and Economics, 2001. pp. 183-190.

[8] Naaman, A.E. : Fiber reinforcements for concrete, looking back, looking ahead. Proc. of the Fifth Internat. RILEM Symp. Lyon, 2000. pp. 65-86.

[9] Balázs, L.Gy., Polgár. L.: Past, present and future of fibre reinforcement concretes.(In Hungarian), Proc. Fibre Reinforced Concrete. Hung. Group of *fib*, Budapest, 1999. pp. 1 -23.

[16] Magyari, B. : Influence of composition on properties of fibre reinforced concretes. As [9], pp114-121.

[18] Hughes, B.P., Fattuhi, N.I. : The workability of steel-fibre reinforced concrete. Magazine of Concrete Research, , 1976. Vol. 28. pp. 157-161.

[23] Mamontov, N.P., Szlivka, J. : Cable-stayed pedestrian bridge, (In Russian), Doklady, Nauchnye Soobshcheniya LPI Lvov, 1994. pp. 608-615.

IMPROVEMENT OF QUALITY OF RECYCLED FINE AGGREGATE

Takayuki FUMOTO and Masaru YAMADA
Faculty of Engineering, Osaka City University
JAPAN

Keywords: recycled fine aggregate, improvement, mortar, particle size

1 INTRODUCTION

Concrete can be recycled by crushing to produce a number of materials. The crushed concrete is virtually used as base course materials and the higher quality ones must be reused as aggregate for concrete. However, it has been suggested that recycled fine aggregate, which consists of particles smaller than 5 mm, is inferior and inadequate for use in concrete, because recycled fine aggregate contains more original paste. Fine aggregate accounts for 40% of recycled concrete, so its reuse is very important.

In this study, the effect of three improvement methods on the properties of aggregate and recycled aggregate mortar were investigated. Laboratory tests were performed to examine the influence of ball milling on the properties of recycled fine aggregate, the effect of improvement by ball milling compared with that by mixing with an ordinary fine aggregate and the influence of particle size on the properties of recycled aggregate mortar.

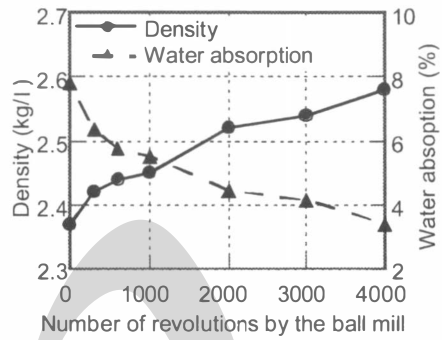

Fig.1 Influence of number of revolutions on density or water absorption

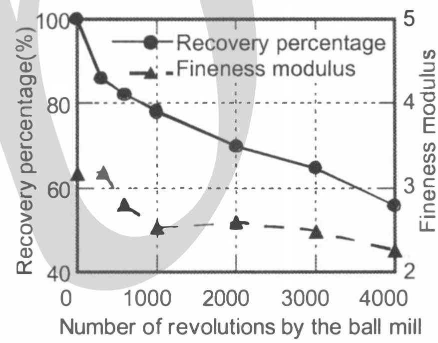

Fig.2 Influence of number of revolutions on fineness modulus or recovery percentage

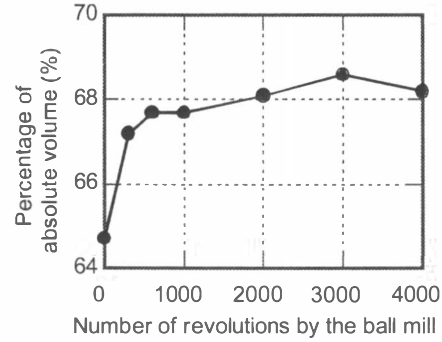

Fig.3 Transition of percentage of absolute volume

2 IMPROVEMENT BY BALL MILLING

Original concrete was made in our laboratory and recycled fine aggregate (RFA: dencity 2.37) crushed the original concrete was improved by ball mill. Figures 1, 2 and 3 show that increasing the number of revolutions improved the quality of the RFA through crushing weak hydration products and decreased the particle size and recovery percentage.

3 IMPROVEMENT BY MIXING WITH ORDINARY FINE AGGREGATE

The effects of ball milling were compared with those of mixing RFA with crushed sand. As shown in Figs.4 and 5, mortar flow using the improved by the ball mill was greater, although compressive strength is approximately equal at the same water absorption of fine aggregate. Water quantity was low in case of the same mortar flow when using RFA improved by ball milling.

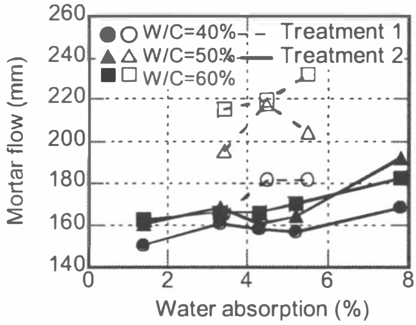

Fig.4 Relations between water absorption and mortar flow

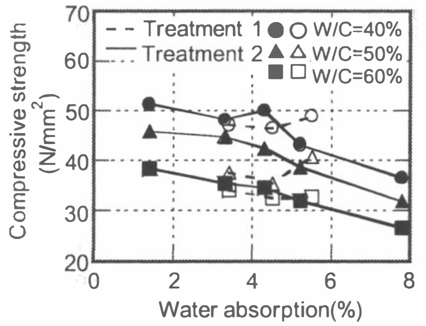

Fig.5 Relations between water absorption and compressive strength of mortar

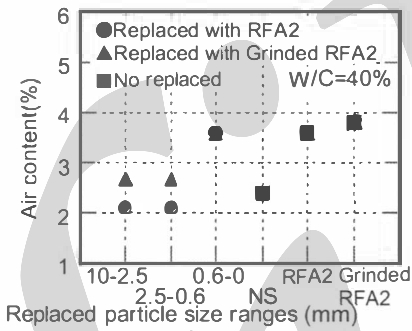

Fig.6 Relations between replaced particle size range and air content of mortar

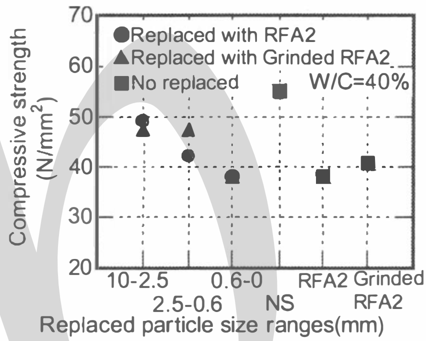

Fig.7 Relations between replaced particle siz e and compressive strength of mortar

4 INFLUENCE OF PARTICLE SIZE OF RECYCLED FINE AGGREGATE

The effects of improvement by mechanical grinding as shown in [1] on particles of another recycled fine aggregate (RFA2: dencity 2.18) were investigated. Figures 6 and 7 show that air content increased and compressive strength decreased, when the replaced particle size range was small. Mechanical grinding had little effect in the range less than 0.6 mm. For this reason, it is considered that particles of less than 0.6 mm have a lot of mortar in original concrete. Hence it will be difficult to improve the particles.

5 CONCLUSIONS

(1) Ball milling increases the density and reduces the water absorption of recycled fine aggregate. However there was a limitation of the improvement due to reduction both of aggregation size and recovery percentage.

(2) Ball milling improves the roundness of the aggregate, thereby increasing the absolute volume and the mortar flow value.

(3) The compressive and splitting tensile strength of mortar made of recycled fine aggregate improved by ball milling were equal to those of mortar made with recycled fine aggregate mixed with ordinary fine aggregate having similar water absorption properties.

(4) Particles smaller than 0.6 mm have a significant influence on the air content, compressive strength and drying shrinkage of mortar, but it is difficult to improve particles including large amounts of mortar.

REFERENCES

[1] Kojima, K., Yonezawa, T., Kamiyama, M. and Yanagibashi, K.; Study of Recycled Concrete Using High Quality Recycled Aggreagte, Proceedings of the Japan Concrete Institute, Cement & Concrete, Vol.22, No.2, pp.1123-1128, 2000(in Japanese).

IMPROVEMENT ON THE QUALITY OF RECYCLED AGGREGATE CONCRETE CONTAINING SUPER FINE MINERAL ADMIXTURES

Dae Joong Moon, Han Young Moon
Department of Civil Engineering
Hanyang University, Korea

Shigeoshi Nagataki, Makoto Hisada, Tatsuhiko Saeki
Department of Civil Engineering and Architecture
Niigata University, Japan

1 INTRODUCTION

Waste concretes demolished from old buildings and constructions are being annually increased in the world, especially in developed countries. Therefore, the utilization of demolished-concrete as recycled aggregate has been researched for the purpose of efficient utilization of resources and protection of environment in some advanced nations. However, there are some problems: the large difference of qualities in recycled aggregates and a minor deterioration of mechanical properties in recycled aggregate concrete in comparison with that of natural aggregate concrete. Therefore, some research has been conducted for improving of the qualities of recycled aggregate concrete by using mineral admixtures and progressing the qualities of recycled aggregate.

In this paper, an investigation to improve the properties of recycled aggregate concrete for containing meta kaolin and silica fume was preformed. Properties of recycled aggregate concrete were investigated regarding compressive strength, penetration resistance of chloride ion and resistance to freezing and thawing.

2 EXPERIMENTAL PROCEDURE

2.1 Material

The cement used was ordinary portland cement (OPC). The mineral admixtures used were meta kaolin (MK) and silica fume (SF). The fine aggregate was river sand with density of 2.60g/cm^3, absorption of 0.90. The coarse aggregates used were a crushed stone (CS) and 4 kinds of recycled aggregates. The recycled aggregates were two kinds of source-recycled aggregates (SA) made from Non-AE source concrete; from a 30x30x30cm cubic specimen, and 2 kinds of demolished-recycled aggregates (DA) made from real concrete structures.

2.2 Specimens' size and test

Compressive strength was measured by the cylinder specimens of $\phi100\times200$mm at the age of 7, 28 91days. Penetrated resistance of chloride ion was carried out as the cylinder specimen of $\phi100\times50$mm in accordance with ASTM C1202. The penetrated depth of chloride ion was measured by 0.1gN nitric acid aqueous solution. Resistance to freezing and thawing was conducted in accordance with ASTM C 666 procedure A on 100x100x400mm prismatic specimens.

2.3 Mixture proportions

Mixture proportions of concrete were set of water cement ratio of range 30% and 55% . Meta kaolin and silica fume were replaced with portland cement of 10% in concrete mixture with DA1 and SA1. Slump and air content was 8 ± 2cm, 4 ± 0.5% respectively in each mixture proportion.

3 RESULTS AND DISCUSSION

Compressive strength of concrete made with crushed stone, 4 types of recycled aggregates and MK, SF in water cement ratio of 55% was shown in Fig.1. The compressive strength of recycled aggregate concrete without mineral admixture was about 40N/mm^2 and tends to be similar to that of concrete with crushed stone at the age of 28days. The compressive strength of recycled aggregate concrete by MK and SF was a little increased compared to that of recycled aggregate concrete without mineral admixtures because that $Ca(OH)_2$ by the pozzolanic activity reaction of MK and SF are consumed.

Passed charge of chloride ion of recycled aggregate concrete was higher than that of concrete with crushed stone in water cement ratio of 55% in Fig. 2. Passed charge of recycled aggregate concretes without mineral admixtures was high penetration above 4,000 coulombs. Passed charge of recycled aggregate concretes with MK and SF was below 3,000 coulombs. On the other hand, penetrated depth of recycled aggregate concrete without mineral admixture was above 30mm, but was below 20mm by MK and SF. As it was, penetration resistance of recycled aggregate concrete with MK and SF was improved in comparison with that of recycled aggregate concrete without MK and SF and passed charge of chloride ion was decreased 2 times.

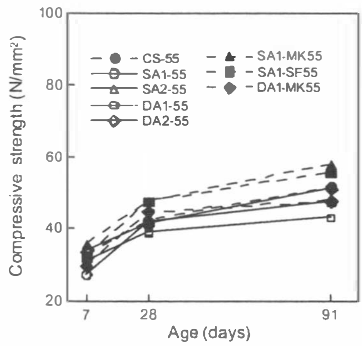

Fig.1 Compressive strength

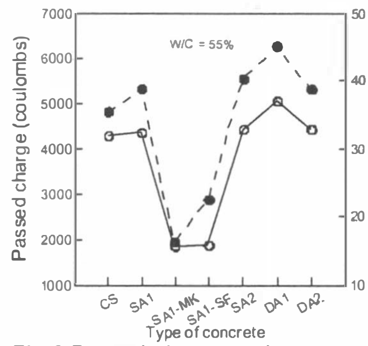

Fig.2 Passed charge and penetrated depth

Relative dynamic modulus of elasticity of concrete in the water cement ratio of 55% was shown in Fig.3. Relative dynamic modulus of elasticity of concrete with crushed stone was about 85% in the freezing thawing cycle of 300. However, relative dynamic modulus of elasticity of concrete with recycled aggregate was below 60% before the freezing thawing cycle of 150 in relation with or without MK and SF. Furthermore, concrete with DA1 recycled aggregate was most weak in comparison with other recycled aggregate concrete about the resistance of freezing and thawing. As it was, the resistance to freezing and thawing of recycled aggregate concrete was deteriorated in comparison with that of concrete with crushed stone because that the adhered mortar on recycled aggregate did not include entrained air.

Effectiveness of compressive strength, passed charge and durability factor of recycled aggregate concrete with MK and SF were shown about each property of recycled aggregate concrete without mineral admixtures of 100 in Fig. 4. The qualities of recycled aggregate concrete by MK and SF were improved about the compressive strength, penetration resistance and resistance to freezing and thawing. Especially, penetration resistance was most highly improved. Therefore, the improving effect of recycled aggregate concrete by MK could be expected in compared to SF.

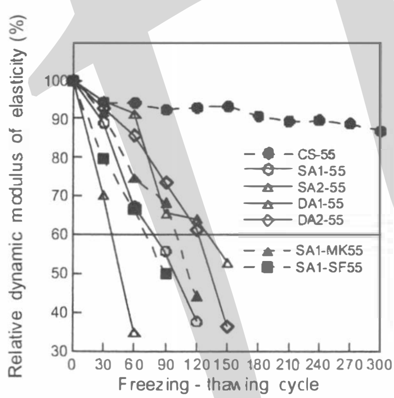

Fig.3 Relative dynamic modulus of elasticity

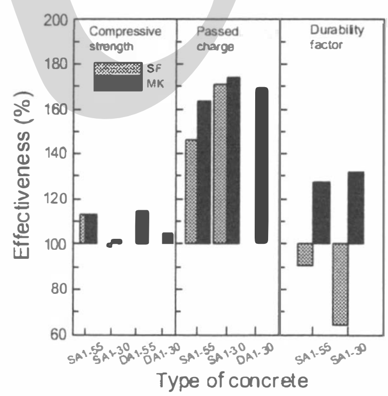

Fig.4 Effectiveness of recycled aggregate concrete by MK and SF

4 CONCLUSIONS

(1) Compressive strength, passed charge and relative dynamic modulus of elasticity of recycled aggregate concrete with MK and SF was highly improved in comparison with recycled aggregate without mineral admixtures.

(2) Effectiveness of penetration resistance of recycled aggregate concrete by MK and SF was remarkably shown about 60% in comparison with concrete without mineral admixtures. The qualities of recycled aggregate concrete by MK could be expected more the improving effect in comparison with using SF.

FUNDAMENTAL PROPERTIES OF CONCRETE MIXED WITH RECYCLING WASTE FOUNDRY SAND

Han Young Moon
Prof. of Civil Engineering
Han Yang Univ., Korea

Yun Wang Choi
Prof. of Civil Engineering
Se Myung Univ., Korea

Yong Kyu Song
Deg. of PhD. of Civil Engineering
Han Yang Univ., Korea

Keywords : clay bonded sand, CO_2-silicate bonded sand, recycling waste foundry sand

1. INTRODUCTION

WFS is classified into clay bonded sand(CLW), furan resin bonded sand, CO_2-silicate bonded sand(COW), α -set sand, resin coated sand etc. in accordance with types of foundry molds. When a casting is manufactured in Korea, the total amount of WFS is about 300 million tons per a year, and the amount of the waste foundry sand produced in Korea is over 800,000 tons per a year, but most WFS has been buried and in these days only 5~6% WFS is recycled as construction materials.
In addition, when it is reclaimed under ground the problems of a site contamination, disposal cost and underground water pollution are occurred. The tipping fee reaches as high as $ 50 per a ton, so the total cost of environmental compliance is occupied approximately 5% on the direct cost to produce a casting. In this study first of all fundamental properties of CO_2-silicate bonded sand, clay bonded sand, washed seashore coarse sand (WCS) in which salt was removed are evaluated. And then WFS is used as a fine aggregate for concrete. Concrete aimed at the specified strength of 270 kgf/cm^2 were mixed with WCS in which salt was removed, COW and CLW.
Moreover, basic properties such as air contents, setting time, workability and slump loss of the fresh concrete with COW and CLW were tested and compared with those of the control concrete mixed without WFS. In addition, both compressive strength of hardened concrete at each ages and its tensile strength at the age of 28 days were measured and discussed.

2. MATERIALS

Specific gravity and unit weight of COW and CLW are similar to each other but absorption and fineness modulus of them are different with each other. Fine aggregates including of COW and CLW have enough to being used as fine aggregate for concrete from the result of organic impurity test. On the other hand, maximum size of coarse aggregate is 25mm, and physical properties of these aggregates are shown in Table 1.

Table 1. Physical properties of aggregates

Type \ Item	Specific gravity	Absorption (%)	Unit weight (kg/m^3)	Percentage of solids (%)	Fineness modulus	Organic impurity	Abrasion value (%)
WCS	2.60	0.78	1,653	63.6	2.97	Good	-
COW	2.60	2.30	1,537	59.1	2.39	Good	-
CLW	2.62	1.12	1,539	58.7	1.40	Good	-
Coarse aggregate	2.65	0.78	1,741	65.7	6.51	-	28.6

3. PROPORTIONS

From the results of preliminary tests mortar mixed in the range of 0~100% of COW and CLW, COW and CLW replaced with natural fine aggregate of WCS from 0% to 50% are chosen and mixed by KS L 5105 in mortar mixtures. In addition, flow value is tested, and compressive strength is also measured at the age of 3, 7 and 28 days respectively. In concrete mixture, specified compressive strength of concrete with COW and CLW was 270kgf/cm^2, the range of air content is 4.5±1% and target slump is 12±1.5cm. The concrete specimens, in which COW and CLW are replaced as fine aggregates at the rate of 0, 20, 30, 40 and 50% are respectively manufactured. And then compressive strength, elastic modulus and tensile strength of concrete with WFS are measured at the age of 3, 7, 28 and 56 days.

4. RESULTS AND DISCUSSION

The compressive and tensile strength of concrete in accordance with replacement ratio of COW, CLW in W/C 50% at the age of 7, 28 and 56 days are shown in Fig. 1. The compressive and tensile strength are the highest in the case of concrete replaced with COW 30% irrespective of ages.

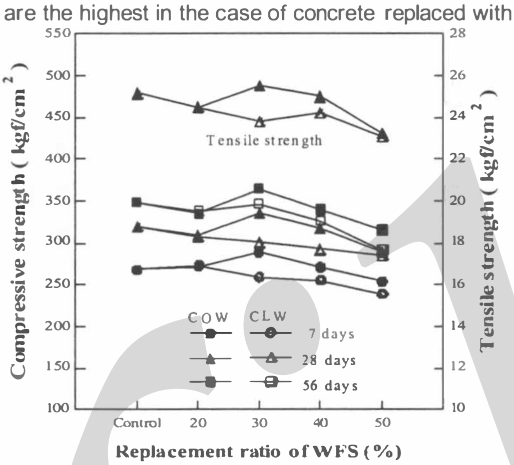

Fig. 1 Comp. and tensile strength of concrete

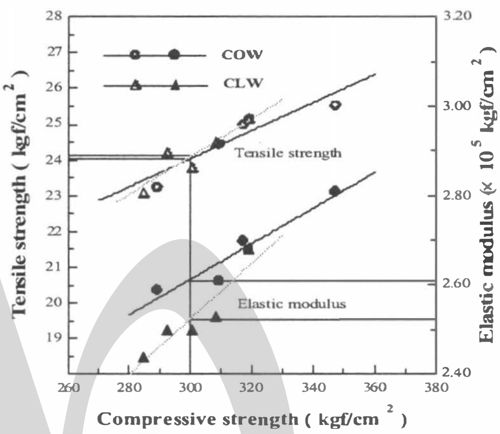

Fig. 2 Relationship tensile str. & elastic modulus to comp. str. of concrete

It is attributed to minimizing the porosity due to the reaction of silicic acid sodium encircled in the surface of COW. On the other side, on a certain occasion of concrete with CLW it is decreased with increasing replacement ratio of CLW. Thereafter Fig. 2 shows the relationship between tensile strength & elastic modulus and compressive strength of concrete with COW and CLW. Tensile strength and elastic modulus of concrete is increased in proportion to compressive strength irrespective of the replacement of WFS. It is indicated that linear relationship in concrete with COW is inclined to be similar to that in concrete with CLW as 83.3% of coefficient of determination in case of tensile strength to compressive strength, however, elastic modulus to compressive strength of concrete with COW and CLW makes different to each other, and coefficient of determination shows 91.8% and 85.1% respectively. This paper contains fundamental properties of concrete mixed with WFS, however, hereafter efflorescence problem of concrete mixed with WFS, and durability of concrete like freezing and thawing, carbonation for the sake of using WFS(COW,CLW) as fine aggregate for concrete will be measured and published.

5. CONCLUSIONS

(1) Flow value and compressive strength of mortar with COW and CLW are decreased with increasing the replacement ratio of COW and CLW due to inappropriate grading curve, fineness modulus and particle shape of COW and CLW.

(2) In the case of concrete mixed with COW of 30%, compressive and tensile strengths of concrete are higher than those of any other concrete without COW. In conclusion, optimum replacement ratio of COW is the about 30%.

REFERENCES

[1] Paul Tikalsky, Mike Gaffney, and Ray Regan : Properties of Controlled Low-Strength Material Containing Foundry Sand, ACI Materials Journal, Vol. 97, No.6 Nov.-Dec., 2000.

[2] Tarun R : Application of Foundry By-Product Materials in Manufacture of Concrete and Masonry Products, ACI Materials Journal, Vol. 93, No.1 Jan.-Feb., 1996.

CHARACTERISTICS OF THE HIGH STRENGTH LIGHTWEIGHT AGGREGATES MADE OF FLY ASH AND APPLICATION OF THESE AGGREGATES TO CONCRETE BRIDGE GIRDER

Hidetaka Umehara
Nagoya Inst. Of Tech

Hiroyuki Ikeda, Norio Suzuki
Japan Highway Public Corpration

Mikio Hara, Koji Hamaoka
Nippon P.S CO.,Ltd

Keywords: Fly ash , Nonfoamed type , Artificial light weight aggregate ,High strength ,PC bridge

1 INTRODUCTION

Lightening of prestressed concrete, hereafter abbreviated as “PC”, constructions had been considered a problem from the point of view of improving earthquake resistance, economics, and aesthetics of structures. As means of lightening weight, there are the method of reducing unit mass adopting lightweight aggregate concrete, and that of increasing compressive strength of concrete and reducing size of the concrete cross section that is subject to compressive force of the tendon. However, with conventional lightweight aggregate concrete, strength as high as that of normal aggregate concrete could not be expected, while the low static modulus of elasticity of the concrete also was a constraint, so that it was not adopted being considered not very effective as a means of cutting weight. Consequently, high-strength fly ash artificial aggregate, hereafter abbreviated “HFA aggregate”, concrete was taken up and lightening weights of PC structures was attempted.

HFA aggregate is a dense, nonfoamed type aggregate manufactured by adding a density regulator, such as calcium carbonate powder and a caking additive, such as bentonite, as auxiliary raw materials to the principal raw material, 90 percent of which latter is coal ash (an industrial waste) coming from thermal power stations, palletizing, and calcining[1]. Accordingly, it is an aggregate which is extremely useful in dealing with environmental problems since ash that had conventionally been disposed of as waste in land fill and other forms was now being used effectively in a positive manner. The category of this aggregate is Artificial Lightweight Aggregate and although corresponding to JIS A 5002, “Lightweight aggregate for structural concrete”, its properties differ from those of conventional artificial lightweight aggregate, and except for specific gravity which is 1.8 and low, are close to aggregate of normal weight[1].

This report describes studies of the effects of using HFA aggregate and the problems to still remain in the future.

2 CONFIRMATION TESTS OF CONSTRUCTION EXECTION[2]

2.1 Confirmation Tests of Concrete Properties

The flexural and tensile strengths were more or less equal to the strengths indicated by the calculation formulae in Standard Specification for concrete by Japan Society of Civil Engineers, while static modulus of elasticity was a value about 15 percent lower than for normal concrete.

2.2 Confirmation Tests of Place ability

2.2.1 Confirmation of Space Filling properties, Aggregate Distribution

It was confirmed that HFA aggregate concrete could be placed using only rod vibrators because of good flowability, and that the bottoms of hollow forms were accurately filled. Further, on cutting whole cross sections of specimens into 5 layers to confirm the state of aggregate distribution, the error of in coarse aggregate area ratio was within 3 percent.

2.2.2 Confirmation of Finishing at Top surface of Girder

With HFA aggregate concrete, by providing appropriate mixture proportions, although aggregate pieces were visible at the top of girder, there were none seen floating loose and finishing was possible to the same degree, as normal crushed stone aggregate concrete.

2.3 Confirmation Tests of Main Girder Properties

Regarding relations of applied load with deflections at middles, both indicated similar behaviors as shown in **Fig.1**.

The ultimate states were top fiber compressive failure of concrete for both, and no difference was seen. It may be judged by these results that an HFA aggregate girder possesses ample strength comparable to a crushed stone girder.

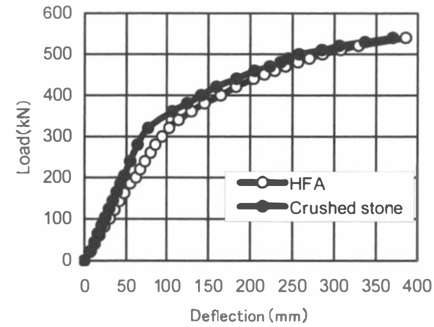

Fig.1 Relation of load and deflection

3 LOADING TESTS OF ACTUAL BRIDGE

The results of measuring deflections and concrete strains at span center are shown in **Fig.2** and **Table 1**, respectively.
Substantial differences from large bridges in general were not seen in the results of the loading tests of the actual bridge,

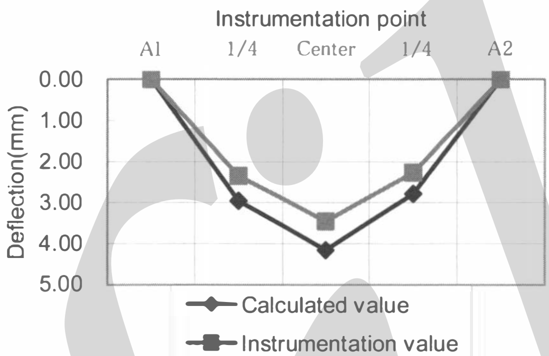

Fig.2 Results of measuring deflection

Table 1 Strain of concrete (Span Center)

Instrumentation Point (Span Center)		Calculated Value (μ)	Instrumentation Value (μ)
Bottom fiber	G1	33	34
	G3	33	36
	G4	33	37
	G8	34	39
Top fiber	G3	-28	-21
	G4	-28	-24

4 CONCLUSIONS

This was the first time that HFA aggregate concrete had been used in main girders of a PC bridge (pretensioned hollow slab bridge). On putting together results of the various confirmation tests, it may be judged that a bridge performance equal or better than normal aggregate concrete can be obtained.

Further, together with reduction of girder height and the low unit mass, there was a lightening of main girder weight by 22 percent and overall dead load reaction force by 16 percent[3], while there were also trial calculation results which indicated that when the lightening effect was extended to the substructure, pile diameter could be reduced about 10 percent. It is considered that reduction effect of the cost of the bridge as a whole could be expected.

It is thought that the HFA aggregate used here is an ideal material for lightening weight while maintaining performance of concrete. The economic effect that high-strength concrete can be obtained without using a special admixture like silica fume or special mixture proportions can also be looked forward to. Today, when depletion of stocks and quality deterioration of natural aggregate for concrete are causes of great concern, an aggregate produced by reutilization of resources and which is artificial and of stable quality is thought constitutes a promising means of satisfying the demand of aggregate.

REFERENCES

[1] Sone: High Strength Artificial Aggregate Using Coal-Ash as Raw Material, pp.3-10 Concrete Journal Vol.36, NO.12, Dec. 1998

[2] Hara, Suzuki, Ikeda, Watanabe, Suzuki and Takimoto: Design and Construction of PC Girder Bridge Applied High-Strength Concrete Using Artificial Coarse Aggregate, pp.141-148 Proceedings of JCI Symposium on High Performance Structural Lightweight Concrete, Aug. 2000

[3] Hara: Invertigation on Manufacturing of Pre-Cast Concrete Members Made with Concrete Using High-Performance Artificial Coarse Aggregate, pp.55-58 Concrete Journal Vol.38, NO.5, May. 2000

RESEARCH ON CONCRETE CONTAINING CUTTER POLISHING RESIDUE SLUDGE AS FINE AGGREGATE

Seiichi Watanabe, Shin Murakami , Aya Taniguchi

Sugiyama Jogakuen Univ., School of Human life Science
17-3 Hoshigaoka - Motomachi Chikujsa-ku Nagoya, 464-8662 , Japan
E-mail : shin@he.sugiyama-u.ac.jp (S.Murakami)

Key Words: cutter polishing residues, sludge mixed concrete strength, slump, creep, drying shrinkage

1. INTRODUCTION

Seki City in Gifu Prefecture is known as the largest production district of cutter products in Japan, where 1,600 tons of sludge of cutter polishing residues is yield a year. The sludge has piled up as industrial waste in disposal sites of controlled landfill type.The nature and the conditions of sludge produced during the process of cutter polishing vary widely according to the types of whetstone to be used for a range of cutter products including kitchen knives and scissors.

The currently available whetstones can be grouped into cement--based whetstones (MG: magnesia cement type, polishing particle: alumina Al_2O_3) for both grinding and polishing and resin-based whetstone (MB: epoxy type, polishing particle: alumina Al_2O_3) for polishing. The former, the cement-based whetstone, is more frequently used because of its low cost.

The sludge produced during this polishing process is mainly composed of fibrous metal debris, a powdered part of whetstone and grinding liquid. It is naturally moist, but is also often changed into muddy or semi-solid matter under different storage conditions

Length and thickness of metal fibers as well as size of fragments of whetstone, all of which are mixed into the sludge, vary according to the kind of the cutter product and the product number of whetstone (which indicates a specific level of grinding/polishing performance within the range from “rough” to “finishing”.)

We can tell the difference of conditions even from a broken dried sludge lump by its specific texture. Disposal sites expressed an increasing demand for development of a measure for effective use of such sludge. Recently, we have noted some effort toward putting the sludge into a practical use as a roof tile. We also have a strong interest in this material in terms of alternative use as a part of fine aggregates to be contained in concrete, and performed some tests to determine characteristics of sludge-mixed concrete, including workability of fresh concrete, strength performance, elastic modulus, drying shrinkage and creep. We would like to discuss the prospective of practical use of the new concrete.

2. MATERIALS AND METHODS

2.1 Physical properties of the concrete mixed with Type E sludge

For this test, we prepared a normal type of concrete, for which we set the following referential standard: Fc value = 21N/mm^2, slump = 18 cm, and mix proportioning strength Fc is 27N/mm^2. In addition to this, we set a model of lightweight concrete and modified it by replacing 30% of its fine aggregates with E type sludge which was considered to be most inappropriate for use in lightweight concrete. **Table 1** shows their mix proportions.

1) Strength and elastic modulus of sludge mixed concrete

The test results of the sludge mixed concrete are shown in **Table 2**

2) Drying shrinkage / creep strain and creep modulus

Fig. 1 and **2** show the test results of drying shrinkage and creep modulus.

Table 1 Mix Proportions

	G max (mm)	Slump (cm)	Air (%)	W/C (%)	Water (kN/m^3)	Weight (kN/m^3) C	Weight (kN/m^3) S	Weight (kN/m^3) G	sludge (kN/m^3)	water-reducing agent (N/m^3)
normal	20	18	5	60.8	1.66	2.94	6.77	10.82	-	7.35
normal +sludge	20	18	5	60.8	1.66	2.94	4.74	10.82	2.03	7.35
light weight	15	18	5	55.4	1.62	2.94	5.57	4.53	-	7.35
lightweight +sludge	15	18	5	55.4	1.62	2.94	3.90	4.53	2.03	7.35

Table 2 The Test Result

	Slump (cm)	1 Week			4 Week		
		compressive strength (N/mm^2)	tensile strength (N/mm^2)	elastic modulus (N/mm^2)	compressive strength (N/mm^2)	tensile strength (N/mm^2)	elastic modulus (N/mm^2)
normal	17.0	19.78	1.83	2.15×10^4	25.34	1.99	2.18×10^4
normal +sludge	5.4	14.52	1.48	1.36×10^4	18.92	1.52	1.67×10^4
lightweight	21.5	17.03	1.99	1.26×10^4	21.55	1.49	1.37×10^4
lightweight +sludge	7.5	17.04	1.49	1.14×10^4	20.19	1.52	1.24×10^4

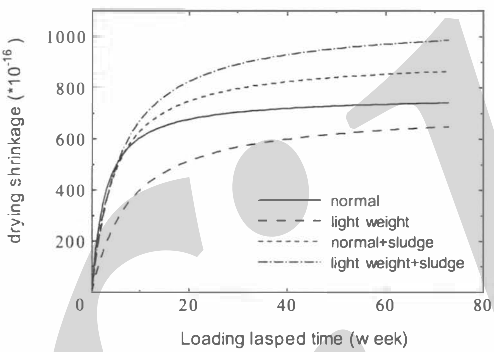

Fig.1 Drying Shrinkage

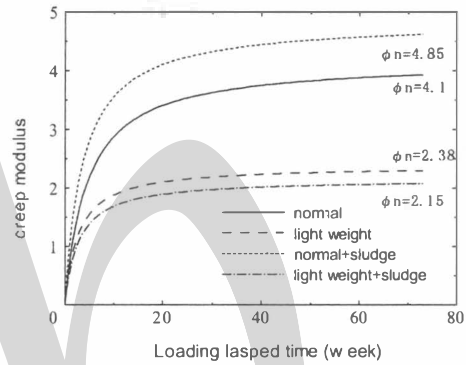

Fig.2 Creep Modulus

3. CONCLUSION

In this research, we obtained the following overall findings about partial replacement of fine aggregates of concrete with sludge from cutter polishing residues:

1) Strength decreased in proportion to increase of amount of added sludge. The magnitude of decrease varied according to the kinds of added sludge, but an average of 10% decrease was observed when mix ratio of sludge increased up to 30%. Smaller rates of strength decrease were observed in the lightweight concrete specimens compared to the normal concrete specimens.

2) Workability of fresh concrete decreased significantly when mixed with sludge. However, there were wide variances between different kinds added sludge.

3) The effects of addition of sludge on drying shrinkage and creep modulus were less significant than those observed for strength and elastic modulus.

As a conclusion based on the results of the series of tests, use of cutter polishing residue sludge in replacement of fine aggregates can be expected to produce concrete of practical use, even when it is normal type concrete, as long as its mix ratio is limited less than 30%, although a large decrease in workability may possibly occur due to use of some kinds of sludge. We were able to obtain generally more favorable results from the lightweight concrete specimens.

REFERENCES

1) Seiichi Watanabe, Rumiko Gotou, Takako Ukawa, Tomoe Mashuo, The Research on Concrete Which Used the Cutter Polishing Residues Sludge as a Fine Aggregate , Proceedings of JAPAN concrete Institute,Vol22, No.2,pp.1177-1182,2000

2) Seiichi Watanabe, Shin Murakami, Aya Taniguchi, Research on Characteristics of Drying shrinkage and creep of Artificial Lightweight Aggregate concrete by the Difference of the Aggregate Grading, Proceeding of Japan Concrete Institute, Vol.23, No.2, pp745-750, 2001

INFLUENCE OF ABSORPTION OF COARSE AGGREGATE ON FROST RESISTANCE AND STRENGTH OF RECYCLED CONCRETE

Katsuyuki Konno
Hokkaido Institute of Technology, JAPAN

Yasuhiko Sato
Hokkaido University
JAPAN

Osamu Katsura
Hokkaido Prefectural Cold Region Housing and Urban Research Institute, JAPAN

Moriaki Kumagai
Hokkaido Regional Development Bureau
JAPAN

Keywords: absorption ratio, compressive strength, frost resistance

1 INTRODUCTION

There have been many researches of recycled concrete, but most of recycled aggregate are being used as subbase course material in Japan. A few recycling plant have the technology to make the recycled aggregate of low absorption ratio with low cost, therefore most of the recycled aggregate are not low absorption ratio and those are used for subbase course material. The authors investigated the strength and frost resistance of recycled concrete[1]-[3], then this paper report that the recycled aggregate of low average absorption ratio, which is less than 3 %, can be used to make concrete of enough quality.

2 FROST RESISTANCE OF RECYCLED CONCRETE IN LONG TERMS

The frost resistance of recycled concrete was investigated[1] by using the recycled aggregate whose absorption ratio was about 5 % as shown in Table1. Mix proportion of concrete were shown as Table 2. The symbol 1R and 2R stand for the recycled aggregate and the recycled aggregate that was recycled again respectively. Figure 1 and 2 are the durability factor and the ratio of mass decrease respectively. The recycled concrete whose water cement ratio was 0.50 and 0.65 indicated over 60 % of durability factor. And the recycled concrete whose water cement ratio was 0.35 and

Table 1 Property of the aggregate

Coarse aggregate	Absorption ratio (%)	Specific gravity
N (virgin)	1.55	2.72
Ra (recycled)	5.15	2.47
Rc (recycled)	5.39	2.47

Table 2 Mix proportion of concrete

Specimen	f'_c (MPa)	C (kg)	W (kg)	s (kg)	G (kg)	AE agent (g)	W/C (%)	s/a (%)	Air (%)	Slump (cm)	Aggregate
N65	27.8	267	174	811	(V) 1081	133	65.0	43.0	4.0	18.0	N
1R65-100	30.3	267	174	811	(R) 982	133	65.0	43.0	4.0	19.0	Ra
1R50-100	40.9	340	170	739	(R) 1016	171	50.0	40.0	3.5	11.5	Rb
1R35-100	50.8	475	166	650	(R) 1014	238	35.0	37.0	3.0	2.0	Rb
2R65-100	24.4	267	174	811	(R) 982	133	65.0	43.0	4.0	20.0	Rc
2R50-100	38.9	340	170	739	(R) 1012	170	50.0	40.0	3.5	6.0	Rc
2R35-100	41.7	478	167	653	(R) 1015	239	35.0	37.0	2.5	2.0	Rc

※V : Virgin aggregate, R : Recycled aggregate

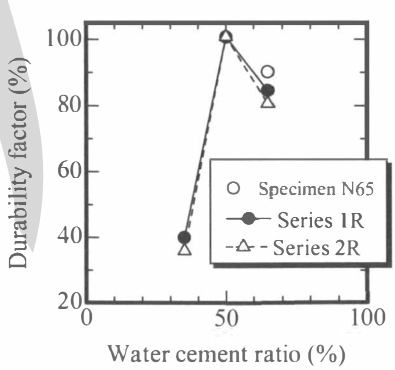

Figure 1 Durability

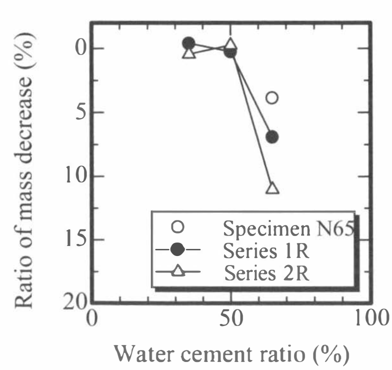

Figure 2 Mass decrease

0.50 showed the low value of the ratio of mass decrease. As a result of this experiment, the recycled concrete that have about 5 % of the absorption ratio of aggregate have enough frost resistance when the water cement ratio was 0.50. But it is difficult to use recycled aggregate whose absorption ratio is more than 5 % as the material for concrete without virgin aggregate.

3 AVERAGE ABSORPTION RATIO

Better material property of recycled aggregate should be used to obtain enough strength and durability of recycled concrete with any mix proportion. The compressive strength and frost resistance of recycled concrete was investigated by using the recycled aggregate which was mixed with virgin aggregate to decrease the absorption ratio[2],[3] as shown in Table 3.

Table 3 Mix ratio of the aggregate

Specimen	Absorption ratio of recycled aggregate (%)	Average absorption ratio of the aggregate (%)	Mix ratio (%)	
			Recycled	Virgin
A-1	2.0	—	0	100
B-1	2.5	2.9	50	50
C-1	2.9	2.9	100	0
C-2	2.9	4.6	35	65
C-3	2.9	6.2	22	78
D-1	4.6	4.6	100	0
D-2	4.6	6.2	63	37
E-1	6.2	6.2	100	0

There was difference among specimens of series C and D about compressive strength however the average absorption ratio was same[2].

Figure 3 shows the relative dynamic modulus of elasticity of recycled concrete whose properties are shown in Table 3. The legend of 40w, 50w and 60w in Fig.3 are the water cement ratio. Even if the absorption ratio of recycled aggregate was 6.2%, the recycled concrete had enough frost resistance by using the recycled aggregate mixed with virgin aggregate. It was shown that the recycled aggregate whose absorption ratio was more than 3% can be used when the average absorption ratio was about 3%[3]. But the relationships between the average absorption ratio of the recycled aggregate and the compressive strength and frost resistance were not considered. In this paper more experimental data were added and the influence of the average absorption ratio of the aggregate is investigated.

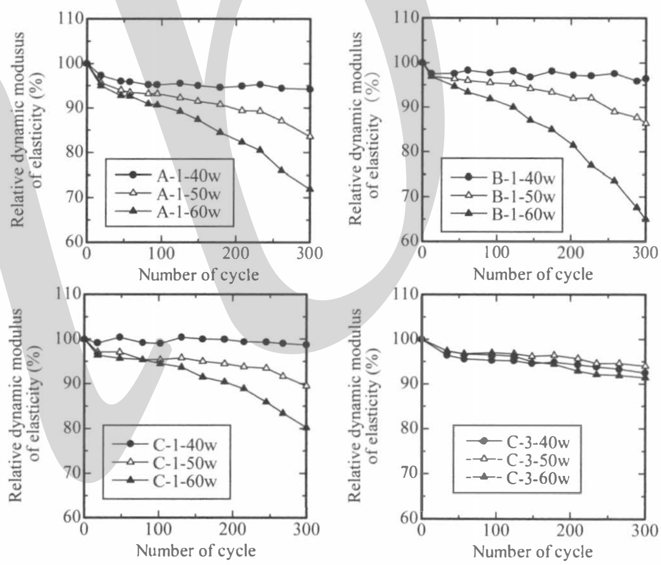

Figure 3 Frost resistance of recycled concrete

REFERENCES

[1] Katsuyuki KONNO, Yasuhiko SATO and Yoshio KAKUTA : Frost resistance of recycled concrete, Influence of characteristic of recycled aggregate to compressive strength of recycled concrete, Proceedings of the 55th annual conference of the Japan society of civil engineering,5, October,2000

[2] Hidetoshi OKUYAMA, Yasuhiko SATO, Masazumi ITO and Kunio SHINDO : Influence of characteristic of recycled aggregate to compressive strength of recycled concrete, Proceedings of the 56th annual conference of the Japan society of civil engineering,5, October,2001

[3] Katsuyuki KONNO, Yasuhiko SATO, Osamu KATSURA and Moriaki KUMAGAI : Frost resistance of recycled concrete by Using recycled aggregate with normal aggregate, Influence of characteristic of recycled aggregate to compressive strength of recycled concrete, Proceedings of the 56th annual conference of the Japan society of civil engineering,5, October,2001

MIX DESIGN METHOD OF ROLLER COMPACTED CONCRETE USING FLY ASH AS THE SUBSTITUTE OF FINE AGGREGATE

Eiji Matsuo Sumio Hamada
Yamaguchi University
JAPAN

Masanori Ogi
Sanin Kensetsu Co.
JAPAN

Tadashi Saitoh
Chugoku Electric Power Co. Inc.
JAPAN

1 INTRODUCTION

Recently, the circulatory system in the total society has become a great subject from a standpoint of preservation of earthly environment. Effective use of various particles is one of this theme, which are the industrial waste or by-product and the amount of them have been increasing year by year. In Japan, Fly Ash (FA) that is produced from the coal thermal power plants is one of these wastes. It has been increasing drastically as the energy demand increases. Furthermore it is getting extremely hard to produce the fine aggregate of high quality because the over-producing of sea sands, which influences environment of the sea. FA particles are typically spherical and it can be compacted quite densely by vibrating compaction with adequate amount of water. Authors have been reporting the strength property of Roller Compacted Concrete (RCC), in which fine aggregate is replaced to FA in large volume.

In the present study, the target amount of fine aggregate is zero, which is all replaced to FA. Reduction of the unit weight of water has been expected, which is the most important subject. The mix design method for such materials is herein proposed. The most proper mix design method is for the target compacting ratio and strength.

2 TEST METHOD

2.1 Used material and mix design

High early strength Portland cement and crushed andesite stone with a maximum size of 20mm as coarse aggregate were mixed in all the present concrete. FA corresponds to the 2nd classification of JIS except the amount of ignition loss and the index of activation at 28 days. Any admixtures were not used in all of concretes to simplify the mix design conditions. Unit volume of coarse aggregate is 81, 91 and 100% for the percentage by solid volume.

2.2 Compacting method

The necessary weight of materials were calculated on the assumption that the aimed compacting ratio is 96% in the rectangular of 10 × 10 × 40cm. The half weight was weighed and casted to the flame, and then they were spread out by a hand spoon. After that, they were compacted by the vibrating compaction machine wholly and evenly until the paste would get fluidity. The second layer was casted in a similar way until the compaction thickness would amount to the aimed thickness of 10cm.

Table 1 Mix proportion of strength test

W/C (%)	W/(C+FA) (%)	Coarse agg. (l/m^3)	Unit weight (kg/m^3)			
			C	W	FA	G
54.8	23	590	270	148	372	1599
49.7			300	149	349	
45.8			330	151	325	
42.2			360	152	302	

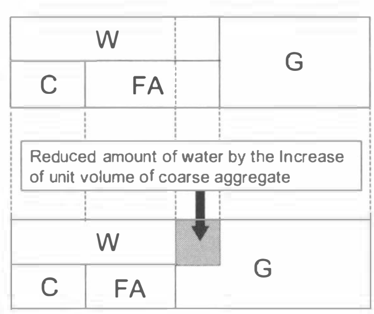

Fig.1 Concept of mix design method

3 COMPACTING RATIO

The amount of fly ash can be reduced by the increase of the unit volume of coarse aggregate, in order to reduce the unit weight of water to the minimum. **Fig.1** illustrates the concept of mix design method. For the purpose of reducing of unit weight of water within the range of sufficient workability, the influence of the unit volume of coarse aggregate to the compacting ratio was investigated. **Fig.2** shows the relationship between W/P ratio and the compacting ratio. The figure indicates that compacting ratio increases as the increase of W/P ratio, which implies the good compactability. W/P ratio at the compacting ratio of 96%, which is the target compacting ratio of RCC, is approximately 23%.

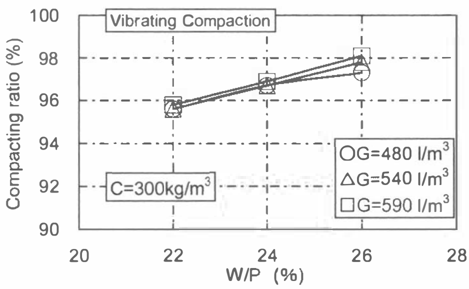

Fig.2 Relationship between W/P and compacting ratio

4 STRENGTH AND MIX DESIGN

A W/P ratio of 23% and unit volume of coarse aggregate of 590 l/m^3 were determined as the most proper mix proportion, which satisfied the target compacting ratio (96%) of conventional RCC by the materials in this study. The minimum amount of cement in concrete was determined, as satisfied the proportioning strength of 5.7Mpa. **Figs.3 and 4** show the relationship between the unit weight of cement and the compressive strength, and the relationship between the unit weight of cement and the bending strength at the curing age of 7, 28, 56 and 91days, respectively. Paying attention to the early age strength till 28 days, the strength had reached the ceiling at the unit weight of cement of 300kg/m^3. It is apparent that the strength of this concrete wouldn't always be in proportion to the amount of cement in early age. The proportioning strength of 5.7MPa could be obtained at 28 days for concrete with the unit weight of cement of 300kg/m^3. From this result, when targeting the sufficient early strength, the necessary and minimum amount of cement is estimated 300kg/m^3.

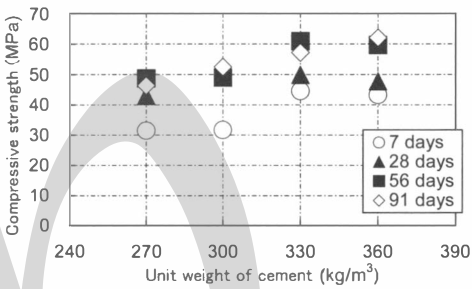

Fig.3 Relationship between unit weight of cement and compressive strength

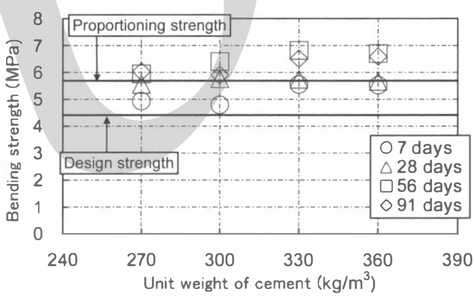

Fig.4 Relationship between unit weight of cement and bending strength

On the other hands, paying attention to the long-term strength from 28 days till 56 days for concrete with the unit weight of cement of 330kg/m^3 and 360kg/m^3, the both of compressive and bending strength increased large. The target structure in this study is a pavement that is expected to open early traffic, and the minimum amount of cement of 300kg/m^3 is required, as well as from the economical viewpoint. From the above results, the mix design method of no sand fly ash RCC was proposed.

5 CONCLUSION

1) Vibrating compaction is more effective than tamping compaction. The difference is clear when the unit volume of coarse aggregate is large or W/P ratio is small.
2) By vibrating compaction, sufficient compacting ratio is obtained without segregation even when the unit volume of coarse aggregate increases to the percentage of solid volume.
3) Compaction effect of vibration does not correlate with the amount of coarse aggregate or cement. It can be evaluated only by W/P ratio.
4) The target bending strength of 5.7MPa is obtained from concrete with the unit weight of cement of 300kg/m^3 at 28 days.

Session 11 | Safety of concrete structures

EVALUATION OF STRENGTH AND MAINTENANCE METHODS FOR RAILWAY REINFORCED CONCRETE STRUCTURES WITH AGED DETERIORATION

Matsuda Yoshifumi[1], Aramaki Satoshi[1], Kitago Yukio[2]
[1]West Japan Railway Company, [2]JR West Japan Consultants Company

Keywords: reinforced concrete, aged deterioration, maintenance, corrosion, carbonation, chloride ion

1 INTRODUCTION

At present, the total length of railway track in Japan, including the Shinkansen lines, is approximately 27,400 kilometers. Many of the concrete railway structures that were built prior to the 1950s, the decade in which Japan's conventional railway line system was nearly completed, have remained in sound condition with absolutely no repair work at all since the initial construction, or with only partial reinforcements or repairs. However, some of the concrete structures built in the 1970s, a period of high-level economic growth, began to show signs of early deterioration in less than 30 years since the structures were constructed.

In this report, we provide an introduction to the current conditions of JR-West evaluations of soundness and maintenance management for railway concrete structures that have undergone age-related deterioration, as well as to the future directions the company is taking with regard to these matters.

2 OVERVIEW OF THE INVESTIGATION CONDUCTED BY THE "SAN-YO SHINKANSEN LINE CONCRETE STRUCTURE INVESTIGATION COMMITTEE"

In June and October 1999, there were two cases of accidents caused by concrete pieces falling from tunnel lining surfaces [1]. Likewise, for the problem of concrete falling from viaducts, etc., emergency inspections were performed, loose concrete was hammered off in the areas of delamination, and necessary measures were taken in order to prevent further accidents. Furthermore, with the goal of obtaining plans to maintain the soundness of concrete structures on the San-yo Shinkansen line, the "San-yo Shinkansen Concrete Structure Investigation Committee" (Chairperson: Professor Shigeyoshi Nagataki, Niigata University) (hereafter, calling "Investigation Committee") was established in the Railway Technical Research Institute under the guidance of the Ministry of Transport.

The committee took approximately 400 samples from viaducts on the San-yo Shinkansen Line, and for each sample, tested the cover, depth of carbonation, the degree of corrosion in the reinforcing steel, and the chloride ion content. The final findings of the committee were presented in a report in July 2000 [2]. The following is an overview of the results of the investigation conducted by the committee.

2.1 Causes of Deterioration

Fig. 1 shows the relationship of the level of reinforcing steel corrosion to the residual carbonation (= cover – depth of carbonation) and the chloride ion content in structures such as viaducts. A trend can be seen in which the ratio of area occupied by reinforcing steel corrosion level I or lower increases as the residual carbonation increases. For chloride ions, the ratio of area occupied by reinforcing steel corrosion level I or less shows no trend for increasing even when the chloride iron quantity increases.

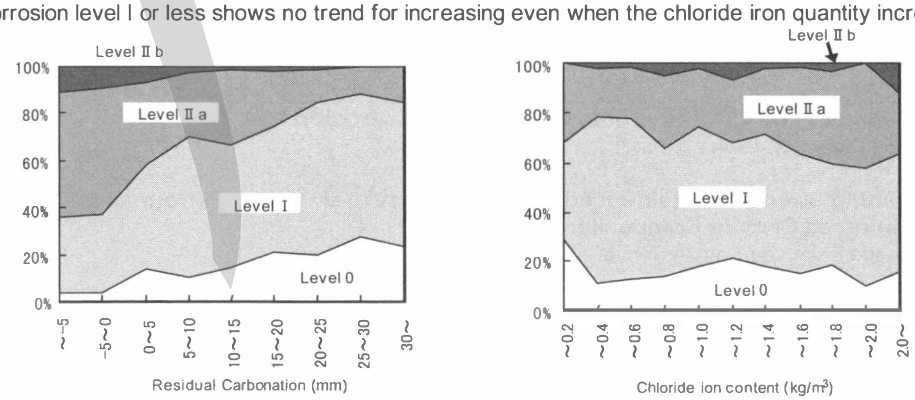

Fig.1 Relationship between the Degree of Reinforcing Steel Corrosion and Residual Carbonation, Chloride Ion Content

2.2 The View of Application of Maintenance Methods

Although there is no structural problem with current structures, it is necessary to maintain them. Therefore, in the Investigation Committee, the view of application of maintenance methods was proposed. This proposal, which is based on currently applicable maintenance methods, is a method for selecting the most effective maintenance plan for the present, taking factors such as the level of condition modification (the ratio of hammered off concrete), residual concrete carbonation, chloride ion content, and the degree of corrosion in the reinforcing steel into consideration. This proposal will also form the basis for the creation of future maintenance plans for viaducts.

3 MAINTENANCE OF REINFORCED CONCRETE RIGID-FRAME VIADUCTS

Reinforced concrete structures on the San-yo Shinkansen Line (total length, approximately 209 km) consist of approximately 16,000 sets of structures. Comprehensive Inspections on the San-yo Shinkansen Viaducts, etc. (hereafter, calling "Comprehensive Inspections") were performed in order to obtain fundamental data about the depth of carbonation, chloride ion content, etc., for each structural set. The following is a summary of the results of the comprehensive inspections.

- The average depth of carbonation progression is approximately 22 mm, and this carbonation is progressing faster than expected for the age of the structures. This is thought to be due to internal factors, such as the quality of the concrete and the quality of the construction work.
- Carbonation is a primary cause of the reinforcing steel corrosion in overhead line bridges and similar structures on the San-yo Shinkansen Line. A trend has also been verified by which reinforcing steel corrosion progresses in relation to the increase in the chloride ion content.

4 MAINTENANCE MANAGEMENT PROJECTS

The considerations and undertakings of JR West are summarized in **Table 1**.

Table 1 Maintenance Management Considerations and Undertakings

	Considerations	Undertakings
Inspection	a. Improvement of inspection precision	Introduction of an infrared camera spalling detection system
	b. Incorporating measurement results into a database	Construction of a database system for viaducts, etc
	c. Improvement of the work capacity of the inspection personnel	Introduction of a qualifications certification system, worker education
Repairs	a. Development of new materials · Improvement of the durability of lining materials · Verification of the performance of desalination and re-alkalization · Verification of cathodic protection · Improvement of concrete chipping technologies using water jets	 · Test work, exposure tests and follow-up surveys · Test work and follow-up surveys · Test work and follow-up surveys · Development of a water jet chipping robot vehicle
	b. Improvements to repair quality · Technical expert education and training	· Drafting of repair manuals and education using these manuals · Introduction of a qualifications certification system for on-site construction managers

5 IN CLOSING

Considering the length of the life of the railway concrete structures, our efforts have just started and will run through the 21st century. In order to keep these structures sound and provide the passengers with the reliable transportation services, we are going to conduct appropriate inspections, take suitable measures, and make constant efforts for the maintenance management.

REFERENCES

[1] Kondo, T. and Ichida M. : Comprehensive Safety Inspection of Sanyo Shinkansen Tunnels, Proceedings of the International Conference on Modern Tunneling Science and Technology (IS-Kyoto 2001), Kyoto, Japan, Vol.1, pp.333-336, October 2001

[2] Report from the San-yo Shinkansen Concrete Structure Investigation Committee, July 2000

ENHANCING THE DURABILITY OF STAY CABLE

Yves Bournand
Head of New Developments
VSL International
St Quentin en Yvelines – France

Keywords: stay cables, durability, anchorages, corrosion protection

1 INTRODUCTION

Today, structures as bridges are generally designed for a life of 100 / 120 years. Consequently we can say that nowadays durability is the most important requirement for the stay cable system, with the fatigue strength.

This paper will analyze the conditions of the durability of stay cables to guide the designers and consultants in their evaluations.

This analysis will dress the list of the main factors, which conduct to the ageing of stay cables with their effect.

The second part of the paper will review the evolutions of the main recommendations about durability. The last revision of the PTI (Post Tensioning Institute) document and the new stay cable document issued by the French committee of the CIP (Commission Interministerielle de la Precontrainte) proposed new recommendations taking into account the last evolutions and requirements to ensure the new expected durability of the cable-stayed structures.

The third part of the paper will introduce a new stay cable System: the VSL SSI 2000.
The presentation of the SSI 2000 will be focused on the durability: the durability analysis of the system has conducted to adapt the components design of the anchorages according to the expected durations and the environmental conditions.

2 MAIN FACTORS TO BE CONSIDERED FOR THE DURABILITY OF STAY CABLES

This chapter will dress the list of the main factors, which conduct to the ageing of the cables.

2.1 The mechanical solicitations

a) The variations of tension in the cable due to the service loads.

b) The rotations of the deck at the level of he cable anchorage.
These rotations introduce flexural stresses in the cable, in the anchorage zone.

c) Deflection of the cable due to the wind, rain or combination of wind and rain.
We can have cable vibrations with very quickly a high level of cycles.
Vibrations contribute particularly to flexural fatigue of stay cables.

d) Statical flexural stresses in the cable due to a misalignment of the anchorage.

2.2 The temporary solicitations during construction

2.3 The environnemental solicitations

The expected aggressiveness of the environment during the whole service life of the structure shall define the level of the necessary corrosion protection. Redundant protection is recommended in the design of a stay cable system.

We will note that in some cases, the aggressiveness of the environment may be variable, for example with the installation of an industrial area near the bridge. The environment will be characterized for each project, to define the level of corrosion protection.

3 THE VSL SSI 2000 STAY CABLE SYSTEM

Modern engineering is setting stringent new standards for cable-stayed bridge systems.
Throughout the world, designers and authorities are all expressing a demand for increased durability, easier monitoring and inspection procedures, and outstanding fatigue and static load performance levels.

The VSL SSI 2000 stay cable system (see Fig. 1) is designed to meet these demands. It incorporates multiple independent and hard-wearing protection layers to guarantee long term performance, and also allows easy inspection and, where required, cable replacement.

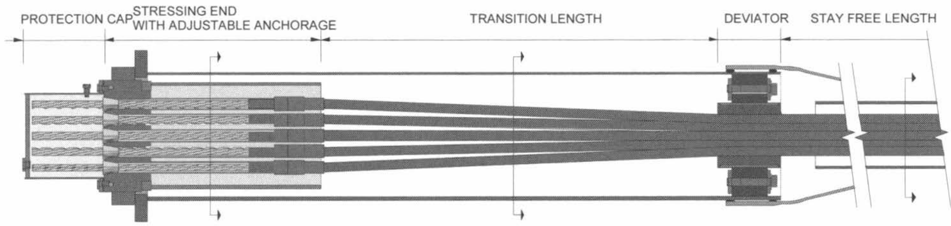

Fig. 1 – VSL SSI 2000 stressing anchorage

The anchorage has been submitted to some fatigue tests and to the new leak test as defined by the PTI. Laboratory accelerated ageing tests have been achieved on samples of HDPE stay pipes, to have a better understanding and better control of the performance and durability of the colored stay pipes. Each parameter of the durability has been evaluated.

To limit our presentation in this paper, we will consider only one parameter: the evaluation of the corrosion protection of the anchorage.

4 THE CORROSION PROTECTION OF THE SSI 2000.

To answer to the future specifications of high durability in the most aggressive environments, a durability analysis has been achieved on each component of the anchorage. This analysis has conducted to adapt the geometry of some components, to use new types of assemblings with adapted material, and to define adapted systems of corrosion protection, according to the specifed objectives.

The first step in the durability analysis was to define the environmental conditions. To define, in a rational way, the impact of the bridge environment on the protection systems of the anchorage, we used the standard ISO 12944-2. This standard defines some typical environments and classifies the atmospheric corrosivity into 5 categories.

Then, for each component of the anchorage, we have considered its accessibility and its replaceability, particularly during the maintenance operations.

The systems of corrosion protection of the SSI 2000 anchorage have been defined with a design life up to 100 years, within the most aggressive environments.

During this design life, the first maintenance operations will be envisaged at 25 years, and the subsequent at regular intervals of 15 years, on the accessible and replaceable components. Inaccessible parts have a system design life for the entire 100 years life without maintenance.

5 CONCLUSION

Durability and fatigue strength are the two most important requirements for stay cables. The SSI 2000 stay cable system has features for a design life of 100 years.
And particularly, to achieve this level of durability:

- The corrosion protections have been defined according to the results of a rational analyse of the environment
- The system has been designed with efficient possibilities of inspection and maintenance.

But the durability of stay cables depends to a large extend of the quality of their assembly and installation.

WHAT WE CAN LEARN FROM ONE OLD BRIDGE BEFORE ITS DEMOLITION ?

Ľudovít Naď
Assoc. Prof., MSc., PhD.
Faculty of Civil Engineering, Technical University in Košice, Slovak Republic

Keywords: bridge, load test, precast beams

1 INTRODUCTION

„The prefabrication period" in bridge construction is well recognizable in many countries all over the world. Former Czechoslovakia was not an exception. Nice and statically very effective precast prestressed beams of different shapes were frequently used in fifties and sixties. Several thousands of bridges are now 40 – 50 years old and are approx. in the middle of their suggested design service-life.

Paper presents an extraordinaire occasion – "strong" static load test and dynamic load test of a 35 years old bridge as well as the "total" – destructive load test of 5 precast 21,4 m long beams, excavated from this bridge before its demolition. There are almost 700 bridges built of this type of precast beams in Slovak Republic. Results, their analysis and conclusions from these load tests serves as basic material for guideline for evaluation of existing precast bridges.

Investigated precast post-tensioned beams of shape of Π were designed to be transversally prestressed in the bridge structure. Because of serious technological problems during the placement of prestressing units in to the gains, later it was decided to not use the transversal prestressing. Of course, it means two different types of static behaviour of the bridge. The first is very stiff in comparison to the second one.

However, some of beams in the bridge structure are seriously damaged by corrosion of prestressing steel, the behaviour of whole bridge during the load test was satisfying. The reason is a relatively good state of transversal prestressing, which assure very stiff transversal connection of precast beams.

2 DESCRIBTION OF THE BRIDGE

The bridge was built in 1964 and is situated on the national road I/50 over the river Hornád near heating plant in Košice. According to the newly constructed route, it was decided that the old bridge has to be demolished. The structure is straight, skew with crossing angle 49°. Vertical alignment is horizontal. The bridge structure comprises of 14 precast post-tensioned prestressed, 22 m long girders type so called "VLOŠŠÁK" in each of 3 statically independent bridge spans (Fig. 1).

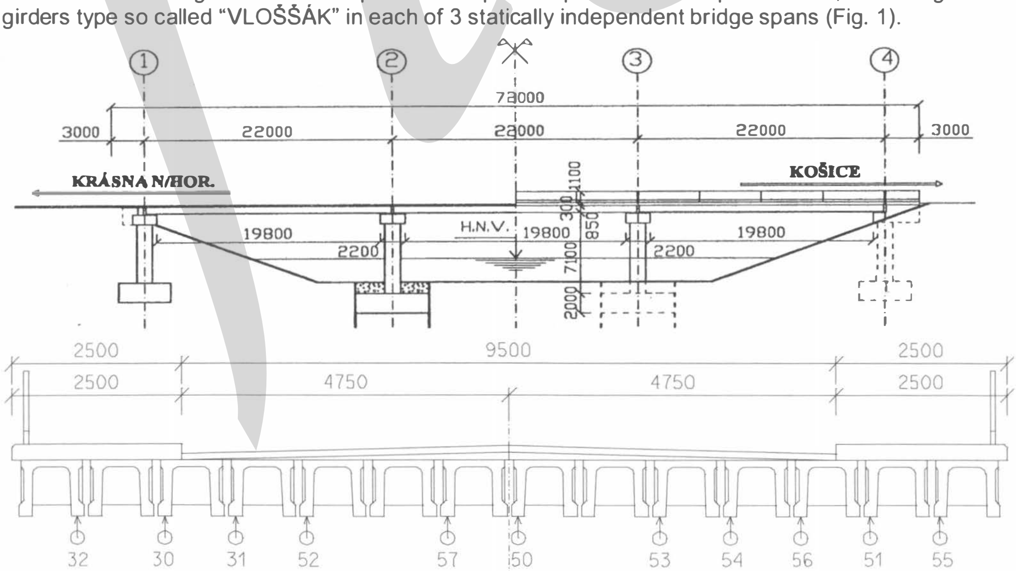

Fig. 2 Longitudinal section and cross-section of the bridge

3 RESULTS

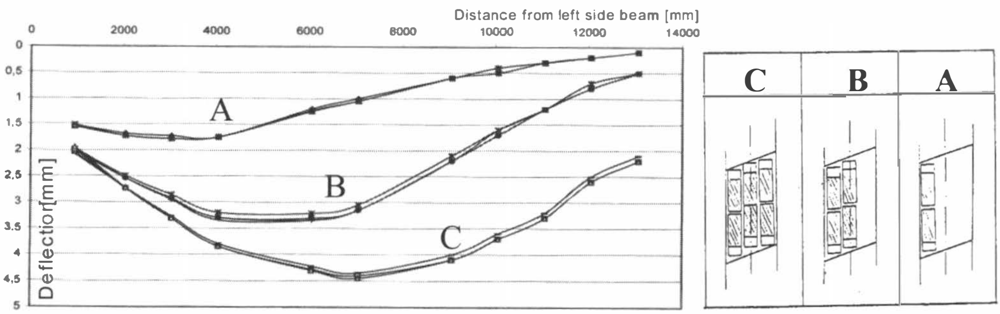

Fig. 3 Deflection of the bridge in transversal direction (in midspan) under three load stage (A – 1 couple of lorries, B – 2 couples of lorries, C – 3 couples of lorries)

"Strong" static load test and dynamic load test of the bridge were executed. Five beams excavated from bridge were tested up to collapse. To illustrate the results, there are the deflection diagrams from bridge load test (Fig. 3) and from beam load test (Fig. 4). Big differences between the real load-carrying capacity of beams and behaviour of whole bridge structure were observed. The bridge has high reserve.

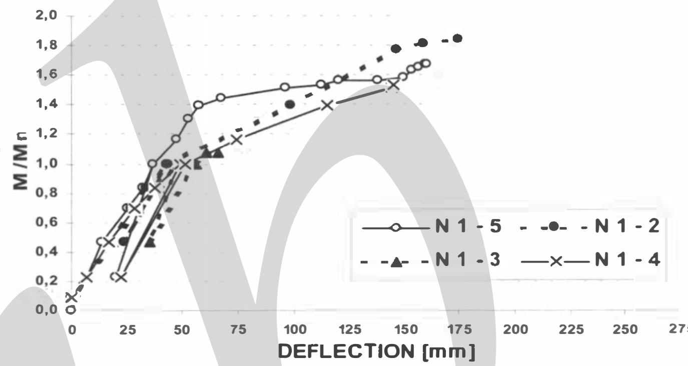

Fig. 4 Working diagram „deflection vs. relative moment" for individual beam N1 tested in couple with N2; N3; N4; N5

4 CONCLUSION

However, the bridge structure is seriously damaged by longitudinal reinforcing and prestressing steel corrosion in some beams, the behaviour of whole bridge structure during the load test – static as well as dynamic can by consider as satisfying. The reason for that is the transversal prestressing (which is in good condition) and not all the beams have corroded prestressing cables. Transversal prestressing "increases" rapidly the transversal stiffness of the structure. It means that most important part of diagnosis is to determine with highest possible precision the state of transversal prestressing and the quality of concrete.

According to the current Slovak Standard [4], dynamic coefficient of the highway bridges is defined in dependency only on span L by formula $\delta = 1 / (0{,}95 - (1{,}4\ L)^{-0{,}6})$. The dynamic coefficient of tested bridge comes out greater, when it is defined on dependency of the bridge basic frequency.

Load carrying capacity limitation according to existing codes is not adequate to real capacity of the bridges of tested type comparing to real as well as perspective traffic load. This constatation is valid for transversally prestressed bridges

REFERENCES

[1] Nad', Ľ. et all.: Dynamic influences and investigation of the vibration of concrete bridges. Final report. Department of Concrete Structures and Bridges, Technical University Košice, Faculty of Civil Engineering. Košice, 2000.

[2] Nad', Ľ. – Krištofovič, V.: Extraordinaire Load Test of Small Precast Prestressed Beam Bridge. In: Proceedings „Roads and Bridges in Europe, 8th International Road Conference, ISBN 963 00 6881 8, Budapest, May 2001 (Proceedings on CD)

[3] The Slovak Standard No. 73 6209 Loading test of bridge.

[4] The Slovak Standard No. 73 6203 Bridge loading.

[5] Vítek, J.L., Křístek, V. : Deflection and strains of prestressed concrete bridges. Proc. Of the 16th Congress of IABSE structural Engineering for Meeting Urban Transportation Challenges. IABSE, Lucerne, Sept. 18-21, 2000, pp. 94-95, ISBN 3-85748-101-5

SYNTHESIS OF SAFETY LEVELS APPROVED IN EAST- AND WEST-EUROPE IN THE EUROCODE

György Farkas, professor
Tamás Kovács, research assistant
Kálmán Szalai, professor
Department of Civil Engineering, Budapest University of Technology and Economics
Budapest, HUNGARY

Keywords: safety, risk, design code, Eurocode, partial safety factor

1 INTRODUCTION AND HISTORICAL BACKGROUND

Hammurabi's laws became necessary because of the tragedies during construction of buildings and other types of structures in Babylon. At that time the builders often reduced the sizes of the cross sections and did not apply durable materials with high strength in order to reduce the cost of the building. In this way, the safety level of structures was gradually decreasing and the number of accidents during construction was growing. The investigation of those accidents and their consequences inspired the researchers' minds. The question of optimal (required and sufficient) level of safety came into the foreground of civil engineering sciences after Newton's and Galileo's work in this field. At the end of the 19th and at the beginning of the 20th centuries the design codes prescribed to verify the adequacy of structures by the allowable stress design method using a single safety factor based on a linear elastic analysis. Parallel to using smaller sizes for the cross sections and more slender structures than before the safety level of structures decreased in the course of time. In addition to the elastic calculation models applied to the check of the serviceability of structures the non-elastic calculation models came into the foreground verifying the sufficient load bearing capacity of structures. The Hungarian G. Kazinczy (1913) analysed the load bearing capacity of a steel beam fixed on both sides by an elastoplastic material model [1]. Then the German M. Mayer (1926) proposed to use the partial safety factor method in structural design [2]. The adoptation of these initiations to the design codes was delayed for some time because of the particular responsibility of structural designers. Then the Russian A. Gvozgyev (1946) recommended the structural design based on the limit state design method [3]. After the World War II, the East-European countries turned to the partial safety factor design method due to the particular economical and political situation [4]. The gradual decrease of safety level of structures started in Hungary at that time and continued until 1986 because the economy planned by the government had continuously demanded the decrease of the building costs. At the end of seventies when the calibration of the CEB-FIP Model Code to the European structural codes took place, the safety level of structures designed according to the Hungarian Code (HC) was found significantly lower than that according to the West-European codes. *Fig. 1* shows the required amounts of bending reinforcement (ρ_{sl}) of a simply supported beam designed according to the Eurocode (EC) and all the consecutive design codes issued in Hungary up to the present [7].

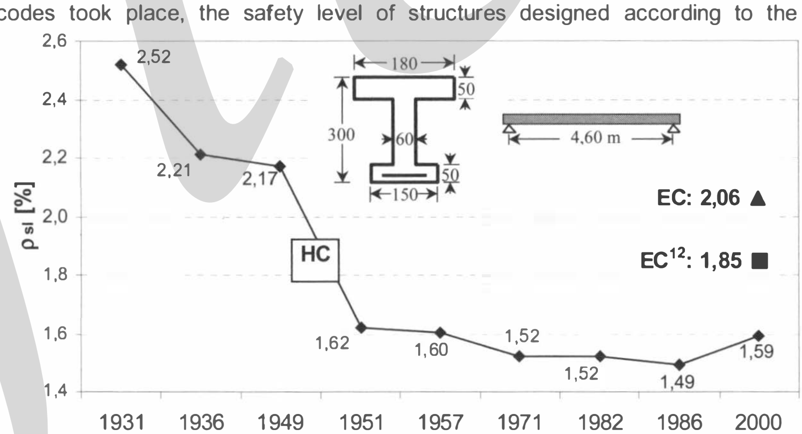

Fig. 1 Required amounts of longitudinal reinforcement

Turning to the market economy, in Hungary in the nineties, the system of governmental warranty was replaced by the private insurance system. This involved the risk of a sudden rise of insurance fees of structures built in Hungary and designed according to the HC compared to that built in Hungary and designed according to the EC because of the lower safety level of the HC. For the sake of decreasing the difference in the safety level between the HC and the EC, the new HC-2000 increased the partial safety factor of permanent actions.

2 OUTLINED COMPARISON BETWEEN THE HUNGARIAN CODE AND THE EUROCODE

2.1 The optimum risk

A "full-scale experiment" testing the safety level of the current design code in the real building industry had practically been going on in Hungary as well as in the East-European countries for almost 50 years in the second part of the last century. The main question was to find out the optimum risk/cost ratio of structures and the corresponding safety elements of the design codes. The optimal value of risk was determined in Hungary by minimizing the complex cost function, which is as follows [5]:

$$C = C_0 + C_1 + p_{opt} D$$

where C_0 is the construction cost, C_1 is the maintenance cost, D is the cost of failure and the probability of its occurrence is p_{opt}. D contains both the loss arising from the injuries and deaths of people and the loss of profit. As a result of the analyses $p_{opt} = 10^{-4}$ was found in Hungary.

2.2 The comparison of the safety levels

Some results of this process were probably used to setting the safety level of the EC by allowing the use of alternative combinations (marked by EC^{12} in *Fig.1* and by EC^1 and EC^2 in *Fig. 2*) containing smaller safety elements (partial safety factors and combination factors) instead of the basic combination of actions (marked by EC in *Fig. 1* and *Fig. 2*) for the verification of the requirements of the ultimate limit states in permanent and transient design situation. The levels of action effects based on the design combination of actions according to the HC and the EC plotted against the ratio of the live load and the total load ($Q/(G+Q)$) are illustrated in *Fig. 2* taking into account only one variable action and neglecting the effects of prestress.

This decrease in the safety level of the EC induces a significant cost saving for the West-European countries compared to the previous periods of time. On the other hand, joining the European Union requires to increase the safety level in Hungary, which induces significant extra cost for the Hungarian building industry [6].

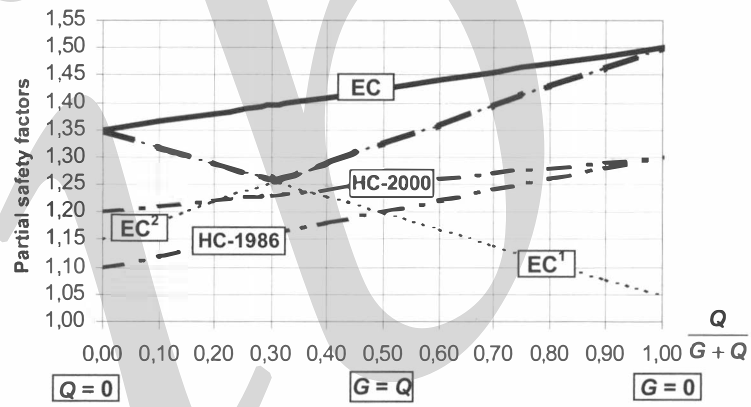

Fig. 2 Comparison of the design effects of actions

The harmonization of the partial safety factors and the synthesis of the safety levels of the West- and East-European design codes in the Eurocode can be considered after all as the final result of optimising the risk/cost ratio in the field of structural design, as well as a scientific result in the field of design theory. If the safety level decreased in the next revised Eurocode versions, it could mean the more efficient utilization of the East-European experiences in this field.

REFERENCES

[1] Kazinczy, G.: *Experiments on fixed beams*, Betonszemle, Budapest, 1913
[2] Mayer, M.: *The safety of structures and their calculation based on ultimate strengths instead of allowable stresses*, Verlag von Julia Springer, Berlin, 1926
[3] Gvozgyev, A.: *Calculation of the load bearing capacity of structures based on the plastic equilibrium method*, Gosztrojzdat, Moscow, 1949
[4] Menyhárd, I.: *New design method of concrete structures. The calculation procedure based on the partial safety factors and the theory of failure*, Építőipari Könyv- és Lapkiadó Vállalat, Budapest, 1951
[5] Kármán, T.: *On the optimum level of safety of structures*, ÉTI, Budapest, 1965
[6] Farkas, Gy.: *Status of domestic and European codes in Hungary*, 6th Hungarian Conference on Load Bearing Structures, Budapest, June 26, 2000
[7] Szalai, K. – Kovács, T.: *Change of the ultimate design requirements in the 20th century; a comparison with the Eurocode*, Vasbetonépítés, Budapest, Vol. II, No. 3, 2000, pp. 76-82

STRUCTURAL ANALYSIS AND SAFETY ASSESSMENT OF EXISTING CONCRETE STRUCTURES

Konrad Bergmeister, Prof., Dipl.-Ing. DDr.
Alfred Strauss, Univ. Ass. Dipl.-Ing.
Institute of Structural Engineering, University of Bodenkultur, Vienna, AUSTRIA

Eva M. Eichinger, Univ. Ass. Dipl.-Ing.
Johann Kolleger, Prof., Dipl.-Ing. Dr.
Institute for Structural Concrete, University of Technology, Vienna, AUSTRIA

Drahomir Novak, Prof., Dipl.-Ing. Dr.
Institute of Mechanics, Technical University Brno, CZECH REPUBLIC

Radomir Pukl, Project Manager, Dr.
Vladimir Cervenka, Project Manager, Dr.
Cervenka Consulting, Prague, CZECH REPUBLIC

Keywords: Inspection, Statistical Analysis, Non-linear calculation, Database, Latin Hypercube Sampling, Reliability, Assessment

1 INTRODUCTION; CONCEPT OF THE PROJECT *SARA*

The project is based on a 2D/3D non-linear analysis program ATENA developed by Cervenka Consulting. This FEM program will be adapted to a probabilistic analysis concept. The necessary handling and treatment of the statistical data of structures – loading and resistance in general - needs special sampling methods. The examination and the inclusion of these methods in the existing non-linear analysis program are main parts of the project. The other major parts of the project, which are responsible for the statistical data needed for the sampling methods, are the investigation of stochastical models of materials (with and without degradation of strength), the investigation of proof loading models (Permanent Load, Variable Load and Traffic Load) - and the recording and utilisation of Structural Monitoring Systems. The draft allows a reliable analysis of concrete structures accompanied by a probabilistic structural identification.

2 SAMPLING METHODS AND TECHNIQUES

The multi-purpose probabilistic software for statistical, sensitivity and reliability analysis of engineering problem FREET [1] is based on efficient reliability techniques. The probabilistic methods utilized in the program FREET were explained in more detail e.g. in [4]. They are summarized below.

A special type of numerical probabilistic simulation called Latin Hypercube Sampling (LHS) makes it possible to use only a small number of simulations [2]. The range of the cumulative distribution function of each random variable is divided into *N* intervals of equal probability *1/N* (*N* is the number of simulations). The regularity of sampling over the range of the cumulative distribution function ensures an efficient sampling of random variables.

Statistical correlation among input random variables can be considered. A special stochastic optimization technique called simulated annealing is utilized to adjust random samples in such a way that the resulting correlation matrix is as close as possible to the target (user-defined) correlation matrix. Note that the approach allows working also with non-positive definite matrix on input, which can be the result of lack of knowledge of the user. This technique generates samples as close as possible to a positive definite matrix (mathematically and physically correct).

The programs FREET and ATENA are integrated in order to allow for a probabilistic fracture analysis of engineering structures. The basic aim of statistical nonlinear fracture analysis is to obtain the estimation of the structural response statistics (failure load, deflections, cracks, stresses, etc.).

3 MATERIAL DATABASE

The material database is a support of the sampling methods. These concepts of probability calculation and design based on FEM needs suitable basic variables.

Generally a resistance model for concrete structures m_R ,e.g.,can be described by the basic variables of concrete strength $f_{c,ij}$, steel strength $f_{y,ij}$, the steel section area A_s and geometrical dimensions of cross sections b, h. First, the challenge was to create a suitable database structure readable for the sampling methods which contains the necessary basic variables.

4 STOCHASTIC NONLINEAR ANALYSIS OF A PRESTRESSED CONCRETE BRIDGE

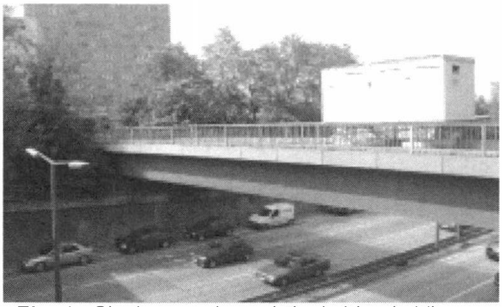

Fig. 1 Single-span box-girder bridge in Vienna, Austria

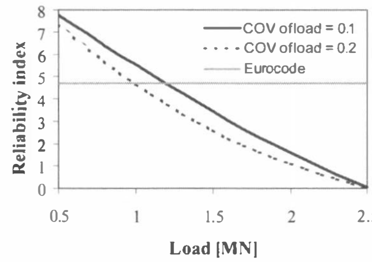

Fig. 2 Reliability assessment

The single span bridge to be assessed is located in Vienna, Austria and is 25 years old. It is a fully post-tensioned box-girder bridge made of 18 segments with lengths of 2,485 m each. The total length of the bridge is 44.60 m, the width 6.40 m and the height 2.10 m. The segmental joints are filled with epoxy resin. Due to an ongoing construction project the bridge has to be demolished. Before the demolition a range of non-destructive tests as well as finally a full-scale destructive load test will be performed. The presented stochastic simulation is part of the predictive numerical study for planning and optimizing the test setup. The segments were cast from concrete B500 and are reinforced with mild steel St 50. The post-tensioning tendons consist of 20 strands St 160/180. The bridge structure was analyzed using the stochastic nonlinear simulation package described above.

4.1 Material properties for the Stochastic Analysis

Mean values of the material parameters for concrete B500 were generated using ATENA defaults (based on recommendations by CEB, fib, RILEM etc.)

Under assumption of normal probability distribution for both R and S a simple possibility of utilization of obtained statistical characteristics of ultimate load for reliability calculation can be drawn. Considering different levels of load S (mean values) and two alternatives of variability (coefficient of variation 0.1 and 0.2), reliability index is plotted in Fig. 2. The horizontal line represents target reliability index as specified by Eurocode [3] (4.7 for 1 year).

5 REFERENCES

[1] D. Novák et al., "FREET – Feasible Reliability Engineering Efficient Tool", Program documentation, Brno University of Technology, Faculty of Civil Engineering, Institute of Structural Mechanics / Červenka Consulting, Prague, Czech Republic, 2002

[2] D. Novák, B. Teplý, and Z. Keršner, "The Role of Latin Hypercube Sampling Method in Reliability Engineering", *Structural Safety and Reliability (ICOSSAR-97)*, Balkema, Rotterdam, The Netherlands, 1998

[3] "Eurocode – Basis of structural design", CEN, Brussels, Belgium, (2001)

[4] Novák, D., Vorechovský, M., Cervenka, V. and Pukl, R., "Statistical Nonlinear Analysis – Size Effect of Concrete Beams", *Fracture Mechanics of Concrete Structures (FraMCoS 4)*, Eds. R. de Borst, Balkema, The Netherlands, pp. 823-830, 2001

ONSET OF CATASTROPHIC FAILURE IN CONCRETE FRAMES: SAFETY ASSESSMENT BY ACOUSTIC EMISSIONS

A. Carpinteri, B. Chiaia and G. Lacidogna
Department of Structural Engineering, Politecnico di Torino, 10129 Torino, Italy

Keywords: Acoustic emissions, stable crack propagation, brittle collapse

Fracture in concrete develops as smeared microcracking or single macrocracks. Both phenomena, occurring for instance in the inelastic hinging regions of beams or frames, cause the moment-curvature diagram to exhibit postpeak softening. Thus, plastic limit analysis is invalidated because the capacity for energy absorption is reduced, leading to poor inelastic moment redistribution.The evaluation of safety and reliability of aged concrete frames represents a complex problem. Therefore, monitoring techniques are progressively assuming greater importance in the field of structural engineering.

A non-destructive technique, originally applied to industrial steel elements and nowadays commonly adopted to identify defects and damage in concrete manufacts, is based on the Acoustic Emission (AE). By means of this technique, a particular methodology has been put forward to monitoring crack propagation, and assess its stability, in structural elements under service conditions, see Fig.1. The highest frequency of AE events occurs at a stress level corresponding to about 80% of the ultimate load. Thus, the AE technique becomes particularly effective when coupled with Fracture Mechanics arguments. It is possible, in fact, to evaluate the relations between diffused micro-cracking, coalescence of defects at the meso-scale, and macroscopic crack propagation leading to collapse.

In Fig. 2, the cumulative counts of emissions and the advancement of the cracks are reported and compared. Notice that, at any stage of the test, the oscillation count is proportional to crack propagation and that a reduction of AE density is directly related to crack arrest in the proximity of the upper beam (where a significantly larger toughness is attained due to steel reinforcement). Since the highest number of AE counts detected during the test corresponds to the maximum velocity of propagation, we can deduce that the local maxima of the AE distribution function correspond to the most critical stages of propagation.

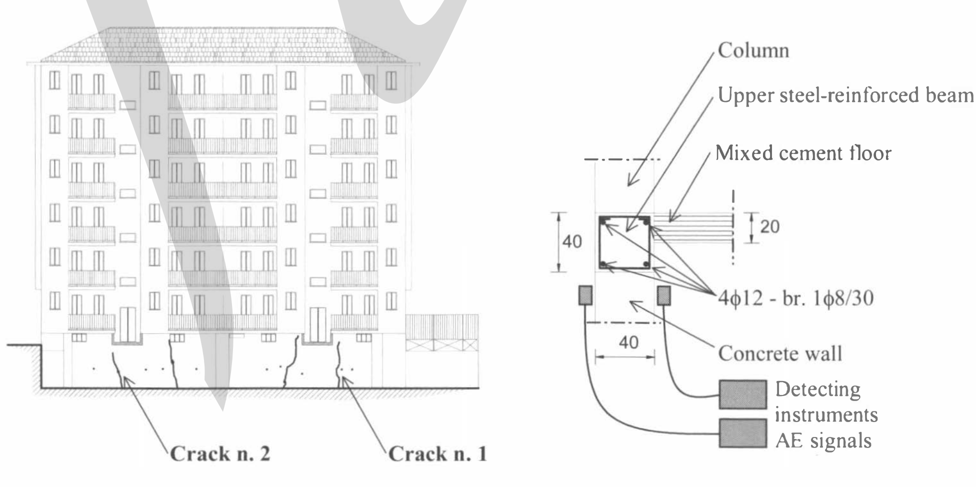

Fig.1 Building in with concrete structure. Cracking framework and location of transducers on the concrete wall

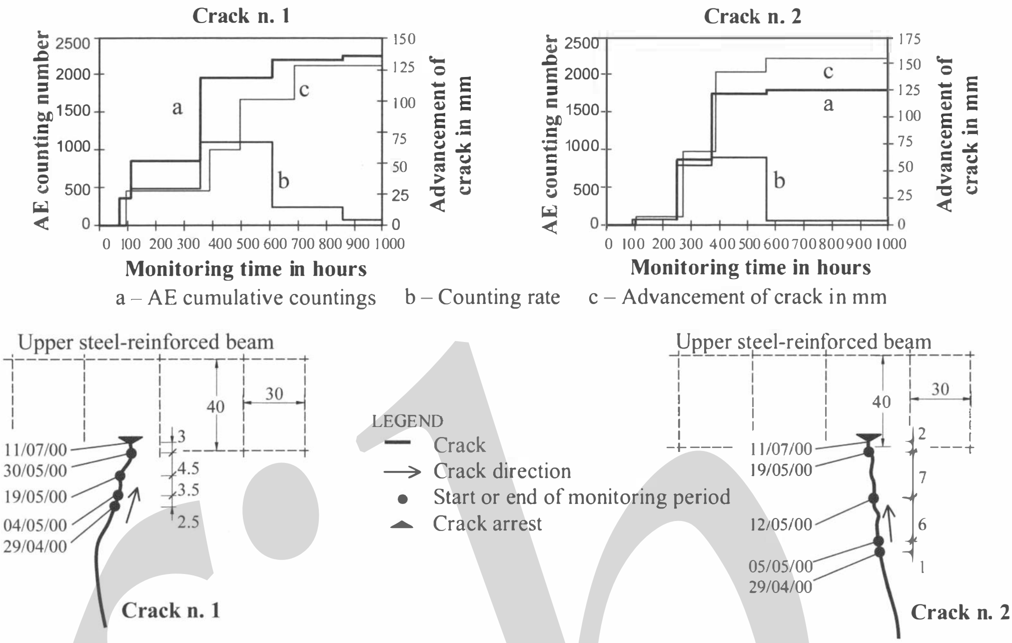

Fig.2 Results of monitoring with the AE technique

When dealing with highly heterogeneous materials like concrete, subjected to constant or increasing stress fields, experimental tests provide a typical power-law relation, like the Gutenberg-Richter law, between the amplitude of AE events (which is related to the released energy) and their frequency. This suggests that the evolution of damage follows a self-organized critical path, implying that correlations among single fracture events (even at a considerable distance) tend to a critical scale-invariant state. This means that damage is not confined below certain scales, but can extend indefinitely, culminating in the macroscopic collapse of the structural element.

The Renormalization procedure (Fig. 3) permits the critical value of the controlling parameter (which can be the load multiplier, the material strength, or any degradation parameter) to be found. At the critical point, the behaviour of the system bifurcates into two attraction basins. One is represented by points corresponding to catastrophic collapse, while the other contains the situations where structural damage is confined below a certain scale.

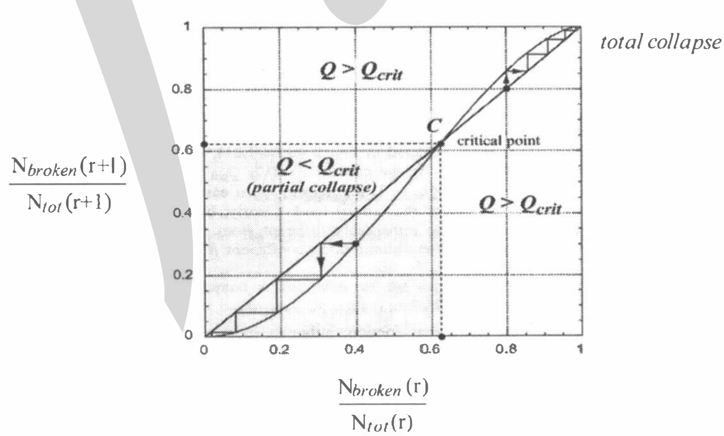

Fig.3 Renormalization curve of collapse events

ON THE USE OF COMMERCIAL PACKAGES FOR THE AUTOMATED DESIGN OF REINFORCED CONCRETE BUILDINGS

Paulo B. Lourenço
University of Minho, Department of Civil Engineering, 4800-058 Guimarães, PORTUGAL
Tel. +351 253 510 200, Fax +351 253 510 217, E-mail: pbl@civil.uminho.pt

Keywords: Safety, commercial software, reinforced concrete frame structures

1 INTRODUCTION

Due to the continuous evolution of computational software and hardware, computers and commercial packages for design and analysis are an indispensable tool for designing concrete structures. The use of adequate software packages is a necessary condition for the final quality of structural design but it is not a sufficient condition. The most important step in design is the conception, where several options are analyzed so that the most adequate solution can be found. Deficient conceptions lead to poor results in terms of safety and economy, even if sophisticated tools of analysis are used and code requirements are fulfilled. In fact, it is believed that modern analysis tools can be a mean of easily producing inadequate solutions or gross errors, due to the blind confidence of the user in the results.

The paper discusses the results of a comparison between several commercial packages for the design of reinforced concrete frames, available in Portugal. To keep the analysis feasible, the three software packages most popular in the Portuguese market were adopted. For the purpose of this study, the programs will be denoted as Program A, B and C. The reference solution, obtained with the finite element method (FEM), will be denoted as Program D. The issues believed to be of relevance in the comparison of the analyses, which have been addressed, are: modeling of the joints, modeling of slabs, dynamic analysis and amount of reinforcement in a complete design analysis. Here, only this last issue is shown.

2 COMPARATIVE ANALYSIS OF COMPLETE DESIGN

For the adopted six-story building, large and unclear differences could be found between different commercial packages, in terms of internal forces and amount of prescribed reinforcement. Fig. 1 illustrates the results obtained in a selected beam and column, in terms of envelope of bending moments and of amount of reinforcement, respectively. The differences are significant.

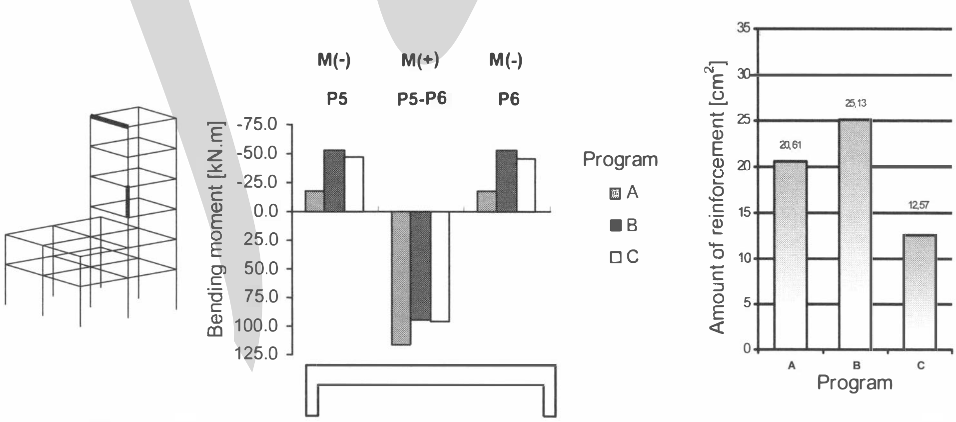

Fig.1 Comparison of the envelope of bending moments in a selected beam and column

Globally, in the structure, the amount of reinforcement, as calculated by the software package, exhibits a variation up to +50% in the beams and up to +80% in the columns, using the minimum value as a reference, see Table 1. For the foundations, both steel and concrete as relevant and no geometry input is required for the analysis. Adopting typical construction costs in Portugal, the values in Table 2 are found. Globally, a difference up to +95% is found in the cost of the foundations, mostly due to the default option of a minimum footing height in program A. In any case, the values encountered are clearly unacceptable for practice and impossible to justify only by the detailing automated procedures.

Table 1 Total amounts of reinforcement obtained with the three different packages

Program	Steel in beams (kg)	Steel in columns (kg)
A	3335	1852
B	3798	3356
C	2548	1956

Table 2 Quantities and cost of foundations

	Concrete (m^3)	Steel (kg)	Cost concrete (75€/m^3)	Cost steel (0.55€/kg)	Total (€)
Program A	47.1	276.2	3532	152	3684
Program B	24.2	531.9	1815	293	2108
Program C	21.0	564.9	1575	311	1886

3 MAIN ISSUES RESULTING FROM THE COMPARATIVE ANALYSIS

3.1 Comparison between the commercial packages

For a given structure, designed with three different commercial packages, it was possible to find (a) differences in the amount of reinforcement of 1:3 in selected beams and 1:2 in selected columns; (b) differences of around 50% in the total amount of beam reinforcement and around 120% in the total amount of column reinforcement.

For a number of different structures, the dynamic results indicated up to 50% difference in the shear base force.

3.2 Aspects related to a single commercial package

A reduction factor for the bending stiffness of the columns of the last floor was found in one of the programs. The variation of the base shear force due to this reduction factor can be up to 30%.

A low stiffness connection between walls, modeled with shell elements, and beams, modeled with beam elements, was found in one of the programs. This low stiffness connection resulted in negative bending moments up to 50% of the expected elastic values.

For the analysis of a symmetric structure, diagonal vibration modes were found in one of the programs. The consequence is that the seismic action was increased up to 30%.

The maximum bending moment in one of the programs is associated with the divisions considered in the beam and does not represent the actual maximum.

A simplified method to calculate the stiffness matrix associated with the modal analysis was found in one of the programs. No reference on this simplification could be found in the user's manual.

In one of the programs, the change in the Young's modulus of the section type does not reflect a change in the members associated with this section. In order to make the change real, the section type must be reattributed to the members.

4 CONCLUSIONS

In the present paper, the results of two benchmarks analyzed by five experienced users (personnel from the software distributors) and five commercial packages resulted in a large variation of results. Several difficulties were found to understand the results provided by the software distributors and the hypotheses adopted by the software developers. For this reason, a single user exhaustively tested three popular software packages in Portugal. The significant differences in the obtained results (up to 1:3 in selected beams and 1:2 in selected columns) demonstrate the need to adequately master and understand the adopted design tools.

Finally, it seems absolutely necessary that modern analysts develop a critical attitude and not an excessive confidence in the results obtained by software.

FINITE ELEMENT ANALYSIS OF STRESS CORROSION CRACK GROWTH OF PRESTRESSED BARS

Lin Bing
School of Civil Engineering and Mechanics
Shanghai Jiao Tong University
Shanghai 200240, P.R.China

Lu Guanglu
Bridge Department
Tongji University
Shanghai 200092, P.R.China

Keywords: Stress Corrosion, finite element method, crack growth

1 INTRODUCTION

High-strength prestressed bars are widely used in prestressed concrete structures. These bars are in high stress status. Some times they are under the conditions of aggressive environments, and easily attacked by corrosion media. Therefore, these bars fracture even if the stress caused by external load is far below the yield strength of materials, and the delayed failure of the bars occurs in the region of the lower potential (cathodic regime). Under this condition, the failure of the bars is caused by hydrogen-induced stress corrosion cracking. The stress lying in the bars will induce hydrogen diffusion and concentration[1], especially at the crack tip zone where the higher stress is produced, and moreover, at this zone, the interaction of the concentrated hydrogen and the stress result in the acceleration of the crack growth. At the same time, the materials at the crack tip zone are yielded. In this case, elastic-plastic fracture mechanics method could be used to calculate the stress intensity factor K_I of the crack tip.

With the help of some experiment data provided by J.Toribio etc.[2], this paper indicates that the elastic-plastic finite element method is more correct than the elastic one in calculating the stress intensity factor K_I of the crack tip, especially in the high stress status.

2 PROBLEM DESCRIPTION

2.1 Geometry and material

The schematic representation of the axisymmetric notched bar is shown in Fig.1. The Young's modulus and 0.2% proof stress of the specimen are 199GPa and 600 MPa respectively.

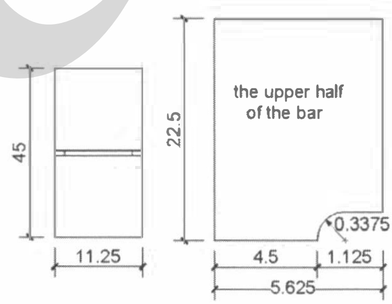

Fig.1 Notched geometries

3 FINITE ELEMENT MODEL

3.1 Finite element method

Due to axisymmetry, only the upper half of the specimen is modeled. Eight-node axisymmetric elements are used.

3.2 Material models

When an elastic analysis is applied, the material model is chosen as isotropic linear elastic. But when considering the plastic characteristic of materials, an elastic-plastic analysis is applied and the material model is chosen as plastic-multilinear.

4 HYDROGEN CONCENTRATION

In the process of the stress corrosion cracking (SCC), the crack growth is very slow. Therefore, the hydrogen diffusion can be assumed to be the steady state, and there is a long duration in which the hydrogen concentration in front of the crack tip is allowed to reach equilibrium state. According to Fick's laws, the hydrogen concentration in front of the crack tip can be obtained[1]:

$$C_H = C_0 \exp[\sigma_h \frac{V_R}{RT}] \qquad (1)$$

where C_H is the hydrogen concentration induced by the applied stress field around the crack tip, C_0 is a bulk hydrogen concentration, σ_h is the hydrostatic stress, R is the universal gas constant, T is the absolute temperature, and V_R is the partial molar volume of hydrogen.

5 CRACK GROWTH RATE da/dt

Untill the hydrogen concentration C_H reaches the critical value, the hydrogen-induced crack would not be nucleated. The hydrogen in the solution is decompounded to form hydrogen atoms, and then the hydrogen atoms enter the specimen and diffuse to reach the expanding crack tip. By this time, a hydrogen-induced crack would continue to expand.

The experiment results[2]show that, in the process of the hydrogen-induced SCC, da/dt vs. K_I curve is divided into three stages: (I) the first stage: just as K_I exceeds K_{IH} (critical stress intensity factor), the crack suddenly accelerates to grow; (II) the second stage: the da/dt is independent of K_I and only controlled by chemical processes; (III) the third stage: the da/dt is obviously dependent on K_I again. The crack length is close to the critical fracture value.

In the first two stages, the da/dt could be expressed as follows respectively[3]:

The first stage: $$\left(\frac{da}{dt}\right)_I = \frac{AC_0DK_I}{T} \quad (2)$$

The second stage: $$\left(\frac{da}{dt}\right)_{II} = \frac{BC_0D}{T} \quad (3)$$

where D is the diffusion coefficient, both A and B are constants relating with crystal structures.

6 CALCULATED RESULTS

When the tensile stress σ is applied at the both ends of the bar, the calculation results of the K_I are shown in Fig.2 The curve a represents the relationship between K_I and σ by the elastic analysis, and the curve b represents the relationship between K_I and σ by the elastic-plastic analysis.

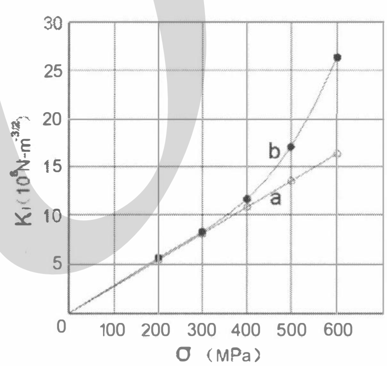

Fig. 2 the curve of K_I vs.σ

7 CONCLUSIONS

On the basis of the above-mentioned results, the following conclusions could be got:

1) According to the equation (1), (2) and (3), it can be concluded that the stress has a great influence on the hydrogen concentration and crack growth around the crack tip zone. Moreover, the equation (2) show that the crack growth rate da/dt is in direct proportion to K_I in the first stage in the process of SCC.

2) According to the Fig.2, when σ<400 MPa, the differences of K_I values got by the elastic and elastic-plastic methods are small, but if σ = 600 MPa, the values of K_I have a great difference. So if the stress in materials is very high, the elastic method is not correct for calculating the crack growth rate in the process of SCC.

3) In order to obtain the crack growth rate in the process of SCC correctly, it is very important to know the stress-strain state around the crack tip zone.

REFERENCES

[1] M.A.Astiz, in C.Taylor, B.R.J.Owen and E.Hinton(eds.), Computational Methods for Non Linear Problems, Pineridge, Swansea, 1987, pp.271-299

[2] Toribio,J., Lancha, A. M. and Elices,M. : Factors influencing stress corrosion cracking of high strength pearlitic steels, Corrosion Science v 35 n 1-4 pt 1 Jun 28-Jul 3 1992 1993

[3] Chu, W.–Y., Qiao, L.–J., Chen, Q.Z. and Gao, K.W. : Fracture and Environmental Fracture, Science Press, 2000 (in Chinese)

YIELD LINE ANALYSIS OF STEEL CONNECTION BETWEEN PRECAST CONCRETE MEMBERS IN EFFECT OF ECCENTRIC LOADING

M. R. Adlparvar
School of Railway Engineering
Iran University of Science and Technology (IUST)

Keywords: Yield line, PrecastConcrete,Cleat connector, Shear friction, Web and Flange.

1 INTRODUCTION

Yield line theory was proposed for the first time by Ingerslev [1] in 1923 and substantially pioneered by Johansen[2] 1943. It is essentially an ultimate – load theory for concrete slab design and is based on an assumed collapse mechanism and the plastic properties of under-reinforced concrete slabs. The assumed collapse mechanism is defined by a pattern of yield lines, along which the reinforcement has yielded and the location of which depends on the loading and boundary conditions.

The result of the yield line method gives an upper bound solution to the collapse load. Ideally, there should be a wide range of collapse mechanisms than the collapse load. The one chosen from this range may not be considered in order to show the mechanism gives the unique solution. Fortunately, in the field of reinforced concrete slabs where most of the yield line work has been carried out, a considerable amount of experimental work has indicated the successful application of upper bound solutions, thus giving confidence to the use of this method in design.

The yield line method neglects the effect of strain-hardening of the reinforcement and ignores the effect of membrane forces.

2 YIELD LINE IN RIGHT HAND HALF OF THE SEATING PLATE

Assuming the yield line pattern in this case for half the horizontal plate in the structural Tee (cut from a Universal Column) given in Fig.3 deforming under point load 'f ' in the bolt.The Principle of Virtual Work (PVW) is used to determine the plastic collapse load using the yield line method. First a virtual deformation Δ' is assumed at the bolt position 'g'.

3 YIELD LINE IN LEFT HAND HALF OF THE SEATING PLATE

Consider the yield line pattern based on the failure pattern in the test results, where bearing is maintained between beam soffit and plate on rectangular area.

The external virtual energy (Ee) can be defined as follows:

$$E_e = T_y \phi \qquad (1)$$

The yield torque capacity of the seating cleat assuming one hinge in the web is equal to:

$$T_y = \left[m_{pf} \left(\frac{\ell}{\tan\alpha_1} + \frac{L}{\sin^2 \alpha_1} \right) + m_{pf}\, \ell \left(\mathrm{Cotan}\alpha_2 + \mathrm{Sec}\alpha_2 \mathrm{Csc}\alpha_2 \right) + m_{pw} L \right] \qquad (2)$$

The yield torque capacity of the seating plate in the beam-to-column joint without considering the shear friction effect of the concrete and grout in the narrow joint depends on the following factors:

i) The thickness of the horizontal plate in the cleat (tw) is that of the web of U.C off-cut. The stiffener plate is fabricated from any suitable thickness plate (ts).
Plots of these results in terms of varying thickness are shown in Fig.1. As can be seen, the yield torque increases with increasing thickness of the horizontal cleat plate and reaches a maximum with tw = 19.2mm.

ii) Increasing the width of the seating cleat also affects the yield torque capacity of the cleat, because the contact bearing area of the precast concrete beam to cleat and the lever arm are also increased. The change in the torque capacity of the cleat with an increase of width from 180mm to 300mm for a range of U.C. off cuts is shown in Fig.2.

iii) The distance 'z' between the contact bearing area of the edge beam to the vertical face of the seating cleat can be very significant. This should be kept to a minimum in order to increase the yield torque capacity of the cleat and torsional stiffness.

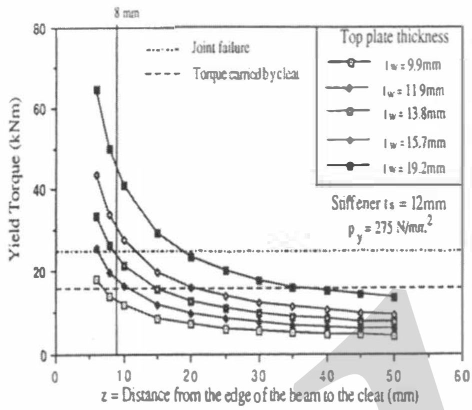

Fig.1. Yield torque capacity of the seating cleat with different thickness of bearing plate (bearing width = 180mm).

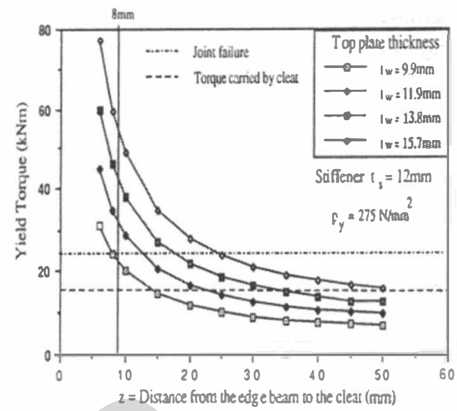

Fig.2. Yield torque capacity of the seating cleat with different thickness of bearing plate (bearing width = 300mm).

As can be seen from Fig.1 and 2 the yield torque capacity increases gradually with decreasing distance 'z'. For the particular beam/column connection the value 0f z=8mm (allowing for root radius). The maximum yield torque capacities of the cleat are Ty=14 kNm for tw=9.9mm and Ty=32kNm for tw=15.7mm (see Fig.1. for bearing width=180mm). On the other hand if the bearing width of the precast concrete beam to cleat is increased from 180mm to 300mm, the maximum yield torque capacity of the cleat becomes Ty=22kNm for tw=9.9mm and Ty=54kNm for tw=15.7mm (see Fig.2 for bearing width= 300mm).

4 DISCUSSION AND CONCLUSIONS

The test results in cleat type of connector was used for the beam-to-column connection has shown the failure of the joint in effect of eccentric loading at very low load level. The shear friction in the joint between the beam and column broke down at T=24.2kNm. After this the torsional moment (torque) carried by the cleat connector was recorded T=16kNm. A yield line theory was adopted to study this behavior and it has been possible to calculate the yield torque capacity of the cleat. As described above, the maximum yield torque capacity of the cleat (Ty) is based on Eq.2.

The yield torque capacity of the seating cleat could be increased by using two methods as follows:

1) Increasing the thickness of the horizontal plate (tw in Fig.1).
2) Increasing the width of the cleat to the maximum 300mm (if possible), which is equal to the width of the precast concrete beam and column.

To prevent the early failure (at low load level) in the joint two types of connector are suggested for use in the beam-to-column connections. These are either (1) using a cleat cut from U.C. with web thickness tw=13.8mm in which the yield torque capacity increases to Ty=24kNm, or (2) using a cleat with 300mm width and the same thickness used previously (tw=11.9mm) in which the yield torque capacity increases to 32kNm. There are many alternative choices in terms of different thickness and widths of cleat to increase the yield torque capacity of the seating cleat as shown in Figs1 and 2 as required.

The object of increasing the torque capacity of the cleat is to prevent the type of rapid failure observed in the test procedure.

REFERENCES

[1] Ingerslev A.,: The strength of rectangular slabs. Structural Engineers, Vol.1, No.1, January 1923, pp3-14.

[2] Johansen K. W., : Yield line theory. Cement and Concrete Association, London 1943.

NEW PLASTIC DESIGN MODEL OF HYPERSTATIC PRESTRESSED CONCRETE STRUCTURES

Zheng Wen Zhong   Li He Ping
School of Civil Engineering, Harbin Institute of Technology, Harbin, 150090, R.P China

Keywords: prestressed concrete; hyperstatic structures; plastic design; new model.

1 STATE-OF-ART INSIDE AND OUTSIDE CHINA[1-3]

Plastic calculation theory and design method of hyperstatic prestressed concrete structures are one of problems thought highly in theory and engineering. After going into it inside and outside China, lots of experimental data are accumulated. At the same time, three plastic design models are obtained. In these design models, design moments of support at critical section are shown respectively

$$M = (1-\beta)(M_{Load} + M_{\sec}) \tag{1}$$

$$M = (1-\beta)M_{Load} + M_{\sec} \tag{2}$$

$$M = (0.7+\xi)M_{Load} + 20/3(\xi - 0.15)M_{\sec} \qquad (0.15 \le \xi \le 0.3) \tag{3}$$

We suggest that the value (M_{load}+M_{sec}) be modulated, and the same of moment modulation coefficient be used in M_{load} and M_{sec}. As we know, in the condition of invariable concrete relative depth of the equivalent stress block of the section ξ, if effective prestressing in tendons, and proportion of tendons and nonprestressed reinforcing are different, plastic angle rotation θ_p is not the same, so extent of moment modulation is different.

2 CALCULATION OF ULTIMATE CURVATURE AND NOMINAL YIELDED CURVATURE

2.1 Calculation of ultimate curvature φ_u

In terms of the assumption of plane section, since compressive force in the concrete is equal to the sum of forces in the prestressing tendons and nonprestressed reinforcing in tensile zone, the coordinate value (σ_p, ε_p) in stress-strain diagram of prestressing tendon at strength state of normal section can be obtained. Therefore, the depth of compressive zone of section c can be worked out at this state. The ultimate curvature (φ_u) of section in prestressed beam is given by

$$\varphi_u = \varepsilon_{cu} / c \tag{4}$$

2.2 Calculation of Norminal yielded curvature φ_y

In terms of the assumption of plane section, since compressive force in the concrete is equal to the sum of forces in the prestressing tendons and nonprestressed reinforcing in tensile zone, the coordinate value (σ_c, ε_c) in stress-strain diagram of compressive concrete can be obtained when stress of nonprestressed reinforcing is yielded strength. Therefore, the depth of compressive zone of section X can be worked out at this state. The norminal yielded curvature φ_y of section in prestressed beam is given by

$$\varphi_y = \varepsilon_{sy} / (h_s - X) \tag{5}$$

3 THE VALUE OF PLASTIC MOMENT

3.1 Determination of plastic hinge rotation of section

Plastic hinge rotation θ_p can be obtained as follows

$$\theta_p = (\varphi_u - \varphi_y) l_p \tag{6}$$

In prestressed concrete structures, l_p can be given as follows

$$l_p = K'C_aC_b(1-1.2n')h_0 \tag{7}$$

3.2 Establishment of the formula of moment modulation coefficient β

In terms of the thought and method of φ_u and φ_y, the result of experiment data inside and outside China being adjusted with Eq. (6) and (7), can be illustrated in Fig.1, where plain rectangular coordinate system treats relative plastic hinge rotation θ_p/h_0 as cross axis and moment modulation coefficient β as longitudinal axis. The lower line owned 95% reliability limits experimental data in Fig.1. Moreover, the formula of moment modulation coefficient β can be obtained as follows

$$\beta = \begin{cases} 0.047(10^5\theta_p/h_0)+0.015 & (10^5\theta_p/h_0)) \le 5 \\ 0.25 & (10^5\theta_p/h_0) > 5 \end{cases} \tag{8}$$

Thus, the design value of plastic moment of support critical section can be calculated as follows

$$M = (1-\beta)(M_{Load} + M_{\sec}) \tag{9}$$

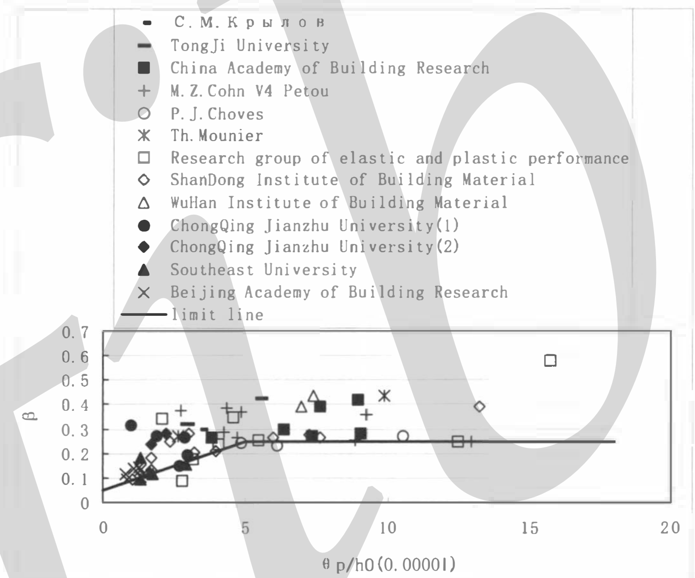

Fig.1 Compare with calculation and experimental data of moment modulation coefficient

REFERENCE

1. ACI318-95. Building Code Requirements for Structural Concrete and Commentary.
2. Shi Ping Fu. Internal Force Redistribution and Moment Modulation in Partially Prestressed Concrete Hyperstatic Structures.. Southeast University, 1995.
3. Design Code of Concrete Structure（Contributions on solicited opinions）. Design Codes of Concrete Structure. National Standard Management Group, 1999.8 .

ANALYTIC METHOD OF LATERAL RESTRAINT IN PRESTRESSED CONCRETE STRUCTURES

Zheng Wen-zhong Zhou Wei
School of Civil Engineering, Harbin Institute of Technology, Harbin, 150090, R.P China

Keywords: prestressed concrete; lateral restraint; secondary axial force; secondary moment; two-stage-working principle of prestressing tendons

1 INTRODUCTION

Most indeterminate prestressed concrete structures, except the few structures for example, continuous beams, etc, are ones with lateral restraint. Lateral restraint is defined as vertical members such as columns, shear walls and tubes, etc, in prestressed concrete frames, the flat plate-column prestressed concrete structures and tall prestressed concrete structures. Lateral restraint restricts axial compressive deformation of beams and slabs. So it influences prestress transfer in horizontal flexural members, and the effect becomes more evident when sections of vertical members are large.

Traditional method, which is based on work principle of continuous prestressed concrete members, can be used in designing structures without lateral restraint. For structures with lateral restraint, it can be applied under the assumption that axial compressive and tensile rigidity in plane floor is infinite. In the condition of small lateral restraint, the calculating result can be accepted. For structures with large lateral restraint, the calculation value of flexural member's strength is bigger than that of real one, and deflection and crack width will be smaller. When traditional method is applied to design structures with large lateral restraint not considering the influence of lateral restraint for prestress transfer and calculating result, the construction is not safe. Therefore, research on analytic method of lateral restraint in prestressed concrete structures is meaningful both theoretically and practically in designing constructions.

2 ANALYTIC METHOD OF LATERAL RESTRAINT

2.1 Load-carrying capacity formulae of traditional method

The following is the load-carrying capacity formulae of singly flexural prestressed concrete section of traditional method

$$\begin{cases} M_{Load} + M_{\sec} = f_y A_s (h_{0s} - \frac{x}{2}) + f_{py} A_p (h_{0p} - \frac{x}{2}) \\ f_{cm} bx = f_y A_s + f_{py} A_p \end{cases} \quad (1)$$

2.2 Lateral-restraint modulus

Lateral-restraint modulus η is defined as ratio of prestress compression considering lateral restraint to that not considering.

2.3 Secondary axial force method considering the influence of lateral restraint of flexural member's strength

It illustrates secondary axial force and the calculation of load-carrying capacity of singly section of flexural member with secondary axial force considering the influence of lateral restraint.

2.4 Two-stage-work principle method considering the influence of lateral restraint

This paper divides the function processes of tendons into two stages. In the first positive stage, from completion of tendons being pulled to prestress down to effective prestress (σ_{pe}) in tendons due to loss of stress, prestressing equivalent loads play the same role of external (dead) load. In second passive stage, after termination of prestress process, tendons work as material just as reinforced bar in prestressed concrete structures only to resist external loads effects and the strength of tendons leaves residual (f_{py}- σ_{pe}) of tendon Code strength (f_{py}) minus effective prestress (σ_{pe}).

Based on two-stage-work principle of tendons and definition of lateral restraint modulus, formulae of load-carrying capacity of single section of flexural member without and with lateral restraint are derived

$$\begin{cases} M_{Load} + M_p = A_s f_y (h_s - \frac{x}{2}) \\ \quad + A_p \sigma_{pe} (h_p - e_p - \frac{x}{2}) \\ \quad + A_p (f_{py} - \sigma_{pe})(h_p - \frac{x}{2}) \\ f_{cm} bx = A_s f_y + A_p \sigma_{pe} \\ \quad + A_p (f_{py} - \sigma_{pe}) \end{cases} \quad (2)$$

$$\begin{cases} M_{Load} + M_p = A_s f_y (h_s - \frac{x}{2}) \\ \quad + A_p (\eta \sigma_{con} - \sigma_l)(h_p - e_p - \frac{x}{2}) \\ \quad + A_p (f_{py} - \sigma_{pe})(h_p - \frac{x}{2}) \\ f_{cm} bx = A_s f_y + A_p (\eta \sigma_{con} - \sigma_l) \\ \quad + A_p (f_{py} - \sigma_{pe}) \end{cases} \quad (3)$$

2.5 Renewing the definition method of secondary moment considering the influence of lateral restraint

Renewing primary moment is defined as the prestressing compression N_p =(η σ_{con}- σ_l)A_P times its eccentricity e, i.e. M_l= N_p . e. Balancing prestressing moment M_p is the moment under prestressing equivalent loads. Therefore, renewing secondary moment is M_{sec}=M_p-M_l.

2.6 Internal force due to lateral deformation method considering the influence of lateral restraint

Internal force due to axial shortening of beams or slab causes the secondary moment, which can be added into traditional secondary moment to consider the influence of lateral restraint.

2.7 Constructional ways to deal with lateral restraint

Three constructional ways as hinged joint in beam end, pin joint, and sub column in column end can be used to eliminate or weaken effects of lateral restraint.

3 CONCLUDING REMARKS

This paper presents some design methods and constructional ways for rationally calculating effects of lateral restraint.

Effects of lateral restraint are connected with structure style, construction program and sequence of tendons being pulled, etc. This will be studied carefully later.

REFERENCE

[1] Zheng wenzhong, Wang Ying: Unified design method and example of prestressed concrete building structures. Helongjiang science and technology publishing house, 1998

[2] Lu Zhitao, Meng Shaoping: Design of modern prestressing. Architectural Industry Publishing House of China, 1998

FIRE DESIGN OF CONCRETE
Materials, structures and modelling

Gabriel Alexander Khoury - *Imperial College, London, UK*
Yngve Anderberg - *Fire Safety Design, Malmo, Sweden*
Kees Both - *TNO, Delft, Netherlands*
Joris Felinger - *TNO, Delft, Netherlands*
Carmelo Majorana - *Padua University, Padua, Italy*
Niels Peter Hoj - *Cowi, Copenhagen, Denmark*

Keywords: Concrete, Fire, Modelling, FIB, Spalling, Properties

Investigation into the effect of fire on concrete and concrete structures has been conducted since at least 1922 primarily in relation to buildings. Up to about a decade ago, fire research was focused upon the behaviour of *normal strength* concrete at high temperatures, and engineers mainly employed *prescriptive* methods of design to ensure structural stability in fire for a sufficient period of time to allow people to escape and fire services to extinguish the fire. Since then, there have been two major developments in this field, namely: (a) the increasing use of high performance concrete (HPC) in buildings, tunnels and bridges allowing the use of more slender and complex structures but with a higher tendency to experience explosive spalling in fire, and (b) the growing acceptance of the use of performance based fire engineering calculations for the structural analysis and design against fire.

Damage to HPC in recent high profile tunnel fires in Europe has provided impetus for research into improving: (a) tunnel safety, and (b) concrete performance in fire. The departure from traditional concrete mixes and structures requires a design based on scientific principles, rendering inappropriate simple extrapolation of existing practice. Traditionally, concrete has been regarded as "fireproof" because of its inflammability and thermal insulating properties. The two main problems experienced by traditional concrete in fire, namely (a) deterioration in mechanical properties, explosive spalling can be addressed by careful mix design. Recent tests have shown that concrete containing the appropriate type and amount of polypropylene fibres will significantly reduce the risk of spalling even when subjected to a tunnel fire that is more severe than an ISO 834 or a hydrocarbon fire. In fact, sprayed concrete containing pp fibres is used as a fire barrier to protect tunnel linings. Careful design can also produce concrete with improved mechanical properties for temperatures as high as 300-600°C. Research to date has shown that concrete is a versatile material and, if appropriately designed, can be inherently fire resistant. This has led to the current era of "bespoke" fit for purpose concrete mix design against fire, but which also holistically serves the structural and architectural function of the material.

At the structural level, the impetus for the development of fire engineering assessment methods came from the limitations inherent in the traditional prescriptive methods of design. Several countries have already developed performance-based codes (e.g. U.K., Sweden, Norway, New Zealand and Australia) and many more countries are in the process of doing so. While the U.K. has led in this field with the publication in 1992 of the Building Regulations Approved Document B3, performance based structural design and analysis methods are still not as widely used by engineers in the UK as they are in Scandinavia. This topic is currently the focus of much discussion, research and development worldwide. This has led to new ideas for improving fire safety, thus encouraging the engineer to develop new creative solutions. Traditionally fire safety was a set of conventions rather than a rational approach with engineering tools. To move forward it is essential that the whole package of conventions, and requirements, are re-examined in a holistic and scientific manner.

[AND 92a] Anderberg, Y. and Pettersson, O. Manual on Fire Engineering Design of Concrete Structures. Swedish Board for Building Research, 1992. ISBN 91-540-5448-6, T13:1992, Part 1.

[BAZ 96] Bazant, Z. and Kaplan, M., Concrete at high temperatures, Longman Group Ltd., 1996, pp. 412, ISBN 0-582-08626-4.

[KHO 00] Khoury, G.A., Effect of fire on concrete and concrete structures. Progress in Structural Engineering and Materials, Volume 2, No. 4, Oct-Dec 2000, pp. 429-447.

[SCH 86] Schneider U. (Ed.), Properties of materials at high temperatures - Concrete. RILEM-Report 44-PHT, 2nd Ed., Kassel, June 1986

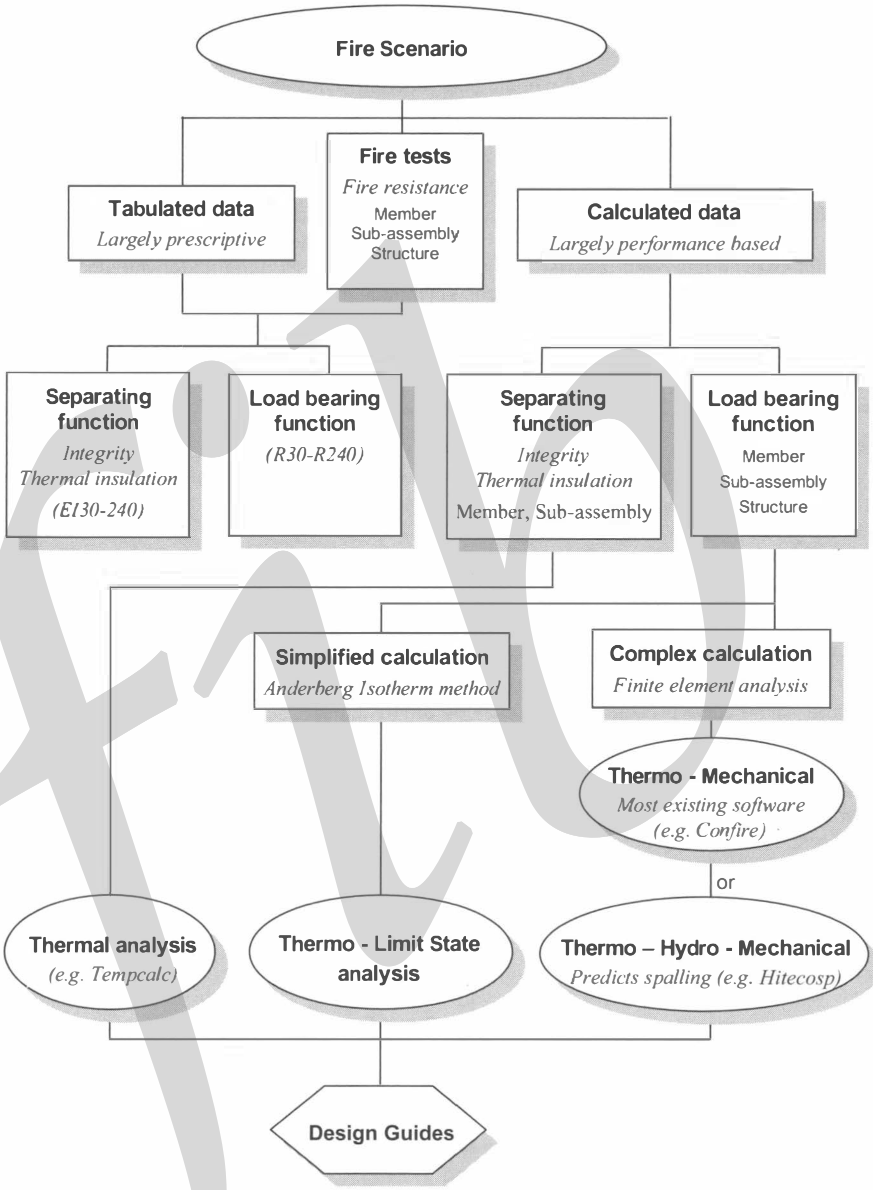

Figure 1. Three main options of concrete fire assessment and design process [KHO 00].
Note: Calculation based methods are becoming acceptable in an increasing number of countries.

AN ESTIMATION METHOD FOR FIRE RESISTANCE OF REINFORCED CONCRETE ELEMENTS CONSIDERING SPALLING

Takeshi Morita, Akira Nishida, Hiroshi Hashida and Nobuyuki Yamazaki
Institute of Technology, Shimizu Corporation

Keywords: fire, high-strength concrete, reinforced concrete, synthetic fiber, spalling

1 INTRODUCTION

High strength concrete indicates inconsistent behavior 'spalling' when exposed to fire. When a structural fire safety design of reinforced concrete elements and structures is performed, designers must know the degree of spalling. Moreover, though the effectiveness of polypropylene (PP) fiber in the prevention of spalling has been reported, an optimum amount of PP fiber added into concrete mixture has not been clearly established. A practical estimation method for fire resistance of reinforced concrete elements considering spalling is proposed in this paper. The study focuses mainly on the derivation of experimental data useful in structural fire safety design and application.

2 EXPERIMENTS

2.1 Materials, specimens and methods

(1) Fire tests of small specimens of concrete mixed with PP fibers: Materials used for concrete were moderate-heat Portland cement, crushed sand stone, land sand and superplasticizer. The W/C ratio of concrete was 0.25. Specimens were heated under the fire temperature – time curve prescribed in ISO834 for 60 minutes.

(2) Fire tests of unloaded reinforced concrete elements: Different W/C ratios were applied in the experiments to get the relationships between W/C ratio and spalling degree, and the relationship between spalling degree, W/C ratio and dosage of PP fibers. The geometry and configuration of reinforced concrete specimens are as follows: section: 70cm * 70cm, height: 140cm, cover thickness: 40mm and 110mm, amount of main re-bar: 2.14% and 3.21%. Specimens were heated under the fire temperature – time curve prescribed in ISO834 for 180 minutes.

2.2 Results

(1) Effectiveness of PP fiber for reduction of spalling

The influence of diameter and length of fibers on the spalling reduction was investigated. According to the fire test results, PP fibers with smaller diameter and longer length are favorable for the reduction of spalling. It can be said that the higher the volume of fibers in concrete, the less the spalling. Moreover, smaller diameter is advantageous for the reduction of spalling.

(2) Spalling degree of reinforced concrete columns

Fig.1 shows the specimens after the fire tests. It is very clear that a lower W/C ratio of concrete leads to deeper spalling. Spalling depths were measured on the lateral surfaces of the column specimens. Simple regression equations, Eq.1, Eq.2 and Eq.3, are obtained from measured depths. In these equations, D_b is the averaged depth of spalling measured on lateral surfaces of a reinforced concrete element made without fibers (mm), W is the weight of water in unit volume of concrete (kg/m^3), C is the weight of cement in unit volume of concrete (kg/m^3), and t_c is the age of concrete (days).

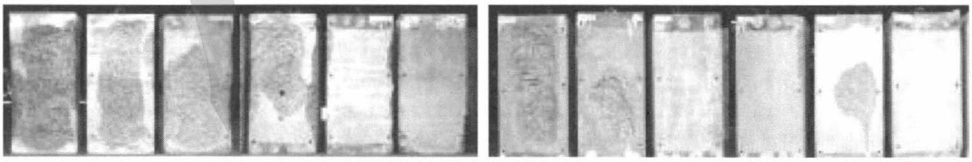

Fig.1 Columns after fire test - effect of water-cement ratio of concrete to the spalling

D_b = 83-157*(W/C) (W/C<0.275, W/C=0.275) (1)
D_b =70+0.235t_c - (109+0.854t_c)*(W/C) (0.275<W/C, and 56<t_c<365 days or t_c =365days) (2)
D_b =156-421*(W/C) (0.275<W/C, and 365 days<concrete age) (3)

The authors have carried out fire tests on more than 20 reinforced concrete elements. An index of the reduction of spalling by PP fibers, 'spalling reduction ratio' is introduced here and defined as Eq.4. In Eq.4, α is the spalling reduction ratio, D_f is the averaged spalling depth measured on lateral surfaces of a reinforced concrete element (mm). The relationship between the spalling reduction ratio and dosage of fibers in concrete are shown in Fig.2, and the relationship between the spalling reduction ratio and W/C ratio of concrete are shown in Fig.3. The multiple regression analysis on α, V_f and W/C leads to Eq.5. In Eq.5, V_f is the volume percentage of fibers in unit volume of concrete (vol%).

α =(D_b – D_f)/D_b (4)
α =V_f*(43.9*(W/C)-7.43) (5)

3 ESTIMATION OF STRUCTURAL FIRE RESISTANCE OF REINFORCED CONCRETE ELEMENTS

A flowchart for structural fire safety design for reinforced concrete elements can be proposed based on the work described in this paper and the previous works by the authors. The flowchart is shown in Fig.4. The important point of the flowchart is that the spalling can be taken into account for calculations of temperatures and structural behavior of reinforced concrete elements by estimating the spalling depths in advance of those calculations. It is safer estimation from the point of fire safety design that the calculation of temperatures and structural behavior are done with a sectional area reduced by spalling depth.

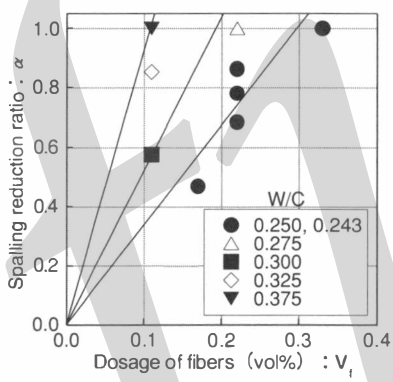

Fig.2 Spalling reduction ratio .vs. dosage of PP fibers

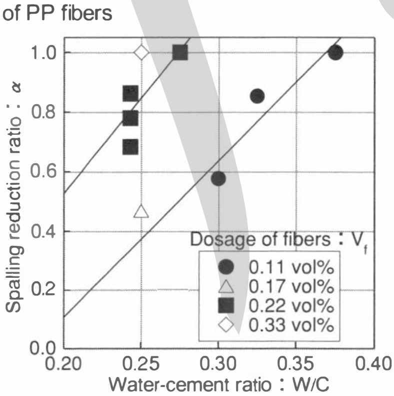

Fig.3 Spalling reduction ratio .vs. W/C ratio

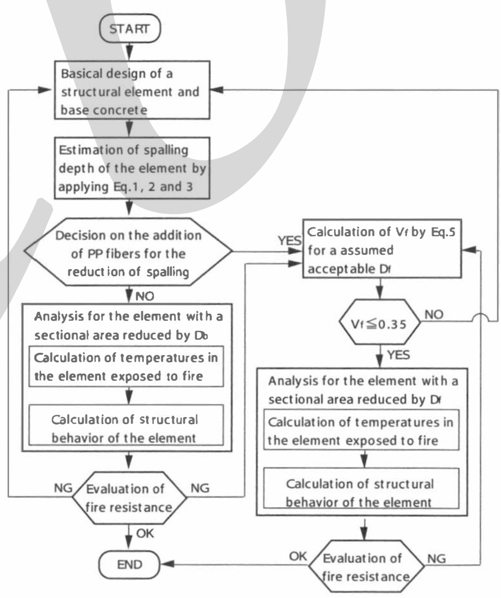

Fig.4 Flowchart for structural fire safety design for reinforced concrete elements

FIRE PERFORMANCE OF REINFORCED CONCRETE COLUMNS USING HIGH-STRENGTH CONCRETE WITH POLYPROPYLENE FIBERS

KUROIWA Shusuke, KOBAYASHI Yutaka and BABA Shigeaki
Building Engineering Research Institute
Technology Center, Taisei Corporation, JAPAN

Keywords: high-strength concrete, spalling, fire resistance, fire test under load, polypropylene fiber

1 INTRODUCTUON

Over the past five years, a number of residential buildings have been constructed in Japan [1] with concretes of specified design strengths of up to 100 MPa, mainly used in columns. The primary objective of incorporating thus high-performance concretes in these projects was to provide more space to architects by reducing the number of columns. One of the major concerns of such concrete is its fire resistance. The standard specification for reinforced concrete structures, JASS5 [2], published by the Architectural Institute of Japan, requires in case of fire that: the concrete shall not cause deformation, failure, or spalling deleterious to the fire resistance and structural yield strength. Therefore, in some of our earlier high-rise RC projects, the most straight-forward measure was taken to avoid the fire concerns: to provide additional finishing with normal-strength mortar layers all over the column surface. On the other hand, it has been known that the inclusion of polypropylene fibers improves the fire resistance of high-strength concrete by creating a pore structure that enables steam to dissipate. At 160°C, polypropylene fibers start to melt, leading to a reduction in volume of the fibers, and produce small voids within the concrete. The voids that remain create routs that let the water vapor escape. In this way, the vapor pressure is released and the thermal gradient becomes loose, and the explosive spalling is avoided [3]. The objective of this study is to experimentally investigate the effectiveness of such a methodolgy to our concretes, whose binder consists of ordinary portland cement, blast-furnace slag, gypsum, and silica fume [4].

2 EXPERIMENTAL PROGRAM

Sixteen fire tests were carried out on reduced-scale column models measuring 800mm high by 400mm square (Fig.1). Under an axial compression of 30% design load applied by a 20-MN loading system (Fig.2), the columns were subjected to the fire temperature history specified in ISO 834. The test variable were: water-binder ratio or concrete strength, coarse aggregate type, amount and length of fibers, and drying period. The compressive strength at the age of testing ranged from 100 MPa to 150 MPa depending on the test parameters.

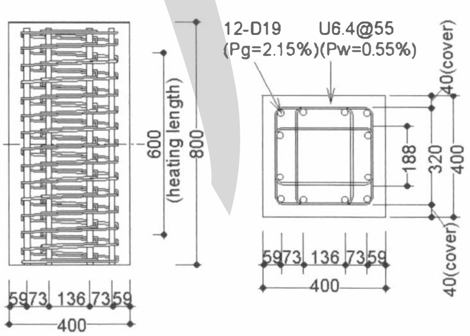

Fig.1 Elevation and cross-section of columns

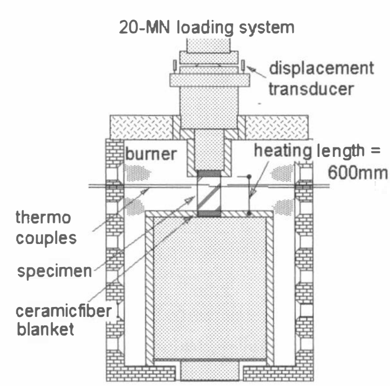

Fig.2 Test set-up

3 EXPERIMENTAL RESULTS

3.1 Influence of water-binder ratio and fiber contents

Fig.3 shows that the fiber content to reduce the spalling increased as the concrete strength increased. For all the models with a specific design strength ranging from 80MPa to 100MPa (W/B>=0.20), spalling was significantly reduced by adding polypropylene fibers of 1.0kg/m^3, and the column fire resistance reached more than 4 hours. Furthermore, the fiber inclusion of 1.5kg/m^3 eliminated spalling and thus significantly reduced the fire-induced deformation of the column specimens.

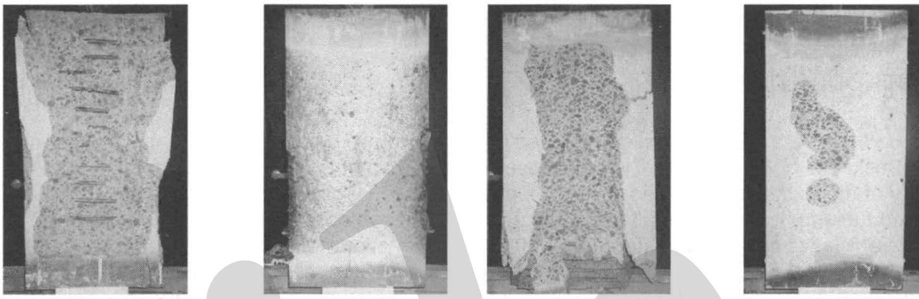

Fig.3 Columns after the fire tests. (left to right) 115MPa concrete without fibers: exposed reinforcement. 110MPa concrete with 1.0kg/m^3 fibers: no spalling. 128MPa concrete with 1.0kg/m^3 fibers: spalling without exposed reinforcement. 129MPa concrete with 1.5kg/m^3 fibers: slight spalling.

3.2 Influence of length of fibers

Columns (W/B=20, at a dosage of 1.0kg/m^3) using 20mm / 10mm long fibers were compared. Columns using 20mm fibers experienced spalling though the reinforcement was not exposed directly to fire and the load was supported during 4 hours. On the other hand, the column with 10mm fibers exposed the reinforcement due to severe spalling, and its fire resistance reached only approximately 197 minutes. The fiber length is, therefore, an important factor in terms of spalling reduction efficiency if at the same dosage.

3.3 Influence of coarse aggregate type

Columns (W/B=20, at a dosage of 1.0kg/m^3) made with andesite, limestone and hard sandstone aggregates were compared. Though spalling was observed in all columns, all the columns showed fire resistance of more than 4 hours. The spalling of limestone concrete was the severest. Moreover, it is inferred from the comparison of axial deformation that the use of hard sandstone aggregate resulted in the best performance.

3.4 Influence of drying period

Most column models (W/B=30, at a dosage of 0.75kg/m^3) were dried only for 2 months, and its fire resistance reached more than 4 hours, though some spalling was observed. On the other hand, columns dried for about 1 year, showed no spalling at all. The same tendency was observed for columns with a 18 % W/B ratio at a dosage of 2.15kg/m^3. This means that lengthening the drying period reduces the risk of the explosive spalling in high-strength concrete.

REFERENCES

[1] Jinnai H., Namiki S., Kuroha K., Kawabata I. and Hara, T.: Construction and Design of High-rise Buildings Using 100 MPa HSC. 5th International Symposium on Utilization on High Strength/ High Performance Concrete, Sandefjord Norway, pp.809-818, 1999.6

[2] F. Tomosawa, S. Nakane, K. Kuroha, and N. Yamasaki: AIJ Standard Specification(JASS) for High-Strength concrete Works. 5th International Symposium on Utilization on High Strength/ High Performance Concrete, Sandefjord Norway, pp.1331-1338, 1999.6

[3] Long T.Phan, Nicholas J.Carino, Dat Duthinh, and Edward Garboczi: NIST Special Publication 919, International Workshop on Fire Performance of High-Strength Concrete, NIST, Gaithersburb, MD, Proceedings, 1997.2

[4] K. Goto, K. Kuroha, S. Namiki and H. Jinnai: Experimental Study on High Strength Cast-in-Place Concrete with 100MPa. 4th International Symposium on Utilization of High Strength / High performance Concrete, Paris France, pp.125-134, 1996.5

THEORETICAL AND EXPERIMENTAL STUDY ON CONCRETE SPALLING IN TUNNEL FIRES

Karen Paliga and Dietmar Hosser
Institute for Building Materials, Concrete Construction and Fire Protection
Braunschweig, GERMANY

Keywords: concrete spalling, tunnel fire, moisture transport

1 INTRODUCTION

Reinforced concrete tubbings, which are used in connection with shield-driven tunnel linings, normally have a thickness of 30 to 50 cm. These relatively thin components have to guarantee the load-carrying capacity of the tunnel in a fire and it must be possible to repair them with a justifiable expenditure, as damaged tubbings cannot be replaced. The temperature development in a tunnel fire with typical road and rail vehicles is completely different from the one in an apartment fire. For this reason, in Germany the so-called RABT curve was developed for the design of tunnel constructions, which contains an extremely rapid temperature increase up to 1200°C within 5 minutes, a stationary phase with 1200°C over 30 minutes as well as a cooling phase. Reinforced concrete tubbings subjected to a tunnel fire tend to have extensive and explosive spalling which reduces the thickness of the tubbings. The fire in the Euro tunnel showed that under unfavourable conditions the reduced thickness can lead to a loss of the load-carrying capacity of the tunnel lining.

Explosive concrete spalling is mainly influenced by a thermo-mechanical and a thermo-hydrological process [1]. The process causes internal stresses in the cross section that support spalling. The thermo-hydrological process comprises mass transport in the form of water, vapour and air through the pore system of the concrete, which effect pore pressure. These causes are intensified by the extreme temperature rise of a tunnel fire.

At present systematic investigations on the concrete spalling behaviour are carried out within the framework of a research project sponsored by DFG (German research foundation) with the help of experimental and theoretical calculations of normal weight concrete by means of the FE method this contribution reports about.

2 EXPERIMENTAL INVESTIGATIONS

The emphasis of the tests was the measurement of temperature and moisture during the heating of the concrete in order to be able to retrace the processes of spalling. The temperatures are measured with the help of thermocouples, the moisture distribution in the concrete as relative moisture with the help of optical sensors. The temperature increase is almost the same with all specimens at a component depth of 1,5 cm. In the test series V3 and V4, the higher moisture content causes a longer stationary phase at 100°C. At larger depths, the

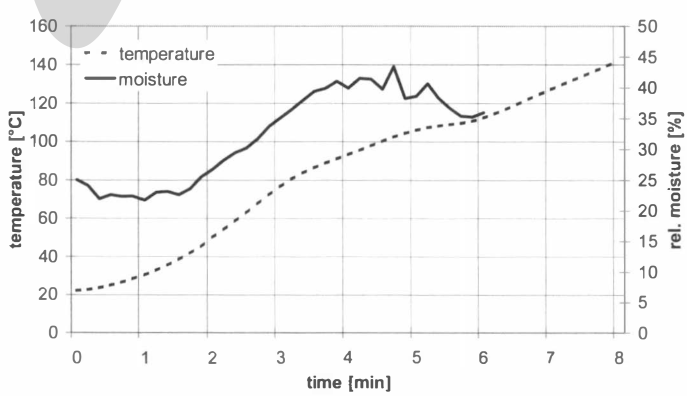

Fig. 1: Measurement of relative moisture and temperature in the concrete

influence of the lower thermal conductivity of limestone becomes recognizable, the temperature rise is lower here.

Fig. 1 shows the moisture development along with the temperature development in the concrete with an aggregate containing lime at a depth of 2 cm. This relative moisture increases from approximately 40°C on and reaches its maximum between 90 and 105°C. After that there is a decrease.

In [2] Ahmed describes the moisture and heat transport while the concrete heats up. When the concrete has sufficiently heated up at a certain component depth, free and bound water evaporates and causes pore pressure. The pore pressure presses vapour to the component surface as well as into the concrete, where it cools and condenses. While the concrete heats up, the evaporation front moves into the component.
Due to the increasing moisture in the inner concrete, pore pressure in the area of the evaporation front becomes higher, which can lead to spalling. If the moisture content can be reduced by a network of pores, pore pressure is lower.

3 THEORETICAL INVESTIGATIONS

The concrete is replaced by a network of finite elements following Wittmann [3]. By a separate modelling of aggregate and mortar matrix, different material behaviour can be considered in the calculation. A FE network is chosen according to the arrangement of aggregate and mortar matrix. Contact elements are arranged between these two components that simulate the properties of the interface. The calculations are carried out with the help of the ANSYS programme. At first, the model was validated with the help of linear material laws and known results. In further validation calculations, non-linear material laws were used and the results were verified by results of own computer codes. After the validation calculations, some of the parameters that are responsible for spalling are to be investigated. These are:

- concrete moisture
- load
- temperature-time curve
- content of polypropylene fibres
- type of aggregate

It is the objective of the investigations to ascertain the influence and interaction of different parameters on the spalling behaviour and to gain information about the production of spalling-resistant concrete.

REFERENCES

[1] Kalifa, P.; Menneteau, F.-D.; Quenard, D.: Spalling and pore pressure in HPC at high temperatures. Cement and Concrete Research 30, p. 1915-1927, 2000.

[2] Ahmed, G. N.; Hurst, J. P.: An Analytical Approach for Investigating the Causes of Spalling of High-Strength Concrete at Elevated Temperatures. International Workshop on Fire Performance of High-Strength Concrete, p. 95-108, 1997.

[3] Wittmann, F. H.: Herstellen und Eigenschaften des numerischen Betons. Baustoffe `85, Bauverlag, Wiesbaden, p. 251-255, 1985.

THE STUDY ON CONCRETE STRUCTURAL ANALYSIS FOR ROAD TUNNEL UNDER THE INCIDENT OF FIRE

Yoshikazu Ota
Ota Engineering
JAPAN

Kenji Horiuchi
Chiyoda Engineering Consultants
JAPAN

Keywords: fire, heat distribution, tunnel structure, concrete, spalling

1 INTRODUCTION

In recent years road tunnel fires have erupted in many locations around the world, which calls for the necessity to adopt more fire-effective and economical tunnel construction practices, having systematically analyzed the entire system of the tunnel. In this study, for probing into the basic characteristics pertaining to the thermal effects on tunnel structures, it is aimed at developing some fundamental literature on fire proofing measures of tunnels by setting up standard conditions and then focusing mainly thermal environmental analysis of flow field and concrete members by numerical simulations, thereby clarifying the thermal distribution of each type of tunnel structure. It was clarified that, assuming the same fire scale, circular tunnels are advantageous (in terms of thermal environment) compared to rectangular tunnels.

In this study, for probing into the basic characteristics pertaining to the thermal effects on tunnel structures, it is aimed at developing to the mitigation of fire protection systems for concrete structure, ventilation conditions and other sage system, which will be exposed in the thermal environment.

The thermal environmental analyses are implemented by computational fluid dynamics (CFD). The results of CFD, we compared with suitable references to thermal environment.

2 BASIC CONDITIONS FOR FLUID DYNAMICS SIMULATION

Heat output in the incidence of fire depends on the scale of fire. Here we assume a heat output of 30 MW due to burning of a Heavy Goods Vehicle (HGV), and the maximum temperature inside the tunnel to reach 1000 Celsius (PIARC Report 1999).

On the other hand, based on the EUREKA Report in the case of heavy goods vehicle fire, the maximum heat release rate will exceed by 100 MW with the time duration 10 - 20 minutes. This heat release rate seems to be maximum value for HGV fire without dangerous goods transportation.

Figure 1, presents of time, heat release rate for 50MW fire and 100MW fire. These figures are not authorized or regulated by public sectors for the tunnel design, it is just arranged for this study based on several researches and information to reference.

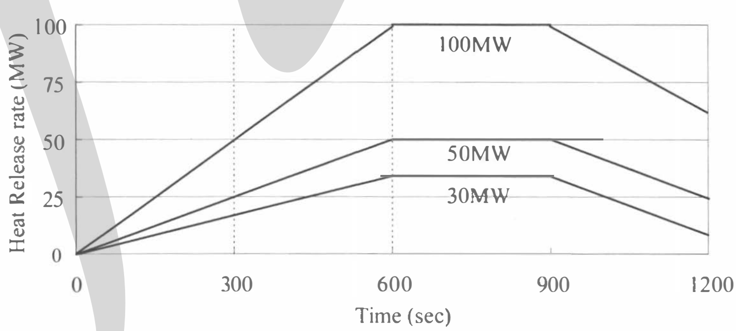

Fig. 1 Heat release curve in tunnel in the incidence of fire

Circular and rectangular cross-sections are used in the present analysis, as shown in Figure 2.

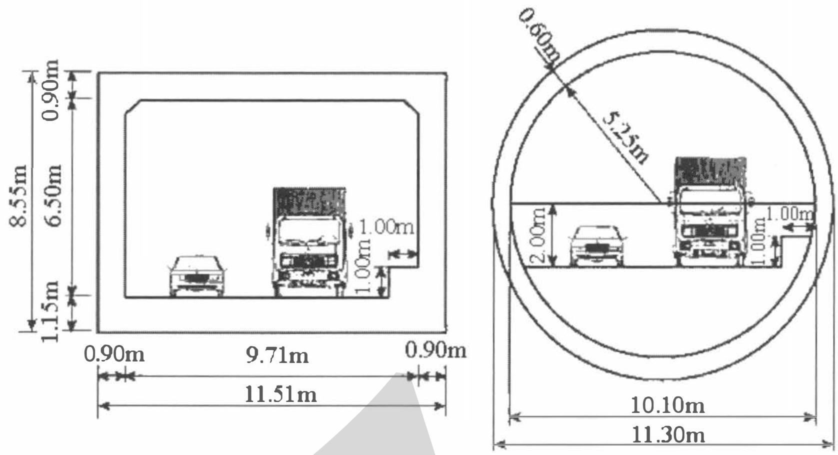

Rectangular section Circular section

Fig. 2 Cross-section of road tunnels used in this study

The basic equations of fluid dynamics (Continuity equation, Navier-Stokes equation and Energy equation) have been applied for forecasting air flow and temperature based on numerical analysis. Further, the κ - ε model has been used to make turbulent flow realistic here.

3 CONCLUSIONS

Regarding the deterioration of strength in concrete and necessity of fire protection mitigation, it is a well known fact that the strength of concrete reduces once the material is subject to a temperature in excess of a certain level.

The deterioration of strength in concrete is be controlled by basic strength of aggregates, water-cement ratio, moisture ratio, density, condition of stress and strain, etc.

Generally, concrete temperature up to 200°C, the basic performance of concrete assumed at 100%. However, Dr. E. Richter[1] mentioned following issues to concrete performance under the thermal condition, "as lasting plastic deformations in the reinforcement are avoided through temperatures 300°C, it is assured that only a short period is required to repair the tunnel after the fire."

Based on this knowledge, in the case of predicted results exceed 300°C, appropriate fire protection mitigations should be adopted to the concrete structure.

In the case of 30MW fire within circular cross section, the maximum temperature at concrete in the surface does not exceed 300°C. On the other hand, at ceiling of rectangular cross section exceed 300°C, the concrete surface of overburden of reinforcement will be spalled out and collapsed, the fire protection mitigation will be required. However, the lower part of side wall near the road surface dose not exceed the critical temperature, fire protection dose not seem to necessary.

In the case of 50MW, 100MW fire adopted to the fire protection design to the tunnel structures. The circular cross section is still better thermal environment than rectangular cross section. However both type of cross section will be occurred very serious damage near the fire source, therefore the fire protection mitigation seems necessary.

The reasons differency between thermal environment of circular cross section and rectangular cross section, in spite of same heat release rate, are as follows.

(1) The distance from fire source to ceiling within rectangular cross section is shorter than circular section.

(2) The flow field of longitudinal air flow rate by mechanical ventilation and thermal flow field from fire source within circular cross section is bigger than rectangular cross section.

Due to these two major differences between rectangular and circular cross section, the value of maximum temperature at concrete surface is controlled.

REFERENCES

[1] Tunnel 6/2001, September

SHEAR RESISTANCE OF PRECAST PRESTRESSED HOLLOW CORE SLABS UNDER FIRE CONDITIONS

Jean-Claude Dotreppe
Professor
University of Liège, Belgium

Arnold Van Acker
Federation of Concrete Industry FeBe
Belgium

Keywords: shear, precast elements, prestressed concrete, slabs, fire resistance

1 INTRODUCTION

The design under normal conditions of precast prestressed hollow core slabs is based essentially on ultimate limit state (ULS) of bending, but other ULS and serviceability limit states (SLS) have sometimes to be considered. Usually adequate detailing is provided [1].

Under fire conditions, the structural design according to Belgian national recommendations [2], to international recommendations [3] and to the appropriate Eurocode [4] is based on bending conditions of single structural elements. Nothing is mentioned about the analysis of the shear capacity, though tests have shown that premature failure due to shear near the supports can be observed. However experimental results also show that connections obtained by appropriate detailing and restraint due to the surrounding elements influence favourably the behaviour of the slabs.

In order to examine the influence of the detailing measures usually adopted in practice, a research study has been performed in Belgium about the shear resistance under fire conditions of this type of element. The results obtained and conclusions are presented in this paper.

2 STRUCTURAL BEHAVIOUR UNDER NORMAL AND FIRE CONDITIONS

Under normal conditions the ultimate limit state of bending is generally governing, which means that failure is due to yielding of the tendons or, more rarely, to crushing of concrete in compression.

Under fire conditions the failure mode of concrete beams and slabs considered in Eurocode 2-1.2 [4] is failure due to bending. However the probability of exceeding the shear capacity is more important under fire conditions than under normal conditions.

At elevated temperatures an additional phenomenon is observed : thermal tensile stresses appear in the central part of the cross section.

The consequence of this phenomenon for an isolated slab on simple supports is the occurrence of quasi vertical cracks in the middle of the cross-section due to the fact that there exists very little or no prestressing in the anchorage zone near the supports. This decreases the shear capacity, and it has been observed that failure may be due to excessive inclined tensile stresses (Fig. 1).

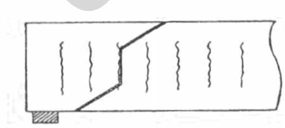

Fig. 1 Failure due to excessive inclined tensile stresses

3 DESIGN PHILOSOPHY

In designing fire safe prestressed hollow core floors, provisions are to be taken to realise the necessary coherence between the units in order to obtain an effective force transfer through cracked concrete sections. The possible design provisions are the following:

- reinforcing bars in cast open cores or in the longitudinal joints;
- peripheral ties;
- restraint due to the surrounding floors and to the supporting construction;
- reinforced topping.

4 RESEARCH STUDY PERFORMED IN BELGIUM

This research project has been carried out at the University of Liège in Belgium, while the fire tests have been performed at the University of Ghent. The tests were conceived to simulate as much as possible the conditions of a real hollow core floor: longitudinal, transversal and peripheral tie reinforcement and a structural topping, but also the blocking effect of the surrounding floor structure and of the edge beams.

Numerical simulations have been realised with the computer code SAFIR developed at the University of Liège. SAFIR has been used for the design of the test units as well as to compare experimental with numerical results. SAFIR is based on the finite element method. It can perform thermal as well as mechanical non linear calculations. With this tool it has been possible, for example, to analyse the evolution of the cracked zone in the central part of the element as shown in Fig. 1.

The practical part of the project included 4 fire tests of approximately 2 hours at the Laboratory of the University of Ghent. The test set up was designed in such a way as to enable the testing of a maximum number of parameters. The dimensions of the test fumace are 6 x 3 m. The results of the 4 tests are given in Table 1.

Table 1 Results of the 4 tests

Test		Failure load (kN)		Failure type
		Without topping	With topping	
First test:	slab 1	178		Bending
	slab 2		(50 mm) 254	Bending
Second test:	slab 1	292		Bending
	slab 2	324		Bending
Third test :	slab 1	267		Bending
	slab 2	254		Bending
Fourth test:	slab 1	305		Bending
	slab 2		(30 mm) 305	Shear

The first test was interrupted after 83 minutes due to spalling on the horizontal face, but no failure was observed. The three following tests were stopped after 120 minutes fire exposure. After that the load was increased, and all slabs failed in bending, with the exception of one, which showed a shear failure. The underside of this floor was more damaged than the one of the others, which might explain the shear failure. All failure loads are very high in comparison to the test load of 100 kN, which has to be considered as a normal loading during a fire. They prove that the hollow core units still had a large remaining resisting capacity both in bending and shear.

5 CONCLUSIONS

The theoretical and experimental study of the fire resistance of prestressed hollow core slabs has clearly demonstrated that the units are keeping their high performances in bending and shear during standard ISO fire tests. However, this requires the presence of a number of connection and tie reinforcements in the design in order to ensure a coherent flooring system, for which the design philosophy is described in the FIP Recommendations on prestressed hollow core floors [1].

REFERENCES

[1] FIP Commission on Prefabrication: FIP Recommendations on Precast Prestressed Hollow Core Floors. Thomas Telford Ltd., London, 1988.

[2] Dotreppe, et al.: Résistance au feu des structures. Principes généraux et Recommandations à l'usage des auteurs de projet. Commission Nationale Belge de Recherche Incendie, Université de Liège et Rijksuniversiteit te Gent Ed., 1983.

[3] Comité Euro-International du Béton: Fire design of concrete structures in accordance with CEB-FIP Model Code 90. Bulletin d'Information du C.E.B., N°208, Lausanne, 1991.

[4] Comité Européen de Normalisation: ENV 1992-1-2. Eurocode 2 : Design of concrete structures Part 1-2 : General rules – Structural fire design. CEN, Bruxelles, 1995.

RESTORATION OF LONG SPAN FLAT PLATE, POSTTENSIONED WITH UNBONDED CABLES – AFTER FIRE

Izhak Z.Stern M.Sc. P.E.
I. Stern – Y.D.E. Engineers LTD 10 Hafets Hayim Street, Tel-Aviv Israel 67441
E – Mail: sternyde@netvision.net.il Tel. 972-3-6956122 Fax. 972-3-6954299

Keywords: restoration, unbonded cables, rebars, posttensioned slab.

1. INTRODUCTION

A fire broke out underneath posttensioned concrete slab in a complex of commercial and residential buildings in Tel-Aviv, at the final stage of construction. *

The slab was 50 cm thick, 16 meters span, design to support a landscape plaza. The fire caused spalling of the concrete at the bottom of the slab over area of approximately 200 m^2, exposing and distorting mild reinforcement and cables. Some of the cables were broken due to the fire and their anchor jumped out off the wall at the end of the slab. The goal was to restore the original slab capacity in minimum cost and deviation from the original design geometry. This goal was successfully accomplished with minimum delay to the occupation of the building. This paper describes the actions taken to achieve this goal.

2. CASE DESCRIPTION

The slab is shown in Fig. 1. The slab was placed in 4 segments with intermediate anchors between the segments. Typical cross section of the slab shown in Fig.2. The fire occurred underneath segment # 3. The Concrete have been detached and fallen down from the slab. Steel rebars were hanging exposed. Cables were broken, suspended and exposed. It was possible to conclude immediately that severe damage had been occurred to the structural capacity of the slab. Segments 1 & 2 were undamaged since these segments were placed before segment 3 & 4 and the intermediate anchors have not been affected by the damage caused to the cables at segment # 3.

3. DAMAGE ASSESSMENT

The results of the following tests enable a spatial mapping of the damage, Three types of concrete tests were conducted: Strength testing by destruction of drilled cores, Carbonization testing of drilled cores and Schmidt hammer strength testing. The conclusion was that the concrete slab beyond the distorted and spalled concrete, are sound. Mechanical properties tests of segments of cables show no significant change in the mechanical properties. Chlorides contains test results is acceptable.

4. REPAIR WORKS OF THE SLAB

The repair works of the slab include the following: Removal of damaged concrete. Cutting and removal of damaged and exposed rebars. Cutting and removal of damaged cables. Adding rebars to replace damaged ones and increasing ultimate capacity of the slab. Reconnection and restressing of cables. Placing new concrete. See Fig.3 and Fig.4.

5. ANALYSES AND DESIGN OF THE SLAB AFTER THE FIRE

The original analysis and design of the slab was accomplished by using "Equivalent frame method" and 2D finite elements analysis demonstrating the 2 way action of the slab.

* The original design of the posttensioned slab and the design of the restoration, were made by – I. Stern - Y.D.E Engineers LTD.

After reconnecting and stressing the cables, we conclude that no more than 10% of the strength and prestressing force have been lost. On the safe side we assumed that only 50% of the interface between the new and old concrete are in contact for transferring horizontal shear. In lieu of Equivalent frame, a continuous beam have been analyzed, using 2D finite element model made of vertical elements.
This model had three versions - See Fig.5a, Fig.5b and Fig.5c. The stresses and the moments from the second and third model were combined together for the final condition. These results were compared to the results of the first one and to the original Equivalent frame analysis. Additional bottom mild reinforcement was required, controlled by the volume of tensile stresses in the new concrete. The final calculated ultimate strength of the slab is larger than in the original design.

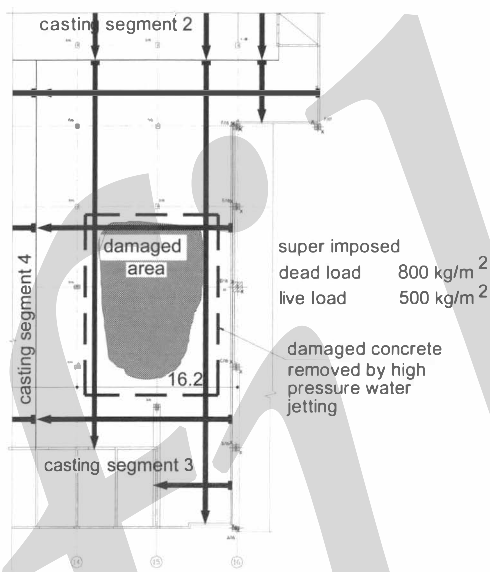

Tel Aviv Tower slab over shopping mall
Fig.1 Partial general layout with schematic p.t. cables arrangement (dimensions in meters)

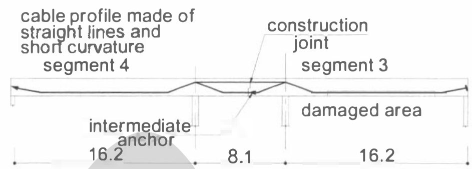

Fig.2 Typical cross section at segment 3 & 4

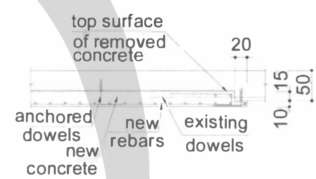

Fig.3 Typical cross section at damaged area after repair (cables not shown)

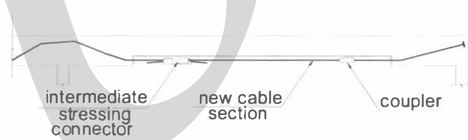

Fig.4 Typical cross section at damaged area after reconnecting cables before placing new concrete (mild reinforcement not shown)

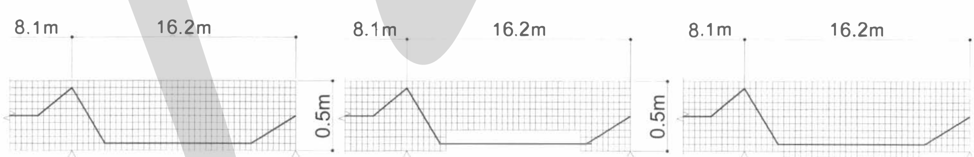

Fig.5a **Fig.5b** **Fig.5c**

Fig.5 Posttensioned beam finite elements model

6. CONCLUSION

The results of the calculation indicate that the goal of the repair was achieved, with close inspection of the repair work, the designer had good confidence in the strength capacity of the slab, so that no loading test was required.

STUDY ON EVALUATION METHOD FOR STRUCTURAL INTEGRITY OF PCCVS AT OHI NUCLEAR POWER STATION

Toshihiro Ikeuchi[1)] Masahiko Ozaki[1)] Hiromi Ohashi[2)] Katsuhiro Suzuki[3)]
1)The Kansai Electric Power Co.,Inc. 2)The Kanden Kogyo Corporation 3)Obayashi Corporation

Keywords: PCCV, concrete strain, tendon tensile force, creep, shrinkage

1 INTRODUCTION

For the reactor containments of Ohi power station unit No.3/4, PCCVs (Prestressed Concrete Containment Vessel) were adopted.

After construction, tendon tensile force which changes with time is evaluated in order to confirm the structural integrity. For the time being, the method used for this evaluation is direct measurement of residual tensile force at tendon anchoring ends. However, much efforts and cost are needed for this measurement. Therefore the evaluation method of tendon tensile force based on concrete strain has been proposed as a more reasonable one ([1]~[3]).

In September 2001 at Ohi unit No.3, the measurement data at the 10th year since the initial operation were obtained. Using the data accumulated to date including these data, the adequacy of the evaluation method has been studied this time, and the result is here reported.

Type of reactor (Output capacity)	PWR (1,180Mwe)
Dimensions	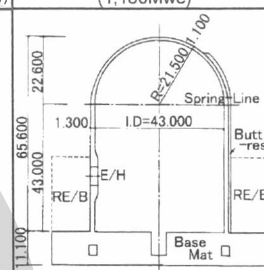
No.of buttress	2
Tendon capacity	10,000kN Class
Prestressing sys.	VSL(Unbonded type)
Concrete strength	44.1N/mm2

Fig.1 Outline of PCCV

2 OUTLINE OF OHI UNIT NO.3/4 PCCVS

PCCV consists of the cylindrical wall and the hemispherical dome, and the steel liner of 6.4mm thickness covers the whole inner surface. The tendon capacity for tensile force is 10,000kN class and VSL (unbonded type) is adopted for prestressing system. The outline of PCCV is shown in Fig.1 and the tendon arrangements in Fig.2.

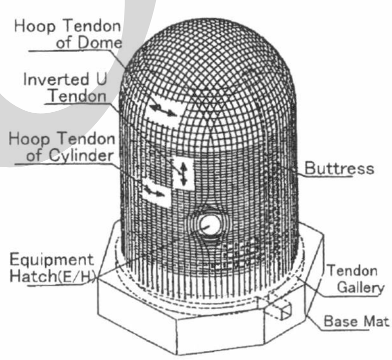

Fig.2 Tendon arrangements

3 EVALUATION METHOD OF TENDON TENSILE FORCE

As a reasonable method for the evaluation of tendon tensile force, the estimation method of tendon tensile force based on measured concrete strain has been proposed([1]~[3]). The concept of this evaluation method is shown in Fig.3.

In this method, tendon tensile force is evaluated indirectly through comparing measured strain values with estimated strain values.

In order to demonstrate the adequacy of this evaluation method, the comparison between measured values and estimated values was made regarding each of concrete strain and tendon tensile force.

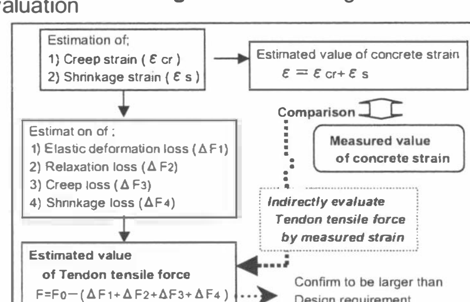

Fig.3 Tendon tensile force evaluation method based on concrete strain

4 MEASUREMENT AND ESTIMATION OF CONCRETE STRAIN

Concrete strain has been measured by rebar strain gauges containing thermocouples embedded in the whole concrete of PCCV, in 184 points for one unit, periodically in general twice a year (summer and winter). Measured strain includes thermal strain due to stress caused by temperature distribution in the section. Therefore, the thermal strain is eliminated from the measured strain value based on measured temperature by thermocouples.

An estimated value of concrete strain are calculated as the sum of creep strain and shrinkage strain, for each of the longitudinal and the circumferential direction. Concrete strain is known to fluctuate periodically with seasonal change in environmental condition, particularly in humidity. Therefore, PCCVs are also considered to receive the effect by seasonal humidity change and the effect is taken into account in the calculations as shown in the reference[3].

A representative example of measured results of concrete strain for Ohi unit No.3 with the estimated values is shown in Fig.4. At the general portion of PCCV the correspondence between the estimated and the measured values comparatively seems good.

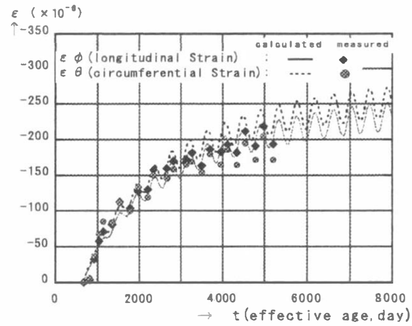

Fig.4 Measured and estimated concrete strain(at Spring-Line)

5 MEASUREMENT AND ESTIMATION OF TENDON TENSILE FORCE

Tendon tensile force has been measured as the lift-off load at the anchoring end by the filler gauge method[1], at the 1st, 3rd, 5th and 10th year since the initial operation.

An estimated value of tendon tensile force is obtained from the initial tensile force (lock-off load: F_0) at the time of construction by subtracting elastic deformation loss of concrete due to tensioning of tendons, relaxation loss of tendon, and creep loss and shrinkage loss of concrete. The estimation method[1] for these losses are as follows.

(1) Elastic deformation loss (ΔF_1)
: computed by FEM analysis of PCCV model
(2) Relaxation loss (ΔF_2) : by Larson-Miller method
(3) Creep loss (ΔF_3) : estimated from creep strain
(4) Shrinkage loss (ΔF_4) : estimated from shrinkage strain

In estimating ΔF_3 and ΔF_4, the influence by seasonal fluctuation is taken into account as in the case of the concrete strain estimation.

A representative example of measured results of tendon tensile force with the estimated values is shown in Fig.5. And from all the measured results for Ohi unit No.3, the measured value/ estimated value ratios range 0.99～1.04. It can be said that the correspondence between the measured and the estimated values to date is good and the tendon tensile force behavior can be estimated with enough accuracy.

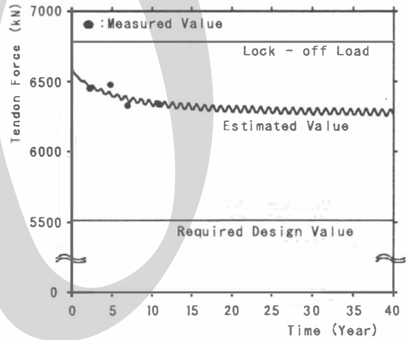

Fig.5 Measured and estimated results of an inverted U tendon tensile force

6 SUMMERY

As a result of the above demonstration using measurement data obtained in the PCCV, it is confirmed that concrete strain and tendon tensile force are estimated with adequate accuracy to date. By this evaluation method, the behavior of tendon tensile force with time can be evaluated using the concrete strain. As the method to confirm the structural integrity of PCCV, the method to evaluate the tendon tensile force by actual measurement of the lift-off test is currently adopted. However, if the adequacy of the above method becomes well proved by future measurement data, it will be possible to confirm the structual integrity of PCCV by the evaluation of the tendon tensile force based on the measurement of concrete strain.

REFERENCES

[1] Kitano,T., Setogawa,S., Yamaguchi,T. et al.: Prediction of time-dependent behavior of tendon force for a PCCV. Summaries of technical papers of Annual Meeting AIJ, pp1603-1604, Sept.,1993, in Japanese.
[2] Ozaki,M., Abe,T., Murazumi,Y., Aikawa,Y.: Study on the evaluation of the prestressing force prediction of PCCV tendons using Monte Carlo simulation. SMiRT-13, Vol.H, pp.83-88,Aug.,1995.
[3] Ozaki,M., Abe,T., Watanabe,Y., Kato,A. et al.: A prediction method for long-term behavior of prestressed concrete containment vessels. SMiRT-13, vol.H, pp.143-148, Aug. 1995

GLOBAL FE ANALYSES OF A REINFORCED CONCRETE CONTAINMENT VESSEL UNDER ULTIMATE INTERNAL PRESSURE

Yoshinori Mihara [3], Yasuaki Fukushima [3], Hiroo Ito [3], Masashi Goto [2], Yasumi Kitajima [1]
1) Nuclear Power Engineering Corporation, Japan
2) Toshiba Corporation, Japan
3) Kajima Corporation, Japan

Keywords: RCCV, FEA, liner tear, ultimate pressure, concrete model

1. INTRODUCTION

In the ABWR (Advanced Boiling Water Reactor) nuclear power plants, RCCV (Reinforced Concrete Containment Vessel) has the important function to prevent the release of radioactive material to the environment. The Nuclear Power Engineering Corporation (NUPEC) has been conducting Containment Integrity Tests to investigate the structural behavior of containment vessels under internal pressure that exceed the design pressure for the severe accident and finally up to ultimate strength. One of the projects is a RCCV test. According to the internal pressure test of the 1/6 scaled RCCV model by Sandia National Laboratories in the United States, liner tearing near penetration occurred about 3.2 times design pressure resulting into the loss of leak-tight function. It is the final objective to evaluate the ultimate strength of the whole RCCV under internal pressure by improved and verified analytical method. In this paper, preliminary FE analyses (FEA) of RCCV under ultimate internal pressure are presented through two analytical procedures of RCCV global model and submodel analyses to evaluate the severe strain localization of liner plates around the opening.

2. CONCRETE MODEL for FEA

It is important to select the robust constitutive law on concrete for RCCV failure analysis. The plastic damage model is proposed by Lee and Fenves (1998) [1] for the dynamic analysis of plain concrete structures. The model is fairly robust even at the failure stage of concrete. Therefore, the plastic damage model is selected to perform preliminary RCCV analyses under ultimate internal pressure. The basic concept of the plastic damage model is described as follows based on [1] and [2].

For in-plane shear problem, the result for variable Ψ and μ =0.0 is shown in Fig.1. According to the past pure shear test [4], 30 degree of Ψ is appropriate for the average of test results and the value between 20 and 30 degree of Ψ is suitable for the lowest limit. Also, compressive damage variable affect the stress-strain curve after the maximum shear stress. . The result for variable μ and Ψ=20 degree is shown in Fig.2. For μ =0.01, the stress is permitted to be extremely outside of the yield surface. Thus the value of the viscosity parameter μ should be defined below 0.01.

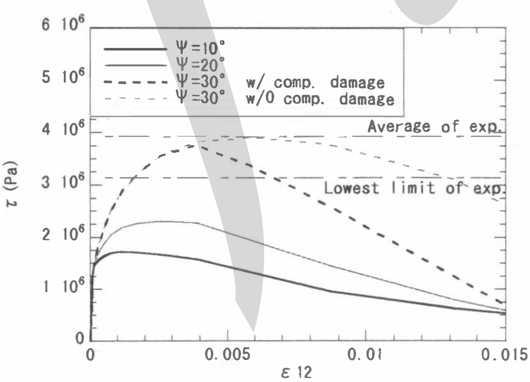

Fig.1 Result of shear problem

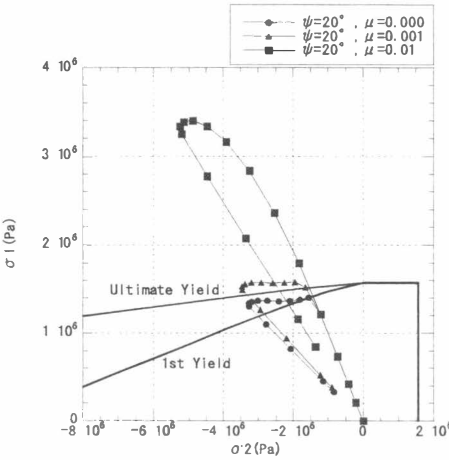

Fig.2 Result for variable μ and Ψ=20 degree

3. ANALYTICAL RESULTS

3.1 Global model FEA of RCCV

Global model FEA of RCCV is performed mainly using the 3D layered shell element under ultimate internal pressure. The analysis is completed up to 5.2 times Pd (pressure of design, 1.0Pd =0.310N/mm^2). Fig.3 shows the equivalent plastic strain contour on inner liner surface and also Fig.4 shows the maximum principal strain contour on outer RC surface. As the results, the critical locations on the severe strain localization are ① around RCCV lower drywell (L/D) circular tunnel, ② lower part of RCCV wall and ③ joint part between RCCV wall and top slab.

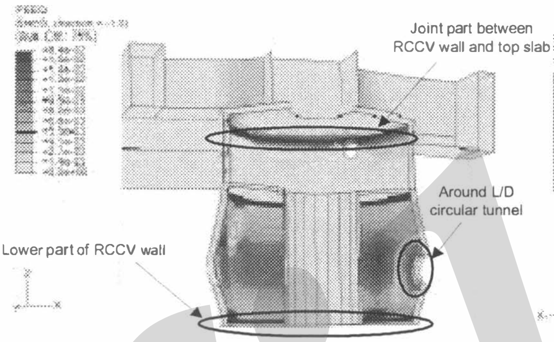

Fig.3 Equivalent plastic strain contour

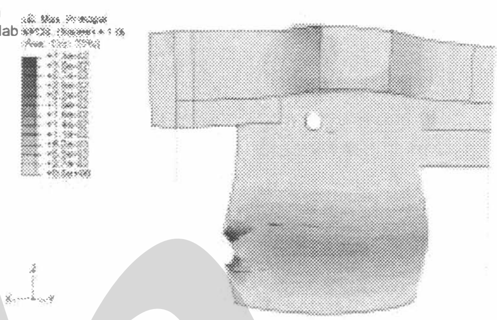

Fig. 4 Maximum principal strain contour

3.2 Submodel FEA around Opening

Submodel FEA around the opening is performed mainly using 3D solid element for concrete and the 3D layered shell element for liner. The analysis is completed up to 4.5 times Pd (pressure of design, 1.0Pd=0.310N/mm^2). Fig.5 shows the equivalent plastic strain contour on the inner liner surface. Radial displacement versus internal pressure relationship near the opening is shown in Fig.6. The internal pressure level beyond 4.5 times Pd is quite close to ultimate pressure level because the extreme degradation occurs in radial displacement versus internal pressure curve From the viewpoint of liner tearing, the strain localization occurs at the boundary between thick insert liner plate and relatively thinner liner plate near the opening and lower part of RCCV. The value of the equivalent plastic strain is about 1 to 4 % for the severe strain localization parts. Also shown in Fig.6, the internal pressure level beyond 4.5 times Pd is quite close to ultimate pressure level because the extreme degradation occurs in radial displacement versus internal pressure curve.

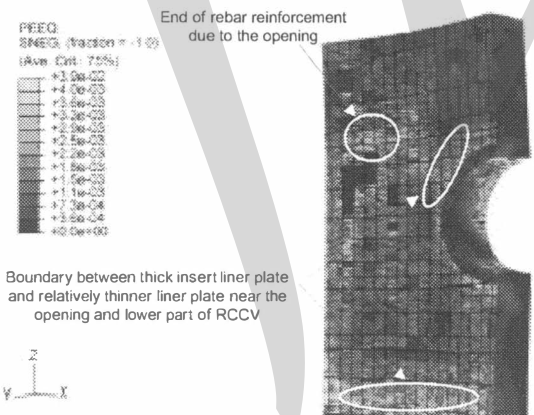

Fig.5 Equivalent plastic strain contour

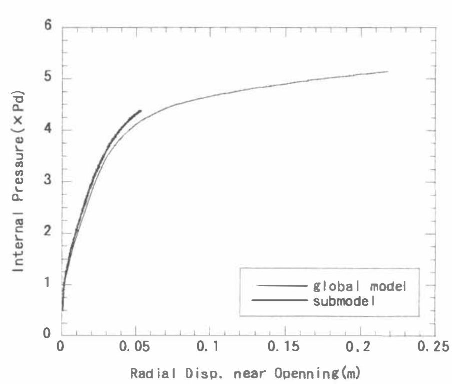

Fig.6 Radial displacement-Internal pressure relation near the opening

4. REFERENCES

[1] Lee, J., and G. L. Fenves, : A Plastic-Damage Concrete Model for Earthquake Analysis of Dams,' Earthquake Engineering and Structural Dynamics, vol. 27, pp. 937-956, 1998.
[2] HKS Inc. : ABAQUS Theory Manual Ver.6.3 Prerelease3, 2002

INTEGRITY TEST FOR REINFORCED CONCRETE CONTAINMENT VESSEL (RCCV)

PART 1.TEST RESULTS UNDER BI-AXIAL TENSION

T. Hasegawa T. Hirama
H. Kumagai, K. Kanemoto
Shimizu Corporation, Japan

Masashi Goto
Toshiba Corporation
Japan

Y. Kitajima
Nuclear Power
Engineering Corporation
Japan

keywords: RCCV, severe accident, liner tear, ultimate strength

1. INTRODUCTION

The Nuclear Power Engineering Corporation (NUPEC) has been conducting Containment Integrity Tests to investigate the structural behavior of containment vessels under internal pressure that exceed the design pressure in the severe accident and finally up to ultimate strength. One of the projects is a RCCV Test. Based on analytic studies and previous experiments partial wall element model with penetration under bi-axial tension have been selected and conducted in this project to investigate the structural performance and failure mode of liner tearing caused by strain concentration around the penetration. This part reports the wall element test results and simulation analysis results are reported in Part 2.

2. TEST PROCEDURE

2.1 Bi-axial tension test model

As the structure of FDW (Feed Water) portion is common with the other major penetrations, it is selected as the test portion and 1/2 scale is chosen to represent liner tearing mode. Figure 1 shows the test apparatus and the configuration of the specimen. Specimen is 3.4m square (test portion is 2.7m square) and is half-thickness of 0.5m because of the test in membrane force. Two specimens are used, one is standing for existing structure with liner plate and the other is without liner.

2.2 Material properties

The specified design compressive strength is 33 N/mm2 in the existing plant. The main reinforcing steel bar used was the same material of SD390 (in JIS standard) as actual plant and the steel liner plate and insert plate for reinforcement of the penetration in the specimen was SM490A (in JIS standard) of which mechanical properties are close to that used in the actual plant.

2.3 Test system

Bi-axial tension was applied in the ratio of 2 to 1 in X and Y direction in accordance with the membrane force in the hoop direction and meridional direction respectively in actual cylindrical wall of RCCV subjected to internal pressure.

3. Test results and conclusion

At 3 times design pressure of 0.316MPa (called "3Pd") steel liner yielded and at 5Pd reinforcement rebar yielded. When loading increased up to about 6Pd, rebar strain at the peripheral portion just adjacent to the end of reinforcement for opening developed about 1.5%. Rebar strains around the opening were rather small about 0.25% due to sufficient reinforcement provided. Therefore the failure mode can be judged the tensile membrane failure. This is common to the test specimens with liner and without liner.

Strain concentration of 3% maximum was recorded at the conjunction at 6Pd between the thick insert plate and liner plate, which was 10 times average strain but not leading to rupture.

After the test, test specimen was cut across the center line and cone-shaped concrete cracking around the liner anchorage was observed, which indicates the separation between the anchorage and concrete structure resulting into reduction of strain concentration of steel liner.

4. ACKNOWLEDGEMENT

The authors wish to express their sincere gratitude to Prof. Akiyama, Nihon University, Prof. Takiguchi, Tokyo Institute of Technology and Prof. Noguchi, Chiba University for much helpful advices.

REFERENCES

[1] D.S. Horschel : Experimental results from pressure testing a 1:6-scale nuclear power plant containment, NUREG/CR-5121, SAND88-0906, Sandia National Laboratories, Albuquerque, NM, January 1992

[2] B.L. Spletzer et. al. : Testing and analyses to investigate liner tearing of the 1:6-scale reinforced concrete containment building, Nuclear Engineering and Design 145, December 1993

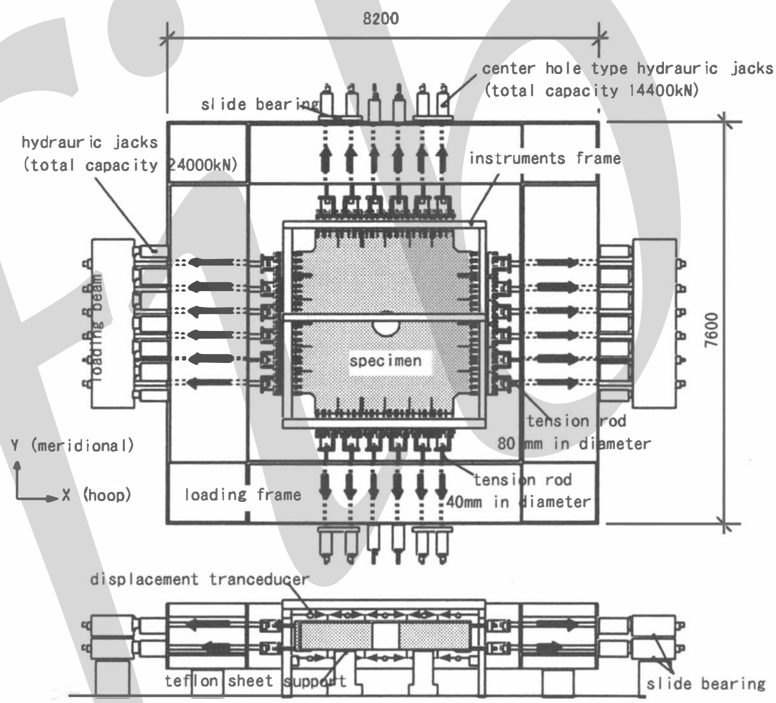

Figure 1 Test apparatus and configuration of specimen

INTEGRITY TEST FOR REINFORCED CONCRETE CONTAINMENT VESSEL (RCCV) PART 2. SIMULATION ANALYSIS OF BI- AXIAL TENSION TESTS

Toshihiko Hirama [3], Toshiyasu Hasegawa [3], Toshiaki Hasegawa [3], Ryosuke Ikeda [3], Masashi Goto [2], Yasumi Kitajima [1]
1) Nuclear Power Engineering Corporation, Japan
2) Toshiba Corporation, Japan
3) Shimizu Corporation, Japan

keywords: RCCV, FEM, nonlinear analysis, layered shell, bi-axial tension

1. INTRODUCTION

The Nuclear Power Engineering Corporation (NUPEC) has been conducting Containment Integrity Tests to investigate the structural behavior of containment vessels under internal pressures that exceed the design pressure for a severe accident up to ultimate strength. One of the tests is a RCCV Test. In this project, experiments have been conducted on partial wall models with penetration under bi-axial tension to investigate the structural performance and failure mode of liner tearing due to strain concentration around the penetration point. The final objective is to evaluate the ultimate strength of the whole RCCV under internal pressure using an improved and verified analytical method through simulation analysis of the test results. This part reports that the nonlinear behavior of a reinforced concrete structure with and without a liner plate under bi-axial tension are analyzed using finite element models and the validity of nonlinear analysis method.

2. ANALYTICAL METHODS

2.1 Test Specimens

Two specimens with penetration under bi-axial tension were conducted to investigate the structural performance. One is standing for existing structure with liner plate and the other is without liner plate to verify validity of non-linear analysis method of reinforced concrete structure. The test specimen modeled the actual steel boundary structure as accurately as possible at 1/2 scale. The liner plate is 3.2mm thick and is anchored to the RC structure by a T-shaped steel beam.

2.2 Analysis model

Figure 1 shows the mesh of the reinforced concrete (RC) element and the loaded portion. The load, which is defined as a monotonic static load, is set with a ratio of force component in the hoop (X) direction to that in the meridian (Y) direction of 2:1, as in the experiment. The anchor was modeled by two methods. In the first, the spring stiffness in the X and Z directions for modeling the anchor were assumed to be infinite. In the other method, the stiffness and strength of the spring were assumed as the previous experimental values. In addition, the degree of freedom for the spring of the Y direction anchor was free in both methods.

2.3 Analysis case

For the analysis using the RC model, two different concrete tensile strengths ft are assumed, based on previous studies on the tensile strength of concrete: fc' (in kgf/cm^2) and 1.3 fc'. The liner and RC model have the following two cases: the liner anchor with a rigid spring and a non-linear spring, using the experimental values.

3 .ANALYTICAL RESULTS

3.1 Analytical results using RC model

Figure2 shows the load - displacement relations. The first breakpoint near 1.5Pd (3000kN) in analysis case of 1-1 under the condition of ft= fc'. agrees with the test results. For the bi-axial tensile analysis of the reinforced concrete structure, good agreement was shown between analysis results and test results over the load range of initial to maximum for the load-displacement relation, nonlinear behavior of the rebar strain and the liner strain.

3.2 Analytical results using the liner and RC model

The effect of the spring model between liner anchor and concrete for the concentration of liner-strain was studied. Figure3 shows the strain in the liner plate near the opening. The strains in the rigid model in case2-1 are much more localized than those in the nonlinear spring model in case2-2. Thus, the rigid spring model estimates the liner strain with a certain safety margin.

4 .CONCLUSIONS

1) The nonlinear behavior of a reinforced concrete structure with and without a liner plate under bi-axial tension was analyzed by the finite element method. Good agreement was obtained between analysis and test results for the load-displacement relation and nonlinear behavior of rebar strain and liner strain. The validity of nonlinear finite element analysis was confirmed.
2) The effect of the spring model between liner anchor and concrete for the concentration of liner-strain was studied. The rigid spring model estimates the liner strain near the opening with a certain margin in comparison with the nonlinear spring model. In the generic portion, no difference was observed between the two models.

5. ACKNOWLEDGEMENT

The authors wish to express their sincere gratitude to Prof. Akiyama, Nihon University, Prof. Takiguchi, Tokyo Institute of Technology and Prof. Noguchi, Chiba University for much helpful advices.

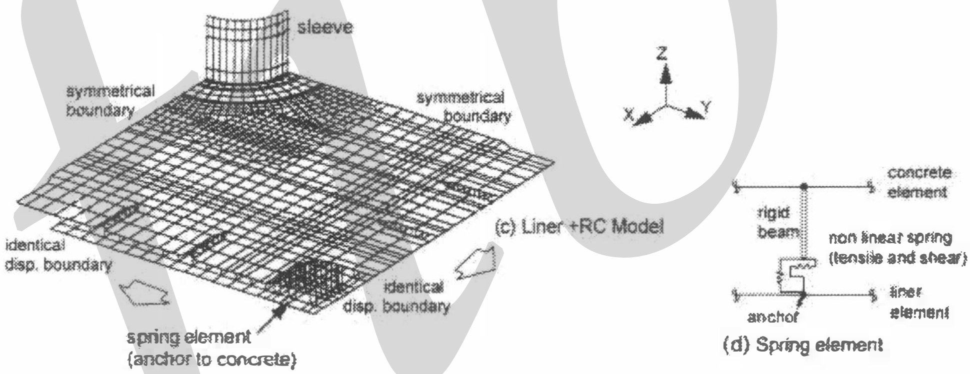

Fig.1 Liner and RC Model

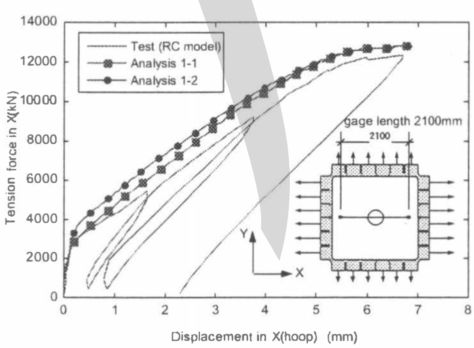

Fig.2 Relationship between Tension and Disp. in X(center of specimen) of RC model

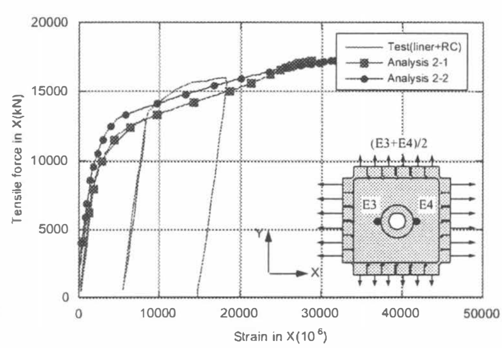

Fig.3 Relationship between Tension and Liner Strain in X(around opening) of Liner+RC model

DESIGN AND TESTING OF THE RECONSTRUCTED PAG BRIDGE

Zelimir Simunic Jelena Bleiziffer
Croatian Institute for Bridge and Structural Engineering
CROATIA

Jure Radic Zlatko Savor
Faculty of Civil Engineering
University of Zagreb
CROATIA

Keywords: reinforced concrete arch bridge, reconstruction, testing, non-linear analysis

1 INTRODUCTION

The Pag Bridge was built in 1968 to link the island of Pag with the Croatian mainland. It is a reinforced concrete arch bridge spanning 193.2 m. The original concrete superstructure comprised a series of simply supported grillages. The columns were precast and connected to the arch by prestressed tendons.

Extremely aggressive maritime environment combined with inadequate detailing, poor workmanship, exceptionally small concrete cover and damages caused by aircraft missiles led to the rapid structural degradation: cracking of concrete, peeling off of concrete cover, reinforcement corrosion and failures of bearings. Structural deterioration required the reduction in the traffic speed and volume. Over the years various repair techniques were tried on the superstructure and columns, but none proved efficient. The arch was repaired in 1991 with the removal of the damaged concrete cover, grouting all visible cracks and placing an additional reinforcement mesh on all external surfaces covered by a fine 4-cm thick concrete layer. Planned replacement of the superstructure and column strengthening had to be postponed due to the war activities in the region.

2 DESIGN OF THE PAG BRIDGE RECONSTRUCTION

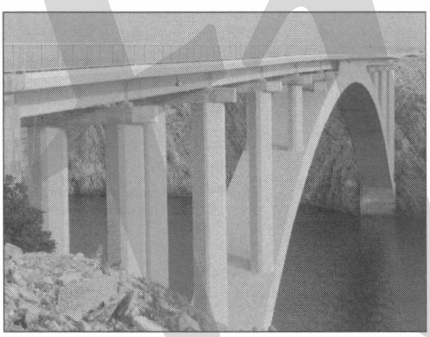

Fig. 1 View of the reconstructed Pag Bridge

The reconstruction commenced in 1999. Two independent continuous steel superstructures were constructed with span lengths 5×23.30+11.65=128.15 m and 4×23.30+11.65=104.85 m. The structural solution comprising steel was favoured since it provided reduction in the weight of the structure. This was important since the traffic loads according to the current codes are almost double the traffic loads to which the original bridge was designed. Both superstructures comprise two 1.5 m deep steel plate girders connected by a 12-mm thick orthotropic deck with open stiffeners. Such structural solution benefited the bridge's durability as it provided access to all steel structural members.

Existing columns were encased in 12-mm thick steel casings while leaving a 12-cm wide gap between the casing and the original column. This space was filled with fine aggregate low shrinkage concrete. Disability to ascertain whether the columns are fixed or pinned at their bottom presented additional problem in the design since new pot bearings would be installed to support the new steel superstructures, thus substantially changing the overall stability of the bridge.

Calculations were carried out with respect to the actions and combinations of actions as defined in DIN 1072, except for the wind loading which was anticipated larger than that required in the code. The deviation of the actual arch axis from the designed one was taken into account as a strong discontinuity with the displacement from the designed arch axis of 26 cm was detected at approximately quarter of the arch span on the side facing the island of Pag. Execution stages comprising the sequence of dismantling the old concrete superstructure and erection of the new steel superstructure had to be carefully checked, especially their influence on the arch behaviour.

The new superstructure is lighter than the original one, but since the arch axis is designed as a thrust line for certain permanent load, the distribution of lighter permanent load can be unfavourable and adversely affect the arch behaviour. The calculations revealed that the arch is capable of withstanding new loading within the designated threshold level only if the arch reinforcement contributes in the compressive zone and if the actual measured compressive concrete strength corresponding to C-50 grade instead of C-35 anticipated in the original design is accounted for.

3 LOAD TESTING OF THE RECONSTRUCTED BRIDGE

The load testing of the reconstructed bridge was performed in 1999, prior to the bridge's re-opening to the service. Both the static and dynamic tests were conducted with controlled traffic loads. The static tests were performed with 27 different arrangements of various number of test vehicles (30-ton trucks). Deflections were measured at 58 points along the superstructure. 8 strain-gauges, 17 accelerometers and 5 displacement transducers were used to record the bridge's response to vertical loads.

The results of the static tests were compared with the stresses and deflections calculated using the same finite element model as in the design calculations. Linear structural analysis was used for calculating deflections and stresses in the bridge superstructure. In addition to the linear structural analysis, a non-linear analysis of a simplified FE model of the bridge taking into account the measured concrete grade of C-50 was used to assess the stresses in the arch.

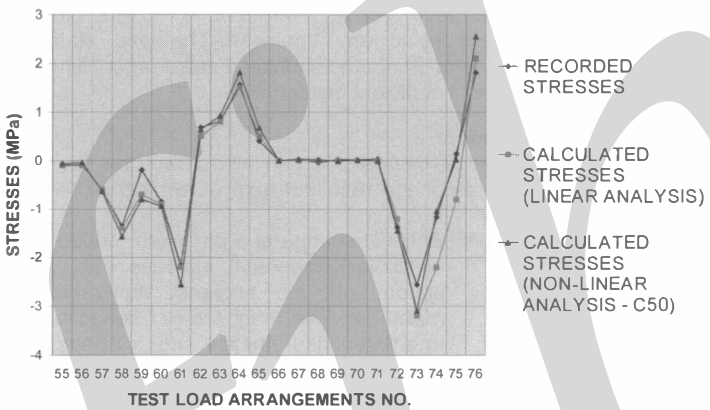

Fig. 2 Comparison of the recorded and calculated stresses in the arch

The numerical and experimental results agree very well, so it was concluded that the FE model used in the reconstruction design calculation was adequate. But, this also confirms that the stresses in the arch under the designed traffic loads are indeed approaching ultimate allowable values.

The dynamic tests comprised single or a pair of test vehicles (30-ton trucks) crossing the bridge at different speeds (20, 40 or 60 kph) and positions, with and without braking, with and without placing an obstacle on the roadway to create an additional dynamic impulse. The same sensors setup was used as in the static tests.

All the experimental natural frequencies are higher than the numerical ones, thus once more confirming the accuracy of the FE model used in the bridge reconstruction design. The recorded dynamic properties were compared with the results of the dynamic tests performed in 1993, prior to the reconstruction. The recorded natural frequencies of the mode shapes in the vertical plane are higher for the reconstructed than for the original bridge. This is a consequence of the 20% lighter mass of the overall structure, but also of an increased modal stiffness of the reconstructed bridge in the vertical plane. This is especially evident in the comparison of the frequencies of the mode shapes which are characteristic for the superstructure.

4 CONCLUSION

Extreme severity of the exposure conditions combined with the exceptionally small concrete cover, inadequate detailing, poor workmanship and maintenance led to the rapid structural degradation of the arched Pag bridge. In 1999, the bridge was thoroughly reconstructed with the replacement of the original simply-supported bridge superstructure with the new continuous steel superstructure and columns strengthening by steel and concrete casings. This has reduced the weight of the overall structure and since the arch axis was designed as a thrust line for certain permanent load, it had to be checked to what degree does the redistribution of the total permanent load in relation to the original design change stresses in the arch. The static and dynamic testing of the reconstructed bridge proved the accuracy of the assumptions incorporated in the reconstruction design calculations. But, this also confirms that the stresses in the arch under the designed traffic loads are indeed approaching ultimate allowable values. This issue is of the utmost importance in planning repair of an arch bridge.

SERVICEABILITY LIMIT STATE OF PRESTRESSED CONCRETE BRIDGES

Vladimir Křistek Alena Kohoutková
Czech Technical University in Prague
Faculty of Civil Engineering
CZECH REPUBLIC

Keywords: serviceability, prestressed concrete bridges, deflections, creep, shrinkage, shear lag

1 MATERIAL ASPECTS

1.1 Prediction of concrete creep and shrinkage

There are many reasons for the deflection increases that are usually coupled together. The paper is directed to two of them, material aspects being among them. Realistic prediction of concrete creep and shrinkage is a basic requirement for achieving appropriate prediction of deflection variations in concrete bridges. Such an analysis is obviously able to take into account all changes of the structural system during the construction process. The authors developed an Internet page [1], which makes a realistic creep and shrinkage prediction is accessible to any engineer. The web address is www.fsv.cvut.cz/~kristek. This design tool gives values of creep and shrinkage strain (after filling in the boxes for all data on the concrete) as well as the creep coefficient instantly.

1.2 Effects of differential shrinkage and drying creep

Shrinkage causes an axial shortening of the bridge beams and can also affect the box girder deflections due to the nonuniform development of shrinkage resulting from different thicknesses of flanges.

It has been found that the curvatures due to the differential shrinkage of a box girder bridge in the cantilever stage first increase over a long period. Later they decrease after reaching a maximum. The magnitude of deflections due to differential shrinkage strongly depends on the flange thickness differences. The maximum point is reached at a relatively very old age of concrete. After the maximum point, the shrinkage rate of the thick bottom flange becomes greater (eventually much greater) than the shrinkage of the thinner top flange (which has essentially finished its shrinkage at that time). The result is a delay in the onset of significant downward deflections of box girder, which gets shifted to a much later period than it would be expected according to common level of understanding.

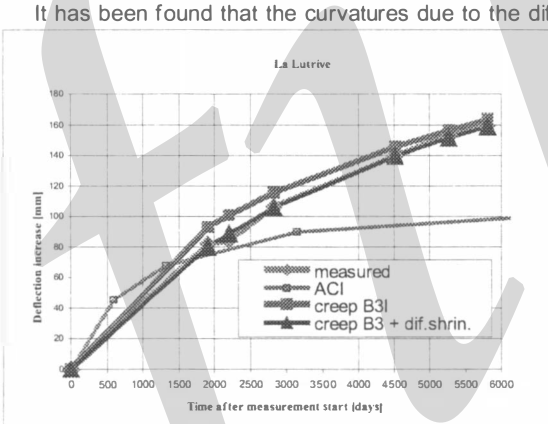

Fig.1 La Lutrive bridge, deflections - measured and predicted by various models

It can be concluded that the differential effects, particularly the differential shrinkage, are the cause of delay of deflections leaving them to develop to much longer ages. As a result of these tricky interactions the deflections are reduced in the first period due to the drying shrinkage and latter, they increase.

The *La Lutrive* Bridge, built in 1973 in Switzerland, with hinges at midspans, was considered in a comparative analysis. The midspan deflections gradually increased, as depicted in Fig.1; and in 15 years they exceeded 150 mm. Fig. 1 shows the diagram of the measured deflection increase at the midspan hinge of the bridge during the period of 6000 days after the start of monitoring of the bridge and development of deflection increase estimated by: (i) the analysis applying the B3 model considering the mean cross sectional approach, (ii) the more realistic analysis applying the B3 model and simultaneously respecting via B3 model the differential shrinkage and (iii) the oversimplified obsolete ACI 209R-92 model.

A maximum deflection at the midspan hinge of the bridge due to differential shrinkage of about 25 mm was reached at an age of concrete of 1300 days. A time lag is seen in the posterior prediction of the deflection evolution respecting the differential shrinkage (the fourth curve in Fig. 1 which exhibits the best fit to the measured values) in comparison with the mean approach.

2 STRUCTURAL ASPECTS

When predicting the overall performance of the bridge, the effects of the shear lag and shear deformations of the webs have to be taken into considerations. The analyses applied in the design practice must necessarily take into account all the changes of the structural system during the construction process as well as the creep and shrinkage of concrete. The approaches to the analysis belong to one of the three following levels: (i) usual calculation taking only the action of bending moments into account (i.e. disregarding the shear deformations and thin-walled effects like the shear lag), (ii) a frame analysis taking the shear deformations of webs into account but disregarding the shear lag, (iii) an advanced analysis taking the shear deformations of webs as well as the shear lag into account.

In design practice, short-term as well as long-term structural analyses of box girder bridges are - unfortunately - still often based on frame idealisation of the level (i) neglecting both shear deformations of webs and the shear lag. This can result in underestimation of deflections due to the action of *vertical loads. The prestressing effects*, being accompanied by no or minor shears, are, on the other hand, predicted by this elementary bending theory rather satisfactorily. Therefore *the common concept of effective widths*, if they are assumed the same for evaluation of effects of vertical loads and prestressing, is *completely wrong* in the case of prestressed concrete bridges.

The 3D finite element analyses (level iii) would provide more accurate results, but from the practical point of view they are still hardly applicable for bridges with many changes of the structural system during the construction process. This is why the authors have developed an improved method of analysis based on the frame model but involving the shear deformations and as well as the shear lag effect to serve as a practical design tool.

The influence of shear lag on the deflections of box girder bridges can satisfactorily be expressed in every-day structural analysis by introducing a reduced cross-section shear area

$$A_{s,r} = \rho \, A_{s,} \tag{1}$$

where ρ is a reduction coefficient given by

$$\rho = \frac{1}{1 + \dfrac{L^2 A_s}{96\,(1+\nu)}\left(\dfrac{1}{\beta \cdot I_{yd} + I_{ys}} - \dfrac{1}{I_{yd} + I_{ys}}\right)} \tag{2}$$

in which

A_s is the shear area of the cross section (cross sectional area of webs), I_{yd} is the second moment of area of the top and the bottom flanges about the centroidal axis of the whole cross section, I_{ys} is the second moment of area of the webs, L is the span length, and ν is Poisson's coefficient.

Coefficient β is given by

$$\beta = e^{-\frac{h}{L}\left(\frac{9 \cdot \pi \cdot b}{L}\right)^{\frac{4}{5}}} \tag{3}$$

in which h is depth of the cross section and b is width of the cell.

ACKNOWLEDGMENT

The support of the Grant Agency of the Czech Republic Grant Project No. 103/02/1005 entitled "Serviceability Limit States of Prestressed Concrete Bridges") and No. 103/00/0604 (entitled "Creep and Shrinkage Effects in Concrete Structures") and the support of the CTU Prague Grant Project J04/98:210000003 are gratefully acknowledged.

REFERENCES

[1] Křistek, V., Petrik, V., Pilhofer, W-H-: Creep and shrinkage prediction on the web, ACI International, January 2001

[2] Křistek V., Bažant, Z. P. Zich, M. and Kohoutková, A: Differential Shrinkage and Drying Creep Effects on Deflection Evolution in Prestressed Concrete Box Girder Bridges

EFFECT OF CREEP AND SHRINKAGE ON LOAD CARRYING CAPACITY OF CABLE-STAYED COMPOSITE GIRDER BRIDGES WITH SEGMENTAL CANTILEVER ERECTION

Yoshiaki Okui
Saitama University
Japan

Masatsugu Nagai
Nagaoka University of Technology
Japan

Yasuto WATANABE, Narioki AKIYAMA
Nihon University
Japan

Keywords: cable-stayed composite girder, creep and shrinkage, load-carrying capacity

1 INTRODUCTION

In this paper, we investigate effects of creep and shrinkage of the concrete slab on the load-carrying capacity of cable-stayed composite girder bridges. In order to consider effects of stress history in construction stages and different concrete ages of precast segments, first creep and shrinkage analysis following construction sequences is carried out, and then load-carrying capacity analysis including material and geometrical nonlinearity is conducted.

2 ANALYTICAL METHOD

A fiber beam element is employed for modeling the composite girder and tower to account for material nonlinearity. In the beam element, cross sections of the girder and tower are considered to consist of thin steel or concrete layers. The tangential stiffness of the beam element is evaluated in accordance with the tangential Young's modulus of the nonlinear stress-strain relation. The large displacement effect is also considered by including a geometric stiffness. In the creep analysis, Kelvin chain model is used to evaluate increments of creep strain in each time increment. The shrinkage is modeled as an eigen strain as a function of time. The aging effect of concrete is neglected.

3 MODEL BRIDGE AND NUMERICAL CASES

Figure 1 shows the considered model in the analysis. All members are sized in accordance with the allowable design method specified by a Japanese highway bridge code. The time-independent material characteristics are summarized in Fig.2. The creep coefficient and shrinkage strain are assumed to be 1.1 and 100 μ, respectively.

The following three different numerical analyses were carried out:

- Case 1: Neglecting all creep and shrinkage effects, then evaluate load-carrying capacity of complete system,
- Case 2: Neglecting creep and shrinkage effects during construction and considering these effects after completion, then evaluate load-carrying capacity,
- Case 3: Considering creep and shrinkage effects both during construction and after completion, then evaluate load-carrying capacity.

4 CREEP AND SHRINKAGE ANALYSIS

Figures 3 shows the stress histories at the top of the concrete in the main girder at the tower position. Comparing Case 1 and 3, the stress transfer due to creep and shrinkage is very large, and especially in the steel girder the stress increase attains 50 % of the stress in Case 1. The comparison between Case 2 and 3 shows that the effect of the construction sequence on stress is influential within about 100 days after completion.

5 LOAD-CARRYING CAPACITY

Figure 4 shows relationships between the load factor and the deflection at the span center. It is shown that the maximum load factor in Case 3 at day 1330 is reduced to 85% of that in Case 1 without creep and shrinkage effects. The maximum load factor in Case 3 decreases from 2.21 at day 330 to 2.13 at day 1330. This represents that the load-carrying capacity decreases as creep and shrinkage effects develop. The reduction of the load-carrying capacity after completion, however, is not so large and less than 4 % by the present analysis. Comparing Case 3 at day 1330 and Case2 at day 1090, the effect of creep and shrinkage during construction on the load-carrying capacity is negligible at 1000 days after completion.

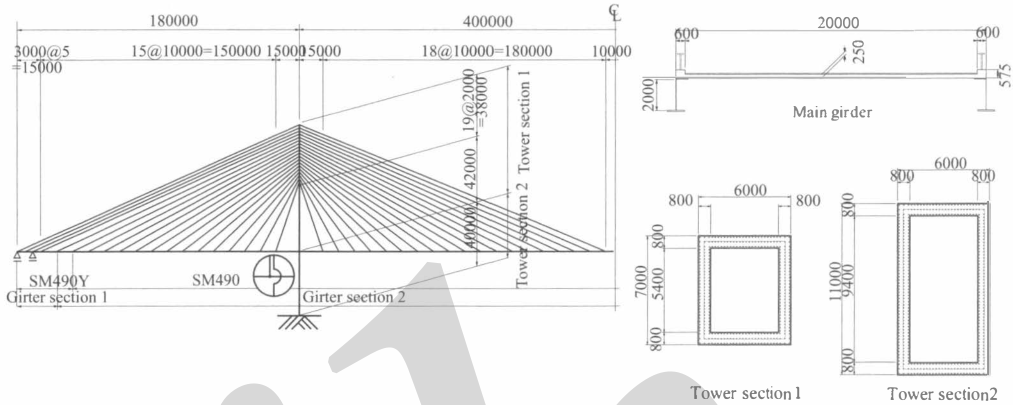

Fig.1 Side view and cross section of model bridge (in mm)

	SM490	SM490Y	SD345
σ_u	416.8MPa	456.4MPa	442.4MPa
σ_y	320MPa	360MPa	345MPa
ε_y	0.0016	0.0018	0.0013

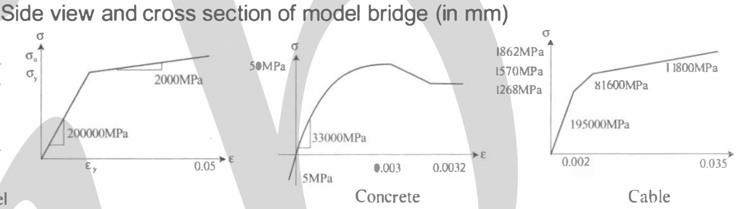

Fig.2 Time-independent material characteristics of steel, concrete and cable

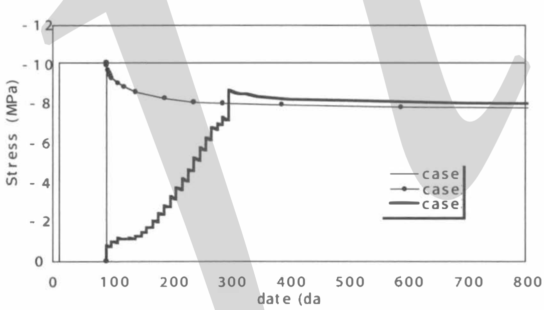

Fig.3 History of stresses at top of concrete deck at the span center

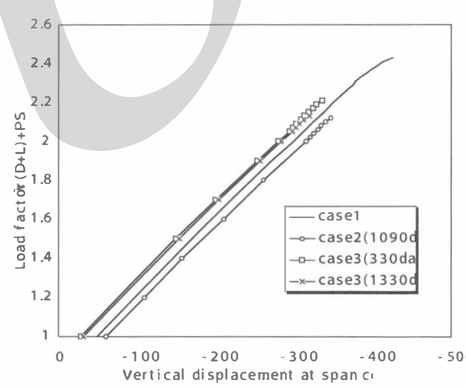

Fig.4 Load factor vs. vertical displacement at the span center

6 SUMMARY

The following conclusions can be drawn from these studies:

(1) The creep and shrinkage have a significant effect on the geometry of composite cable-stayed bridges under cantilever election.

(2) The load-carrying capacity of a completed cable-stayed bridge would be overestimated if creep and shrinkage effects were not included in the analysis.

(3) The effect of creep and shrinkage during construction on the load-carrying capacity of a completed cable-stayed bridge is not so significant, and less than 5 % in the present numerical example.

VIBRATION CHARACTERISTICS OF "TORIZAKI RIVER PARK BRIDGE" AN INNOVATIVE PC BRIDGE WITH LARGE ECCENTRIC EXTERNAL TENDONS

Hiroo Shinozaki
Mitsui Construction Co., Ltd.
Tech. Res. Inst., JAPAN

Hiroshi Kamazawa
Mori Town Office
JAPAN

Michifumi Hojo
CES Co., Ltd.
JAPAN

Shin-ichi Takemoto
DPS Bridge Works Co., Ltd.
Hokkaido Branch, JAPAN

Keywords: large eccentric external tendons, vibration test, vibration characteristics, serviceability

1 INTRODUCTION

As a possible extension of external prestressing, the authors have developed an innovative PC bridge, where external tendons are provided with large deviation from the axis of main girder. This structural concept maximizes the structural performance of the PC bridge and decreases the dead weight of the girder, amount of reinforcing bars and prestressing cables. The authors have carried out research on the structural characteristics of this concept with many loading tests and FEM analyses using scaled models, and it was proven from design simulations that such bridges are superior to the conventional ones in terms of economical and structural aspects.

Photo 1 Torizaki River Park Bridge

Based on this research and development, the "Torizaki River Park Bridge," a two-span continuous PC bridge was designed and constructed in Hokkaido, Japan (**Photo 1**)[1]. In this bridge, the external tendons were placed below the girder in the mid-span region by means of steel struts, and at the intermediate support region it is placed above the bridge deck. The tendons in the support region were arranged in a fin-shaped concrete web member. In this type of bridge, since the rigidity of girder and dead weight are comparatively smaller than conventional PC bridge, the dynamic response to the live load was of concern. As such, a vibration test and simulations under live loads were conducted on the actual bridge in order to check results of preliminary analysis and serviceability of this bridge.

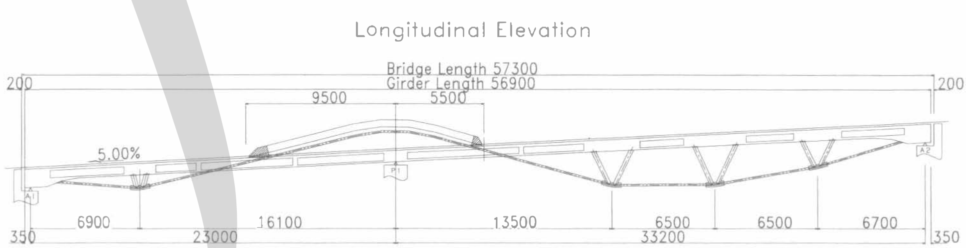

Fig. 1 Dimension of the bridge

2 VIBRATION TEST FOR THE BRIDGE

Vibration test on the actual bridge was conducted in April 2001, about two months after the bridge was completed. The test was conducted in two stages. In the first stage, frequencies and damping ratios by free damping waveform were obtained by one point excitation, while in the second stage serviceability of the bridge was checked by marching test in different patterns to simulate the walking of pedestrians. To obtain the free damping waveform, excitation was created by jumping by two persons at the mid of longer span at a pre-calculated frequency (mode 1). Marching by two or five persons according to measured frequency obtaining in first stage (mode 1) was performed in 4 patterns. An analytical model for the bridge was developed based on the 2D frame structure model. Maximum values of acceleration from test for each case are compared with results of simulation as shown in **Table 1**. The simulation results agreed well with the experimental results

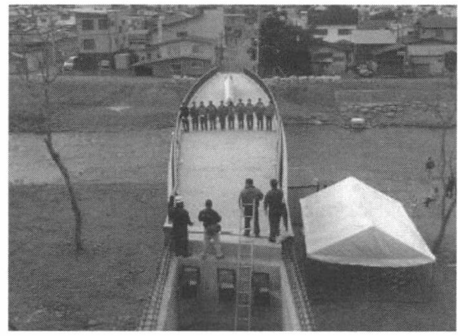

Photo 2 An experimental situation

3 EVALUATION OF SERVICEABILITY

In some past research, acceptance limits of vibration level have been proposed [2-4]. The values of maximum acceleration obtained in this particular test on the actual bridge are plotted together with these proposed limits as shown in **Fig. 2**. It can be seen that even in the worst case under vibration (5 persons crossing), the level of acceleration was well below the accepted limits. As such, it is believed that under normal walking conditions of pedestrians, the vibration of this bridge would be well within comfortable limits without causing any displeasure to the users.

Table 1 Maximum values of vibration data

Simulation Case	Acceleration(mm/s^2)	
	Cal.	Exp.
2 Persons in one direction	101.2	122.6
5 Persons in one direction	254.9	218.9
2 Persons crossing	102.5	103.2
5 Persons crossing	258.0	246.6

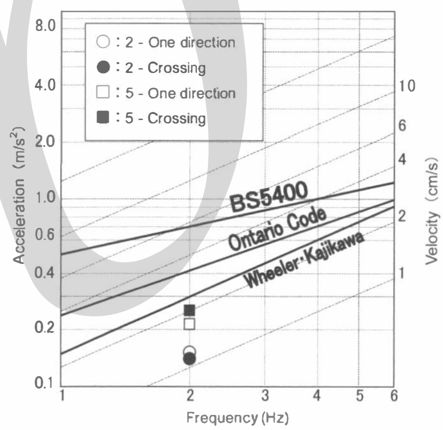

Fig. 2 Relation between comfort limit and frequency

4 CONCLUSIONS

A vibration test of an innovative bridge with continuous spans having large eccentric external tendons was conducted and the following conclusion could be drawn.

1. In eigenvalue analysis or walking simulation of this bridge, it is better to assume that external tendon is fixed at the deviators.
2. From the test results, it was confirmed that the vibration characteristics of this bridge could be predicted well using a simplified 2D frame model consisting of beam elements for the main girder and truss elements for tendons in the structural analysis.
3. Even under the worst case of simulation, it was found that the accelerations were within the accepted limits. Therefore, it is believed that under normal walking condition, this bridge would not cause any displeasure to the pedestrians.

REFERENCES

[1] Matsui, T., Kamazawa, H., Hojo, M., Kaneko, H. : Design and construction of Torisaki river park bridge a two span continuous innovative PC bridge with large eccentric external tendons. Proc. of the 11th Symposium on Developments in Prestressed Concrete, pp.315-320, Nov., 2001 (in Japanese)
[2] Wheeler, J.E. : Prediction and control of pedestrian induced vibration in footbridges, Proc. of ASCE, VOL.108 No.ST9, pp.2045-2065, Sep., 1982
[3] Kajikawa, Y. : Some considerations on ergonomical serviceability analysis pf pedestrian bridge vibration, Proc. of JSCE, VOL.325, pp.23-33, 1982.9
[4] BSI : Steel, Concrete and Composite Bridges, Part 2. Specification for loads, 7.1.5 Vibration serviceability, BS5400,1978

PROTOTYPE FALLING WEIGHT IMPACT TEST ON PRC GIRDERS FOR ROCK-SHEDS

Hisashi Konno
Civil Engrg. Research
Inst. of Hokkaido, JAPAN

Norimitsu Kishi
Muroran Inst. of Tech.
JAPAN

Shin-ichi Takemoto
DPS Bridge Works
JAPAN

Kenji Ikeda
Civil Engrg. Research
Inst. of Hokkaido, JAPAN

Keywords: impact test, PRC girder, tensioning rate, shear-bending capacity ratio, rock-shed

1. INTRODUCTION

In this study, in order to establish a rational impact design method for Prestressed Reinforced Concrete (PRC) girders with high impact resistant capacity, falling-weight impact tests were conducted using a 3,000-kg steel weight. Under the condition keeping shear-bending capacity ratio α constant, impact resistant behaviors of prototype four types PRC girders were investigated, in which the rate of introduced pretension force in the PC tendon (hereinafter, tensioning rate), material property and volume of axial rebar, and girder height were taken as variables.

2. OUTLINE OF THE EXPERIMENT

2.1 Test procedure

Figure 1 shows an experimental setup. The impact load was subjected freely falling a 3,000-kg weight onto the span center of the girders. In this study, the ultimate state of the girder is defined as that when its maximum residual displacement reached 1/100 of the clear span length to keep away from danger. The impact load was subjected by means of single loading method and the falling height of weight was exclusively 22.5 m.

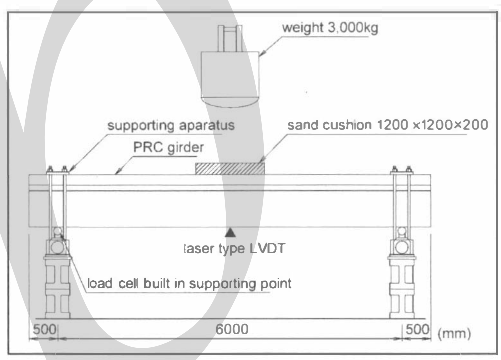

Fig. 1 Experimental setup

In this experiment, acceleration of the falling weight, reaction force excited at supporting points (reaction force R), and mid-span displacement (displacement δ) were measured and recorded continuously.

2.2 PRC girders

Four types PRC girders used in this experiment are listed in Table 1. All the PRC girders have similar static shear-bending capacity ratio α (the ratio of static shear capacity to static bending capacity). The four types PRC girders are: 1) Type 1 girder is designed according to the conventional design code; 2) Type 7 girder is let a tensioning rate be 0.5 with reference to the value for Type 1 girder; 3) Type 9 girder is let rebars be arranged in two rows in the lower edge; and 4) Type 10 girder is let high-strength deformed bars be arranged in the lower edge instead of normal rebars.

Table 1 List of PRC girders

Specimen	Tensioning rate	Lower rebar, nominal name* × number	Shear-bending capacity ratio α	Girder height (cm)
Type 1	1.0	D16×4	1.30	90
Type 7	0.5	D16×4	1.30	90
Type 9	0.8	D16×8	1.30	90
Type 10	0.5	G23×4	1.31	65

* D: deformed bar, G: high-strength deformed bar

Note: Static bending capacity and shear capacity are approximately 1.5 MN and 2.0 MN, respectively.

Figure 2 shows the dimensions for cross section of each girder. All the girders were PRC ones with a simple T-section constructed based on the pretensioning system. The PC tendon was SWPR7BN- ϕ 15.2 (yield strength f_y = 1770 MPa). SD345-D16 (f_y = 394 MPa) and high-strength deformed bar ϕ 23(f_y = 1070 MPa) were used for lower rebars.

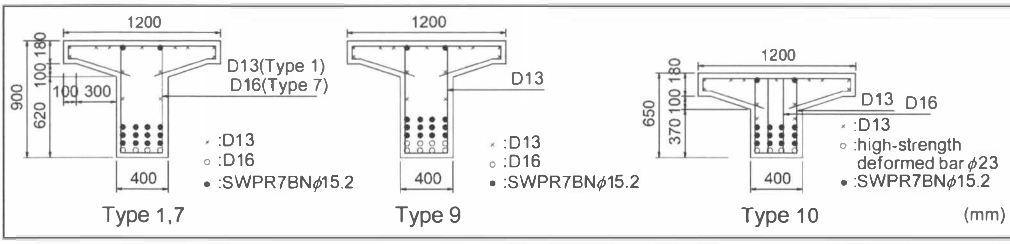

Fig. 2 Dimensions for cross section of PRC girders

3. EXPERIMENTAL RESULTS

3.1 Hysteretic loops of reaction force - displacement

Figure 3 shows hysteretic loops of the reaction force and displacement $R-\delta$ obtained from the experimental results. The result for Type 1 girder shows a triangular hysteretic loop with a wide base, which means that the girder has reached the ultimate state with a shear failure mode. The shapes of hysteretic loops for Type 7, 9 and 10 girders are different slightly from one another because the tensioning rate and the material property and number of lower rebars were different. Although the hysteretic loop for Type 10 girder indicates a simple triangular distribution, this girder has a tendency to freely vibrate with small displacement after unloading. This means that it has not reached the ultimate state yet.

3.2 Max. & residual disp. and absorption energy

Table 2 shows the maximum displacement, residual displacement and absorption energy. The absorption energy was estimated by using the area of the hysteretic loop in the positive loading state in Fig.3. While the residual displacement for Type 1 girder comes up more than 20 cm as a result of shear failure, those for the other three types of girders were slightly bigger than the reference value (6 cm) at the ultimate state. Then, it is seen that these three types of girders were in the ultimate state defined in this study but still have been stiff and freely vibrated.

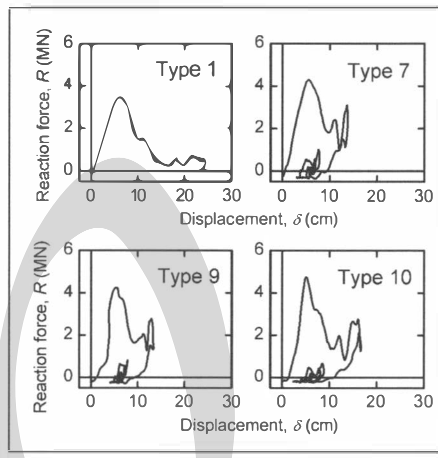

Fig. 3 Hysteretic loops of $R-\delta$ relation

Table 2 Experimental results

Specimen	Max. disp. δ_{max} (cm)	Residual disp. δ_r (cm)	Absorption energy E_s (kJ)
Type 1	24.2	21.5	303.2
Type 7	13.7	6.3	311.0
Type 9	13.4	6.5	256.7
Type 10	16.6	6.8	325.2

Comparing impact resistance among three types girders except Type 1 girder, Type 10 girder, in which high-strength deformed rebars were arranged in the lower edge and a girder height was 25 cm lower than that of the other type girders, has not reached real ultimate state even though both maximum and residual displacements were the largest among three types of girders. Then, it can be judged that Type 10 girder has the most effective section among three types of girders.

4. CONCLUSIONS

From this study, it is revealed that under the condition keeping shear-bending capacity ratio α constant, reducing the tensioning rate of PC tendons to around 0.5 and arranging high-strength deformed bars in the lower edge of PRC girders, the impact resistant capacity can be increased effectively. Furthermore, construction costs for PC rock-sheds can be reduced by downsizing the girder height comparing the conventional PRC girders while withstanding the same rockfall load.

A STUDY ON FALURE MODE OF CARBON FIBER-SHEET-REINFORCED CONCRETE 3-POINT BENDING SPECIMEN WITN A V-NOTCH*

Huang Pei-yan Zhou Xu-ping Luo Yi
South China University of Technology, China

Liu He-ping Wang Xiao-Tian Luo Li-feng
Guangdong Province Highway Bureau, China

Keywords: carbon fiber-sheet, V-notch beam, over-stress area, failure mode, concrete member

1 INTRODUCTION

Reinforcing or repairing concrete structures with high strength fiber-sheet is an advanced new way to raise load-bearing capacity and extend life. Since 1995 the studies related with fiber-sheet reinforced concrete (FSRC) have been more and more valued by researchers[1,2]. For presenting an optimum design method and a reasonable and economical reinforcing technique, it is necessary to study deeply the failure mechanism of these kinds of beams. In this paper, some concrete 3-point bending specimens reinforced by carbon fiber-sheet (CFS) are used to numerically and experimentally study their failure modes, with several different depth of the V-notch and different length of the CFS.

2 NUMERICAL ANALYSIS

2.1 Analysis model

The analysis model is a 3-point bending specimen (beam) with a V-notch (Fig. 1). The size of the specimen is 0.1 x 0.1 x 0.45m, the depth of the V-notch is 0.02m and the angle of the notch tip is 30° . The basic material is C40 concrete, based on which the proportioning (by weight) is determined. The quality characteristics of the concrete are as follows[2]: Young's Modulus Ec=300GPa; Poisson ratio ν =0.20; bending strength σ_l=5.15MPa. The imported carbon fiber, T300-3K, is used. Their characteristics are as follows: tensile strength σ_{fb}=3500MPa; Young's Modulus E_f=400GPa; elongation=1.5%. The matrix of the CFS preimpregnated strip is an epoxy resin, and the quality characteristics of the CFS strip are as follows: thickness t_f =5$\times 10^{-4}$ m; Young's Modulus E_{cf}=240MPa; tensile strength σ_b= 2100MPa; Poisson ratio ν =0.29.

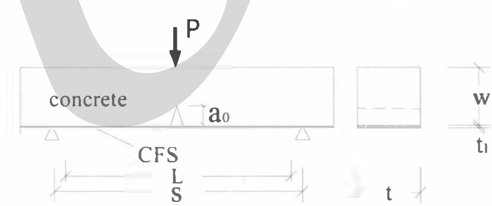

Fig.1 FSRC 3-point bending specimen

2.2 Numerical analysis results and discussion

Adopting the above calculation model (Fig.1), the stress field of the CFS reinforced concrete specimen with a V-notch under the load P=20KN is analyzed numerically using the software ANSYS5.5. In these calculations, the variation of the length of the affixed CFS, L, and the depth of the crack, a_0, is taken into account. The chosen length is 0.2m, 0.3m, 0.4m and 0.45m, while the depth of the crack is 0.01m, 0.03m and 0.05m. Also the failure process and failure mode of the specimen is predicted.

2.2.1 Over-stress areas

While a higher load being applied to the specimen, the FEM analysis results show that there are two "over-stress areas" on the specimen, where the stress is higher than the bending strength of the concrete (σ_l =5.15MPa). One of the areas near the V-notch tip, the other is on the concrete side of the

* This study is subsidized by National Natural Science Foundation of China (19972020) and Guangdong Province Natural Science Foundation (990567).

interface between concrete member and CFS.

For the case near the V-notch tip, the relationship between the tensile stress σ_I(MPa) on the "nominal crack tip"[2] and the crack size a (mm) is given by:

$$\sigma_I=-0.0039a^2+0.178a+8.62 \qquad (1)$$

Eqn.(1) shows that "over-stress area" near the mode-Ⅰ crack tip will decrease gradually, and finally vanish after the crack has propagated a longer distance under the same load.

For the case on the concrete side of the interface, the FEM analysis results show that the length of the CFS, L, has a great effect on the stress field on the interface as follows:

1) When L/S<3/8 (S is the distance between two fulcrums) and load level is higher, there will be an "over-stress area" on the concrete side of the interface, and the width of the area exceeds the length, L.

2) When L/S≥3/8, the "over-stress area" evolves into two areas: one (width: D_1) in the field affixed with the CFS is bigger, the other (width: D_2) in the outside of the field is smaller.

3) The relationships between D_1, D_2, and L/S can be given by:

$$2D_1/S=-1.22\alpha^4+5.14\alpha^3-7.88\alpha^2+5.25\alpha-0.780, \qquad (\alpha=L/S) \qquad (2)$$

$$2D_2/S=0.854\alpha^4-4.32\alpha^3+7.40\alpha^2-5.35\alpha+1.41, \qquad (\alpha=L/S) \qquad (3)$$

Using eqn.(2) and eqn.(3), the variations of the "over-stress area" on the interface of the concrete member and CFS, and then the failure mode of the specimen can be predicted conveniently.

2.2.2 Prediction of the failure modes

The predicting results from eqn.(1) - (3) show that the failure modes and fracture processes of the specimens are as follows:

1) The "over-stress area" will cause the mode-Ⅰ (opening mode) crack initiation and propagation on the V-notch tip.

2) The mode-Ⅰ crack will be propagated rapidly when the loading is increased continuously. Following the crack propagation, the stress level on the V-notch tip is down, and the "over-stress area" will disappear, then the crack propagation is arrested.

3) Some macro diagonal cracks exist in the "over-stress area" on the concrete side of the interface after the mode-Ⅰ crack propagation is arrested. These cracks will form a main crack (diagonal crack), then the main crack will be propagated rapidly under bending loads, and that leads the concrete members of the specimen to be ruptured.

4) However, the differentiae of place and width of the "over-stress area" may cause some different failure modes on the specimens. When L/S<3/4, a main crack will be initiated on the bottom of concrete beam near the end of the CFS, then leads the crack to growth and the specimen to fail; When L/S≥3/4, the main crack will initiate in the area D_1 (the range affixed with CFS), then propagates on the concrete member of the specimen. The debonding fracture on the interface between CFS and concrete member will happen after the main crack extends to a certain size, then the specimen to be ruptured for the latter case.

3 EXPERIMENTAL VERIFICATION

For testing and verifying the above prediction about the failure modes of the specimens, 30 specimens are divided into 10 groups based on several different depths of V-notch and different lengths of CFS as same as the FEM analyses. All tests are carried out with MTS machine. The experimental results correspond with that obtained from the prediction by FEM.

REFERENCES

[1] Wakui, H. , and Matsumoto, N. : Seismic strengthening of railway concrete viaduct with fiber plastic sheets. JSCE, 82(May), pp.10-12, 1997 (in Japanese)

[2] Huang P. Y., Long Z. Q., Lou Y., et. : Experimental study on load-carrying capacity of carbon fiber-Sheet-reinforced concrete three-point bending specimen with a V notch. Proc. SPIE Vol.4537, pp.95-98, 2002

THE APPLICATION OF MULTI-AXIAL STRENGTH THEORIES IN THE ANALYSIS OF RC CHIMNEY WALL

Qin Likun[1 2] Song Yupu[1] Zhao Dongfu[1] Yao Jiawei[3]
Dalian University of Technology, CHINA[1] Dalian Yalong Decoration Co. CHINA[3]
Dalian University, CHINA[2]

Keywords: RC(Reinforced Concrete) chimney Wall Multi-axial strength axial Crack Stress

1. INTRODUCTION

This paper applies multi-axis strength theory of pure concrete to the analysis of the result of RC plate experiment in document 1. Which proves that the multi-axis strength theories of pure concrete can be directly applied to RC structure analysis, i.e. it can be introduced into the calculation of RC chimney wall. Also, the strength of concrete chimney wall, the concrete crack stress and concrete stress permissible value can be analyzed with multi-axis strength theory. All the past experiment results prove it more practicable to analyze the RC chimney wall with concrete multi-strength standard.

Chimney wall is subjected to the effect of weight, wind, earthquake and temperature. Among them, the stress caused by the effect of weight, wind and earthquake is longitudinal force. The inner and outer surface of the chimney wall have different temperature, which generate compressive stress to the inner surface and tensile stress to the outer surface. Years of engineering practice demonstrate that longitudinal and annular cracking are common on the chimney, and the main cause of the cracking is temperature and contraction effect. In addition, in studying the stress state caused by deformation variation, the analysis of the stress state caused by loading variation is used, that is, Duhamel Resemblance, also named equivalent loading method, is used.

To design the chimney wall under compressive and tensile stress with uni-axial strength theory is another reason to cause the crack, since it overestimates the tensile strength of concrete. Therefore, using multi-axial strength theory to analyze the RC chimney wall is more in accordance with the actual stress state of the chimney wall.

2. ANALYTICAL METHODS

2.1The Applicability of Plain Concrete Multi-axial Strength Theory in RC Structure

Analyze the result of RC plate experiment in Document 1 (see Document 1 for experimental survey). Use the concrete failure criteria theory in Document 2 to analyze the cracking stress. According to octahedral stress space concrete failure criteria theory, the positive stress on the octahedron σ_{oct} is:

$$\sigma_{oct} = \frac{1}{3}(\sigma_1 + \sigma_2 + \sigma_3) \tag{1}$$

Among them, σ_1, σ_2 and σ_3 are positive stress from three directions. The sheer stress on the octahedron τ_{oct} is:

$$\tau_{oct} = \frac{1}{3}\sqrt{(\sigma_1-\sigma_2)^2 + (\sigma_2-\sigma_3)^2 + (\sigma_3-\sigma_1)^2} \tag{2}$$

The mathematical expression of octahedral stress space concrete failure criteria is:
The tensile meridian plane:

$$\frac{\tau_{ot}}{f_c} = 0.05073 - 0.8816\frac{\sigma_{oct}}{f_c} - 0.06426(\frac{\sigma_{oct}}{f_c})^2 \tag{3}$$

The compressive meridian plane:

$$\frac{\tau_{oc}}{f_c} = 0.0688 - 1.072\frac{\sigma_{oct}}{f_c} - 0.0699(\frac{\sigma_{oct}}{f_c})^2 \tag{4}$$

2.2 Establish the Wall Strength , Stress Computation Expression According to RC Multi-axial Strength Theory

1.Analyze the Strength of the Chimney Wall According to the RC Multi-axial Strength Theory

The inner surface of the lee side wall is in bi-axial stress state, so space RC stress failure criteria can be applied for analysis. We can establish the computation expression of the strength of the chimney wall at its maximum loading ability state.

$$Ne \le [\sigma_{3t}A_1 + f_{ct}(A - A_t)]\frac{r_1 + r_2}{2}\frac{\sin\alpha\pi}{\pi} + f_{st}A_s r_s \frac{\sin\alpha\pi + \sin\alpha_t\pi}{\pi} \qquad (5)$$

In it, N is the design value of longitudinal eccentric force the section can endure; e is the eccentricity of the longitudinal force to the annular section centroid; f_{ct} is the design value of axle center tensile strength of RC under the effect of temperature; A is wall section surface area; r_1, r_2 are respectively the inner and outer radius of wall. α ,α_t are respectively the half-angle coefficient in compressive zone and the half-angle coefficient of tensile reinforcement bar. f_{st} is the tensile strength design value of reinforcement bar under the effect of temperature; A_s is the surface area of tensile reinforcement bar and r_s compute the circle radius on the section where the reinforcement bars are installed

2.Analyze RC Stress Allow Value According to Multi-axial Strength Theory

σ_{cwt} is the RC compressive stress of the wall on lee side under the joint effect of loading standard

$$\sigma_{cwk} \le 0.5\sigma_{3k} \qquad (6)$$

value and temperature andσ_{3k} denotes the standard value of the compressive strength under the effect of temperature, which has obtained according to the multi-axial strength theory computation.

2.3paint performance

Study the inner surface of the facing wind side wall. Get data of σ_{cw} and σ_{ct} from Document 3. Since$\sigma_1/\sigma_2 = \sigma_{cw}/\sigma_{ct}$, apply equation (1)-(4), we can get the concrete cracking stress of the facing wind side wall under the joint effect of temperature and load. See Table-1 for computation results, f_{tt} in the table denotes the concrete strength designed value considering temperature effect under uni-axial stress state, the data can be obtained from Document 3. From Table-1, we know that using multi-axial stress state theory to analyze the concrete cracking stress of the facing wind side wall under compressive and tensile state, the cracking stress is smaller than we use the uni-axial stress state theory, thus it is not safe enough.

Table 1 Contrast of Computation of the Facing wind side Wall RC Cracking Stress Value According to Multi-axial and uni-axial Strength theory

Sectio-n	σ_{cw}	σ_{ct}	$\frac{\sigma_c}{\sigma_{ct}}$	$\alpha = \frac{\sigma_1}{\sigma_2}$	f_c	σ_{oct}	τ_{oct}	θ	σ_1	f_{tt}	$\frac{\sigma_1}{f_{tt}}$
4	0.52	-1.91	-0.27	-0.27	12.5	$0.24\sigma_1$	$0.55\sigma_1$	11.64^0	0.85	1.03	0.825
6	1.25	-2.10	-0.60	-0.60	12.5	$0.13\sigma_1$	$0.66\sigma_1$	21.79^0	0.89	1.03	0.864
8	1.08	-2.21	-0.49	-0.49	12.5	$0.17\sigma_1$	$0.62\sigma_1$	18.81^0	0.88	1.07	0.822
10	0.87	-2.12	-0.41	-0.41	12.5	$0.20\sigma_1$	$0.59\sigma_1$	16.52^0	0.87	1.06	0.820
12	0.34	-2.54	-0.13	-0.13	12.5	$0.29\sigma_1$	$0.51\sigma_1$	6.30^0	1.17	1.05	1.110

REFERENCES

[1] Zuo Kewei, Kang Guyi and Chen Yunxia: The Softening Function of Concrete under Plate Stress state, Journal of Building Structures, 1993, 10.(in Chinese)

[2] Song Yupu and Zhao Guofan: The Finite Unit Method of RC Structure Analysis, Dalian University of Science and Technology Publishing House, 1994. (in Chinese)

ARCH MECHANISM IN REINFORCED CONCRETE BEAMS WITH WEB OPENINGS

Seijiro Iida, Nihon University, Japan
Ryuichiro Uchida, Matsui Construction, Japan
Hiromitsu Suetsugu, Nihon University, Japan
Masayuki Hamahara, Nihon University, Japan

Keywords: arch mechanism, openings, unbonded axial reinforcement, shear span ratio

1 INTRODUCTION

It is widely recognized that the arch mechanism is difficult to exist in the reinforced concrete beams with openings. Taking this situation into consideration “AIJ structural design guidelines for reinforced concrete buildings” requires that the shear carried by the arch mechanism shall be ignored in calculating the ultimate strength of the solid portion of the beams with web openings. The truss mechanism is difficult to form in the members like precast concrete jointed by prestress, which has poor bond performance in longitudinal reinforcement. Therefore, to prepare openings in such members is almost impossible. Hamahara[1)] et al. performed the reversed cyclic loading testes on the precast prestressed concrete beams with rectangular web openings. From this investigation it was found that the ultimate strength of the test beams was accurately predicted by lesser value of that in solid portion (Q_u) or that in the openings in the test beams (Q_{uo}). This result indicates that the openings can be prepared in the arch mechanism in contradiction to “AIJ structural design guidelines for reinforced concrete buildings”.

Monotonic loading tests on beams with web openings having axial reinforcement without bond were performed, in order to investigate the effect of bond characteristics of axial reinforcement on shear transfer mechanism.

2 OUTLINE OF THE TEST

Table1 shows the outline of specimens. Fig. 1 shows the loading system. Details of a typical test beam are shown in Fig. 2.

Table 1 Outline of specimens

Specimens	L_o*×H_o** (mm)	a/D
SR10-L_o30-H_o15	300×150	1.0
SR15-L_o30-H_o15	300×150	1.5
SR20-l_o30-H_o15	300×150	2.0
SR10-L_o9-H_o9	90×90	1.0
SR15-l_o9-H_o9	90×90	1.5
SR20-L_o9-H_o9	90×90	2.0

*Height of openings **Width of openings

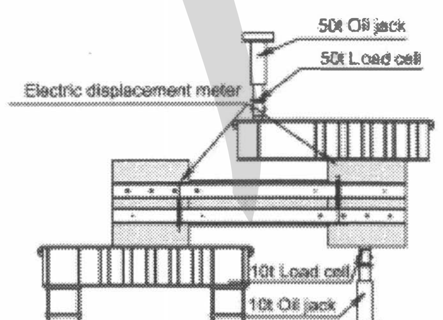

Fig. 1 Loading system

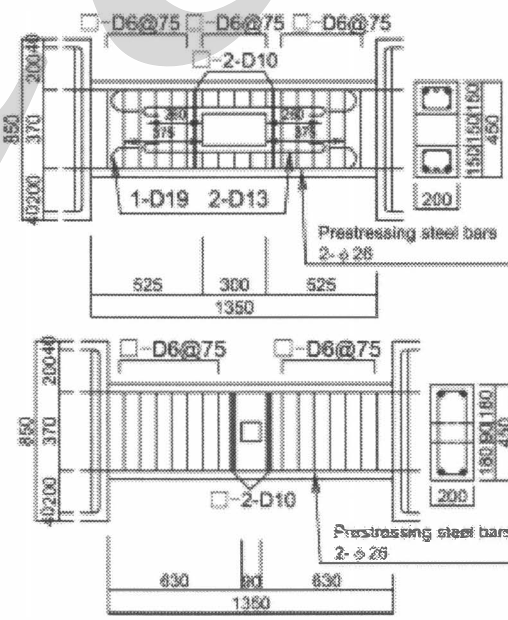

Fig. 2 Details of a typical test beam (SR1.5)

3 TEST RESULTS

The modes of failure were classified two as follows.
(1) Diagonal tension failure of chord members **(DT)**.
(2) Compression failure of solid portion in maximum bending moment regions **(C)**.
Fig. 3(a), (b) and (c) show the load-rotation angle relationship of each test beams. From these figure, the unbonded reinforced concrete beams with rectangular web openings have sufficient ultimate strength, when the premature failure at the openings is avoided.

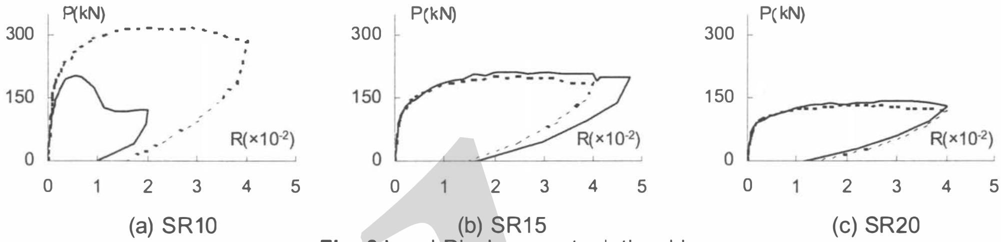

Fig. 3 Load-Displacement relationship

4 STRAIN OF CONCRETE

Fig. 4 show longitudinal strain distribution of test beams whose shear span ratio are 1.5. The strain distribution at each section indicates that:
The strain at each section takes a maximum value at the compressive fiber and decreased in proportion to the distance from the compressive fiber. "Plane section remains plane", i.e. linear strain distribution, was established in concrete, and the strain corresponded to the bending moment distribution. This result indicates that the direct concrete struts, i.e. the arch mechanism does not exist in unbonded reinforced concrete beams.

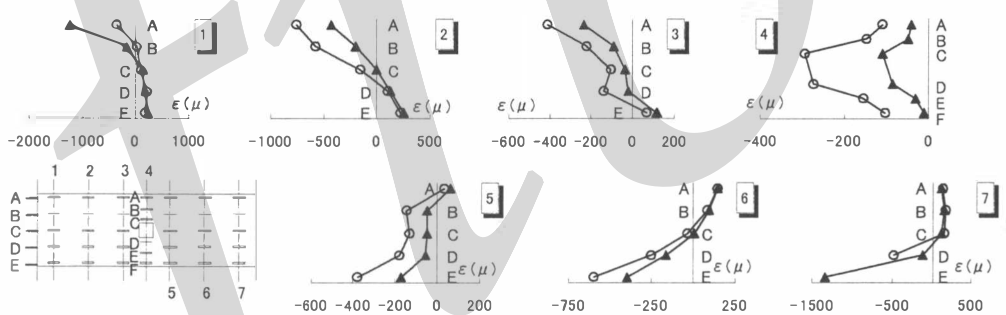

Fig. 4 Strain distribution of concrete

5 CONCLUSIONS

The following conclusion can be derived from the test.
(1) Unbonded reinforced concrete beams with web openings had sufficient ultimate strength when the premature failure at the openings is avoided.
(2) It seems that the direct concrete struts do not exist in unbonded reinforced concrete beams.

REFERENCES

[1] Hamahara M., Tsuji E. and Moritaka H.: "Experimental Study on Behavior of Prestressed Concrete Beams with Web Openings", Journal of Prestressed Concrete, Vol.41, No.3, pp14-19, 1999(in Japan)
[2] AIJ: "Design Guidelines for Earthquake Resistant Reinforced Concrete Buildings Based on Ultimate Strength Concept", Maruzen Co., Ltd pp106-146, Oct. 1990

EXPERIMENTAL BEHAVIOUR OF SMOOTH BARS ANCHORAGES IN EXISTING R.C. BUILDINGS

G. Fabbrocino G. M. Verderame G. Manfredi E. Cosenza
Department of Structural Analysis and Design
School of Engineering, University of Naples, Naples - 80125, ITALY

Keywords: Structural assessment, existing r.c. buildings, smooth rebars, bond, anchorage details.

1 INTRODUCTION

The first step in upgrading strategies of existing concrete structures is the assessment of current performances of materials and structural systems.

The aim of assessment is the reliable evaluation of the actual conditions of the building in order to ensure satisfactory structural performances against current and exceptional loads, and develop a rehabilitation process when potential damages occurred. This circumstance applies particularly in the field of seismic vulnerability of underdesigned reinforced concrete structures, which is relevant in many European countries, i.e. Italy, Greece and Portugal. In fact, many existing constructions have been designed only for gravity loads or according to outdated seismic rules resulting in low available ductility and lack of strength hierarchy. The measure of global ductility for frames is the interstorey drift ratio that for r.c. frames is dependent upon different contributions like the beam plastic rotation, the column flexural behaviour and the beam to column joint region deformation. The latter is generally divided in two components related to shear deformation of the panel zone and to the fixed-end rotation that is predominant in underdesigned structures and depends on bond properties of reinforcement and anchoring devices.

The present paper deals with smooth reinforcing bars widely used up to 1970's in a very large number of existing constructions and characterised by poor bond performances resulting in mandatory anchoring end details able to ensure the required levels of interaction.

As a consequence, behaviour of anchored smooth bars is a key issue in development of reliable procedures for evaluation of remaining carrying and/or displacement capacity of buildings based on refined structural analyses taking into account actual measured dimensions, critical sections and regions, test data of the concrete and reinforcement. Basic properties of bond and response of bar end details used in critical regions are examined with specific reference to typical circular hooks with 180° opening angle and the related stress-slip response under static loads.

2 SUMMARY OF RESULTS

The experimental program is based on two different types of test set-up: beam-test for evaluation of bond properties of straight bars and hooks up to yielding; pull-out tests to analyse the response of hooked anchorages both under service and ultimate load. At the present stage more than 30 tests have been carried out varying the concrete cover, casting direction and diameter. The tested reinforcement consists of smooth rebars still available for secondary purposes in r.c. structures; their mechanical properties are similar to steel classified as Aq42 in Italian design Code utilised in 1960's; yielding stress is about 320 MPa, ultimate stress is equal to 430 MPa and ultimate uniform strain is about 20%.

The beam test and pull-out specimens are reported in Figure 1.a and 1.b respectively; in the first case the hook slip is calculated starting from a reference point slip, in the second case a direct measure of hook slip has been carried out. The results showed some particular aspects of the behaviour under monotonic loading. The slippage due to anchoring devices is relevant, especially in large post-yielding field; mechanisms governing stress-slip response of hooks allow a reduced yielding spreading in the anchoring devices, so that at yielding, the hook slip does not show a plastic plateau and increases only when strain hardening starts. The concrete cover plays a role in the large post-yielding field, since splitting type failure have been observed in END specimens that fit the bar embeddement in external beam to column regions. Casting direction seems to have an influence on the behaviour together with the relative position of the hook respect to the top surface of the concrete specimen. These experimental evaluation is a base point for modelling of the behaviour of critical details governing the failure modes of underdesigned r.c. frames.

3 TEST RESULTS

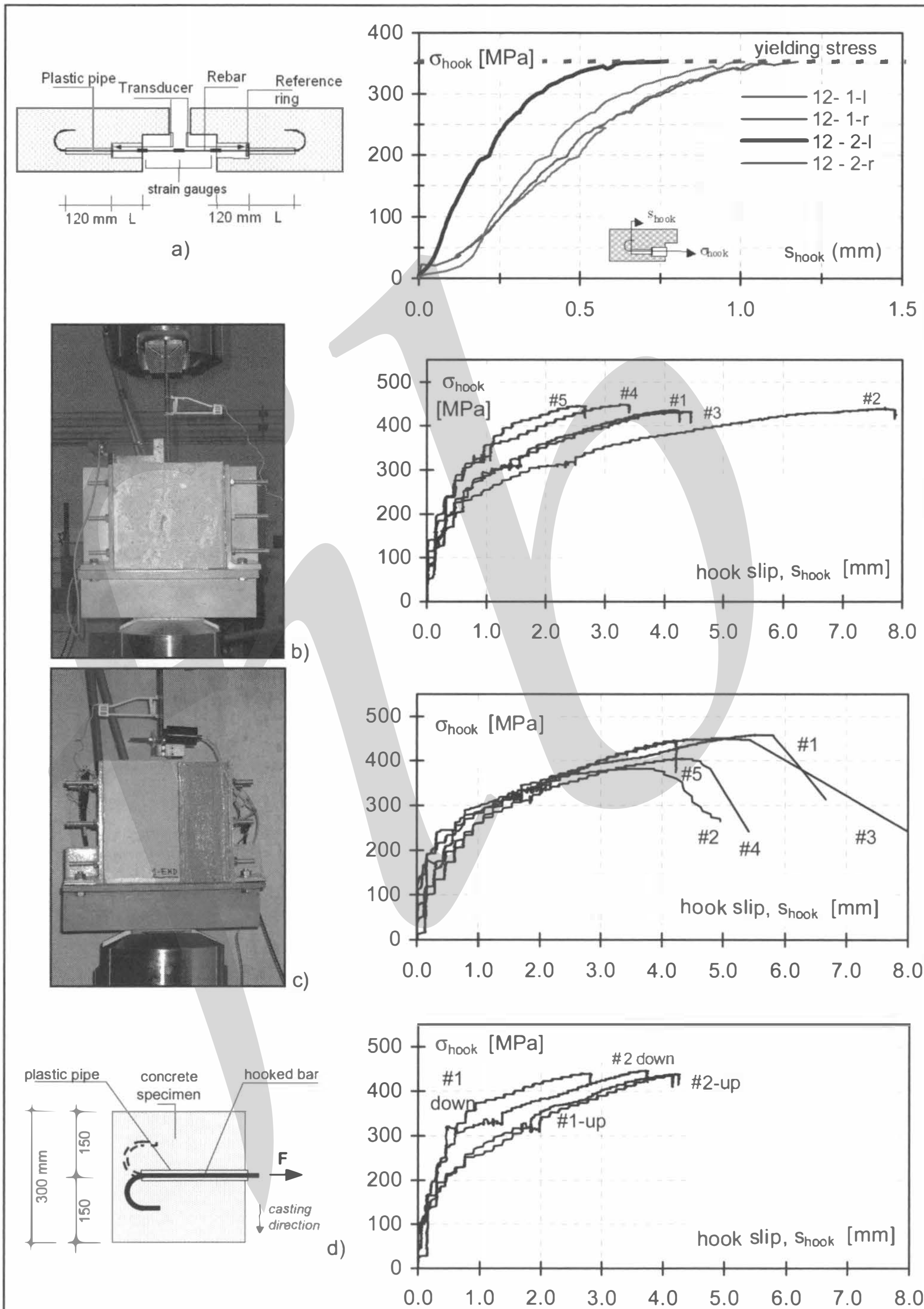

Fig. 1: Experimental results from beam tests (a), FULL (b), END (c), FULL-H (d) pull-out specimens.

THEORETICAL AND EXPERIMENTAL ANALYSES OF PRECAST PRESTRESSED CONCRETE ROOF ELEMENTS FOR LARGE SPAN

Beatrice BELLETTI Roberto CERIONI Ivo IORI.
Department of Civil Engineering, University of Parma

Keywords: reinforced concrete, cracking, failure, design.

1 INTRODUCTION

This work aims at demonstrating that NLFE analysis, supported by a well-documented and verified constitutive relationship, has become a practical and powerful tool not only for research purposes but also for ordinary design of reinforced concrete structures. Authors, after defining and testing a constitutive stiffness matrix (PARC) for reinforced concrete membrane elements [1], have inserted this one in the multipurpose finite element package ABAQUS. In this work theoretical and experimental analyses of precast prestressed concrete roof elements for large span have been developed. The experimental tests have been simulated through a non-linear finite element model, using a mesh of layered SHELL elements. This numerical procedure, recently proposed by the Authors [3], allow an assessment of service and ultimate loads, collapse mode, displacements and cross-section deformations, crack openings, stress and strain in concrete and steel, etc.

2 EXPERIMENTAL PROGRAM

In October and November 1999, an experimental program was carried out at the laboratory of RDB S.P.A. (Italy) ([3]). Shear tests relative to THOR elements, which are a kind of precast prestressed roof element made by RDB S.P.A., were performed (Fig. 1 and 2). Two shear tests, called THOR T1 and THOR T2, have been carried out, Fig. 3a shows structural schematisation of tests.

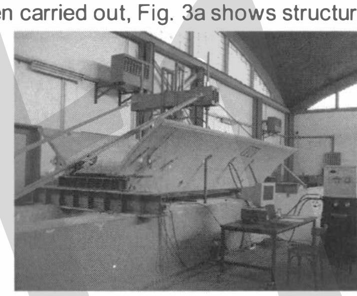

Fig.1 The precast prestressed roof element THOR.

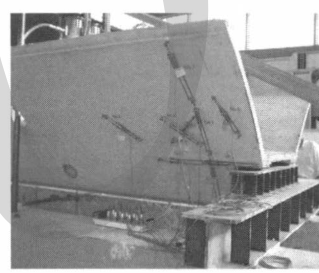

Fig.2 The head of THOR element.

To better knowledge of the behaviour of dapped ends of elements, 18 LVDTS with bases ranging from 24 to 42 mm, have been placed near the support nearest of load (Fig. 2).

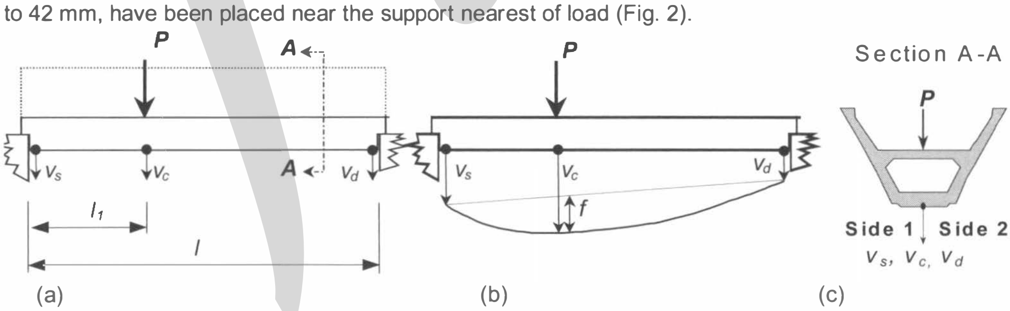

Fig.3 Schematisation of shear tests: (a) structural schematisation; (b) calculation of element deflection at the point of application of load; (c) transversal cross section.

3 NON – LINEAR FINITE ELEMENT APPROACH

NLFE analyses have been carried out using the multipurpose finite element package ABAQUS ([3]) that enables user to introduce subroutine to define material constitutive relationship; details of NLFE analysis are provided in the following. Three - dimensional SHELL elements have been adopted for describing the midsurface shape of precast prestressed reinforced concrete roof elements (Fig. 4b).

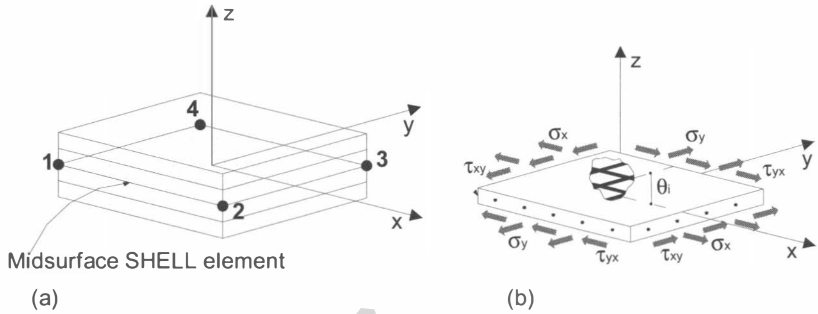

FIG. 4 (a) Composite SHELL finite element adopted, (b) one layer of SHELL element.

Layered finite element SHELL (Fig. 4a) is used to define a laminate shell made of one or more materials, each layer behaves as a reinforced concrete membrane element (Fig. 5). Constitutive relationship of these reinforced concrete layers, subjected to plane stresses, is evaluated by a stiffness matrix proposed by the Authors called PARC ([1]).

4 COMPARISON BETWEEN EXPERIMENTAL OBSERVATIONS AND NLFEA RESULTS

Comparison between experimental and numerical results has shown a good agreement, regarding both structure displacements and local behaviour, confirming the effectiveness of the proposed model within the design of these special roof elements. Fig. 5 shows, for example, comparisons between experimental and numerical load – deflection curves for THOR T2 respectively.

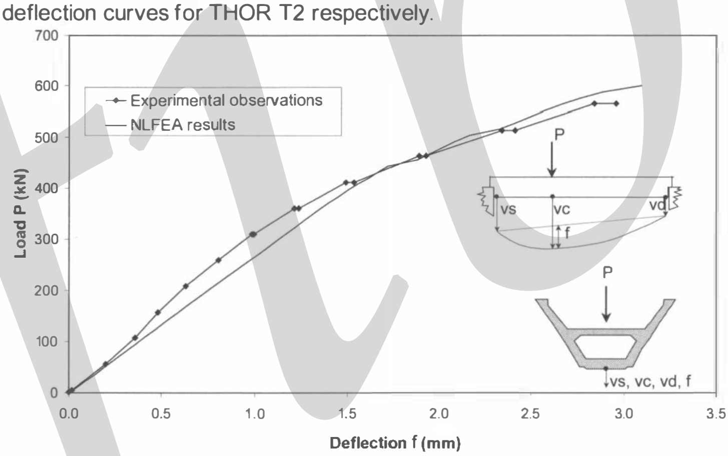

Fig.5 THOR T2 test: comparison between experimental and NLFEA results.

5 CONCLUSIONS

NLFE analyses proposed, more demanding than traditional LFE analyses, have made it possible to obtain numerical results in good agreement with experimental ones, not only for service loads but also at failure. Numerical analyses provide several quantities such as displacement, crack opening, strains and stresses in concrete and steel, useful not only in the research field but also for the design.

REFERENCES

[1] Belletti, B., Cerioni, R. and Iori, I. : A Physical Approach for Reinforced Concrete (PARC) membrane elements. J. Struct. Engrg., ASCE, 127(12), 1412-1426, December 2001

[2] Belletti, B., Cerioni, R. and Iori, I. : A numerical approach for the analysis of reinforced concrete deep beams. Workshop Strut & Tie, Florence, 16 March 2001 (in Italian)

[3] Belletti, B., Cerioni, R., Gazzola, G., Iori, I., Meroni, R. : A Precast Prestressed Reinforced Concrete Roof Element. XVII° International Conference BIBM, Istanbul, 1-4 May 2002.

THE SHEAR DESIGN OF

REINFORCED AND PRESTRESSED BEAMS

Robert E. Loov Ahmed El Metwally
Dept. of Civil Engineering, The University of Calgary, CANADA

Keywords: high-strength concrete, prestressed concrete, reinforced concrete, shear, shear-friction

Revised equations for shear supported by concrete and stirrups

In a 1998 paper, Loov[1] derived a general equation, for the shear strength along a potential failure plane as in Fig. 1. With some changes of symbols, V_c, the factored shear supported by concrete is:

$$V_c = 2V_{45}\left[\sqrt{\frac{F}{V_{45}}+\cot^2\theta}-\cot\theta\right]\left(1+\cot^2\theta\right)-F\cot\theta \qquad (1)$$

where F is force in longitudinal reinforcement, V_{45} is shear supported by a crack inclined at 45°, and θ is angle between longitudinal axis and a potential inclined shear plane.

$$V_{45} = \lambda\,\phi_c\beta_v\sqrt{f'_c}\,A_w \qquad (2)$$

where λ is lightweight aggregate factor, ϕ_c is material resistance factor, β_v calibrates equation to test results, f'_c is concrete strength, and A_w is shear cross-section. Shear resistance does not increase in proportion to the square root of f'_c nor in proportion to beam depth.

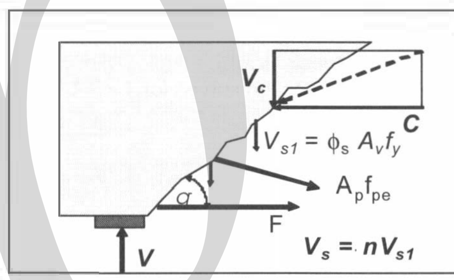

Fig. 1 Free-body diagram

$$\beta_v = 0.36\left(\frac{30}{f'_c}\right)^{0.25}\left(\frac{500}{h}\right)^{0.25} \qquad (3)$$

where h is the overall beam depth. The cross-section assumed to resist shear is $b_w h$ for rectangular sections. T-beams have a higher shear strength than rectangular sections of the same size[2][3].

The concrete shear strength predicted by Eq. (1) reaches a maximum of

$$V_c = V_{45}\tan\alpha \qquad (4)$$

When

$$F \ge F_o = V_{45}\left(2+\tan^2\alpha\right) \qquad (5)$$

Fortunately, this equation applies to most practical cases although Eq. 1 still governs for beams with low steel ratios and in anchorage regions.

The shear supported by the stirrups, V_s is:

$$V_s = V_{s1}\left(\frac{d_{ev}\cot\alpha}{s}-1\right) \qquad (6)$$

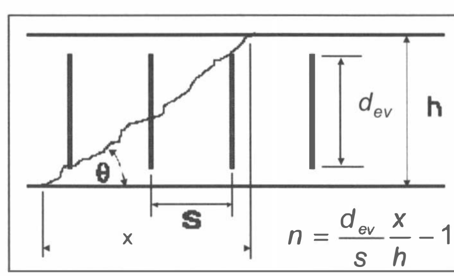

Fig. 2 Number of stirrups crossed by crack

where s is stirrup spacing and d_{ev} is effective length, $V_{s1} = \phi_s f_y A_v$, is shear supported by one stirrup, ϕ_s is material resistance factor for steel, f_y is yield strength of stirrup steel, and A_v is area of each stirrup.

The need to exclude 1 stirrup as can be seen in Fig. 2 has been noted by Marti[5] and by Hoang[6] (see also page 447 of Nielsen[4]). Nielsen has mentioned a similar conclusion by Ichinose[7].

Shear strength of beam based on pessimum angle

The factored shear resistance, V_r, is shear supported by concrete plus shear supported by stirrups.

$$V_r = V_c + V_s \tag{7}$$

Using the simple equation for V_c, this becomes:

$$V_r = V_{45}\tan\theta + V_{s1}\left(\frac{d_{ev}\cot\theta}{s} - 1\right) \tag{8}$$

As seen in Fig. 3, high strengths occur for both high and low angles. The lowest resistance occurs at an intermediate angle. The pessimum angle (i.e. the weakest angle) is:

$$\tan\theta = \sqrt{\frac{V_{s1}d_{ev}}{V_{45}s}} \tag{9}$$

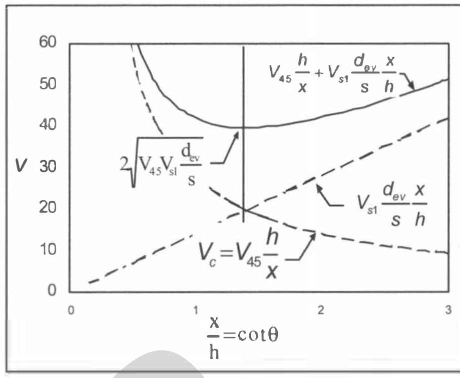

Fig. 3 Variation of shear strength with angle

The shear supported by concrete and stirrups is exactly equal except that the one stirrup that misses the crack needs to be subtracted. Therefore

$$V_r = 2\sqrt{V_{45}V_{s1}\frac{d_{ev}}{s}} - V_{s1} \tag{10}$$

For prestressed beams the transverse component of prestress force, V_p, adds to the shear resistance.

When the longitudinal force across a shear crack is lower than F_o, the concrete shear resistance is reduced below that given by Eq. (4) so that Eq. (1) is applicable. Unfortunately, differentiation of the general equation leads to a complicated solution for the pessimum angle. Although easily solved using root-solving methods, it does not lead to a simple closed-form solution for θ because it requires the solution of a cubic equation. A satisfactory approximate solution has, however, been obtained.

Because the computations are based on residual strength after formation of a crack along the weakest possible plane as well as a more conservative estimate of the stirrup contribution, it is unnecessary to add additional spacing requirements for ultimate load. In particular, the equations inherently include a check of the strength of the possible shear failure plane that could pass between adjacent stirrups.

REFERENCES

[1] Loov, R.E.: Review of A23.3-94 simplified method of shear design and comparison with results using shear-friction, Canadian Journal of Civil Engineering, Vol. 25, No. 3, June 1998, pp. 437-450.

[2] Hoang, L.C.: Shear strength of non-shear reinforced concrete elements, Part 2 - T-Beams, Department of Structural Engineering and Materials, Report R, No. 29, 1997

[3] Peng, L. : Shear strength of beams by shear-friction, M.Sc. Thesis, U of Calgary, 1999.

[4] Nielsen, M.P.: Limit analysis and concrete plasticity, 2nd Edition, CRC Press, 1999

[5] Marti, P.: Staggered shear design of concrete bridge girders, Proceedings of the second international conference on short and medium span bridges, Ottawa, Ontario Canada, Vol. 1. pp. 139-149, 1986.

[6] Hoang, L.C.: Shear strength of lightly shear reinforced concrete beams, Department of Structural Engineering and Materials, Technical University of Denmark, Series R, No. 65, 2000.

[7] Ichinose, T. and Hanya, K, : Three dimensional shear failure of R/C beams, Concrete under Severe Conditions, E & FN Spon, Vol. 2, 1995, pp. 1737-1747.

SHEAR TRANSFER MECHANISM IN REINFORCED CONCRETE BEAMS WITH UNBONDED LONGITUDINAL REINFORCEMENT

Masayuki Hamahara
Nihon University
Japan

Seijiro Iida
Nihon University
Japan

Ryuichiro Uchida
Matsui Construction
Japan

Tsuyoshi Fukui
PS Co.Ltd.,
Japan

Keywords: arch mechanism, bond performance of longitudinal reinforcement, linear strain distribution

1 INTRODUCTION

Many investigators have accepted the hypothesis that the arch model can be applied if the longitudinal reinforcement is not bonded with the surrounding concrete or to "short beams". As a consequence, short beams containing longitudinal reinforcement with no bond have been adopted in order to investigate the shear transfer mechanism in the arch action. Many shear transfer models (e.g. [1]-[3]) have been established based on the hypothesis mentioned above. In spite of the intensive investigations into the shear transfer mechanism in the arch action, the compressive stress field that diagonally flow from the free end to the support, i.e. the arch action, has not been verified yet.

Test [4] on a short beam having unbonded longitudinal reinforcement showed that almost 100% of the total deformation of the test beams was due to flexure and the shear deformation was not observed. This result suggests that the assumption "plane section remain plane" can be established in the short beams having unbonded longitudinal reinforcement, which is contradictory to the arch theorem mentioned above.

Monotonic loading tests on 4 short beams were conducted in order to investigate the bond performance of longitudinal reinforcement on the shear transfer mechanism.

2 OUTLINE OF TEST

The test variables included the amount of web reinforcement and bond performance of the longitudinal reinforcement, i.e. bonded or unbonded. Table1 shows the outline of the test beams. Fig. 1 shows the loading system. The details of a typical test beam are shown in Fig. 2.

Table 1 Outline of test beams

Specimens	Concrete		Stirrup					Longitudinal reinforcement**
	f_c' (N/mm^2)	E×10^4 (N/mm^2)	p_w* (%)	dia (mm)	Spacing (mm)	f_y (N/mm^2)	E×10^5 (N/mm^2)	
PW00-B	31.5	3.09	0	------	------	------	------	bond
PW00-NB	34.7	3.00	0	------	------	------	------	no bond
PW04-B	27.8	3.01	0.4	D6	75	319	1.80	bond
PW04-NB	32.9	2.90	0.4	D6	75	319	1.80	no bond

p_w*=a_w/(bx) Where a_w and x denote sectional area of a group of stirrup and spacing of stirrups respectively
3-D25(f_y=379N/mm^2, E=185000 N/mm^2) were used as top and bottom longitudinal reinforcement

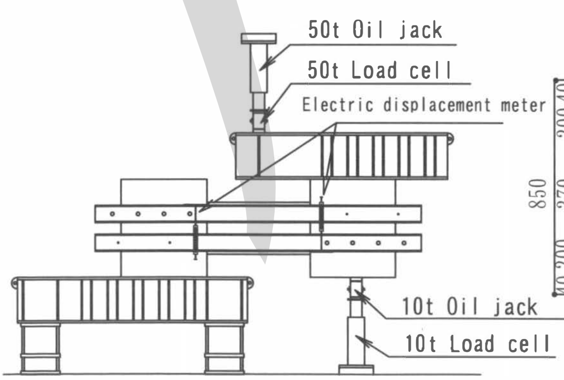

Fig. 1 Loading system

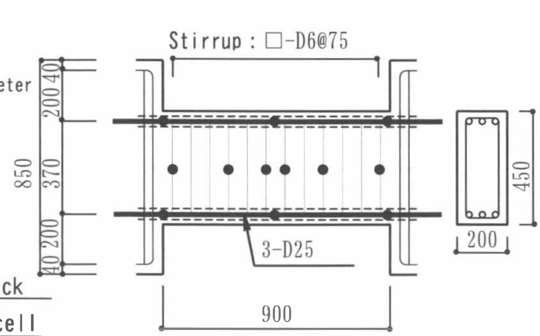

Fig. 2 Detail of test beam

3 TEST RESULTS

All of the test beams failed due to the formation of the diagonal tension crack as shown in Fig.3.

(a) PW00-B (b) PW00-NB (c) PW04-B (d) PW04-NB

Fig. 3 Modes of failure

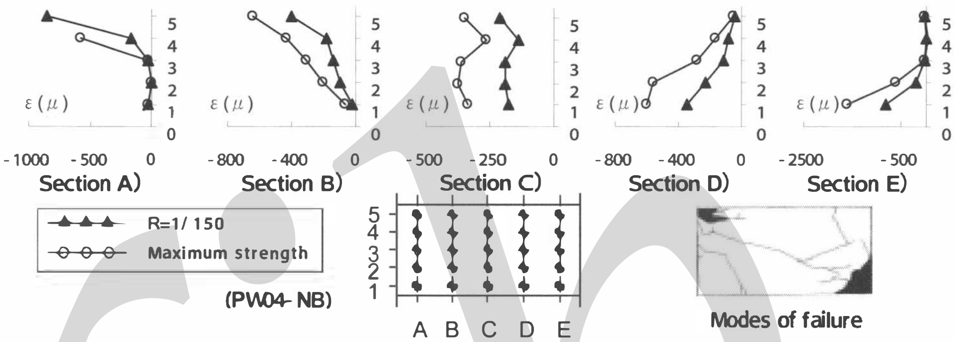

Fig. 4 Strain distribution of concrete

Fig.4 shows the longitudinal strain distribution of test beam, PW04-NB. From this figure, it is found that the strain in each section increases in proportion to the distance from the neutral axis and the curvature at each section increases in proportion to the distance from the contra-flexure point, These results indicate that the assumption of “plane sections remain plane” was established in the concrete and the direct concrete struts, i.e. the arch mechanism, does not exist in unbonded reinforced concrete beams. The diagonal tension crack forms under the condition of the linear strain distribution. Fig. 5 shows the distribution of the principal strain at the rotation angle of 1/150. Similar to Fig. 4 the flow of the diagonally inclined compressive stress,i.e. the arch action, does not observed.

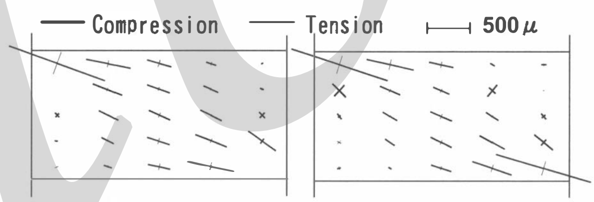

(a) PW00-NB (b) PW04-NB

Fig. 5 Distribution of the principal strain

4 CONCLUSIONS

The following conclusion can be derived from the test.

(1) All of the test beams failed due to the formation of the diagonal crack.

(2) The assumption “plane sections remain plane” was established and the direct concrete struts do not exist in reinforced concrete beams having longitudinal reinforcement with no bond.

REFERENCES

[1] J. Schlaich, k.Schafer and M. Jennewein: ”Toward a consistent design of structural concrete”, PCI journal, pp.75-149, May-June, 1987

[2] AIJ: “Design Guidelines for Earthquake Resistant Reinforced Concrete Buildings Based on Ultimate Strength Concept”, Maruzen Co., Ltd pp106-146, Oct. 1990

[3] P. Marti: “Basic tool of reinforced concrete beam design”, ACI journal, pp.46-56, Jan.-Feb., 1985

[4] Umemura H., Matsumori T. and Otani S.: ”Experimental study on resisting mechanism of R/C short span beams (Part2 Mechanism of shear resistance)”, Summaries of technical paper of annual meeting AIJ Ⅳ-C-2, pp.535-536, Aug., 1995 (in Japanese)

EXPERIMENTS ON SHEAR BEHAVIOR OF PRECAST PRESTRESSED CONCRETE BEAMS

Tsuyoshi Fukui
P.S. Corporation
JAPAN

Ryuichiro Uchida
Matsui Construction Co.Ltd
JAPAN

Masayuki Hamahara
Nihon University
JAPAN

Keywords: precast prestressed concrete members, anchorage condition of longitudinal reinforcement, web reinforcement ratio, truss and arch mechanism

1 INTRODUCTION

Recently Many investigators have intensively conducted the experiments on the mechanical behavior of precast prestressed concrete members. These experiments have clarified the flexural behavior of the beams, shear behavior of the beam-column joint and direct shear transfer behavior in the joint mortar. However, little is known about the behavior of the precast prestressed members subjected to shear, since there have been very few investigations. In current AIJ code the ultimate shear strength of prestressed concrete members is expressed as the sum of the truss and arch mechanism on the basis of the plastic theorem. When applying the theorem to precast prestressed concrete members, the following problems arise.

Typical precast prestressed concrete members resist external forces by prestressing steels, since the ordinal longitudinal reinforcement is cut off in front of the joint mortar. The bond performance of typical prestressing steels is inferior to that of the ordinal deformed steel bars. Consequently the truss mechanism may not form in these members.

The purpose of this study is to clarify the influence of the anchorage condition of longitudinal reinforcement and the amount of the web reinforcement on the shear behavior of precast prestressed concrete members.

2 OUTLINE OF TEST

2.1 Test specimens and mechanical properties of material

In this test 6 test beams were subjected to cyclic reversed bending and shear. The test variables included the web reinforcement ratio and the anchorage condition of longitudinal reinforcement (i.e. anchored into stub or cut off in front of the stub). The experiment consists of two series, that is,

Series-A : The longitudinal reinforcement is anchored into the stub.
Series-NA: The longitudinal reinforcement is cut off in front of the stub.

A detail of a typical test beam is shown in **Fig.1**.

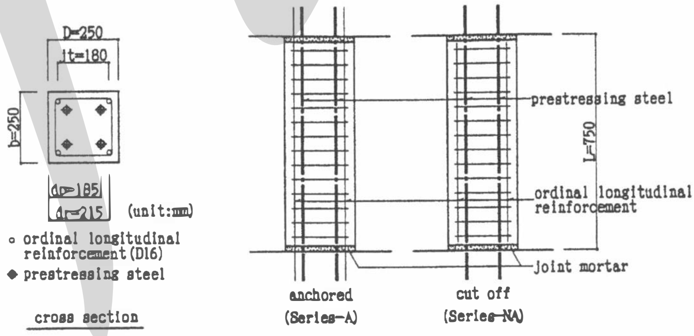

Fig.1 Detail of a typical test beam

3 APPLICABILITY OF SHEAR CODE IN AIJ PC STANDARD TO TEST RESULTS

In AIJ PC Standard [2], the shear strength of prestressed concrete members is given as the sum of the shear carried by the arch and truss mechanism. That is:

$$Q_u = b \cdot j \cdot p_w \cdot {}_w f_y + b \cdot D\left(\nu \cdot \sigma_B / 2 - p_w \cdot {}_w f_y\right) \cdot \left[\sqrt{(L/D)^2 + 1} - L/D\right] \quad (1)$$

where, p_w and wfy denote web reinforcement ratio and yield strength of web reinforcement respectively.

ν denotes effectiveness factor of concrete compressive strength which is given as:

$$\nu = 0.25 \cdot \{1 + (\sigma_g / \sigma_B)\} L / D \quad (2)$$

but $0.65 \le \nu \le 1$

σ_g and σ_B denote prestress and compressive strength of concrete respectively.

Ultimate flexural strength (Q_{mu}) was calculated using Umemura's E - function method, which is on the basis of the assumption that plane sections remain plane. **Fig. 2** shows the relationship between the maximum load and ultimate strength given by **Eq. (1).** From this figure the followings can be pointed out. The applicability of **Eq.(1)** to the test beams of Series-A, whose longitudinal reinforcement is anchored into the stub, is considerably high. On the other hand, with respect to the test beams of Series-NA, the little effect of web reinforcement ratio on the ultimate strength was observed. Accordingly the calculated ultimate shear strength tends to overestimate the test results with the increase of the amount of the web reinforcement.

Fig. 3 indicates that applying the equation ignoring the shear transferred by the truss action in Eq.(1) to the Series-NA, the calculated results agree well with the test results .

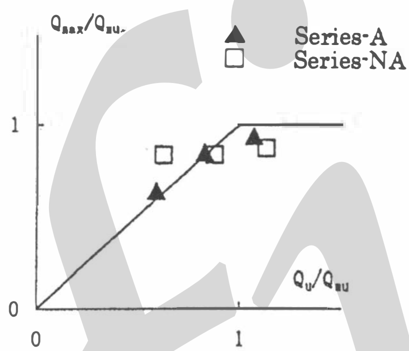

Fig.2 Relationship of maximum load – ultimate strength given by Eq.(1)

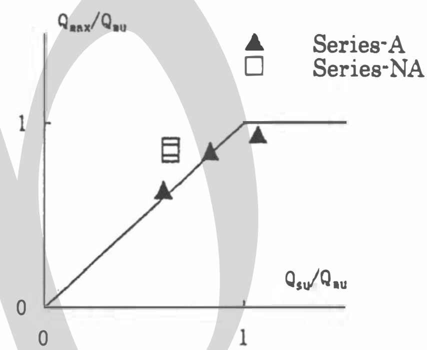

Fig.3 Relationship of maximum load - ultimate strength given by Eq.(1) ignoring truss action to Series-NA

REFERENCES

[1] G.N.J Kani: "The riddle of the shear failure and it's solusion", *Jour. of ACI*, pp.441-467, Apr., 1964

[2] "The standard for structural design and construction of prestressed concrete structures", Architectural institute of Japan, 1998

SHEAR STRENGTHENING WITH PREFABRICATED CFRP L-SHAPED PLATES

Christoph Czaderski
EMPA
Civil Engineer FH/ETH/SIA
Dübendorf, Switzerland

Keywords: Shear strengthening of reinforced concrete, CFRP L-shaped plates, post-strengthening design, shear design, post-strengthening of a preloaded structure

1 INTRODUCTION

Post-strengthening of reinforced concrete (RC) structures with CFRP (Carbon Fibre Reinforced Plastic) plates, in contrast to steel plates, have the advantage of being substantially lighter. The handling on site is therefore much easier. The CFRP plates are also corrosion-resistant and exhibit excellent fatigue strength. This material can be used for the strengthening of concrete members for flexure, shear or torsion as well as confinement.

Prefabricated "CFRP L-shaped plates" (Sika® CarboShear L®) can be used to shear strengthen RC T-beams. In a previous test series, EMPA was able to demonstrate the feasibility of these CFRP L-shaped plates for shear strengthening. To obtain a better understanding of the load-bearing behaviour of this strengthening system, a new systematic test programme was performed in partnership with a Swiss industrial company (Sika AG, Zurich). A test beam specially designed for high shear loads was tested with different arrangements of the shear reinforcement. See Table 1. Most of the existing structures which have to be strengthened are already bearing a load, so that the concrete and the internal reinforcement steel are under stress. A further beam was therefore tested to demonstrate the load-bearing behaviour of a preloaded and subsequently strengthened beam. Using an extensive measurement concept, a number of useful items of information have been gathered from the tests.

One significant problem in the shear strengthening of T-beams is the anchorage in the compression zone. For this reason, strengthening with FRP-fabrics, which is used in many places, is less suitable. The CFRP L-shaped plates can be glued in drill holes through the flange and therefore they have a better anchorage.

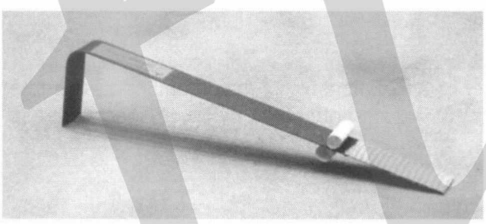

Fig. 1 CFRP L-shaped plate.

The prefabricated CFRP L-shaped plates consist of carbon fibres in an epoxy matrix. The 90° bend has a radius of 25 mm. The thickness of the plate is approximately 1.4 mm, the width 40 mm. The Young's modulus is 120'000 MPa. It is a product from Sika® known as Sika® CarboShear L®. The plates have to be bonded to the concrete with a solvent-free, thixotropic, epoxy-based two-component adhesive mortar named Sikadur®–30.

2 LARGE-SCALETESTS

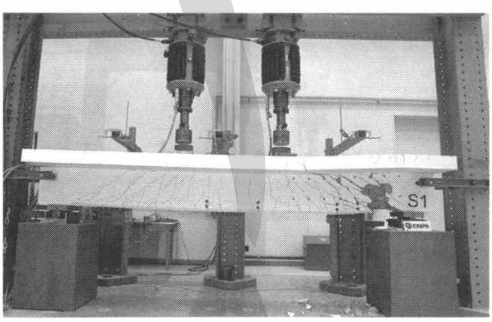

Fig. 2 Beam without external strengthening after the test, shear failure

Fig. 3 Detail of the CFRP L-shaped plates after failure

Table 1 Overview of the tests (s = spacing), beam S5 was preloaded and subsequently strengthened

	Type of Test	Shear Reinforcement	
		internal steel stirrups	external post - strengthening
S1	static failure test	ø8 s = 150 mm	without
S2	static failure test	without	without
S3	static failure test	without	CFRP L-shaped Plates s = 300 mm
S4	static failure test	ø8 s = 150 mm	CFRP L-shaped Plates s = 300 mm
S5	static preloading test	ø8 s = 150 mm	CFRP L-shaped Plates s = 300 mm

3 DESIGN PROPOSAL

Similar to the flexural strengthening with CFRP plates, the following states for the shear design of a RC member can be distinguished:

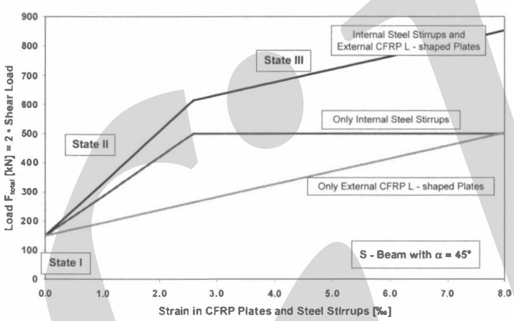

Fig. 4 Load–strain diagram of the shear reinforcement in the S-beams

State I: Uncracked cross-section, i.e. no shear cracks exist, the concrete bears the whole load, no stress in the shear reinforcement.

State II: Shear cracks exist, the internal steel stirrups are in the elastic region, the internal steel stirrups and the external CFRP plates bear the load in proportion to their stiffness.

State III: Shear cracks exist, the internal steel stirrups yield, the external CFRP plates bear the whole increase in the load.

The shear resistance of a member can be calculated as the sum of the contributions of the concrete, the internal steel stirrups and the external CFRP L-shaped plates.

For the verification of the CFRP L-shaped plates contribution the following failure modes have to be considered:

- Opening of the overlapping of the CFRP L-shaped plates
- Anchorage pull-out of the CFRP L-shaped plates
- Peeling-off and CFRP plate fracture

4 CONCLUSIONS

CFRP L-shaped plates can increase the shear failure load so that a structure can bear higher live loads (ULS). Furthermore, the brittle failure mode "shear failure" can be changed to a ductile behaviour with yielding of the internal flexural reinforcement. The CFRP L-shaped plates can also be used to obtain better behaviour in the serviceability limit state (SLS) with a reduction of the shear deformations anddd the strains in the internal steel stirrups.

The concrete, the internal steel stirrups and the externally applied CFRP L-shaped plates act together to bear the shear load. The strains in the shear reinforcement depend on the stiffness of the concrete, steel stirrups and CFRP L-shaped plates. With the simple design concept described, it is possible to understand the three states I, II and III in the post-strengthened RC structure. In addition, the possible failure modes of the CFRP L-shaped plates are described. The strut inclination is limited to $\alpha \geq 45°$.

Preloading of the structure before the strengthening only reduces the load, which the structure can bear at SLS after the strengthening. The ULS and the accidental situation are not influenced.

ESTIMATION OF PUNCHING SHEAR STRENGTH FOR RC SLABS UNDER ECCENTRIC LOAD

Hiroshi Higashiyama
Dr. and Assistant Professor
Department of Civil & Environmental Engineering
Kinki University, JAPAN

Shigeyuki Matsui
Dr. and Professor
Department of Civil Engineering
Osaka University, JAPAN

Keywords: reinforced concrete slab, punching shear strength, eccentric load

1 INTRODUCTION

The punching shear strength of highway bridge slabs is an important factor in evaluating the fatigue durability. Previous researches [1-3] into the punching shear strength of reinforced concrete slabs have conducted by many experimental works. In these experiments, formulae are experientially derived based on a failure mode of reinforced concrete slabs, which have been subjected to a concentrated load at the middle of the slab. However, wheel positions of moving vehicles on highway bridge slabs are not fixed at the center of the slabs. The wheel position follows a normal probability distribution, which can be obtained from the results of measurements [4]. Therefore, a certain breadth of the slab is excessively subjected to randomly running wheels, which are depending on the characteristics of structural dimensions, especially the spacing of main girders. This investigation was carried out to verify the effects of eccentric load. Static failure tests were conducted on square reinforced concrete slabs supported simply at all edges. From the limited experimental results, the characteristics of punching shear strength under the eccentric load are estimated.

2 DESCRIPTION OF TESTS

A total of 22 square reinforced concrete slabs were prepared for the tests as summarized in Table 1. All test slabs were reinforced with 10mm-diameter deformed bars in the main and distribution bar directions. The effective depth and the ratio of reinforcement are expressed with the average value of the main and distribution bar directions, respectively. The average yield strength and young's modulus of reinforcement were f_y=391N/mm^2 and E_s=187kN/mm^2, respectively.

Table 1 Details of test slabs

Specimen	Breadth B (mm)	Span L (mm)	Thick. t (mm)	Effective depth d (mm)	Dia.-pitch (mm)	Ratio of reinforcements p (%)	Loading pad a (mm)	Eccentricity e (mm)	Concrete strength f_c' (N/mm^2)	Young's modulus E_c (kN/mm^2)
A-1 A-2 A-3	2200	2000	100	75	D10-80	1.18	100	0 320 640	33.2	28.2
B-1 B-2 B-3	1700	1500	100	75	D10-80	1.18	100	0 240 480	35.2	26.1
C-1 C-2 C-3	1700	1500	100	75	D10-80	1.18	100	0 80 160	21.5	23.5
D-1 D-2 D-3	1700	1500	100	75	D10-120	0.79	150	0 120 240	23.6	26.6
E-1 E-2 E-3 E-4	700	600	80	55	D10-50	2.60	50	0 90 0 90	34.5 34.5 28.9 28.9	29.4 29.4 27.5 27.5
F-1 F-2 F-3 F-4 F-5 F-6	700	600	80	55	D10-50	2.60	60	0 48 96 96 144 192	18.5	22.3

The positions of the concentrated load were moved as a eccentricity from the center of the slab in the main bar direction. Table 1 shows the description of all test slabs and loading positions from the middle of the slab. The loading pad used for the test was also a square steel plate.

3 ESTIMATION OF PUNCHING SHEAR STRENGTH

Fig. 1 shows the ratios between the failure load of the eccentrically loaded slabs against the failure load of centrally loaded slab and the eccentricity of the loading position. The failure loads remarkably varied with the distance of the loading position. And it appears that there is turning point in the punching shear strength from a certain eccentricity. Increasing the eccentricity, the failure load starts to re-increase again due to changing of the failure mode. It is believed that the failure load closely correlated with the internal shear force in the slabs. Therefore, for all test slabs, maximum shear force was calculated by numerical analysis using the orthotropic plate theory. Fig. 2 shows the relation between the ratios of the maximum shear force based on the maximum shear force of the centrally loaded slab, which is noted as α, and the eccentricity of the loading position. With increasing the eccentricity, the internal shear force increases as a quadratic function. Therefore, combination with the ratios of experimental failure loads and the calculated internal shear forces is considered as shown in Fig. 3. P_{exp}/P_0 multiplied by $\alpha^{2.3}$ is independent upon the eccentricity of the loading position.

4 CONCLUSIONS

From the test results, it was found that the punching shear resistances of reinforced concrete slabs are affected by the eccentricity of the loading position. Punching shear strength is related to the amount of the shear force in the slab. By the combination with the experimental failure load and the calculated shear force, the punching shear strength is independent upon the eccentricity of the loading position. However, this is only a preliminary conclusion, which requires the experimental works to make up the reliability of the relation.

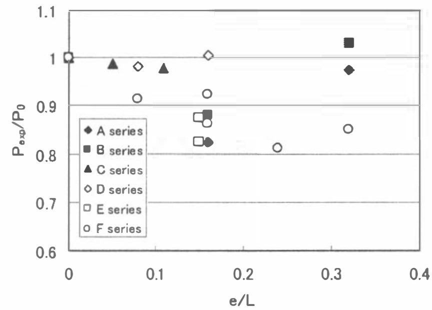

Fig. 1 Relation between the ratios of failure load and the eccentricity of loading position

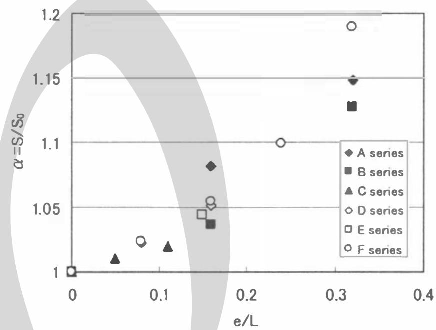

Fig. 2 Relation between the ratio of maximum shear force and the eccentricity of loading position

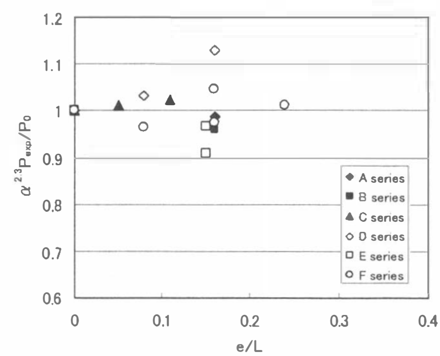

Fig. 3 Results of punching shear strength under eccentric load

REFERENCES

[1] Yitzhaki, D.: Punching Strength of Reinforced Concrete Slabs, Journal of ACI, Vol.63, No.5, pp.527-540, May 1966

[2] Kakuta, Y., Itoh, A. and Fujita, Y.: Experimental Study on Punching Strength of Reinforced Concrete Slabs, Journal of JSCE, Vol.229, pp.105-115, Sept. 1974 (in Japanese)

[3] Maeda, Y. and Matsui, S.: Punching Shear Load Equation of Reinforced Concrete Slabs, Journal of JSCE, Vol.348/V-1, pp.133-141, Aug. 1984 (in Japanese)

[4] Fukumoto, Y., et al.: Development of High Technology in Short and Medium Span Bridge Structures, Report of Dept. of Civil Engineering, Osaka Univ., pp.179-189, Mar. 1991 (in Japanese)

STRUCTURAL CHARACTERISTICS OF PLATE ANCHORED BARS FOR SHEAR REINFORCEMENT AND ITS EFFICIENCY IMPROVEMENT IN CONSTRUCTION WORKS

Toshihiko Tsuka Weijian Zhao Yoshihiro Tanaka Technology Center, Taisei Corporation, JAPAN

Keywords: plate anchored bar, shear reinforcement, construction, covering concrete, ductility, confinement

1 INTRODUCTION

After the Hanshin-Awaji earthquake in 1995, seismic design specification of major building codes [1], [2] changed and semi-circular hooks or 135 degrees bent hooks are presented as standard. However, in most cases of constructing highly dense reinforcing bars (re-bars), it is so difficult to place re-bars with those bent hooks afterwards that complicated procedures of construction or machinery connections are needed.

To solve this problem, Nakamura et al. [3] presented plate anchored reinforcing bars (PA bars) shown in Fig.1.

In this paper, the design method of optimized anchor plates as well as effects on ductility as earthquake-proof performance is discussed. In addition to the design matters, two construction works with PA bars are introduced and good efficiency improvement is indicated.

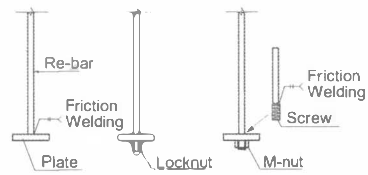

Fig.1 Examples of anchor plates

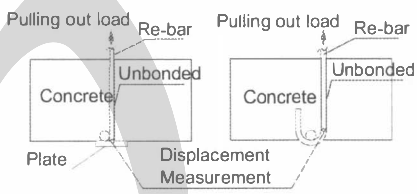

Fig.2 Pulling out test model

2 DESIGN OF ANCHOR PLATES

An anchor plate should have performance of anchoring equal to or more than that of an ordinary semi-circular hook anchoring.

The criterion of deciding a size and thickness would be the following: a plate and surrounding concrete should not fail before a re-bar yields. For a reasonable and efficient design of an anchor plate under this criterion, it is necessary to inspect a behavior of pulling out PA bar and evaluate displacements and stresses of a plate and surrounding concrete. In this study, axisymmetric FEM analysis is applied and inspected.

As an example, a D22 PA bar was designed under the above-mentioned conditions.

The behavior of pulling out is shown in Fig.3. Test results of pulling out displacements of a D22 semi-circular hook and a PA bar are shown in Fig.4, as well as the analysis results. The analysis results agree well with the test results.

This design method gives a minimum size of a circular plate, which is necessary for anchoring re-bars.

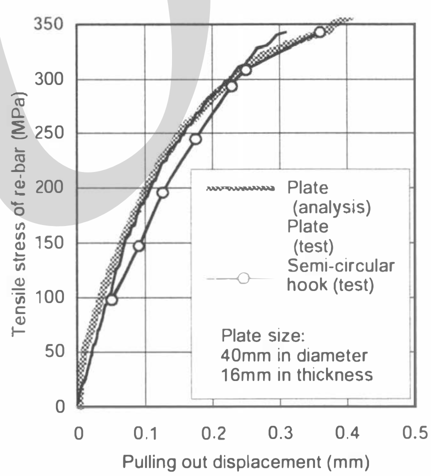

Fig.3 Pulling out displacement of anchor

3 EARTHQUAKE-PROOF PERFORMANCE

To evaluate PA bars' effects on member strength, a reverse cyclic loading test of a wall installed with both PA bars and semi-circular hooks was conducted. A shear re-bar has both an anchor plate and a semi-circular hook on both ends, so that the effects of PA bars can be evaluated with the same specimen.

Observing that the strength ratio of the final to the maximum is 0.72 for the semi-circular hook side, and 0.87 for the PA bar side, the drop of strength is lower on the PA bar side. The reason is a confinement effect by anchor plates of PA bars (see 3.2 (2)). The above proves that ductility of members with PA bars is greater than those with semi-circular hooks.

The specimen at the final displacement of 10 δ_y is shown in Fig.4. On the side of semi-circular hooks, the hooks came out of the surface, the horizontal re-bars loosened and core concrete behind re-bars fell down. On the other hand, core concrete did not collapse on the PA bar side. The above indicates that anchoring performance and confinement effect of PA bars is excellent and a PA bar is a better option than a semi-circular hook as an anchorage.

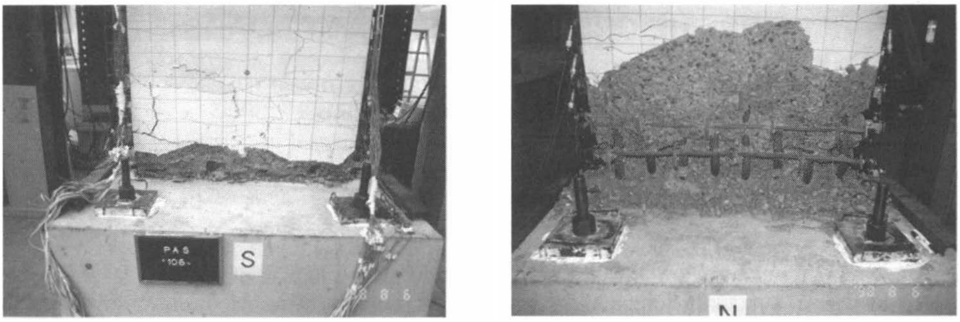

(a) PA bar side (b) Semi-circular hook side

Fig.4 Final conditions of specimen at the displacement of 10 δ_y

4. EFFICIENCY IMPROVEMENT IN CONSTRUCTION WORKS

(1) Slabs of an underground vertical tunnel structure

PA bars were used in top and bottom slabs of an underground vertical tunnel structure for shield machines. The top slab was 2.5m in thickness and the bottom slab was 3.0m in thickness. Because of highly dense re-bars U-shaped shear re-bars with semi-circular hooks were replaced with PA bars. A PA bar has a plate on one end and a semi-circular hook on the other end. The comparison of the periods of construction is shown in Table 1. It indicated that PA bars reduced 25% of the total construction period of re-bars.

Table 1 Efficiency improvement of construction (Ex1)

Total weight of re-bars	850 tons
Total construction period of re-bars w/ traditional shear re-bars (estimated)	48 days
Total construction period of re-bars w/ PA bars (practical)	36 days
Reduction of construction period	approx. 25%

Table 2 Efficiency improvement of construction (Ex2)

Total weight of re-bars	1,860 tons
Total construction period of re-bars w/ traditional shear re-bars (estimated)	210 days
Total construction period of re-bars w/ PA bars (practical)	166 days
Reduction of construction period	approx. 20%

(2) Walls and slabs of an underground railway station

PA bars were used in upper sidewalls, lower sidewalls, top slabs, middle slabs and bottom slabs of an underground railway station. Instead of pairs of U-shaped parts with semi-circular hooks on each end, PA bars were used so that the construction period should be reduced. A PA bar has a plate on one end and a semi-circular hook on the other end. In comparison to traditional U-shaped shear re-bars, it was estimated that the construction period of re-bars decreased 20%, as shown in Table 2.

5. CONCLUSION

In this study a design method of PA bars was presented and effects of PA bars on strength and ductility were discussed based on the results of numerical analyses and the reverse cyclic loading test of a wall. And efficiency improvement in construction works was discussed on examples of slabs and walls installed with PA bars. The conclusions are the followings:

(1) Design of PA bars can be done with an axisymmetric analysis of a pulling out test.
(2) It is not necessary to consider the effect of falling down of covering concrete outside plates in design
(3) PA bars have significant effects on confinement of concrete.
(4) Decrease of strength under reverse cyclic loadings is less with PA bars than with semi-circular hooks and PA bars improve ductility of concrete.
(5) PA bars improve significantly improve efficiency of construction of re-bars.

REFERENCES

[1] Japan Society of Civil Engineers: Standard specifications for concrete - Seismic design -, 1996 (in Japanese)
[2]Japan Road Association: Specifications for highway bridges - Seismic design -, 1996 (in Japanese)
[3] Nakamura, T., et al.,: Plate anchored shear reinforcement bars, Concrete Journal, Vol.36, No.9, 1998, pp.8-14
[4] Dilger, W. and Ghali, A.: Double-head studs as ties in concrete, Concrete International, No.6, '97, pp.59-66
[5] Dyken, T. and Kepp, B.: Properties of T-headed reinforcing bars in high strength concrete, Nordic Concrete Research, No.7, 1988, pp.41-51
[6] Nakamura, T. et al..: Applying plate-anchored shear reinforcing bars to highly dense reinforcement, Proceedings of JSCE 53rd Annual conference, VI-192, 1998, pp.384-385
[7] Japan Society of Civil Engineers: Standard specifications for concrete - Design -, 1996 (in Japanese)

STRENGTHENING OF HIGHWAY BRIDGES IN PERU WITH CFRP FOR THE CROSSING OF HEAVY LOADS

Jack López Acuña Jack López Jara
J.L. Ingenieros s.a. , PERU

Keywords: CFRP, reinforcement, strengthening.

1 INTRODUCTION

The problem of how to maintain in service existing concrete infrastructures has been always a challenge for structural engineers. In the case of bridges, the structural reinforcement responds to the need of keeping old structures compatible with new (usually more demanding) design specifications, to correct construction or design defects, or to allow the crossing of heavier and extraordinary loads.

For a long time the use of steel plates bonded to the concrete was considered an adequate procedure for the strengthening of concrete members. Several factors limit the use of steel plates. Some of those factors are: (1) The weight of the plates may make its installation difficult, and limit its use for long spans, (2) A considerable effort is needed to adapt the plates to the concrete surface, and (3) Due to potential corrosion / debonding problems, a regular maintenance is required.

In recent years the use of Carbon Fiber Reinforced Polymers (CFRP) has been established as one of the most promising methodologies in the field of structural rehabilitation of concrete structures. The inherent advantages of CFRP are: (1) Easy Installation, (2) Light weight, (3) Flexibility, (4) To be non-corrosive

2 BACKGROUND

This paper describes the process of strengthening a group of 13 bridges by externally bonding CFRP reinforcement. The bridges were retrofitted in order to allow the crossing of several trucks carrying heavy loads up to 173 tons (1698 KN), used for the construction of a hydroelectric plant in Aguaytia – Peru.

2.1 Structural Evaluation

The existing structures were designed according to the AASHTO specifications, using the HS-20 design load. Since no structural drawings were available, it was necessary to perform a detailed "in-situ" field inspection of the bridges. With the information collected, structural analyses, demand calculations and capacity checks were conducted. Reduction factors on the capacity calculations were used to account for the state of conservation of the structures. A detailed comparison between the capacity of the members and the maximum demands determined that 13 of a group of 22 bridges required reinforcement.

2.2 Structural Reinforcement

Several alternatives for the reinforcement of the structures were evaluated. The use of CFRP fibers was considered the best solution because it allowed to obtain a reliable design, its installation was relatively easy and permitted minimize the time of installation. CFRP strips were used for the reinforcement of the girders and CFRP sheets were used for the reinforcement of the slabs.

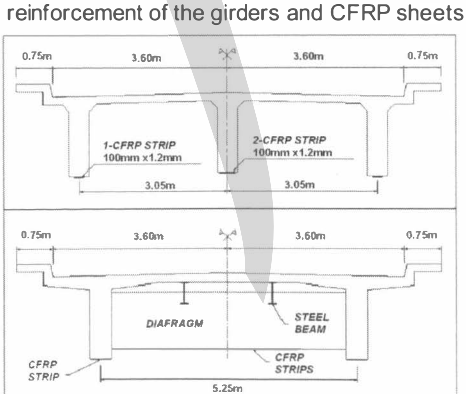

Fig.1 Typical Deck Cross Section after reinforcement

Fig.2 Crossing of Heavy Loads through a reinforced bridge

3 NON-LINEAR INELASTIC FINITE ELEMENT MODELING OF CONCRETE ELEMENTS WITH CFRP REINFORCEMENT

Finite element analyses were performed to study the behavior of the concrete deck of the bridges reinforced with CFRP strips. The program ADINA was selected for the analysis due to the capacity of this program to directly model the inelastic behavior of the concrete and the reinforcement steel, and also due to the option of this program to activate certain elements of the model at specific times during the analysis. This is an interesting feature of the program, which permits the generation of stress-free elements that can simulate the installation of CFRP sheets on an existing structure. Several types of elements were used to model the 3 fundamental components of the structure: concrete sections, steel rebars and CFRP strips.

Once the model was created, a time dependant analysis was performed in which the loads were applied as functions of time. The self-weight and superimposed dead loads were applied initially to the model, and after these loads were fully applied and the structure had deflected, the elements modeling the CFRP strips were generated on a stress-free condition at the bottom of the girders. The live loads were applied after the installation of the CFRP to ensure composite action only for live loads.

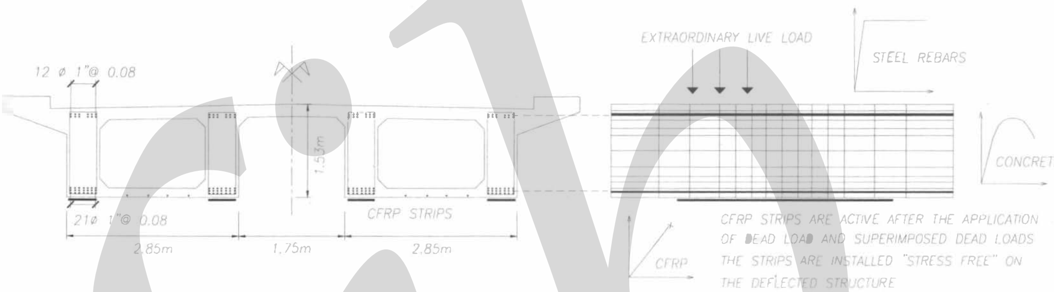

Fig.3 ADINA Modeling - Concrete Bridge Deck

4 APPLICATION OF THE CFRP REINFORCEMENT

It is extremely important to have a strict control of the process of placing the CFRP strips and sheets on the concrete surface. Prior to the application of the reinforcement, both concrete and CFRP surfaces should be carefully prepared to obtain an adequate bonding. For the concrete, large cracks and imperfections should be repaired. The substrate should be prepared and Pull-out tests should be conducted to verify an adequate strength of the concrete-adhesive interface. The temperature and humidity conditions at the site during the installation of the reinforcement should be carefully monitored, since a thin layer of water exuding from the concrete may negatively affect the performance of the adhesive material. Due to the especial conditions of the site (high temperatures and humidity) no CFRP reinforcement was placed unless the right conditions were present.

In the case of 3 bridges it was decided not to retrofit the structures because the deteriorated conditions of the surface and the poor quality of the concrete (as it was observed from in-field “Pull-Out” Tests). For these cases temporary false work was placed under the structures for the crossing of the loads.

5 PERFORMANCE OF THE REINFORCED STRUCTURES

It was possible to observe the performance of the retrofitted structures when trucks carrying a total load of more than 170tons (1,697 KN) crossed the bridges. During the crossing of the trucks a detailed control of deflections and displacements was performed. The observed deflections were very close to the values obtained from the FE analysis. No noticeable permanent deformations were observed. The structures returned to their original configuration after the loads were applied.

6 CONCLUSIONS

An application of CFRP for the strengthening of concrete bridges was successfully conducted. This method of reinforcement showed advantages due to its simplicity, reliability and easy installation. It was possible to evaluate the performance of the design when heavy trucks carrying loads of more than 170 tons (1,697 KN) crossed the reinforced structures without problems.

An evaluation of the structures after the crossing of the trucks showed no damages and no permanent deformations. This confirmed the adequacy of the CFRP reinforcement provided and validated the analytical studies and procedures performed prior to the application of the loads.

THE COLLAPSE OF THE KOROR BRIDGE

Man-Chung Tang, Chairman and Technical Director
T.Y. Lin International, San Francisco, USA

Keywords: bridges, long span bridges, prestressed concrete bridges, bridge failure, rehabilitation, creep and shrinkage.

1 INTRODUCTION

On September 26, 1996 the Bridge, which spans the Tongel Channel between the islands of Koror and Babeldaob, collapsed. Most part of the bridge fell into the channel causing two deaths and severed the connection between these two islands.

At the time of its completion and dedicated on April 26, 1977, the 790 ft (241m) long main span of the Koror bridge was the longest concrete bridge span in the world. It is located in a very remote area in the south Pacific, a US Trust Territory at that time.

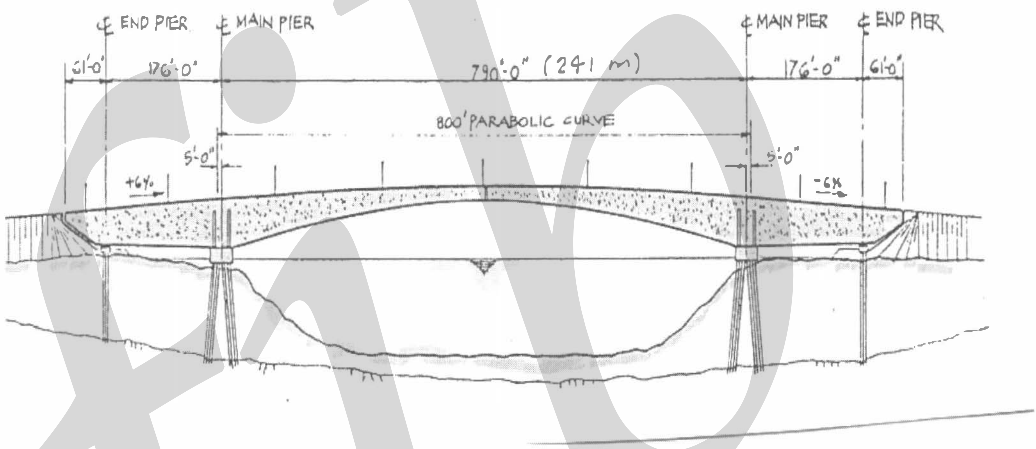

Fig. 1 Elevation of the Bridge

Due to the remoteness of the project location, low maintenance was of utmost importance. The main piers, being near the channel edges, were subjected to splashes from the waves and wind. Consequently it was prudent not to use any moveable bearing at the main piers. This lead to the use of monolithic connection between the superstructure and the piers.

Because the large span and the fixity of the main piers, it became obvious that a hinge at the mid-span was required to allow longitudinal movement due to creep, shrinkage and temperature changes. This was the reasoning behind the chosen structural system.

Therefore a box section was selected with a small overhang slab each side. The girder was 12 ft deep at the midspan and increased to 46 feet at the main piers. This deeper box was chosen for two reasons: to increase the stiffness of the box and to convey an appearance of an arch. The higher stiffness would reduce both elastic and plastic deflections. The cylinder strength of concrete used in the design was 5,000psi (34.4 Mpa).

The elastic deflection based on the original design was around 0.62 ft. (190mm) at the mid span. So even with a creep coefficient of 3.0, the ultimate long term deflection should be about 1.86 ft (570mm). However, much higher deformation was detected after several years. In 1985, eight years after completion, the bridge had deflected 850mm. By 1990 the deflection was found to have increased to 1030mm.

Tests found that the creep deformation was significantly higher than normal, due to unexplainable reasons. And the concrete was still creeping after over 10 years of loading, which was very exceptional. However, the conclusion was that the bridge was structurally sound and safe. The Authority decided to rehabilitate the structure. A contractor initiated rehabilitation scheme was less expensive and was used to repair the dip. This scheme introduced two major changes to the structure:

1. It froze the mid span hinge and made the bridge continuous after pushing the two halves of the bridge apart by a large force, and
2. It added a substantial amount of longitudinal posttensioning running from one end to the other end of the bridge, draped in the area of the mid span.

About two months after the rehabilitation was completed, the bridge collapsed into the water.
Subsequent calculation showed that the rehabilitation added a significant amount of compressive stresses in the top slab. Because there were many layers of prestressing tendons in the top slab, the concrete underneath the tendons may be weaker. In the original design, this was not important because the compressive stress was very low. The high compression induced by the rehabilitation created expansion in the vertical direction of the slab, thin layers of concrete may have formed under this effect and creep effect. After the top slab delaminated into thin layers of concrete, it could not resist the high compression force and buckled. The effect of creep explained why there was a delay of two months after completion of the rehabilitation before it failed.

2 POSSIBLE FAILURE MECHANISM

Based on the above observation, the failure mechanism appears to be as follows:

1. After the top slab of the girder above the Babeldaob main pier had buckled, the cross section would not be able to resist the bending moment at this location. With the top slab failed, the axial compression in the web increased significantly and might have caused them to either buckle or crash as evidenced by the overlapping of the web plate at this area.
2. After the webs at this location failed, the combined action of compression and shear crushed the bottom slab at the Babeldaob pier.
3. The buckling and crush caused a release of the bending moment at this location.
4. This release of bending moment transferred load of bridge towards the Koror side. This increased the negative bending moment in the girder at the Koror main pier. This caused the main span to bend downward thereby lift up the Koror end span. The tie downs at the end pier and the ballast had provided a safety factor of 1.50 against overturning of the main pier so the bending moment must have increased much more than 50%.
5. The increased bending moment in the girder at the Koror main pier caused the bottom slab at that location to crash. The crash of the bottom slab in turn relieved the bending moment at this point.
6. With less bending moment at the main pier, the Koror end span fell back down and hit the end pier. This impact caused the double punching shear failure of the girder at this location. This explains the vertical dislocation of the girder at both sides of the end pier.
7. At the same time the main span became a simple beam spanning between the main piers with some residue bending moment at both ends. This increased the positive bending moment in the girder way over its capacity. The girder did not have the capacity to carry its own weight through such a structural system, so it bent down, causing many large vertical cracks starting from the bottom slab, and fell into the water.
8. By impact with the water and the channel bed, the bottom of the girder cracked up in longitudinal pieces.
9. As the girder bent downward, the continuous tendons had to elongate locally and created high uneven forces at the two sides of a deviator. This force could rip a deviator off the girder.

Most relevant information about the collapse was sealed after some court cases. But the failure mechanism described above appears to be able to explain all damages observed in the bridge after the collapse.

THE STRENGTHEN METHOD BY CARBON FIBER SHEETS FOR R.C. SLABS OCCURRED FATIGUE DETERIORATION

Koichi Sugioka, Shigeru Matsumoto,
Hanshin Expressway Public Corporation
Osaka, Japan

Kazuhiro Kuzume
Kokusai Structural Engineering Corp.
Osaka, Japan

Keywords: reinforcing, carbon fiber sheet, reinforced concrete slab, fatigue, infrared thermography

ABSTRACT

Hanshin Expressway Public Corporation (HEPC) had been repairing reinforced concrete slabs showing deterioration from fatigue by bonding steel plates to the slabs with epoxy resin. Recently, however, studies have been in progress on the use of carbon fiber sheets which provide reinforcing effects without increasing dead load of superstructures.

This paper firstly describes a design method for reinforcing slabs with carbon fiber sheets contemplated based on fatigue tests and their analysis results. Further, the applicability of nondestructive testing by an infrared thermography system as a technique for maintenance after reinforcing is also undergoing study.

1 SELECTION OF REINFORCING METHOD

At the HEPC the standard procedure is to adopt the epoxy-bonded steel plate method as the reinforcing method for RC slabs of old design or which show deterioration exceeding a certain level.[1)] However, when it is difficult to apply the epoxy-bonded steel plate method because of cramped space or when the increase in dead load due to addition of steel plates will have adverse effects on the entire bridge system, adoption of the CF sheet bonding method is permitted for strengthening RC slab of low degrees of damage.

When reinforcing with CF sheets, the number of CF sheets in principle is one layer for slabs of thickness 17 cm or more designed after August 1970. In this case, one sheet bonded in the direction perpendicular to the bridge axis and one sheet in the direction of the axis are considered as one layer.

Since in reinforcing a slab the CF sheet's crack inhibiting effect will be of importance, a high-elasticity type is made the standard, with the tensile Young's modulus to be not less than $(39\pm 2.9)\times 104$ N/mm^2, the tensile strength being a reference value.

Further, the filament weight of a CF sheet is taken to be 300 g/m^2.

2 EVALUATION OF RC SLAB FATIGUE DURABILITY BY TRAVELING WHEEL LOAD TESTING APPARATUS

Test results may be summarized as follows:

(1) With the CF sheet bonding method, ample improvement in durability is obtained with only a small number of reinforcing layers.

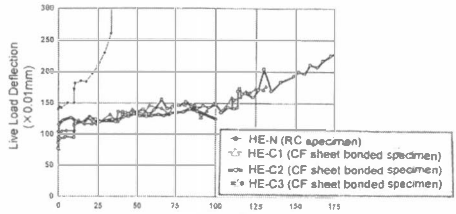

Fig.1 Deflection from Live Load at Span Center

(2) The efficient quantity of reinforcing sheets is one layer each in the main reinforcing bar direction and the distribution bar direction.

3 REINFORCING EFFECT OF CF SHEET BONDING METHOD

Considering single-layer reinforcing, comparisons were made of Model B assuming a high-strength type for the CF sheet and Model D assuming a high-elasticity type, and the results are shown in Figs.2 and 3. It may be judged from these results that the high-elasticity type has restraining effects on both deflection and crack opening quantities. Furthermore, when the fact that failure due to rupture of CF sheet was not produced even when using high-elasticity type, it may be judged using the high-elasticity type rather than the high-strength type will have a greater effect of restraining growth of cracking and is more desirable.

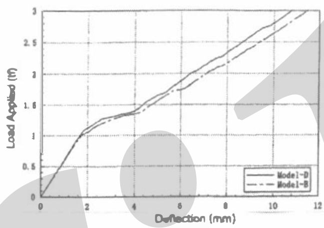

Fig. 2 Comparison of Deflections (Analytical Values of Models B, D)

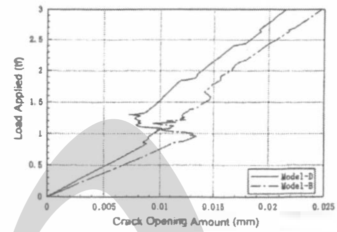

Fig.3 Comparison of Crack Openings (Analytical Values of Models B, D)

4 EXAMINATION OF INSPECTION TECHNIQUES IN MAINTENANCE

At the HEPC, sophistication of inspection techniques is aimed for in order to achieve rational maintenance of concrete structures, and expectations are rising with regard to infrared thermography as an approximate inspection method.[2)] The infrared thermography system is easily affected by weather and meteorological conditions, and insolation on and soiling of the structure so that it is desirable for an evaluation system to detect changes including relations with the observation environment and detected temperature resolving power to be built up.

5 CONCLUSIONS

The fundamental matters concerning the method's design and related maintenance examined through tests and analyses are summarized as follows:

(1) The carbon fiber sheet bonding method provides ample improvement in durability with the minimum number of sheets for reinforcement, and the most efficient number is one layer each in the main reinforcing bar and distribution bar directions.
(2) It is more effective and desirable to use carbon fiber sheets of high elasticity rather than high strength to restrain growth of cracks.
(3) It is advisable for the reinforcing effect of carbon fiber sheet bonding to be evaluated focusing on deflection of the slab, and design of the number of sheets to be bonded may be determined so that the slab deflection ratio will be within the range of allowable values.
(4) For improving detecting accuracy of the infrared thermography system as a detection technique for maintenance, it is necessary to build a system capable of quantitatively evaluating the relationships with the observation environment and detected temperature resolving power.

REFERENCES (IN JAPANESE)

1) Hanshin Expressway Public Corporation: Investigation and Study Work Report Concerning Soundness of Concrete Structures, Mar.1982
2) Hanshin Expressway Public Corporation: Outline of Nondestructive Testing in Construction and Maintenance of Urban Expressways, Rikoh Publications, Jan.2000

STUDY ON IMPACT RESISTANCE OF PC BEAMS WITH BUFFER LAYER MADE OF DUCTILE FIBER REINFORCED CEMENTITIOUS COMPOSITES

Keitetsu Rokugo, Minoru Kunieda
Department of Civil Engineering
Gifu University, JAPAN

Hiroshi Sakai, Masahiro Suzuki
P.S. Corporation
JAPAN

Keywords: impact resistance, PC beams, DFRCC, drop-weight tests

1 INTRODUCTION

In this study, drop-weight test with gradually increasing drop-height was adopted to evaluate the impact resistance of steel fiber reinforced concrete PC beams. The specimens with buffer layer made of Ductile Fiber Reinforced Cementitious Composites (DFRCC) were also investigated through the fracture behavior focusing on the size of local damaged concrete (i.e. cracks, spalling of concrete portions). One of DFRCC named Engineered Cementitious Composites(ECC)[1] was applied for the buffer layer of PC beams subjected to impact loads.

2 OUTLINE OF IMPACT TESTS

Three kinds of members were used: prestressed concrete beams (PC), PC beams reinforced with short steel-fibers (SF-PC), and SF-PC with buffer layer made of ECC. The fiber content in the SFC was about 1.0% of the concrete by volume.

Water to cement ratio of ECC was 30%, and the Polyethylene fiber having the diameter of 0.012mm and length of 12mm was used. Fiber content was 1.5% by volume. Two levels of prestressing in concrete were prepared: 6MPa and 12MPa. The size of specimen was 200×200×3,000mm (height ×width×length).

A repeated impact drop-weight test with increasing drop-height was used, as shown in Fig. 1. The drop-height was initially set at 100mm, and increment of 100mm was given at each impact. When the displacement of the beam specimen after striking of the drop-weight (residual displacement) exceeds the value of 20mm, the loading was terminated.

3 APPLICABILITY OF ECC TO BUFFER MATERIAL AGAINST IMPACT LOADING

As for the most beam specimens reinforced with short steel-fibers, the impact resistance became higher than that of PC6 specimen. Especially, the maximum impact reaction force in SF-PC6 was highest in all series. For SF-PC12, it seems that too much prestressing increased the localized damage in concrete. It can be concluded from this study that the proposed impact testing method with increasing drop-height at increment of 100mm was efficient for the evaluation of relative impact resistance of PC beams.

Figure 2 shows the crack patterns of each specimen with buffer layer. The global failure behaviors of both specimens were originated from the delamination of the buffer layer at ultimate stage. However, using the buffer layer imparted the impact resistance to the specimen through reducing both the local damaged part struck by the drop-weight and tensile cracks due to bouncing out of the specimens. As shown in Fig. 2, only the crack located at the center of the specimen propagated after occurring the delamination of the buffer layer in SF-PC6-buffer (pre-cast) specimen. However, SF-PC6-buffer (placing) specimen exhibits many

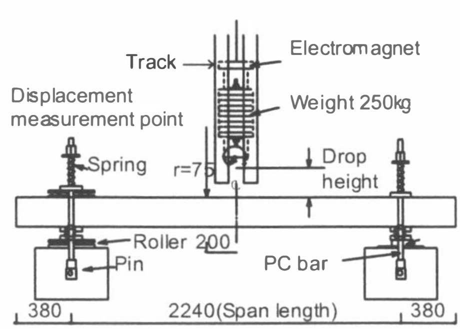

Fig. 1 Test setup

cracks, in which the length of each crack was almost the same, and has large deformation capacity.

In impact reaction force-maximum displacement relations as shown in Fig. 3, the maximum impact load and ultimate displacement of SF-PC6-buffer (placing) became larger than those of SF-PC6-buffer (pre-cast). It became clear from these tests that the bond properties at interface between the buffer layer and substrate was important and should be improved in order to utilize ECC for buffer layers.

Drop height (m)	SF-PC-buffer (placing)	SF-PC-buffer (pre-cast)
0.5	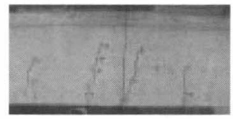	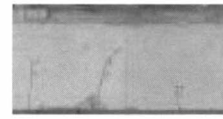
1.0	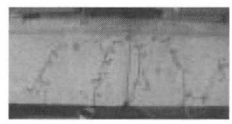	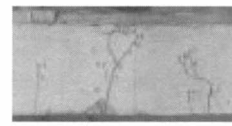
1.5		 (1.4m)

Fig. 2 Crack patterns of specimens with buffer layer

4 CONCLUSIONS

The PC beams reinforced with short steel-fibers were developed, and tested through "repeated impact drop-weight test" to evaluate their impact resistance. And also, ductile fiber reinforced cementitious composite (ECC) was applied to the buffer material against impact loading. The following results were obtained:

(1) The reinforcing with short steel-fibers imparted the impact resistance to PC concrete beams. However, too much prestressing increased the localized damage in concrete. There would be a best combination between the steel-fiber content and the amount of prestressing.

(2) The proposed impact testing method with increasing drop-height at increment of 100mm was efficient for the evaluation of relative impact resistance of PC beams.

(3) Using buffer layer made of ductile fiber reinforced cementitious composite (ECC) was effective method to reduce the spalling of concrete portions.

(4) The failure behaviors of both specimens with buffer layer were originated from the delamination of the buffer layer itself. However, the difference in crack patterns and impact reaction force-displacement curves related to the bond properties at interface could be observed. The bond properties at interface between the buffer layer and substrate was important and should be improved in order to utilize ECC for buffer layers.

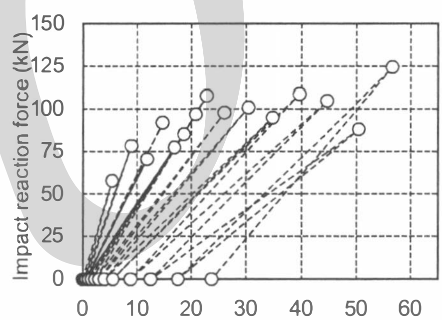

(a) SF-PC6-buffer(placing)

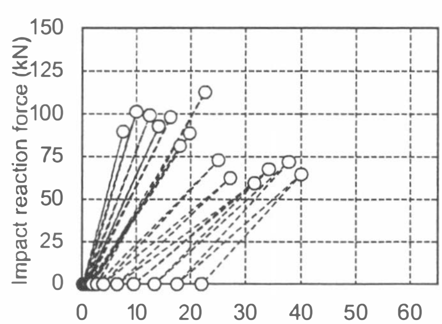

(b) SF-PC6-buffer(pre-cast)

Fig. 3 Relationship between impact reaction force and maximum displacement at each impact

REFERENCES

[1] V.C. Li and T. Kanda: Engineered Cementitious Composites for Structural Applications, ASCE, J. Materials in Civil Engineering, No.10, Vol. 2, pp.66-69, 1998

DESIGN AND CONSTRUCTION OF THE REINFORCEMENT FOR THE SUPERSTRUCTURE OF THE IWABUCHI BRIDGE (RAPID RETROFIT UTILIZING A WATERJET AND ARAMID FRP RODS)

N. Ando
Sumitomo Construction Co., Ltd., JAPAN

M. Kuroyanagi
Japan Highway Public Corporation, JAPAN

K. Kondo
M. Kameyama
Sumitomo Construction Co., Ltd., Shizuoka office., JAPAN

Keywords : Aramid FRP rod, waterjet, retrofit

1. INTRODUCTION

The Iwabuchi Bridge is a three-span post-tensioning T-girder bridge located at the crossing of the Tomei Expressway and Tokaido Shinkansen railway in Shizuoka prefecture. In 1998, its girders were made continuous using external cables to handle the increased live load. Although the bridge crosses the Tokaido Shinkansen railway, it was only equipped with guardrails, sound barriers and a safety net. During this construction, the guardrails were replaced with concrete barrier curbs to ensure traffic safety and new girders were added outside of the existing exterior girders to support the increased weight caused by the addition of the concrete barrier curbs and enlargement of the sound barriers.

Prefabricated precast girders were used for the reinforcement girders and the construction was performed using cranes positioned on the bridge slab. The reinforcement and existing girders were combined by Aramid FRP rods, with the holes for the latter being drilled using a waterjet.

The construction was completed successfully despite the many restrictions imposed by the need to protect traffic on the Tomei Expressway and Shinkansen railway, the emphasis on night-time working, and power to the rails only being removed for a few hours each night. This paper details the design and construction of a new structure that is consolidated with the existing bridge by focusing on the use of waterjet and Aramid FRP rods.

2. OVERVIEW

The reinforcement girders were combined with the existing girders using cross beams. Since they were close to the overhead wiring of the Shinkansen tracks, they were joined using nonconductive Aramid FRP rods. Photo 1 shows the

Photo 1 Bridge overview

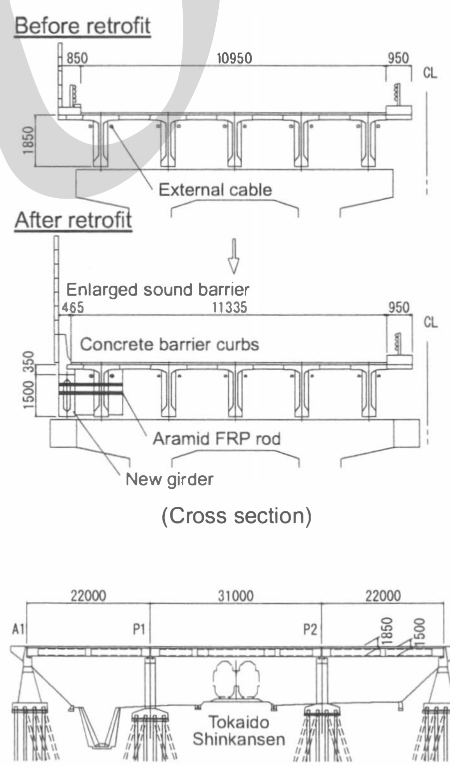

Fig. 1 General diagrams

bridge overview and Fig. 1 shows the general diagrams.

3. DESIGNING THE SUPERSTRUCTURE

3.1. Designing the main girder

The existing bridge was a thirty-five-year-old T-girder bridge utilizing a post-tensioning system and creeping and drying shrinkage of concrete had settled. Therefore, it was decided to allow the reinforcement girders to age for 180 days to minimize the effect of the restraining force by allowing creeping and drying shrinkage to occur prior to construction. Also, as the girders were to be erected in three steps, structural variation was taken into account in the design.

3.2. Designing the cross beam

The Aramid FRP rods were used as tendons. Due to its lightness, high strength and excellent corrosion resistance, Aramid FRP rod was a more appropriate material than steel rebar for the Iwabuchi Bridge. It excelled in the following areas:

(1) As it did not conduct electricity, it was unaffected by the adjacent high-voltage overhead wiring of the Shinkansen tracks.

(2) It's lightness provided excellent workability within the narrow girder, eliminating the need for heavy equipment and special scaffolding.

(3) It's excellent corrosion resistance and compatibility with concrete enabled pretensioning (bonding) without anchorage elements. These qualities also allowed smooth surfaces over the filled-in tendon holes.

4. CONSTRUCTION OF THE SUPERSTRUCTURE

4.1. Erecting the reinforcement girders

A total of six girders had to be erected within Tomei Expressway's nighttime road closure schedule and outside the operating and maintenance hours of the Tokaido Shinkansen railway, and so the working hours were extremely limited.

4.2. Drilling the cross beams

The reinforcement and existing girders were joined using Aramid FRP rods. Core drilling for the cross beams carried a high risk of cutting the steel rebar or stirrups, which were dense there. Therefore, the location of the steel was determined radiographically before drilling and the waterjet method was used for those sections. Fig. 2 shows the waterjet drilling procedure.

4.3. Installing the Aramid FRP rods

The Aramid FRP rods were inserted into the existing girders and side beams and attached to the steel anchorage elements. Then, the pedestals were fitted to apply tension. Fig. 6 shows the installation procedure for the Aramid FRP rods and Photo 3 shows an Aramid FRP rod and an anchorage element.

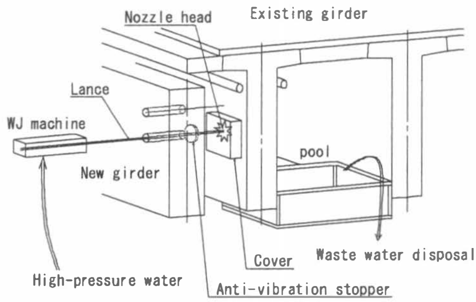

Fig. 2 Waterjet drilling procedure

(1) Constructing the joint cross beam
Drilling the existing girder

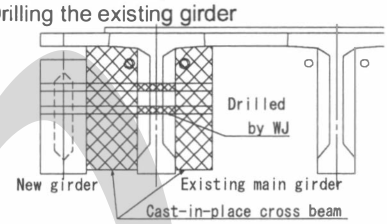

(2) Applying tension to the Aramid FRP rods
Pedestal installation / Tensioning / Grouting

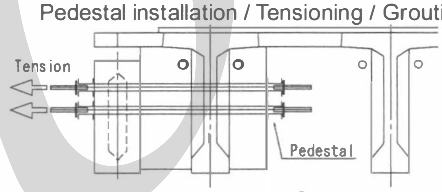

(3) Post treatment
Cutting Aramid FRP rod / Trimming

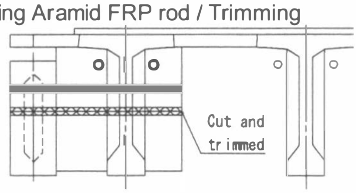

Fig. 3 Installation procedure of Aramid FRP rod

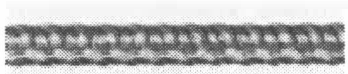

Aramid FRP rod (ϕ7.4)

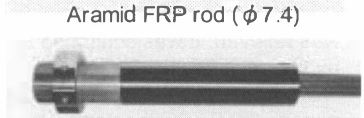

Anchorage element

Photo 3 Aramid FRP rod

BASIC ELEMENT TESTS OF REINFORCED CONCRETE CONTAINMENT VESSEL WITH ANTI-PLANE PRESSURE

Naohiro Nakamura[3)] Yasumi Kitajima[1)] Makoto Fujii[2)] Masahiro Sugata[3)]
Atsushi Kambayashi[3)] Naoto Yabushita[3)]
1) Nuclear Power Engineering Corporation, Japan 2) Toshiba Corporation, Japan
3) Takenaka Corporation, Japan

Keywords: RCCV, liner, anti-plane pressure, loading experiment, non-linear analysis

1 INTRODUCTION

Reinforced concrete containment vessels (hereafter referred to as RCCV) used in reactor buildings of ABWR nuclear power plants are important structures for the prevention of the leak of radioactive materials in the case of an accident. The RCCV is designed with a satisfactory safety margin for design basis accidents such as the loss of coolant accident. However, in cases where an accident exceeding the design basis accident (the severe accident) occurs, it may well be that the inner pressure in the containment vessel will increase to a value higher than that for the maximum serviceability pressure.

Therefore, this experiment aims at understanding the characteristics of the basic structural behavior for the RCCV by exerting both the anti-plane pressure equivalent to the inner pressure and the tension load corresponding to the hoop tension simultaneously on the specimen made simulating the vicinity of the opening. Furthermore, an evaluation method as well as modeling technology is studied carrying out simulation analyses for the experiment results.

2 OUTLINE OF EXPERIMENT

Fig.1 shows the structural outline of the RCCV and the simulated part for the specimen. The vicinity of the opening is one of the most critical elements with regard to the pressure resistance limits for the RCCV. Therefore, a 1/2-scale specimen was made as a rectangular parallelepiped simulating the vicinity of the opening. Five different test specimens were made using variable of the three items; anti-plane pressure, flat bar and distance of liner and anchor. Table 1 shows the list of the parameters and the specimens. As representative specimens, the shapes, dimensions and element names of No.2 and No.5 each of which is equipped with a flat bar are illustrated in Fig.2.

Fig.3 shows the photograph of the loading setup for the experiments.

3 TEST RESULT

Fig.4 illustrates the relationship between tension load and axial displacement for all specimens. The yielding load for specimens No.2 and No.5 both of which are equipped with flat bars is slightly larger than that for the other specimens without a flat bar. Except for this, the load-displacement relationships for all specimens were nearly similar to each other. Fig.5 illustrates the final cracking conditions for specimen No.1.

4 SIMULATION ANALYSIS

Fig.6 illustrates the analysis model utilized. Fig.7 shows the comparison between experiment and analysis values with regard to the load-displacement relationship for specimen No.1. Fig.8 shows the comparison of deformation between experiment values and analysis values for liners and liner anchors for specimen No.1. The analysis values correspond almost well to the experiment values.

5 CONCLUSION

- In the specimen with anti-plane pressure, strain concentration occurred between the taper and the first liner anchor (the experimental area). However, tearing did not occur due to the fact that strain concentration was relieved by concrete cracks occurring in the proximity of the liner anchors.
- Tearing in the experimental area of the liner in specimens without anti-plane pressure did not occur. This is so because the liner anchor separated toward an anti-plane direction and strain concentration was relieved. It was confirmed from these experiments that the separation of a liner anchor is caused by the eccentricity of a liner and that anti-plane pressure can restrain this separation.
- With regard to specimens No.2 and No.5 equipped with flat bars, strain concentration occurred on experimental area located on the extended line of the flat bar and that tearing occurred eventually.
- It was confirmed from the simulation analyses that the behavior obtained from these experiments can almost be simulated.

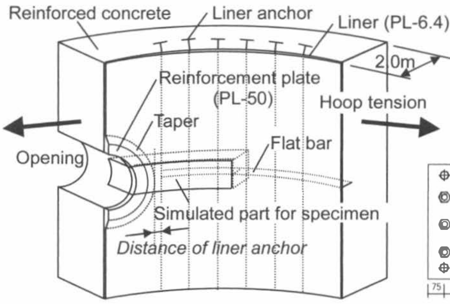

Fig.1 Configuration of RCCV and simulated part for specimen

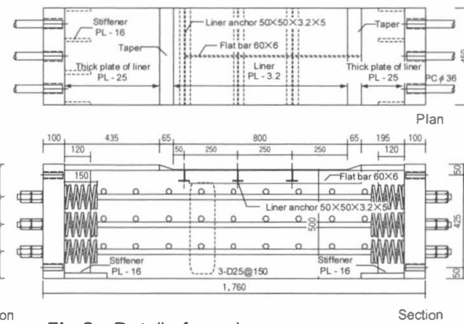

Fig.2 Detail of specimen

Table 1 Parameters and specimens

Specimen	Parameter: Anti-plane pressure	Parameter: Flat bar	Parameter: Distance of liner anchor	Loading pattern
No.1	Yes	No	50	p_2, P_1, P_1
No.2	Yes	Yes	50	p_2, P_1, P_1
No.3	Yes	No	100	p_2, 100, P_1, P_1
No.4	No	No	50	P_1, P_1
No.5	No	Yes	50	P_1, P_1

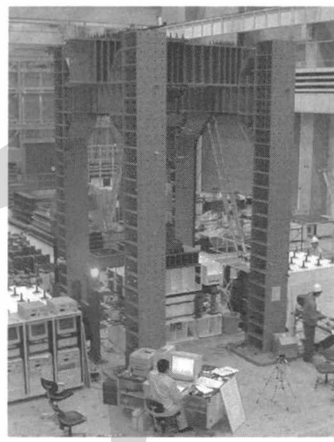

Fig.3 Loading setup

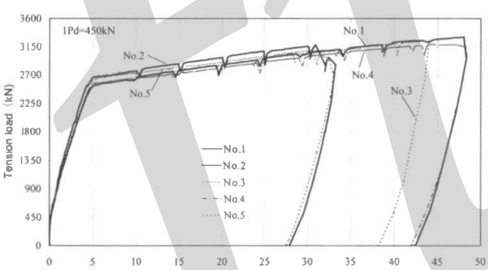

Fig.4 Load-displacement relationship

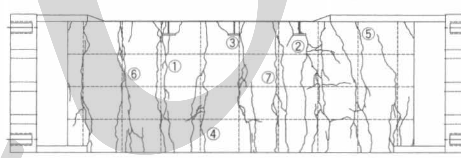

Fig.5 Crack patterns of specimen No.1

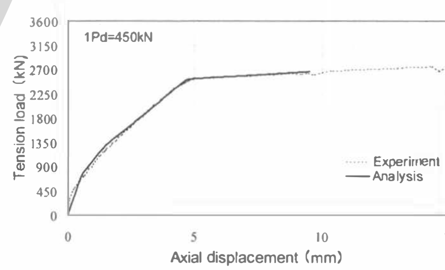

Fig.7 Comparison of load-displacement relationship between experiment and analysis (specimen No.1)

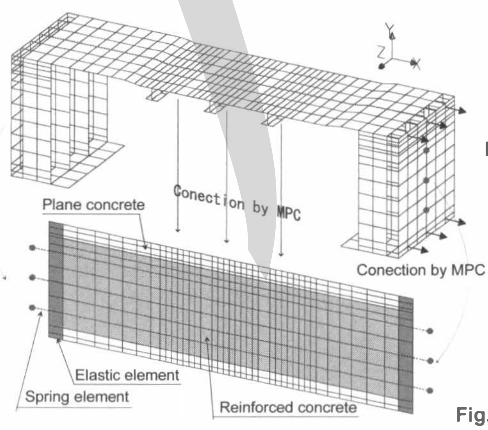

Fig.6 Analytical model

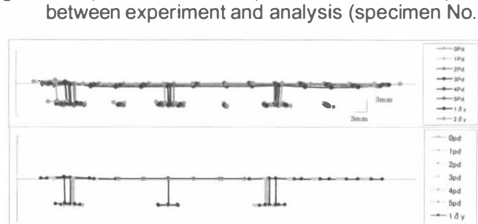

Fig.8 Comparison of deformation of liners and liner anchors between experiment and analysis (specimen No.1)

INSPECTION OF REINFORCED CONCRETE STRUCTURES, USING "THE HEIGHT ELEVATION INSPECTION VEHICLE"

Nozomu Hirabayashi Hiroshi Ueki Naomi Tamura
Technology Center of Metropolitan Expressway, JAPAN

Keywords: Inspection, High Elevation Inspection vehicle, pole

1. FOREWORD

We conduct visual checks of concrete structures of urban expressways for the purpose of quickly detecting deformities in them. From a point directly underneath a bridge, however, it is difficult to make a visual check of places that come within a dead angle due to the existence of the crossbars of a bridge pier or an attachment, etc., to the bridge.

Moreover, the space under an elevated structure of an expressway in Tokyo is usually limited, and there are places where enough of an inspection cannot be made by using an ordinary manned high-ranger maintenance truck.

The high-elevation inspection vehicle (**Fig. 1**) to be introduced here is a tool that makes inspections of bridge parts that are in dead angles, such as supports and slabs' under-surfaces, possible and easy by remote control from the ground.

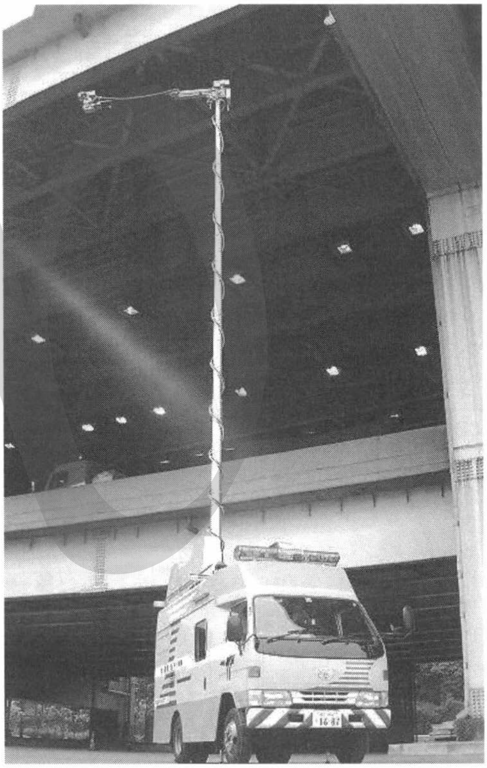

Fig. 1. The high-elevation inspection vehicle (with the pole extended)

2. OUTLINE OF THE SYSTEM

The high-elevation inspection vehicle must be compact so that it can be operated in small spaces, such as the space underneath an elevated expressway. For this reason, we structured one using a 2-ton truck's chassis as the basis.

The inside of the vehicle consists of three spaces: the driver's cab, the operating room and the storage space. In the operating room, there is a remote-controlling mechanism for the high-elevation inspection system, an image monitor and a recorder. A single operator conducts the checks here. In the storage space, there is the high-elevation inspection system and an electric power generator. Besides, there is a space to store such things as collar cones.

The high-elevation inspection system borne on the vehicle consists of a multi-stage expansion pole that can be stretched up to 15 meters from the ground surface, a horizontal arm that can be stretched to 3 meters from the apex of the pole and a camera mounted at the end of the horizontal arm.

3. CHECK BY A HIGH-ELEVATION INSPECTION VEHICLE

Usually, concrete structures are checked visually from a distance. But the ends of girders and the supports, which are important parts to be inspected, are hidden behind the piers or girders. Here we will explain the inspection of the supports, where the high-elevation inspection vehicle displays its strength, and the slabs, which are dark due to the existence of equipments.

3.1. Inspection of supports

Because the supports above the piers are invisible from under an elevated structure, the arm is elevated to the height of the support and lit up (**Fig. 2**). As a result, inspection of the entire supports by means of the inspection camera becomes possible (**Fig. 3**). By using the zoom mechanism, it is possible to capture the details of the supports and detect abnormalities, such as cracks

3.2. Inspection of a slab

Fig. 4 shows a slab being checked. Because slabs exist in a dark place, the camera is elevated through cross beams and brought nearer to a slab's surface, and is rotated by 90 degrees upward, and the object to be inspected is lit up. **Fig. 5** shows an image taken by a camera. When it is difficult to distinguish between a crack and a pattern, an enlarged picture is taken by zooming in on the target, and then judged.

Fig. 2 Inspection of a support

Fig. 3 Image of a support given by the inspection camera

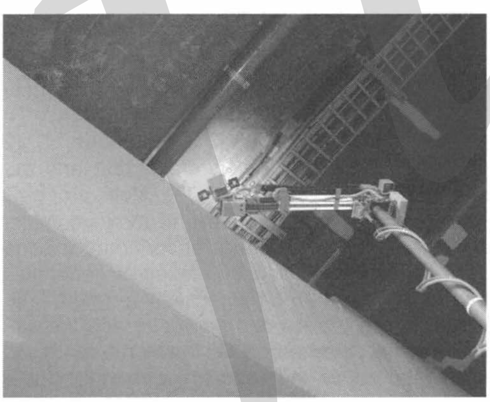

Fig. 4 Checking a slab

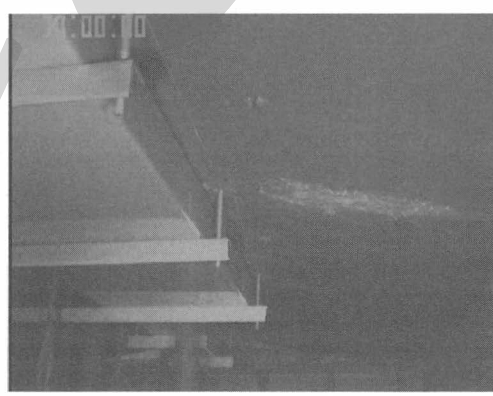

Fig. 5 Image of a slab from the camera

4. CONCLUSION

The inspection system introduced here displays its strength particularly in a spot inspection in an emergency. In the recent examination, the operability has been improved and the adaptability to diverse conditions under which the system is used has been increased, and the system has acquired characteristics that make it suited to inspections of a higher efficiency. We want to improve its functions furthermore through actual measurement.

SAFETY REDUCTION OF R.C. STRUCTURES DUE TO REBAR CORROSION

Z. Rinaldi
Università di Cassino
Cassino (FR), ITALY

C. Valente
Università "G. d'Annunzio"
Pescara, ITALY

L. Pardi
Autostrade S.p.A
Roma, ITALY

Keywords: corrosion, residual strength, residual ductility, experimental tests, concrete beams.

1 INTRODUCTION

Corrosion is one of the most common causes of deterioration of r.c. structures. It weakens the mechanical and geometrical characteristics of both steel and concrete and their bond and affects the serviceability and ultimate condition of r.c. members. Beams designed for obtaining a flexural failure can show shear collapse for certain level of rebars and stirrups corrosion and, similarly, ductile designed members can experience brittle failure when pitting localizes strains [1]. Aim of the paper is to contribute to the evaluation of the residual safety ranges of corroded r.c. structures by setting up theoretical models validated against experimental results. The study is part of a larger research, funded by Autostrade SpA, aiming at providing a rational approach for assessing the residual life of bridge grillages affected by reinforcement corrosion. A proper numerical model is used to carry out a large parametric investigation to evaluate the sensitiveness of strength and ductility to the different effects of the corrosion attack. The results are exploited to design sound and corroded beams able to experience different failure modes depending on the effects of the chemical attack for different damage levels. These elements are then realised, corroded and subjected to experimental tests. The results are used within comparative analyses in order to validate the proposed theoretical models.

2 SIMULATION AND TESTS OF CORRODED BEAMS

Conventional theoretical models have been revised and adjusted to incorporate corrosion effects in terms of steel strength and ductility reduction and of the concrete damage and cover delamination. A fibre model has been used for the analyses to find out where the collapse conditions change from steel to concrete failure. Each corrosion effect was analysed in its own and then they were all combined together. The load has been increased up to failure and the response curves constructed according to prefixed corrosion levels in the range 0% (sound) - 100% (max assumed corrosion). The following effects have been considered, according to the main assumptions in the literature [1], [2]: diameter reduction of the longitudinal reinforcement (max = 12.5%); diameter reduction and step increase of the transverse reinforcement (max = 25% and 50%); variation of the steel properties (max = 10% ε_{su} decrease, 16.7% σ_{su}/σ_{sy} decrease); concrete cover reduction (max = complete delamination). In this paper the study has been restricted to bending mode failures for both the sound and the corroded beams and the relevant results have been summarised by means of generalized load–displacement diagrams [1]. An average loss of about 30% and 65% respectively for the bearing capacity and for the member ductility is detected depending on the section geometry and the steel percentage. These results agree with the available experimental data reported in the literature [3].

An experimental program has been set up to validate the above theoretical model and 21 beam specimens have been designed accordingly and chosen, among other requirements, to have comparable results with similar specimens reported in the literature, Fig. 1. The longitudinal and transversal reinforcement has been designed to get always flexural failure when testing the sound beams and to get flexural or shear failure when testing the corroded beams. All the beams have identical geometry, steel reinforcement and concrete mix, so that they differ from one another only for the different corrosion patterns and levels and the test conditions. The maximum assumed corrosion level corresponds to a 12.5% loss of steel mass. In order to get working flexibility and to check the results repeatability, the beams have been collected in 7 different groups of 3 beams each. Presently, only the first group has been completely realized and tested.

The three beams tested relate to 3 limit conditions: (1) sound beam S_t; (2) beam with maximum corrosion C_{t100}; (3) beam corroded at the cracking limit state $C_{t,cr}$. The corrosion was artificially induced using a properly selected current density, but no provisions were taken to control the corrosion distribution among the longitudinal and transversal reinforcement, that is corrosion could spread freely resembling on site "uncontrolled" conditions. The material adopted, concrete mixture and steel of the rebars, comply with the standard materials used for bridge construction. The beam specimens are tested according to a 4PBT. The applied load, the strains at midspan and the vertical displacements are measured to monitor the beam behaviour. Each test is composed by a sequence of 4 static loading cycles: (1) cracking load L_{cr} ; (2) intermediate load L_i ($L_i = 2L_{cr}$ and about 1/3 of L_y); (3) yield load L_y; (4) ultimate load L_u .

3 RESULTS

At the end of the corrosion process the C_{t100} beam presented a single longitudinal crack and an extended delamination of the concrete cover. The longitudinal tensile rebars were uniformly, yet slightly, corroded whereas the stirrups were subjected to a strong pitting attack that led in several cases to a total consumption of their section. The C_{tcr} beam showed cracking initiation for very low values of the corrosion attack ($\approx 50\mu m$) well comparable with literature data [2]. The experimental results indicate a certain similarity of the response between the sound S_t and the corroded C_{t100} beams, as a direct consequence of the corrosion attack experienced by beam C_{t100}, Fig. 2. The monotonic response up to L_{cr} ($\approx$ 27 kN), do not show large stiffness variations between S_t and C_{t100} notwithstanding the delamination. As the load is increased up to the L_i ($\approx$ 54 kN = 2 L_{cr} and about 1/3 of L_y) level an unexpected small stiffness drop of the S_t beam is observed. However, this drop is apparent since it is related to the different loading rates adopted for the two tests: ratio 1 to 3 between S_t, (slow test) and C_{t100} (fast test). This aspect should constitute a matter of careful consideration and calls for a standardization of these type of tests. At higher load levels, L_y ($\approx$ 135 kN), the unloading - reloading cycles still no remarkable differences in stiffness between the two beams. The S_t beam approaches the yield limit more gradually than the C_{t100} beam where a sharper transition is observed for the first loading branch it can hence be argued that the sound beam is capable to better distribute the state of stress. No such distinction is yet observable for the subsequent loading cycles. The yield limit of the S_t beam is slightly greater than that of the C_{t100} beam, about 2%, but no difference is detected for the ultimate capacity, case in which the C_{t100} beam presents a more regular behaviour. The present results, do no allow to draw definite statements concerning ductility.

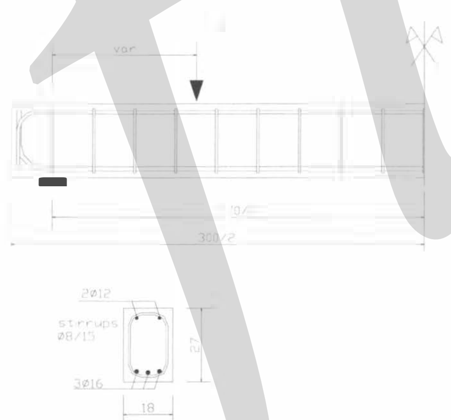

Fig. 1 - beam geometry

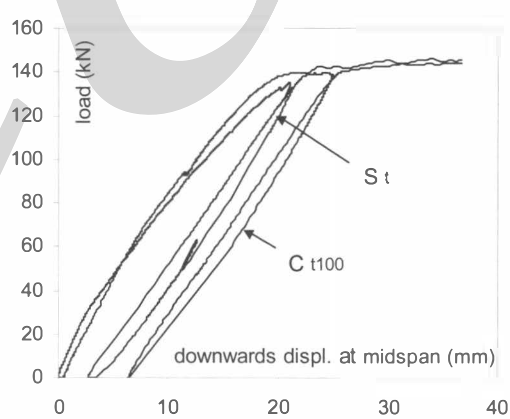

Fig. 2 - Load deflection responses

REFERENCES

[1] Pardi, L., Rinaldi, Z., Valente, C., Strength and ductility changes in bridge decks due to corrosion effects. Proc. Structural Faults & Repair 2001. London, July 2001.

[2] Rodriguez J., Ortega L., Casal J., Diez J.M. "Assessing structural conditions of concrete structures with corroded reinforcement" Int. Conf. Concrete in the Service of Mankind, Dundee, U.K., June 1996.

[3] Castel, A., Francois, R., Arliguie, G. Mechanical behaviour of corroded reinforced concrete beams – Part 1: experimental study of corroded beams. Materials and Structures, RILEM, Vol. 33, November 2000, pp. 539-544.

BOND SPLITTING STRENGTH IN REINFORCED CONCRETE BEAMS USING HIGH PERFORMANCE FIBER REINFORCED CEMENT COMPOSITE

Masaki Maeda, Kim Va, Satoshi Tomita
Tohoku University
Japan

Satoru Nagai, Tetsushi Kanda
Kajima Technical Research Institute
Japan

Keywords: High Performance Fiber Reinforced Cement Composite (HPFRCC), bond splitting strength, lateral reinforcement, bond length

1. INTRODUCTION

The authors have been developing structural members with High Performance Fiber Reinforced Cement Composite (HPFRCC) instead of normal concrete (NC) [1]. HPFRCC using Poly Vinyl Alcohol (PVA) fibers is a kind of Engineered Cement Composites (ECC) developed to achieve high seismic resistant performance. Its material characteristics retain lower elastic modulus and high ductility of about over 1% in tension because of multiple-cracking effect as shown in Fig.1. Tensile ductility of HPFRCC is expected to improve bond splitting behavior of longitudinal bars in reinforced concrete members, which is generally governed by tensile failure in concrete. In this study, simply supported beams were tested to investigate bond splitting behavior of beams using HPFRCC and NC.

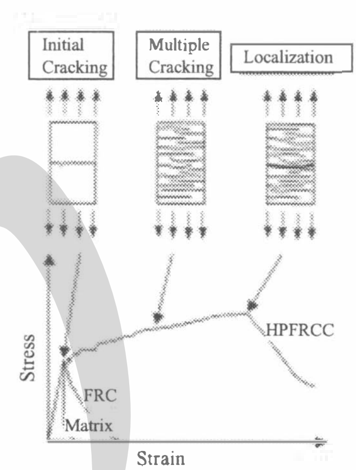

Fig.1 Tensile stress – strain of HPFRCC

2. OUTLINE OF EXPERIMENT

Six simply supported beams were designed following specimens tested by authors [2]. Figure 2 shows reinforcing details of a specimen. The specimens were designed to fail in bond splitting (side splitting mode) along longitudinal bars (test bars). The variables of specimens were:(1) Type of concrete (HPFRCC, NC), (2) Lateral reinforcement ratio, p_w (p_w = 0, 0.32%, 0.63%), (3) Arrangement of lateral reinforcement, (4) Bond length of test bars ($12d_b$(300mm), $24d_b$(600mm)), (5) Number of test bars (3-D25, 4-D25), and (6) Position of test bars (top, bottom).

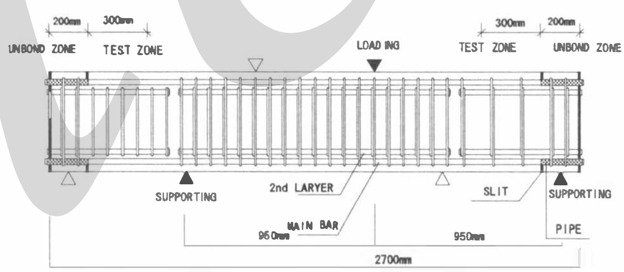

Fig.2 Side elevation of a specimen

3. RESULTS OF EXPERIMENT AND ANALYSIS

3.1. Failure mode

Every specimen failed in bond splitting along test bars in the test zone. Photo 1 shows a comparison of crack patterns of NC and HPFRCC specimens without lateral reinforcement (p_w=0%) after loading. Bond splitting cracks were observed on top and side faces along test bars in the test zone. Many straight short cracks, "multiple-cracks", were observed in specimens using HPFRCC. Crack width remained less than 0.1-0.2mm, which were narrower than in specimens using NC, until bond stress reached the maximum.

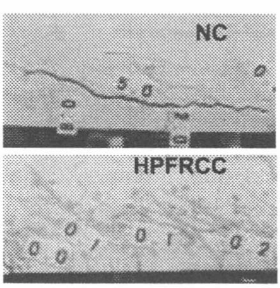

Photo.1 Crack patterns after Loding

3.2 Bond stress-free end slip curve

Figure 3 shows relations of bond stress and free end slip in test zones without lateral reinforcement (p_w=0%). Bond stress in NC with p_w=0% reached maximum with very small slip and decreased rapidly with expansion of bond splitting cracks along test bars. On the contrary, bond stress in HPFRCC with p_w=0% maintained bond stress until approximately 1mm slip, and bond deterioration was gradual comparing to NC. No significant difference was found between bond stress – free end slip relations of NC and HPFRCC with p_w=0.63%, although maximum bond stress of HPFRCC was rather higher.

The use of HPFRCC improves not only bond splitting strength but also bond deterioration after bond splitting failure occurred especially in specimens without or with few lateral reinforcements.

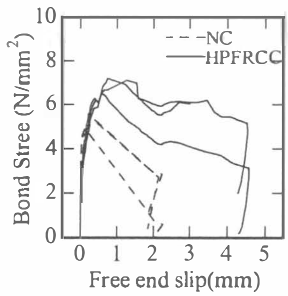

Fig.3 Bond stress-free end slip

3.3 Maximum bond stress

The ratio of average maximum bond stresses τ_{maxav} in specimens using HPFRCC to those using NC are shown in Fig.4. The ratio increased with the decrease of lateral reinforcement ratio p_w. In case of p_w=0%, maximum bond stresses of HPFRCC were 1.27 times (4-D25) - 1.32 times (3-D25) larger than those of NC for specimens with bond length of 12d_b(300mm), 1.64 times (4-D25) for specimens with bond length of 24d_b(600mm). In case of p_w=0.63%, 1.02 times (4-D25) - 1.07 times (3-D25) for specimens with bond length 12d_b(300mm), 1.30 times (4-D25) for specimens with bond length 24d_b(600mm). These results indicate that the contribution of HPFRCC to improve bond splitting strength was larger as lateral reinforcement ratio p_w decreased.

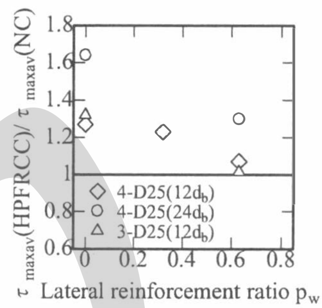

Fig.4 The ratio of maximum bond strength of HPFRCC to NC

3.4 Influence of bond length

The relationships between maximum bond stress τ_{max} and bond length are shown in Fig.5. As pointed out in previous researches, bond splitting strength of NC decreases with the increase of bond length because bond splitting failure and bond deterioration occur gradually from tensile side to another side along longitudinal bars. On the other hand, in specimens using HPFRCC bond stress along test bars was maintained after occurrence of bond splitting due to its ductile tensile characteristics. Therefore influence of bond length on splitting strength was not observed.

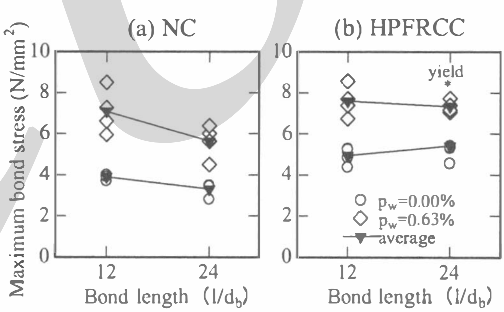

Fig.5 Influence of bond length

4. CNCLUSIONS

Main findings in this study can be concluded as follows:

1. Multiple-cracks were observed in the specimens using HPFRCC and crack width remained less than 0.1 - 0.2mm until bond splitting failure occurred along longitudinal bars.
2. Bond splitting strength in the specimens using HPFRCC were 10 – 60% higher than those in the specimens using normal concrete. The effect of HPFRCC on improvement of bond splitting strength increased as the lateral reinforcement ratio decreased.
3. Use of HPFRCC improved not only bond splitting strength but also ductility after maximum bond strength. As a result, influence of bond length on decrease in bond strength was not observed in the specimens using HPFRCC.

REFERENCES

[1] Kanda, T.: Design Technology of High Performance Reinforced Cementitious Composite at present state. Concrete Research and Technology, JCI, Vol.38, No.6, pp.9-16, Jun., 2000

[2] Maeda, M., Otani, S., Aoyama, H.: Experimental Research on Bond Splitting Strength of RC members. Proceedings of the Japan Concrete Institute, Vo.13, No.2, pp145-150, Jun., 1991

A DESIGN METHOD FOR PRECAST CONCRETE RETAINING WALLS CONNECTED WITH COUPLER JOINTS

Katsuhiro Nagatomo
Takamatsu National College of Technology
JAPAN

Tetsuya Matsuyama, Seiichi Shimomura, Nozomi Motomura, Tsuyoshi Kameyama
Nihonkogyo Corporation
JAPAN

Keywords: precast concrete, retaining wall, coupler joint, design method

1 INTRODUCTION

A cast iron coupler recently developed can connect precast concrete(PCa) elements easily and reliably only by tightening anchor bars which are welded to the couplers and embedded in the elements on both sides of a joint. In this study, tests for full scale PCa retaining walls which have a joint section and are connected with couplers are conducted and the results are reported. The purpose of the study is to establish a design method for vertical walls on the basis of the comparison between the measured and calculated results. Primary design considerations of walls include (1)stresses of concrete and reinforcement, (2)horizontal displacement distribution of the vertical wall, and (3)widths of major cracks formed in the wall.

2 TEST SPECIMENS

Figure 1 shows the test specimen with a joint. In the right circle in Fig. 1, the detail of a coupler joint made from cast iron is shown. Entire tensile force acting on the joint due to bending moment was sustained by the couplers and transmitted to other reinforcing bars and their surrounding concrete in both PCa segments through anchor bars. Reinforcing bars of 15.9 mm diameter set along the anchor bars are called 'lap bars'; a further set of longer bars set on both sides of the lap bars are called 'middle bars'. Hollowed areas around the couplers are referred to as 'pockets', into which mortar was cast later.

3 CRACKING PATTERN AND FAILURE MODE

Only three types of horizontal cracks appeared on the vertical wall; a crack appeared at the base of the wall, a crack occurred at the joint, and cracks passing through the upper face of the pockets. The design load of the wall was less than the cracking load. The maximum loads for the specimens were governed by flexural failure at the base section of the bottom slab. For the vertical wall base and joint sections, the experimental strengths were greater than those calculated from the Specification of JSCE.

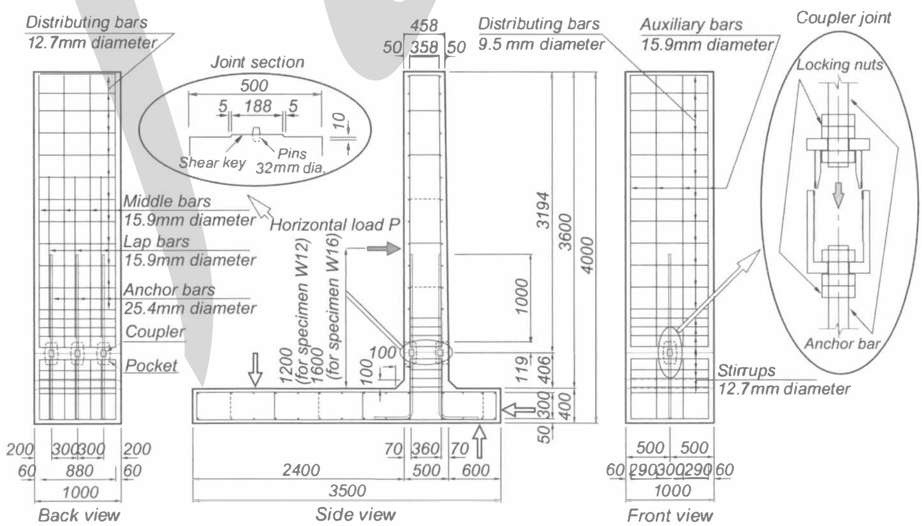

Fig.1 PCa retaining wall (in mm)

4 STRESSES AT TENSIONING

Two-dimensional finite element (FE) analyses for a vertical wall were conducted. Bond linkage elements were inserted between concrete and bar elements, where the initial stiffness 'k_b' was evaluated by the authors' empirical equation[1] as

$$k_b = \frac{\tau_x}{S_x} = \frac{\frac{1}{3}\left\{0.51\left(\frac{C}{D}-2.5\right)+1.38\right\}\cdot\sqrt{f_c'}}{0.0035\cdot C} \qquad (1)$$

where C(mm), D(mm) and f_c' (MPa) represent the concrete cover for the bars, diameter of the bar, and concrete compressive strength, respectively. Lap and middle bars were ignored. The measured stresses in concrete agree with computed ones despite the simplified analyses.

The differential equations for the bond stress-slip relation were used to calculate stress distributions for anchor bars. The obtained stress distribution agreed well with experimental one by using the value of 'k_b' determined from Eq. (1). Both stresses in the lap and middle bars estimated near the joint were approximately 3.5 MPa, which could be neglected.

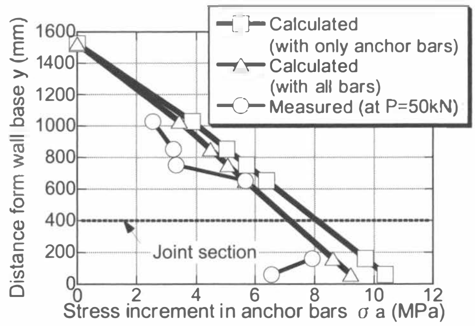

Fig.2 Measured and calculated stress increment distributions for anchor bars at a load of 50 kN before cracking (for specimen W16)

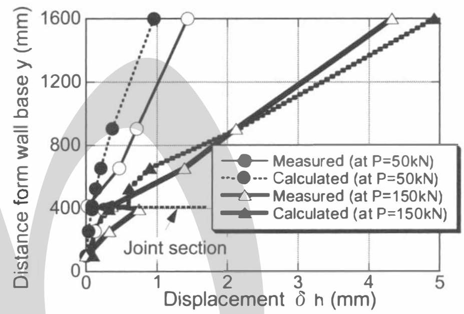

Fig.3 Horizontal displacement distributions of the vertical wall before and after cracking (for specimen W16)

5 STRESSES BEFORE CRACKING

In the following sections, only stress increments caused by a horizontal load will be treated to simplify the discussion, so the authors shall omit stresses due to fastening couplers.

The stress increments in used materials, concrete and vertical bars, can be estimated by the conventional elastic bending theory, in which an uncracked section with all vertical bars is used and an appropriate stress reduction factor for the computed values is required. Figure 2 shows measured and calculated stress increment distributions for anchor bars as an example. It is noted that lap and middle bars, except for 'the development region' over approximately 200 mm in length on both sides of the joint, can sustain almost the same tensile force as anchor bars, despite being cut close to the joint.

6 STRESSES AFTER CRACKING

The stress increments in used materials can be estimated by the conventional elastic bending theory, in which a cracking section with all vertical bars is used and an appropriate stress reduction factor for the computed values is required. According to the results, it is concluded that anchor bars act not only in the same fashion as connecting bars, but also as ordinary main tensile bars, and that lap and middle bars act like continuous main tensile bars, although they are actually cut.

7 DEFLECTION AND CRACK WIDTH

The horizontal displacements of the vertical wall 'δ_h' at various locations are calculated as the sum of elastic deformations for a cracked RC cantilever beam and additional displacements caused by rotation 'θ_j' defined as S_j / z, where 'z' is the flexural lever arm and 'S_j' (j = 1 - 3) are slips at the sections of the main cracks assessed by employing the differential equations for the bond stress-slip relation. The predicted lines are in close agreement with the measured lines as shown in Fig. 3.

8 CONCLUSION

Design Methods were proposed for concrete and bars stresses at three stages; tensioning couplers, before cracking and after cracking, and for horizontal deformation and crack width of PCa vertical walls.

REFERENCE

[1] Nagatomo, K., : Fundamental Study on Bond Characteristics of Deformed Bars and Their Modelling, Doctoral Thesis, Toyohashi University of Technology, 1993 (in Japanese).

PREDICTION OF CHLORIDE PENETRATION AND LIFE-CYCLE COST OF CONCRETE BRIDGES

Shoichi Ogawa, Tamio Yoshioka
Research Laboratory,
Oriental Construction Co., Ltd., JAPAN

Takafumi Sugiyama
Department of Civil Engineering,
Gunma University, JAPAN

Keywords : life-cycle cost, durability, chloride attack, diffusion

1.INTRODUCTION

Due to the large volume of existing concrete bridges, durability concerns have grasped considerable attention worldwide. The corrosion of the reinforcing bars in concrete due to chloride ingress is a serious problem for the durability of concrete bridges. In case of bridges that are located in severe marine environments, such damage may occur in an unexpectedly short time. In order to avoid this problem, it is necessary to perform suitable protection measures. To achieve good durability, the durability and design performance concepts encourage the use of LCC value, which is evaluated by considering the maintenance and repair costs. Therefore, prediction of chloride penetration into concrete structures is indispensable to evaluate the LCC.

In the present study, mathematical models governing the chloride penetration process are used to simulate the penetration of chloride and its effect on the LCC. The factors considered in this study are the amount of air-borne chloride as environmental conditions, concrete cover thickness and the water-cement ratio (W/C) of concrete. Their influence on the LCC values are analyzed. Furthermore, the effect of applying a paint layer at the initial construction as one of the protection measures is investigated. Fig.1 summarizes the various factors considered in this study. The life-span of bridges under consideration is extended over 100 years and repair operations and paintings are maintained during the life-span period. LCC is estimated as the sum of initial construction cost and total repair/painting cost values.

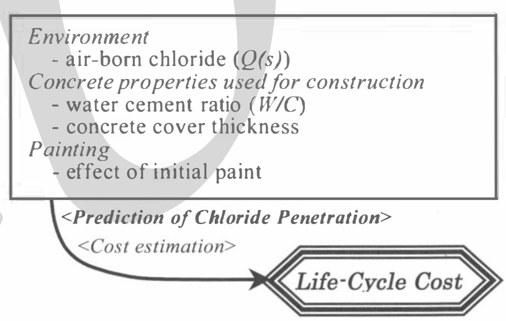

Fig.1 Factors considered in this study

2. ANALYTICAL METHODS

2.1 Analysis of chloride penetration

Two basic solutions are used to analyze the chloride ingress into concrete, fixing boundary conditions at the surface and calculating the diffusion into concrete. Boundary conditions, developed by Yamada et al. [1], are fixed by assuming that only a part of air-born chloride reaching the surface of concrete can penetrate into concrete. Furthermore, painting is considered to prevent chloride penetration at the concrete surface and performance of painting decrease with age. The air-borne chloride is assumed to be 20 mg/cm^2/year, which represents a severe marine environment. On the other hand, the amount of 1 mg/cm^2/year represents a non severe case. Diffusion equations, developed by Saetta et al.[2], are used to evaluate the diffusion of chloride into concrete considering the influence of humidity, temperature, and the hydration rate of cement.

$$\frac{\partial Ct}{\partial t} = div\left[D_a grad(Ct)\right] \tag{1}$$

2.2 Model bridges and repair schedule

The concrete bridge model, considered in this study, consists of two span post-tensioned T-section girders. All girders are made with 40% W/C concrete and a cover thickness of 40 mm. This concrete bridge model is investigated as the basic type girder.

The life-span of bridges under consideration is extended over 100 years, and repair operations and paintings are maintained during the life-span period. LCC is estimated as the sum of initial construction cost and total repair/painting cost values. Also repair works consist of the replacement of the cover concrete, and are repeated whenever chloride concentration reaches the threshold value, 1.0% by weight of cement at the reinforcing bar. The required repair and painting are repeated until the age of 100 years.

3. RESULTS AND DISCUSSIONS

3.1 Effect of air-borne chloride

The effects of air-borne chloride on the LCC are investigated since the concrete structures located near the coastline are damaged in a short time in some cases. Using mathematical models governing the chloride ingress, chloride concentrations of concrete for the basic type girder are simulated and the chloride concentrations are shown in Fig.2. As a result, repair is required twice and painting three times. In the same procedure, the number of repair and painting operations under the condition of 1 mg/cm^2/year air-borne chloride are estimated.

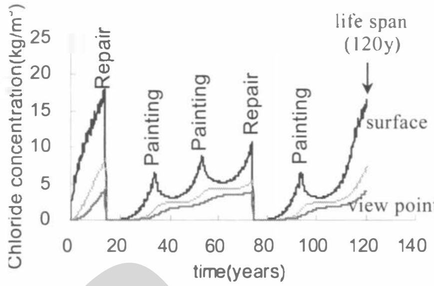

Fig.2 Chloride concentration on the basis type girder (($Q(s)$)= 20 mg/cm^2/year)

Fig.3 shows the initial construction cost (ICC), total repair/painting cost and LCC, as a normalized value to ICC. From this result, the LCC of post-tensioned bridges located in a large air-born chloride environment is more than four times higher than ICC. The difference of the amount of air-born chloride that reaches the concrete surface is effective on the LCC value.

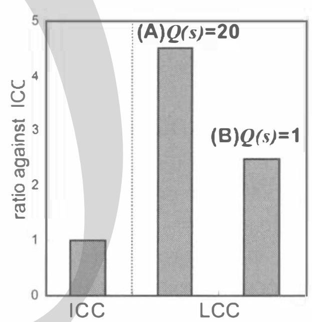

Fig.3 Comparison of costs

3.2 Effect of protection measures on LCC

Two types of girder bridges, Type A girder which increased the cover thickness from 40 to 50 mm and decreased W/C from 40 to 30%, and Type B girder which has a paint layer initially using the basic type girder, are assumed as protection measures. Their effects on LCC are investigated on deferent air-borne chloride. Estimated LCC are shown in Fig.4, as a ratio of LCC on the basic type girder bridge.

In the type A girder, the LCC does not decrease if the bridges are located in high amount of air-borne chloride environment. However, if this type of girder is located in low amount of air-borne chloride environment, LCC may results in a decrease of the LCC significantly. On the other hand, in the case of type B girder, which has an initial paint layer, LCC may undergo a reduction of about 25% if they are located in a high air-borne chloride environment. From these results, it can be stated that the selection of suitable protection measures is highly dependent on the amount of air-borne chloride that may reach the surface of the concrete. The prediction of chloride penetration process can therefore help design structures where low LCC may be obtained.

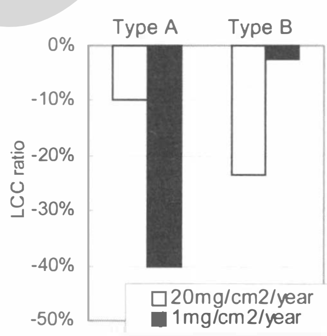

Fig.4 Change in predicted LCC for different air-borne chloride

REFERENCES:

[1]Yamada, Y. et al.: Analytical study on chloride penetration into concrete exposed to salt-laden environment. J. Struct.Constr. Eng., AIJ, No.501, pp.13-18, Jul., 1997 (Japanese)

[2]Saetta, A.V., Scotta, R.V. and Vitaliani, R.V. : Analysis of chloride diffusion into partially saturated concrete. ACI Materials Journal, Vol.90, No.5, Sep-Oct, pp.441-451, 1993

LIFE CYCLE COST EVALUATION TO EFFICIENTLY REPAIR AND MAINTAIN THE REINFORCED CONCRETE BRIDGES APPLIED BY RISK MANAGEMENT METHOD

Hitoshi Takeda Tetsushi Uzawa Hiromitsu Izumi Yoshihiro Tanaka Tsuyoshi Maruya
Taisei Corporation, Technology Center, JAPAN

Satoru Koyama Takaaki Nakamura
Shinozuka Research Institute, JAPAN

Keywords: life cycle cost, deterioration model, risk evaluation, probability, repair/maintenance, chloride attack

1 INTRODUCTION

This study aims at developing the decision support system for repair and maintenance of deteriorating concrete structures. In this study corrosion of reinforcing bars cased by chloride attack is regarded as the main deterioration behavior. The influence of carbonation on corrosion progress is also considered. As taking account of the accuracy of presumption for predicted corrosion grade, the probabilistic statistic method is availed. The developed system regards the performance degradation as a risk and adds it to the life cycle cost of the structure.

2 MODEL DEVELOPMENT

The decision support system consists of four subsystems as shown in Fig.1. The deterioration model can output the present and future status of deterioration corresponding to input values, such as chloride ion concentration, depth of carbonation, thickness of covering concrete and the information obtained from the inspection in addition. And further, the probabilistic and statistic technique added to the deterioration evolution formula. The risk evaluation model regards the performance degradation due to deterioration as the risk presented in the form of the expected loss R. R can be obtained from Equation 1 where P indicates an occurrence probability and C denotes a loss.

$$R = P \times C \tag{1}$$

The probability P is defined as a probability that the load exceeds the strength. The deterioration model after repair can estimate the deterioration evolution after the proposed repair executed by inputting various conditions such as a time, measures and an expense of the repair in the proposed method. The planning of repair and maintenance provides accumulative total costs expected to be required during the structure's life including the risk due to the performance degradation.

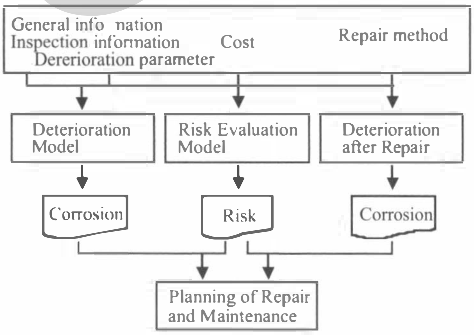

Fig.1 Flow of decision support system for repair and maintenance

3 APPLICATION OF THE DETERIORATION MODEL AND EXAMPLE

The applicability of the deterioration model was examined using a beam of the actual pier utilized for 20 years. The present deterioration states were judged I=0.78, II=0.18, III=0.03,IV=0.01 and the future deterioration states were presumed as shown in Fig.2. If the deterioration states were judged I=0, II=0.5,III=0.5,IV=0 by the visual inspection the posterior distribution would be changed as shown in

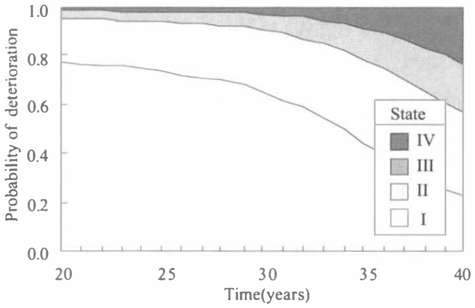

Fig.2 Prediction of deterioration for concrete cover depth=70mm

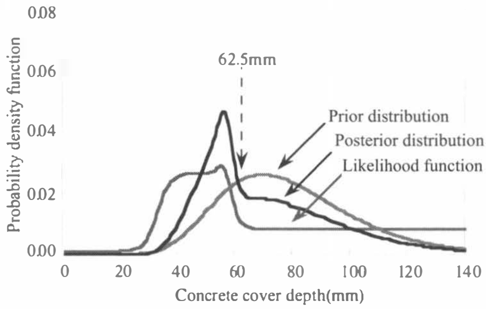

Fig.3 Distribution by Bayesian analysis

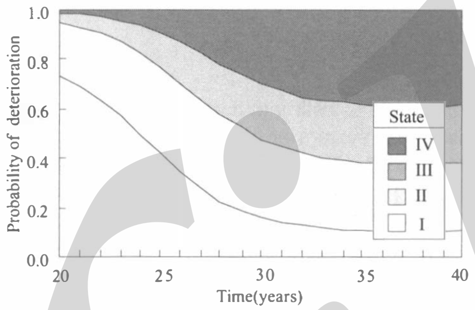

Fig.4 Prediction of deterioration for concrete cover depth=62.5mm

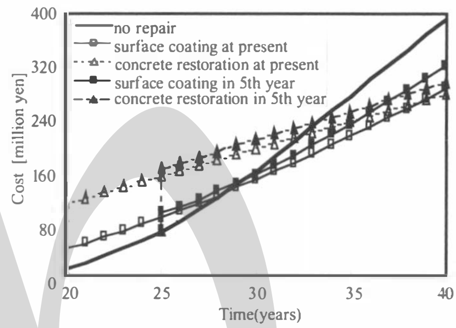

Fig.5 Comparison of a life cycle cost

Fig.3 by Bayesian analysis. Since the visual inspection revealed the deterioration state was worse than that obtained from assumption of 70mm concrete cover depth, the median of concrete cover depth became 62.5mm in the posterior distribution. According to this procedure the concrete cover depth would be modified taking present inspection data into account. It can be expected that the future deterioration states are presumed more accurately by this method (Fig.4). Finally, two cases that is repair and no repair were compared from a viewpoint of a life cycle cost. Four cases of repair were studied that is surface coating at the present, concrete restoration at the present, surface coating at 5 years later and concrete restoration at 5 years later. The results were shown in Fig.5. The results suggest the life cycle cost at 20 years later attains the highest in the case of no repair and the lowest in the case of repair at the present.

4 CONCLUSIONS

This paper presents the deterioration model that is one of the subsystems in the decision support system. The deterioration model was composed of combining the probabilistic technique with the past deterioration prediction model. An example simulation analysis was carried out to verify this model.

REFERENCES

[1] Ohya, T. and Mizutani, M.: On optimization of maintenance strategy for highway bridge slab panels, Structural Safety and Reliability, ICOSSAR, pp.229-236, 1997

[2] Hsu, K. L., Takeda, H. and Maruya, T. : Numerical simulation on corrosion of steel in concrete structures under chloride attack, Concrete Library of JSCE, No.37, pp.175-189, Jun., 2001

[3] Takeda, H. and Maruya, T.: Prediction of reinforcement corrosion in concrete structures by neural network, Concrete Research and Technology, VOL.9, No.1, pp.133-141, 1998 (in Japanese)

[4] Mochizuki, T. and Nakamura, T.: Statistical inference of seismic fragility curve by multinomial response model, Proceeding of the Second Real-time Earthquake Disaster Prevention Symposium, JSCE, pp.47-50, 2000 (in Japanese)

AN INTEGRATED DESIGN AND COST ESTIMATION ENVIRONMENT FOR PRESTRESSED CONCRETE HOLLOW SLAB BRIDGES BY PRODUCT AND PROCESS MODELS

Nobuyoshi Yabuki Masaya Furukawa Muroran Institute of Technology, JAPAN
Kenichi Matsui Yoshitaka Kato National Institute for Land & Infrastructure Management, JAPAN
Tsutomu Yokota Oriental Construction, Co., Ltd., JAPAN
Tetsushi Konishi Kawada Construction, Co., Ltd., JAPAN

Keywords: product model, process model, integration, prestressed concrete hollow slab bridge

1 INTRODUCTION

In the management of concrete structures, it is desirable to estimate the construction cost of the structure and select an optimized and appropriate structural system at the early stage of the design process, especially in the coming era of performance-based design. However, the lifecycle of the structure consists of various tasks including planning, design, estimation, construction, and maintenance, and these tasks are done in a spatially and chronically distributed manner by a number of different organizations and professionals. Although some of these tasks are automated by computers, the data transfer from one application system to the other is done manually, since the interchangeability of data among such heterogeneous systems is quite low. This leads to the problem of low productivity, the lack of true design optimization, and low motivation of innovative design.

In order to solve this type of "islands of automation" problem and to enable interoperability of data among heterogeneous applications, 3D product and process models would be needed because 3D data are necessary for design checking, quantity calculation and cost estimation [1].

In this paper, we propose and develop 3D product and process models for prestressed concrete hollow slab bridges, and we develop a design checking system, estimation system, and construction scheduling system for this type of bridges, and integrate these systems by the product and process models by using a 3D CAD system. We test this prototype environment by applying it to a bridge project and find that efficiency is improved and that the construction cost can be estimated smoothly.

2 PRODUCT AND PROCESS MODELS

Product models represent the data of the product in a formal and generic manner so that the model can be applied to any kind of products in the same category. A process model represents the construction process such as placement of concrete and rebars, etc. in a hierarchical structure. ISO's Standards for the Exchange of Product model data (STEP) [2] and IAI's Industry Foundation Classes (IFC) [3] are being developed and are well known as international standards of product models.

We developed product and process models for prestressed concrete hollow slab bridges. The developed product model consists of hierarchical classes. Each class has its attributes such as length, number, materials, etc. Instances are actual objects and they are classes of which attributes have real values. We used Extensible Markup Language (XML) to implement the product and process models.

The information such as which part of the concrete structures would be placed by concrete is represented by the link from the instance in the process model to the corresponding instance of the product model. Each class in the process model contains attributes including necessary days for the process, machinery to be used, the number of workers, pre- and post-processes, etc.

3 INTEGRATION OF APPLICATION SYSTEMS

In this research, we developed prototype application systems for design checking, quantity calculation – cost estimation, and construction scheduling. Then, we integrated these systems with a 3D CAD system, AutoCAD 2000i, by the product and process models for prestressed concrete hollow slab bridges.

We developed a user interface, Converter I, for data input for the selected CAD system so that the interface system makes both 3D CAD data and corresponding 3D product model data simultaneously. Converter I can also transfer the product model data to the 3D CAD system.

The prototype design checking system was developed for a simple straight prestressed concrete hollow slab bridges, on the basis of the provisions of the Japan's Highway Bridge Specification [4] by using Java. We also developed a data transfer program, Converter II, which obtains the data necessary for the design checking system from the product model data by using Java.

The bottleneck when executing cost estimation is typically the manual quantity calculation, which is cumbersome, error-prone, and time consuming. We developed a prototype quantity calculation and cost estimation system by using Microsoft Excel and Visual Basic for Application (VBA). Then, we developed a data conversion system, Converter III, which analyzes the product model and obtains necessary data including coordinates and dimensions of the design members from the product model, and which computes quantities such as concrete volume, the length of hollow pipes, weight of rebars, etc., based on the obtained data. Then, the quantity data are inserted into the cost estimation system, and unit prices are computed. The unit prices and quantities are inserted into a table, direct and indirect costs and the total cost are computed.

We developed a construction scheduling system by using Microsoft Project 2000, and a data conversion system, Converter IV, which obtains necessary data from the process model and transfers it to the scheduling system, by using VBA. The scheduling system automatically draws a construction bar chart shown, based on the data transferred from the product model smoothly by Converter IV. Since the product model and the process model have mutual links, 4D CAD simulation is possible. 4D CAD is a combination of 3D CAD and the dimension of time, which is represented by the process model. 4D CAD can simulate and demonstrate the construction process.

We integrated the above-described application systems in this research and investigated the data interoperability among systems and their performances by applying the systems to a sample bridge project. The result shows that the data interoperability among systems is smooth and efficient. Thus, the productivity can be improved significantly by applying the integrated system.

4 CONCLUSIONS

Performance-based design will give designers and contractors chances for more innovative design. But at the same time, in order to utilize the concept of performance-based design effectively, a fully integrated and automated project processing environment would be necessary from conceptual design through construction planning and cost estimation. Because a number of different design plans have to be considered and compared for optimization. However, the "islands of automation" problem exists and thus, the interoperability among heterogeneous application systems is necessary.

In this research, we proposed and developed prototype 3D product and process models for prestressed concrete hollow slab bridges. Then, we developed a design checking system, quantity calculation – cost estimation system, and construction scheduling system. Furthermore, we integrated these systems and a 3D CAD system by the product and process models and converter programs, and we tested the data interoperability among the systems. We found and demonstrated that the data transfer among the systems was smooth and efficient and that the productivity can be improved significantly by the integrated and automated environment.

ACKNOWLEDGMENT

This research has been partially supported by Japan Prestressed Concrete Constructors Association. The authors would like to acknowledge their support.

REFERENCES

[1] Yabuki, N. and Shitani, T.: An integrated design system for connections of steel structures. Proc. from the specialty conference on fully integrated and automated project process, Ed. Songer, A. et al., Blacksburg, VA, USA, ASCE, pp.58-65, 2001.

[2] International Organization for Standardization: ISO 10303, Industry automation systems and integration – product data representation and exchange, 1994.

[3] International Alliance for Interoperability: http://iaiweb.lbl.gov/

[4] Japan Highway Association: Highway bridge specification and commentary, 1996 (in Japanese).

INQUIRY AND ANALYSIS REGARDING THE TECHNICAL LEVEL OF ENGINEERS ENGAGED IN CONCRETE CONSTRUCTION WORK

Yasushi KAMEZAWA
Taisei Corporation
JAPAN

Hiromichi MATSUSHITA
Kyushu University
JAPAN

Hiroaki TSURUTA
Kyushu University
JAPAN

Keywords: concrete construction work, level of engineers, compactness, performance-based standard

1 INTRODUCTION

To ensure compactness, the minimum quality standard for the quality of durability of concrete structures, the technical abilities and awareness of problems about compactness on the part of engineers at each stage in the process play an extremely important role, and it is thought that their importance will continue to grow. However, at present, almost no studies have been conducted regarding the technical level of these engineers and their awareness of problems about compactness.

In this study, the authors conducted a survey and analysis of the technical level of engineers and their recognition of problems related to concrete compactness in an effort to determine the technical environment related to concrete work.

2 SURVEY

2.1 Summary

This study targeted engineers involved in the ordering (administration), design and construction stages of the process of constructing concrete structures. A survey was conducted in order to find out the technical level of engineers and their degree of awareness of problems related to compactness of concrete. The questions on the survey related to the attributes of the individual respondent (age, education, type of organizational affiliation, nature of work), degree of self-recognition of technical ability, level of specialist knowledge, awareness of current problems related to compactness of concrete, etc.

2.2 Respondent

Valid responses (including partial responses) were returned from 1090 engineers in all. The respondents were categorized as "owners", "designers", or "site-engineers." Persons affiliated with national or local governments and public corporations, public utility corporations and other contracting organizations were classified as "owners." Persons affiliated with consultant organizations were classified as "designers." Persons affiliated with general contractors, PC specialist companies and sub-contractors were classified as " site-engineers."Of these responses, the average age was 39.3 years. About 62% of respondents had graduated from universities or graduate schools.

3 ANALYSIS OF AVERAGE LEVEL OF SPECIALIST KNOWLEDGE

In Japan, Standard Specification for Design and Construction of Concrete Structures (hereinafter "Standard Specification") is assumed to be the standard for design and construction of concrete structures, and a manual with which engineers working with concrete should naturally have a thorough knowledge.

As shown in **Fig. 1**, in terms of their knowledge of the content of Standard Specification, about 66% had only browsed through the manuals at most, and about 10% answered that they have never read them. Regarding the revision of the Construction part of Standard Specification in 2000(characterized by the introduction of performance-based standards), approximately 87% of all respondents answered that they were either unaware of the revisions or had no knowledge of its content.

It is presumed that quite few of the respondent actually understand the content of the Standard Specification to some degree. The situation was serious enough that 52% of "owners" were not even aware that the Standard Specification had been revised.

From the above results, it can be seen that, in objective terms, the level of technical knowledge of respondents was by no means high, and the level of specialist knowledge even on the part of "owners" who were comparatively highly educated was not high. The level of technical knowledge on the part of "designer" engineers is thought to be slightly higher than the other two categories, but it can by no means be considered adequate. These results suggest that there is a high degree of danger that the personnel on the upper levels (planning and design) of the building construction process do not have an adequate knowledge and understanding of construction.

4 AWARENESS OF PROBLEMS RELATING TO COMPACTNESS

About 70% of the engineers of general contractors and sub-contractors often recognized problems in drawing to ensure compactness. In other words, these responses show that problems at the drawing stages are common in actual practice. However, these percentages dropped dramatically when it comes to consultant engineers. Nearly 80% of them responded that there were almost never any problems at the drawing stage. Thus there is a huge difference between the perceptions of these two groups (design and construction). This suggests that there is not much consideration for the compactness of concrete at the design stage.

Fig. 2 shows the ratio of respondents with experience in offering or receiving proposals for correcting drawings at the stage at which problems with compactness have developed.

About half of the general contractors engineers answered that they sometimes proposed changes in order to improve compactness. However, around 90% of the consultants and owners who should be receiving these proposals responded that there were rarely any proposals, and just under 60% said that they have never received such proposals.

The figures for the offering of proposals and the receipt of proposals may not necessarily match perfectly. However, these results show that, in actuality, the information (proposals for improvement) from construction engineers is not being communicated properly, and that there is an enormous information gap.

Without the flow of information, proposals cannot be properly utilized, and it is conjectured that improvements to securing compactness are being made by construction site-engineers at the so-called field level.

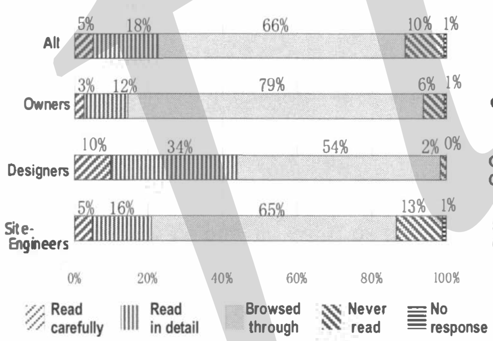

Fig.1 Degree of Awareness of Standard Specification (Design)

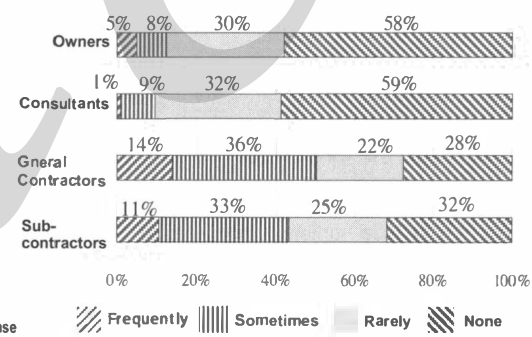

Fig.2 Offering of Proposals to Correct Problems at the Design Stage (Drawings)

5. PROPOSAL FOR STANDARDS TO ASSESS COMPACTNESS

This study has made it clear that, at present, the technical level of engineers is by no means high. In this situation, in order to ensure that the concept of performance-based evaluations is being adequately employed and secure the compactness of concrete, naturally we must find a way to improve the technical ability of relevant engineers. Moreover, we must create a system in which even the average engineer, whose technical level is currently not very high, is able to determine pros and cons in advance with respect to compactness and, if improvements are necessary, to propose and adopt appropriate corrective measures. In other words, we propose that judgment standards that we call "compactness prior assessment standards" should be created so more competent judgements related to ensuring compactness can be made in a simpler and easier manner.

DESIGN METHODOLOGY FOR FLEXURAL UPGRADING OF RC BEAMS USING BONDED STEEL PLATES

Bimal Babu Adhikary and Hiroshi Mutsuyoshi
Department of Civil and Environmental Engineering, Saitama University, Japan

Keywords: epoxy bonding, flexural upgrading, RC beams, steel plates, strengthening

1 INTRODUCTION

Bonding of steel plate with epoxy adhesive on the tensile side of an RC beam is one of the widely used techniques for flexural strengthening. In this paper, simple approximate closed form expressions are developed for the interface stresses at concrete-epoxy-steel plate joint for beams with tension-face plate. The expressions are modified for the inclusion of nonlinear and inelastic effects from the parametric study conducted using the finite element model developed by the authors [1]. A design methodology for strengthening of concrete beams in flexure with epoxy bonded steel plate is presented. Checks for avoiding debonding and ripping failure are suggested and a design example is presented.

2 EXPRESSIONS FOR INTERFACE STRESSES

In this section, analytical expressions are developed for shear and normal stresses in interface by the theory of constant modulus of displacement [2]. The assumptions made in the formulation are homogeneous isotropic linear elastic behaviors for concrete and the strengthening materials, plane sections remain plane and linear strain distribution along the 'x' and 'y' axes and that the adhesive takes no longitudinal forces. The maximum shear stress and normal stress at the plate cut-off point are given by eq. 1 and eq. 2 respectively.

$$\tau_0 = t_P \frac{n y_b}{I_{tr}} \left\{ M_0 \sqrt{\frac{K_S}{t_P E_P}} + V_0 \right\} \tag{1}$$

$$\sigma_0 = -\tau_0 t_P \left(\frac{K_n b_P}{4 E_P I_P} \right)^{\frac{1}{4}} \tag{2}$$

where, M_0 and V_0 are bending moment and shear force due to external load at the plate cut-off point.

3 PARAMETRIC EVALUATION

On the basis of numerical parametric analysis, the expressions for shear and normal stresses are modified to include nonlinear and in-elastic effects by multiplying eq. 1 by ω and eq. 2 by α.

$$\omega = 0.9 + \varsigma / 21 \quad \text{and} \quad \varsigma = \frac{V_0}{f_c' t_P e}, \quad \alpha = 0.7 \tag{3,4}$$

4 DESIGN METHODOLOGY

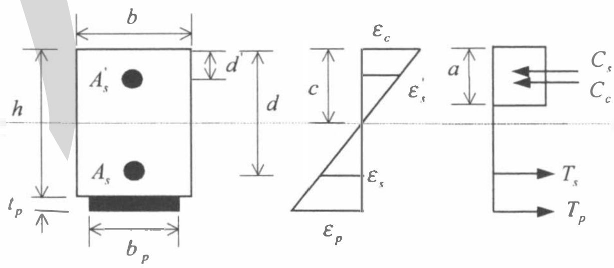

Fig. 1 Beam model for strengthening design for flexure

For steel plate bonded beam, failure may be categorized as 1) Flexural cracking, yielding of internal reinforcement and steel plate leading to crushing of concrete, 2) Compression failure of concrete before yielding of plate and steel re-bar and 3) pre-mature debonding and ripping failure at the plate cut-off point due to high stress concentrations at the interface.

1. Assuming that the compression steel yields at failure, suitable values for b_p and t_p are assumed.
2. Distance of neutral axis is determined and verified that both steel reinforcement and steel plate yield, if not, assume smaller value of t_p and start again.
3. Calculate resisting moment M_r and check if $M_r \geq M_u$, if not, start all over again.
4. Check t_{pb} and see if $t_p \leq t_{pb}$.

To avoid pre-mature debonding and ripping failure, interface stresses must be checked at plate cut-off point. The maximum shear stress at the interface at which debonding starts is given by eq. 5.

$$\tau_{deb.} = \frac{5.0}{1 + K_0 \tan 30^0} \text{ (in MPa)} \tag{5}$$

From the tooth model by Zhang et al. [3], the maximum shear stress for ripping failure is given by eq. 6.

$$\tau_{rip.} = \left(\frac{f_t L_c}{6d_c}\right) b / b_p \tag{6}$$

The allowable shear stress at the interface can be set to minimum of eq. 5 and eq. 6.. Allowable principal stress for tension-tension state is given by eq. 7 [4].

$$\sigma_{all} = 0.295 f_c'^{2/3} \text{ (in MPa)} \tag{7}$$

5 DESIGN EXAMPLE

An RC beam spanning 8m was designed for a factored moment of 384kNm. It was decided to strengthen the beam for additional factored moment of 192kNm using steel plate. Design parameters are: b=350mm, h=600mm, d=535mm, d'=45mm; Concrete: f_c'=30MPa, E_c=24647MPa; Reinforcement: A_s=2400mm^2, A_s'=400mm^2, E_s=210GPa, f_{ys}=400MPa; Steel plate: E_p=210GPa, f_{yp}=350MPa.

Solution:
1. Calculating the moment of resistance of existing beam M_{re}=470.5kNm>M_{fe}=384kNm OK
2. Computing factored moment to be carried by strengthened beam M_f=576kNm>M_{re}=470.5kNm
3. Selecting 330mm wide, 6mm thick and 7400mm long steel plate, t_p=6mm, b_p=350-20=330mm
4. Taking ε_{cu} =0.0035,following result is obtained: M_r=797.3kNm>M_f=576kNm, Safety Factor=1.38 OK
5. Computing t_{pb}=17.8mm>t_p=6mm OK
6. Computing allowable stresses at plate cut-off point e=300mm using n=8.52, K_s=60MPa/mm, K_n=144MPa/mm, d_c=45mm, L_c=250mm, f_t=2.9MPa: $\tau_{deb.}$ =4.4MPa, $\tau_{rip.}$=2.85MPa, $\sigma_{all.}$=2.85MPa
7. Computing stresses at plate end: τ_o =2.34MPa<2.85MPa<4.4MPa, $\sigma_{max.}$=2.62MPA<2.85MPa OK

6 CONCLUSIONS

Analytical expressions for shear and normal stresses at the concrete-epoxy-steel plate interface are developed and modified for the inclusion of nonlinear and inelastic effects. Stepwise design procedure for flexural strengthening of RC beams with soffit bonded steel plate is described. Checks for interface stresses to avoid debonding and ripping failures are suggested and a design example is presented.

REFERENCES

[1] Adhikary B.B. and Mutsuyoshi H. (2002) 'Numerical simulation of steel plate strengthened concrete beams by nonlinear FEM model' Construction and Building Materials (in press).

[2] Tepfers, R. (1980) 'Bond stress along lapped reinforcing bars' Magazine of Concrete Research, 32 (112): 135-142.

[3] Zhang, S., Raoof, M. and Wood, L.A. (1995) 'Prediction of peeling failure of reinforced concrete beams with externally bonded steel plates' Structures and Buildings, 110: 257-268.

[4] Saadatmanesh, H. and Malek, A.M. (1998) 'Design guidelines for flexural strengthening of RC beams with FRP plates' Journal of Composites for Construction, ASCE, 2 (4): 158-164.

CONCRETE STRUCTURES AND SUSTAINABLE DEVELOPMENT

Ma Baomin
Tsinghua University Building Design
and Research Institute, Beijing, China

Lu Youjie
Dept of Construction Management
Tsinghua University, Beijing, China

Keywords: concrete, quarry, aggregate, fly ash, environment

1 INTRODUCTION

The number of buildings of over 10 floors high has grown rapidly in recent two decades in China[1]. 90 percent of the buildings are made of reinforced concrete. The annual output of concrete has exceeded 500 million cubic meters. Having made living conditions more comfortable the concrete built environment has become the "containers" or "forests" that trap the urban residents in a restricted space. The trapped residents are desperately struggling out of the "containers" and the "forests" for larger open space, fresh air, clean water and beautiful natural scenery.

2 CONCRETE STRUCTURES AND NATURAL RESOURCES

Increasing demand for concrete has caused aggregate to be in short supply. More and more coarse aggregate has to be obtained from quarries in remote hills. Unplanned quarries have destroyed original vegetation causing serious environment problems. The poor environment awareness of the people combined with outdated quarrying methods have produced huge amount of waste that cannot be effectively used. There has emerged a sign that the exhausting quarry is depleting the rock resources.

3 CONCRETE STRUCTURES AND ENVIRONMENT

3.1 Concrete structures and ecological environment

The ecosystems interact with and exchange energy and substance with their environment in a sustainable way. The exchange has never wasted anything. Output of one ecosystem is input to another. The self-adaptation and inter-adjustment mechanism will go wrong when their environment is disturbed to a certain extent.

Wide use of concrete contributes more than other materials to the human shelters in both positive and negative terms.

Any additional concrete building in a place is actually an additional invader to the local ecosystem that forces the local ecological colony to migrate or die. The people involved in the invasion have not realized this. The ecosystems from which stone materials are taken away and the surrounding environment have been damaged as well.

Quarry and moving away of the materials to urban centers have changed both the geographical distribution of energy and substance and the distribution of stress and hydrological field. The changes may evolve into some kind of disasters to the local community.

3.2 Concrete structures and physical environment

The production, use and disposal of concrete may cause a number of environmental problems.

(1) Dust pollution due to quarry
(2) Damage to landscape
(3) Uncontrolled carbon dioxide discharge
(4) Difficulty in future use of sites

4 WASTE PRODUCED IN MAKING CONCRETE

Vast amount of waste is produced during production, transportation, storage and use of concrete. If the buildings or other structures made of concrete are anyway demolished when they are in service long enough or not needed any longer, debris will become a headache to both the present and the future generations.

5 EXTERNALITY AND FULL COST OF CONCRETE CONSUMPTION

The market price of concrete represents only a small portion of the life cycle and full cost. It does not include the disposal cost when concrete is demobilized nor the external cost that some one else in the society has to pay. We have actually already paid and will continue to pay for use of concrete as building materials much more than it has appeared to us.

6 DURABILITY OF CONCRETE STRUCTURES IN THE PERSPECTIVE OF SUSTAINABLE DEVELOPMENT

The works made of concrete have been exposed to an increasingly poorer condition since they are put in service. There have occurred already many accidents caused by the decreased strength, stability and durability due to the deteriorating service conditions. It has become urgent to improve the condition to which the concrete works are exposed.

We dream of a kind of concrete that can reduce to reusable raw materials as soon as it is discarded. The rationale behind both the considerations is sustainability of construction and all human activities.

High performance concrete has been under development for a number of years in China already. A concept of “green concrete” has been perceived in China [2]. The idea is to make a durable and environment-friendly concrete.

7 CONCRETE *VS* OTHER BUILDING MATERIALS

Having realized the problems caused by unlimited use of concrete as a building material a great deal of effort has been made in China to reduce consumption of natural stone and sand and the resultant damage to physical environment.

The governments in China have imposed restrictions on usage of clay brick in recent years to conserve the scarcely available farming land. As a result concrete as an alternative to clay brick has been used rapidly not only in urban but also rural areas, which has caused a number of problems as described above.

China’s government has realized that making use of industrial waste such as fly ash generated by coal-fueled power plants is a way out. It is actually a strategy that can “kill three birds with one stone”. China’s governments have been encouraging substituting fly ash ceramsite for natural stone materials already for over three decades.

The timber and/or bamboo shall be used as structural and wall enclosure materials in rural and/or mountain areas instead of using so much concrete as in urban areas upon condition that planting and cutting are kept in balance.

In addition to seeking the alternatives to concrete as building materials attention have been drawn to the recycling of ordinary and asphalt concrete in China.

8 CONCLUSIONS

The rapid economic growth and social development and the resultant urbanization in China seem to have exceeded the limit and caused shortage of construction materials in some places, such as a few coastal urban centers and increasing damage to physical environment.

The situation has alerted the government officials and academics of the issue. As a part of sustainable development strategies much effort has been made and alternatives have been sought to reduce the pace of consumption of natural building materials and to recycle industrial waste including building waste in China.

REFERENCES

[1] Ma Baomin, Lu Youjie: Tall buildings and sustainable development. The 16th National conference on structures of tall buildings, proceedings, Shanghai, pp.7, October 2000

[2] Lian Huizhen, Lu Xinying: Issues in development of concrete works in China. Architecture Technology, Vol. 31, No.1, pp.10-14, 2000

REALISM IN SERVICE LIFE DESIGN OF CONCRETE STRUCTURES – THE DESIGNERS POSSIBILITIES

Steen Rostam, MSc, PhD - Chief Engineer. sro@cowi.dk, sro-privat@get2net.dk
COWI A/S, Denmark
Chairman ***fib*** Commission 5

Keywords: Concrete, deterioration modelling, reliability, service life design, contracting, education

1 INTRODUCTION

1.1 Deterioration modelling

Recent years recognition of the deterioration mechanisms for concrete structures and their governing parameters has lead service life modelling to become a realistic tool for the designer to provide quantified service life designs, see figure 1 and 2.

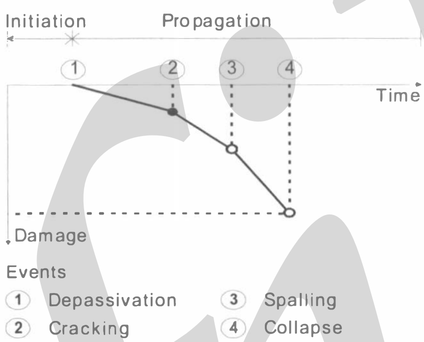

Figure 1 Events related to the service life.

Figure 2 Bridge piers exposed to a marine environment. Extensive damage due to chloride induced reinforcement corrosion

2 RELIABILITY BASED SERVICE LIFE DESIGN

The introduction of probabilistic methods to treat the inherent uncertainties in concrete quality and environmental aggressivity does now allow the level of reliability of such service life designs to be quantified. A comparison of a specific deterministic calculation and a probabilistic calculation of the concrete cover is presented in figures 3 and 4. The probabilistic approach illustrates the interrelations between the design cover thickness and the probability of corrosion - or of the "Design Service Life".

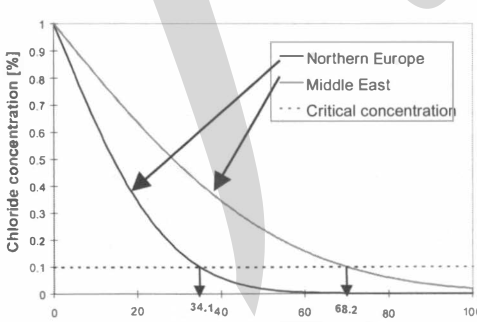

Figure 3 Deterministic approach.
Required concrete cover to ensure 50 years service life and assuming a chloride threshold value of 0.1% by weight of concrete.

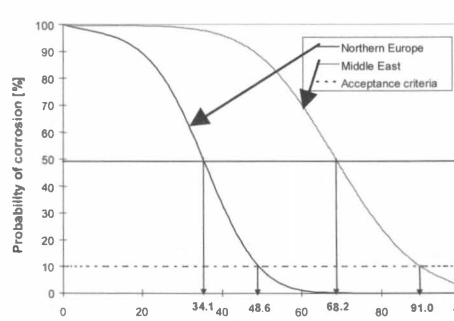

Figure 4 Probabilistic approach.
The deterministic approach provides only 50% probability of avoiding corrosion at the age of 50 years. Accepting 10% probability of having corrosion results in considerably larger covers.

3 "BIRTH CERTIFICATE" AND SERVICE LIFE UPDATING

When then the real qualities of the concrete in the structures is determined, e.g. at handing over in the form of a "Birth Certificate" of the structure, and later followed up during regular inspections, then an updating of the service life forecast can be made with ever increasing reliability.

These new possibilities may lead to much more well-performing structures as well as to very considerable savings in future maintenance and repair costs of concrete structures if the true potentials and their consequences are taken seriously into account by the construction industry as well as by the owners.

4 CHANGES NEEDED IN DESIGN REQUIREMENTS AND IN CONTRACTING CONDITIONS

One example could be that - due to the nature of concrete and the performance of concrete structures - fundamental changes in the very traditional ways of approaching service life requirements from the owners' side would be needed.

Revised types of contracting and liabilities would also be needed, if true improvement shall be obtained.

5 INTERNATIONAL CODES AND STANDARDISATION

The messages above have now come across to international code and standardisation organisations like CEN and ISO, as well as to the corresponding activities within ***fib***. The latter activities are currently in progress within ***fib*** Commission 5, Task Group 5.6 "Model Code for Service Life Design". Service Life is also being incorporated in the planning of the new ***fib*** Model Code. In the foreseen future updating of the new Eurocode 2 on the design of concrete structures is also incorporating service life design as a priority issue. ISO TC71 SC6 was recently established with the aim to develop an international standard on "Service Life Design".

The above is valid also for updating the service life estimations of repaired and re-designed structures. In this respect it is particularly promising that such reliability based service life designs can be based on the same load-and-resistance-factor-design methods (LRFD) as generally used for design for physical loads, see figure 5.

Thus, it is foreseen that future structural designs will focus considerably more than in the past on durability, service life and controlled requirements for maintenance, figure 6 would - among many others - represent such structures.

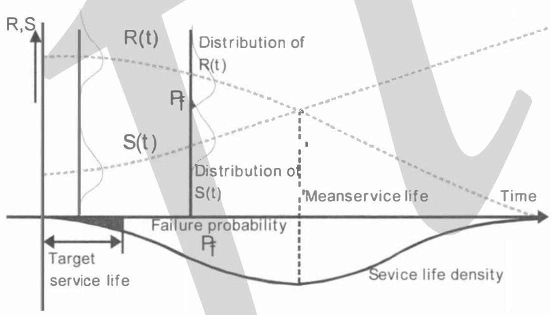

Figure 5 Failure probability and target service life. Load-and-resistance-factor-design (LRFD)

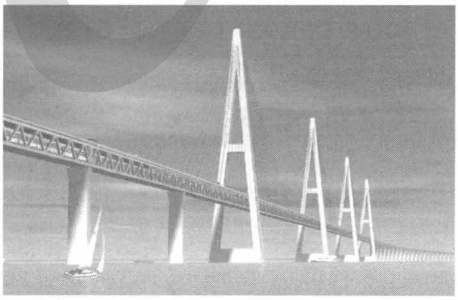

Figure 6 Crossing of the Strait of Gibraltar. Such future mega-projects require reliable service life designs - but so does all other structures.

6 CHALLENGES TO R&D AND TO ENGINEERING EDUCATION

Such advancements in durability designs pose challenges to research and developments as well as to future engineering education. It is particularly disturbing that such education has suffered year-long public neglect in comparison to other more short-term technical disciplines

7 STRUCTURAL ENGINEERING HAS BECOME A LOW-PRESTIGE EDUCATION

It must unfortunately be recognised that in spite of the fact that societies largest long-term investments are made in constructing buildings and infrastructure, structural and construction engineering has developed into a low prestige profession seldomly attracting the most gifted engineering students and professionals. The long-term economic consequences of this development may become very serious and develop into an unforeseen societal burden.

DEVELOPMENT OF CONSTRUCTION METHODS FOR INTERNATIONAL MEGA-PROJECTS

Prof. Dipl.-Ing. Dipl.-Kfm. Christian Brockmann
University of Applied Sciences, Bremen

Keywords: Construction industry, construction methods, mega-projects, innovation, R&D

1 INTERNATIONAL MEGA-PROJECTS

When describing the essence of mega-projects, it is best to characterize them by those dimensions, which set them apart from the rest of the construction projects. The most appropriate dimensions are:

- Complexity
- Novelty
- Factor specificity

The set of alternate items which constitute a project and their possible interconnections determine the overall complexity. If a project requires a new technological approach, the degree of novelty for this task will be high. Standard solutions then will not provide for a satisfying outcome and innovation in design and in construction methods are essential. The third dimension of a mega-project is the specificity of the input factors. For such projects highly specialized equipment is normally procured from the world market. The supervisory team must have experience and knowledge of similar previously employed technologies. The know-how and the organization of the company must be such that progress in developing construction methods is facilitated.

Mega-projects can then be described as being highly complex projects, where the most appropriate construction technique is innovative and where specific input factors (know-how, organization, manpower, equipment) are required. Describing mega-projects in an international environment signifies the impact of a specific situation. First, mega-projects often become feasible only on the international level. Second, this environment introduces in each case a very specific set of constraints. These might be political, economical or social constraints.

2 DEVELOPMENT OF CONSTRUCTION METHODS FOR MEGA-PROJECTS

The rationality concept which applies best to construction is that of bounded rationality as introduced by the Nobel prize economist Simon [1]. Our rationality as engineers is restricted by uncertainty of future outcomes and we are wise to acknowledge this fact. The uncertainty also includes the algorithms with which to determine the solution. There are no general criteria for optimality.

Since we are unable to find optimal solutions, we must be content with such, which are exceeding our own level of expectations. This behavior was termed satisficing by Simon. It is a search among the alternatives which stops once an acceptable solution has been found. There may be more than one solution satisfying subjective judgment or just one. In both cases the solutions will have to undergo a process of intended rational critique. By this an objectivity of the search is reached. As the philosopher Popper explains: "The so-called objectivity of science consists of the objectivity of the critical method; this means most of all, that no theory can be deliberated from critique but also that the logical tools of critique – the category of logic contradiction – are objective." [2, translation from German by the author].

More so, within the framework of the theory of computational complexity, Gödel's theorem proves that any mathematical theory is incomplete and that even moderately complex problems cannot always be solved consistently within a certain time. This has nothing to do with the capacity of computers but with the underlying theory.

Fig. 1 depicts a flowchart of the general procedure in developing construction methods. Starting from the set of solutions known to a company (or a consortium), the already realized construction methods will be varied to find a better fit to the new task. From this slowly evolve new solutions by gradually changing the different approaches more and more. This process is cyclical, always involving product design, cost and time. At any point the question must be answered, whether the developed innovative construction method can be executed by the company (or consortium). This is the question, whether the solution is part of the technology space mastered. The technology space can of course be expanded but hardly by great leaps while minimizing cost. Great leaps always require investments and in construction these must be amortized on the focal project. Some of the innovations for construction methods can still be considered major.

It is always possible that an original solution will be found. This is, however, a rare circumstance and not much a result of intentionally rational search.

The next step describe the satisficing behavior: the subjective evaluation, whether a personal level of acceptance is surpassed. Then follows testing of the solutions by the critical method and thereby introducing objectivity into the procedure. Finally a decision will be taken and a special construction method chosen. Once this is done and after some further detailing, the contract commitment will take place. After signing the contract month of further detailing become necessary before the plans for a construction method can be transformed into equipment and manhours.

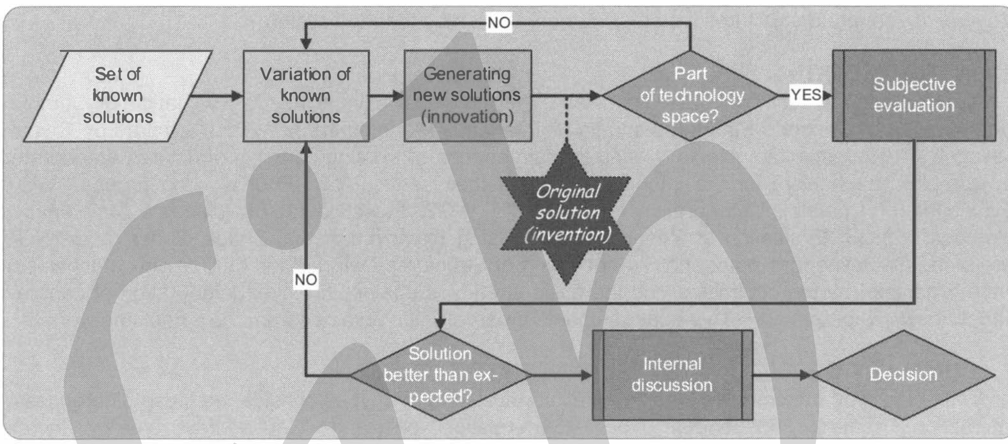

Figure 1: Development of new construction methods

The chosen construction method will be tested during the execution of the project and the assumptions are continuously monitored by the contractor. In this trial and error period, only the contractor has the detailed target data and gathers the detailed actual data. Only he will be able to learn fully from the experience. Even though the owner or a professional construction manager working as a consultant accompany the whole project, monitor the progress, collect data and write reports, they never become privy to the cost data of the construction company. In summary, most of all construction companies can further technological progress in construction in collaboration with the owner (favorable contractual framework) and the designer (appropriate design).

3 REFERENCE

[1] Simon, H.A.: A Behavioral Model of Rational Choice. Quarterly Journal of Economics, pp. 99-118, 1955

[2] Popper, K.R.: Logik der Sozialwissenschaften. Kölner Zeitschrift für Soziologie und Sozialpsychologie, Vol. 14, pp. 233-248, 1962

MAINTENANCE SYSTEM OF CONCRETE STRUCTURES DETERIORATED BY COMPLEX MECHANISM

Toyoaki Miyagawa, Kyoto University, Japan
Yoshihiro Masuda, Utsunomiya University, Japan
Hidenori Hamada, Port and Airport Research Institute, Japan

Katsunobu Demura, Nihon University, Japan
Takahumi Noguchi, Tokyo University, Japan
Atsuro Moriwake, Toa Corporation, Japan
Takao Ueda, Tokushima University, Japan

Keywords: concrete structures, complex deterioration, maintenance system

1 INTRODUCTION

Japan Concrete Institute (JCI) organized "The Technical Committee on Evaluation of Complex Deterioration of Concrete Structures and Its Maintenance Planning (1998 - 2000)" chaired by Toyoaki Miyagawa, to investigate subjects relating to maintenance of existing concrete structures deteriorated by complex mechanism for the intended period of their service life. Four working groups, "WG1: Evaluation of Complex Deterioration Mechanism", "WG2: Investigation of Adequate Maintenance Methods", "WG3: Evaluation of Repair Methods Using Removed Actual Bridge Girder" and "WG4: Preparing Guideline for Repair and Strengthening of Structures Deteriorated by Complex Mechanism" were organized by the committee and the basic strategies against complex deterioration of concrete structures were proposed. This paper presents a part of fruits obtained from the committee work.

2 SUMMARY OF THE COMMITTEE'S ACTIVITY

WG1 classified the complex deterioration into three different types considering these differences of interaction, namely "Independent type", "Synergistic type" and "Cause-effect type". In the independent complex deterioration, each deterioration occurs simultaneously, but a synergistic effect doesn't occur and a speed of deterioration is similar to the case of single deterioration. In the synergistic complex deterioration, a synergistic effect of combination of deteriorations accelerates the process of deterioration, compared with the case of single deterioration. In the cause-effect complex deterioration, a certain phenomenon caused by one deterioration mechanism initiates or propagates the other deterioration mechanism. In this case, one deterioration goes ahead of the other and usually each deterioration appears at the different time.

WG2 investigated to propose the way of thinking how to choose adequate maintenance measures against complex deterioration. Repair or strengthening methods are chosen to recover the degraded performance of deteriorated structures. Such countermeasures against complex deterioration were evaluated on the basis of " Protection from deterioration factors", "Restriction of the deterioration process", "Removal of the deterioration factor/inhibition of steel corrosion" and "Restoration of load bearing ability, rigidity and ductility". WG2 proposed the table which shows adequate countermeasures against the complex deterioration. In this table, applicable countermeasures are indicated by double or single circles in combination with each deterioration degree. By using this table, applicable countermeasures can be selected easily. However, as concrete structures have diversity, this selection method should be modified according to the condition of the structures.

Based on the above investigation, the committee has drafted the guidelines of countermeasures against complex deterioration. The guideline proposes the basic process and procedure of maintenance for concrete structures deteriorated by complex deterioration. Outline of the maintenance system is shown in **Fig. 1**. This figure shows two flows of procedures. An ideal maintenance way is that the performance degradation of structures due to complex deterioration is evaluated quantitatively and next, remedial measure is selected by performance verification referring to the evaluation of performance restoration due to applying the remedial measure. However, it is technically difficult to evaluate such performance degradation or restoration exactly at present. Therefore, more practical way is proposed in this guideline, that is, adequate remedial measures can be selected by considering deterioration degree or dominant deterioration mechanism. This guideline will be brushed up through further investigation or research for practical applications against complex deterioration.

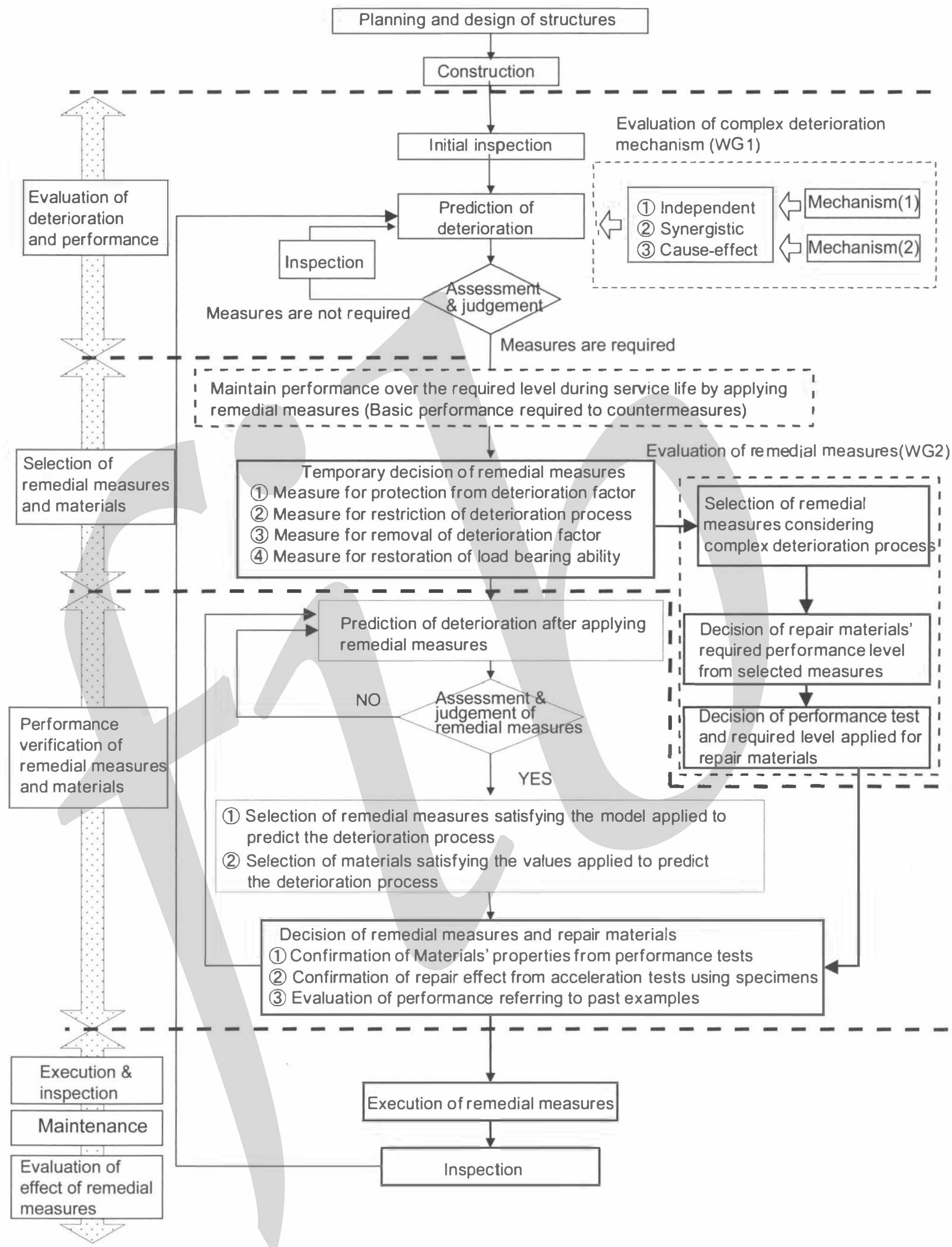

Fig. 1 Basic maintenance procedure for concrete structures considering the complex deterioration

TECHNOLOGY MANAGEMENT OF PRESTRESSED CONCRETE CONSTRUCTION COMPANIES: ITS NECESSITY AND PRACTICE

Kiyoroku Fukayama Kiyokazu Shinagawa Yo Takebe
PC Bridge Co., Ltd.
JAPAN

Jun Yamazaki
Nihon University
JAPAN

Keywords: technology management, prestressed concrete construction industry, human resources

1 INTRODUCTION

Japan's prestressed concrete (PC) construction industry has grown over the past fifty years by focusing on efforts to advance PC technology to meet demand for construction of better quality. Today, Japan is about to experience unprecedented changes both socially and economically.

This report suggests the technical guidelines which the PC construction industry should follow in the surroundings and discusses the technology management of PC construction companies.

2 CHANGE IN THE PC CONSTRUCTION INDUSTRY'S SURROUNDINGS

In Japan, the PC construction industry has, over the past fifty years, been engaged in the addition of applied technologies of its own development to PC technologies developed in Europe and the U.S. These technologies have been adapted mainly to the construction of bridges, and thereby have contributed to the development of social infrastructure such as roads and expressway networks. PC technology applications in 1999 [1] included bridges (84 percent), containers (5 percent), architecture (5 percent), disaster prevention facilities (2 percent), and other applications (4 percent).

It is not too much to say that the PC construction industry's growth to date is largely attributable to demand for the maintenance of social infrastructure, and, therefore, the industry is heavily dependent on national policies. The hottest issues in Japan include the assessment of the necessity and efficiency of social infrastructure investments and the reconsideration of a road construction fund as part of "structural reform", both of which have important implications for the PC industry.

Japan's industries, especially manufacturing and construction, are now experiencing the types of rapid environmental changes that had not taken place in the past fifty years. The PC construction industry is now at a critical turning point, just as all other industries are. **Fig. 1** shows the major elements of the new environment for the PC construction industry. It should be noted that these elements are linked together by an incentive chain, rather than working independently of one another.

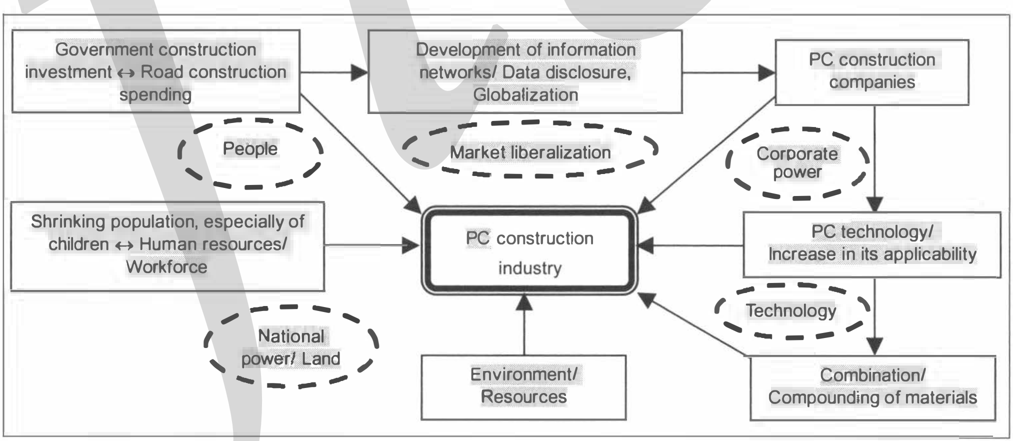

Fig. 1 New environment for the PC construction industry

3 CHALLENGES TO THE PC CONSTRUCTION INDUSTRY AND THEIR SOLUTION

PC technology has advanced in parallel with the development of social infrastructure, which has called for improvement in the quality of construction materials. The importance of PC in building up a stock of social infrastructure is emphasized by its increase in use as a material for road bridge extensions over the past twenty years. While the use of steel and RC has almost tripled and doubled, respectively, PC has shown a much greater increase, about 500 percent [2]. This is largely attributable to the advancement of PC technology.

The PC construction industry is an order-initiated industry and cannot survive solely through its own efforts. It is critical for the PC industry to escape from this fate and differentiate PC technology from its rivals, steel and RC.

The construction market is expected to shrink, increasing competition among steel, RC, and PC as major construction materials. The most appropriate response to this situation seems to be to develop technology for reducing impact on the entire society, e.g., environmental impact. Indicators of load reduction may include, industry-wise, improvement of labor productivity and, technology-wise, reduction of environmental impact and cut down of the life-cycle cost. To this end, it is important to shift focus from construction sites to product improvement and switch over from decentralized to intensive production systems, which, in our opinion, make it necessary to precast members.

4 NECESSITY OF TECHNOLOGY MANAGEMENT IN PC CONSTRUCTION COMPANIES

Technology management, as shown in **Fig. 2**, is a way to account for technology as a new element of the management resources of a company, in addition to the traditional elements of human resources, goods, and money. Technology management includes strategic and tactical planning and management of all stages of technology from its research and development to its application.

Technology management in the PC construction companies has to be shifted from the corporate management consisting of hardware such as financial resources, facilities and human power to the management focusing on software such as human resources and technology. The significance of this technology management is being recognized as a means to improve the vitality of companies.

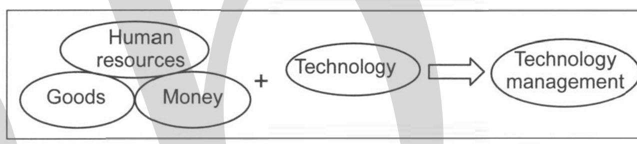

Fig. 2 Major elements of management resources

The requirements of the management of a PC construction company in the future are believed to have clear differences from those of its competitors. In order to differentiate itself from its competitors, it is necessary for a company to understand what kinds of technology it has accumulated and decide in which fields it is strong or weak in an objective manner. From the viewpoint of technology management, a company needs to know the technology it has based on a detailed analysis.

A PC construction company must aim to reduce the size of the balance sheet and yield profits by concentrating on its business using the unique technology it has, rather than simply expanding the company. It also needs to maintain and reconstruct its business by participating in maintenance, renewal and overseas markets aggressively. In order to do so, it is important to establish technology management unique to the company. It needs to have a clear picture of what it should be like in the future and inject management resources, instead of sticking only to maximizing current profits.

5 CONCLUSION

The most important guidelines for the mid- and long-term development of the PC construction industry are improvement of labor productivity, reduction of environmental impact and cut down of the life-cycle cost. As an effective way to achieve these goals, the "promotion of precast" is suggested.

Practice of "technology management" is necessary for the PC construction companies, which is in the severe surroundings. The practice will, we believe, lead to the development of PC technology. It would be emphasized, in particular, that the development of core engineers is what is required in "technology management".

ACKNOWLEDGMENT

The authors would like to thank Prof. Ryo Hirasawa (National Graduate Institute for Policy Studies in JAPAN) for his advise and support of this study.

REFERENCES

[1] Japan Prestressed Concrete Contractors Association: *Prestressed Concrete Year Book* 27, 2000 version, October 2000.

[2] Road Bureau, Ministry of Construction (current Ministry of Land, Infrastructure and Transport,): *Road Statistics Annual Report*, October 2000.

SOCIO-ECONOMIC IMPACT OF HONSHU-SHIKOKU BRIDGES

K. Yoshinaga, S. Kinoshita, S. Ohe, and K. Imai
Honshu-Shikoku Bridge Authority, Kobe, Japan

Keywords: big projects, innovative infrastructure, socio-economic Impact

1 INTRODUCTION

The land of Japan consists of four main islands, Hokkaido, Honshu, Shikoku, and Kyushu. Transportation by ships and airplanes had been often interrupted by bad weather such as winds, waves, or fogs. To eliminate such inconvenience and to promote balanced development of entire country, the government decided to construct three routes to connect between Honshu and Shikoku and established Honshu-Shikoku Bridge Authority (HSBA) to construct and maintain Honshu-Shikoku bridges in 1970.

Since Honshu and Shikoku are separated by the Seto-Inland Sea, long span bridges were needed to be constructed. Fig. 1 describes three routes of Honshu-Shikoku bridges. HSBA started its construction in 1970 and completed in 1999. These long span bridges were designed based on the design lifetime of 100 year. To provide the continuous highway network, many short and middle span bridges also had been constructed.

Although all three routes were opened in 1999, HSBA has tried to investigate the impact of Honshu-Shikoku bridges. Based on the investigations, this paper describes the socio-economic impact of Honshu-Shikoku bridges, which has been investigated until now.

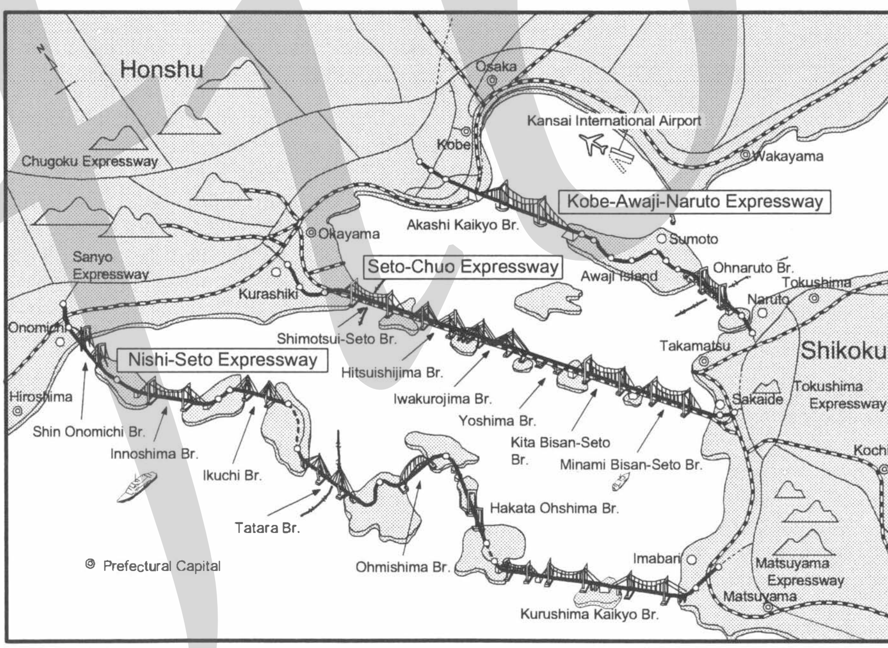

Fig. 1 Honshu-Shikoku Bridges

2 IMPACT OF HONSHU-SHIKOKU BRIDGES

After the completion of the Honshu-Shikoku bridges, traveling times between Honshu and Shikoku have been extremely reduced. It took about 270 minutes between Kobe and Tokushima before Kobe-Awaji-Naruto Expressway was opened to traffic. It was reduced to 100 minutes after the expressway was in service. It can also be found that the traveling times between Honshu and Shikoku by using Seto-Chuo and Nishi-Seto expressway were reduced to one third of those by ferry. Furthermore, traveling time between Okayama station and Sakaide station was reduced to one-forth after JR Seto-Ohashi line was in service.

Because of the reduction in traveling time, the traffic volume between Honshu and Shikoku increased from 16,951 vehicles per day in 1984 to 42,132 vehicles per day in 2000 as shown in Fig. 2. The traffic volume had increased approximately 2.5 times within this period. Since the increase of traffic volume in Japan within the same period was approximately 1.5 times, the traffic volume between Honshu and Shikoku was significantly increased.

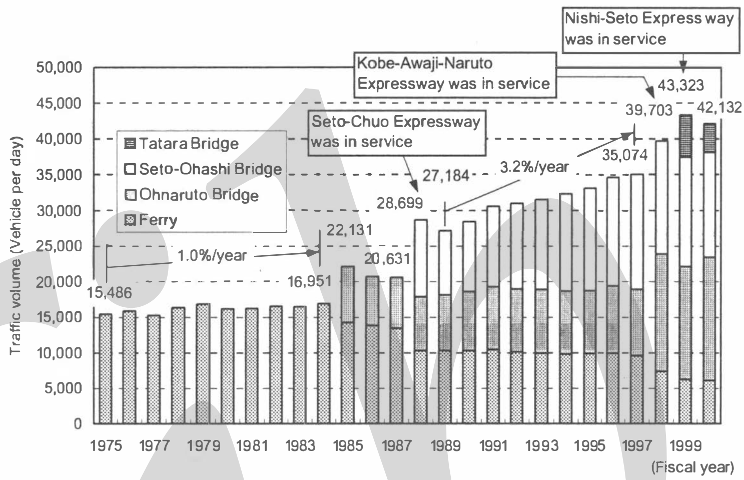

Fig. 2 Traffic volume between Honshu and Shikoku [1]

The Honshu-Shikoku bridges drastically reduced the psychological distances in the minds living in both Honshu and Shikoku. Therefore, in various human activities such as commuting and going to school, people traveling between Honshu and Shikoku have increased.

The time reduction in traveling time promoted such economic activities as agricultural, fishery, and manufacturing productions. Therefore, transportation of these products has been increased.

Since human and economic activities are activated, investments were also increased. New factories in Shikoku from 1988 to 1999 were 1.25 times of those from 1976 to 1987. This surpasses the national average of 1.13. This proves that proper conditions to deliver products on demand can be established in Shikoku by Honshu-Shikoku bridges and highway networks.

The above impacts have been measured by using a macro economic model and a direct benefit analysis. The total amount of direct benefit in 2000 is estimated to be 250 billion yen. Furthermore, the total amount of direct benefit over 40 years from 2000 is estimated and discounted to be 8.7 trillion yen as today's value. On the other hand, sum of construction and maintenance costs is estimated and discounted to be 5.2 trillion yen as today's value. The benefit over cost, therefore, is 1.7.

Current trends of personal income and population in Shikoku proved that Honshu-Shikoku bridges have promoted balanced development of entire country.

Various investigations revealed that Honshu-Shikoku bridges activated human and economic activities, increased investments, and contributed to balanced development of entire country. Therefore, Honshu-Shikoku bridges have become an indispensable social infrastructure in Shikoku, Chugoku, and Kinki regions.

REFERENCES

[1] Economic department, Planning division, Honshu-Shikoku Bridge Authority: Linkage, Socio-economic impact of Honshu-Shikoku bridges. Jul., 2001 (in Japanese)

WEB-BASED SAFETY MANAGEMENT SYSTEM IN CONSTRUCTION OF PRESTRESSED CONCRETE BRIDGES

Jiandong Zhang
P.S. Corporation
JAPAN

Michiyuki Hirokane
Kansai University
JAPAN

Hideyuki Konishi
Japan Bridge Corporation
JAPAN

Keywords: safety management, accident, web-based system, xml

1 INTRODUCTION

In the present study, we attempted to develop the safety management system for workers and site foremen who are working in the erection sites of PC bridges. The information on accidents can be retrieved and inputted by using a microcomputer. The database for this system was described in extensible markup language (XML) so that workers and site foremen can retrieve information from any erection sites through the world wide web (Web) and use these information for their safety planning and management. For example, after an erection method was decided, workers and their site foreman will retrieve information on accidents associated with the erecting method and, using of the retrieved information, make safety planning. Moreover, as the XML is used in this system as mentioned above, information can, by adding tags to specific items of information, be analyzed by type of accident, date and time, age, years of experience, degree of injury, and so on. Furthermore, by using one and the same format, information can be shared among all concerned and a large number of accident cases can be accumulated easily.

2 SAFETY MANAGEMENT SYSTEM

After accessing to the address for this system, the top page shown in **Fig.1** is displayed. Here, one operation can be selected from 3 menus such as input, retrieval and analysis of accident case.

2.1 Input of accident cases

In this research, the past actual accident cases are described in XML, but they are still insufficient for diffusing safety consciousness. It is important to grasp enough of the causes and the measures of actual accidents for preventing similar accidents. For this purpose, it is necessary to accumulate the past accident cases as much as possible. At the same time, it is necessary to prepare the friendly interface so that workers and their site foreman can input easily the information for accidents that may occur in the near future.

This system with the above interface was constructed by using JAVA language. **Fig.2** is a part of page for input of accident information that had occurred in the erecting method of false-work. It was considered to realize the simplification of input by the check box or the pull-down menu as much as possible. By realizing the above input method, information can be standardized and shared among all concerned, and a large number of accident cases can be accumulated easily.

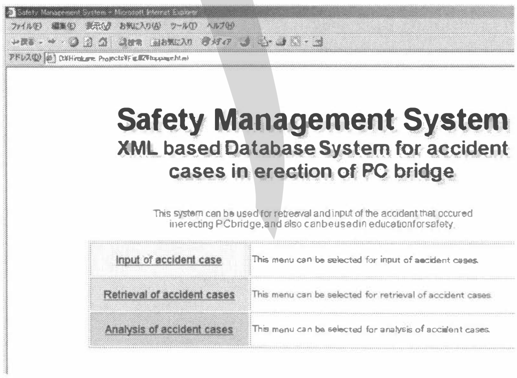

Fig.1 Top page

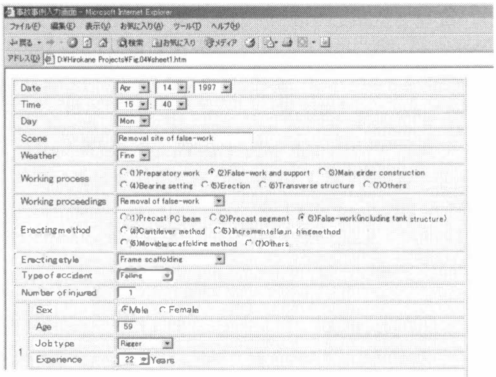

Fig.2 Page for input of accident case

2.2 Retrieval of accident cases

In case that the user accesses to this system and selects the retrieval of accident cases in the top page shown in **Fig.1**, the top page for the retrieval of accident cases appears on the display, which is the first step of retrieval of relevant information. On this screen, the user selects how to retrieve the accident cases. If the user selects the retrieval method by the working process / proceeding, the list for the working process and proceeding appears on the display shown in **Fig.3**. In case that the user selects the categories for the working process and proceeding in order, a list of relevant accident cases appears on the display, the page of detail for the selected accident case is browsed.

2.3 Analysis of accident cases

The circle graph of **Fig.4** shows an example of analysis results, the relation between the years of experience and the number of accidents. The years of experience is classified into 6 sections. About 40% of all accidents are occurring among the workers with experience less than 5 years. As the years of experience build up, the number of accidents decreases. The high frequency of occurrence of accidents among workers with experience less than 5 years seems to imply that there is a high risk of accidents when they get used to work. Among the workers with experience less than 1 year, 5 % of all accidents are occurring. This number is less than the rate of the workers with experience 1 to 5 years because the workers with experience less than 1 year aren't engaged in the dangerous works.

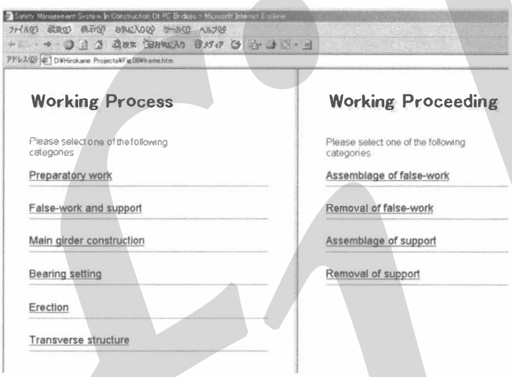

Fig.3 selection of working process/proceeding

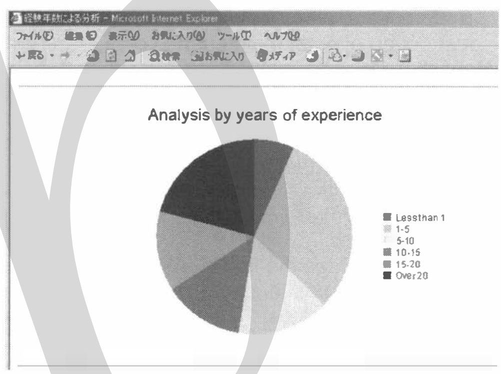

Fig.4 Analysis by years of experience

3 CONCLUSIONS

The safety management system for workers and site foremen to retrieve and input information on accidents occurred in the erection work of PC bridges was developed. The features of the system are summarized below.

(1) Easiness of Operation

This system was developed by the language that can be used on the Web such as HTML, XML, JAVA and so on. Therefore, the workers and the site foremen can, from anywhere that a microcomputer and a telephone line are available, retrieve the relevant information from the database through the Web. Besides, by making good use of the system, the workers and the site foremen at various erection sites can improve their safety programs in accordance with the erecting style, and safety education and training can also be conducted effectively.

(2) Information Sharing

By using one and the same format, it is possible to standardize and share accident information among all concerned, and a large number of accident cases can be accumulated easily, which enable us to develop a more practical and effective system.

(3) Visualization of Accident Cases

This system offers visualized information on the situations in which accidents occurred so that the workers and the site foremen can have pseudo experience of accidents in their offices. Besides, after the erecting method is decided, they can retrieve information on accidents associated with the erecting method and, using the retrieved information, make safety planning. Moreover, as each accident case is described in XML, the accident information can, by adding tags to specific items of information, be analyzed by type of accident, time, years of experience and so on.

A PRACTICAL BRIDGE MANAGEMENT SYSTEM FOR EXISTING CONCRETE BRIDGES

Ayaho Miyamoto
Prof., Dr. Eng., Dept. of Computer & Systems Engineering,
Yamaguchi University, Ube 755, Japan

Keywords: Bridge Management System, Concrete Bridge, LCC, Optimal Maintenance Planning

Recently, the maintenance planning of existing bridges has become a major social concern, because the number of deteriorated bridges is increasing owing to factors such as the increasing volume of traffic, increasing weight of road vehicles, and structural aging. Thus, the necessity of developing a computer-aided decision support system that includes not only a serviceability assessment system but also a life cycle cost minimization system has been pointed out for maintenance, diagnosis, repair and rehabilitation of existing bridges [1].

The authors have been developing a practical Bridge Management System that is referred to as the Japanese Bridge Management System (***J-BMS***) integrated with the Concrete Bridge Rating Expert System (***BREX***) that can be used to evaluate the serviceability of existing concrete bridges [2,3,4]. The J-BMS uses multi-layered neural networks to predict deterioration processes in existing bridges, construct an optimal maintenance plan for repair and/or strengthening measures based on minimizing life-cycle cost and maximizing quality, and also estimate the maintenance cost. In this system, the Genetic Algorithm (GA) technique was used to search for an approximation of the optimal maintenance plan. In this paper, it will be demonstrated concretely how the J-BMS works on a computer by using some screen displays. And also, by applying this system to an existing bridge, it has been verified that employed system is effective.

Fig. 1 shows the overall configuration of the J-BMS. The type of bridge considered for the purposes of this study is the reinforced concrete (RC) bridge, and main girders and deck slabs are the members considered here.

In the J-BMS, as the first step, the system was divided into three major components according to the basic flow of maintenance (inspection→diagnosis→corrective action). They are the "Recording Section", the "Diagnosis & Evaluation Section" and the "Decision & Remedies Section". The arrows in Figure 1 show the directions of data flow.

The data acquisition in the J-BMS makes a combination of a large number of detailed visual inspections and some simple nondestructive inspections for a target existing bridge, and stores inspection results into a data base ((1)), and, using the inspection data and bridge inventory data thus obtained, performs a damage assessment of the target bridge under consideration ((2)). Then, deterioration is predicted on the basis of the degree of structural soundness determined through deterioration assessment ((3)). An optimal maintenance plan is then drawn up according to a deterioration status report output by the deterioration prediction function ((4)). The deterioration factor inference function infers damage-causing factors from the inspection and bridge data collected thus far ((5)). Repair or strengthening methods to be recommended are selected in view of the damage-causing factors thus inferred ((6)).

Fig. 2 shows the startup screen of the BMS. Clicking on one of the buttons shown starts the corresponding system. On the screen, clicking on the "Concrete Bridge Rating Expert System (BREX)/Maintenance Plan Optimization System" button or the "Maintenance Decision Support System" button activates the process shown in the left half of **Fig. 1** (deterioration assessment→deterioration prediction→optimization of maintenance plan) or the process in the right half (inference of deterioration factors→selection of maintenance measures), respectively. Clicking on the "Data Base Management System" button starts the data base system.

Since the three systems can be run independently, the user can start the BMS from any of the three systems (functions). For example, to view a bridge inventory or inspection log or to enter new data, the user clicks on "Data Base Management System." To use an existing inspection data file in the data base or perform damage assessment or maintenance planning based on new inspection data, the user starts the "Concrete Bridge Rating Expert System (BREX)" or the "Maintenance Plan Optimization System". To infer factors contributing to the damage encountered or make a decision as to maintenance actions to be taken to slow the progress of damage, the "Maintenance Decision Support System" can be activated.

Sound evaluation of existing bridges based on on-site investigations and inspections often depends on domain experts' knowledge and experience and is not necessarily made quantitatively. Infrastructure including bridges, however, is expanding steadily, and the number of structures to be maintained is increasing, necessitating the development of methodologies of rational and economical maintenance. One option is to develop and put to practical use decision support systems utilizing the computer and information technologies. In this paper, the authors did their best to show detailed examples, wherever possible, of various functions of the newly developed bridge management system designed mainly for concrete bridges.

REFERENCES

[1] J.E. Roberts, "Bridge Management for the 21st Century", *Maintaining the Deteriorating Civil Infrastructures* (Edited by Miyamoto, A., and Frangopol, D. A.), Yamaguchi University, Yamaguchi, pp 1-13, (2002).

[2] Miyamoto, "Development of a Bridge Management System (*J-BMS*) in Japan", *Life-Cycle Cost Analysis and Design of Civil Infrastructure Systems* (Edited by Frangopol, D. A. and Furuta, H.), ASCE, Virginia, pp 179-221, (2001).

[3] K. Kawamura, H. Nakamura, and A. Miyamoto, "Development of Concrete Bridge Rating Expert System (*BREX*) in Japan", *Life-Cycle Cost Analysis and Design of Civil Infrastructure Systems* (Edited by Frangopol, D. A. and Furuta, H.), ASCE, Virginia, pp 161-178, (2001).

[4] Miyamoto, et al, "Development of a bridge management system for existing bridges", *Journal of Advances in Engineering Software Computers & Structures*, Vol. **32/10-11,** pp. 821-833, (2001).

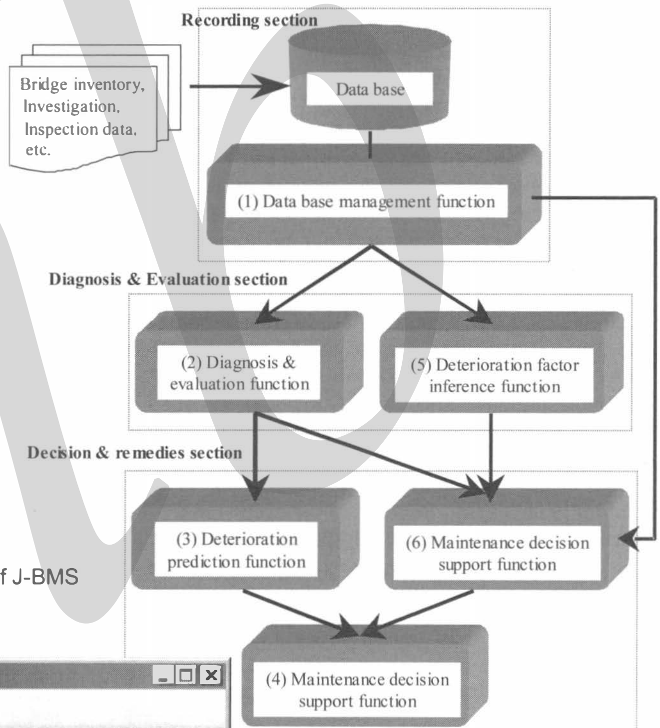

Fig. 1 System configuration of J-BMS

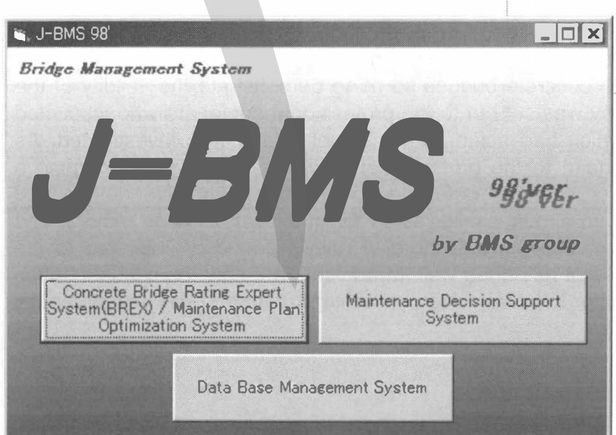

Fig. 2 Starting screen of J-BMS

BRIDGE MAINTENANCE STRATEGIES CONSIDERING DETERIORATION FACTORS IN BRIDGE MANAGEMENT SYSTEM

Hideaki Nakamura
Yamaguchi University
JAPAN

Hiroshi Yokoyama
Abe Kogyosho Co., Ltd
JAPAN

Kei Kawamura
Yamaguchi University
JAPAN

Keywords: Bridges maintenance, BMS(Bridge Management System), Cause-Effect Network

In Japan, many concrete bridges were constructed during the period of high economic growth. However, many of theses bridges have seriously deteriorated in resent year. In order to use the concrete bridges for a long period, it is necessary to maintain the concrete bridges appropriately. Many bridges must be repaired or strengthened depending on the severity of their deterioration. However, due to the limited budget for maintenance, it is impossible to perform all the demanded maintenance works[1]. Therefore, the bridges must be maintained reasonably and effectively within the limited budget. In order to maintain the bridge effectively, it is important to restore the bridge damage as well as to suppress the deterioration factors.

Under such a background, authors have been developing a Bridge Management System (J-BMS) as an integrated system which enables to support the bridge maintenance works[2]. In this study, a new sub-system was developed as a function of the J-BMS. This sub-system presumes the deterioration factor from the inspection data and non-destructive testing. The position of this sub-system in the J-BMS is shown in **Fig.1**.

Technical specification data, inspection data, and various data concerning bridge maintenance are stored in the data base (①). The performance of the each bridge members is evaluated using the obtained inspection data and the technical specifications of the target bridge. This evaluation is performed using a program referred to as the Concrete Bridge Rating Expert System (②). Then, based on the results of the expert system, the present state of deterioration can be characterized and the remaining life of the bridge can be estimated using the predicted function of deterioration (③). If the present remaining life calculated by the J-BMS does not exceed the expected service life, the rehabilitation strategy is obtained from the prediction curve according to the cost and effect of repairs and strengthening. This strategy includes various maintenance plans provided by cost minimization or quality maximization (④). However, the maintenance strategy planned in the present J-BMS does not consider the deterioration factor. Therefore, the deterioration factor keeps acting even if damage is restored, so the same damage might happen again, and the output maintenance strategy by the system is inefficient. In order to solve this problem, the deterioration factor estimation system which presumed the deterioration factor from the inspection data was newly constructed (⑤). Furthermore, the maintenance strategy was planned from the maintenance strategy planning system (⑥). This sub-system involves arranging various causal relations of the damage occurring in the bridge and the acting deterioration factor. The deterioration factor is reasoned according to the cause-effect network expressed the causal relation[3]. The cause-effect network for the bridge slab is shown in **Fig.2** as an example of the cause-effect network. The square shows damage, and the circle shows the deterioration factor in the figure. The flow of the inference is shown in **Fig.3**.

This sub-system was applied to existing concrete bridges so as to demonstrate the validity of the proposed system. The questionnaire survey was set out to the professional engineers who inspected the bridge and the deterioration factor which had acted on the target bridge was investigated. As compared with the result of the questionnaire to the professional engineers, this system outputs a different score for the deterioration factor such as defective construction, defective design and defective material. This system outputted an almost similar score for other deterioration factors, and could reason well. In order to solve this problem in the future, a rule is added or improved to the system for the deterioration factor which is not reasoned well. In addition, not only the causal relation between damage and the deterioration factor but also rules concerning traffic and the environmental condition are added to this system.

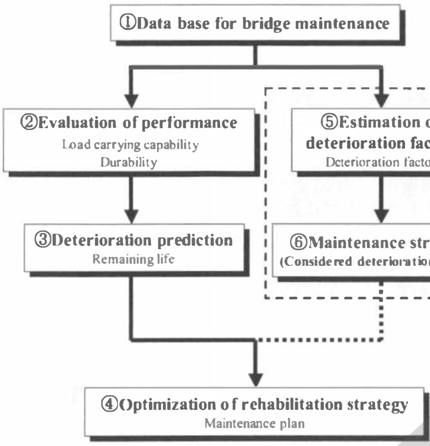

Fig.1 Position in the J-BMS

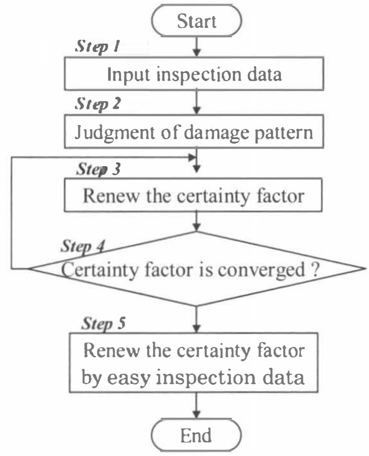

Fig.3 Flow chart of inference process

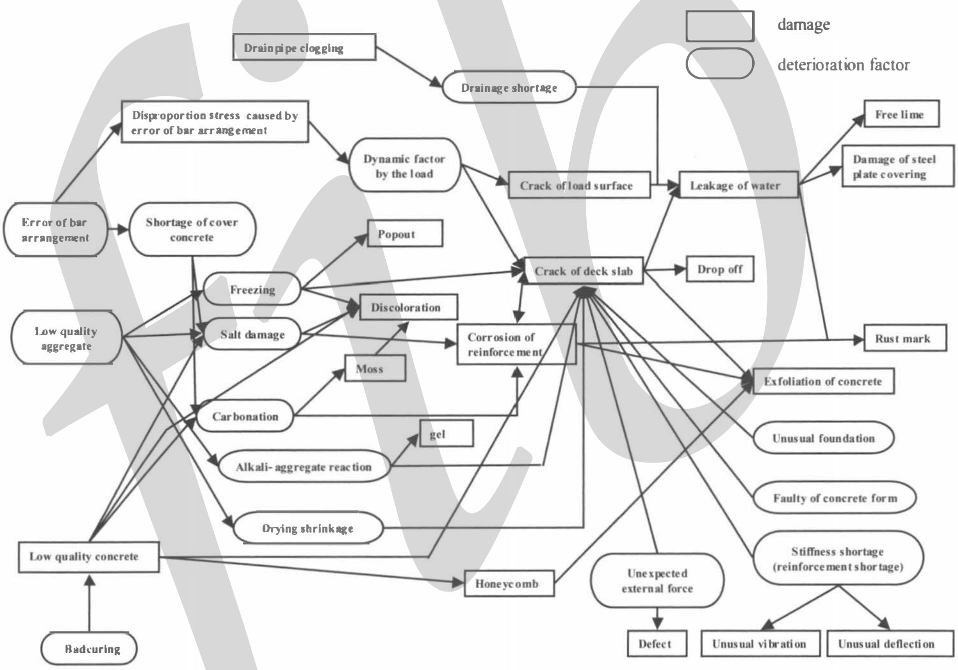

Fig.2 Image of cause-effect network (deck slab)

REFERENCES

[1] Kazuhiro Nishikawa, "Longevity and maintenance of road bridge", *Journal of structural mechanics and earthquake engineering*, JSCE, No.501/I-29 pp.1-10 (1994).(Japanese)

[2] Ayaho Miyamoto, Kei Kawamura and Hideaki Nakamura, "Multiobjective optimization of maintenance planning for existing bridges by using bridge management system (BMS)", *Journal of construction management and engineering*, JSCE, No.588/VI-38 pp.191-208, (1998). (Japanese)

[3] Ichizou Mikami, Chitoshi MIKI, Shigenori Tanaka and Takanori Tsuchida, "Inference procedure for selection method of retrofitting fatigue damages in steel bridge based on cause-effect network", *Journal of Structural Engineering*, JSCE, Vol.36A, pp.1003-1014, (1990). (Japanese)

BRIDGE DECK INSPECTION AND MAINTENANCE MANAGEMENT DATABASE SYSTEM USING UBEIS

Mohammed E. Haque, Ph.D., P.E.
Associate Professor, Department of Construction Science
Texas A&M University, College Station, TX 77843-3137, USA

Keywords: bridge deck inspection, bridge elements, bridge management system, condition rating, load rating

INTRODUCTION

The planning and programming of remedial and preventative maintenance and repair work, or even bridge-deck replacement, with the minimum effect upon traffic, are dependent upon systematic and detailed inspection and the expert assessment of data. An effective, timely, and economic rehabilitation or repair to a highway bridge deck structure demands a proper understanding of its existing condition through in-depth inspection. The "2001 Report Card for America's Infrastructure", which was released by the American Society of Civil Engineers (ASCE), United States' bridges received the Grade of "C" (where grade A = Exceptional, B= Good, C = Fair, D = Poor, and F = Inadequate). The Federal Highway Administration's (FHwA's) strategic plan states that by 2008 less than 25% of the nation's bridges should be classified as deficient. They are either in poor physical condition, not structurally capable of supporting today's legal truckloads, or not capable of meeting current minimum geometric standards. A major effort is now needed to define which bridges need attention and to rehabilitate or replace these structures. With ailing bridges as with ailing people, the first step to a cure is a proper diagnosis. Any effective rehabilitation or repair to a given structure demands first a proper understanding of its existing condition.

This paper addresses an innovative way of managing bridge deck inspection records using a **U**niform **B**ridge **E**lement **I**dentification **S**ystem (*UBEIS).* This system generates a grid of structural deck segments within a single span, and each of these grids is uniquely identifiable. The *UBEIS* is a generalized multi-dimensional coordinate system, which consists of a string of alphanumeric characters to provide a unique global identification for bridge structural elements. It does not require any structural detail drawings, such as framing plan, cross-sections, etc., to identify a unique structural element. This system is very easy to use for short to very long span bridges including cable suspension, truss bridges, and viaducts.

UBEIS – A GENERALIZED COORDINATE SYSTEM FOR BRIDGE ELEMENTS

Each bridge can be divided into sections identified by the bridge identification number (BIN) [1]. BIN is a unique seven-character designation assigned to each individual bridge. In UBEIS, the numbering sequence in each BIN increases along the length of the bridge, from the beginning to the end of the BIN. The numbering system for the bridge transverse direction increases from left to right, with the observer (inspector) looking towards the end of the BIN. Each BIN structure is divided into spans, and each span is divided into panels by the floor beams [2-3].

A few examples of UBEIS are provided in this section to illustrate how the uniform bridge element identification system provides a unique designation for each bridge element. The author in his earlier paper [3] published the details of UBEIS.

Stringer: A stringer location is defined by span, the panel and the position within the panel, and can be expressed as (Fig. 1):

SN xxx P xxx ST xxx

Where SN = span; P = panel; ST = stringer; and xxx = three digit location number. For example, in Fig. 1, the SN 004 P 002 ST 002 designates the second stringer from left with the inspector looking towards higher span (i.e., towards the end of the particular BIN) for the second panel of span 4.

Bridge Deck: Bridge deck is identified by span, panel, and deck subpanel (Fig. 1) and listed as

SN xxx P xxx DST xxx

where DSP = Deck subpanel, which is in between two adjacent stringers/girders.

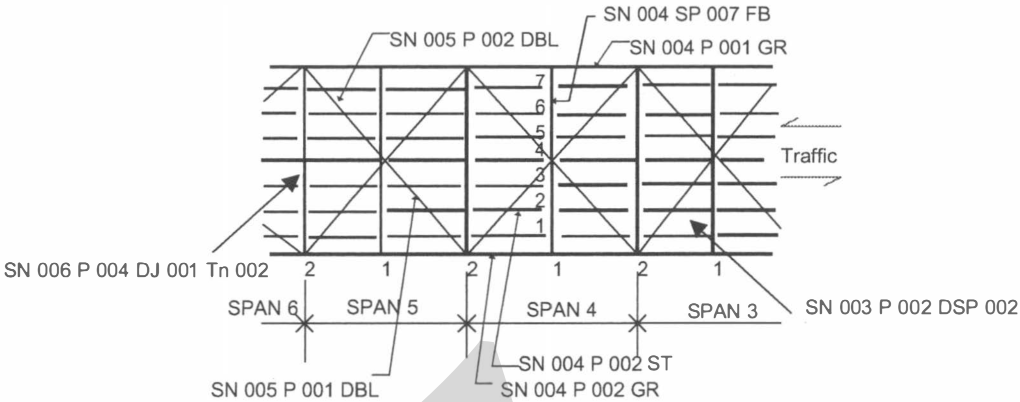

Fig. 1 Typical superstructure elements

UBEIS can be easily implemented to a bridge management system database using Window based EXCEL, LOTUS 1-2-3, or some other database systems, such as Access, Dbase, FoxPro, etc. This type of system can be used to track the life long history of the bridge components, to identify the needs for future repair actions, to determine the members need to be inspected/monitored more frequently, and to estimate related costs and other impacts. Each bridge element represents a record in the database system for which an array of information can be stored. As an example, a record which is defined by UBEIS, includes the information - bridge name and BIN, structural type and element classification, structural and paint condition ratings and information, inventory and operating load ratings, both as-built and actual condition, structural and safety flag information, special emphasis inspection intensity categories, inspection report including photographs, scanned field sketch, drawings, etc., date of inspection, inspection company and inspector, and comments.

CONCLUSIONS

This paper addresses an innovative way of managing bridge deck inspection records using a **U**niform **B**ridge **E**lement **I**dentification **S**ystem (*UBEIS*). This system generates a grid of structural deck segments within a single span, and each of these grids is uniquely identifiable. The *UBEIS* is a generalized multi-dimensional coordinate system, which consists of a string of alphanumeric characters to provide a unique global identification for bridge structural elements. It does not require any structural detail drawings, such as framing plan, cross-sections, etc., to identify a unique structural element. UBEIS is easy to implement into a menu driven database system, geared to easy data entry, sorting, updating and report generation. Each one of the bridge elements can be represented as a record in the database for which an array of information, such structural and paint condition ratings, load ratings, structural and safety flag information, structural importance, field sketches, photographs, scanned/CADD drawings and technical specifications, etc. can be stored. This type of system enables the engineer to evaluate future rehabilitation needs, to track the condition of structurally deficient members, and to keep rehabilitation/replacement history of the bridge. All this information can be stored on compact discs, which certainly eliminate the mass of document-management problems.

REFERENCES

[1] Bridge inspection manual-82. New York State Dept. of Transportation, (1982).
[2] Haque, M.E., and Pongponart, K.,"Integrated Multimedia Uniform Bridge Element Identification System Database for Bridge Inspection and Maintenance," *Transportation Research Record: Journal of the Transportation Research Board*, pp. 1-5, Record No. 1697, (2000).
[3] Haque, M.E., "Uniform Bridge Element Identification System (UBEIS) for Database Management for Roadway Bridges," *ASCE Journal of Bridge Engineering*, Vol. 2, No.4, pp. 183-188, (1997).

DEVELOPMENT OF BRIDGE MANAGEMENT SYSTEM FOR EXPRESSWAY BRIDGES IN JAPAN

Kazuaki YOKOYAMA Tadashi KANNO Koichiro SHITOU Yoshiyuki MOMIYAMA
Expressway Research Institute of Japan Highway Public Corporation, JAPAN

Keywords: Bridge, Life cycle, Management system, Repair, Replacement

1 INTRODUCTION

The key issues for minimizing the life cycle costs for bridges from the construction to the maintenance are to design and build bridges economically and with high durability in the construction phase and to maintain the bridge structure by the optimum methods at the optimum timing in the maintenance phase. As the number of bridge structures to be managed will increase further, it will be essential to establish a Bridge Management System (BMS) as soon as possible in order to ensure the progress in bridge maintenance according to the plan.

This BMS optimizes the repair methods, timing and costs in correspondence with the soundness of bridge structures and the predictions of their deterioration through an analysis of bridge maintenance database. The database includes the bridge inventory, initial inspections and the record of subsequent follow-up inspections.

This study describes a systematic overview of the practical development of a system (BMS prototype). It also discusses the determination of the optimum repair and the timing in order to achieve life cycle cost optimization for bridges.

2 OUTLINE OF BMS PROTOTYPE

2.1 SYSTEM CONFIGURATION OF BMS PROTOTYPE

As can be seen in Fig.1, the BMS prototype developed in this research was developed as a system for supporting repair and improvement planning while accessing to the integrated maintenance database storing bridge inventory, inspection records and repair/improvement histories. It is also intended for the deterioration prediction, the structural soundness evaluation, and the determination of the repair and improvement methods of bridges. A large number of the bridge maintenance information and extensive research findings are available in academic studies on this topic.

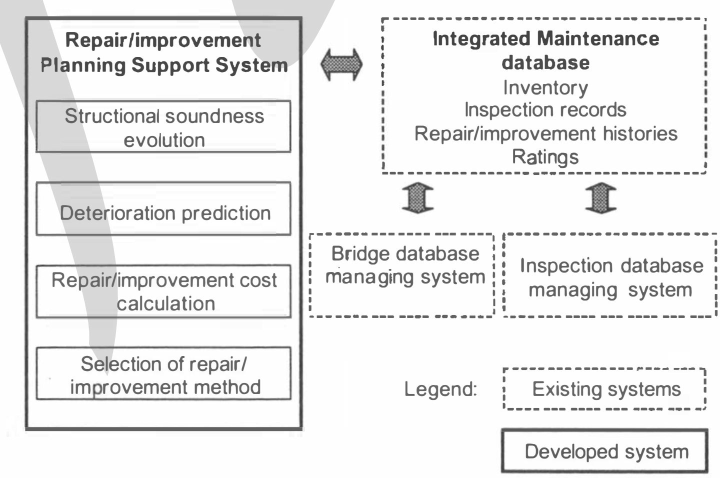

Fig.1 System Configuration of the BMS Prototype

2.2 STRUCTURAL SOUNDNESS EVALUATION

Regarding the reinforced concrete deck, the structural soundness was evaluated according to cumulative damage rule focusing on the punching shear strength. As for the bearing and joint, the replacement cycle was determined from the analysis of the repair. (See Fig.2 for example.)

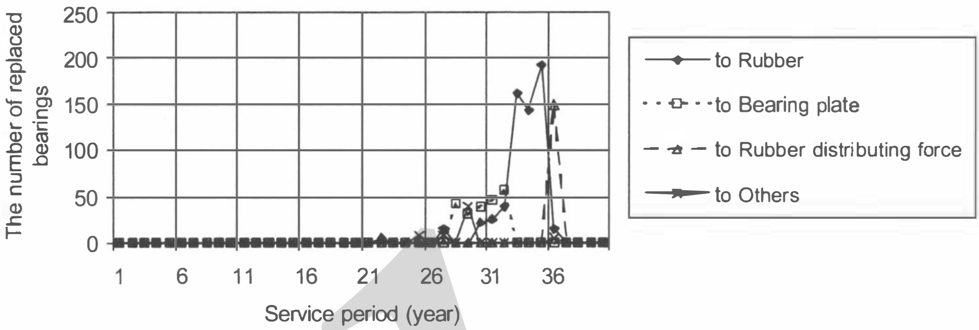

Fig.2 Replacement Cycle of Linear Bearings

2.3 LIFE CYCLE COST ACCOUNTING

As for life cycle cost accounting, a system capable of outputting the total cost estimation has been developed. To do this, the average unit repair cost was calculated statistically and the time of repair execution was optimized from analyses of the present maintenance, improvement costs and deterioration curve. The applicable deflator and social discount rate are taken into consideration.

The repair/improvement method and its unit cost for the bridge member can be revised and/or added at any time in response to future acquisition of maintenance information and introduction of new technology and new construction methods. We have also calculated the life cycle cost of life scenarios assumed to be performed on various repairs and improvements that have been applied to the individual bridge members. The results are shown on the screen, with the scenario resulting in the smallest life cycle cost given as the optimum proposal.

3 PERSPECTIVE OF STUDY

The presented study had been undertaken to develop a BMS prototype on a tentative use to support for decision making extensively that is required for bridge maintenance and management.

The problems that will be solved in the near future are summarized as follows:

1. BMS prototype should be put in the actual service environment to be criticized from the viewpoint of the bridge administrator.
2. Deterioration prediction must be extended to all elements in the same way. Structural soundness can be considered as assembly of structural soundness of members.
3. The prototype will also be applied to concrete bridges by allowing for the various types of deterioration factors including salt damage and neutralization problems that were described in "Concrete Practice, Maintenance and Management, The Japan Society of Civil Engineers" published in January 2001.
4. Development is scheduled in order to launch a system that can evaluate cost-benefit ratio through a linkage on the intranet with other management systems for road structures.

REFERENCES

[1] Kanno T, Y. Kamihigashi and H. Ishida: Experimentally Derived Cost-Effective Planning of Bridge Deck Rehabilitation by Steel Plate Bonding, Transportation Research Record 1642, pp21-26, 1999.

[2] Thompson P. D, E. P. Small, M. Johnson and A. R. Marshall: The Pontis Bridge Management System, Structural Engineering International, pp303-308, 1998.4

HEALTHINESS EVALUATIONS DERIVED FROM EXPERIMENTS, STATISTICAL ANALYSES AND EXPERT SYSTEM

Yoshiyuki Momiyama Tadashi Kanno Kazuaki Yokoyama Koichiro Shito Tsutomu Akiba
Expressway Research Institute of Japan Highway Public Corporation CTI Engineering Co.,Ltd

Keywords : maintenance, inspection, efficiency, BMS, neural network

1 INTRODUCTION

As of March 2002, the total length of roads managed by Japan Highway Public Corporation (JH) is 6,949 km, and bridges account for 14.5% of that total. The average service life of a road is about 18 years. Since the total length of bridges continues to increase as new bridges are constructed to form a road network, there is an urgent need to build a bridge management system (BMS) for systematic maintenance of bridges.[1],[2],[3],[4]

Bridge inspections conducted by JH consist mostly of visual inspections. At bridge sites that are not accessible for visual inspection, such as sites in urban or mountain areas, inspection ratings tend to be affected by the experience of individual inspectors. Inspection results reported by inspectors are then evaluated by bridge experts for soundness rating, and these experts also have varied experience. It was decided, therefore, to develop a soundness assessment technique using the neural network method suitable for the formulation of rules of knowledge and experience of inspectors and bridge experts, which are difficult to quantify.

In this study, changes over time in soundness ratings calculated from inspection results for different bridge elements (see Figure 1) were analyzed statistically, and soundness ratings of bridge elements by experts and results obtained from a neural network model were compared. The comparison showed a percentage of agreement with domain expert ratings of 74 percent, indicating that the soundness rating method using a neural network model is reliable.

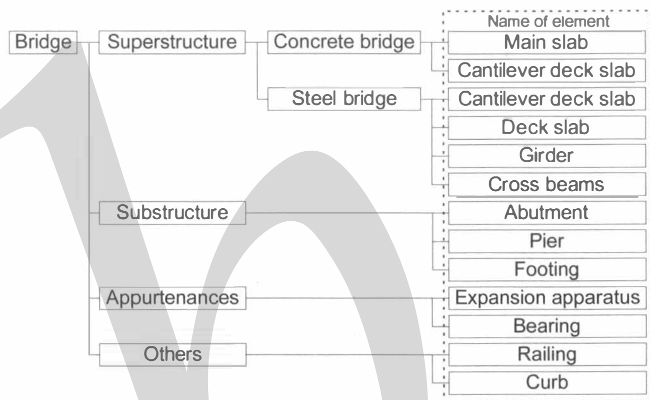

Fig. 1 Bridge elements

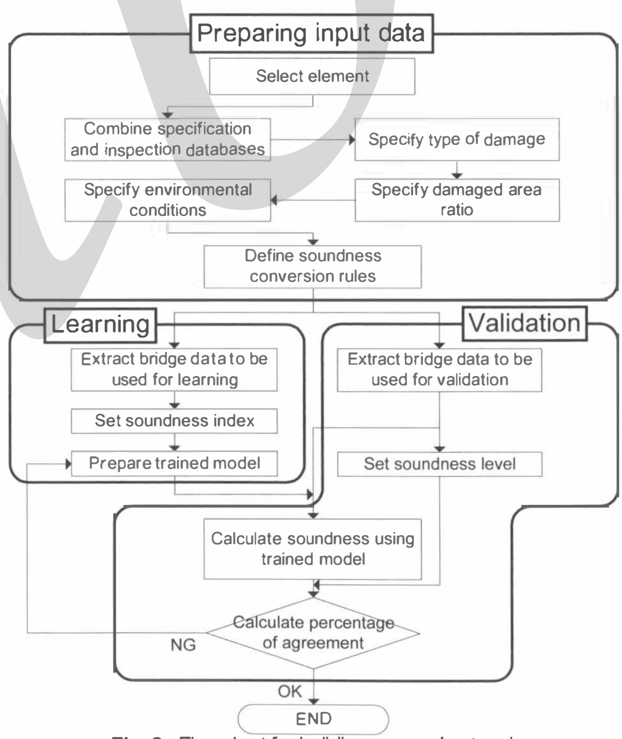

Fig. 2 Flowchart for building a neural network model for soundness rating

2 BUILDING A NEURAL NETWORK MODEL FOR SOUNDNESS RATING

The work flow for building the neural network model is shown in Fig. 2. A neural network model for soundness rating was built using JH's inspection database for the bridge elements concerned.
To prepare the parameters of the neural network model, the results of soundness rating made by bridge experts and the inspection database were used as teacher data. Outputs of the model were compared with expert ratings of bridges whose data had not been used for the teaching, and validity of the model outputs were evaluated in terms of the percentage of agreement with expert ratings.

Reinforced concrete hollow-slab bridges account for 27.7% (more than any other type of bridge) of all bridges under JH's jurisdiction. For this reason, it was decided to consider main slabs of reinforced concrete hollow-slab bridges for the purposes of this study.

3 VALIDATION OF THE NEURAL NETWORK MODEL

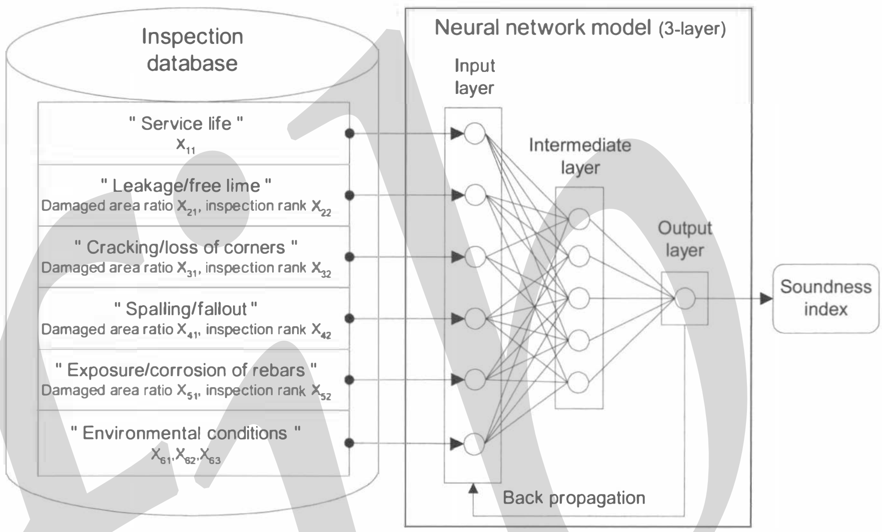

Fig. 3 Neural network model for soundness rating

Input data were prepared by following the steps shown in Fig. 3.The data used to evaluate the validity of the neural network model were prepared by randomly extracting 250 data sets (i.e., data for 250 bridges) from the inspection database (different from the data used for learning).

Fig. 4 compares soundness ratings given by experts and the neural network model. For 186 out of the 250 bridges, the rating given by the neural network model agreed with the ratings given by the experts (percentage of agreement: 74%). The coefficient of correlation R, which indicates the degree of reliability of the model, was 0.710. Thus, validity of soundness rating using the neural network model was confirmed.

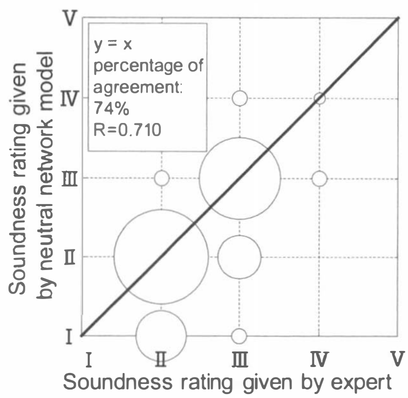

Fig. 4 Comparison of soundness ratings

REFERENCES

[1] Momiyama, Y.: Concrete structure management system (in Japanese). Prestressed Concrete, Vol. 43, No. 1, 36-43. 2001.
[2] Yokoyama, Kanno, Shito and Momiyama: Development of Bridge Management System for Expressway. Yamaguchi University LCC Workshop. 2001.
[3] Thompson, P., Small, E., Johnson, M. and Marshall, A.: The Pontis Bridge Management System. Structural Engineering International, Vol. 8, 303-308. 1998.
[4] Hawk, H. and Small, E.: The BRIDGIT Bridge Management System. Structural Engineering International, Vol. 8, 309-314. 1998.

APPLICATION OF ELECTROCHEMICAL TECHNIQUES FOR MAINTENANCE OF CORRODING REINFORCED CONCRETE STRUCTURES

C. L. Page
University of Leeds, School of Civil Engineering, Leeds LS2 9JT, UK

Keywords: service-life prediction, reinforced concrete, cathodic protection, cathodic prevention, sacrificial anodes, realkalisation, electrochemical chloride extraction.

1 INTRODUCTION

There is little difficulty in designing reinforced concrete structures for a corrosion-free 'safe-life' in most conditions by specifying the quality and thickness of the cover concrete appropriately. This is not so, however, when structures are exposed to chloride-laden environments for long expected lifetimes. Although efforts are now being made to improve service-life models and performance specifications for concrete subjected to chloride ingress, the prospects of a robust, generally applicable design methodology emerging are considered somewhat remote.

In the author's view, there is now a clear need for greater emphasis to be put on developing 'fail-safe' supplementary corrosion control measures for reinforced concrete structures subjected to severe chloride-containing environments. This implies a preference for protective measures of the sorts which can be: (i) readily monitored to check their continuing effectiveness, and (ii) easily reapplied or modified in the event of premature failure. Numerous improvements in the relevant monitoring techniques have been made in recent years and a number of supplementary corrosion prevention measures that are easy to reapply or modify in the event of failure are now available. In particular, substantial progress has been made in developing electrochemical techniques for improving the reliability of protection afforded by concrete to embedded steel and for restoring protection cost-effectively once corrosion has been initiated.

2 ELECTROCHEMICAL METHODS OF TREATMENT OF CORROSION IN CONCRETE

2.1 Cathodic protection and prevention

Over the past 20-30 years, major developments in controlling chloride-induced corrosion in reinforced concrete have been made by application of cathodic protection (CP) [1]. It is now generally accepted that this can provide an effective remedial approach and many corroding structures have been successfully treated by impressed current CP systems of various types. The main areas of research have been concerned with: (i) developing anode systems that are suitable for different types of structure and environmental exposure conditions, (ii) minimising the risk of undesirable side effects, and (iii) devising monitoring systems and criteria for establishing the effectiveness of operation of the technique. Substantial progress has been made in all of these areas and a European Standard has recently been published.

An important advance has been the demonstration that, if steel reinforcement is subjected to a very small, continuous CP current density before the concrete surrounding it becomes significantly chloride-contaminated, then the initiation of 'pitting' corrosion can be suppressed indefinitely, despite subsequent ingress of substantial amounts of chloride. This condition, known as 'imperfect passivity', provides the rationale for the method of 'cathodic prevention', in which new structures are treated by CP at very low current density before they become contaminated with chloride salts [2].

Other useful developments have been concerned with galvanic (sacrificial anode) cathodic protection systems, which require no permanently installed power supply or regular maintenance. Specially designed systems of this type, incorporating small, discrete zinc anodes encased in mortars of controlled composition, offer a promising way of eliminating the 'incipient anode' problem that is often encountered when cementitious patch repairs are used for the rehabilitation of structures suffering from chloride-induced corrosion [1]. The sacrificial anodes serve to maintain the potential of the reinforcement in the vicinity of the repair patches at a level that induces 'imperfect passivity' (i.e. cathodic prevention). Discrete sacrificial anodes may also be useful for maintaining reinforcing steel in a state of 'imperfect passivity' (cathodic prevention) even in cases where 'pitting' corrosion had already been initiated, providing that the steel is subjected to cathodic pre-treatment at a current density high enough to repassivate existing pits so that 'perfect passivity' is first restored (see Fig. 1).

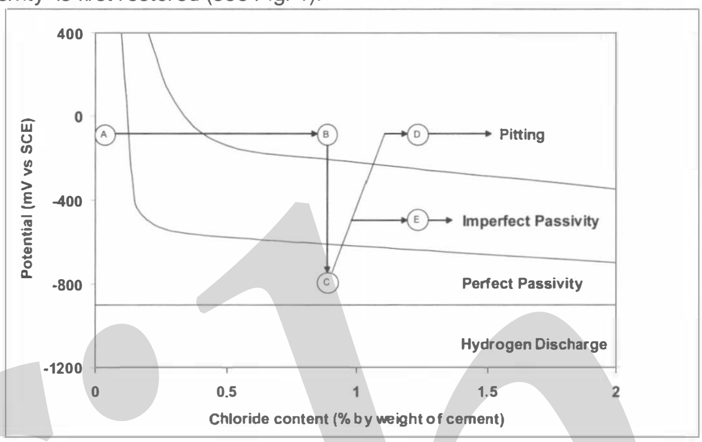

Fig. 1 Temporary Cathodic Protection with Subsequent Galvanic Cathodic Prevention: After chloride contamination has induced pitting (A→B), the steel potential is depressed sufficiently to achieve 'perfect passivity' by temporary application of a fairly high cathodic current density (B→C). Steel will subsequently be vulnerable to renewed 'pitting' (C→D), but this may be prevented by means of galvanic coupling of steel to discrete sacrificial anodes to preserve 'imperfect passivity' (C→E).

2.2 Electrochemical realkalisation and electrochemical chloride extraction

While cathodic protection of reinforced concrete is a permanently-installed form of corrosion treatment, other electrochemical techniques that have been developed involve relatively short-term application of much higher cathodic current density to the embedded steel. Both realkalisation, aimed at restoration of passivating conditions in carbonated concrete, and electrochemical chloride extraction, aimed at removing chloride ions from salt-contaminated concrete, are of this nature. A state-of-the-art review dealing with these techniques was produced in 1998 by the European Federation of Corrosion - Working Party 11 'Corrosion of Reinforcement in Concrete' [3].

In the case of realkalisation, research has been directed towards improved understanding of the mechanisms of the process and, in particular, the role of electro-osmosis, which has provoked some controversy. Further work has also been aimed at devising acceptance criteria to demonstrate that the treatment has been applied adequately to induce durable repassivation of the steel. Aspects of electrochemical chloride extraction, which have been studied extensively during the last ten years, include factors affecting the induction of potentially deleterious side-effects, the efficiency of chloride removal as a function of the time and intensity of current application, optimisation of process variables and development of reliable acceptance criteria. The last-mentioned of these has been problematic because many factors can influence chloride threshold levels for corrosion of steel in concrete.

REFERENCES

[1] Page, C. L. and Sergi, G.: Developments in cathodic protection applied to reinforced concrete, J. Mater. Civ. Eng. (ASCE), Vol. 12, No. 1, pp. 8-15, 2000; also Discussion by G. K. Glass and authors' closure: ibid, Vol. 13, pp. 396-398, 2001.

[2] Pedeferri, P.: Cathodic protection and cathodic prevention, Construction and Building Materials, Vol. 10, No. 5, pp. 391-402, 1996.

[3] Mietz, J. (ed.): European Federation of Corrosion Publications, No. 24, Electrochemical Rehabilitation Methods for Reinforced Concrete Structures, The Institute of Materials, 1998.

JSCE - STANDARD SPECIFICATION FOR CONCRETE STRUCTURES –2001 "MAINTENANCE"

Toyoaki MIYAGAWA
Kyoto University
Japan

Nobuaki OTSUKI
Tokyo Institute of Technology
Japan

Hidenori MORIKAWA
Kobe University
Japan

Atsuro MORIWAKE
Toa Corporation
Japan

Hidenori HAMADA
Port and Airport Research Institute
Japan

Keywords: concrete structures, maintenance, JSCE, specification

1 INTRODUCTION

In 2001 January, the first edition of "JSCE - Standard Specification for Concrete Structures –2001 "Maintenance" was issued based on the preparation of almost 10 years. The background of this issue is a great number of accumulations of concrete structures during the later half of the 20th century in Japan. Relatively high percentage of these structures have deteriorated gradually, therefore it is supposed that these structures require great numbers of maintenance work in the 21st century. Based on this background, JSCE (Japan Society of Civil Engineers) established technical committee on maintenance problem of concrete structures about 10 years ago. Through almost a decade discussions of committee members from all fields of concrete technology, the principle of maintenance procedure of concrete structures is developed, and this "JSCE - Standard Specification for Concrete Structures –2001 "Maintenance" is issued.

This standard specification shows a principle of maintenance procedure adopted for all kinds of concrete structures, and indicates the specialized procedures applied to "Carbonation induced deterioration", "Chloride induced deterioration", "Frost attack", "Chemical attack", "Alkali aggregate reaction", "Fatigue of RC slab of road bridge" and "Fatigue of RC beam of railway bridge".

This paper presents a brief introduction of this specification, by describing the basic idea of maintenance adopted in this specification, background of formulation, and outline of this specification.

2 BASIC IDEA OF MAINTENANCE

A concrete structure is strongly expected to retain the required level of its functions for the required period of service life. In engineering discussions, "a function" is difficult to be dealt with quantitatively, it can be translated into that "the performance of the structure shall be retained above the required level with adequate reliability during the structure's designed service life". This means that an adequate maintenance work is inevitable for every concrete structure. In order to perform the rational maintenance, it is necessary to seize the time-dependent changes of performance of the structure during their service life. However, such changes, in most cases, cannot be strictly analyzed at the current engineering level. Therefore, they are mostly verified by considering a limit state of the structure in consideration of the durability under the expected deterioration mechanism, by using the deterioration model.

The level of maintenance is closely related to the level of the design and the construction execution. This means, for example, that when no maintenance is carried out, design and construction execution shall be carried out to provide sufficient margins of performance to the structure. On the other hand, when frequent maintenance is carried out, the margins of performance can be set to be rather small. Therefore, it can be said that performance of a concrete structure can be clearly specified only with a service life scenario incorporating their maintenance strategy.

3 BACKGROUND OF FORMULATION

In consideration of the importance of maintenance, "JSCE Concrete Committee" organized a subcommittee on maintenance of concrete structures, to publish "Recommendations for Maintenance of Concrete Structures (draft)[1]," which is a groundbreaking code of maintenance for concrete structures, in October 1995, hereafter referred to as "Recommendations". However, after the publication of "Recommendations", the necessity of maintenance has been increasing. And also, new findings have been accumulated based on the progress in concrete technology. Incorporating these sets of technological knowledge with additional investigations' results, "Standard Specification for Concrete Structures –2001 "Maintenance"" is completed. With the completion of this specification, a series of Standard Specification becomes to cover the all areas of concrete structures' life cycle, from "Design", "Construction", to "Maintenance".

4 CONTENT OF "JSCE - STANDARD SPECIFICATION FOR CONCRETE STRUCTURES –2001, MAINTENANCE"

Total content of this specification is as follows.

Part 1: Maintenance Fundamental

Chapter 1 General
Chapter 2 Required Performance of Concrete Structures
Chapter 3 Principle of Maintenance Procedure
Chapter 4 Identification of Deterioration Mechanism
Chapter 5 Initial Inspection
Chapter 6 Routine Inspection
Chapter 7 Regular Inspection
Chapter 8 Detailed Inspection
Chapter 9 Extraordinary Inspection
Chapter 10 Techniques of Testing and Surveying
Chapter 11 Measures Toward Deterioration
Chapter 12 Records

Part 2: Maintenance Standard

Chapter 13 Standard Maintenance Method for Carbonation Induced Deterioration
Chapter 14 Standard Maintenance Method for Chloride Induced Deterioration
Chapter 15 Standard Maintenance Method for Frost Attack
Chapter 16 Standard Maintenance Method for Chemical Attack
Chapter 17 Standard Maintenance Method for Alkali Aggregate Reaction
Chapter 18 Standard Maintenance Method for Fatigue of RC Slab of Road Bridge
Chapter 19 Standard Maintenance Method for Fatigue of RC Beam of Railway Bridge

REFERENCE

[1] Guideline (Draft) for Maintenance of Concrete Structures, Concrete Library No.81, Oct. 1995, JSCE (Japan Society of Civil Engineers) (in Japanese).

CONDUCTIVE CEMENT-BASED COMPOSITE AS ANODE FOR THE CATHODIC PROTECTION OF REINFORCED CONCRETE STRUCTURES.

Luc Westhof
Master Builders Belgium
Belgium

Masami Motouri
NMB
Japan

"Keywords": Impressed current cathodic protection, cementitious conductive anode, activated titanium mesh, ease of installation, adhesion tests/durability.

1. INTRODUCTION.

Steel reinforcement is passivated by the high alkaline environment of the concrete, and therefore does not corrode. Active corrosion of the reinforcement can however occur when chlorides penetrate through the concrete cover and destroy the passivation layer, or through carbonation of the concrete. The corrosion of the reinforcement, an electrochemical process, is successfully stopped, mitigated or prevented with the use of several electrochemical methods. Cathodic protection for reinforced concrete is such an electrochemical method, which is used with success for the last 50 years.
A durable, conductive, polymer modified, cementitious mortar has been developed which serves as a secondary anode for the cathodic protection of steel in concrete. The electrical conductivity of this composite is obtained through the incorporation of nickel coated carbon fibres. The composite provides a uniform current distribution.
The major benefits over an activated titanium mesh anode system, used for the cathodic protection of steel in atmospherically exposed concrete, are its ease of installation and cost reduction. Typical applications for this conductive cement-based anode system include car parks, jetties, bridges etc. Galvanostatic tests have shown the excellent durability of the nickel coated carbon fibres in this cement-based mortar. This conductive material has been successfully tested in laboratory tests and in the field, and has been successfully used to protect more than 20,000 m² of reinforced concrete (figures 1-3)

Fig. 1 First CP 60 field trial

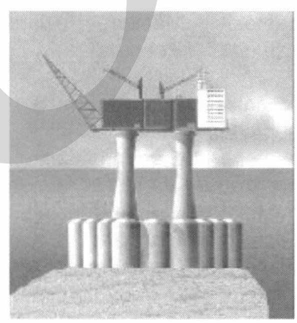

Fig. 2 Oseberg A oil platform

Fig. 3 Bridge in Holland

2. CP of reinforced concrete with Thoro CP Anode 60 conductive mortar system.

It is interesting to examine the evolution of anodic systems used in reinforced concrete cathodic protection (1-5).
The development of anode materials was approximately 30 years oriented towards mesh systems applied on the external surface of the structure to be protected, and anchored by a concrete layer. These activated titanium mesh anodes have proven themselves in a variety of applications since then. The activated titanium mesh anodes exhibit good mechanical and electrochemical properties leading to good lifetime properties. The major problems encountered with this type of anode material, are its high material cost and the application method.
Master Builders Technologies has therefore oriented its research in the late 1980's towards the development of an anode system (Thoro CP Anode 60) which combines the ease of installation of a conductive paint system with the good durability of the activated titanium mesh system.
The Thoro CP Anode 60 anode system is based on the use of a conductive overlay, which behaves as an inert anode system. The Thoro CP Anode 60 mortar, a PCC mortar, is a complex composite material consisting mainly out of a Portland cement matrix, a non-reactive filler material, and a polymer. The Thoro CP Anode 60 conductive mortar is having a bulk resistivity of < 10 ohm.cm. The electron micrograph (figure 4) of a section of hardened CP 60 Anode shows the distribution of the fibres and the Nickel coating.

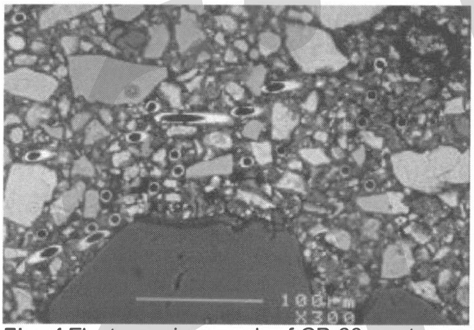

Fig. 4 Electron micrograph of CP 60 mortar

The operations required for the application of the Thoro CP Anode 60 anode system on site are simple: primary anode (or current feeder) installation; then spraying of the conductive cement based mortar in the same way as other wet spray applied mortars to an average layer thickness of 8 mm. The current feeders bring the current into the conductive mortar, which then uniformly distributes the current over the area to be protected.
While showing similar protection levels of the steel reinforcement, and lifetime expectancy as activated titanium mesh systems, Thoro CP Anode 60 has following advantages over the distributed mesh anodes:
- Ease of application/installation
- Cost strongly reduced
- Reduced application/installation time resulting in less down-time
- High adhesion, even after long term energisation

REFERENCES

1. F. De Peuter, L. Lazzari, “New Conductive Overlay for CP in Concrete: Results of long term testing”, Proceedings of NACE 1993 conference-New Orleans (US), paper n° 325, 1993
2. K. Kendell, Proceedings of UK Corrosion ’86, Birmingham, November 1986
3. C.J. Mudd, G.K. Mussinelli, P. Pedeferri, M. Tettamanti, Materials Performance, pp 18-24 Sep. 1988
4. M. Grandi, L. Lazzari, “Cathodic Protection Experiences on Highway Bridge Decks”, Proceedings of 11th ICC, 2-6 April 1990? Florence, Italy, p 2.481.
5. J.P. Broomfield, “The North American Approach to Protection Measures”, Proceedings of Int. Conf. On Structural Improvement through Corrosion Protection of Reinforced concrete, Doc.E7190, 2-3 June 1992? London (1992)

INFLUENCE OF REINFORCING STEEL CORROSION ON FLEXURAL BEHAVIOR OF RC MEMBER CONFINED WITH CFRP SHEET

Takashi Yamamoto, Atsushi Hattori and Toyo Miyagawa
Department of Civil Engineering, Kyoto University, JAPAN

Keywords: reinforcing steel corrosion, carbon fiber sheet, confined concrete, ductility, flexural member

1 OBJECTIVE

The objectives of this study are to establish the application scheme of strengthening by confinement using CFRP sheet for a member in which rebar corrosion has already occurred and to clarify the performance change on ductility due to rebar corrosion after strengthening by confinement has been applied for a flexural member. In order to examine these points, reversed cyclic loading test was carried out for RC beams, with corroded longitudinal rebar, confined using CFRP sheet.

2 EXPERIMENTAL PROCEDURES

2.1 Specimens

Dimension of RC beams is shown in Fig.1. The 2-D10 (SD295A) were arranged as longitudinal rebar in both upper and lower sections symmetrically (p=0.81%). These were cast using rebar beforehand corroded by spraying salt water. The details of RC beams strengthened by confinement using CFRP sheet are shown in Fig.2.

2.2 Test parameters

The corrosion mass loss rates, C_r were 0.0%, 3.3% and 23.0% in central 700mm length of longitudinal rebar. The volumetric confinement ratios of CFRP sheet, ρ_{CF} were 0.00%, 0.17% and 0.66%. One and three loading cycles at (2n-1) times the yield displacement were adopted.

2.3 Loading test procedures

Reversed cyclic load was applied to two symmetrical points. The yield displacement, δ_y, was determined from the bent of load-displacement curve in sound specimen without strengthening. The ultimate state was defined as the point at which the load dropped below 80% of the maximum load.

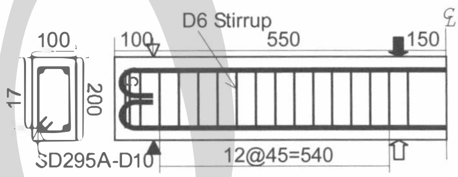

Fig.1 Dimension of RC beams (unit: mm)

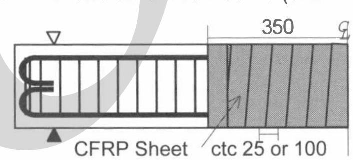

(unit: mm)

Fig.2 RC beams confined with CFRP sheet

3 TEST RESULT AND DISCUSSION

3.1 Ultimate failure mode

In one loading cycle, although from C_r=0.0% to C_r=3.3% compression failure occurred, rupture of rebar occurred at 23.0%. When three loading cycles of each step and C_r=3.3% were adopted, compression failure occurred with ρ_{CF}=0.00% and ρ_{CF}=0.17%. However, rupture of longitudinal rebar occurred with 0.66%.

3.2 Maximum load

Influences of C_r on maximum load are shown in Fig.3 with the derived curves obtained by sectional M-ϕ analysis. In this analysis, the stress-strain model of JSCE [1] for plane concrete and that for confined concrete using CFRP sheet [2] were used. The model of JSCE [1] was used for rebar was used. The sectional area of corroded rebar was calculated assuming that sectional area loss rate was corresponding to C_r due to longitudinally uniform corrosion. From the experimental result, at C_r=3.3% maximum load did not decrease in any ρ_{CF}. However, that one in 23.0% was reduced approximately by 10% from that of sound specimen.

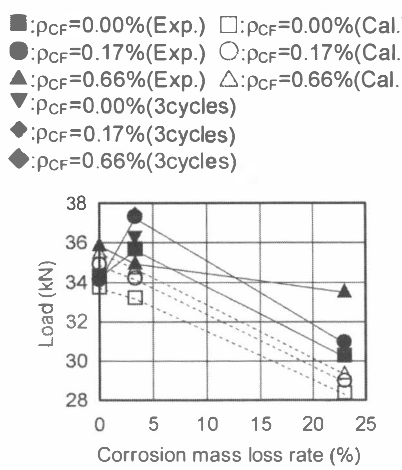

Fig.3 Maximum Load

Comparison of calculated values with experimental one indicated very good agreement on the ratio of reduction.

3.3 Ductility

Influences of Cr on displacement ductility factor, μ (=$\delta_u(0.8P_m)/\delta_y$) are shown in Fig.4. In little Cr, μ of specimen confined using CFRP sheet was larger than that of specimen without strengthening. However, in 23.0% μ decreased remarkably from that of sound specimen, because rupture of rebar occurred ahead of compression failure. Furthermore, in three loading cycles, μ of ρ_{CF}=0.66% in which rupture of rebar occurred was about the same as that of 0.17%. From the above discussion, confinement by CFRP sheet for the flexural member, in which little rebar corrosion occurred, can restore or improve the ductility. However, at the significant corrosion, it is difficult to determine that confinement using CFRP sheet can improve ductility dramatically over the sound member. Moreover, even if corrosion is slight such as 3.3%, excessive confinement should be avoided and the combined use of confinement and flexural strengthening is required in the case that reversed cyclic load works in the post-peak region.

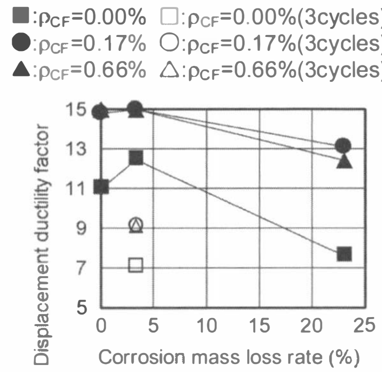

Fig.4 Displacement ductility factor

3.4 Estimation of ultimate failure mode

The following procedure conducted during estimation of ultimate failure mode: 1. Obtain the relation between C_r and strain of rebar in lower section when concrete strain of upper extreme fiber is ultimate in each ρ_{CF}. 2. Obtain the relation between C_r and ultimate strain of corroded rebar by linear regression on the results of previous studies [3]. 3. Compare relation 1. with relation 2. In this analysis, the same stress-strain models of concrete and rebar as 3.2 were used. Results of analysis are shown in Table 1. Rupture of rebar occurred ahead of compression failure in small C_r, as ρ_{CF} increased. Rupture of rebar occurred in all ρ_{CF} at C_r=23.0% corresponded to experimental one. However, when three loading cycles and C_r=3.3% were adopted in experiment, rupture of rebar occurred at ρ_{CF}=0.66%.

Table 1 Estimation of C_r that rupture of rebar

ρ_{CF} (%)	0.00	0.17	0.66
C_r (%)	21.6	19.1	13.3

4 CONCLUSIONS

The conclusions obtained in this study are as follows:

(1) From the result of loading test for specimens which had corroded rebar and strengthened by confinement using CFRP sheet, at corrosion mass loss rate of 3.3% maximum load did not decrease. However, that at corrosion mass loss rate of 23.0% was reduced approximately by 10% from that of sound specimen.

(2) Ductility of specimen confined using CFRP sheet was larger than that of specimen without strengthening in little corrosion mass loss rate. However, at significant corrosion, ductility decreased remarkably from that of sound specimen, because rupture of rebar occurred. Furthermore, in three loading cycles, the specimen with corrosion mass loss rate of 3.3% and volumetric confinement ratio of 0.66% resulted in rupture of rebar. Therefore, excessive confinement using CFRP sheet should be avoided and the combined use of confinement and flexural strengthening is required in the case that reversed cyclic load works in the post-peak region.

(3) Estimation of ultimate failure mode was conducted by comparing the relation between corrosion mass loss rate and strain of longitudinal rebar in lower section at the ultimate state with the relation between corrosion mass loss rate and ultimate strain of corroded rebar. The result is that rupture of rebar occurs ahead of compression failure in small corrosion mass loss rate, as volumetric confinement ratio increased.

REFERENCES

[1] JSCE: Standard Specification for Design of Concrete Structures., Mar., 1996 (in Japanese)
[2] Hosotani, M., Kawashima, K. and Hoshikuma, J.: A Stress-Strain Model for Concrete Cylinders Confined by Carbon Fiber Sheets. Jour. of Materials, Concrete Structures and Pavements, JSCE, No.592/V-39, pp.37-52, May, 1998 (in Japanese)
[3] Ooi, T.: Evaluation of Reinforcing Steel Corrosion in Concrete Cylinder., Proc. of the 25th JUCC Congress on Cement and Concrete, JUCC, pp.111-116, Oct., 1998 (in Japanese)

CONCRETE PATCH REPAIRS:

TIME FOR A RISK-BASED STRATEGY?

T.D.Gerard Canisius Nadia Waleed

Centre for Concrete Construction, BRE Ltd., Garston, Watford, WD25 9XX, ENGLAND

Keywords: concrete patch repair, risk analysis, risk-based implementation

1 INTRODUCTION

The authors use this paper to address the question of whether we need a risk-based approach to structural concrete patch repair (where the deteriorated concrete is taken out and replaced with new repair material) and, if yes, how we could start laying the foundation for it. The authors do this with a presentation of some aspects of structural concrete patch repair and a discussion.

2 THE LITERATURE REVIEW

The authors' conducted a literature review concentrated upon the question of whether a structure should be propped during patch repair or left unpropped [1]. The main technical argument in favour of leaving a structure unpropped is that, when the repair is on the tension side, depropping after the repair is likely to result in the cracking of the repair patch and this can pose durability related problems. On the other hand it can be argued that without propping (which is expensive) the structural behaviour will change and the repair patch will not participate fully in resisting loads. In addition to this, in the absence of propping, sometimes parts of a structure away from the repair patch may become overloaded, giving rise to cracks and durability problems. According to an industrial source, there have been situations where even reinforcing bars have distorted or failed in anchorage on exposure during the unpropped patch repairs of car park slabs. However, if temporary props are used to relieve load from the member and/or to prevent significant redistribution of stresses within the member during and immediately after repair, then these consequences of altered structural behaviour may be minimised.

Although this document concentrates more on the 'structural' behaviour related to propping and not propping, the structural properties and loading conditions are not the only factors that affect a repair operation. This is because it is not only the stresses present during and after repair that affect the short and long term behaviour of a repaired structure, but also other aspects such as environmental conditions and compatibility of the repair material with the original concrete (the 'substrate'). That is, the considerations for implementation of patch repair are two-fold, viz. the material aspects and the structural aspects, including the compatibility between the repair and the substrate. This paper discusses the authors' literature review on the structural aspects, viz. the behaviour of concrete members with reinforcement exposed during repair, and the behaviour of repair patches under propped and unpropped repair implementation, together with information on the material aspects.

3 DISCUSSION AND CONCLUSION

An important observation to be made on the conclusions put forward in the literature is their inapplicability in general to all structures and situations. This is because the available conclusions have been based upon, and with respect to, a limited set of conditions considered by the tests and/or analyses. For example, most of the available investigations are in relation to simply supported beams excavated or repaired on the tension side. There do not seem to have been attempts, perhaps through follow-up projects, to examine the validity of those conclusions when applied to other situations. This is very much so for the case of repair of plates and shells: the authors did not discover any similar paper on the subject. In fact, industry sources have indicated that there is a lack of guidance, although various problems can be encountered in the repair of plates (slabs), for example, in car parks.

It was also observed that most research work has concentrated on addressing a single or a few issues in isolation. For example, when the benefits and shortcomings of propped and unpropped repair were investigated with respect to the repair patch, little or no consideration seems to have been given to accompanying effects such as cracking elsewhere and the possible changes in structural capacity and durability due to this. This approach seems to have led to the following differences in the conclusions of researchers.

- According to [2], a successful repair needs the stresses to flow through the repair patch, instead of around it through the substrate. This requires the repair patch to possess a stiffness *greater* than that of the substrate. However, Mangat and O'Flaherty [3] have recommended that the stiffness (Young's modulus) of the repair patch be *smaller* than that of the substrate.
- Emberson and Mays [4,5], who considered the structural aspects of repair excavation, have suggested the need for propping during repair. However, Mangat and O'Flaherty [6], who considered the cracking of the repair patch, have suggested the opposite.

These indicate that comprehensive studies, which consider the various effects simultaneously, could help in achieving a 'system approach' to patch repair; as has been called for by Emmons and Vaysburd [7].

3.1 The need for a risk-based approach to answer patch-repair questions

The literature survey indicated that there are three main aspects that researchers have considered, albeit independently, to evaluate the possible need for propping of a structure. They are as follows.

- Should loads on the structure and, by association, stresses within it be relieved during repair so that the repaired structure behaves as a new one?
- Should propping or shoring be provided, with or without relieving load, so that there is no distress to the structure during repair, and its ultimate strength in the repaired state is not detrimentally affected?
- Should propping be avoided as it may crack a repair patch on depropping?

It is the authors' opinion that these questions should be raised simultaneously while considering safety, serviceability and durability of the whole structure, including the repair patch. However, due to the uncertainties and difficulties involved, such an action needs a common basis for comparison of options and this seems to be lacking at present. A risk-based approach could provide this common basis. While not all information necessary for a full probabilistic implementation may be available at present, ***it is certainly timely to start development of a risk based approach*** and laying the foundation for collecting the necessary data and developing the associated methodologies.

REFERENCES

[1] Canisius, T.D.G. and Waleed, N. : The behaviour of concrete repair patches under propped and unpropped conditions: Critical review of current knowledge and practices. FBE Report 3, March 2002.

[2] Wood, J. G. M., King, E. S. and Leek, D. S. : Defining the properties of concrete materials for effective structural application. Proc. Conference on Structural Faults & Repair, London, 1989.

[3] Mangat, P. S. and O'Flaherty, F. J. : Influence of elastic modulus on stress redistribution and cracking in repair patches. Cement and Concrete Research, 30, pp. 125-136, 2000.

[4] Emberson, N. K. and Mays, G. C.: Significance of property mismatch in the patch repair of structural concrete. Part 1: Properties of repair systems. Magazine of Concrete Research, Vol. 42, No. 152, pp. 147-160, Sep., 1990.

[5] Emberson, N. K. and Mays, G. C. : Significance of property mismatch in the patch repair of structural concrete. Part 2: Axially loaded reinforced conc. members. Magazine of Concrete Research, Vol. 42, No. 152, pp. 161-170, Sep., 1990.

[6] Mangat, P. S. and O'Flaherty, F. J.: Factors affecting the efficiency of repair to propped and unpropped bridge beams. Mag. of Conc. Research, Vol. 52, No. 4, pp. 303-319, Aug. 2000.

[7] Emmons, P. H. and Vaysburd, A. M. : Factors affecting durability of concrete repair, the contractor's viewpoint. Proc. Fifth International Conference on Structural Faults and Repair, Vol. 2, pp. 253-267, June 1993.

CONSTRUCTION INDUSTRY IN ASIA AND MODEL CODE FOR MAINTENANCE

Tamon Ueda
Hokkaido University
JAPAN

Keywords: construction industry, cement consumption, Asia, model code, maintenance

1 CONSTRUCTION INDUSTRY IN ASIA

It is often said that the 21st century is the century of Asia which is the most populous and fastest developing in the world. The current size of the construction industry in major Asian countries is compared with that of the rest of the world in Fig.1 [1]. Japan is the second largest in construction industry, followed by China, Korea and India who are 4th, 10th and 12th respectively. USA tops Japan as the largest construction industry, while Germany, ranking 3rd in the world and 1st in Europe spends slightly more than China. Approximately one third (31%) of the world construction industry spending was in Asia in 2000, while the other two thirds were in Europe and North/South America [1]. In many Asian countries the construction industry contributes more than 10% of GDP [1]. The construction industry in Asia takes a greater role in its economy than that in many developed countries.

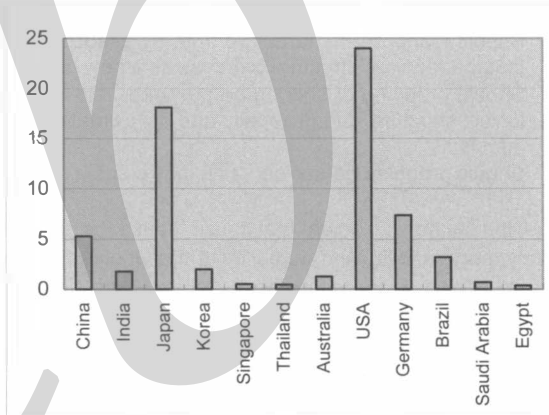

Fig.1 Construction market share of Asian and other countries (% of the world construction market) [1]

Construction industry quantified by money value may not reflect the real size of the industry because the money value varies greatly among countries. Consumption of cement can be a better index for measuring the volume of construction works. Countries consuming cement per capita most in 1999 were NICs (Singapore: 1542kg, Korea: 954kg, Taiwan: 857kg, Hong Kong: 654kg) not the economic giant Japan (558kg) [2]. Major cement consuming countries in Asia consume more than most of the other countries except for some of the Middle East and European countries. In order to see the development of construction industry in Asia a chronological change in cement consumption in the world is given in Fig.2 [2]. The cement consumption in

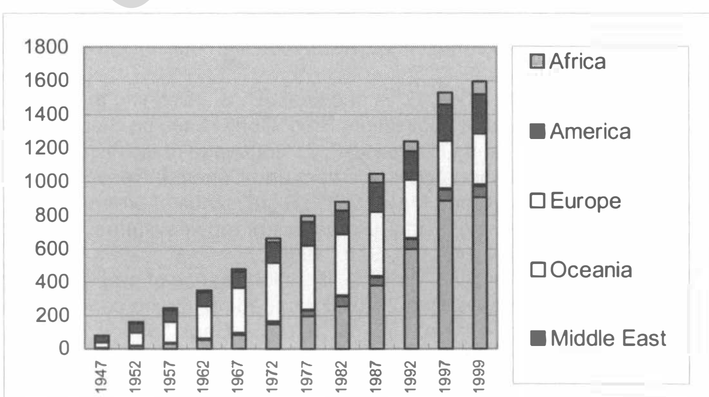

Fig.2 Chronological change in cement consumption in the world (million ton) [2]

Asia excluding the Middle East grew quicker than the rest of the world and reached over 50% of the world consumption in 1990s. China, who ranks 1st in the world in terms of cement consumption, has been showing a much faster growth in cement consumption than other countries such as India, USA and Japan who rank 2nd, 3rd and 4th respectively in 1999 [2].

In 1990s the construction industry in Japan shrunk due to the burst of the bubble economy. Despite the economic slump the ratio of maintenance work to the total construction work increased steadily. The percentage of maintenance work in Japan reached 19.5% in 2000 [3], while that in France, Germany and USA was around 30% in either 1993 or 1995 and that in UK was almost 50% in1995 [4]. It is expected in Japan that the share of maintenance work would reach 50% soon and become even more. The same scenario can be expected in other Asian countries.

2 MODEL CODE FOR MAINTENANCE

The maintenance work is expected to be a major work in construction industry in Asia for this century. In order to tackle the common task international collaboration is preferable. At present codes for maintenance work have not been well prepared in most of the countries in the world. In Asia the level of ability to prepare codes and the surrounding conditions for structures which affect maintenance works are so diverse, which means that many maintenance codes should be prepared there. It is, however, not feasible for each Asian country, especially rather small countries, to prepare her own codes for maintenance by herself. Instead it would be more practical for the Asian international community to prepare their maintenance codes.

There are two types of the maintenance codes to be prepared. The first type is a common code or a model code, which would contain only a basic frame of maintenance and act as a model for each practical code for a particular type of structure in each country, which is the second type. The first type is to be prepared by international collaboration, while the second type by respective country. A practical maintenance code for similar structure in similar condition can be prepared by multiple countries who have a common need.

With the same concept above the International Committee on Concrete Model Code for Asia (ICCMC) published the Asian Concrete Model Code (ACMC) in March 2001 [5]. ACMC consists of three parts, one of which is Maintenance. The Vietnam government is preparing a national code for maintenance of concrete structures, based on ACMC.

5 CONCLUDING REMARKS

Asia's construction industry accounting for one third of the worldwide construction market at present is still growing. The maintenance work is vital for Asia if it were to be responsible for sustainable development of the world. For the efficient preparation of maintenance codes in Asia implementation of a model code by international collaboration is suggested. The model code can also be a good model for the future ISO code. Through code drafting Asian participation on ISO will increase.

International collaboration in Asia is vital for Asia to become an equal partner of Europe and North America. On the other hand the only international organization in the world concrete society, *fib*, should take a stronger leadership role for harmonization and further development of concrete technology worldwide.

REFERENCES

[1] Engineering New Record, Vol.245, No.22, McGraw Hill, New York, 4 December 2000.

[2] Data on the cement consumption in the world provided by Dr Ouchi Masahiro of Kochi Institute of Technology, Japan and the Cement Shimbun Co. Ltd., Japan

[3] Japan Federation of Construction Contractors : Handbook of Japanese Construction Industry in 2002 (Kensetsugyo Handbook), http://www.nikkenren.com/ (in Japanese)

[4] Nihon Keizai Shimbun, Inc., 19 February 1998 (in Japanese).

[5] International Committee on Concrete Model Code for Asia : Asian Concrete Model Code 2001, ICCMC, March 2001.

MAINTENANCE OF CONCRETE STRUCTURES OF TOKYO METROPOLITAN EXPRESSWAY

Okada Masasumi
Kojima Hiroshi
Sasaki Kazuya
Design and Research Division
Maintenance and Facilities Department
Metropolitan Expressway Public Corporation

Keywords: inspection, repair work, lifecycle, prevent maintenance

1. INTRODUCTION

With a total length of approximately 270km, the Tokyo Metropolitan Expressway handles an average traffic volume of around 1.16 million vehicles (about 10% of which are heavy-duty cargo vehicles) and about 2 million people daily. It has two or three lanes in each direction, making a total of four or six lanes in both directions. The expressway accounts for 13% of Tokyo's entire trunk road system in terms of length, but the traffic volume (vehicle-km) is approximately 28% and goods transport volume is 38%. These figures underscore the expressway's importance in supporting life and industry in the greater metropolitan area of Tokyo.

Over 80% of the structures are elevated constructions, which, together with tunnels and subsurface structures, account for 95% of the expressway's total length. Approximately 15% of these elevated structures are made of concrete, and have a total length of 38km. Sections opened to the public in 1962 are expected to have a life span of nearly 40 years. Routes in use for over 30 years account for roughly a third (36%) of the entire expressway, while routes opened over 20 years ago amount to roughly half (52%).

Maintenance procedure for these structures consists of three phases: collecting inspection data, classifying the data based on the degree of damage, and executing maintenance and repair work. The first step is to inspect and observe the deterioration in the concrete structures. This is carried out through daily inspections, periodic inspections and emergency inspections. The second step is to classify the inspection data according to the degree of damage. These data form the basis for decisions regarding subsequent repair work. ① Concrete floor slabs subject to repeated vehicular loads are strengthed with carbon fiber sheets. ② Glass fiber sheets are used for preventing delamination of concrete from pier beams and parapets. These two types of repair work are presently under way (Photo1, 2 and 3).

This paper outlines the maintenance work carried out on the concrete structures under the administration of the Metropolitan Expressway Public Corporation (MEPC).

2. MAINTENANCE AND MANAGEMENT

Road administrators are responsible for managing road structures more equitably and efficiently. For this, it is necessary to minimize the lifecycle cost of road facilities and add it to the traditional notion of short-term economic consideration. Lifecycle cost may be calculated using the following equation:

$$LCC=I+M+R \qquad (1)$$

LCC: Lifecycle cost, I: Initial cost. M: Maintenance cost, R: Renewal cost

This principle involves the total consideration of initial costs, maintenance costs and renewal costs throughout the road's operational life. Since maintenance and renewal costs are greatly influenced by the condition of the structures, it is necessary to gather the inspection data with which to assess the conditions of the structures.

There is another concept for damage repair and strengthening, which is the main purpose of facilities maintenance. In contrast to implementing measures after damage is discovered, the method aims to "prevent maintenance" by regulating traffic while implementing intensive measures before damage is revealed.

Photo 1 : Daily Inspection
Inspection personnel observe the appearance of the structures by using binoculars.

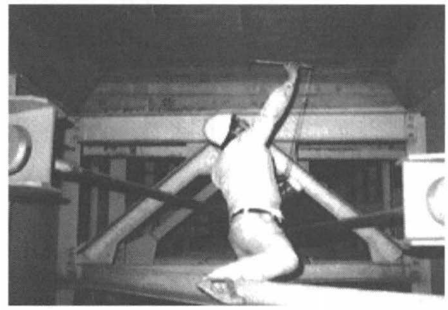

Photo 2 : Hammer inspection
Inspection personnel search for possible detachment or delamination of concrete by tapping suspected sites with a hammer and comparing the sound with that of undamaged parts nearby.

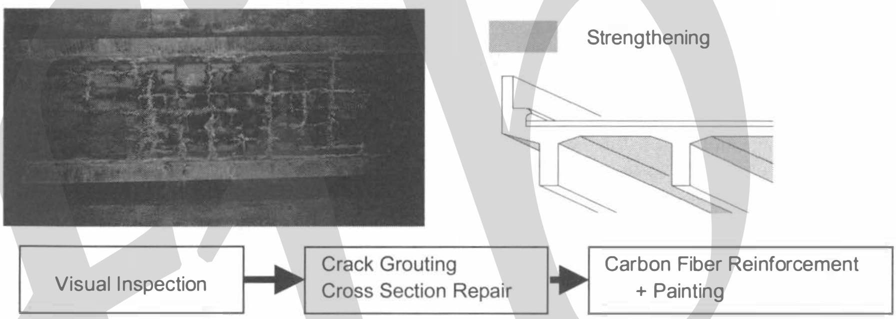

Photo 3 : Damages and Countermeasures (Concrete Floor Slabs)

REFERENCES

[1] Road Maintenance and Management on the Most Heavily Used Expressway in the World - The Tokyo Metropolitan Expressway, H. Mitani, K. Izumi. Dec. 2000

[2] Inspection Specifications for Structures, April 2001, Metropolitan Expressway Public Corporation, Maintenance and Facilities Department

[3] Inspection Specifications for Structures (Precedents of Assessments Issue), April 2001, Metropolitan Expressway Public Corporation, Maintenance and Facilities Department

MANUAL FOR MAINTENANCE OF DURABLE PRESTRESSED CONCRETE BRIDGES

Hideaki KITAZONO*・Yuzuru HAMADA**・Yoshinobu ISHIKAWA***
Minoru MIZOE****・Toyoaki MIYAGAWA*****

*ABE Kogyo Sho Co., Ltd., Tokyo, Japan, **DPS Bridge Works Co., Ltd., Tokyo, Japan,
***Oriental Construction Co., Ltd., Tokyo, Japan, ****Japan Highway Public Corporation, Tokyo, Japan,
*****Kyoto University, Kyoto, Japan

Keywords: Prestressed Concrete Bridges, Manual for Maintenance, Technical Specifications

SUMMARY

The Japan Prestressed Concrete Engineering Association (JPCEA) has taken initiatives toward development of durable prestressed concrete structures. The Research Subcommittee on Improvement in Durability of Prestressed Concrete Bridges was set up by JPCEA in 1998. "Manual for Maintenance of Prestressed Concrete Bridges" was established as one of the final output of this subcommittee.

This paper outlines the Manual for Maintenance of Prestressed Concrete Bridges.

1. INTRODUCTION

In 1994, JPCEA established the Research Committee on Technical Specifications for Prestressed Concrete Structures (chair person: Shouji Ikeda) to draft design codes, taking into consideration the recent development of prestressed concrete technologies. Following research for improving the durability of prestressed concrete bridges, the Committee set up the Subcommittee for Improvement of Prestressed Concrete Structure Durability. The first stage of the research of the Subcommittee (between 1994 and 1996, headed by Hiroyuki Ikeda) included research on damage and deterioration of existing prestressed concrete bridges. The results of the first stage were compiled in the Design and Construction Manual for Durable Prestressed Concrete Bridges issued in March 1997 [1]. The Second Subcommittee was formed in 1998, under the chairmanship of Prof. Toyoaki Miyagawa. In the first stage of the research of the Second Subcommittee, examples of deteriorated prestressed concrete bridges were collected. In the next stage, repair and strengthening methods used in such bridges were investigated. Furthermore, the relation between deterioration cases and repair/strengthening methods was analyzed, and the "Manual for Maintenance of Durable Prestressed Concrete Bridges [2]" was issued in 2000. This paper briefly explains the contents of the "Manual for Maintenance of Prestressed Concrete Bridges," which was produced by incorporating the results of the research.

2. MANUAL FOR MAINTENANCE OF PRESTRESSED CONCRETE BRIDGES

2.1 Outline of the Manual

The JPCEA manual was produced based on the following concepts:

(1) The principal purpose of the manual is codification of repair measures for prestressed concrete bridges with serious deterioration, rather than deterioration prevention and maintenance. In other words, the manual covers the concept of measures to be taken after the occurrence of deterioration.

(2) The JPCEA manual has combined many prescriptive criteria so that it would be easily used by site engineers. The contents of the manual are shown in Table 1.

As shown in Fig. 2, each factor is assessed according to the normal maintenance procedure.

Table 1: Contents of JPCEA Maintenance Manual

CONTENTS

2.2 Features of the Manual

The features of the Manual are summarized as follows:

(1) Although the manual covers the fundamentals mainly for the maintenance of prestressed concrete bridges, it is also designed to serve as a reference for selecting strengthening methods for other structures, such as prestressed concrete slabs for steel bridges, external tendons for reinforced concrete bridges, prestressed concrete tanks, and prestressed concrete buildings.

(2) Specific aspects about prestressed concrete bridges such as creep and shrinkage behavior, and decrease in performance of accessories are presented, as well as general aspects of the deterioration mechanism such as chloride-induced corrosion, carbonation-induced corrosion, frost damage and alkali-aggregate reaction.

(3) The evaluation of the deterioration of prestressed concrete bridges, and the selection of repair and strengthening methods depend on the initiation limit state of corrosion of prestressing tendons. This indicates that the performance of prestressed concrete members is greatly affected by tendon corrosion.

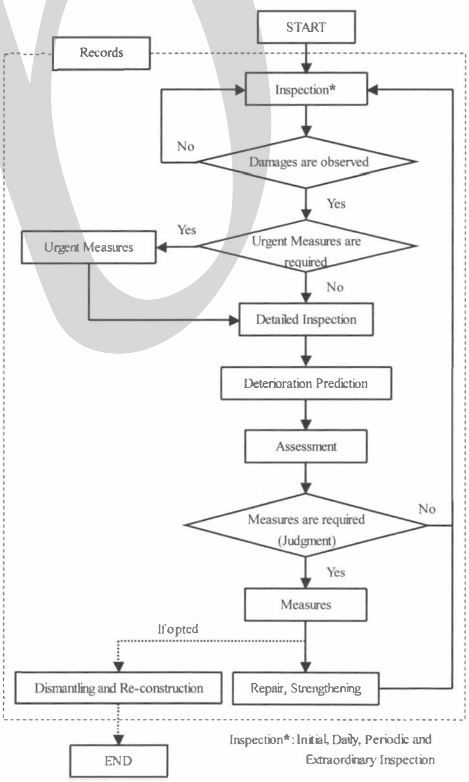

Fig. 2: Flow of maintenance process

REFERENCES

[1] JPCEA: Design and Construction Manual for Durable Prestressed Concrete Bridges, Mar., 1997.
[2] JPCEA: Manual for Maintenance of Prestressed Concrete Bridges, November 2000.
[3] JSCE: Standard Specification for Maintenance of Concrete Structures, January 2001.
[4] R. J. Woodward and F. W. Williams : Collapse of Ynys-y-Gwas Bridge, West Glamorgan, Proceeding of The Institution for Civil Engineers Part 1, Aug. 1988

EVALUATION OF LOAD CARRYING CAPACITY AND DURABILITY THROUGH THE FIELD EXPERIMENTS FOR RC GERBER'S BRIDGE SERVICING FOR 63 YEARS

Yoshihiro Tanaka
Taisei Corporation
JAPAN

Naoshige Nomura
Road Management Technology Center
JAPAN

Takeuki Yokooka
New Structure Engineering LTD.
JAPAN

Tetsushi Uzawa
Kazuhiko Iida
Taisei Corporation
JAPAN

Keywords: Gerber's bridge, diagnosis for the bridge deterioration, load carrying capacity, corrosion

1. INTRODUCTION

Arakawa Bridge on the national highway route number 4 was completed in 1938. The bridge length and the width are 134.5 m and 7.5 m, respectively. The type of this bridge is the so called "Gerber's type" with which more than 300 bridges have been constructed in Japan. It is planned that this old bridge should be replaced because of the lack of the traffic flow capacity in February 2001 by a new wider bridge. The Road Management Technology Center organized the working research group of road bridge maintenance to carry out the material tests of bridge concrete and round bars as well as the structural experiments of the Gerber's hinge member. In 1999, the working group conducted the first field investigation of Nasuno Bridge which is also Gerber's type reinforced concrete bridge constructed in 1936 and some variable information were obtained [1]. In 2001, this working group achieved again the field and laboratory investigation and the experiments to clarify the concrete material strength, carbonation and mixed material proportion through the non-destructive test and core sampling. The shear loading capacity test in the job site for the Gerber hinged girder and its structural evaluation for the shear resistance were conducted to verify the prediction method of the structural diagnosis for the similar type of bridges. It is also planning that the verification data would be obtained through conducting the accelerated deterioration experiment using the RC beams cut from Arakawa Bridge in order to clear the relationship between the structural deterioration and the corroded reinforced concrete.

2.MATERIAL TESTS

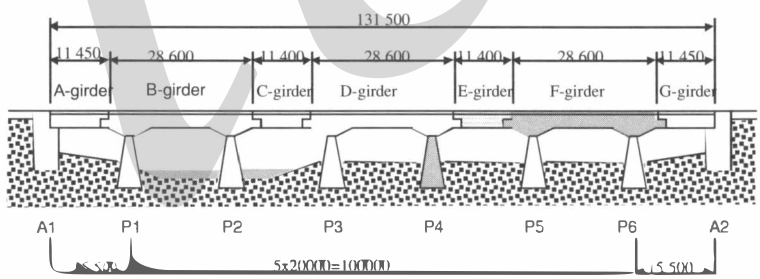

Fig.1 Overview of Arakawa Bridge

Awakawa Bridge as shown its overview in Fig. 1, is composed of three main girders and 7 spans. The material physical and chemical tests were conducted for the core test specimen sampled from the main girder and the outer girder of "F-girder". The detection of concrete cover thickness and round bar location was carried out by both the electromagnetic reflection method and the electromagnetic inductance method, then the round bar location and the concrete cover thickness were inspected by chipping the cover concrete to verify the measurement errors. It is noted that the complex method combined with the Schmidt concrete test hammer and ultra sonic velocity method can estimate more accurately. The concrete mix proportion of Awakawa Bridge is estimated according to the method recommended by Japan Cement Association. The estimated results of the concrete mix proportion of Arakawa Bridge and Nasuno Bridge are similar to each other. Those estimations are based on "Concrete standard specification" issued by JSCE in 1931. The compressive strength values obtained from 150mm diameter cores of Arakawa Bridge are 13 ~ 25N/mm^2 for the main girder and 22 ~ 25N/mm^2 for the pier. On the other hand, the compressive strength values of Nasuno Bridge are 22~ 48N/mm^2 for the main girder and 38 ~ 57N/mm^2 for the pier. Comparing those two values, the compressive strength of Arakawa Bridge are smaller than those of Nasuno Bridge. After 20 cycles of freezing and thawing, the relative dynamic elastic coefficient decreased down to zero; i.e. this means that this concrete is very poor for the resistance to freezing and thawing. One of the reasons is that this concrete is non-AE concrete. It is said that the entraining air agent was applied to concrete for the first time in 1949 in Japan. Therefore, this concrete must be a plain concrete. Through the appearance check, the severe deterioration of surface concrete was not observed. According to the risk distribution of frost damage in Japan, the area of Arakawa Bridge is classified level-1 (small risk of frost damage). It should be noted that the severe maintenance check should be focused on the RC structures made of non-AE concrete in the years of 1930 ~ 1940's in cold regions.

3. STRUCTURAL EXPERIMENT

The load carrying capacity test has been conducted on the site for the hinge member of the "F-girder", after removing the "G-girder". The main purpose of the structural loading experiment is to confirm the shear strength of the hinge member. In order to provide a testing load for the middle specimen girder, the reaction H-shaped steel beam was installed in the center of the deck as illustrated in Photo 1.

Poto1 Loading test on the site

As a result of loading test, the loading force versus the displacement at the loading point is illustrated in Fig. 2. For the first loading, the cracks existing before loading started to open at the load of about 1,000kN. For the second loading, those cracks opened rapidly at the load of 1,400kN and accordingly the stiffness became lower and lower. At the load of 1,750kN, the crack width at the corner of the hinge member became 4.4mm, and then the member could not sustain the load. The simulation results of crack distribution at the maximum load by the fixed crack model and the rotational crack model are compared in Fig. 2. Both models simulated well the loading experimental behavior that the initial crack on the corner of the hinge member started to open at the load 300kN and the diagonal reinforcement bars begun to yield.

4. ACCELERATED CORROSION TEST

The test specimen for the chloride penetration test was cored out from "E-girder". The test core was divided into four pieces of specimen and the side surface and one cut surface were sealed by epoxy resin. The test pieces were placed into the penetration liquid that is 3% density of NaCl and the penetrated chloride ions from the surface were investigated every three months. Three pieces of the accelerated corrosion experiment specimen were cut out from "E-girder". One of three specimen girders is loaded without accelerating corrosion experiment to clarify the bending moment load carrying capacity in the laboratory. The maximum load is 1,130kN and the destruction is typical bending failure mode. Using the concrete and round bar constitutive laws obtained from the material test data, non-linear analysis applying a fiber model is carried out. The calculation agrees well with the experimental result. The accelerating corrosion is repeating the conditions of spraying the salty water and drying. Monitoring the chloride content ions and the electrochemical potential mapping, the accelerated corrosion test is now carryied out.

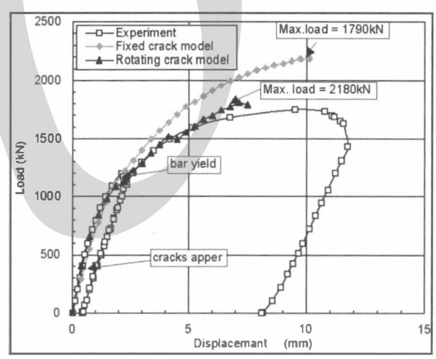

Fig.2 Test result and simulation

5. CONCLUDING REMARKS

We hope this report may be used for the maintenance, the inspection system as well as the retrofit for the similar type of Gerber Bridge or the similar aged bridges. It is judged that the environment of Arakawa Bridge was good condition in terms of the durability from the material tests and field inspections. Compared with the similar period Nasuno Bridge, concrete of Arakawa Bridge is more carbonated and more deteriorated than Nasuno Bridge.

REFERENCE

[1] Nomura, N., Tanaka, Y. and Yokooka, T. :Durability and structural safety evaluation for RC Gerber's bridge servicing for more than 60 years, UJNR 99, Tokyo, November 1999.

MANUAL FOR IMPROVEMENT IN DURABILITY OF PRESTRESSED CONCRETE BRIDGE (DESIGNING / CONSTRUCTION EDITION)

Yoshimitsu Shibata
Yachiyo Engineering Co., Ltd.
Japan

Jun Sakamoto
Taisei Corporation
Japan

Kouta Yamaguchi
Pacific Consultants Co., Ltd.
Japan

Yoshinobu Ishikawa
Oriental Construction Co., Ltd.
Japan

Minoru Mizoe
Japan Highway Public Corporation
Japan

Toyoaki Miyagawa
Kyoto University
Japan

Keywords: Prestressed concrete bridge, durability improvement, grout, initial inspection

1. INTRODUCTION

The Japan Prestressed Concrete Engineering Association has established the Subcommittee to examine the methods for improving the durability of prestressed concrete bridges. In the first phase subcommittee (1994 - 1996), designing and construction guideline (proposal) to improve the durability of newly constructed prestressed concrete bridges was published. It also introduced technical methods for repairing and strengthening the existing prestressed concrete bridges.

Later, many cases of deteriorated concrete construction were reported in Japan, drawing attention to concrete durability as a social problem. As to the prestressed concrete bridges, deterioration due to insufficient grout filling became a serious problem, which made if necessary to urgently prepare a standard incorporating new information on durability. Therefore, the second phase subcommittee was established in 1998. The second phase subcommittee aimed to improve durability of both new and existing prestressed concrete bridges, and summarized a manual consisting of "Designing / Construction Edition" and "Maintenance / Management Edition." This document reports on the "Designing / Construction Edition."

This manual mainly describes materials, designing and construction as the basics in facilitating durability of prestressed concrete road bridges to be constructed newly. It also covers the expansion joint, the drainage system, and the shoe which largely influence the durability of the prestressed concrete bridge main body.

Furthermore, since newly constructed bridges are the subject of this manual, it positions the completion test as the initial inspection and strongly recommends performing inspections to collect basic data for later maintenance and management as well as to learn whether there is any initial fault, damage, or deterioration.

In recent years, bridges incorporating new structures and new technologies are drawing attention for their rationality. However, these bridges have many unclear points on their durability because they have short history or records. Therefore, this manual summarizes with reference to various designing standards the matters to be noted for higher durability when prestressed concrete bridges adopting new structures or new technologies (bridge adopting external cables, PPC structure, composite structure, precast segment) are to be constructed.

2. PRESTRESSED CONCRETE BRIDGE DURABILITY IMPROVEMENT MANUAL

Though this manual describes the basic measures to improve new prestressed concrete road bridges and specifies the initial inspections to be implemented at the time of completion, this section introduces the overview of corrosion prevention in PC tendon and initial inspection.

PC tendon may be corroded by invasion of chloride ions, water, or air from outside even if they are contained in concrete. Especially when the PC tendon under high stress is corroded, the section of the PC tendon may decrease and cause the tendon to break. Some of the preventive ways to avoid PC tendon corrosion are ensuring grout filling, corrosion prevention on PC tendon surface, and use of tendons which is difficult to be corroded. Recently, there is also new development of methods requiring no PC grout injection into the duct after PC tendon is tensioned. Figure-1 shows the methods to prevent tendon corrosion.

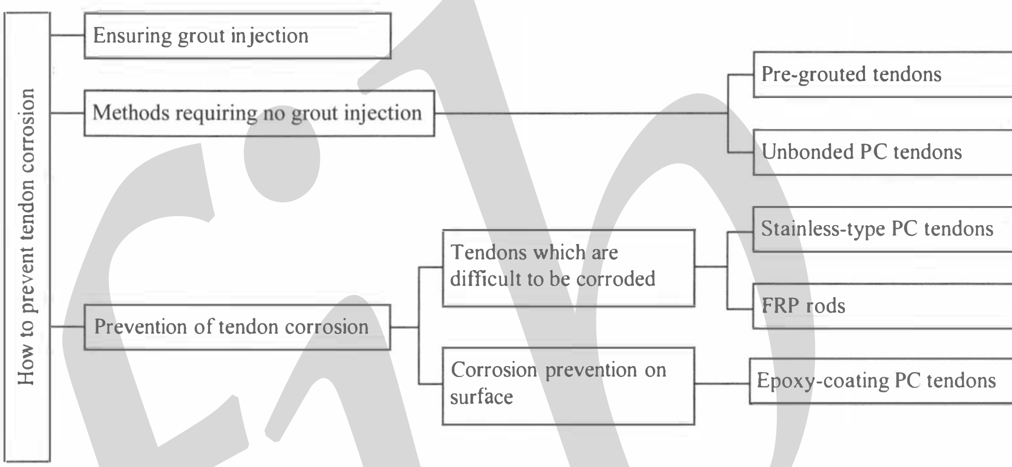

Fig.1 Examples of Tendon Corrosion Prevention

It was agreed that this manual would specify initial inspection as an inspection to predict structure deterioration after the prestressed concrete bridge is put to use in addition to confirmation of whether the quality specified in designing documents is ensured to be performed after the bridge is completed and before it is put to use. Inspection items are visual inspection of concrete surface states, concrete and grout quality inspection by confirmation of quality control results at the time of construction, and examination of reports on results of construction management using PC grout flow meter as an inspection of grout filling. If these inspection results show a possibility of not ensuring the specified quality, various nondestructive tests should be performed to confirm the quality, and the results are to be included in evaluation and judgment of inspection results. In addition, the inspection results here should be used as the initial data on deterioration in the later maintenance and management evaluations.

REFERENCES

(1) Prestressed Concrete Construction Association Corporation: Construction Manual for Prestressed Concrete Grout & Pre-grouted Tendon, 1999.11

(2) Japan Society of Civil Engineering: Standard Concrete Specifications [Construction] 1999 Fiscal Year Edition, 2000.1

REVIEW OF CROSS BEAM CONNECTION METHOD FOR THE EXISTING

PC POST-TENSION T BEAM

Shigeru Matsumoto Akiko Tabata Hideaki Teraguchi
Hanshin Expressway Public Corporation Nippon PS Corporation
JAPAN JAPAN

Keywords: cross beam connection, bond strength of concrete, flexible pier

1 INTRODUCTION

To eliminate or minimize damage in an expansion joint of a viaduct is considered as a very important subject from the viewpoint of a management of a viaduct. Because if it occurs, it may create a traffic accident, and also it causes a traffic conjunction during the repair work.

Hanshin Express Way Public Corporation has traditionally applied a seamless joint, which has less damage risks, to small span PC beams which expansion volume is relatively small. However it has been difficult to apply the seamless joint to the long span PC beams which length is 25m or more.

To resolve this problem, the cross beam connection method is intended to disuse the expansion joints themselves by connecting the existing adjoining end cross beams with prestressing steel bar.

Before adopting this method, we compared the life cycle cost estimation and ensured its applicability. This paper discusses, the verification test which was performed in terms of the adoption of this method, and the result of the study.

2 VERIFICATION TEST

2.1 Verifying shear strength at a joint section of a main beam and a cross beam

Because bonding reinforcing bars were not installed between the main beam and the cross beam in a PC post tension T beam which was constructed during Showa 40's (1965 - 1974), the verification is needed to declare whether the surface between the beams have the enough shear strength to propagate the stress. We performed the net yield strength experiment with the test piece which is shown in Fig.1, varying the prestressing load which affects the shear strength in the faying surface.

The result is shown in Fig.2. As seen in this figure, the obtained friction coefficient is almost equivalent to a general value, μ=0.5. And in the term of shear strength, it is found that the bond strength of concrete is also effective, other than the compression stress by prestressing.
Converting into the experimental revel, a prestressing force loaded into a joint section of a real structure is corresponding to 40kN as shown in Fig. 2, and the shear strength capacity is estimated to be approximately 200kN. In this situation, the shearing force at a real structure is computed to be 50kN which value is less than the shear strength capacity. Therefore it was verified that the joint section has enough capacity of shear strength to transfer the stress.

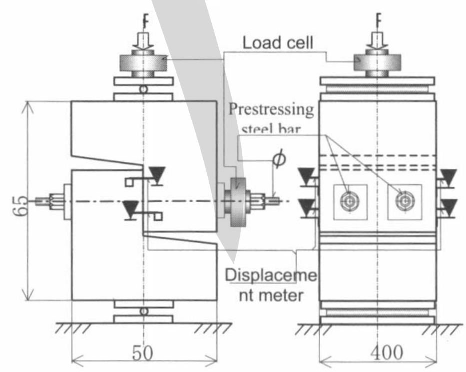

Fig.1 Test piece

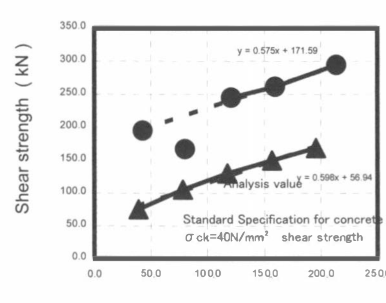

Fig.2 Prestress – shear strength

2.2 Static Loading Experiment

This experiment was performed to ensure the connection effect of cross beam connection method.

The test piece was connected form of the length of one main beam. Applying one-sided load, we measured the deflection and the opening width within the connecting part. Fig. 3 shows the load and the deflection.

Comparing the experimental value with the calculated value for 100% rigidity in the connecting part (equal to the rigidity in the main beam), it is found that as the load becomes higher, the modulus of rigidity decreases. When the load became the equivalent value of B live-load (14t)that defined in Japanese Specifications for highway bridge ,2002, it decreases to 5 - 20%. And on the B live-load, slippage did not occur between the main beam and the cross beam, and the measured opening width was only about 0.04 mm and it corresponds to about 0.1 mm in a real structure level, therefore it is considered that there is no problem in the durability of continuous paving.

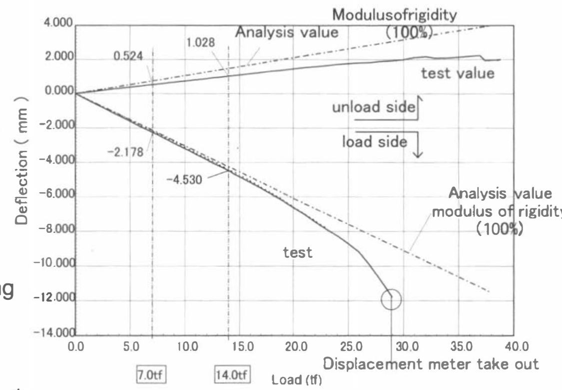

Fig.3 Load – deflection

Furthermore, remarkable damage did not occur when applying up to double of the design load. The subsequent destruction transferred from the breaking in the connecting part to the main beam, and did not lead extremely dangerous breakdown.

2.3 Cycles Loading Experiment

This experiment was performed to ensure the safety of the cross beam connecting part against fatigue. The test piece is the part from the connecting part, in which the negative bending may occur. Fully loading the B live-load, measurement was performed respectively in the cases of 100% and 20% rigidity of the connecting part. In the former experiment, it is ensured that the range of rigidity of the cross beam connecting part is 5 - 20% of the continuous beam. The 20% is the rigidity in which the negative bending becomes the maximum within this range.

According to the experiment, in the case of 100% rigidity of the connecting part, slippage between the main beam floor slab and the cross beam occurred in N=5,700, the edge between the main beam and the cross beam was broken apart completely in N=1.3 million. In the case of 20% rigidity of the connecting part, just a small opening occurred even after 2 million times loading, there is no slippage between the main beam and the cross beam nor decline in the yield strength. From this result, the safety against the fatigue in the connecting part has been ensured.

3 LIFE CYCLE COST

For 40 spans and 41 piers in Higashi Osaka Line, one of the lines of Hanshin Express Way, we compared the cost for the case in which the cross beam connection method is adopted and the case in which the maintenance for expansion is performed without beam connection work. According to the result, the initial cost is nearly equivalent. Considering the life cycle, the cost for the former case of adopting the cross beam connection work is to be cheaper.

REFERENCES

[1] Standard Specification for Concrete (Japan Society of Civil Engineers, constituted in 1996)

[2] Hayashi, Kawamura, Teraguchi, Joudai: “Loading Tset of Prestressed Concrete Girders Connecting End Diaphragms”, Proceedings of the 8th Symposium on Developments in Prestressed Concrete, October, 1998

[3] Hayashi, Hayashida, Uchida, Saito: “Experiment on Shear Strength of the Match-Cast Concrete between PC Girder and its Cross Beam”, Proceedings of the 8th Symposium on Developments in Prestressed Concrete, October, 1998

[4] Hayashi, Kawamura, Uchida, Joudai: “A Fatigue Failure Behavior of Coupling Structures in Prestressed Concrete Girders Connecting End Piaphragms”, Proceedings of the 9th Symposiums in Developments of Prestressed Concrete, October, 1999

Session 13 | Failure mechanism and non-linear analysis for practice

PRACTICAL USE OF NONLINEAR ANALYSIS ON DAMAGE DETECTION OF RC STRUCTURES

Yoshio KANEKO Hirozo MIHASHI Naruaki KANEZASHI Akira MITA

Tohoku University
JAPAN

Keio University
JAPAN

Keywords: Nonlinear FEM analysis, structural health monitoring, reinforced concrete structure, story stiffness, rotation angle of column-base

1 INTRODUCTION

A system identification technique is aggressively employed in the field of airplane and offshore-platform, in which the occurrence of damage, the level and the location are detected. The change of natural frequency and vibration mode are examined employing the vibration measurement for an earthquake, a micro tremor and a forced vibration [1]. Though the methodology to evaluate the global characteristics has been studied, there is little study on the quantitative correlation between the dynamic characteristics and the local damage level. Therefore, the quantification of correlation between the damage level of members and global response of framing system is expected.

In this paper, the relation between the change of mechanical characteristics of the framing system due to an earthquake and the damage level of the structural members is numerically examined, based on the fact that the natural frequency of structures is changed before and after an earthquake.

2 STRUCTURAL FRAME FOR ANALYSIS

The interior column-beam joint was considered as shown in Fig. 1. The frame was modeled assuming a part of intermediate story in a typical six-storied reinforced concrete building and the structure was designed as a weak beam/strong column moment frame. A pushover analysis was carried out for the framing system shown in Fig. 1. At the first loading step, the column axial force N_L was applied without both vertical supports of the beam. At the subsequent loading steps, N_L and the vertical displacement due to N_L at the supports of the beam was kept constant, and the lateral force Q_H was increased step by step in both positive and negative directions. The frame was assumed to be in a state of plane stress except the column-beam joint. We considered two cases: (1) column-beam joint in a state of plane stress for weak orthogonal restraint; (2) column-beam joint in a state of plane strain for strong orthogonal restraint.

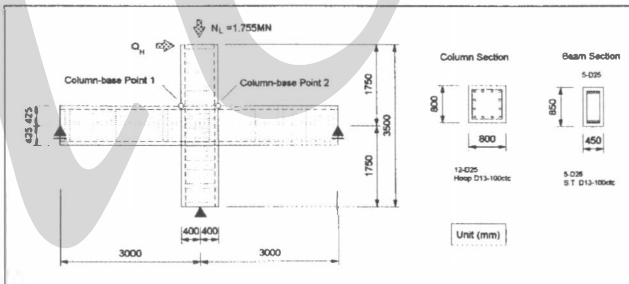

FIG. 1 Framing Configuration and Loading Condition

3 NONLINEAR FINITE ELEMENT ANALYSIS

The two dimensional pushover analysis was carried out using ATENA Finite Element Program developed by V. Cervenka et al. [2]. A smeared crack approach using a rotating crack model was employed. Finite plane stress/strain elements consist of quadrilaterals. The stress-strain relation of reinforcement is assumed as perfectly elasto-plastic. The main reinforcement is modeled by a discrete truss bar element, which is embedded and passing through the quadrilateral elements. The truss bar element has only axial stiffness and is in the uniaxial stress-state. The shear reinforcement is modeled by a smeared reinforcement which axial stiffness is considered in the quadrilateral element.

In the present analysis, two constitutive models for concrete were employed in order to examine the model-dependency: (1) damage model in the plane stress state and (2) fracture-plasticity model in both the plane stress state and plane strain state.

4 ANALYTICAL RESULTS

The eminent story stiffness reduction is observed at the relatively small drift ratio (see Fig. 2a). In addition, the stiffness associated with micro deformation after large deformation has high correlation with the secant stiffness at large deformation (see Fig. 2b).

The linear correlation between the rotation angle of the column-base and the drift ratio is kept even in the nonlinear response level (see Fig. 2c).

5 APPLICATION FOR STRUCTURAL HEALTH MONITORING

Based on the findings obtained in the analysis, potential systems for a structural health monitoring are explained as follows: (1) The good correlation between the stiffness associated with micro deformation and the secant stiffness at large deformation implies that the story stiffness identified from the micro tremors may indicate the ever-experienced deformation in a particular story; (2) Since the story drift has a good correlation with the rotation angle of the column-base, it may be useful to develop a damage index sensor that can memorize the maximum rotation angle of the column-base. Then, the drift ratio is evaluated examining the rotation angle of the column-base and finally the damage level is evaluated based on the known drift ratio.

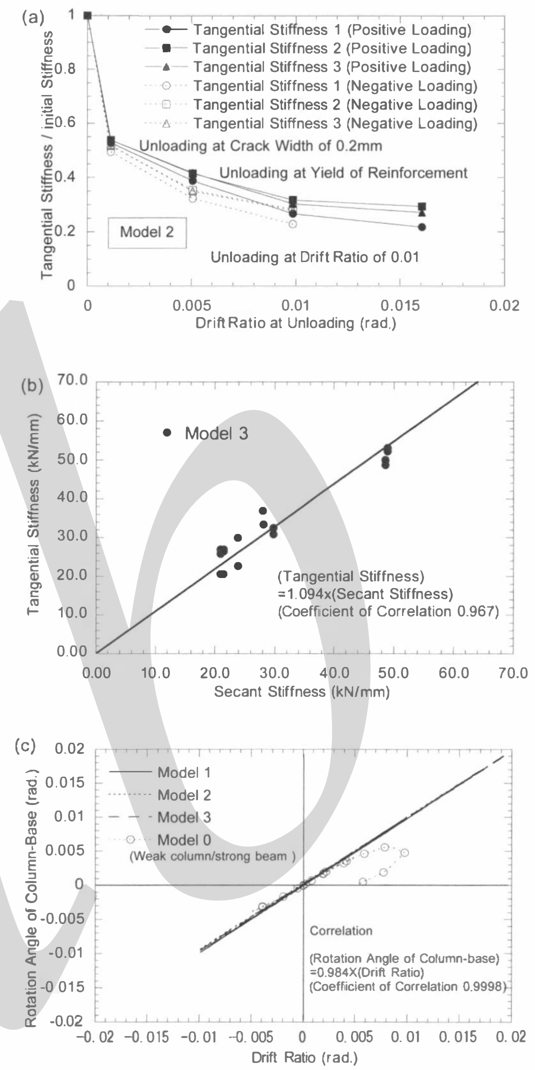

FIG. 2 (a) Story Stiffness Reduction vs. Drift Ratio; (b) Tangential Stiffness vs. Secant Stiffness; (c) Rotation Angle vs. Drift Ratio

6 CONCLUSION

In this paper, a practical use of nonlinear FEM analysis is introduced, employing a part of the weak beam/strong column moment frame. The story shear-drift ratio relation is analyzed numerically in association with the damage level. The correlation between the story stiffness/the rotation angle of the column-base and the damage level of members in the frame under lateral loading is clarified. Based on the numerical analysis, the methodology of the reliable structural health monitoring system is indicated.

REFERENCES

[1] Doebling, S. W., Farrar, C. R., Prime, M. B., and Shevitz, D. W.: Damage Identification and Health Monitoring of Structural and Mechanical Systems From Changes in Their Vibration Characteristics: A Literature Review, Los Alamos National Laboratory Report LA-13070-MS, May 1996.

[2] Cervenka Consulting: ATENA Computer Program for Nonlinear Finite Element Analysis of Reinforced Concrete Structures, Program Documentation, Prague, May 17, 2000.

A NEW PROCEDURE FOR MODELLING CREEP UNDER VARIABLE STRESSES

Hugues Somja, Engineer
Vincent de Ville de Goyet, Dr. Engineer
Greisch Engineering, Belgium

Jean-Claude Dotreppe, Professor
University of Liège, Belgium

Keywords: creep, time-dependent effects, stress history

1 INTRODUCTION

The usual basis for the evaluation of creep of concrete under variable stresses is the principle of superposition. This article presents a numerical technique which, by using only a few variables, obtains the same final strain as the one from the superposition principle and presents at intermediate stages a maximum difference in strain of 5 %.

This method is based on the fictitious loading age method (FLAM). The original method cannot represent the recovery of creep. Furthermore differences of 20 % with the superposition principle are often observed. The article shows how the new method, called FLAM2, solves these two problems.

2. DESCRIPTION OF FLAM2 METHOD

According to the superposition principle, if a stress σ_1 is applied at time t_1, and a stress σ_2 at time t_2, the concrete strain at time $t > t_2$ is given by :

$$\varepsilon=J(t,t_1)^*\sigma_1 + J(t,t_2)^*\sigma_2. \qquad (1)$$

$J(t,t_0)$ is the compliance function.

FLAM method replaces these two terms by only one:

$$\varepsilon=J(t,t_{fla})^*(\sigma_1+\sigma_2) \qquad (2)$$

t_{fla} is calculated in order to respect the strain continuity at time t_2 (Fig.1).

This method has two major limitations :

- Recovery cannot be represented
- The final strain is not the same as the one given by the superposition principle, though in practice the difference remains acceptable.

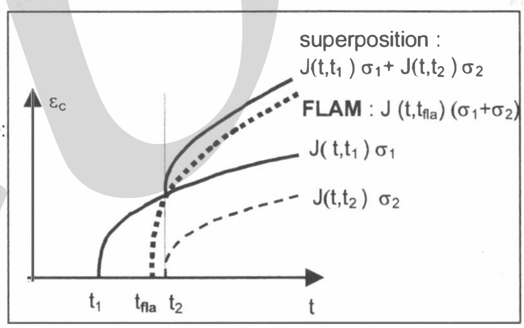

Fig. 1 Strain evolution from FLAM and from the superposition principle

The first problem has been solved by Philippe Boeraeve [1].

The second one has been worked out in FLAM2. The superposition principle is replaced by the equation :

$$\varepsilon=J(t,t_{fla})^*(\sigma_1+\sigma_2) + \varepsilon_{base} \qquad (3)$$

Two conditions have to be expressed to determine t_{fla} and ε_{base}. In the method proposed here the strains obtained by FLAM2 and the superposition principle are set equal at two particular times, t_2 and t_∞.

Another way of solving the same problem has been proposed by Kretz and Peyrac [2]. Instead of adding a free variable like ε_{base}, they use the value of the compliance function J_∞ at time t_∞ as a parameter. This approach is usually called "Incremental Method".

3 NUMERICAL TEST

FLAM, FLAM2 and the incremental method are compared with the superposition principle by studying the behaviour of a concrete specimen submitted to varying stresses (Fig. 2).

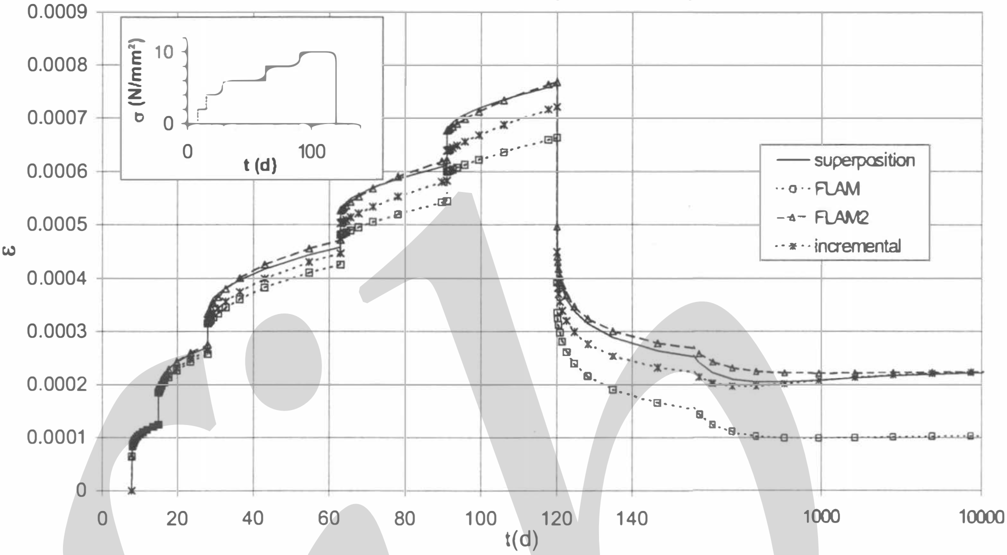

Fig. 2 Strain evolution for varying stresses

While the stress increases, the method which is closer to the superposition principle is FLAM2.
After total unloading, during recovery, the residual strain given by the incremental method is very close to the one given by the superposition principle.
It can be seen that the strain predicted by the superposition principle increases during recovery, while the stress on concrete is equal to 0. This is a well known shortcoming of the superposition principle, mentioned already by Bazant, but with very few practical consequences.

4 CONCLUSIONS

The purpose in developing FLAM2 was to obtain a simple and efficient tool, to be used for the calculation of structures in which creep is one of the problems that has to be taken into account. From this study, it can be concluded that this objective is reached.

- From a technical point of view :
  - The final state is identical to the one given by the superposition principle
  - As shown in examples, the differences at intermediate stages are small.
- From a numerical point of view :
  - Only 6 variables must be stored
  - Updating at each step is done by solving only one equation with one single unknown.

REFERENCES

[1] Boeraeve P.: Contribution à l'analyse statique non linéaire des structures mixtes planes formées de poutres, avec prise en compte des effets différés et des phases de construction. Thèse de doctorat, Université de Liège, 1991.
[2] Kretz T. and Peyrac P. : Le fluage du béton : les limites des modèles classiques appliqués aux ouvrages d'art. Les perspectives du modèle incrémental. Bulletin du Laboratoire des Ponts et Chaussées (LCPC), Spécial XX, pp 41-48, 1998.

EFFECTS OF SCALE AND RIB SHAPE ON BOND STRENGTH OF DEFORMED BAR

Changde Fu Toshikatsu Ichinose Yuji Kanayama Yoshiki Inoue John E. Bolander
Nagoya Institute of Technology, Japan University of California, Davis, USA

Keywords: Scale effect; rib shape; bond strength; concrete cover thickness; and splice

1 Introduction

This paper investigate the effects of scale and rib shape of deformed bars on bond strength using lap splice specimens. The cause of the scale effect in bond splitting is discussed, which leads to a set of design equations for lap splice strength, revising recent proposals by Zuo and Darwin [1].

2 Description of tension lap splice test and load method

Figure 1 shows the specimens geometry and loading system for the lap splice test. Two forces were monotonically applied as shown in Fig. 1 (a) to produce a constant moment over the splice length, l_s. Each specimen had two splices of 12.6 d_b in length.Table 1 indicates the parameter settings for the six series of tested specimens.

3 Result of tension lap splice test

The relation between bond strength and bar diameter is plotted by logarithm scale in Fig. 2 for all the splice specimens. The solid lines show the result of regression analyses. Figure 3 shows the relationship between the bond strength and the scale effect, as given by the slope of the regression lines in Fig.2. In general, the scale effect decreases as the bond strength increases due to larger confinement. The scale effect is larger for the bars with higher ribs.

4 Proposed equation for splice without stirrups

The following equation, based on Zuo and Darwin's equation, is proposed to calculate the concrete contribution in consideration of the scale effects in the case without stirrups.

$$T_c = \left[61 l_s (c_m + 0.5 d_b) + 2251 A_b \cdot d_b^{-0.4}\right] \cdot \left[0.1\left(\frac{c_M}{c_m}\right) + 0.9\right] \cdot f'_c{}^{\frac{1}{4}} \quad (1)$$

Note that the power on d_b, -0.4, should be larger in magnitude than the value of -0.3 plotted in Fig. 3 because the scale-effect is considered in one of the two terms in Eq. (1). Figure 4 compares the computed results with the experimental results given in the database of Zuo and Darwin [1] and in this paper.

Table 1 Parameters of lap splice specimens

Specimens		d_b	bond length	stirrup diameter	stirrup spacing	Number of specimen
		(mm)				
with stirrups	LS17L / LS17H	17.4	220	4	24.5	3
	LS35L / LS35H	34.8	440	8	49	2
	LS52L / LS52H	52.2	660	12	73.5	1
without stirrups	LC17H	17.4	220	-	-	3
	LC35H	34.8	440			2
	LC52H	52.2	660			1

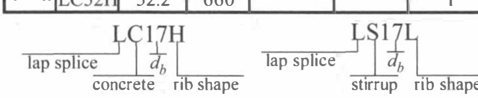

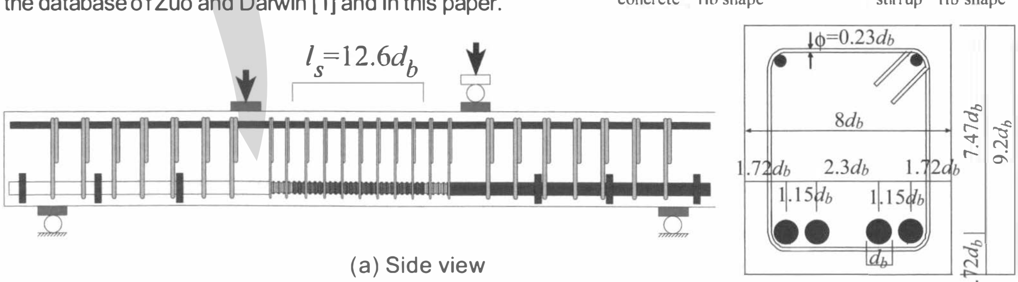

(a) Side view

Fig.1 Splice specimen (with strirrups)

(b) Cross-section

The relation between the bond strength plotted by logarithm and the main bar diameter is shown in Fig. 2 by the chained lines.

5 Proposed equation for splice with stirrups

We propose the following equation for calculating the confining steel contribution of specimens with stirrups:

$$T_s = \left[165 \cdot R_r \cdot d_b^{\,0.2-1.8\cdot R_r} + 22\right] \cdot \frac{NA_{tr}}{n} \cdot f'_c{}^{\frac{3}{4}} \tag{2}$$

The term R_r (ratio of rib height to rib spacing) had to be included in the power on d_b, since the scale effect in the specimen with low rib height was so small. The chained lines in Figs. 2 show the results computed by Eqs. (1) and (2). The relation between experimental results and the value computed from the formula (1) and (2) is shown in Fig. 5.

6 Conclusions

The experimental work reported here investigated the dependence of bond strength over a range of specimen scales, including those for bar sizes currently outside the limits prescribed by ACI318-02. The results clearly showed a strong scale effect on the bond strength. More specifically:

1. The effect of scale without confining steel reinforcement was larger than that with such reinforcement.
2. The larger rib height/interval ratio, which affects the strength of splices confined by stirrups results in larger scale effect.

The design equations for bond strength proposed by Zuo and Darwin [1] have been modified to better represent the scale effect witnessed in this experimental program. The modified equations also agree well with the experimental database presented by Zuo and Darwin [1].

REFERENCES

[1]. Zuo, J. and Darwin, D., 2000, "Splice Strength of Conventional and High Relative Rib Area Bars in Normal and High-Strength Concrete, ACI structural journal, Vol. 97, No. 4, pp. 630-641

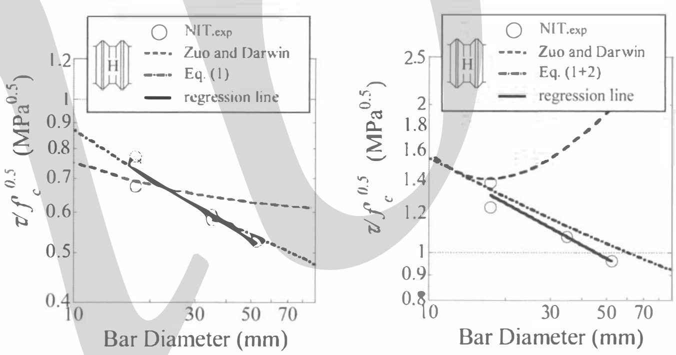

(a) Type H (without stirrups) (b) Type H (with stirrups)

Fig. 2 Bond strength-bar diameter relation for all lap splice specimens

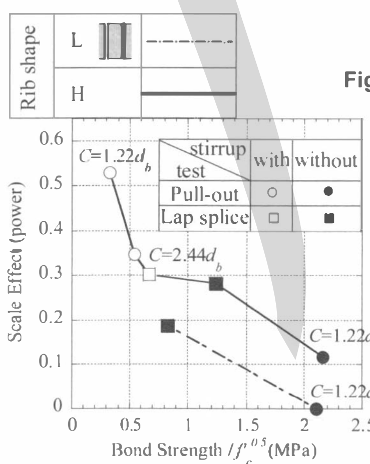

Fig. 3 Scale effect-Bond Strength

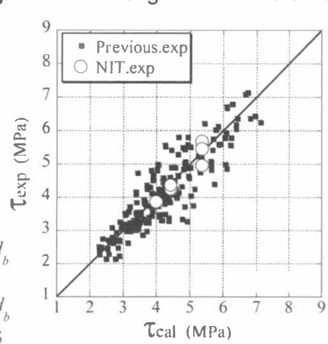

Fig. 4 Comparison between calculated and experimental results (without stirrups)

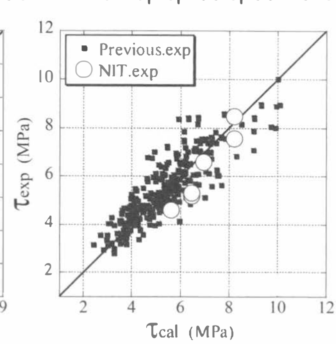

Fig. 5 Comparison between calculated and experimental results (with stirrups)

MODELLING OF NON-LINEAR TIME-DEPENDENT EFFECTS OF CREEP AND SHRINKAGE IN PRESTRESSED CONCRETE BRIDGES

Stuart G Reid
Department of Civil Engineering
University of Sydney, NSW 2006
Australia

David Coker
Department of Civil Engineering
University of Sydney, NSW 2006
(now with SMEC Australia)

Keywords: creep, shrinkage, deflection, prestressed concrete bridges, Bayesian updating

1 INTRODUCTION

The time-dependent effects of creep and shrinkage are particularly important with regard to the deformations and serviceability of prestressed concrete bridges. The prediction of creep and shrinkage effects is important not only for the purposes of initial design, but also for the purposes of monitoring structural performance with regard to the rate of development of deformations. If structural monitoring shows that measured deformations at an early age are greater than expected, theoretical models should be used to produce revised (updated) predictions of the deformations at later ages.

In principle, the statistical method of Bayesian updating can be used to improve the theoretical model predictions taking account of measured deformations, and accounting for the variability of the model parameters and the distributions of likely responses related to the range of values of the model parameters. In practice, however, Bayesian updating is difficult to apply to the prediction of prestressed concrete bridge deformations because there are many variables involved in the relevant theoretical models and it is difficult to assess the relevant likelihood functions (based on laborious time-step analyses of finite element models).

The present study concerns the modelling of time-dependent effects of creep and shrinkage in prestressed concrete bridge units in the Douglas Park Twin Bridges located near Sydney, Australia. These effects are not only time-dependent but also non-linear due to the non-uniform development of creep and shrinkage effects throughout the structure (resulting in continuous redistributions of internal stresses).

Theoretical results have been obtained from time-step analyses of finite element models, incorporating three alternative numerical models of elemental concrete creep and shrinkage. The theoretical results have been compared with measurements of the actual bridge deformations recorded over a period of 20 years.

Also, a simplified Bayesian updating technique has been proposed to extrapolate beyond the measured values of bridge deformations to predict the most likely values of subsequent deformations (based on theoretical modelling and accounting for the uncertainty of the theoretical model parameters and the sensitivity of deformations to uncertain variations of those parameters).

2 NUMERICAL MODELLING

Numerical modelling of the non-linear time-dependent effects of creep and shrinkage in the prestressed concrete bridge units has been carried out using time-step analyses, including finite element modelling of the structural effects of concrete creep and shrinkage strain increments.

Due to the prestress, the concrete is uncracked and the concrete strains have been described using creep and shrinkage models for uncracked concrete. The modelling of strain increments within each bridge element was carried out using three alternative numerical models of creep and shrinkage: the BP model, the CEB-FIP (1978) model and the calculation model given in the Australian Standard AS3600 (all described in [1]).

The finite element modelling of the structural effects of the concrete creep and shrinkage strain increments was carried out using equivalent thermal stress analyses based on the finite element program Strand7. For the purposes of analysis, the bridge was divided into elements with essentially uniform creep and shrinkage characteristics throughout each element .

The calculated deflections based on the BP, CEB-FIP and AS3600 models were compared and found to be similar. The calculated deflections were also compared with measurements of the actual bridge deformations recorded over a period of 20 years. Figure 1 shows a typical comparison between calculated deflections (based on the BP model) and measured deflections at a hinged joint.

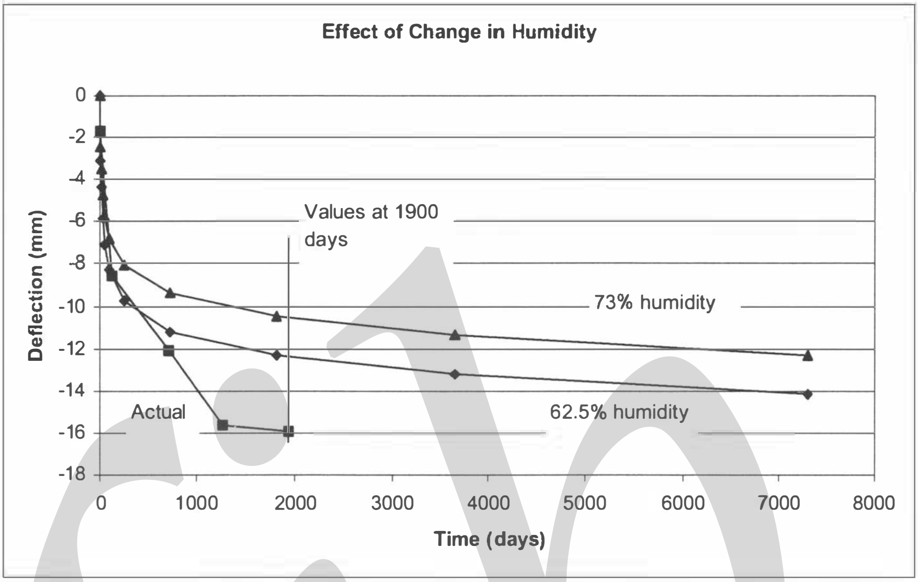

Fig. 1 Measured and calculated deflections (showing calculated effect of change in humidity)

The numerical models predicted the general trend of the deflections up to about 3,000 days (although the measured deflections were generally greater than predicted for that period). Beyond 3,000 days, the numerical models predicted only very small increases in the deflections, but survey results have shown significant increases in the deflections over the period from 3,000 to 8,000 days. Accordingly, the measured long-term deflections due to creep and shrinkage are much larger than predicted and significant growth of the deflections has continued over a much longer period of time than predicted.

2.1 Bayesian Updating

A simplified method of Bayesian updating has been proposed to extrapolate from measured deflections. The simplified method identifies the most likely values of uncertain model parameters x_i consistent with the measurements. The most likely value of the model variable x_l (with mean value m_l and standard deviation σ_i) that would predict an observed response u^* (relative to the expected response u based on expected values of the variables m_i) is given by

$$x_i^* = m_i + \alpha_i \beta \sigma_i$$

$$\alpha_i = \frac{\partial u}{\partial x_i}\sigma_{x_i} \Bigg/ \left(\sum_i \left(\frac{\partial u}{\partial x_i}\sigma_{x_i} \right)^2 \right)^{\frac{1}{2}} \qquad \beta = \left(u^* - u\right) \Bigg/ \left(\sum_i \left(\frac{\partial u}{\partial x_i}\sigma_{x_i} \right)^2 \right)^{\frac{1}{2}}$$

Following this approach, it is concluded that the 'most likely' values of the model bias factor k and humidity h consistent with the observed deflection shown in Figure 1 (at 1900 days) are k^*=1.276 and h^*=0.60. These 'most likely' values could be used in numerical modelling to obtain updated estimates of subsequent deflections. However, it should be noted that this (or any other updating procedure) would improve the deflection estimates only as long as the values of k and h do not vary with time.

REFERENCE

[1] Gilbert, R.I.:Time Effects in Concrete Structures. Elsevier, Sydney, 1988

A MECHANICAL MODEL FOR THE CONFINED COMPRESSED CONCRETE OF RC BENDING ELEMENTS

Alessandro P. Fantilli — Paolo Vallini
Department of Structural and Geotechnical Engineering
Politecnico di Torino, Italy

Ivo Iori
Department of Civil Engineering
University of Parma, Italy

Keywords: RC beams, compressed concrete, confined concrete, ductility.

1 INTRODUCTION

In the ultimate structural analysis of reinforced concrete bending members, a constitutive law for the compressed concrete, which should be able to encompass the crushing and the subsequent expulsion of v-shaped concrete block, is needed. In the stress-strain diagram for the concrete in compression, after the compressive strength, the softening branch indicates the concrete failure that localizes around sliding planes.

Due to recent developments of fracture mechanics, the crushing of concrete in uniform compression can be modelled more effectively. In several works the experimental softening behaviour of various concrete cylinders is shown with a single curve in the post-peak compressive stress -inelastic shortening diagram. The curve seems to be independent of the specimen length, therefore within the element, as in tension problem, it is possible to identify a localized damage surface and the relevant compressive fracture energy. Some authors attribute the softening branch of the σ-ε diagram to two different localized damage zones where, respectively, the splitting cracks and the local deformation are allocated. Other authors proposed a damaged band of uniaxial splitting crack, in which buckling of concrete slabs between two cracks takes place. Although a revision of the classical definition of the post-peak behaviour of uniform compressive concrete, when brittle or quasi-brittle failure occurs, has been proposed, its mechanisms remain unclear. This localized phenomenon appears both in the uniaxial and eccentric compression, when the compressive strength is reached. It may be analysed with the sliding model proposed in [1], where the softening branch of stress-strain law depends on the strain gradient (i.e. curvature) and on the dimension of concrete in compression. For bending beams without stirrups, a good agreement between numerical and experimental computation of the ductility has been obtained.

The crushing of compressed concrete, and the subsequent softening branch in the post-peak response of RC members, are more visible in over-reinforced concrete elements. This is evident in the experimental results of Mansur et al. [2], where four point bending beams, having the same cross section and longitudinal reinforcement, have been tested. In these tests, to increase the ductility of RC members, a different amount of transversal reinforcement (i.e. stirrups) has been introduced. To analyzed these aspects, in this work the post-peak behaviour of concrete in compression is also computed when a confinement is present. In point of fact, closed stirrups in a beam may restrain the vertical displacement of the concrete that slides along the failure planes. Therefore, the vertical strain of compressed zone, obtained from a numerical procedure, could be considered as an implicit action affecting the stirrups, those are stressed without any shear actions.

2 THE PLASTIC ROTATION AND ITS SIZE EFFECTS

Mechanical models based on stress-strain relationships for compressed concrete, are not able to show the size effects of ductility. On the contrary, the variation of the plastic rotation, observed in the some tests, could be reproduced with the proposed model. Taking into account the proposed approach, size effects are inevitably considered, since in each point of concrete in compression the stress is function of both the curvature and the depth of compressed zone.

For these reasons, some numerical results obtained with the proposed model are presented in the present section. The object of these applications is to investigate the effects of structural dimensions and transverse reinforcement on the ultimate limit state (and ductility) of RC beams. In particular, the cross sections of these beams are obtained multiplying the dimensions of Fig. 1a by a factor scale. The conventional plastic rotation θ of a block of length H could be considered as a measurement of ductility:

$$\theta = \mu \cdot H \tag{1}$$

where μ is the cross section curvature obtained from the moment curvature relationship of Fig. 1b.

In the present study, the plastic rotation θ has been calculated with Eq.(1) both at the maximum moment, where $M = M_{max}$ and $\mu = \mu_{max}$, and in the point of softening branch where $M = 0.98\ M_{max}$ and $\mu = \mu_u$ (Fig. 9b). In Fig. 1c, the plastic rotations, obtained in the cases of confined (with stirrups) and unconfined concrete (without stirrups), versus the scale factor are plotted. In the same diagram are also considered the plastic rotations obtained from the application of CEB model [3] for compressed concrete.

In Fig. 1c an appreciable size effect of ductility is measured both at peak load ($\mu = \mu_{max}$) and after the peak load ($\mu = \mu_u$). For beams with confined concrete, plastic rotations are higher than the unconfined ones, even if the difference (due to the stirrups confinement) decreases with increasing in the scale factor. No dimensional effects can be evaluated through the application of CEB model [3] for compressed concrete, for $\mu = \mu_{max}$ and $\mu = \mu_u$, with or without stirrups.

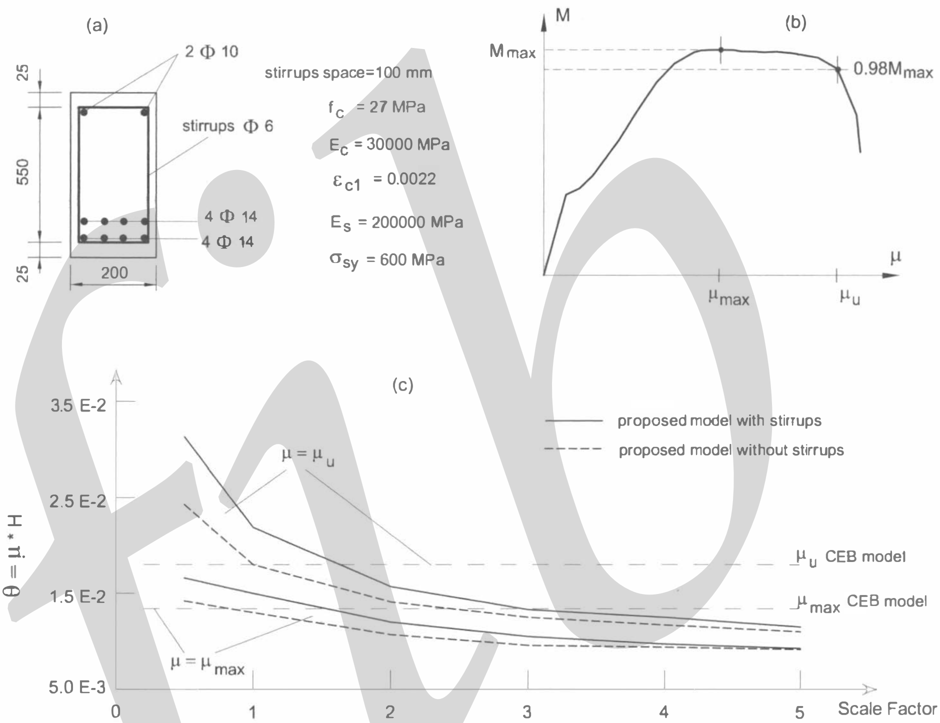

Fig.1 Plastic rotation and its size effects: (a) cross-section of beams; (b) M-μ diagram; (c) plastic rotations versus scale factor

3 REFERENCES

[1] Fantilli, A. P., Ferretti, D., Iori, I., and Vallini, P. “A Mechanical Model for the Failure of Compressed Concrete in R/C Beams.” J. Struct. Engrg., ASCE, 128(5), pp. 637-645, 2002.

[2] Mansur, M. A., Chin M. S., and Wee T. H. “Flexural behavior of high-strength concrete beams.” ACI Struct. J., 94(6), pp. 663-674, 1997.

[3] CEB, Comité Euro-International du Béton. “High performance concrete - recommended extension to the model code 90”. CEB Bulletin d'Information No. 228, Comité Euro International du Béton, Lausanne, 1995.

NON LINEAR ANALYSIS AND SAFETY FORMAT FOR PRACTICE

G. Mancini
Department of Structural Engineering and Geotechnics - Politecnico di Torino, Turin
e–mail: mancinig@athena.polito.it

Keywords: analysis, format, practice

1 INTRODUCTION

Non linear analysis in concrete structures nowdays cannot be considered only as a research tool to improve the understanding of structural behaviour, but it is also a useful mean to design more and more enhanced structures and to estimate the actual safety level in existing structures. As a consequence it becomes necessary the definition of a proper safety format for the use of non linear analysis within the frame of semiprobabilistic approach to the structural safety, the most common method currently used in practice by the designers.

In the following, after a retrospective revue of main issues on this subject, a proposal for non linear analysis safety format is presented, able to take into account all the model uncertainties currently defined within the most update safety codes and to fullfill the safety verifications both in scalar and vectorial combination of internal actions.

2 NEW PROPOSAL FOR SAFETY FORMAT IN NON LINEAR ANALYSIS

Mantaining the approach of a global safety coefficient, the safety format should be applied in the external and internal actions domain, that is:

$$S(\gamma_G G + \gamma_Q Q) \le R\left(\frac{q_u}{\gamma_{Gl}}\right) \tag{1}$$

where q_u is the maximum level of direct/indirect actions reached in non linear analysis, performed with materials strength $0.85 f_{ck}$ and f_{ym}.

In such a manner:

- the safety format eq.(5) is consistent with the semiprobabilistic approach;
- the comparison between S and R automatically takes account of structural behaviour;
- model uncertainties both on action and resisting side may be explicitely taken into account splitting the $\gamma_G, \gamma_Q, \gamma_{Gl}$ coefficients.

In agreement to this last point the inequality (1) may be modified into:

$$\gamma_{Rd} S(\gamma_G G + \gamma_Q Q) \le R\left(\frac{q_u}{\gamma_{gl}}\right) \quad \text{or} \quad \gamma_{Sd}\gamma_{Rd} S(\gamma_g G + \gamma_q Q) \le R\left(\frac{q_u}{\gamma_{gl}}\right) \tag{2}$$

with $\gamma_{Sd} = 1{,}15$, $\gamma_{Rd} = 1.08$ and $\gamma_{gl} = 1{,}2$.

The inequalities (2) should be alternatively used as safety format for non linear analysis, according to the importance assumed by model uncertainties on the action side within the specific design.

The definition of uncertainties covered by γ_{Sd} and γ_{Rd} partial factors may be assumed in agreement to Eurocode – Basis of Structural Design, that is:

- γ_{Sd} takes account of uncertainties in modelling the effects of actions and, in some cases, in modelling the actions;
- γ_{Rd} takes account of uncertainties in the resistence model and of geometric deviations not explicitely modelled.

It appears then clearly the necessity to introduce the γ_{Rd} and, eventually, γ_{Sd} partial factors in the safety evaluation of a non linear process.

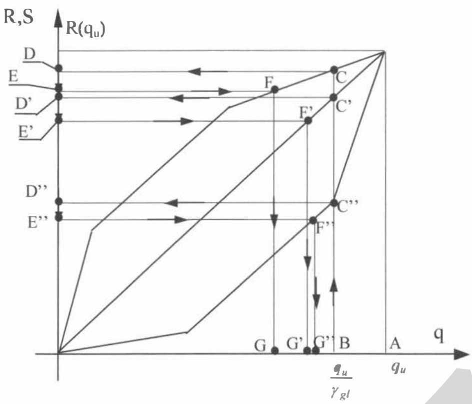

Fig. 1 – Application of safety format for scalar problems

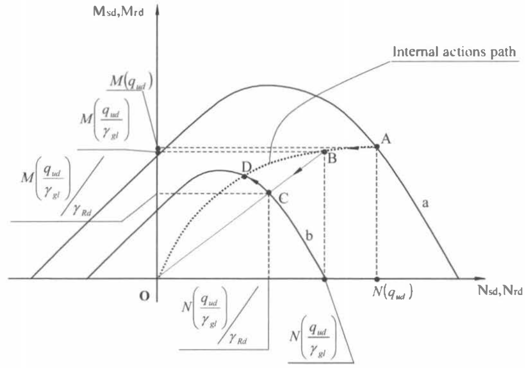

Fig. 2 – Safety format application for vectorial (M,N) underproportional behaviour in M

The application of safety format described in (2) requires further comments according to wether the safety verification is performed within the scalar or vectorial field. In fig. 1 the application of proposed safety format ($\gamma_{Sd} = 1$, $\gamma_{Rd} = 1{,}08$) is shown for three different internal action path in the scalar field: overproportional, linear, underproportional; the corresponding final point of procedure G, G', G'' defines the maximum value of action combination $(\gamma_G G + \gamma_Q Q)$ compatible with the required safety level.

In case of vectorial combination of internal actions, like N, M_x, M_y or n_x, n_y, n_{xy}, the safety format application is shown in fig. 2 (considering for the sake of semplicity only N, M_x combination).

Point A is the analysis final step and the curve "a" represent the safety domain N,M built with the same material strength used for the analysis. By the application of γ_{gl} one shifts from point A to B along the internal action path; at this point the linearization should be performed vectorially reducing vector $\overline{OB}$ by the ratio γ_{Rd}. Now point C is reached, which distance from the safety domain is a misure of the safety level required. In general point C does not belong to the internal action path. Can be individuated, then, a point D, that has the same safety level than C, at the intersection of the curve "b", omothetic domain to "a" passing by C, with the internal action path.

The final verification requires that the point representing the design combination $M(\gamma_G G + \gamma_Q Q)$; $N(\gamma_G G + \gamma_Q Q)$ remains along the internal action path inside the omothetic safety domain "b".

Same procedure applies tridimensionally in case of combination of N, M_x, M_y or n_x, n_y, n_{xy}. It is then clear that in case of vectorial combination of actions the safety format requires the knowledge of safety domain related to the same strength distribution used in the analysis.

3 CONCLUSIONS

A new proposal for the safety format in non linear analysis field is suggested; the procedure is able to take into account the internal action path in the region in which failure is reached and model uncertainties both on resistence and actions side. This proposal is also consistent with the safety approach within the semiprobabilistic level, the most common method currently used in design. Nevertheless this solution is contained within the well known frame of semiprobabilistic approach to structural safety and is based on engineering judgement, a calibration with level 2 method should be performed in a near future, to evaluate the scattering in β value of structures designed with such an approach and able to give rise to a very large variety of internal actions paths.

SIZE EFFECT ANALYSIS OF REINFORCED CONCRETE MEMBERS USING MULTI EQUIVALENT SERIES PHASE MODEL

Toshiaki Hasegawa
Institute of Technology, Shimizu Corporation
JAPAN

Keywords: nonlocal constitutive model, Enhanced Microplane Concrete Model, shear, bending

1 INTRODUCTION

The role that size effects play in the failure of concrete structures is extremely complicated. Numerical simulations are, consequently, an efficient means of exploring their causes and establishing design codes that take them into account. Size effects in the shear failure of reinforced concrete deep beams and in the flexural failure of reinforced concrete slender beams are simulated using both the Multi Equivalent Series Phase (MESP) Model [1] and the Enhanced Microplane Concrete (EMPC) Model.

2 MULTI EQUIVALENT SERIES PHASE MODEL

In the MESP Model, fracture localization at the microscopic level is modeled using a series phase consisting of fracture and unloading phases. Through a simple homogenization procedure for the individual series phases, based on a constant plastic fracture energy law, the orientation and size characteristics of series phases in a concrete volume element are taken into account in the resulting nonlocal macroscopic constitutive relation. This yields regularization of the MESP Model. The incremental form of the stress-strain relation for the MESP Model is written as

$$d\sigma_{ij} = D_{ijrs} d\varepsilon_{rs}$$

$$D_{ijrs} = \frac{3}{2\pi}\int_{\theta=0}^{\theta=2\pi}\int_{\phi=0}^{\phi=\pi/2}\Big[n_i n_j n_r n_s D_N^E + \frac{1}{4}\left(k_i n_j + k_j n_i\right)\left(k_r n_s + k_s n_r\right) D_{TK}^E + \frac{1}{4}\left(m_i n_j + m_j n_i\right)\left(m_r n_s + m_s n_r\right) D_{TM}^E \Big] \cdot \sin\phi \, d\phi \, d\theta$$

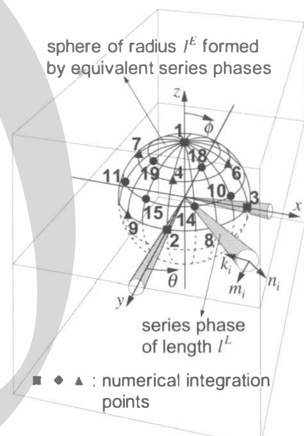

Fig.1 Concrete volume element

in which θ and ϕ = the spherical angular coordinates (Fig.1); n_i, k_i, and m_i = the unit coordinate vectors of series phase; and D_N^E, D_{TK}^E, and D_{TM}^E = incremental stiffnesses for the equivalent series phase. The MESP Model and the EMPC Model are implemented in the program DIAMESP (FASCOS) based on the general-purpose finite element system DIANA for practical and structural calculations.

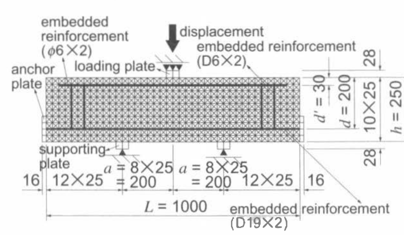

Fig.2 Analysis case B1

3 SIZE EFFECT ANALYSIS

Shear tests carried out on three similar reinforced concrete deep beam specimens by Matsuo (effective depth d =200, 400, and 600 mm) are analyzed in analysis cases A, B, and C. Full structure models are considered in analysis cases B (Fig.2) and C, but symmetric structure models in analysis cases A. In analysis cases D, bending tests on three similar reinforced concrete flexural beams by Mizumachi et al. (d = 154, 308, and 462 mm) are simulated. Reinforcing bars are modeled using the embedded reinforcement elements of the Von Mises elasto-plastic constitutive model, taking into account the tension stiffening effect of concrete. The elements around the tension reinforcing bar are assumed to be bond concrete elements to take into account tension stiffening. The EMPC Model, a local constitutive law, is assumed for the bond concrete, and the MESP Model is used for concrete elements other than the bond concrete elements.

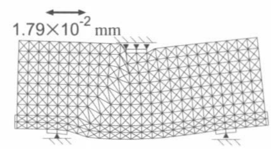

Fig.3 Incremental deformation at V_u (Analysis case B3)

3.1 Reinforced concrete deep beams

Figure 3 shows the incremental deformation of analysis case B3 ($d = 600$ mm) at the maximum shear load V_u. The analysis reflects the experimental crack pattern in a relatively good manner (Fig.4). The incremental deformations and cracking pattern look almost symmetrical in analysis case B1 ($d = 200$ mm), but are obviously unsymmetrical in analysis cases B2 ($d = 400$ mm) and B3 ($d = 600$ mm). This indicates that the shear fracture does not propagate symmetrically through the left and right spans, and the bifurcation from symmetrical to unsymmetrical modes arises as the size of the specimen increases. Regarding the size effect of shear strength in reinforced concrete deep beams this analysis using the MESP and EMPC Models is able to make accurate predictions (Fig.5).

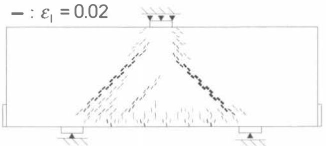

Fig.4 Cracking pattern at V_u' (Analysis case B2)

3.2 Reinforced concrete flexural beams

In Fig.6 the calculated displacement δ/l of beam is compared with the experiment by Mizumachi et al (l = loading span length). The predicted flexural response agrees with the experiment very well. This analysis technique correctly predicts that there is no size effect of yield and ultimate strengths in reinforced concrete flexural beams. However, it indicates that there is no size effect of deformation capacity, i.e., yield, ultimate, and failure displacements, which is consistent with the experimental results obtained by Alca et al. but contradicts the experiment by Mizumachi et al. The analysis provides reasonable simulation of the localization of flexural and shear cracks, and crack spacing as well as compressive splitting cracks in the experiment, as shown in Fig.7. A detailed examination of the analysis results reveals that analysis cannot be continued further into the post-peak regime because of a premature termination of the numerical calculation due to spurious kinematic modes [2] of certain (shaded) finite elements as a consequence of the strain softening constitutive model for tension (Fig.8).

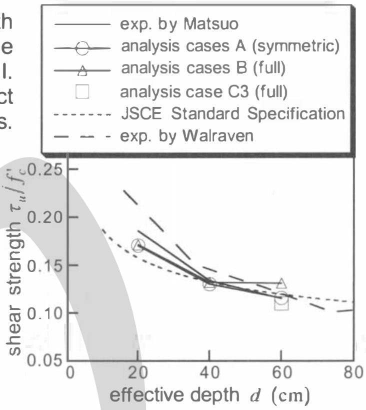

Fig.5 Size effect of shear strength

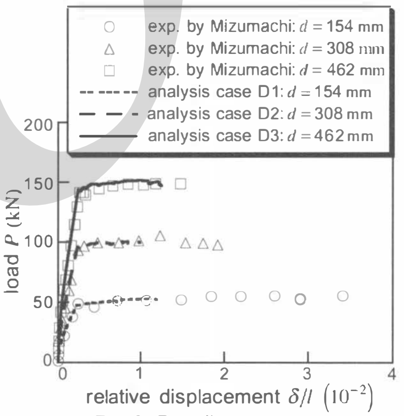

Fig.6 Bending response

4 CONCLUSIONS

The MESP and EMPC Models can simulate cracking, shear deformation, shear-compressive failure localization, unsymmetrical shear failure mode, and size effect of shear strength in reinforced concrete deep beams. The models are also able to predict yield and ultimate strengths, flexural response, crack localization, and compressive softening failure in reinforced concrete flexural beams. However, the size effect of deformation capacity does not appear in the analysis due to spurious kinematic modes of certain finite elements as a consequence of the strain softening constitutive model for tension.

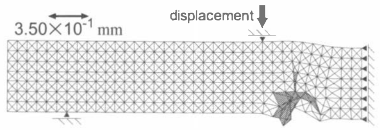

Fig.8 Incremental deformation ($d = 154$ mm)

REFERENCES

[1] Hasegawa, T. : Multi equivalent series phase model for nonlocal constitutive relations of concrete. Fracture Mechanics of Concrete Structures, pp.1043-1054, AEDIFICATIO Publishers, 1998

[2] De Borst, R. : Analysis of spurious kinematic modes in finite element analysis of strain-softening solids. Cracking and Damage: Strain Localization and Size Effect, pp.335-345, ELSEVIER Science Publishers, 1989

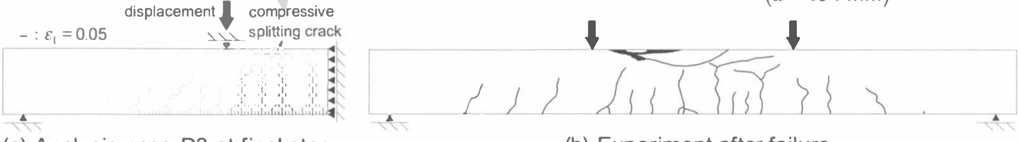

(a) Analysis case D3 at final step (b) Experiment after failure

Fig.7 Cracking pattern ($d = 462$ mm)

THE MECHANISM OF SIZE EFFECT ON THE SHEAR STRENGTH OF REINFORCED CONCRETE MEMBERS

Kazuhiko Hayashi
Faculty of Engineering, Yokohama National University, JAPAN

Kei Oriji
Graduate School of Engineering, Yokohama National University, JAPAN

Takahiro Yamaguchi
Kyokuto Kogen Concrete Shinko Co., Ltd., JAPAN

Shoji Ikeda
Faculty of Engineering, Yokohama National University, JAPAN

Keywords: Size Effect, Shear, Diagonal Tension Failure, Aggregate Size, Reinforced Concrete

1. INTRODUCTION

A great number of researches on the shear mechanism of reinforced concrete (hereafter, RC) members have been performed and many of them have been published so far. Especially, many researches have treated with a so-called size effect by which shear strength decreases as the structural size increases. And eventually the influence of the size effect is related to $d^{-1/4}$ (d: effective depth) in the Japanese design code [1] based on the result of large-scaled experiments carried out in Japan. Although the fundamental mechanism of the size effect has not been necessarily clarified yet, the size effect is being recognized as an inherent character in the reinforced concrete.

To obtain the basic fact of the size effect problem, it is crucial to compare the shear behavior of RC members with those of the members having different size consisting of ingredients the each size of which is proportional to the size of the related cross section. However, it is almost impossible to realize such RC members because it is difficult to proportionate the size of particles perfectly. On the other hand, the influence of the size was not shown in the shear test of the RC pier specimens having 350mm-1400mm in height of the cross section [2]. In that study, the maximum size of the aggregate and the diameter of reinforcement were proportional to the cross sectional size of the specimens. The result of that study indicates the necessity of the further study on the size effect problem. Moreover, it was reported that concrete drying shrinkage and the direction of placing would influence the diagonal tensile strength [3]. In general, concrete is not homogeneous after it hardens due to bleeding and subsidence in the fresh concrete condition. Therefore, it is necessary to consider a characteristic heterogeneity to evaluate the mechanical behavior of the concrete members.

From the above mentioned circumstance, an comprehensive and basic mechanism of the size effect of RC members in the shear behavior are investigated in the logical manner by systematic experiments having essential parameters such as specimen size, maximum size of coarse aggregate, concrete placed direction, type of concrete, diameter of reinforcement, thickness of cover, and support condition.

2. SPECIMENS AND EXPERIMENTAL METHOD

Sixty two specimens were made and were tested.

Three sizes were selected, i.e., large, medium, and small ones where the effective depths were 560mm, 280mm, and 140mm, respectively. The ratio of shear span to effective depth, a/d, is 2.5. Maximum sizes of coarse aggregate were determined to be three sizes. Four cases of concrete placed direction were defined as **Fig.1**. To investigate the influence of the segregation of concrete, three types of concrete, i.e., Normal, High-bleeding, and Non-bleeding, were made. Influence of diameter of reinforcement, thickness of cover, and existence of support restraint, were examined.

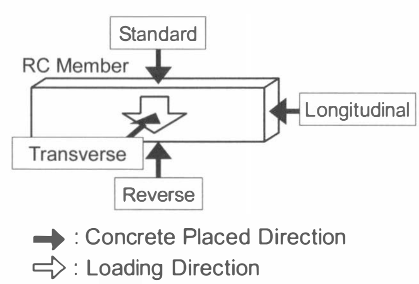

Fig. 1 Relation between Concrete Placed Direction and Loading Direction

3. EVALUATION OF SIZE EFFECTT

Considering the past and present experimental results, a comprehensive formula was proposed here to evaluate the diagonal tension failure strength as shown by Eq.(1). Here the following parameters are included in the formula: Effective depth, maximum size of coarse aggregate, ratio of reinforcement, diameter of reinforcement, and influence of loading condition.

$$\tau_{cal}=0.4 \cdot k_1 \cdot k_2 \cdot k_3 \cdot k_4 \cdot k_5 \cdot f_{ct} \qquad \text{Eq.(1)}$$

where,

τ_{cal}: Calculated shear strength of diagonal cracking

$$k_1 = 1.25\frac{S \cdot d}{M},\quad k_2 = 0.5+\frac{p}{2\,p_0},\quad k_3 = \sqrt[4]{\frac{20}{d/G_{max}}},\quad k_4 = \sqrt[4]{\frac{100}{d/\varphi}},\quad k_5 = 1$$

f_{ct}: Tensile strength of concrete($f_{ct} = 0.23 f_c'^{2/3}$)

M, S: Bending moment and shear force at the location of diagonal crack. The location is at the center of the shear span in case of the concentrated load, or 1.5d from support in case of uniformly distributed load.

d: Effective depth, p: Reinforcement ratio [%]

p_0: Standard reinforcement ratio (p_0=1%)

G_{max}: Maximum size of coarse aggregate

ϕ: Diameter of reinforcement

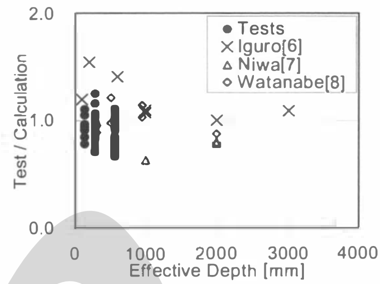

Fig. 2 Test / Calculation

The comparison of the experimental values with the values calculated by Eq.(1) is shown in **Fig. 2**. The proposed equation is fairly good to evaluate the diagonal tension strength of reinforced concrete beams with non-dimensional manner. Hence, shear strength of concrete is not related directly to the effective depth. Therefore, the so-called size effect which has been evaluated so far can be recognized as an apparent phenomenon rather than the matter of mechanics.

4. CONCLUSION

Following conclusions are obtained from this study.

1) It was proven that concrete shear strength of the reinforced concrete member was influenced greatly by the ratio of the size of maximum coarse aggregate to the effective depth, the tensile reinforcement ratio, and the diameter of reinforcement.

2) From the experimental results including other researcher's results, the authors were able to formulate a comprehensive equation for the evaluation of diagonal tension cracking strength of reinforced concrete members without shear reinforcement in which the size was included in the non-dimensional manner. This means that the size effect attributes to the heterogeneity of concrete.

3) When the cover of longitudinal reinforcement is thickened, there is a tendency for concentrated flexural cracks to propagate to diagonal cracks.

4) Even though the size and proportion were identical, it was shown that shear strength of reinforced concrete members without shear reinforcement could vary significantly according to the heterogeneity due to the material segregation before hardening, and the fracture pattern happened to be different. On the contrary consistent behavior was observed in the experiment where the concrete had no material segregation by using non-bleeding agent.

5) When the supports of a simple beam specimen were restrained to move horizontally, there was a tendency of increasing shear strength. Therefore insufficient support condition would apparently enhance the shear strength of the test beam.

REFERENCES

[1] Japan Society of Civil Engineers: Standard Specifications for Design and Construction of Concrete Structures (Design), March 1996

[2] Osada, K., Igase, Y., Suda, K., Ikeda, S.: Shear Behavior of Real-scale Reinforced Concrete Piers Strengthened with Carbon Fiber Sheets, *Proceedings of the Japan Concrete Institute*, Vol.23, No.1, June 2001, pp.877-882 (in Japanese)

[3] Hayashi, K., Oriji, K., Yamaguchi, T., Ikeda, S.: Size Effects on Shear Behavior of Reinforced Concrete Members, *Proceedings of the Japan Concrete Institute*, Vol.23, No.3, June 2001, pp.973-976 (in Japanese)

FLEXURAL CONSTITUTIVE RELATIONSHIP OF CRACKED TENSILE CONCRETE FOR DEFORMATIONAL ANALYSIS OF CONCRETE STRUCTURES

Gintaris Kaklauskas, prof., dr. habil. (dr. sc.)
Vilnius Gediminas Technical University, Lithuania
Sauletekio al. 11, 2040 Vilnius, e-mail: Gintaris.Kaklauskas@st.vtu.lt

Keywords: deformation, tensile concrete, constitutive relationship

1. INTRODUCTION

Present research is dedicated to investigation of tension stiffening effect in lightly reinforced concrete flexural members subjected to short-term loading. Most of the constitutive relationships for cracked tensile concrete [1] have been derived on the basis of tension or shear tests. Due to this in the flexural deformational analysis, empirical design code methods give more accurate results [1] in comparison to those obtained by numerical simulation.

Recently a method [1,2] has been developed for determining the average concrete stress-strain relations in tension (including the descending branch) from experimental moment-strain (curvature) diagrams of reinforced concrete beams. The stress-strain relations are computed incrementally from equilibrium equations for the extreme surface fibers. The computation is based on an idea of using the previously computed portions of the stress-strain relations at each load increment to compute the current increments of the stress-strain relations. The stress-strain relations for cracked tensile concrete were obtained [2] for 14 beams tested by L. A. Clark and D. M. Speirs.

The objective of developing a simple and accurate statistically verified deformational model and a new constitutive relationship for cracked tensile concrete based on experimental data of flexural R/C members was set for the present work. The simplicity criteria were assumed as follows: 1) minimal number of empirical relationships and factors; 2) integral and smeared estimate of complex phenomena; 3) applicability of the constitutive model to classical formulae of strength of materials and numerical techniques.

2. FLEXURAL CONSTITUTIVE RELATIONSHIP FOR CRACKED TENSILE CONCRETE

Using the method proposed [1,2], 16 new average stress-strain relations of tensile concrete, $\sigma_t - \varepsilon_t$, were derived from moment-curvature, $M - \kappa$, diagrams of lightly reinforced beams ($p \geq 0.16\%$) reported by Figarovskij. Present research deploys experimental data of the first and third series, i.e. rectangular cross-section specimens reinforced with plain and deformed bars, respectively. The experimental $M - \kappa$ diagrams for the beams of the first series are shown in Fig. 1. The computed $\sigma_t - \varepsilon_t$ curves for these diagrams are presented in Fig. 2. Based on $\sigma_t - \varepsilon_t$ curves of present and previous [2] research, a new flexural constitutive relationship for tensile concrete shown in Fig. 3 has been proposed. An empirical dependence has been established for flexural members between the factor β reflecting the length of the descending branch and the reinforcement ratio p (Fig. 4).

3. PREDICTION OF DEFLECTIONS OF EXPERIMENTAL BEAMS

The accuracy of the proposed constitutive relationship has been investigated by the calculation of deflections/curvatures for a large number of experimental beams. For that purpose, the flexural constitutive relationship was incorporated into a simple iterative technique based on the layered approach. Statistical comparison of the deflections has been carried out with the predictions made for design code methods of different countries and well-known constitutive relationships of tensile concrete. For the beams with average and high reinforcement ratio, accurate predictions of relative deflections have been made by all the methods with standard deviations of relative deflections ranging from 8.8 to 10.3%. However, as shown in Table 1, predictions for lightly reinforced beams ($p \leq 0.7\%$) were far less accurate. These risen inaccuracies are related to the increased influence of tensile concrete the strength of which is a highly dispersed value. Based on the results presented in Table 1, it can be concluded that the proposed deformational model as a universal, simple and accurate tool, can serve as an alternative to the design code methods.

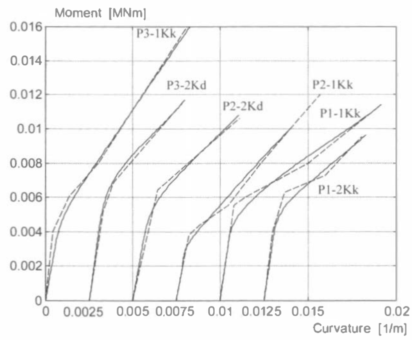

Fig. 1 Experimental moment-curvature diagrams for beams with plain bars
- - - - measured —— averaged

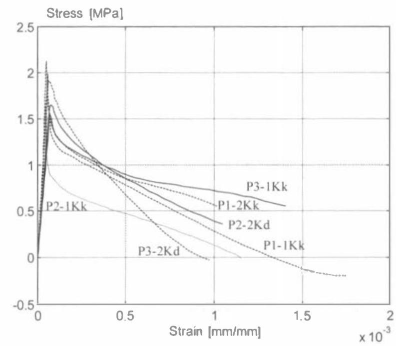

Fig. 2 Computed $\sigma_t - \varepsilon_t$ curves for beams with plain bars

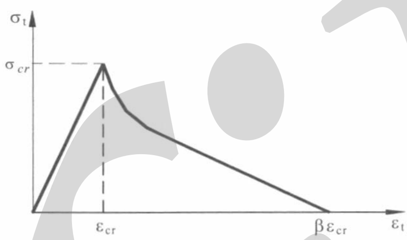

$$\sigma_t = 0.625\sigma_{cr}\left(1 - \frac{\overline{\varepsilon_t}}{\beta} + \frac{1+0.6\beta}{\beta\overline{\varepsilon_t}}\right)$$

$$\overline{\varepsilon_t} = \varepsilon_t / \varepsilon_{cr}\,; \qquad \varepsilon_{cr} = \sigma_{cr} / E_c$$

Fig. 3 Flexural stress-strain relationship for tensile concrete

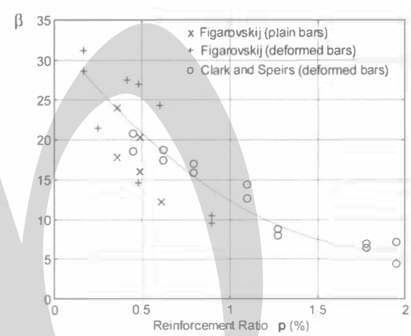

Fig. 4 Relationship between reinforcement ratio p (%) and parameter β

Table 1 Mean value and standard deviation of relative deflections ($f_{th} / f_{\exp}$) for beams with small reinforcement ratios (p <0.7%)

Method/ author	ACI	EC2	SNiP	Vecchio-Collins	Hsu	Prakhya-Morley	Flexural
Mean	0.980	1.224	0.955	0.865	1.122	1.180	0.922
Standard	0.220	0.372	0.201	0.216	0.398	0.446	0.140

4. CONCLUDING REMARKS

A new flexural constitutive relationship of tensile concrete for short-term deformational analysis of concrete structures has been proposed. The relationship in a simplified integrated manner takes into account complex effects of cracking, bond (including tension stiffening) and shrinkage. This constitutive model can be applied not only in a finite element analysis, but also in a simple iterative technique based on classical principles of strength of materials extended to the layered approach. The latter technique as a universal, simple and accurate tool can serve as an alternative to the design code methods.

REFERENCES

[1] Kaklauskas, G.: Integral constitutive model for deformational analysis of reinforced concrete members. Habil. Dr. (Dr. Sc.) thesis, Vilnius Gediminas Technical University, Lithuania, 2000
[2] Kaklauskas, G. and Ghaboussi, J.: Stress-strain relations for cracked tensile concrete from RC beam tests. J. of Struct. Eng., ASCE, Vol. 127, Issue 1, Jan., pp. 64-73, 2001

SIMPLIFIED MODEL FOR ESTIMATING PUNCHING RESISTANCE OF RC SLABS

Wijaya Salim and Wendel Sebastian
1.60 Queens Building, Department of Civil Engineering, University of Bristol, U.K

Keywords: punching shear, concrete slabs

1 INTRODUCTION

Few problems in concrete have been studied more extensively than the punching shear failure of concrete slabs. Despite considerable experimental as well as theoretical work, it has been proved extremely difficult to develop a consistent yet meaningful theoretical approach for punching shear failure. As a consequence, design codes of practice have relied on either purely empirical or semi-empirical approaches for predicting punching loads. Therefore, there remains a real need to develop a theoretical model in which the important physical characteristics are clearly and properly represented. To that end, two main modelling approaches, namely the Upper Bound approach based on plasticity theory, and the Lower Bound approach founded on satisfying equilibrium requirements, have enjoyed encouraging success.

Kinnunen and Nylander [1] developed a mechanical model for the analysis of punching shear failure in concrete slabs. Predictions from this model showed good agreement with experimental punching loads. However, the expression for the punching shear strength of concrete slabs suggested by Kinnunen et al is quite lengthy and thus not attractive to practicing engineers. For this reason, there was a need to derive a simpler rational method which can compete with the simplicity of empirical formulae.

In the following section, a simple model to estimate the punching strength of the slab-column connections is briefly outlined. This model has the same general aspect as the more complete one developed by Shehata. [2]

2 PROPOSED MODEL

From the observed typical crack pattern of test specimens (Fig. 1) and the linear deflection profiles obtained, it is considered that the slab is divided into rigid radial segments which rotate around a centre of rotation (CR) located at the column face and at the level of the neutral axis. This implies that bonded reinforcement crossing the tangential crack at the column yields. In addition, it is assumed that at near failure, a rigid wedge element, bounded by the internal inclined crack and the initial circumferential crack, is detached from each radial segment and rotates independently around the centre of rotation (CR). Experimental and numerical data [1-2] show that the angle of inclination of the internal crack surface can be approximated as 20°. The concrete in compression at the column face is considered to be in the plastic state.

The forces involved in the analysis of each radial segment of the slab are:

a) The external applied load $P(\Delta\phi / 2\pi)$, at radius $r = r_p$;
b) The radial component of the resultant ring tension forces $F_{st}\Delta\phi$ due to slab deformation;
c) The radial component of the resultant ring compression forces $F_{ct}\Delta\phi$ due to slab deformation;
d) Forces in the concrete at the face of the column, dF_{cr};
e) The radial net force dF_{sr}; and
f) Dowel forces dD of the steel cutting across the inclined crack. These forces are ignored here since in all practical cases, steel is reaching its yield strength at the time of punching failure and hence the dowel resistance of the bar is zero.

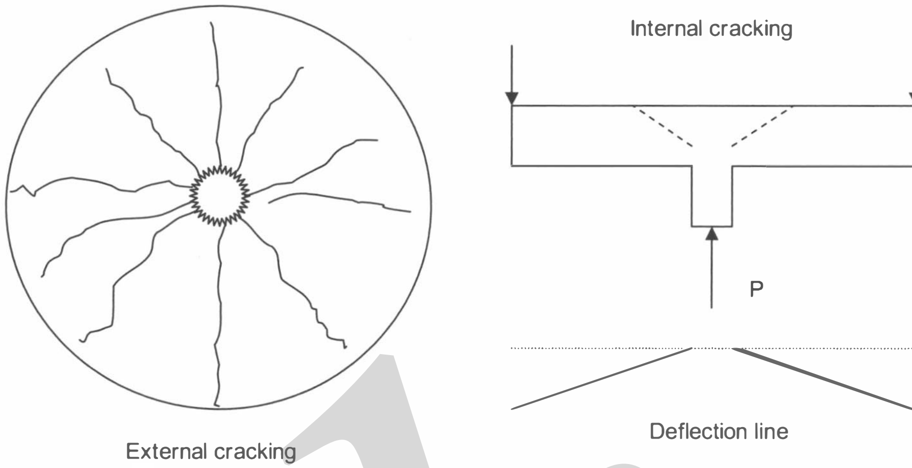

Figure 1. Typical test specimen in punching shear

By considering the equilibrium of forces, the punching shear can be evaluated as follows:

$$P = 2\pi r_0 \cdot x \cdot n_c \cdot f_c \cdot \tan 10^\circ \cdot \left(\frac{191}{d}\right)^{0.5707}$$

The overall correlation of experimental to predicted punching loads is shown in (Fig. 2). It can be seen that the analysis shows good agreement with the experimental punching loads.

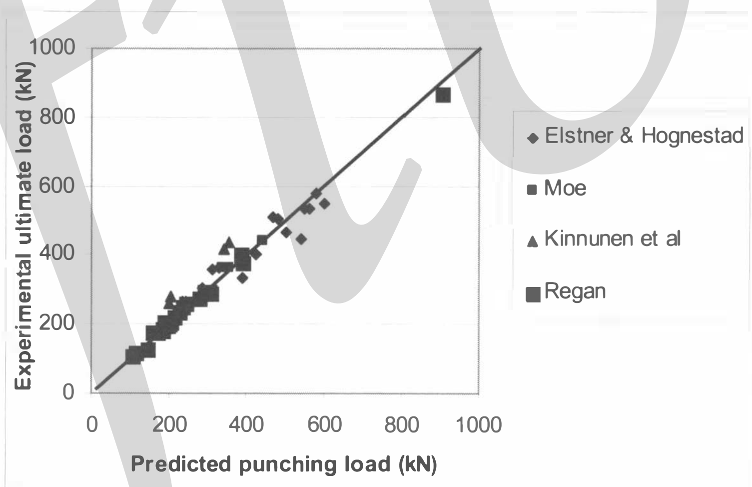

Figure 2. Overall correlation of predictions with 47 test results

REFERENCES

[1] Kinnunen, S., and Nylander, H., "Punching of concrete slabs without shear reinforcement", *Transactions of the Royal Institute of Technology*, Stockholm, Sweden, No. 158,1960, 112 pp.

[2] Shehata, I.A.E.M., *Theory of punching in concrete slabs*, PhD. Thesis, University of Westminster, U.K, 1985.

NUMERICAL SIMULATION OF FRACTURE PROCESS OF PLAIN CONCRETE BY RIGID BODY SPRING METHOD

Kouhei Nagai, Yasuhiko Sato, Tamon Ueda
Hokkaido University
JAPAN

Keywords: Rigid Body Spring Method, random geometry, fracture process, meso level

1 INTRODUCTION

Concrete is a composite material consisting of aggregate and mortar in meso level. Evaluation of the fracture process in this level is useful to quantify concrete properties in macro level in which homogeneity is assumed. In this study, numerical simulation of compression and tension tests of mortar and compression tests of simplified aggregate-mortar concrete model are conducted by Rigid Body Spring Method (RBSM). And the constitutive models for mortar and aggregate-mortar interface are presented in meso level. For formulating the arbitrary crack direction, random meshing of the model is introduced using the Voronoi diagram. The fracture process and behavior of each component are examined and the macroscopic stress-strain curves are compared with experimental results.

2 CONSTITUTIVE MODELS

Normal springs and shear springs set on the boundary of the elements develop normal stresses (σ) and shear stress (τ), respectively (Fig.1). Elastic modulus of the spring is determined by the material properties assuming the plane stress condition. Springs act elastic fundamentally. For the mortar part, τ_{max} criteria is set as shown in Fig.2. Shear stress can increase until τ_{max} criteria which depends on the normal stress(σ) in the range that the normal stress is less than tensile strength (f_t). Fracture happens between the elements when the normal stress reaches f_t, and the normal stress and shear stress become dependent on crack width and decrease linearly with crack width. For the interface between mortar and aggregate, failure criteria is set as shown in Fig.3. After generated normal and shear stresses reach to the criteria, spring can transfer only the compressive stress of normal spring.

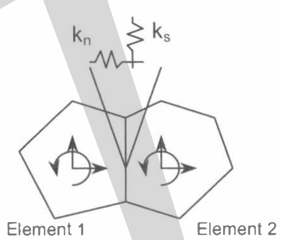

Fig.1 Interconnected elements

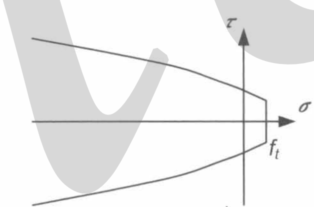

$$\tau_{max} = \pm 2\{(-\sigma + f_t) f_t\}^{\frac{1}{2}} \quad (\sigma \leq 0)$$
$$\tau_{max} = \pm (2 f_t - \sigma) \quad (0 < \sigma \leq f_t)$$

Fig.2 τ_{max} criteria for mortar

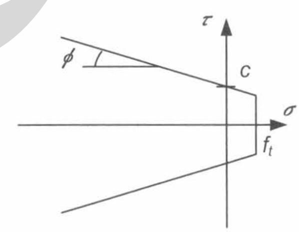

$$\tau = c + \sigma \tan \phi$$

Fig.3 Failure criteria for interface

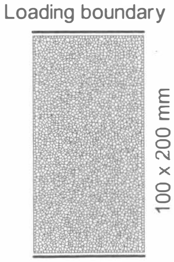

Fig.4 Analytical model

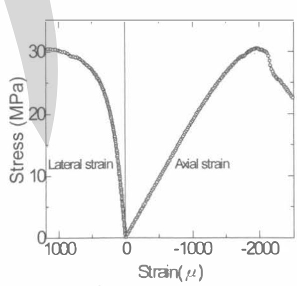

Fig.5 Stress-strain curve

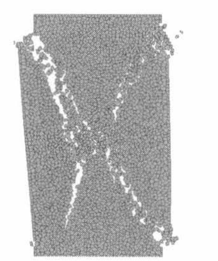

(Deformation is enlarged 10 times)

Fig.6 Failure deformation

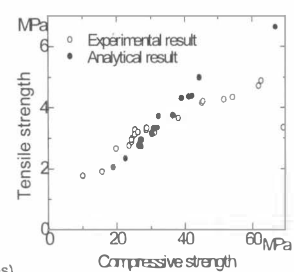

Fig.7 Strength relations of mortar

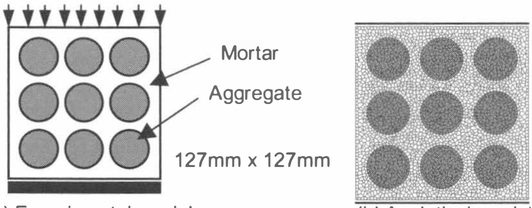

(a) Experimental model (b) Analytical model

Fig.8 Experimental and analytical model

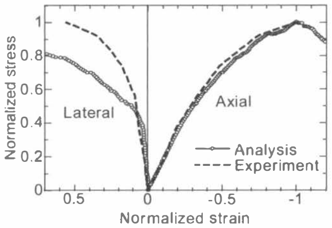

Fig.9 Stress strain curve

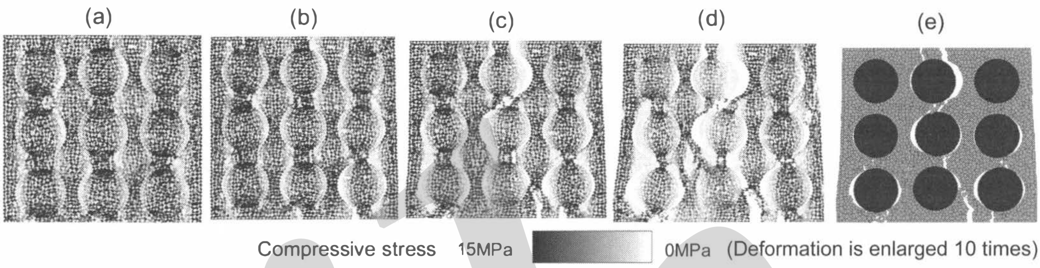

Fig.10 Change in stress distribution and failure deformation in analysis

3 ANALYSIS OF MORTAR

Numerical analysis of uniaxial compression test of mortar is carried out. Fig.4 shows the analytical model. Number of the element is 3046. Top and bottom boundary is fixed in lateral direction. In this study, experimental data of mortar are derived from the previous study [1]. Fig.5 and Fig.6 show the analytical result of stress-strain curve and deformation at failure, respectively. These results are similar to usual experimental results. Some analyses of compression and tension tests of mortar models are carried out and the relationship between compressive strength and tensile strength of mortar are examined. Fig.7 shows the experimental and analytical results. From Fig.7, analysis can predict the compressive-tensile strength relations of mortar well except for the high compressive strength range.

4 ANALYSIS OF PLURAL AGGREGATE MODEL

Analysis of compression test of the simplified concrete model in which nine aggregates exists as shown in Fig.8 (a) and (b) is carried out and compared with experimental result [2]. Material properties are obtained from experimental result [2]. Boundaries on top and bottom side are not fixed in lateral direction. Number of the element in the analysis is 3230. Fig.9 shows the experimental and analytical results of stress-strain relation. Results are normalized by maximum stress and axial strain. Analysis can predict the axial stress-strain curve well in axial direction. Disagreement of lateral strain may be because boundary condition in the experiment is not presented precisely in the analysis. Fig.10 (a)-(d) show the changing of deformation and stress distribution from around the peak load in analysis. Propagation of axial crack through the interface between mortar and aggregate is simulated. Fig.10 (e) shows the deformation at failure in the analysis. Fracture process and deformation at failure are similar to experimental result [2].

5 CONCLUSIONS

(1) RBSM developed in this study can simulate the fracture process of the mortar and concrete model.
(2) Compressive-tensile strength relation of mortar can be predicted by RBSM except for high compressive strength range.

REFERENCES

[1] Y. Kosaka, T. Tanigawa and F. Ota: Effect of gravel on failure process of concrete, J. Struct. Const. Eng., AIJ, Vol228, Feb., pp.1-11, 1975 (in Japanese)
[2] Buyukoztork, O., Nilson, A. H. and Slate F. O.: Stress-Strain Response and Fracture of a Concrete Model in Biaxial Loading, ACI Journal, Aug, pp.590-pp.599, 1971

CRACK PROPAGATION CONTROL WITH PRE-EXISTING SLITS AND CRACKS IN CONCRETE

Pimanmas Amorn
Sirindhorn International Institute of Technology, THAILAND

Maekawa Koichi
Department of Civil Engineering
University of Tokyo, JAPAN

Fukuura Naoyuki
Taisei Corporation, JAPAN

Keywords: shear failure, crack propagation control, pre-cracking, shear anisotropy, crack arrest

1 INTRODUCTION

In general practice, growth of crack in reinforced concrete is mainly controlled by reinforcing bars. For a linear member like beam and column, flexural crack growth is controlled by longitudinal bars whereas the diagonal shear crack growth is controlled by transverse ones (stirrups). When sufficient amount of reinforcement is provided in directions where cracks are expected to form, for example, 2-way reinforcement for arbitrary in-plane cracks and 3-way reinforcement for arbitrarily space crack, RC exhibits ductile failure.

However, full use of reinforcing bars for controlling crack growth may bring about difficulty for some large 2- and 3-D structures such as RC slab, foundation, etc. For these structures, large amount of shear reinforcement cannot be placed physically and economically. In fact, there are some provisions that specify no placement of transverse bars in slab and foundation structures. These structures are therefore classified as lightly reinforced and are prone to localized failure characterized by the propagation of few dominant cracks.

In this paper, the authors aim to propose a new method of controlling crack propagation without using reinforcing bars. We raise the idea of specifying paths of crack propagation by installing pre-slit made from pre-cracks and metallic/non-metallic plates embedded in RC members. These pre-slits will alter the stress distribution inside the member and lead to a change in failure characters and the overall behavior of the member. Here the authors present the structural behavior of RC beams containing pre-slits and conduct the finite element analysis for these beams. The target is to study how pre-slits alter the path of shear crack propagation in RC members.

2 EXPERIMENTAL PROGRAM

The authors conducted two experimental programs to investigate the structural behavior of beams containing pre-slits. In the first experimental program, pre-cracking is created in the beam by reversed flexural loading before shear loading. In the second experimental program, artificial pre-slits made from metallic and acrylic plates are embedded in the beam. The comparison of load-displacement relations for pre-cracked beams is shown in Fig. 1. It is found that the pre-cracked beam can reach much higher loading capacity, displacement ductility and energy dissipation compared to non pre-cracked control beam. For the control beam, the failure behavior is governed by a localization of a single diagonal crack (Fig. 1). But, in pre-cracked beam, the diagonal crack cannot propagate continuously but it is arrested at the pre-crack. This phenomenon is identified as 'crack arrest and diversion'. The behavior of pre-cracked beam is rooted in the interaction between diagonal crack and vertical pre-cracking. The 'crack arrest and diversion' is viewed as another method to control crack propagation. Then, the authors conduct the shear experiment on beams containing artificial pre-slits made from metallic and acrylic plate (*Artificial crack device*: ACD) as shown in Fig. 2. The experimental load-displacement relations (Fig. 2) show that the ACD-embedded beam can reach much higher shear capacity compared with control beam. The crack arrest and diversion control is experimentally demonstrated.

3 NUMERICAL ANALYSIS

Pre-slit (pre-cracking and artificial crack device: ACD) creates shear anisotropy inside RC members. In case of pre-cracked beams, two systems of cracks (vertical pre-cracking and diagonal crack) are interacting. The authors apply the finite element method to simulate the structural response

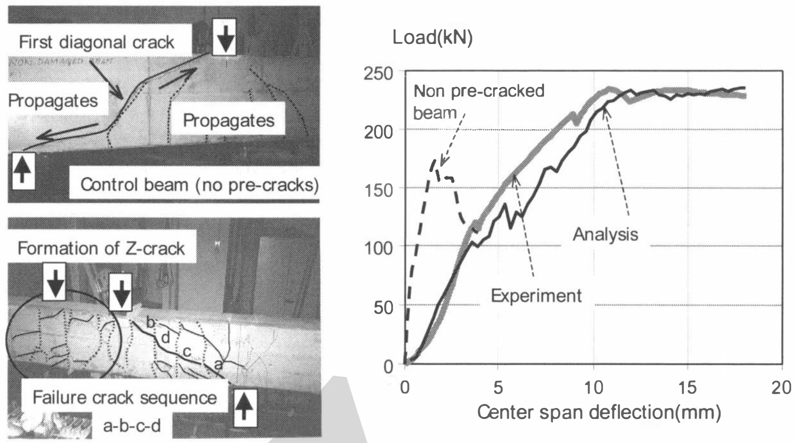

Fig. 1 Shear experiment of pre-cracked beam [1]

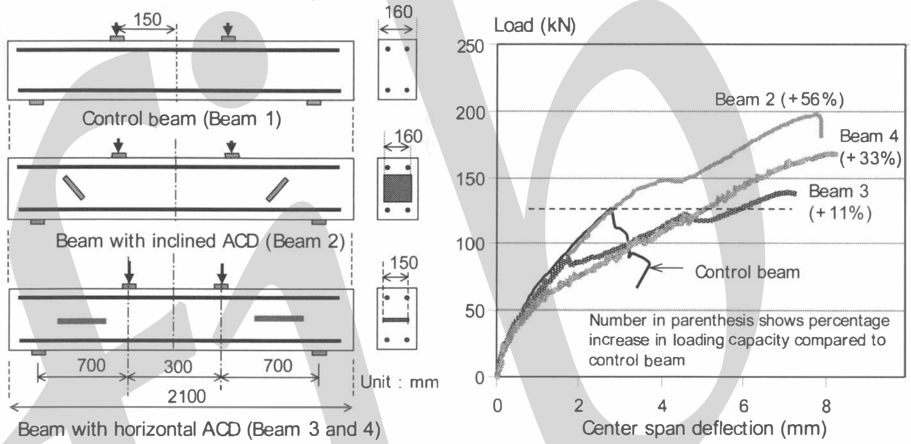

Fig. 2 Shear experiment of ACD-embedded beam [2]

of both pre-cracked and ACD-embedded beams. The four-way fixed crack model is adopted for modeling cracking since it can deal with shear anisotropy and multi-cracking. The combination of interfacial discrete elements and multi-directional smeared crack modeling can work as the simulator for failure of RC beams with pre-cracks, metallic and non-metallic sheets that cause artificial shear anisotropy in the member. The failure behavior and crack formation process can be reasonably predicted.

4 CONCLUSIONS

A new method for controlling crack propagation is proposed by using pre-slits to arrest and divert the crack propagation. Experiments are conducted to demonstrate the crack propagation control by using pre-cracking and artificial metallic/acrylic plates. Numerical finite element analysis is conducted to reproduce the failure character of beams containing pre-slits. Good agreement between experiment and analysis is found.

5 REFERENCES

[1] Pimanmas, A. and Maekawa, K.: Influence of pre-cracking on reinforced concrete behavior in shear, Concrete Library of JSCE, No.38, pp.207-223, Dec., 2001
[2] Pimanmas, A. and Maekawa, K.: Control of crack localization and formation of failure path in RC members containing artificial crack device, J. Materials, Conc. Struct. Pavements, JSCE, No.683/V-52, pp.173-186, Aug., 2001

ESTIMATION OF THE LOCALIZED COMPRESSIVE FAILURE ZONE OF CONCRETE BY AE METHOD

Ken Watanabe*1, Mitsuyasu Iwanami*2, Hiroshi Yokota*2 and Junichiro Niwa*1
*1 Department of Civil Engineering, Tokyo Institute of Technology, JAPAN
*2 Structural Mechanics Division, Port and Airport Research Institute, JAPAN

Keywords: localized compressive failure, compressive failure zone length, AE method, peak-amplitude, deep beam

1 INTRODUCTION

When a concrete specimen is subjected to uniaxial compression, the failure is sometimes also localized. The localization of the failure governs structural behaviors of concrete, especially the post-peak behavior. In addition, it is rather difficult to understand the mechanism of compressive failure because the failure is volumetric and depends on test conditions, such as specimen size, compressive strength, and loading speed. Therefore, the extent of the failure zone has not been quantitatively estimated. One remarkable example of the compressive failure of concrete in RC beams is that occurred in RC deep beams. In the previous study, the size effect in shear exists for RC deep beams without the transverse reinforcement because the failure of concrete is localized. It is interesting to find out the size of the localized failure volume in order to take account into the size effect.

In this study, a series of uniaxial compressive loading tests has been conducted. The compressive failure zone length was quantified by the AE method, which was compared with the results of visual observation of cracks, the distribution of local energy by the acrylic bar method. Then, AE method has been also applied to RC deep beams and compared the result with the results of previous study.

2 OUTLINE OF EXPERIMENT

Four concrete specimens, three prisms and one cylinder were made with lateral dimensions (D) of 100 or 150 mm. The height to depth ratio (H/D) of the specimen is fixed to be four in order to bring the localized failure based on the previous researches [1]. A deformed acrylic bar was embedded inside one of the four specimens and a set of strain gauges was attached on its surface to capture the localized compressive failure zone length. The local strains were measured by strain gauges attached to the acrylic bar embedded in the specimen. To divide the specimen longitudinally into 2 parts AE signals were measured by four or five AE sensors (150 kHz resonant type) attached to surfaces of the specimen at the interval of 50 mm or 100 mm (**Fig.1(a)**). AE measurement was conducted under the gain level of 60 dB and the threshold level of 60 dB.

On the other hands, **Fig.1(b)** shows the details of the tested RC deep beam without the transverse reinforcement. The width of the specimen was 150 mm. These conditions are referred to the previous study [2] to compare with the test results. To distinguish the failure zone from the non-failure zone, AE signals were measured by five AE sensors attached to one side of the specimen as shown in **Fig.1(b)**. AE measurement conditions are same as conditions in uniaxial compression test.

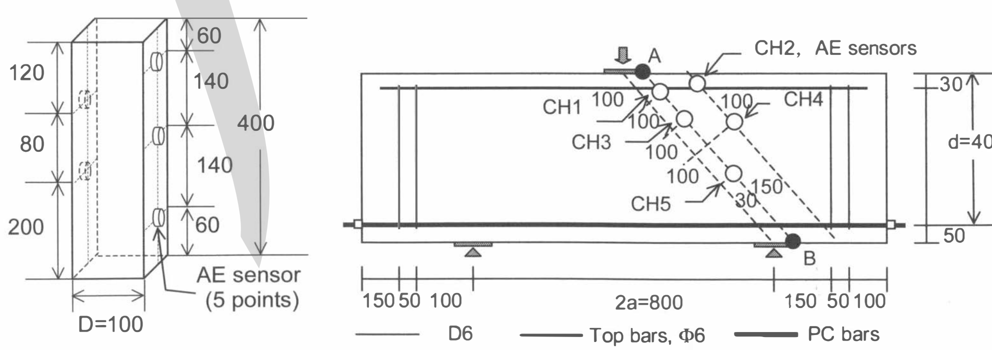

(a) The uniaxial test specimen (PS10-40.ac)

(b) The RC deep beam specimen

Fig.1 Schematic drawing of the RC deep beam specimen (Unit : mm)

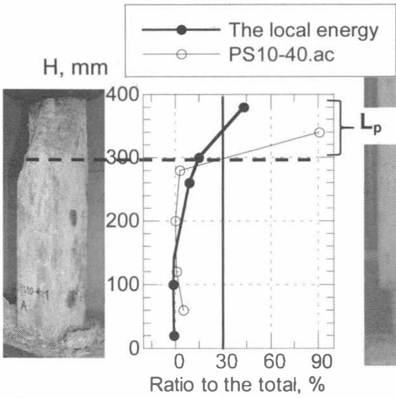

Fig.2 Comparison of failure zone and distribution of peak-amplitude

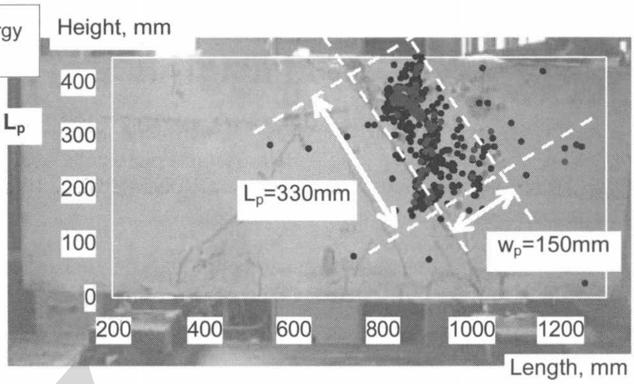

Fig.3 AE source location in case of RC deep beam

3 EXPERIMENTAL RESULTS AND DISCUSSIONS

3.1 Uniaxial compression test

Referring to the clearly localized case of PS10-40.ac as shown in **Fig.2**. Since AE signals were hardly recognized to the post-peak region, where cracks were remarkable, the value of AE signals detected up to the peak was utilized in this study. **Fig.2** shows the longitudinal distribution of local energy calculated based on the local strain measured by acrylic bar method. This curve shows L_p is equal to 103 mm. And the accumulation of the peak-amplitude of AE signals, which is closely correlated to the magnitude of damage, is also shown. Both curves are the values as the ratio to the value summed up throughout the specimen. By comparing these curves, the failure zone defined by the concept of local energy distribution coincided with that based on the accumulation of peak-amplitude indicated in both specimens. This criterion of 30% could be applied to other cases of which the size of specimen was different.

3.2 Application for the deep beam

The failure zone was estimated through the two-dimensional distribution of AE sources in the span of the RC deep beam (**Fig.3**). However, there is no AE source location in the area right under the loading point in spite of many cracks being observed. Because of many cracks, the information to estimate the AE source locations could not be captured by AE sensors. From **Fig.3** AE signals generated only local portion inside the white line, the length, L_p of 330 mm, and the width, w_p of 150 mm. These values were almost the same as the value obtained from previous study [2,3].

4 CONCLUSIONS

In uniaxial compression tests, on the basis of the accumulation of peak-amplitude detected up to the peak stress, the criterion to evaluate the localized failure zone was proposed. The length of failure zone was defined as the region of more than 30% of the sum of values detected by all sensors with any shape and size of specimens. AE method could be also applied to the estimation about the size of localized compressive failure zone in RC deep beam by considering the two-dimensional distribution of AE sources.

REFERENCES

[1] Lertsrisakulrat, T., Watanabe, K., Matsuo, M. and Niwa, J.: Experimental Study on Parameters in Localization of Concrete Subjected to Compression. Journal of Materials, Concrete Structures and Pavements of JSCE, No.669/V-50, pp.309-321, Feb., 2001.

[2] Lertsrisakulrat, T., Yanagawa, A., Matsuo, M., and Niwa, J.: Concept of Concrete Compressive Fracture Energy in RC Deep Beams without Transverse Reinforcement. Proceedings of the JCI, Vol.23, No.3, pp.97-102, Jun., 2001

[3] Niwa, J.: Equation for Shear Strength of Reinforced Concrete Deep Beams Based on FEM Analysis, Concrete Library of JSCE, No.4, pp.283-295, Dec., 1984

FRACTURE MECHANICS AND FROST RESISTANCE OF CONCRETE

Siarhei Leonovich
Belarussian Polytechnic Academy
BELARUS

Keywords: modified and self-stressed concrete, frost resistance, stress intensity factors

1 INTRODUCTION

On the climatic influences, alternate freezing and thawing and the number of such cycles per year are decisive for some types of concrete structures. The severity of a climate relative to the concrete structures is determined by the number of freezing and thawing cycles and the mean minimum annual temperature. The more often freezing (particularly if caused by a sudden drop of temperature) and thawing alternate, the more deleteriously the climate affects durability of concrete structures.

2 CONCRETE MIXES AND SPECIMENS

The specimens were saturated by water during 96 hours. The specimens are frozen until temperature -50 °C, then they are thawed until temperature +20 °C in water or on air.

Table 1 Concrete mixes

Series	Content of concrete mixes, kg/m^3						Density, kg/m^3	Compressive strength, MPa
	Cement	Sand	Crushed Stone	Water	Super-plasticizer	Air-entrainer		
1	480	680	1100	180	-	-	2440	34.0
2	465	655	1160	165	3.72	-	2445	44.5
3	528	620	1100	195	-	0.3	2350	40.3

Table 2 Self-stressed concrete mixes

Series	Content of concrete mixes, kg/m^3				Slump, cm	Compressive strength, MPa (1 day)
	Stressed cement	Sand	Crushed stone	W/C		
C1	455	680	1120	0.40	-	-
C2	440	695	1130	0.40	-	-
4	400	669	1214	0.38	1.0	20.1
5	500	620	1125	0.35	1.7	20.5
6	550	598	1085	0.35	2.0	23.7

3 THE RESULTS AND DISCUSSION

The compressive strength of concrete specimens (series 1) after 20 cycles of freezing-thawing decreased by 22 % (from 34 to 26.5 MPa). At the same time, compressive strength of concrete, modified by superplasticizer S-3, increased by 11.2 % (from 44.5 to 49.5 MPa). Compressive strength of concrete, modified by air-entrance admixture SNV, increased 6% (from 40.3 to 42.7 MPa), however then after 28 cycles decrease by 5.2 % (to 38.2 MPa). The tensile strength, as the stress intensity factor, is the most sensitive characteristic and is the most suitable for correct estimation of destructive process by cyclic freezing-thawing. The concrete tensile strength is decreased during cyclic freezing-thawing accordingly 29.3; 50.3 and 47.5 % for series of specimens 4, 5, 6. The increasing of stressed cement content practically doesn't influences on concrete frost resistance. The character of change of compressive strength of self-stressed concrete differs from ordinary Portland cement concrete and modified concretes with superplasticizer and air-entrained modificator. After 15 accelerated cycles freezing-thawing the compressive strength increased from 49.7 to 60.5 MPa (22 %). After 25 cycles compressive strength was more, than initial strength 3 % and only after 27 cycles it was increasing of compressive strength (4 %). The stress intensity factors of normal pull out and transverse shear of series 1 after 20 cycles freezing-thawing decreased by 21 % and by 25 % accordingly. At the same time, stress intensity factors of normal pull out and transverse shear of concrete, modified by superplasticizer S-3, increased by 14 and by 8 % accordingly, but after 23 cycles these parameters decreased by 16 and by 7 %. The increasing of crack resistance parameters of concrete, modified by air-entrance admixtures was estimated before 20 cycles of freezing-thawing. The stress intensity factors of normal pull out of concrete specimens series 3 after 27 accelerated cycles freezing-thawing was higher, than initial value 25 %. However, the value of stress intensity factor of transverse shear after 27 cycles decreased by 20 %. Stress intensity factors by normal pull out of self-stressed concrete under action of cyclic freezing-thawing are decreased, but stress intensity factors by transverse shear of self-stressed concrete are increased.

CONCLUSIONS

The complex experimental investigations were allowed to assess poly-parametrical model (compressive and tensile strength, modulus elasticity, residual and cryogenic deformations, stress intensity factors by normal pull of and transverse shear) of frost destruction of self-stressed concrete. The experimental examination of theoretical concrete durability prediction for different types of pore structure was carried out. The correlation was established between changes of concrete porosity and stress intensity factors under action of cyclic freezing-thawing. The results obtained show that, although the addition superplasticizer S-3 confers a lower porosity to the cement paste, which means, in general, a higher durability for the concrete, for high resistance to frost a certain amount of air is needed even in concrete mixes with superplasticizer.

The computing fracture mechanics allows to evaluate in terms of force and power parameters the kinetics of frost destruction for any combinations of a structure of concrete and cryogenic effects, that enables to calculate the stress-deformed condition of existing reinforced concrete constructions in the actual conditions of exploitation (unilateral freezing, sharp cooling of a thin-walled construction, cyclical freezing-thawing in conditions of water-saturation etc.).

REFERENCES

[1] Leonovich S. N., Guzeev E. A. Prediction o concrete structures durability — Another look. Proc. of 13. Congress FIP. Amsterdam, Netherlands. 1998.

[2] Leonovich S. N. Crack resistance and durability of concrete structures in the terms of force and energetic criteria of fracture mechanics. Minsk: Tydzen, 1999.

[3] Guzeev E. A., Leonovich S. N., Piradov K. A. Fracture mechanics of concrete: problems of theory and practice. Brest: BPI, 1999.

[4] Watkins J., Fracture toughness test for soil-cement samples in mode II. Int. J. Fracture, 23, 1983.

THE USE OF ADVANCED NON-CONTACT MEASUREMENT SYSTEMS FOR THE DEVELOPMENT OF COMPREHENSIVE NON-LINEAR SIMULATION MODELS

Daniel Kuchma, University of Illinois at Urbana-Champaign, Assistant Professor
2114 Newmark Laboratory, 205 N. Mathews Ave., Urbana IL 61801 kuchma@uiuc.edu

Keywords: Computation, Design, Instrumentation, Validation, Verification

1 INTRODUCTION: THE ROLE OF COMPUTATIONAL TOOLS IN STRUCTURAL ENGINEERING PRACTICE

Engineers who design bridges and buildings typically use linear-elastic frame and finite element analysis programs to determine the distribution of loads in structures and then use design code specifications to dimension and detail the individual structural components. Over the last several years, vendors have been integrating design code specifications with linear-elastic analysis tools to create "complete" computer-based design programs. While this has streamlined the design process, it has not improved the correctness of design practice. Firstly, this is because structural systems are built using highly non-linear materials that crack, slide, creep, yield, expand and otherwise deform in non-linear manners in response to applied loadings, temperature changes, and the passage of time. As a result, the "true" distribution of loads and thus the required capacities of members are not properly determined using linear-elastic analysis tools. Secondly, building code specifications often provide poor estimates of capacity due to the need for these code specifications to consist of simple rules and broadly applicable relationships.

Computational tools that consider geometric and material non-linearities are extensively used in the design of structures in which optimization in design is essential, such as aircraft, automobiles, and other mass manufactured products. These non-linear computational tools are also used for the design of specialized civil engineering structures such as offshore oil platforms and nuclear power facilities. While these non-linear computational tools can theoretically be used for the design of typical building and bridge structures, the current versions of these tools are generally viewed by structural engineers as time-consuming "black-boxes" that can be tweaked to give any answer desired by the user. This lack of uniqueness is particularly frustrating to the typical structural engineer who feels ill-equipped to understand the underlying basis for these tools and to properly select parameter values.

The next step in the evolution of structural engineering design practice is to use non-linear computation tools for the design of typical building and bridge structures. But for these tools to be accepted in the structural engineering community, they will have to be comprehensive, transparent, and verifiable. These issues are being address by *fib* Task Group 4.4 on "Computer Based Modelling and Design". Within this task group, Working Party 4.4.4 "Benchmark Tests and Validation Procedures", which is chaired by the author of this paper, was formed to examine what improvements in experimental research practice and in methods of model assessment are required to promote the development of non-linear computational models for structural engineering design practice. The initial results from this work are reported in this paper. The 3 parts of this paper will present non-contact measurement technologies, the requirements for data-visualization and knowledge-integration tools, and the state of development in model verification and validation procedures.

2 NON-CONTACT MEASUREMENT TECHNOLOGIES

While conventional measurement devices such as strain gauges and displacement transducers have been the mainstay in structural research, the effort, expense, and space required by each of these gauges limits their usefulness in collecting the detailed data that is necessary for the development, calibration, and validation of more comprehensive computational tools. Over the last few years, there has been a tremendous growth in the capabilities of non-contact instrumentation methods for measuring displacements and strains at a very large numbers of individual points. Three non-contact measurement technologies which have the potential of revolutionizing the amount of information available to researchers are described below.

Coordinate Measurement Machines are able to measure the position of up to 256 small (8 gram and 8 mm diameter) light emitting diode markers in three-dimensional space to an accuracy of plus/minus 0.02 mm at a sampling rate of up to 3000 individual readings per second. One such system consists of a portable housing containing three 2048 CCD line-element cameras. The camera system has an effective measurement volume of 17 m^3. To utilize this system, the researcher hot-glues small plastic caps in a configuration of their choice to the surface of the test specimen, and then inserts a LED marker into each cap. Visit www.krypton-intl.com for more information.

Full-Field non-contract stress/strain measurement systems can be used to measure the distribution of strain over the surface of a selected region. To use such a system, an application of a thin (0.25 mm) plastic coating (photoelastic material/epoxy) is applied to the surface of the test specimen. A light source is then used to emit circular polarized light and a 320 by 240 pixel digital camera is used to measure the resulting fringe patterns. Unlike with traditional photoelasticity, the these systems do not count fringe lines to determine stress levels; rather, they measures small variations in the patterns of circular light. As a result, reliable sub-fringe level accuracy can be obtained with up to 500 stress/strain levels being resolved. At each of the camera's 240 by 320 pixel locations, the system returns the magnitude and directions of principal strains. For more information, visit www.stressphotonics.com.

Over the last several years, there have been tremendous advancements in high-resolution digital cameras, high performance computers, and image processing software. This has led to the development of vision-based measurement systems for a wide variety of applications. In a recent application in the field of structural engineering, a close-range photogrammetric system was developed to measure the positions of targets placed on the surface of reinforced concrete beams from which strains, crack widths, and other features were monitored. This was conducted at Aachen University of Technology in Germany [2]. As many as ten cameras were used to capture 500 circular target points spaced uniformly in 25 mm grids covering an area of 250 mm x 1000 mm.

3 DEVELOPMENT OF DATA-VISUALIZATION AND KNOWLEDGE-INTEGRATION TOOLS

A major hindrance to advancements through structural engineering research has been inadequate tools for the analysis of raw experimental test data and for the comparison of the measured behavior with the predictions of computational tools. A first step in overcoming this difficulty is to develop a data visualization and knowledge integration tool that has the following capabilities:
(i) Provides similar capabilities for the display of experimental test data as a post-processing tool does for the results from a finite element program. This includes the ability to display the exaggerated and contoured states of deformation, strain, and cracking in both 2 and 3 dimensions.
(ii) Unlike when processing the results from a finite element analysis, the tool for displaying the measured experimental response must deal with incomplete as well as redundant and therefore contradictory test data. As a result, the post-processing tools for experimental data must be able to integrate, interpolate, and extrapolate the results from all forms of measurement (knowledge sources) to create a picture of the state of the test specimen at each stage in the loading history.
(iii) In addition to the integration of experimental test data, this tool must enable a statistical comparison to be made of the experimentally measured response versus the computationally predicted response at all reference points using measures that will support parameter estimation and model validation.
A data-visualization and knowledge integration tool to have the capabilities described above is currently under development by the author and the National Center for Supercomputing Applications at the University of Illinois at Urbana-Champaign.

4 DEVELOPMENT, VERIFICATION, AND VALIDATION OF NUMERICAL SIMULATION MODELS

The 1998 book by Patrick J. Roache "*Verification and Validation in Computational Science and Engineering*" sparked the developments of methods for model verification and validation. One of the most significant public efforts is by a ASME group on "Verification and Validation in Computational Solid Mechanics". The mission of this group is "To develop standards for assessing the correctness and credibility of modeling and simulation in computational solid mechanics." This group has drafted discussion papers on many topics including calibration, a posteriori error estimation, data requirements, and constitutive modeling. Please visit http://www.usacm.org/vnvcsm/ for additional information on the activities and accomplishments of this group.

5 REFERENCES

1. ACI Committee 318, "Building Code Requirements for Structural Concrete (ACI 318-99) and Commentary (ACI 318R-99)," American Concrete Institute, Farmington Hills, Michigan, 1999, 391 pp.
2. Roache, Patrick J. "Verification and Validation in Computational Science and Engineering", Hermosa Publishers, 1998

3D FEM ANALYSIS OF PUNCHING SHEAR FAILURE OF STEEL-CONCRETE SANDWICH SLABS

Ryosuke TAKAHASHI Yasuhiko SATO Tamon UEDA
Graduate School of Engineering, Hokkaido University, Sapporo
, JAPAN

Keywords: Punching shear failure, steel - concrete sandwich slab, RC slab, 3DFEM

1 INTRODUCTION

In this paper, effort has been given to differentiate between sandwich and RC slabs by non-linear 3D-FEM analysis, which can accurately visualize crack pattern and strain/stress distribution inside the slabs and finally this mechanism was taken into account to formulate design equation for punching shear strength capacity of open sandwich slab.

So, in future, the authors expect the necessity of this equation as a powerful tool for performance base design of sandwich slab.

2. THREE-DIMENSIONAL CONSTITUTIVE LAWS

Non-linear three-dimensional analysis in this paper is based on finite element program (3D-FEM), which was developed at Hokkaido University for analysis of composite members. When cracks take place, the strains in global coordinate system are transformed into the strains in local coordinate system, which is based on the crack plane. After calculating stresses from the strains in the crack coordinate system by some constitutive laws, the stresses are retransformed into stresses in the global coordinate system and averaged.

3. VERIFIABLE ANALYSIS OF PUNCHING SHEAR FAILURE OF RC SLAB

Experimental result of punching shear failure of RC slab was verified with that of the analysis by the program. Specimen No.1 experimented by Yawaka, et al. [1] was chosen for the analysis

Fig.1 shows a typical load - displacement curve of both experimental and analytical one. Good agreement between the experimental and analytical result can be seen. Analytical peak load is 156.5 KN, whereas 161KN for experimental one, and produces an error of 3%.

It can be assumed that FEM program is appropriate to some extent for analyzing a behavior of punching shear failure of RC slab supported by two edges and loaded at center.

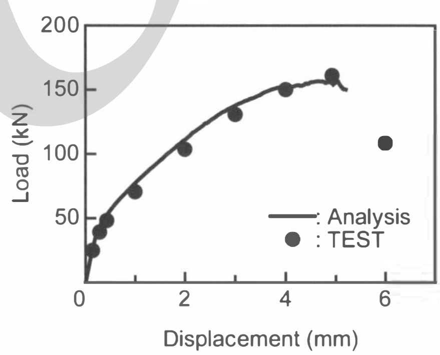

Fig.1 Load – displacement curve

4.ANALYSIS

Experimental specimen of open sandwich slab in author's experiment [2] was the model for analysis. Two analytical specimens for open sandwich slab, namely OP1 and OP2, where bond link element was adopted between concrete and steel for the first and interface was perfectly bonded for the second, were modeled.

To investigate the effect of thickness of cover concrete on punching shear behavior, two types of analytical RC slab specimens with two different cover concrete thickness (1cm and 5cm) with same effective depth and reinforcement ratio as in open sandwich slab, were modeled. Since it is difficult to determine the effective concrete area in tension, the height of RC element that is

Table 1 Analysis specimen

	Type	h(cm)
OP1	SW (bond element)	17.725
OP2	SW (perfect bond)	17.725
C1	RC(c = 2 cm)	18.500
C5	RC(c = 10cm)	23.500
D5	RC(c = 2 cm)	23.500

twice of cover concrete for specimen C1 and C5. The height of RC element for specimen D5 was the same as that of C1 to investigate the effect of undertaking area of RC element.

5. RESULTS AND DISCUSSION

5.1 Load - displacement relationship

The result of OP1 in Fig.2 (a) holds good agreement with the experimental result. However, the peak load of specimen OP2 is as greater as 45 % than the experimental one which gives a clear indication that in open sandwich slab the bond mechanism between concrete and steel plate greatly affects its punching shear strength capacity.

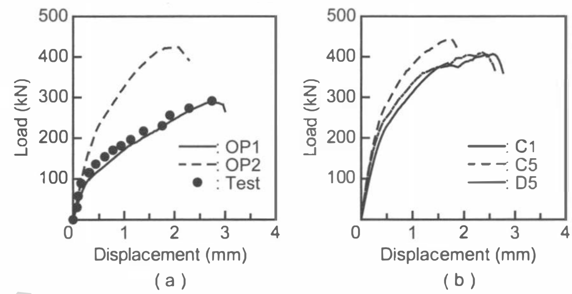

Fig.2 Load – displacement relationship

The comparison between the results of C1 and D5 in Fig.2 (b) shows that the size of area of RC element substantially affects punching shear behavior. The facts indicated in Fig.2 (b) clearly shows that the size of concrete area effective for tension stiffness should be modeled reasonably for accurate prediction of punching shear behavior and that the difference in the size of effective concrete area between sandwich and RC slabs may differ their punching shear behavior.

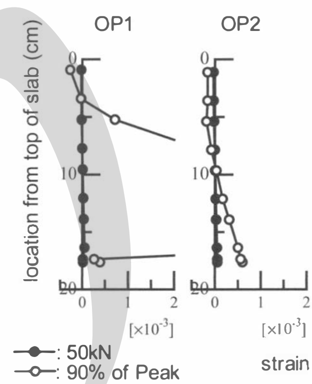

Fig.3 Strain distribution in height at center

5.2 Strain distribution

Fig.3 shows stress distribution along height under loading plate of OP1 and OP2. When the applied load is about 90% of each peak load it is clear that the depth of the neutral axis of OP1 is much less than that of OP2. Though the position of neutral axis could be a one of the indicator, there are many mechanisms involved that have a sizeable effect on punching shear capacity of slab. They are mutually related to each other, which make the total procedure more complex.

6. CONCLUSION

The following conclusions can be drawn considering the facts found in this study:

- Stiffness of bond between concrete and steel plate substantially affect the position of neutral axis. It is likely that the property of the interface between concrete and steel plate, namely stud, is one of the causes for the reduction of punching shear capacity in comparison with RC slab. It is important for making design equation for punching shear capacity of open sandwich slab with consideration of the interface property.
- It becomes quite clear from analytical result that the size of area of RC element (or tension stiffness area) affects the punching shear capacity of RC slab. Further clarification is necessary for the effect of concrete cover on the punching shear behavior of both RC and sandwich slabs that affects the size of tension stiffness by conducting both experimental and numerical investigation.

REFERENCES

[1.] Yawaka, M., Higai, T., Nakamura, H. and Saito, S.: Analysis of Punching Shear Failure in RC Slabs by 3-D FEM, Journal of structural engineering, JSCE, vol.47A, pp.1339-1346, Mar. 2001

[2.] Takahashi, R., Furuuchi, H. and Ueda, T.: Study on the mechanism of punching shear failure of steel-concrete open-sandwich slab, Proceedings of Hokkaido Chapter of JSCE, JSCE Hokkaido branch, No.55 (A), pp.462-467, Feb. 1999

ANALYSIS OF SLAB-COLUMN CONNECTIONS USING C^0 SHELL FINITE ELEMENTS

Maria Anna Polak
Department of Civil Engineering,
University of Waterloo,
Waterloo, Ontario, Canada

Keywords: punching shear, shell finite elements, failure, analysis, material modelling

1 INTRODUCTION

The paper presents a formulation which allows to use C^0, degenerate, layered shell elements for the analysis of reinforced concrete shells and slabs subjected to concentrated transverse loads. The presented formulation of the elements allows the use of three-dimensional models for reinforced concrete and the implementation of transverse reinforcements in the analyses. Punching or flexural mode failures are predicted through consideration of three-dimensional states of strain and stress in each layer of the element.

The paper presents and discusses features of the proposed formulation, which are related to the transverse shear model. Modelling of transverse shear transfer mechanisms is examined. Formulation of shear modulus for concrete and constitutive modelling, especially modelling of reinforced concrete in tension, are discussed. The comparison between experimental and analyical results for slab-column connections subjected to transverse loads and moments is presented.

2 THREE-DIMENSIONAL FINITE ELEMENT FORMULATION USING SHELL ELEMENTS

The finite element formulation is based on degenerate shell elements. In particular, Lagrangian quadratic elements are used with nine nodes per element and five degrees of freedom per node: u,v, w, θ_x,θ_y. The presented finite element model adopts isoparametric formulation of the elements. Integration through the element thickness is done using a layered model (shell is divided into a series of concrete and reinforcement layers). The transverse reinforcement is modelled as a property of a concrete layer by adding appropriate stiffness in the direction of the reinforcement. The analysis accounts for nonlinearities due to constitutive behaviour in the form of nonlinear elastic formulation, and due to changing structural geometry by adopting total Lagrangian formulation The nonlinear solution algorithm is based on an iterative, full-load, secant stiffness formulation. The final load can be approached through intermediate load levels. The convergence criteria are based on changes in deformations and residual forces (Polak, 1998).

The material principal directions are assumed to coincide with the directions of principal strains. The material is assumed to be orthotropic The constitutive model is nonlinear elastic based on the assumption that principal directions of strains and stresses coincide. The material stiffness matrix is evaluated in principal directions using the adopted stress-strain relationships from which secant material moduli are determined.

3 EFFECT OF MATERIAL MODELLING ON PREDICTIONS

Shear modulus formulation reflects shear force carried in compression and tension zones. In case of degenerate shell elements the formulation enforces constant shear strain distribution though the thickness of a shell. Actual transverse shear strains are not constant but depend on a state of stress or strain (e.g. degree of cracking or amount of compression) at a given point along the height. These actual strains increase with the increase of transverse load. The theoretical transverse strains also increase with load. Thus, they can be considered an indicator of the amount of transverse straining of a slab.

Since the constant transverse strain is an approximation, the formulation for reduction in shear stiffness for concrete should be simple. A linear function was adopted in the analyses presented in the paper for experimental corroboration. Tension modelling for cracked reinforced concrete is done using a linear formula. It influences predicted deflections at service loads but does not significantly influence punching failure load predictions. Dowel action of longitudinal reinforcement is included in the formulation by adding an appropriate term in the reinforcement material stiffness matrix. The transverse reinforcement is specified as a property of a given concrete layer. It can be present in any number of concrete layers and contributes to the stiffness in the direction of the reinforcement.

4 COMPARISON WITH EXPERIMENTAL RESULTS

The test specimens used for experimental corroboration represented a portion of slab-column edge connection bounded by the lines of contraflexure around the column (El-Salakawy et al. 1999). The presented experimental comparisons include slabs SF0 (with 150x150 mm opening in front of the column and SF0-R (same as SF0 but with shear studs) and XXX and XXX-R (with shear studs), both without openings. The slabs were subjected to a constant moment to shear force ratio of M/V=0.3 The results of the analyses are shown in Fig. 1. The collapse loads are predicted within 10% accuracy. The type of failure, flexural or punching shear, is predicted well.

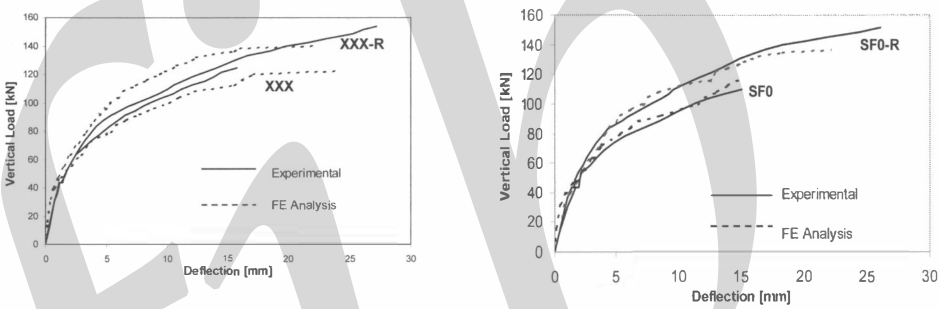

Fig 1 Comparison with experimental results: slab-column edge connections

REFERENCES:

[1] Polak, M.A., (1998), "Shear Analysis of Reinforced Concrete Shells Using Degenerate Elements", Computers and Structures, 68, 17-29.
[2] El-Salakawy, E.F., Polak, M.A. and Soliman, M.H., (1999). "Reinforced Concrete Slab-Column Edge Connections With Openings", ACI Structural Journal, Vol. 96, No. 1, Jan.-Feb., pp. 79-87.

THREE-DIMENSIONAL FEM ANALYSIS OF RC ECCENTRIC BEAM-COLUMN JOINTS SUBJECTED TO SEISMIC FORCES

KASHIWAZAKI Takashi
Research Associate

NOGUCHI Hiroshi
Professor

Dept. of Design and Archit., Fac. of Engrg., Chiba University, JAPAN

Keywords: reinforced concrete, beam-column joint, eccentricity, three-dimensional analysis, FEM

1 INTRODUCTION

In Tokachi-Oki Earthquake 1968 and Hansin Awaji Earthquake 1995, it was recognized that the remarkable damages of eccentric beam-column joints in RC buildings were observed by the intensive input shear forces produced by the additional torsion moment. Regarding the eccentric beam-column joints, it was expected that the severe earthquake damages and brittle shear failure in a joint would occur because joint input shear forces have concentrated to the eccentric side in a joint.

Therefore, it is necessary to establish the more rational shear design method for the eccentric beam-column joints subjected to seismic forces. In this study, three-dimensional FEM analysis of eccentric beam-column joint has been carried out in order to discuss the story shear force and story drift angle relation, failure modes, the joint shear resistance mechanisms and the deterioration of joint shear capacity.

2 OUTLINE OF FEM ANALYSIS

Two two-third-scale RC interior beam-column joints, specimens No.34 and No.35 [1] have been selected as reference specimens in this study. All specimens have an interstory height of 2m and a beam span of 3.5m. Specimen No.34 is a non-eccentric joint. On the other hand, the beam axis of specimen No.35 has an eccentricity of 7.5cm from the column center. During the experiment, the beam flexural yields occurred on both specimens No.34 and No.35 in the experiment. Properties of specimens are shown in Tables 1.

This analysis was carried out by using a three-dimensional nonlinear FEM program developed by Uchida K. and Noguchi H. [2]. Concrete was represented by 8-node solid elements. It was modeled as orthotropic material, based on the hypoelastic formulation, using the equivalent uniaxial strain concept proposed by Darwin-Pecknold, modified by Murray et al. for the three-dimensional FEM analysis. Saenz model was used for the ascending compressive stress-strain relationships of concrete. Confined effect by lateral reinforcement on the compressive descending stress-strain relationships were represented by Kent-Park model. The longitudinal and lateral reinforcement in columns and beams was modeled by linear elements. The stress-strain relationships of the longitudinal and lateral reinforcement were assumed to be bilinear and trilinear, respectively.

3 ANALYTICAL RESULTS

Distributions of joint shear stress at the maximum story shear force obtained from FEM analytical results of specimens No.34 and No.35 are shown in Fig.1. The locations of estimated elements in a joint are shown at the top of Fig.1. As shown in this figure, the elements from C to F and from B to E are within a beam width of specimens No.34 and No.35, respectively. It was recognized that the shear stresses on elements from C to F in specimen No.34 have concentrated to the center of a column. The shear stress of specimen No.34 showed the asymmetric distributions in a joint. On the other hand, the distributions of shear stresses in specimen No.35 with eccentricity of 7.5cm concentrated to the eccentric side in a joint. The

Table 1 Properties of specimens

Specimen		No.34	No.35
Eccentricity		0cm	7.5cm
Column	Section Main bars Lateral reinforcement	50cm x 50cm 4-D19 + 8-D22 4-D10@80, 0.71%	
Beam	Section Main bars Lateral reinforcement	50cm x 30cm Upper: 4-D25 Bottom: 4-D25 4-D10@65, 0.71%	
Joint	Lateral reinforcement	2-D10@40, 0.71%	

shear forces calculated by accumulation of shear stress in some elements were shown in the same figure. The total shear forces within and outside a beam width in specimen No.34 were 695kN and 418kN, respectively. The shear forces within a beam width were 66% higher than that outside a beam width. On the other hand, as for specimen No.35 with eccentricity, the total shear forces within and outside a beam width were 705kN and 375kN, respectively. The shear forces within a beam width were 88% higher than that outside a beam width. From these analytical results, it was recognized that the concentrated shear force was applied to the eccentric side in a joint.

4 CONCLUSIONS

The deterioration of maximum story shear force of eccentric beam-column joints by the additional torsion moment was not observed in case when beam flexural yields occurred without the joint shear failure and the eccentricity of beam axis toward the column center was relatively small as of 7.5cm. It was recognized that the shear stresses of eccentric beam-column joint concentrated to the eccentric side in a joint compared with the non-eccentric beam-column joint. The concentrations of shear stress in eccentric beam-column joints must be considered at the shear design of beam-column joints.

REFERENCES

[1] Hayashi, K., Kanoh, Y., Teraoka, M. and Mollick, A. A.: Experimental Study on Reinforced Concrete Interior Beam-Column Joints When Axis of Beam and Axis of Column are not Concurrent, Proc. of the Japan Concrete Institute, Vol.13, No.2, pp.507-512, 1991 (in Japanese).

[2] Uchida, K. and Noguchi, H.: Analysis of Two Story, Two Bay Frame Consisting of Reinforced Concrete Columns and Steel Beams with Through-Beam Type Beam-Column Joints, Journal of Structural and Construction Engineering, No.514, pp.207-214, Dec., 1998 (in Japanese).

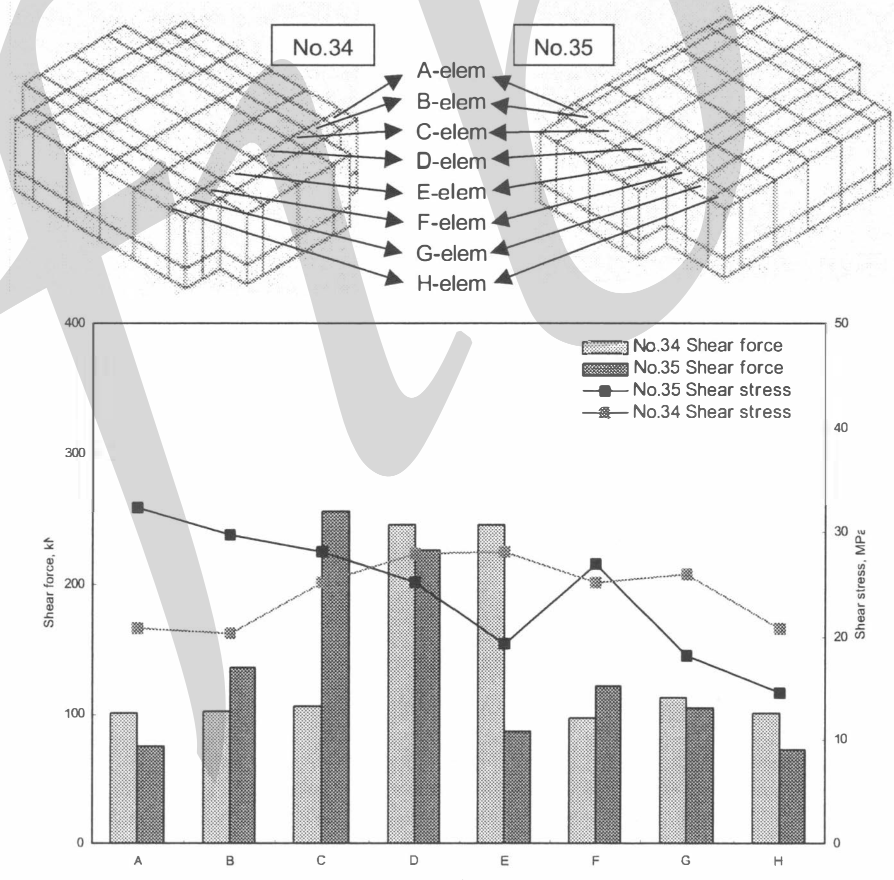

Fig.1 Distributions of shear stress and shear force in a joint

3D FINITE ELEMENT MODELING OF REINFORCED CONCRETE STRUCTURES

Helmut Hartl Christoph Handel
Graz University of Technology, Institute for Structural Concrete
AUSTRIA

Keywords: 3D (three dimensional) analysis; bond slip; embedded reinforcement, finite element analysis

1 INTRODUCTION

A nonlinear finite element tool for reinforced and prestressed concrete structures is presented. The program is designed as a lucid analysis tool for engineers. The user has to be still experienced and cautious but he does not have to be an expert who is dealing with nonlinear finite element analyses every day. This is realized by following two key ideas: First, model the geometry of the structure as it is given in physical reality and second, employ only such material parameters which are easily accessible and understandable to an engineer.

2 REPRESENTATION OF THE REINFORCEMENT

The first idea requires that the concrete geometry is discretized correctly. Favorably, a mesh with a high regularity should be employed. The same principle applies for the reinforcement. The reinforcement should enter the model exactly at that location where it is present in nature without any restriction. Modifications of the concrete mesh or the reinforcement layout should not cause time consuming challenges. These requirements can be fulfilled employing the embedded approach, presented by Elwi [1]. Anchorage loss or even bond slip along the entire rebar can be formulated in different ways, Elwi [1], Hartl [2, 3].

2.1 Embedded formulation allowing slip

This new developed form of the embedded approach allows the rebar to slip within the parent concrete element. Fig. 1 presents a brick element with parabolic shape functions and one embedded rebar. In this special case the size of the element stiffness matrix is increased for the slip degrees of freedom from 60 to 63. The first form of this approach is presented in Elwi [1]. A new easy to follow derivation of this approach is given in Hartl [3].

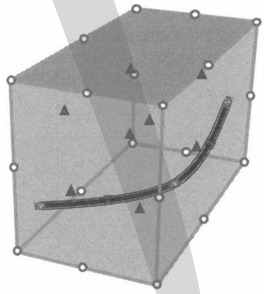

Legend:
- Node point of parent element (DOF, appears in the vector of nodal element displacements)
- Rebar point (DOF, appears in the vector of nodal element displacements)
- ▲ Integration point of the parent element (local coordinates of the Gauss points are known)
- ⧗ Integration point for the rebar (local coordinates and rebar orientation have to be determined)

Fig. 1 Embedded reinforcement bar allowing slip

3 CONCRETE MODELING

Concrete failure is incorporated in terms of plasticity for its simplicity in concept. Engineers are used to this approach and to the associated parameters. Concrete crushing is modeled by the Ottosen model and concrete cracking is implemented by a rotating fictitious crack model based on Hillerborg's theory. Creep and shrinkage is a very important phenomenon in concrete. It is incorporated along the recommendations given in fib bulletin No 1, with storing the entire stress history.

4 EXAMPLES

4.1 Beam with one post tensioned bonded and one post tensioned unbonded tendon

The example shown in this section is supposed to illustrate the performance of the supplementary slip model. The analyzed beam is shown in Fig. 2. The concrete is assumed to behave solely linear elastic and no creep and shrinkage is considered at all. Additional mild reinforcement is not taken into account as well. Hence, only the capability of the supplementary slip model is pointed out here.

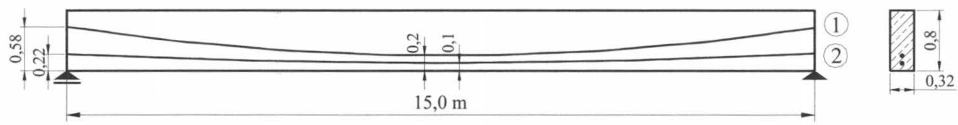

Fig. 2 Analyzed beam

Following load cases get applied to the beam

- Load case 1: Apply a prestress force of 0.785MN to tendon ① + 50% of dead load
- Load case 2: Apply a wedge-pull-in of 1.50mm to the live anchor (left side) of tendon ①
- Load case 3: Apply a prestress force of 0.779MN to tendon ② + 50% of dead load
- Load case 4: Apply a wedge-pull-in of 1.50mm to the live anchor (left side) of tendon ②
- Load case 5: Grout the duct of tendon ② and apply a boundary load q=32.20kN/m
- Load case 6: Apply an additional boundary load q=128.0kN/m

The stress resulting from the loads applied are shown in Fig. 3a and get discussed in the full-length paper.

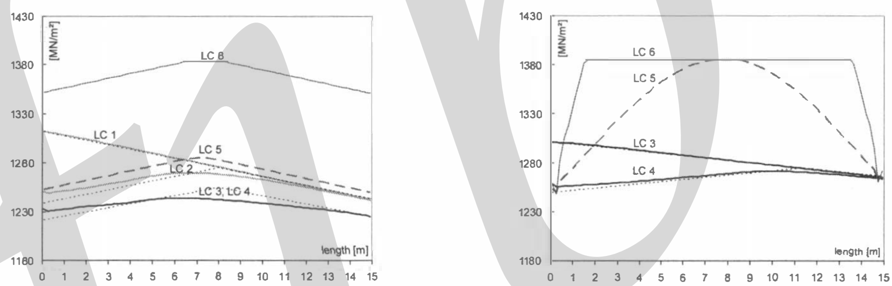

Fig. 3 a)Stresses in unbonded tendon ① b) Stresses in bonded tendon ②

5 CONCLUSION

A finite element tool taylored for reinforced and prestressed concrete structures is developed as an extension to an existing finite element program BEFE [4]. Today's standard computers are on the edge to allow such programs to become a lucid office tool for engineers. The material models are comparable simple in concept. The parameters can be obtained easily. Nevertheless, the results until now are very promising. The program is employed in teaching and for expert studies in industry with success.

6 REFERENCES

[1] Elwi A.E., Hrudey T.M., "Finite Element Model for Curved Embedded Reinforcement", Journal of Engineering Mechanics, ASCE, 115, pp. 740-754, 1989

[2] Hartl H., Sparowitz L, Elgamal A., "The 3D computational Modeling of Reinforced and Prestressed Concrete Structures", Bergmeister K. (ed.), Proceedings of the 3rd International PhD Symposium in Civil Engineering, Vienna, vol. 2, pp 69-79, 2000

[3] Hartl H., "Development of a Continuum-Mechanics-Based Tool for 3D Finite Element Analysis of Reinforced Concrete Structures and Application to Problems of Soil-Structure Interaction", Doctoral Thesis, Graz University of Technology, 2002

[4] Beer G.,"BEFE user's, reference & verification manual", CSS, Graz, 2001

THE ROLE OF FEM ANALYSIS OF RC STRUCTURES IN RELATION WITH EXPERIMENTAL STUDIES AND STRUCTURAL DESIGN

Hiroshi NOGUCHI
Department of Architecture, Chiba University
1-33 Yayoi-cho, Inage-ku, Chiba-City, JAPAN
e–mail: noguchi@archi.ta.chiba-u.ac.jp

Keywords: FEM analysis, RC structure, experimental study, analytical research, structural design, macroscopic model, microscopic model, basic test, verification analysis

1 INTRODUCTION

The analytical method of concrete structures is remarkable for its development. However, the analytical method had not evolved independently. The improvement of the analysis method had been made in the form of trial and error in the beginning in order to reproduce the experimental results of load-deformation relationships. The experiment at that time was not intended to be utilized for the analysis. The performance of structural members was tried to be grasped only from the experiment.

Afterwards, the analysis was started to be utilized as the reliability of the analysis was improved. The experiment was complemented by the parametric analysis. The internal stress condition which is difficult to grasp in the experiment could be also utilized for investigating the process of the failure progress in the structures. However, even at this stage, the analysis had been supplementary for understanding the experimental results more deeply. The experiment had not been concerned with the analysis.

Recently, such a basic experiment that develops and verifies a FEM microscopic model or a macroscopic model has come to be carried out. In the future, when the analysis is made advanced furthermore, how will the relation of the analysis with the experiment change? Will the age when the experiment is not necessary come from that the behaviour of various structures is possible to predict only by the analysis?

As shown in Fig. 1 [1], the researches on concrete structures are divided broadly into the following three categories: experimental research, macroscopic model analytical research and FEM microscopic model analytical research. These three categories researches are closely connected and the research fruits are applied to several codes and structural design methods in the area of structural design. These researches are also connected with structural design engineers.

In this paper, the role of FEM analysis of RC structures is mainly discussed in relation with experimental studies and structural design.

2 DISCUSSIONS

1) Collins' Panel Test is introduced. The test's target was laid on the calibration of analytical models. This corresponds to the flows 1 and 2 in Fig. 1.
2) Collins' Shell Tester is introduced. This test was conscious of the analysis. This corresponds to the flow 1 and 3 in Fig. 1.
3) The relations from experimental study to macroscopic models, FEM microscopic models are discussed. The JCI selected specimens for verification of analytical models are introduced. This corresponds to the flows 1 and 3 in Fig. 1.
4) Basic experiments with the aim of improving the accuracy of structural analysis are introduced. These correspond to the flows 1 and 3 in Fig. 1.
5) The relations between macroscopic models, FEM microscopic models and shear design method in structural design are discussed. These correspond to the flows 5, 6, 8 and 9 in Fig. 1.

3 CONCLUSIONS

The study of RC structures had been originally composed of experiment, and there are still many researchers based on only experiment. If the ability of the experiment is high, the test results may be reliable. But three-dimensional deformation and internal stress distribution are very difficult to measure in the experiment. The applicable area of the obtained information is not so wide. There is also demerit in the experiment about that it is difficult to explain why the behaviors are occurred.

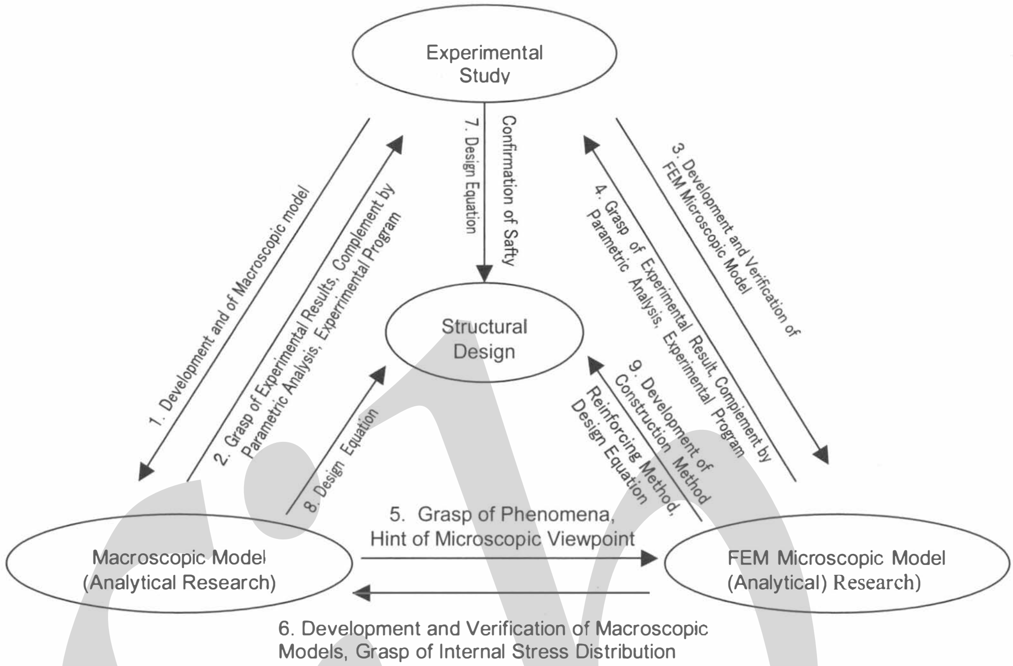

Fig. 1 Relationship between Research and Design of Concrete Structures [1]

In the future, the development of the research will be difficult without analytical support or understanding in order to investigate the structural performance more rationally. In the case, not only crack patterns and load-deformation curves from the experiment but also internal stress state, progress level of failure damage and failure mechanisms will be useful.

The flows 2 and 4 in Fig. 1 are actions of analytical researches based on the macroscopic model and FEM microscopic model to experimental researches. The actions include that the analytical researches are useful for understanding the experiment more deeply. The analytical researches complement the experimental parameters and they can make up for lack of number of test specimens. The analytical researches are also useful for experimental planning by predicting the behavior of the test specimen in advance.

The flow 5 in Fig. 1 means that the macroscopic model researches which can grasp the phenomena well give a hint to the microscopic view. The flow 6 in Fig. 1 means that the microscopic model researches are useful for the development of macroscopic models and the verification of models and assumptions. The grasp of internal stress distribution is useful for the macroscopic models.

The flow 7 in Fig. 1 shows that the experimental studies have been useful for the confirmation of safety which is required for the structural design, and the design equation based on the experiment have been useful for the structural design.

In this way the analytical researches and experimental studies, and also analytical researches between macroscopic and FEM microscopic models are complementary to each other. In future, it will be necessary for researchers on the experiment, microscopic model analysis and FEM microscopic model analysis to make close information exchange and apply the experimental and analytical research fruits to the practical structural design. For example, this will be an ideal research approach. Before the experiment on the structural performance of RC structures on members, it is desirable to predict the behavior and resting mechanisms of the objective test specimens using macroscopic models or FEM microscopic models for the selection of the target specimens in the experimental planning.

REFERENCES

[1] Noguchi, H., "The Relations between Analytical Researches and Experiment," Concrete Journal, Japan Concrete Institute, Vol. 39, No. 9, pp.27-31, Sept. 2001 (in Japanese).

SHEAR DEFORMATION OF R.C. BEAMS

Pier Giorgio Debernardi   Maurizio Taliano
Dep. of Structural and Geotechnical Engineering,
Politecnico di Torino, ITALY

Keywords: crack pattern, bending and shear interaction, shear strain

1 INTRODUCTION

In the design of r.c. beams the traditional calculation methods are quite simple and, in general, give good practical results. They in fact consider bending moments and shear separately. In reality, experimental behaviour is rather complex: the pattern of cracks changes with the increase of loads and cracks have inclinations along the beams which can vary as a function of the interaction between the moment and shear. This implies some stress transfer mechanisms that evolve with the loads and which depend on the opening and the slip between the crack edges. States of stresses, such as the well-known dowell and interlock effects and shear friction, which substantially contribute to the equilibrium, are associated to these displacements.

The available models in literature mainly deal with the evaluation of the strength at the ultimate limit state without giving any indications on the deformation or, not even, on the behaviour during service conditions. These models can be classified into two groups: truss models, which are based on a lattice-like behaviour and smeared models [1], which consider the mean behaviour of a cracked solid.

Although several experimental works were carried out on either thin web beams or elements subjected to composed states of stress, the discussion on the two calculation methods is still controversial. A clarification can only be made thorough experimental investigations which have to examine not only the global and macroscopic aspects of structural behaviour, such as crack inclination and structural resistance, but also all the local aspects, i.e. strains, crack openings and slips when the load effects increase.

This research is part of this framework: it has the aim of determining either the global aspects concerning deformations, in particular the influence of shear on the moment – mean curvature and shear – mean shear strain diagrams, or the local strains and relative displacements. An experimental methodology was set up using a thick triangulation network of mechanical extensometers which were arranged on the web of the beams.

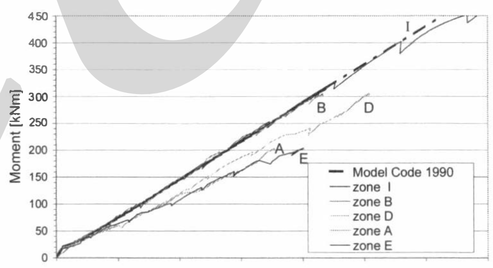

Fig.1 Beam TR2:
moment – mean curvature diagram

2 EXPERIMENTATION

The experimental investigation was carried out on six 600 mm high and 100 mm wide, simply supported r.c. beams with the same transversal section.

They are subjected to two symmetrical loads (beams TR1 and TR2) or a symmetrical (beams TR3 and TR4) or anti-symmetrical (beams TR5 and TR6) load.

3 EVALUATION OF THE GLOBAL DEFORMATION

The influence of shear on the deformation of the bottom and top chords clearly appears in Fig.1 in which the mean curvature is represented as a function of the acting moment.

The mean shear strain γ_m is determined on the basis of the deformations of the

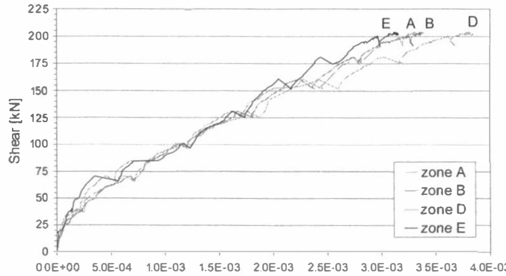

Fig.2 - Beam TR2: T-γ_m diagram

measuring lattice. These values are expressed as a function of shear, as it results from the classic theory. However, it is influenced by the effects of the moment, which play an important role (Fig.2).

4 ANALYSIS OF LOCAL BEHAVIOUR

4.1 Displacements of the vertexes of the measuring network

An examination of local effects can be made from the analysis of the strains and mutual displacements that occur in the web of the beams. It is interesting to compare the displacements of the points, at the same moment, in zones with no shear (zone C) and with shear (zone D). The results of Fig.3 show a remarkable influence of the shear on the local deformation.

4.2 Crack opening and slip

As an example, in the TR6 beam, first, the vertical crack formed and, then, when the load increased, the inclined CD crack formed. The trend of the crack opening along an CD alignment is shown for several loads in Fig.4.

4.3 Mean strain on the web of beams

The trend of the mean strains ε, which are determined along several directions around the middle of zone D of TR1 beam, is shown in Fig.5 by means of a polar diagram. The results give an indication of the evolution of the principal directions of the mean strains when loads increase.

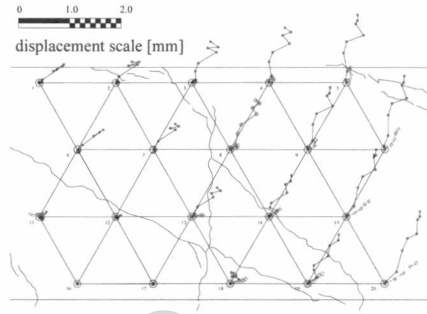

Fig.3 Beam TR1: displacements of points of the zones C and D at the same moment

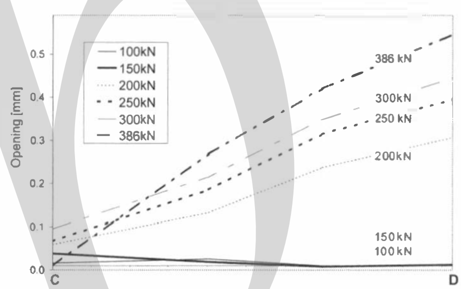

Fig.4 Beam TR6: crack opening along CD alignment (F zone)

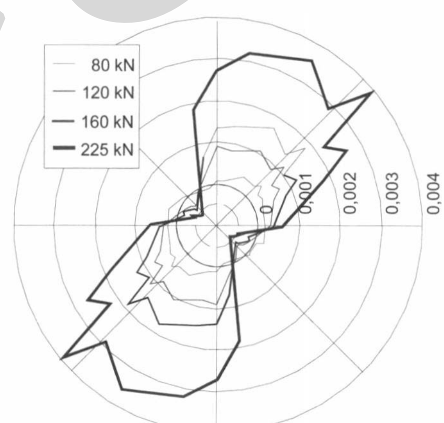

Fig.5 Beam TR1: polar diagram of strains related to the middle of zone D

REFERENCES

[1] Collins, M.P. : Towards a rational theory for RC members in shear. Journal of structural division, ASCE, 104 (4), pp.649-666, 1978

[2] Di Prisco, M., Gambarova, P. : Comprehensive model for study of shear in thin webbed RC and PC beams. ASCE Journal of Structural Engineering, vol. 121, No.12, pp.1822-1831, 1995

[3] ASCE-ACI Committee 445 on shear and torsion: Recent approaches to shear design of structural concrete. Journal of structural division, ASCE, 124 (12), pp.1375-1417, 1998

SHEAR STRENGTH ANALYSIS OF RC DEEP BEAMS INCORPORATING THE CONCEPT OF CONCRETE LOCALIZED COMPRESSIVE FAILURE

Torsak Lertsrisakulrat   Junichiro Niwa   Manakan Lertsamattiyakul   Tomohiro Miki
Department of Civil Engineering, Tokyo Institute of Technology, JAPAN

Keywords: localization in compression, reinforced concrete deep beam, localized compressive failure volume, compressive fracture energy, shear strength analysis

1 INTRODUCTION

It has been recently realized that the failure of concrete in compression is localized. Several attempts had been carried out to clarify its behavior by measuring the internal (local) strain inside concrete specimens [1, 2]. The parameters of localized failure such as the localized compressive failure volume, V_p, and the compressive fracture energy, G_{Fc}, were formulated based on the uniaxial compression tests [1] and were verified with the structural RC deep beams [2].

The purpose of this research is to utilize the concept and parameters of concrete localized compressive failure previously established [1, 2] in the formulation of material model of concrete under compression. Then, the proposed material model is utilized in the analysis of RC deep beams using the Lattice Model Analysis [3]. Finally, the experimental results [2] are compared with the analytical results of which the localized compressive failure concept is incorporated. The analytical results without considerations on the localized compressive failure concept are also illustrated.

2 ANALYSIS OF RC STRUCTURAL MEMBERS AND COMPRESSIVE σ–ε RELATIONSHIP

In this research, based on the simplicity and the objectivity in the post processing of calculated results and the simple representation of the shear resisting mechanism, the Lattice Model Analysis [3] was selected. The continuum body of the RC deep beam is converted into an assembly of truss components consisting of concrete and reinforcement members. The existence of concrete diagonal tension members of the web concrete and the arch member is one of the special characteristics of the lattice model. The web concrete is divided into truss and arch parts. The ratio of the width of the arch member to the beam thickness, b, is assumed to be t which is approximated to be the ratio that minimizes the total potential energy for the whole structure when assuming a unit shear force acting on the beam with a specified t value ($0<t<1$). The height of the lattice model, in this research, with square mesh, equal to d is used. The concrete diagonal compression (and the compression arch) and diagonal tension members are aligned at the angle of 45 degree and 135 degree to the specimen axis (horizontal axis), respectively. Figure 1 shows outlines of the lattice model in this study.

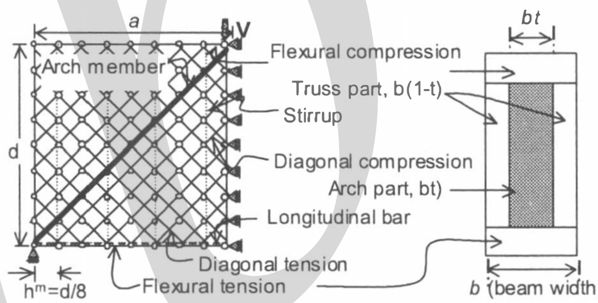

Fig. 1 The lattice model of a RC deep beam

The stress-strain relationship proposed by Vecchio et al. [4] in Eq. (1) has been used as the material model for concrete in compression in the conventional Lattice Model Analysis (Fig. 2(a)). The reduction in compressive strength of cracked concrete is taken into account by introducing the compression softening factor, η. However, in this study, the concept of the localized compressive failure of concrete is incorporated and the post-peak curve (descending path) is modified into Eq. (2) (Fig. 2(b)).

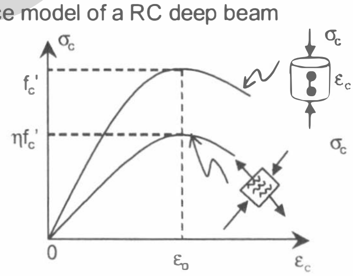

(a) Vecchio's model

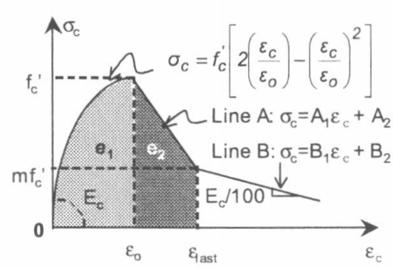

(b) Bi-linear post-peak model

Fig. 2 Compressive σ–ε relationship

$$\sigma_c = -\eta f_c'\left[2\left(\frac{\varepsilon_c}{\varepsilon_o}\right)-\left(\frac{\varepsilon_c}{\varepsilon_o}\right)^2\right] \qquad (1)$$

$$\sigma_c = \eta f_c'\left[2\left(\frac{\varepsilon_c}{\varepsilon_o}\right)-\left(\frac{\varepsilon_c}{\varepsilon_o}\right)^2\right] \quad ;\varepsilon_c < \varepsilon_o \qquad (2)$$
$$= \eta(A_1\varepsilon_c + A_2) \quad ;\varepsilon_o \le \varepsilon_c \le \varepsilon_{last}$$
$$= \eta(B_1\varepsilon_c + B_2) \quad ;\varepsilon_c > \varepsilon_{last}$$

where
f_c' = concrete cylinder strength(N/mm^2), ε_o = 0.002

$\eta = \dfrac{1}{0.8-0.34(\varepsilon_t/\varepsilon_o)} \le 1.0$ and ε_t=tensile strain (perpendicular to the compression member (minus)).

From the energy concepts and the parameters of the localized compressive failure of concrete, i.e. V_p and G_{Fc}, it was finally found that,

$$A_1 = \frac{(m^2-1)\ \ f_c'^2}{2e_2},\quad A_2 = f_c' - \frac{(m^2-1)\ \ f_c'^2}{2e_2}\varepsilon_o,\quad B_1 = -E_c/100 \ \text{ and } \ B_2 = mf_c' + \frac{E_c}{100}\left(\varepsilon_o + \frac{2e_2}{(1+m)f_c'}\right)$$

where m= percentage of the last level of loading (%) = $-14(1200/d-1)+r_w^2+30(1200/d-1)r_w+30$
(d= effective depth of the RC deep beam (mm), r_w= transverse reinforcement ratio (%)),
e_2= energy consumed within the post-peak region (N-mm/mm^3) =$[G_{Fc}V_p/V_c](K_V/K_E)-(2/3)\varepsilon_o f_c'$,
K_V= volume amplification factor, K_E= energy reduction factor,
K_V/K_E=1.14 and 1.82 for beams without and with transverse reinforcement, respectively,
G_{Fc}= compressive fracture energy (N/mm^2) = $0.086f_c'^{1/4}$, E_c=concrete Young's modulus (N/mm^2),
V_p= localized compressive failure volume (mm^3) = L_pA_c, L_p=localized compressive failure length (mm),
V_c= volume of compression member (mm^3) = L_cA_c, L_c= member (element) length (mm),
L_p/D^* = 1.36 ;D^*<100
= $-3.53\times10^{-5}D^{*2}+1.71$;$100\le D^*\le180$
= 0.57 ;D^*>180
D^*= equivalent cross-section width (mm)
= $\sqrt{A_c}$, A_c= cross-sectional area (mm^2).

3 ANALYSIS OF RC DEEP BEAMS

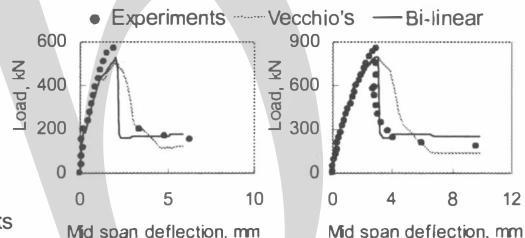

(a) d=400 mm, r_w=0.0% (b) d=600 mm, r_w=0.0%

Fig. 3 Experimental and analytical results

Figures 3 show samples of the analytical results by the Lattice Model Analysis for both when the concepts of localized compressive failure are incorporated into the analysis (Bi-linear), and those utilizing Vecchio's original compressive σ–ε relationship (Vecchio's). It is obvious that the analysis using the Lattice Model Analysis, incorporating the bi-linear post-peak compressive σ–ε relationship, yields a very good complete history of the load-deformation curve, especially within the post–peak region, compared with the experimental results.

4 CONCLUDING REMARKS

Based on experimental results and the concept of the localized failure of concrete in compression from the previous studies [1, 2], the conventional compressive stress-strain relationship [4] is modified. The so-called bi-linear post-peak compressive stress-strain relationship is proposed by taking into account the parameters of localized compressive failure (V_p and G_{Fc}) and is employed as the material modeling for compression members in the Lattice Model Analysis [3].

It was found that the load-mid span deflection curves, especially within the post-peak region, of the selected experimental results from the previous study [2] can be excellently predicted by the analysis incorporating the concept of the localized compressive failure.

REFERENCES

[1] Lertsrisakulrat, T., Watanabe, K., Matsuo, M. and Niwa, J.: Experimental Study on Parameters in Localization of Concrete Subjected to Compression. Journal of Materials, Concrete Structures and Pavements, JSCE, No.669, Vol.50, pp.309-321, Feb., 2001
[2] Lertsrisakulrat, T., Niwa, J., Yanagawa, A. and Matsuo, M.: Concepts of Localized Compressive Failure of Concrete in RC Deep Beams. Journal of Materials, Concrete Structures and Pavements, JSCE, No.697, Vol.54, Feb., 2002 (In publication)
[3] Niwa, J., Choi., I.C. and Tanabe, T.: Analytical Study for Shear Resisting Mechanism Using Lattice Model. Concrete Library of JSCE, No.26, pp. 95-109, 1995
[4] Vecchio, F.J., and Collins, M.P.: The Modified Compression Field Theory for Reinforced Concrete Elements Subjected to Shear. ACI Journal, pp. 219-231, 1985

EFFECT OF SHEAR REINFORCEMENT ON MECHANICAL BEHAVIOR OF RC DEEP BEAMS

Maki Matsuo Torsak Lertsrisakulrat Akinori Yanagawa Junichiro Niwa
Department of Civil Engineering
Graduate School of Science and Engineering
Tokyo Institute of Technology, JAPAN
2-12-1, O-okayama, Meguro-ku, Tokyo, 152-8552

Keywords: deep beam, confinement, size effect, compressive strength and tied-arch mechanism

1 INTRODUCTION

This study focuses on a short beam and a deep beam. These kinds of beams have a small *a/d* (shear span / effective depth ratio) not exceeding 2.5. The failure mode of these beams is much different from that of slender beams because of their geometries. These beams reach to the end by shear compression failure. Special features of this failure mode are that the beams can be loaded further after the occurrence of an inclined crack, the strong tied-arch mechanism is built and finally the concrete adjacent to the loading point is crushed. Therefore the behavior of an arch concrete subjected to compression has a dominant effect on the failure of a short beam and a deep beam.

Main aims of this study are (1) to clarify the occurrence of size effect of the deep beams, which fail by compression mode and (2) to explain the mechanism of shear reinforcements in deep beams. Tests for deep beams having various effective depths and shear reinforcement ratios were carried out.

2 OUTLINE OF EXPERIMENT

The details of the specimens are listed in Table 1. In Table 1, d (mm) is the effective depth, r (mm) is the width of bearing plate, and r_w (%) is the shear reinforcement ratio, respectively.

For all specimens, ①a shear span / effective depth ratio a/d = 1.0, ②a width of bearing plate / effective depth ratio r/d = 0.25, ③a width of the specimen b = 150 mm and ④a distance between the support and the edge of the specimen = 300 mm are kept constant.

3 FAILURE MECHANISM OF RC DEEP BEAM

3.1 IDEALIZATION OF RC DEEP BEAM

The following two results were obtained by the experiments: ① shear reinforcement is effective on the increase in v (nominal shear strength) of RC deep beams and ② shear reinforcement has a dominant effect on the specimens with lower d. It is well known that a deep beam has a strong tied-arch mechanism. A longitudinal reinforcement and a concrete between the loading point and the support has functions as a tie and an arch, respectively. Therefore, it may be important to comprehend the behavior of concrete of the arch portion subjected to compression.

The concrete in arch portion subjected to compression may expand and the shear reinforcement may confine this expansion. Hence, it was assumed that the confinement of shear reinforcement led to the increase in shear strength of RC deep beams with a/d=1.0. Figure 1 shows the model of an idealized RC deep beam. For this model, it was assumed that a strut was subjected to the constant compressive stress σ'_c (N/mm^2)

Table 1 Properties of specimens

Series	No.	d (mm)	r (mm)	r_w (%)
DN	DN200	200	50	0
	DN204			0.42
	DN208			0.84
	DN400	400	100	0
	DN404			0.42
	DN408			0.84
	DN600	600	150	0
	DN604			0.42
	DN608			0.84
DL	DL200	200	50	0
	DL202			0.21
	DL204			0.42
	DL400	400	100	0
	DL402			0.21
	DL404			0.42
	DL600	600	150	0
	DL602			0.21
	DL604			0.42
	DL800	800	200	0
	DL802			0.21
	DL804			0.42

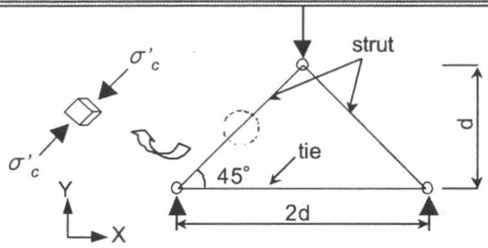

Fig.1 Model of idealized RC deep beam

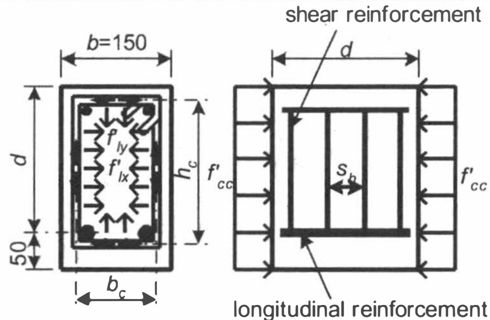

Fig.2 Confined arch portion

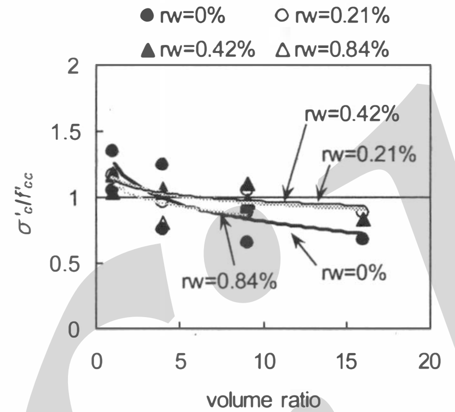

Fig.3 σ'_c/f'_{cc} vs. volume ratio relation

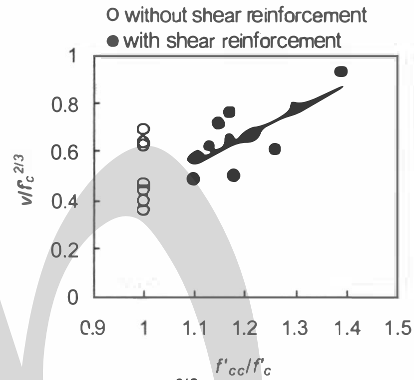

Fig.4 $v/f'^{2/3}_c$ vs. f'_{cc}/f'_c relation

and that the cross sectional area of a strut was the width of bearing plate r (mm) multiplied by the width of specimen b (mm). The confined arch portion was assumed to be a rectangular solid with shear reinforcement subjected to compression as shown in Fig.2. The effectively confined core area $b_c \times h_c$ is shown in Fig.2. In consequence, the enhanced concrete compressive strength f'_{cc} (N/mm^2) to f'_c (N/mm^2) ratio can be obtained by reference [1].

3.2 EFFECT OF SHEAR REINFORCEMENT

Figure 3 shows the relation between σ'_c/f'_{cc} and strut volume. The strut volume of the specimen with d=200 mm is assumed to be 1.0. Concerning Fig.3, σ'_c/f'_{cc} of the specimens with shear reinforcement was nearly equal to 1.0. On the other hand, σ'_c/f'_{cc} of the specimens without shear reinforcement decreased with the increase in strut volume.

Figure 4 shows the relation between $v/f'^{2/3}_c$ and f'_{cc}/f'_c. As regards the RC deep beams with shear reinforcement, the linear relationship was observed. It is possible that the shear strength v will be directly proportional to the confinement effect. However, v of the RC deep beams without shear reinforcement decreased with the increase in d because of no confinement.

Finally, it was found that the proposed idea was in agreement with the failure mechanism of the RC deep beams with shear reinforcement. The effect of shear reinforcement in RC deep beams can be related to the confinement. Furthermore, it became clear that the compressive strength σ'_c of the arch portion decreased with the increase in effective depth d of the RC deep beam without shear reinforcement and that the decrease in σ'_c brought the decrease in shear strength v.

4 CONCLUSIONS

(1) The confinement effect exists in RC deep beams with shear reinforcement. This effect helps the increase in shear strength.

(2) The shear strength of RC deep beams with no shear reinforcement decreases with the increase in volume of the arch portion.

5 REFERENCES

[1] Mander, J.B., Priestley, M.J.N. and Park, R. : Observed stress-strain behavior of confined concrete, Journal of Structural Engineering, Vol.114, No.8, pp.1827-1849, August 1988

SHEAR FAILURE ANALYSIS OF RC BEAMS USING HIGH STRENGTH MATERIALS

Satoshi Tsuchiya
COMS Engineering Corporation
JAPAN

Tetsuya Mishima
MAEDA Construction Co., Ltd.
JAPAN

Koichi Maekawa
University of Tokyo
JAPAN

Keywords: shear failure, RC beam, self-compacting high strength concrete, high strength reinforcing bars, FE nonlinear analysis

1 INTRODUCTION

For dealing with shear failure of RC beams using high strength materials, material constitutive models for high strength concrete has been proposed, based on the existing original models for normal strength materials [1] from the view of engineering approach. The proposed analytical method can evaluate the following peculiar behaviors of RC beams using high strength materials, which have been observed through experimental investigations [2].

2 CHARACTERISTICS OF SHEAR FAILURE OF RC BEAMS USING HIGH STRENGTH MATERIALS

The increase of concrete compressive strength scarcely affects nominal shear strength carried by concrete in the higher range than 50 [MPa], and size effect in shear became considerable. If normal strength reinforcing bars are used for stirrups with high strength concrete, even though crack surface is smoother, reinforcement effect equivalent to yield strength of stirrup can be obtained. If high strength reinforcing bars are used for stirrups, the reinforcing effect differs greatly depending on concrete strength. In the case of high strength concrete, reinforcement effect equivalent to yield strength of stirrup may be expected. However, in the case of normal strength concrete, reinforcement effect equivalent to yield strength of stirrup cannot be ensured. On crack and damage distribution, the position where the first diagonal crack progresses seemed to be more toward the loading points than in the case of normal strength concrete.

3 SUMMARY OF NONLINEAR ANALYSIS METHOD

In high strength concrete, aggregates are split and crack surface becomes smooth. For this reason, transferred stress along crack planes decreases. This cannot be expressed simply by merely changing strength value in the existing constitutive models for normal strength materials. Then, the two-dimensional nonlinear FE analysis based on path-dependent material constitutive models considering the smooth crack planes is employed. This study focuses on two issues as peculiar properties of high strength concrete; tension softening of plain concrete after cracking and the reduction of stress transfer along crack planes.

For the former issue, a fracture energy formula including high strength concrete proposed by Uchida et al [3], described in Eq. (1), is applied in plain concrete element.

$$G_f = \alpha_f f_c'^{1/3}, \quad \alpha_f = 10 d_{max}^{1/3} \tag{1}$$

where, G_f is fracture energy (N/m) and d_{max} is maximum aggregate size (mm).

For the latter issue, the authors had adopted a contact density model for normal strength. In the case of high strength concrete, however, stress transfer mechanism changes. Here, the stress transfer equation can be simplified by multiplying the shear transfer

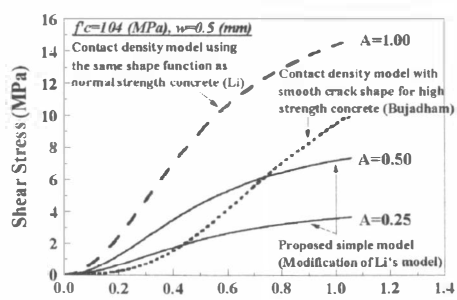

Fig.1 Shear transfer model

envelop (Eq. (2)) of the contact density function model that assumes rough crack surface of normal strength concrete by a reduction coefficient A (< 1.0), as shown in Fig. 1.

$$\tau = A\tau_{normal} = Af_{st}\frac{\beta^2}{1+\beta^2} \tag{2}$$

where, t is shear stress transferred along crack plane, A is shear transfer reduction coefficient (A = 1.0 in the case of high strength), t_{normal} is basic shear stress transferred along crack surface, f_{st} is ultimate shear transfer strength (= 3.83f'_c1/3) and ß is ratio of shear slip and opening displacement on crack surface.

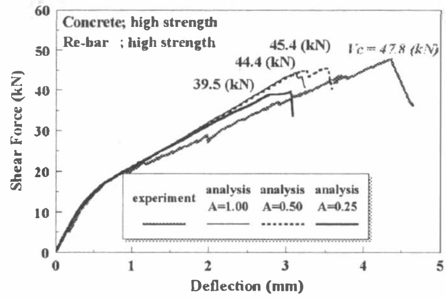

Fig. 2 Sample of comparative analyses

4 APPLICATION OF TWO-DIMENSIONAL FINITE ELEMENT ANALYSIS

In order to identify the shear transfer reduction coefficient and to consider the influence of smoothing crack planes to structural response, comparative analyses are carried out here, by comparing with our experimental results [2]. Parametric analyses are conducted with the shear transfer reduction coefficient A changed to 1.00, 0.50 and 0.25 (Fig. 2).

Judging from the relationship between shear force and displacement and the cracking distribution, it is learned that using the shear transfer reduction coefficient of 0.50 generally resulted in a good correlation with the experimental results. In the shear transfer test conducted for a single crack formed by creating a linear slit, the reduction rate was approximately 0.25. In contrast, in the sensitivity analysis performed for cracking in an actual structure, a value of 0.50 gives good results. This difference may be dependent on the degree of meandering in the cracks produced in the structure.

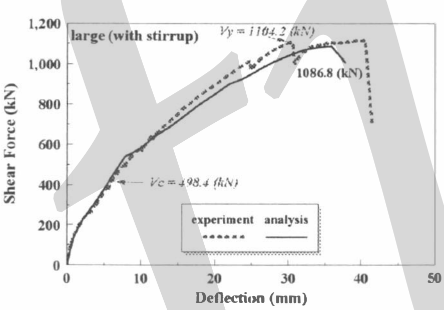

Fig. 3 Specimen with stirrups (large size)

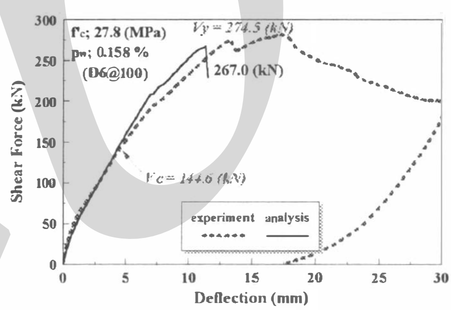

Fig. 4 Specimen with normal strength concrete

Next, the proposed method with shear transfer reduction coefficient of 0.50 has been applied to the other suggestive experiments [2] for verification and discussion. Fig. 3 and Fig.4 are examples of analytical results. It is verified that the proposed analytical method can accurately evaluate response behaviors of RC beams using high strength materials failed in shear. These results indicate that the size effect of shear capacity of concrete and the increase in capacity after shear reinforcement yielding are directly represented. Moreover, shear failure can generally be evaluated for not only combinations with high strength concrete but also a combination with normal strength concrete, whose capacity cannot be predicted by the design equation.

REFERENCES

[1] Maekawa, K. et al. : 2D and 3D multi-directional cracked concrete model under reversed cyclic stresses, Modeling of inelastic behavior of RC structures under seismic loads, ASCE, 2001.
[2] Tsuchiya, S. et al. : Shear failure and numerical performance evaluation of RC beam members with high strength materials, Proc. of JSCE, No.697/V-54, pp.65-84, February 2002. (in Japanese)
[3] Nakamura, S. et al. : Discussion on standard evaluation method for tension softening properties of concrete, Concrete Research and Technology, JCI, Vol.1, No.1, pp.1151-164, 1991. (in Japanese)

DIAGONAL TENSION FAILURE MECHANISM OF REINFORCED CONCRETE BEAM WITHOUT SHEAR REINFORCEMENT

Yasuhiro Takaki Manabu Fujita Kaori Matsumoto
Institute of Technology & Development, Sumitomo Construction Co., LTD.
Japan

Keywords: diagonal tension failure, lateral crack, spiral hoop reinforcement, ductility

1 INTRODUCTION

The shear failure mode of reinforced concrete beams without shear reinforcement can be divided by shear span ratio into diagonal tension failure and shear compression failure. Of these two categories, diagonal tension failure results from a slight increment in load after diagonal cracking has occurred. Ultimate failure occurs when lateral cracking develops along the tension reinforcement or diagonal cracks penetrate near the loading point. In addition, according to research by Kim et al [1], the development of flexural shear cracking to the compression zone depends on the development of the lateral cracks. As a result, determining the behavior of lateral cracking is thought to be important when considering the shear load-carrying mechanism after diagonal cracking occurs.

For this reason, in this study basic tests were conducted regarding the effect of lateral cracking on diagonal tension failure. First, shear tests were conducted with the aim of grasping the diagonal tension failure mechanism and differences in the failure mechanism caused by the compression strength of the concrete. Based on the results, verification tests were conducted using reinforced specimens. A study of the mechanism by which diagonal tension failure occurs was also tried by using numerical analysis to reproduce this mechanism.

2 TEST USING COMPRESSIVE STRENGTH AS A PARAMETER

First, in order to examine the status of the occurrence of diagonal cracking and lateral cracking, static load tests were conducted using three test specimens. The shear span ratio (*a/d*) was set at 3. The concrete compressive strength was planned in three levels: 30(SP1), 60(SP2) and 90(SP3) N/mm^2. In this test, PI displacement transducers were provided in the horizontal, vertical and diagonal directions, and accelerometers were placed at the top and bottom of the beams along the diagonal cracks.

From test results, the diagonal tension failure is surmised to occur by means of the following mechanism.

1) After diagonal cracking occurs, lateral cracking occurs along the tension reinforcement in the direction of the support, starting from the intersection between the diagonal cracking and the tension reinforcement.
2) The cracking at the intersection opens in the vertical direction (meaning that lateral cracks developed), and the member shifts out of place in the vertical direction.
3) This opening of crack becomes the origin, and diagonal cracking penetrates all at once up to a point near the loading point.

The above indicates that it is possible that diagonal tension failure of reinforced concrete beams without shear reinforcement may be caused by the sudden development of lateral cracks. For this reason, the place where lateral cracking occurs was reinforced with spiral hoop reinforcement.

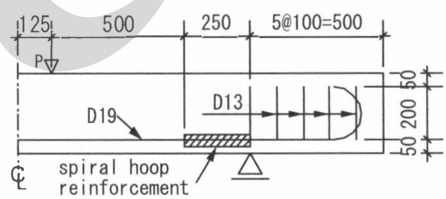

Fig. 1 Specimens geometry

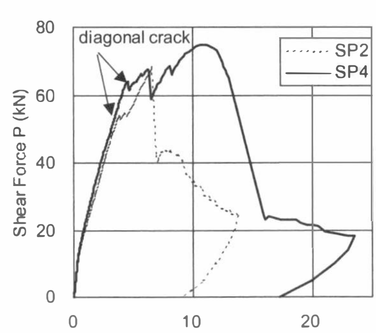

Fig. 2 Shear force – Deflection relation at midspan for specimens.

3 REINFORCEMENT TEST FOR LATERAL CRACK POSITION

Since the range of the lateral cracking in SP2 was approximately 1d from the support in the loading point direction, this range was reinforced (**Fig.1**).

Compared to SP2, diagonal cracking occurrence load and shear capacity of SP4 increased, and the fracture became more ductile (**Fig.2**). This indicates the possibility that diagonal tension failure is triggered by sudden development of lateral cracks.

Table 1 Material Property

No.	Compression※1			Tension※1		
	Zone1	Zone2	Zone3	Zone1	Zone2	Zone3
1	C1	C1	C1	T2	T3	T1
2	C1	C1	C1	T2	T3	T3
3	C1	C1	C2	T2	T3	T4
4	C1	C1	C3	T2	T3	T5

※1:stress-strain curve(C1-3,T1-5 : refer to Fig.4)

4 NUMERCIAL ANALYSIS

4.1 Outline of analysis

An attempt was made to reproduce this behavior through numerical analysis. Analysis was performed with the finite element analysis program DIANA.

The analysis model was divided into three zones. The analysis was performed for the four cases (**Table1**). In particular, material properties are changed in Zone3 that took into consideration whether or not there was any adhesion of the tension reinforcements and the concrete, and the effect of spiral hoop reinforcements.

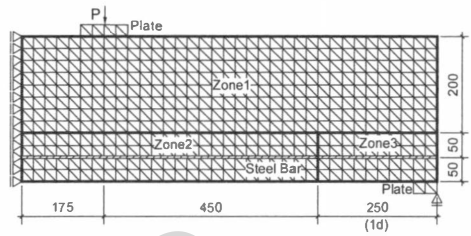

Fig.3 Analytical Model

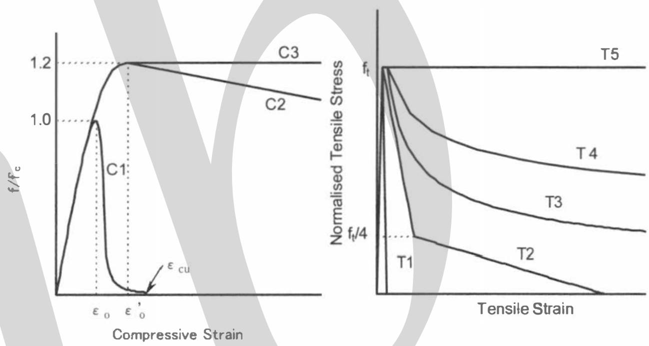

(a) Property of compression (b) Property of tension

Fig. 4 Analytical Material Model

4.2 Results of analysis

The load at which diagonal cracking occurred increased slightly from No. 1 to No. 4, which is consistent with the test results (**Fig.4**). The behavior of each of the cases after the occurrence of diagonal cracking was as follows. For No. 1, the load decreased sharply. For No. 2, the load remained almost constant, and only deformation progressed. For No. 3, the maximum load was greater than load when diagonal cracking occurred, the results were extremely similar to those for the test specimen that had been provided with spiral hoop reinforcement. For No. 4, a firm tied arch was formed and shear compression failure occurred. The test using spiral hoop reinforcement is thought to fall between No. 2 and No. 4.

As shown above, changes in the shear load-carrying mechanism due to reinforcement of the lateral cracking position were confirmed qualitatively through numerical analysis as well. In other words, the shear load-carrying mechanism after the occurrence of diagonal cracking was controlled by lateral cracking, and restraining the ring tension and dowel action at the lateral cracking position enables the shear load-carrying capacity and deflection ductility to be increased.

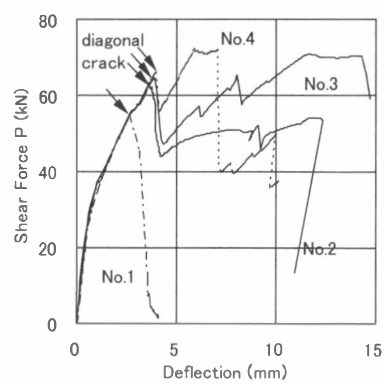

Fig. 5 Shear force – Deflection relation

REFERENCES

[1] Woo Kim, Richard N, White : Shear-Critical Cracking in Slender Reinforced Concrete Beams, ACI Structural Journal, Vol.96, No.5, September-October 1999.

SOME ASPECTS ON THE BEHAVIOUR AND DESIGN OF REINFORCED CONCRETE BEAMS WITH LARGE OPENINGS -THEORETICAL RESULTS AND TEST SETUP-

Prof. Dr.-Ing. Martina Schnellenbach-Held, Dipl.-Ing. Stefan Ehmann, Dipl.-Ing. Carina Neff
Institute of Concrete Structures and Materials
Darmstadt University of Technology, Germany
{schnh, neff}@massivbau.tu-darmstadt.de

Keywords: beams, large openings, reinforced concrete, structural design, nonlinear Finite-Element analyses

1 INTRODUCTION

Openings are often provided in beams in order to install service lines. So beams with large openings are applied in the structures of almost every building. These openings affect the beams' behaviour in the ultimate and the serviceability limit state. In Europe two concepts which are based on very few experimental investigations of the 1960's are applied. Ongoing comprehensive experimental investigations have been done by Mansur and co-authors [1] in the 1980's and 1990's.

During the past three years extensive studies concerning the load bearing behaviour of reinforced concrete beams with one large web opening have been conducted. The first part of the research program which dealt with nonlinear Finite-Element analyses of beams with one large opening has been completed [2]. The results of these studies will be presented. In the second part of the research program eight laboratory tests will be conducted. The test setup will be illustrated.

2 RESULTS OF THE FINITE-ELEMENT ANALYSES

The theoretical studies have shown that the maximum stresses do not occur directly at the end of the chords. In Fig. 1 the locations of possible plastic hinges (as a result of the nonlinear Finite-Element analyses) have been marked.

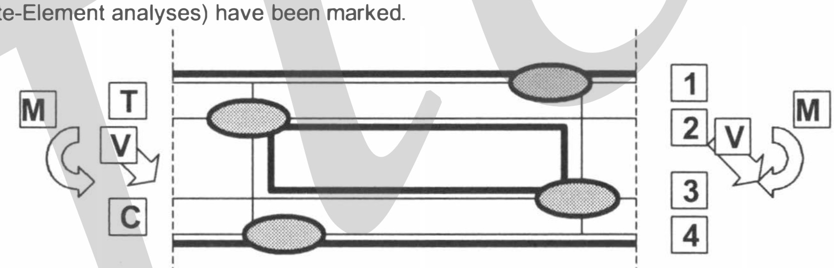

Fig. 1: Locations of possible plastic hinges

The point of contraflexure in the chord members is characterized by the following parameters: opening length l_o, the proportion of the reinforcement α_t in the regarded chord and the location of the opening represented by the ratio of the internal forces M/V [m]. While a linear influence of M/V and α_t can be recognized, the influence of l_o approaches a logarithmic function. The secondary bending moment does not occur if the opening length drops below a boundary value.

The shear force distribution on the chord members is characterized by exceeding the concrete's tensile strength. The physical nonlinear Finite-Element computations show that behaviour. They enable to record the data for the curve's trend for the first time. The conducted studies point up the influences of the M/V-ratio, the amount of the tension chord's reinforcement and the opening's length on the shear force distribution.

The theoretical investigations show that the crucial parameters on the load bearing capacity are the amount of the chords' reinforcement and the opening's geometry. The location of the opening represented by the M/V-ratio does not affect the load bearing capacity as it is presumed frequently. The maximum load is reduced if there is an insufficient quantity of stirrups right next to the opening (A_{sH}) and also in a particular distance to the opening's border (A_{sH2}). Additional stirrups in a particular distance to the opening's border increase the load bearing capacity by obtaining a proportion of the compression chord's shear force and anchorage forces from the chord's reinforcement.

3 TEST SETUP

In order to verify the results of the FE-calculations eight tests will be carried out. The special test setup offers the possibility to create the bending moment and the shear force independently and so control the internal forces separatly from each other.

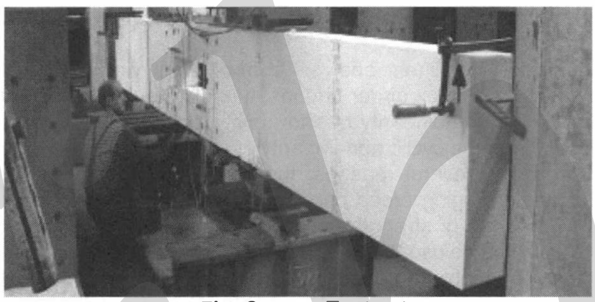

Fig. 2: Test setup

In the test program several parameters will be varied:

- Different M/V-ratios.
- The length of the opening.
- Variations of the reinforcement areas and distribution of the reinforcement of both chords.

During the tests the deformation of the chords and the strains in the reinforcement will be measured. It is the aim to find the exact location of the plastic hinges of the reinforcement as well as to determine the forces in the stirrups close to the opening. Therefore strain gauges and position encoders are arranged around the opening.

Supplementary the deformations of the compression and tensile chords will be measured by photogrammetry. Therefore various points are marked at the surfaces of both chords. During the increasing load-steps pictures will be taken. Afterwards the deformation of every marked point can be computed. So the results of the photogrammetry and the measurement by strain gauges can be compared.

4 CONCLUSION

The results of the FE-calculations provided a basis for the design of beams with large openings. The distribution of shear forces on the tension and on the compression chord can be determined now. Furthermore it is possible to choose the area of the stirrups close to the opening and to compute the deformation. Within the next year tests with realistic sized specimens will be conducted in order to verify the FE-calculations.

REFERENCES

[1] Mansur, M. A.; Tan, K.-H.: Concrete Beams with Openings – Analysis and Design. National University of Singapore, 1999

[2] Ehmann, S.: Zum Trag- und Verformungsverhalten von Stahlbetonträgern mit großen Öffnungen, submitted Dissertation, TU Darmstadt, Institut für Massivbau, October 2001

COMPUTING FORCE FOR PRACTICE, A REVIEW OF NON-LINEAR OPTIONS

Johan Blaauwendraad
Delft University of Technology
The Netherlands

Keywords: bridge models, fire, contact elements, young concrete, deep beam design

1. OVERVIEW IN A NUTSHELL

In research circles analysis methods which account for non-linear material behaviour and gross deformations are in use for many years. The majority of general-purpose FEM-packages offer such options, be it in a larger variety for metal structures than for brittle material structures like concrete and masonry. Gradually more such non-linear software starts playing a role in design of structures. This paper intends to give an overview in a nutshell of practical applications and wants address a limited number of such non-linear analyses.

We can address the subject of non-linear analysis from different viewpoints. One can start from the category of structures: shear walls, box girder bridges, tunnels, pavements, composite structures, etc. or from the actions. Deviations from linearity due to gravity loads are different from deviations due to fire, and these are different from the cyclic non-linearity at earthquake excitations.

Material non-linearity can have several reasons: the concrete can be cracked under tension, can become plastic in compression, aging creep can be the source, or swell and shrinkage may occur. Failure will occur due to passage of strength limits or by fatigue. A modern trend is not to speak in terms of cracks and plasticity, but to use the concept of damage for the loss of structural integrity.

A special class of non-linear analyses consists of the modelling of hydration processes in young hardening concrete. This is done to control the tensile stresses during the curing process in order to prevent early cracking. Another category of non-linear behaviour consists of contact problems. The material itself can stay elastic, but the geometry of the structure may change. This can be found in tunnel linings, which are built up from pre-cast concrete elements. The elements itself are considered to stay elastic, but the joints have non-linear characteristics.

2. PROGRAM TYPES

One cannot find designer oriented software, which will cover all possible sources of non-linearity. In practise different kinds of software exist for different applications. Here we will mention a few:

General-purpose FEM packages like Diana, Marc, Ansys and Abaqus. It is software to check a design, not to make a design. The design of structural concrete with the Strut-and-Tie method can be supported by software, which accounts for the stiffness of tensile members in a cracked state.

Special FEM software, which has been developed for a class of structure, say shear-walls. Now special attention is paid to user-friendliness and nice showing of results. The programs Atena and SPanCAD are examples of this type of software.

A class of programs, which has not yet been widely distributed is based on classic theory of plasticity and optimisation techniques. The universities of Zürich and Copenhagen have worked on this subject.

Some programmes are in circulation in which assemblages of rigid parts and lumped masses, springs and dashpots are applied, sometimes in combination with a limited set of standard continuous finite elements. An example is the New Zealand package Ruaumoko.

3. WHAT THE DESIGNER SHOULD KNOW

The applicant of any software is asked to provide data on the structure to be designed. He or she must understand what information is asked. He has to understand the meaning of softening parameters for regions tension and compression. A completely new field of material data regards fibre-reinforced concrete. The materials composition can be engineered and the fracture characteristics can be manipulated. A separate story is the data needed for cyclic loadings. A correct choice of model and data is of major importance for a proper simulation of the hysteresis nature of the structure and therefore for the capacity to absorb energy. In case of fire deteriorating strength and stiffness data are needed which depend on temperature. The same applies for studies of the development of strength and stiffness in young concrete. In this case a complex coupled problem of heat generation and ´ripening´ must be solved and data are needed which are unfamiliar to civil engineers.

4. APPLICATIONS

4.1 Bridge composed of box-girders

A bridge with a span of 27 meter which is composed of five box girders is modelled in three different ways: a slab model (2D), a shell model (2.5D) and a solid model (3D). The latter is shown in figure 1. The shell model and solid model yield similar results. The transverse bending moments in the slab model deviate quite a bit, at least for the transverse bending moments. This may lead to wrong conclusions about the need of post-tensioning in transverse direction.

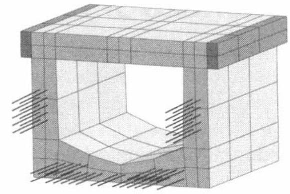

Fig. 1 Solid model of box girders bridge

4.2 Fire on top of covered LNG-tank

Fire on the domed roof of an LNG-tank is the subject of this section. The finite element mesh of the tank under consideration is shown in figure 2. In case of over-pressure of the gas a safety valve starts to open and the gas is burned on top of the tank. Burning of the gas heats the domed-roof and extreme strains and stresses are determined. The non-linear analysis is done in an iterative way by an elastic FEM analysis in combination with a non-linear company module.

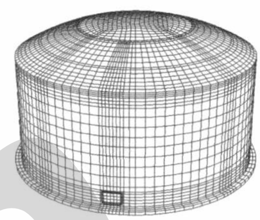

Fig. 2 Finite element model of safety tank

4.3 Segmented tunnel lining

In order to gain better understanding of the complex structural behaviour in shield driven segmented tunnel linings for soft soil conditions, a full-scale test set-up has been realized in the Netherlands. The focus in this study is on contact elements in order to model joint behaviour as good as possible, see figure 3. The joint behaviour is introduced in the analysis by means of a user-defined subroutine. The computed curvatures in tangential direction are compared with experimental results. Further refinement of the joint modelling is still needed.

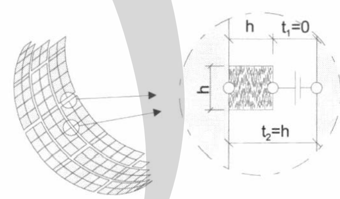

Fig. 3 Joint schematisation

4.4 Prevention of cracking in curing concrete

An important computing facility to serve designers is software to predict the development of temperature, stiffness and creep and quantities, instantaneous strength and stresses of young concrete. All these quantities develop in time during the curing process of hardening concrete. The chosen example are the walls in the approach road to the tunnel under the Western Scheldt, which is the open connection of Antwerp to the North Sea. Fig. 4 shows a typical result for the process development in time. The stress keeps lower than 50% of the tensile strength.

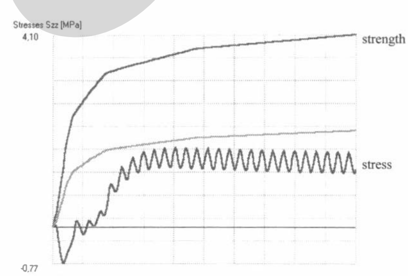

Fig. 4 Stress and strength development

4.5 Design of deep beam

In this section the headlines of a design program are introduced for the structure of figure 5.

The software is based on AutoCAD, which for the purpose is enriched with analysis commands. The designer takes the lead in an interactive design process. In three steps the design of a deep beam is improved. Sufficient strength is the goal for the ultimate limit state and sufficient crack-width control for the serviceability state.

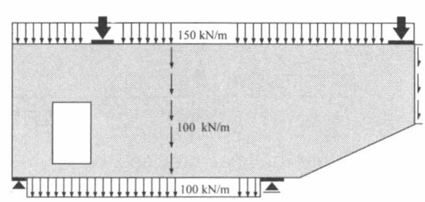

Fig. 5 Design example

A STUDY ON FLUCTUATIONS IN ULTIMATE STATICALLY INDETERMINATE FORCES OF PRESTRESSED CONCRETE CONTINUOUS BEAM

Kenji Umezu Manabu Fujita
Sumitomo Construction Co., Ltd. JAPAN

Keywords: indeterminate force, secant stiffness method, no-joint, failure mechanism, nonlinear analysis

1 INTRODUCTION

We investigated the ultimate bending behavior and failure mechanism of prestressed-concrete continuous beams by conducting static load experiments and nonlinear analysis. The test specimen was reduced-scale model of a prestressed-concrete continuous-girder bridge in which single girders of an existing highway bridge are connected by a no-joint construction method and are reinforced with external tendons. The no-joint construction method consists of removing expansion joints.

2 TEST SETUP AND PROCEDURE

The test girder is two-span continuous beam, and the geometry and dimensions of it is shown Fig.1[1]. An equal load was placed in two locations per span, in symmetrical positions on the left and right of the span, and the load was increased gradually until the girder suffered bending failure.

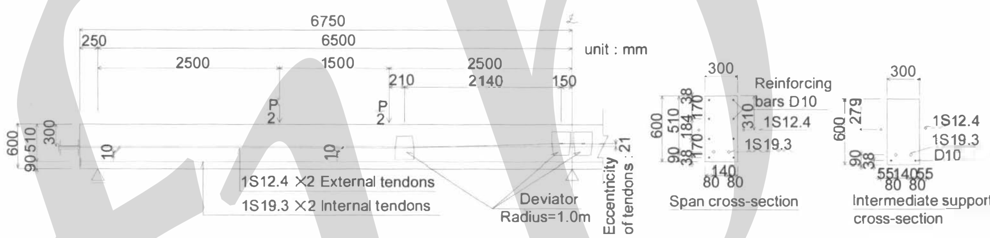

Fig.1 Geometry, dimensions of the test girder

3 TEST RESULT

3.1 Formation of plastic hinges and redistribution of moments

At the intermediate support part, the degree of opening after cracking occurred was significant, because the tensile edge is unreinforced. A plastic hinge was formed sooner in the intermediate support part than in the span.

Between loading points of the span, the lower-edge reinforcing bar and the internal tendons yielded, and an increase in the curvature of the girder was observed. These are judged to be the times at which plastic hinges form in the left and right spans.

The moment redistribution rate at maximum load reached the conspicuous values of 32% in span *Mmax.* cross-section and − 70% in intermediate support cross-section (Fig.3).

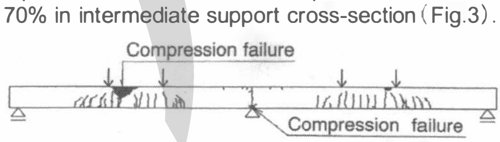

Fig.2 State of final cracking

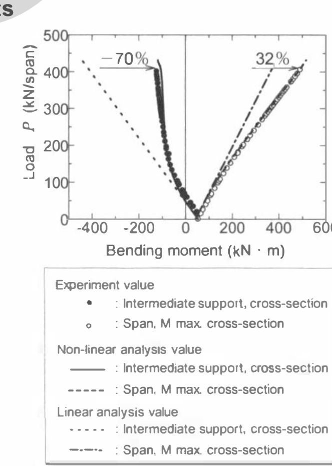

Fig.3 Relationship between load and bending moment

3.2 Failure mechanism

Compression failure was found in the left span upper edge concrete at load peak. Thereafter the load carrying capacity gradually decreased as the compression failure portion of the concrete slowly spread from the edge toward the cross-sectional centroid, and the deflection of the left span kept progressing. Thus the structure became unstable, so it led to the failure mechanism.

4 ANALYSIS USING SECANT STIFFNESS

4.1 Secant stiffness

The secant stiffness EA and EI of members, which are the gradients of the secant that joins the origin with an arbitrary point on the $N-\varepsilon$ diagram and $M-\phi$ diagram as shown in Fig.4.

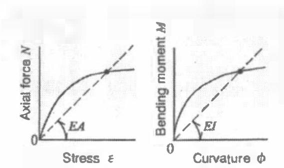

$$EA = \frac{N}{\varepsilon}, \quad EI = \frac{M}{\phi}$$

Fig.4 Secant stiffness

In order to apply the widely used framework elasticity analysis method to linearly reproduce an arbitrary state subsequent to entering the plastic region in an overall structure system, it can be done by loading the overall effect load at that time onto a structure system consisting of members evaluated by secant stiffness at that time.

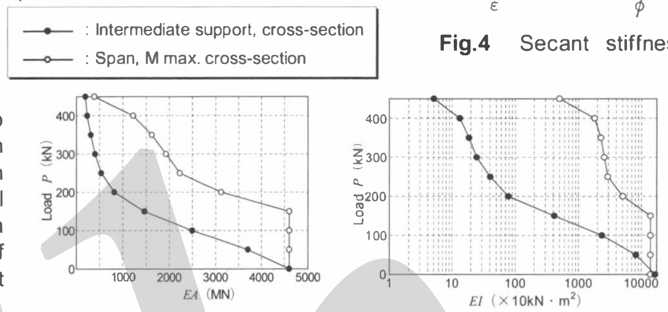

Fig.5 Relationship between EA and EI and the load on the main cross-section

4.2 Changes of support reaction

Fig.6 shows the changes under a gradual increase in load when the support reaction is decomposed by the secant stiffness method into components due to each load. As the stiffness declines with increasing load, the reaction due to dead load moves a little from the intermediate support to the end support, and the indeterminate reaction due to prestressing decreased.

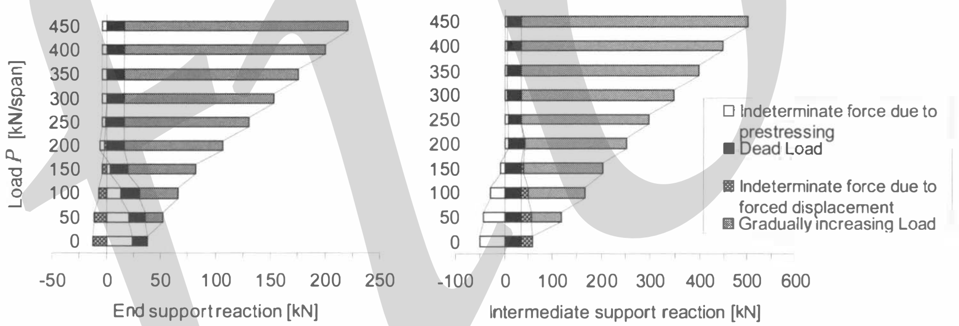

Fig.6 Analysis of support reaction by the secant stiffness method

And in this research, the nonlinearity in the behavior of a statically indeterminate beam structure seen in this test girder made it clear that the effect of the reduction in flexural stiffness is greater than the axial stiffness of the member. But it was shown that once the main tensile steel member yields, the effect of the reduction in the axial stiffness of the member cannot be ignored.

5 CONCLUSION

The indeterminate forces due to forced displacement of a support and the indeterminate forces due to prestressing fluctuate with the reduction of the member stiffness, a change in the stiffness ratio between members, and the movement of the centroid axis when the load is increased. In this test girder, the state in which the indeterminate forces due to prestressing diminishes was obtained by the change in the ratio of the stiffness between members accompanying a exceeding decline of the flexural stiffness at the intermediate support part.

REFERENCE

[1] Tsuno,K., Fujita,M., Umezu,K., Seki,H. :Ultimate bending behavior of external tendon-reinforced prestressed-concrete girders made continuous by no-joint methed. Journal of Materials, Concrete Structures and Pavements, Japan Society of Civil Engineers,No.641,pp.87-100,Feb.,2000

NONLINEAR FINITE ELEMENT ANALYSIS OF PRESTRESSED CONCRETE MEMBERS

Makoto Kawakami — Kozo Keikaku Engineering Inc., Japan
Tadahiko Ito — Nishimatsu Construction Co., Ltd., Japan

Keywords: nonlinear finite element analysis, prestressed concrete, crack, crush, contact

1 INTRODUCTION

Nonlinear finite element analysis of prestressed concrete (PC) members were performed based on two load test results: [1] for a PC column which included material nonlinearities (concrete cracking/ crushing and rebar plasticity), and [2] for a pecast segmental PC beam which included goemetrical nonlinearities (large displacement and contact/separation between the segments) as well as material nonlinearities. For the calculation, the general-purpose finite element code ADINA was used.

2 PRESTRESSED CONCRETE COLUMN

2.1 Load test [1]

Fig. 1 shows the test specimen. The PC bar had no bond with the concrete. The horizontal displacement was statically applied.

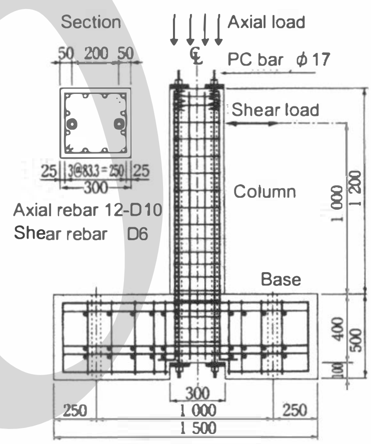

Fig.1 Test specimen

2.2 Analysis model

Only the column was analyzed using a two-dimensional finite element model. Concrete and steel bars were modeled using plane stress elements and truss elements, respectively. All of the nodes on the column baseline were fixed. The concrete material model included nonlinear stress-strain relationship, biaxial stress failure envelope, linear tension stiffening, smeared cracking model, etc. [3]. The steel were bilinear elastic-plastic. The PC bar pretension was modeled using initial strain of the truss element. Static analysis based on the small displacement formulation was performed using the simple incremental approach.

2.3 Analysis results

Fig.2 shows the calculated cracking and crushing extents at various load levels. The calculated failure sequence was as follows: bending cracks occurred on the tension side of the column base; the cracking progressed upward; tensile rebar yielded; the cracking propagated through the depth of the column in a slanted direction; vertical cracking and crushing occurred along the compression side of the column base. Nonlinear load-displacement relationship and elastic-plastic behavior of the rebars were observed. These nonlinear behavior obtained from the calculation were compared with the tested results.

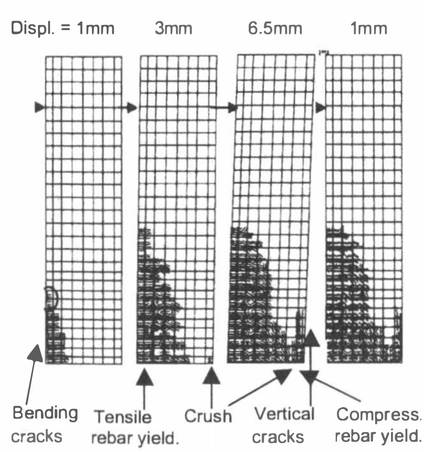

Fig.2 Crack and crush distribution

3 PRECAST SEGMENTAL PRESTRESSED CONCRETE BEAM

3.1 Load test [2]

Fig. 3 shows the test specimen, which consists of six precast segments assembled into a beam using pretension of four external cables. The axial rebars were not connected to the adjacent segments. The simply supported beam was statically subjected to the vertical load.

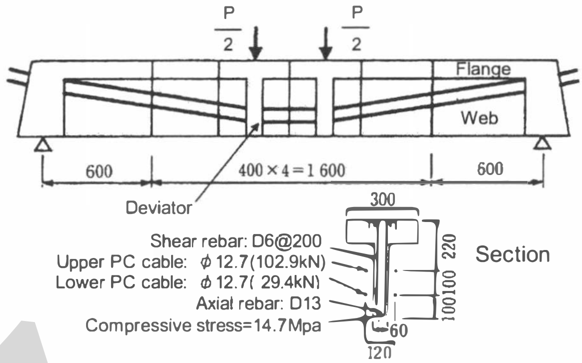

Fig.3 Test specimen

3.2 Analysis model

Because of the symmetry condition at midspan, only the right half (three segments) of the beam was modeled using a two-dimensional finite element model. Concrete and steel bars/cables were modeled using plane stress elements and truss elements, respectively. The concrete and steel material models were the same as described in section 2.2. The PC bar pretension was modeled using initial strain of the truss element. The contact surface calculation enabled the transmission of the pressure and friction forces at the point of contact and no force at the separated parts between two adjacent segments. The vertical shear load was applied. Static analysis based on the large displacement formulation was performed using the incremental approach with the equilibrium iterations.

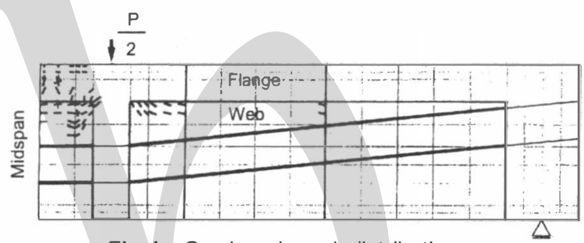

Fig.4 Crack and crush distribution

3.3 Analysis results

Gap openings between the segments were observed at the bottom face of the beam. Fig. 4 shows the cracking and crushing distribution at the final state in the calculation. The material failure was concentrated at the segment adjacent to the midspan boundary and the failure sequence was as follows: horizontal cracks occurred at the upper part of the web; cracking progressed at the flange and the right web of the midspan segment; crushing occurred at the top face. The load-displacement and load-strain relationships for the concrete and the PC bars were compared with the tested results.

4 CONCLUSIONS

The calculated results were in good agreement with the tested results in terms of properties such as the concrete cracking/crushing process, the gap opening/closing between the segments, the load-displacement relationships, and the load-strain relationships for the rebars, the PC bars/cables, and the concrete. Therefore, the analysis models presented here were found to be very effective for gaining detailed knowledge of the nonlinear behavior of PC members.

REFERENCES

[1] Ito, Yamaguchi, Ikeda: Seismic performance of reinforced concrete piers prestressed in axial direction, Japan Concrete Institute Conference Proceedings, Vol.19, No.2, pp.1197-1202, 1997

[2] Ito, Yamaguchi, Ikeda: Experimental study on flexural shear properties of precast segmental beams, Journal of Prestressed Concrete, Japan, Vol.39, No.1, pp.83-96, 1997

[3] Bathe, et al.: Nonlinear Analysis of Concrete Structures, Computers & Structures, Vol.32, No.3/4, pp.563-590, 1989

MULTI-SEGMENT MODEL FOR NONLINEAR ANALYSIS OF EXTERNALLY PRESTRESSED CONCRETE BOX GIRDER

Navakumar Poologasingam
Graduate student
Yokohama National University

Tatsuya Tsubaki
Member of JPCEA
Yokohama National University

Keywords: multi-segment model, friction factor, joint element, shear stress, ultimate moment capacity

1 INTRODUCTION

Prestressed concrete box type structures are used because of its reduced self-weight and high torsional stiffness. The use of external prestressing in such a structure is considered as the advanced technique used for strengthening and rehabilitation of existing structures as well. The effect of friction at the deviator on the ultimate moment capacity of the structure, however, is not well known because the bond behavior is not known with the deformation of the structure.

In order to get accurate overall response of that type of structure, the shear stress in a box type cross section must properly be obtained so that the cracking load and where the cracking occurs are properly estimated, in particular, for a tapered box type cross section.

In this paper, therefore, nonlinear multi-segment model [1] is used to analyze a concrete girder with a hollow cross section or a solid cross section. The crack pattern, effect of friction and behavior of joint element for a precast segmental bridge are examined.

2 MULTI-SEGMENT MODEL

The engineering shear stress distribution across the thin-walled cross section is assumed to be reasonable in this study with the Bernoulli-Euler beam theory taking into account the material nonlinear models for concrete, reinforcement and PC tendon [1]. The finite element model is formulated with the arbitrary shape of cross section as shown in Fig.1. Each segment could have different thickness and is divided into a number of layers perpendicular to the centerline of the segment axis to take into account the material nonlinearity and the shear stress distribution along the segment.

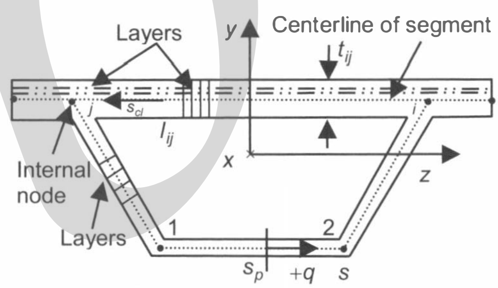

Fig. 1 Multi-segment model

2.1 Shear stress

The normal stress across the cross section is calculated using the strain-displacement relation with the assumed displacement field and the displacements at the nodal points in the finite element analysis [1]. The stress equilibrium at each point is considered across the segment of the cross section. Then, the continuity of the shear flow over the closed single cell is taken into account for the calculation of the shear stress. The crack pattern obtained from the stress distribution is plotted for the transverse cyclic loading at the 7-th cycle for a simply supported box girder as shown in Fig. 2. The simulated crack pattern is in agreement with test data.

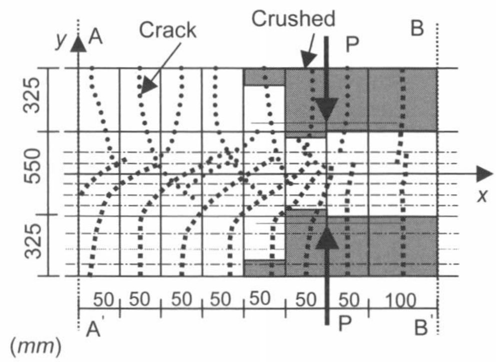

Fig. 2 Crack pattern

2.2 Friction at deviator

Usually, for the analysis of externally prestressed structures, the effect of friction at the deviator point is neglected considering free-slip condition.

An equation is proposed for the cable strain ε with the elongation ratio $\Delta l / l$:

$$\Delta\varepsilon_{pi} - \Delta\varepsilon_{pi+1} = k_i\left(\frac{\Delta l_i}{l_i} - \frac{\Delta l_{i+1}}{l_{i+1}}\right) \qquad (1)$$

where k_i is friction factor. For different values of friction factor, the flexural response of the structure is simulated under monotonic loading and is compared with the test data as shown in Fig.3.

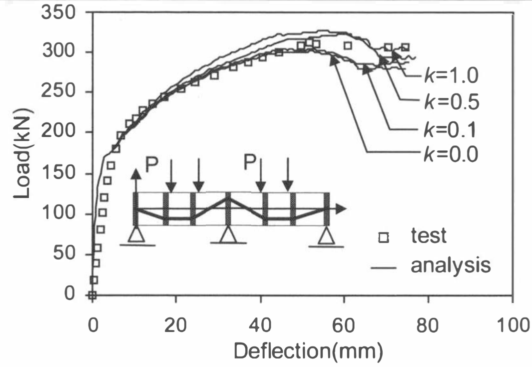

Fig. 3 Effect of friction factor

2.3 Joint opening

To calculate the ultimate moment capacity of the precast segmental concrete structure, the nonlinear behavior of joint opening with the deformation of the structure has to be considered. Discontinuity of joint starts while the joint opens. A simplified joint element is introduced for the discontinuity of the structure with the reduction of flexural stiffness as de-bonding occurs. Simulated results for the joint opening of the Bangkok second stage expressway bridge [2] is shown in Fig.4.

The joint element between precast segments is shown in Fig.5 where h_c is the compression zone, h is the thickness of the segment and Δa is the crack opening.

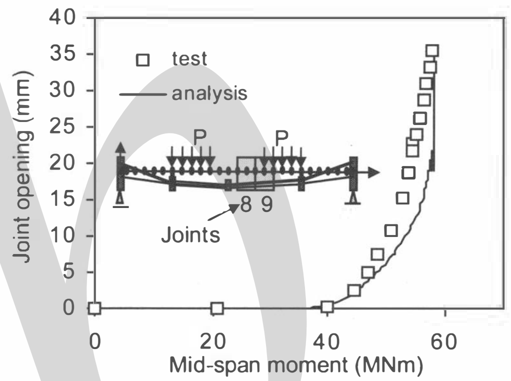

Fig.4 Joint opening near to mid-span

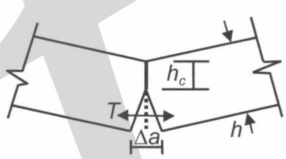

(a) Join opening between segments

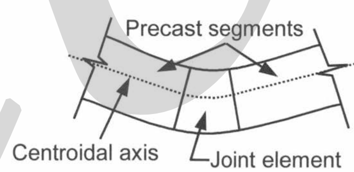

(b) Joint element between segments

Fig. 5 Joint between segments

3 CONCLUSIONS

Nonlinear multi-segment model is used to analyze a prestressed concrete structure taking into account the material nonlinearity, shear stress distribution, friction at the deviator, and joint element for the discontinuity at the joint between the precast segments. The analytical results are in agreement with the test data.

With the present multi-segment model, it has been confirmed that the crack pattern, the effect of friction at deviator, and the joint behavior between precast segments are properly simulated.

REFERENCES

[1] Navakumar, P. and Tsubaki, T. : Numerical simulation model for hysteretic behavior of prestressed concrete box girder. Proc., 11-th Symposium on Developments in Prestressed Concrete, JPCEA, pp.1-6, 2001.

[2] Takebayashi, T., Deeprasertwong, K. and Leung, Y.W. : A full-scale destructive test of a precast segmental box girder bridge with dry joints and external tendons. Proc. Instn Civ. Engrs Structs & Bldgs, No.104, pp.297-315, Aug., 1994.

PRETEST AND POSTTEST ANALYSES FOR NONLINEAR BEHAVIOR OF 1/4 PCCV MODEL SUBJECTED TO INTERNAL PRESSURE

Kenji Yonezawa[1)] Katsuyoshi Imoto[1)] Asao Kato[2)] Masahiko Ozaki[3)]
Kazuhiko Kiyohara[4)] Yasuyuki Murazumi[5)] Kunihiko Sato[6)]

1) Obayashi Corporation, JAPAN
2) The Japan Atomic Power Company, JAPAN
3) The Kansai Electric Power Co.,Inc., JAPAN
4) Kyushu Electric Power Co.,Inc.,JAPAN
5) Taisei Corporation,JAPAN
6) Mitsubishi Heavy Industries,LTD.,JAPAN

keywords: PCCV, FEM analysis, ultimate capacity, internal pressure

1 INTRODUCTION

An increasing number of prestressed concrete containment vessels (PCCVs) are being constructed in Japan as final barriers to hypothetical severe accidents in nuclear power plants. A JAPAN-US cooperative research project on the ultimate capacity of nuclear reactor containment vessels subjected to internal pressure was established by the Nuclear Power Engineering Corporation (NUPEC) and the Nuclear Regulatory Commission (NRC) [1] [2]. As a part of this research, ultimate capacity pressure tests were carried out on a 1/4 scale PCCV model of existing PCCVs in Japan in September, 2000 in Albuquerque, USA [1][2]. In addition, before and after the tests, Round Robin pretest and posttest analysis meetings were held, in order to improve the existing analysis methods for the nonlinear behaviors of PCCVs. The Japan PCCV research group consisted of above six companies participated in this meeting and presented the pretest analysis results obtained in our research program. Many types of global and local pretest analyses were conducted and carried out on the 1/4 PCCV model to establish an analysis methodology that can predict the nonlinear behaviors of actual PCCVs subjected to internal pressure.

This paper discusses the reliability of the pretest and posttest analysis methods developed by the Japan PCCV research group mainly for the structural nonlinear behaviors of 1/4 PCCV up to ultimate internal pressure by comparing the analysis and test results.

2 OUTLINE OF 1/4 PCCV TEST MODEL

The PCCV model is a uniform 1/4 scale model of actual PCCVs used in Japan. The model includes a steel liner and scaled representation of opening and penetrations, such as the equipment hatch (E/H), personnel airlock (A/L), main steam (M/S), and feed water (F/W). The configuration of the PCCV model is shown in Fig.1. The test was terminated by out of nitrogen gas due to leakage of liner tearing portions at a pressure of 1.32MPa.[2]

3 ANALYSIS MODELING

The computer code used here is FINAL [3] using finite element method, which was developed by Obayashi Corporation for nonlinear analysis of concrete structures. Three types of global and local analysis models were conducted. Computational grids of two global analyses and a local analysis are shown in Fig.2.

The 3D90° model idealizes a one quarter section (azimuth 180° ~270°) of the test model. The 3D180° model idealizes a half section (azimuth 90° ~270°) of the test model. Both analyses are performed to quantitatively determine the global nonlinear behaviors of the test model, and to obtain boundary condition for local analyses.

The local 3D E/H model idealizes the entire E/H opening. It is performed to grasp the mechanisms of the liner tearing in the test.

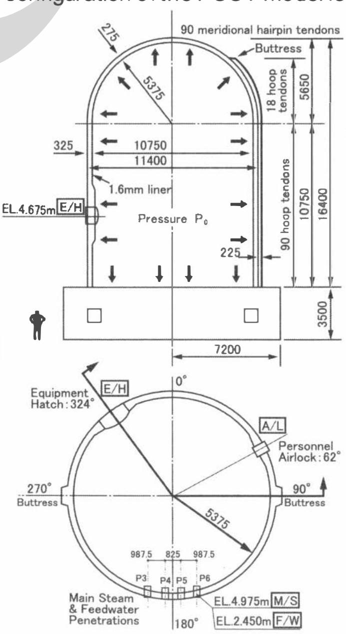

Fig.1 Config. of 1/4 PCCV model

4 PRE- POSTTEST ANALYSIS RESULTS

Fig.3 compares the pressure - displacement relationships obtained from pre-posttest analyses and test results at the 8 measuring points. It is found from these figures that pretest analysis predicted the structural nonlinear behaviors of the test model fairly well, except the nonlinearity due to concrete cracking. After investigating the reasons for this difference, it was found that the tensile strains of concrete due to drying shrinkage might be as large as the cracking strain at time of the tests. Therefore, posttest analyses were performed by only modeling the influence of drying shrinkage of concrete. Nothing was changed in the posttest analyses from the models of the pretest analyses except the tensile strength of concrete according to the study on dying shrinkage. As a result, the nonlinear behaviors obtained from the posttest analyses agreed much better with the test results than those by the pretest analyses.

The von Mises strain contours of the liner obtained from Local analysis are shown in Fig.4. The local analysis can simulate the strain concentration in detail at the same locations as in the test.

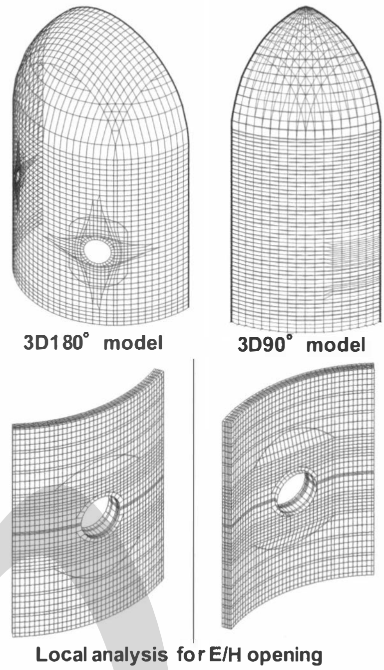

Fig.2 Computer grids

5 CONCLUSION

1) Pretest analysis predicted the nonlinear behaviors of the test results up to the ultimate state with good accuracy. However, a little difference between these two were found at the first turning points.
2) Nonlinear behaviors according to the posttest analysis taking into account the effects of the drying shrinkage of concrete agreed with the test results much better than those of the pretest analysis.
3) It is necessary to conduct several types of analytical models for analyzing the nonlinear behaviors of very complicated RC structures like PCCVs.
4) Therefore, it can be used to evaluate the nonlinear behaviors of actual PCCVs subjected to internal pressure.

Note: The test date is quoted from [2].

REFERENCES

[1] Pretest Round Robin Analysis of a Prestressed Concrete Containment Vessel Model, NUREG/CR-6678 Report, USA, SAND 00-1535
[2] Containment Integrity Test Report of NUPEC, March 2001.
[3] Takeda T., et al: Report on Tests of Nuclear Prestressed Concrete Containment Vessels, Concrete Shear in Earthquake, Edited by T. C. C. Hsu, S. T. Mau, Elsevier Applied Science, pp.163-172, 1992.

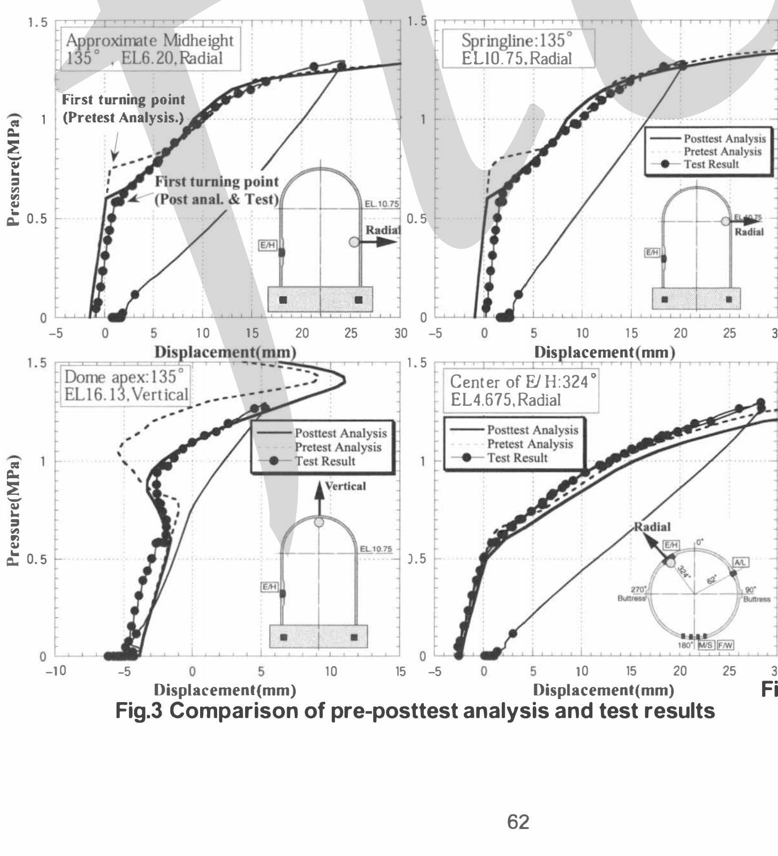

Fig.3 Comparison of pre-posttest analysis and test results

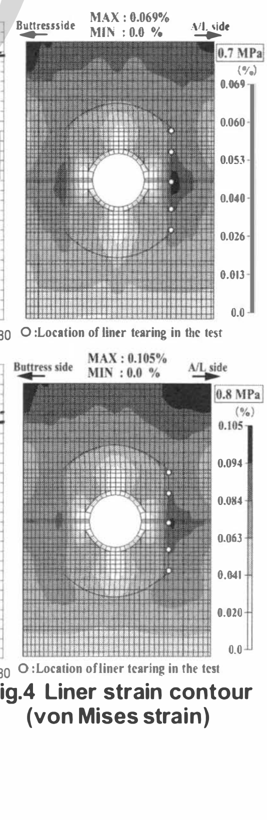

Fig.4 Liner strain contour (von Mises strain)

COMPUTER SIMULATION OF FAILURE OF CONCRETE STRUCTURES FOR PRACTICE

Vladimir Cervenka
Cervenka Consulting, Prague, Czech Republic

Keywords: non-linear analysis, fracture mechanics, plasticity, failure, pre-stressed concrete

1 INTRODUCTION

Non-linear analysis of concrete structures became a novel design tool. It employs the power of computer simulation to support and enforce the creativity of structural engineers. Although it is frequently used in research and development its potential for engineering practice has not been yet fully discovered. In the new design standards for concrete structures, such as Eurocode 2 (1992), the non-linear behaviour of concrete is described by a uni-axial stress-strain diagram. However, this is only a fraction of the available knowledge of material models and theories discovered and validated by research. The finite-element-based failure analysis can take advantage of rational and objective theories such as fracture mechanics, plasticity and damage mechanics. It makes possible a "virtual testing" of building structures under designed loading and environmental conditions. The implementation of these advanced methods and techniques introduces new possibilities for the engineer, not only in research and development but also in practical design. Computer simulation is a modern tool for optimisation of structures, which can contribute to better economy in design. The aim of the paper is to describe the features of non-linear finite element analysis used for computer simulation on the example of the program ATENA and illustrate its potential for practical application.

2 NON-LINEAR FINITE ELEMENT ANALYSIS

Computer simulation is based on the non-linear finite element analysis where four levels of modelling can be recognised: 1.structural model, 2.finite element, 3.material point and 4.non-linear solution technique. An approach of balanced approximation should be accepted on all levels of the model. In case of reinforced concrete structures the choice of a realistic constitutive model at a material point is the crucial factor deciding about the quality of simulation.

Concrete is a quasi-brittle material with a low tensile strength and a strong confining effect in compression. It has been recognised that this behaviour can be described by models based on fracture mechanics, damage mechanics and plasticity. The most important feature of concrete, the crack development, can be adequately simulated by the crack band model based on fracture energy. In this model a discrete crack is approximated by a band of localised strains with a finite width **L** as shown on the example of a crack in the shear wall in Fig.1.

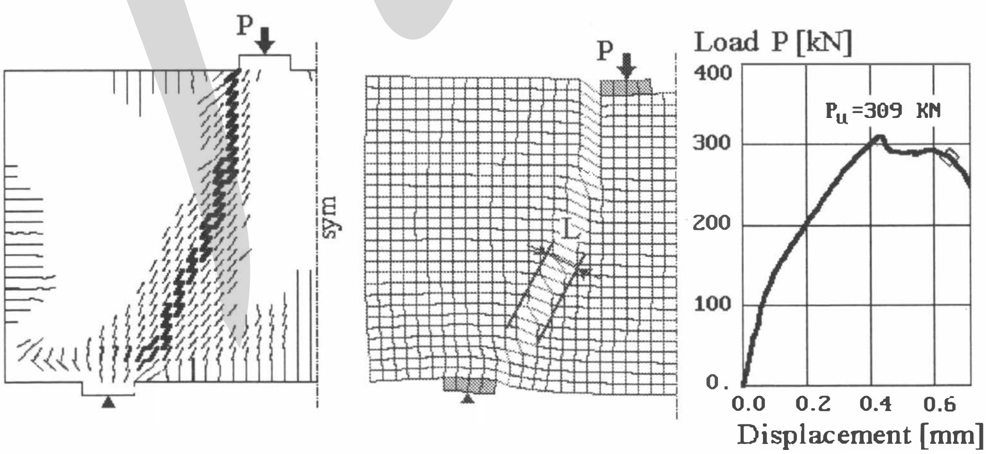

Fig.1 Example of a crack band in the shear wall.

The objectivity of numerical models must be validated by comparison with experiments. The authors have performed extensive studies for this purpose. They confirmed, that the crack band method gives acceptable results for the assessment of crack pattern and crack width and for prediction of failure load in brittle failure modes. In a certain range these results are independent of the finite element mesh size [3], [4].

3 APPLICATION

The full paper shows four cases of practical applications accomplished with the help of the program ATENA: Crack analysis of girder with openings (2D plane stress); Punching of slab (2D axial symmetry); Crack analysis of frame corner (2D and 3D); Box girder bridge (3D analysis). An example from the last case in Fig.2 shows deformations and crack opening in the box girder bridge.

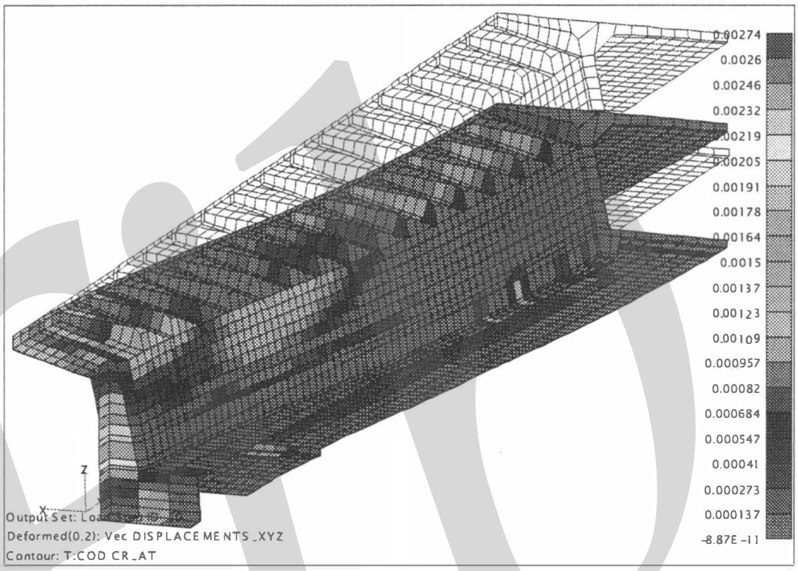

Fig.2 Simulation of cracks and deformations in the box girder bridge in Prague.

4 CONCLUDING REMARKS

Non-linear finite element analysis based on advanced constitutive models can be well used for simulation of a real behaviour of reinforced concrete structures. Computer simulation is a relatively new and robust tool for checking the performance of concrete structures in design and development. Such simulation can be regarded as virtual testing and can be used to confirm and support the structural solutions with complex details or non-traditional problems and can serve to find an optimal and cost-effective design solution. Simulation is useful in such cases, which are not well covered by the code of practice provisions. An interesting application is also in assessment of the remaining structural capacity of existing structures and investigating the causes of damage and failures. It can support the creativity of engineers and contribute to safety and economy of designed structures.

REFERENCES

[1] ATENA Program Documentation, Cervenka Consulting, Prague, Czech Republic, 2000.

[2] CERVENKA, V., 'Simulating a Response', *Concrete Engineering International*, 4 (4) (2000) 45-49.

[3] Cervenka, V. & Pukl, R. - Mesh Sensitivity Effects in Smeared Finite Element Analysis of Concrete Structures. In: Proceedings of the Second International Conference on Fracture Mechanics of Concrete Structures (FRAMCOS 2):1387-1396, Ed. F. H. Wittmann, AEDIFICATIO, ETH Zürich, 1995, Switzerland.

[4] Cervenka, V. – Simulation of shear failure modes of R.C. structures, Proc. of EURO-C 1998, Badgastein, Austria, pp.833-838.

CRITICAL ASPECTS IN MODELLING THE SEISMIC BEHAVIOR OF PRECAST/PRESTRESSED CONCRETE BUILDING CONNECTIONS AND SYSTEMS

Stefano Pampanin
Department of Structural Mechanics
University of Pavia, Italy

Minehiro Nishiyama
Global Environment Engineering
Kyoto University, Japan

Keywords: Precast/prestressed buildings, analytical modelling, section analysis, unbonded tendons, strain incompatibility

Recent developments in the research of precast/prestressed concrete structures for seismic areas have resulted in the experimental validation of different innovative typologies of ductile connections for moment resisting frames or wall systems, either in accordance or alternative (U.S. PRESSS program, [1]) to the "emulation of cast-in-place concrete" approach, typically required by major current design codes. As a result, a wide range of alternative arrangements for connections of precast structural members is available, in the form of a continuous set of solutions from monolithic to precast jointed connections (Fig. 1).

Significant differences in the behavior at both local and global level are expected, depending on the adopted solutions for the longitudinal reinforcement (prestressed, post-tensioned, mild steel or combination of the above), on the characteristics of bond conditions (from fully bonded to fully unbonded) as well as on other structural details in the anchorage solutions (mechanical, lap splice, end-hooks).

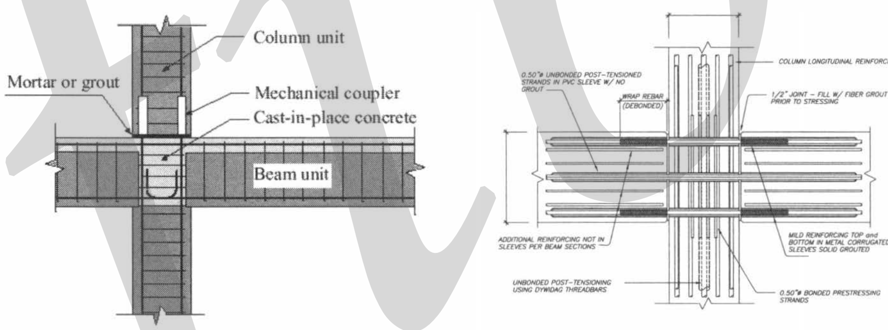

a) emulative approach

b) jointed system

Fig. 1- Alternative arrangements of precast beam-column connection according to a) emulation approach b) jointed system

In this contribution, an overview of alternative analytical approaches, at different levels of complexity, to model the seismic behaviour of different precast/prestressed connections/systems is provided. Particular attention is given to simplified methods, based on section analysis approach, which may represent viable tools for reliable prediction of the response of subassemblies and whole frame or wall systems (Fig.2).

A procedure for the definition of the monotonic moment-rotation curve for connections with unbonded reinforcements which violate strain compatibility between steel and concrete is presented [2]. Based on a member compatibility concept, the method relies on an analogy with equivalent cast-in-place solutions, named "monolithic-beam-analogy". The cyclic behaviour can ultimately be defined as an adequate combination ([2], [3]) of self-centering or energy dissipation contributions (hybrid system), modelled with rotational springs in parallel with appropriate hysteresis properties (Fig. 3).

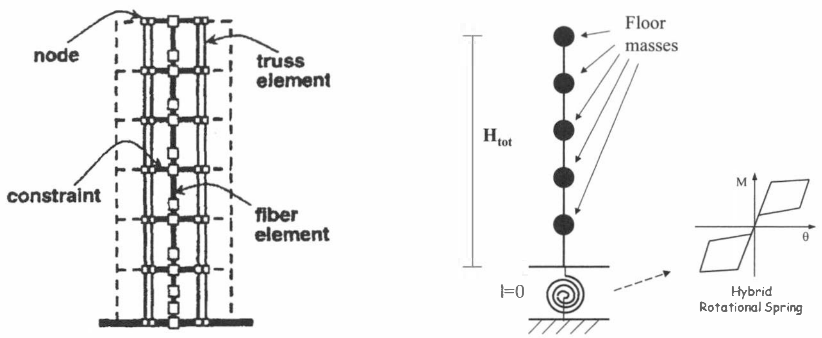

Fig. 2- Alternative modelling approaches for jointed wall system:
a) fiber model b) concentrated plasticity model

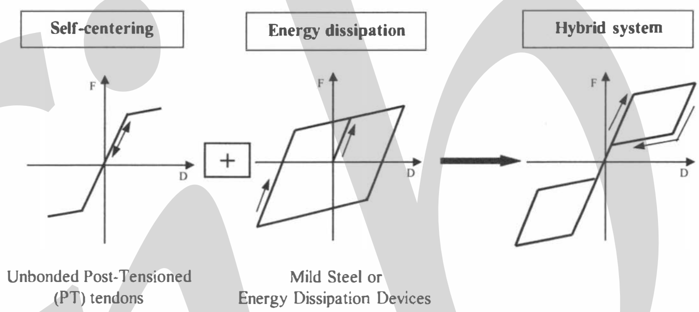

Fig. 3- Combination of self-centering and energy dissipation contributions in a hybrid hysteresis rule

The proposed simplified procedure, applicable to the general case of a precast hybrid system, represents a viable tool to model, according to a concentrated plasticity model, alternative to a refined fiber model, the seismic behaviour of general precast/prestressed systems, being the inelastic demand concentrated at the critical section and correctly described by rotational spring with appropriate hysteresis characteristics (Fig.2 right side). The section analysis approach is presented referring to the mechanism of a general hybrid beam-column connection. In conclusion, immediate extensions when modelling jointed wall system with or without additional energy dissipation devices are discussed.

REFERENCES

[1] Priestley, M.J.N., Sritharan, S., Conley, J.R. and Pampanin, S.: Preliminary results and conclusions from the PRESSS five-story precast concrete test-building, PCI Journal, 44(6), 42-67, 1999

[2] Thompson, K.J. and Park, R. : Seismic response of partially prestressed concrete. Journal of Structural Division, ST8, pp. 1755-1775, 1980

[3] Pampanin, S., Priestley, M.J.N, Sritharan, S.: Analytical modelling of the seismic behaviour of precast concrete frames designed with ductile connections. Journal of Earthquake Engineering (JEE), Imperial College Press, Vol. 5, No.3, pp.329-367, 2001

A MODEL FOR STRESS-STRAIN RELATION OF PRESTRESSING STEELS UNDER CYCLIC LOAD

Masashi HIRAO
Neturen Co. Ltd.
JAPAN

Tadashi NAKATSUKA
Assoc. Prof., Osaka Univ.,
Dr.Eng., JAPAN

Shigeru MIZOGUCHI
Neturen Co. Ltd.
JAPAN

Keywords: Stress-strain relation, Prestressing steel, Hysteresis curve, Menegotto-Pinto model, Random cyclic load

1. INTRODUCTION

Stress-strain relations of prestressing steels under cyclic loading are essential information to predict load-deformation characteristics of prestressed concrete flexural members, along with the ones for reinforcing bars. For ordinary reinforcing bars, several models are have been proposed, such as Ramberg-Osgood model which expresses strain in terms of stress. In contrast, there are few papers and models for stress-strain relations for prestressing steels under various types of cyclic loading.

This paper describes the cyclic stress-strain models for prestressing steels, that is, Menegotto-Pinto model[1,2] which has easier applicability because it gives stress as a function of strain.

2. OUTLINE OF EXPERIMENT

As listed in Table 1, the experimental variables adopted in the tests were types of PC steels and loading hysteresis. Specimens consisted of four types, specimen (1) for deriving the proposed model, specimens (2) to (4) for examining the general applicability of the proposed model to all PC steels.
Eight types of loading hysteresis, including monotonous tension and monotonous compression, were used as shown in Fig. 1. Hysteresis types 1 and 2 were monotonous loading, 3 to 6 were cyclic loading, and type 7 simulated pseudo-random loading to examine the applicability of the model over the range from regular cyclic loading to wide-range.

Table 1 Outlines of Specimens

Specimen	Purpose of Experiment	Manufacturing Method	Size Strength	Hysteresis Type
(1)	Hysteresis model consuruction	Induction heating quenched and tempered	ϕ36 mm C1	1~7
(2)	Applicability to PC bar	Stretching and Blueing	ϕ32 mm B2	1~6
(3)	Applicability to PC strand wires	Patenting, cold drawn and buleing	12.7mm B	1'
(4)	Applicability to random loading	Induction heating quenched and tempered	ϕ23 mm B1	1,2,6,7

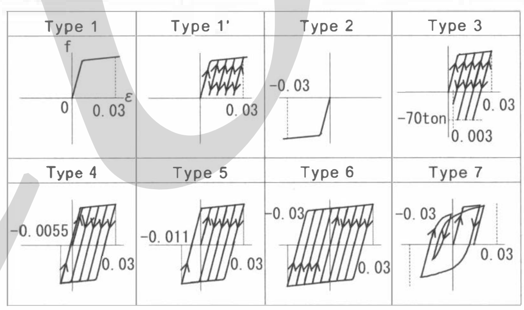

Fig. 1 Schematic Diagram of Loading Hysteresis

3. OUTLINE OF HYSTERESIS MODEL

An outline of the hysteresis model based on the Menegotto-Pinto expression is illustrated in Fig. 4. The following two points are basic to this model: (1) an envelope for the cyclic stress-strain curves, and (2) a half-cycle hysteresis curve starting from the loading reverse, expressed by Eq. (1) with the coefficient R determining the shape of the hysteresis curve.

$$f_s = f_0 + (\varepsilon_s - \varepsilon_0)\, E_m \,(Q + (1-Q) / (1 + |\, E_m (\varepsilon_s - \varepsilon_0) / (f_{ch} - f_0)\,|^{R})^{1/R}) \qquad (1)$$

From the examination of the test results, following rules were derived.

1. Tangent modulus at the half-cycle starting point (E_m) and ultimate-range asymptote of the cyclic stress-strain curve are assumed to be equal to those of the monotonous stress-strain curve.
2. The coefficient R, for example, is given for following cases as shown below.
   In the case that the strain at the previous half-cycle starting point (ε_{p0}, f_{p0}) is greater than or equal to any earlier strain in the same loading direction.
   R = 10; when ε_{pl} (%) ≤ 0.2, R = 5; when $0.2 < \varepsilon_{pl}$ (%) ≤ 0.3
   R is determined from regression formula shown in Fig.3 ; when $0.3 < \varepsilon_{pl}$ (%) (≤ 3.0)

Where, $\varepsilon_{pl} = |\, (\varepsilon_0 - \varepsilon_{p0}) - (f_0 - f_{p0}) / E \,|$ (2)

ε_{pl} (> 0): plastic strain developed in the previous half cycle

ε_{p0}, f_{p0}: strain and stress at the starting point of the previous half cycle

3. For PC steel enhanced in strength by stretching and blueing, ε_{pl} should be evaluated by adding virtual plastic strain $\overline{\varepsilon}_{st}$ (=1.0%) to ε_{pl}.

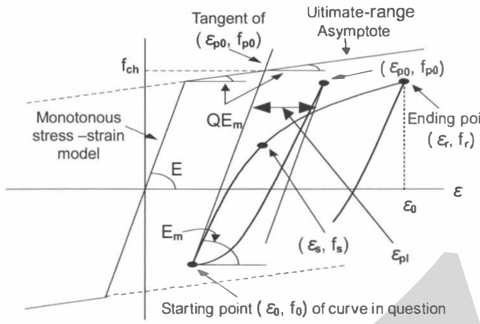

Fig. 2 Schematic illustration of Menegotto-Pinto Model

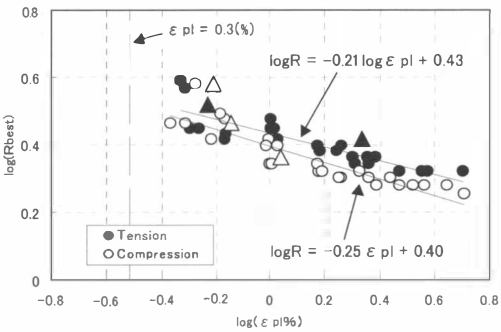

Fig.3 Relationship between R and ε_{pl}

4. SUMMARY

The main results of the present study are summarized below.

1) The characteristics and coefficients required for a Menegotto-Pinto expression-based model were formulated from the results of the experiment with induction heating quenched and tempered PC steel bars.

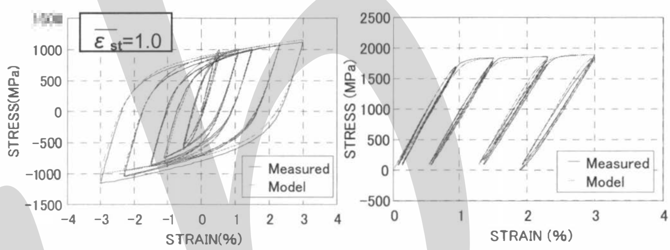

(a) Specimen (2) (b) Specimen (3)

Fig. 4 Applicability of Model to Experimental Results

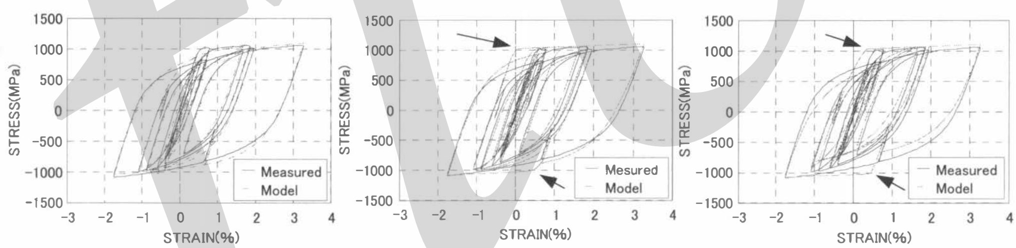

(a) Proposed Model (b) Nishiyama Model (c) Ciampi Model

Fig. 5 Applicability of Proposed Model and Existing Model

2) The hysteresis model proposed in 1) can be satisfactorily applied to PC strand wires, PC steel bars subjected to stretching and blueing and PC steel bars that are identical in manufacturing method to, but different in diameter and strength from, those used in 1).

3) The present model is more highly applicable to the results of the experiment than existing models based on the Menegotto-Pinto expression.

5. REFERENCES

[1] J.F.Stanton and H.D.McNiven, The development of a mathematical model to predict the flexural response of reinforced concrete beams to cyclic loadings, using system identification, Report No.79-02, Earthquake Engineering Reseach Center, Jan. 1979

[2] Hirao M, Nakatsuka T, Mizoguchi S, A Model for Stress-Strain Relation of Prestressing Steels under Cyclic Load, Journal of Structural and Construction Engineering, AIJ, No.550, pp.7-14, 2001.12 (in Japanese)

INFLUENCE OF LARGE ECCENTRIC EXTERNAL TENDONS ON SHEAR BEHAVIOR OF PRESTRESSED CONCRETE BEAMS

Eakarat Witchukreangkrai, Hiroshi Mutsuyoshi
Department of Civil and Environmental Engineering, Saitama University, JAPAN

Thiru Aravinthan
DPS Bridge Works Co., Ltd., JAPAN

Muneki Watanabe
Mitsui Construction Co., Ltd., JAPAN

Keywords: prestressed beams, shear capacity, external prestressing, large eccentricity

1 INTRODUCTION

The concept of external prestressing with large eccentric external tendons has been recently developed for the construction of an innovative pedestrian bridge structure [1]. In this type of structure, external tendons are placed at the level below or above the main girder by means of intermediate steel-strut deviators. To adopt this concept for a real bridge structure, however, an understanding of the shear behavior of such beams becomes necessary. The main objective of this study is to investigate the effect of tendon configuration–tendon area, tendon eccentricity and effective prestressing force–on the ultimate shear strength of beams prestressed with large eccentric external tendons by conducting a parametric evaluation based on a nonlinear finite element approach.

2 ANALYTICAL METHODOLOGY

A nonlinear finite element approach (WCOMD Ver.5 [2]) was used to predict the shear behavior of externally PC beams with large eccentricity. The concrete beam was modeled by using the 8-node RC plate element, which is based on the smeared-crack concept. The external tendon and steel-strut deviator were modeled by using truss element. The applicability of the numerical program was verified by comparing the analytical predictions with test data of shear behavior of PC beams having large eccentric external tendons [3]. A reasonable agreement with the test data is obtained, implying that the numerical program is capable of predicting the shear behavior of a concrete beam prestressed with large eccentric external tendons. Based on the analytical model as shown in Fig. 1, the amount of force in external tendon (F_{ps}) can be calculated as follows.

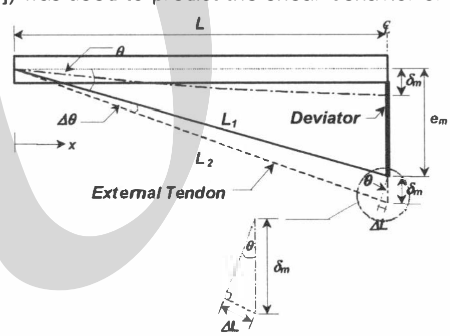

Fig. 1 Force increase in external tendon

$$F_{ps} = F_{pe} + \Delta F_{ps} = F_{pe} + E_{ps} A_{ps} \cos^2\theta \frac{\delta_m e_m}{L^2} \tag{1}$$

3 PARAMETRIC EVALUATION

Parameters that influence the ultimate force in external tendon, which consequently affect the shear capacity of the beam, were investigated by conducting a parametric study. These include tendon eccentricity (e_m), tendon area (A_{ps}), magnitude of effective prestressing force (F_{pe}), and ratio of nonprestressed reinforcement (p_w). The ranges of each variable are summarized in Table 1. The

Table 1 Variables used in parametric study

No.	Parameter	Range of values	No. of cases
1	Tendon depth ratio, d_p/h	1.33, 2.17, 3.00	3
2	Prestressing steel ratio, A_{ps}/bh (%)	0.09, 0.15, 0.23	3
3	Effective concrete stress, F_{pe}/A_c (MPa)	0.17, 0.47, 0.83	3
4	Reinforcing steel ratio, A_s/bd_s (%)	2.5, 3.0, 3.5	3

results of parametric study were discussed in terms of the relative shear strength ($V_u/V_{u,RC}$), which is defined as the ratio of the ultimate shear capacity of a PC beam with external tendon to that of an identical RC beam. In other words, this parameter indicates the magnitude of shear capacity contributed by the presence of large eccentric external tendon

According to the analytical results in Fig. 2, for a particular value of tendon eccentricity, the relative shear strength decreases with the main reinforcement ratio. This means that the contribution of external tendon to the shear capacity tends to decrease as the amount of main reinforcement becomes larger. The reason may be attributed to the fact that, in beam having high ratio of main reinforcement, the failure mode is likely to be non-ductile, in which small deformation occurs at ultimate. This causes a small increase in external tendon force and a consequently reduction in shear strength. The effects of tendon area and effective prestressing force on the relative shear strength are very similar to that of tendon eccentricity.

The influence of reinforcing steel ratio on shear capacity of PC beams with external tendon is illustrated in Fig. 3. It can be seen that the predicted values of both flexural and shear strength increase with the amount of main reinforcement, in which the predicted flexural strength shows a higher rate of increase than that of the shear strength. For the value of p_w less than 2.5%, the calculated shear strength of beam with F_{pe} of 25 kN is slightly higher than that with lower F_{pe} (10 kN). From Fig. 3, the values of reinforcing steel ratio ($p_{w,cr}$) that yield the same theoretical flexural and shear capacity is higher in beam with higher F_{pe}. This clearly indicates the influence of F_{pe} on preventing a shear failure of a PC beam.

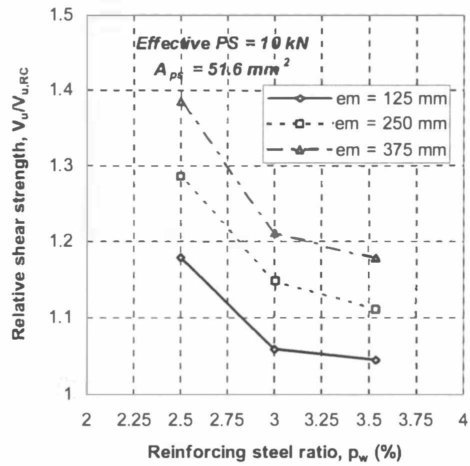

Fig. 2 Effect of tendon eccentricity

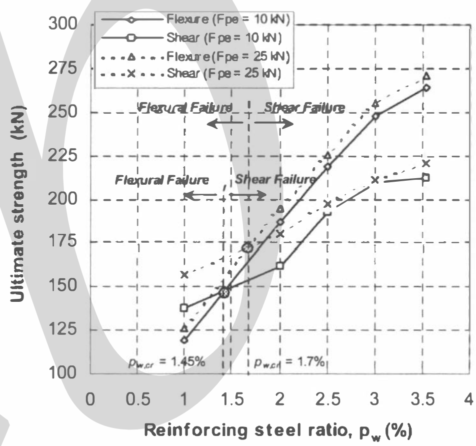

Fig. 3 Effect of reinforcing steel ratio

4 CONCLUSIONS

Based on the findings of this study, it can be concluded that the tendon configuration, in terms of tendon eccentricity, tendon area, and effective prestressing force, appears to have a significant effect on the shear strength of PC beams with large eccentric external tendon. This is because the increase in tendon force is directly related to these parameters. The larger the value of tendon eccentricity, tendon area and effective prestressing force, the higher is the ultimate shear capacity. However, in beam with high reinforcing steel ratio (p_w > 3%), the influence of large eccentric external tendon on shear carrying capacity was found to be insignificant. This may be attributed to the fact that the failure mode of such beams is likely to be non-ductile, in which small deformations occur at ultimate. This results in a small increase in external tendon force and a consequently insignificant contribution to the shear capacity from large eccentric external tendon.

REFERENCES

[1] Mutsuyoshi, H. et al.: New PC Truss Bridge Using External Tendons with Large Eccentricity. 16th IABSE Congress Report, Lucerne, pp. 124-125, Sep., 2000

[2] Okamura, H. and Maekawa, K.: Nonlinear Analysis and Constitutive Models of Reinforced Concrete. Gihodo Press, Tokyo, 1991

[3] Witchukreangkrai, E. et al.: Effect of Tendon Configuration on Shear Strength of Externally PC Beams with Large Eccentricity. Proceedings of the Japan Concrete Institute, pp. 667-672, Vol.23, No. 3, 2001

PC MEMBERS UNDER UNIAXIAL CYCLIC LOAD; EXPERIMENT AND ANALYSIS

Mohammadreza Salamy
Yamanashi University,
JAPAN

Tamio Yoshioka
Oriental Construction Co.
JAPAN

Keywords: Pre-stressed concrete, uniaxial, cyclic load, residual cracks, bond effect

1 INTRODUCTION

The objective of this study is to evaluate pre-stressed concrete structures subjected to direct cyclic tension. The experimental results of this study were first to investigate occurrence of the residual cracks after severe earthquake in pre-stressed concrete water tanks. Second aim of the experimental as well as the work was to examine the influence of the bond between PC tendons and surrounding concrete. The experiment consists of two sets of specimens called A series, B series totally 7 specimens with bonded and un-bonded tendons (RC specimens A1 and B1 along with five PC specimens A2, A3, A4, B3 and B4). Bond is set to be perfect for smeared reinforcements and bar reinforcements are fixed between nodes and embedded within finite elements. Influences of pre-stressing tendon as well as reinforcement ratio variation in the specimen's response in terms of unloading-reloading inclination is also examined and presented.

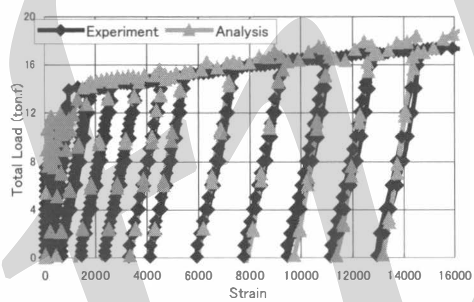

Fig.1 RC Specimen A1 under cyclic load

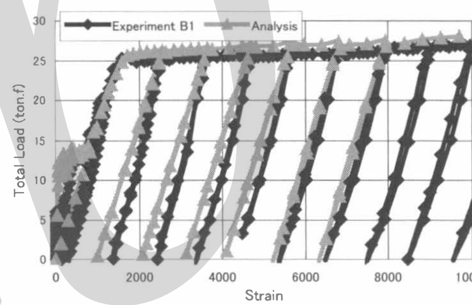

Fig.2 RC Specimen B1 under cyclic load

2 EXPERIMENTAL AND ANALYTICAL RESULTS

Results are presented in **Fig.1** to **7** briefly. Based on the experimental and analytical results of this study, the following conclusions are drawn:

1. Monotonic and Cyclic load

Comparison has been made with the envelop of cyclic response, where in some cases, analytical results are in excellent agreement with experiment particularly in RC specimens and A3 but in some other cases (A2, A4, B3 and B4), analytical responses show higher load capacity than those observed in experiment. Apparently, cyclic responses of the over-mentioned specimens are higher. In case of cyclic behavior, two parts of loading including unloading and reloading branches can be categorized due to the descending and ascending inclination and also histeresis loops in specimen response. Both

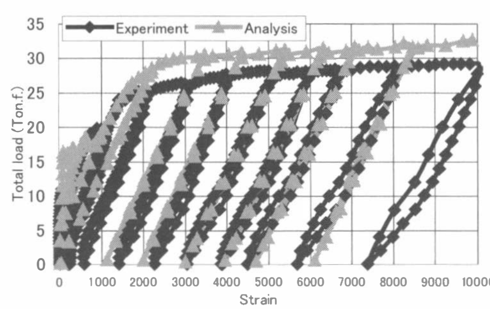

Fig.3 PC Specimen A2 under cyclic load

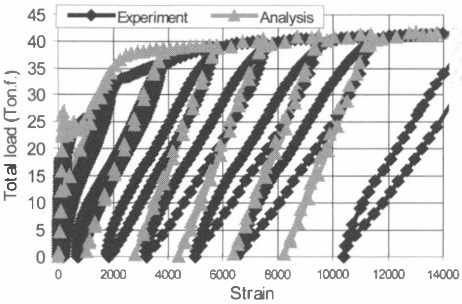

Fig.4 PC Specimen A3 under cyclic load

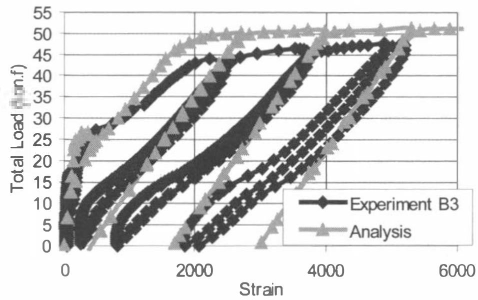

Fig.5 PC Specimen B3 under cyclic load

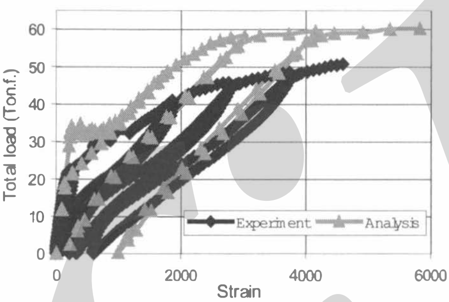

Fig.6 PC Specimen A4 under cyclic load

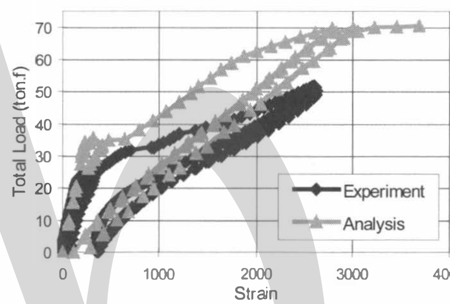

Fig.7 PC Specimen B4 under cyclic load

of the mentioned behaviors are partly relevant to constitutive model of concrete in tension and crack opening expression of the model. In analyses, histeresis loops are smaller than those observed in the experiment which manifest lack of the model in bond deterioration simulation. Next trial is to examine specimens without bond between concrete and PC tendon analytically and experimentally.

2. Loading and unloading inclination

Loading process contains both loading and unloading branches according to the experiment load history. Since inclination of descending and ascending branches are due to the structure rigidity, relevant parameters should be considered in detail. As for RC specimens, the results show agree well with experiment while in PC specimens, obtained behavior of the structures in analyses are stiffer than those of experiments. In each series of specimens, amount of reinforcing steel is kept constant but amount of pre-stressing tendons vary from zero to a maximum in A4 and B4. Based on analytical observation, the greater tendon yields the stiffer behavior. A possible reason for this problem out to be stated here is the effect of bond between tendon and concrete through grouting material. In other words, perfect bond is assumed here therefore no sliding as well as bond deterioration, which have considerable effects specially in cyclic response of RC and PC structures, can be detected in the analysis. In **Fig.8** summary of the loading-reloading inclination of last cycles (based on analysis) is presented.

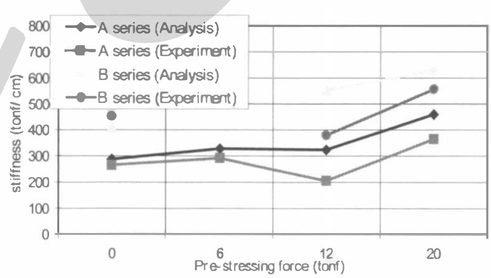

Fig.8 Last cycles Unloading-reloding inclination

REFERENCES

[1] ATENA Program Documentation, : Vladimir Cervenka, CERVENKA CONSULTING, Prague 2000

[2] Gopalaratnam, V.S. and Shah, S.P. : Softening response of plain concrete in direct tension. J. ACI, Proceeding V.82, No.3, pp.310-323, May-June 1985

FINITE ELEMENT ANALYSIS OF REINFORCED CONCRETE SHEAR WALLS OF CRANK TYPE UNDER CYCLIC LOADING

Makoto Ohya
Matsue National College of Tech.
JAPAN

Shiro Kato Shunsuke Shimaoka
Toyohashi University of Tech.
JAPAN

Makoto Takayama
Kanazawa Institute of Tech.
JAPAN

Keywords: RC shear wall, lattice model, crank, cyclic loading, reinforcing ratio

1. INTRODUCTION

A system of reinforced concrete (RC) shear walls is well known as one of the most significant elements of architectural structures for resisting against earthquakes. The walls are thin and are subjected to cyclic loading such as earthquake loadings. Crank typed shear walls, which has a crank in its plane, is often used as partitioning walls in buildings of apartment house and hotels. Despite of much adoption, there have been few investigations on the crank typed shear walls [1].

The present paper aims, first, at a finite element analysis of crank typed shear walls under cyclic loading. The shear walls analyzed in the paper are the ones to which experiments were performed previously to see how the behavior for the crank and the ratio of reinforcing steel bars by the fourth author using crank typed shear walls [1]. The constitutive equations in the finite element are based on Ring Typed-Lattice Model [2], which was applied also in the previous researches to an analysis of RC structures subjected to cyclic loading. Second, from the comparison between the experiments and analyses, this study aims to show the extensive applicability of the constitutive equations based on Lattice Model analysis, and finally, to investigate in detail the structural behavior RC shear walls with a crank and the effect of the ratio of reinforcing steel bars subjected to cyclic horizontal loading.

2. NUMERICAL ANALYSIS

In the present numerical analysis of crank typed shear walls, an isoparametric degenerated shell element is applied with an additional use of the nine-node Heterosis element. The selective integration rule is used. The geometric and material nonlinearities are taken into account. A layered approach is used to describe the material nonlinearities through thickness. The displacement incremental scheme is used. Five specimens, designated CE-0, CE-1/2, CE-1/4, CE/30S and CE/20S, are analyzed. The numerical model of CE-1/2 is shown in Fig.1. And, Fig.2 shows the load Q(kN) - displacement δ (mm) relations for CE-1/2. The solid lines denote the numerical responses, and the solid lines with filled diamond marks denote the experimental ones. The ratio of experimental to numerical results of the ultimate load Q_{ult} falls on 0.96 to 1.12, and the ratio of those for R=1/100 ranges from 0.83 to 1.06. From the comparison between experimental and numerical results, fine agreements are obtained with

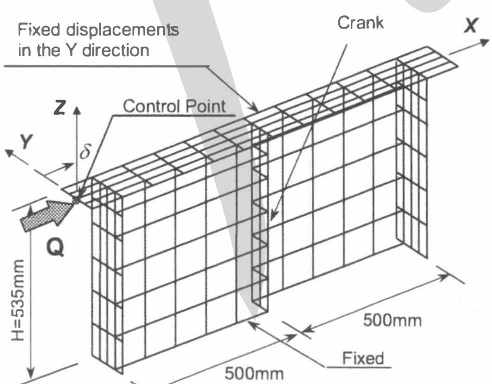

Fig.1 Finite Element Mesh for CE-1/2(CE/40S), CE/30S, CE/20S

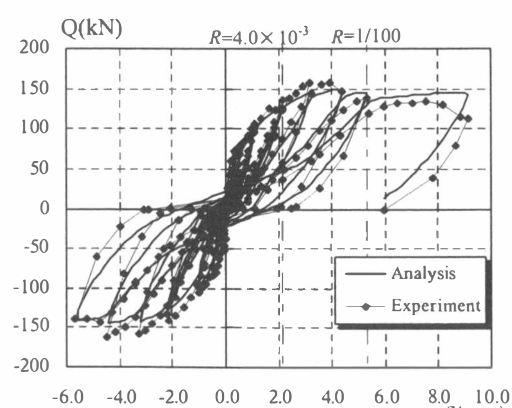

Fig.2 Load-Displacement Relations for CE-1/2

respect to both of the ultimate loads and area of hysteresis loops. The ductile deformation and low carrying capacity for crank typed shear wall are found, since a relatively large sway is produced for the crank typed walls. Judging globally, not only the ultimate load but also the total behavior of deformation of the shear walls under cyclic loading may be simulated based on Lattice Model.

3. ULTIMATE SHEAR STRENGTH WITH A CRANK

In order to examine the effect of reinforcing ratio on shear strength, the non-dimensionalized quantities are adopted as follows.

$$\chi = \frac{v_u}{f_c'} = \frac{Q_{ult}}{A_w f_c'}, \quad \omega = \frac{\rho_s f_{sy}}{f_c'} \tag{1}$$

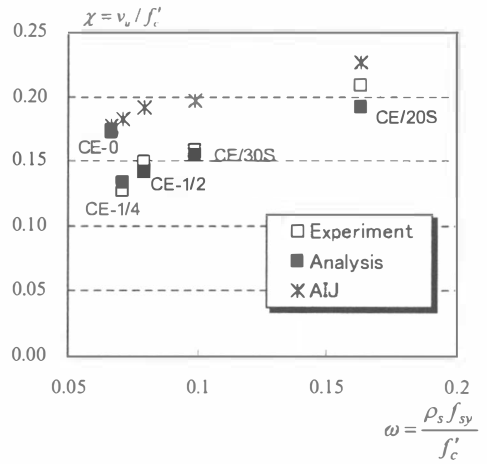

Fig.3 Ultimate Shear Strength with AIJ Strength

where Q_{ult}, v_u, A_w, f_c', ρ_s and f_{sy} are respectively the ultimate load, ultimate shear strength, cross section of the horizontal wall section, compressive strength as of cylinder test, reinforcing ratio in the horizontal direction of the wall part and yield strength of reinforcing steel bar.

The non-dimensionalized ultimate shear strengths for both the experiments and analyses are shown in Fig.3 with the predicted ultimate shear strength of ordinary shear wall according to AIJ Code [3]. In Fig.3, the empty squares, solid squares and asterisks are the results of experiment, analysis and AIJ Code, respectively. The ultimate shear strength for CE-0 is similar than the predicted ultimate shear strength according to AIJ Code. It is found that the ultimate shear strength with a crank, of which position is located at its center or a quarter, tends to decrease due to the presence of the crank approximately by the order of 20% and 25% than those without cranks. Comparison among CE-1/2(CE/40S), CE/30S and CE/20S reveals the effects of reinforcements; the ultimate shear strength increases with increase in proportion to the reinforcement in both cases of the experiments and analyses. The ultimate shear strength with a crank decreases at most by the order of 30% than the predicted ultimate shear strength determined according to AIJ Code.

4. CONCLUSIONS

In this paper, the cyclic behavior of the shear walls with and without crank is examined both numerically and experimentally. The conclusions are drawn as follows.

1. The validity and applicability of the constitutive equations based on the Lattice Model for RC shear walls with and without crank subjected to cyclic loading is confirmed.
2. In the present numerical analysis, the ductile deformation is found for the crank type shear walls as depicted in the experiment, however, with slightly smaller shear strength than ordinary shear walls.
3. The ultimate shear strength with a crank is smaller by the order of 30% than the predicted ultimate shear strength according to AIJ Code.

REFERENCES

[1] Takayama, M. and Fujita, K. : Elasto-plastic behavior of crank type reinforced concrete shear walls, Proc. of 6th Asian Pacific Conference on Shell and Spatial Structures, pp.485-492, 2000
[2] Kato, S., Ohya, M., Maeda, S. and Yoshino, F. : The formulation of constitutive equation for concrete based on the ring type-latticed model and its application to finite element analysis of reinforced concrete shells, Journal of Structural Engineering., Vol.44B, pp.441-454, 1998 (in Japanese)
[3] AIJ : Design Guidelines for Earthquake Resistant Reinforced Concrete Buildings Based on Inelastic Displacement Concept, 1999 (in Japanese)

COLLAPSE AND DUCTILITY OF HIGH-STRENGTH FIBER-REINFORCED STRUCTURAL ELEMENTS

A. Grimaldi
Università di Roma "Tor Vergata"
Roma, ITALY

Z. Rinaldi
Università di Cassino
Cassino (FR), ITALY

Keywords: high strength fiber reinforced concrete, local ductility, ultimate behaviour.

1 INTRODUCTION

The definition and application of new materials, suitable to grant the best performances of new or existing constructions, is nowadays considered of topical interest, both in the research and in technological fields.

The advantages given by steel, glass or polymeric fibers, constitute a present and widely discussed theme, as well as the study on the properties and the possibility provided by high strength, high performance and light-weight concrete. The interest about this topic, and about its economical implications, is witnessed by the recent bibliography.

The present study aims at evaluating the characteristics of structural elements made with high-strength fiber reinforced concrete.

As well known the high-strength concrete allows the development of a great compression strength (above 100 MPa), but it is characterised by a limited behaviour in tension, and by a lack of ductility. The addition of fibers could improve the structural behaviour, giving rise to a new material working in compression and tension, with good plastic capacity.

The evaluation of the structural behaviour of a high-strength (HC) or fiber reinforced high-strength (FHC) element can not neglect the fundamental aspects related to the non-linearity of the materials, to the tension stiffening effects, and to the localization of the steel strain near the cracks. In this paper the evaluation of the strength and ductility characteristics of FHC beam elements will be performed by adopting suitable models. In a first phase an analytical model is formulated, able to take account of the non-linear behaviour of the materials (concrete, steel) and to consider the presence of a slip between them. Furthermore the model allows pointing out the phenomena connected with the cracks formation and with the localization of steel strain.

In a second phase a numerical model of a cracked FHC element is studied. Particular care is devoted to the simulation of the crack formation and growth and to the slip between concrete and steel. The results obtained with the two models are compared and discussed.

2 ANALYTICAL MODEL OF THE BEAM-COLUMN ELEMENT

2.1 Analytical model

Aim of the present paper is the evaluation of the influence of the fiber addition on the inelastic behaviour of r.c. structures. This purpose is pursued by adopting the local model proposed in [2] that allows to define a relationship between resultant forces and mean deformations, taking account of the inelastic behaviour of the materials and considering the tension stiffening effects.

The analyses are performed with reference to an r.c. element with a length l equal to the crack distance, subjected to tensile load, or loaded by bending moment and axial forces. The mean strain applied at the element is the loading parameter and the structural behaviour is analysed for subsequent steps by means of equilibrium conditions, up to the failure, defined by the achievement of the ultimate strain in one of the constitutive materials.

After an initial elastic phase, the cracking in the concrete and the slip between the materials occur, with subsequent redistribution of stress and strain. The values related to a single section lose their importance and it is necessary to refer to mean values along the element. By increasing the applied strain, the steel yielding is reached firstly in the cracked section, then the plastic deformation spreads along the element up to the attainment of the ultimate condition in the concrete or in the steel.

In the whole methodology the hypothesis of perfect bond is removed and the inelastic behaviour of the materials and the presence of slip at the concrete-steel interface are taken into account.

2.2 Results

The proposed model has been used in order to evaluate the influence of the fiber addition in normal and high strength concrete. A parametric inquire has been performed by varying the geometrical and mechanical characteristics of the cracked element, and the constitutive relationship of the materials.

A typical result is reported in the following figure, where the ultimate bending moment M_u and the ductility ratio (ρ_{mu}/ρ_{my}) are plotted vs. ω_s, for normal concrete (NC), high strength concrete (HC), fiber reinforced concrete (FNC) and fiber reinforced high strength concrete (FHC).

The ultimate bending resistance always increases with the rebars increase, but a higher gradient appears for HC and FHC. The addition of fiber in NC and HC slightly affects the ultimate moment value.

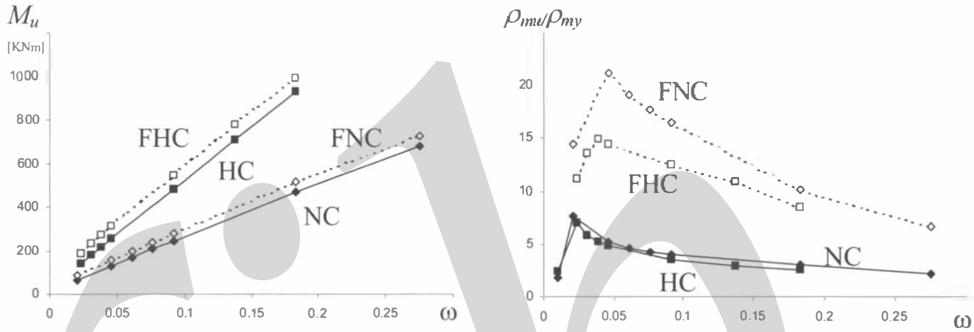

Fig. 1 a) Ultimate bending moment vs mechanical percentage; b) ductility ratio vs. mean curvature mechanical percentage.

The "ductility" curves for all the qualities of concrete show the typical peak sharing the steel failure from the concrete crisis. For the analysed geometry, no significant differences appear between NC and HC. The addition of fiber, instead, sharply modifies the ductile behaviour. The peak of the curve related to fiber reinforced concrete is shifted towards higher value of the steel percentage and the increase of the ductility ratio can reach the value of 300% for FNC respect to NC, and the value of 200% for FHC respect to HC. The differences between the ductile behaviour of FNC and HNC diminish when the steel rebars increase.

The results obtained by a numerical model validate the proposed analytical model.

REFERENCES

[1] Faisal, F. W., Ashour S.A.: Mechanical properties of High-strength fiber reinforced concrete. ACI Material Journal, Vol. 89, No. 5, Sept-Oct 1992, pp.449-455.

[2] Fib Bulletin. Bond of reinforcement in concrete – state of the art report. Fib. August 2000.

[3] Grimaldi, A., Rinaldi, Z.: Influence of the steel properties on the ductility of r.c. structures. Proc. 12WCEE World Conference on Earthquake Engineering, Auckland New Zealand, January-February 2000.

[4] Lim, T.Y., Paramasivam, P., Lee, S.L.: Bending behaviour of steel fiber concrete. ACI Structural Journal, November-Dec. 1987, pp. 524-536.

[5] Nataraja, M.C., Dhang N., Gupta A.P.: Stress-strain curves for steel fiber reinforced concrete under compression. Cement & Concrete Composite 21, Elsevier 1999, pp. 383-390.

SERVICEABILITY BEHAVIOUR OF D-REGIONS

V.I. Carbone L. Giordano G. Mancini
Department of Structural Engineering and Geotechnics
Politecnico di Torino, Turin

Keywords: strut, tie, serviceability

1 INTRODUCTION

The physical models developed for the ultimate limit state design and verification of short corbels of D regions in reinforced concrete can be rated as sufficiently well-tested and reliable from both the scientific [1] and the codification viewpoint; moreover, practising engineers can find in the literature several approaches to the identification of optimal strut-and-tie mechanisms [2] [3]. An aspect which has not yet been sufficiently cleared up, however, is the serviceability behaviour of D regions designed at the ultimate limit state, especially with regard to the control of crack formation and hence to the detailing of secondary reinforcement, i.e. the reinforcement not strictly necessary to ensure equilibrium in the ultimate configuration envisaged.

The aim of this study is to work out secondary reinforcement dimensioning criteria ensuring the opening of cracks of pre-determined width in serviceability conditions.

2 ADINA IMPLEMENTATION MODALITIES

The operational modalities of ADINA presuppose that:

- cracks are formed when concrete tensile strength f_{ct} is reached and run parallel to the principal compressive stress in concrete;
- the direction of the cracks remains the same throughout the process of crack propagation (non rotating crack);
- the evolution of crack opening will take place orthogonally to its direction;
- both normal and tangential stresses can be transferred across the cracks.

With these assumptions, the determination of the relative spacing and width of cracks can be performed by means of the Tension Chord Model. For the caracterisation of concrete behaviour, a limit state function of the material is described in the program. This function, worked out through the procedure proposed by von Grabe and Woruschka, is compatible with Sargin's law. Steel behaviour is described according to a hardening bilinear relationship. The limit state behaviour of concrete is identified by the tensile and compressive failure surfaces, of which the former is based on the control of the principal tensile stress and the latter corresponds to the proposal formulated by Kotsovos.

3 NUMERICAL ANALYSIS OF A SERIES OF WALLS WITH OPENING

Ten walls whit openings were subjected to tests at the University of Lisbon in 1995 [2]. The reinforcement of nine walls was dimensioned according to three strut-and-tie mechanisms, of which the first is based on the formation of a transverse compressive stress field, the second on the presence of transverse tensile stresses, and the third on a combination of the previous two. In the tenth wall, the reinforcement was arranged on the basis of results of a finite element elastic analysis.

Table 1 summarises the significant aspects of crack formation in serviceability conditions ($\gamma = P_u / P_k = 2$) and compares maximum crack width as determined experimentally and numerically (expressed in mm).

Table 1 Comparison between experimental and numerical values of crack width

Corbel	w_{exper}	w_{ADINA}	Corbel	w_{exper}	w_{ADINA}
MB1ee	0.210	0.222	**MB2ae**	0.400	0.460
MB1ee1	0.150	0.135	**MB3ee**	0.210	0.171
MB1aa	0.330	0.280	**MB3aa**	0.230	0.203
MB1ae	0.233	0.308	**MB4ee**	0.100	0.108

As can be seen, the experimental results are in good agreement with the corresponding numerical values.

4 NUMERICAL ANALYSIS OF A SERIES OF DEEP BEAMS

The four deep beams subjected to numerical analysis belong to a series of sixteen tested experimentally by Foster and Gilbert [3]; two were subjected to a single concentrated load and two to concentrated load pairs.

The experimental and numerical failure loads are given, and compared, in Table 2. It can be concluded that the procedure described above makes it possible to approximate the experimental results quite closely. On the other hand, experimental vs. numerical crack width results could not be compared, since the experimental values had not been documented.

Table 2 Comparison between experimental and numerical failure loads

Corbel	$P_{u,\,exper}$ (kN)	$P_{u,\,ADINA}$ (kN)	Error (%)	Failure mode
B2.0-1	1590	1516.7	4.6	A_s yielding
B2.0A-4	1900	1885.6	0.8	A_s yielding
B3.0-1	1020	1033.9	1.4	A_s yielding
B3.0A-4	1550	1521.5	1.8	A_s yielding

5 NUMERICAL EVALUATION OF CRACK FORMATION AS A FUNCTION OF THE PROVIDED SECONDARY REINFORCEMENT

Now that the proposed procedure has been sufficiently validated, we can proceed with the assessment of the quantity of secondary reinforcement needed to ensure the opening of pre-determined cracks; the procedure has been applied to the series of deep beams described above, this type of structure being used very widely. The procedure consists of the following steps:

- consider different values of the secondary reinforcement, the main one remaining unchanged, so as to obtain average crack widths of 0.1 / 0.2 / 0.3 mm, and not controlled one;
- determine the ultimate load P_u corresponding to the selection of the secondary reinforcement, which affects the overall response and define the serviceability load as $P_k = P_u / 2$ for each condition.

The geometric percentages of the horizontal and vertical reinforcement, ρ_h and ρ_v , are shown in fig. 1; as can be clearly seen, to restrict the opening to cracks to 0.3 mm it must be $\rho_h \cong 0.0025$, $\rho_v \cong 0.0035$

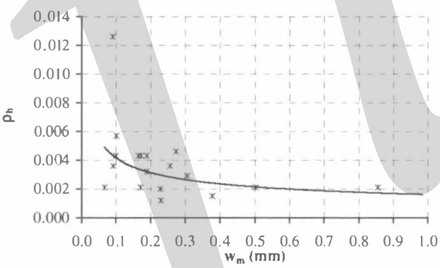

(a)

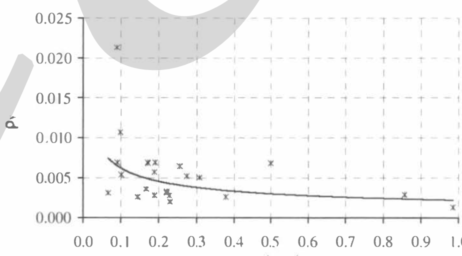

(b)

Fig 1 Horizontal (a) and vertical (b) reinforcement geometric percentages

REFERENCES

(1) Schlaich J., Schäfer K., Jennewein, M., "Toward a Consistent Design of Reinforced Concrete Structures", *PCI Journal*, v. 32, no. 3, May-June 1987, pp. 74-150

(2) Filho J.B., "*Dimensionamento e Comportamento do Betao Estrutural em Zonas com Descontinuidades*", Tese submetida para a obtencao do grau de Doctor em Engegneria Civil, Universidade Tecnica de Lisbona, May 1995

(3) Foster S., Gilbert R.I., "Experimental Studies on High-Strength Concrete Deep Beams", *ACI Structural Journal*, v. 95, no. 4, July-August, 1998

SAFETY VERIFICATION IN NON-LINEAR ANALYSES THE PROBLEM WITH 2ND ORDER EFFECTS EVALUATION

João Vinagre
Director of Escola Superior de Tecnologia do Barreiro of Polytechnic Institute of Setúbal
Assistant Professor, IST, Technical University of Lisbon, PORTUGAL

Keywords: 2nd order effects, non-linear analysis, safety formats

1 INTRODUCTION

The paper discusses the various methodologies that are usually applied for the safety verification of reinforced concrete structures, when adopting non-linear analyses and is based on the studies performed by the author [1]. This verification is linked to securing a minimum collapse probability of structures, which may be calculated in an explicit way or performed indirectly, by using partial safety coefficients.

The different techniques usually adopted are briefly explained. The difficulties involved in adopting safety coefficients for actions are discussed and the major objectives of their application are defined. The associated difficulties are illustrated and the way to avoid them is discussed.

In respect to the application of safety coefficients to concrete and steel, the major methodologies are presented: global safety coefficients applied to the cross sections' resistance or distinct partial safety coefficients for both materials. The advantages and disadvantages of both models are referred to and an illustration is given based on simple examples. The rules of the most important European codes are also referred, as they reflect the major current opinions on this subject.

2 SAFETY FORMATS

In the modern structural reliability theory, it is accepted that no absolute safety guarantee can be achieved for any structure, some collapse risk having to be accepted. The main objective of structural design thus consists in assuring, within an acceptable level of probability, that the structure (total or partially) maintains its capacity to correctly function and resist when subject to all actions.

Structural safety can be operated at three levels that differ from each other according to the kind of calculations performed and the accepted approximations. Level 3 constitutes an exact or regulating level, where the collapse probability is explicitly calculated. At level 2, collapse probability is calculated either by means of approximate methods or indirectly, by changing the multidimensional problem into several unidimensional ones. Finally, at Level 1, actions and resistances are represented by characteristic values and are compared by expressions that include partial safety coefficients. The main reason for adopting partial safety coefficients as opposed to global safety factors is that only those can lead to reasonable and consistent reliability standards. The safety format usually used for reinforced concrete structures is included in this category. The safety verification models involve the comparison of fairly reduced values of the capacity resistance of the elements and actions combinations values, obtained through combinations rules that include the characteristic action values.

3 PARTIAL SAFETY COEFFICIENT FOR ACTIONS

In order to design a structure for a particular set of actions with different types it is necessary to establish rules for actions combination. The study of structural safety for action combinations is very important from a practical point of view because of the significant savings obtained if the right coefficients are chosen. Simplified rules enabling the combinations of actions are derived from the results obtained. The combinations of actions are obtained through the characteristic values of all different actions that act on the structure. Although the application of safety coefficients to actions raises some particular problems, the main questions concern the introduction of coefficients that reduce the material's properties, in particular as regards to concrete.

4 MATERIALS SAFETY COEFFICIENTS

After presenting the constitutive laws usually adopted for steel and concrete, safety formats based on global or partial coefficients are analysed. From the analysis of a simple problem (constant cross-section cantilever), the difficulties associated to load path dependency in physically non-linear analysis when using global coefficients were referred. The incoherence of the same safety format in non-linear geometrical problems is shown.

Another way of applying the safety format in a non-linear analysis of reinforced concrete structures is to adopt partial safety coefficients applied directly to the materials' stress relationships. Taking in account that the usual design process if a physically non-linear analysis is performed using materials' design stress relationships, collapse will be achieved for a load near the one considered at design. This feature is, without any doubt, one of the major advantages of this methodology. After knowing the collapse load given by that analysis, it is possible to estimate and quantify the importance of geometrically non-linear effects from the load parameter reduction, $\Delta\Lambda$, obtained in a totally non-linear analysis (physical and geometrical). The adoption of design values for the constitutive relationships of the materials properties, for one and the same acting load level, leads to bigger deformations than those obtained with medium values, in non-linear analysis. Consequently, the resulting displacements can be overestimated. This constitutes one of its major shortcomings. It should however be referred that the over-measurement of the structural deformability will influence the results of 2nd order sensitive structures analysis. The over-measurement of structural displacements will also be associated to a structural design whose 2nd order effects are more significant than the actual ones and, therefore, to a safety design.

5 NEW PROPOSAL FOR DESIGNING WITH NON-LINEAR ANALYSES

Being generalized the use of non-linear analysis in design, almost all codes, enable and specify its use for design of concrete structures. Unfortunately, although the principles for non-linear analysis are set, the codes do not give any orientations for designing with this powerful tool. When 2nd order effects are important, the designers have to decide how to include them in the design process and how to achieve a safety solution. Several studies developed by the author and others enabled to conclude that a consistent and simple way to design with non-linear programs and taking into account 2nd order effects can be done by executing the following steps:

1. determination of elements' elastic stresses (linear analysis);
2. section's design (quantification of reinforcement amounts needed for elastic stresses);
3. execution of a physical and geometrically non-linear analysis, till collapse, with design constitutive relationships for steel and concrete and determination of the load parameter at collapse, Λ_{NLFG};
4. redesign of all critical sections for the internal stresses obtained in 3, multiplied by $1.50/\Lambda_{NLFG}$ (assuming that the design process' objective was to achieve a load parameter of *1.50*);
5. execution of a new non-linear analysis with the obtained reinforcement.

The process described above should be repeated (steps 3 to 5) till achieving an acceptable difference between the load parameter objective (usually *1.50*) and the non-linear analysis load parameter, Λ_{NLFG} (lower than *5%*, for example). The method converges in two or three iterations, gives excellent results (the 2nd order effects will automatically be taken into account) and constitutes a coherent and complete guide for concrete structures' designers.

6 CONCLUSIONS

Different safety formats were analysed and their most important variables, as well as the uncertainties and difficulties associated to structural reliability. Of all available formats, those based on safety coefficients (level 1 formats) are well adapted to reinforced concrete structures. That is why they are usually used in non-linear analysis. The application of safety coefficients to actions and to the materials' relationships was discussed. With regard to the coefficients applied to the materials relationships, global and partial methodologies were analysed and reviewed. The major difficulties connected to their application were analysed and the conclusion was drawn that it is advisable to adopt partial safety coefficients to the materials relationships. Finally, a simple method using non-linear analyses for reinforced concrete structures' design, with important 2nd order effects, was presented. This method constitutes a complete and coherent design tool for project.

REFERENCES

[1] Vinagre, J. : Avaliação dos efeitos de 2ª ordem em edificios de betão armado. PhD Thesys, Instituto Superior Técnico, March, 1997 (in Portuguese).

[2] Castro, P. M. R. P. : *Modelos para análise da encurvadura em pórticos de betão armado*. PhD Thesys, FEUP, October, 1998, (in Portuguese).

NUMERICAL SIMULATION OF DEBONDING BEHAVIOR OF FRP SHEET STRENGTHENING RC BEAMS

Guangfeng Zhang Norimitsu Kishi Hiroshi Mikami Masato Komuro
Muroran Institute of Tech, JAPAN
Mitsui Construction, T.R.I, JAPAN
Muroran Institute of Tech, JAPAN

Keywords: RC beam, AFRP sheet, nonlinear analysis, discrete crack, peeling action

1 INTRODUCTION

In this study, in order to establish a numerical analysis method to appropriately evaluate the failure behavior of flexural strengthened RC beams with FRPS, three-dimensional elastic-plastic Finite Element (FE) analyses were carried out using commercial FE package DIANA (DIANA7.2). Furthermore, experimental results obtained from four-points bending test and analytical results by means of Multi-Section Method (MSM) were used to confirm an applicability of the FE analysis method.

2 NONLINEAR FE ANALYSES

Two failure type of flexural strengthened RC beams with Aramid FRPS (AFRPS) were used in this research. One is Debonding Failure type (hereafter, DF type), the other is Flexural Compressive Failure type (hereafter, FCF type) [1]. Considering the geometrical and structural symmetry of the RC beam, only a quarter of it was three-dimensionally modeled. Details of the two beams and the FE model of the DF beam are shown in Fig. 1. In these models, concrete was modeled using 8-nodes solid elements and/or 6-nodes solid elements along the diagonal cracks. Main rebar and AFRPS were also modeled by 8-nodes solid elements. Embedded reinforcement elements were used to model the upper axial rebar and stirrups. Furthermore, considering the geometrical discontinuities, opening of the cracks developed in concrete and debonding of AFRPS were modeled by discrete cracking model; slipping along the rebar was modeled by bond-slip model.

3 ANALYTICAL RESULTS

Load-midspan deflection (Load-deflection) curves of the experimental results are shown in Fig. 2 comparing with the analytical results by means of both FE and MSM. From the results of the DF beam (Fig. 2 a), it can be observed that the stiffness obtained from experimental result is reduced distinctly at point (i) and point (ii). These may be due to opening of the flexural cracks and yielding of the main rebar respectively. After the main rebar yielded, the load-deflection curve almost linearly distributes and finally dropped suddenly by AFRPS being fully debonded. The analytical results obtained from FE method is in good agreement with the experimental results up to near the ultimate stage of the experiment. On the other hand, because the MSM analysis was performed based on the hypothesis that concrete and AFRPS are under full bond condition during whole the analysis, flexural stiffness of the RC beam after the rebar yielded is higher than that of the experimental and the FE analytical results.

Comparison for the results of the FCF beam is shown in Fig. 2(b). Even though MSM is formulated

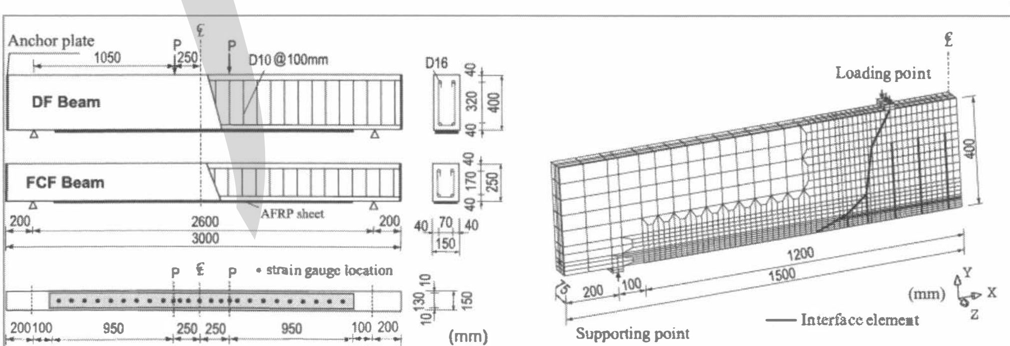

Fig. 1 Details of specimens and FE analysis model of DF beam

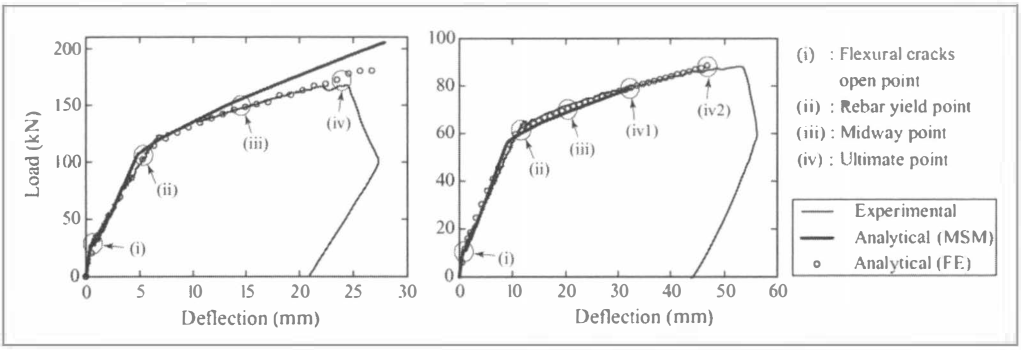

(a) DF beam (b) FCF beam

Fig. 2 Comparison of load-midspan deflection curves

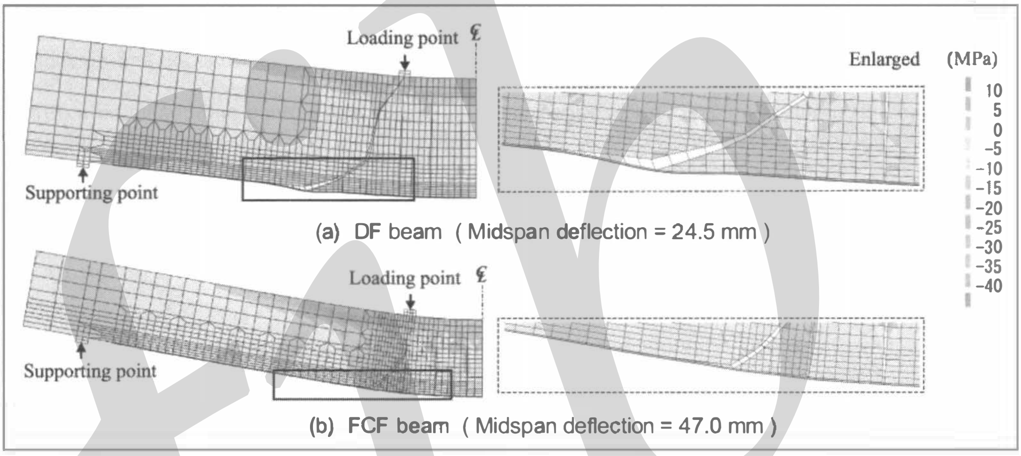

Fig. 3 Opening of discrete cracks and principal stress distributions at ultimate state in FE analysis

under the full bond condition between concrete and AFRPS, the results obtained from MSM is in a good agreement with the experimental results as well as the FE analysis results. This suggests that in case of FCF beam, AFRPS has not been debonded distinctly from concrete surface until the upper concrete near loading points reaches the ultimate state.

Figure 3 shows deformation configuration of the RC beams, opening of discrete cracks and principal stress distributions at the ultimate point for the two beams. In case of DF beam, a debonded length of AFRPS at the experimental ultimate point was estimated as about 200 mm by the FE analysis. Although whole debonding of AFRPS can not be simulated, it can be seen that the debonding behavior of AFRPS was simulated well. From the results of FCF beam shown in Fig. 3(b), it is observed from FE analysis that AFRPS has not been debonded remarkably up to ultimate point in FE analyses. These analytical results are similar to the experimental one.

4 CONCLUSIONS

Modeling main cracks, rebar slipping and AFRPS debonding from concrete with interface elements using discrete cracking model and bond-slip model, debonding behavior of AFRPS due to peeling action of concrete block formed in the lower cover concrete can be numerically analyzed by means of proposed FE analysis technique.

REFERENCES

[1] Kishi, N., Mikami, H., Matsuoka, K. G., Kurihashi, Y.: Failure behavior of flexural strengthened RC beams with AFRP sheet. *FRPRCS-5*, pp.87-95, 2001.

BOND, PRESTRESSING, CRACK OPENING AND FLEXURAL BEHAVIOR

Rezende Martins, P.C.
University of Brasilia
BRAZIL

Regis, P.A.
Federal University of Pernambuco
BRAZIL

Tavares, M.E.N.

BRAZIL

Keywords: bond, crack opening, prestressed concrete, flexural behavior.

1 INTRODUCTION

The effect of bond between concrete or cement paste and steel (strands or bars) is of fundamental interest for the description of the equilibrium state and deformability of concrete structures. In case of cracked elements this interaction becomes of prime importance and modeling of bond evolution around cracks/ joints if more than necessary for a precise description of deformations and equilibrium of the structure.

The research program focused in this paper started in the 80`s in France and continued in Brazil. The French part was developed at the CEBTP laboratory, ref. [1]. The brazilian part has been conducted by Martins and the other two authors [2], [3]. The aim of the research is to establish the influence of bond and to compare the behavior of beams prestressed by internal bonded strands and/or external unbonded strands. For this purpose an experimental program was executed in Brazil, as explained below.

2 GENERAL DESCRIPTION OF TESTS

A first series of hyperstatic beams with different ratio of extemal/internal cables and technique of construction were tested. The results of the two first beams were presented at the FIP Congress, in Amsterdam, by Martins and Regis [4].

A second series of isostatic beams was tested. They were erected by segmental method, with internal bonded tendons, intending to furnish data about bond effects on the behavior of prestressed beams. The basic parameter was the length/height ratio of the segments (from short till long ones).

3 EXPERIMENTAL PROGRAM

Figure 1 presents the data of the hyperstatic beam, prestressed by one internal bonded tendon and two external tendons, as detailed in references [2] and [4].

Data about the second series, as described and detailed in ref. [3], are summarized in figure 2. All beams were tested under similar conditions, based on a numerical analysis performed by CARPE, the computer program designed by MARTINS [1], in 1989, and improved by his team since 1994 till now.

4 CONCLUSIONS FROM TESTS

Since the main goal of tests was to provide information for the development of the theoretical model of flexural behavior of beams taking into account bond-slip interaction around open joints or cracks, the experimental program focused the stress and strain distribution in steel and concrete around the joints between segments. The main conclusions are:

a) if a segment may be considered as a short one (length/height ratio smaller than 1,4) no cracks appear inside the segment, its behavior is governed by that of joint sections, deformed sections do not remain plane and bond between steel and concrete can not be considered perfect any more all along the segment;
b) in case of long segments (l/h bigger than 1,5), segments also do not behave under the Bernoulli-Navier hypothesis along a length of 0,7 of the height from the joint section;
c) even in the case of severe bending moment gradient acting inside the segments, there is no significant changes in their behavior, which means that the hypothesis made for the model of constant bending inside short segments may remain valid also for this other case.

5 GENERAL CONCLUSIONS FOR MODEL

Three important conclusions arise from this study: (i) theoretical model presented in ref. [1] is largely confirmed by all tests and is able to explain and justify the real behavior of elements with opened cracks or joints and the divergences that appear when they are treated by classical theory; (ii) it may be foreseen a new way of modeling the equilibrium and deformation of concrete elements, under the simultaneous action of shear and bending, when cracks are inclined to the longitudinal axes of the elements; (iii) it enables researchers and professionals to evaluate accurately equilibrium, deflection and crack opening of beams, even under pathological situation.

This is the subject of the current research program undertaken by a brazilian group working simultaneously at three brazilian universities.

REFERENCES

[1] Regis, P. A. : Theoretical and experimental study of the behavior of externally prestressed beams. D.Sc. thesis, COPPE, The Federal University of Rio de Janeiro, 1997, Brazil (in portuguese)

[2] Tavares, M. E. N. : Experimental study of prestressed concrete beams – influence on bending of bond-slip interaction between steel and concrete. D.Sc. thesis, COPPE, The Federal University of Rio de Janeiro, 2001, Brazil (in portuguese)

[3] Rezende Martins, P. C., Regis, P. A. : Mixed prestressing in hyperstatic beams. In Challenges for concrete in the next millennium, FIP Congress, pp. 923-926, Amsterdam, 1998

[4] Rezende Martins, P. C., Regis, P. A. : Mixed prestressing in hyperstatic beams. In Challenges for concrete in the next millennium, FIP Congress, pp. 923-926, Amsterdam, 1998

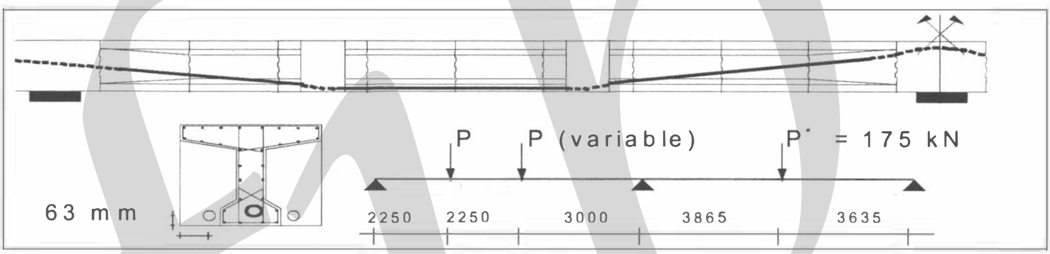

Fig. 1 General lay-out and characteristics of tested hyperstatic beam

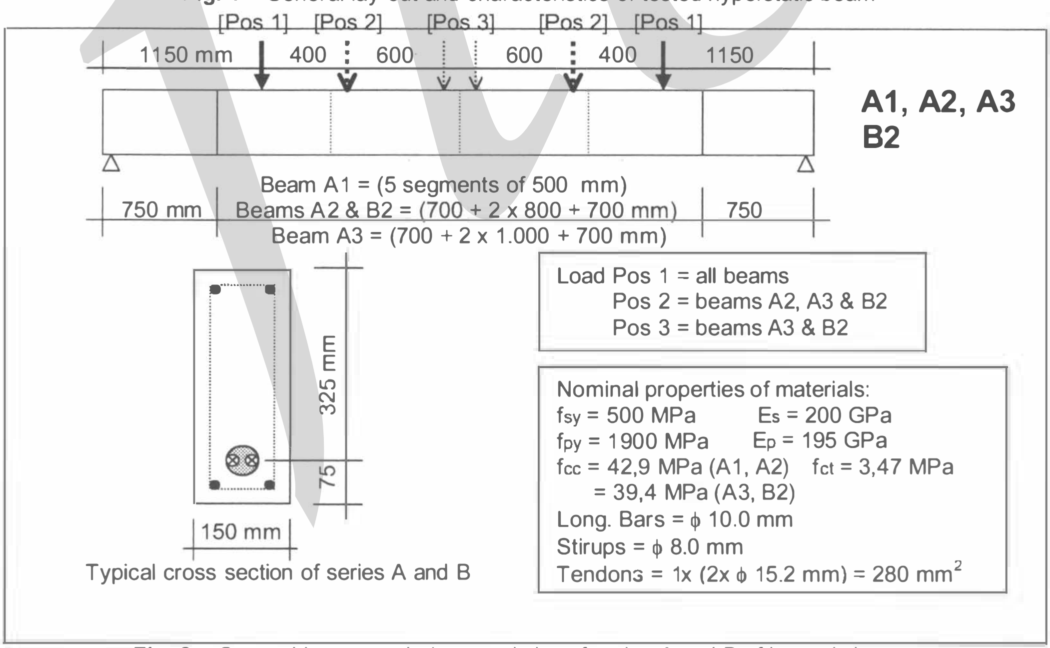

Fig. 2 General lay-out and characteristics of series A and B of isostatic beams

NUMERICAL SIMULATION OF THE FAILURE MECHANISM OF CORRODED 'DRY' BUTT-JOINED POST-TENSIONED BEAMS

Istvan Bodi
Budapest University of Technology and Economics, HUNGARY

Eduard Klopka
Neimar Engineering Ltd.
YUGOSLAVIA

Zoltan Klopka
Construct-Trade Ltd.
HUNGARY

Keywords: prestressed beam, numerical simulation, tendon corrosion

1. INTRODUCTION

Post-tensioned beams assembled of precast elements in 'dry' butt-joint technology were widely used type of beams for industrial hall bays of large spans in the 1960's in Yugoslavia. However, these members are very sensible to deterioration in time, especially the corrosion of tendons represents a serious hazard to the load-bearing capability.

The recent collapse of one structure, where the post-tensioned, precast 'dry-bonded' beams were used raised series of questions about these structures. Some of these questions addressed the failure mechanism of the 'dry-bonded' pre-cast post-tensioning system.

2. DRY BUTT-JOINED POST-TENSIONED BEAM

The hall building of the Wire Production Plant in Novi Sad, Yugoslavia is a four-bay hall made of prefabricated skeletal elements. The beams, spanning 20.5m are made of three separately moulded parts which are connected together by means of post-tensioned prestressing (Fig. 1). The individual elements are joined in a 'dry' technology, which means that only the prestressing force safe-guards the connection. The columns are prefabricated, and they are fixed in the foundations.

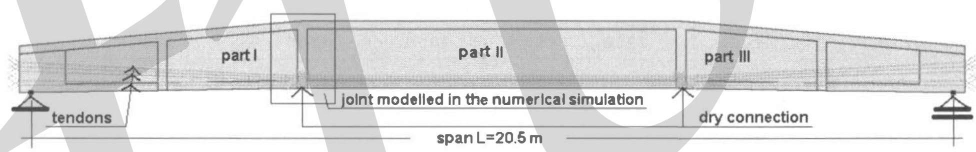

Fig 1. Elevation of the prestressed beam

The analysis of the collapsed structure and structural elements made by the Technical University of Novi Sad found stated that among another reasons the main reason of failure was the corrosion of some of the tendons. The load-bearing capability of the sound of tendons was not enough to balance the increased loading, and these tendons failed in tension. The member collapsed rapidly without any significant warning sign.

3. NUMERICAL SIMULATION

The numerical simulation of the behaviour of the prestressed member was conducted to try to envisage and understand the behaviour of the member near the state of collapse. Although no eye witnesses were at site at the time of collapse, the assumed failure mechanism is thought to be rapid and sudden. Obviously, a sudden failure of the structure probably needs a more detailed analysis of the ultimate limit state if not a larger level of safety (higher partial safety factors) than the usual approach provides.

It is also an important question, what is the amount of corrosion or what is number of corroded tendons which still assures the soundness of the structure.

The process of corrosion progresses in time so a nonlinear approach was needed. The numerical simulation was conducted in two steps. In the first step (Fig. 2) the overall usability of the model was studied, and comparisons were made to the results obtained by the first order analysis and the traditional design method. The second step was thought to be the modelling of the corrosion process of the tendons.

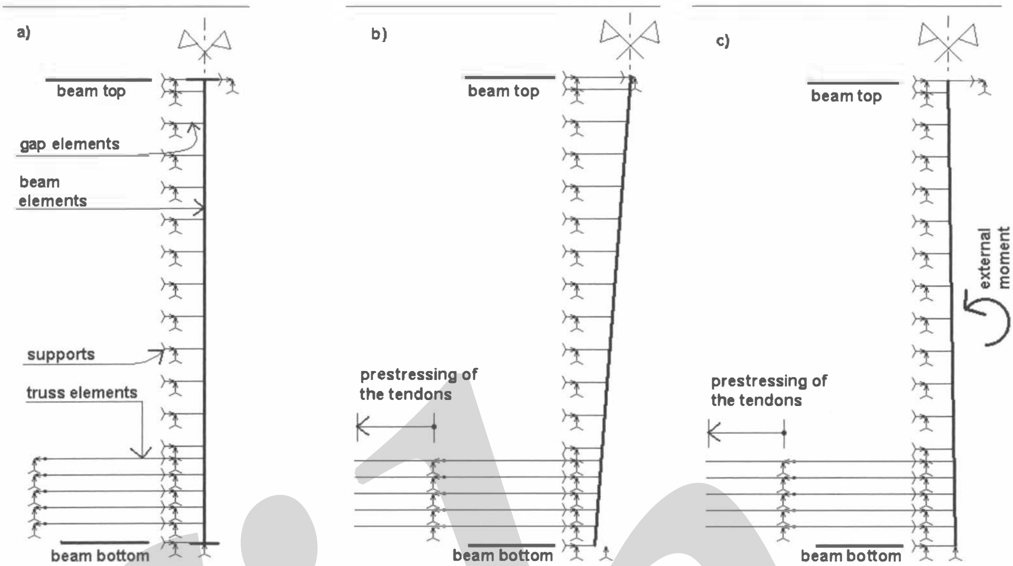

Fig. 2 The models a) without loading b) the state of prestressing c) state in exploitation

4. PROPOSED REPAIR AND STRENGTHENING METHOD

The choice of the strengthening method was made with regard to the costs, available materials and tools, and the execution flexibility. The chosen method introduces additional load-bearing capability in the structure by means of post-tensioning, namely 'lowering' the tendons. After the lowering process of the tendons the protective tubes were grouted and sealed. The computer image of the strengthened beam can be seen in Fig. 3.

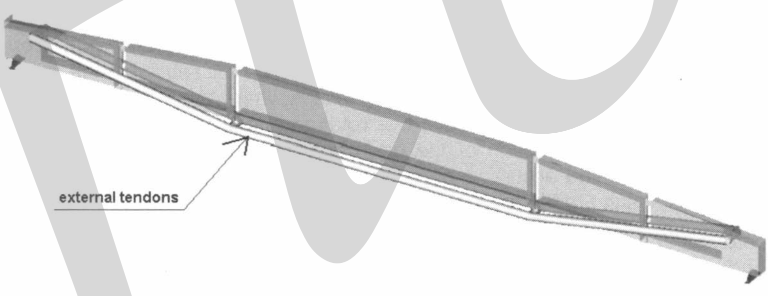

Fig 3. Computer image of the strengthened prestressed beam

5. CONCLUSIONS

A recent collapse of a 'dry' butt-joined post-tensioned beam has pointed out the weakness of such structures on corrosion of the tendons. The simple model developed for the numerical analysis of the corrosion process has performed satisfactory in describing the state of the prestressed members. Further the model will be tested on various problems considering the corrosion of prestressed structural details, where the failure occurs rapidly without warning, to qualitative describe the ultimate limit state and to estimate the load-bearing capability of the structure. This information is often valuable, since a large number of prestressed structures have been built in Hungary using grouting material highly aggressive on steel.

COMPARATIVE STUDY OF FEM BASED REINFORCED CONCRETE ANALYTICAL MODELS AND THEIR NUMERICAL IMPLEMENTATION: SOFTWARE PACKAGE FELISA/3M

HRISTOVSKI Viktor,
Post-Doctoral Researcher, Dept. of Design & Archit., Faculty of Engineering, Chiba University, 1-33 Yayoi-cho, Inage-ku, Chiba City 263-8522, JAPAN

NOGUCHI Hiroshi,
Professor, Dept. of Design & Archit., Faculty of Engineering, Chiba University, 1-33 Yayoi-cho, Inage-ku, Chiba City 263-8522, JAPAN

Keywords: rotating cracks, shear-slip, tension-stiffening, aggregate interlock

1 INTRODUCTION

Cracking of concrete is one of the major factors contributing to its non-linear behavior. Two distinguished cracking modes have generally proved to influence significantly the overall structural response: *normal mode*, caused by principal tensile stresses acting perpendicularly to the crack plane, and *tangential mode*, resulting from shear-stresses in the crack plane, causing shear-slip phenomenon. In spite of its discontinuity nature, these phenomena have been more or less successfully simulated over the last 30 years using continuum-based approaches. The *smeared crack models* for the normal mode have particularly become very popular because of their convenience to be easily implemented into finite element programs. Within this study performed by adopting the smeared crack approach, both cracking modes have been discussed. Regarding the normal mode, a *hypo-elastic rotating crack model* has been considered, and as for tangential mode, the *Walraven's shear-slip model* (Ref. [1]) including the effects of aggregate interlock, has been adopted.

The proposed constitutive models have been implemented into the original software package FELISA/3M. Using this program, the particular contribution of each cracking mode has comparatively been considered, finding reasonable agreement between the analyses and the experiments.

2 PROPOSED CONSTITUTIVE MODELS AND VERIFICATION

The proposed models based on hypo-elasticity use the *equivalent uniaxial strain* formulation for bi-axial stress-strain state (Ref. [2]). The principal stresses and strains are allowed to rotate in coaxial directions during the loading process that is necessary condition for satisfying the form invariance of the crack-induced orthotropic material behavior. In the cases where a large rotation is expected (as in the analysis of beam-column joints), control of this rotation becomes necessary in order to prevent numerical instabilities during calculation of the equivalent uniaxial strains. Therefore, according to Noguchi (Ref. [2]), the improved accuracy is provided by transformation of the principal axes in the case when the rotation relating to the original state becomes greater than 45 degrees.

The *ultimate surface* adopted in the model is based on the Kupfer's yield curve for bi-axial stresses, taking into account the influence of the strength reduction of cracked concrete in compression, according to Noguchi (Ref. [3]). Hence, particularly, for the combination of stresses "tension-compression", when tension strain is greater than cracking strain, the following expression has been used:

$$\sigma_{c2} = \frac{f_c}{0.27 + 0.96\left(\dfrac{\varepsilon_{u1}}{\varepsilon_{cu}}\right)^{0.167}} \geq f_c \qquad (1)$$

In Eq. (1) σ_{c2} is ultimate stress in principal direction, f_c is uniaxial concrete strength in compression, ε_{u1} and ε_{cu} are equivalent uniaxial strain function in principal direction 1 (in tension) and uniaxial strain in compression for the corresponding strength f_c, respectively. For the normal crack mode, the Shirai's function (Ref.[4]) for accounting the tension-stiffening effects has been used, as follows:

$$\sigma_{u1} = f_t(1 - 2.748\xi + 2.654\xi^2 - 0.906\xi^3) \qquad (2a)$$

$$\xi = \frac{\varepsilon_{ul} - \varepsilon_{cr}}{\varepsilon_m - \varepsilon_{cr}} \tag{2b}$$

where σ_{u1} is equivalent uniaxial stress on tension, f_t is the concrete uniaxial tension strength, ε_{cr} is a concrete cracking strain and ε_m is a tension strain for zero stresses (adopted in the analyses: ε_m =20 ε_{cr}). The tangential crack mode has also been treated within this hypo-elastic smeared-crack formulation, based on the stiffness portion of Walraven's shear-slip relationship (Ref. [1]) for the cracked surfaces, as follows:

$$\delta = \frac{\tau_c}{1.8\,w^{-0.8} + (0.234\,w^{-0.707} - 0.2)\,f_{cc}} \tag{3}$$

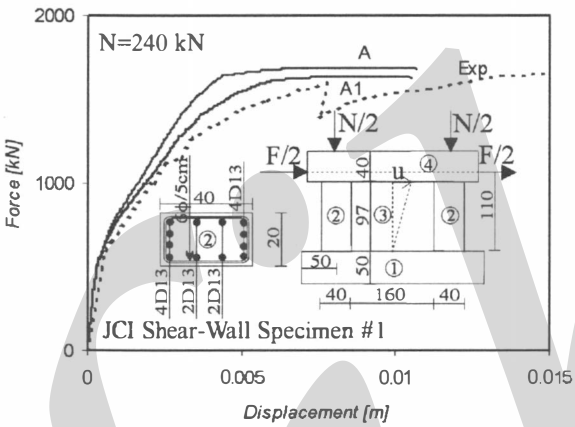

Fig.1 JCI Specimen #1: Geometry and comparison of analytical (A1 – with shear-slip effects, A – without shear-slip effects) and experimental (EXP) force-displacement diagrams

In Eq. (3) δ is the tangential slip along the crack (in mm), ***w*** is the crack width (in mm), f_{cc} is the cube concrete compressive strength (in MPa) and τ_c is the local shear stress acting along the crack (in MPa).

Verification of the models has been done using the results from experiments conducted on samples of reinforced concrete columns, beams and shear-walls, recommended for model verification by Japan Concrete Institute (JCI) and Architectural Institute of Japan (AIJ). In **Fig. 1** the comparative results from the analyses and experiment of the JCI shear-wall specimen #1 (tested by Aoyama et al.) is shown. It can be seen that the analysis including the both cracking modes ("A1") has simulated the force-displacement relationship closer to the experimental one, compared to the performed analysis taking into account only the normal cracking mode ("A").

3 CONCLUSIONS

From this study it can be concluded that the model including only the normal cracking mode could be acceptable for the case of members with basically flexural and mixed failure modes. However, the integral model (including both cracking modes) has shown to be more appropriate for correct simulation of the failure progress for members with predominant shear behavior. It is also recognized that the influence of the slippage between the parts of the specimen with different thickness should be considered in the future, since it can significantly improve the overall force-displacement prediction.

REFERENCES

[1] Walraven, J.C. : "Fundamental Analysis of Aggregate Interlock," ASCE Journ. of Structural Engineering, Vol.107, No.11, 1981, pp.2245-2270

[2] Noguchi, H. : "Analytical Models for Reinforced Concrete Members Subjected to Reversed Cyclic Loading," Proc., Seminar on Finite Element Analysis of Reinforced Concrete Structures, Volume 2, JSPS, Tokyo, May 21-24, 1985, pp.93-112

[3] Noguchi, H., Ohkubo, M. and Hamada S. : "Basic Experiments on the Degradation of Cracked Concrete under Biaxial Tension and Compression," Proc. of JCI, Vol.11, No.2, 1989, pp.323-326 (In Japanese)

[4] Shirai, N. and Sato, T. : "Bond-Cracking Model for Reinforced Concrete," Trans. of the JCI, Vol. 6, 1984, pp. 457-468

DESIGN INSTRUMENT SPANCAD FOR SHEAR WALLS AND D-REGIONS

Johan Blaauwendraad Pierre C.J. Hoogenboom

Delft University of Technology
Faculty of Civil Engineering and Geosciences
Delft, The Netherlands

Keywords: reinforced concrete, shear walls, software, stringer-panel model, design procedure

1 INTRODUCTION

Shear walls and deep beams of complicated geometry frequently occur in civil engineering structures. Design of these elements is a considerable challenge for the responsible structural engineer. Often such an element is subdivided in B-regions and D-regions. Obviously, B-regions are the parts of a structure in which the classic beam theory applies and for which we can think in terms of the familiar bending moments and shear forces (Bending). The remaining part of the structure consists of D-regions in which the fore-mentioned classic state is disturbed (Disturbance). Examples are beam column joints, openings in the web of a beam and dented beam-ends. A shear wall with an irregular shape needs to be considered as one large D-region. The software SPanCAD has been developed for design of such elements.

2 SPANCAD

The objective of this new software is to offer an alternative design tool, which combines a number of advantages and releases a number of drawbacks. It aims for:

- PC environment, under Windows, ready while you wait,
- The same model for elastic state and failure state,
- The same model for different load combinations,
- Information about crack-widths and displacements,
- Interactive design tool; the engineer is on the lead.

The program SPanCAD is based on a special type of element method. In the standard finite element method it is practice to apply a mesh as fine as possible, but SPanCAD is developed to apply the coarsest mesh for a given geometry. This has been obtained by feeding much concrete mechanics intelligence into the elements. The second special feature of SPanCAD is the type of elements. Only two types exist, a stringer element (straight bar) and a panel element (rectangle or quadrilateral) (Fig. 1). The non-linear characteristics of the stringers is based on the Eurocode. The behaviour of the panels is based on the modified compression field theory.

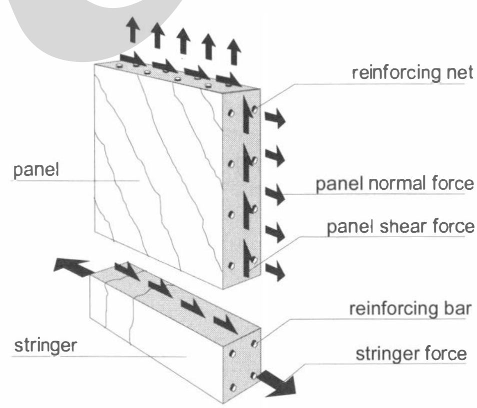

Fig. 1 Stringer and panel element

3 A THREE-STEP DESIGN PROCEDURE

First step, elastic analysis

A structural design is made in three steps. In the first one a linear-elastic model is used. In this step the stringer-panel model carries all normal forces in the stringers only and carries all shear forces in the panels. In this first step the force flow is not much influenced by the sizes of cross-sections assigned to the stringers. The structural engineer makes rough estimates using experience and rules of thumb. The software performs the linear-elastic analysis for all load combinations.

Second step, non-linear analysis

In the second step the structural engineer selects reinforcement based on force flow computed before. Subsequently, the software performs a non-linear analysis. The model used accounts for concrete cracking in the tensioned stringers and panels. The reinforcement of the stringers is kept linear-elastic but the panel reinforcement can yield. In step 2 the stress state in the panels is extended to shear and normal stresses.

A non-linear analysis is successively made for each load combination. The load is controlled by a load factor that starts at zero and is increased in small increments until 1 at which the full load combination is at the model. The structural engineer can follow the progress of the analysis on the screen where a load-displacement graph is drawn.

Third step, simulation

The structural engineer improves the reinforcement using the just computed force flow and crack widths. Normal dimensioning formulae can be used available in codes of practise. Subsequently, SPanCAD performs a simulation for each load combination. In the simulation no restrictions are imposed on the non-linear response of the model. If everything goes well the result of these computations shows that all performance criteria are satisfied and the design is completed.

4 DESIGN EXAMPLE

A deep beam is simply supported and has a large opening (Fig. 2). The stringer-panel model of this beam is shown in Figure 3. Two independent concentrated forces F_1 and F_2 act on the beam. The loading for the service limit state consists of 3 load combinations. The loading for the ultimate limit state consists of 4 combinations. Figure 4 shows the force flow in the non-linear stringer-panel model for one of the load combinations. The final design is shown in figure 5.

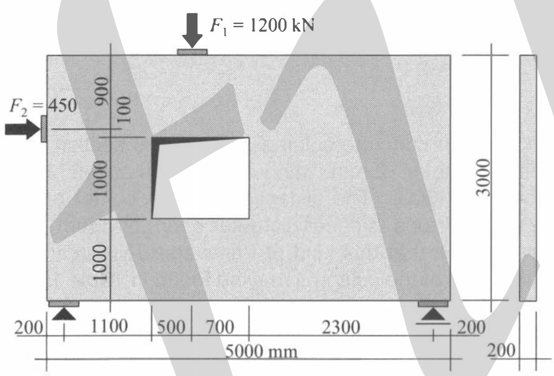

Fig. 2 Deep beam with opening

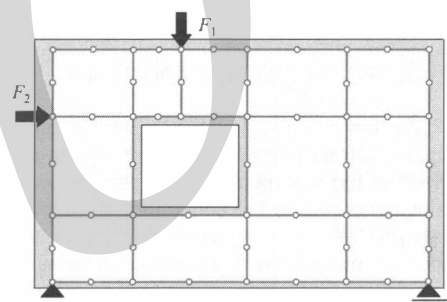

Fig. 3 Stringer-panel model of the deep beam

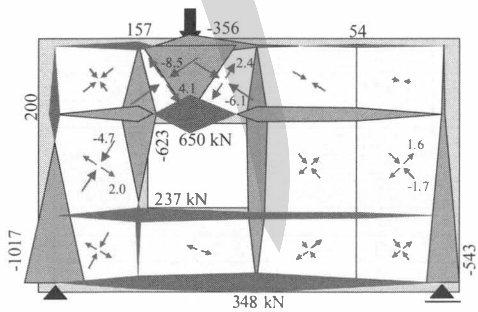

Fig. 4 Nonlinear force flow for one of the load combinations

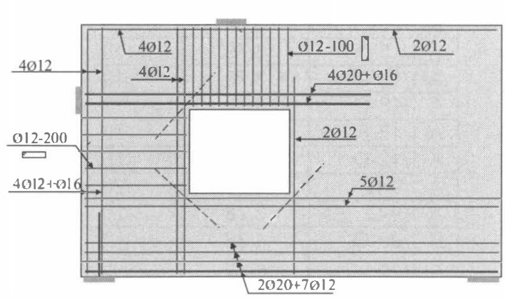

Fig. 5 Final reinforcement of the deep beam

CARRYING CAPACITY AND POST PEAK BEHAVIOUR OF SLENDER HIGH STRENGTH REINFORCED CONCRETE COLUMNS

Olivier Germain Bernard Espion

Department of Civil Engineering (194/4)
University of Brussels (ULB)
B 1050 Brussels, Belgium

Keywords : Slender columns, high strength concrete, buckling tests, numerical modeling

1 INTRODUCTION

With the advent of high strength concrete, the question of the verification of the ultimate limit state induced by structural deformations (*i.e.* buckling) needs to be considered in particular design situations. For instance, when high strength concrete is used to reduce the dimensions of the cross section of columns, their slenderness is increased by comparison with columns in normal strength concrete of similar length and supposed carrying capacity, which in turns increases the possibility that the ultimate load of high strength columns may sometimes be governed by instability rather than by strength. Up to now, very little work has been done in order to know if the computation methods which are used to check the stability of slender reinforced concrete columns made of normal strength concrete (e.g. the CEB column model method) remain valid for slender columns made in high strength concrete.

2 EXPERIMENTAL PROGRAMME

We have tested 12 slender, two hinged, high strength concrete columns. The cross section was square 180 mm by 180 mm and reinforced by 4 bars diameter 12 mm (with yield strength at 542 MPa), which is the minimum column reinforcement allowed by EC 2. The distance from the center of the reinforcing bars to the concrete surface was 37.2 mm. Stirrups in either diameter 6 mm or 8 mm (see Table 1) were placed with a spacing of 140 mm. It is felt that this kind of transverse reinforcement does not provide any particular confinement. Other details of the columns may be found in Table 1.

Table 1 Details of test columns and results

Column designation	Effective length [m]	Load eccentricity [mm]	Stirrup diameter [mm]	Cylinder strength[1] [MPa]	Cylinder Strength[2] [MPa]	Maximum load [kN]
A-1/36-R	3.78	5	8	82.6	86.9	1750
A-1/36-O	3.78	5	8	87.1	87.3	1640
A-1/18-R1	3.78	10	6	89.5	92.0	1922
A-1/18-Q	3.78	10	8	88.8	89.3	1524
A-1/18-O	3.78	10	6	94.3	91.4	1489
A-1/18-R2	3.78	10	8	80.0	85.9	1479
A-1/12-O	3.78	15	6	86.7	89.4	1256
A-1/9-R	3.78	20	6	92.5	91.8	1140
A-1/9-O	3.78	20	6	97.8	94.3	1100
B-1/90-O	4.38	2	6	90.4	92.0	1388
B-1/36-O	4.38	5	6	94.6	93.1	1315
B-1/18-O	4.38	10	6	91.6	91.3	1153

[1] Cylinders cured under moist conditions
[2] Cylinders cured under laboratory drying conditions

By comparison with the experimental data published by previous investigators, our test series includes some larger columns, columns with larger slenderness ratios, with minimum reinforcement, and with lower relative eccentricities. But more fundamentally, another important point which differs from previous test series is the loading mode: whereas previous investigators tested their columns either by load control or by controlling the displacement of the actuator of the testing machine (*i*.e. the axial deformation of the column), our columns were tested in a closed loop testing machine where the controlling parameter was the transverse displacement, i.e. the curvature of the columns. All our columns reached their maximum load by instability (not by material failure).

3 DISCUSSION OF RESULTS

The columns have been modeled by two methods proposed by the CEB: the finite differences (FD) method and the simplified column model (CM) method [1]. The stress-strain for the HSC concrete in compression comes from [2]. To obtain a good agreement between experimental and computed load deflection curves for low loads (below 600 kN), an accidental eccentricity had to be taken into account. This accidental eccentricity is at most equal to 7.5 mm, which is less than the accidental eccentricity that has to be used for the verification of the ultimate limit state of buckling. A summary of the results concerning the maximum loads is represented in figure 1 where the maximum loads (either computed or experimental), reduced by the “squash” load

$$N_R = 0.85\ f_c\ A_c + f_y\ A_s \qquad (1)$$

are plotted in function of the relative modified eccentricity. Both methods capture the influence of the eccentricity and the slenderness ratio on the maximum load.

The post peak behaviour is influenced by tension stiffening effects and damage localization, none of which are taken into account in the modeling. However, a careful examination of the load deflections curves computed with the modified eccentricities shows that the FD curves follow more closely the experimental curves than the CM curves. But the ultimate deflection (at material failure) predicted by the FD method is always less than the measured ultimate deflection, whereas the ultimate deflection predicted by the CM method is sometimes significantly larger than the experimental ultimate deflection (Fig. 2).

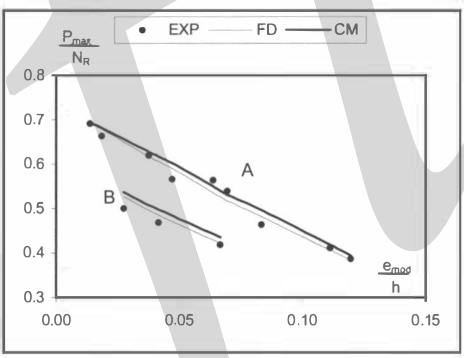

Fig.1 Maximum loads

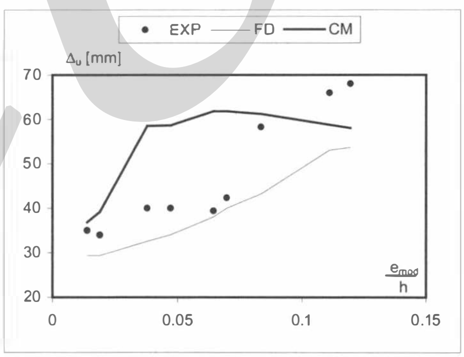

Fig.2 Ultimate deflections (A series)

REFERENCES

[1] CEB, Manual on Buckling and Instability, Bulletin d'Information du CEB, N°123, 1977.
[2] fib : Structural Concrete, vol.1, Bulletin fib, N°1, 1999.
[3] Germain, O. : From buckling tests of high strength concrete columns to their analysis with numerical models, M.Sc. Thesis, University of Brussels, 2001 (in French).

COMPUTER AIDED DESIGN ON SELF-ADJUSTABLE ARRANGEMENT OF REINFORCING BARS WITH SMART FICTITIOUS MATERIAL MODELING

An Xuehui Maekawa Koichi
Department of Civil Engineering
The University of Tokyo, Japan

Kikuchi Tatsuya
Kajima Corporation
Japan

Kishi Kanako
Department of Civil Engineering
The University of Tokyo, Japan

Keywords: nonlinear analysis, FEM, RC structures, computer aided design

1 INTRODUCTION

Nonlinear analysis programs are already being used to check completed designs. As the results from using a linear analysis cannot consider the cracking behavior of concrete, the initial design may need to be improved many times during the design cycles (Fig.1a).

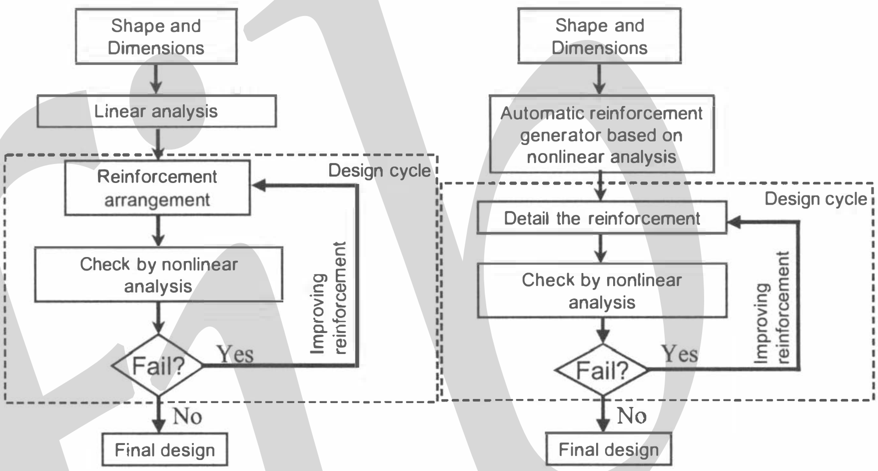

(a) Nonlinear analysis only used as a checker (b) Nonlinear analysis used also as a generator

Fig.1 Different flow charts for designing an RC structure

In this study, instead of using a linear analysis to arrange the reinforcement, the nonlinear finite element analysis is adopted as an automatic reinforcement generator. If the reinforcement is generated while considering the location and amount of the cracks, a good initial design can be made and time saved in the successive steps of the design process. This concept allows a new computer based optimization design procedure (Fig.1b).

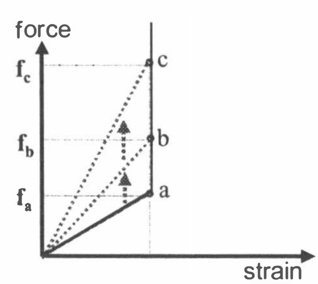

Fig.2 A smart fictitious material model with strengthening behavior

2 FEM ANALYSIS OF SELF-ADJUSTABLE ARRANGEMENT OF REINFORCING BAR

The basic design rule of RC structures is that the reinforcement will carry a force under the design load and does not accept any yielding. After cracks occur in the RC structures, the stress carried by concrete at the cracking location will be transferred to the reinforcement. During the process of increasing the load applied to the RC structure up to design load level, initial cracks may happen inside concrete, and stresses will be redistributed. The cracked locations with very low reinforcement ratio start to yield. If we want the material to carry this stress without yielding, we have to strengthen it locally, for example, increase the reinforcement ratio. Subsequently, the material behaves according to curve b and the load is increased again (Fig.2).

When the ultimate elastic strain is reached again and the load is to be increased, once more we need to strengthen the material and curve c is obtained. During FEM analysis, by switching the steel model in the existing nonlinear FEM program into this smart fictitious material model, the reinforcement ratio needed to carry the force at each element can be calculated. The reinforcement generating procedure can be carried out as follows:

① Set initial reinforcement ratio after deciding shape and dimensions of the RC structure
② Perform the nonlinear analysis for design load, get the output of generated reinforcement
③ Summarize the output reinforcement ratios from all load combinations.

3 EXPERIMENTAL VERIFICATION

An experiment has been conducted by following the new design procedure. A beam with openings in the spans has been reinforced according to the output reinforcement ratio automatically generated (Fig.3). The purpose of this experiment is to check the shear capacity of this beam, that is, whether the automatically generated reinforcement in Y-direction is enough to carry the shear force. Considering the output results of reinforcement ratio, 3 steel bars with diameter of 10mm will be safe under the design load (20tonf). Here, two types of arrangement of steel bars are adopted. Type A, normal shear reinforcement type is put into side A of the beam, and Type B, with the same reinforcement amount but surrounding the opening, is put into side B (Fig.4).

The capacity for side A is 22.4 tonf and for side B is 26.7 tonf. Both are higher than the design load. Side B is much stronger than side A as the horizontal part of shear reinforcement of Type B contributes significantly.

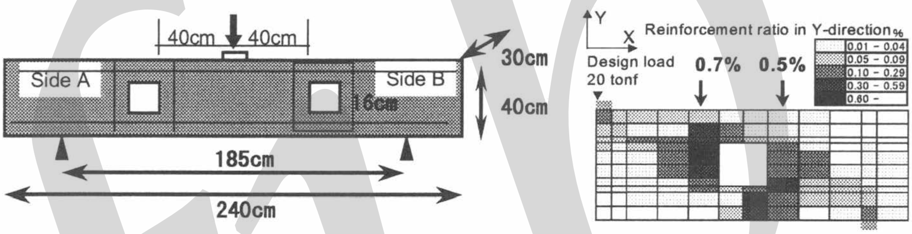

Fig.3 Shape and dimensions of the beam and the output reinforcement ratio map (Y-direction)

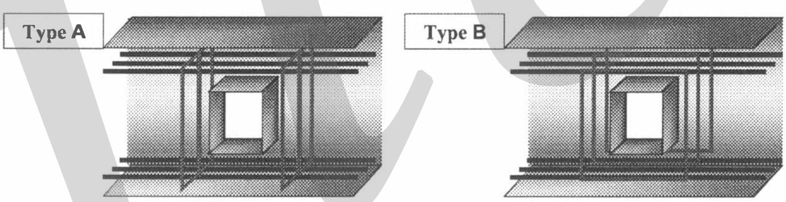

Fig.4 Two types of shear reinforcing bars used to strengthen the opening

4 CONCLUSIONS

An automatic reinforcement generator program, based on nonlinear analysis, has been developed for a new design procedure of RC structures. The smart fictitious material model with strengthening behavior is adopted to improve the reinforcement according to the applied force. An RC beam with opening has been designed by using this new procedure and the test results proved that the shear capacity is secured. The test result for different layouts of steel bars shows that the detail of reinforcement, such as anchorage, will affect the behavior of the real structure.

REFERENCES

1. Okamura, H., and Maekawa, K.: Nonlinear analysis and constitutive models of reinforced concrete, Gihodo-Shuppan Co. Tokyo, 1991

2. Hoogenboom, P.C.J.: Discrete elements and nonlinearity in design of structural concrete walls, Dissertation, Delft University of Technology, 1998.

NONLINEAR ANALYSIS OF REINFORCED CONCRETE SHELLS SUBJECTED TO CYCLIC LOAD

Tae-Hoon Kim Kwang-Myong Lee Hyun Mock Shin
Department of Civil and Environmental Engineering, Sungkyunkwan University
300 Chunchun-dong, Jangan-gu, Suwon, Kyonggi-do, 440-746, KOREA

Keywords: reinforced concrete, shell, nonlinear analysis, cyclic load

1 INTRODUCTION

In recent years reinforced concrete shells have been widely applied to underground tanks, nuclear waste containers, and offshore structures. Finite element analysis of such structures has become increasingly important because it is generally not possible to obtain the deformation and failure behavior by conventional procedures, and experimental studies on these structures are very expensive.

In the present study, models for material nonlinearity include tensile, compressive and shear models for cracked concrete and a model of reinforcing steel where the smeared crack approach is incorporated. Furthermore, the emphasis is on its ability to model cyclic behavior by proper theoretical representation of the material parameters.

The primary objective of this study was to develop a new finite element formulation for the nonlinear analysis of shell structures. In order to analyze reinforced concrete shells with highly nonlinear behavior, the layer method was introduced, assuming that several thin plane stress elements are layered in the direction of thickness. The cross section of reinforced concrete is divided into concrete and steel layers. Each layer consists of 4-node flat shell elements. The flat shell element was developed by combining a membrane element with drilling degree of freedom and a plate bending element. Thus, the developed element possesses 6 degrees of freedom (DOF) per node, which permits an easy connection to other types of finite elements with 6 DOF per node and greatly improves the element behavior.

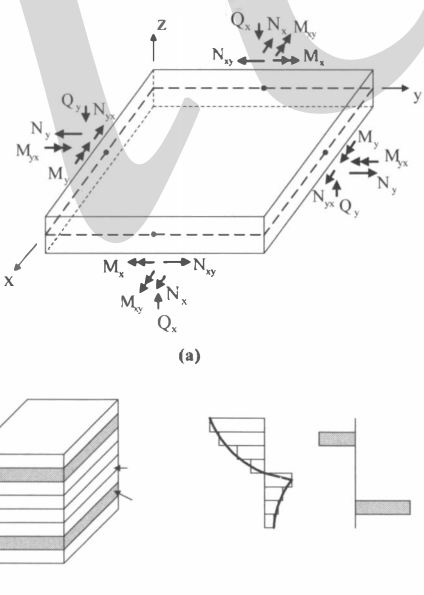

Fig. 1 Shell element: (a) Forces acting on RC shells; and (b) Layered element

2 FINITE ELEMENT FORMULATION

For the analysis of reinforced concrete shells the finite element formulation of a 4-node quadrilateral thin flat shell finite element, which has six DOF per node, is presented herein. The sixth DOF is obtained by combining a membrane element with a normal rotation θ_z, the so-called the drilling degree of freedom, and a discrete Kirchhoff plate element.

In order to analyze reinforced concrete shells with nonlinear behavior, the layer method is used, assuming that several thin plane stress element is layered in the direction of thickness. Fig. 1 gives the illustration of layered element and forces acting on the shells.

3 NONLINEAR MATERIAL MODEL FOR REINFORCED CONCRETE

Reinforced concrete is highly nonlinear material. The nonlinear material model for the reinforced concrete is made up of models for concrete and a model for the reinforcing bars. Models for concrete may be divided into models for uncracked concrete and cracked concrete. The basic model adopted for crack representation is a non-orthogonal fixed crack approach of the smeared crack concept, which is widely known to be a robust model for crack representation [1, 2].

4 ANALYSIS PROGRAM BY FINITE ELEMENT METHOD

The proposed structural element library RCAHEST(**R**einforced **C**oncrete **A**nalysis in **H**igher **E**valuation **S**ystem **T**echnology) is built around the finite element analysis program FEAP [3] developed by Taylor. FEAP is characterized by modular architecture and by the facility of introducing any type of custom elements, input utilities and custom strategies and procedures. The FEAP will help alleviate many of the difficulties commonly encountered in maintaining the integrity of existing software components during the development of new research capabilities. FEAP permits users to add their own element modules to the program. Accompanying with the present study, we will attempt to implement such constitutive models for reinforced concrete and reinforced concrete shell element.

ACKNOWLEDGEMENTS

The study described in this paper was supported by the Korea Science and Engineering Foundation (KOSEF) through the Korea Earthquake Engineering Research Center (KEERC) under Grant No. 2000G0203. The authors wish to express their gratitude for the support received.

REFERENCES

[1] Kim, T. H. and Shin, H. M. : Analytical Approach to Evaluate the Inelastic Behaviors of Reinforced Concrete Structures under Seismic Loads. Journal of the Earthquake Engineering Society of Korea, EESK, Vol.5, No.2, pp.113-124, 2001

[2] Kim, T. H., Lee, K. M., Yoon, C. Y. and Shin, H. M. : Inelastic Behavior and Ductility Capacity of Reinforced Concrete Bridge Piers under Earthquake. I: Theory and Formulation. Journal of Structural Engineering, ASCE, 2001, (Accepted)

[3] Taylor, R. L. : FEAP - A Finite Element Analysis Program, Version 7.2 Users Manual, Volume 1 and Volume 2, 2000

ANCHORAGE OF HEADED BARS IN DETAILING RC STRUCTURES

M. Keith Thompson (Graduate Student)
James O. Jirsa (Professor)
John E. Breen (Professor)
The University of Texas at Austin
10100 Burnet Rd., Building 177
Austin, Texas 78758 USA

Keywords: anchorage, headed reinforcement, strut-and-tie modeling, CCT nodes

1 INTRODUCTION

Anchorage of reinforcement at the nodes of strut-and-tie models is frequently difficult due to the limited distances available for transferring forces from bars (tensions ties) to the concrete (compression struts or nodes). Headed bars provide a potential solution to the problems of node anchorage in strut-and-tie modeling. Current code provisions do not provide guidelines for the use of headed reinforcement. To address these issues, a test program was developed to study headed bars anchored in Compression-Compression-Tension (CCT) nodes.

2 TEST PROGRAM

Sixty-four CCT node specimens were tested. The basic test specimen is shown in Figure 1. The width of the specimens and the bearing plate was always 6 bar diameters ($6d_b$) and the strut angle was varied by changing the placement of the load ram. The details of the node are shown in Figure 2. Concrete strengths varied between 21 to 29 Mpa. The variables of the test program included:

- Anchorage Type: non-headed, hooked, and headed bars
- Head Size: net head area (A_{nh}) varied from 0 to 10.4 bar areas (A_b)
- Head Orientation: rectangular heads oriented with long axis vertical or horizontal
- Bar Size: 25 and 36 mm diameter bars
- Strut Angle: 30°, 45°, and 55°
- Confinement: unconfined or 10 mm stirrups at 75 or 150 mm

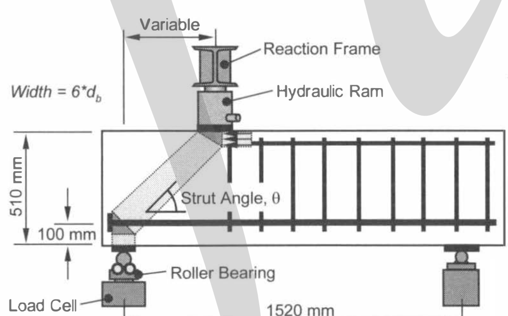

Figure 1 Typical CCT node test specimen

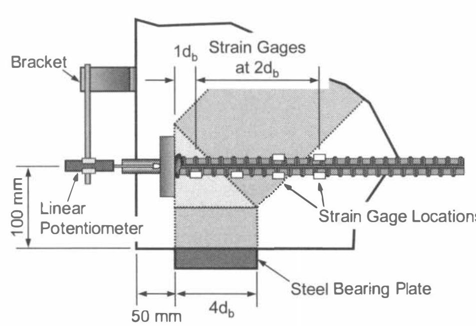

Figure 2 Detail of typical CCT node

3 HEADED BAR ANCHORAGE BEHAVIOR

The stages of headed bar anchorage in a CCT node are illustrated in Fig. 3. Cracking occurred in stages with cracks forming closer to the node as load was applied. The largest increases in bar force occurred when these cracks formed. When crack 2 formed, the head began to carry most of the bar force.

Head slip data from four 35 mm headed bars tests are plotted in Figure 4. Head sizes varied from non-headed (A_{nh}/A_b = 0.0) to a very large head size (A_{nh}/A_b = 9.3). The primary effect of a larger head size was to increase the load at which slip initiates. Once slip began, the behavior of the bars with relative head areas of 4.8 or less was similar with dramatic increases in slip for small increases in bar stress. For those bars, the initiation of slip served as a precursor to anchorage failure.

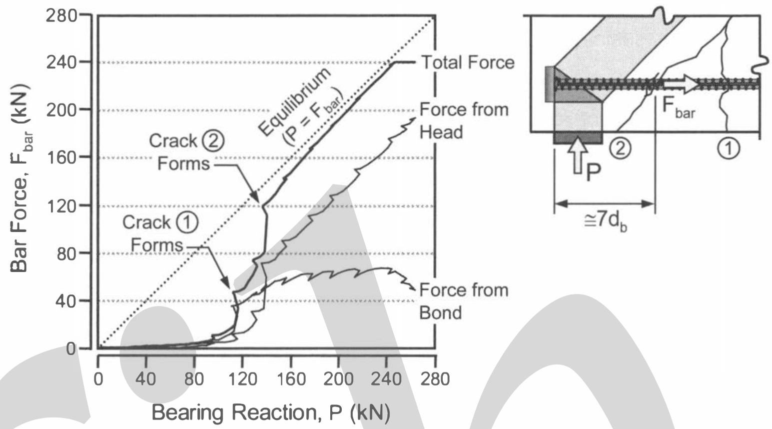

Figure 3 Stages of bar anchorage and contributions from bond and head bearing

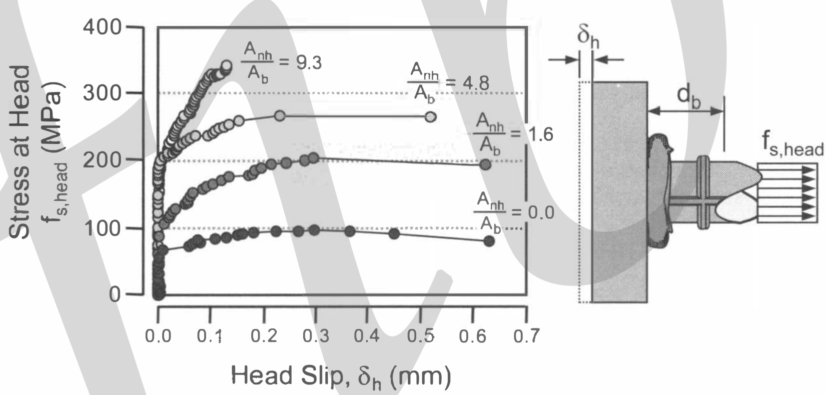

Figure 4 Head slip for bars of various head sizes

4 SUMMARY

The following observations were made:

- Initially bar force was transferred by bond but as bond deteriorated the head became the primary anchoring mechanism.
- Increasing head size improved the resistance of the head to slip and anchorage capacity.
- Decreasing strut angle increased the anchorage length of the bar over which bond acted.
- Failure of CCT nodes anchored by non-headed bars was by pullout of the bar.
- CCT nodes with headed bars failed by rupture of the node and the diagonal compression strut.
- Headed bars could achieve better anchorage in CCT nodes than hooked bars.
- Headed bars behave similar to deeply embedded anchor bolts or rigid plates bearing on concrete.
- Capacity could be predicted by considering bond and head bearing contributions separately.

RESEARCH ON DEFLECTIONS OF THE CONTINUOUS REINFORCED CONCRETE BEAMS

Mieczysław Kaminski   Mariusz Szechinski   Sebastian Tos
Wroclaw University of Technology
POLAND

Keywords: deflections, sustained loads, reinforced concrete, continuous beams

INTRODUCTION

Deflection of the straight axis of the bar is derivative of curvature, that is deformation of two previous parallel cross sections, in sequence of the bending moment action. It is possible to derive this dependence from geometrical and physical dependences.

DEFLECTIONS OF REINFORCED CONCRETE ELEMENTS

In the case of the reinforced concrete elements it is not possible to use relationships of isotropic materials. Basic differences are:

- different values coefficients of elasticity of concrete and steel; for concrete this value is depended on time and on the level of loads;
- cracking of the cross-section in the stretched zone for higher loads levels, it causes changes of the moment of inertia of the cross-section while increasing bending moment;
- plasticity of concrete, it implicates the false of geometrical proportions used for derivation the equations of deflections of elastic elements;

During the process of loading it changes the stiffness of reinforced beam. Main reasons:

- change of material characteristics of concrete caused by loads and time;
- change of geometry of concrete cross-section (cracking);

Generally, stiffness of bended element is the function of three parameters:

- loads
- localization of cross-section
- time

In Euro Code and Polish Code there are made several assumptions (like for example constant stiffness for the whole bended element) which are far from reality. But these methods are sufficient for practical purposes and simplification is huge.

CONCEPTIONS OF STIFFNESS DISTRIBUTION IN REINFORCED CONCRETE ELEMENTS

There are four main conceptions of assuming of stiffness of reinforced concrete elements:

1. Conception of constant stiffness in segments [1].
2. Conception of continual distribution of stiffness [2].
3. Conception of jumped distribution of stiffness.
4. Conception of waved distribution of stiffness [3].

Different functions of stiffness shown upper allow to get deflections of reinforced concrete beams, working under short- and long-term loads. This problem can be solved in many ways. It is quite important because according to standard recommendation of Euro Code, every procedure is allowed which helps to get deflections of reinforced concrete element.

CALCULATIONS OF LONG TERM DEFLECTIONS USING *CEB* METHOD

In order to calculate deflections of two-span reinforced concrete beam, working in *II* phase, one can use nomograms made by *CEB* (*Commité Européen du Béton*). The allow to take into consideration such factors like creeping and shrinkage which depend on relative humidity, degree of concrete reinforcement, overall dimensions, composition of concrete (proportion of cement to water) and time.

Main equation allowing to calculate deflection of reinforced concrete element is $y = (1+\Phi)y_E + \frac{l^2}{8}\cdot\frac{\varepsilon_{sc}}{z}$, where y_E – calculated deflection of element without creep and shrinkage; Φ – factor taking into consideration creep of material; ε_{sc} – factor taking into consideration shrinkage of material; l – length of bended element.

Value y_E can be calculated by integration of axis of deformation of beam.

General equation for stiffness is: $B = \dfrac{d_{02}}{\left[\dfrac{\sigma_{c0}}{E_c} + \dfrac{\sigma_{sa0}}{E_s}\right]}$. Values σ_{c0} and σ_{s0} depend on phase in which element works. They change with change of shape of a graph of stresses in cross-section

As soon as one gets values of immediate deflections one can take into consideration such factors like creeping and shrinkage. According to *CEB* recommendations shrinkage influence is given by relationship $\varepsilon_s = \psi\alpha_s\beta_s(1-0{,}1\rho_0)$ .When one wants to get deformations in time interval $t_n - t_i$: $\varepsilon_{st_n} = \varepsilon_s(\rho_{t_n} - \rho_{t_i})$. When one wants to take into consideration influence of creeping it is very similar procedure. According to *CEB* recommendations shrinkage influence is given by relationship:

$\Phi = \varphi_0 \cdot \alpha_p \cdot \beta_p \cdot \zeta(1-0{,}1\rho_0)\rho_{(t_n-t_i)}$. All coefficients are taken from experimental received nomograms.

EXAMPLE CALCULATIONS

Two-span reinforced concrete beam was researched. Element was loaded during 76 days.

As soon as one enters data into proper relationships one received B_{Ia}= 480,45 kN·m^2.

Deflection in the middle of span is $y_E = 5{,}30 \cdot 10^{-5}$m. Shrinkage influence: $\varepsilon_s = 2{,}01 \cdot 10^{-5}$.

Creep influence: $\Phi = 1{,}05$. Total deflection of 100 days old two-span reinforced concrete beam (with creep and shrinkage) in the middle of span is: $y = 1{,}09 \cdot 10^{-4}$ m.

LABORATORY RESEARCH

The laboratory test were made on two span reinforced concrete beams.The beams were loaded for long term in creep machines. Together with beams a concrete and steel samples were made for tests of material properties as elasticity, ultimate strength, creep and shrinkage. Receive values were used in analytical calculations. Results of tests and calculations are shown on Fig 1.

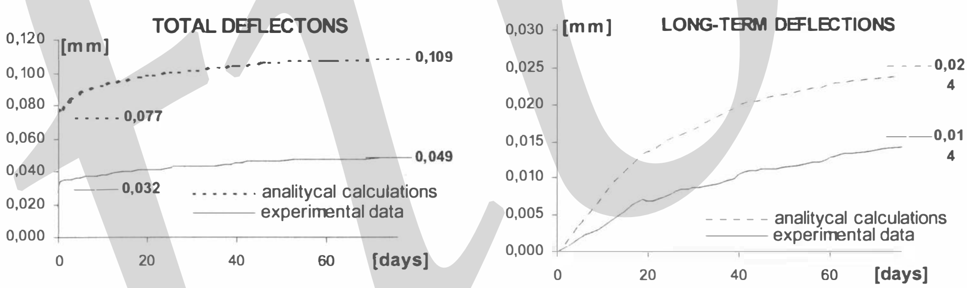

Fig. 1 – Total and long-term deflections of reinforced concrete beam.

CONCLUSIONS

Received results show that long-term deflections of the reinforced concrete two span beams may be calculated using presented *CEB* simple method. Relationship between experimental and analytical data is faithful. In test are beams with more spans and different shapes of cross-sections, Results will be presented soon together with calculations using another methods given in point 2.

REFERENCES

[1] MURASOV V.J., SIGALOV E.E., BAJKOV V.V., Reinforced Concrete Structures, Moskva, Stroijizdat, 1962

[2] KUCZYNSKI W., Reinforced Concrete Structures, Continuous theory of bending of the Reinforced Concrete Structures. Warszawa. PWN. 1971

[3] SZECHINSKI M. *Deflections of long-term loaded Reinforced Concrete Beams.,* Oficyna Wydawnicza Politechniki Wroclawskiej. Wroclaw, 2000

[4] BORCZ A., General conception of Mechanics of Reinforced Concrete Structures. Oficyna Wydawnicza Politechniki Wroclawskiej. Wroclaw, 1980

HIGH-PERFORMANCE OF REINFORCED CONCRETE MEMBERS BY USING HIGH-STRENGTH REINFORCEMENT

Makoto Sudo ingérosec
Tetsukazu Kida, Kiyoshi Kato, Kazuhiko Minakuchi, Tadashi Abe, Makiko Takano
Nihon University
Naoki Kato
Asano Institute of Technology
Tomiaki Kamisawa
Neturen
JAPAN

Keywords: high-strength rebar, heavy confinement, load-carrying capacity, self-induced prestress

1 INTRODUCTION

The upper-bound equations estimating the compressive load-carrying capacity of reinforced concrete columns are used all over the world, based upon the ultimate limit state design, but the common equations include both the elastic terms and the plastic one without a unification concept. In recent years, the high-strength type reinforcement (SBDP type) has been used frequently in the RC column and beam in Japan. Now, the common equations can not apply to the case of the high-strength primary reinforcement of the RC column[1]. This paper describes the generalized practical equation for the load-carrying capacity considering the buckling affection of primary rebars and further the flexural characteristic of the confined column with the high-strength rebars by virtue of the self-induced prestress.

2 FUNDAMENTAL UPPER-BOUND EQUATION OF DESIGN COMPRESSIVE LOAD-CARRYING CAPACITY OF RC COLUMN AND SELF-INDUCED PRESTRESS

2.1 General upper-bound equation of load-carrying capacity of RC column

The common equation regarding the primary rebar as a short column should be modified such as Eq. (1), by using the characteristic compressive strength f'_{ck} in place of the design compressive strength f'_{cd}.

$$N'_{oud} = (0.85f'_{ck}A_c + f'_{yd}A_{st}) / \gamma_b \quad (1)$$

where, N'_{oud} is the upper-bound for the design axial compressive load-carrying capacity, A_c is the area of concrete section, f'_{yd} is the compressive yield strength, A_{st} is the cross-section of primary rebars, γ_b is the member-factor and so on. Figure 1 illustrates a damaged highway bridge pier subject to a great earthquake and Figure 2 expresses the simplified buckling model of its reinforcement cage. When both ends of rebar are pin-connections, the buckling stress σ_s by the Rankine's equation can be given by Eq.(2).

where, λ is the slenderness ratio, obtained by $l/(\phi/4)$, l and ϕ are the length and the diameter of rebar, respectively, and E_s is the elastic modulus of rebar. Thus, the upper-bound of load-carrying capacity N'_{oud} of RC column considering the buckling effect of primary rebars, basically, can be expressed by Eq.(3), assuming A_e to be the core area.

$$\sigma_s = f'_{yd}/[1 + f'_{yd}\lambda^2/(\pi E_s)^2] \quad (2)$$

$$N'_{oub} = A_e f'_c + A_s \sigma_s \quad (3)$$

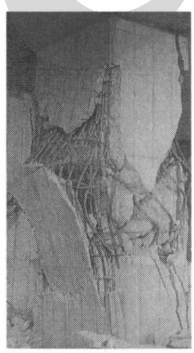

Fig.1 Damaged pier due to earthquake

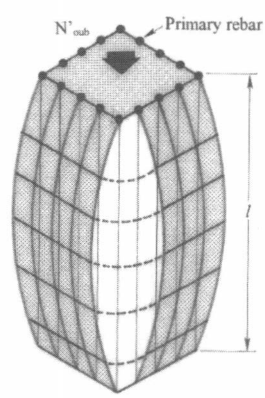

Fig. 2 Modeling of buckling of primary rebar in RC column

2.2 Experimental verification

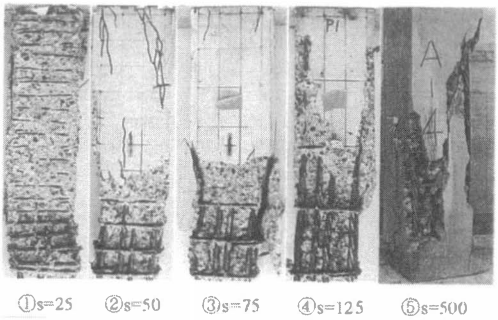

Fig.3 Failure mode of SBPD type RC column

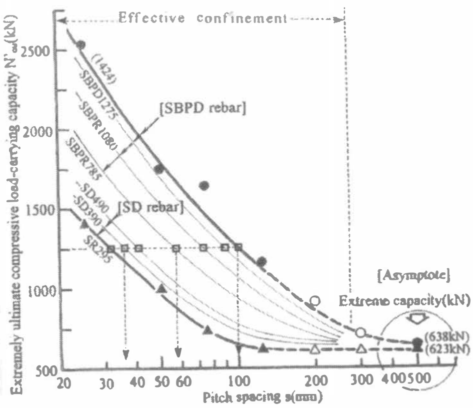

Fig.4 Three-factors relation diagram

D13(ϕ =12.7mm; SD295 type) and U13(ϕ =13.1mm; SBPD1275 type) for the primary rebars were used for preparation of the reinforcement cages. The column model size was 150×150×530mm. The nominal pitch spacing were five kinds of 25mm, 50mm, 75mm, 125mm, and 500mm. Figure 3 shows the typical failure modes. Figure 4 has made the useful relationship among the load-carrying capacity, the pitch spacing and the design yield strength to be clear. Especially, a large attention must be paid to the fact that the load-carrying capacity gradually approaches an asymptote, that is," the upper-bound of load-carrying capacity"in spite of the difference in quality of primary rebars of RC columns. The load-carrying capacity of confined RC column can be evaluated by Eq.(3) by using the " double pitch spacing"as the buckling length of primary rebar, that is $l \equiv 2s$ from the phenomenal viewpoint. The "double pitch method"fairly well agrees with the experimental values and the " Mander´s method"[2] is approx. 1.5 times larger than them.

2.3 Self-induced prestress due to deflection

The case of the nut anchorage for the primary rebar concerning the confined column-beam indicates about two times as much load-carrying capacity as that of the straight anchorage as shown in Fig. 5. Both the perfect anchorage and the strengthening of primary rebar bring forth the self-induced prestress due to flexure, and contribute to the larger deflection recovery, being important for the improvement of durability of the RC structure.

3 CONCLUSION

(1) The buckling behavior of primary rebar must be taken in the common equation of RC column.
(2) The present " double pitch"method estimates well the load-carrying capacity for the confined RC column.
(3) The high elastic recovery of deflection by using the high-strength reinforcement con- tributes to the high-performance and the improvement of durability.

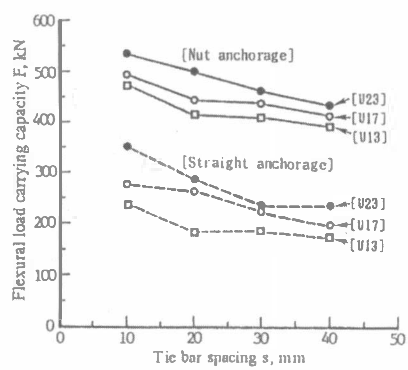

Fig.5 Tie bar spacing vs. flexural load-carrying capacity relation

REFFERENCES

[1] Sudo, M., Kida, T., Kato, K., Abe, T., Kuroda, I., Kato, N. and Kamisawa, T.: Upper-Bound Equation of Compressive Load-Carrying Capacity of RC Column Considering Characteristic of Material and Buckling of Primary Rebar, Theor. and Appl. Mech., 49, pp. 117-125, 2000
[2] Mander, J. B., Priestly, M. J. N. and Park, R.: Theoretical Stress-Strain Model for Confined Concrete, Jour. Struct. Eng., 114, 8, pp. 1804- 1826, 1988

ANALYTICAL PREDICTION OF BEHAVIOR UP TO ULTIMATE LIMIT STATE OF CONCRETE SLENDER COLUMNS

Jun Yamazaki, Nihon University, Japan
Nobuo Kasuya, Mitsui Construction, Japan
Hiroki Kouno, Kosei Ido, Nihon University, Japan
Makoto Sudou, SEEE Corporation, Japan

Keywords: Concrete Slender Column, Nathan's method, N-M Interaction

SUMMARY

Behavior of slender concrete columns such as tall piers,pylons or piles in soft ground is govemed by geometrical and material nonlinearity. The criteria for determining the partial safety factors conceming the confidence of structural behavior and analysis for the limit state design have not been prescribed in codes because of complexity of behavior and lacking information on influences of diverse structural parameters. The analysis method referred herein is economical in that it does not require convergence procedure, and by utilization of deflected shapes of the structures, affording visual perception which suites for design calculations interactively performed on computers with graphic display (utilizing "CDC"). The method is transparent. One can see on display a group of columns subjected to various states of loading. This allows one to notice change of state of column with variation in load. Moment-curvature relationship throughout the length of the column is also visible. Thus, one can judge whether the limit state is materials failure or instability. Confidence of the method should be enhanced by experimental verification. Load tests were referred for reduced scale cantilever model subjected to eccentric axial load for the predicted ultimate limit state of the instability that precedes materials failure. The tested mode of failure agreed with predicted behavior of instability. For further narrowing the safety factor, expansion of the scope of the experiment is necessary.

HOW TO USE THE "CDC" IN DESIGN PROCESS

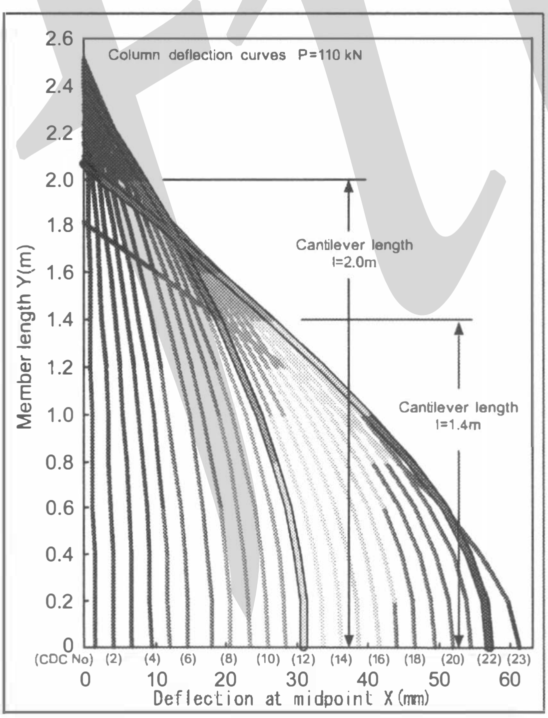

Fig.1 Instability limit state to be tested and "**CDC**"

Compression members are widely used to support heavy superstructures.

Compression members are frequently built into a straticlly indeterminate structure, and hence, loss of bearing capacity of single member does not mean collapse of the structure.

For conceptual design phase of compression members designers are free to choose whether a compression member shoud behave rigidly followed by some inelasticity, or more elastically with lesser ultimate resistance.

For the latter choice slender columns are suitable.

The use of the "Column Deflection Curves" in such design process is illustrated by an example as follows.

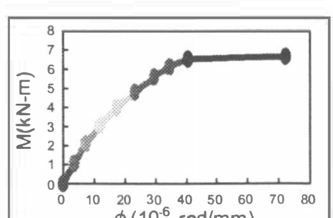

Fig.2 M-ϕ curve

EXAMPLE:

1 PROBLEM

Condition :

An axial load "P" with an eccentricity "e" acts on the member end of the cantilever beam. The cross section of the cantilever beam and the axial load "P" are known. The eccentricity "e" is unknown.

(1) In case of "short column"

When the member is in the condition of the ultimate limit state due to the failure of the cross section, How long is the column length when the moment induced in the critical section of the column is very close (for example, 94%) to the ultimate? How does the shape of that column deflection curve (CDC) look like?

(2) In case of "slender column"

When the member is in the condition of the ultimate limit state due to instability of the member, How long is the column length? How does the shape of that CDC look like?

Find out one example of each of two cases. Use the CDC group given in Fig.1. Values required to draw the CDC group are calculated by the following conditions.

- By axial load only, a uniform axial stress, P/A is equal to 11 N/mm^2.
- The cross section is 100mm × 100mm square section. • Let the side length be denoted by "a".
- The tension reinforcement ratio is 1.6%. • The section is doubly reinforced symmetrically.
- Moment- curvature rerationship of this section is shown in Fig.2.

2 ANSWER

(1) In case of "short column" : The member length is 1.4m. (2L/a=28)

- The moment of the critical section is 6.3 kN-m. The section strength is 6.7 kN-m.
- The moment of the critical section corresponds to 94% of the section strength.
- The shape of the CDC is shown by CDC No.22 in Fig.1.
- The eccentricity "e" with which an axial load acts on the member end is 26.2mm.
- The member end moment is M=Ne=(110)(26.2/1000)=2.9 kN-m.

(2) In case of "slender column" : The member length is 2.0m. (2L/a=40)

- The moment of the critical section is 3.6 kN-m.
- The moment of the critical section corresponds to 54% of the section strength.
- Accordingly, this condition is within the service limit state.
- Accordingly, the section is not subject to any damage.
- The shape of the CDC is shown by CDC No.12 in Fig.1.
- The eccentricity "e" with which an axial load acts on the member end is 8.05mm.
- The member end moment is M=Ne=(110)(8.05/1000)=0.9 kN-m.
- This value corresponds to only 31% of the member end moment of the short column.

3 SOLUTION METHOD

How to get the CDC of the ultimate limit state of the cantilever beam of an arbitrary length "L"? In the Fig.1, a horizontal line which passes through a coordinate "L" which locates on the Y axis line is drawn. This horizontal line and 23 columns make 23 cross points. The point of the largest eccentricity "e" is selected from these 23 cross points. Find out the CDC which passes through that point.

4 WHAT IS THE "CDC"?

Fig.1 is a collection of the "Column Deflection Curves" that are in equilibrium when axial load acts along Y axis. We selected 23 columns but the number of selection is arbitrary. The color of the columns represents the moment acting on that section. The value of the moment can be found from the portion of the same color on the moment - curvature relationship shown in Fig.2. Consider any arbitrary length L. Plot a point at coordinate L on Y axis. Draw a horizontal that passes through that point. Consider the group of column deflection curves below this line. These are cantilever beams each of which is acted on an axial load with member end eccentricity equal to the distance of the tip of cantilever column to Y axis, "e". The member end forces composed of axial force N with eccentricity e are identical to axial force N and moment M=N•e.

REFERENCE

[1] Nathan, N.D. (1972), "Slenderness of Prestressed Concrete Beam Columns". PCI Joumal, Vol.17,No.6.

STUDY ON THE NON-LINEAR DYNAMIC ANALYSIS OF RC ARCH BRIDGES SUBJECTED TO LONG PERIOD WAVES

Xia Qing
Doctoral course student
Kyushu University

Hisanori Otsuka
Professor
Kyushu University

Keywords: dynamic analysis, material and geometric non-linearities, long-period seismic wave

1 INTRODUCTION

The studied bridges are a 600m-span reinforced concrete arch bridge and a 100m-span half-through type reinforced concrete arch bridge. This paper compared the behavior of bridges subjected to long-period and short-period waves, and it also reveals the effects of material and geometric non-linearities in the dynamic analysis for two bridges with large seismic waves.

2 STUDIED BRIDGES

Two types of bridges were chosen in this study. **Fig.1** shows the outline of these bridges. The 600m-span RC arch bridge is a bridge studied in JSCE committee[2)] and the half-through type RC bridge is the largest existing one of this type in Japan.

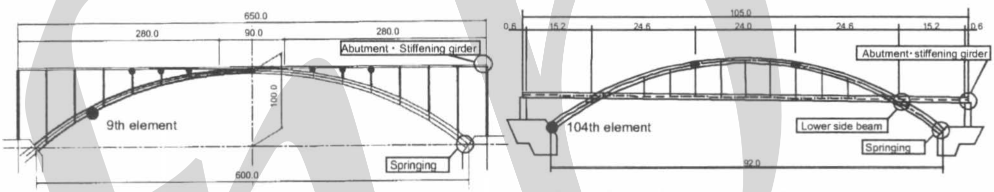

Bridge A: 600m-span reinforced concrete arch bridge

Bridge B: 100m-span half-through type reinforced concrete arch bridge

Fig.1 Outline of the studied bridges (in m)

3. LONG-PERIOD SEISMIC WAVE

Because both bridges have long natural periods that are more than 2.0 sec, it is an interesting topic to study the effect of a long-period seismic wave. The direction of inputted waves is decided considering the amount of the effective mass, therefore the direction of inputted wave is transverse for the bridge A and longitudinal for the bridge B, respectively. Newmark ß method (ß=0.25) was used, and the time interval in numerical calculation is 0.001 sec.

The response acceleration spectra of seismic waves type 112 and type 212 are shown in **Fig.2**. Type 112 is a plate boundary earthquake wave and type 212 is near fault earthquake wave.

In order to grasp the behavior of the rib, the displacement and the moment time-histories of the 9th element for the bridge A are shown in **Fig.3** and **Fig.4** respectively. Acceleration response of type 112 wave is larger than that of type 212 wave for the natural period of 7.0 sec. It is the reason why the responses for type 112 wave are larger than that for type 212 wave.

Inputting type 112 wave, both the periods of the displacement and the moment time-histories are about 7.0 sec until the maximum response value, and this period is same to first natural period of the bridge A. But

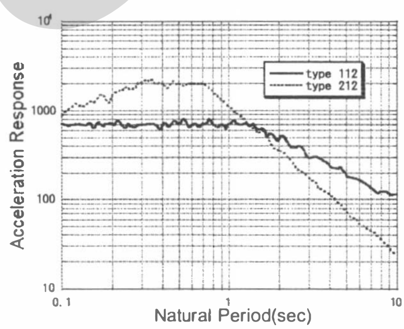

Fig.2 Response acceleration spectra of inputted waves

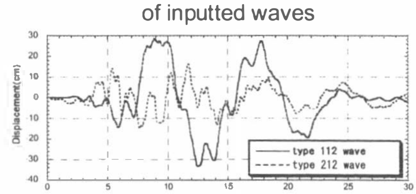

Fig.3 Displacement time-history of the 9th element

the period became longer after that time, i.e. 9.0 sec, because a part of the bridge members entered the plastic range.

While inputting type 212 wave, the period of displacement is about 1.5 sec until the maximum displacement, this period is close to the 5th natural mode. After the maximum point, the period became up to 7.0 sec. The responses of the bridge B show the same inclination as the bridge A.

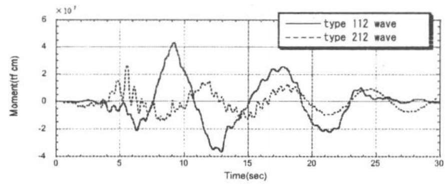

Fig.4 Moment time-history of the 9th element

4. MATERIAL AND GEOMETRIC NON-LINEARITIES

In this section, two analytical cases for bridge A and B are selected. In the case A-1 and B-1, only material non-linearity is considered, and in the case A-2 and B-2, both non-linearities are considered. The waves are inputted in three directions, and type 111 and type 112 waves are used for horizontal directions and observed waves at same site, JMA KOBE_ud is used for vertical direction.

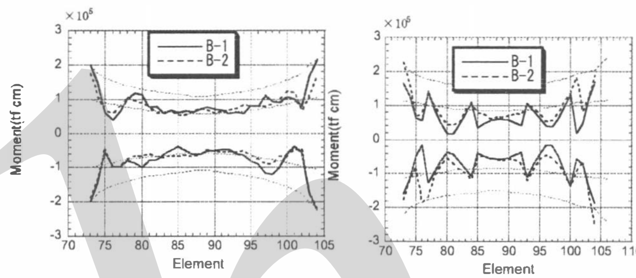

Fig.5 Maximum moment of arch rib (bridge B)

The maximum moments of arch ribs for the bridge B are shown in **Fig.5**. The out-of-plane bending moment in B-2 becomes larger than that in B-1, and over the yield moment.

The time-history of out-of-plane bending moment for 104th element is shown in **Fig.6**. The period of moment is about 1.0 sec for both cases, but after 9.0 sec that is the time when the moment is over the yield point, the moment in case of considering the both non-linearities can not come back to the 0 axis.

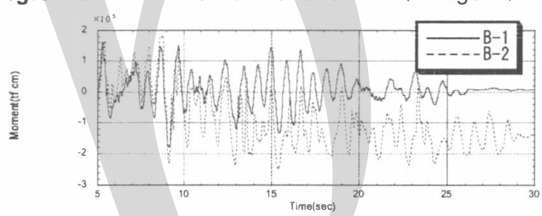

Fig.6 Bending moment of out of plane time-history in the 104th element(bridge B)

On the other hand, the moments of the bridge A are almost same amount in both cases. The period of moment became longer when geometric non-linearity is considered. But the amplitudes of response are almost same for both cases.

The span of the bridge A is much longer than bridge B, but the effect of geometric non-linearity is larger in bridge B.

5. CONCLUSION

The following conclusions may be drawn by this study:

1) The natural periods became longer by considering geometric non-linearity.

2) For the 600m-span arch bridge (bridge A), the response for type 112 wave is larger than those for type 212 wave, the reason is that the bridge has long natural period and the acceleration response for type 112 is larger for this period.

3) In case of the bridge B, the response differences by two inputting waves are large, because of the members enter the yield zone and the decreasing rate of moment becomes very slow.

4) The effect of both non-linearities in the bridge B is larger than that in the bridge A, because of the plastic behavior of members in the bridge B.

The paper shows the effects of long-period wave and necessity of considering geometric non-linearity, and it clarifies the importance considering the long period waves and both non-linearities for the dynamic analysis of an arch bridge.

REFERENCES

1) Japanese specification of seismic design for highway bridges, 1996

2) T.Mori, T.Yamamoto,N.Tamehiro and J.Niwa: The state of the Art and The Future Prospects on Long-span Concrete arch Brides, Concrete Journal, Vol.39, No.3, Mar.2001

ON HOW CONCRETE SPATIAL STRUCTURES CAN BE BEAUTIFUL

Mamoru Kawaguchi
Hosei University
JAPAN

Keywords: esthetics, design of structures, concrete shells, spatial structures, beauty of structures

INTRODUCTION

In 1912 Max Berg realized a concrete arched dome "Jahrhunderthalle" in Breslau (currently Wroclaw in Poland) having a span of 65m, recording the first concrete spatial structure that had a span exceeding that of Pantheon in Rome. Concrete thin shell structures started to be built in 1922 when a planetarium of 16m in diameter was constructed in Jena by Walter Bauersfeld and Franz Dischinger. The record of Jahrhunderthalle was renewed in 1928 by a market hall in Leipzig designed by Hubert Ritter, having a span of 76m. Then many concrete shells followed, first in Europe and then all over the world. Eduardo Torroja played an important role in development of shell structures, when he suggested the possibility of creating novel shell forms not only by choosing from among geometrical surfaces with boundary conditions favorable for analytical solution, but also by attempting freer forms with freer boundaries on the basis of sound intuition and experimental methods of confirming structural safety. In Japan joint works of Kenzo Tange and Yoshikatsu Tsuboi created several new, beautiful examples of concrete shell structures after the World War II.

Fig.1 A Residence in Matsumoto

The future of shell structures thus seemed prosperous until around nineteen sixties, but then they became to be built less and less, and today it is often said that the concrete shell structure is dying. The present paper reviews this issue first, and then describes the author's attempts to realize rational and esthetic shell and spatial structures, citing the built examples as follows in which he has been involved as the structural designer.

THE AUTHOR'S ATTEMPTS

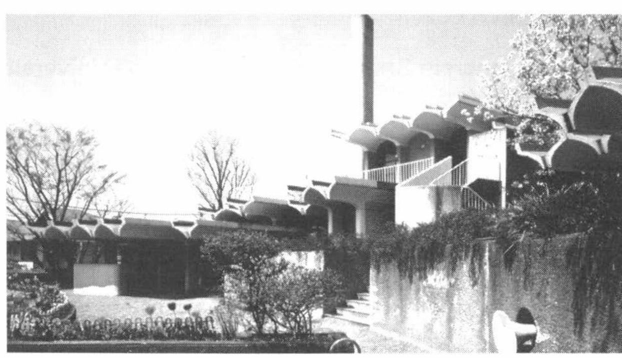

Fig.2 A Kindergarten with Prestressed Concrete Roof

In the first example of a residence, the function of the building is divided into two parts: the living part and the "shelter" that protects it. The living part should be changeable so that the family can enjoy their lives in it to the highest extent at any time, while the shelter should protect the lives as long as possible without changing its structure. The residence has been accomplishing its task so far in the above direction. The concrete shell roof designed as a part of the shelter having deep, cantilevered eaves of hyperbolic paraboloids is esthetically satisfactory as well.

In the second example of a kindergarten the roofs are constituted by cylindrical units having the sectional shape of a flying bird, prefabricated and prestressed in the site. The shape and the dimension of the roof are suitable for a kindergarten. Prefabrication in the site was the most economical solution for making the cylindrical units, and simple prestressing along the axis of the cylinder was sufficient to put the most part of the shell in compression.

The third example of a convention center shows the possibility of high computational ability of our age that can be applied to a shell with a peculiar boundary which would have been impossible to solve without the aid of computers. The shape of the shell with the peculiar boundary shape has a certain architectural impact. The shell was prestressed by a sophisticated arrangement of the cables for the most efficient stress distribution in the shell.

The effect of structural "articulation" is discussed in the fourth example of a football stadium. By structural articulation it is possible to find structural components that are stressed in pure compression.
Concrete is an ideal material for such components. In the present example prefabricated, prestressed concrete piles are used for those components. This technique satisfied the architect's dream of the roof that was "floating in a copse".

Natural stone such as granite is a material that is very close to concrete in the sense that both materials are strong only against compression. In design of a footbridge as the fifth example the author adopted granite blocks for the deck of the bridge which is the upper chord of the lenticular structure. To make the whole deck "monolithic" it is prestressed in the longitudinal direction. This idea together with the concept of "incomplete truss" made the bridge rational and esthetically satisfactory.

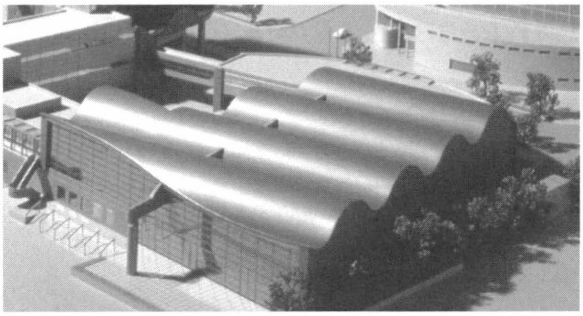

Fig.3 Kitakyushu International Convention Center

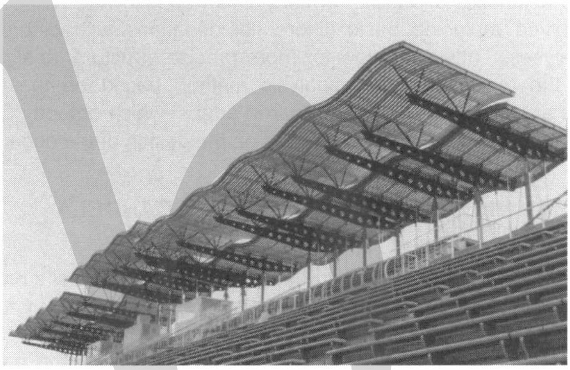

Fig.4 Tochigi Green Stadium

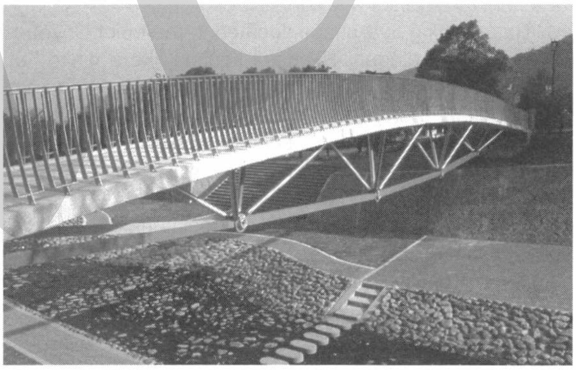

Fig.5 "Inachus" Granite Footbridge

REFERENCES

1) Kawaguchi, M. et al.: Design of prestressed concrete sinusoidal shells with irregular boundaries. 5th Int. Conf. on Concrete, Sept., 1990.
2) Ohta, K.: The House in Matsumoto City (in Japanese). Kenchikubunka, Feb.,1971
3) Tange, K.: The Yukari Bunka Kindergarten (in Japanese). Shinkenchiku, Sept., 1967
4) Kawaguchi, M.: A few examples of prestressing in spatial structures. IASS Int. Symp.,Nov., 1997

HYPERBOLIC PARABOLOIDAL SHELL AND FELIX CANDELA

Mutsuro SASAKI Eisuke MITSUDA

Nagoya University ,Nagoya ,JAPAN *Sasaki Structural Consultants ,Tokyo ,JAPAN*

Keywords : membrane stress theory, free edge design, Aesthetics of Felix Candela

1. INTRODUCTION

In general, a realistic design for hyperbolic paraboloidal shell(HP shell) starts with an accounting of membrane stress theory, followed by a rough estimate and grasp of the overall qualitative characteristics of shells. Formerly, this was followed by the conventional direct analysis method, which involved replacing basic differential equations with difference equations and performing numerical analyses. Today, to allow for more precise structural analysis, detailed structural design is performed by the direct numerical analysis method based on the finite element. I would like to clarify the characteristics of HP shell with free edges, which embody Candela's structural rationality and sense of beauty, with a particular emphasis on the design of the edge beams at the boundaries.

2. SAN VICENTE DE PAUL BY FELIX CANDELA

Fig.1 Hyperbolic paraboroidal roof of San Vicente de Paul

I would now like to introduce the work of a typical structuralist of the mid-20th century, the San Vicente de Paul by Felix Candela. In this work, Candela sought to fuse structural rationality to artistic formations of reinforced concrete shells working on the basis of the membrane stress theory. Candela's Catholic Church is a typical architectural design of multiple reinforced concrete HP shell. The effects of HP shell are apparent in an interior space filled with characteristic skylines and lights.

This building is a chapel located in the quiet Coyoacan district in Mexico City, an elegant HP shell floating like a white hat in a green grove. The building was completed in 1959 in collaboration with Enrique de la More, an architect, representing a work in the Candela's prime. Three HP shells with a span of 17.385 m x 14 m, a height of 14 m, and average thickness of a mere 4 cm, are laid out on a flat equilateral triangular surface with a single side of 34.67 m, nestling close to each other. The shells are supported by three inclined columns (resultant forces from the edge beams of the respective shells are applied) located at the center of the respective sides of the triangle. The lateral thrusts from the inclined columns are designed to abut tie beams to prevent disturbing the position of the base.

The 17.385-m long upturned tips are cut off from hyperbolic paraboloidal surfaces by straight lines, giving the HP shells an air of lightness and dynamism, with sharp-looking free edges. These light edges were made possible by the ingenious design of edge beam sections. Outside the building, all edge beams are 8 cm thick, for visual harmony. Inside the building, they gradually increase the depth as they descend. Edge beams with light non-uniform sections give an impression of grace and lightness. There are also slots for toplights at the connecting sections of the three HP shells. The respective sections are connected with steel lattices, with sheets of fixed stained glass. This creates a beautiful fusing of the rising hyperbolic paraboloidal surfaces and lights, creating soaring and floating interior spaces. A structural solution to the boundaries with the use of steel lattices is very unique.

The marvelous HP shell designed by Candela were based on fundamental membrane theory. Now, for reference, I would like to provide the results of detailed analyses of stresses and deformations of accurate analytical models, which integrate peripheral edge beams and internal steel lattices, based on the finite element method, which is the general analytical method in use today. We learn from these analytical results that membrane theory offers only an incomplete model with which to perform calculations and does not necessarily recreate the flows of the forces of actual HP shell. For instance, according to membrane theory, uniform sheer forces are generated within shells, and principal stresses of the same values, which become compression and tension, are generated at upward- and downward-facing parabolas oriented at 45 degrees to the axial bus bars. But this is incorrect. In fact, peripheral edge beams are deformed toward the inside of shell surfaces, thus generating no tensile principal stresses at the downward parabola. The load of a roof is transmitted to edge beams or support structures (inclined columns) primarily by the arches that transmit the compressive principal stresses within the upward parabola. Therefore, since the axial forces of the edge beams are decreased by these values, which are considered to be generated by tensile principal stresses under membrane theory, the sections of edge beams can ultimately be minimized and designed almost like free edges. When intermediate support points are not provided for edge beams, the deflections at the tips appear to be small, and the mullions serve as secondary supports. It is possible to build steel lattices using delicate members used in actual shells. Candela must have understood these things intuitively. Even with today's technology, designing and building of such sophisticated HP shell is difficult. This sophisticated design would not have been possible ,if Candela had not consistently sought to develop HP shell with free edges. This was a feat of which only Candela was capable.

Results of analyses based on the finite element method

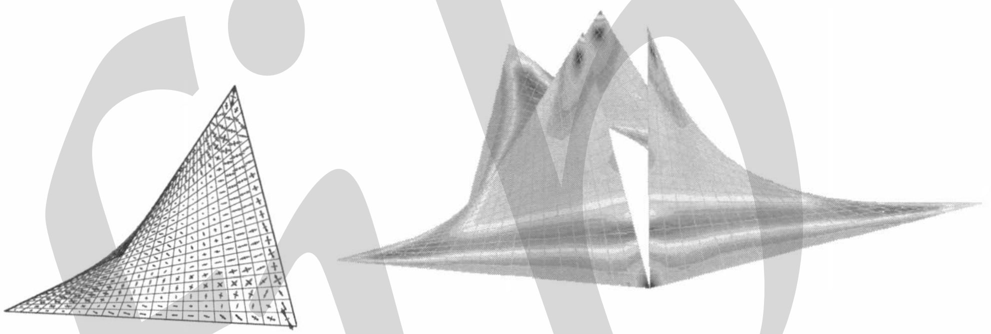

Fig.2 Drawing of the principal stress of the shell

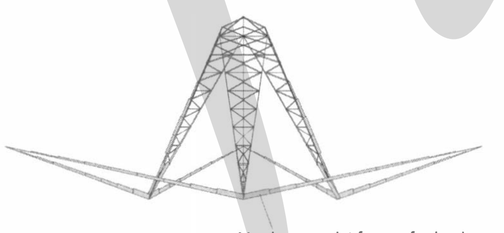

Fig.3 Drawing of the axial forces of edge beams and steel lattices

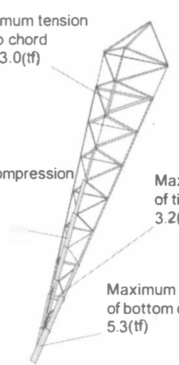

Fig.4 Axial forces of lattice members

REFERENCES

1: Wataru Kato,Toshio Nishimura : design of curved plate structure, Shokokusha,1963
2: Yutaka SAITO,et al.: Felix Candela, TOTO-publications,1995

ACHIEVING CONCRETE AESTHETICS THROUGH "TOTAL DESIGN"

Arata Oguri
Senior Associate
Arup Japan

Bob Cather
Associate Director
Arup Research & Development

Shigeru Hikone
Principal
Arup Japan

Keywords: Concrete, Appearance, Structures, Microstructure, Design

1 INTRODUCTION

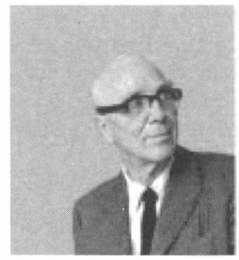

Fig. 1 Sir Ove Arup (1895-1988)

In 1970, the founder [**Fig. 1**] of the authors' practice stated; "It (a structure) should be pleasing aesthetically, for without that quality it doesn't really give satisfaction to us or to others." Then, he introduced a concept of Total Architecture where "all relevant design decisions have been considered together and have been integrated into a whole by a well organised team empowered to fix priorities." It is this belief that has led the practice to the Total Design approach, in that "a desired result would be produced by intimate integration of the various parts or the various disciplines".

Since then, the practice has been associated around the world with a number of building and civil projects where aesthetics plays a definitive role in their fame. Amongst those, there are several notable projects where the authors believe the aesthetics in concrete was one of the key factors for their success, for which a close collaboration between designers, architects, structural engineers and contractors (and in some cases precast concrete manufacturers) from early stages of the projects was essential.

This paper proposes the classification of concrete aesthetics into two categories. Then, by illustrating recent project examples for each category, various aspects of concrete aesthetics and its driving forces are discussed.

2 TWO CATEGORIES OF CONCRETE AESTHETICS

To analyse the concept of concrete aesthetics, it is judged that the aesthetics in concrete can be considered in the following two categories;

- Aesthetics in FORM
  which is related to either an overall form or an elemental shape of concrete structures, and
- Aesthetics in the MATERIAL
  which is the matter of constituents and microstructures of concrete.

Each of the above two categories is separately discussed and the concept is elaborated by examining specific issues related to concrete aesthetics in the design and construction of actual project examples from around the world.

3 AESTHETICS IN FORM

The aesthetics in FORM is achieved by integrating the following elements;

- the sharing of design intention among project team members,
- discovery of rational geometry and structural form, and
- due consideration to be given to buildability, ie consideration of the interaction of the design and the construction processes.

Fig. 2 Sydney Opera House, NSW, Australia

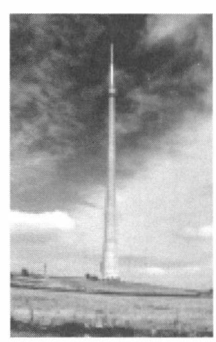

Fig. 3 Emley Moor Television Tower, UK

Some of the unique characteristics of concrete have been fully exploited to achieve the aesthetics, namely high compressive strength, high durability and high plasticity.

In the quest for height, a tall building and a tubular shell with a unique profile were realised by utilising high compressive strength of concrete when hardened. Various architectural forms were achieved, such as

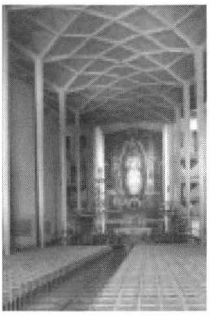

Fig. 4 Coventry Cathedral, UK

ribbed arch roof, long spanning wave-form folded plate floor, double layer shell and floating spaceship, all by repeating a limited number of types of standard shaped precast units and by laying them out side by side. Changing section profiles were easily achieved for rotated footbridge, tapered slender columns and candlestick-like columns due to high plasticity (ie. easily moulded into any desired shape) while still wet. Even a 'concrete catenary' was successfully completed.

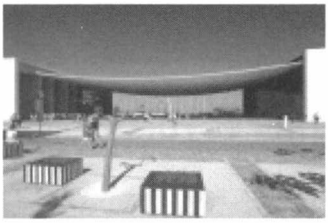

Fig. 5 Portuguese National Pavilion, Lisbon

4 AESTHETICS IN MATERIAL

The aesthetics in the MATERIAL is achieved by combination of;

- recognising the potential for colour and texture,
- the contributions of the individual concrete component materials and the resulting microstructural response of the concrete,
- recognition of the need to communicate the desired quality to all those in the construction chain,
- awareness of the critical interaction of the construction processes with design.

Fig. 6 Judge Institute, Cambridge, UK (not Arup).

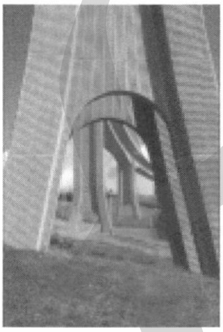

Fig. 7 Byker Viaduct rib piers

There are particular technical aspects that should be considered and used as route markers to achieve the desired and pleasing outcome. One of the more difficult aspects of concrete aesthetics is for the creator or the imaginer to convey to others the nature of the desired outcome and what, if any, departure from 'perfection' is acceptable. Concrete in structures is not a perfect and fully homogeneous material. Therein lies some of its attractiveness.

Some of the aspects of concrete, such as colour, texture, visual defects and weathering or in-service performance, are described with project examples where the materials of concrete and their combination influence and contribute to the ultimate appearance.

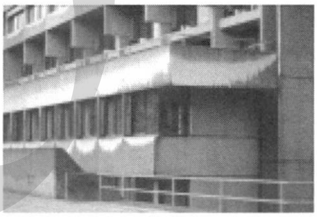

Fig. 8 uneven or uncontrolled water flow

5 CONCLUSIONS

It is shown that there are some essential ingredients to achieve the excellent aesthetics in concrete, not to mention a thorough understanding of clients brief. The in-service performance, particularly retention of pleasing appearance, stems from both structural form and details and from the component materials and their combination into a concrete.

The Total Design approach is an integral part in the achievement of concrete aesthetics and all those concerned should always have the totality and interdependency of this necessary approach in their minds throughout the planning and implementation stages of projects.

REFERENCE

[1] Sir Ove Arup: The Key Speech, given on 9 July 1970 at an internal meeting of Ove Arup Partnership (obtainable at http://www.arup.com/about/pdfs/key_speech.pdf)

TOWARDS THE FUSION OF ARCHITECTURAL DESIGNS AND STRUCTURAL TECHNOLOGIES ---FOR THE DESIGN AND EXECUTION OF THE SAITAMA PREFECTURAL UNIVERSITY---

Katsunori Kaneda
Structural Designer, Structural Design PLUS ONE Inc.

Keywords: beauty of concrete as a material, structural system,precast prestressed concrete

1 PREFACE

Precast concrete ("Pca") in architecture may be divided into two types: PCa mainly for curtain walls, internal walls and other such non-structural member uses and PCa for such uses as columns, girders, seismic-resistant walls and other such structural members. In Japan, despite being the same PCa, both types have undergone different processes of evolution into different pricing systems and different manufacturers to date.

But, if sectional shapes of members should be optimized, if studies should be made to make member-to-member connections in esthetically agreeable form, and if product PCa members can be handled with proper care and caution, PCa as a structural member would eliminate the need for additional finishing materials for it. Here, PCa as a finishing material and PCa as a structural material become fused as one and the same, thus demonstrating the full potential of its rationality.

As an example of this basic concept, the author wishes to introduce an outline of the recently designed Saitama Prefectural University, for reference.

Fig.1 View from 1st floor

Fig.2 View from 2nd. floor

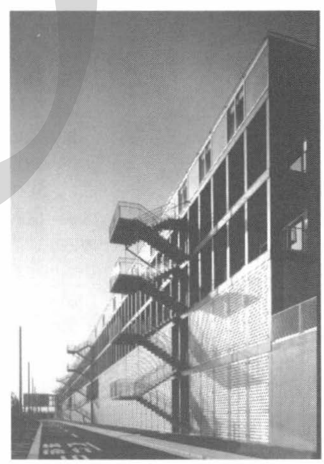

Fig.3 Exterior View

2 BASIC CONCEPT OF THE DESIGN

In the past, universities were often finely divided into numerous study rooms and laboratories for mutual nonintervention. Here, in this new university, in order to create space which visually achieves the oneness to facilitate the daily learning of interpersonal relationships, the whole structure has been given as high transparency as circumstances permit.

Consequently, by minimizing the size of structural members, the design sought to minimize the presence of obstructions to lines of sight wherever practicable. Further, excluding anything decorative, the design sought to explore the possibility of forming space by the use of outdoor daylight and straight-line structural components alone.

3 GENERAL PLAN

In order to make this concept the column size were reduced 230mm x 630mm.

Also, flat girders, with height held down to 400mm, were adopted. In addition, to secure seismic safety, steel-reinforced concrete earthquake-resisting walls, which are to bear most of horizontal forces at times of earthquake, were provided at every four grids (30.8m).

In this manner, it became possible to design the main frame structure as a rigid-frame structure consisting of columns, which were so narrow in width as to look like louvers and were also thin, and girders which were so heavy and thick as slabs.

To resolve many problems, and also to secure structural strength and express the beauty of concrete as a material, it was decided to design as many sections of the structure as possible as a precast-prestressed concrete ("PCaPC") structure.

On this project, by designing the structure as a PCa system, the system itself was applied as a rule common to the structural design, equipment designs and all the segments involved. Thus, once the system had been completed, many sections of the building were determined as if they were derived from the system.

Consequentially, the systematized PCa structure, not only being important structurally, but also came to have a meaning of added importance as one major determinant affecting the character of the whole building.

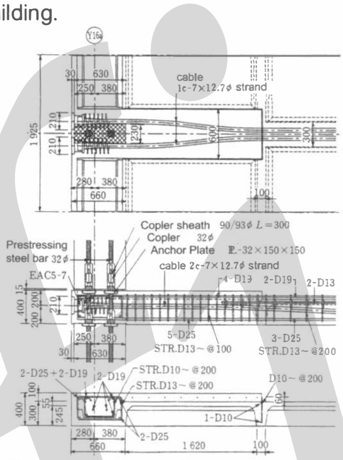

Fig.4 Detail of PCaPC members

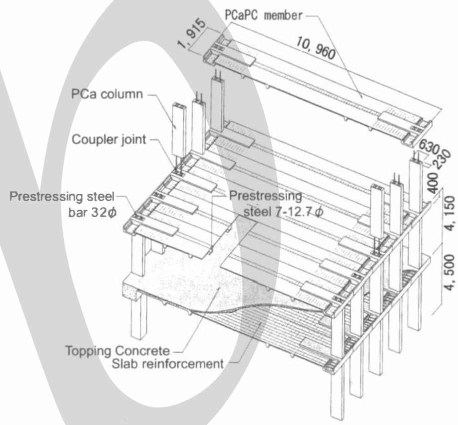

Fig.5 Assembly diagram

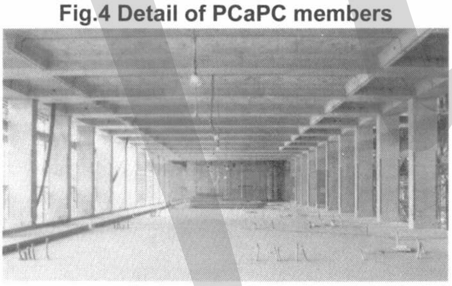

Fig.6 View of PCaPC

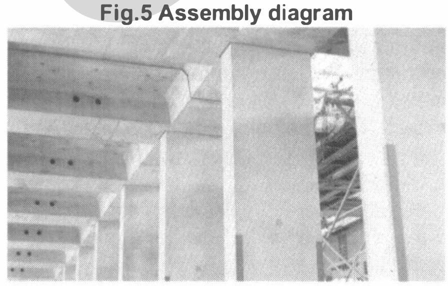

Fig.7 Detail of joint

4 CONCLUSION

The PCa PC structure, despite its 80-year-long history since its first use for bridge girders in the 1920's, cannot be said to have come into widespread use today.

Nevertheless, against the background of the mounting concern over the global envir9onment and increasingly acute shortages of skilled labor at construction sites in recent years, cases in which PCa is used throughout the structure in one way or another are beginning to increase in numbers.

It is both useful and necessary to use PCaPC to its unique advantage and keep on proposing to society such PCaPC structures as to fully demonstrate their worth in responding to diverse needs of future structures.

COMFORTABLE AND BEAUTY IN SMALL ARCHITECTURE

Masahiro Ikeda
Masahiro Ikeda Architecture Studio

Keywords : Architecture, beauty, comfortability

1 INTRODUCTION

Concrete has some characteristics compared to steel; the strength of concrete is not as high as that of steel, but it is easy to make plain or curved surface according to the concept of architects, and then it is durable material against fire. The designing of architectures is based on the better understanding the characteristics of both materials and to create a comfortable figure for humankind. The "Figure " expresses the both outside shape of the architecture and inside structure of it, and it contains some spiritual aspects or awareness of the architects. How to inform the figure to people?, this is the point where architects are now confronted with. There is something to exist before phenomenon will occur, this is to say "Original Figure", and many musicians and poets have been struggled with the original figure in order to express them by means of sounds and words. Architects are in the same circumstance and try to express their original figures by means of concrete and steel. The following designs are the expression by an architect who feels and aware the inspiration from the landscape and the interesting combination of materials and forms.

2 STANDPOINTS OF ARCHITECTS

There are some standpoints of architects who try to express their original figure to their architectures; scale, structure, beauty and comfortableness.

Scale;

When we design small architectures, we must think about human scale

Structure;

Strength is not only the characteristics of materials, but also the result of combination of forms and materials, but at the same time, we also think about safety and economy of architectures. It means that we need strong and economical structures.

Beauty and comfortableness;

Sometimes architect and structural engineer want contrary things. It is very often that the opinions about aesthetics are different from each other. Even though they require beauty and comfortableness, the outputs are different, so it is very unique for each professions to mix their opinions and collaborate each other. When we express different opinions and discuss about them, we can sometimes design something new. It will give comfortableness to many people as well as beauty. This is why I design architecture on the point of both architect and structural engineer.

3 EXAMPLE

Here are three examples of small architectures of concrete structure. One is pure concrete structure and the other is hybrid of steel and concrete.

Y house	architect = Keiichi Irie and Masahiro Ikeda	construction = concrete
A house	architect = Yasuhiro Yamashita and Masahiro Ikeda	construction=concrete and steel
Natural Unit	architect= Masaki Endo and Masahiro Ikeda	construction=concrete and steel

1) Y-house

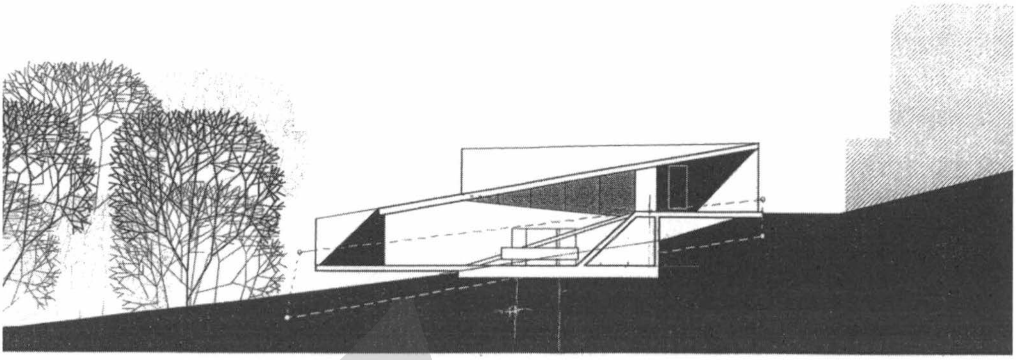

2) A-House

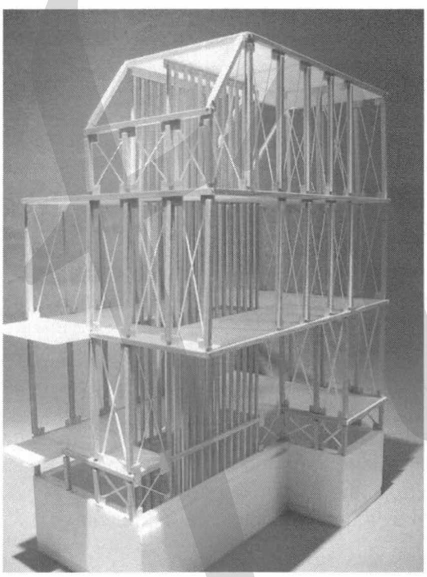

3) Natural Unit

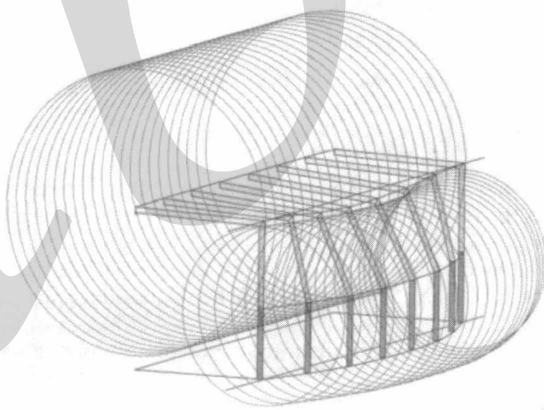

PURSUIT OF IDEAL PLANE STRUCTURE BY FULLY UTILIZING CHARACTERISTICS OF CONCRETE -CREATION OF SPACE BY ADAPTING "BOX STRUCTURE"-

Hirokazu TOKI
Nikken Sekkei,JAPAN

Keywords: Box Structure ,Plane Structure

1.INTRODUCTION

Materials that compose architectural space have their own characteristics and intrinsic values. Any architectural space that is created making the most of the particular advantages of materials used is beautiful. Concrete as a construction material has the following two great advantages unique to it.

1)Concrete is plastic material and can be formed into almost any shape.

2)By using concrete, plane structure, which is not a structure consisting of linear structural members but a structure consisting of plane structural members, can be built.

The author is proposing the use of the "box structure" as structural frame which makes the most of the favorable taste of the continuous structure. This paper is to discuss the structural characteristics and space-making advantages of such box structure.

2.BOX STRUCTURE

"Box structure" is based on a concept which considers the whole building as one box forming a space making the most of the characteristics of concrete Every part of the box structure building takes part in stress resistance while on the other hand contributing to the space formation and functions of the building.

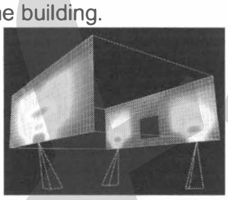
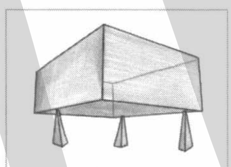
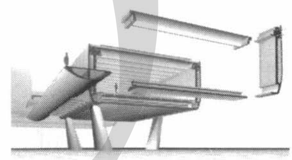

The advantages of space creation by this "box structure" include the harmony with the surroundings as "open system" while securing the functions of the interior space as "closed system" which is foreign to the surroundings.

Based on two actual examples, discussions will be made of techniques to attain harmony between the functions of the internal space and the surroundings using the "box structure" technology.

○A building which fits into its surroundings and satisfies the functions required of a museum

This is a building located in a national historical site, which used to be the site for an ancient castle.

Each museum building was so planned as to be floated up in the air and supported by three columns to avoid disruption of the rich natural environment by locating buildings and,to avoid disturbing the excavated old roads crossing the site.

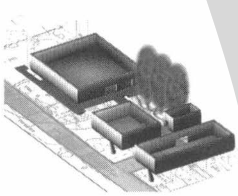
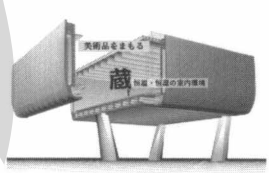
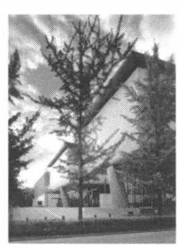
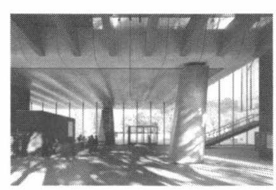

Furthermore, an internal environment like that of so-called "warehouse" was targeted creating double structure wall sandwiching heat-insulating materials in between. To solve the problem of how to actualize the buildings afloat on those seemingly instable three legs, the idea occurred was the "double-skin box", which may well protect the works of art. "A closed box is strong!" Is it not possible to depend on this philosophy? Let us assume the whole building to be one box. And it was decided to fabricate this double-core structure having a complicate configuration as a precast concrete structure.

Complicated expressions can be taken in while the products are being moulded in the factory . In designing these buildings, efforts were made to have the "box structure" of PcaPC embody the "commodity" or the function as warehouse to protect works of art, the "firmness" or a rigid box structure, and "delight" or the facade of a museum in the midst of nature.

○Configuration without a feeling of offence to the surroundings with functions as experimental facility and sufficient research space, -safe, comfortable and dynamic, all by the "PC Box Structure" and "Seismically Insolated Independent Legs" -

This building is located on a site close to a housing area and consists of experiment rooms and researchers' offices. Therefore, it was proposed that the office building with the seismic isolation mechanism be placed upon the experiment rooms/storages building to create one composite building symbolically demonstrating the safety of a seismically isolated building and generating ample outdoor open space within the site.

And, it was decided that the entire walls be deemed to be one integral structure with holes(windows) occurring at regular intervals. In other words, the entire structure was considered to be a box to be supported by independent columns. In the case of this building, flexible space can be pursued in its interior as its perimeters are rigidified with "rigid box".

An attempt was made to express the feeling of security that a seismic vibration isolated building posseses by the dynamic appearance of the "box structure" afloat in air consisting of the "box structure" and the "seismically isolated independent columns" and to create an internal space, open and integral, by rigidifying the perimeters by means of the box structure combined with steelframework


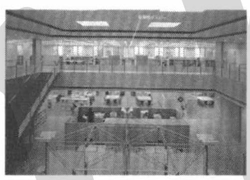
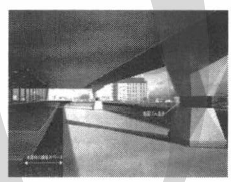

3.COMBINATION OF "SURFACES" AND "LINES"

Concrete, which generates plane structures, is able to create a variety of space when combined with other materials. Left figure shows examples of combination with steel. These are historical museum buildings planned on a site halfway up the mountain looking out on the town.Right figure shows an example of combination with wood. The building is the auditorium of a kindergarten located in the mountain's breast

In the exterior, the feeling of narrowness is alleviated and melting into the surroundings by lifting up the structure and, in the interior, the "lines" by wood and steel made of gently and elegant envelopes . respectively with the line material, steel, timber.

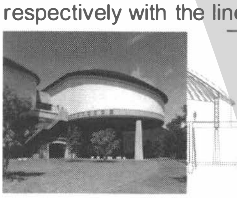
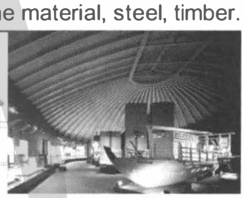
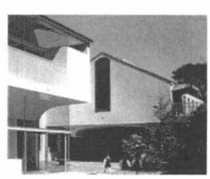
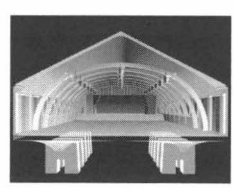

4.CONCLUSIONS

The greatest characteristics of concrete as construction material are that it is capable of forming a continuous structural body which is not a combination of parts.This paper has discussed the creation of exterior and interior space by the "box structure", which takes the advantages of the characteristics of plane structure, showing some actual examples.

It must be used to incarnate the "function of inner space". Potentials for space creation are ever increasing through upgrading of the performances of materials and development of techniques. It is necessary for structural engineers to pursue the characteristics of materials as well as the optimal space creation by means of the optimal structural engineering.

AN APPROACH TO STRUCTURAL BEAUTY IN SMALL-SCALE REINFORCED CONCRETE BUILDINGS

Alan Burden DEng MSc DIC CEng MICE MIStructE
Structured Environment Limited / Kanto-Gakuin University, Japan
www.structured-environment.com alanburd@tka.att.ne.jp

Keywords: beauty, unified design, structural system, reinforced concrete

1. INTRODUCTION

This paper describes the structural aspects of three small buildings in reinforced concrete designed recently by the Author. Special attention is paid to the relationship between the structural and spatial design in each. In particular, the attempts made in each to unify the structural and functional aspects of the design are investigated.

2. HOUSE IN TOKYO

The first project is a typical RC house project in Tokyo. The building is known in Japanese publications as 'House in Tokyo'. A four-storey structure was required in order to accommodate the desired floor area on the small site (Figure 1). A mix of shear wall and moment-frame structural systems was employed to achieve a tall narrow form with an open facade facing the street (Figure 2).

Figure 1 General view

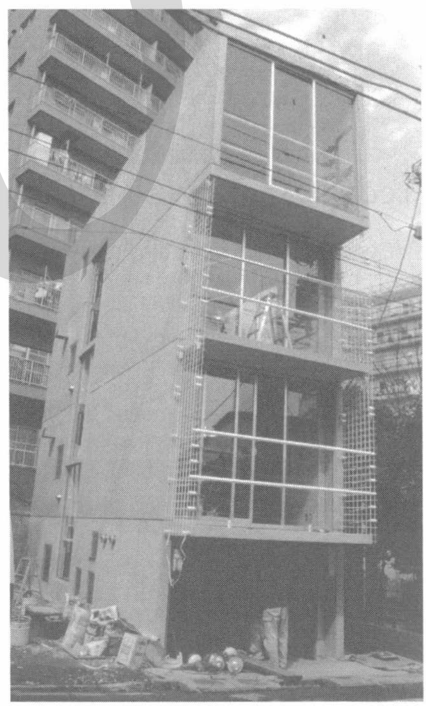

Figure 2 Front facade

3. ORANGE FLAT, SENDAI

The second project, known as 'Orange Flat', is a three-storey condominium located in Sendai (Figure 3). Flat plate construction is used (still rare in Japanese RC buildings). The building is divided into two blocks with a communal courtyard between. The structural system spans this courtyard on the second and third levels with diagonal concrete link bridges. These serve to link the slabs on either side with sufficient stiffness to almost eliminate the eccentricity of the building mass with respect to the shear wall shear center (Figure 4).

Figure 3 General view

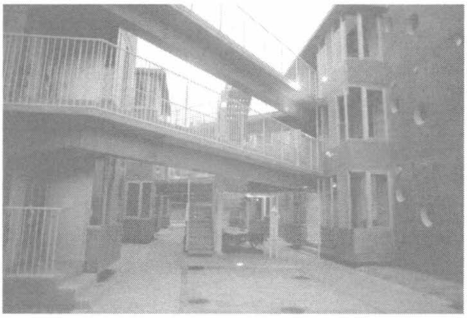

Figure 4 Link bridges over courtyard

4. HOUSE IN HODOGAYA 2

The final project is known as 'House in Hodogaya 2'. A parking area was required on the ground level of the triangular site. This was formed by making a cut across the site. An RC slab and retaining walls were used to stabilize the space thus formed (Figure 5). A further slab was the cast to form the second level floor structure. This was supported on its periphery by a series of stainless steel flat bars cast into the concrete. Finally the main living space was constructed in timber over two storeys on top of the second level slab (Figure 6).

Figure 5 General view

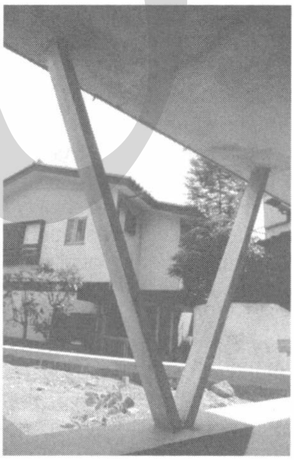

Figure 6 Second level slab support struts

5. PROJECT DETAILS

House in Tokyo: architect – Hideyuki Yamashita; contractor – Kadowaki Construction; completed – 1999
Orange Flat: architect – Itsuko Hasegawa Atelier; contractor – Ando Construction; completed – 2000
House in Hodogaya 2: architect – Mitsuhiko Sato Architects; contractor – Daido Contstruction; completed - 2001

DESIGN CONCEPT OF THE ENVIRONMENTALLY COMPATIBLE SPATIAL STRUCTURE

Structural design architect: Norihide Imagawa
Prof. Tokyo Denki University / TIS & PARTNERS Co., Ltd.
JAPAN

Keywords: Structural design epistemology, Plate & shell structures
Low stress concrete structures, Economical construction system

1. INTRODUCTION

What is a compatible architecture?

This is a worldwide theme of architectural field during the last decade. Engineers and we structural designers have wrestled with this theme and tried to realize "compatible architecture" using the technique which we mastered through 20th century. We approach to compatible architecture through various aspects…

By using data related on actual environmental pollution
By considering how to bring out material performance
By controlling emission energy of architecture and structure from construction to maintenance
By defining architectural durability
By searching material character not in use and considering recycling…

I already designed more than one thousand and five hundred architectural spaces in Japan and foreign countries during the last quarter century. I used various materials such as stone, brick, timber, steel, concrete, synthetic, fiber, glass etc., and I realized it was important to understand primary form, which was the basic form to each material. I categorize structural materials into three primary forms, which are massive, linear, and shell type.

I designed massive type of spatial structure using stone or steel…
I designed linear type of spatial structure using timber or steel…
I designed linear and shell type of spatial structure using concrete and so on…

On January 17th 1995, a great earthquake hit Kobe, Japan. More than 6,000 people have died, many buildings, highways and bridges were torn down. Structural engineers have to face the fact that they could not clearly explain performance and quality of collapsed structural engineers have to face the fact that they could not clearly explain performance and quality of collapsed structures. From this happening, I realized "Architecture should bridge as long time as possible" and "Environmentally Compatible Architecture could be designed when its end user confirms architectural sustainability".

2. TO REALIZE ENVIRONMENTALLY COMPATIBLE STRUCTURE

To explain professionally structural analysis or criteria of a structure is not the first priority to realize environmentally compatible architecture for a society and an end user. The first is to explain performance of each material (stone, timber, steel, concrete, glass, synthetic fiber etc…). It is important to explain how material is related to architectural performance.

Agreement on performance of environmentally compatible structure can be confirmed by using my structural design epistemological function F_{SD}

$$F_{SD} = F(M_x, S_y, L_z, C_\alpha, D_\beta, E_\gamma) \geqq$$

- natural conditions
- social environments
- required performances
- architectural worth

Structural Design epistemological Function (F_{SD}) consists of 6 factors: M_x: material, S_y: skeleton, L_z: load, C_α: cost, D_β: durability, and E_γ: erection. Result of function consisting above factors should not be less than the right side of an equation, natural condition, social environments, required performances and architectural worth.

3. STRUCTURAL DESIGN TO REALIZE ENVIRONMENTALLY COMPATIBLE AND SUSTAINABLE ARCHITECTURE IN PRACTICAL FIELD

It is understanding structural design epistemological 7 point the following;

1. Structure not obstructing spatial organization
   - ☐ Realize space with minimum surface from minimum members
   - ☐ Make use of spatial forms for structural design
2. Structure making use of material characters
   - ☐ Use nature and character of material in fill effect
   - ☐ Find out material character not in use
   - ☐ Find out method of material re-use
   - ☐ Use suitable materials in suitable area
3. Structure making use of local materials and techniques

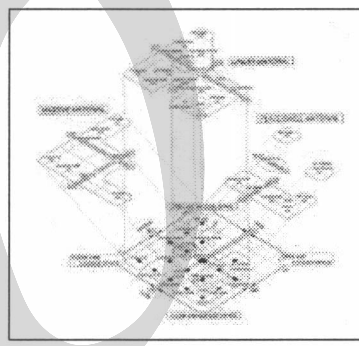

Fig.1 Structural Design and Primary Form

4. Structure using minimum fabrication and construction energy
   - ☐ Make use of gravity for fabrication and construction
   - ☐ Schedule order of erection considering direction of assembly
   - ☐ Use temporal structure of tensile resistant members for efficient construction
5. Structure with suitable on –site joint methods which determine architectural sustainability
6. Structure with complete “Confirmation Design” of its performance
7. “Renewal Design” of structure making use of characters and material performance of original building

4. HOW TO DESIGN ENVIRONMENTALLY COMPATIBLE REINFORCED CONCRETE STRUCTURE USING FROM LINEAR MATERIAL TO PLATE/SHELL MATERIAL.

I will introduce several special Environmentally compatible reinforced concrete structures.

MEETING AESTETIC REQUIREMENTS IN ARCHITECTURAL CONCRETE USING COMPUTER SIMULATIONS

Konrad Bergmeister
Institute of Structural Engineering,
Vienna, AUSTRIA

Vladimir Cervenka
Cervenka Consulting,
Praha, CZECH REPUBLIC

Keywords: Architectural Design, Structural Analysis, Computer Simulation

1 INTRODUCTION

Aesthetics and creativity play an important role in the design process of concrete structures. A structure must be safe, serviceable and durable during its lifetime. In addition, a designer must always be aware that a structure should be practical and economical to construct and should fulfill not only functional but also aesthetic needs. This results in an optimization process taking into account structural mechanics, material behavior as well as technological constraints.

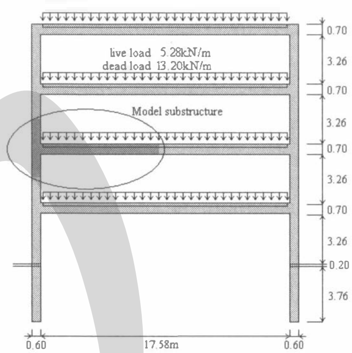

Fig. 1 Frame with model substructure

In the following paper the process itself and the various solutions will be discussed on an example of a new structure for the University of Brixen – Italy. The whole area consists in several buildings, where the structure with the largest span will be presented. The building serves as a lecture aula. The frame structure has span of 18 m and 6 levels above the ground. The most stressed frame corner is visible on the background of the large glass facade.

Two solutions had been developed: one based on a prestressing concept and the other using ordinary reinforcement. The verification of the structural performance was done using non-linear analysis based on the state of the art algorithms. The paper describes in detail the crack pattems, widths and deflections of the proposed solutions for the construction and the final phase. The various design approaches: strut- and tie-model, elastic FE-analysis, non-linear 2D and 3D analysis have been compared

For the optimization process the 3-dimensional nonlinear finite element analysis has been carried out by using the simulation software ATENA. The program is based on the non-linear finite element analysis and is specially designed for concrete and reinforced concrete structures. In ATENA the tensile cracking is based on the fracture energy-based crack band model. This enables to calculate mesh-independent crack widths.

2 RESULTS OF SIMULATION

The load history applied to the model included serviceability as well as ultimate loads. It can be seen from the example of the load vs displacement diagram.

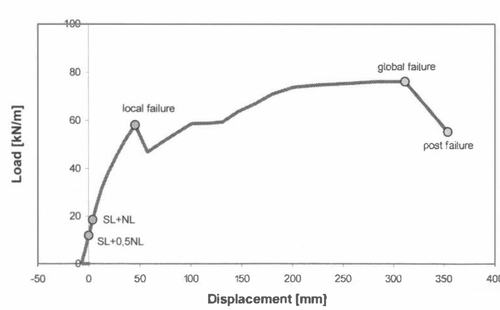

Fig. 2 Load – displacement diagram

The results available form the simulation will be demonstrated on example of the case with 2 prestressing cables with account for the long time effects of shrinkage and creep. Design load level includes dead and live loads (SL+NL).

The results show details of behavior in the whole loading history. Under service load the most interesting are the crack widths and deflections. They were compared with the code requirements and the structure was optimized in order to reach sufficiently small cracks. The failure mode can be analyzed from the stress and damage state at the peak and post-peak stages. It is interesting to compare the moment distribution in girder in service and ultimate states.

The simulation in the plane stress state shows a brittle type of failure due to concrete in compression at the anchoring region. It was realized, that this region is subjected to a three dimensional stress state and therefore a 3D analysis was performed as illustrated in the 3D figure.

The analysis shows that the cracks in 3D model (max crack width 0.28 mm) are significantly reduced comparing to 2D model (max crack width 0.55 mm).

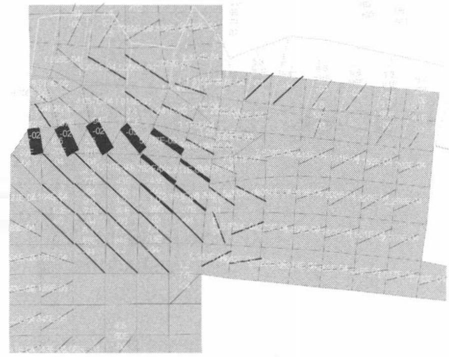

Fig. 3 Crack pattem in the frame corner

3 CONCLUSIONS

Computer simulation offers an advanced tool for virtual testing of a structure under design conditions. It is a new technique similar to a "design by testing", which was previously used as an ultimate tool for assessment of the designed structures. However, unlike in real testing the virtual testing has much wider limits imposed by structure size and cost of testing. Moreover, the computer simulation allowed to satisfy not only structural needs, but also aesthetic requirements.

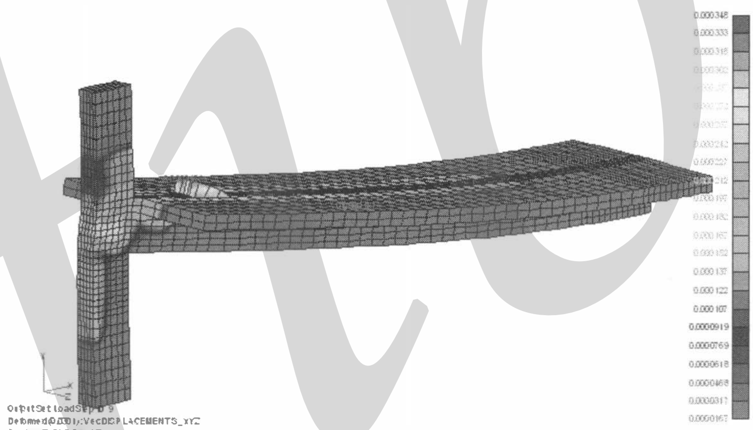

Fig. 4 3D-simulation of crack width development

REFERENCES

[1] Cervenka V., Bergmeister, K., Nichtlineare Berechnung von Stahlbetonkonstruktionen. Beton- und Stahlbetonbau 94, Heft 10, S.413-419 (1999)

[2] MacGregor, James, Reinforced concrete. Mechanics and Design. Prentice Hall, (1988)

[3] Vollum, Robert, Strut and tie modeling of external beam-column joints. Structural concrete – the bridge between people. Fib Symposium Prague, pp. 301 – 306, (1999)

THE NEW BRIDGE STRUCTURES OF DELHI: IMPROVED AESTHETICS & TECHNOLOGY

BY
Prof Mahesh Tandon
Managing Director, Tandon Consultants Pvt Ltd, New Delhi, India
Distinguished Visiting Professor at IIT Kanpur & IIT Roorkee

Keywords: aesthetics, incrementally launched, precast segmental, integral bridges

1. INTRODUCTION

The new generation of bridges in Urban Delhi are changing the city's skyline. Prestressed concrete is the dominant construction material used. New structural forms and technologically advanced techniques have been adopted. These bridges and flyovers demonstrate the possibilities of creating environmentally sensitive durable and aesthetic structures, which are appropriate to local conditions from the point of view of constructability as well as cultural settings. Some important examples of such structures designed by the author's consultancy organisation are presented herein.

The implantation of a huge structure on the cityscape imposes great responsibilities on the designer, far beyond the utilitarian function of relieving traffic congestion or providing an alternative route. Human beings have a deep sensitivity to their surroundings, which affect their physical and mental well being. The acid test of an urban bridge is that it is acceptable when viewed from various angles, from varying distances and at different times of the day and night.

2. STRUCTURES OF DELHI MRTS

Fast track elevated MRTS construction includes 14 km long viaduct snaking through the most crowded part of the city. It includes Precast Segmental Viaduct, Incrementally Launched Bridge over River Yamuna, Integral Bridge with a 70^0 skew and large span crossings at important roads Figs A,B,C. The world famous state-of-the-art 200 km long Delhi Metro, planned to be completed in phases upto 2020, will alleviate the woes of the citizens and improve the quality of their lives.

3. PRECAST SEGMENTAL FLYOVERS FOR DELHI GOVT.

Precast segmental techniques were used for the *Flyovers for Delhi Government*. Aesthetically shaped solid rectangular girder elements for the 6-lane flyovers were employed, Fig D. The elements are characterised by weights of only 30t and employ simple erection trusses weighing as little as 50t. The recently opened flyovers were won in open competition and include:

- Two important crossings on Ring Road
- Two important crossings on Outer Ring Road

4. INTERCHANGES AT CHRONICALLY CONGESTED TRAFFIC INTERSECTIONS

The ITO, Dhaula Kuan and AIIMS-Safdarjung Crossings are notorious for their congested, polluted and accident-prone characteristics. These intersections are being re-modelled with new constructions, which include complex bridges where architectural engineering has been given high priority, Figs E,F,G.

5. CONCLUSION

An urban bridge should never be an ungainly structure sticking out like a sore thumb. It must be elegant, graceful, beautiful - a poem in concrete - that merges ever so smoothly in its milieu so as to enhance the environment instead of detracting from it. A well-designed, well-constructed aesthetic bridge not only brings joy to its users, but activates their civic pride and motivates them to protect it against any wanton vandalism of its more vulnerable elements.

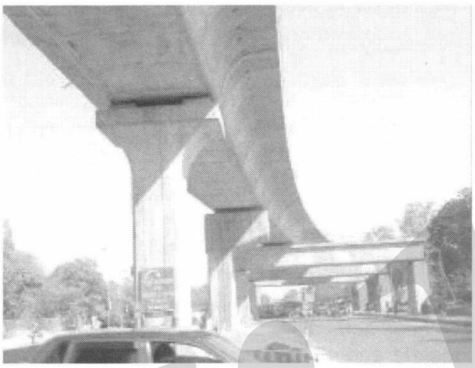

Fig.A: Delhi Metro: Precast Segmental Viaduct
Note: Portals & Different Pier Shapes with changing Alignment

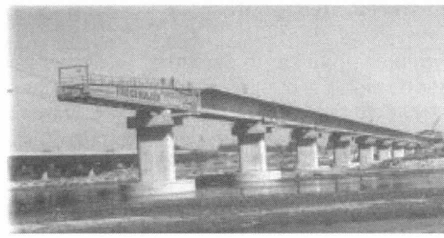

Fig.B: Delhi Metro: Superstructure (554.4m) of Yamuna Bridge being Incrementally Launched

Fig.C: Delhi Metro: Curved Flyover with 70° skew has no bearings or expansion joints on piers/abutments ('Integral Bridge' concept).

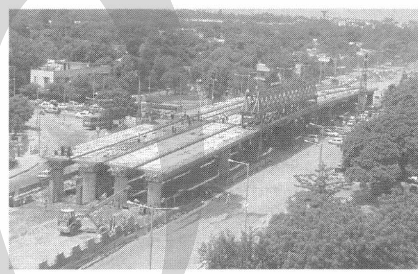

Fig.D: Precast Segmental Flyovers For Delhi Govt. Erection of four independent sub-bridges in progress

Fig.E: Sharply Curved Clover Leaves At ITO Connecting existing IP Estate Flyover

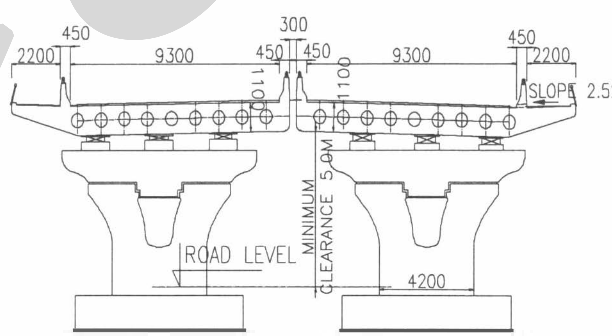

Fig.F: Dhaula Kuan Interchange for Delhi Govt. Straight Bridge (cast-in-situ voided slab)

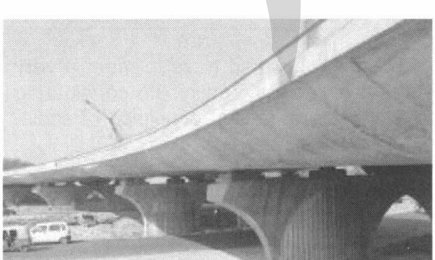

Fig.G: AIIMS-Safdarjung Crossing.
Note: Streamlined shape of deck & architecturally shaped piers

THE AESTHETICS OF RECENT CONCRETE ARCHITECTURE

Morten Gjerde Andrew Charleson
School of Architecture Victoria University
Wellington NEW ZEALAND

Keywords: aesthetics, concrete architecture, structure, precedent, teaching tools

1. INTRODUCTION

Firmness, relating to structural and physical adequacy; Commodity, equating to functional adequacy and Delight, a quality that derives from aesthetic beauty are the three criteria by which to evaluate architectural excellence according to Vitruvius. The sources of Delight in architecture can be elusive and difficult to measure when compared to the sources of Commodity and Firmness, which can be assessed by quantitative means.

Reinforced concrete is one of the most revolutionary construction materials in history, yet it has generally been recognised only for its structural and durability qualities. This view is now changing and the architectural potential of concrete is being recognised. Through their collective work, contemporary designers are revisiting the potential of concrete and it is therefore relevant to examine the aesthetic potential of concrete. The authors aim to review a group of buildings to gain an understanding about the ways in which concrete is being used to achieve aesthetically pleasing architecture. This paper proposes four categories for the consideration of architectural aesthetics of concrete buildings and evaluates buildings published in architectural journals and books over the last five years.

2. A PRIMER ON AESTHETICS

The inquiry into the aesthetics of concrete architecture will benefit from a brief overview of how humans recognise beauty. Perception of aesthetic stimuli can be broken down into three areas: **Sensual, Intellectual and Moral.**

Sensual perception is through each of the five senses and is highly personal. A value judgement is made, conditioned by previous experiences or education. It is a largely personal response.
Intellectual delight varies in the observer according to level of sophistication and in the context of appreciation of architecture can be considered an appreciation of the skills evident in the built form.
Moral pleasure in aesthetic appreciation will also involve considerable judgement and can be affected by building type or by an appreciation of the philosophical approach taken by the designer. These three sources of delight do not occur in isolation and the degree of aesthetic pleasure will be governed by the level of sophistication of the observer.

This overview of perception of aesthetics leads on to the study, which considers the extent to which designers are currently exploiting the unique qualities of concrete to create 'delightful' architecture.

3. BASIS OF THE STUDY

Research was undertaken to establish a database of exemplary concrete architecture for the use of students and staff at Victoria University. The study set out to identify innovative and exemplary concrete architecture in one or more of four different categories noted below.

Architectural Form & Space	Structure	Detailing & Craft	Surface Finish

Before a building could be included in a very select group of buildings it would have to meet a very high standard both in terms of its usage of concrete and overall architectural quality. In considering buildings to be included, regard was given to the recognised architectural design principles of scale, proportion, symmetry, compositional balance, contrast and texture.

4. FINDINGS AND DISCUSSION

Out of a total of more than ten thousand buildings reviewed during the study, fifty-two buildings incorporating exposed concrete were selected. They are in fact not as tightly nor as precisely defined as Table 1 indicates. In most cases a building displays more than one area of excellence or innovation, and in some it is impossible to prioritise them in order of importance.

Table 1: Occurrence of Different Areas of Excellence

	Number of occurrences	As a percentage of the total number of buildings in the database
Architectural Form & Space	**32**	**62 %**
Structure	**23**	**44 %**
Detailing & Craft	**12**	**23 %**
Surface finish	**14**	**27 %**

Architectural form and space
Concrete can be shaped to virtually any form imaginable and this quality is used to great advantage in the buildings that display excellence and innovation in the area of architectural form. The designers of the most successful architectural spaces in the database have introduced natural light to create drama and contrast.

Structure
Structural forms identified in this category contribute significantly to the aesthetic beauty of the building. Of particular note are the spaces defined by repetitive or rhythmically curved skeletal elements

Detailing and craft
Although all buildings selected for the database exhibit high levels of detailing and craft, a number stand out. Generally held limitations of the medium have been exceeded through innovation by the designer and excellence in execution by the builder.

Surface finish
In most cases, innovation or excellence in surface finish amplifies the excellence in the overall aesthetic achievement of the project. An example is a library building in which the designers have permanently formed intricate designs into the concrete surface. This becomes a main feature of the completed project.

5. CONCLUSIONS

The following conclusions may be drawn from the preceding enquiry into the aesthetics of recent concrete architecture.

1. The Vitruvian criteria of 'Firmness', 'Commodity' and 'Delight' must be ably met in any building considered to be exemplary architecture.
2. The sources of Delight in architecture can be summarised to derive from three stimuli, which are **sensual, intellectual and moral**. Designers should make effective use of recognised design tools, have an appreciation of the construction medium and processes as well as a view to innovation to maximise aesthetic beauty in their projects.
3. Concrete has suffered poor reputation through association with some high profile, poorly designed projects during the modern period and through its extensive use as a material in civil engineering projects. Increasingly designers are recognising the architectural qualities of a medium that can be formed to most shapes and sizes imaginable and which has impressive strength characteristics.
4. Designers and constructors have used concrete effectively to create significant architectural forms and spaces, to demonstrate innovative detailing and excellent craft, to design innovative and well-integrated structural systems and to exploit the surface finish possibilities.

BRIDGE AESTHETICS IN JAPAN

Miyoko Ohno
M+M Design, Tokyo, Japan

1. INTRODUCTION

Pre-stressed concrete bridges are presently common not only in Japan, but a great number are built all over the world. In Japan, Europe, and America, there are several differing aspects of building conditions, such as those of the natural environment as well as design criteria. In Japan, in spite of the fact that PC bridges are built among such differing regions as the varied natural environments, farm villages and urban areas, there are several that don't quite suit their surroundings.

In order to solve this problem, let us simply consider the history of the Japanese bridge and try to examine the relationship between the bridge and the natural features of Japan through my research entitled 'Bridge Aesthetics', which I will now present. And in conclusion, I will survey the future of Japanese bridges.

2. HISTORY OF THE JAPANESE BRIDGE – BRIDGES FROM OLD JAPAN TO THE PRE-STRESSED BRIDGE

Traditional bridges of Japan were small-scale and had unique concepts of structural form, and also used material and local traditional building techniques that evoked regional character. In modern and even contemporary Japan, iron and concrete are used and, even now, efforts continue to be concentrated on structural technology introduced from 'advanced nations'. Importance is placed on functionality and ease of construction, yet, is the resultant form suitable for the landscape of Japan?

3. BRIDGE AESTHETICS AND CASE STUDIES

For reference, I list some keywords which characterize the natural features of Japan in consideration of the relation of the bridge to aesthetic characteristics. In addition, I also list concrete cases of aesthetics design.

(1) Gentle mountain range

(2) Rich greenery
Village mountains
Pastoral plains

(3) Wooden townscape
Local culture
Warm atmosphere

(4) Dense urban areas

(5) Close-range visibility

(6) Anti-seismic structure
Seismically isolated structure

(7) High temperatures with moisture

fig.1 Rural village scenery

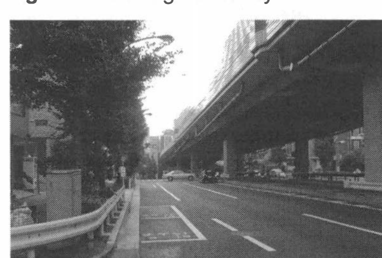

fig.2 Urban scenery

○ Ayunose Bridge (Kumamoto pref.), length: 390m

fig.3 A combination of a single tower cable-stayed bridge with a V-shaped pier; it is a structural form that enhances the scenery of the V-shaped valley.

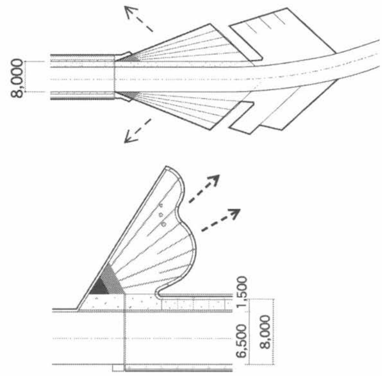

fig.4 Various sized lookouts at the end of the bridge where people gather and can view the valley. Local tuff stone and limestone are used as paving.

4. PROSPECTS FOR THE AESTHETICS OF JAPANESE BRIDGES

I will discuss the direction of bridge aesthetics towards expressing the genuine originality of Japan In the midst of a world of progressing globalization.

<Globalization and Originality>

As initially with steel bridges, the influence of Japanese PC technology came from Europe. And although techniques improved, somewhere, there exists an element of borrowed-ness.
Although functional, the bridge of former times was built by people who had an "aesthetic consciousness" supported by the surety of technology. That "aesthetic consciousness", lined with individual culture, lived continually with people for a long time. Could there be a hidden potential that could give birth to a bridge form of a new originality? Amidst cries for globalization of the world, it is most important to establish the originality of Japan. And for the first time, let us seek out a direction for the globalization of Japan.

<Bridge Construction>

Is there not a method of, for example, making a beautiful bridge utilizing a structural form highly effective against earthquakes through a purely structural trial? For this method to prevail, given conditions, such as site width and structural type, are determined much too soon. It is necessary to reconsider problems of the design procedure. Furthermore, the review process based on reliance on procedure that suppresses originality, while considered to be the safest approach, makes it difficult to create a structural system suitable to the natural features of Japan.

<Regional Space through Bridge Design>

Bridges, unlike cars that can be mass-produced, are created bridge by bridge, in Japan, South-east Asia, Europe and America. In these different regions, culture also completely differs along with the climate and natural features. Moreover, the purpose and scale for each bridge is different. But with each, the notion that the bridge will remain as "a form" in the area is identical. In other words, the examination of the relationship between this "form" and the local region is an aesthetic task for us to consider. And finally, the way that human skill is utilized can reveal the depth of the connection to a particular locale. Isn't it possible to provide the future direction of bridge-making by capitalizing on the human skill and natural features of a region?

RIVER CROSSING EXAMPLES IN V.E.A. (VALUABLE ENVIRONMENTAL AREAS)

Prof. Eng. Enzo Siviero Dr. Arch. Lorenzo Attolico Dr. Eng. Tobia Zordan
University Institute of Architecture in Venice (IUAV), ITALY
I.B.C. (International Bridge Consulting) associates

Keywords: concrete bridges aesthetics, environmental impact

1 INTRODUCTION

During the last few years, the University Institute of Architecture in Venice (IUAV), through the graduation theses of the students on the course of "Bridge Theory and Design", has been focusing on the theme of Bridge Aesthetics. One of the main purposes of the worked out projects, as highlighted also during the International Workshop "The World of Bridges", recently held at the IUAV, is to deal with real problems (encountered on the territory), offering solutions or proposals which are concrete, feasible and useful. In this way the University seeks a comparison with the external world, based on the quality of the project, aware of the fact that project excellence, on all fronts, must be the objective of the years to come.

There's no doubt, in fact, that when the technical knowledge of the field of engineering aspires merely to the production of useful and lasting things, and the only goal is the economical one, often the results cannot aspire to match the definition of "Works of Art", that is probably the most exhaustive definition the Engineering Practice can seek for its realizations.

Of course this is not an easy objective to achieve, but in any case is considered to be a very important one, especially in the eyes of those who feel the ethical responsibility that planning involves, with respect to the present and future generations.

In this sense, designing a bridge is an experience able to offer an extraordinary experience in synthesizing the complementary branches of different specialization typical of the fields of engineering and architecture, because "Bridge Design" contains significant forms of social, cultural and economic conditioning, able to deeply affect the installation area for the years to come.

In the following paper, a selection of three graduation theses carried out by former students and dealing with the complex problem of Bridge Design in Valuable Environmental Areas is presented.
The first thesis put forward the solution for a bow-string bridge spanning the Adige River close to Verona (north-east of Italy), in the open countryside, with the approaching viaducts ascending the river banks in a "pre-mountain" hilly landscape (Fig.3). In the second thesis, an arched bridge linking two urbanized productive areas and spanning the Brenta river near Padua is proposed (fig.4), while in the third thesis is given a solution for a suspended pedestrian crossing inside the Bassano, renowned historical city centre in the province of Vicenza, north-east of Italy (Figg.1-2). This last project deals with the proximity of Alpini bridge, one of the most important Italian historical bridges designed by Andrea Palladio in the XVIth century.

2 DESIGN PROPOSALS THROUGH IMAGES

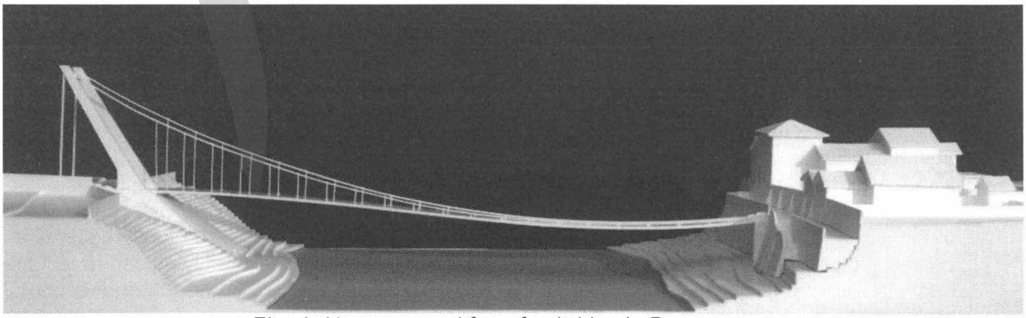

Fig. 1: New proposal for a footbridge in Bassano

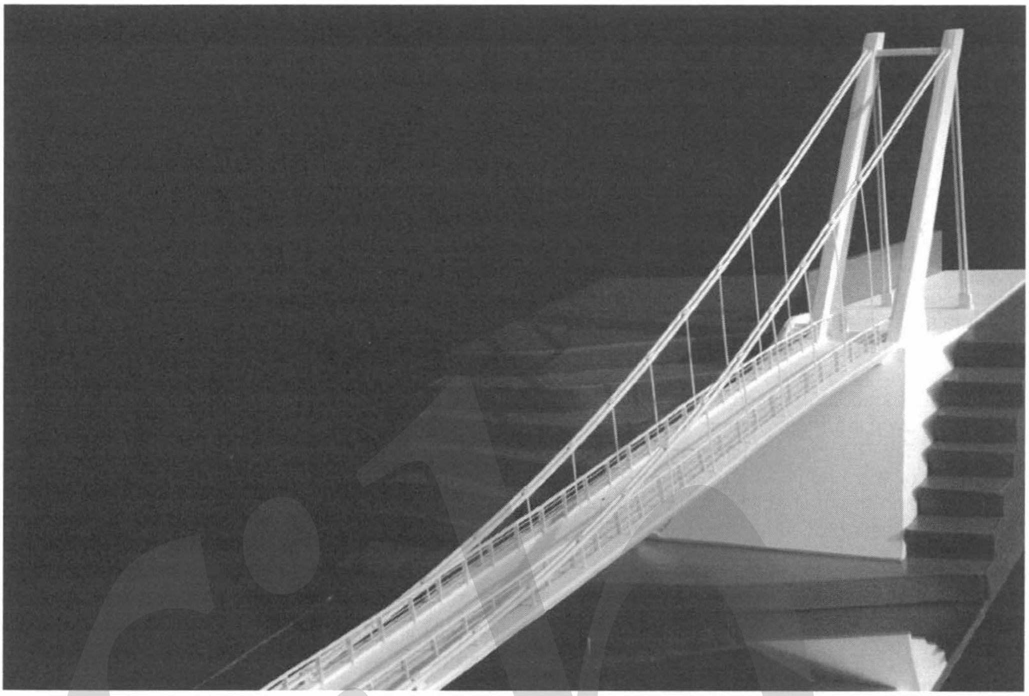

Fig. 2: View of the model

Fig. 3: The new bridge over the Adige river

Fig. 4: Render of the new Bridge over Brenta river

INTEGRATION OF PEDESTRIAN BRIDGES INTO THE COMMUNITY LANDSCAPE: CALGARY, CANADA

Jadwiga Kroman, City of Calgary
Calgary, CANADA

Gamil Tadros, Speco Engineering Ltd.
Calgary, CANADA

Keywords: aesthetics, pedestrian bridges, structural design, reinforced concrete

1 INTRODUCTION

The City of Calgary is located in southern Alberta at the foothills of the Canadian Rocky Mountains. It is a vibrant, fast growing city, situated on both embankments of the Bow River. The need for a pedestrian bridge over the busy four lane, divided Memorial Drive in the city's North West, was identified by a long term transportation plan, and was heartily supported by the local community.

This particular location of the bridge offered an advantage of great natural beauty. The structure, spanning over the major motor artery, presented the opportunity to capture a perspective view of the roadway. The aesthetic quality of the bridge was considered even more important because of the proximity of the bridge to park users. With that focus in mind, equally important was the aspect of durability and maintainability of the structure as means of extending the life of the structure, and thus providing a lasting benefit to the community.

2 CONCEPTUAL DESIGN

The conceptual design process included public consultation, thorough examination of the site, exploration of a variety of alignments and possible structural systems. The sensitivity of the bridge form to the natural environment was of prime importance.

Three conceptual alternatives of the bridge were selected for closer evaluation and presentation to the community. The first option was a non-symmetric two-span cable stay main bridge with multi-span cast in place ramps. The second alternative encompassed girders of trapezoidal cross section, longitudinally shaped into shallow arch spans. The third option consisted of a single spine girder with deep cantilevers, formed into flat parabolic arch spans and gently curved in horizontal alignment. The third option was selected as the design that best addressed the users needs, such as gently curved alignment, rounded corners and good visibility along the bridge (Fig. 1). This option also offered a superior fit with the environment and the elegance of clean curved lines rich in rhythm, harmony and balance.

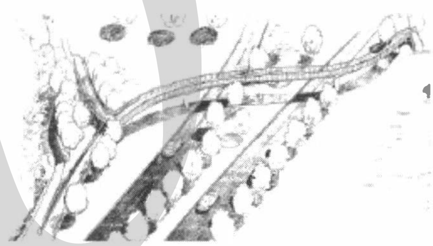

Fig. 1 Option 3: Conceptual Rendering

3 DETAILED DESIGN

The span lengths and superstructure depths were refined during the iterative process of structural balancing and visual harmony. The girder shape and proportions were structurally optimized following a sophisticated structural analysis. Long cantilevers of the bridge deck and variable depth of the girders made an attractive 3-dimesional form, emphasized by a natural play of light and shade (Fig. 2). A particular challenge was to accommodate the structure's response to the environmental loads. A multi-directional movement bearing with an uplift capacity was designed and custom-made to facilitate the structure's movement at the north turning point.

Fig. 2 Bridge Details

The pier design was based on balanced composition of gently curved contours, opened up at the top for visual lightness, complemented by contrast enhancing, textured reveals extending from the lines of the aperture.

4 CONCLUSIONS

This project confirmed that a bridge design in which a clear focus on aesthetics is equally respected with safety, strength, durability and maintainability, does not automatically entail a significantly higher project cost.

The public consultation confirmed the appreciation of fine aesthetic quality of pedestrian bridge appearance and conservation of the environment.

Fig. 3 Bridge Ramp Looking East

This project demonstrated that pedestrian bridges as part of urban infrastructure not only fulfill the utilitarian function but can provide an improvement to quality of life. Hence, the concept of bridge function should integrate the quality of aesthetics and environmental considerations (Fig. 3).

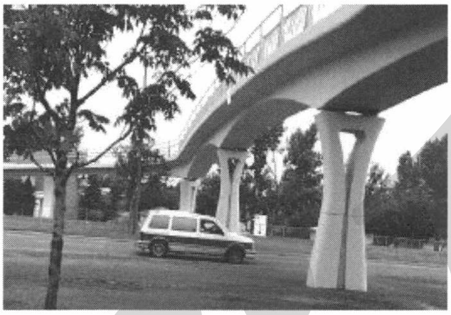

Fig. 4 Main Spans

The elegance of this bridge structure is derived from relatively few structural elements that bring it together: the lines of curved girder, the gracefully shaped piers, and a matching, railing (Fig. 4). A smooth transition of the bridge structure to the at-grade pathway gently winding along the river introduces a visual integration of the structure with the environment (Fig. 5 and 6).

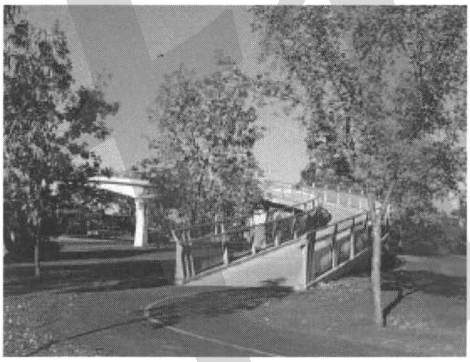

Fig. 5 South West Ramp Entrance

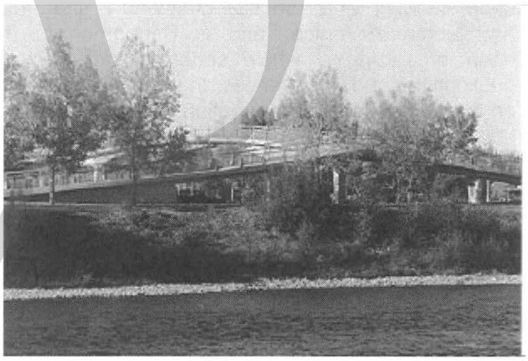

Fig. 6 View of the Bridge from the South Bank of Bow River

DESIGN OF CONCRETE BRIDGES. EXPERIENCE AT THE UNIVERSITY INSTITUTE OF ARCHITECTURE IN VENICE (IUAV)

Prof. Eng. Enzo Siviero Dr. Eng. Bruno Briseghella Dr. Arch. Gigliola Meneghini
University Institute of Architecture in Venice (IUAV), ITALY

Keywords: Bridges, Aesthetics of Concrete Structures

1 INTRODUCTION

One of the problems that the art of modern and contemporary building has been having to cope with for some time now is that of taking the interaction between technique and form into due account in the design process. Engineers and architects, both agents in this activity and both interested in the same goal of building structures for human use, seemed to be standing on the opposite banks of a river, as if awaiting a treaty that would restore their unity, harmoniously blending the fragments of this dispersed knowledge. The former seemed more interested in sophisticated systems of structural analysis, in strictly calculating the structural aspects of the design and its component parts, while the latter seemed intent on its geometrically determined form, starting from a formal, perceptive and utilitarian viewpoint. The need to overcome this dualism is inescapable, because whatever the type of building we consider, from a humble homes to an opera house, to a bridge, our fundamental concern is to consider the structural conception as a cultural conception; to build structures or architectural works through a design effort comprising a conceptual integration of different aspects, so as to satisfy all the requirements - the functional, structural, economic and aesthetic – in order to better the quality of the design as a whole.

It is to facilitate this type of approach, to create a culture of construction, to make the passage between design and construction perceptible, to restore the necessary symbiosis between cognitive understanding and practical know-how, that for several years now the University Institute of Architecture in Venice - and the Department for the Construction of Architecture in particular – has been organizing a whole series of activities, including formal lectures, seminars, exhibitions, publications and conferences, that emphasize the relationship between form and structure and focus on the interaction and integration of the art and science of building in an attempt to identify a way to bring together the two cultures: the "humanistic-literary" and the "technical-scientific".

To illustrate the above considerations, this paper describes three reinforced concrete viaduct projects developed by undergraduates at the IUAV for their dissertations. The students designed these works according to an integrated approach that combined utility with form, technical demands with economic restrictions, concentrating on a global concept of the work that focused constantly on the solution of problems and practical needs, and consequently had to be supported by feasibility studies. The three dissertations presented here, which focused on real situations, demonstrate how these premises can be put into practice and they are an excellent example of the relationship between form and structure.

2 THE PROJECTS

The first thesis develops a project for a viaduct crossing over the River Brenta in Bassano del Grappa (nort-east of Italy). The particular development of the shaping of the longitudinal and cross sections of the viaduct designed stems from a construction philosophy that seeks to establish a direct relationship between the work and its surroundings, lending the form a plastic connotation to express the intimately figurative quality of the construction and giving the work a markedly sculptural texture.

The second thesis proposes a solution for a road network problem affecting the area coming between Bassano del Grappa and Cittadella (nort-east of Italy). The prospect of the bridge is composed of three shallow-arched bays: the two on either side are 51 m wide, while the one in the middle is 90 m. The three arches are characterized by the changing cross-section of the blocks forming the deck and by the slightly-arching vertical elements in the extrados.

The measure considered in the last thesis was a viaduct serving the state road 53 "Postumia" in the municipality of Vedelago, on the stretch of road that connects Cittadella to Treviso (nort-east of Italy). The construction comprises a multi-cellular boxed deck of constant height, forming a continuous curve over eight bays, two at the ends that are 28.8 m and six in the middle that are 36 m long, amounting to a total length of 273.60 m. The deck is made of prestressed reinforced concrete, cast in place by repeatedly using one and the same formwork. Particular attention was paid to the pedestrian and cycle paths. In fact, a pavement was planned on a level with the road while the cycle path was raised 1.5 m above the road by means of a projecting steel structure.

Fig. 1 Render of the new bridge near Bassano del Grappa

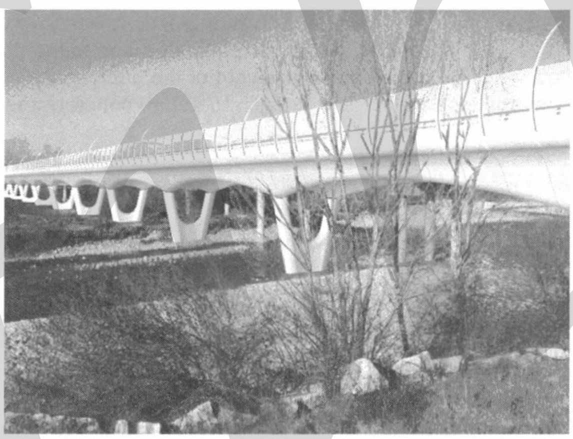

Fig. 2 Render of the new bridge over the River Brenta

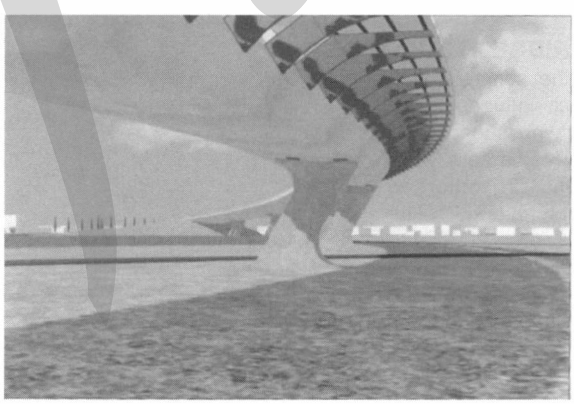

Fig. 3 Render of the new bridge in Vedelago

AESTHETIC DESIGN OF LONG SPAN ARCH BRIDGE -THE IKEDA HESSOKO OHASHI BRIDGE-

Hirohumi ANDO Hidetsugu MOCHIZUKI Kei SUZUKI Yuichi KOGURE
Japan Highway Corporation Kajima Corporation

Keywords: history, aesthetic design, long-span arch bridge, collaboration Kei

1. INTRODUCTION

The history of engineering is not a set of facts, date, and phenomenon, but a process of human thought and challenging of engineers and architects. When we look over the process of the development of some materials and structures, there are some cause and effect relationship between the former and the latter stage. The development of each stage is the result of the organic chain reaction with the former stage. This relationship was revealed by Charles Darwin who presented " Evolution" in his book of " On the origin of species" . But we sometimes made mistakes, if we think that the Evolution is the absolute progress of the latter or the newer is always in a higher position than the older. When a new form of bridge is the result of human thought, the value of the structure is always the same. The form of bride does not evolve, but it metamorphoses (changes gradually) according to human thoughts.

2. HISTORY OF CONCRETE

The usage of concrete metamorphoses according to human thought. In the last half of the 19th century ,concrete was intended to use as a cover of iron member in order to protect it from fire. Francois Hnnebicque (1842-1921), the French architect, tried this idea and found that the quantity of steel became twice as much as the original plan and the weight of the deck became heavier. In order to solve these problems, he gave independent roles to each material, concrete resists compression force and steel resist tension force in one beam. Finally the origin of reinforced concrete was invented in 1878. In 1867 Joseph Monier (1823-1906), a French gardener, patented an idea of flowerpot, a tie for railway where steel mesh is covered with concrete.

Emil Moersh (1870-1950), the professor at Stuttgart University, published his calculation method for fixed arch bridge using elastic theory in Schweizerische Bau Zeitung in 1904. He designed the Gruenwald Bridge (Fig.1)

This is one of the turning points where experience of arch bridge construction and scientific knowledge of calculation are unified.

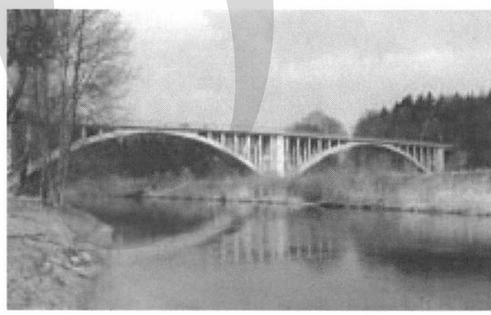

Fig.1 Gruenwald Bridge 1904

3. HISTORY OF ARCH BRIDGE IN EUROPE

In the early 20th century the concrete arch bridge design received much influence of a stone bridge where the arch rib supports all upper loads. Then a plenty of timbers were required for the scaffolding in order to supports the weight of the arch rib (Fig.2). The design of concrete arch bridge metamorphoses from the points where how to reduce the quantity of scaffolding and how to use effectively both the arch deck and the arch rib.

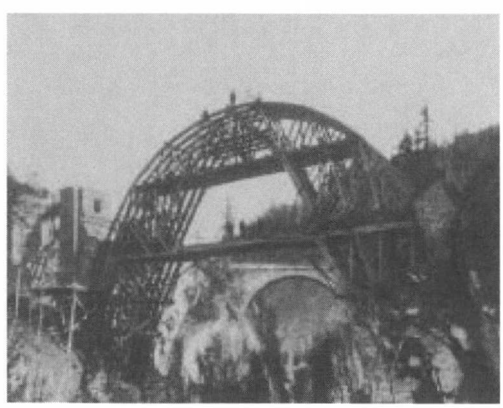

Fig.2 Solis Bridge (Rhaetische Bahn)1902

4. HISTORY OF ARCH BRIDGE IN JAPAN

In 1974, the Hokawazu Bridge with an arch span of 170m was constructed using balanced cantilevering method (Fig.3). This was for the

first time application in the world.
The Beppu-myoban Bridge with an arch span of 235m was constructed in 1990 by using the Pylon and Melan construction method (Fig.4). The characteristics of this construction method are to reduce temporary stay cables and to improve the stability against earthquake during construction This bridge form is harmonized with surroundings and the aesthetic design was admitted in the FIP congress at Hamburg in 1991. By using these construction methods, the possibility of arch bridge design in Japan is extremely enlarged The design of the Ikeda Hesokko Ohashi Bridge, where the main span is three span continuous deck-stiffened arch bridges based on the new construction method. The two formtravelers cantilevers from a pier-head to both directions simultaneously.

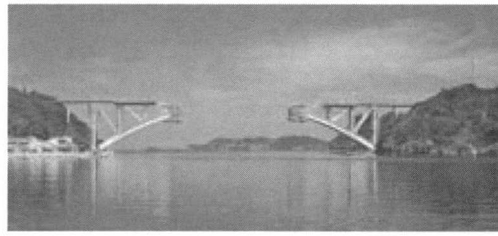

Fig.3 Hokawazu Bridge 1974

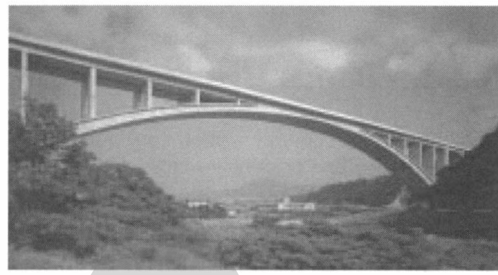

Fig.4 Beppu-myoban Bridge 1990

5. THE AESTHETIC DESIGN OF THE IKEDA HESOKKO OHASHI BRIDGE

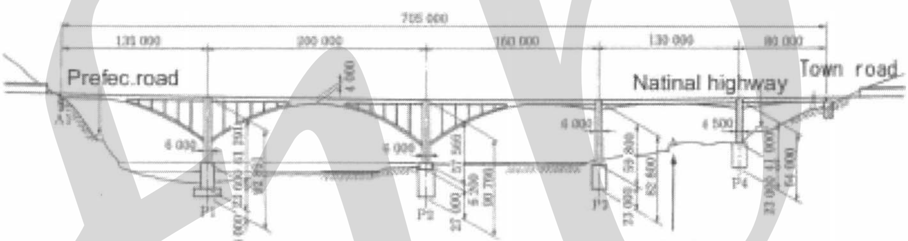

Fig.5 Plan

The Ikeda Hesokko Ohasi Bridge (Fig.5) is situated in Ikeda town of Tokushima prefecture in Shikoku Island. The bridge is situated in the final section for the opening of the Tokushima Expressway. This bridge is the prestressed concrete 5spans continues arch bridge crossing over the Ikeda dame lake in Yoshino River in Shikoku Island. This bridge type was decided according to the structural efficiency, economy and aesthetic judgments. In order to find the design problems, the Psycho-vector method (Fig.6) is applied and estimated from several viewpoints. For the erection of this arch bridge, the simultaneous balanced cantilevering method is for the first time applied. The realization of this bridge design is based on the new construction method as mentioned before and also good relationship between skilled engineers and designers.

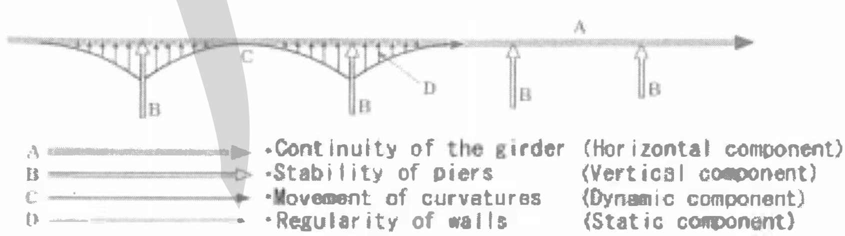

Fig6. Psycho-vectors of the basic plan

BRIDGE IN FLIGHT: HARMONY OF STYLE AND STRUCTURE

Tanja Wilcox
Supervising Designer and
Senior Landscape Architect
J.A. Brennan Associates,
Seattle, WA, U.S.A.

James S. Guarre
Structural Expert and Senior
Vice President
BERGER/ABAM,
Federal Way, WA, U.S.A.

Fredric S. Berger
Project Principal and Senior
Vice President
The Louis Berger Group,
Washington, D.C., U.S.A.

Keywords: aesthetic design, extra-dosed, international collaboration, community involvement, colored concrete

1 INTRODUCTION

Through international collaboration, aesthetic design brought a new perspective to the design of the Rittoh Bridges and possibly to modern Japanese bridge design in general. The Japan Highway Public Corporation (JH) developed a design for two cable stayed, extradosed, corrugated web bridges along the New Meishin Expressway. The expressway will link Tokyo to Osaka, with the Rittoh Bridge functioning as a gateway to the Kansai District. The basic engineered design, although innovative in its advanced technological approach, JH felt was not sufficiently aesthetically pleasing and responsive to the site and its cultural context. To improve the bridges' response to the site, JH engaged a US aesthetic designer, Tanja Wilcox, landscape architect with J.A. Brennan Associates (JAB), BERGER/ABAM and the Louis Berger Group Inc. (LBGI), to develop an aesthetic design for the bridges to fill this gap. The result has been a successful cultural exchange and the design of two bridges, which are technologically advanced and simultaneously aesthetically responsive to their unique context. The design effort benefited from a successful community involvement program.

The project is an example of a unique collaboration between Japanese engineers, their American counterparts and a landscape architect. Over the course of several years, beginning in the fall of 1999 the aesthetic design unfolded through collaboration between the aesthetic design consultant team and JH engineers. Further design refinements were made in cooperation with substructure contractor, Maeda Corporation, and superstructure contractor P.S. Corporation Joint Venture. This collaborative process is necessary to successfully create a harmony between style and structure.

2 AESTHETIC DESIGN PROCESS

The aesthetic design process began with an analysis of the landscape context of the Rittoh bridge project site and research into its cultural context. Several design alternatives were then developed at a preliminary design level. Next, through client and designer discussion and meetings with the local community, a preferred design concept was chosen, which was then taken to the schematic design level. The design development phase refined the concept in greater detail. The concept design was then incorporated into the construction documents and the project was awarded as a design-build contract.

2.1 Landscape context analysis

Current and future conditions surrounding the Rittoh Bridge site that affect the aesthetic design were studied. As the Rittoh Bridge site is located in the Shiga Prefecture Nature Park, minimizing impacts to the natural landscape during construction of the bridges, tunnel, and reservoir was emphasized. The visual character of the landscape was strategically analyzed and considered during design development using views created with a digital terrain model of the mountain landscape and bridge locations.

2.2 Cultural context

An understanding of the cultural context of the project is critical in the aesthetic design process. Through interaction with the community, a design emerged that responds to the culture of the local people, while also responding to the greater community.

Several basic ideas became clear through research conducted in Shiga Prefecture. Shigaraki pottery is clearly an important tradition in the area, and the style of pottery shows the people's appreciation of simple and graceful forms, the power of natural forces, such as fire, and the importance of the local soil, source of the clay for their craft. The study of traditional Japanese gardens assisted in developing an understanding of the Japanese style of creating harmony between buildings and nature. These insights into the local cultural values helped to shape the aesthetic design.

Fig. 1 Japanese Crane

2.4 Bridge in Flight design concept

The Bridge in Flight concept was inspired by the forms of the natural landscape and simultaneously by its cultural context. The Bridge in Flight design creates harmony between structure and nature by responding to the layered repetition of mountain peaks of the Shiga Prefecture Nature Park with repetition of curved forms in each pier across the bridge. Inspiration came from the Japanese love for nature and birds. The design borrows the flowing lines of the nationally significant Japanese Crane, or "Tancho," to create a sculptural form that makes smooth transitions between the towers and girders of the bridge. The repetition of curved lines is reminiscent of the forms in a bird's wing, which gives a dynamic fluid appearance to the bridge span and the impression that the structure is floating over the valley. The sculptural transition between pier column, girder and tower consists of two scalloped concrete forms with a one-meter deep reveal, emphasizing the tapered shape of the pier.

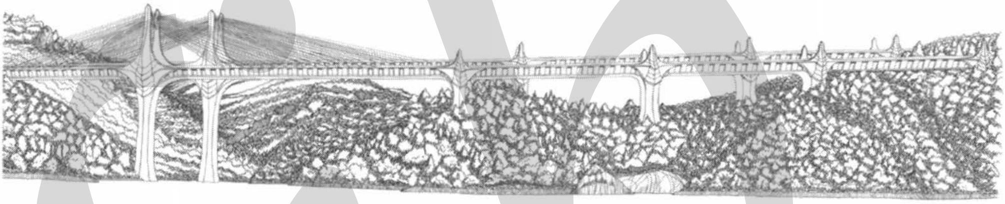

Fig. 2 Bridge in Flight Concept Sketch, View 3

3 DESIGN ASPECTS

Harmony of style and structure was accomplished by addressing a wide range of design aspects that would affect the aesthetic character of the bridge in the landscape. Aesthetic design of the tunnel portals was developed to the preliminary design stage, while detailed aesthetic design of the piers and bridge span was carried through to the completion of detailed shop drawings. The aesthetic design team worked closely with the design/build contractors, reviewing and commenting on shop drawings, three dimensional computer graphics and scale models. Conflicts between structural requirements and aesthetic design requirements were resolved through a creative process and an effective collaborative effort of the aesthetic design team, client and the design/build engineering contractors.

The use of colored concrete became an important part of the aesthetic design. The light sandy colored concrete will blend the bridge into the landscape and relate it to the local granite outcrops, soil and pottery colors. The US aesthetic design team was able to assist the substructure contractor in obtaining the research information needed to develop an integrally colored concrete mix design through the arrangement of a colored concrete study tour.

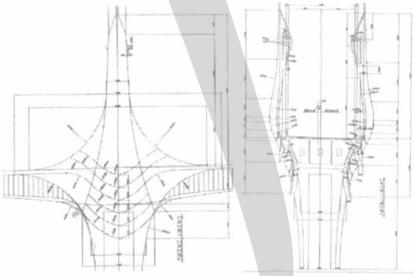

Fig. 3 Bridge in Flight Shop Drawings of Main Tower, by The Rittoh JV

4 CONCLUSION

Harmony of the style and structure of the bridge was accomplished through international collaboration, the aesthetic design process, community involvement, and by working through the detailed bridge design aspects as a multi-disciplinary team.

ENVIRONMENTAL AESTHETIC MEANING OF CONCRETE OBJECTS IN LANDSCAPE

Yoichi Kubota
Saitama University
JAPAN

Keywords: environmental aesthetics, concrete structure, landscape, skeleton system

1 INTRODUCTION

As the elements of physical environment, concrete structures appearing in daily landscape should be considered from various points of view in addition to technical scope by expertise. There is a risk, however, that demotic superficiality might overspread if profound thought is not prevalent. To configure intangible properties of concrete structures appropriately, environmental aesthetics as one of disciplines in human science may provide a certain horizon for contemplation of the broad meaning of concrete structures as visual objects in landscape. This paper endeavors to categorize some environmental aesthetic meanings of concrete structures based on semiotic aspects.

2 CONCRETE STRUCTURE AS AN OBJECT IN LANDSCAPE

Concrete structures are physical objects in landscape that ordinary people can perceive in daily life. This simple fact should be the basis for figuring out what should be considered in designing concrete structures in landscape. It would include epistemological issues or paradigmatic matters on how people perceive and recognize their surroundings with significance for their lives.

The psycholinguistic hypothesis that human thought is governed by daily verbal language acquired through growth process does not compromise by principle with Gestalt psychology that human beings have common perceptual tendencies toward their environment. The former regards that discrimination of object is not possible without acquisition of language, especially vocabularies, and the latter insists that prior to recognition of name or meaning of object, there should be some factors influential to the possibility of perception of object itself. Gestalt theory denies elementary comprehension of phenomena, emphasizing that the whole of the object is recognized as a complete entity with meanings more than as the sum of its consisting parts. Articulation of perceived object by language surely exists, but perception of environment by living creatures that have no verbal language cannot be explained. Recognition with verbal language must have salient significance on the existence of human life. There should be, however, configurative meanings of objects in landscape that cannot be described by verbal language and could be more important than definitive expression by words.

This issue is also significant with respect to concrete structures. According to Gestalt psychology, it is not possible to think that the whole structure is beautiful when its parts are beautifully designed. To contemplate the relationship between parts and the whole seriously should be the fundamental discipline of structural engineers.

For the sake of developing schematic framework to this issue, skeleton system could be a new keyword instead of structure. To think about skeleton system requires flexible view with zooming range together with wholistic sight on object and landscape of surrounding environment.

The fact that an object has a certain form may not be preceded by any languages used by human beings for explanation. No design works will make progress even though many literal phrases might be listed up. No innovative values can be added to the existence of structures even by means of accumulation of superficial aesthetic treatment, which can be merely adhesion of 'concrete meaning' to concrete structure. The key point hereby is how deeply designers can recognize the fact that relevant internal and external configurations of environment that the object faces will affect the process of generating its form. Liberation from daily verbal languages and the recovery of language by form of object itself can be the basis for thoughts on developing the new design of skeleton system. Researches, however, on skeleton form of concrete structures are still rare.

3 MEANINGS OF CONCRETE STRUCTURES AS SKELETON SYSTEM

This paper tries to explore the mechanism how concrete structures become paradoxical objects in landscape by their appearance with implicit or explicit intensions that may lead to the anatomy of concrete structures with concrete form with concrete meaning to be recognized. By quoting semiotic framework, several categorical phases of environmental aesthetic meanings can be discerned.

Skeleton systems designed by civil engineers can be regarded as self-exposure of technological contrivance, symbolizing the progress of human knowledge and wisdom. They are called technoscape for categorizing this specific aspect. Self-reference, or auto-reference, by the structure itself is obvious in technoscape, as they are contrived to be as such. No other expression can explain its meaning without the existence of itself. Self-contentment is original significance of objects unexplainable by literal way.

On the other hand, literal depiction of the skeleton system as an object in landscape may enlarge the meanings of the object beyond what itself denotes. Expression by verbal language is organized socially for categorization to identify objects in other sign system, but subjective interpretation is unavoidable. In short or other words, subjective interpretation can intervene as connotative sense upon denotative significance of skeleton system. Connotative meanings may include emotional or expressive attachment of subjective impression. Interrogative response to poetic sentimentalism is sometimes discussed because of this intervention.

Contrary to connotation, denotation of object is objective in true sense of the word. Objective meaning is functional and utility-oriented, and can be universal by the shape or form of skeleton system. Morphological difference can enhance the meanings of the skeleton system, but mostly it is formative and typological, as typological scheme of comprehension aims at abstract similarity. There are some efforts to enhance respective physical features of skeleton system, which is formative approach to enrich the existence of object itself.

In paradoxical sense, however, concrete objects as products of technical contrivance can be perceived as plain objects of alienation from their surroundings due to their outstanding heterogeneous physiognomy. Even a bridge designed in practical explicit context emerges as an object with implicit aesthetic meanings in the environment where it stands. If a structure is designed to have an explicit form understandable from demotic standpoint, it will force people to perceive itself as something else away from what it denotes. Paradoxical objects with mediocrity by demotics may be produced in such circumstances in order to avoid abstract alienation from the surroundings.

Hereby, significant or what signifies, and signifie or what is signified. If excessive connotative physiognomy is attached to an object, denotative signification will be transformed to something else. Sometimes such situation may occur when people without technological knowledge face with unfamiliar object literally unidentifiable, “what is it?”. More serious situation may happen when an object becomes totally alien existence in its environment like a sculpture. Contextual approach quoting historical, cultural, spatial, natural meanings in surrounding environment of the object is now rather prevalent. Contextual meanings are very important but should be treated with great concern and deliberateness.

4 CONCLUDING REMARKS

Willful engineer works with Promethean self-consciousness in a sense. What is left behind is an expression of spatial context of the place where the skeleton system is built. In order to facilitate transformation from superficial shape to the recovery of wholesome physique of concrete objects as skeleton systems, it is necessary to comprehend what constitute the semiotic context of the place where the skeleton system is constructed. Syntactic approach associated with space-oriented contextualism can be the basis for skeleton systems of the contemporary age.

REFERENCES

Kubota, Y. (2002) Design of Skeleton System, paper for the 48th Symposium of Structural Engineering, Japan Society of Civil Engineers & Architectural Institute of Japan.

Nakamura, Y. & Kubota, Y. (1991) Pedestrian Bridges in Japan, in "Bridge Aesthetics around the World”, Transportation Research Board.

BRIDGES FORMED BY THEIR ENVIRONMENT

Milan Kalny
PONTEX Consulting Engineers Ltd
Czech Republic

Keywords: concrete bridges and structures, integration to environment, aesthetics, conceptual design

1. INTRODUCTION

Protection and improvement of our environment by designing appropriate, elegant and economic structures are among the professional duties of owners, engineers and architects. Besides the obvious concentration on extensive projects with large span bridges we should not miss any small chance to introduce structural concrete as a material corresponding to nature and the human scale. The author is especially concerned with the impact of bridges as a part of transport route to public. Declaring "Less is more" and permanently searching for unity between structures, their details and surrounding environment the author will present examples both favourable and less fitted to urban or countryside conditions in his country, where understanding environment, tradition and culture should be compulsory for consulting engineers.

2. NATURAL AND URBAN LANDSCAPE

Natural landscape is beautiful and full of harmony. High diversity and the "self-repairing" ability of natural forces form quickly appropriate balance of shapes, colours and covering flora for the relevant climate and environment. The passing time in nature undisturbed by man is usually adding and not deteriorating the integrity and quality of environment. In contrast with nature, human activity leads in many cases to chaos or boring uniformity. Our never ending ambitions for growth, speed, records, superiority and spending all available resources are stretching out beyond any limits. Just recall towns where public transport and infrastructure provide a real quality and enhancement for the citizen's life. Or consider the crawling residential and business suburbs around a concentrated metropolis. In our cities there are many significant buildings and structures, however finding their integration into the environment in a creative, delightful and noble way is quite rare. In fact we can find more well-balanced urban environments in traditional locations, where peace, order, education and democratic principles were cultivated in long undisturbed periods.

A logical system of natural roads and links was developed over centuries and is surprisingly stabilised. Planning any new route has a huge impact on the existing environment. No wonder that finding public approval is increasingly more and more difficult. When crossing natural or artificial obstacles, where size is often not the governing factor, one has to point out even higher attention and sensitivity. Bridges have always been from ancient time up to the present human works at the edge of technology, spanning over dividing borders and fulfilling the permanent desire for travelling and connection. Bridge alignments are usually lifted to higher levels and thus visible from long distances. The designer has to study carefully what type of structure and method of construction is more acceptable to local conditions. Sometimes landmarks are welcomed and even domination of a new crossing over the surrounding environment is required. More frequently sensitive adaptation of a new bridge to an existing natural or urban landscape is advisable. All new construction should show respect to the preceding character and activities in the relevant area. From the past we know that thorough planning and urbanism was used before major construction. Perhaps it was easier to create magnificent panoramas and vistas in a less built-up landscape. However let us think twice and always compare all available alternatives before making any decision that is usually irrevocable for a very long time. Our final goal has to be finding improvement of the environment and not a contribution to discord due to ignorance or overbearing superiority.

The most difficult assignment is apparently found, when the owner or the architect gives precedence to symbolic or "innovative" form over functionality. These circumstances can not always be avoided, however a lot of sound scepticism should be involved to prevent spoiling of the landscape by monstrous or extravagant structures.

3. EXAMPLES FROM PRACTICE

Several examples where the author with his colleagues from the design office have endeavoured to implement these ideas into practice are shown below.

3.1. Footbridge at Pilsen - Ejpovice

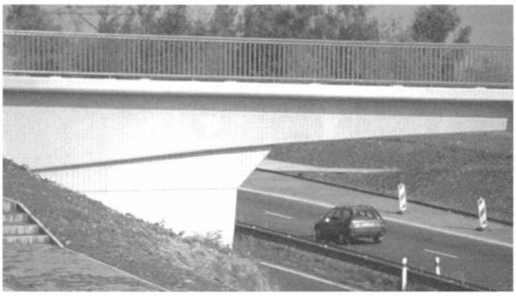

The footbridge contributes to breaking the monotony of a perhaps dull motorway route for the drivers. The design is based on the application of an expressive asymmetrical concept for the superstructure with a natural smooth curve supplemented with painstakingly designed details of the substructure and accessories. The slenderness of the superstructure (ratio of L/h = 43 at the middle of the main span) and a provided camber of some 0.15 m contributed to the smooth shape of the structure.

3.2. Pedestrian bridge at Cerna Street

This bridge connects the pedestrian zone in the suburbs with the center of Opava. The frequently used footbridge is a visually important structure, that should be integrated seamlessly into the city environment. The characteristic elements are the arch-like superelevation, extremely slender superstructure (depth at midspan is 0.70m, resulting in depth/span ratio 1:54) and fluent connection to the approaching footways. The prestressed concrete superstructure crosses the Opava River with one span of 38m and has special illumination.

3.3. Road bridge at Jaselska Street

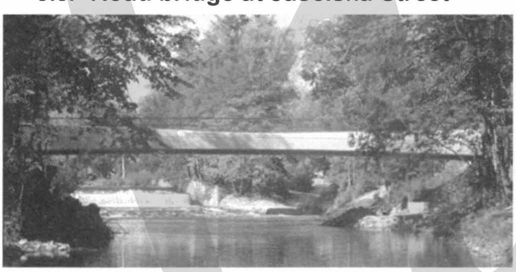

This road bridge across the Opava River serves a little suburban local road. The structure has very low depth at midspan due to its fixed connection to both abutments and strengthening ribs of variable depth. Total span of the superstructure is 36m, while its overall width is 9m. With respect to the bridge's location close to a public park and swimming pool, an aesthetically pleasing structure was a clear target, well positioned to the natural surroundings.

3.4. Footbridge at the Navigation Channel in Podebrady

A new bridge for pedestrians and cyclists has been planned over the navigation channel in the spa of Podebrady in a location with scenic beauty. The main obstacle on the planned path represents a moderate skew span of 35m. The designers chose the alternative option of a slender continuos deck slab supported by the I- and Y-shaped struts of steel twin tubes Ø 150mm and steel strut frame of tubes Ø 280mm acting as composite with the concrete deck slab in the main span. This solution is very economical and blends in with the local environment and landscape.

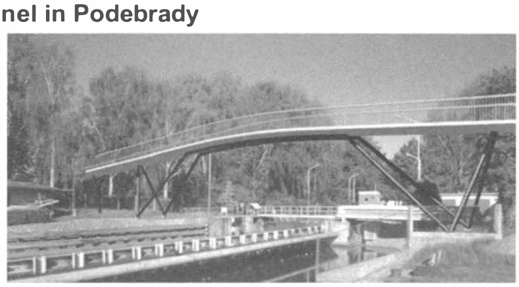

4. CONCLUSION

The search for ecologically viable, technically possible and economically reasonable structures is the most exciting part of work and a challenge for the consulting engineer. The optimum means always to find equilibrium not only in given forces but also to all given conditions. If the new bridge is well adapted to its environment then it truly reflects the aspiration of the designer.

Session 15 | Monitoring

THE REMOTE MONITORING SYSTEM BASED ON INTERNET TECHNOLOGY WITH WIRELESS LAN FOR EXECUTION CONSTRUCTION MANAGEMENT OF SASHIKI BRIDGE

Kunio IMADA	Takatoshi OKABAYASHI	Toru YOSHIMURA	Masafumi HOSOKAWA
Kumamoto Prefecture	The University of Nagasaki	Oriental Construction Co.,Ltd.	Fuji Engineering Co.,Ltd.

Keywords: extradosed prestressed concrete bridge, remote measurement, Internet technology

1 INTRODUCTION

In observing bridges, the efficient management of measurement data is important for the effective use of measurement results. To this end, the remote monitoring is required; it is necessary to construct such systems as unattended operation, and real-time automatic meter reading.

Sashiki Ohashi (Provisional name) is an extra dosed prestressed concrete bridge constructed in Kumamoto prefecture. For construction management of this bridge, field measuring was carried out. We constructed the remote monitoring system for continuous monitoring of observation data obtained at the construction site.

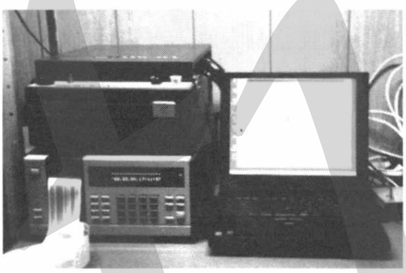

Fig.1 Measurement system (in the measurement room)

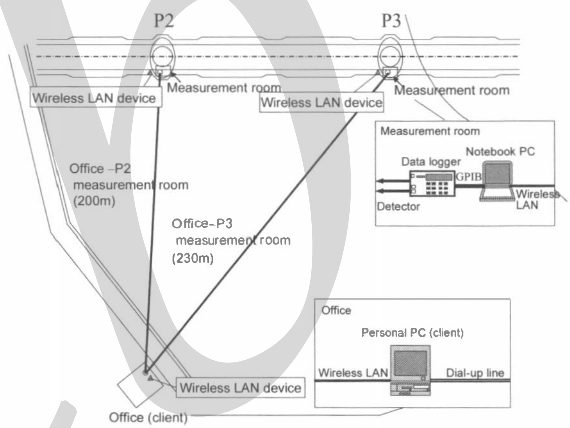

Fig.2 Construction site intranet

2 CONFIGURATION OF REMOTE MONITORING CONTROL SYSTEM

2.1 Remote monitoring system with wireless LAN

The measurement rooms were set up at the P2 bridge support and P3 bridge support respectively for measurement under construction. In the individual rooms, the data loggers are permanently installed. The measurement data of temperature or diagonal member tension are automatically measured, and they are saved in the built-in memory of the data loggers temporarily (Fig.1). In order to manage the actual measurement data, which are obtained from the individual measurement rooms, at the site office approximately 200m away from the measurement rooms, we connected the measurement rooms and the site office with wireless LAN bridge to constitute the construction site LAN. Fig.2 shows the schematic diagram of remote monitoring system with wireless LAN for this bridge.

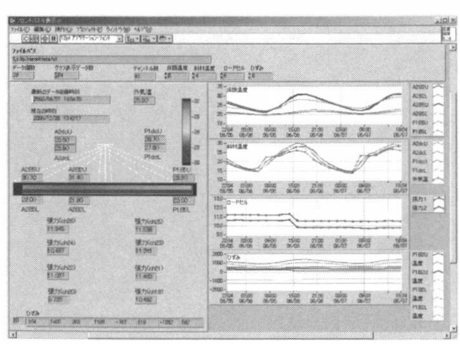

Fig.3 Monitoring screen created with LabVIEW

2.2 Remote monitoring

The personal computers, which were set up in the construction site and the office, were used for remote monitoring of this bridge. They were connected with LAN. On the notebook computers of the construction site, the measurement program was conducted for obtaining measurements, while on the desktop computer of the office, the measurements were monitored using the browse. LabVIEW, virtual measuring instrument software (made by National Instruments), was used for programming. Using the browser, the desktop computer of the site office (client-side) can operate the notebook computers of the measurement rooms (the server side) by remote control. When URL is specified, the screen created with LabVIEW, as shown in Fig.3, is displayed. The current temperature and deflection quantity, and variations for the past 48 hours are displayed on the browser.

3 REMOTE CONTROL FROM OUTSIDE THE CONSTRUCTION SITE

3.1 Remote monitoring control system from outside the construction site

It was performed the remote monitoring and data transfer between Nagasaki University and Sashiki bridge construction site (approximately 80km) by remote monitoring control system for managing experiment from a remote site.

Shown in Fig.4, in order to connect from Nagasaki University to the site intranet at first, we connected dial-up rooters to the computers of Nagasaki University and site office respectively, for communications between them on LAN via dial-up connections using ISDN line. By the configuration of the network, which enables us to connect the computer of Nagasaki University to those of the site for monitoring, as well as connecting the computers of the site office to those of the construction site.

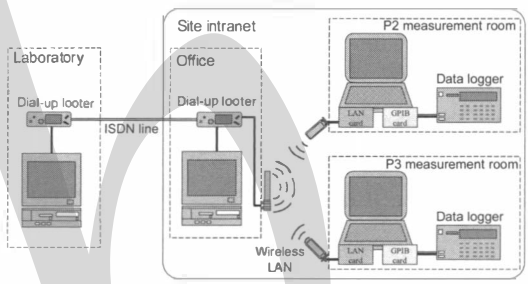

Fig.4 Remote monitoring control system from outside the construction site

3.2 Analysis of measurement values

We compared the actual measurement data with the calculated values with regards to the stay cable tension to analyze them. Fig.5 shows variations of stay cable tension during the course of time. Transition of the stay cable tension showed the behavior of variations during the course of time as calculated. We confirmed the validity of the design condition and calculation model.

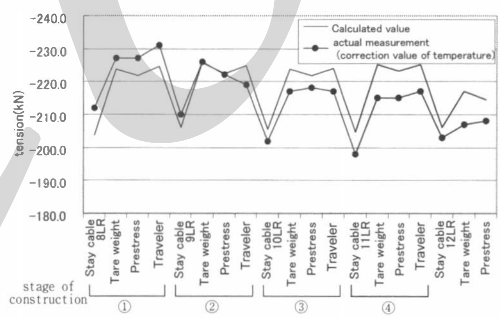

Fig.5 Variations of Stay cable tension during the course of time

4 SUMMARY

For the construction management measurements of this bridge, we adopted the remote monitoring control system with wireless LAN, so that the actual measurement data obtained at the construction site can be managed from the remote site office(Construction of the site intranet).

In addition, we believe that development of the network will be useful in the future, so that the condition state of more than one construction site can be monitored from various points in a wide area. Therefore we performed the wide area monitoring experiment using wireless LAN and ISDN line as initial experiment of development. We confirmed that quantity of information and transfer speed are both feasible.

REFERENCE

[1] Okabayashi, T., Yoshimura, T., Kawamura, S., Hosokawa, M : The telemetry system based on Internet technology with wireless LAN for execution management of bridge construction. Journal of Structural Engineering, Vol.47A, pp.285-292, 2001.3

STRUCTURAL HEALTH MONITORING OF INNOVATIVE BRIDGE STRUCTURES IN CANADA

Aftab Mufti, Gamil Tadros, John Newhook and Roger Cheng
ISIS Canada, Winnipeg, Manitoba, Canada

SUMMARY

ISIS Canada, Intelligent Sensing for Innovative Structures, is a Canadian Network of Centres of Excellence established in 1995 to research and develop innovative uses of fibre reinforced polymers (FRPs) in concrete structures that are prone to deterioration because of corroding steel reinforcements. As a means of documenting the behaviour of FRPs, ISIS Canada also researches and develops structurally integrated fibre optic sensing systems that allow engineers to monitor structures from remote locations. The six projects described in this paper outline the collaborative projects undertaken by ISIS Canada to incorporate fibre optic sensing and remote monitoring in bridges built in Alberta, Nova Scotia, Manitoba, Quebec, and Prince Edward Island/New Brunswick, Canada.

1. BEDDINGTON TRAIL BRIDGE – ALBERTA

This is the first bridge to be instrumented in Canada with fibre optic sensors, and the first bridge known to contain pre-stressed carbon fibre composite cables with Fibre Bragg Grating (FBG) sensors embedded in the concrete girders supporting the bridge. A total of 20 FBGs were installed in 1993. To check the integrity of the carbon fibre cables and the FBGs, measurements were made (November 1999) and 18 of the sensors were still operative. No structural problems were detected.

2. SALMON RIVER BRIDGE – NOVA SCOTIA

This bridge is noteworthy because one span was constructed in 1995 using an innovative steel-free deck consisting of polypropylene fibre reinforced concrete with no internal continuous reinforcement. FBGs were embedded into the fibre reinforced polymer reinforcements during manufacture for use in the adjacent curb sections. Of particular interest in this application is the extensive testing done on a full-scale model incorporating components that were instrumented with both FBGs and foil resistance strain gauges. In all cases, the two sensor systems correlated very well.

3. TAYLOR BRIDGE – MANITOBA

Taylor Bridge is considered to be the world's largest highway bridge reinforced by FRP and monitored using fibre optic sensors (FOS). The 165.1 m long bridge consists of 40 prestressed concrete AASHTO-type girders. Four girders of the Taylor Bridge were prestressed by two different types of carbon fibre reinforced polymer (CFRP) material using straight and draped tendons. The girders were also reinforced by CFRP stirrups protruded from the AASHTO type girders to act in composite action with the bridge deck. A portion of the deck slab is reinforced by CFRP reinforcement. Glass fibre reinforced polymer (GFRP) was also used to reinforce the barrier walls.

FBG sensors were used to monitor the strains in the CFRP reinforcement of the girders and the deck slab of Taylor Bridge, as well as the GFRP reinforcement of the barrier walls. Selective girders reinforced by conventional steel reinforcement were also instrumented using FBG sensors. A total of 63 FBG sensors and two multi-Bragg sensors were glued to the reinforcing CFRP bars.

Twenty-two AD590 electric-based temperature sensors were installed for the purpose of compensation for thermal apparent strain. Temperature sensors provide representative temperature measurements among different girders and at various locations along and through the depth of the girder and the deck slab. The reading of a FBG sensor was used to estimate the temperature-compensated strain.

4. CROWCHILD TRAIL BRIDGE – ALBERTA

The original Crowchild Trail Bridge in Calgary, Alberta was a two-lane, three-span prestressed concrete box-girder bridge. The bridge was found to be under-strength as a result of deterioration over 20 years and increased traffic load on the bridge. Therefore, the bridge superstructure was replaced in June 1997.

The new superstructure is the first continuous span steel-free bridge deck in the world. The removal of internal steel reinforcement is made possible by providing lateral restraint to the supporting steel girders through evenly spaced transverse steel straps placed across the tops of the adjacent girders. Glass fibre reinforcements are used at the regions of interior supports and overhanging cantilevers. Prefabricated glass fibre reinforcing grid, NEFMAC, is used for the reinforcement of side barriers.

A total of 103 strain gauges, two fibre optic strain sensors, and five thermisters were used in the monitoring program. The first tests (1997) consisted of a static truckload test, an ambient vibration test, an effect of temperature test, and dynamic measurements under passing trucks. The second tests (1998) consisted of static and dynamic truckload tests and ambient vibration test.

5. JOFFRE BRIDGE – QUEBEC

The Joffre Bridge, located over the St-François River in Sherbrooke, Quebec, Canada, built in 1950, showed signs of deterioration of the concrete deck slab and girders primarily due to reinforcement corrosion. The City of Sherbrooke and the Ministry of Transport of Quebec reconstructed a significant part of the bridge deck, sidewalk and traffic barrier using carbon and glass FRP reinforcements, and monitored the performance not only to answer the safety concerns, but also to generate valuable data for the research and development of FRP technology for reinforced concrete structures.

The bridge was extensively instrumented with several different types of gauges. A total of 180 critical locations were identified and instruments (fibre optic sensors, vibrating wire strain gauges, and electrical strain gauges) were installed at those locations in the concrete deck slab and on the steel girders.

The bridge was opened to traffic on 5 December 1997. The dynamic responses of different components of the bridge are being regularly recorded using computer aided data logging systems. The interim results indicate confidence in the use of FRP reinforced concrete structures and the use of state-of-the-art instrumentation for continuous long-term structural performance monitoring.

6. CONFEDERATION BRIDGE – PRINCE EDWARD ISLAND/NEW BRUNSWICK

This is the longest bridge over ice-ocean water, spanning 12.9 km from Prince Edward Island to the New Brunswick main land. Its enormous size required the use of the most modern concrete manufacturing process and a hollow core design to incorporate a very large utility corridor. Because this bridge has been designed for 100-year lifetime and must operate in a most severe environment, extensive sensor instrumentation has been employed to monitor the loads and structural performance. Included in the suite of sensors used were FBGs bonded to steel rebars that are embedded in concrete. A total of 15 FBGs are currently in service on both a main girder and in the adjacent drop-in span. Four gauges were left 'unbounded' to provide temperature compensation and a means to compare with bonded thermocouple data. The system installation in 1996 involved engineers from various groups within ISIS Canada and EPC. A more complete description of the installation details and bridge structure can be found in.

CONCLUSIONS

A total of 16 bridges have been instrumented across Canada with various combinations of fibre optic sensors, strain gauges and thermal gauges. Field experience has been gained in terms of the operational performance of fibre optic Bragg gratings over a period of six years. In all cases, very few failures of these sensors have been found when they were properly installed. The examples described in this paper were chosen for the special features associated with the bridge structure, the use of advanced composite materials and fibre optic sensing. Both of these technologies are relatively new in the field of civil engineering structures. However, the emerging need to provide new design concepts taking advantage of new materials necessitates the requirement for long-term monitoring. The FOS, calibrated through several load tests, showed good performance as compared to the conventional electric strain gauges. When embedded in concrete members, FOS are more durable than electric strain gauges. The monitoring system can provide a profile of the bridge, with detailed information on its structural behaviour, as well as health due to applied loads and environmental effects. Fibre optic sensing with its many advantages over conventional electrical resistance strain gauges provides a unique opportunity to use modern telecommunication technologies, which are developing at the same time. The availability of high bandwidth transmission makes possible the task of employing multisensor systems that can serve the long-term 'health' monitoring of new and rehabilitated structures from central sites, and minimize the need to do on-site inspections.

SCANNING PROCEDURE OF IMPACT ECHO FOR DETECTING DEFECTS IN CONCRETE STRUCTURE

Takeshi Watanabe Chikanori Hashimoto Masayasu Ohtsu
The University of Tokushima Kumamoto University
JAPAN JAPAN

Keywords: Impact-Echo, Scanning Procedure, SIBIE,

1 INTRODUCTION

The impact-echo technique is an advanced nondestructive evaluation (NDE) for defects in concrete structures. The technique is based on detecting elastic waves due to a mechanical impact. Conventionally, extracting resonance frequencies responsible for the locations of reflectors, the presence and depth of defects are estimated. Thus, the technique is available to evaluate voids in concrete structures is promising. Although, a variety of attempts have been reported, it is realized that identification of resonance frequencies due to defects has been marginally successful. This is because there exist unresolved problems still to be applied to concrete structures in service. Consequently, to circumvent drawbacks on the identification of peak frequencies, the impact-echo is theoretically studied on the bases of the elastodynamics and the signal analysis. Theoretically, frequency responses of the specimen depend on the size of the member, and the location of the void and P-wave velocity, because wave motions in concrete structures are characterized by material properties, incident waves, and the representative length. The frequency response is investigated in respect to the relationship between the wavelength and the depth of defects. In order to improve the impact echo, a new procedure to evaluate defects in concrete is investigate, applying an scanning procedure. Thus, stack imaging of spectral amplitudes based on the impact-echo (SIBIE) is developed. The procedure is applied to concrete slab which has voids to be detected.

2 IPACT-ECHO METHOD AND RESONANCE FREQUENCY

Concerning the frequency responses of concrete slab and the dimensional analysis, the following two relationships between the wavelength and the depth of the void are known [1][2]. f_{void} and f'_{void} is the resonance frequency of the void in the depth d. C_p is P-wave velocity. 0.96 is a shape factor determined by the geometry and is not directly related with the Impact-echo theory.

$$f_{void} = 0.96\frac{C_p}{2d} , \qquad f'_{void} = \frac{C_p}{d} \tag{1}$$

3 INVERSE SCATTERING AND SCANNING PROCEDURE OF SIBIE

According to the inverse scattering theory in elastodynamics[3], one scanning procedure is developed as SIBIE (**S**tack **I**maging of spectral amplitudes **B**ase on the **I**mpact-**E**cho) [4] .

First, in cross-sections of the specimen meshes are arranged in evenly. Then, the resonance frequencies due to reflections from the element are computed. In this case, the travel distance from the input to the output via the element is calculated as the total distance R.

$$R=r_1+r_2 \tag{2}$$

At the each element, the distance R of reflected path is calculated. Then, resonance frequencies in eq.3 are computed

$$f_1=C_p/(R/2) , \quad f_2=C_p/R , f_3=C_p/2R , \quad f_4=C_p/3R,\cdots\cdots \tag{3}$$

In order to detect carry out the inverse transform, the spectral amplitudes corresponding to these resonance frequencies are summed. Thus, the characteristic function at each element is estimated as a stack image. This scanning procedure is named as SIBIE.

4 EXPERIMENT

A specimen containing voids was tested. Dimensions of the specimen are 900x900x300mm3 type voids which dimensions are 80x80x50mm, 80x80x20mm and 160x160x20mm are buried in 30mm and 150mm depth. As impact tests, two steel balls of 9.5mm and 19.0mm diameter were dropped at 250mm height over the top surface of the specimen. the upper bound frequencies of two steel balls of 9.5mm and 19.0mm diameter are 30.6kHz and 15.3kHz respectively.

The impact-echo tests using the two steel balls were conducted at six point over voids and the center of the specimen without voids. A typical cross section tested is shown in Fig.5. Elastic waves due to the steel balls were detected by an accelerometer. Fourier spectrum of the acceleration was analyzed by FFT.

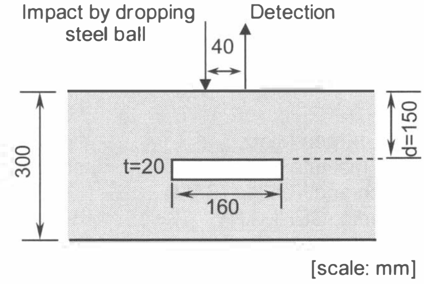

Fig.1 Cross-section performed impact-test.

5 RESULT

In the case of test on void 150mm in depth, frequency spectra due to a steel ball of 9.5mm diameter are detected. In the frequency spectra, the resonance frequency f_{void} is observed around 12.5kHz, although the results demonstrate the difficulty to identify the resonance frequencies due to voids only from the frequency spectra.

The scanning procedure of SIBIE were applied to the frequency spectra detected over voids 150mm in depth. In Fig.2, at cross-section(b) and (c), the high intensity regions due to the voids are observed about 150mm in depth. It is confirmed that the location and presence of the void can be visually identified by SIBIE.

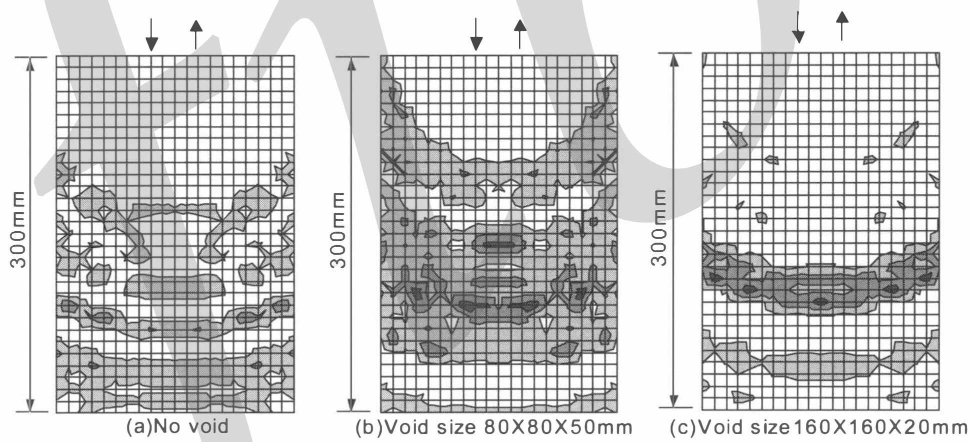

Fig.2 Results of imaging after summing resonance frequencies f'_{void} and f_{void} in the case using the steel ball of 9.5mm diameter.

REFERENCE

[1] Sansalone, M.J. and Streett, W.B : Impact-Echo, Bullbrier Press, Ithaca, N.Y., 1997
[2] Ohtsu, M. : On High-Frequency Seismic Motions of Reinforced Concrete Structures," *J.Materials, Concrete Stru. and Pavements*, JSCE, **544**, 277-280, 1996.
[3] Nakahara, K. and Kitahara. M. : Inversion of Defects by Linearized Inverse Scattering Methods with Measured Waveforms, Proc, Int. Sym. on Inverse Problems in Engineering Mechanics (ISIP2000), 9-18, 2000.
[4] Watanabe, T. and Ohtsu, M. : Spectral Imaging of Impact Echo Technique for Grouted Duct in Post-tensioning Prestressed Cocrete Beam," Nondestructive Testing in Civil Engineering, Elsevier, 453-461, 2000.

INTEGRATED MONITORING SYSTEM FOR REINFORCED CONCRETE STRUCTURES

Jürgen Mietz
Federal Institute for Materials Research and Testing (BAM), Berlin, GERMANY

Michael Raupach
Institute for Building Materials Research, ibac, RWTH-Aachen, GERMANY

Per Goltermann
RAMBOLL, Virum, DENMARK

Keywords: reinforcement corrosion, sensors, inspection, maintenance, bridge management

1 INTRODUCTION

The major part of the infrastructure has reached an age where capital costs have decreased, but where the inspection and maintenance costs rapidly increases and constitute the major part of the costs. Monitoring and inspection systems are used in a variety of industries to ensure safety and reduce costs by early detection of damage (so minor rehabilitation work will stop the deterioration). Such systems can also be applied to civil engineering structures if the necessary probes are available for embedding in structures.

Traditional bridge management usually includes routine, principal or special inspections. The special inspections usually lead to an assessment of the structures performance (safety and functionality) and a prediction of the development over another 5, 10 and 20-25 years in order to estimate the economical and technical consequences of taking or postponing repair actions.

A vital part in this prediction are the models and experiences in e.g. extrapolation of chloride ingress, estimated critical chloride concentration for initiation of corrosion and later loss of reinforcement and structural performance. These models are not precise, but the experience from the sampling of chloride and moisture clearly shows that the main uncertainties are caused by the variations of the input as e.g. the chloride or moisture profile. This uncertainty may be reduced by the use of a monitoring system with sensors, which record the chloride or moisture development versus time in fixed positions and depths.

The current development in structural monitoring is concentrated on the installation of permanently embedded sensors. Theses monitors continuously provide information on structures, which reduces the inspection costs. The main advantages of a permanent monitoring system are as follows:

- more reliable deterioration trends (frequent collection of data)
- more precise assessment of the conditions of the structures
- input for undertaking preventative actions
- input for defining maintenance/repair strategies
- feedback on the effectiveness of repairs
- evaluation of the need for further inspections and additional testing

2 OVERVIEW OF THE SMART STRUCTURES PROJECT

During the SMART STRUCTURES project (no. BRPR-CT98-0751) - an interdisciplinary research project funded by the European Community, eight European partners developed and tested the necessary probes and sensors for monitoring chloride, moisture, pH and corrosion risk in different depths and for strain, crack-widths, vibration frequencies and amplitudes for use in existing concrete structures. These are integrated through an Internet-based software for collecting, storing and treating the monitoring data in order to produce an input to the bridge maintenance.

The Skovdiget Western bridge near Copenhagen in Denmark has been chosen for field testing of the monitoring both for convenient location and because different deterioration mechanisms are contemporarily active on the structure.

In order to reach the desired objective of the research, the project is divided into 7 tasks:

Task 1 describes the state of the art of current practice in the fields of inspection, monitoring and maintenance, both in Europe and in the USA, underlying advantages and possible disadvantages as well. It results in a number of requirements and system specifications for the integrated monitoring system from the end-user point of view.

Task 2 contains the description and correlation of the most relevant deterioration mechanisms for the structures with the parameters that may be measured on-site. The focal point is the determination of the critical levels of both the parameters of the models and of the corresponding measurable parameters.

Task 3 is related to the implementation of portable equipment to measure corrosion activity. This equipment may be used to support the current activity of monitoring and inspection of bridges. It has been successfully tested in laboratory and on-site, in Italy and in Denmark.

The objective of Task 4 is the design, development, and production of a number of sensors to be installed on the structures to monitor their progressive deterioration.They have been firstly tested in laboratory where their performances have been compared to those of sensors and probes available on the market, to be next successfully installed and tested on an existing bridge.

Task 5 aims at designing and integrating the systems for data acquisition and transfer with the software for data treatment and analysis.

Task 6 represents the design and implementation of the whole system at a demonstration structure along with guidelines for the installation of the sensors. Testing has been going on for two years up to now on a bridge in Denmark and it is foreseen to continue for the next five years. Data collected on-site and transferred according to the results of Task 5, are processed to evaluate the progress of deterioration, to define alarm thresholds and to establish maintenance strategies and compute the overall costs.

Task 7 deals with the economic validation of the entire system and the assessment of the existing maintenance and repair strategies and incorporation of the integrated monitoring system and improved lifetime models into those strategies.

2 CONCLUSIONS

During the SMART STRUCTURES project different embeddable sensors for measuring the key parameters of the most common deterioration mechanisms have been developed or improved and tested both in laboratory and on-site. The testing has documented that the sensors functions and are durable in the laboratory and in the test bridge for the duration of the test (12 to 24 months so far). The different sensors are combined through an Internet-based software to an integrated monitoring system. The Internet-based software collects and presents all the monitored data and can be linked to the facilities of management systems and is able to run on the owners Intranet as well. This is a large advantage in utilizing the data for the bridge management.

The integrated monitoring system and the sensors are able to cover existing concrete structures in the infrastructure (roads, bridges, harbors, airports) as well as building structures. Improvements in the data acquisition and transfer facilities will reduce the monitoring costs substantially and will widen the range of applications for the systems. The monitoring system and the sensors establish valuable, additional knowledge about the deterioration mechanisms and the structures performances in practice. It is estimated that the use of this system could generate reductions in the order of 10-20% of the current operating costs, especially through easier access to data and postponing or reduction of extensive repair works.

Further information about the Integrated Monitoring System and the different probes and sensors can be obtained the project web http://smart.ramboll.dk/smart_eu/.

INVERSION BY BEM OF HALF-CELL POTENTIAL MEASUREMENT FOR NDE OF REBAR CORROSION

Je-Woon Kyung
Graduate School of Science and Technology
Kumamoto University
Graduate Student, JAPAN

Masayasu Ohtsu
Graduate School of Science and Technology
Kumamoto University
Professor, JAPAN

Keywords: NDE of corrosion, half-cell potential, BEM, concrete resistivity, polarization resistance

1 INTRODUCTION

Corrosion of rebars is one of the major problems facing engineers today. Because concrete is a porous material, carbon dioxide and chloride can penetrate into it. As a result, the passivity of the steel is destroyed, and then rebars in concrete are corroded. The expansion of corrosion products generates cracks which result in serious defects in reinforced concrete (RC) structures. Thus, nondestructive evaluation (NDE) for corrosion of rebars is to be performed in advance to visible inspection of cracking. So far, two nondestructive techniques of the half-cell potential and the polarization resistance are practically available. The former provides information on the probability of corrosion, while the latter is associated with information on the corrosion rate.

For the half-cell potential measurement, the criterion to estimate the probability of corrosion has been already coded in ASTM C876. It is reported, however, that the potentials measured are too sensitive to moisture content, thickness of concrete cover, surface coating, resistivity of concrete and so forth. Consequently, the estimation of corrosion by the half-cell potential is still inconclusive.

An essential drawback of the half-cell potential measurement results from the fact that the potentials are measured not near rebars but on concrete surface. One compensation is to measure the potentials as close to rebars as that probes of the electrode are embedded in concrete or are inserted into the bottom of bore holes. Another compensation is to determine the potentials around rebars analytically. Although the direct BEM was introduced, three-dimensional (3-D) analysis was not only time-consuming but also impractical.

In the present paper, a simplified inversion by BEM is applied to convert the potentials on concrete surface to those on rebars, taking into account the concrete resistivity. An applicability of the procedure is examined by accelerated corrosion tests of RC slabs.

For practical use, the procedure is developed where results of IBEM are visualized by VRML (Virtual Reality Modeling Language) in three-dimensional space.

2 INVERSION BY BOUNDARY ELEMENT METHOD (IBEM)

To convert the potentials on the surface into those on rebar, previously a simplified inversion by BEM was applied.

$$u_i = \sum_{j=1}^{M}\left[-\frac{\partial G_{ij}}{\partial n} R\right] u_j \Delta S . \tag{1}$$

Here R is the relative coefficient of concrete resistivity. When a void and a determination are identified by radar measurement,

$$R = \frac{R_{nv}}{R_v} , \tag{2}$$

where R_{nv} is the averaged concrete resistivity of intact part and R_v is that of void part.

3 RESULTS

3.1 Concrete Resistivity

The concrete resistivity of void part is higher than that of non-void part. A result of the void specimen is shown in Fig.1. Comparing these two parts, the relative coefficient R is determined by Eq.2. In computation of Eq.1, R is constantly 1.0 for non-void parts.

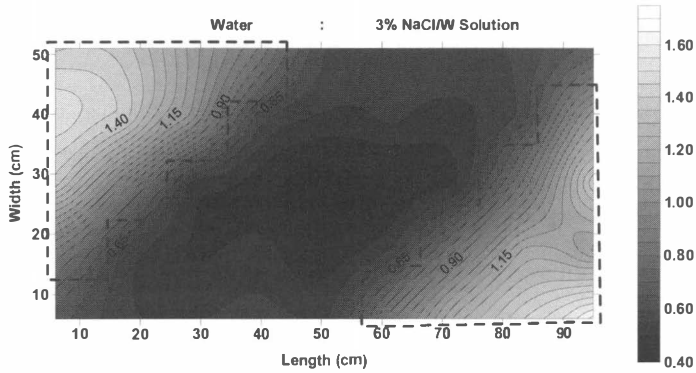

Specimen including void

Fig. 1 Concrete resistivity after 36hrs by an accelerated corrosion test (kΩ).

3.2 Half-cell potentials

The specimen was broken and the rebars were removed to identify the corroded area. Results are shown Fig.2 (a) by VRML. Results of IBEM are given in Fig.2 (b) by VRML. Remarkable agreement between the actual corroded region and the estimated is observed.

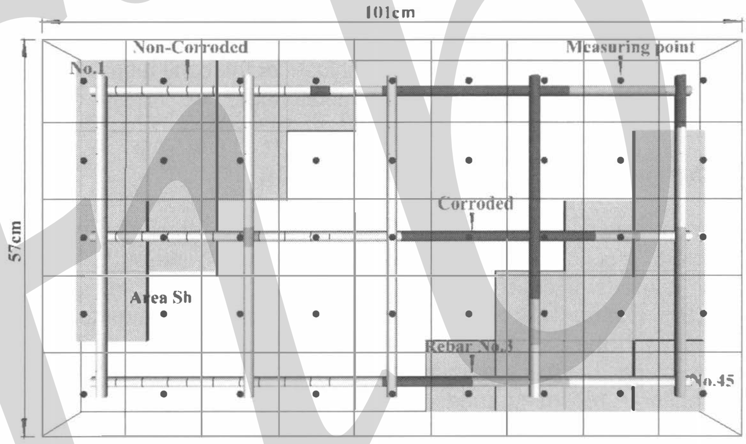

(a) Results of visual inspection

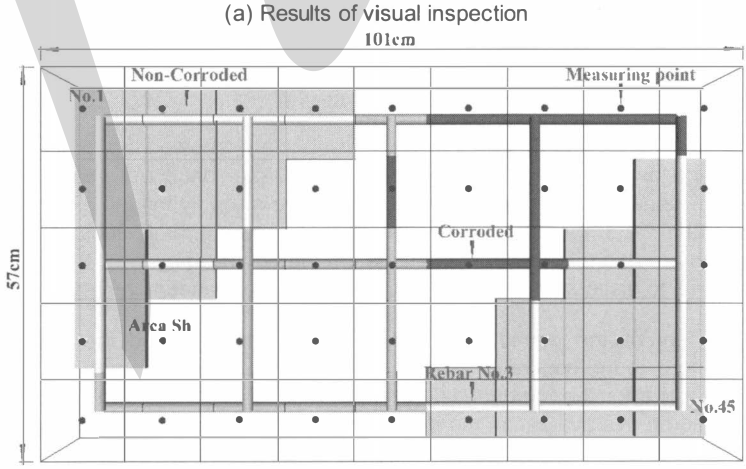

(b) Results of IBEM (R =0.467)

Fig.2 Results of half-cell potential measurement in the specimen with void.

ONLINE-MONITORING OF CORROSION IN REINFORCED CONCRETE STRUCTURES

Yves Schiegg and Hans Böhni

Institute of Materials Chemistry and Corrosion
Swiss Federal Institute of Technology
CH-8093 Zurich, Switzerland

Fritz Hunkeler

Technical Research and Consulting on Cement and Concrete (TFB)
CH-5103 Wildegg, Switzerland

Keywords: monitoring, corrosion, reinforcement, concrete

1 INTRODUCTION

Chlorides from deicing salts are one of the main causes for corrosion damage in concrete bridges and other road structures. The corrosion of concrete constructions is a complex process that is largely influenced by the interaction of the environment with the reinforced concrete. One can distinguish between the initiation state and the corrosion propagation state. During the initiation state chlorides are transported into the concrete leading to localized corrosion of the reinforcement. A theoretical prediction of the corrosion propagation was practically not available up to now. The goal of this work was the acquisition and the assessment of important parameters of rebar corrosion in concrete structures and to provide the fundamentals of corrosion propagation that would enable the engineer to make a better prediction on the development of the corrosion state of the reinforcement. A further goal was the development and testing of a measuring technique for the continuous assessment of important corrosion parameters of concrete structures (online-monitoring).

2 INSTRUMENTATION AND FIELD INVESTIGATIONS

Investigations on corrosion propagation were based on the development of concrete cores equipped with sensors capable to monitor the major parameters involved in the ongoing corrosion processes. The instrumentation consists of concrete cores with chloride, resistivity and temperature sensors as well as isolated active rebars. The cores were taken from concrete structures or prepared in the laboratory. The cores with the sensors were mounted in the boreholes of structures with different exposure conditions along the swiss national highway A13. A special data aquisition system was developed for the continous recording (measuring interval ≥1 minute) of resistivity (concrete humidity), potential (corrosion state, chloride content), corrosion current (material loss) and the climatic parameters such as temperature and relative humidity [1].

3 RESULTS AND DISCUSSION

The measurements taken over a period of two to three years, showed that continous monitoring has a decisive advantage over periodic single measurements (e.g. once per year). Since some of the parameters like the resistivity and the corrosion current are strongly influenced by the environmental conditions (temperature and humidity), short-time changes like e.g. daily fluctuations as well as long-term changes which are due to seasonal variations can be recorded by the new measuring technique. This procedure allows to distinguish between period of low or enhanced corrosion activity.

For an assessment of the humidity exchange in the concrete and the consequences on the corrosion rate, changes in the concrete resistivity had to be separated from the effect of temperature. An evaluation procedure for the exponential correlation of temperature and resistivity over time was developed [2]. Based on this evaluation the influence of exposure conditions on the concrete humidity and the temperature as well as on the corrosion current could be shown and new findings on the humidity exchange of concrete structures and the transport of aggressive substances were found. For all exposure conditions a characteristic course of the concrete resistivities was found. From this behaviour short-term humidity changes which only cause a change of the humidity directly below the surface of the concrete (small incidents) could be distinguished from deep-reaching humidity change with transport zones over 40 mm (large incidents). These results provided a new insight of the chloride transport into the concrete.

From the corrosion current measurements and the determination of active corroding areas on the rebar probes the corrosion propagation (material loss over time) could be calculated. Rebars in structures with direct weathering and/or splash water showed high corrosion rates up to 0.6 mm/year, whereas the propagation in partially wet structures or structures with indirect weathering was much lower (≤0.01 mm/year). The propagation curves showed that the decisive factor for the increase of the corrosion processes was mainly the exposure conditions of a concrete structure and to a minor extent the chloride content in the concrete. The characteristic step-shaped propagation curves had to be attributed to seasonal variations of the temperature and humidity. During the summer season the corrosion rate was approximately a factor of two higher than during the winter months [Fig. 1]. Regarding the predicion of the corrosion propagation a hyperbolic correlation between the concrete resistivity and the corrosion rate was found and an assignment to four different exposure conditions could be made. This enables to estimate the corrosion propagation rates of concrete structures.

On the basis of this new understanding of the transport of humidity and agressive substances as well as of the corrosion propagation specific measures are proposed to increase the initiation stage and to reduce the corrosion rate. Since the exposure conditions of a concrete structure and the concrete resistivity have a decisive influence on the corrosion propagation some measures not only increase the initiation state but also positively affect the corrosion rate. The future application of the online-monitoring aims at developing new repair methods, new materials or optimizing repair products with the help of field investigations [3]. But it can also be used for special problems of corrosion propagation of concrete structures.

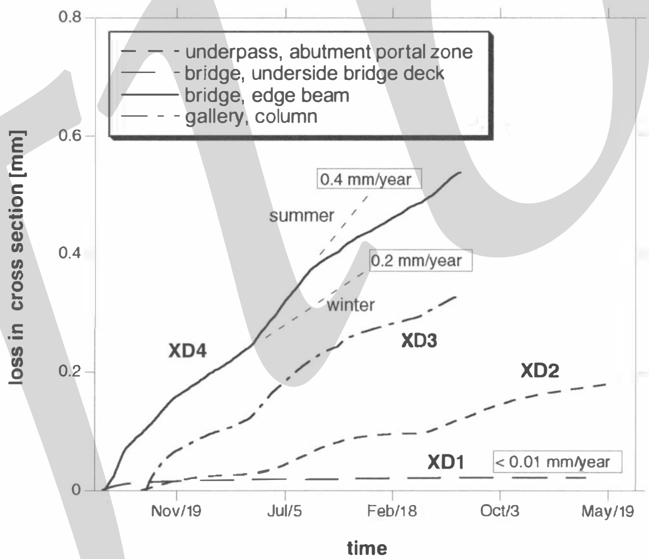

Fig. 1 Corrosion propagation over time of corroding rebar probes in different exposed concrete structures. Exposures XD1: indirect weathering / XD2: spray, partially wet / XD3: splash water / XD4: direct weathering

REFERENCES

[1] Schiegg, Y., Böhni, H.: Online-Monitoring der Korrosion an Stahlbetonbauwerken, Beton- und Stahlbetonbau, Heft 2, p. 92-103, Feb. 2000

[2] Schiegg, Y., Audergon, L., Elsener, B., Böhni, H.: Online-Monitoring of the corrosion in reinforced concrete structures, Proc. Eurocorr'01, Riva del Garda, Italy, 2001

[3] Schiegg, Y., Hunkeler, F., Ungricht, H.: The effectiveness of corrosion inhibitors - a field study, Proc. Eurocorr'01, Riva del Garda, Italy, 2001

HEALTH ASSESSMENT OF A PC BOX GIRDER BRIDGE

Ming L. Wang, Jaroslav Halvonik

Dept. of Civil and Material Engineering
University of Illinois at Chicago, 842 W. Taylor St
Chicago, Illinois 60607, USA

Dept. of Concrete Structures and Bridges
Slovak Institute of Technology
Bratislava, Slovak Rep

Keywords: health monitoring, damage assessment, shear crack, shear stiffness, load test

Abstract

There are hundreds of bridges that for some reason suffer from damages that hinder their proper performance. The damages have a various severity, from cosmetic defects to damages that may cause a sudden collapse of the structure. In bridges, deterioration processes are often accelerated by harsh weather conditions, presence of de-icing agents as well as by overloading due to unpredictable increase of traffic. Then, a small hidden defect may develop into a damage leading to the failure within few years. Therefore methods are needed that enable to detect these damages in time and distinguish their rate of severity.

With increasing experience many non-destructive testing methods have been developed for health assessment of the bridges, from the simplest ones that cover regular inspections and visual controlling, to highly sophisticated methods, which require expensive equipment and highly skilled personnel. This paper presents experiences gained by authors from health assessment of Kishwaukee River Bridge. Dynamic and static methods have been used for evaluation of the health condition of the bridge including two load tests.

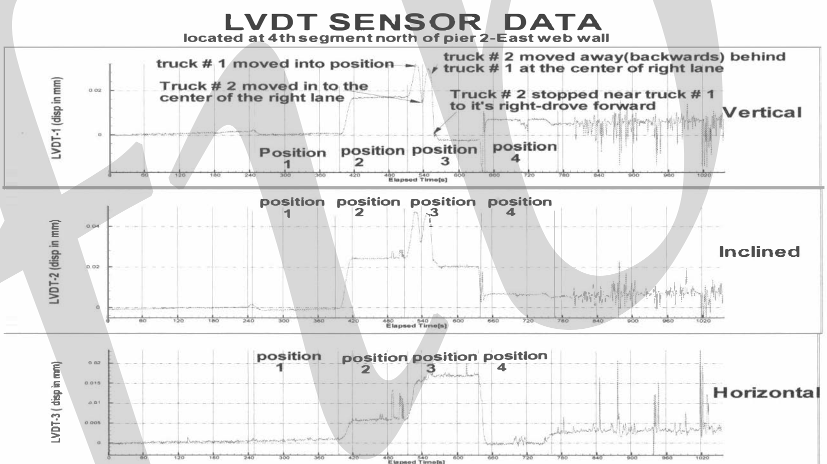

Fig.1 LVDT sensors data record

Table 1: Comparison of vertical natural frequencies

Frequency	Bridge	1.mode	2.mode	3.mode	4.mode	5.mode
*)Measured by CTL	southbound	1.61 -1.65	2.06-2.08	2.64-2.66	-	3.90-3.98
	northbound	1.62 -1.69	2.13-2.18	2.75-2.79	-	3.97-4.05
Measured by UIC	southbound	1.60 -1.65	2.05-2.10	2.65-2.70	2.95	3.95-4.00
	northbound	1.65 -1.70	2.10-2.15	2.70-2.75	2.97	4.00-4.05
Computed	not damaged	**1.650**	**2.132**	**2.767**	**3.010**	**4.032**
*) Measurements made by Construction Technology Laboratory in 1986						

CONCLUSIONS

1) The webs of the Kishwaukee Bridge can be deemed as non-prestressed, because prestressing units are located in the slabs. Therefore an existence of the cracks is expected here and less rigorous crack width limits can be applied. However, inadequate growth of the cracks after retrofit has attracted an attention on the stress rate in shear reinforcement. The web cracking as a damage got further dimension in relation to the design criteria. Besides threat of steel corrosion (durability), the higher steel stresses that had developed during construction might threaten shear strength (safety) of the structure.
2) The retrofit has enhanced shear resistance of the joints, which is a fundamental assumption for development of the shear strength of southbound bridge. However we do not know, how existing crack pattern would influence a flow of internal forces due to ultimate load and how higher steel stresses would affect shear strength of the structure.
3) Unfortunately there are no non-destructive methods that allow direct determination of the ultimate strength. Structure in service must not be subjected to ultimate load because it causes such permanent damages in structural materials, that the structure becomes unfit for further service. Testing can be carried out only by a service load (proof testing). On the other hand, the safety design criteria are usually so strict, that a proper performance of the structure under service conditions automatically ensures required safety. However this rule is not applicable in Kishwaukee Bridge.
4) A small sensitivity of both tests (dynamic and static) to detect this sort of damage from global properties of the structure was observed in Kishwaukee Bridge. These defects had little influence on responses like resonant frequencies, corresponding mode shapes and deflections due to static load. Furthermore, material properties of concrete like modulus of elasticity are variable values that depend on many parameters e.g. on ambient conditions e.g. temperature and moisture. So, the deviations of these properties can be larger than the effect of the damage on the global properties of the structure.
5) If damage location is known, the static load test is shown to be a valuable tool for assessment of the damage severity. The performed static load tests indicated that shear reinforcement in the most damaged web was working elastically when a stress increment was ranging from 8 MPa to 15 MPa, because tangential shear stiffness was reduced only to 45% of the value in uncracked state.
6) Higher shear strains accompanied by a transverse bending moment (trucks located at position #3), caused permanent residual displacements recorded by LVDT sensors. We suppose that the transverse bending moment increased average steel stresses ranging 15 - 28 MPa in shear reinforcement located at exterior surface of the web as the steel could reach the yielding strength and small plastic deformation could occur in some bars. To confirm this theory, further test was proposed with LVDT sensors installed on both sides of the web (inside and outside of chamber).

REFERENCES

[1] NAIR, Shankar R. - IVERSON, James K.: Design and Construction of the Kishwaukee River Bridge, *PCI Journal*, Vol.27, No.6, pp.22-47, 1982

[2] SHIU, Kwok N. - DANIEL, James L. - RUSSEL, Henry G.: Time-Dependent Behavior of Segmental Cantilever Concrete Bridges, 1983

[3] AASHTO LRFD Bridge design Specification, 1998

[4] HSU, Thomas T.C.: Unified Theory of Reinforced Concrete, CRC Press, 1993

[5] COLLINS, Michael P. – MITCHEL, Denis: Prestressed Concrete Structures, Prentice Hall, Englewood, New Jersey 1991

[6] FU, Gongkang: Nondestructive Testing: Load Rating and Condition Rating in Bridge Safety and Reliability, ASCE, 1999

LONG-GAGE SENSOR TOPOLOGIES FOR STRUCTURAL MONITORING

Daniele INAUDI and Branko GLISIC
SMARTEC SA, Via Pobbiette 11, CH-6928 Manno, Switzerland
Tel: ++41 91 610 18 00; Fax: ++41 91 610 18 01; e-mail: smartec@smartec.ch; www.smartec.ch

Keywords: long-gage sensors, structural monitoring, sensor topologies, fiber optic sensors, SOFO

1 INTRODUCTION

The availability of long-gage fiber optic sensors has opened new and interesting possibilities for structural monitoring. Long-gage sensors allow the measurement of deformations over measurement basis that can reach tens of meters with resolutions in the micrometer range. The SOFO sensors developed by SMARTEC SA and the Swiss Federal Institute of Technology in Lausanne constitutes a good example of such a sensor system.

Using long-gage sensors, it becomes possible to cover the whole volume of a structure with sensors enabling a global monitoring of it. This constitutes fundamental departure from the standard practice that is based on the choice of a reduced number of points, supposed to be representative of the whole structural behavior, and their instrumentation with short-gage sensors. This common approach will give interesting information on the local behavior of the construction materials, but might miss behaviors and degradations that occur at locations that are not instrumented. On the contrary, long-gage sensors allow the monitoring of a structure as a whole, so that any phenomena that has an impact on the global structural behavior is detected and quantified.

This contribution discusses the use of long-gage sensors for structural monitoring. The response of these sensors in inhomogeneous material like concrete, possibly including defects (e.g. cracks), is analyzed. The paper also presents the ideal disposition of multiple sensors (topology) to measure different parameters including compression, bending and shear. In particular, an algorithm for retrieving the vertical displacement of bridges instrumented with pairs of horizontal sensors is introduced and analyzed. Finally a number of application examples show how interesting this technique is for the monitoring of different types of concrete structures including bridges, piles and high-rise buildings.

2 LONG-GAGE (DEFORMATION) SENSORS – BASIC NOTIONS

Sensor designed to measure relative displacement between two pre-defined points of a structure is called deformation sensor in this paper. The distance between these two points is called gage-length of the sensor.

Frequently used construction materials, and notably concrete, can be affected by local defects, such as cracks, air pockets and inclusions. For structural monitoring purposes it is necessary to use sensors that are insensitive to material discontinuities.

The long-gage deformation sensor, by definition, is a sensor with a gage-length several times longer than the maximal distance between discontinuities or the maximal diameter of inclusions in monitored material. E.g. in case of cracked reinforced concrete, the gage length of long-gage sensors is to be several time longer than both, maximum distance between cracks and diameter of inclusions.

Main advantage of this measurement is in its nature: since obtained by averaging the strain over long measurement basis it is not influenced by local material discontinuities and inclusions. Thus, the measurement contains information related rather to global structural behavior and not to a local material behavior. Figure 2 illustrates this statement. The measurement performed by the long-gage sensor represents average strain of the cracked reinforced concrete element considered as a homogenous material. On the other hand, the short-gage sensors measure local behavior of material. For example, the sensor g_1 will record the exact strain in concrete at the position where it is placed, while the sensor g_2 will be influenced by crack opening and will record a value very close to the size of the opening. In structural point of view, even if they are at the same level in cross section, they will give a different answer, not related with value of bending moment. Therefore from these measurement it is difficult, or even impossible, to understand structural behavior of the element.

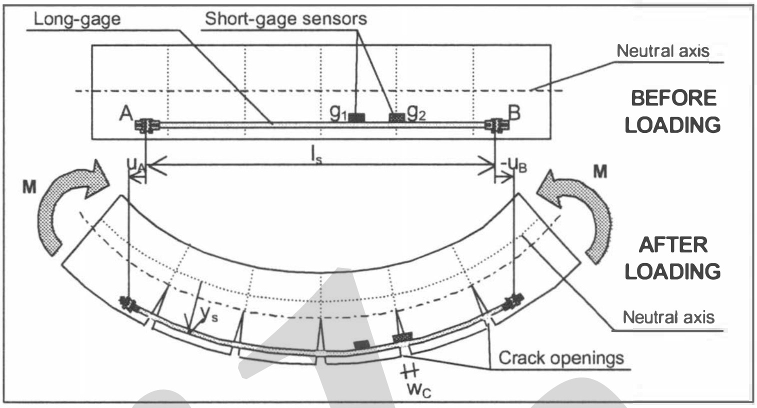

Fig. 2 Difference in deformation measured by the SOFO long-gage and strain (short-gage) sensors

An example of monitoring system that deals with long-gage sensors is the system called SOFO (French acronym for Surveillance d'Ouvrages par Fibres Optiques – Structural Monitoring using Optical Fibers), based on low-coherence interferometry in optical fiber sensors

3 LONG-GAGE SENSOR TOPOLOGIES

Long-gage sensors can be combined in different topologies and networks, depending on geometry and type of monitored structure, allowing monitoring and determination of important structural parameters such as average strains and curvatures in beams, slabs and shells, average shear strain, deformed shape and displacement, crack occurring and quantification as well as indirect damage detection.

To perform a monitoring at a structural level it is necessary to cover the structure, or a part of it with sensors. For this purpose the structure is firstly divided in cells (see Figure 3). Each cell contains a combination of sensors appropriate to monitor parameters describing the cell's behavior. Knowing the behavior of each cell, it is possible to retrieve the behavior of the entire structure. The combination of sensors installed in single cell is called sensor topology in this paper. Totality of sensors is called sensor network.

Sensor topology in each cell is appropriated to the parameter representative for this cell (e.g. strain, curvature, etc.). Sensor network can contain cells with different topologies.

4 CONCLUSIONS

An original structural monitoring method is presented in this paper. The particularity of the method is the use of long-gage sensors combined in different topologies. The idea is to divide the structure in cells, to equip each cell with topology which corresponds to the expected strain field and then to link results obtained from each cell in order to retrieve global structural behavior. In that way a kind of "finite element monitoring" is performed.

Three typical topologies of long-gage sensors are presented, simple, parallel and crossed topology. Real, on-site application of simple and parallel topology illustrates the power of the method. Number of parameters related to structural behavior is monitored or determined from monitoring.

It is demonstrated that long-gage sensors offer large possibilities since they provide measurement that is not influenced by local material defects. Moreover, they are able to monitor defects such as cracks in reinforced concrete. The averaged value obtained by long-gage sensors is fully in accord with philosophy of reinforced concrete where the cracked concrete is considered as homogenous material at macro-level.

ELASTO-MAGNETIC SENSOR UTILIZATION ON STEEL CABLE STRESS MEASUREMENT

Sunaryo SUMITRO*, Andrej JAROSEVIC, and Ming L. WANG
*Research and Development Division, Keisoku Research Consultant Co.,
22-7, Minamioi 3-chome, Shinagawa-ku, Tokyo 140-0013, Japan
E-mail: Sumitoro@krcnet.co.jp http://www.krcnet.co.jp/

Keywords: elasto-magnetic, actual stress, EM sensor, monitoring

ABSTRACT

Maintenance of the huge stock of infrastructures is one of the major concerns in the developed countries in this century. Structure Health Monitoring System development, such as, evaluation of the field condition of existing structures and to monitor the important engineering properties of new structures, can be considered as the first step in resolving of the above problem [1]. New innovative evaluation methods need to be devised to assess the deterioration of infrastructures such as steel tendons, cables in cable stayed bridge and strands embedded in pre- or post-tensioned concrete beams.

However, no accurate and simple method is available for directly measuring the stresses in steel cable in cable-stayed bridges and suspension bridges [2]. The measurement of the stresses is important for monitoring excessive wind or traffic loading to gage the redistribution forces present after seismic events, and for detecting corrosion via loss of cross section of steel. These cables are often very large, containing several hundred wires of 7mm diameter. The cables are sheathed in a plastic protective cover filled with cement grout, and the wires may be coated with lubricating compounds. For these reasons, invasive methods such as strain gages that have been used for much smaller pre-stressing cables are impossible to use with cable stays. Vibration frequency measured at the middle region of a cable is often used to determine the tension force. The uncertainties of the values of parameters such as mass, length, and cross section area can introduce a significant error to the actual force. Moreover, the stress near the anchor point is of real concern.

The Elasto-Magnetic technology is a novel new approach to monitor cable forces in pre-stressed structures and bridge cables [3]. This technology overcomes the above mentioned disadvantages related to vibrating frequency or strain gauge methods while still inhabiting the advantages of normal NDT methods [4]. The Elasto-Magnetic Phenomenon is a simple nondestructive evaluation technique for monitoring stress in steel cables [5]. An experiment to verify the utilization of Elasto-Magnetic phenomenon on stress monitoring of steel cables was constructed. The magnetization phenomenon is performed by two solenoids, i.e., a primary coil and a secondary coil. Basic material parameters such as magnetic permeability, intensity of magnetization and temperature were obtained from calibration tests on 7mm wire. Then, these basic material parameters were used to measure the real stress in a 37x7mm diameter cable.

The magnetization of a material is typically described by the relationship between the magnetic field strength, H (Amp-turns/m), and the flux density, B (Webers/m^2), and for any material can be expressed by the general constitutive equation, $\vec{B} = \underline{\mu}\,\vec{H}$ where, $\underline{\mu}$ is the magnetic permeability tensor [10]. However if the material is macroscopically homogeneous and isotropic, the relationship can be reduced to its scalar form and μ is a scalar. Fig.1 shows a typical magnetization curve for a ferromagnetic material. It is evident that the permeability is not constant, but is dependent on the field strength. It should be noted that μ is not the slope of the magnetization curve, but simply represents the ratio B/H. One of the easiest ways to magnetize a material and study its magnetic characteristics is through the principle of magnetic induction and two solenoids, a primary coil and a secondary coil, with the material whose magnetic characteristics are to be investigated as the core. If a DC current is applied across the primary coil it produces a magnetic field (H) and the magnetic flux density (B) within the specimen. Amplitude permeability is defined as the ratio B/H, and incremental permeability defined as the ratio $\Delta B / \Delta H$ [6]. In both the cases, permeability depends also on "working point" at which it is measured.

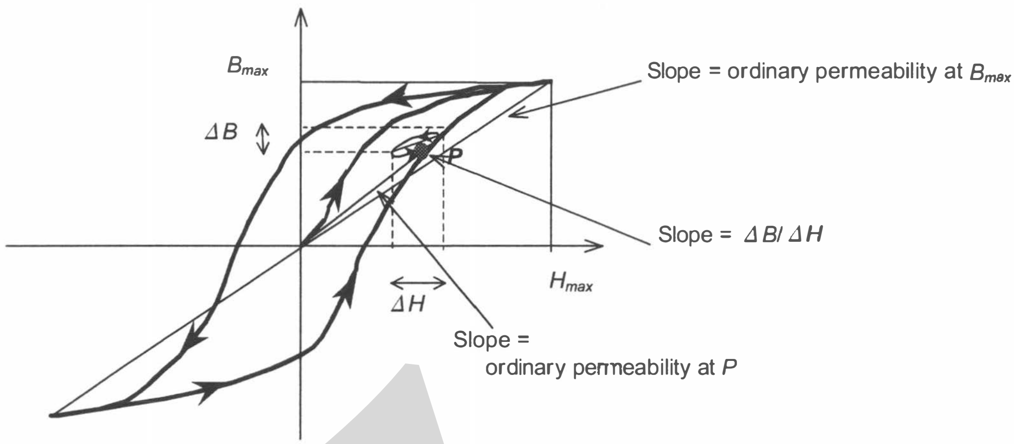

Fig.1 Typical *B-H* curve for a ferromagnetic material

By observing numerous field measurement results, it is confirmed that EM sensor is a non-destructive, no-contact, easy to operate measurement system to measure actual stress of steel wires, bars and cables. Therefore, this measurement technology is suitable for developing a health monitoring system for any pre-stressed concrete (PC) structure.

Some concluding remarks are summarized as follows:

1. EM sensor consists of the input device (magnetizing coil) and the output device (sensing coil). But the real sensor is the 'intelligent' PC structure itself that has high magnetic sensitivity to stress.
2. For PC steel, previously calibrated data can be utilized for the PC from the same specification.
3. Scattering in the stress measurement on PC steels is not influenced by the mechanical properties. Successful application of EM technology, knowledge of magnetic characteristics and its scattering is essential. By observing numerous measurement results, it is confirmed that the scattering of elasto-magnetic characteristics is within 5%.
4. Temperature change influences the magnetic properties of steel and the temperature error is up to about 10N/mm^2 per ℃.
5. EM sensor transfers the stress from the measured element to the sensing coil with the change of the magnetic flux. This phenomenon is not influenced by insulation resistance, however, ferromagnetic surrounding the sensor affects the distribution of the magnetic flux. Therefore, magnetic shielding of the sensor is needed when ferromagnetic surrounding the sensor is not stable.

REFERENCES

[1] Tominaga, M., Sumitro, S., Okamoto, S., Kato, Y., and Kurokawa, S. : Development of monitoring technology for steel and composite structures, J. of Constructional Steel, Vol.9, Nov, pp.575-582, 2001

[2] Sumitro, S, Okamoto, T., Matsui, Y. and Fujii, K. : Long span bridge health monitoring system in Japan, Proc. SPIE 8th Annual International Symposium on Smart Structures and Material, Health Monitoring and Management of Civil Infrastructure Systems, Newport Beach CA, Vol. 4337-67, pp.517-524, 2001

[3] Jarosevic, A., Fabo, P., Chandoga, M., and Begg, D.W. : Elastomagnetic method of force measurement in prestressing steel, Inzinerske Is Stavby, Brastilava, Slovakia, Vol. 7, pp.262-267, 1996

[4] Wang, M.L. : Monitoring of cable forces using magneto-elastic sensors, 2nd U. S. -China Symposium workshop on Recent Developments and Future trends of computational mechanics in structural engineering, May 25-28,1998, Dalian, PRC.

[5] Chen, Z., Wang, M.L., Okamoto, T., and Sumitro, S. : A new magnetoelastic stress/corrosion sensor for cables in cable-stayed bridges using measurement of anhysteretic curve, 2nd Workshop on ATUEDM, Kyoto, July 11-13, 2000

[6] Sumitro, S. : True-stress measurement of PC steels by EM sensor, J. of Prestressed Concrete Japan (JPCEA), Vol.43, No.6, Nov, pp.99-103, 2001 (in Japanese)

MEASUREMENTS OF PRESTRESSING FORCES IN LARGE CAPACITY EXTERNAL TENDONS USING ELASTO-MAGNETIC SENSOR IN KAMIKAZUE VIADUCT

Hideaki Sakai, Chubu Branch, Japan Highway Public Corporation JAPAN
Hiroshi Yasumori, DPS Bridge Works Co., Ltd., JAPAN
Noriyuki Miyamoto, Keisoku Research Consultant Co. JAPAN
Junichi Izumo, Kanto Gakuin University JAPAN

Keywords: EM sensor, external tendons, precast segment, tendon force measurements, full-scale model test

1. INTRODUCTION

The Kamikazue viaduct is a double box girder PC bridge formed by connecting two single box-girder precast segments together by means of RC slab with lapped reinforcement in the form of double loop, first of its kind in the world. This is a 17 span continuous girder bridge that has a length of 630 m and width of 16 m, consisting of 1040 segments. The segments are erected by span-by-span method using movable falsework. The segments are jointed using epoxy resin and prestressed by means of external tendons in each span.

The construction of this viaduct using precast segmental construction and prestressing being completely provided with large capacity external tendons was a challenge in many ways, since experience with such construction was rare in Japan. As such, a full-scale model test was carried out to verify the safety performance of the anchorage blocks and deviators, by tensioning the tendons. While verifying the safety of the individual members, the frictional effect at the deviator was also investigated. This was carried out by measuring the tendon forces at either side of the deviator and computing the friction coefficient from the difference in forces.

The most commonly used method to measure the tendon force is by attaching strain gages to the strands that form the tendons. However, this method is not possible in this viaduct, since epoxy coated strands are used for external tendons. As such, an Elasto-Magnetic (EM) sensor was adopted where the tensile force in a tendon is measured directly using the magnetic strain property of steel. The use of such new technology has been rare, especially for large capacity tendons. This paper describes the use of EM sensor in the Kamikazue viaduct to measure the tensile stresses directly in large capacity tendons and the applicability of such system in future.

2. OUTLINE OF EM SENSOR

The EM sensor is based on the principal that the magnetic properties of a ferrous material change when it is subjected to tension, and the change in the magnetic properties is dependent on the tensile stress of the material. By measuring the permeability ratio of an unstressed external tendon beforehand, it is possible to obtain the tendon force at the time of tensioning, from the relationship between magnetic characteristic and tensile force. Measurement of tendon stress using an EM sensor is shown in Photo 1. Since the measurement of actual stress using EM sensor is a kind of non-destructive and non-contact test, it is considered to be one of the most suitable methods that could measure the stress in prestressing steel easily. EM sensor consists of a primary coil and a secondary coil as shown in Fig. 1, forming a cylinder type coil including a temperature sensor. Since this cylindrical elasto-magnetic gage is not fixed to the prestressing tendon, it can be set to any arbitrary position. When an alternate current is passed in the primary coil, magnetic flux is produced through the measured element (prestressing tendon) within the solenoid, inducing a voltage in the secondary coil. The permeability ratio of

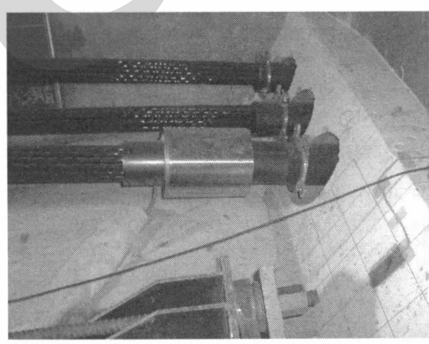

Photo 1 Measurement of tendon force using EM sensor

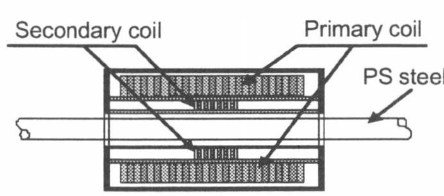

Fig. 1 Structural layout of EM sensor

the prestressing steel can be known from measurement of this induced voltage.

3. FULL-SCALE MODEL TEST

The Kamikazue viaduct is a 17 span continuous box-girder type PC bridge that adopted only external prestressing using epoxy coated multi-strand tendons of type 19S15.2B. The layout of the external tendons is shown in Fig. 2. The external tendons were draped at two deviators and anchored at the diaphragm wall provided at the pier sections. Moreover, the saddle portion of the deviator section was made of double tubular structure consisting of a steel pipe and a polyethylene pipe so that replacement of external tendons was possible. The purpose of measuring the prestressing force by EM sensor was to verify the amount of friction losses of the external tendons at the deviators.

The purpose of this model test was to verify the validity of the friction coefficient used in the design with the actually measured values so that the safety of this viaduct is confirmed, while checking the applicability of EM sensor. In addition, by using this EM sensor, the difference in tension on either side of the deviator was measured directly, and the friction coefficient at the deviator was calculated. The arrangement of sensors and other devices is shown in Fig. 3.

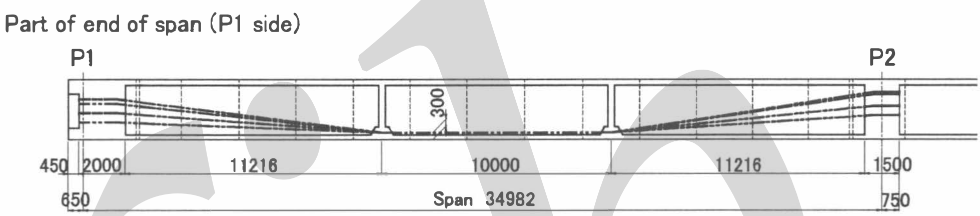

Fig. 2 Layout of external tendons ※Radius of bent R=4000

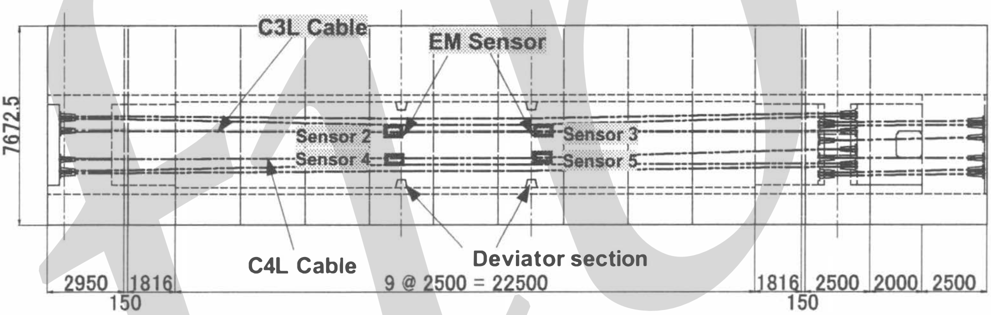

Fig. 3 Layout of measurement devices

The accuracy and the output characteristics of the EM sensor were checked for the individual strands. Later, the whole tendon (19S15.2 mm) consisting of 19 strands was calibrated. The calibration of 19S15.2 mm cable was performed at the factory where the precast segments were prepared. It can be seen that the error was within ±2.0%. However, it should be noted that the error was almost negligible at comparatively high level of tension, indicating that the accuracy of EM sensor is very high at the design prestress level. The coefficient of friction calculated based on the EM sensor measurements at different prestressing levels are shown in Fig. 4.

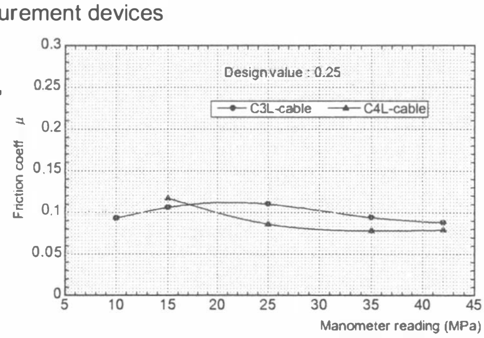

Fig. 4 Variation of friction coefficient μ with prestressing force

In this test, the friction coefficient of PE pipe and epoxy coated tendon combined with the deviator was found to be in the range of 0.078-0.117. Therefore, the friction coefficient between PE pipe and epoxy coated tendons was set to 0.15 in the final design, considering a factor of safety of 1.5.

REFERENCES

1. Ladislav Búci :Strengthening of Segment Bridge by Means of External Tendons, *Journal of Theory, Structures and Elements*, Vol. 42, No.2-3, 1994, pp.111-115

EVALUATION OF GROUTING CONDITION IN TENDON DUCTS OF PRESTRESSED CONCRETE MEMBERS BY IMPCT ELASTIC-WAVE METHODS

Toshiro KAMADA Keitetsu ROKUGO Tsutomu WAKAYAMA Hideaki KITAZONO Katsuji IMAO

Gifu University
JAPAN

Abe Kogyosho Co., ltd.
JAPAN

Keywords: nondestructive test, impact elastic-wave methods, elastic-wave propagation velocity

1 INTRODUCTION

Studies have been conducted on nondestructive methods for detecting voids in grouted tendon ducts using elastic waves. These methods, however, involve a problem of frequency distribution varying under the influence of the striking condition or sensor characteristics. When comparing various frequency distributions, qualitative judgments tend to be made rather than quantitative interpretation. Greater objectivity will therefore be required in understanding obtained data.

Against the above background, the authors have earlier studied parameters for detecting voids using elastic waves and found that the elastic wave propagation velocity could be used for detection [1]. In this study, based on the above study, tests were carried out on a slab specimen and the relationship between the volume percentage of grout and the elastic wave propagation velocity was examined. For identifying the mechanism of variation in elastic wave propagation velocity depending on the voids in grouted tendon ducts, an finite element analysis was also made using a simple two-dimensional model. Tests were also conducted on a 35-m-long full-scale PC girder to examine the applicability of the method to actual structures.

2 TESTS ON SLAB SPECIMEN

The PC slab specimen shown in Fig. 1 was used in the tests. Tendon ducts with volume percentages of grout of 0%, 25%, 50%, 75%, and 100% were placed inside the slab specimen to examine the effect of the percentage of grout on the elastic wave propagation velocity.

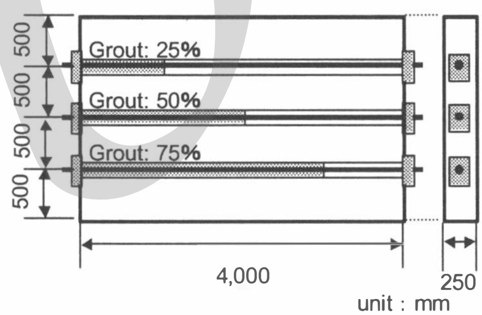

Fig. 1 Slab specimen

The input and received points, where elastic wave were input and detected respectively, are shown in Fig. 2 Elastic wave propagation time was measured by a digital AE measurement system. Elastic wave propagation velocity was obtained by dividing the distance between sensors by propagation time.

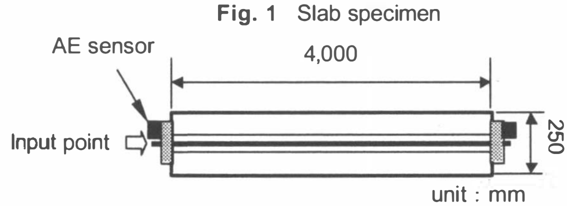

Fig. 2 Elastic wave input point and AE sensor location

Additional tests were conducted using a specimen made by applying concrete covers to both the end portions of the prestressing tendons in the slab specimen.

Fig. 3 shows the relationship between the volume percentage of grout and the ratio of propagation velocity in the slab and concrete-covered specimens. The ratio of propagation velocity here refers to the ratio to the propagation velocity when the volume percentage of grout is 100%. This figure indicates the tendency of the radio of propagation velocity to gradually decrease as the percentage of grout increased whether protective concrete covers are applied or not. When the volume percentage of grout was 0%, input elastic waves propagated only through the prestressing tendon. In the section where the ducts were filled with grout, elastic waves propagated through a composite member incorporating the steel tendon and the grout and exhibited different behavior from that in the case of propagation through a nongrouted tendon.

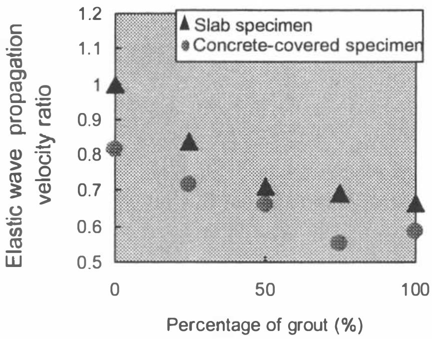

Fig. 3 Relation between grouting condition and elastic wave propagation velocity ratio

3 FINITE ELEMENT ANALYSIS ON ELASTIC WAVE PROPAGATION BEHAVIOR

In order to identify elastic wave propagation behavior, finite element analysis was carried out using a two-dimensional simple model, which was made by combining the prestressing tendon, grout, tendon duct and concrete and impact load was applied at an end to obtain the distribution of response displacement in the model.

It was visually indicated that grouting affected the behavior of elastic waves in respective tendons. When a higher volume percentage of grout, grout had a greater bonding effect, so the distance between the impact input point and the wave front tended to be shorter or the propagation velocity tended to decrease after the same period of time passed. This agreed to the test results shown in Fig. 3. The effectiveness of using the elastic wave velocity was thus verified by analytical results.

4 TESTS ON FULL-SCALE PC GIRDER

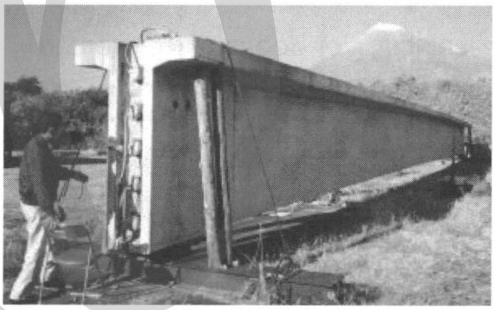

Photo. 1 Whole view of PC girder

Photo. 1 outlines the full-scale PC girder specimen with T-shaped cross section. The specimen size was 1500 mm x 1950 mm x 35000 mm. A total of five tendons were placed curvilinearly. For examining the effect of the volume percentage of grout on the elastic wave propagation velocity, three grouting patterns were adopted: full grouting, partial grouting (volume percentages of grout: 37% and 65%) and nongrouting. Elastic waves were input by the same equipment as used in the tests on the slab specimen. Elastic waves were input at the center of the protective concrete cover at one end of the main girder, at the end of the prestressing tendon and on the surfaces of concrete near the anchor and in the web.

It was confirmed that the elastic waves induced by the striking method well propagated through the length of 35m. It was found that the volume percentage of grout could be estimated using the mean elastic wave propagation velocity through the full length of the girder by inputting elastic waves at one end of the girder as long as the waves could be detected at both ends. When detecting elastic waves on a side of the girder, using propagation velocities in respective sections was found effective.

ACKNOWLEDGMENT

The authors would like to acknowledge the cooperation of Japan Prestressed Concrete Contractors Association in conducting the tests. The assistance of M. Asano and Y. Kunieda, graduate students of Gifu University, is also gratefully acknowledged.

REFERENCES

[1] Kitazono, H., Kamada, T., Yokoyama, H. and Rokugo, K.: Detecting of Voids in Grouted Tendon Ducts of PC Members Using Elastic Wave, Vol.22, No.1, pp.367-372, 2000

CONTINUOUS REMOTE ACOUSTIC HEALTH MONITORING OF TENSIONED ELEMENTS IN STRUCTURES

Jack Elliott
Vice Pdt & General Manager
Pure Technologies, Calgary
jack.elliott@soundprint.com

Thomas Le Diouron
Asia Manager
Advitam, Tokyo
tlediouron@advitam-group.com

Jérôme Stubler
General Manager,
Advitam, Paris
jstubler@advitam-group.com

Keywords: acoustic, monitoring, remote, continuous, wire failure, management, corrosion, fatigue, cable

1. INTRODUCTION

The durability of prestressed concrete structures and cable structures is highly dependent on the condition of tensioned steel wires that are subject to corrosion. Failure of cables as a result of corrosion can lead to catastrophic collapse without warning signs.

Operators and owning authorities are facing the challenges of identifying and addressing these concerns. While routine inspections may not reveal a potential problem, intrusive investigation techniques for detecting early signs of corrosion are inconclusive and expensive. Acoustic monitoring is becoming increasingly popular for prestressed concrete and cable-supported structures, as it is the only way to get comprehensive data on the progression of corrosion.

2. PRINCIPLE OF ACOUSTIC MONITORING

Acoustic sensors (accelerometers) distributed in key locations along a structure will detect the energy released by a fracture event. Each sensor is connected using coaxial cable to an on-site data acquisition unit. The system monitors continuously but collects no data until triggered by an acoustic event falling within pre-set limits. Software filters are then applied to reject events of no further interest. Events that successfully pass these tests may be wire fractures. They are sent via the Internet to a processing center for review by an engineer who will classify, calculate their position and notify the owner. Provided with high quality data of this type, the engineer can appraise a structure with knowledge of the actual failures in tensioned elements, and their locations, in the entire structure over the monitoring period.

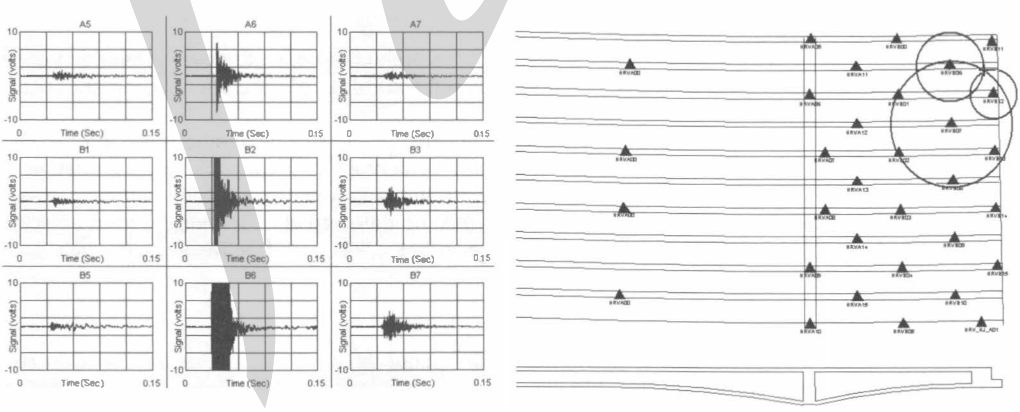

Fig.1 : the acoustic signal collected by each sensor is used to identify and calculate the position of the acoustic event

This continuous acoustic monitoring system has successfully passed several evaluations carried out by independent organizations.

3. IMPLEMENTATION

3.1 Post-tensioned bridges

The performance of the system in “open” and "blind" trials, both in laboratory and on actual bridge approached 100 percent and the location of events was generally achieved within 300mm of the correct position.

3.2 Suspension bridges

Following successful implementation on a suspension bridge in the US, the system has been further developed in order to facilitate its installation: highly sensitive mono-directional sensors allow to capture any single wire break over 150m along the main cable, while wireless data transmission eliminate the tiresome wiring task.

3.3 Stay cable bridges

The monitoring system is particularly suitable for use on cable-stayed bridges. Because of the fact that, after construction is completed, visual inspection of cable components is not possible, the system can provide reassurance about the long-term integrity of the wires.

The capability of the system to detect wire breaks from both ends of the stay was confirmed for all lengths of stay-cables. The monitoring system can be adapted to integrate a vibration monitoring capability so that future vibration performance of the stays can be assessed .

3.4 Containment vessels, reservoirs and pipelines

The system is also applicable to monitor tendon deterioration and concrete cracking in prestressed concrete containment vessels (PCCV), water reservoirs and pipelines.

Fig.2: Investigation based on acoustic data (water reservoir)

4. CONCLUSION

The technology of acoustic monitoring is non-destructive and non-intrusive. It has been demonstrated that it can monitor continuously an entire structure, detect and locate failures or abnormal events. Provided with valuable information about deterioration, engineers and owners can perform focused investigation, optimize the timing of repairs and develop more accurate maintenance budgets.

Acoustic monitoring is a management tool that can assist owning authorities to monitor the residual life of their structures and provide confidence in their structural integrity.

LONG-TERM EVALUATION VS. SHORT-TERM MEASUREMENTS : THE CASE OF THE RIDDES BRIDGES

Olivier Burdet and Jean-Luc Zanella
Swiss Federal Institute of Technology in Lausanne, Switzerland, olivier.burdet@epfl.ch
http://is-beton.epfl.ch

Keywords : **bridge, monitoring, bridge management, long-term measurements, inclinometers, hydrostatic leveling.**

1. INTRODUCTION

Bridge management is a very important part of the sustainable deployment of a quality infrastructure. In order to improve their assessment of the bridges condition, bridge management systems need to improve the information they handle. Presently, these systems mainly include geographical and administrative information complemented by the results from visual site inspections. To improve their efficiency, it is needed that additional information be incorporated, for example results from other types of evaluations of the bridge condition based on analytical models (reliability based for example), and results from site measurements. Such data is often available, at least in part.

Based on the example of the monitoring of the Riddes bridges, the paper shows that monitoring data, and in general measurement data, needs to be considered critically in the process of the assessment of bridge condition. In particular, environmental effects need to be taken into account when assessing the quality of the data on which the evaluation of the structure will eventually be made.

2. THE RIDDES BRIDGES

The case presented in the paper shows how effective measurements can be made to help in the assessment of an important structure in a relatively short time frame using a combination of electronic inclinometers, temperature sensors and hydrostatic leveling.

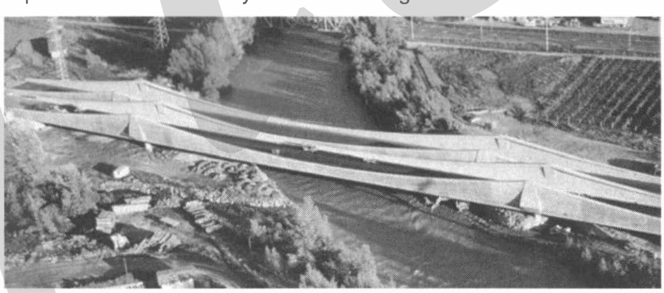

Figure 1: General view of the two Riddes bridges

The Riddes viaducts were built in the late 1980's by the balanced cantilever method for the main span of 140 m over the Rhone river. Because of the construction method, the longitudinal statical system has a hinge at mid-span. Over the years since their construction, both bridges exhibited increasing downward deflections at the middle of the main span, as other similar bridges have in the past [1,2,3]. Additional prestressing added in spare ducts in 1997 had the effect of lifting the bridge, but it was unclear to the owner what the actual behavior of the bridge was in its present condition. It was therefore decided in late 1999 to perform a detailed monitoring of the two bridges, with the aim to quantify the actual behavior of the bridges, to evaluate the efficiency of the previous retrofitting and to help in the decision process leading to a possible strengthening of the superstructure. A network of 14 high-precision inclinometers and 20 temperature sensors was installed in the twin bridges [4]. This method, already used in several other bridges for short- and long-term monitoring, has the advantage of being fully automatic and delivering an absolute value (angular change) that can easily be linked back to the deflected shape of the bridge.

3. PRELIMINARY RESULTS

The bridges exhibit significant displacement under the effect of daily temperature changes. It is not rare to observe daily movement with an amplitude of nearly 50 mm. Figure 2 shows the location of the mid-span of the South bridge over the period of observation starting in July 2000 (bottom curve), along with the ambient temperature underneath the bridge (top curve). The influence of daily temperature variations can be clearly seen (hairy look of the curves). The influence of seasonal temperature changes can also be observed. The white squares are measurements made on a monthly basis by an independent method: a hydrostatic leveling system, operated manually.

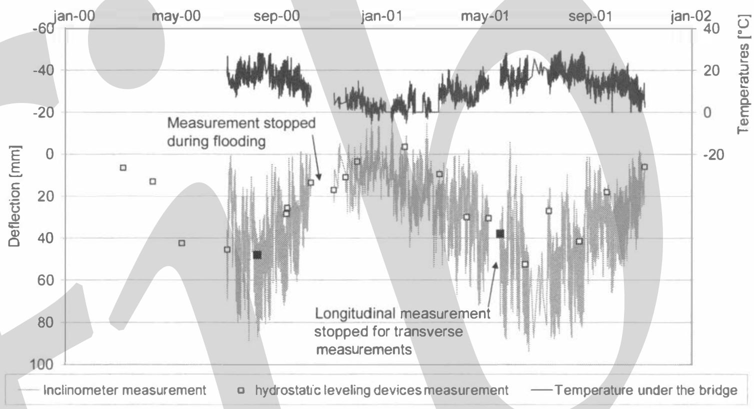

Figure 2: Calculated deflected shape of the South Riddes bridge over the period of monitoring

In less than two years of measurement, the preliminary results presented in the paper showed that the bridges mid-span deflections is increasing only very slowly.

The deciding factors in the success of this operation were :

- use of the proven, stable technology (electronic inclinometers), complemented with a well established, independent system (hydrostatic leveling);
- careful measurement of the temperature condition of the structure, at the same frequency than the other measurements;
- large quantity of measurements, facilitating the identification of reliable data and permitting various numerical treatments.

REFERENCES

[1] **BURDET O.**, *Load Testing and Monitoring of Swiss Bridges*, CEB Information Bulletin, Safety and Performance Concepts n° 219, Lausanne, Switzerland, **1993**.

[2] **BURDET O., BADOUX M.,** Long-term deflection monitoring of prestressed concrete bridges retrofitted by external post-tensioning - examples from Switzerland, IABSE Rio 1999, Rio de Janeiro, Brazil, 1999.

[3] **PATRON-SOLARES A., GODART B., EYMARD R.,** Etude des déformations différées du pont de Savines (Hautes.Alpes), Bulletin du Laboratoires des Ponts et Chaussées, 203, 91-103, Paris, France, 1996.

[4] **BURDET O., ZANELLA J.-L.,** Automatic Monitoring of the Riddes Bridges using Electronic Inclinometers, IABMAS, First International Conference on Bridge Maintenance, Safety and Management, Barcelona, Spain, **2002**.

EXPERIMENTAL STUDY ON DETECTION OF FAULTS IN COVER CONCRETE USING ELASTIC WAVE METHODS

Kazuhiro Kuzume
Kokusai Structural Engineering Corp.

Toshikatu Yoshiara
Non-Destructive Inspection Co.,Ltd.

Toyoaki Miyagawa
Professor, Department of Civil Engineering, Kyoto University

Keywords: nondestructive testing, elastic wave method, ultrasonic method, cover concrete, internal flaw, specimen

ABSTRACT

Studies concerning nondestructive inspection techniques applied to concrete structures traditionally consisted mostly of efforts to evaluate strengths, but techniques by which characteristic of the structure other than strength are evaluated are now on the increase. However, methods capable of detecting flaws such as cracks, voids, and poor bond of construction joints occurring in cover concrete of actual structures are limited.

In nondestructive testing techniques, elastic wave methods which possess histories of having been studied for comparatively long periods and which have substantial track records are taken up in this paper. In particular, the ultrasonic method is picked out from among the various elastic wave methods, with improvements made on both hardware and software aspects to enhance flaw detecting accuracies, and results of experimental studies made are described.

1 IMPROVEMENTS OF MEASUREMENT APPARATUS

Coarse aggregate particles in concrete act to scatter propagation of ultrasonic waves when the wavelengths of the ultrasonic waves are shorter than coarse aggregate sizes. Also, although it is more possible to decrease resolving power by using ultrasonic waves of wavelengths as short as practicable, there is the characteristic that attenuation is greater the higher the frequency. It was decided to use a frequency of about 100 kHz when the thickness of the structure was 300 mm or less and about 50 kHz in case of thickness exceeding 300 mm in this present study.

In this study, sine waves with which high-energy transmission is possible were used. For this purpose, a transmitting assembly incorporating a high-powered amplifier in the transmitter was fabricated. A low-noise wide-band preamplifier was used in the receiving assembly.

2 IMPROVEMENT OF ANALYSIS SYSTEM

By averaging the signal waveforms received while varying the spacing between pickups it becomes possible to emphasize only the waves reflected from flawed parts. It became possible to reduce the influence of scattered noise in concrete by such an averaging method.

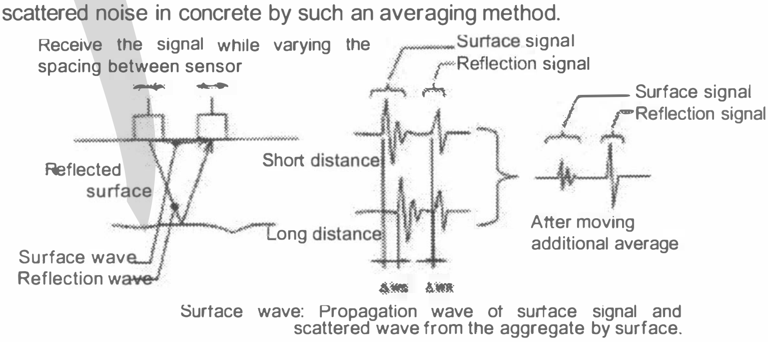

Fig.1 Outline of Averaging Method

3. DETECTION TESTS ON SPECIMEN

Fig.2 shows the specimen configuration, and the location of faults.

A representative example of the results of detecting faults 200x200 mm at 200 mm from the surface is shown in Fig.3. Sound parts were subjected only to the influence of surface waves and waves from the interior were not grasped, but reflected waves from the void and cold joint faults models were recognized.

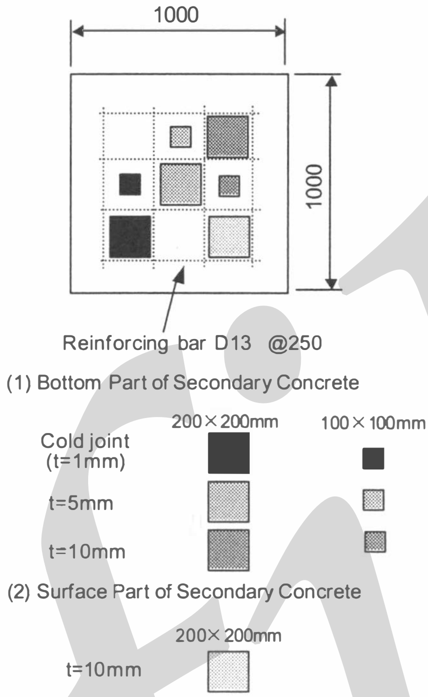

Fig.2 Slabe Type Specimen

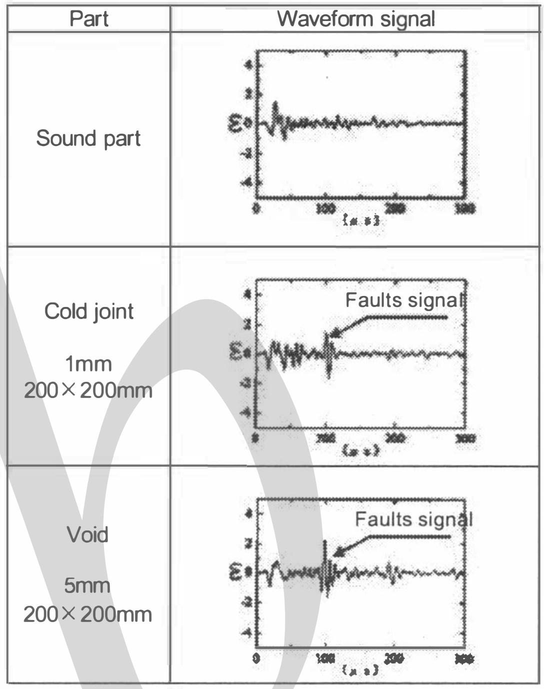

Fig.3 Example of Detection Results

4. CONCLUSION

The ultrasonic wave method was picked from among elastic wave methods of nondestructive testing and its applicability to detection of faults in concrete structures was examined in this study. The following conclusions were drawn concerning measurement of reflected waves from the results of tests on specimens:

(1) At a frequency of 200 kHz or under, using sine waves of high energy and averaging method for received waveforms, it is possible to clearly detect waves reflected from faults.

(2) The results of tests using specimens showed it is possible to detect voids and cold joints existing at depth of 200 to 300mm.

(3) The possibility of an accurate grasp of the size and location of faults in concrete structures, is confirmed by mapping-deal analysis.

REFERENCES

1) Japan Society of Civil Engineers: 2001 Edition, Standard Specifications for Concrete (Maintenance Volume), Jan.2001

2) T.Kojima, H.Hayashi, M.Kawamura, K.Kuzume, Maintenance of Highway Structures Affected by Alkali-Aggregate Reaction, Proceedings of the 11th International Conference on Alkali-Aggregate Reaction, pp.1159-1166

DAMAGE MECHANICS FOR CORE CONCRETE BY AE RATE PROCESS

Masayasu OHTSU Hiroshi WATANABE Makoto ICHINOSE
Graduate School of Science & Technology,
Kumamoto University, Kumamoto 860-8555, JAPAN

Keywords: acoustic emission, rate process analysis, damage mechanics, concrete core

1.INTRODUCTION

To inspect existing concrete structures, acoustic emission (AE) techniques deserve to draw a careful attention. This is because crack nucleation and extension are readily detected and monitored by AE. Measurement of AE activity in the uniaxial compression test of core samples was proposed. To model AE generating behavior under compression, the rate process analysis was introduced. It is demonstrated that the result of AE rate process analysis is closely associated with the presence of microcracks and voids in concrete. Here, the damage parameter in damage mechanics is introduced and is correlated with AE rate process analysis to estimate the decrease of the modulus in concrete as the damage. An applicability of the procedure is investigated by employing concrete samples of controlled damage, which are deteriorated by freezing and thawing action. A field measurement is conducted, and further the database is constructed for practical use.

2. RATE PROCESS ANALYSIS AND DAMAGE MECHANICS

To formulate AE activity under compression, the rate process theory is introduced. The relation between the number of AE, N, and the stress level, V (%), is represented,

$$N = C\,V^{a}\exp(bV). \tag{1}$$

It is found that the evolution of damage is the most dominantly correlated with the rate (coefficient a in Eq. 1). These results lead to the fact that the damage evolution under uniaxial compression is closely associated with the variation of the rate. In the theory of continuous damage mechanics, the damage of concrete is defined as,

$$\Omega o = (1 - Eo/E^*). \tag{2}$$

Here Ωo is the initial damage, Eo is the intial modulus of elasticity, and E* is the modulus of intact state. Since the modulus Eo should be determined as the tangential modulus, the relationship between stress and strain is approximated by a parabolic equation.

3. ESTIMATION OF DAMAGE

To prepare concrete samples of controlled damage, cylindrical specimens of 10 cm diameter and 20 cm height were made. The freezing and thawing tests of samples were conducted for 10 cycles, 20 cycles and 50 cycles. To estimate the damage from damage mechanics, the ratios of the strength were compared with the relative moduli. It is found that the damages introduced are not so severe that the compared data are plotted closely to the two curves based on the damage mechanics.

Because modulus E* is unknown in an actual case, a relationship between the difference of moduli under uniaxial compression and the rate of the samples is studied. For the sake of simplicity, a linear correlation is approximated. Because the rate varies depending on the degree of the damage, it is assumed that the initial modulus is identical to intact modulus in the case where the rate is equal to 0. Thus, intact modulus E* is theoretically determined. Through this procedure, relative modulus Eo/E* was estimated at each freezing-thawing cycle as average values of three samples. It is realized that the ratios Eo/E* obtained slightly overestimate the actual ratios, while the trend of the decrease due to deterioration is in remarkable agreement. This result implies that the damage of concrete can be practically estimated without knowing the modulus of elasticity at constructed stage. Because mechanical properties of concrete at construction are mostly missing when inspection is conducted, the procedure is promising to estimate the degree of the damage as the relative modulus Eo/E* via AE rate process analysis.

The procedure was applied to concrete-core samples taken from bridge supports of an existing bridge. From concrete supports of piers P1, P2 and anchor A2, three cores were taken out and uniaxial compression tests of them were conducted. It is observed that the moduli of cores in the anchor A2 are slightly larger than 1.0, while those of cores in the piers P1 and P2 are a little less than 1.0. This implies that the concrete in anchor A2 is undamaged, while the concrete of piers P1 and P2 is a little deteriorated. This result is found to be in good agreement with a numerical study on fatigue damage of the bridge supports.

In actual inspection, however, many cores can not be taken out to be tested. In this respect, construction of a database was attempted. All data of uniaxial compression tests of concrete samples in a laboratory have been stored and the relation are plotted as a database of AE rate process analysis. The data of core samples are added to the database as shown in Fig. 1. Then relative moduli Eo/E* are again estimated from the relation. Results are shown in Fig. 2. Remarkable agreement between relative moduli estimated and those from the database is observed. Thus, an applicability of the procedure is confirmed. The damage of concrete at the current state could be estimated from AE rate process analysis without knowing the original state at construction.

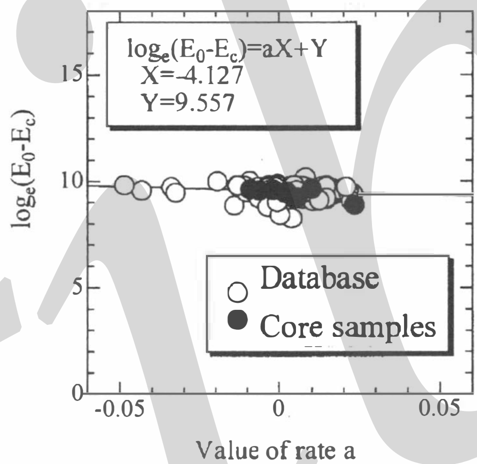

Fig. 1 Relationship between the difference of moduli under uniaxial compression and the rate.

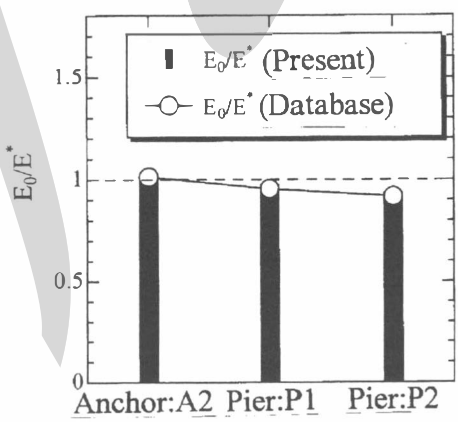

Fig. 2 Relative moduli determined from the present test and from the database.

MONITORING METHOD OF THE STRUCTURAL INTEGRITY AT TSURUGA UNIT 2 AND GENKAI UNIT 3 & 4

Ikurou Kawai
The japan Atomic Power Company,JAPAN

Kazuhiko Kiyohara
Kyushu Electric Power Co.,Inc., JAPAN

Mikio Yamamoto
Obayashi Corporation
JAPAN

Keywords PCCV, ISI, concrete strain, tendon residual force, load cell

1. NTRODUCTION

Since the operation of the Tsuruga Unit No.2 in 1987 which was the first prestressed concrete containment vessel (PCCV) in Japan, 5 power stations with PCCV are now under operation. For the confirmation of the structural integrity of PCCVs, the in-service inspection test (ISI) is put into practice periodically. In this paper, the ISI practice in Japan is introduced together with some results of the series of studies enforced to improve the monitoring method.

2. THE IN-SERVICE INSPECTION

The basic dimensions of PCCV in Tsuruga Unit No.2(GT-2),and Genkai Unit No.3/4 (QGN #3 & QGN #4) are almost the same, where the inner diameter 43.0m and the height 64.5m, a 1.3m thick cylindrical wall of 21.5m inner radius and a 1.1m thick hemispherical dome with 6.4mm steel liner covering the whole inner surface as shown in fig.1. The prestressing system is unbonded BBR and capacity is 1000t class. The ISI of the PCCVs are going to be enforced in the 1st (No.1 ISI), 3rd (No.2 ISI) , 5th (No.3 ISI) ,10th(No.4 ISI) years after commercial operation . From the visual inspection of the exposed concrete, cracks, chipping, rust, and grease leaks were not detected. Measurements of all examined tendons at the lift-off test were large enough compared to the expected required design measurements.

3. MEASUREMENT AND PREDICTED VALUES OF TENDON TENSILE FORCE

The predicted tendon residual force is calculated considering elastic concrete deformation, wire relaxation , concrete creep and shrinkage losses[1],and gives good agreement with measured force having the accuracy of the 0.98～0.99 as shown in fig.2. In the calculation equation, losses by concrete creep and shrinkage are based on calculated value of concrete strain. Calculated concrete strain correspond well to measured value by embedded strain gauges. As shown in fig.2, tendon residual force after design life (40 years) is enough for design force .

4. DEVELOPMENT OF LOAD CELLS

The possibility of using load cells for long-term measurement of residual tendon tensile force has been proposed as a inexpensive method than the conventional lift-off test. But, according to the proc. of the workshop on prestress loss [2],a reliability of the large capacity load cell is quite less. So, load cells for 1000t-category BBR and VSL have been developed for long-term measurement in Japan. Both BBR type and VSL type have been developed with a half-divided design for easy installation both at the construction, and after operation. As for the replacement method for the anchoring end shim plate, a compression type measuring 225mm in thickness has been developed for BBR and a shear type measuring 100mm in thickness for VSL.. Photo.1 shows the load cell for BBR after installation to hoop tendon of GT-2 PCCV . The measurement results of the load cell by the end of January 2002 are shown in Fig.3. The load cell is

In-service stably and continuously, and was able to measure small tendon force changes by the leak rate test (C/V LRT).

5. CONCLUDING REMARKS

The structural integrity is confirmed by lift-of test at ISI. Tendon residual force by lift-of test shows good agreement with calculated predicted force. As an inexpensive method for measuring tendon tensile force which would replace the lift-off test, load cells for BBR and VSL have been developed. These load cells were installed to the existing plant or to the test bed, and it was confirmed that they can be installed to the end part of tendons during as well as after construction, and have good accuracy and stability for long-term measurement.

REFERENCES

[1] Watanabe,Y.,Kawai,I.,Kowada,A.,Akita,S.,Itou,Y.,Sono,Y.,Koyanagi,M.,Yamamoto,M.,In-Service Inspection and R&D of PCCVs in Japan, Nuclear Engineering and Design 200 (2000),pp337-351

[2]Proc. of Joint WANO/OECD-NEA workshop,prestress loss in NPP containment,25-26 August 1997,Poitiers

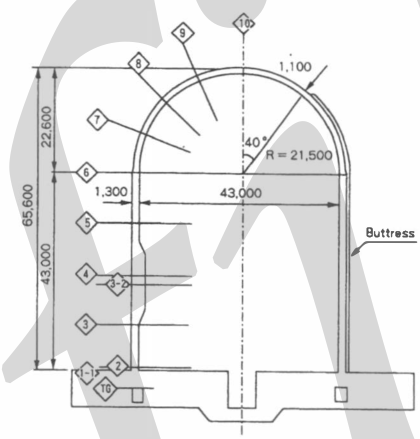

Fig.1 Outline of PCCV

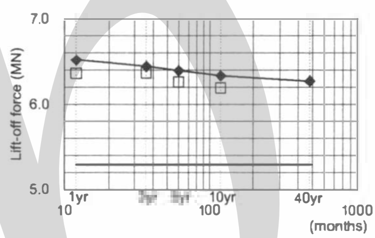

Fig.2 Measured and Predicted Tendon Force

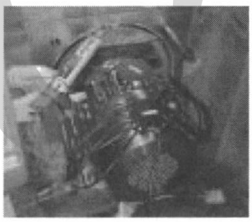

Photo.1 Load cell after Installation

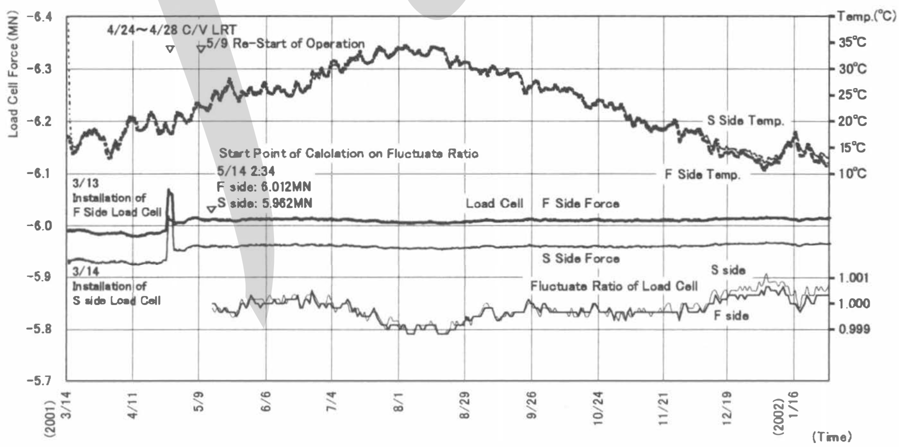

Fig.3 Results of Long-term Measurement of Tendon Tensile Force (GT-2)

INSPECTION BASED HEALTH MONITORING OF PRESTRESSED CONCRETE BRIDGES

Haluk M. Aktan*, Yilmaz Koyuncu and Theresa M. Ahlborn

*Civil and Environmental Engineering Department, Wayne State University, Detroit, MI 48202, USA
E-Mail haluk.aktan@wayne.edu, Web Page: http://www.wayne.edu

INTRODUCTION

The first prestressed concrete (PC) I-girder highway bridge was constructed in 1958 in the State of Michigan. A predominant number of the PC I-girder bridges (345 out of a total of 699) were constructed between 1960 and 1970. Bridge management in Michigan is performed using a relational database integrated under a software program called "Pontis". Inventory, operation, inspection and management data is collected in the relational database. According to the inventory data, there are 5902 bridges under the jurisdiction of Michigan's Department of Transportation (MDOT). Out of this total 2632 are prestressed concrete with design types of an I-girder, box girder or spread box girder of which, 699 are PC I-girder bridges. PC box girders are designed for spans up to 43 meters. AASHTO type PC I-girders are also designed for spans up to 32 meters, and a Wisconsin Type I-girder with a depth of 1800 mm can achieve a span of 46 meters using 48 MPa concrete. Furthermore, prestressed concrete girders are now the choice in freeways bridges subjected to severe exposure conditions with I-girders being the most preferred type. In earlier designs the girders were simply supported on neoprene or steel pads with an unshored composite concrete deck having expansion joints between each span. More recently the deck is cast continuously with the approach pads and monolithically with sizable diaphragms over the piers and the abutments. The girder ends are waxed during the casting of the diaphragms, assuming that rotational freedom is provided. On the deck surface, control joints are cut at the inflection point locations in order to prevent cracking. The primary reason for this detail was to eliminate the leaky joint in order to provide a roof over the beam-ends and pier caps for protection from heavy applications of deicing salts.

An earlier study focusing on the condition of Michigan's PC bridges revealed that while most were in fair or better than fair condition, older structures were beginning to show signs of significant deterioration at the ends of the PC beams. Newer structures (less than 20 years old) utilize joint details that help to deter the deterioration as described above. Major concerns observed with older structures included the corrosion of prestressing strands and high chloride concentrations in concrete. It was reported that the deterioration level was influenced by the location of the bridge, traffic volumes, load limits, and de-icing salt usage. The study brought out the need for clear health monitoring guidelines in appraising the vulnerability of the PC I-girder to deterioration. A careful review of 500 PC I-girder inspection reports showed that 110 bridges exhibit cracking, corrosion and delamination at the girder ends within the first meter. A detailed inspection of 20 such bridges constructed between 1964 and 1998 was conducted and their condition documented. Detailed review of the inspection data indicated that the girder-ends are often cracked as early as the time of erection.

The specific goals of this research were to develop a health monitoring procedure for PC I-girder bridges primarily based on visual inspection and to develop/recommend protection and repair techniques corresponding to each state of health. The primary expectation from the health monitoring procedure is to identify the PC I-girders vulnerable to tendon corrosion. The health monitoring procedure is being based on extensive analysis of the Pontis data, a multi-state survey in the US to learn about the experience of other State Highway Agencies, and the detailed field inspection of twenty highway bridges. It is also important to note that the bridgework activities in Michigan are funded under four categories specified as "Capital Scheduled Maintenance (CSM)", "Capital Preventive Maintenance (CPM)", "Rehabilitation (R1)" and "Replacement (R2)". CPM activities are for sustaining the current condition of the bridges, CSM is to address the needs of bridges in fair condition, and R1 and R2 are for improving the condition of the bridges. The health monitoring procedure is needed to designate the condition states compatible with the funding categories. The protection/repair procedure recommendations were developed. These procedures are based on what is reported in the literature and analytical FE studies of a typical PC I-girder bridge.

HEALTH MONITORING AND VULNERABILITY ASSESSMENT RECOMMENDATIONS

In Michigan, health monitoring of bridges is based on the visual inspections performed every two years. Inspection is performed on each bridge component. Specifically for PC I-girder bridges, rating and comments are provided for the barriers, expansion joints, deck, stringers, diaphragms, bearings, piers, abutments and the drainage system. The rating is a condition state and assigned for each of the inspected components. At this time, two independent instruments are used in defining the condition state. The first instrument is described in the Michigan Pontis Bridge Inspection Manual and primarily intended for fleet management tasks such as scheduling preventive maintenance. The second instrument is described in the Michigan Structure Inventory and Appraisal Coding Guide, used for National Bridge Inventory System (NBIS inspections) with a primary purpose of safety assessment. Pontis has defined pre-determined assessment criteria for an inspector to follow for assigning a condition state and potential feasible actions. In contrast, the Michigan Structure Inventory and Appraisal Coding Guide allows for greater latitude in assigning condition ratings to a structural element. In a Federal Highway Agency manual (Manual 90) for the training of bridge inspectors, it is required that inspectors rate bridge elements, including prestressed concrete I-beams, as a whole, rather than allowing individual locations of distress to lower an element's rating. However, inspectors are expected to modify the condition rating accordingly if an isolated distress (possibly beam end deterioration) influences the load carrying capacity or serviceability of the element. The NBIS inspection condition rating for a superstructure element, such as a prestressed concrete I-girder, is based on a scale of 0 to 9. However, a uniform damage severity classification is not provided for various concrete distresses and assessment is left to the judgment of the bridge inspector.

The PC I-girder vulnerability was defined based on the distress observed at the girder ends. The primary reason for the girder-end distress was the expansion joint and/or the drainage system failure. As a result the surface water together with dissolved deicing salts drain over the girder ends. With sufficient time deicing salts reach and initiate corrosion of the reinforcement and the tendons. The field inspection performed concentrated on documenting the condition of the beam end for the purposes of developing a health monitoring procedure for the corrosion prone beam-ends. A total of twenty bridges between the ages of 3-40 years were inspected. After reviewing the inspection data consisting of 828 girder ends and an equal number of bearings and sole plates, a pattern of deterioration was identified. Five of the bridges were of more recent vintage incorporating the continuous joint detail cast monolithically with the diaphragm and deck. The behavior of newer bridges is significantly different due to the lack of water infiltration (no leaky joint) and lack of subsequent restraint at the pier and abutment reduce sole plate and tearing corrosion. However, the vertical cracking observed at the abutments is perhaps due to the restraining effect of the end diaphragm. The bridges designed before 1980 are truly simply supported systems with expansion joints over each pier. Over the abutments, the girder ends are encased in diaphragms monolithically cast with the deck and approach slab, except that the girder end with the expansion joint is expected to provide the movement capability. Over the piers, the girders are connected near the ends with partial diaphragms. The partial diaphragms depths are not uniform, always ending above the bottom flange but sometimes extending to the deck.

Detailed analytical models of PC I-girder bridges of were developed with typical configurations to provide a clear understanding of the bridge response under the complexities and the variations of the structural system. Using the models, a three dimensional finite element (FE) analysis was conducted in order to evaluate the restraints imposed on the girders due to the continuous deck and diaphragms. The FE model also included the impact of non-functional elastomeric bearing pads on the girder end stresses.

Utilizing the inspection data, a preliminary vulnerability assessment measure has been developed. The measure is based on the state of girder-end cracking in excess of 0.0025 mm, expansion joint condition, functionality of the bearing pads and the state of corrosion of the sole-plate. The vulnerability can directly be determined from the bi-annual visual inspection reports.

REFERENCE:

[1] Enright, M. P. and Frangopol, D. M. (2000). "Survey and Evaluation of Damaged Concrete Bridges", Journal of Bridge Engineering, February, pp. 31-38

[2] AASHTO, "Pontis" (Version 3.4.3), *Computer Software*, American Association of State Highway and Transportation Officials, Washington, D.C., (2001).

GUARANTEEING STRUCTURAL SERVICE LIFE THROUGH MONITORING

Ulrich Santa **Konrad Bergmeister** **Alfred Strauss**
Institute of Structural Engineering, Vienna, AUSTRIA

Keywords: Structural Condition Assessment, Structural Monitoring, Durability

1 INTRODUCTION

The condition assessment of aged structures is becoming a more and more important issue for civil infrastructure management systems. The continued use of existing systems is, due to environmental, economical and socio-political assets, of great significance growing larger every year. The performance of many of these in-service structures has decayed over the years of utilization and the inherent level of safety might be inadequate relative to current design documents. Structural integrity has to be guaranteed by the structural safety under ultimate and serviceability conditions in order to ensure the safety of the structure and its users. For the purpose of developing adequate life extension and replacement strategies, issues such as whole-life performance assessment rules, target safety levels and optimum maintenance strategies must be formulated and resolved from a lifetime reliability viewpoint and lifecycle cost perspective [1].

2 STRAIN AND DEFORMATION MONITORING

When forces are applied to a structure, the components of the structure change slightly in their dimensions and are said to be strained and they may even underlie a certain translational or rotational displacement. Creep, shrinkage, and seasonal temperature changes may result in overall length changes of a bridge or components of a bridge. The measurement of deformation can be approached either from the material or from the structural point of view. On the one hand, observation of local material properties made by a series of short base-length strain sensors can be extrapolated to the global behavior of the whole structure. While strain sensors on a short base length are usually used for material monitoring rather than structural monitoring, long-gauge sensors give information on the behavior and response of structure.

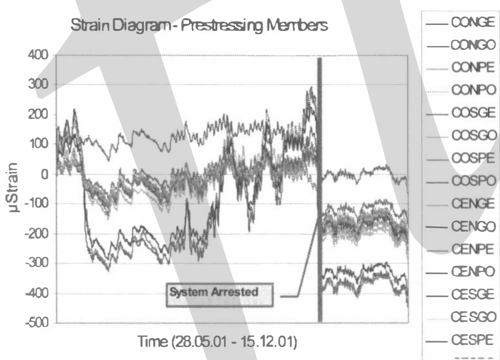

Fig. 1 Strain evolution of prestressing members

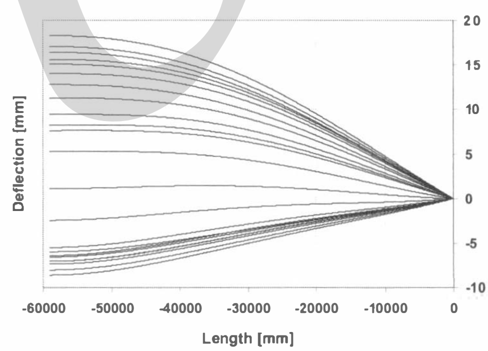

Fig. 2 Cantilever deflection – 24h behavior (7.6.01)

In the present monitoring system realized on the Colle Isarco viaduct on the Italian Brennero-Highway A22, a network of fiber optical long base length sensor was installed for strain (**Fig. 1**) and deformation (**Fig. 2**) measurements. 96 fiber optical SOFO-Sensors with a base length of 10 m were installed on the concrete surface parallel to the neutral axis of the box girders in order to determine the vertical, horizontal, and torsional deformations. Sensors with a base length of 0,5 m were used to measure the strains of 16 selected prestressing members. Another 24 sensors with a base length of 8 and 10 m were installed on the two piles P7 and P8 of the structure. The elongational strain measured by 4 strain sensors in each section and the beam curvature are related according to the Bernoulli-Navier beam theory, the curvature function of each beam section is a second-degree polynomial [2]. The displacement functions can then be obtained by double integration of the curvature functions for each instrumented section (**Fig. 2**), the determination of the rigid body motion is achieved through the application of the inclinometer measurements. For this purpose 36 highly accurate inclinometers were installed on the structure. On the one hand, these inclinometers complete the fiber optical network with information on the rigid body displacements of the structure. On the other hand, given a sufficient number of sensors, vertical deflections can immediately be determined by the simplified relation $h_i=\sin(\tau_i)*l_i$, where h_i denotes the vertical deflection of a section i with length l_i, where a rotation of τ_i was measured. Alternatively, a similar algorithm [2] as applied for the fiber optical network might find application for a more precise representation.

In order to separate the influence of thermal gradients in the structure and other agents (traffic, snow, wind), 60 thermocouples (T-Type, embedment depth 200 mm) have been installed in the girders and on the piles P7 and P8. Further, 10 LVDTs have been installed to instrument movements on the bearings.

3 DURABILITY MONITORING

Steel embedded in good quality concrete is protected by the alkalinity of the concrete pore water. However, penetration of aggressive ions, as e.g. chloride from deicing salt or carbonate from acid rain, will destroy the passivation of the embedded steel. In the presence of oxygen and the right humidity level in the concrete, corrosion of the steel will start and develop continuously [3]. This category of measurements is based on the electrochemical nature of corrosive processes that is comparable to the anode and cathode principle. On 4 selected columns of the Colle Isarco viaduct 12 electrochemical multiprobes have been installed to determine the concentration of free chlorides, corrosion current and the electrochemical potentials at different embedding levels.

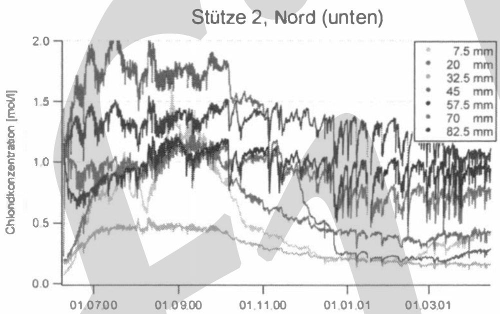

Fig. 3 Chloride concentration measurement [mol/l]

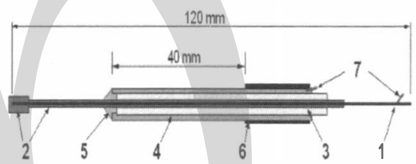

Fig. 4 Chloride sensitive sensor element

4 DATA INTERPRETATION AND SYSTEM MODELING

The installation of sensing elements and a data acquisition system to collect measured data is only the start of monitoring field performance. Interpretation of the acquired data is equally important, namely the comparison of measured and calculated data in order to validate the model assumptions. SARA, a project related to the present monitoring program, is based on the 2D/3D nonlinear analysis program ATENA developed by Cervenka Consulting. This FEM program will be adapted to a probabilistic analysis concept. The structural monitoring data is used to suit the stochastic models, for example with Bayesian updating, or for the derivation and validation of the numerical model assumptions.

REFERENCES

[1] Frangopol, D. M., Bridge Health Monitoring and Life Prediction based on Reliability and Economy. International Workshop on the Present and Future in Health Monitoring, Bauhaus-University Weimar, Germany, (2000)

[2] Vurpillot, S., Gaston, K., Benouaich, D., Clément, D., Inaudi, D., Vertical deflection of a pre-stressed concrete bridge obtained using deformation sensors and inclinometer measurements, ACI Structural Journal, Vol. 95, No. 5, pp. 518, (1998)

[3] Zimmermann, L., Schiegg, Y., Elsener, B., Böhni, H., Electrochemical techniques for monitoring the conditions of concrete bridge structures, Repair of Concrete Structures, Proceedings of Int. Conference, (1997)

MONITORING THE RISK OF REINFORCEMENT CORROSION USING THE EXPANSION-RING-SYSTEM

Michael Raupach
Institute for Building Materials Research
Technical University of Aachen, ibac, Germany

Peter Schießl
Institute for Building Materials
Technical University of Munich, BSI, Germany

Keywords: Corrosion, monitoring, steel, concrete, reinforcement, anode, cathode, sensor

1 INTRODUCTION

Monitoring sensors for the risk of reinforcement corrosion are used world-wide more and more to reduce the risk of undetected corrosion problems, which often cause expensive repair measures when they are detected in a stage, when cracks and spalling appear. Especially in areas with difficult access or in cases, where e.g. traffic lanes have to be closed for a certain time, the automatic inspection using sensors is more cost-effective than on-site inspections.

A sensor system for installation together with the reinforcement before placement of the concrete is available since 1990. This is used world wide in concrete structures exposed to aggressive environment. To enable such monitoring also for existing structures a new system had to be developed. First tests on drilled-in sensors have been carried out already in 1996. After several improvements now suitable sensors and sufficient experience are available to use the system.

2 DESCRIPTION OF THE EXPANSION-RING-SYSTEM

The Expansion-Ring-System consists of the Expansion-Ring-Anode and a Cathode Bar. The Expansion-Ring-Anode and Cathode Bar are inserted into holes, which have to be drilled into the concrete surface. The geometry of the holes has to be very exact. Therefore special drilling equipment has to be fixed to the concrete surface during drilling. The measuring sensor is the Expansion-Ring-Anode. Similar as the six bars of the Anode-Ladder-System the Expansion-Ring-Anode consists of six measuring rings in different distances from the concrete surface, in 1 cm -steps from 1 to 6 cm. In this way the ingress of chlorides and/or carbonation from the concrete surface into the concrete and the subsequent corrosion risk of the reinforcement can be measured in the same way as using the Anode-Ladder-System.

Above, between and below these metal rings altogether seven insulation rings are established to seal the area between the rings, i.e. to prevent water or chlorides penetrating along the drilled surface deeper into the hole of the Expansion-Ring-Anode.

In the head of the Expansion-Ring-Anode a socket is integrated, which allows to insert the plug of the measuring instrument. Between the measurements a sealing cap is put onto the socked to protect it from corrosion. Cables are led from the measuring rings to this integrated socket inside of the Expansion-Ring-Anode. After production of the electrode all inner open spaces are filled with resin and sealing material to ensure that no water or chlorides can penetrate to or within the inner part of the sensor.

The Expansion-Ring-Anode and Cathode Bar are fixed to the concrete by turning nuts at the upper part of the sensors, which leads to an expansion of the rings in a way, that both sensors can be tightened sufficiently. To prevent cracking of the concrete due to the pressure by expansion of the sensors, the increase of the diameter is limited: After a certain torque is reached, the sensor turns itself within the hole preventing high forces to be introduced into the concrete.

3 MEASUREMENTS AND EVALUATION

All measurements can be carried out automatically by computer control or by using hand-held instruments in regular intervals (e. g. one to four times per year). As long as the critical chloride content and the carbonation depth have not reached the surface of the outer anode, all electrical currents are low, i.e. smaller than 10 µA. In the course of time the anode-rings will be depassivated one after the other. By measuring the electrical currents and voltages between anodes and cathodes in regular intervals, the relationship between the depth of the critical chloride content or carbonation and time can be determined.

The time to corrosion of the existing reinforcement can be estimated approximately by extrapolation using appropriate calculation models.

For the measurements an automatic portable instrument has been developed. Using this battery-powered instrument the electrical currents, potentials, electrolytic resistances and the temperature can be measured automatically. The critical values are indicated automatically within the large display. The data of 1000 measurements can be stored and transferred to a personal-computer by the integrated serial port. For further evaluation of the data software is available, which builds up a database and shows the data versus time including alarm-values.

4 RESULTS FROM LABORATORY TESTS AND FIRST INSTALLATIONS INTO CONCRETE STRUCTURES

To investigate the proper functioning of the Expansion-Ring-System extensive tests have been carried out at S+R Sensortec and BAM within the Brite Euram project "Smart Structures". Additionally Expansion-Ring-Sensors have been installed into columns of a parking deck, the coated upper surface of a parking garage and a bridge cap in Germany and into different coastal structures in Norway. Actually more pilot projects are starting.

5 FIELDS OF APPLICATION

The corrosion monitoring system has the following advantages compared to other monitoring methods:

- It is not only shown, whether the reinforcement corrodes or not, but it can also be estimated, when the reinforcement will start to corrode.
- The corrosion monitoring system shows directly the depth of the critical chloride content and not the absolute chloride contents. Compared to the measurement of chloride profiles this is a decisive advantage, because as known from experience the interpretation of absolute chloride contents is always difficult. Therefore the installation of corrosion monitoring sensors can not be replaced simply by taking concrete samples for chloride profiles.
- The use of the corrosion monitoring system is especially economic in locations with difficult access. Leading the cables to accessible locations for the measurements or using automatic data-logging systems is especially possible in cases when the monitoring location is under traffic.

Therefore typical fields of application will be concrete structures exposed to aggressive environment, especially to chlorides, when the traditional methods are difficult to be applied (e.g. difficult access) and when the durability of the structure is uncertain (e.g. when new protection measures like inhibitors, newly developed coatings etc. have been used).

6 OUTLOOK

Laboratory tests and first installations on site have shown, that the critical depth related to reinforcement corrosion can be monitored using the Expansion-Ring-System. The experience from the ongoing and future installations will be presented in further papers.

FIBER OPTIC DISTRIBUTED SENSOR FOR CONCRETE STRUCTURES

Hitoshi Kumagai Keiji Shiba
Shimizu Corporation
JAPAN

Hiroshige Ohno Hiroshi Naruse
NTT Access Network Service Systems Laboratories
JAPAN

Keywords: optical fiber, Brillouin scattering, strain, deflection, concrete structure

1. INTRODUCTION

For the fiber optic distributed sensor described in this paper, BOTDR (Brillouin Optical Time Domain Reflectometer) are utilized. When optical pulses are launched into an optical fiber, some of the light is backscattered. Of this light, the frequency of Brillouin backscattered light changes in proportion to the optical fiber strain. Hence the strain distribution along the fiber can be obtained by measuring the variation in the Brillouin backscattered light power and its arrival time.

Figure 1 shows the fiber optic sensor cable developed in this study. To protect the optical fiber from the shock caused by casting concrete and so on, a two-layer coat is used. Aramid fiber reinforced plastic (AFRP) is used for inner layer and resin is used for outer layer. The resin coat is indented at regular intervals before the heat hardening process, in order to be firmly bond to concrete.

Two types of sensor cable were prepared. Sensor cable with a diameter of 2 mm is mainly used for pasting cable on the surface of the existing concrete structures, and sensor cable with a diameter of 6 mm is used for embedding cable into concrete structures. In this paper, four point bending test on the reinforced concrete slab installed with this new-type fiber optic sensor cable has been reported.

2. TEST PROGRAM

A reinforced concrete slab shown in Figure 2 was tested to investigate the effectiveness of this sensor. The specimen was 1200 mm wide, 300 mm thick and 4000 mm long. The effective span was 3600 mm, and loads were applied 900 mm apart on both sides of mid-span. The specimen was reinforced with 19 mm diameter deformed bars (D19) with spacing of 150 mm on the top and bottom. Compressive strength of the concrete was 46.8 MPa, and yield strength of D19 was 386 MPa.

2 mm and 6 mm sensor cables were installed along the top and bottom bars. They were fixed to the bars with binding wires. 2 mm sensor cables were pasted with epoxy adhesive resin on the top and bottom surfaces.

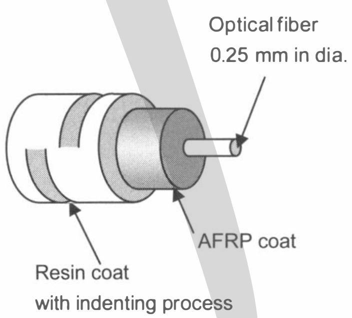

Fig.1 Structure of the sensor cable

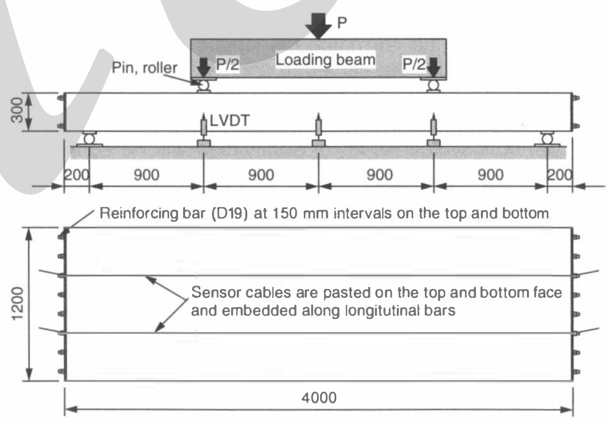

Fig.2 Outline of the specimen

3. TEST RESULTS AND DISCUSSION

Figure 3 shows the load-deflection curve. Circular marks and numbers in the figure indicate BOTDR measuring steps. Flexural cracks were visible at step 2 (P=150 kN), the measured strain in the bottom bar reached its yield strain at step 6 (400 kN) and concrete at the compression edge was crushed at step 12 (550 kN) .Figure 4 shows the strain distribution measured by BOTDR and strain gages at step 6.

The strain distribution measured by BOTDR is in good agreement with that measured by strain gages on compression and tension sides. After step 11, the strain on tension side could not be measured either by BOTDR or strain gages. The strain on compression side could be measured to the last step, but the sensor cables were partially peeled when concrete was crushed.

Curvature distribution can be calculated if sensor cables are installed on the top and bottom sides. Deflection curve can be obtained by integrating the curvatures twice in the longitudinal direction. Figure 5 shows the deflection curve obtained using above mentioned method and the deflections measured by LVDTs in step 6. The deflections by both methods are in good agreement at each of the three points.

4. CONCLUSION

The authors developed this new fiber optic sensor cable suitable for concrete structures, conducted four point bending test on the slab installed with this sensor cable and applied BOTDR. The test results are summarized as follows:

1) The sensor cable developed in this study is available either for pasting on the surface of the structure or embedding into concrete. With a single line of this sensor cable, the continuous strain distribution can be obtained.
2) Comparing the measured strain statistics of fiber optic sensors and strain gages, both are in agreement.
3) The deflection curve can be calculated if the sensor cables are installed on the top and bottom sides of the structural member. The calculated value was in agreement with measured deflection by LVDT.

REFERENCES

[1] Oka, K., Ohno, H., Kurashima, T., Matsumoto, M., Kumagai, H., Mita, A and Sekijima, K.: Fiber Optic Distributed Sensor for Structural Monitoring, Proc. Of 2nd Intl. Workshop on Structural Health Monitoring, pp.672-679, 1999

[2] Shiba, K., Kumagai, H., Watanabe, K., Naruse, H. and Ohno, H.: Fiber Optic Distributed Sensor for Monitoring of Concrete Structure, Proc. Of 3rd Intl. Workshop on Structural Health Monitoring, pp.459-468, 2001

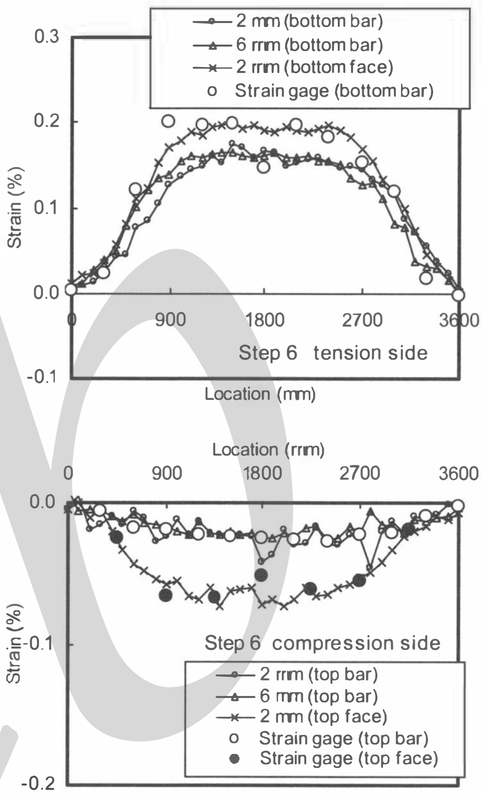

Fig.4 Strain distribution at step 6

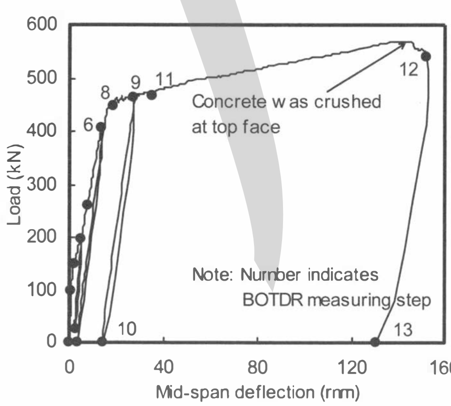

Fig.3 Load-deflection curve

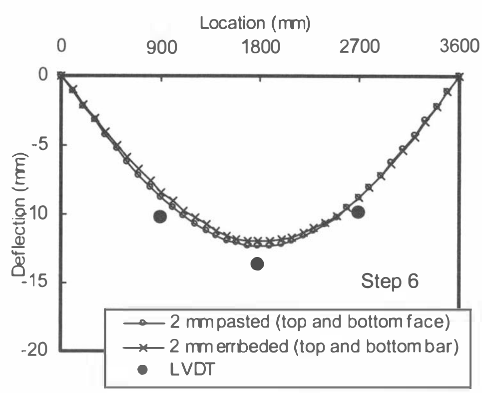

Fig.5 Deflection curve at step 6

ESTIMATION OF STEEL BAR CORROSION IN RC MEMBER BASED ON POLARISATION RESISTANCE

Koichi KOBAYASHI
Chubu University, JAPAN

Toyo MIYAGAWA
Kyoto University, JAPAN

Keywords: Deterioration of RC member, Chloride induced corrosion, Polarisation resistance

1 INTRODUCTION

Deterioration of reinforced concrete structure is caused by several factors, a typical one of which is the corrosion of reinforcing steel. Polarisation resistance method is particularly suitable for theoretically evaluating the corrosion rate of steel bar.

This study investigates into the polarisation resistance methods. Based on the better understanding of these methods, this study aims at clarifying the relationship between the corrosion loss and the polarisation resistance in reinforced concrete beams deteriorated by the chloride induced corrosion, so that the corrosion loss of steel bar can quantitatively be estimated from the polarisation resistance.

2 EXPERIMENTAL PROCEDURE

The specimen shown in Fig. 1 has vertical joints to simulate an uneven chloride ion distribution, which causes a macro-cell corrosion circuit to be formed. The water-cement ratio of concrete was set to be 0.4 and 0.6. Chloride ions were added to them in three differing amounts ranging from 0 to 5.5kg/m^3.

The polarisation resistance of the steel bars was measured by double rectangular pulse method. A copper plate measuring 100mm in width and 800mm in length was used as the counter electrode. The measurements were made every one or two weeks.

The polarisation resistance of the steel bars was also measured using an AC impedance method. The counter electrode used for the AC impedance method was a double-disk type consisting of a main centre disk 40mm in diameter and an enclosing guard disk 108mm in diameter.

Specimen were broken up for removal of the steel bars. The corrosion loss of these steel bars was examined.

3 DEFINING POLARISATION AREA

In order to determine the polarised area, the distributions of the electric potential and the current flow in the specimen being polarised were simulated by a two dimensional finite differential method.

Fig. 2 illustrates an example of a cross section of the specimen with the double-disk counter electrode used in the AC impedance method. It is assumed from these results that all the current flows from the main counter electrode into the upper half of the steel surface adjoining the cover concrete, and that only the upper half of the steel is polarised by the main counter electrode. Regarding the model specimen with the large counter electrode which entirely covers the surface of

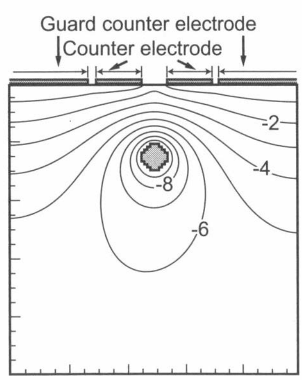

Fig. 2 Example of electric potential distribution in the lateral cross section (unit: mV)

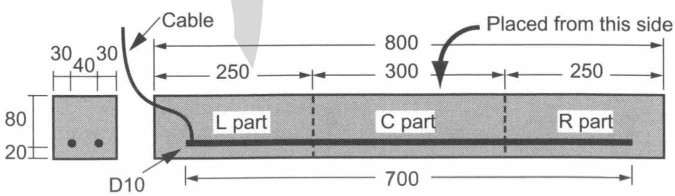

Fig. 1 RC beam specimen (unit: mm)

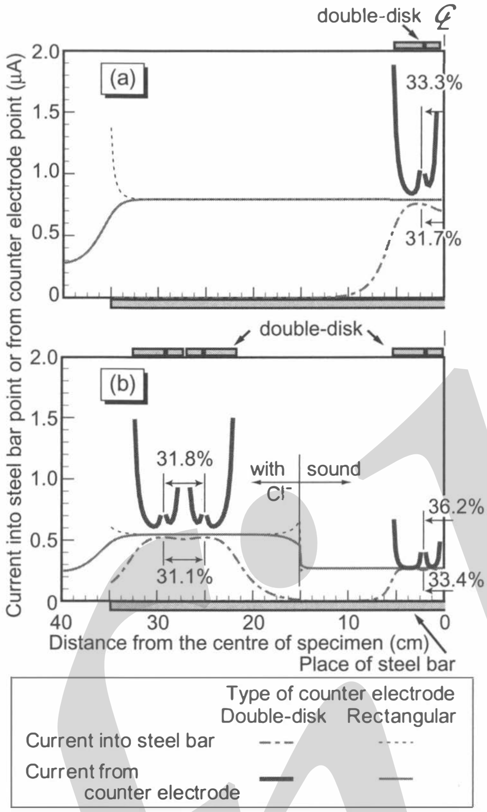

Fig. 3 Current distributions in the longitudinal cross section: (a) Specimen with even chloride distribution. Polarisation resistance was not taken into consideration, (b) Specimen with macro-cell corrosion. Polarisation resistance was taken into consideration.

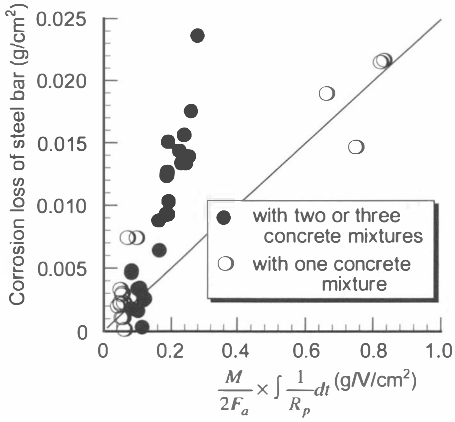

Fig. 4 Relationship between corrosion loss and polarisation resistance by the double-pulse method

the specimen, the current flowing into the steel bar from the lower half or the inner part of the specimen was significantly large.

Fig. 3 shows the current intensity from or into the nodal points of the counter electrode and the steel bar in the longitudinal cross section of the model specimen. The intensity of current flowing out from the main counter electrode of double-disk almost matched the intensity of current flowing into the steel bar just beneath the main counter electrode. Moreover, the intensity of current flowing into steel bar was smaller in the cases in which polarisation resistance was taken into consideration.

4 STUDY OF CONSTANT K

Fig. 4 shows the relationship between the corrosion loss and the integral of corrosion rate index, which is reciprocal of polarisation resistance obtained by the double-pulse method, multiplied by $M/2F_a$ (M : atomic mass of iron (=55.8), F_a : Faraday constant (=96500C)). The corrosion loss per unit surface area was obtained by dividing the total corrosion loss with the surface area of steel bar (210cm^2).

The degree of inclination of this graph corresponds to the constant K in Stern-Geary equation. Accordingly, the constant K was 0.0252(V) in the case of the specimens with uniform chloride distribution.

5 CONCLUSION

The results obtained in this study can be summarised as follows:

(1) The current developed upon polarisation flows largely into the backside of steel bar irrespective of the type of counter electrode.

(2) In the case with the double-disk counter electrode, the amount of current flowing out from the main counter electrode approximately corresponds to that flowing into the cover side of the steel bar.

(3) The polarisation resistance could more precisely be measured by AC impedance method using the double-disk counter electrode.

(4) The polarisation resistance should be taken into consideration when estimating electrical potential distribution in RC member.

QUANTITATIVE EVALUATION OF DYNAMIC COMPACTION PROCESS IN FRESH CONCRETE

Fumitake Kunisue Yoshiyuki Yokoyama Keiichi Nogami Masayasu Ohtsu
Graduate School of Science and Technology, Kumamoto University
JAPAN

Keywords: dynamic compaction, pore pressure, boundary element method, two-phase theory, acoustic emission

1 INTRODUCTION

Although vibrating compaction is extensively applied to fresh concrete, quantitative evaluation of the compaction process is not clarified yet. Because the conventional treatment applied to the quality control of fresh concrete is quite simple, the reliability on the performance of the compaction is limited. In this paper, pore pressure is measured in a vibrating compaction test to investigate dynamic compaction process of fresh concrete. Transition from the unsteady state to the steady on dynamic behavior of concrete is examined by acoustic emission (AE) measurement. Such mechanical parameters as elastic modulus, permeability and wave attenuation of the concrete are measured in the early age. Based on Biot's two-phase mixture theory, the boundary element method (BEM) analysis is applied, taking into account the effect of viscosity and inhomogeneity of permeability in a layer. Pore pressures and volumetric strains are theoretically synthesized and compared with the experimental results.

2 ANALYTICAL METHOD

Concerning displacement **u** and pore pressure p, an equilibrium equation on solid phase at the steady state is derived, based on Biot's two-phase mixture theory.

$$\rho\left(-\omega^{2}\right)u_{i} = (\lambda + \mu)u_{j,ji} + \mu\, u_{i,jj} + p_{,i} \qquad (1)$$

An equation of continuity on liquid phase is represented as well as,

$$p_{,ii} = -\left(\rho^{f}\omega^{2} + \frac{\gamma_{w}}{k} i\,\omega\right)u_{i,i} \qquad (2)$$

where, ρ^{f} is the density of solid phase. ω is the angular frequency. γ_{w} is unit weight of liquid phase. k is the permeability coefficient. λ and μ are Lame's constants.

This two-phase problem coupling eqs.1 and 2 can be analyzed by BEM. Here, complex variables of λ and μ are applied, taking into account viscosity. Two-dimensional dynamic analysis based on BEM is applied to solve the dynamic steady state of fresh concrete.

3 DYNAMIC COMPACTION TEST

Mixture proportions of the concrete are shown in Table1. The fresh concrete is placed into the wooden mold of inner dimensions 30cm×30cm×35cm. Pore pressure meters are set at three depths of 5cm, 15cm, and 25cm. A steel tap of thickness 5mm is placed on the surface of fresh concrete to apply a vibrating load. Dynamic load of 130Hz is applied at 1.74kPa in case of mixture Ⅰ,6.53kPa for mixture Ⅱ respectively. AE sensor of 1MHz resonance is attached to the outside the mold, where the amplification is 60dB gain and the threshold level is 42dB.

Table 1 Mixture Proportions

Mixture	Gmax (mm)	W/C (%)	s/a (%)	Slump (cm)	Admixture (cc)	Weight per volume (kg/m³)				
						W	C	F	S	G
I	20	60	40	21.3	114	228	380	0	690	1035
II	20	50	42.3	7.8	112	178	407	0	714	973
III	20	35	38.5	0	0	113	226	97	780	1274

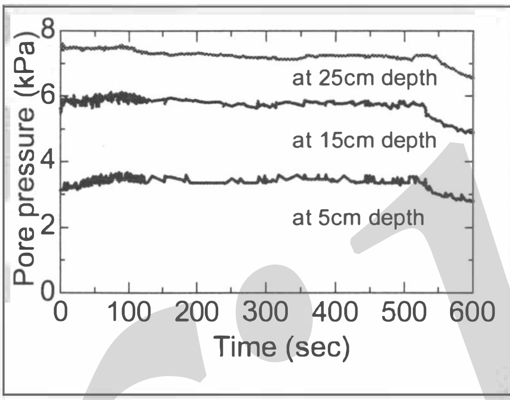

Fig.1 Pore pressure (Mixture I)

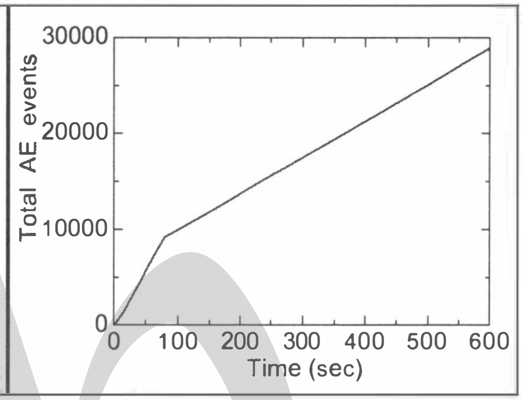

Fig.2 AE events (Mixture I)

4. RESULTS AND DISCUSSION

Pore pressures measured in case of mixture I are shown in Fig.1. At the bottom area of concrete, the pore pressure becomes larger because of hydrostatic pressure prior to dynamic compaction. On the other hand, around the upper area, the pore pressure becomes lower. Pore pressures fluctuate slightly until 100 sec, and then become constant as the steady state.

AE events measured during the tests are shown in Fig.2. Total number of AE events increases linearly until 100sec as time passes, and then increases less than the beginning. The behavior clearly shows the transition from the unsteady to steady state of pore pressure during compaction.

Pore pressures calculated by BEM are shown in Fig.3, compared with experimental results. By changing the permeability coefficient as smaller as the deeper location of concrete, numerical analysis of the inhomogeneous case is conducted. The homogeneous cases result in larger pore pressure distribution than inhomogeneous cases. It is observed that the experimental results closely distribute between the visco-elastic solution and the elastic in the inhomogeneous case. Thus, an applicability of BEM analysis is confirmed in the elastic solution and the visco-elastic.

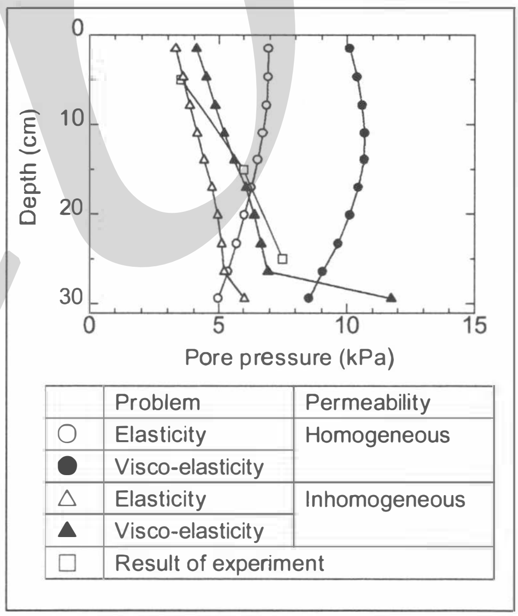

Fig.3 Results of BEM (Mixture I)

REAL TIME INTELLIGENT DATA ACQUISITION AND CONTROL SYSTEMS FOR MONITORING AND MANAGING INFRASTRUCTURE

Prof. A. Emin Aktan, Prof. Alexander Meystel

*Drexel Intelligent Infrastructure Institute
Drexel University, Philadelphia 19104, USA
e-mail: aaktan@drexel.edu, web page: http://www.di3.drexel.edu/

Key words: Health Monitoring, Civil Infrastructure Systems, Long Span Bridges, Information Technology

Abstract. Significance of effectively managing civil infrastructure systems (CIS) throughout CIS life-cycles, and especially during and after natural or man-made disasters is well recognized. Disaster mitigation includes preparedness for hazards to avoid casualties and human suffering, as well as to ensure that critical CIS components can become operational within a short amount of time following a disaster. It follows that mitigating risk due to disasters and CIS managementare intersecting and interacting societal concerns. A coordinated, multi-disciplinary approach that integrates field, theoretical and laboratory research is necessary for innovating both hazard mitigation and infrastructure management. Health monitoring (HM) of CIS is an emerging paradigm for effective management, including emergency response and recovery management. Challenges and opportunities in health monitoring enabled by recent advances in information technology are discussed in this paper. An example of HM research on an actual CIS test-bed is presented.

Experiences with recent natural and man-made disasters indicate the need for real-time data and information management systems that provide timely information to emergency managers regarding the conditions of critical infrastructure following disasters. There are obvious connections between integrated information systems that take advantage of a GIS platform for emergency management, and the health-monitoring (HM) systems that are envisioned for long-span bridges, tunnels and entire regional transportation networks in the realm of next generation intelligent transportation systems. The writers envision that transportation HM systems will take advantage of integrated information systems that will permit officials and engineers to access, review and analyze legacy and recent data and information in addition to real-time data. The data will have many simultaneous modalities, such as satellite images and on-ground streaming-video of traffic and roadway conditions, weigh-in-motion information and critical structural responses including temperatures, accelerations, displacements, tilts and strains. Intermittent and continuous data should be sufficient to evaluate, in real-time, any critical changes in operational safety due to incidents and weather, and structural reliability due to aging, deterioration, damage due to accidents or overloads. These are discussed further in the following. The similarities between transportation HM systems and the real-time earthquake damage assessment and disaster mitigation systems envisioned by the earthquake disaster mitigation research community are obvious[1].

We define the health of a bridge as its system reliability to possess adequate capacity against any probable demands that may be imposed on it in conjunction with the limit states (LS). Performance is a consequence of health, i.e. how the bridge actually meets the reasonable peak-level demands related to utility, operation, serviceability, durability and safety. We note that there has not yet been an adequate discussion for the critical limit-states for defining performance within the civil engineering community, therefore, an ASCE SEI Committee has been recently formed for this purpose. To initiate discussion, we venture the ranges of return periods for peak-demands during the serviceability-durability, safety and conditional limit-state events maybe taken as 25-75 years, 250-500 years and 2500-5000 years, respectively, given the related discussions in the earthquake engineering community for seismic performance.

In reliability analysis it is common to use the “Second Moment Reliability Index β” as a measure of health or reliability as this relates to the deterministic “Safety Factor” or “Load Rating” most engineers use in practice. For example if Capacity and Demand are independent and normal random variables, $\beta = 0$ corresponds to a Health or $1-P_f$ of 0.5, $\beta = 3$ corresponds to a Health of 0.999, and $\beta = 4.75$ corresponds to a Health of 0.99999. The latter corresponds to one in a million chance of inadequate capacity.

HM concept may be described best in terms of the goals of preventive health management in medicine: anticipate and prevent highly probable, common ailments before they occur; and, diagnose and intercept less common ailments at a sufficiently early stage while they are more curable. The principal advantage is pro-actively intercepting "ailments" before they take their toll. The potential in applying this concept in mature industries such as manufacturing, aerospace, automotive and electronics are well established and the US bridge engineering community has already started to recognize the need for such a concept in view of the perceived "insufficient" condition of a large percentage of the bridges.

Given the limitations and shortcomings in the current practice, and also given that available bridge program funds permit replacement or upgrade of only a small percentage of the posted and deficient bridges in the National Bridge Inventory every year, we need effective strategies for leveraging technology and improving the objectivity, reliability and efficiency in the manner we manage our current investment into highway bridges. HM may be considered as a new paradigm powerful enough to serve as an overall framework for leveraging technology to impact the practice of bridge engineering. If we are able to make a sufficient number of proper and successful implementations, in the long-term we would accumulate sufficient data and information, gain knowledge and insight .

Given the potential impacts and benefits of HM we note that HM is much more than just a group of technologies. HM involves the tracking of any aspect of performance or health by reliably measuring data and interpreting this in conjunction with domain specific knowledge and heuristic experience so that the health of a bridge for the LS events that are of concern and interest may be quantified objectively. Therefore we should recognize that HM requires the integration of a considerable number of analytical, experimental and information technologies as well as heuristic knowledge and experience ***through a well-coordinated multi-disciplinary team effort and within a systems-engineering framework.***

We strongly recommend government agencies such as FHWA, NSF and NIST to establish joint programs and initiatives to promote research and further development of HM as a most promising paradigm for infrastructure management.

REFERENCES

[1] Housner, G.W. et al. (1997), "Structural Control: Past, Present, and Future", Special Issue, *Journal of Engineering Mechanics*, Sep. 1997, Vol. 123, No.9.

[2] ASCE Official Register (2001), The Structural Engineering Institute (SEI), Committee on Performance-Based Design and Evaluation of Civil Engineering Facilities, p.412.

[3] AASHTO LRFD Bridge Design Specifications,American Association of State Highway Officials,Washington,DC, 1994.

[4] Ang, A.H. and Tang, W.H. (1975), "Probability Concepts in Engineering, Planning and Design," Vols. I and II, John Wiley and Sons, N.Y.

[5] Frangapol, D. M. and Kong, J.S. "Bridge Management Based on Reliability States and Whole Life Costing: From Theory to Implementation," Proceedings of the 3rd International Workshop on Structural Health Monitoring, Stanford University, Stanford, CA, Sept. 12-14, 2001, p.403-419.

EFFICIENT MANAGEMENT OF INSPECTION AND MONITORING DATA FOR A BETTER MAINTENANCE OF INFRASTRUCTURE

Thomas Le Diouron
Asia Manager
Advitam, Tokyo
tlediouron@advitam-group.com

Jérôme Stubler
General Manager,
Advitam, Paris
jstubler@advitam-group.com

Keywords: management, monitoring, inspection, maintenance

1. INTRODUCTION

In North America, Europe and Japan, government agencies and large private owners are now facing the challenge of maintaining with limited resources large stocks of vital infrastructure that has not been designed to be easily repaired or replaced, and that is getting older and more vulnerable.

People involved in the infrastructure management have developed extensive technical methods and tools to monitor the condition of the structure and establish the diagnosis. Each authority has been developing its own maintenance manual, taking into account their specificity, their different priorities, safety requirements, resources and range of competence.

In most cases visual inspections are used to detect deteriorations, rank structures, define priorities, estimate repair costs... These visual inspections require to record, report, analyze and store for years large quantities of data (inspection records, drawings, photos...) and it is easy to get lost in the clerical work. Moreover a number of decision steps (inspection record, ranking of defects, long-term analysis) are still highly subjective and can greatly affect the quality of the final diagnosis.

An inspection-based management software system has been developed to optimize this process and provide decision-makers with objective information on the condition of the infrastructure. The system is a comprehensive management system which integrates: database of structural defects, on-site computerized record, analysis, maintenance, diagnosis, repair and budgetary functionalities.

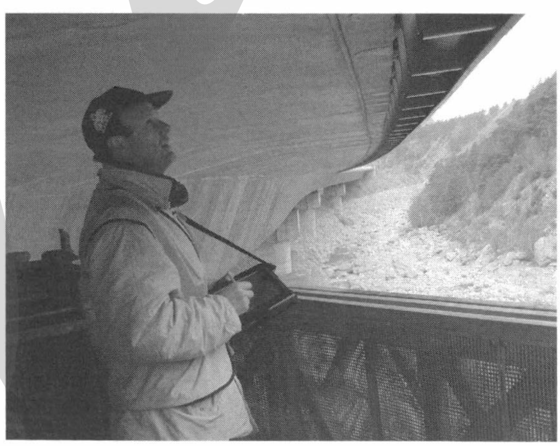

Fig.1: Site inspection using pen-touch computers

2. DESCRIPTION OF INSPECTION-BASED MANAGEMENT SOFTWARE

The inspection-based management software comprises of several components specifically designed to handle the tasks of each people involved in the maintenance process (Table 1).

Software components	Tasks	Designed for
Infrastructure Management	-database of detailed information on structures (drawings, design- construction-inspection-repair data), -ranking of structures according to preset rules, -management of the database, -budgetary tools, -scheduling of tasks, -management of repair works	-operators of infrastructure, -consultants, -specialized inspection companies
Inspection Management	-preparation of inspections, -transfer of data from mainframe to mobile inspection units	-inspectors, -specialized inspection companies, -consultants
Inspection	-on site recording of deterioration (on pen-touch light computers) -reference available	
Photo-based inspection	-time-effective survey of deterioration based on photos	
Report	-reporting of site-records, -automated standard report	
Analysis	-advanced analysis functions, -detailed investigation, -detailed repair definition	-engineers, -consultants, -contractors

Table 1: components of the inspection-based management software

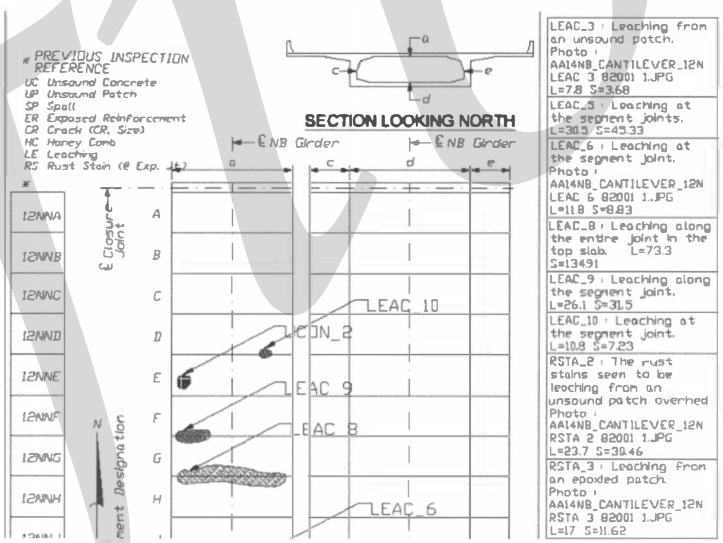

Fig.2: Example of standard output

3. IMPLEMENTATION AND EFFICIENCY OF THE SYSTEM

The system is currently used in the management of various structures in Europe, USA and Japan. It has proven its capabilities to significantly simplify the tasks of inspectors, engineers and decision makers.

ADVANCES IN THE CORROSION RATE MONITORING IN REAL STRUCTURES

I. Martinez and C. Andrade*

Institute of Construction Science "Eduardo Torroja", CSIC.
C/Serrano Galvache s/n. 28033, Madrid. Spain

1. INTRODUCTION

It is recognised worldwide that reinforcement corrosion is the main distress behind the present concern regarding concrete durability. However in spite of the very numerous papers published on the subject, relatively few are devoted to the development of measurement of on-site techniques in general, and even less to the measurement of corrosion. However, it is recognised the importance of an accurate (non destructive) on-site identification of the zones suffering corrosion, and in these zones, to appraise the importance of this corrosion, that is the achieved loss in cross section and the rate of its progress. In the present paper, a review is made on existing on-site techniques, and on the recent development of new ones, including embedded sensors, as well as the needed treatment of their expected evolution and integration on time, in function of the changes in the climatic conditions of the environment surrounding the concrete structure.

2. EXPERIMENTAL TECHNIQUES

The main techniques used on-site for appraising corrosion of reinforcements are of electrochemical nature. Because of its simplicity, the measurement of Ecorr (rest or corrosion potential) is the method most frequently used in field determinations. From these measurements, potential maps are drawn which reveal those zones that are most likely to undergo corrosion in the active state. However, such measurements have only a qualitative character which may make data difficult to be interpreted. This is due the potential only informs on the risk of corrosion and not in its actual activity. The same that said for the potential can be stated on Resistivity, ρ, measurements, which sometimes are used jointly with Ecorr mapping. The ρ values indicate the degree of moisture content of the concrete, which is related to the corrosion rate when the steel is actively corroding, but which may mislead the interpretation in passive conditions.

The only electrochemical technique with quantitative ability regarding the corrosion rate is the so called Polarization Resistance, R_p[1]. This technique has been extensively used in the laboratory. It is based on the application of a small electrical perturbation to the metal, the $\Delta E/\Delta I$ ratio defines the R_p. The corrosion current, I_{corr}, is inversely proportional to R_p, $I_{corr} = B/R_p$ (Stern- Geary ecuation), where B is a constant.

Direct estimation of True R_p values from $\Delta E/\Delta I$ measurements is usually unfeasible in large real concrete structures. This is because the applied electric signal tends to vanish with distance. There are several ways of accounting on-site for a True R_p value, among which the most extended one is the use of a guard ring[2] in order to confine the current in a particular rebar area. However, not all guarded techniques are efficient. Only that using a "Modulated Confinement" controlled by two small sensors for the guard ring control, placed between the central auxiliary electrode and the ring, is able to efficiently confine the current within a predetermined area (Figure 1).

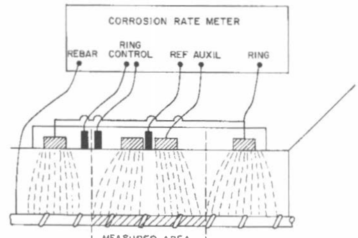

Figure 1: Modulated confinement of the current (guard ring) method

When the concrete is very wet, its resistivity may be so low that the confinement by the guard ring of the current cannot be well achieved because the area polarized is very large. For these conditions, another measurement method has been developed, the so called measurement of the potential attenuation with the distance[3] which is based in the direct measurement of the critical length (length o rebar really polarized). This method is not applied for normal non-wet concretes due to it cannot, in these cases, localize well the isolated corroding areas.

A new advanced technique of corrosion measurements has been recently developed. This technique is called "Passivation Verification Technique" (PVT). It has been developed for being applied on cathodically protected structures, and is possible to know the efficiency of the protection system without switching off the current. It uses the confinement sensor for delimitating the area and is based in applying an A.C current (instead of a D.C step). The response is analysed at a set of different frequencies. The PVT can be also applied when no cathodic protection is operating for simply verifying if the reinforcement is actively corroding or not. Although still more results are needed, the PVT may be used in the future to complement Rp measurements in order to find out whether a particular result is reliably informing on the corrosion state.

Other alternative to the periodic measurements is the use of monitoring systems based on the introduction of small sensors in the interior of the concrete, usually when placing it on-site. It is one of the most promising developments in order to monitor the long term behaviour of the structures. The most usual, as in the case of non-permanent on-site techniques, is to embed reference electrodes or resistivity electrodes. They can inform of the presence of moisture and on evolution of corrosion potential. Others events that can be monitored are the advance of the carbonation or chloride fronts, the oxygen availability, temperature, concrete deformations and the corrosion rate.

The most challenging aspect of on-site measurement, is the fact that the electrochemical parameters are weather dependent and, therefore, its instantaneous value will depend on the particular climatic conditions around the structure. When a single value of the corrosion current is measured on-site, it may happen that the concrete is dry at the time of measurement and therefore, mislead the deduction of its corrosion state. A methodology for obtaining a Representative on-site I_{corr} is presented. Two main alternatives exist: a) to take several readings during a certain period of time, a year for instance, and averaging them, or b) making a single isolated I_{corr} and ρ on site measurements, and drilling cores where I_{max} could be measured in the laboratory to average the on-site values.

Concerning the state of the art on on-site corrosion techniques, themselves, it is necessary to remark that the advances achieved are much more important than in other metal-electrolyte systems. In spite of it, several aspects remain to be improved in order to achieve the goal of making measurements of reinforcement corrosion a necessary and routine technique for any structural assessment of corroding structures.

3. REFERENCES

1. Andrade, C. and Gónzalez, J.A., "Quantitative measurements of corrosion rate of reinforcing steels embedded in concrete using polarization resistance measurements", *Werkst. Korros.*, **29**, 515 (1978).

2. Feliú, S. , González, J.A., Feliú, S.Jr., and Andrade, C., "Confinement of the electrical signal or in-situ measurement of Polarization Resistance in Reinforced concrete," *ACI Mater. J.*, **87**, pp 457. (1990)

3. Feliú S., Gonzalez J.A., Andrade C.**,** "Multiple-electrode method for estimatinfg the polarization resistance in large structures". *Journal of applied electrochemistry* **26**. Págs 305-309. (1996)

NEW PRESTRESSING FORCE MEASUREMENT SYSTEM FOR PRESTRESSED CONCRETE CONTAINMENT VESSELS

Masahiko Ozaki
The Kansai Electric Power Co., Inc., Japan

Ikuro Kawai
The Japan Atomic Power Company, Japan

Hiromi Ohashi
The Kanden Kogyo Inc., Japan

Yasuyuki Murazumi Shinichi Takezaki
TAISEI Corporation, Japan

Keyword: PCCV, anchored load, lift-off load, in-service inspection

1. INTRODUCTION

In Japanese PWR type nuclear power plants, periodic measurement of prestressing force at tendon anchorages (anchored load) in prestressed concrete containment vessels (PCCV) has been carried out to verify that they have required ability after completion as shown in references [1], [2] and [3].

VSL unbonded prestressing system is used for Ohi power station unit 3, 4. In the anchored load measurement in each periodic inspection, two filler gages (0.3 mm thick, stainless steel) are inserted between the bearing plate and the anchorhead at selected tendon ends by pulling the tendons with a hydraulic jack. Next, the tendon is pulled again by the jack gradually. When the filler gages are pulled out because of anchorhead movement, the jacking load at the moment (lift-off load) is regarded as anchored load. Schematic drawing is shown in Fig. 1.

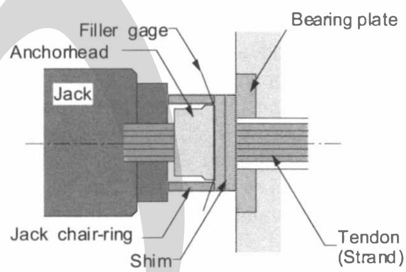

Fig. 1 Lift-off load measurement by filler gage method

The measurement work is required to be carried out more rationally from the viewpoint of time and cost.

Considering these present conditions, we developed simpler and easier method for the measurement, which can keep the same measuring accuracy as existing method.

We, for our purpose, utilized hydraulic type load cells, which were used for prestressing force measurement of permanent anchors in sloped soil and others.

This measurement system is composed of a hydraulic type load cell, a hydraulic pump, an amplifying cylinder, and other measuring devices. The load cell is permanently set between the bearing plate and the anchorhead. The anchor load is obtained in the manner that the oil pressure is measured at the time the rams of the load cell move.

We carried out two tests to realize this system in existing PCCVs. They are reduced-model test and full-scale mode test.

2. OUTLINE OF THE TESTS

In reduced-model test, ring-shaped 1 MN class load cell was made. It is divided in two like shims to be installed to the prestressing system without detension.

The load cell is set between the bearing plate and anchorhead and functions as shims usually does. When the prestressing force is measured, the oil is injected by hydraulic pump and hose into the load cell, and the prestressing force is obtained by measuring the oil pressure in the load cell by a pressure gage. Outline of this system is shown in Fig.2. The amplifying cylinder is used to increase the pressure made by portable low pressure pump.

In full-scale model test, the load cell has just the same size and configuration as shims in existing 10 MN class tendon anchorage in PCCVs, because we plan to set the load cells between the bearing plates and the anchorheads by replacing the shims which were set in existing PCCVs without detension. The load cell consists of two parts as 1 MN class shim–type load cell does. Each part has seven oil cells. The material of the load cell is nickel chromium molybdenum steel.

VSL system 10 MN class tendon anchorage was modeled in concrete block (W:1.1 m, H:1.1 m, L:1.6 m). 10 MN class shim-type load cell is set at the end and tested.

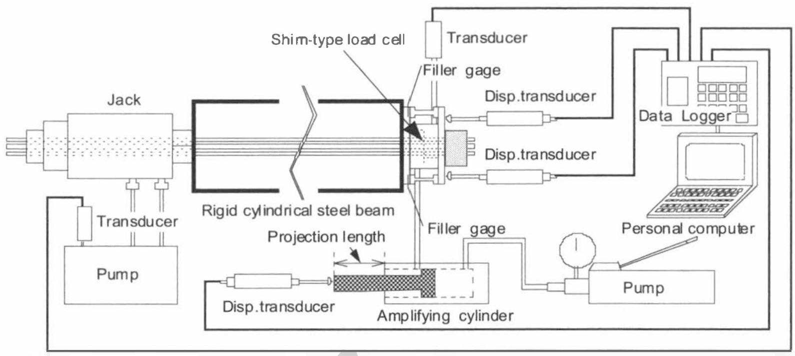

Fig. 2 Outline of measuring system (1MN class)

3. TEST RESULTS

Figure 3 shows, as an example, the relation between the load cell load and the projection length of the amplifying cylinder, which is in proportion to injected oil quantity to the load cell in the reduced model. The relation between the load cell load and the uplift displacement of the anchorhead and lift-off load obtained by filler gage method are also plotted in the figure.

The projection length increased linearly and gradually up to the first pull out of the filler gage. The length increased rapidly after the pull out. The reason is that when the load cell load exceeded the prestressing force, the load cell lifted the anchorhead, and injected oil to the load cell increased rapidly.

Observing the relation between the load cell load and the projection length of the amplifying cylinder, we could obtain anchored load with good accuracy.

The replace work without detension was carried out smoothly in full-scale model test.

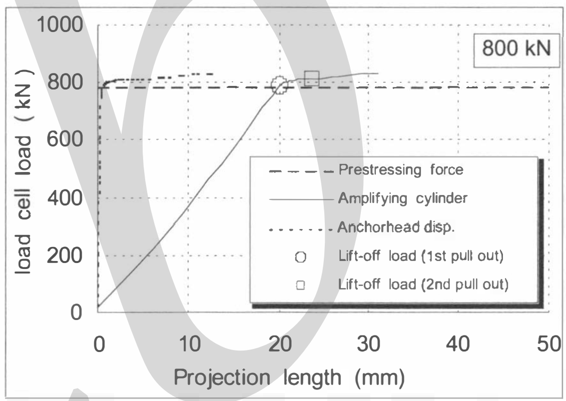

Fig. 3 The relation between the load cell load and the projection length of the amplifying cylinder

4. CONCLUSION

The conclusions obtained by the reduced-scale model test and full-scale model test are as follows:

(1) There are no fundamental technical problems in applying the system we propose here as a measuring system of anchored force measurement of PCCV tendons.

(2) Lift-off load and the change of projection length of the amplifying cylinder which express the change of injected oil quantity to the load cell show close relation to each other.

(3) The difference between anchored load and evaluated load by our method is within 2% in reduced model. However, the accuracy in the full-scale model test was a little lower than that in the reduced-scale model. The better evaluating method is a further research subject.

Further tests on the influence of weather condition, time depending factor, heated grease on the reliability, and measuring accuracy of the load cell are also in execution or planed.

REFERENCE:

[1] Tamura,S. et al. : A Delayed Phenomena Evaluation of Prestressed Concrete Containment Vessel at Tsuruga Unit No.2 Power Station. SMiRT-11, Div.H, pp.305-310, Aug., 1991

[2] Ozaki,M. , Abe,T. , Murazumi,Y. , Aikawa,Y. : Study on the evaluation of the prestressing force prediction of PCCV tendons using Monte Carlo simulation. SMiRT-13, Volume IV, pp.83-88, Aug., 1995

[3] Ozaki,M. , Abe,T. , Watanabe,Y. , Kato,A. et al. : A prediction method for long-term behavior of prestressed concrete containment vessels. SMiRT-13, Volume IV, Div.H, pp.143-148, Aug.1995

LONG TERM STRESS MONITORING ON PC BEAM BY USING ELASTO-MAGNETIC SENSOR

Shoji KUROKAWA, Sunaryo SUMITRO*, Keiji SHIMANO, and Ming L. WANG

*Research and Development Division, Keisoku Research Consultant Co.,
22-7, Minamioi 3-chome, Shinagawa-ku, Tokyo 140-0013, Japan
Email: Sumitoro@krcnet.co.jp http://www.krcnet.co.jp/

Keywords: maintenance, EM sensor, actual stress, fatigue, monitoring,

ABSTRACT

Steel together with concrete is the main structural material of the infrastructures. Along with social development, steel materials have been used for a variety of structures, such as, highway bridges, railroad bridges and buildings. In recent years, many structures have been deteriorating. In order to carry out maintenance management of the structures economically and rationally, it is necessary to evaluate their life cycle cost (LCC) based on the following stages, i.e., construction, inspection, repair, maintenance management, destruction and/or dismantlement [1]. Research on the optimization of maintenance plan has been reported by taking into account inspection expense and inspection accuracy on a description model of the LCC of civil engineering structure [2]. In considering a maintenance plan for Pre-stressed Concrete (PC) structure which aims to reduce its LCC, it is requested that the measurement system should fulfill "AtoE" characteristics, i.e., (A)ccuracy, (B)enefit , (C)ompact, (D)urable and (E)asy to operate, besides enable to measure the actual stress of the PC tendon, non-destructive to the PC tendon itself and no damage to its protection sheath [3]. However, the stress measurement method that fully satisfies such characteristics was not found.

Elasto-Magnetic (EM) actual stress measurement method by utilizing the sensitivity of incremental magnetic permeability due to stress change has been being developed [4,5,6]. Numerous tests of various steel materials by applying this measurement method in which satisfy above-mentioned characteristics have been conducted [7]. It has been proved that EM measurement method enable to measure actual stress of steel wire, PC bar and PC strand precisely without destroying their polyethylene covering sheath [8]. For a PC structure member, although pre-stressing measurement by the load-cell installed at a jack end can be performed before fixation, but the problem becomes difficult after fixation of the PC tendon. Therefore, in order to solve the problem, the steel tendon stress measurement test on outer cable PC beam was conducted by utilizing EM sensor. By comparing with load-cell and strain gage measurement results, the actual stresses of the outer PC tendon in the following conditions are clearly investigated: actual mechanical properties of PC wire under tension test, pre-stress change due to set-loss at PC tendon fixation stage, pre-stress change due to PC tendon relaxation, concrete creep and shrinkage at long-term pre-stressing stage, PC tendon pre-stress change of PC beam under cyclic fatigue loading and actual pre-stress change due to re-pre-stress process.

The loading system is conducted by a Pulsator Fatigue Machine with maximum load 200kN as shown in Fig. 1. The movable rotation supports at both sides were set in the span of 2000mm. The outer cable PC beam specimen was constructed in the length of 2100mm, the width of 150mm, and the height of 180mm. The end of the PC beam was made as a rectangular form to fix PC tendon and a ditch was formed inside the PC beam to enable to install PC tendon and EM sensor.

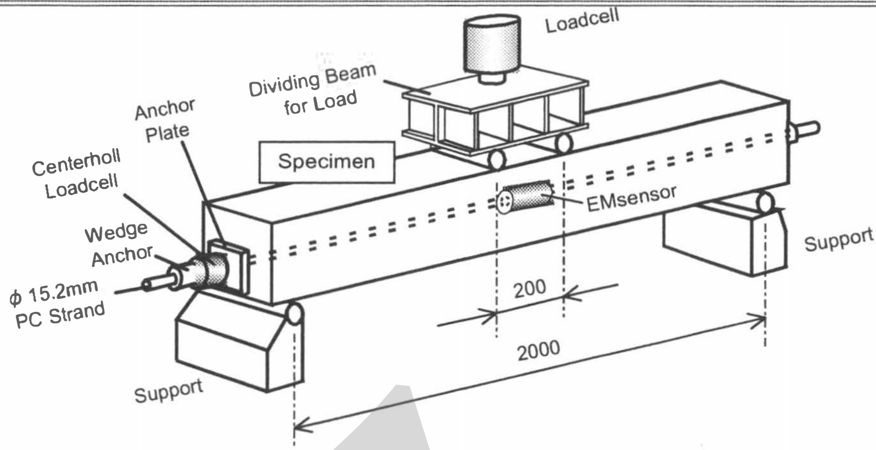

Fig. 1 Specimens and loading system

The concluding remarks of the stress measurement by utilizing EM sensor technology can be summarized as follows:

1. For PC wire under tension loading, EM sensor can perform highly precise stress measurement in the range from zero stress stage to yielding stress stage.
2. As the result of stress measurement at the pre-stress introducing stage, comparing to strain gage and load-cell install at fixation end, EM sensor measurement is the nearest result to the result showed by the load-cell at the jack.
3. In the case of long term pre-stress measurement, stress measurement by utilizing EM sensor has a good agreement with the data recorded by load-cell at jack, therefore, it is confirmed that EM sensor is a suitable measurement device to monitor long-term pre-stress changes.
4. By observing the result of PC beam under static loading test, it is verified that regardless to previous loading history, the easy install EM sensor enable to perform accurate and reliable stress measurement for PC structures at various loading stages.
5. Stress measurement on the pre-stress tendon of PC beam under cyclic fatigue loading test was performed by load-cell and EM sensor. All sensors data shows the same tendency of the stress change which respect to number of loading cycles, however, there is a large difference in pre-stress force quantity. It may be influenced by the restraint of the load-cell setting under severe cyclic load. On the other hand, EM sensor is set-free and does not receive any external force, therefore, it is considered that EM sensor can perform more rational measurement on PC structures under cyclic loading.

REFERENCES

[1] Tominaga, M., Sumitro, S., Okamoto, S., Kato, Y., and Kurokawa, S. : Development of monitoring technology for steel and composite structures, J. of Constructional Steel, Vol.9, Nov, pp.575-582, 2001 (in Japanese)

[2] Honjo, Y., Ueki, J., Sumitro, S., Matsui, Y., and Kato, T. : Influences of quality and frequency of inspection on maintenance of civil engineering structures, Proc. of JSCE Annual Conference, Vol.56, CS6-004, Oct, pp.262-263, 2001 (in Japanese)

[3] Sumitro, S, Okamoto, T., Matsui, Y. and Fujii, K. : Long span bridge health monitoring system in Japan, Proc. SPIE 8th Annual International Symposium on Smart Structures and Material, Health Monitoring and Management of Civil Infrastructure Systems, Newport Beach CA, Vol. 4337-67, pp.517-524, 2001

[4] Chen, Z., Wang, M.L., Okamoto, T., and Sumitro, S. : A new magnetoelastic stress/corrosion sensor for cables in cable-stayed bridges using measurement of anhysteretic curve, 2nd Workshop on ATUEDM, Kyoto, July 11-13, 2000

[5] Sumitro, S. : True-stress measurement of PC steels by EM sensor, J. of Pre-stressed Concrete Japan (Japan Prestressed Concrete Engineering Association), Vol.43, No.6, Nov, pp.99-103, 2001 (in Japanese)

Author Index

Volume 1	**Plenary papers, Primary papers, Condensed papers(1)**
Volume 2	**Condensed papers(2)**
Volume 3～8	**Keynote papers, Contributed papers**